OPTICAL COHERENCE TOMOGRAPHY
of OCULAR DISEASES

Carmen A. Puliafito
Michael R. Hee
Joel S. Schuman
James G. Fujimoto

Optical Coherence Tomography of Ocular Diseases

CONTENTS

CHAPTER 1

Principles of Operation and Technology

Measuring Microstructural Information
Tomographic Imaging
OCT Instrumentation
Summary

Optical Coherence Tomography (OCT) is a new medical diagnostic imaging technology which can perform micron resolution cross-sectional or tomographic imaging in biological tissues [1-4]. The operation of OCT is analogous to ultrasound B-mode imaging or radar except that light is used rather than acoustic or radio waves. OCT is especially suited for diagnostic applications in ophthalmology because of the ease of optical access to the anterior and posterior eye.

Imaging techniques which can provide tomographic or cross-sectional images of intraocular structures can yield powerful diagnostic information which is complementary to conventional fundus photography and fluorescein angiography. Techniques such as X-ray computed tomography (CT) and magnetic resonance imaging have been applied for diagnostic imaging in ophthalmology [5-7]. However, these approaches have not been widely used in routine diagnostic applications in ophthalmology because of their limited resolution and preclusive cost and complexity.

This chapter presents an overview of the principles of operation and the technology of OCT. This information, while not directly relevant for clinical diagnosis, will provide the interested reader with a knowledge of how OCT functions and how OCT imaging compares to other diagnostic imaging such as ultrasound. In addition, we will describe the technology which governs OCT and how OCT instruments function. A more detailed discussion of the physical principles of OCT is included in the Appendix. This information is useful for the researcher who wishes to understand the factors which govern OCT imaging resolution and performance.

MEASURING MICROSTRUCTURAL INFORMATION

Optical Tomography Versus Ultrasound

Ultrasound imaging is widely used clinically for quantitative measurements of intraocular distances as well as imaging the anterior eye and globe [8-9]. Since ultrasound imaging depends on the reflection of sound waves from intraocular structures, it requires direct contact of the ultrasound measuring device to the cornea or immersion of the eye in a liquid which facilitates the transmission of sound waves into the globe.

The resolution of ultrasound measurement depends directly on the frequency or wavelength of the sound waves which are used. For typical ultrasound systems, sound wave frequencies are in the ten megahertz (10 MHz) regime which yield spatial resolutions of approximately 150 microns. Ultrasound imaging also has the advantage that sound waves are readily

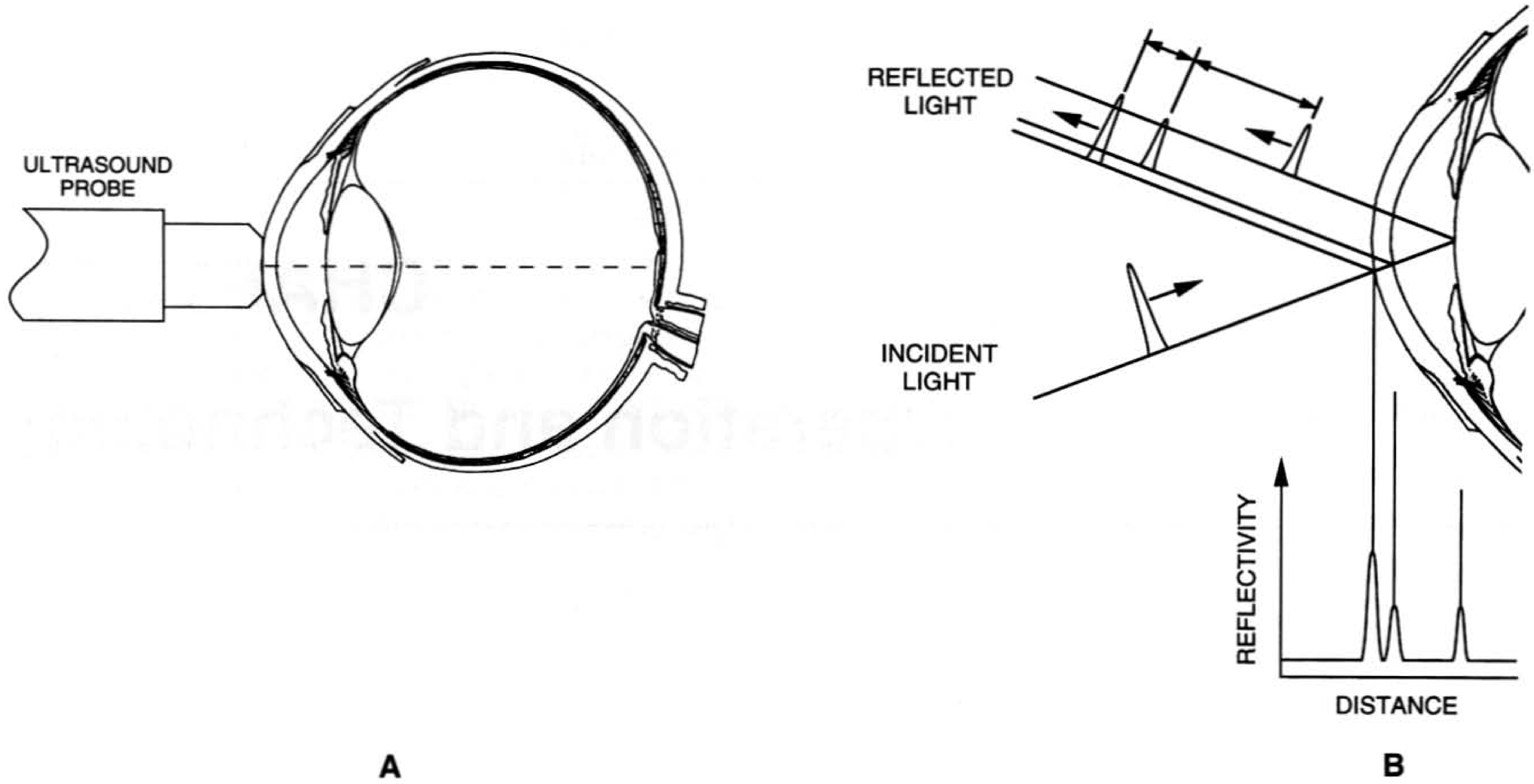

Figure 1-1. Reflection of light and sound from the eye. (A) Ultrasonic axial measurement (A-mode) and imaging (B-mode) function by measuring the time delay for sound to be reflected from different intraocular structures. Ultrasound measurement requires direct contact with the eye in order to transmit and receive the sound waves. (B) Optical axial ranging and imaging function by measuring the time delay when light is reflected from different structures. Optical techniques have higher spatial resolution than ultrasound and do not require direct contact with the eye.

transmitted into most biological tissues and therefore it is possible to obtain images of structures deep within the body. Recently, high resolution ultrasound imaging systems have been developed which use higher frequency sound waves and which have resolutions on the 20 micron scale [10]. However, higher frequency ultrasound is strongly attenuated in biological tissues. Imaging can be performed to depths of only 4 to 5 mm, limiting the application of high resolution ultrasound to the anterior eye.

In contrast, optical measurement and imaging techniques rely on the use of light rather than sound waves. For this reason, optical diagnostics can be performed without physical contact to the eye, thereby minimizing patient discomfort during examination. In addition, the use of light rather than sound waves provides a significantly higher spatial resolution than possible with ultrasound. Current OCT imaging technologies yield images which have approximately ten times higher resolution than standard ultrasound B-mode imaging. The inherently high resolution of OCT permits the imaging of fine structures within the retina as well as anterior eye, thus facilitating the diagnosis of a wide range of clinically relevant pathologies. The principal disadvantage of optical techniques is that light is highly scattered or absorbed within most biological tissues and therefore optical imaging is constrained to tissues which are optically accessible either directly or via endoscope or catheter. OCT is ideally suited for ophthalmology, however, because of the ease of optical access of the eye.

In order to perform cross sectional or tomographic optical imaging in biological systems, it is first necessary to have an approach which can measure the internal structure of biological tissues. In OCT, the first step in measuring a tomographic image is the measurement of axial distance or range information within the tissue. Figure 1-1 shows a schematic which contrasts the use of sound waves versus light waves for measurement of distances in the eye.

In ultrasound measurement, a high frequency sound wave is launched into the eye from an ultrasonic probe. The sound wave travels into the eye and is reflected from different boundaries between microstructural features in the eye. The time behavior or echo structure of the sound waves which are reflected back to the ultrasonic probe are then measured and distances within the eye are determined from the echo

delay of the sound from different boundaries within the eye. This principle of operation is similar to that used in radar detection of aircraft.

In OCT, measurements of distance and microstructure are performed by reflecting light waves from different microstructural features within the eye. For the purposes of illustration, it is possible to conceptualize the operation of OCT by thinking of the light beam as being composed of short optical pulses. However, it is important to note that although OCT may operate using short pulse light sources, most OCT systems operate using a continuous beam of what is termed short coherence length light. The operation of OCT is based on an optical measurement technique known as low-coherence interferometry. A detailed description of the physical principles of operation of low-coherence interferometry is presented in the Appendix.

Echo Delay

When a beam of light is directed onto the eye, it is reflected from boundaries between different tissues as well as scattered differently from tissues which have differing optical properties. The distances and sizes of different tissue structures in the eye can be determined by measuring the "echo" time it takes for light to be reflected or backscattered from the different structures at varying axial (longitudinal) distances [11-12]. This principle of operation is identical to ultrasonic

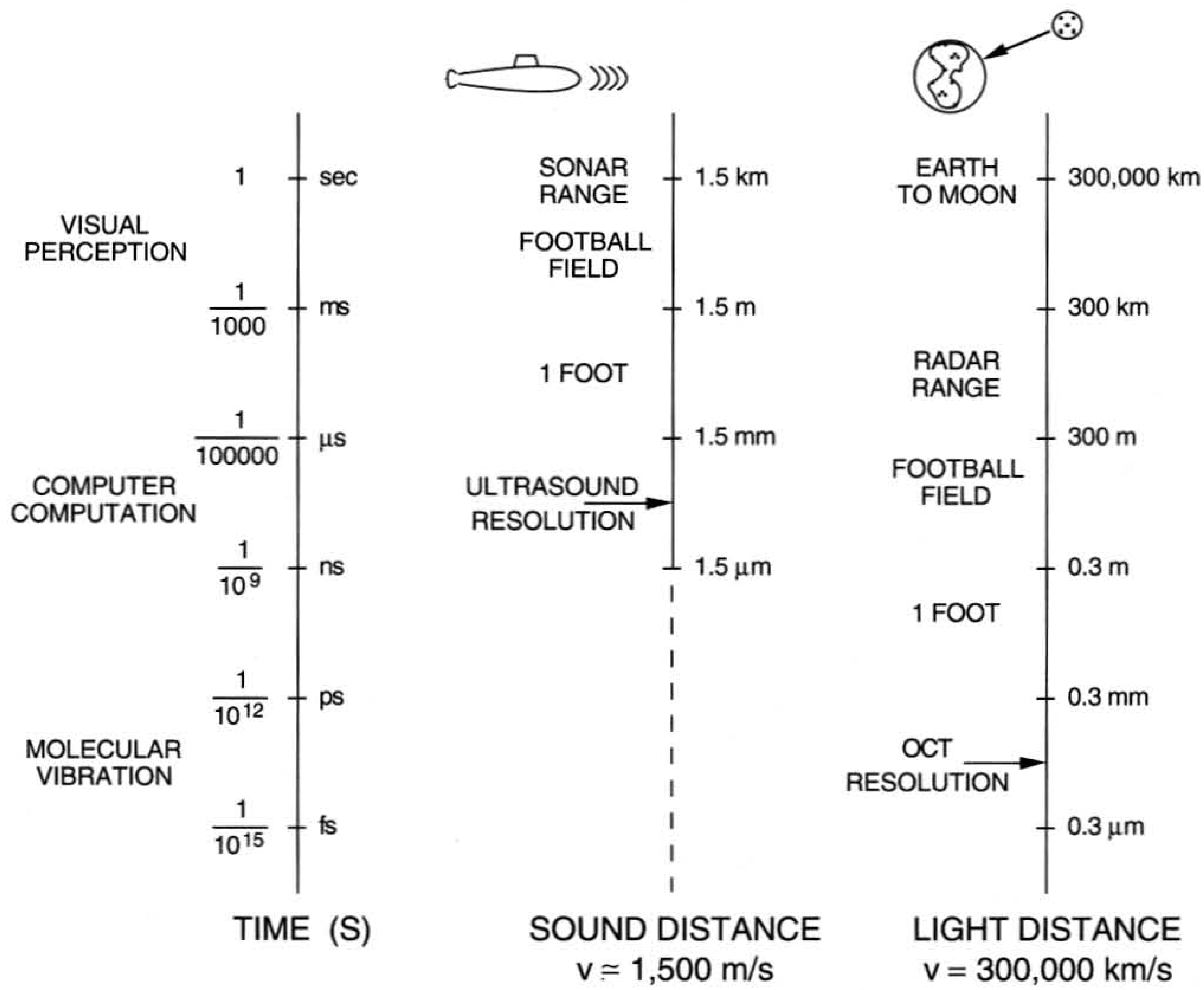

Figure 1-2. Distance and time scales for light and sound. The characteristic time and distance scales for light and sound are dramatically different. The velocity of sound is approximately 1500 meters/sec while the velocity of light is 3×10^8 meters/sec. Standard ultrasound has a resolution limit of 150 microns, which corresponds to a time measurement of 100 ns, (100×10^{-9} sec). In contrast, standard OCT technology has a resolution of 10 microns, corresponding to a time measurement of 30 fs (30×10^{-15} sec). Thus, the use of light for measuring short distances implies very high resolution time measurement. The above scales are logarithmic, each vertical division represents a factor of 1000. Note that light from the moon takes about 1.3 sec to reach the earth.

A-mode ranging except that light rather than soundwaves are used. As discussed previously, optical techniques provide significant advantages over ultrasound.

The principal difference between ultrasonic and optical imaging is speed: the speed or velocity of propagation of light is nearly a million times faster than the speed of sound. Since distances within the biological tissue are measured by measuring the "echo" time delay of reflected sound waves or light waves, this implies that distance measurement using light requires ultrafast time resolution.

Figure 1-2 describes the conversion of distance and time scales for light and sound. The velocity of sound in water is approximately 1500 meters per second, while the velocity of light is approximately 3×10^8 meters per second. Distance or spatial information may be determined from the time delay of reflected echoes according to the formula $\Delta T = \Delta d / v$ where ΔT is the echo delay, Δd is the distance that the echo travels, and v is the velocity of the sound wave or light wave. Thus, the measurement of distances and structure with a resolution on the 100 micron scale, which would be typical for ultrasound, corresponds to a time resolution of approximately 100 ns (100×10^{-9} s). In contrast, measurement of structure with a resolution on the 10 micron scale, which is achieved by OCT, corresponds to a time resolution of approximately 30 fs (30×10^{-15} s). Fortunately, it is possible to perform high resolution optical range and corresponding time measurements using relatively simple optical techniques.

Low-Coherence Interferometry

Optical Coherence Tomography uses low-coherence or white light interferometry to perform high resolution range measurements and imaging. The basic technique of white light interferometry is well established and in fact was first described by Sir Isaac Newton [13]. During the last several years, low-coherence interferometry was developed as a measurement technology for performing high resolution optical measurements in fiber optics and optoelectronic components [14-16]. In order to perform high resolution structure measurements with tens of micron resolution (corresponding to echo delay times of tens of femtoseconds), it is necessary to use an optical instrument which compares or correlates one optical beam or lightwave with another. This measurement may be performed by an optical device known as an interferometer.

Figure 1-3 shows a schematic of an optical interferometer. An optical beam from a laser or light source which emits either short optical pulses or short coherence length light is directed onto a partially reflective mirror (optical beamsplitter). The partially reflecting mirror splits the light into two beams; one beam is reflected and the other is transmitted. One light beam is directed onto the patient's eye and is reflected from intraocular structures at different distances. The reflected light beam from the patient's eye consists of multiple echoes which give information about the range or distance and thickness of different intraocular structures. The second beam is reflected from a reference mirror at a known spatial position. This retro-reflected reference optical beam travels back to the partial mirror (beamsplitter) where it combines with the optical beam reflected from the patient's eye.

The operation of the system can be understood

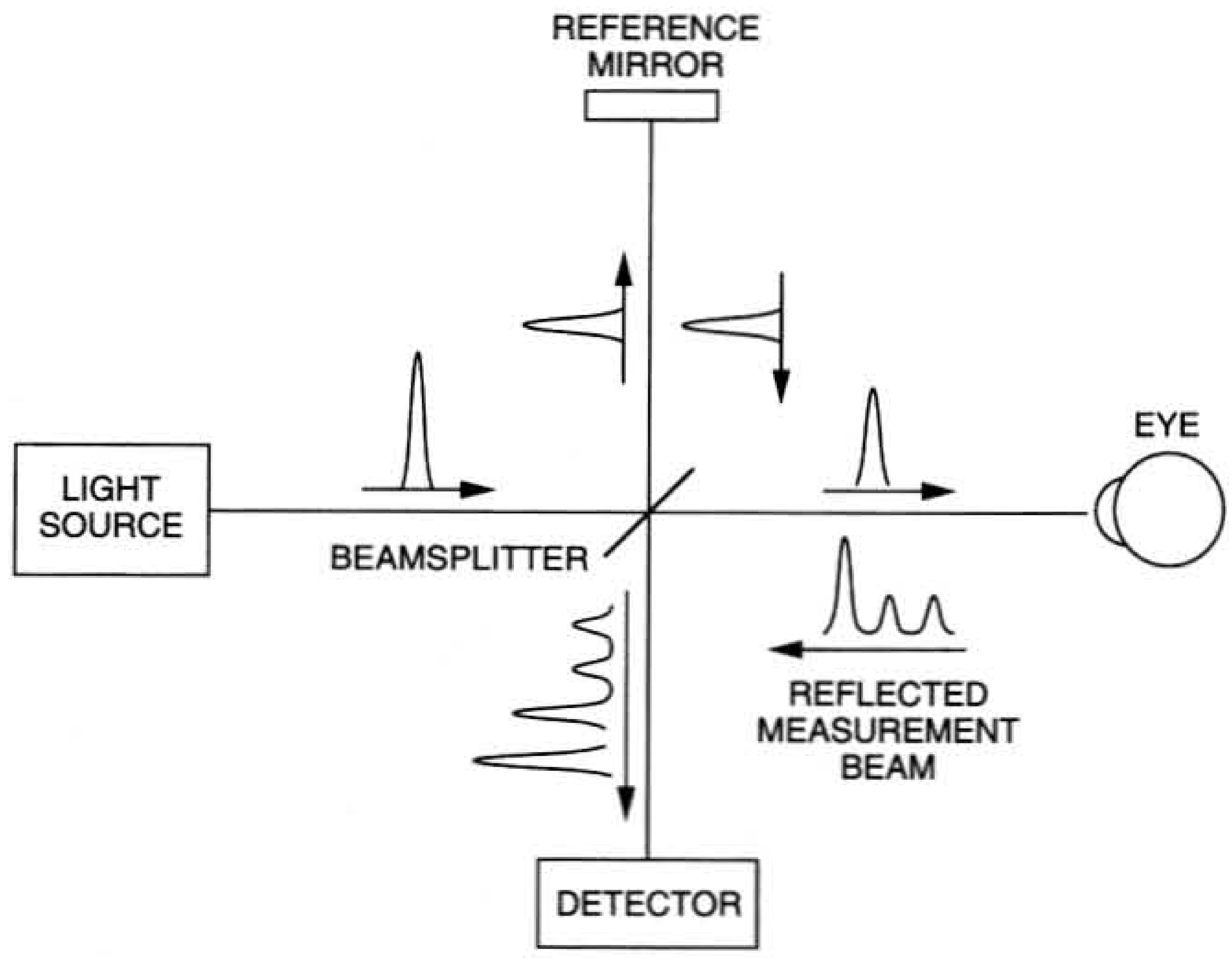

Figure 1-3. The optical interferometer: a technique for high resolution time and distance measurement using light. High resolution time and distance measurement may be performed by comparing or correlating one light beam with another. Light from a source is directed onto a partially reflecting mirror and is split into a reference and a measurement beam. The measurement beam is reflected from the specimen with different time delays according to its internal microstructure. The light in the reference beam is reflected from a reference mirror at a variable distance which produces a variable time delay. The light from the specimen, consisting of multiple echoes, and the light from the reference mirror, consisting of a single echo at a known delay are combined and detected. The echo structure of the reflected measurement beam may be determined by electronically processing the detector output while varying the position of the reference mirror to produce different time delays for the reference light. A detailed discussion of the operation of this device is provided in the appendix.

qualitatively if one thinks of the light beam as being composed of short pulses of light. In this case, the pulse of light reflected from the reference mirror will coincide with the pulse of light reflected from a given structure in the patient's eye, only if both pulses arrive at the same time. This will occur only if the distance that light travels to and from the reference mirror precisely matches the distance that light travels when it is reflected from a given structure in the patient's eye. When the two light pulses coincide they produce a phenomenon known as interference which is measured by a light sensitive detector (photodetector).

In order to measure the time delays of light echoes coming from different structures within the eye, the position of the reference mirror is changed so that the time delay of the reference light pulse is adjusted accordingly. The signal from the detector will then follow the echo structure of the light reflected from the eye. If there are multiple reflections, there will be a peak observed each time the reference pulse is delayed so that it coincides with an echo pulse from a particular structure in the eye. Thus the interferometer can precisely measure the echo structure of reflected light and perform high resolution measurements of the distance and thickness of different tissue structures [17-20].

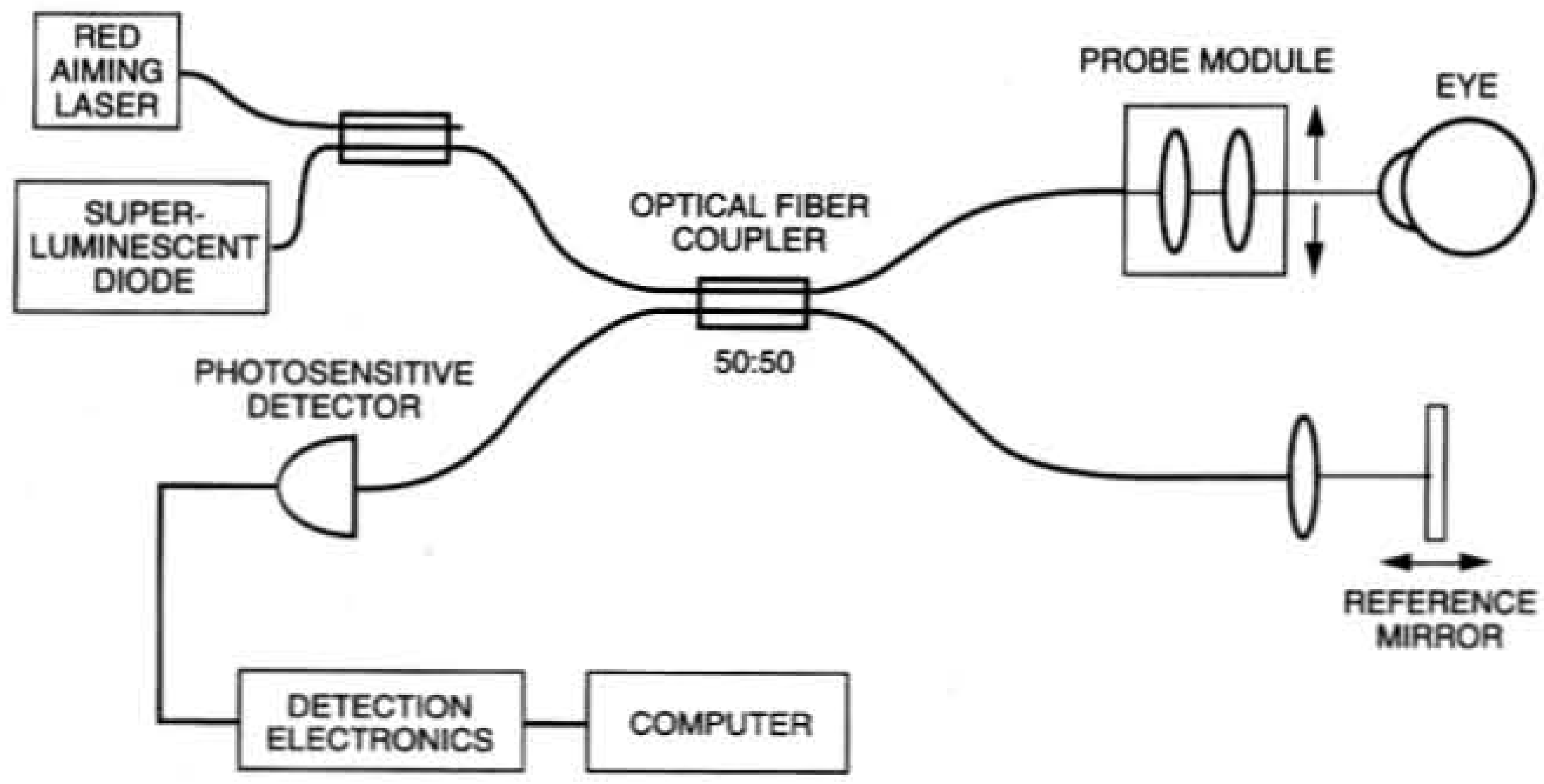

Figure 1-4. Fiber-optic interferometer OCT system. The optical interferometer shown in Fig. 1-3 can be built using fiber optic components to contstruct a compact and modular system. The light source used in most OCT systems is a low-coherence, superluminescent diode which is directly coupled into an optical fiber. The interferometer is built using an optical fiber coupler (splitter) where one fiber forms the measurement path of the interferometer and the other the fiber forms the reference path of the interferometer. The fiber in the measurement path is engineered as a remote probe which may be interfaced to a variety of ophthalmic instruments.

A more detailed description of how the interferometer operates is presented in the Appendix. For the purposes of the current discussion, the key feature of the interferometer is that it can measure the time delays of optical echoes by comparing the reflected light beam with a reference beam. While the explanation presented here assumes that the light is composed of short optical pulses, the measurement may also be performed using non-pulsed, or continuous light with a short coherence length [17-20]. For this reason the measurement technique has been termed "low-coherence interferometry."

Recent technological advances in fiber optics and optical communications technology have made it possible to engineer an extremely compact, robust, and low cost measurement system using optical fibers and diode light sources [21]. Figure 1-4 shows a schematic representation of a fiber-optic version of the interferometer. The light source for the interferometer is a compact superluminescent diode, which is coupled directly into an optical fiber. This light source is similar to laser diodes used in optical compact disc players, except in OCT, the diode source is designed to emit short coherence length light. The interferometer is constructed using a fiber-optic coupler which functions analogously to a beamsplitter. The arm of the interferometer which consists of the reference mirror is located within the instrument, while the optical fiber in the second arm of the interferometer is connected to the OCT ophthalmic instrument resembling a slit-lamp biomicroscope or fundus camera. In other applications, the fiber optic probe can be interfaced with endoscopes or catheters for measurement of images at distal points. The technological base for the instrument is well developed because of its widespread use in fiber-optic communications networks. Thus, its inherent reliability and robustness is exceedingly high. In addition, the use of a fiber-optic technology is well suited for interfacing to different instruments for clinical imaging.

Axial Range, Distance, and Thickness

The simplest type of measurement that can be performed by OCT is a measurement of axial range analogous to ultrasound A-mode ranging. Range information and tissue distances or thicknesses are determined by electronically measuring the signal from the light sensitive detector and then processing the signal electronically and displaying it by computer. Figure 1-5 shows an example of axial range measurements performed in the anterior chamber [17-20]. The graph shows the intensity of the reflected light from different structures within the anterior eye as a function of

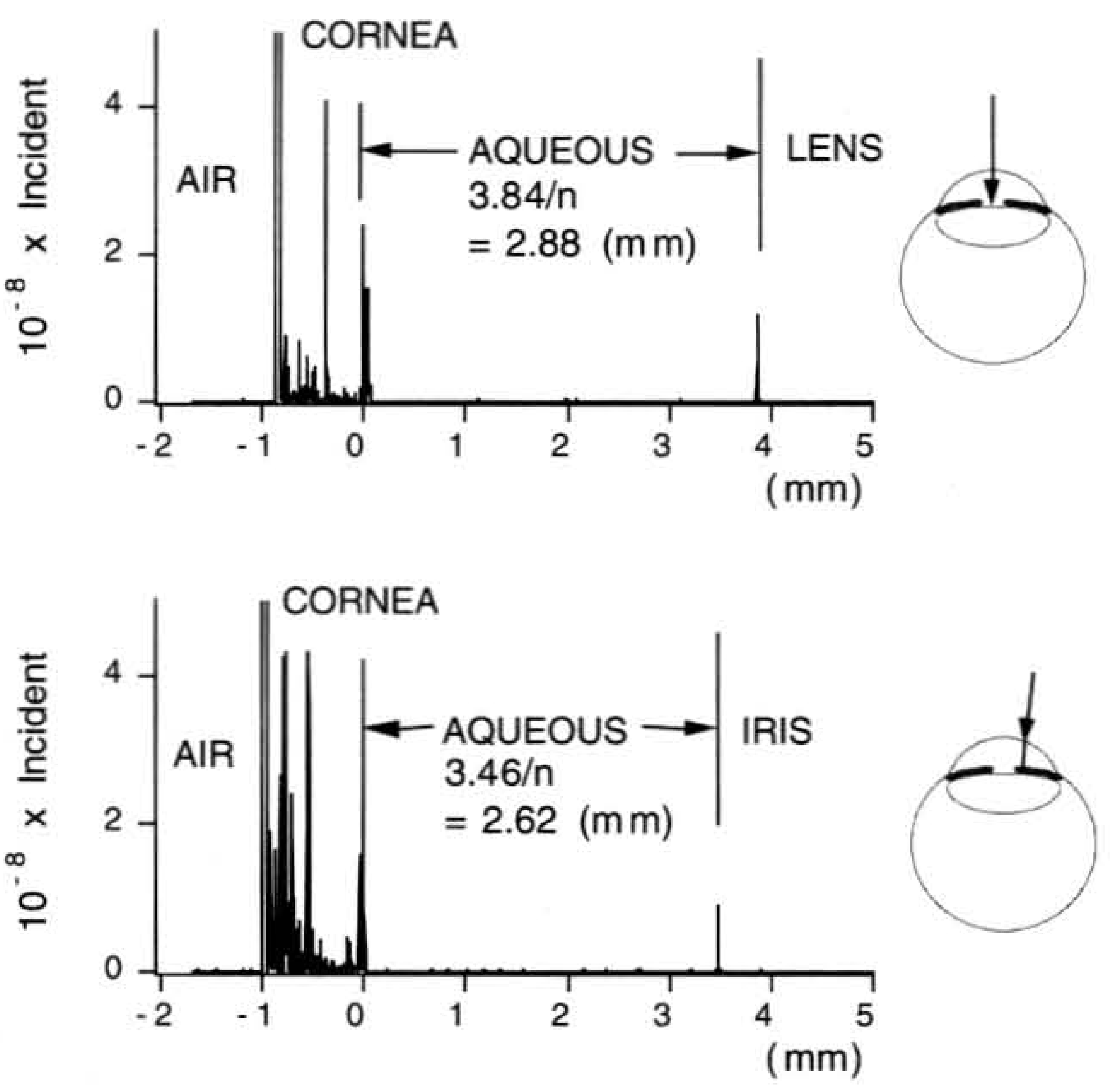

Figure 1-5. Measurement of the anterior chamber depth using optical low-coherence interferometry. The graphs display the magnitude of the reflected optical intensity as a function of distance. The measurement is analogous to ultrasound A-mode ranging, except that light is used rather than sound. A large reflection is observed from the anterior surface of the cornea while smaller reflections originate from the posterior corneal surface (cornea-aqueous boundary), and the lens or iris. Note the presence of scattered light which originates from within the cornea. The data plots show the structural features which occur along the axis of the optical beam. If the transverse position of the optical beam is changed, then different features are measured (the depth of the anterior chamber versus the depth to the iris).

echo delay or distance (axial or longitudinal range). Echoes may be observed from the anterior and posterior surfaces of the cornea as well as from the anterior capsule of the lens. The intensity of reflections is a measure of the discontinuity of the optical properties of the tissue. The reflection of the optical beam from the anterior surface of the cornea is relatively large; however, reflections from internal structures occurring at boundaries between different tissue types (*i.e.*, such as between the cornea and aqueous, or different layers of the retina) are relatively small. In addition, the scattering of light from different tissues (*i.e.*, such as within the cornea and lens, or, in the posterior eye, within different layers of the retina) can also be measured.

The axial range measurement shown in Figure 1-5 permits a direct measurement of corneal thickness as well as anterior chamber depth. The thickness of the tissue is calculated by measuring the optical echo delay and multiplying it by the speed of light in the tissue. The speed of light in the tissue is given by the speed of light in vacuum times the index of refraction of the tissue. Thus, measurement of physical thickness from OCT relies on knowing or assuming a value for the index of refraction of the tissue. The strength or magnitude of the reflected light is extremely small, on the order of approximately 10^{-5} to 10^{-9} (-50 dB to -90 dB) of the incident light power. Thus, very high detection sensitivity to very weak reflected echoes is required for ranging or measurement of structures within the eye.

Once an axial range measurement has been made, the relative positions of different structures may be measured by changing the transverse position or aiming of the optical beam within the eye. Figure 1-5B shows a second axial range measurement with the optical beam aimed on the iris rather than the anterior capsule of the lens. Because the light beam can be focussed to a small spot size, the transverse position of the beam can be known with high precision. Thus, information on both the axial or longitudinal as well as the transverse microstructure of tissue can be measured. This is the basis for performing optical tomography or cross sectional imaging.

TOMOGRAPHIC IMAGING

Constructing Tomographic Images from Successive Axial Range Scans

Tomographic or cross sectional imaging of the tissue is achieved by performing successive axial or longitudinal measurements of the tissue at different transverse points [1-4]. Figure 1-6 schematically illustrates how an optical coherence tomogram of the anterior chamber is acquired. Successive rapid axial measurements are performed while scanning the optical beam in the transverse direction. The result is a set of axial range data similar to that shown in Figure 1-5 where each trace represents the magnitude of reflection or backscattering of the optical beam as a function of depth in the tissue. Conversely, each trace describes that axial (or longitudinal) information at a different transverse position. For purposes of visualization, it is more convenient to process this data by computer and display it as a two dimensional grey scale or false

color image.

Grey Scale and False Color Representation of Images

Figure 1-7 shows an example of a tomographic image of the anterior chamber displayed in grey scale. The image consists of 200 pixels (horizontal) by 500 pixels (vertical). The vertical direction corresponds to the direction of the optical beam and the axial (longitudinal) data sets. The optical beam was scanned in the transverse direction and 200 axial measurements were performed. The intensity of the backscattered optical signal is represented on a logarithmic scale with varying degrees of brightness. The white corresponds to the highest reflection or backscatter of the optical signal, while dark grey and black correspond to weaker back reflection. The image is displayed on the logarithmic scale with the maximum signal approximately -50 dB or 10^{-5} of the incident signal, and the minimum detectable back reflection is approximately -95 dB, or 10^{-10} of the incident optical signal. The dynamic range of the image is approximately 45 dB.

The grey scale tomographic image clearly delineates structure in the anterior eye including corneal thickness as well as curvature of the anterior and posterior surfaces of the cornea. The depth of the anterior chamber may also be readily measured as well as structures within the iris and lens. Shadowing of structures is also observed in a manner analogous to ultrasound. If a tissue lies behind a highly optically scattering tissue, then the optical beam may not penetrate the highly scattering tissue and the deeper tissues will appear dark in the image. This can be observed in the area of the lens behind the iris and also in the area of the image behind the sclera.

In order to enhance the differentiation of different structures within the image, the image may also be displayed in a false color representation as shown in Figure 1-8. In this case, the logarithm of the optical reflection or backscatter is represented by different colors. In this image, the intensity of the optical signal is mapped onto the color scale using the standard "rainbow" order of colors. The highest back reflection or scattering is represented by red and white colors, and typically corresponds to -50 dB of the incident signal, while the lowest backscattering is represented by blue and black and typically corresponds to -100 dB of the incident signal. Thus tissues which have different optical reflection or scattering properties will be displayed in different colors on the false color image. It is important to note that although the tomographic image represents the true dimensions of the structure (knowing the optical index of refraction) being measured, the coloring of different structures represents

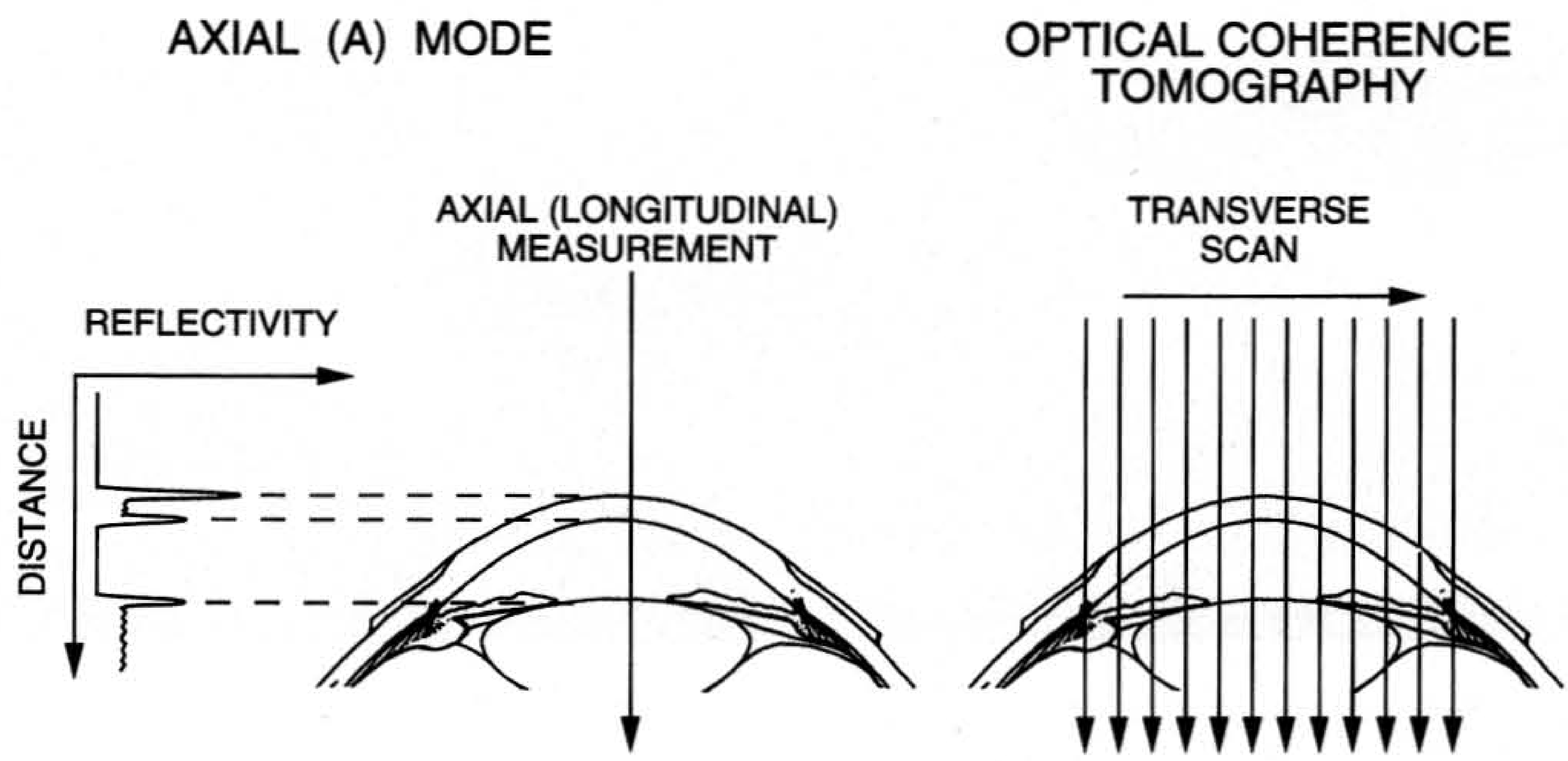

Figure 1-6. Image measurement using Optical Coherence Tomography. Tomographic images are constructed by performing rapid, successive axial (longitudinal) measurements at different transverse points. Each axial measurement represents optical reflection and backscatter from microstructures which are intercepted by the optical beam. By scanning the beam transversely while performing axial measurements, a two dimensional set of data may be measured which is a cross-sectional map of the reflection and backscatter within the tissue.

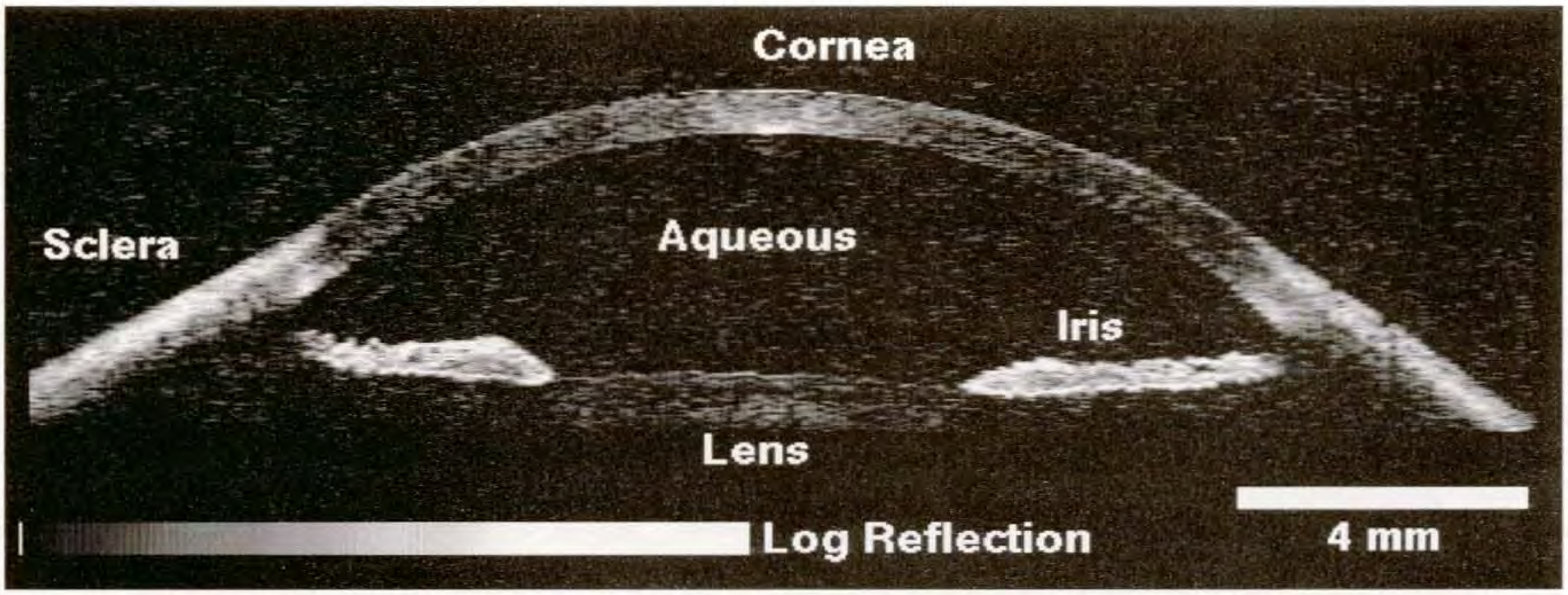

Figure 1-7. Grey scale Optical Coherence Tomography image of the anterior chamber of a human eye obtained *in vivo*. The image contains 200 pixels (horizontal) by 500 pixels (vertical) and spans 21 mm across by 6 mm deep. The image is displayed using a logarithmic mapping of the measured optical signal to brightness. The maximum signal is approximately -50 dB of the incident signal, while the minimum detectable signal is approximately -95 dB.

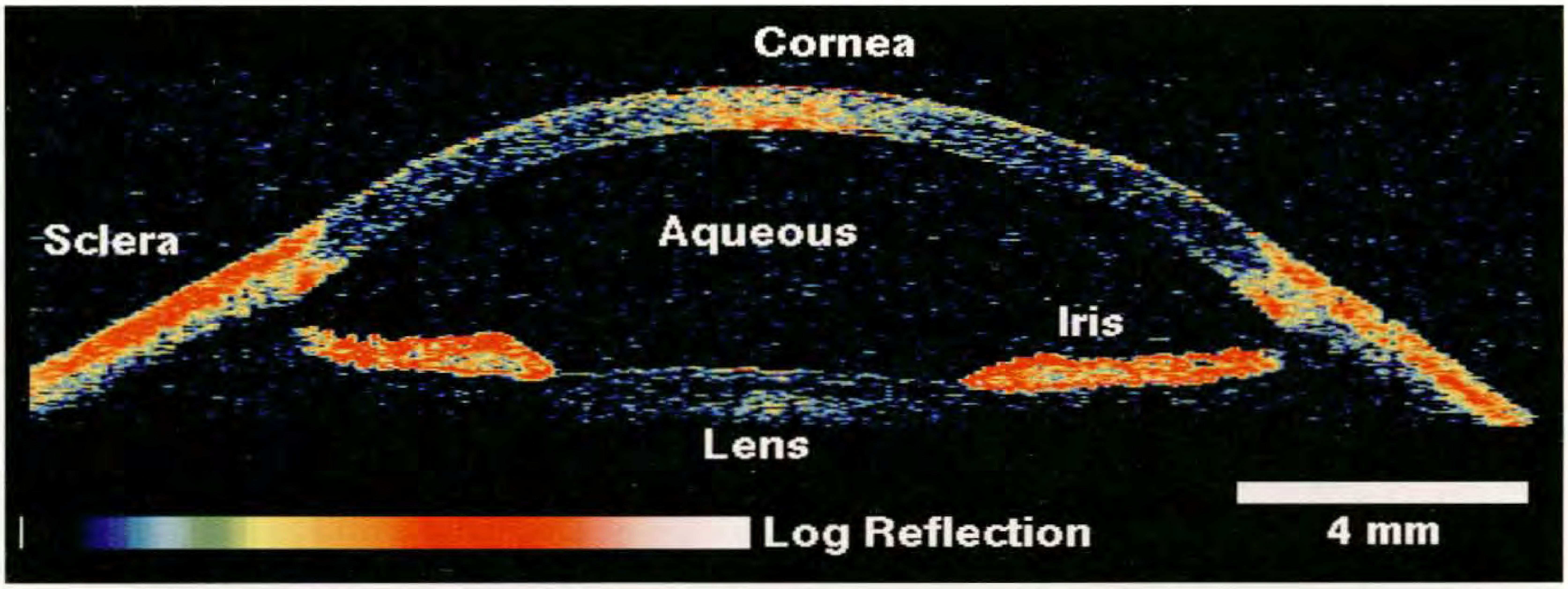

Figure 1-8. False color representation of the same Optical Coherence Tomography anterior eye image shown in Figure 1-7. The image is displayed using a logarithmic mapping of the measured optical signal to brightness. The maximum optical reflection and backscattering (-50 dB of the incident light) are represented by red-white colors, while the minimum detectable signals (-95 dB) are represented by blue-black colors. As in other medical imaging modalities, the use of false color does not necessarily correspond to microstructural features, but can aid in differentiating different structures in an image.

different optical properties and not necessarily different tissue morphology. Care must be taken to avoid interpreting images analogously to conventional histopathology. OCT imaging is similar to ultrasound where different degrees of ultrasound backscattering correspond to different color or grey levels except that in OCT images, different optical reflection and scattering properties are measured.

Image Resolution

The image resolution of OCT in the axial (or longitudinal) versus transverse directions is determined by different mechanisms. A more detailed description of the factors governing image resolution is presented in the Appendix. The quantitative information presented here is intended only as a rough guide to image resolution since different OCT systems can have significantly different performance depending upon their design and intended application.

The resolution of the image in the axial (longitudinal) direction is determined by the resolution of the optical ranging measurement. This is determined by the physical properties of the light source which is used for the measurement. If a short pulse laser source is used, the axial resolution is determined by the pulse duration. Conversely, if a continuous, low-coherence light source is used, the axial resolution is determined by the "coherence length" of the light source. For typical systems, the axial resolution is approximately 10 to 20 microns. This number represents the apparent width on a linear scale of an isolated reflection and is a measure of the smallest feature that can be differentiated in the image. It is important to note that the measurement of distance or tissue thickness can, in practice, be performed with significantly higher resolution than this limit.

The transverse resolution of the image is determined by the size of the focussed optical beam. This is a function of the optics used to project the beam onto the eye and is determined by factors such as whether imaging is performed over a large depth, such as in the anterior eye, or whether the focussing angle is restricted, as in imaging the retina. Typically, the transverse resolution is in the range of 20 to 50 microns and depends upon whether imaging is performed in the retina or the anterior eye, respectively.

The image resolution is also a function of the size of the tomogram that is desired. If a larger area is to be scanned, the image may be constructed with a larger number of axial (longitudinal) data sets which correspond to more transverse points (or pixel elements) in the image. For most intraocular structures it is not necessary to image with the full resolution possible in the transverse dimension to permit clinical diagnosis. Since the image acquisition time depends on the number of transverse pixel elements as well as the depth of the image being acquired, faster image acquisition may be obtained if very high resolution imaging is not required.

Computer Image Processing and the Correction of Eye Motion

Since the resolution of OCT is extremely high, it is essential to compensate for motion of the eye during image acquisition, since eye motion can cause image blurring. Movements of the eye can be caused by a variety of processes including fluctuations in intraocular pressure produced by pulse, microsaccades and tremor, and changes in the patient's fixation point. Since OCT measures the absolute distance or range of the tissue specimen, it is essential to correct for motion of the eye. This problem is addressed by powerful yet simple computer image processing techniques which can be used to dramatically enhance imaging performance by virtually eliminating image blurring from involuntary patient eye motion.

Figure 1-9 shows an optical coherence tomogram of the fovea showing the raw image data without image processing and the image achieved after processing to correct for eye motion. The dominant motion which blurs the image occurs in the axial (longitudinal) direction because retinal structure in this direction has dimensions on the micron scale. These changes in the longitudinal position of the eye may be corrected because the optical ranging measurement itself determines the longitudinal position of the retina. The tomographic image is constructed by performing sequential axial (longitudinal) ranging measurements at different transverse positions within the eye. However, if the eye moves on a micron scale in the longitudinal direction, between the time that successive axial range data sets are acquired, then the positions of different features will be observed at different axial (longitudinal) ranges. Thus, the motion of the patient's eye in the axial (longitudinal) direction may be measured, by correlating adjacent axial data sets. Figure 1-10 shows an example of this measurement.

Once the axial position of the patient's eye is known, the scans in the optical tomographic image may be displaced in the axial direction so that microstructural features will be aligned. Changes in transverse eye position are not eliminated using image processing. Thus, drifts in patient fixation are not compensated for. However, small changes in transverse position do not produce significant degradation in image quality because the typical features in the trans-

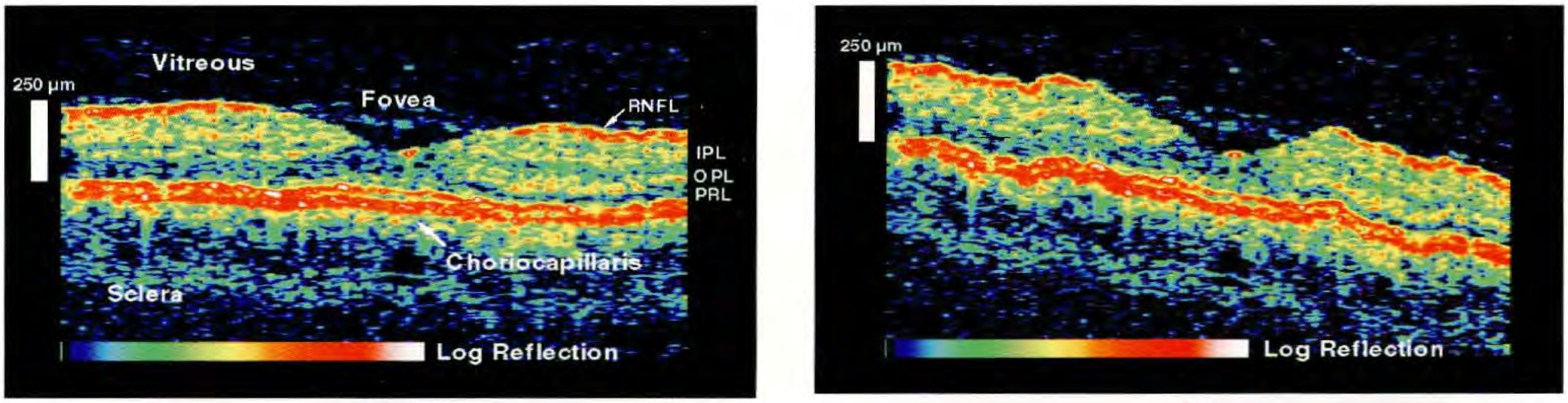

A B

Figure 1-9. Optical Coherence Tomography images of the macula showing the use of computer image processing to correct for patient eye motion. (A) Processed image. Identifiable structures include the vitreous, fovea, retinal nerve fiber layer (RNFL), photoreceptor layer (PRL), inner and outer plexiform layers (IPL, OPL), and choriocapillaris. The inner and outer nuclear layers appear as unlabeled darker regions posterior to the plexiform layers. The image consistes of 100 pixels (horizontal)by 250 pixels (vertical). The horizontal scale has been compressed by a factor of two to aid in viewing. (B) Original, unprocessed tomogram corresponding to the image presented in (A). Ocular motion creates small variations in the depth of each axial reflectivity profile which may be corrected with a cross-correlation scan re-registration technique.

Figure 1-10. The axial deviations caused by ocular motion may be estimated by cross-correlating adjacent longitudinal (axial) data sets. The plot shows the index of the peak cross-correlation between adjacent scans and is a measure of longitudinal eye motion. Low-pass filtering of the contour estimate nominally removes high spatial frequency motion artifacts while preserving the actual variations in surface profile. Scan re-registration is accomplished by comparing the original and filtered contour estimates.

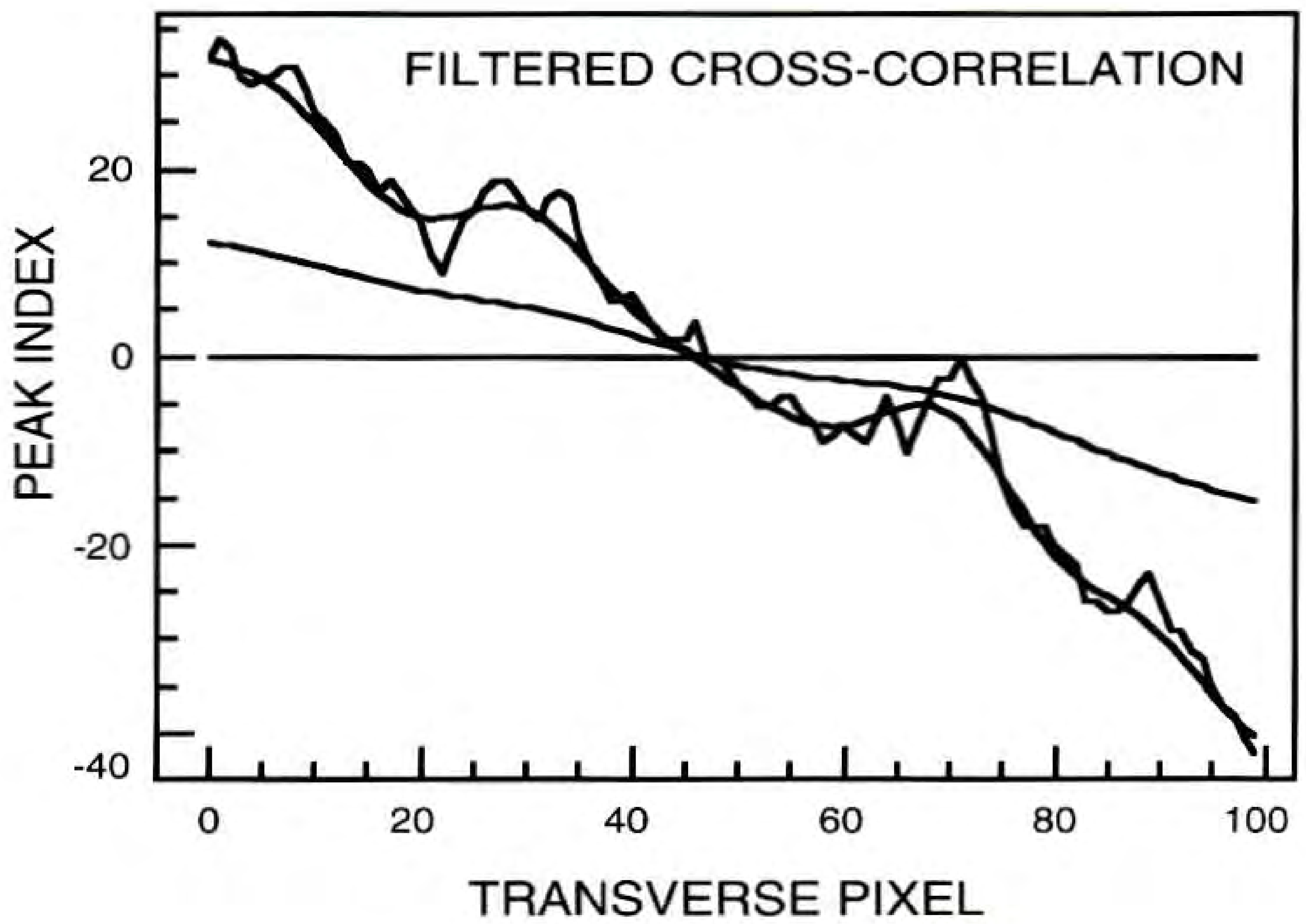

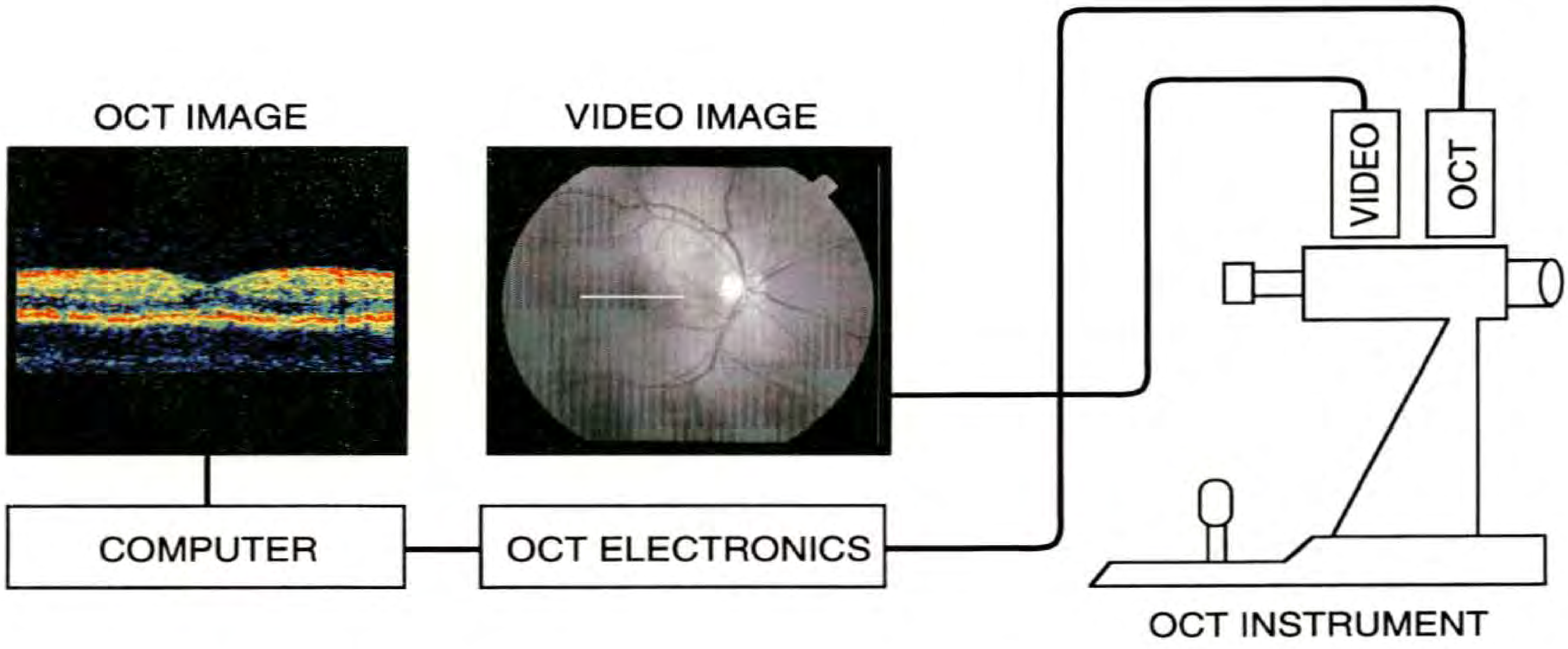

Figure 1-11. Schematic diagram of a typical Optical Coherence Tomography system for ophthalmic examination. The instrument for ophthalmic examination is similar to a slit-lamp biomicroscope or fundus camera. OCT images are processed by computer and displayed as they are acquired on a high resolution color monitor. The portion of the retina or anterior eye that is being tomographically imaged is viewed on a video monitor. Images are stored for the diagnostic record via computer.

verse dimension occur on a significantly larger distance scale than in the axial (longitudinal) direction.

OCT INSTRUMENTATION

There are two principal modes of operation for optical coherence tomographic imaging in the eye, depending on whether imaging is performed in the anterior segment or in the retina. In this section, we will describe the instrumentation and optical imaging techniques which are used in these two generic cases. The instruments used for anterior segment and retinal imaging operate along similar principles to the slit-lamp biomicroscope and fundus camera, respectively. Figure 1-11 shows a block diagram of the OCT system. The instrument permits the operator to view either the part of the anterior segment or retina which is being tomographically imaged either directly through an ocular or using a video camera.

From the functional viewpoint, the acquisition of tomographic images is extremely simple. The optical beam which is emitted from the OCT device is aimed at the structure which is to be imaged, and axial (longitudinal) range information is measured by computer while the beam is scanned in the transverse direction. The scan pattern of the tomographic beam can be controlled by computer, and thus cross sectional images along arbitrary cross sectional planes or curved surfaces can be measured.

The operating wavelength of the OCT probe beam is typically in the near infrared (~ 800 nm), and thus it is minimally visible to the patient. This minimizes patient discomfort during the examination. The position of the OCT measurement beam and hence the position of the tomographic scan can be observed by the clinician using an infrared sensitive video camera. Alternately, if the anterior segment or fundus is viewed directly by the clinician, a visible laser beam is coupled along the optical path of the OCT measurement beam to assist in aiming.

The beam scans under computer control and it is possible to directly view the portion of the anterior segment or fundus which is being imaged in tomographic cross section. The optical coherence tomogram is displayed in either grey scale or false color on a high resolution computer screen or monitor. The image is computer processed and may be displayed continuously as it is acquired. When the image is recorded for the patient record, the computer can store both the OCT image as well as the conventional image showing the registration or exact area of the structure which has been tomographically imaged.

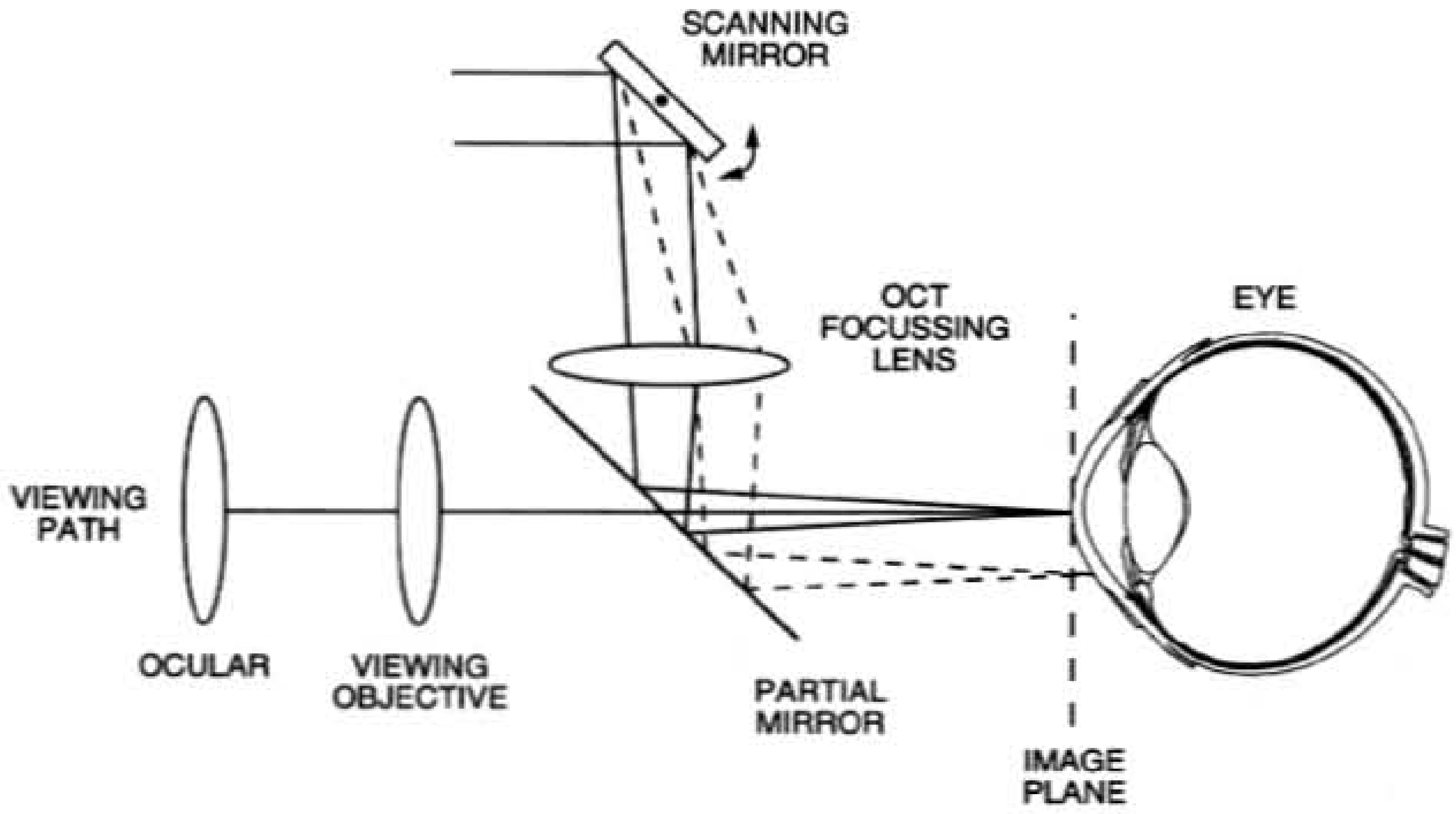

Figure 1-12. Schematic of the optical system for OCT imaging in the anterior eye. Operator viewing is provided by a standard imaging system with the image plane on the anterior eye. A computer controlled scanning mirror is used to position and scan the OCT measurement beam. The OCT measurement beam is focussed with a lens onto the same image plane as the operator view.

Instrumentation for Anterior Segment Imaging

Figure 1-12 shows a schematic diagram of the optical imaging system for tomographic imaging of the anterior segment. The basic diagnostic instrument is similar in design to a slit-lamp biomicroscope. In this case, the microscope images structures in the anterior segment directly and the operator can view them through an ocular or with a video camera. The OCT measurement beam is coupled along the viewing path of the device using a partially reflective mirror and the focal point of the OCT probe beam is coincident with the image plane of the biomicroscope. The position of the OCT optical beam is controlled by a scanning mirror or pair of mirrors which aims the beam position the coronal plane (x,y directions).

The operator's view of the anterior segment is determined by the magnification of the ophthalmic instrument or slit-lamp biomicroscope. The depth of field or range over which the OCT beam remains focussed is also determined by the imaging optics used to focus the beam onto the coincident image plane for the slit-lamp biomicroscope. For studies in the anterior segment, the depth of field is often set to be relatively large and thus the transverse spot size of the OCT beam is usually large. The resolution of the OCT image in the transverse direction is coarse with low transverse magnification of the OCT image.

Instrumentation for Retinal Imaging

The second general type of ophthalmic imaging which can be performed using OCT is imaging the posterior segment of the eye or the retina. In this application, the instrument operates analogously to a fundus camera. Figure 1-13 shows a schematic diagram of the imaging optics which are used for retinal OCT imaging. In this case, a high power condensing lens is used so that the retina may be imaged onto a plane within the instrument. The instrument then reimages the retinal plane to permit viewing by the operator. The OCT measurement beam is coupled into the optical path of the instrument using a partially reflective mirror or beamsplitter. The magnification of the retinal image is determined by the refractive power of the condensing lens and the magnification of the ocular. The OCT measurement is focused onto the retinal image plane using a focusing lens. Since the retinal thickness is quite small, the depth of focus is relatively shallow, and the spot size for the OCT beam can also be made small.

The transverse position of the OCT measurement beam is controlled by a mechanical scanning mirror system within the instrument. A typical field of view at lowest magnification is 30°. The fundus image can

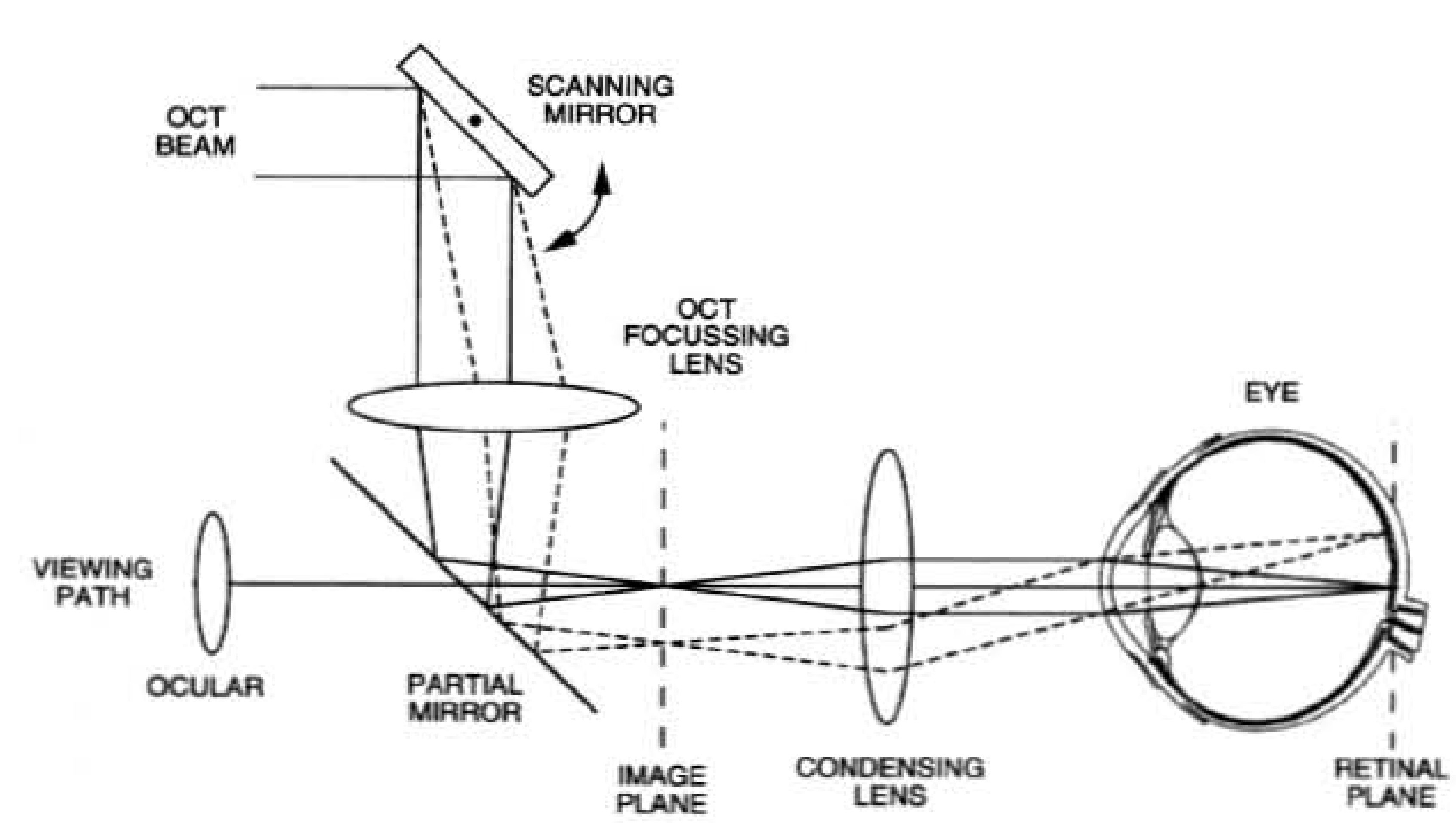

Figure 1-13. Schematic of the optical system for OCT imaging of the retina. A condensing lens is used to image the retina onto a plane inside the instrument. Operator viewing of the retina is provided by a standard imaging system. A computer controlled scanning mirror is used to position and scan the OCT beam. A focussing lens is used to focus the OCT beam onto the image plane where the retina is imaged. The condensing lens, in turn, relays the image of the OCT beam onto the retina. The OCT beam delivery is designed so that the OCT beam pivots about the pupil of the eye as it is scanned, thereby minimizing vignetting and distortion.

be viewed either directly through the ocular or via a video camera. When the beam is scanned, it produces a scan pattern on the retina which is visible to the operator (as well as to the patient). Thus the exact location of the tomographic image on the fundus can be determined. Instrument magnification can be adjusted depending on the examination which is being performed. Furthermore, since the scanning pattern of the OCT beam on the retina can be controlled by computer, different scan patterns can be designed and adopted as part of the diagnostic protocol for different retinal diseases. Imaging of typical retinal features and use of different scan patterns is described in more detail in the next chapter.

SUMMARY

Because OCT permits simultaneous viewing of the position on the ocular structure which is being scanned as well as its transverse cross-section, it can be used either in real time to diagnose characteristic morphologies in the anterior eye or the fundus or it can be used to create a diagnostic record similar to fundus photography. Because OCT images can be acquired extremely rapidly and the OCT measurement beam is in the infrared, patient discomfort during the examination is minimized. The rapid acquisition time of OCT images permits many images to be acquired on different cross-sectional planes in the anterior segment or fundus. Furthermore, OCT images contain quantitative information on dimensions of intraocular structures and have the potential to stage disease progression or response to therapy.

REFERENCES

1. Huang D, Swanson EA, Lin CP, Schuman JS, Stinson WG, Chang W, Hee MR, Flotte T, Gregory K, Puliafito CA, Fujimoto JG. Optical coherence tomography. Science 1991; 254:1178-1181.
2. Swanson EA, Izatt JA, Hee MR, Huang D, Lin CP, Schuman JS, Puliafito CA, Fujimoto JG. In vivo retinal imaging by optical coherence tomography. Opt Lett 1993; 18:1864-6.
3. Izatt JA, Hee MR, Swanson EA, Huang D, Lin CP, Schuman JS, Puliafito CA, Fujimoto JG. Micron-scale resolution imaging of the anterior eye in vivo with optical coherence tomography. Arch Ophthalmol 1994; 112:1584-9.
4. Hee MR, Izatt JA, Swanson EA, Huang D, Schuman JS, Lin CP, Puliafito CA, Fujimoto JG. Optical coherence tomography of the human retina. Arch Ophthalmol 1995; 113:325-32.
5. Chang DF, Ophthalmic examination. In: Vaughan DG, Asbury T, Riordan-Eva P eds. General Ophthalmology. Norwalk, CT: Appleton and Lange; 1992:30-62.
6. Seiler T. Magnetic resonance imaging of the eye and orbit. In: Masters BR, ed. Noninvasive Diagnostic Techniques in Ophthalmology. New York: Springer-Verlag; 1990:17-31.
7. Taveras JL, Haik BG. Magnetic resonance imaging in ophthalmology. In: Masters BR, ed. Noninvasive Diagnostic Techniques in Ophthalmology. New York: Springer-Verlag; 1990:32-46.
8. Olsen T. The accuracy of ultrasonic determination of axial length in pseudophakic eyes. Acta Ophthalmol. (Copenh) 1989:67; 141-144.
9. Pavlin DJ, Sherar MD, Foster FS. Subsurface ultrasound microscopic imaging of the intact eye. Ophthalmology 1990; 97:244-250.
10. Allemann N, Chamon W, Silverman RH, Azar DT, Reinstein DZ, Stark WJ, Coleman DJ. High-frequency ultrasound quantitative analysis of corneal scarring following excimer laser keratectomy. Arch Ophthalmol 1993; 111:968-973.
11. Fujimoto JG, De Silvestri S, Ippen EP, Puliafito CA, Margolis R, Oseroff A. Femtosecond optical ranging in biological systems. Opt Lett 1986; 11:150-152.
12. Stern D, Lin WZ, Puliafito CA, Fujimoto JG. Femtosecond ranging of corneal incision depth. Invest Ophthalmol Vis Sci 1989; 30:99-104.
13. Born M, Wolf E. Principles of Optics, 6th ed. New York: Pergamon Press; 1980.
14. Youngquist RC, Carr S, Davies DEN. Optical coherence-domain reflectometry: a new optical evaluation technique. Opt Lett 1987; 12:158-160.
15. Takada K, Yokohoma I, Chida K, Noda J. New measurement system for fault location in optical waveguide devices based on an interferometric technique. Appl Opt 1987; 26:1603-1606.
16. Gilgen HH, Novak RP, Salathe RP, Hodel W, Beaud P. Submillimeter optical reflectometry. IEEE J Lightwave Technol 1989; 7:1225-1233.
17. Fercher AF, Mengedoht K, Werner W. Eye-length measurement by interferometry with partially coherent light. Opt Lett 1988; 13:1867-1869.
18. Huang D, Wang J, Lin CP, Puliafito CP, Fujimoto JG. Micron-resolution ranging of cornea anterior chamber by optical reflectometry. Las Surg Med. 1991; 11:419-425.
19. Hitzenberger CK. Optical measurement of axial eye length by laser Doppler interferometry. Invest Ophthalmol Vis Sci 1991; 32:616-624.
20. Fercher AF, Hitzenberger C, Juchem M. Measurement of intraocular optical distances using partially coherent laser light. J Mod Opt 1991; 38:1327-1333.
21. Swanson EA, Huang D, Hee MR, Fujimoto JG, Lin CP, Puliafito CA. High-speed optical coherence domain reflectometry. Opt Lett 1992; 17:151-153.

CHAPTER 2

Interpretation of the OCT Image

OCT is a new method for high-resolution, cross-sectional visualization of tissue [1,2]. The physical basis of imaging depends on the contrast in optical reflectivity between different tissue microstructures. When combined with the conventional clinical techniques of direct and indirect ophthalmoscopy, fluorescein angiography, and visual field testing, OCT is a powerful diagnostic tool for a variety of ocular diseases. In many cases, a definitive diagnosis may be established directly from the OCT images. Because OCT is an inherently digital technique, quantitative measurements may be easily extracted from the tomograms, and automated computer image processing techniques may be applied to the problem of image interpretation. The availability of quantitative information makes OCT useful for longitudinally tracking small changes in tissue structure and the development or resolution of disease processes.

This chapter will provide a brief explanation of light propagation through tissue, describe the anatomical features visible on OCT tomograms of the normal anterior eye, macula, and optic disc, and provide a framework for interpreting OCT images of retinal pathology.

OPTICAL PROPERTIES OF TISSUE

OCT is analogous to conventional clinical ultrasound, except that the optical rather than the acoustic properties of tissues are measured. Like ultrasound, cross-sectional images of reflectivity in tissue are obtained that can differentiate internal tissue structure. Since light incident on and reflected from deeper tissue layers must pass through more superficial layers before detection, the reflections from internal tissue structures depend critically on the effects of overlying tissue. An understanding of the general concepts of light propagation through tissue is essential to develop a basis for interpretation of OCT images.

Light incident onto a scattering or turbid medium such as tissue is either transmitted, absorbed, or scattered. Absorbed light is converted into heat in the tissue and is effectively removed from the incident beam. Absorption occurs because tissue chromophores, such as hemoglobin, have internal energy transitions which match the energy of the incident light. Transmitted light remains unaffected, and is free to interact with deeper tissue layers. Scattering is a fundamental property of a heterogenous medium, and occurs because of microscopic spatial variations in the refractive index within tissue. A scattering event causes light to experience a random directional change. Light that completely reverses direction when scattering is known as backscattered, or reflected light.

Three parameters are typically used to statistically summarize the optical properties of a scattering medium, and to define the ensemble effects of absorption and scattering on the incident light beam [3-5]. The *absorption coefficient*, with units of inverse distance,

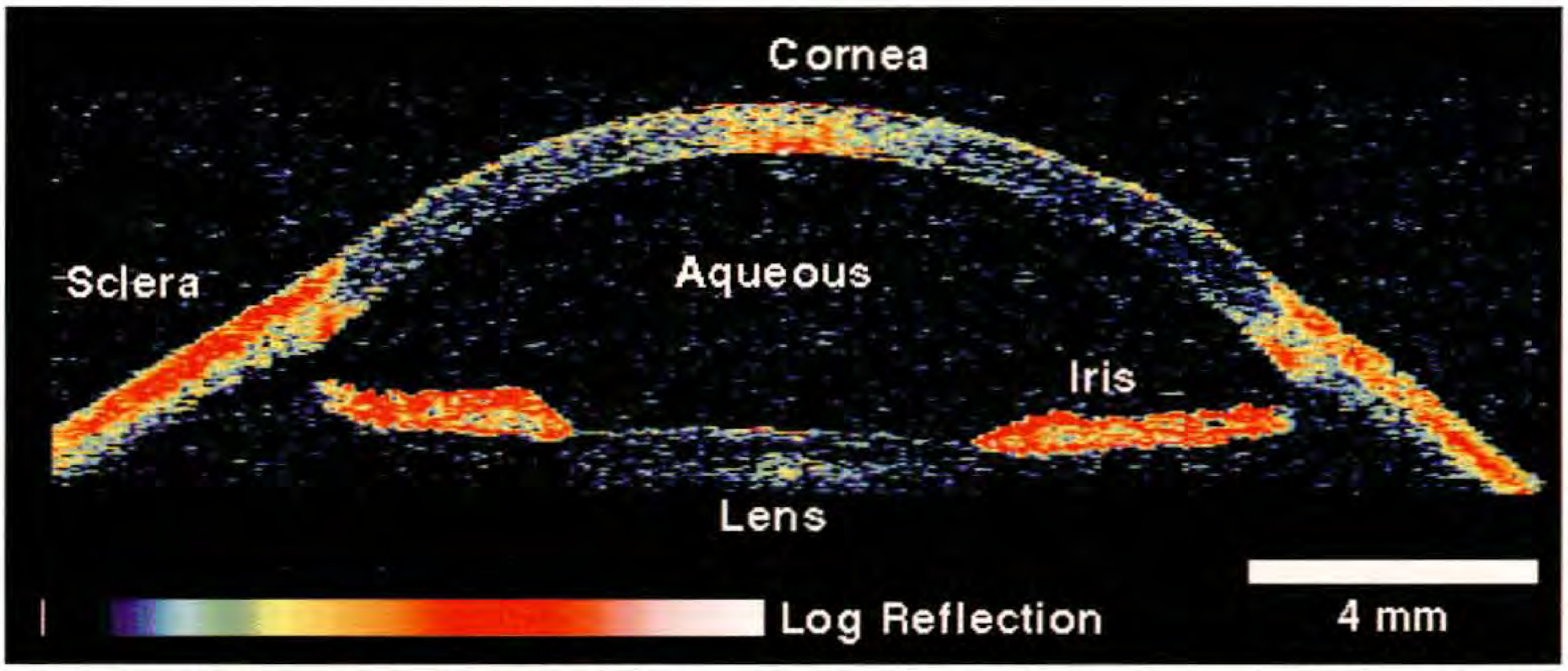

Figure 2-1. OCT image of a normal anterior eye chamber. Optical backscatter is visible through nominally opaque structures, such as sclera and iris, and from within transparent structures such as cornea and lens.

defines the fraction of incident light absorbed by the tissue after the light propagates an infinitesimal distance through the tissue. In a purely absorptive medium, the intensity of the incident beam would decrease exponentially with distance, with a rate determined by the absorption coefficient. The *scattering coefficient*, also with units of inverse distance, similarly defines the fraction of incident light scattered by the tissue in an infinitely small distance. A purely scattering medium would correspondingly attenuate the incident light exponentially with increasing depth, with a rate dependent on the scattering coefficient.

The effects of absorption and scattering on the incident light beam are indistinguishable, so that transmitted light will be attenuated exponentially with distance into the tissue by a combination of both processes. In most tissues, however, light scattering predominates over absorption, and at a given time, a scattering event is about ten times more likely than an absorption event [4]. Therefore, most major differences in the attenuation of light propagating through different tissues derive from differences in tissue scattering, rather than absorption properties. Absorption only becomes an appreciable factor if a high concentration of a chromophore is present with a specificity that matches the wavelength of the incoming beam.

The *scattering anisotropy* factor describes in a statistical manner the probable direction of light scattering events. A medium with isotropic scattering, for example, is equally likely to scatter incident light into all possible directions. In contrast, the scattering events in most tissues are predominantly forward directed [4].

The OCT system is in principle sensitive to two types of reflected light. The dominant contribution to the OCT signal is derived from light which propagates to a particular layer in the tissue without scattering or absorption, experiences a single scattering event in the backwards direction, and returns to the detector without further scattering or absorption. In contrast to this singly backscattered light, light that has undergone multiple scattering events, but no absorption, may also be detected if it happens to take a path which returns to the detector. The optics of the OCT system make it improbable that multiple scattered light will travel on such a path, because the confocal and interferometric nature of the detection process places additional requirements on the temporal and spatial coherence of the detected light. Thus, for all practical purposes, the OCT signal may be considered to be exclusively comprised of light that has undergone just a single backscattering event at the tissue layer of interest.

The strength of the OCT signal at a particular tissue layer is defined by the amount of incident light which is transmitted without absorption or scattering to that layer, by the proportion of this light which is directly backscattered, and by the fraction of the directly backscattered light which returns to the detector without further attenuation. The proportion of the incident light which is directly backscattered by a tissue structure defines the *reflectivity* of that structure. Thus, the OCT signal from a particular tissue layer is a combination of its reflectivity and the absorption and scattering properties of the overlying layers. The internal reflectivity of a homogenous tissue layer depends on both the layer's scattering coefficient and its scattering anisotropy. A highly reflective tissue will have both a high scattering coefficient and a strong

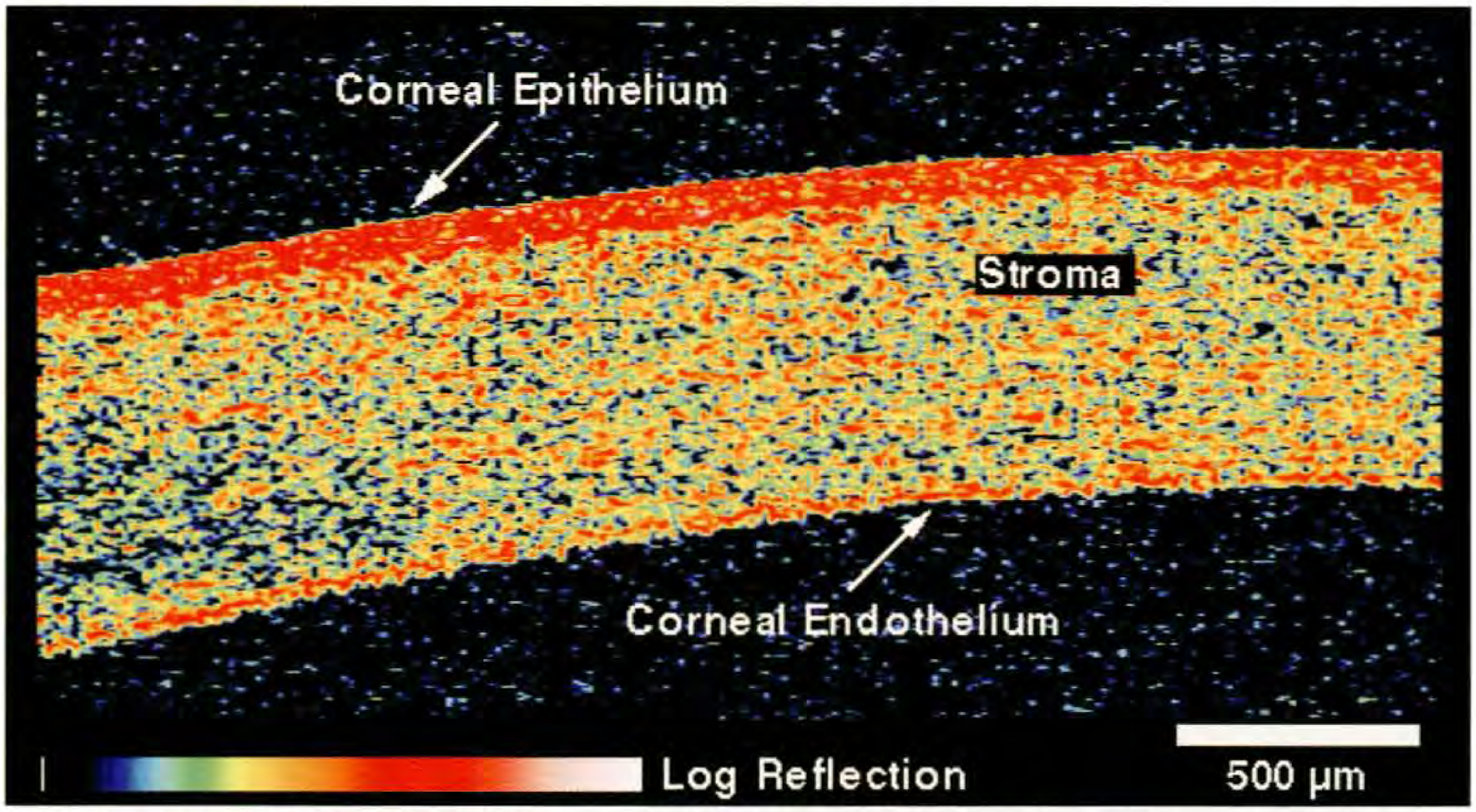

Figure 2-2. Narrow field-of-view OCT image of a healthy cornea showing the contrast in optical reflectivity between the corneal epithelium, stroma, and endothelium.

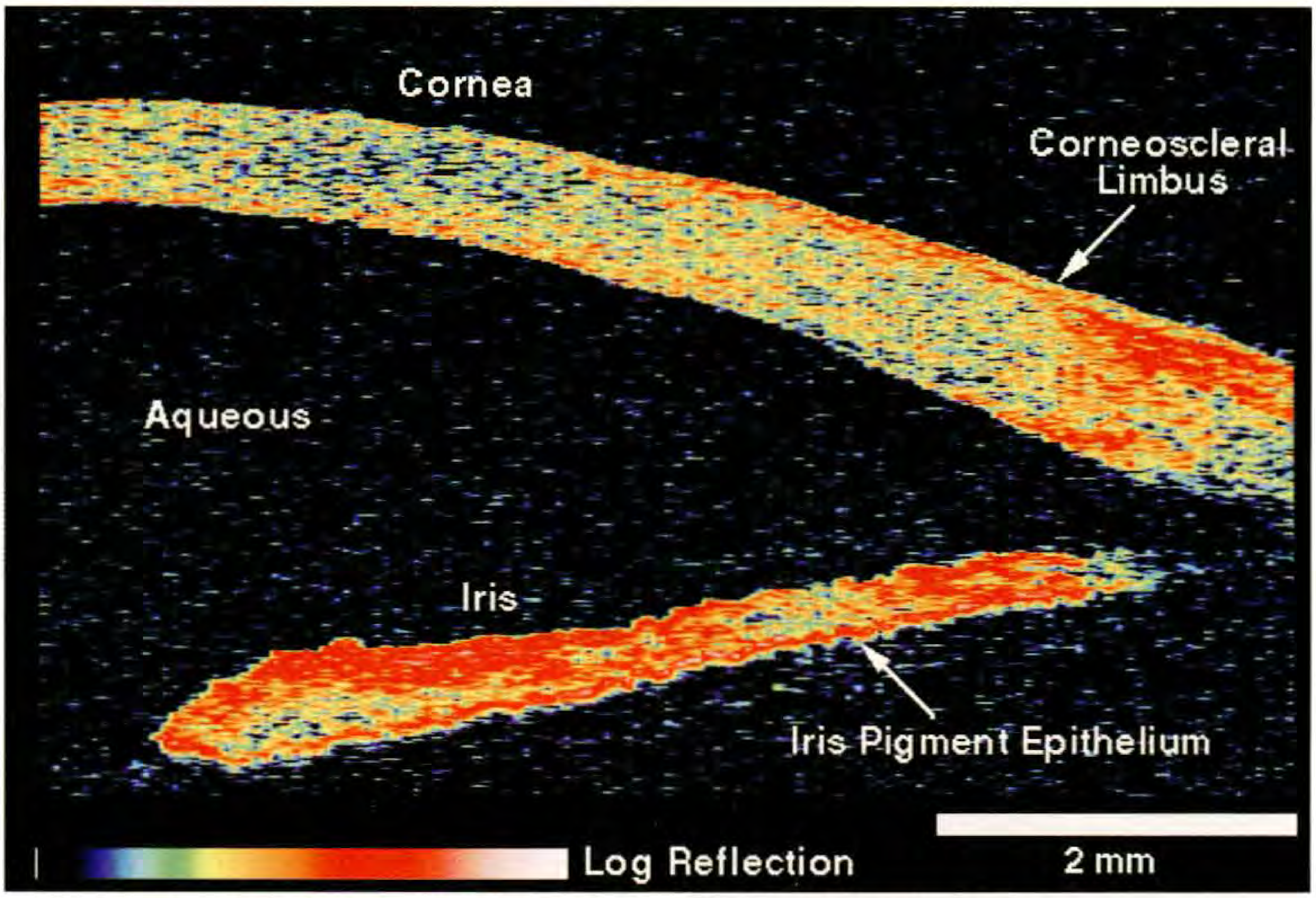

Figure 2-3. Narrow field-of-view OCT image of a healthy anterior chamber angle.

disposition to scatter light in the perfectly backwards direction. Strong reflections also occur at the boundaries between two medias, for example, between two materials of different refractive indices.

NORMAL ANTERIOR EYE

Anterior Chamber

Figure 2-1 displays an OCT image of a normal anterior chamber obtained from a healthy human eye [6]. The image is composed of 200 A-scans, and plots the logarithm of optical reflectivity mapped to a false color scale. Clearly identifiable structures include the cornea, sclera, iris, and lens anterior capsule. The strongest reflected signals arise from the epithelial surface of the cornea, and the highly scattering sclera and iris. Smaller amounts of backscatter are visible from within the nominally transparent cornea and lens. The backscatter intensity gradually decreases from central to peripheral cornea. This signal fading may be attributed to highly angle-dependent backscattering from the stromal collagen lamellae, which run parallel to the corneal surface. The limbus appears as the angled interface between the cornea and the sclera. The normal "watch glass" insertion of the cornea into the sclera is clearly visible.

Cornea and Angle

By narrowing the field-of-view, OCT can be used to obtain high resolution images of corneal microstructure. A magnified OCT image of the cornea appears in Figure 2-2, which differentiates the corneal epithelium, Bowman's layer, stroma, Descemet's membrane, and endothelium based on the differences in their optical properties. A close-up view of the angle region (Figure 2-3) shows the iris contour and epithelium, the corneoscleral limbus, and the anterior chamber angle. Structures in the angle region such as the trabecular

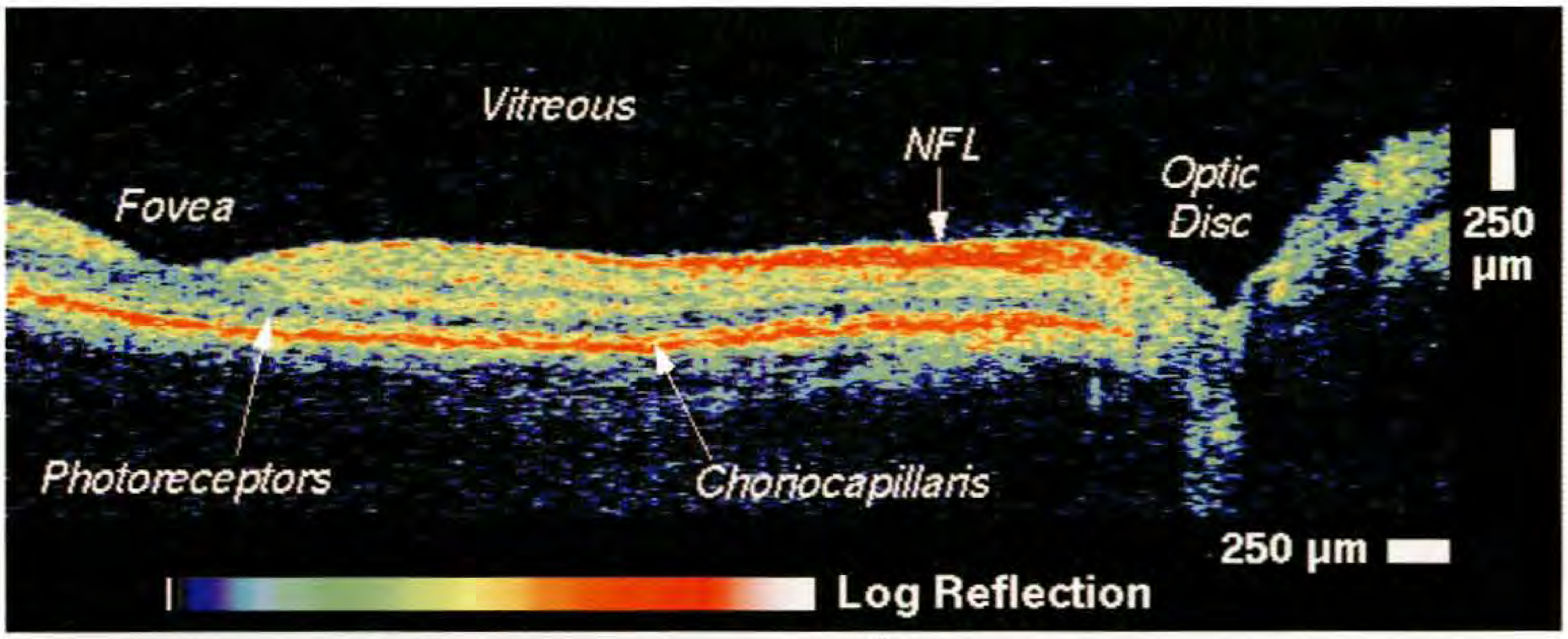

A

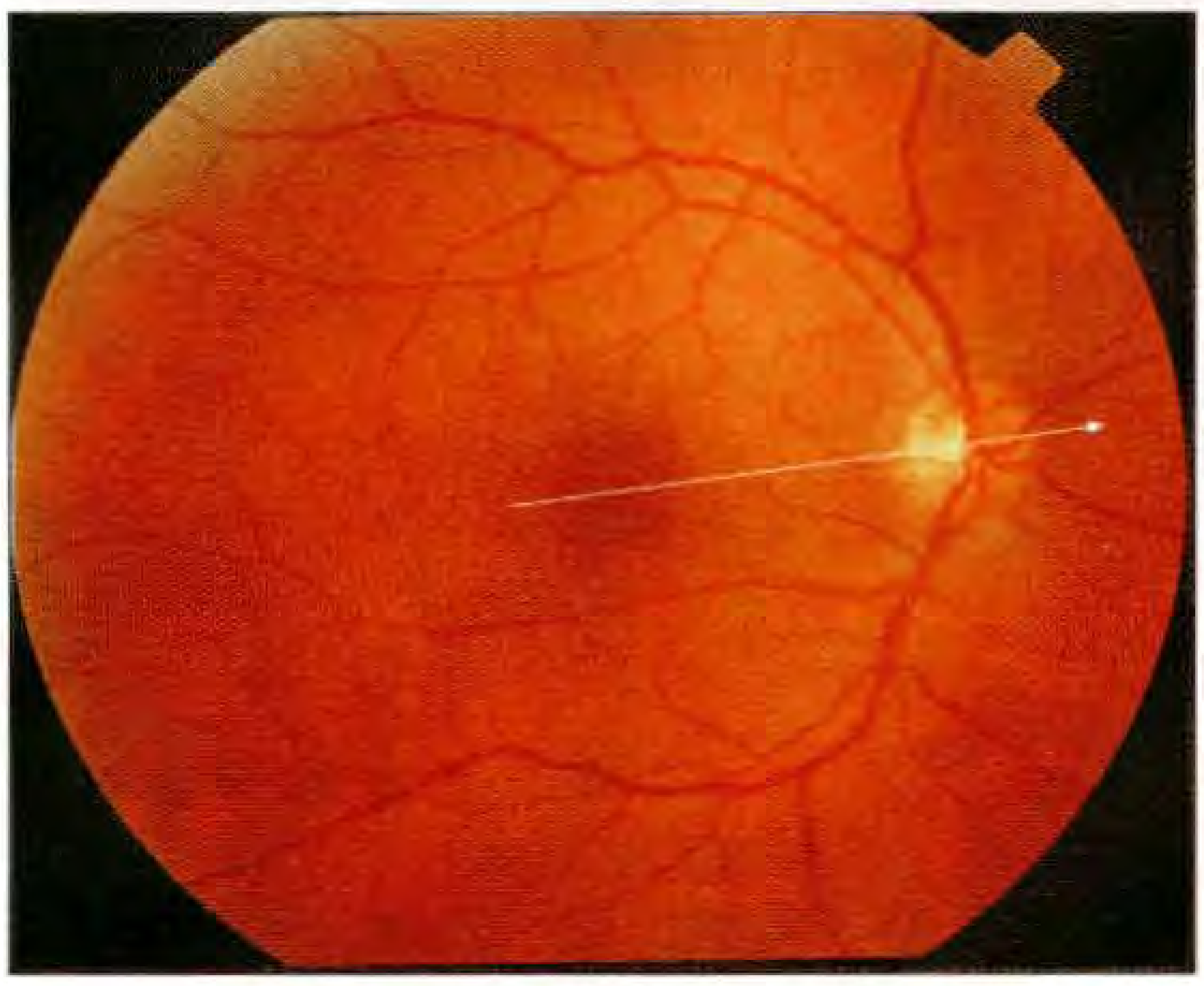

B

Figure 2-4. OCT tomogram (A) of a normal fovea and optic disc taken along the papillomacular axis. The location of the scan is shown on a corresponding fundus photograph (B). The fovea and optic disc are identifiable by their characteristic morphology and the layered structure of the retina is apparent. The retinal nerve fiber layer (NFL) is highly reflective and increases in thickness towards the disc.

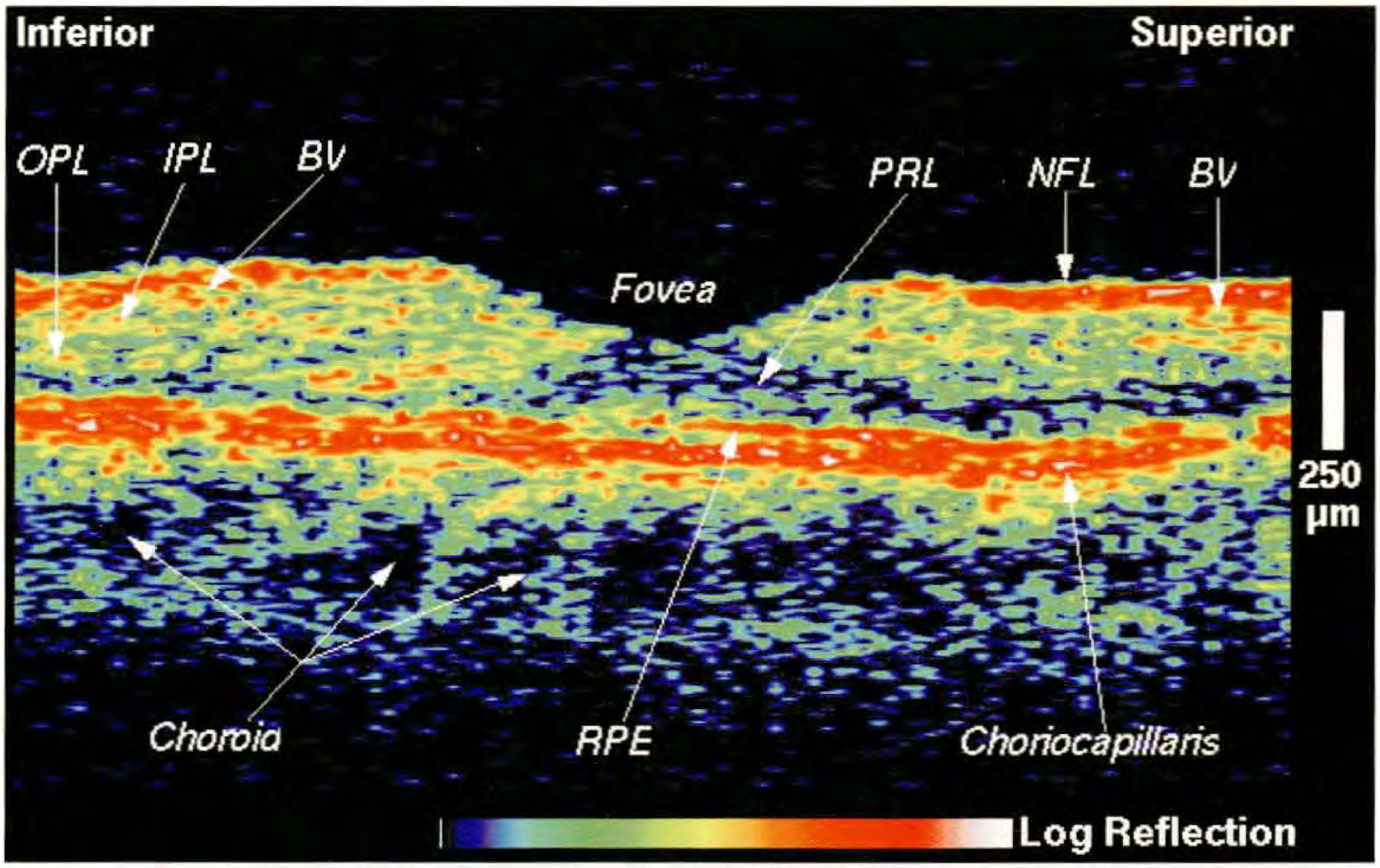

A

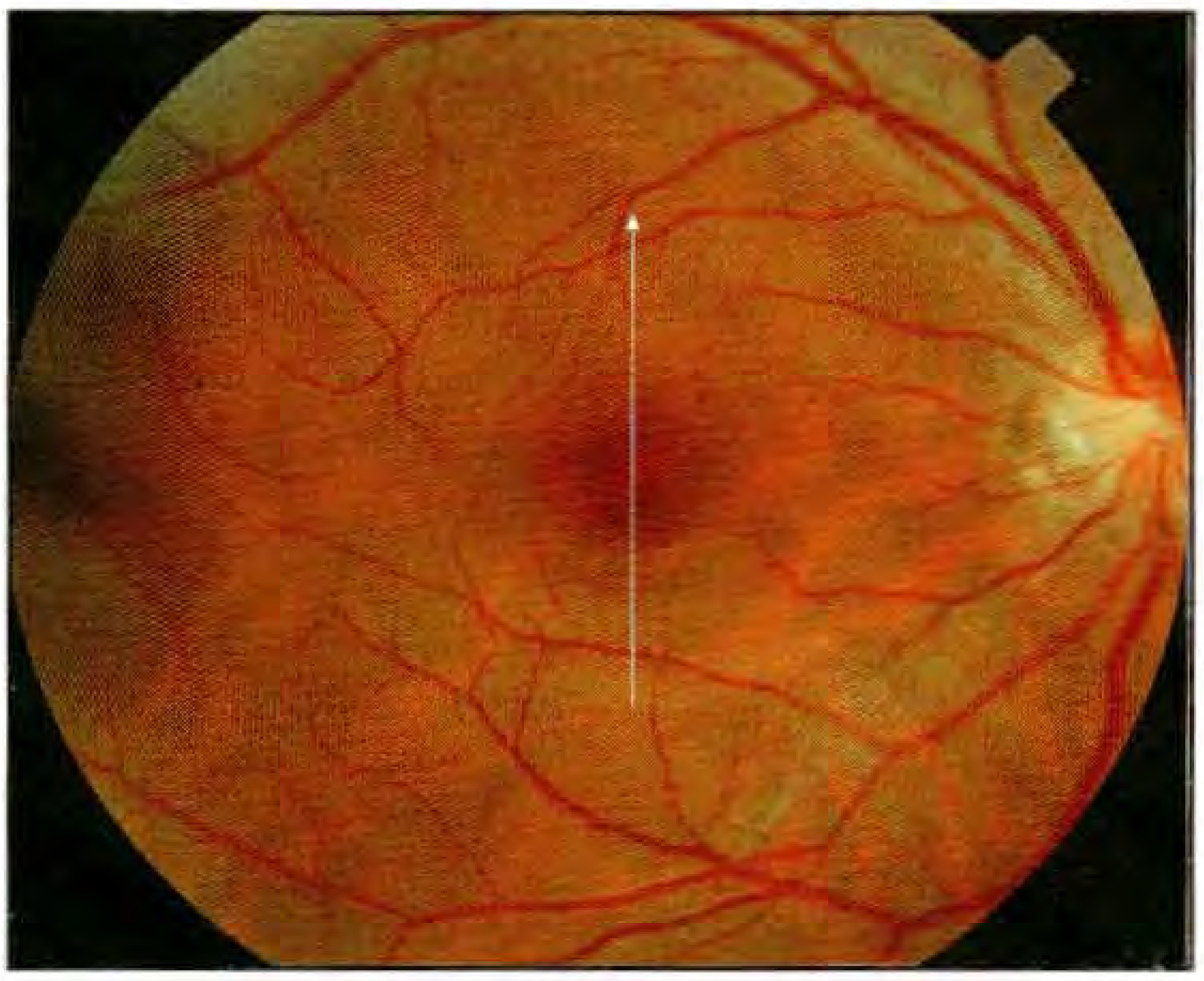

B

Figure 2-5. Higher magnification OCT tomogram (A) of a healthy fovea showing the layered structure of the retina. The image is displayed twice expanded in the vertical direction for better readability. The location of the scan is shown on a corresponding fundus photograph (B). The retinal pigment epithelium (RPE) and choriocapillaris form a highly reflective boundary at the posterior neurosensory retina. The nerve fiber layer (NFL) is also highly backscattering. Intermediate reflectivity is observed from the inner and outer plexiform (IPL, OPL) layers, which are more reflective than their respective nuclear layers. The photoreceptor layer (PRL) exhibits minimal backscatter signal. Retinal blood vessels (BV) are identifiable by their increased reflectivity and by their shadowing of the reflections from the RPE and choriocapillaris. Larger choroidal vessels appear as dark spaces in the tomogram.

meshwork and canal of Schlemm are not clearly visualized in the tomogram since the incident and backscattered light is highly attenuated after traversing the overlying scleral tissue.

NORMAL RETINA

Papillomacular Axis

Figure 2-4 shows a large field-of-view OCT tomogram of a healthy retina including both the macula and peripapillary region [7]. Large scale anatomic features, such as the fovea, optic disc, and retinal profile are evident in the tomogram and are identifiable by their characteristic morphology. The vitreoretinal interface is demarcated by the contrast between the non-reflective vitreous and the backscattering surface of the retina. The fovea appears to the left in the tomogram as a characteristic thinning of the retina and shows the lateral displacement of the retina anterior to the photoreceptors. The optic disc appears to the right in the tomogram, showing the optic nerve head contour and evidence of normal cupping.

A highly reflective red layer delineates the posterior boundary of the retina in the tomogram, and corresponds to the retinal pigment epithelium (RPE) and choriocapillaris. This posterior layer terminates at the margin of the optic disc consistent with the termination of choroidal circulation at the lamina cribosa. Below the choriocapillaris, relatively weak scattering returns from the deep choroid and sclera, due to attenuation of the signal after passing through the neurosensory retina, RPE, and choriocapillaris . A dark layer indicative of minimal reflectivity appears just anterior to the choriocapillaris layer, and represents the outer segments of the retinal photoreceptors. The intermediate layers of the retina anterior to these segments exhibit moderate backscattering. The inner margin of the retina shows another area of bright backscattering, a red layer that corresponds in location and in anatomical variation to the retinal nerve fiber layer (NFL). According to the tomogram, the NFL increases in thickness from the macula to the optic disc as expected from normal anatomy.

Fovea

A narrow field-of-view image (Figure 2-5) of a normal fovea further delineates the contrast between different retinal layers. The anterior and posterior margins of the retina are again defined by highly reflective layers corresponding to the NFL and RPE / choriocapillaris. The RPE appears distinct from the choriocapillaris directly beneath the fovea, where the pigmentation is the heaviest. Above the minimally reflective photoreceptors, alternating layers of moderate and low reflectivity reveal the stratified structure of the retina. Moderate backscattering is observed from the inner and outer plexiform layers (IPL, OPL), which like the NFL, consist of a fibrous structures running perpendicular to the incident beam. In contrast, minimal backscattering is noted from the nuclear layers, in which, like the photoreceptors, the cell bodies are oriented parallel to the incident light. Retinal blood vessels are identified by their increased backscatter and by their shadowing of the reflections from the RPE and choriocapillaris. The larger choroidal vessels also appear in the image and have minimally reflective, dark lumens.

Serial Sagittal Tomograms Through the Macula

In analogy to X-ray computed tomography (CT) or magnetic resonance imaging (MRI), information on three-dimensional structure may be obtained by using the optical sectioning capability of OCT to acquire serial images of consecutive slices through the retina. As an example, six sagittal tomograms were obtained consecutively from the macula of a human subject with a lateral displacement of 225 μm between each image (Figure 2-6). The locations of each tomogram on the retina are labeled on a corresponding fundus photograph.

Characteristic features of the retina appear consistently in the serial sections. The anterior and posterior surfaces of the neural retina are demarcated by backscattering at the NFL and vitreoretinal interface, and the highly backscattering red layer representing the RPE and choriocapillaris. The sequence of tomograms shows the development and resolution of the foveal depression, which reaches its maximum depth at the fovea centralis. Retinal blood vessels derived from the superior and inferior branches of the central retinal artery are evident in the tomograms from the partial shadowing of the deep retinal structure beneath the vessels.

Serial Radial Tomograms Through the Optic Disc

Figure 2-7 displays OCT sections taken through different radial planes, each passing through the center of the optic nerve head, which are useful in com-

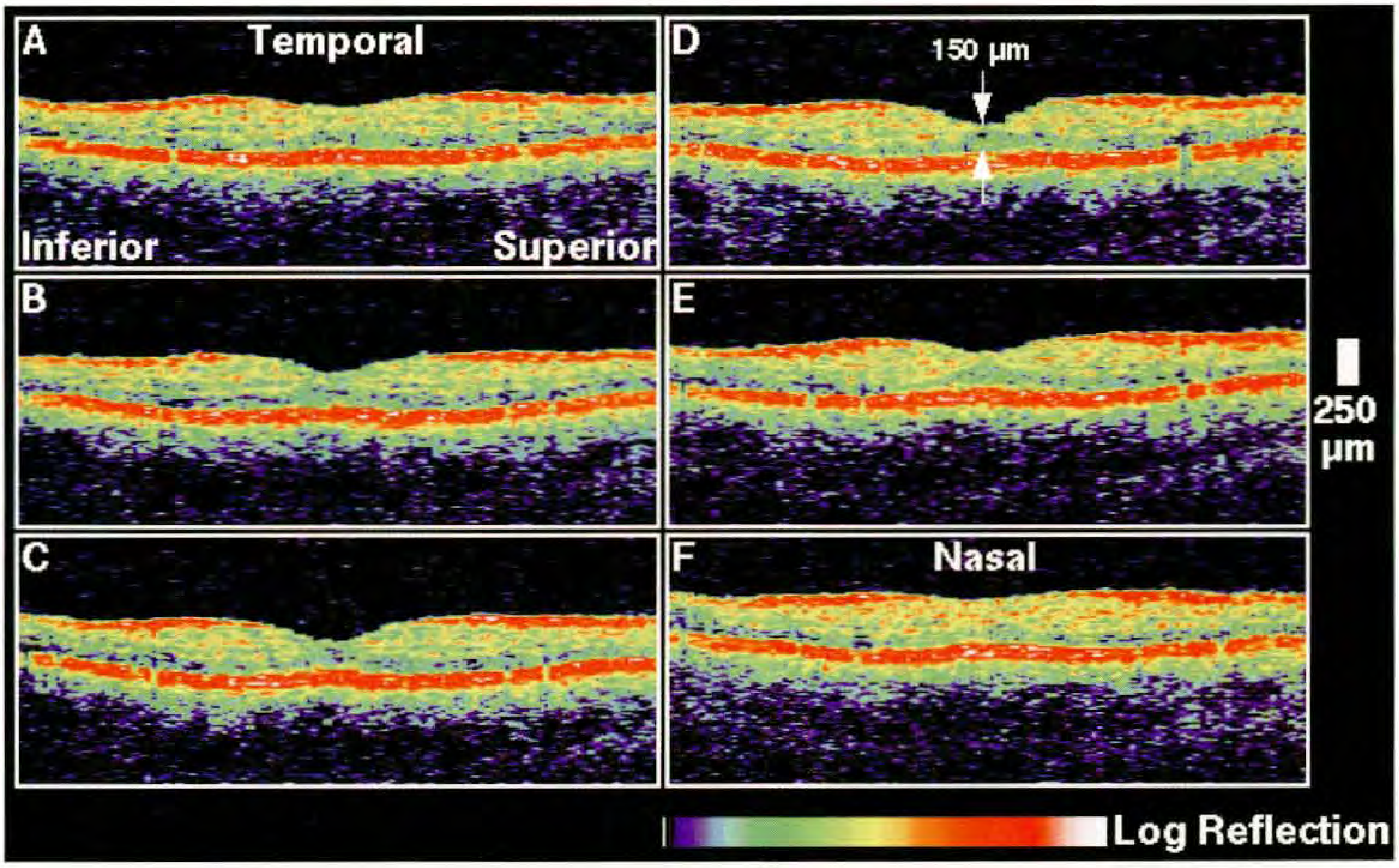

A

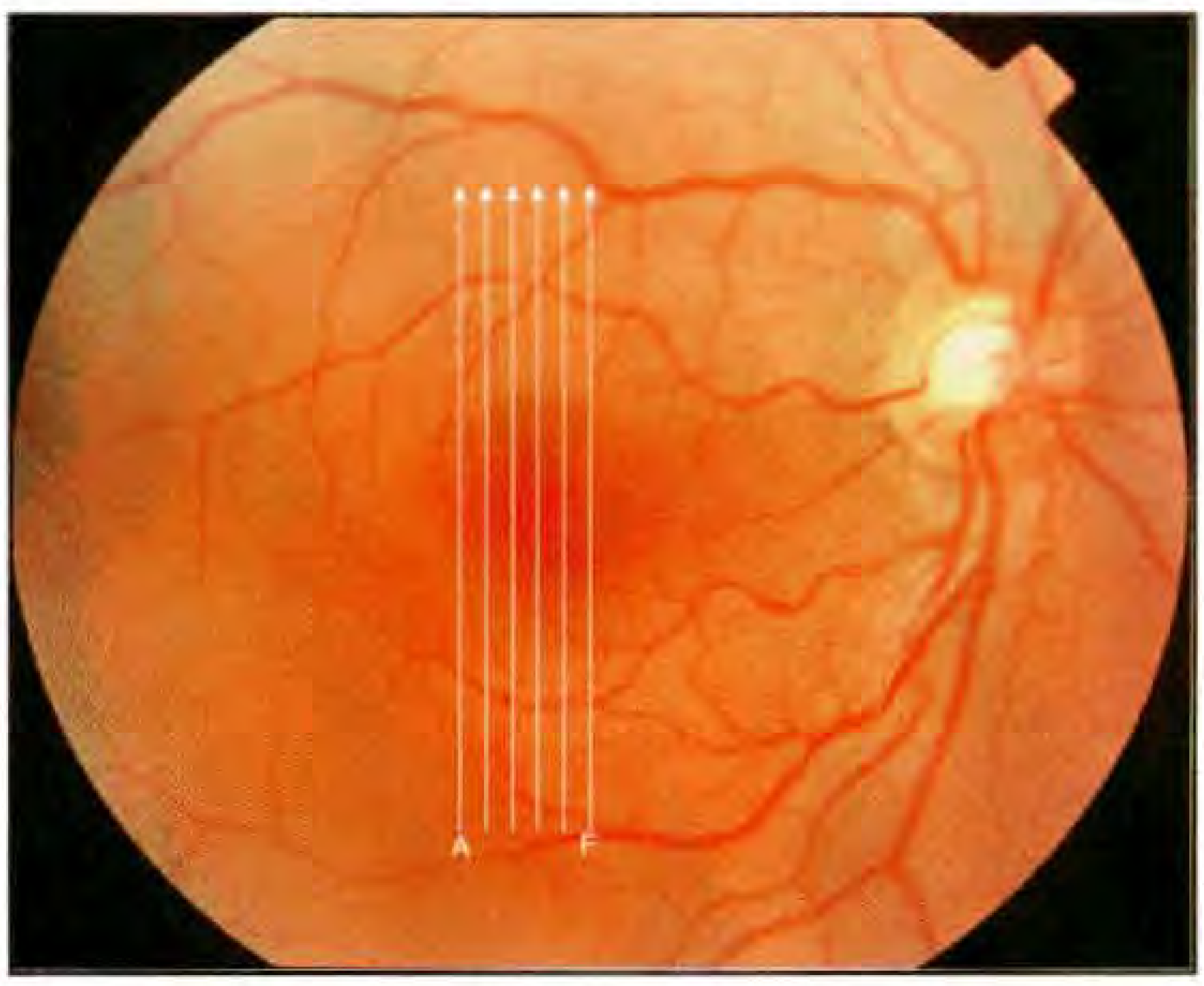

B

Figure 2-6. Serial sagittal tomograms through a healthy macula (A) showing the three-dimensional structure of the fovea. The images are displayed twice expanded in the vertical direction. The location of the scans is shown on the corresponding fundus photograph (B). The central foveal thickness measured directly from the tomogram is 150 µm.

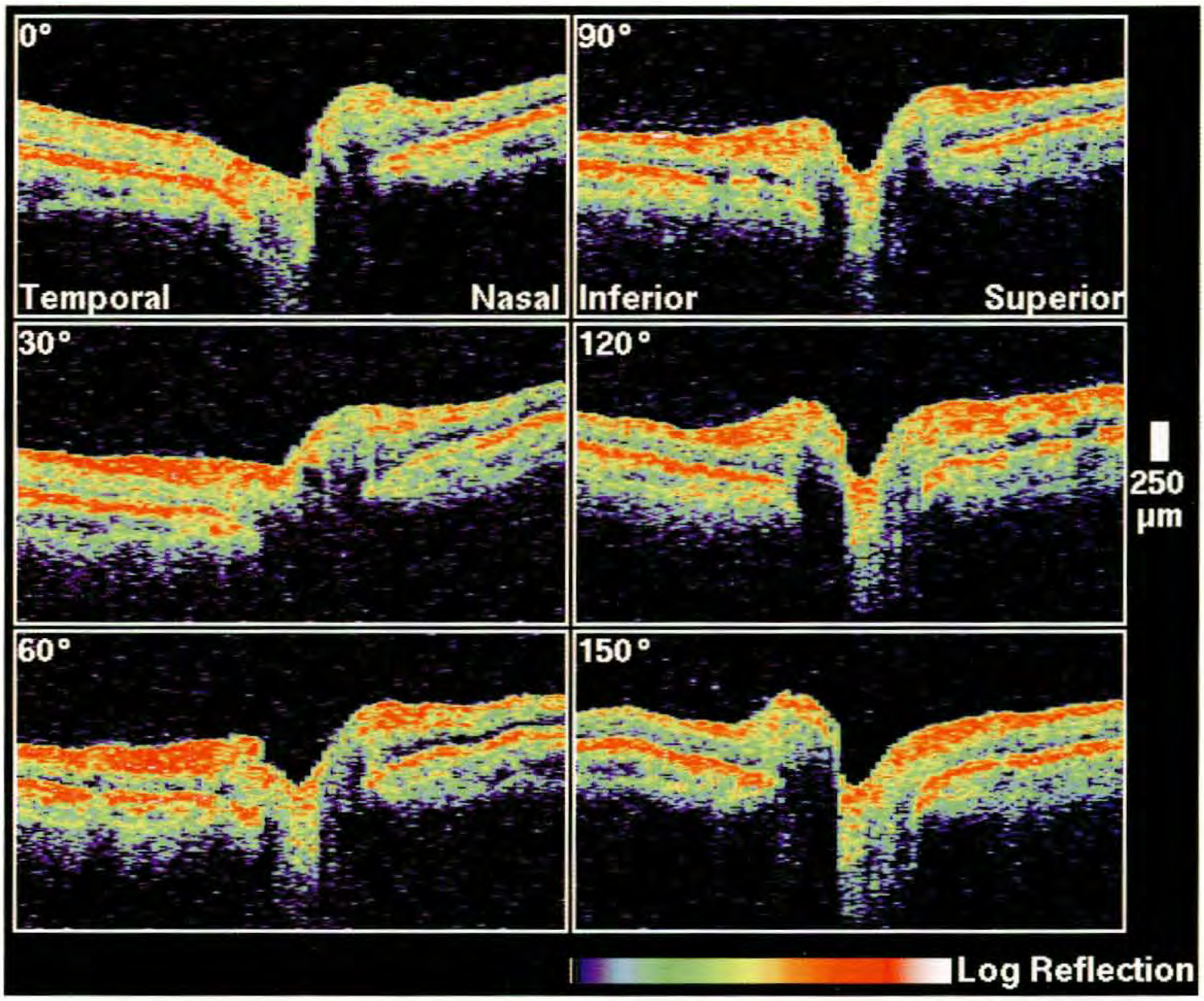

A

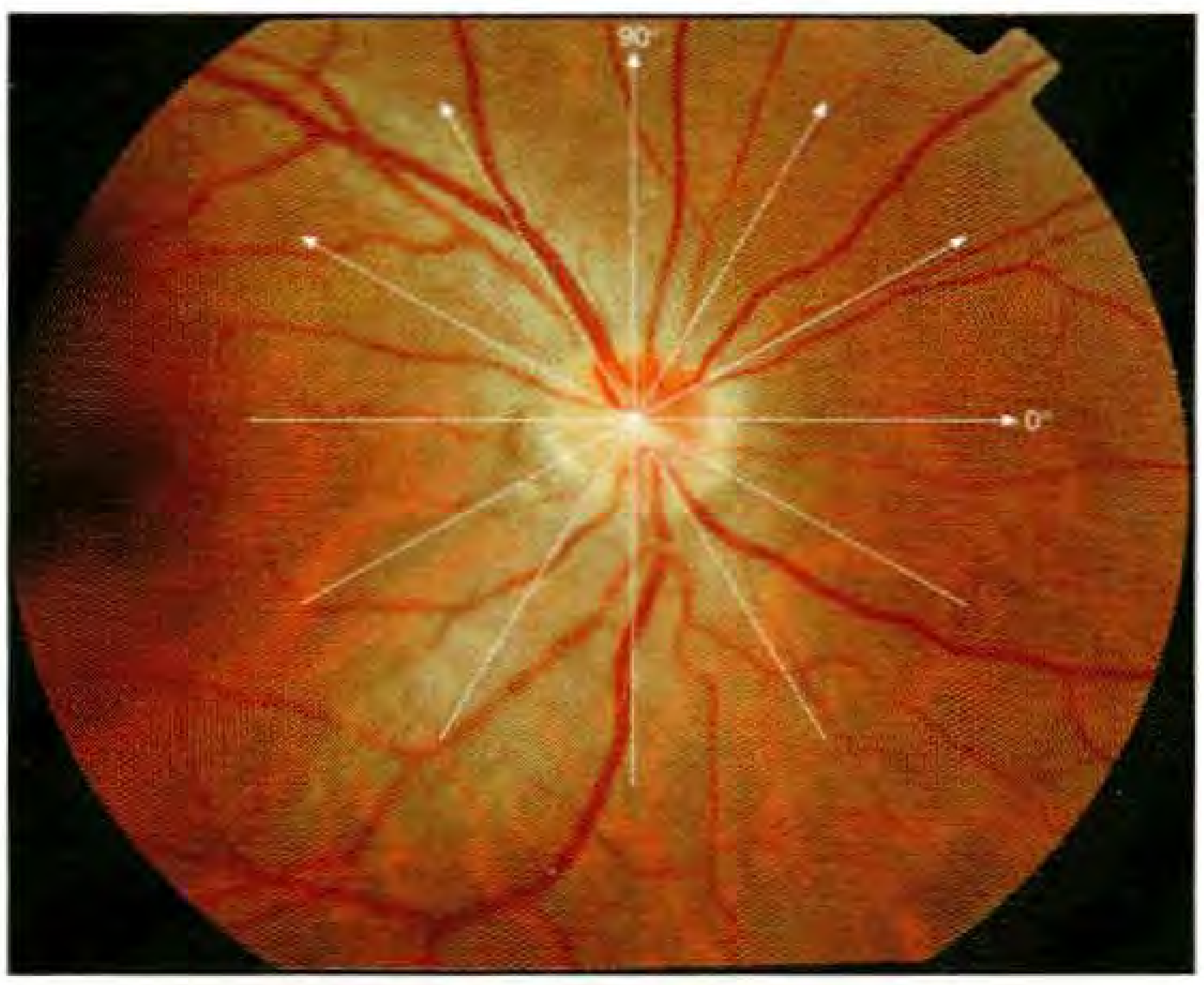

B

Figure 2-7. Radial OCT sections (A) through the optic disc and peripapillary region taken at equally spaced angular orientations showing the three-dimensional structure of the disc. The contour of the disc, including cupping, is well visualized. The images are displayed twice expanded in the vertical direction. The location of the scans is shown on the corresponding fundus photograph (B).

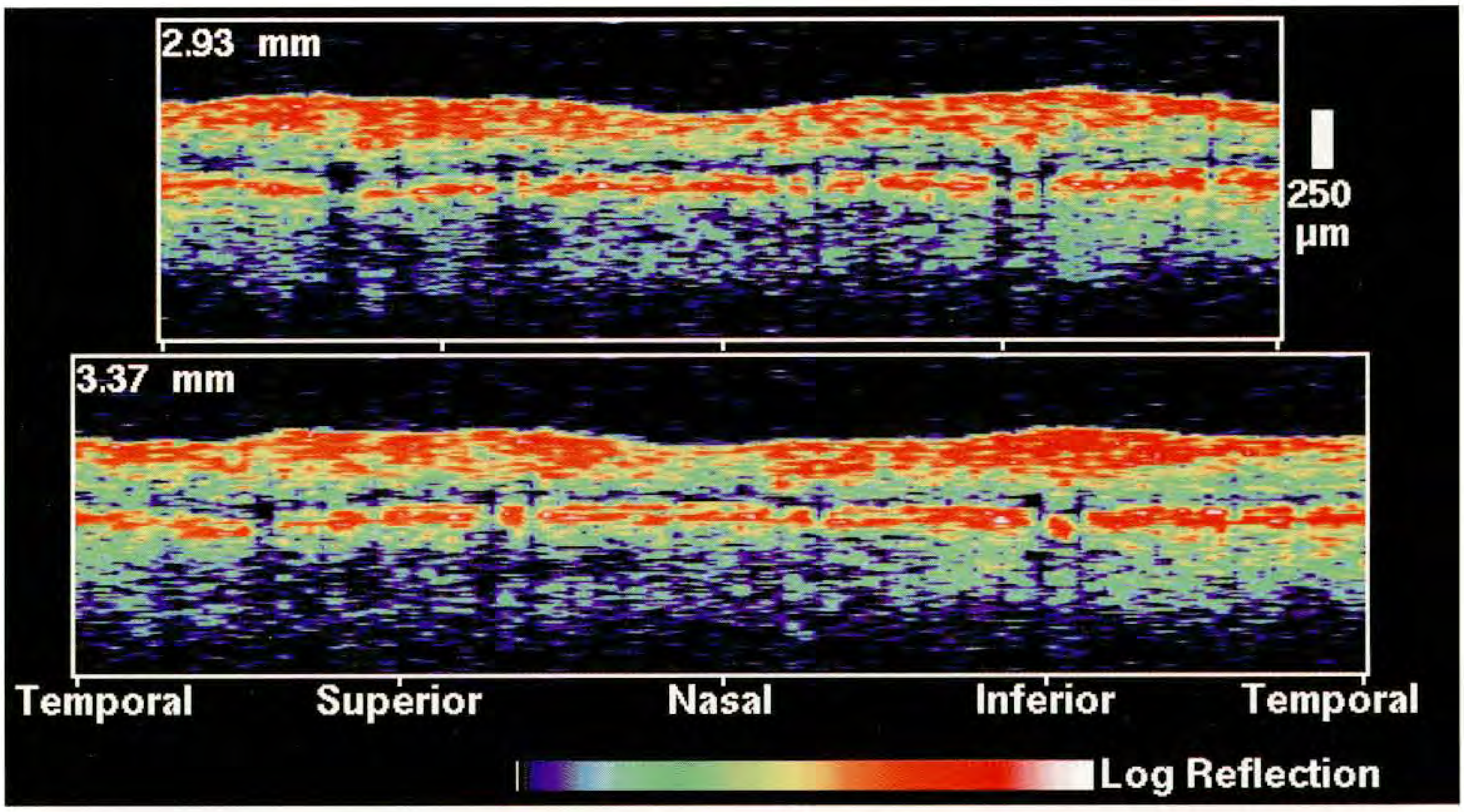

A

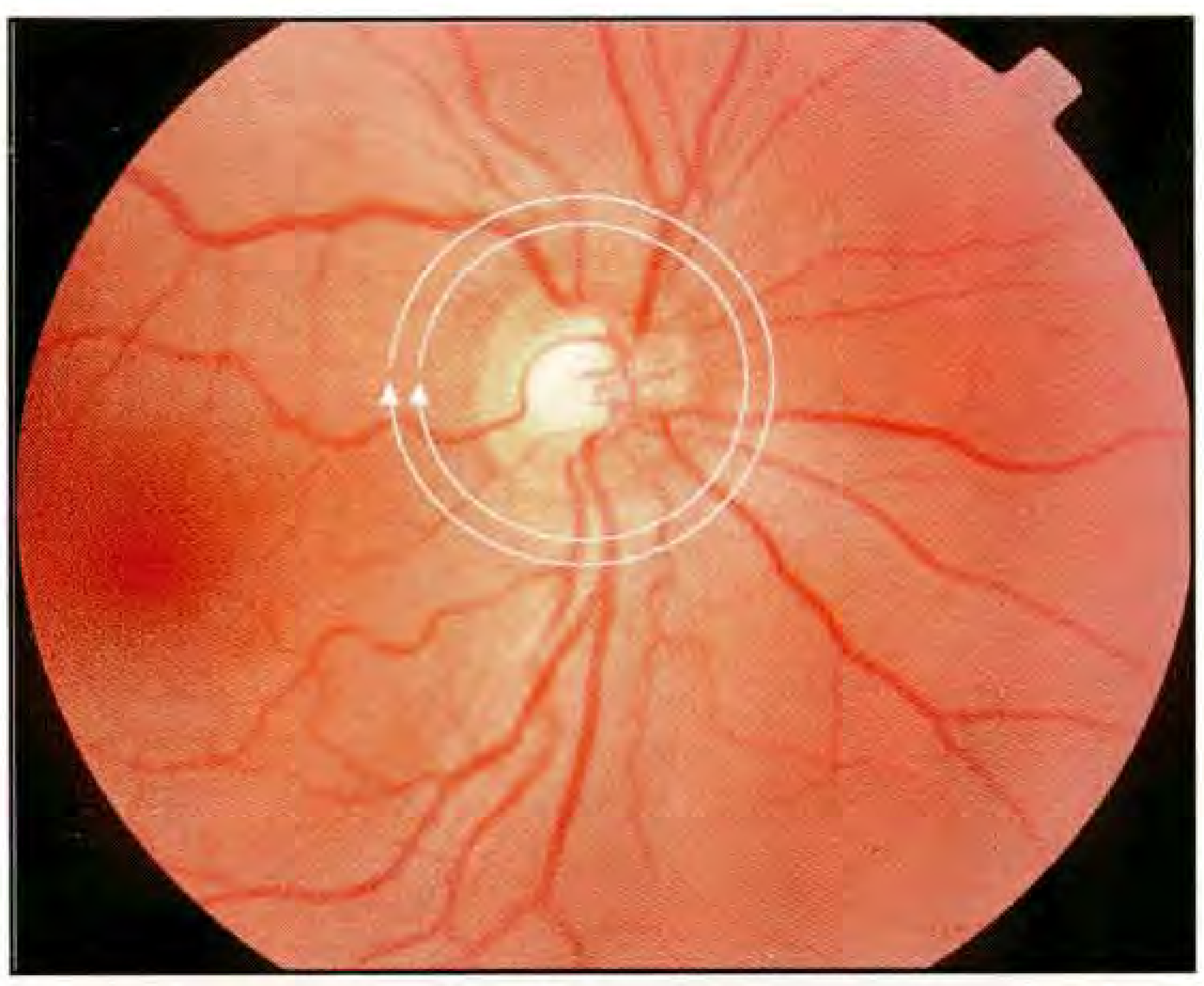

B

Figure 2-8. Peripapillary circular OCT tomograms (A) acquired around the optic disc at diameters of 2.3 mm and 3.4 mm. The cylindrical sections correspond to a clockwise scan around the disc and are displayed unwrapped. The superotemporal and inferotemporal bundling of the nerve fiber layer is evident. Retinal blood vessels are evident by their shadowing of the reflection from the retinal pigment epithelium and choriocapillaris. The location of the scans is shown on the corresponding fundus photograph (B).

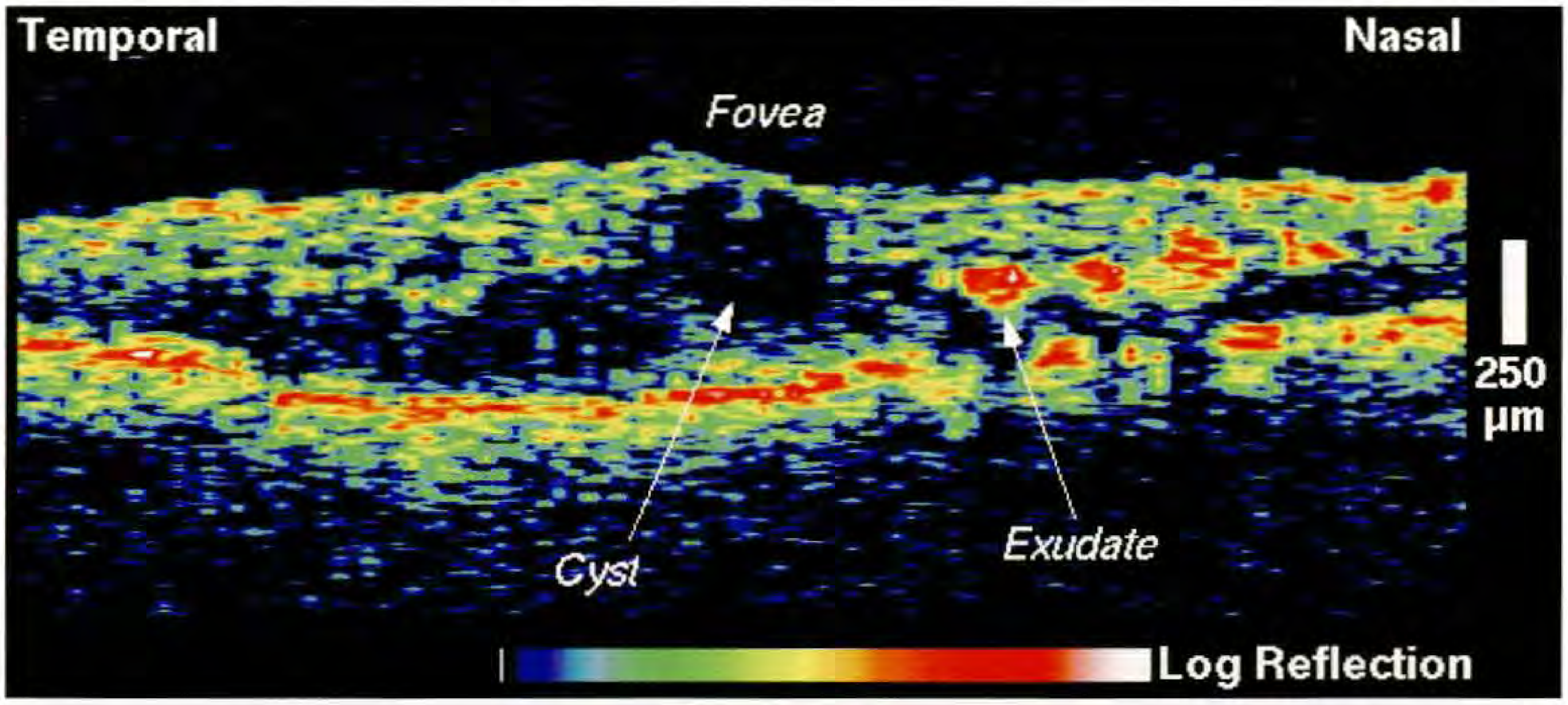

Figure 2-9. OCT tomogram acquired through fixation of a patient with cystoid macular edema secondary to non-proliferative diabetic retinopathy. The retina is significantly thickened, with loss of the normal foveal pit contour. Intraretinal fluid accumulation leads to the development of non-reflective cystic spaces and reduced reflectivity from the neurosensory retina. Focal areas of high backscattering which shadow the retinal layers below correspond to hard exudate.

paring nerve fiber thickness through different planes and in assessing the profile of the optic disc. The location of each tomogram on the retina is labeled on a corresponding fundus photograph. In the 90° tomogram (taken perpendicular to the papillomacular axis), high backscattering (red) is visible from the NFL and from a band defining the posterior boundary of the sensory retina, corresponding to the RPE and choriocapillaris. The tomogram shows the NFL expanding towards the optic disc to occupy nearly the entire retinal thickness, commensurate with the presence of the inferior and superior arcuate nerve fiber bundles. In comparison, the 0° tomogram (taken parallel to the papillomacular axis) exhibits a thinner NFL, consistent with fewer nerve fibers in this area. The surface contour and normal cupping of the disc are visualized in all of the tomograms. The termination of the choroid at the lamina cribosa is also delineated.

Circular Tomograms in the Peripapillary Region

Documentation of nerve fiber layer thickness and degeneration in the peripapillary region may be important in the diagnosis and treatment of glaucoma and other neurodegenerative diseases. A useful way of assessing the NFL in this area is to image cylindrical tissue sections centered around the optic disc. Figure 2-8 shows two circular OCT tomograms with different diameters, each centered on the nerve head. Each tomogram is displayed unwrapped and corresponds to a clockwise scan around the optic disc. The location and orientation of both tomograms on the fundus also depicted.

The anterior and posterior highly backscattering layers represent the NFL and choriocapillaris/RPE, respectively. The inferotemporal and superotemporal nerve fiber bundles are evident in both tomograms as localized thickenings in both the NFL and retina. The bundling becomes more diffuse in the images as the distance from the optic nerve head increases with a larger scan diameter, as expected from normal anatomy.

INTERPRETATION OF OCT IMAGES

The evaluation of OCT tomograms depends on the ability of the observer to identify both differences in the relative reflectivity of different tissue layers and morphological changes in tissue structures [8]. In some cases, because of the high axial resolution of the OCT images, small changes in morphology may be difficult to assess by direct observation of the images. In these cases, automated computer image processing tools may be used to extract precise quantitative measurements from the images.

Retinal Thickness

Retinal thickness is an important consideration in the assessment of many macular diseases. The high axial resolution of OCT combined with the well-defined contrasts in reflectivity at the anterior and posterior boundaries of the retina make OCT uniquely suited for measurement of this parameter.

Retinal thickness may be increased with edema. The accumulation of intraretinal fluid will lead to both an increased retinal thickness, and also a change in the scattering properties of the tissue. An important location to measure retinal thickening is directly in the fovea, where edema can have a profound effect on visual acuity. This type of measurement can be particularly useful in tracking patients with macular edema due to diabetic retinopathy (Figure 2-9), or for screening and following patients with cystoid macular edema following cataract surgery [9].

Retinal edema may be differentiated from retinal traction by the identification of cystic spaces within the retina, indicative cystoid macular edema, or by visualization of the posterior hyaloid or an epiretinal membrane, which may be causing retinal traction.

Decreased retinal thickness often occurs with atrophy or scarring and may be either focal or diffuse.

Reflectivity

Changes in retinal architecture or cellular morphology result in changes in optical properties which may be observed on the OCT tomograms. The apparent reflectivity measured by OCT is a combination of the actual reflectivity and the scattering and absorption characteristics of the overlying media. Thus, the apparent reflectivity for retinal imaging may be af-

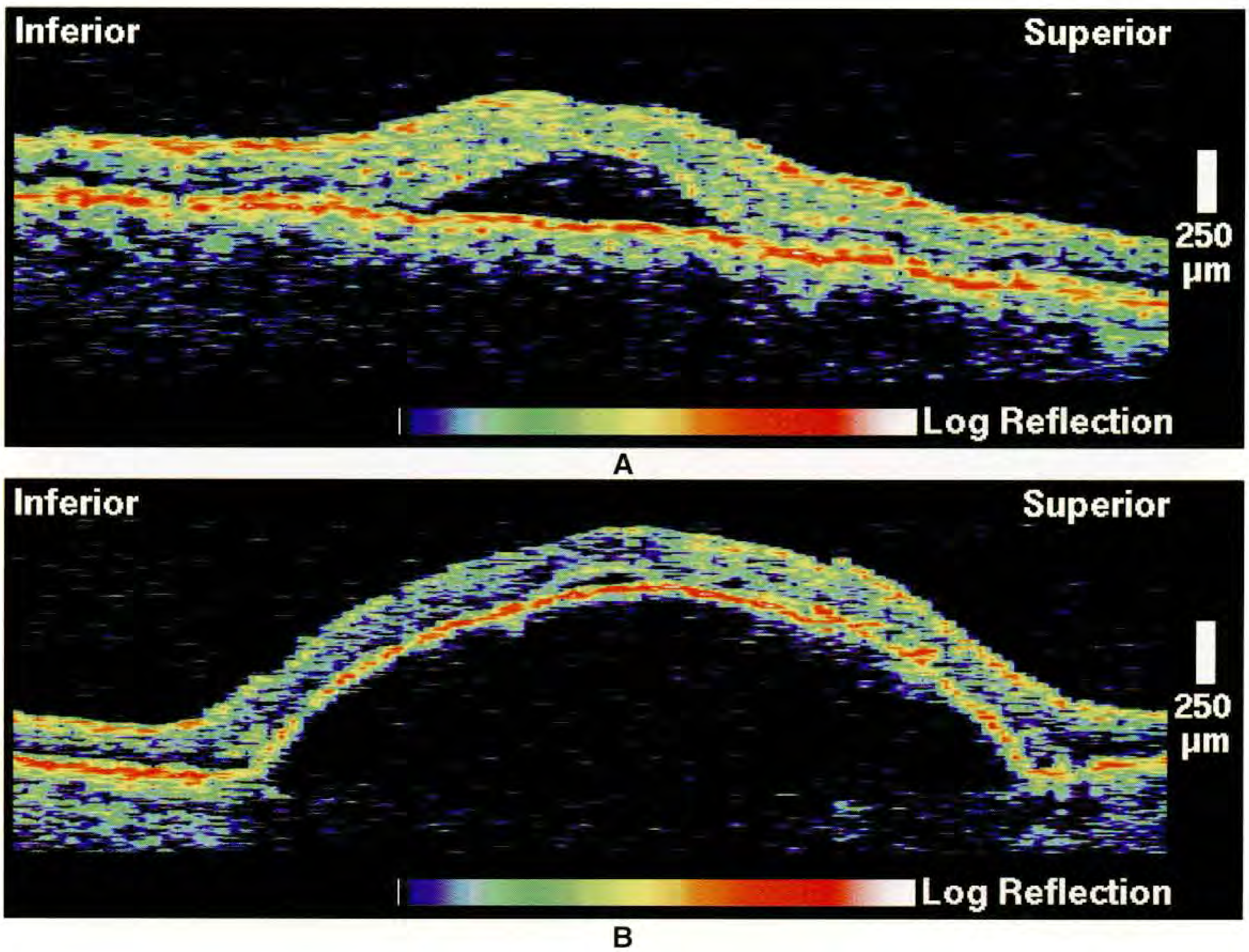

Figure 2-10. OCT tomograms of a neurosensory retinal detachment (A), and a serous detachment of the retinal pigment epithelium (B). Both detachments exhibit an elevation of the retina over an optically clear space corresponding to serous fluid accumulation. In the pigment epithelial detachment, however, the red band defining the posterior sensory retinal boundary is also elevated and the detached RPE severely shadows the reflections from the choroid below.

fected by abnormalities in the cornea, aqueous, lens, vitreous, and anterior retinal layers.

Causes of increased or hyper-reflectivity include inflammatory infiltrate into any layer of the retina or choroid, fibrosis, such as in a disciform or other scar, hard exudate, and hemorrhage. Hard exudate is highly reflective, but completely blocks the reflections from the deeper retinal layers (Figure 2-9). Blood also has a high scattering coefficient, which has two effects. The amount of backscattering from blood is great, leading to a bright reflection from hemorrhage; however, the scattering is also significant, leading to a rapid attenuation of the incident light as it propagates through the blood. Thus, blood vessels are most readily identified by their shadowing effect on the reflection from the RPE and choriocapillaris. The attenuation of the incident light depends on the thickness of the scattering medium. Thin hemorrhages appear as thin, highly reflective bands that have little effect on the underlying tissue. Thick hemorrhages, however, completely attenuate the probe light after more than approximately 200 μm.

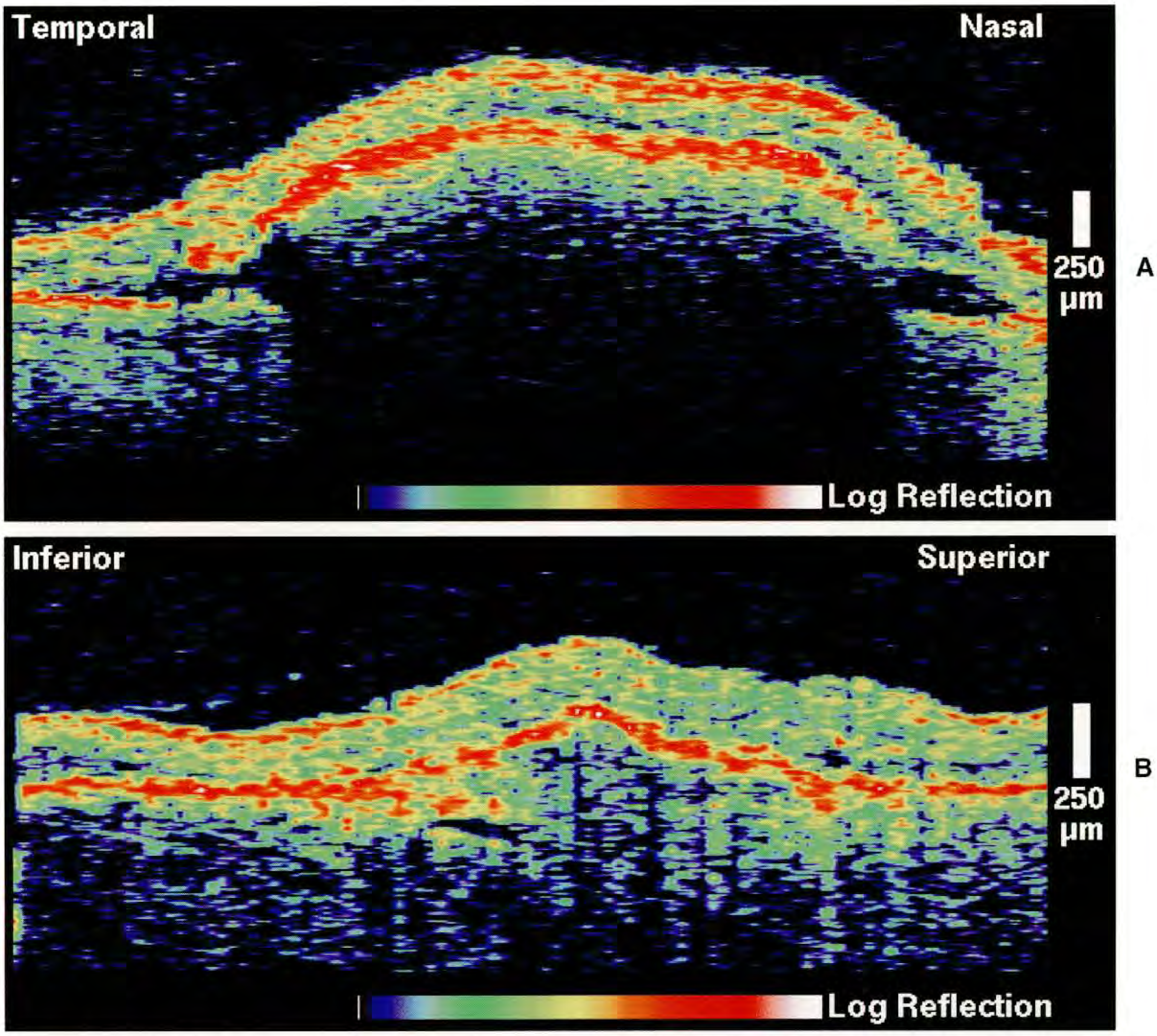

Figure 2-11. OCT tomograms of a hemorrhagic (A) and a fibrovascular (B) detachment of the retinal pigment epithelium (RPE). The hemorrhagic detachment displays high reflectivity just beneath the RPE corresponding to the hemorrhage. The incident light is attenuated by the superficial blood, completely shadowing the reflections from the deeper hemorrhage and choroid. In contrast, the fibrovascular detachment shows moderate backscattering throughout the sub-RPE space. Minimal reflection from the choroid is also visible.

Decreased, or hypo-reflectivity may be caused by retinal edema, in which fluid accumulation leads to a decreased density of microscopic scatterers and a corresponding reduction in the scattering coefficient (Figure 2-9). Alterations in cellular structure such as hypopigmentation of the RPE may also result in reduced reflectivity.

These morphological causes of reduced backscattering must be distinguished from alterations in the incident light caused by dense cataracts, cloudy media, astigmatism, poorly centered intraocular lens implants, or poor alignment of the OCT instrument while imaging. Abnormalities in the intervening structures typically cause a diffuse hypo-reflectivity throughout the OCT image, in all retinal layers. Focal decreases in reflectivity may be caused by shadowing from hyper-reflective tissues, such as hemorrhage, hard exudate, or a detached RPE. Local reductions in backscattering may also occasionally occur through silhouetting of the scanning probe beam by a narrow pupil. In this case, the reflectivity from all retinal layers is proportionately reduced, and the region of reduced reflectivity dynamically changes with alterations in the alignment of the delivery system.

The distinction between blood, serous fluid, and exudate is also made on the basis of reflectivity. The scattering coefficient, which along with anisotropy determines reflectivity, is essentially proportional to the concentration of particles in the fluid. Serous fluid, containing few cells, is optically transparent, so its accumulation is immediately recognized on OCT as a region devoid of backscattering. Blood, in contrast, has a large number of cells and a very high scattering coefficient, leading to both enhanced reflectivity and increased attenuation of the incident light. Cloudy exudate typically has an intermediate appearance between blood and serous fluid on OCT images.

Detachments of the Neurosensory Retina and Retinal Pigment Epithelium

OCT is extremely useful for evaluating detachments of the neurosensory retina and RPE [10]. Neurosensory detachments appear as a shallow elevation of the retina, with an optically clear space between the retina and RPE (Figure 2-10). The backscattering from the normally minimally reflective photoreceptors is increased, resulting in a well-defined fluid-retina boundary.

Serous detachments of the pigment epithelium have a distinctly different appearance (Figure 2-10) The reflective band corresponding to the RPE is focally elevated over an optically clear space. Like the photoreceptors in the neurosensory detachment, the detached RPE is more highly reflective than normal, perhaps due to a refractive index difference between serous fluid and the choriocapillaris, or due to decompensation and morphological changes in the RPE cells themselves. The increased reflectivity from the RPE strongly shadows the backscattering signal from the choroid below the detachment, often even obscuring the reflective boundary between the serous fluid and the basement membrane. The angle of the detachment is also more acute in a pigment epithelial as compared to a neurosensory detachment because of the tight adherence of RPE cells to the basement membrane at the edge of the detachment, which supports an increased fluid pressure.

The increased reflectivity from the photoreceptors in a neurosensory detachment may mimic the high reflectivity from the pigment epithelium, but rarely does it significantly shadow the reflections from the RPE and choroid. Thus, the distinction between a neurosensory and a pigment epithelial detachment relies on assessing the strength of the reflection below the serous fluid collection, and evaluating the angle of the detachment.

Neurosensory detachments may occasionally be confused with severe retinal edema on OCT, since in many cases the fluid accumulation and reduced backscattering which occurs with edema is preferentially seen in the outer retinal layers. It is important in these cases to identify a smooth and continuous fluid-retina boundary to establish the diagnosis of a sensory retinal detachment.

Hemorrhagic detachments of the RPE have all of the characteristics of a serous RPE detachment, except that an optical backscatter signal corresponding to blood is observed directly beneath the detached RPE (Figure 2-11). The blood usually appears moderately, rather than highly, backscattering because of the attenuation of the incident light through the detached RPE. The optical penetration through both the detached RPE and hemorrhage is usually less than 100 μm.

Fibrovascular pigment epithelial detachments also show some optical backscatter within the sub-RPE space (Figure 2-11). However, a lower scattering coefficient compared to blood results in reduced apparent reflectivity from the fibrovascular proliferation and increased penetration of the probe light, which often reaches the choroid. Other lesions, such as a vitelliform lesion, may have a similar appearance of constant mild to moderate reflectivity extending between an elevated RPE and the choroid.

Confluent soft drusen may be mistaken for small pigment epithelial detachments. However, no shad-

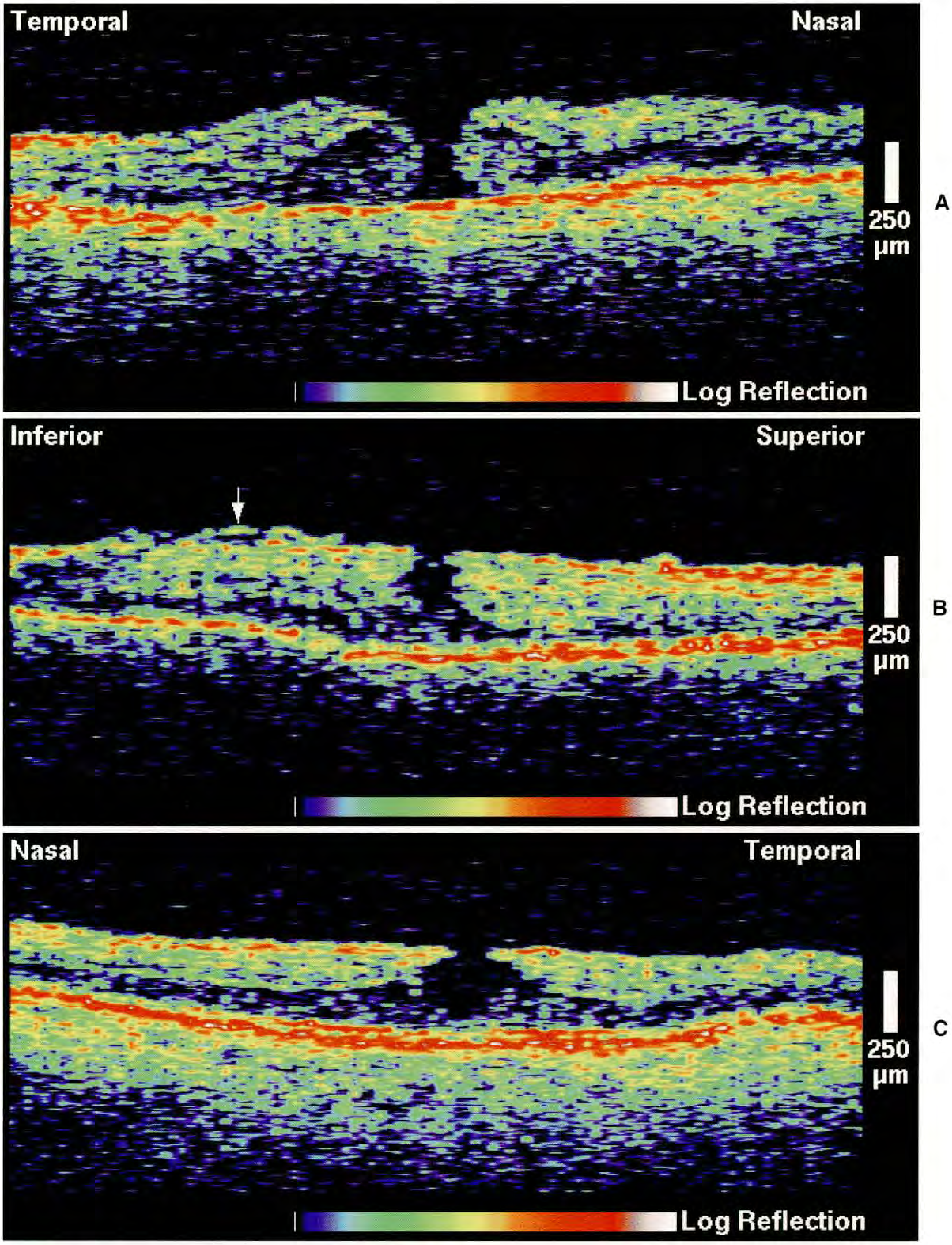

Figure 2-12. OCT images comparing an idiopathic full-thickness macular hole (A), a macular pseudohole due to an epiretinal membrane (B), and a lamellar or partial-thickness hole (C). The full-thickness hole displays a complete loss of retinal tissue in the fovea and surrounding retinal edema. The pseudohole and lamellar hole, however, exhibit an intact photoreceptor layer in the fovea. The pseudohole is characterized by a steepened foveal pit contour due to traction by the epiretinal membrane. The membrane is sometimes visible when it is separated from the sensory retina (B, arrow). The foveal contour of the lamellar hole is indicative of the rupture of a central cyst.

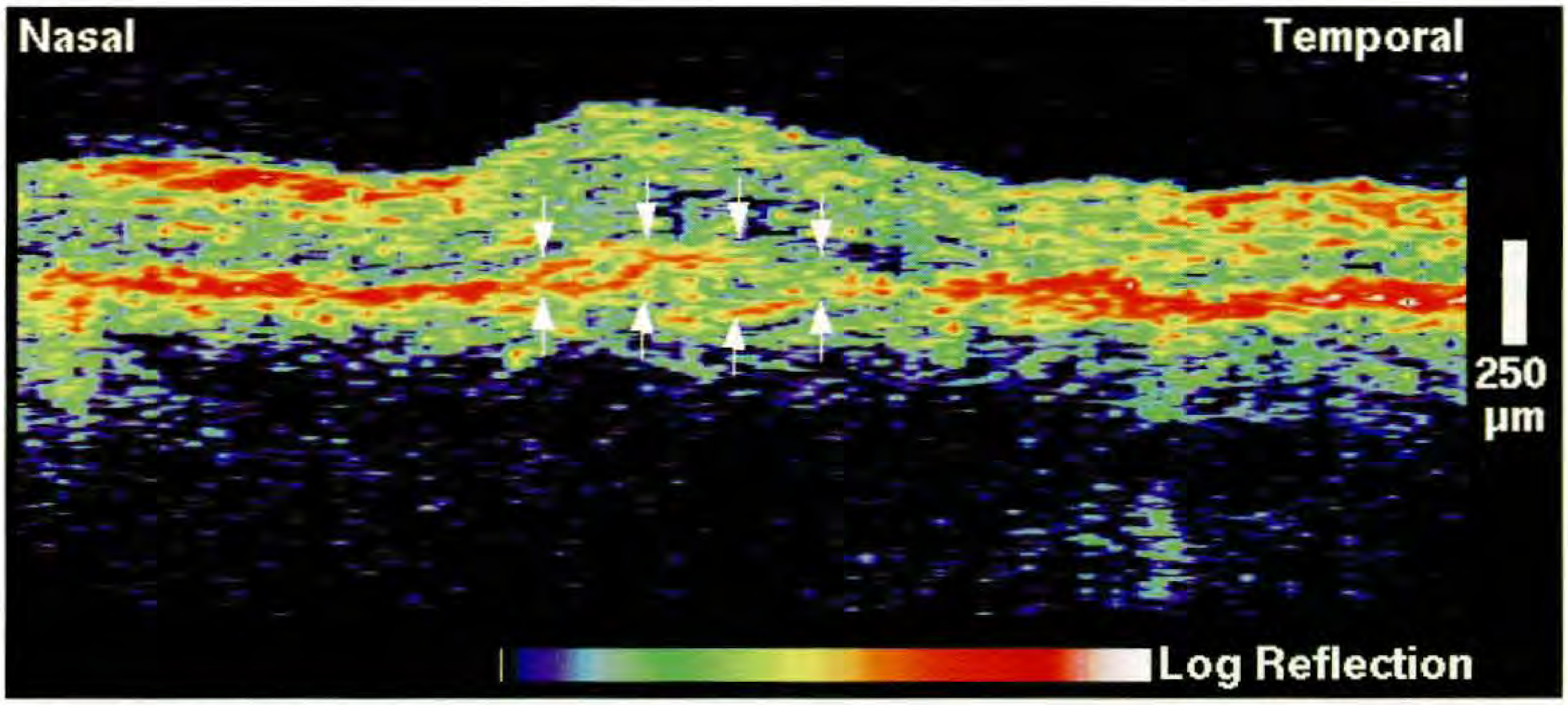

Figure 2-13. A choroidal neovascular membrane appears as a disruption and thickening of the reflective band corresponding to the retinal pigment epithelium and choriocapillaris. Subretinal or intraretinal fluid or hemorrhage may be visible above the membrane.

owing occurs with soft drusen and mild reflectivity, often indistinguishable from the choroidal reflectivity, extends from the elevated RPE down the choroid.

Fovea

Changes in the morphology of the fovea are often indicative of disease on the OCT image. Loss of foveal photoreceptors can be assessed with OCT, as occurs with full-thickness macular holes (Figure 2-12), central scarring or fibrosis, and other macular lesions. Steepening of the foveal contour is commonly associated with epiretinal membranes and macular pseudoholes or lamellar holes (Figure 2-12). Loss or flattening of the foveal contour may occur with impending macular holes, foveal edema, or foveal neurosensory detachments. Vitreomacular traction may result in flattening or protrusion of the fovea [11].

Retinal Pigment Epithelium and Choriocapillaris

While the RPE and choriocapillaris are difficult to distinguish on the OCT tomogram, their combined reflection, which defines the posterior boundary of the neurosensory retina on the OCT image, provides useful information on chorioretinal pathologies such as age-related macular degeneration and choroidal neovascularization.

Hyperpigmentation of the RPE leads to increased reflectivity, mild thickening of the posterior reflective boundary, and concomitant shadowing of the backscattering from the choroid. Detachments of the RPE also lead to choroidal shadowing, as discussed above. Disciform scars and other fibrosis appear as a severely thickened posterior reflection due to the high reflectivity and extension of fibrotic structures into the retina.

Hypopigmentation or pigment epithelial atrophy results in decreased reflection and an associated window defect, enabling increased penetration of the probe beam to the choroid, and higher reflectivity from the deeper layers.

Disruption of the reflection corresponding to the RPE and choriocapillaris is a good indicator of choroidal neovascularization (Figure 2-13). The ingrowth of new blood vessels through breaks in Bruch's membrane results in fragmentation and thickening of the posterior reflection due to the architecture of the neovascular membrane. This fragmentation and thickening may sometimes be difficult to discern, but may be associated with a thickening of the overlying neurosensory retina due to intraretinal or subretinal fluid leakage from the new vessels.

Vitreous and Vitreoretinal Interface

Many diseases of the vitreous and retina affect the vitreoretinal interface. The normal vitreous gel is optically transparent, providing a high contrast bound-

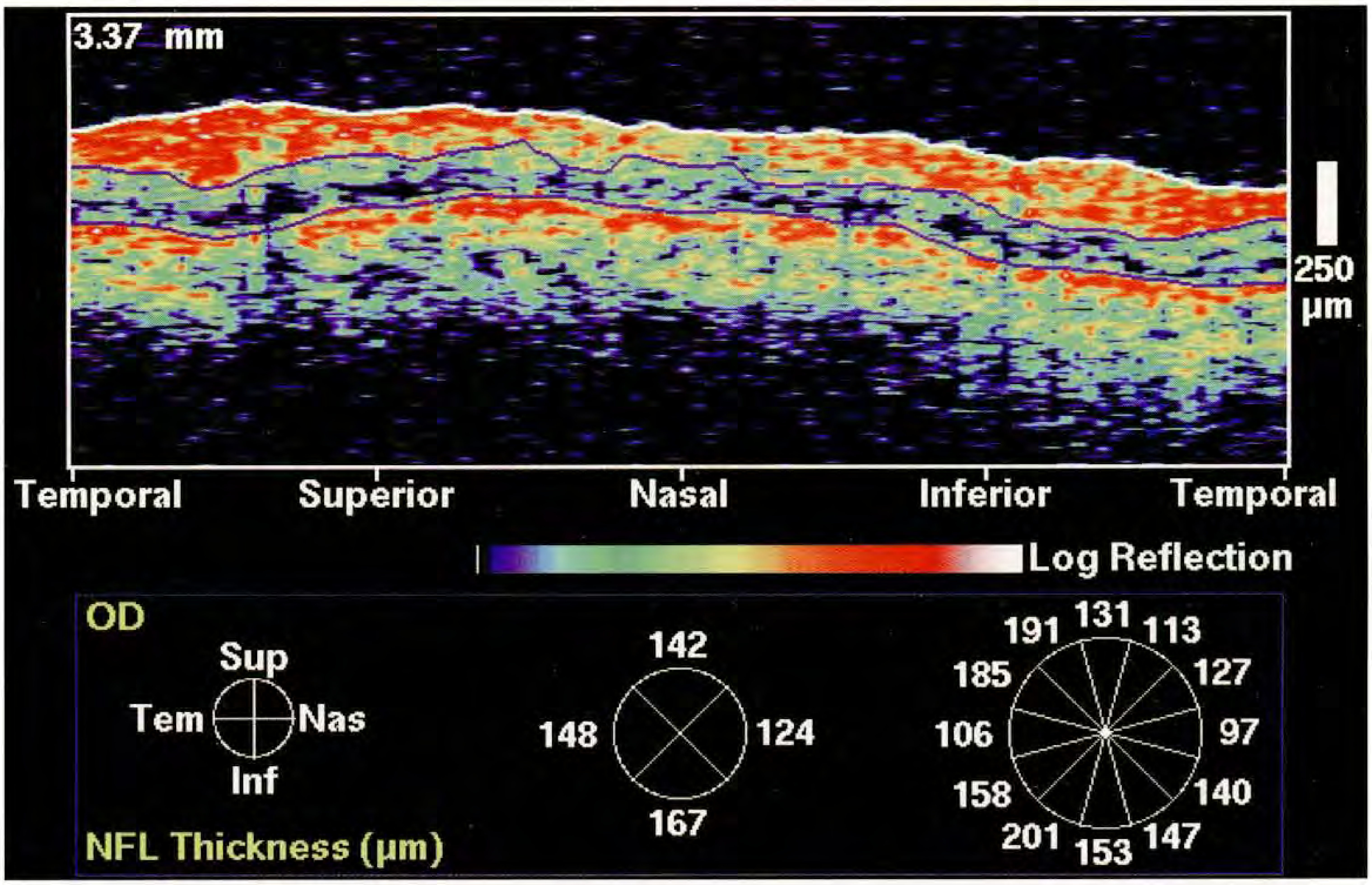

Figure 2-14. Circular tomogram representing a cylindrical section around the optic disc at a diameter of 3.4 mm. White and blue lines indicate the computer generated profiles of the anterior and posterior retinal boundaries, and the posterior margin of the retinal nerve fiber layer. Thicknesses are displayed averaged over quadrant and clock hour.

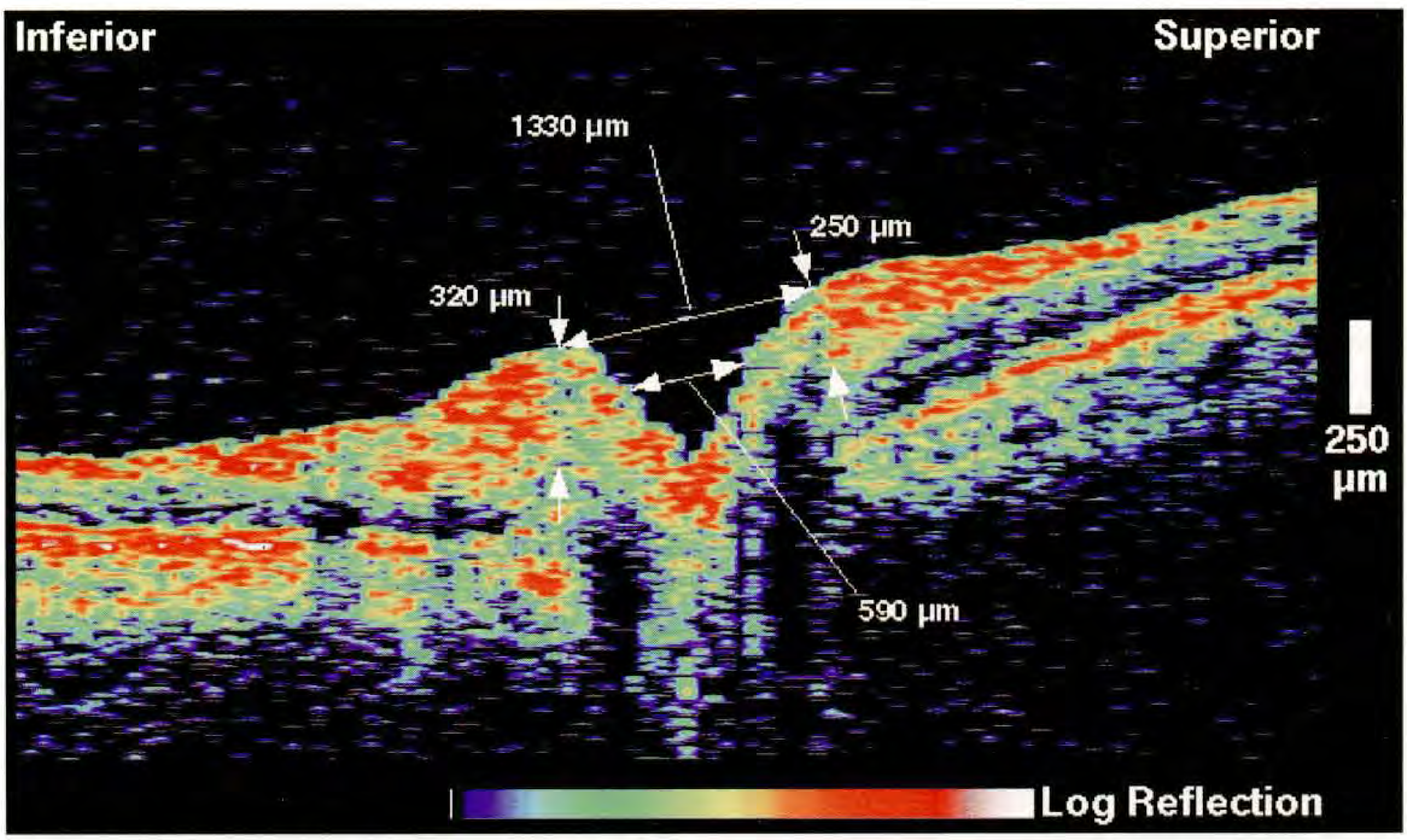

Figure 2-15. A vertical linear tomogram showing the cross-section of the optic nerve head. Disc parameters such as cup and disc diameter, neuroretinal rim area, and cup-to-disc ratio may be estimated from the image as shown.

ary between the vitreous and retina. Significant backscatter signal may be observed from the vitreous with inflammatory infiltrate, vitreous condensations, or hemorrhage. An operculum or pseudo-operculum may also present as a focal, thin area of backscatter anterior to the retinal surface. The posterior hyaloid membrane is nominally indistinguishable from the superficial retina on the OCT image, but becomes apparent when the posterior vitreous is detached [11]. The reflection from the posterior hyaloid is typically weak and often appears patchy because the vitreous gel and the intervening fluid have similar indices of refraction.

An epiretinal membrane may be observed easily if it is separated from the neurosensory retina. Often, however, the membrane will be tightly adherent to the retinal surface, in which case the distinction between it and the retina depends on differences in optical reflectivity, and on the presence of secondary features, such as a macular pseudohole, or traction detachment of the retina. The reflection from an epiretinal membrane is usually stronger than that observed from the underlying retinal tissue.

An epiretinal membrane which is separated from the retina is distinguished from the posterior hyaloid based on the membrane's higher reflectivity, greater thickness, and differences in contour. A contracted epiretinal membrane usually has a flatter contour than a detached posterior hyaloid, indicating greater tension.

Nerve Fiber Layer

Alterations in the thickness of the retinal nerve fiber layer may be a powerful indicator of the onset of neurodegenerative diseases such as glaucoma. The NFL appears in the OCT images as a highly backscattering layer in the superficial retina and exhibits increased reflectivity compared to the deeper retinal layers. NFL thickness may be assessed at individual points on a cylindrical or linear tomogram in the peripapillary region. Alternatively a computer algorithm can be used to evaluate both retinal and NFL thickness. Figure 2-14 shows a clockwise circular tomogram around a normal optic disc. Computer generated profiles of the NFL and retinal boundaries are displayed, and the NFL thicknesses are reported as either averages over each quadrant or clock hour [12].

Careful inspection of the circular tomograms is required to identify focal NFL defects, which must be distinguished from normal variations in reflectivity and NFL thickness. The observation of depressions from both the anterior and posterior margins of the NFL is a helpful indicator of actual thinning.

Linear tomograms through the optic disc are useful for assessing disc and cup parameters (Figure 2-15). The points at which the choriocapillaris terminates at the lamina cribosa may be used to determine the boundaries of the disc. Extrapolation of these points to the retinal surface defines a line segment which measures the disc diameter. Total retinal and retinal nerve fiber layer thickness can also be assessed at these points. The cup diameter may be estimated by choosing a line segment parallel to the line segment defining the disc diameter, but taken at a certain depth into the cup. Throughout this text, we have used a depth of 140 μm to define the cup diameter. The disc and cup diameters can provide an estimate of disc, cup, and neuroretinal rim areas.

SUMMARY

Although the basic principles of image interpretation have been outlined in this chapter, future developments in OCT technology will likely lead to enhanced images and exploit other optical properties of tissue. High-resolution OCT systems, for example, will lead to better distinction between retinal layers and perhaps the ability to examine cellular morphology. Tomography with multiple optical wavelengths or polarizations [13] will use spectroscopic or birefringent properties of tissue to provide increased contrast, allowing the detection and differentiation of various disease states.

REFERENCES

1. Huang D, Swanson EA, Lin CP, Schuman JS, Stinson WG, Chang W, Hee MR, Flotte T, Gregory K, Puliafito CA, Fujimoto JG. Optical coherence tomography. Science 1991; 254:1178-1181.
2. Swanson EA, Izatt JA, Hee MR, Huang D, Lin CP, Schuman JS, Puliafito CA, Fujimoto JG. In vivo retinal imaging by optical coherence tomography. Opt Lett 1993; 18:1864-6.
3. Bohren CF, Huffman DR. Absorption and Scattering of Light by Small Particles. New York: John Wiley & Sons; 1983.
4. Cheong W, Prahl SA, Welch AJ. A review of the optical properties of biological tissues. IEEE J Quantum Electron 1990; 26:2166-85.
5. Patterson MS, Chance B, Wilson BC. Time resolved reflectance and transmittance for the non-invasive measurement of tissue optical properties. Appl Opt 1989; 28:2331-6.
6. Izatt JA, Hee MR, Swanson EA, Huang D, Lin CP, Schuman JS, Puliafito CA, Fujimoto JG. Micron-scale resolution imaging of the anterior eye in vivo with optical coherence tomography. Arch Ophthalmol 1994; 112:1584-9.
7. Hee MR, Izatt JA, Swanson EA, Huang D, Schuman JS, Lin CP, Puliafito CA, Fujimoto JG. Optical coherence tomography of the human retina. Arch Ophthalmol 1995; 113:325-32.

Section II

MACULAR DISEASES

CHAPTER 3

Macular Hole and Vitreomacular Traction

Idiopathic Macular Holes
Atypical Macular Holes
Vitreomacular Traction Syndrome

Lesions that ophthalmoscopically resemble various stages of macular hole development include lamellar holes, macular cysts, foveal detachments of the neurosensory retina or pigment epithelium, and epiretinal membranes with macular pseudoholes [1,2]. OCT can effectively distinguish these pathologies in cross-section [3]. Full-thickness macular holes show a clear loss of retinal tissue in the fovea extending to the pigment epithelium on OCT. In contrast, lamellar holes and pseudoholes only develop a partial loss of retinal tissue and a steepened foveal contour. Macular cysts and retinal detachments show a localized intraretinal or subretinal accumulation of optically clear serous fluid.

OCT is effective in staging idiopathic macular holes according to the criteria developed by Gass [3,4], which may be important in evaluating surgical intervention. Stage 1 impending macular holes may be distinguished by a reduced or absent foveal pit and the presence of an optically clear space beneath the fovea suggesting a foveolar detachment. Evidence of traction by the posterior hyaloid on the fovea may be present. Stage 2 holes have an attached operculum corresponding to a partial break in the outer retinal tissue. A full-thickness retinal dehiscence with a complete break in the outer retinal tissue and variable amounts of surrounding macular edema is observed in a Stage 3 hole. An operculum may be present and is completely separated from the edges of the hole. Stage 4 holes are characterized by their complete loss of tissue and a detachment of the posterior hyaloid involving the fovea and optic disc.

Vitreomacular traction has been implicated in the pathogenesis of hole formation [4-9]. OCT can assess the status of the vitreoretinal interface which is useful in evaluating the risk of hole formation, especially in the fellow eyes of patients with a unilateral macular hole [3]. Several studies have shown the protective value of vitreous detachment in preventing hole formation [8,9]. OCT tomograms identify a detached vitreous by the presence of a faint membrane anterior to the retina corresponding to the posterior hyaloid. Fellow eyes with a high risk of progression to a full-thickness hole display a perifoveal vitreous detachment with foveal adhesion and loss of the normal foveal pit contour. This perifoveal vitreous detachment characteristically heralds the onset of a Stage 1 hole and emphasizes the role of vitreous traction in hole formation.

Quantitative information may be directly extracted from the OCT tomograms, including the diameter of the hole, and the extent of surrounding subretinal fluid accumulation. The high resolution obtained in the tomograms suggests that OCT may be a useful method of precisely monitoring hole progression, or recovery after surgery. OCT images of successful surgical repair of macular holes demonstrate complete hole closure with a normal appearing fovea, providing an *in vivo* alternative to histopathology [10-11].

Atypical macular holes do not exhibit the typical inverse anvil shape of a classic Stage 3 hole with surrounding retinal edema. Many occur in the setting of age-related macular degeneration, displaying irregular edges, retinal thinning and atrophy, and increased reflectivity from the choroid due to pigmentary atrophy or chorioretinal scarring.

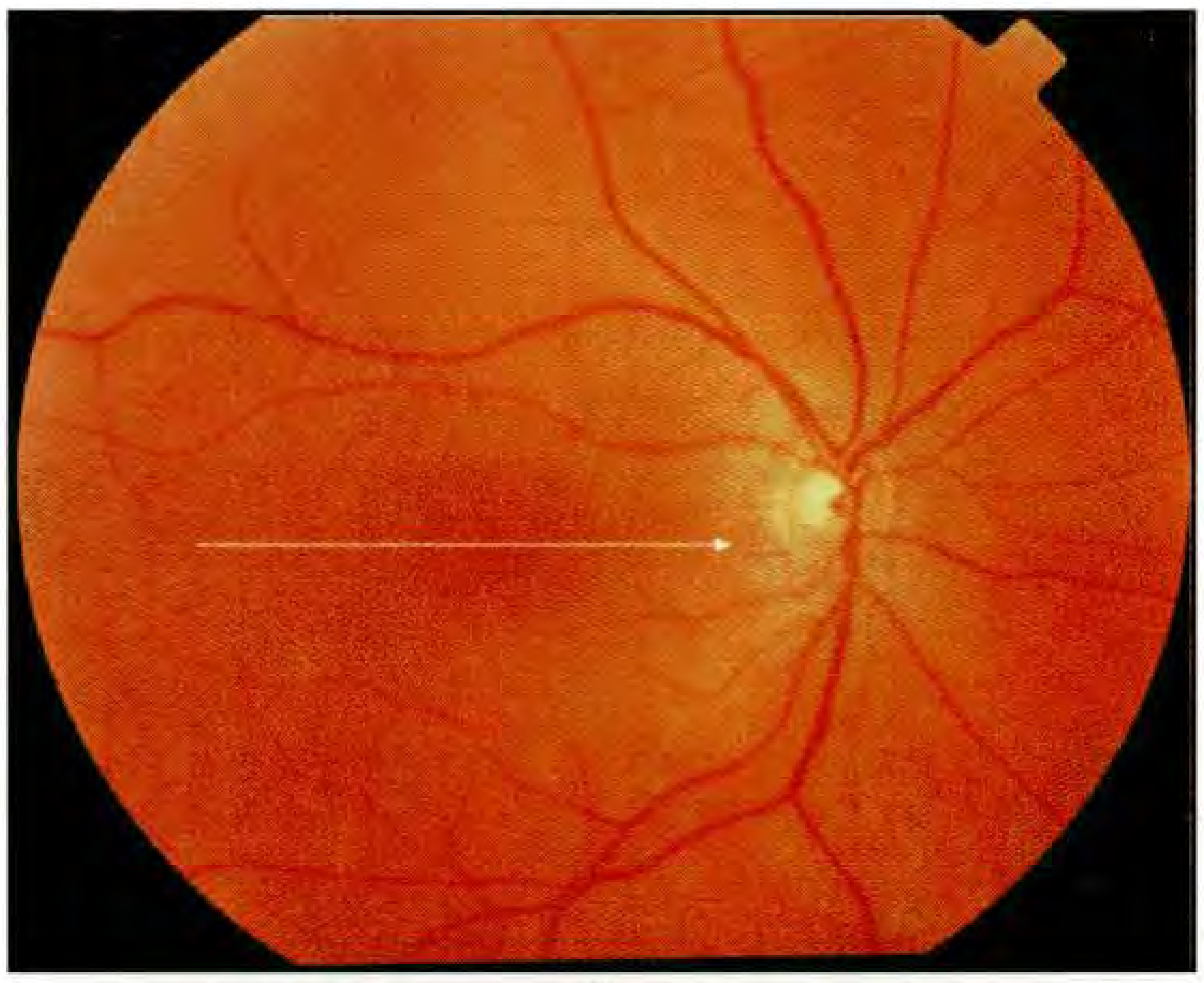

A

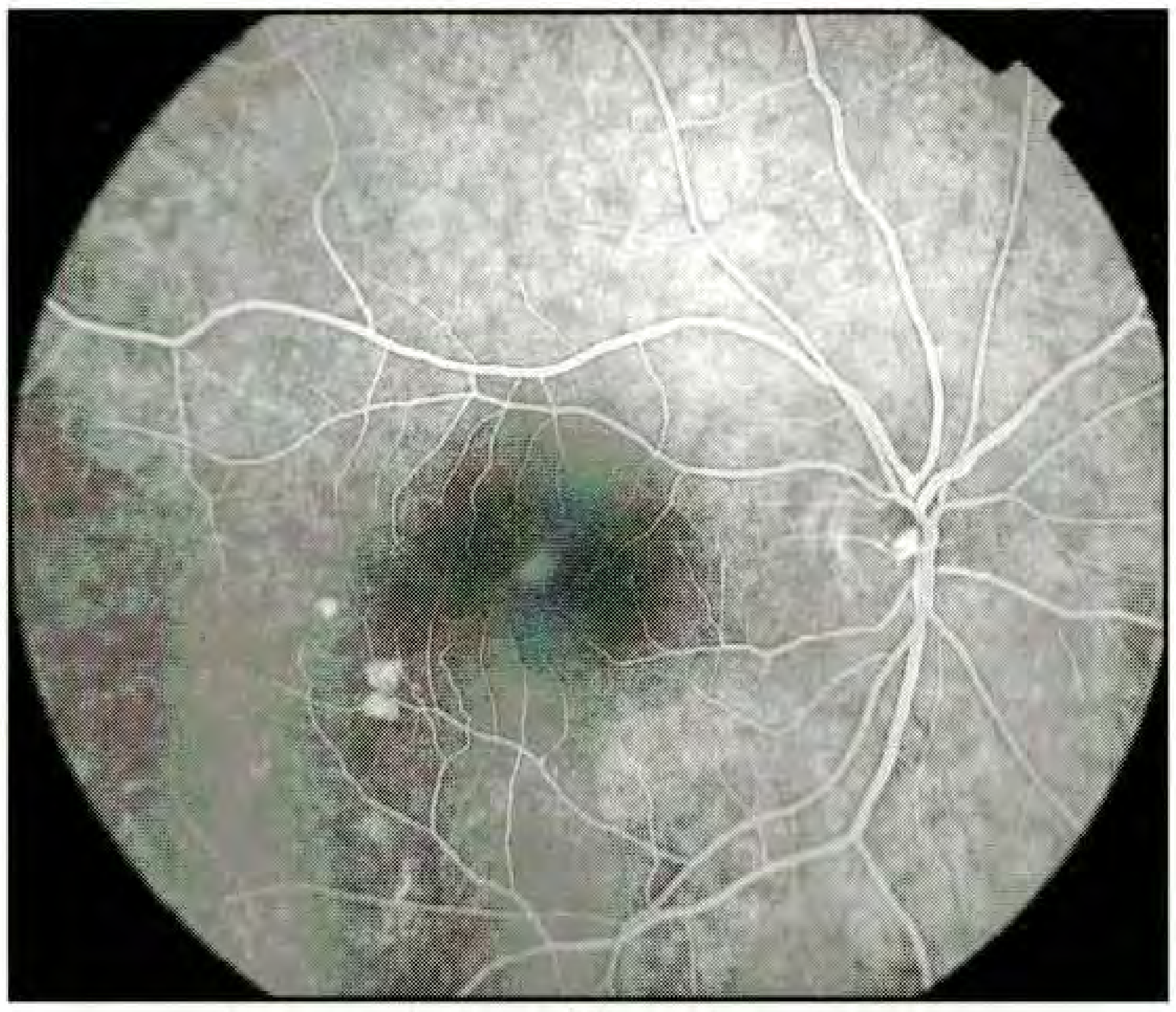

B

Case 3-1. Stage 2 Macular Hole and Successful Surgery

Clinical Summary

A 54-year-old woman was examined after she noted worsening vision in her right eye over several months. Her visual acuity in this eye was 20/70. Dilated ophthalmoscopy (A) revealed a full-thickness macular hole with a surrounding cuff of subretinal fluid. Fluorescein angiography (B) demonstrated a faint, focal area of hyperfluorescence in the fovea consistent with a window defect and a partial break in the retinal tissue

Optical Coherence Tomography

OCT examination (C) was performed and showed a full-thickness loss of tissue in the fovea with a diameter of approximately 350 µm. A small operculum was attached to the edge of the hole consistent with a partial break in the outer retina and a Stage 2 classification. A region of slightly reduced optical reflectivity and increased retinal thickness was evident in the region surrounding the hole correlating with the clinical finding of fluid accumulation. The retinal thickness reached a maximum of 370 µm in this area compared with a measurement of approximately 200 µm at the temporal margin of the image.

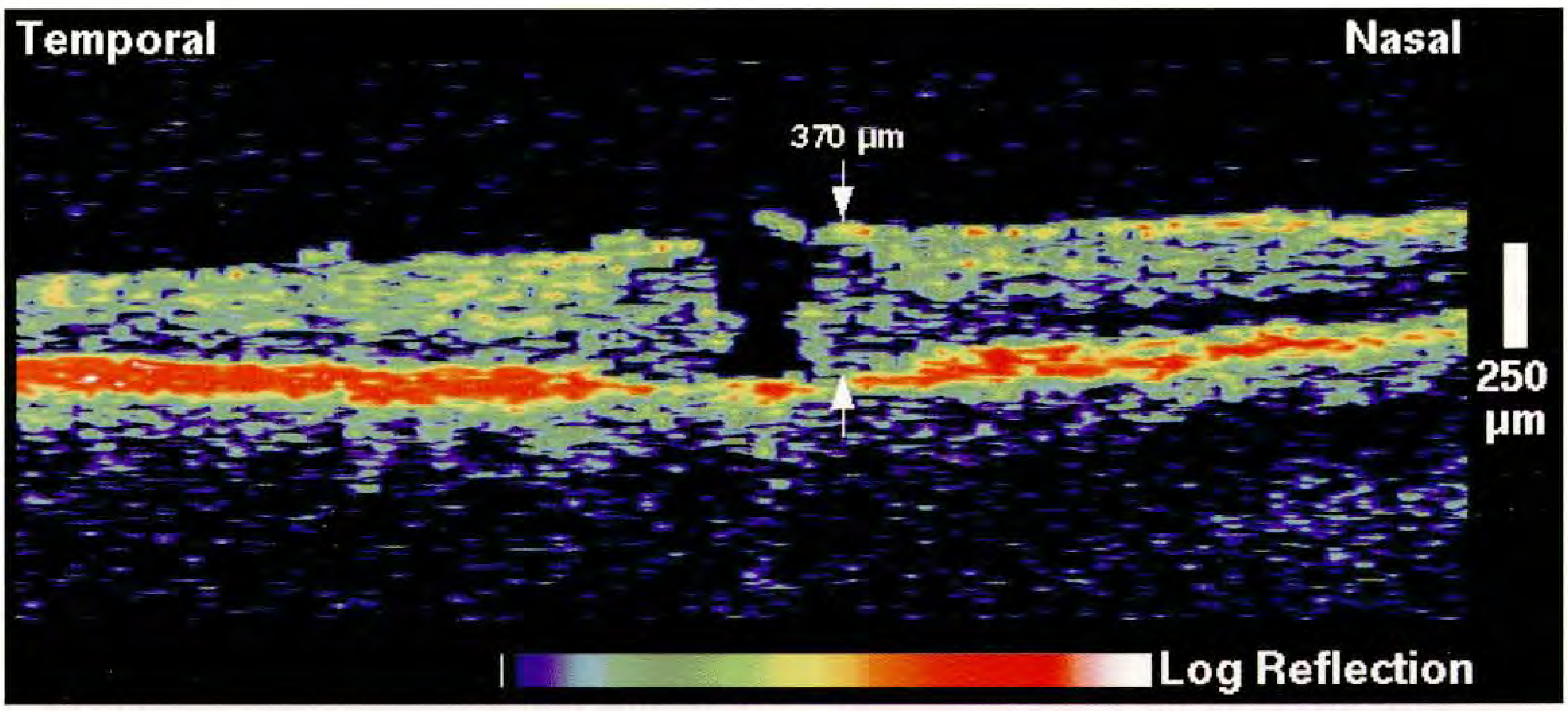

C

Case 3-1 continued

Follow-up Examination

One week later the patient underwent pars plana vitrectomy, injection of autologous serum, and post-operative intraocular gas tamponade with SF_6. Six weeks after the operation her vision had improved to 20/20 and fundus examination (D) showed reapproximation of the edges of the hole.

Optical Coherence Tomography

A post-operative OCT image (E) also demonstrated hole closure with an apparently intact photoreceptor layer.

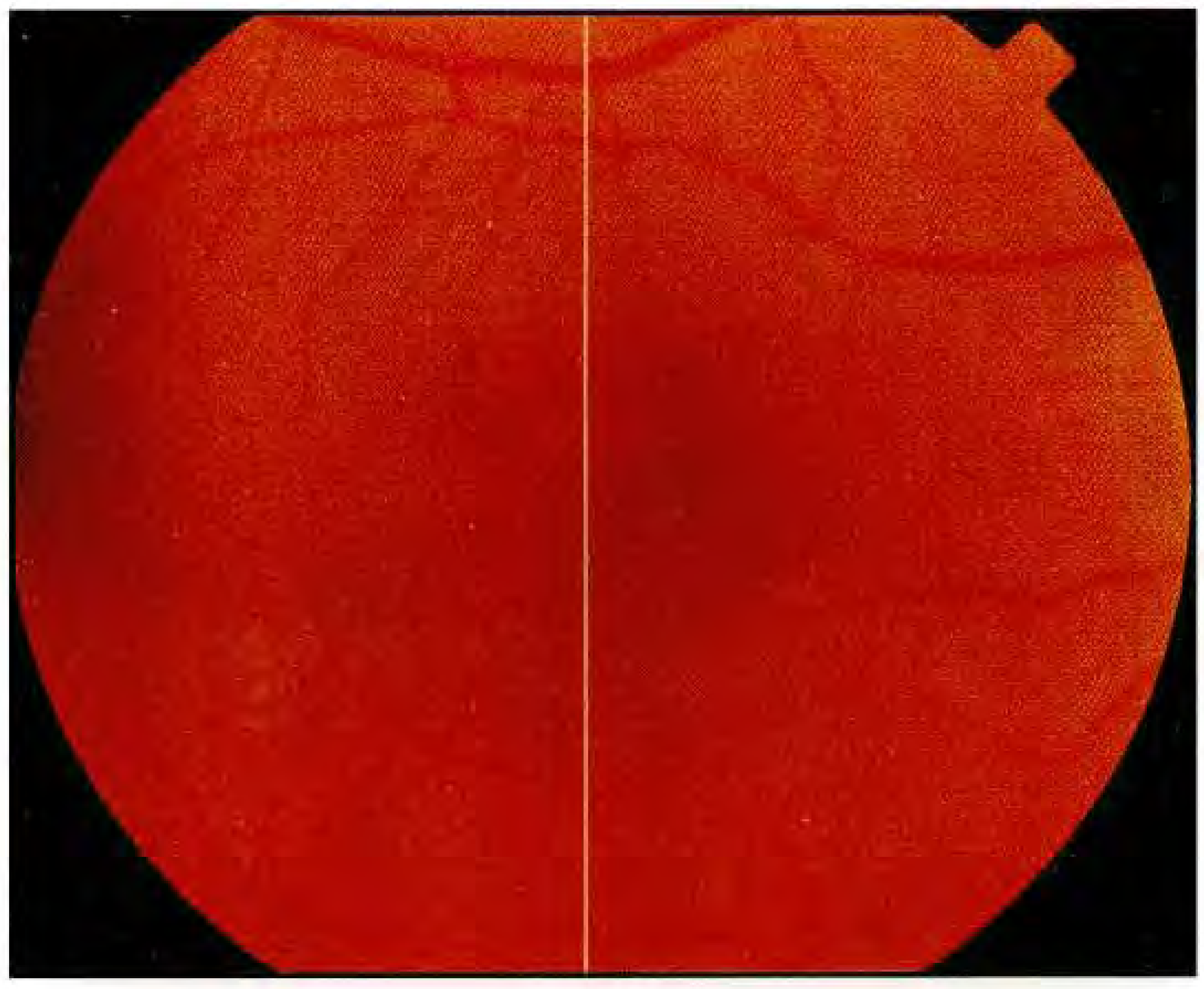

D

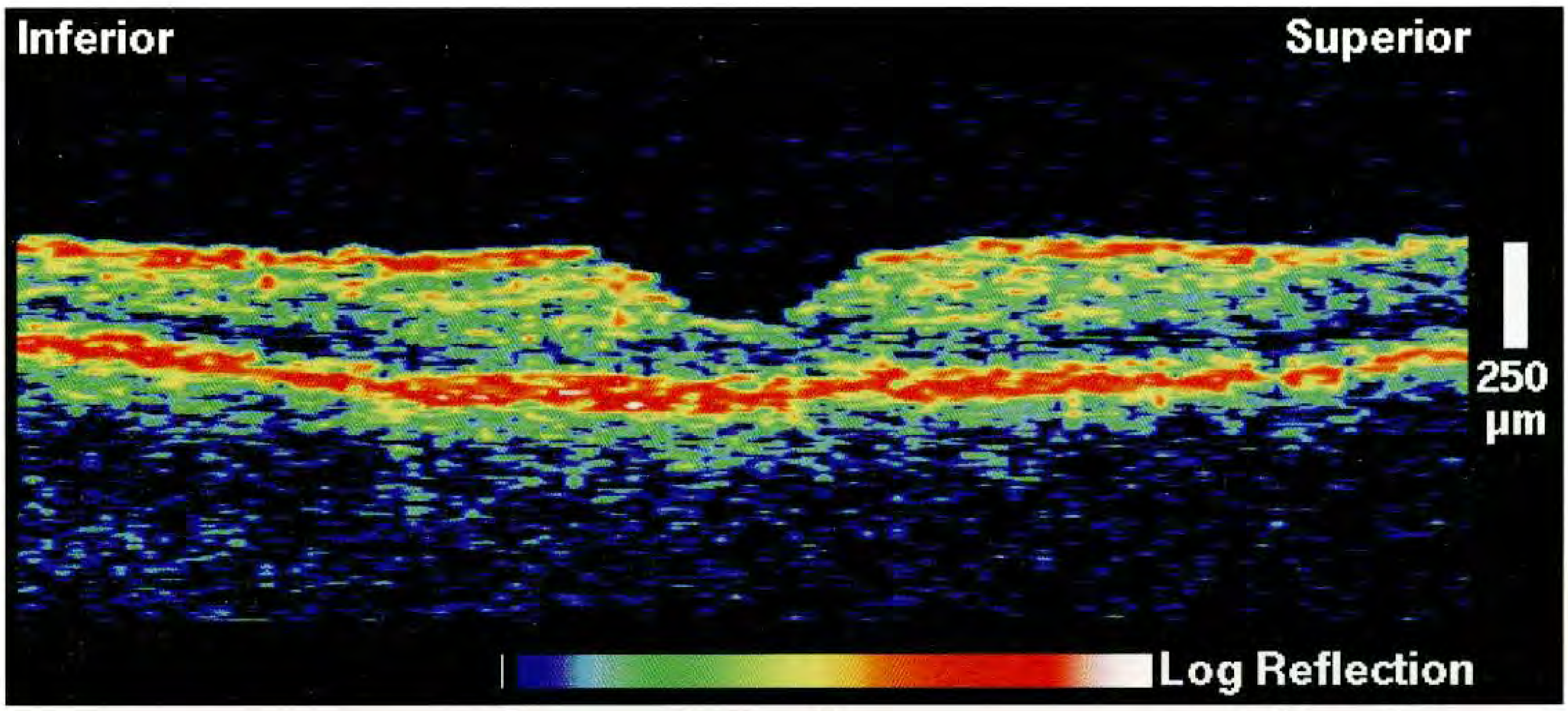

E

A

Case 3-2. Stage 2 Macular Hole and Surgical Treatment

Clinical Summary

A 72-year-old man was referred for evaluation of a macular hole in his right eye. On examination, his visual acuity in this eye was 20/70, and a small Stage 2 hole was identified in the macula (A).

Optical Coherence Tomography

A horizontal OCT scan (B) showed a narrow, full-thickness retinal dehiscence with a thin, attached operculum consistent with a Stage 2 classification. There were significant cystic changes surrounding the hole which were manifest by retinal swelling and decreased intraretinal optical reflectivity.

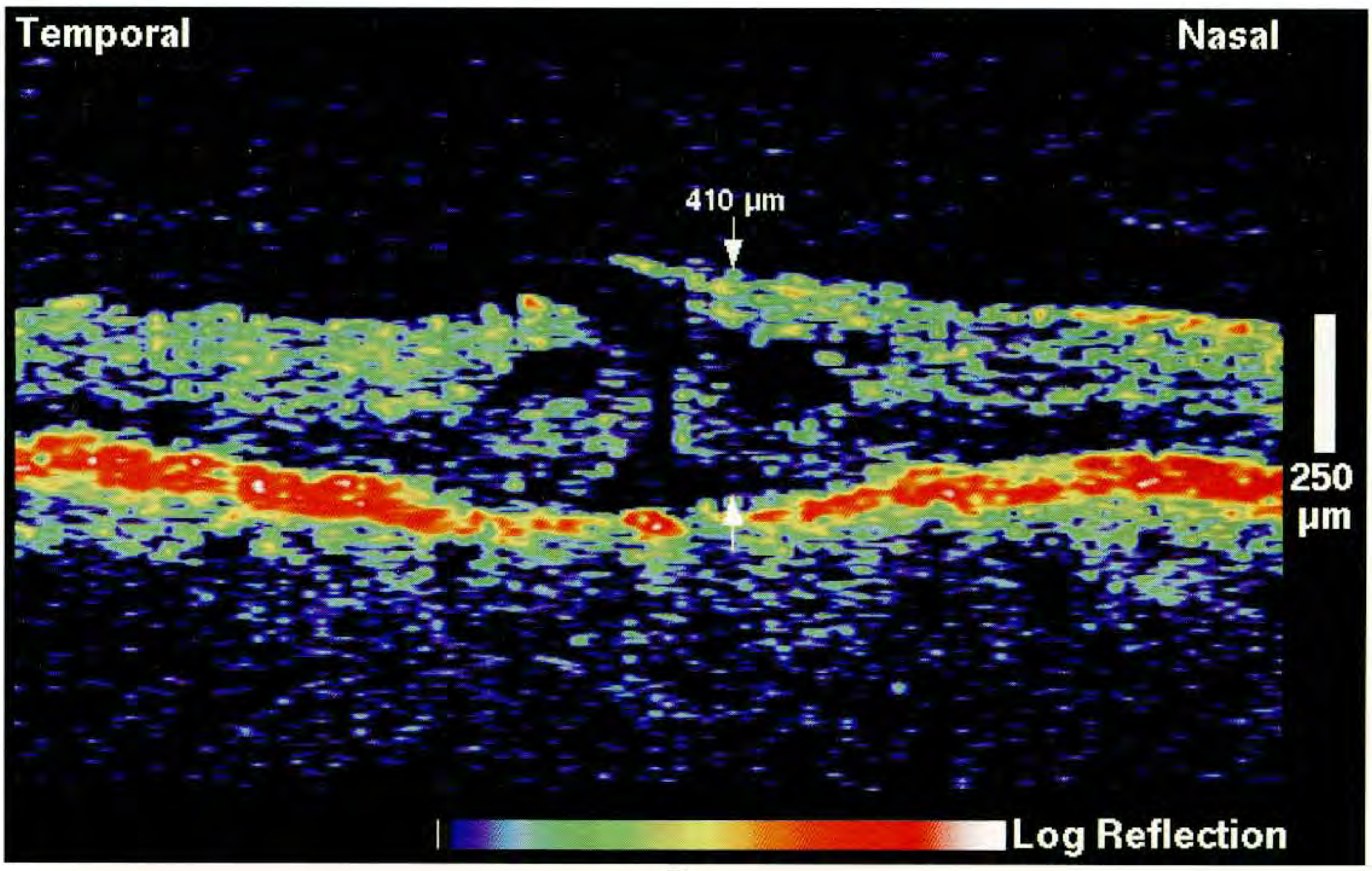

B

Case 3-2 continued

Follow-up Examination

Pars plana vitrectomy surgery was performed with autologous serum and injection of 15% C_3F_8. Three weeks after surgery, the patient's visual acuity was 20/200. Dilated fundus examination revealed a partial gas fill and closure of the hole (C).

Follow-up Optical Coherence Tomography

OCT (D) showed reapproximation of the edges of the hole and a reduction in the amount of surrounding retinal edema. A residual subretinal space was identified below the fused edges.

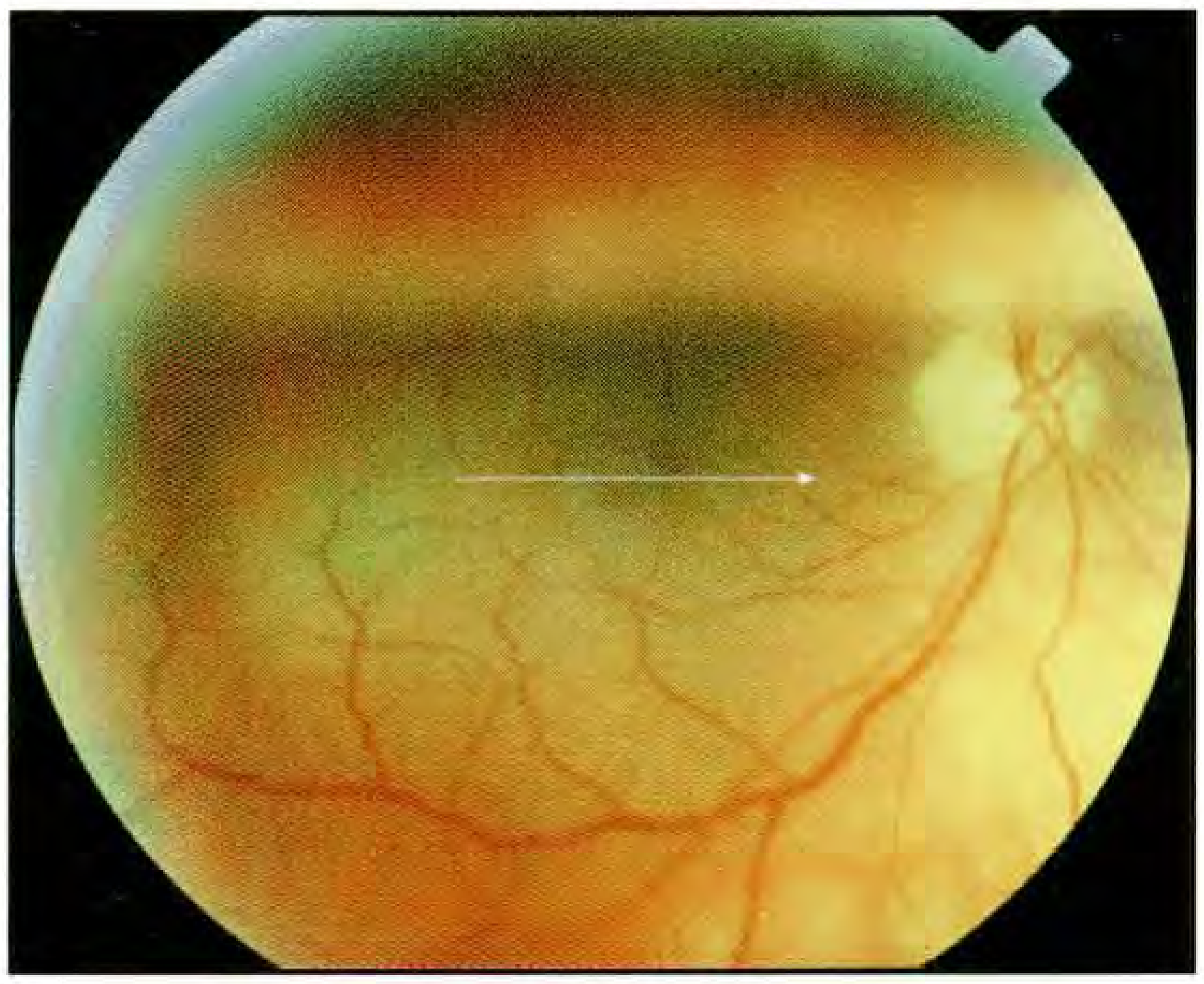

C

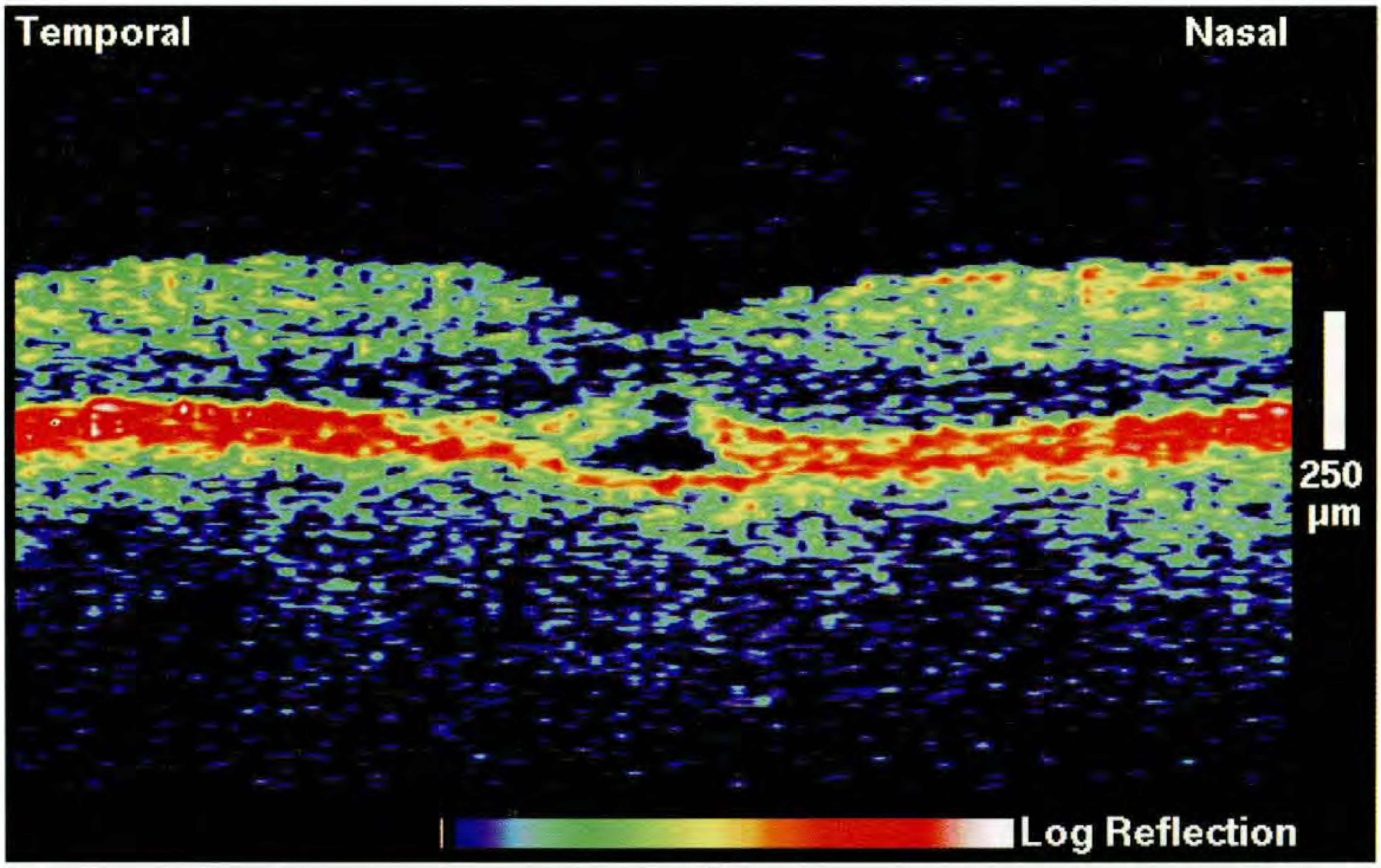

D

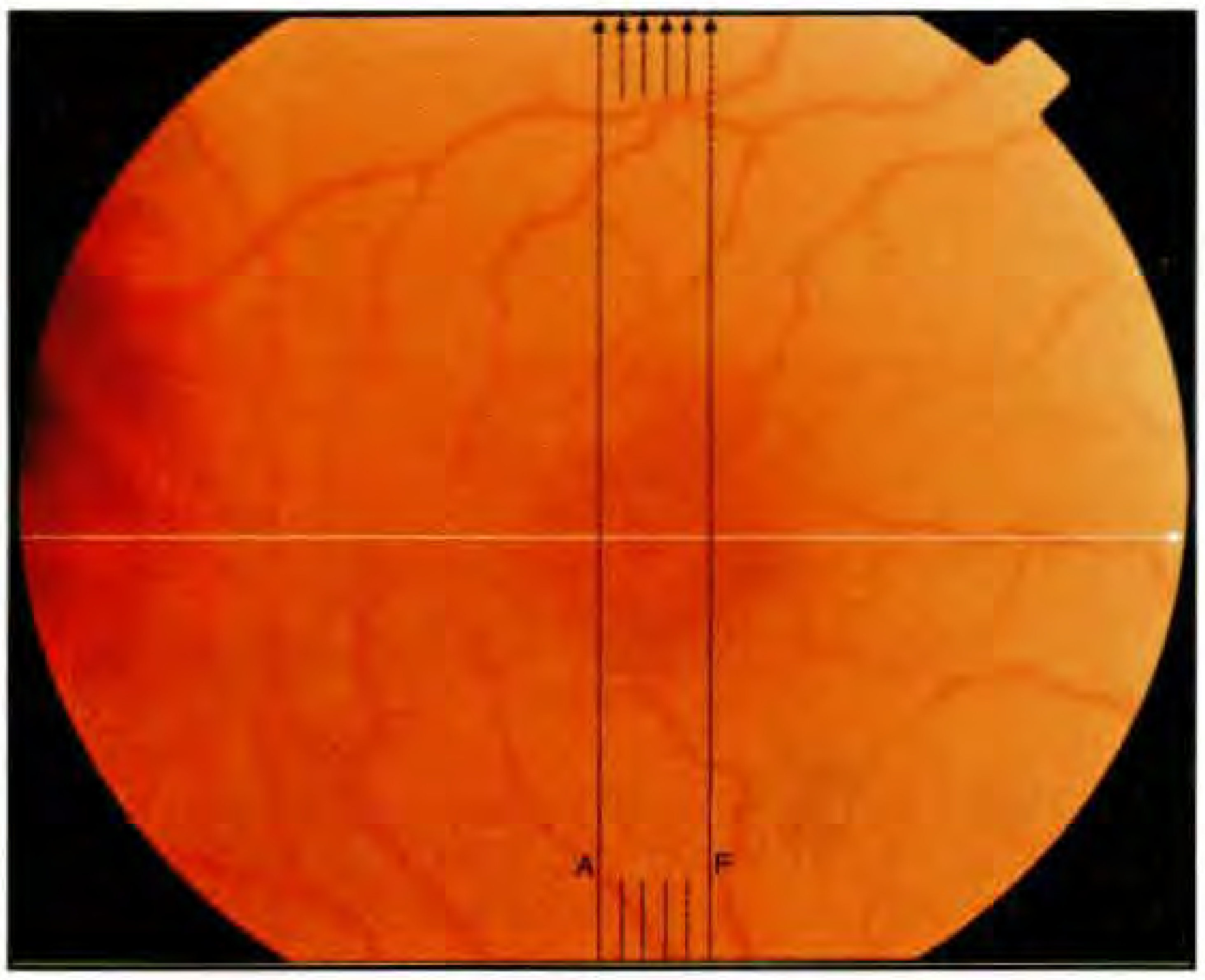

A

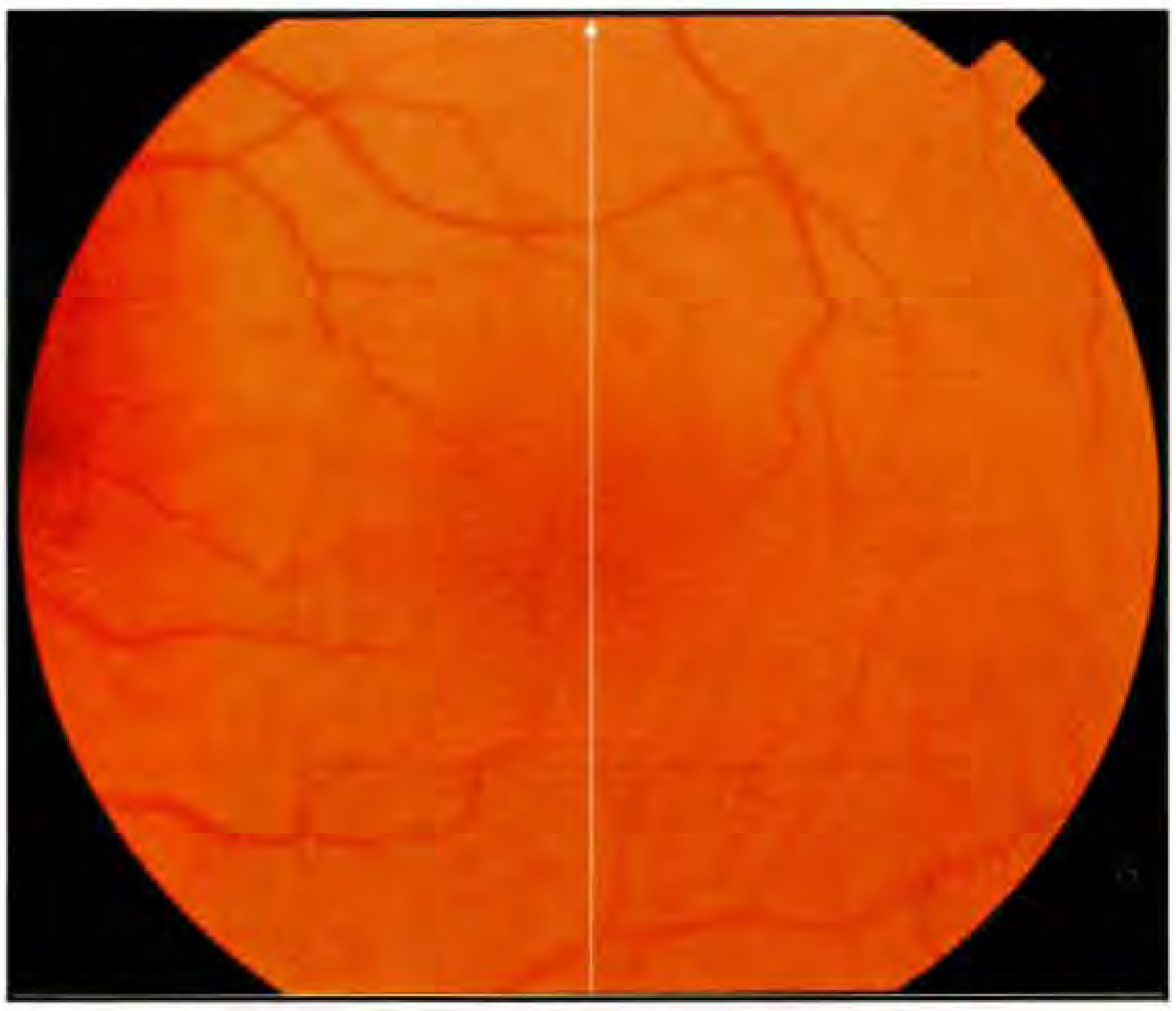

B

Case 3-3. Stage 2 Macular Hole and Macular Hole Development

Clinical Summary

A 59-year-old woman was referred for declining vision in her right eye. Her visual acuity was 20/200 in this eye and dilated fundus examination (A) revealed a Stage 3 or Stage 4 macular hole with a cuff of retinal thickening. In the fellow eye (B), a subtle increase in foveal redness and a reduced foveal reflex was observed. The visual acuity was 20/20.

Optical Coherence Tomography

A horizontal OCT section (C; white line on A) through the hole in the right eye showed a full-thickness loss of retinal tissue with two non-reflective spaces within the neurosensory retina corresponding to cysts. The posterior hyaloid appeared as a faint, minimally reflective membrane approximately 400 µm anterior to the retina. The reflection from the posterior vitreous was patchy in the foveal region, but the membrane seemed to arise from the proximity of the hole and increase in separation from the retina distally. A sequence of vertical OCT tomograms (D; black lines on A) demonstrated a partial break in the outer retinal layers and an operculum attached to the edge of the hole, suggesting a Stage 2 classification. The minimally reflective band corresponding to the posterior hyaloid appeared to be attached to the operculum in scans C and E of the collage.

A vertical OCT tomogram (E) acquired through the fellow eye exhibited a normal appearing fovea with a perifoveal detachment of the posterior vitreous.

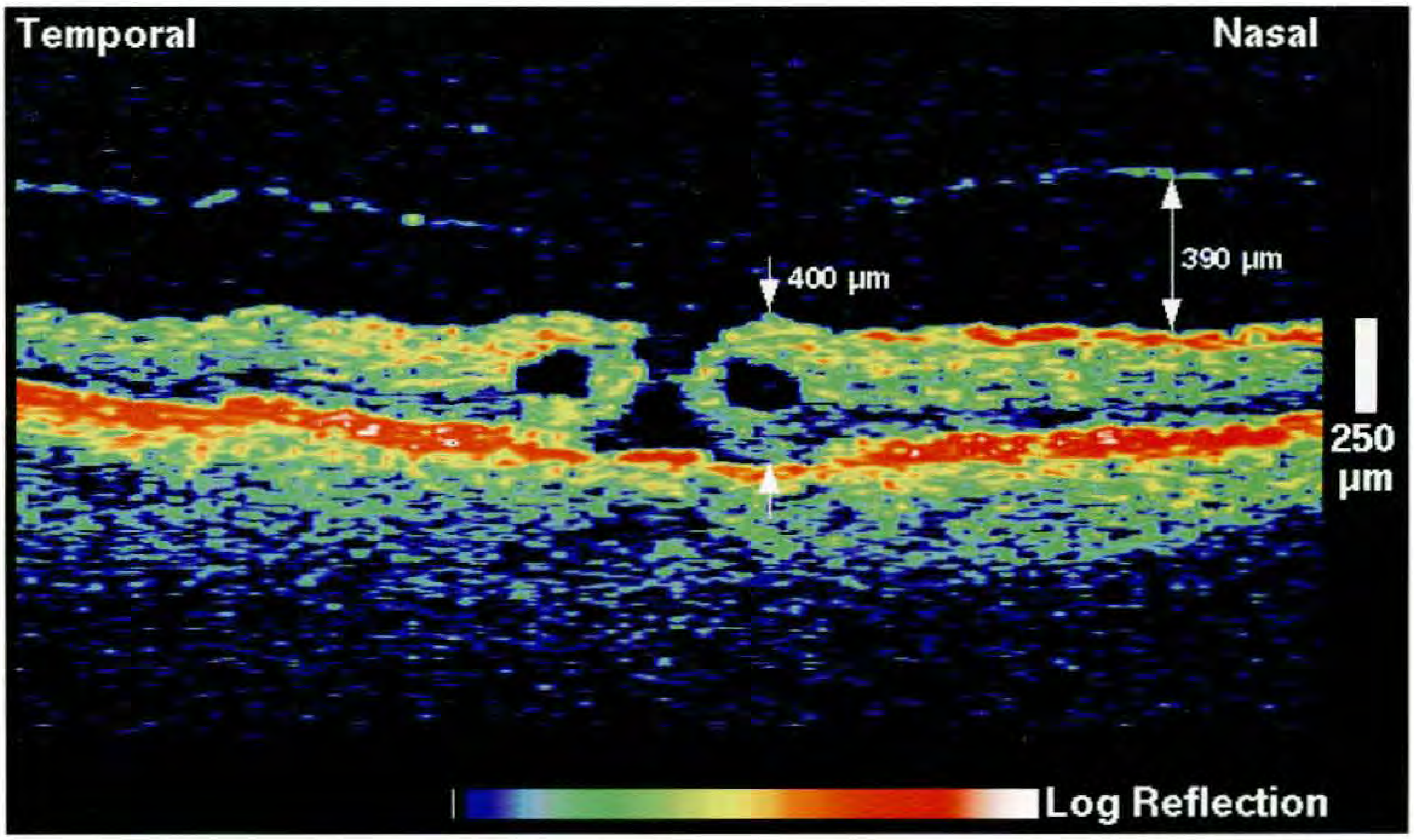

C

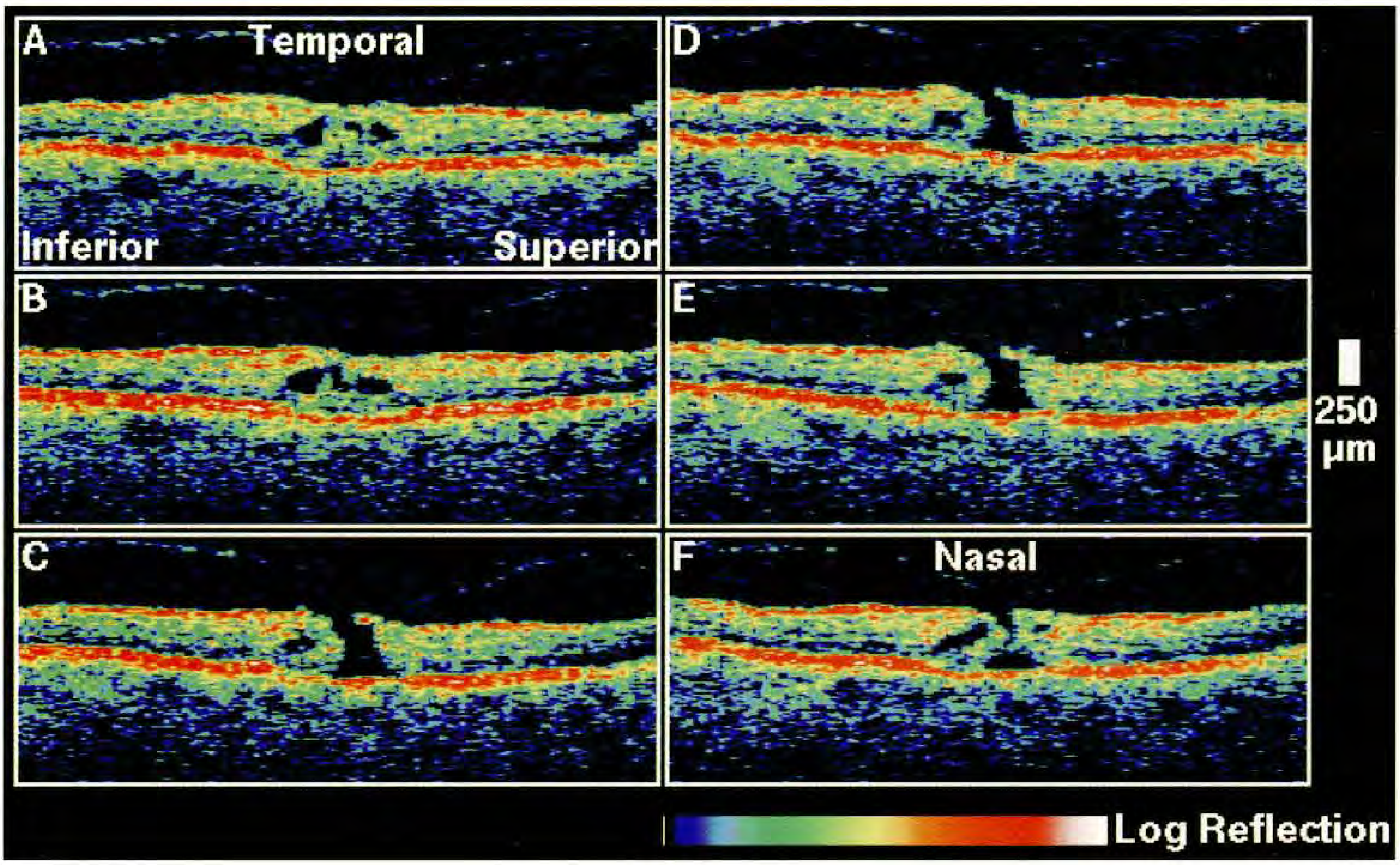
A
Temporal
Inferior
Superior
B
C
D
E
F
Nasal
250
µm
Log Reflection

D

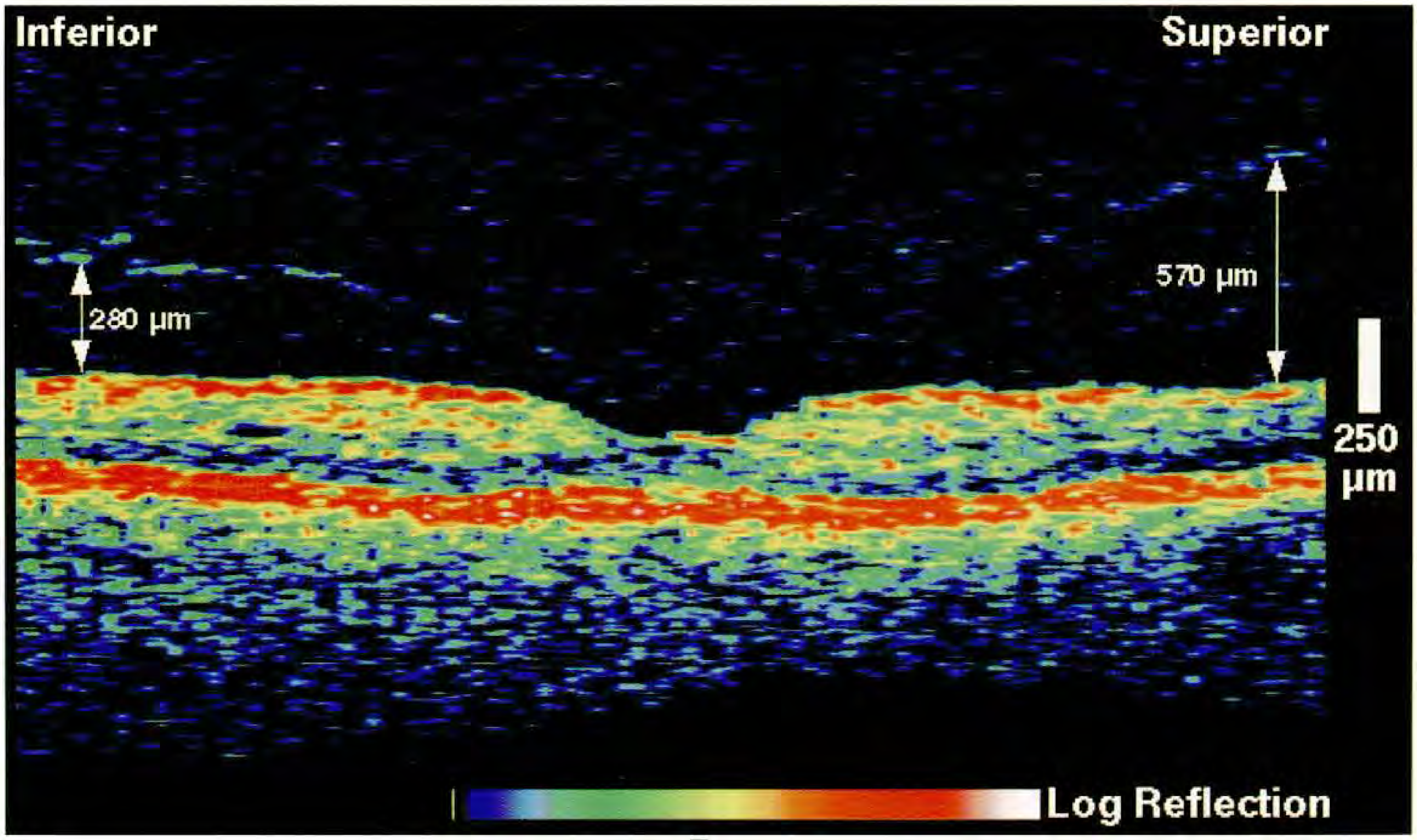
Inferior
Superior
280 µm
570 µm
250
µm
Log Reflection

E

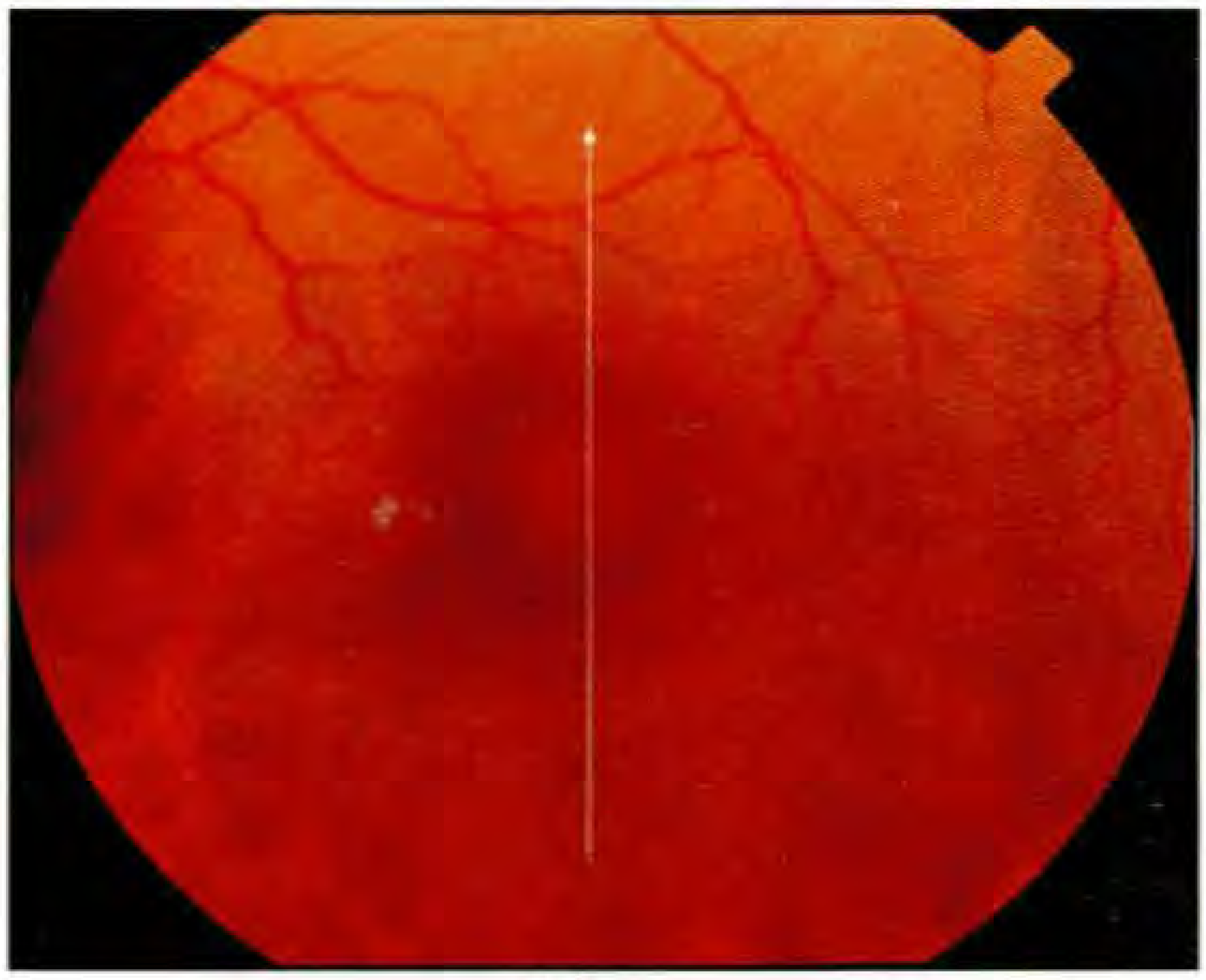

F

Case 3-3 continued

Follow-up Examination

Six months after initial presentation, the patient returned with a decrease in visual acuity in her left eye from 20/20 to 20/80. A small neurosensory foveal detachment was identified (F) consistent with a late Stage 1b hole.

Follow-up Optical Coherence Tomography

A vertical OCT image (G) showed flattening of the foveal contour and a non-reflective intraretinal space without a full-thickness retinal dehiscence. The posterior hyaloid was visible superior to the fovea as a lightly reflective membrane separated from the retina. The membrane appeared to exert traction on an attached operculum which was slightly elevated compared to the surrounding inner limiting membrane.

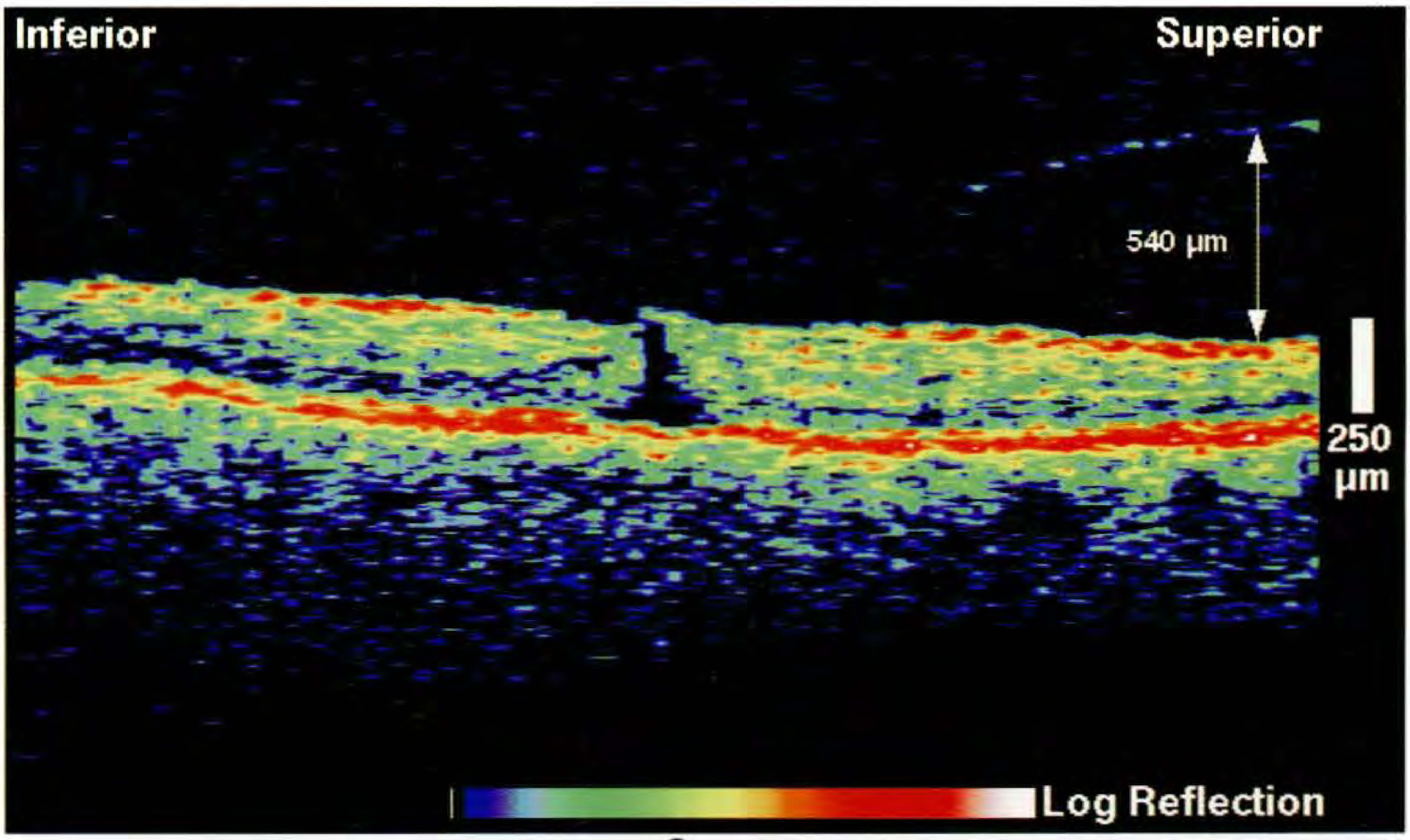

G

Case 3-3 continued

Follow-up Examination

One month later, the visual acuity in the patient's right eye remained at 20/80. Dilated fundus examination (H) revealed progression to an early Stage 2 hole.

Follow-up Optical Coherence Tomography

OCT (I) demonstrated the development of a full-thickness retinal dehiscence with a partially attached operculum consistent with a Stage 2 classification. Cystic changes and increased retinal swelling were noted surrounding the hole. The posterior hyaloid membrane was not visible in the image.

This sequence of OCT images (E,G,I) demonstrates the development of a full-thickness macular hole from an initial perifoveal vitreous detachment with foveal adhesion.

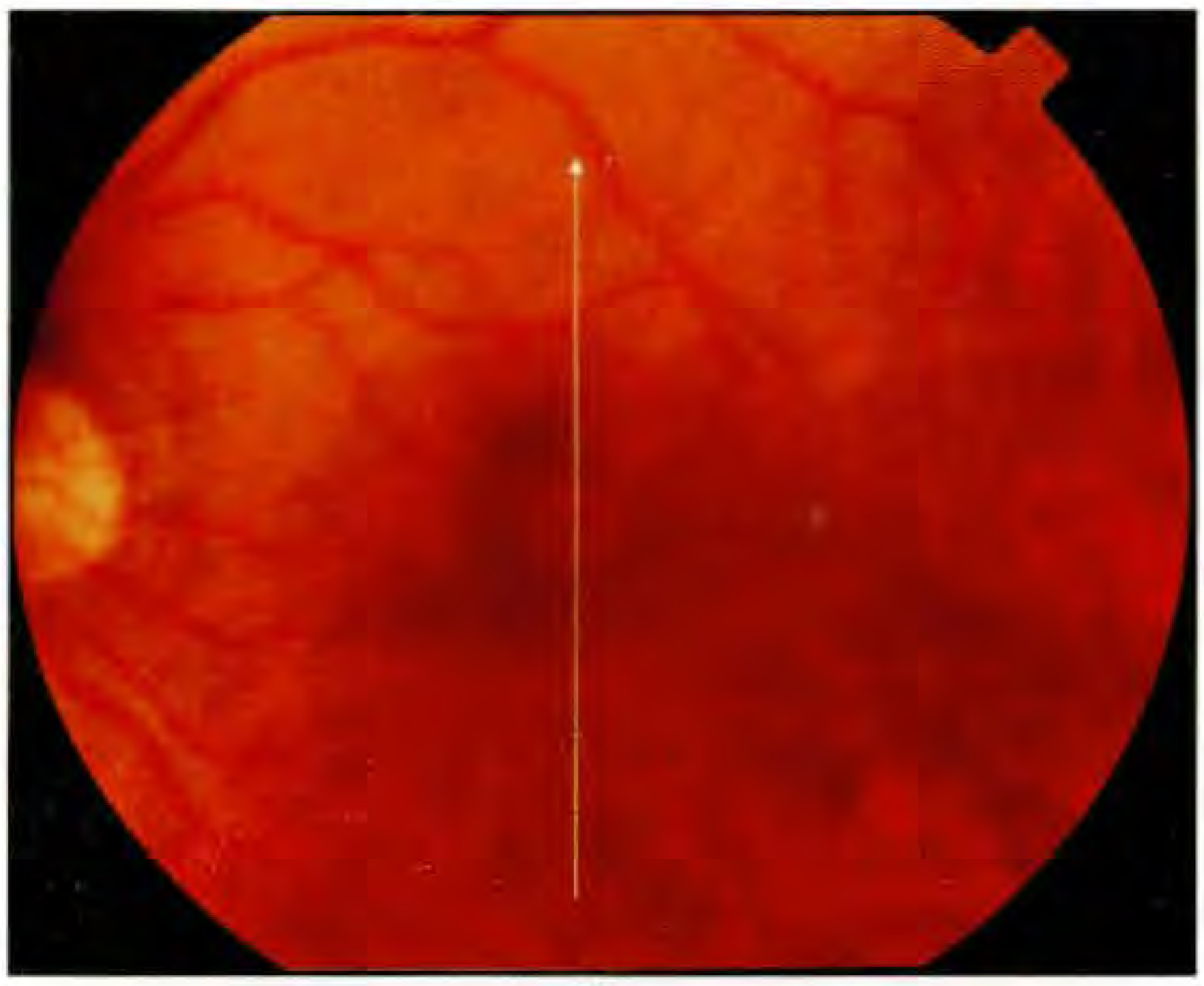

H

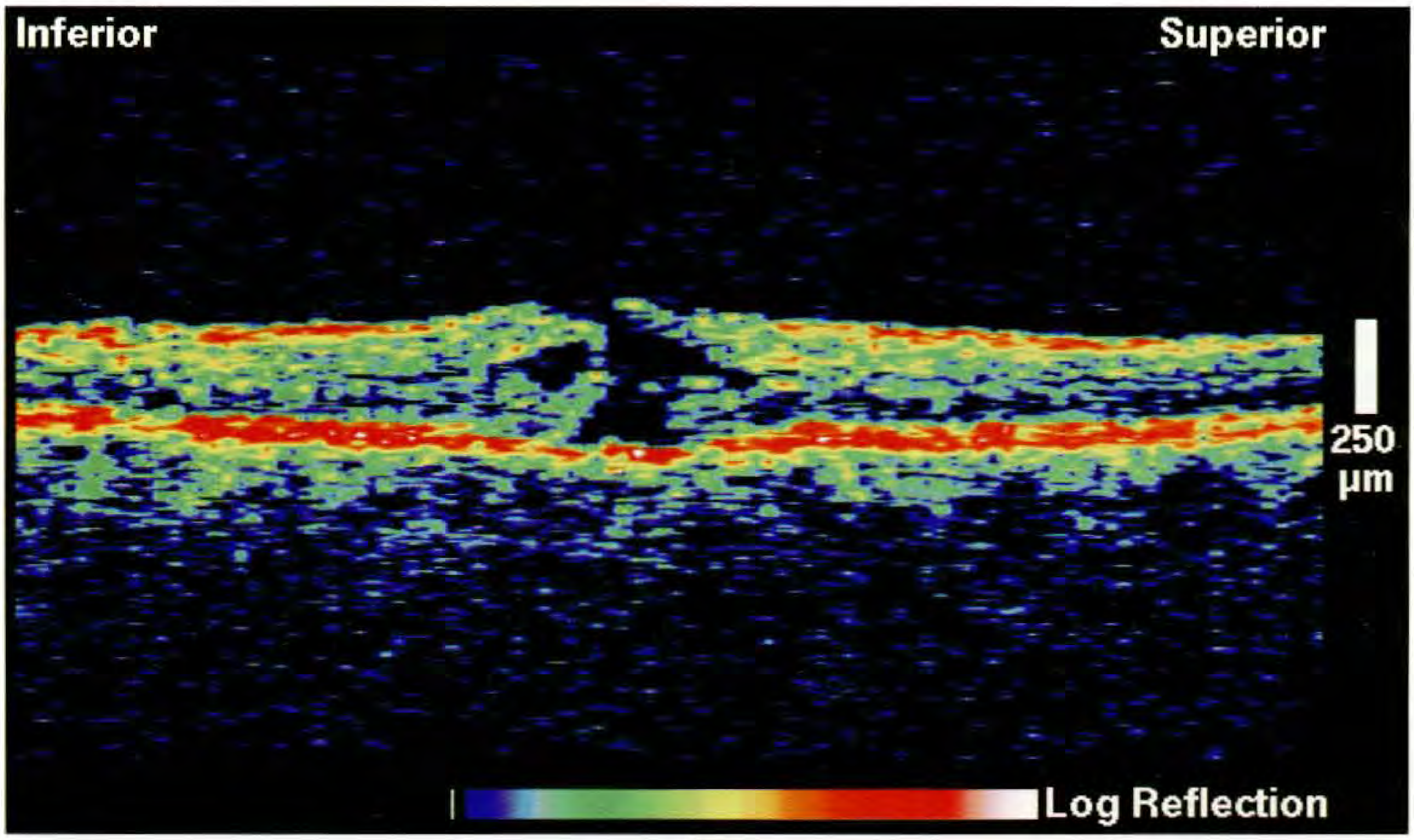

I

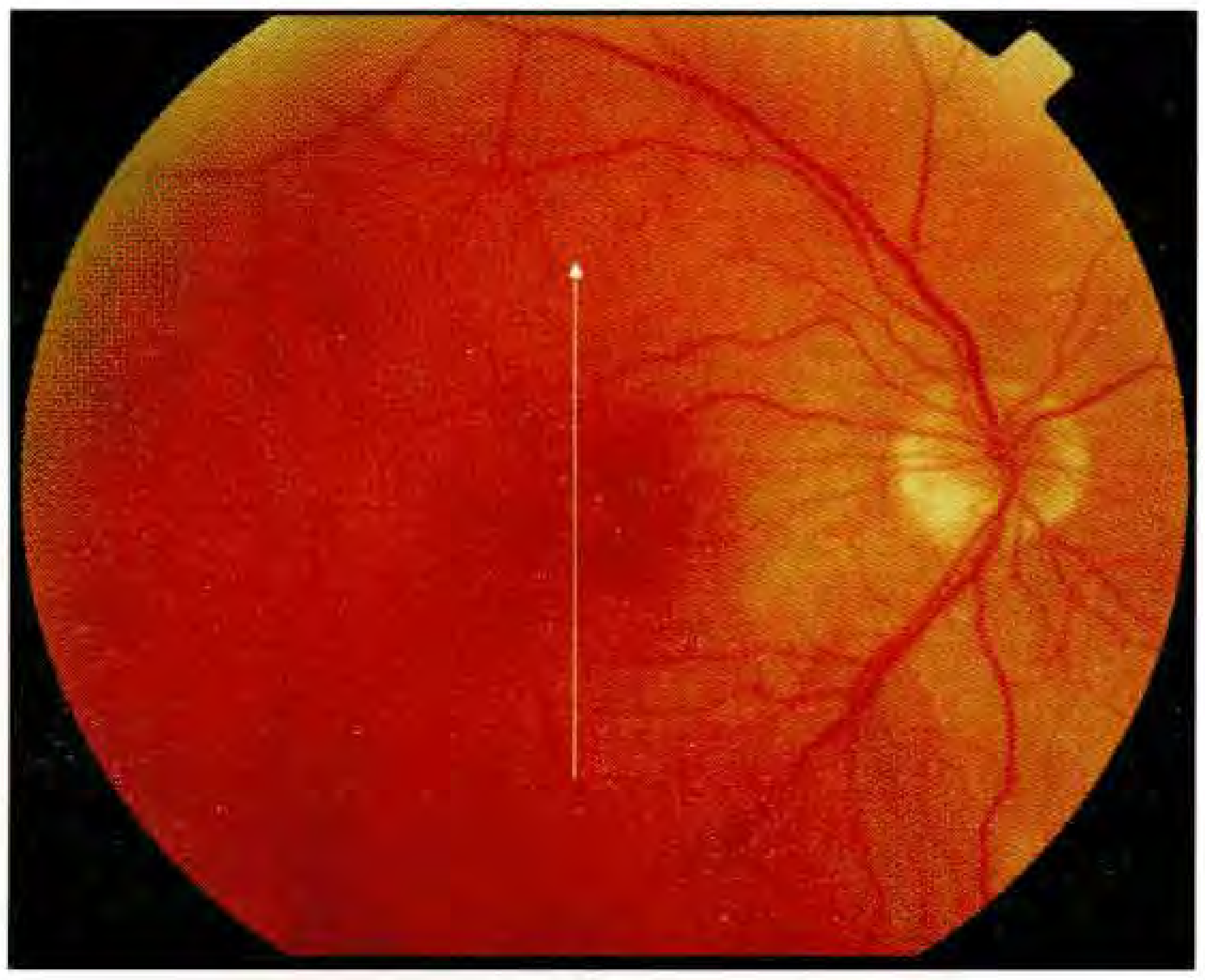

A

Case 3-4. Stage 3 Macular Hole

Clinical Summary

A 58-year-old man was referred for evaluation of a macular hole in his right eye. His visual acuity in this eye was 20/50. Slit-lamp biomicroscopy (A) revealed a small, full-thickness hole in the central macula. The Watzke's sign was positive.

Optical Coherence Tomography

A vertical OCT image (B) was obtained through the fovea which confirmed the full-thickness defect in the neurosensory retina. The diameter of the hole measured directly from the OCT tomogram was 200 µm. Small regions of reduced optical reflectivity were noted in the immediate surrounding retina and corresponded to cystic spaces. The fluid accumulation was associated with an increased retinal thickness, which was measured to be 470 at the inferior margin of the hole.

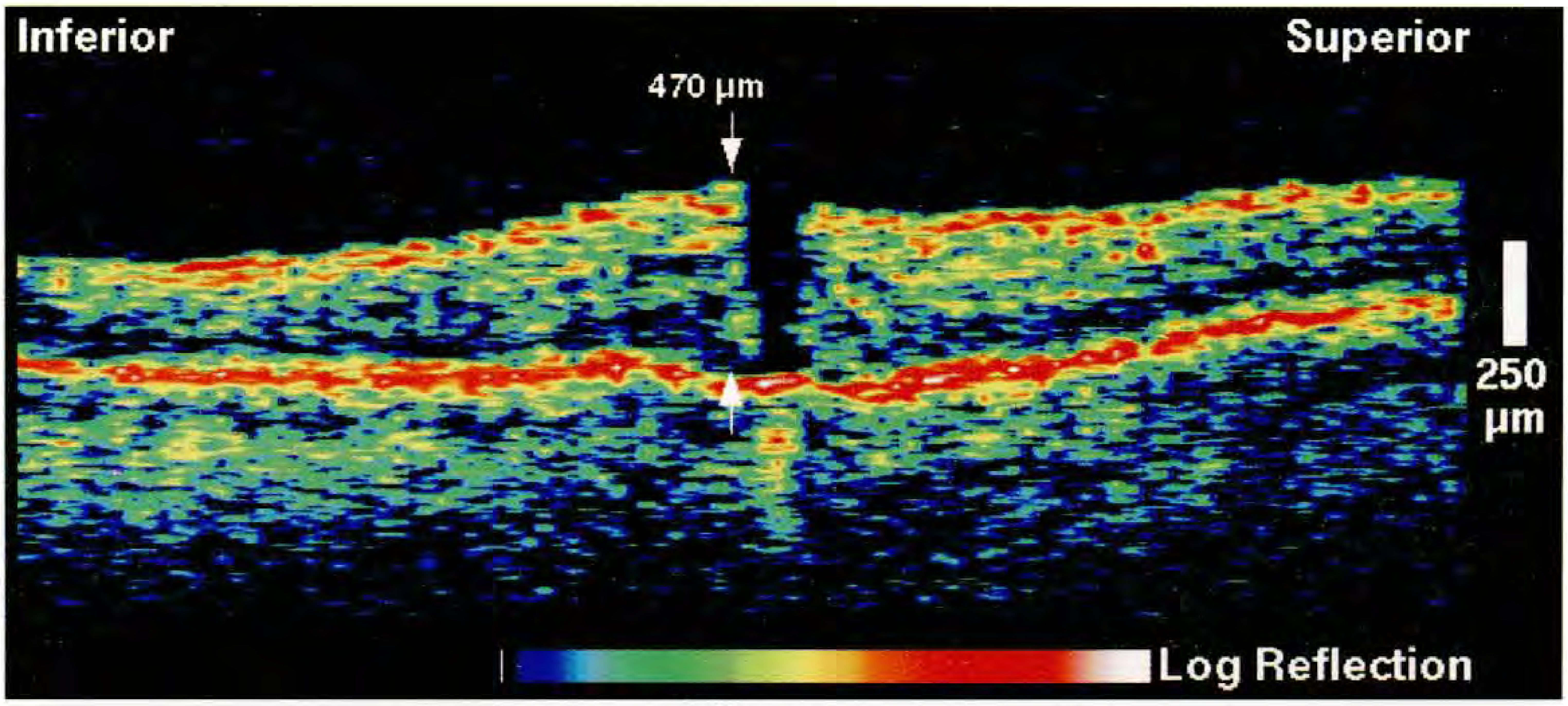

B

Case 3-5. Stage 3 Macular Hole with Operculum

Clinical Summary

A 66-year-old woman had a full-thickness macular hole in her left eye with a large surrounding cuff of subretinal fluid (A). Her visual acuity was 20/300 with a positive Watzke's sign.

Optical Coherence Tomography

A horizontal OCT section (B) taken through the macula illustrated a classic Stage 3 hole with a large operculum situated approximately 800 μm in front of the retina. The diameter of the hole was measured to be about 430 μm at its minimum point in the image. The surrounding neurosensory retina exhibited both a large halo of retinal detachment and decreased reflectivity in the outer retinal layers corresponding to cystic changes and fluid accumulation. A significant increase in the retinal thickness surrounding the hole was apparent, which reached a maximum of 480 μm in the tomogram.

A

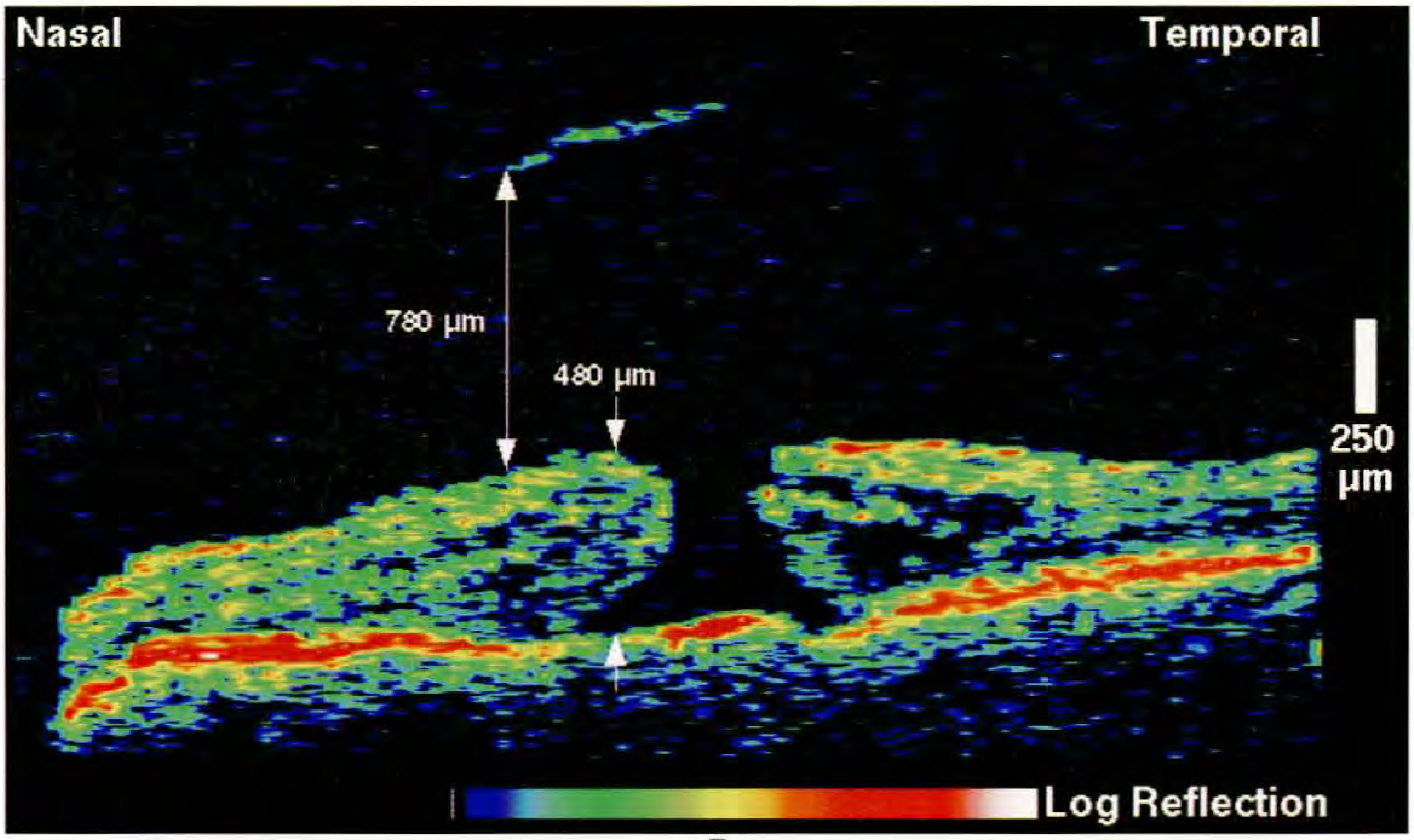

B

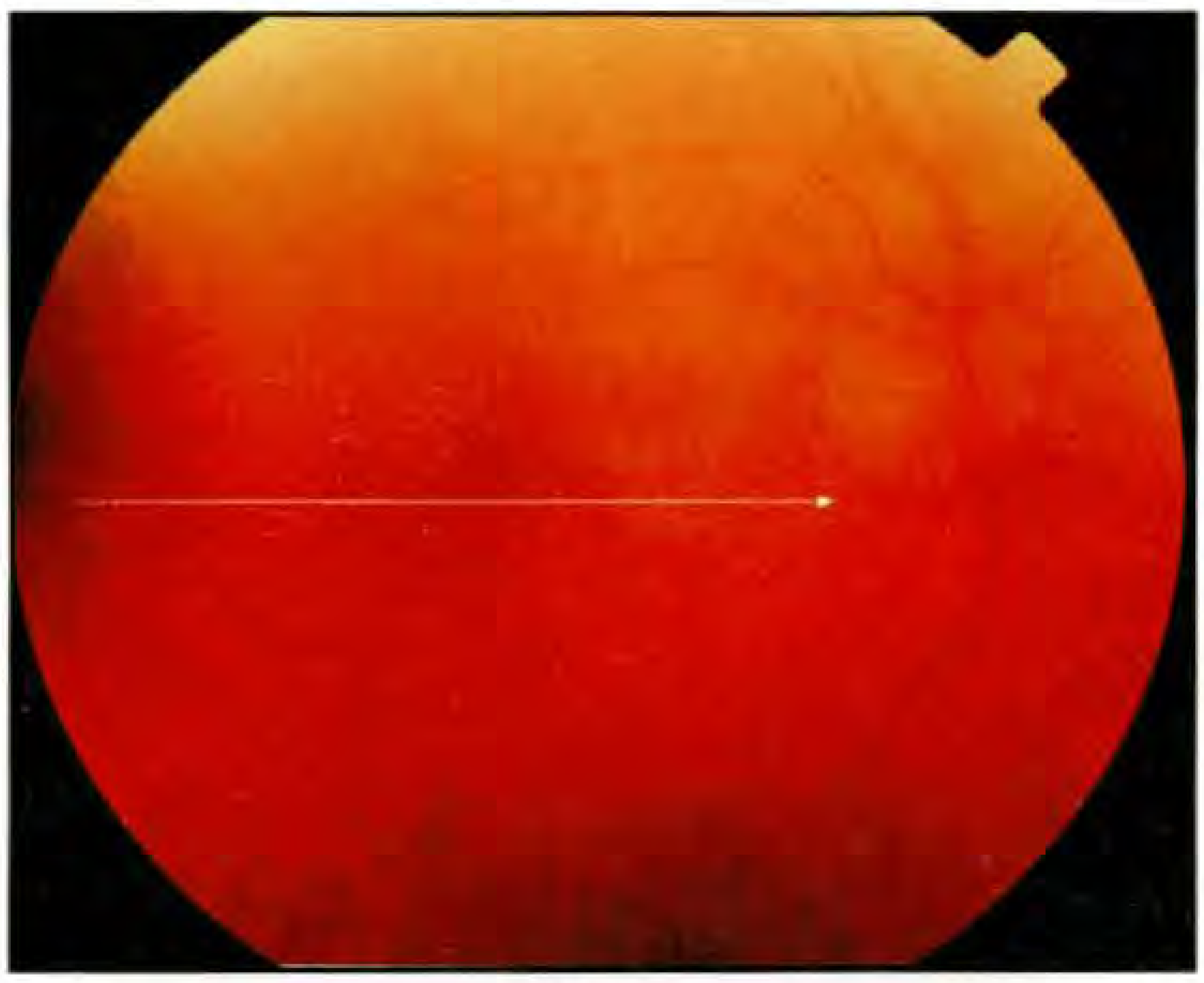

A

Case 3-6. Stage 3 Macular Hole with a Developing Stage 1 Hole in the Fellow Eye

Clinical Summary

An 81-year-old woman reported a one week history of vision loss in her right eye. On examination, her visual acuity was 20/100 in this eye, and a full-thickness macular hole was diagnosed after slit-lamp biomicroscopy (A). There was 2 to 3+ nuclear sclerosis of the crystalline lens bilaterally.

Optical Coherence Tomography

A horizontal OCT tomogram (B) confirmed the diagnosis of a Stage 3 macular hole in the right eye. The inner diameter of the hole was approximately 350 µm. Moderate retinal edema surrounded the hole and the retinal thickness reached a maximum of 380 µm at the hole margin. A small piece of tissue was identified about 400 µm anterior the retina consistent with an operculum.

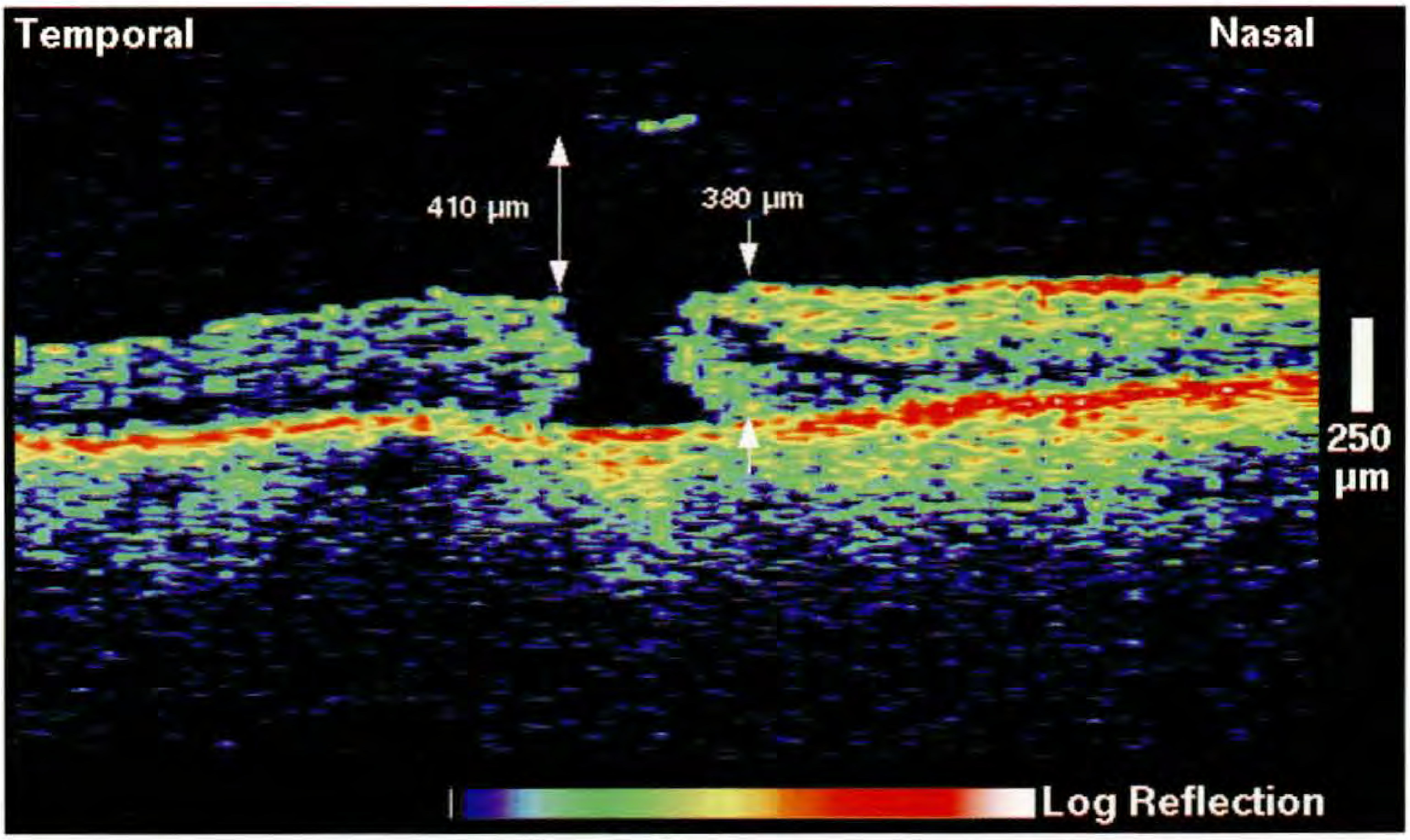

B

Case 3-6 continued

Clinical Summary

Clinical examination of the left eye (C) revealed only mild pigment mottling in the macula. The visual acuity in this eye was 20/30.

Optical Coherence Tomography

An OCT image (D) obtained through the left macula illustrated a loss of the normal foveal contour associated with vitreomacular traction and a perifoveal detachment of the posterior hyaloid membrane with foveal adhesion. This configuration suggested a developing Stage 1 macular hole and an increased risk of progression to a full-thickness macular hole in this eye.

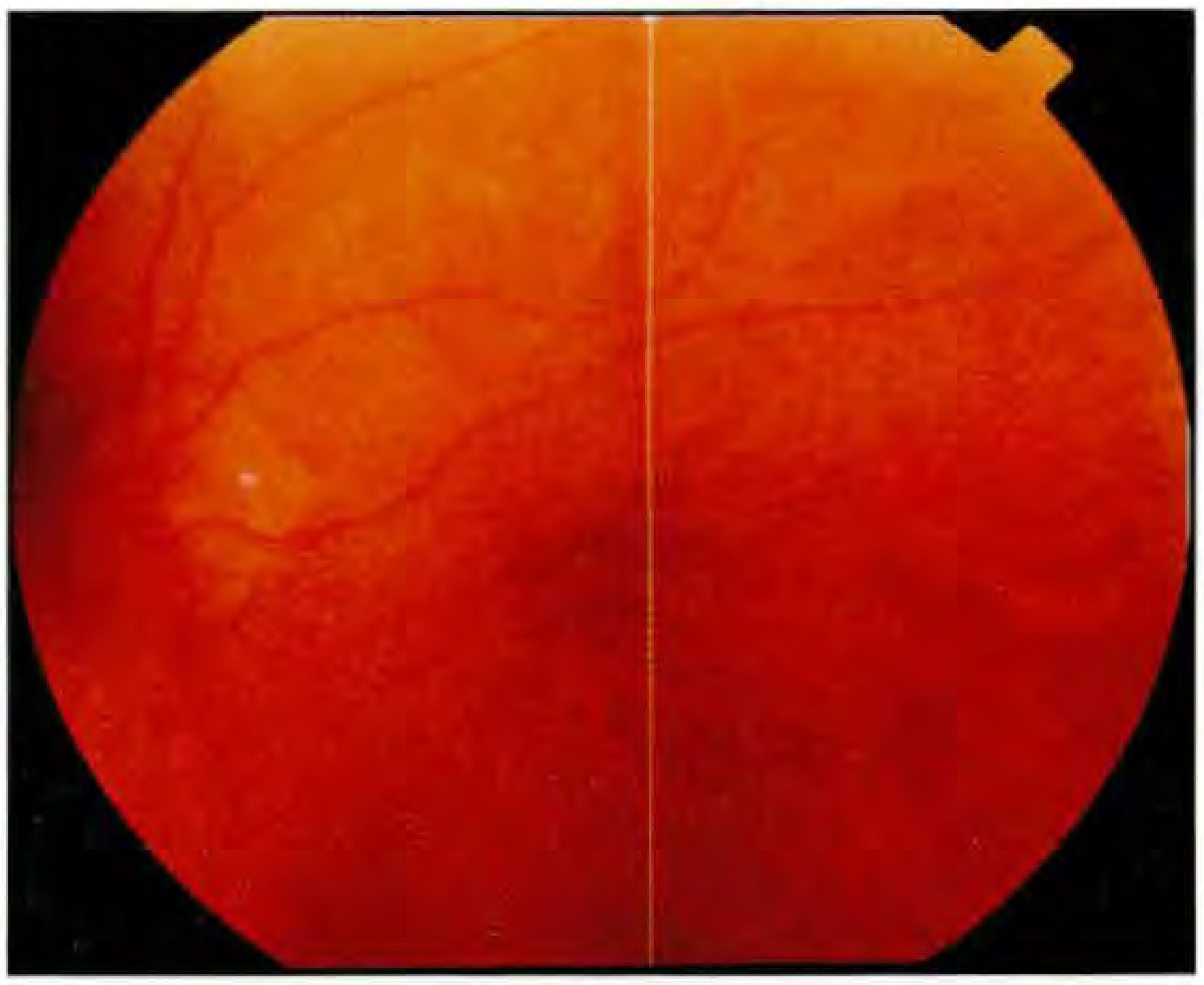

C

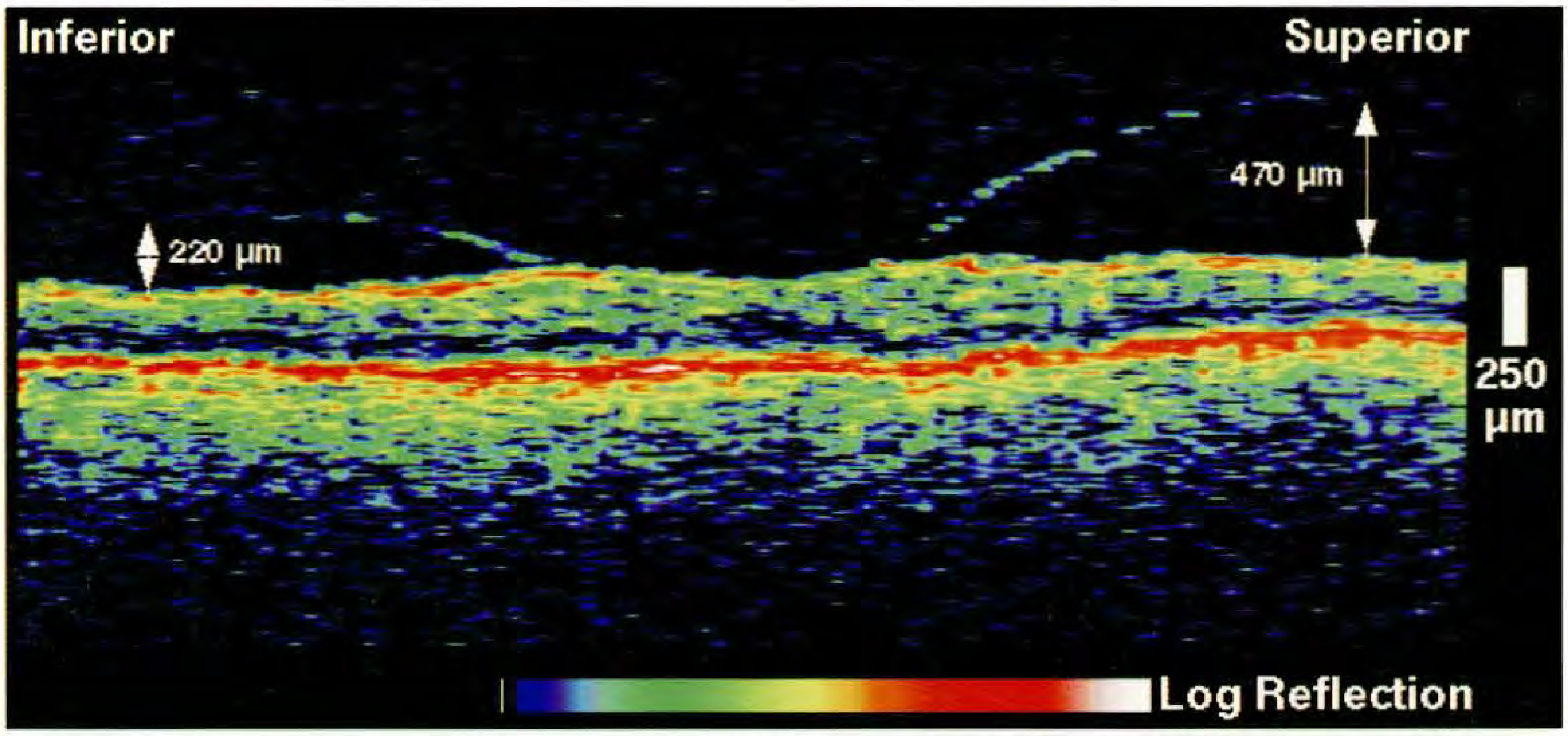

D

A

B

Case 3-7. Stage 3 Macular Hole with Vitreomacular Traction in the Fellow Eye

Clinical Summary

A 67-year-old woman was referred for worsening vision in her left eye. Her visual acuity in this eye was 20/80. Indirect ophthalmoscopy (A) revealed a small, full-thickness macular hole, surrounding cystic edema, and an attached vitreous. There was a positive Watzke's sign. Hyperfluorescence was observed in the fovea on fluorescein angiography (B) consistent with a window defect.

Optical Coherence Tomography

The OCT tomogram (C) displayed a Stage 3 full-thickness hole with a surrounding cuff of retinal edema, and a minimum inner diameter of approximately 300 μm. The retinal thickness was increased to 420 μm at the edge of the hole. Decreased reflectivity was noted in the outer retinal layers surrounding the hole corresponding to cystic changes.

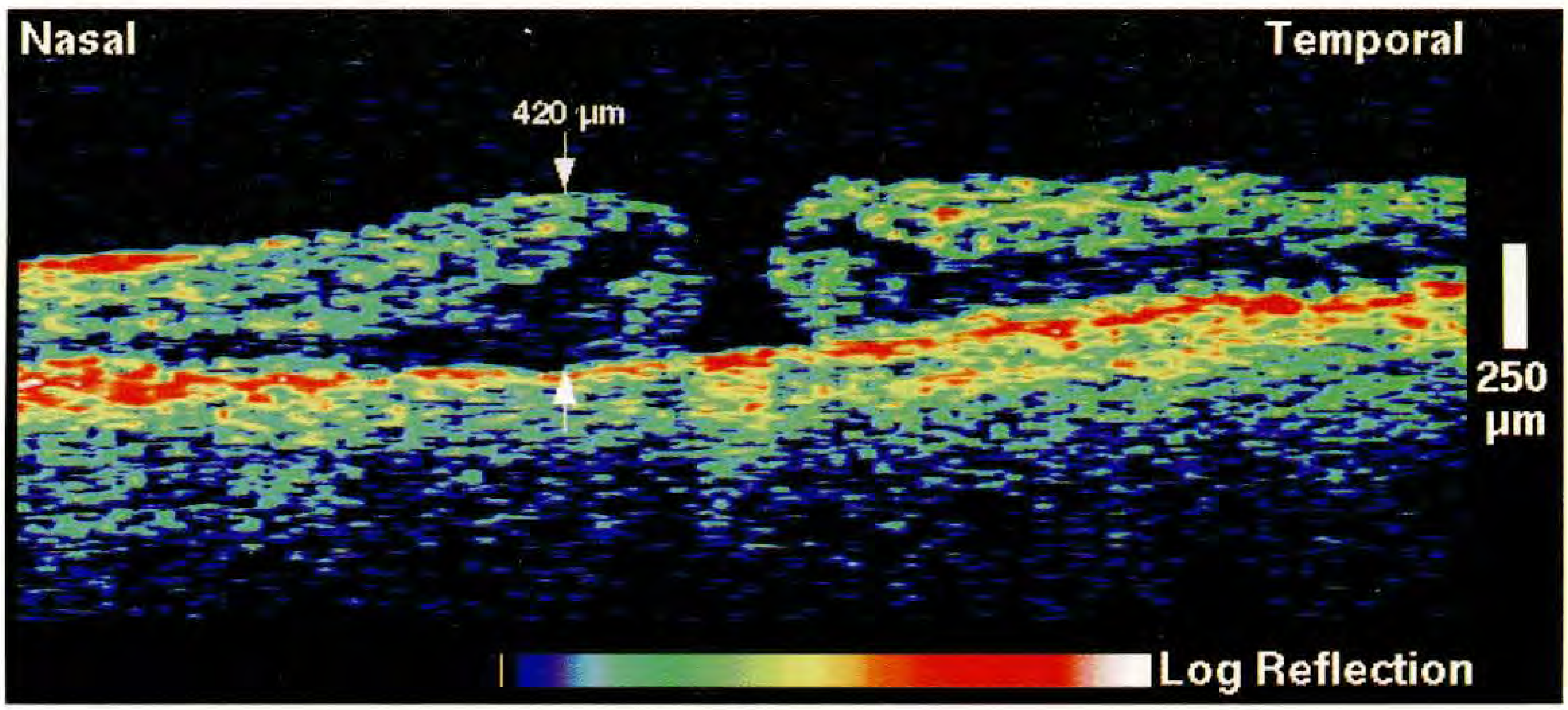

C

Case 3-7 continued

Clinical Summary

Dilated fundus examination (D) of the patient's right eye revealed mild mottling of the retinal pigment epithelium and an apparently attached vitreous. A subtle cyst or pseudohole was observed in the fovea. The patient's visual acuity in this eye was 20/25. Fluorescein angiography (E) appeared normal.

Optical Coherence Tomography

OCT examination (F) demonstrated an elevation of the inner retina above an optically clear space consistent with a cyst directly in the fovea. The minimally reflective band corresponding to the posterior hyaloid appeared to be attached to the fovea, but separated from the more peripheral retina by approximately 300 μm. This finding was not visible ophthalmoscopically.

D

E

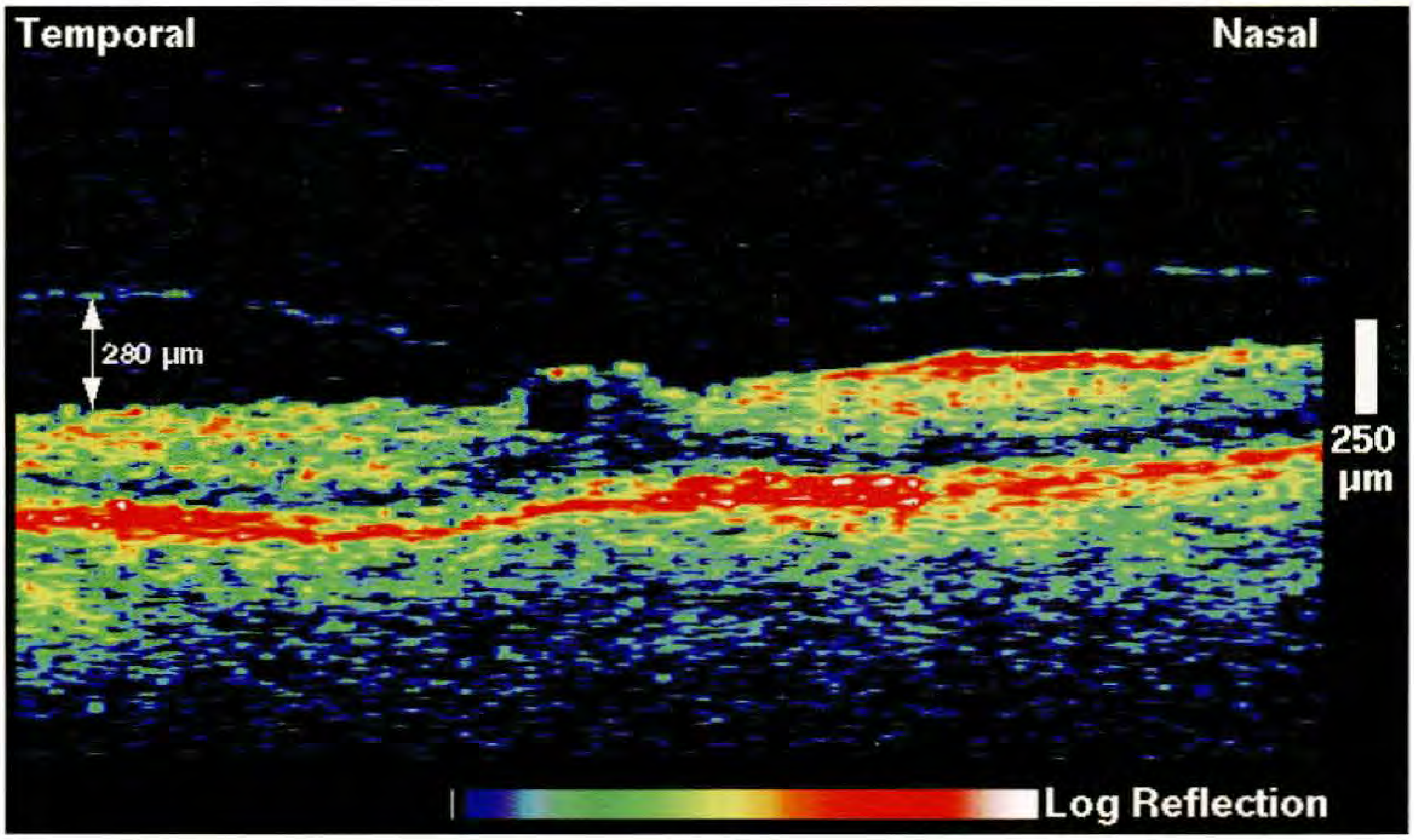

F

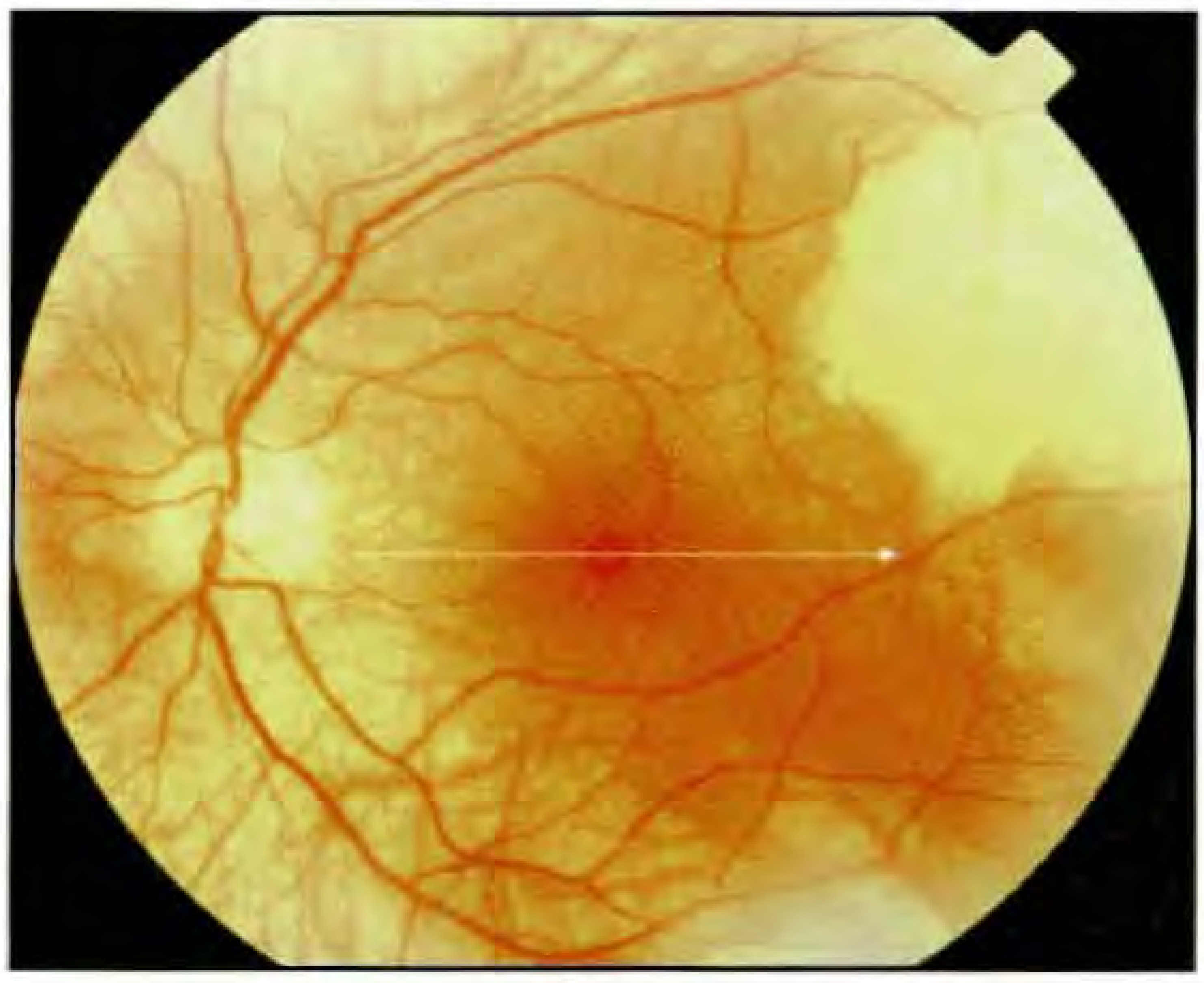

A

Case 3-8. Stage 3 Macular Hole with a Posterior Vitreous Detachment in the Fellow Eye

Clinical Summary

A 65-year-old woman presented with a Stage 3 macular hole in her left eye associated with a visual acuity of 20/200 (A). An area of retinal pigmental epithelial atrophy was noted superotemporal to the macula.

Optical Coherence Tomography

An OCT tomogram (B) through the macula delineated a full-thickness hole with a minimal surrounding retinal edema. The retinal thickness was 360 μm at the edge of the hole.

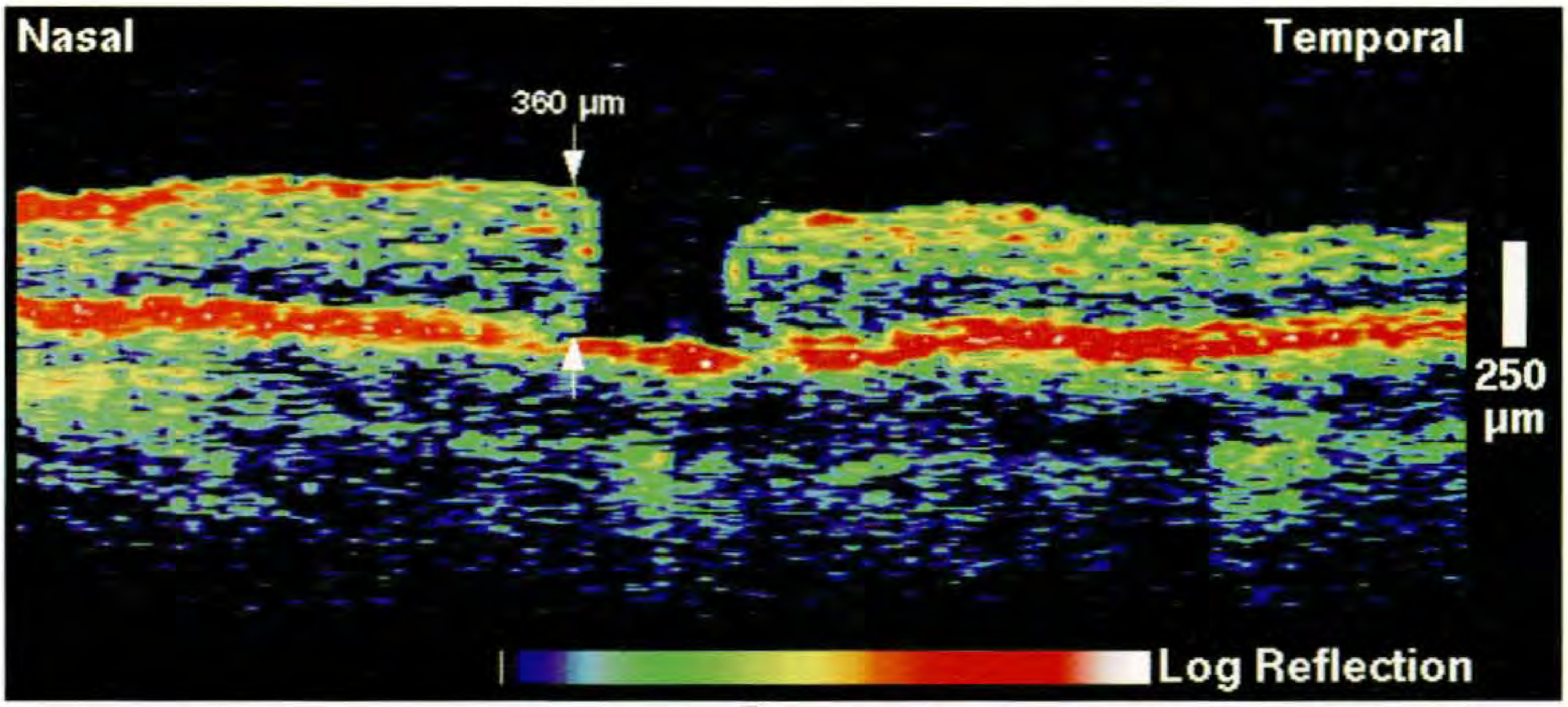

B

Case 3-8 continued

Clinical Summary

The patient's fellow eye was normal on slit-lamp examination (C) with a visual acuity of 20/20.

Optical Coherence Tomography

OCT (D) also showed a healthy fovea. The posterior vitreous face was observed to be detached from the retina, including the fovea, by approximately 500 µm indicating a negligible risk of macular development in this eye.

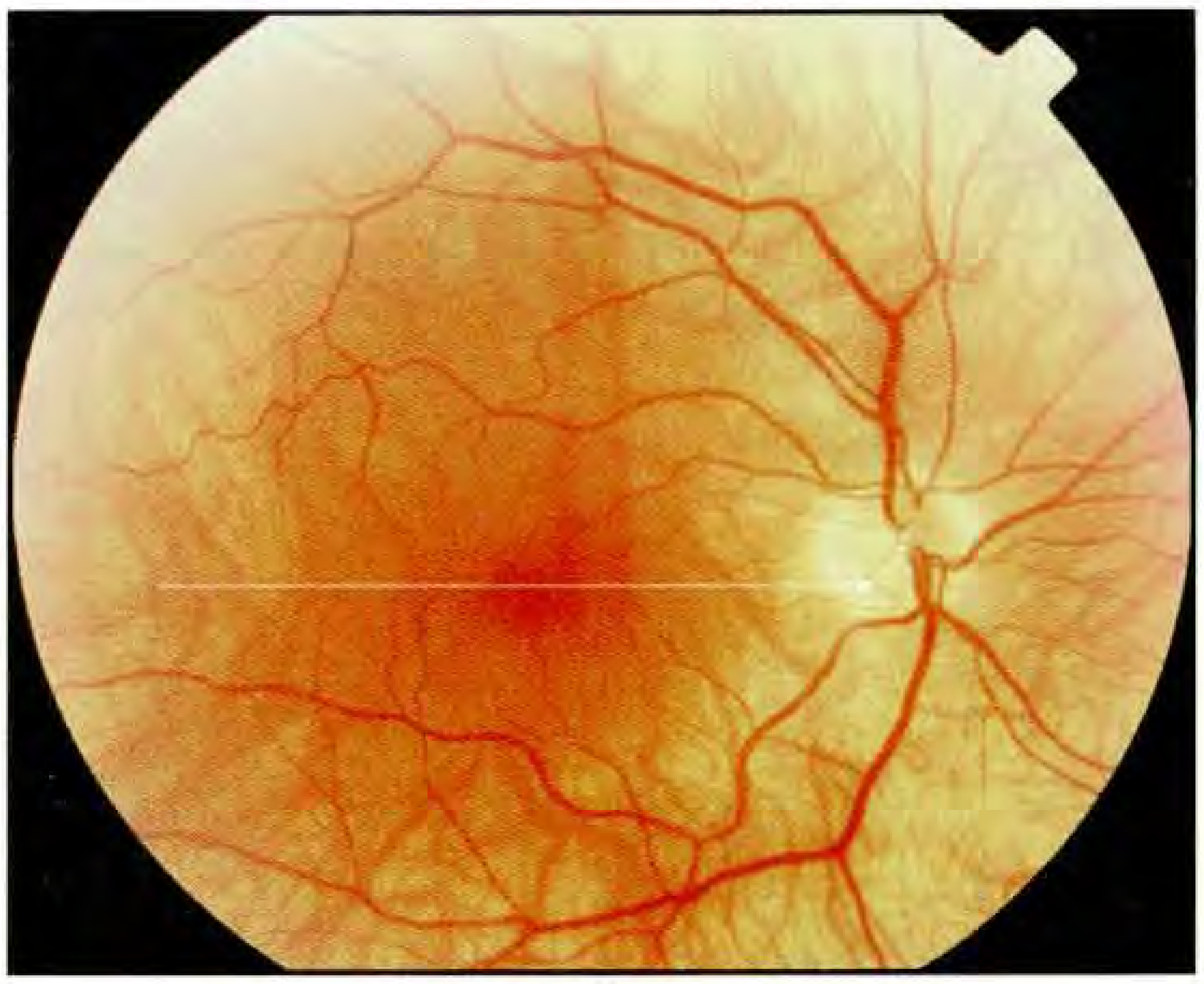

C

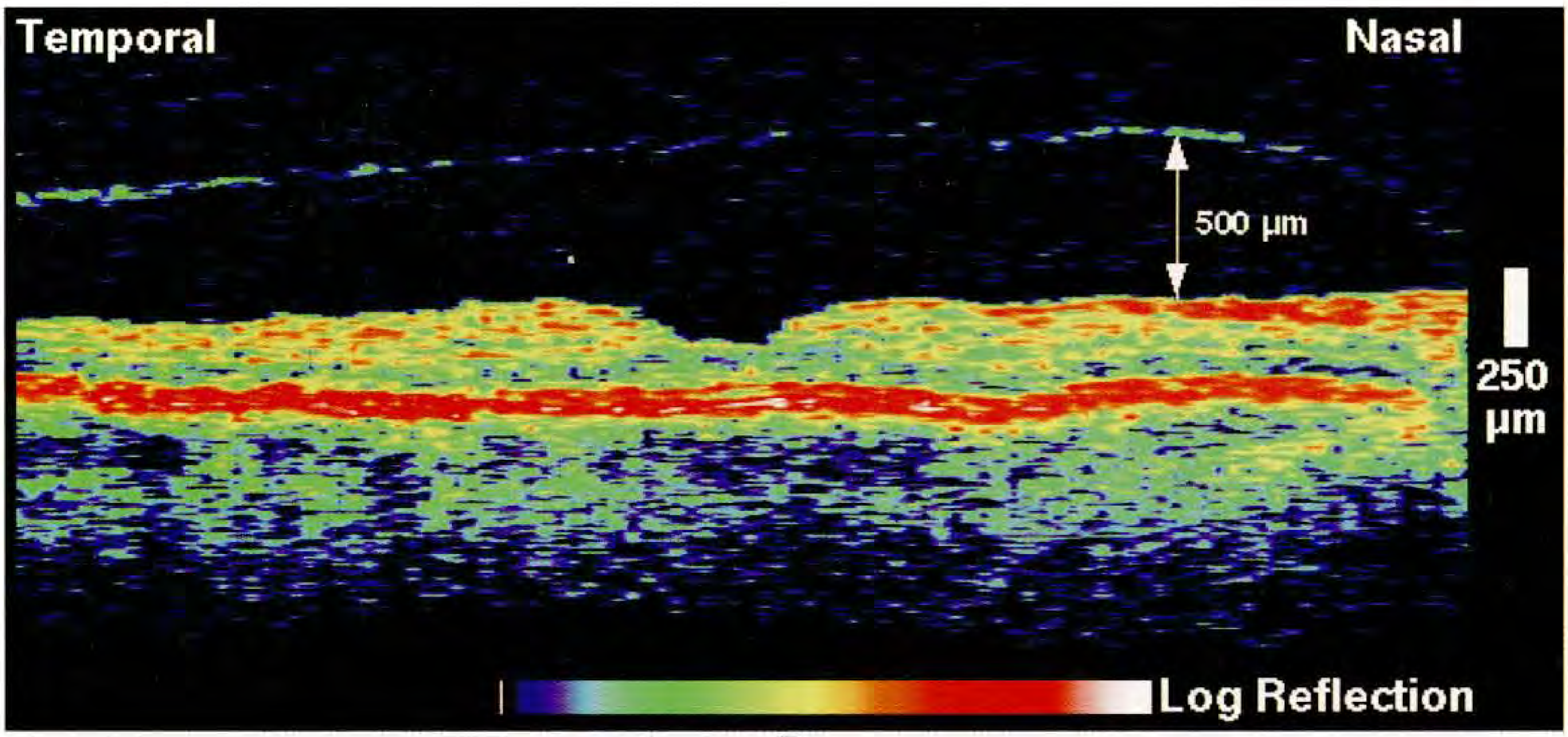

D

A

B

Case 3-9. Stage 3 Macular Hole with a Posterior Vitreous Detachment in the Fellow Eye

Clinical Summary

A 68-year-old man had a Stage 3 full-thickness macular hole in his left eye with a surrounding halo of macular edema (A). Hyperfluorescence in the fovea was observed on fluorescein angiography (B) consistent with a central window defect.

Optical Coherence Tomography

A horizontal OCT section (C) revealed a full-thickness loss of retinal tissue in the fovea with an inner diameter of approximately 275 µm . A small piece of tissue consistent with an operculum appeared about 500 µm anterior to the retina. An operculum was not visible biomicroscopically. Large cystic spaces and fluid accumulation in the outer retinal layers were observed in the retina just surrounding the hole.

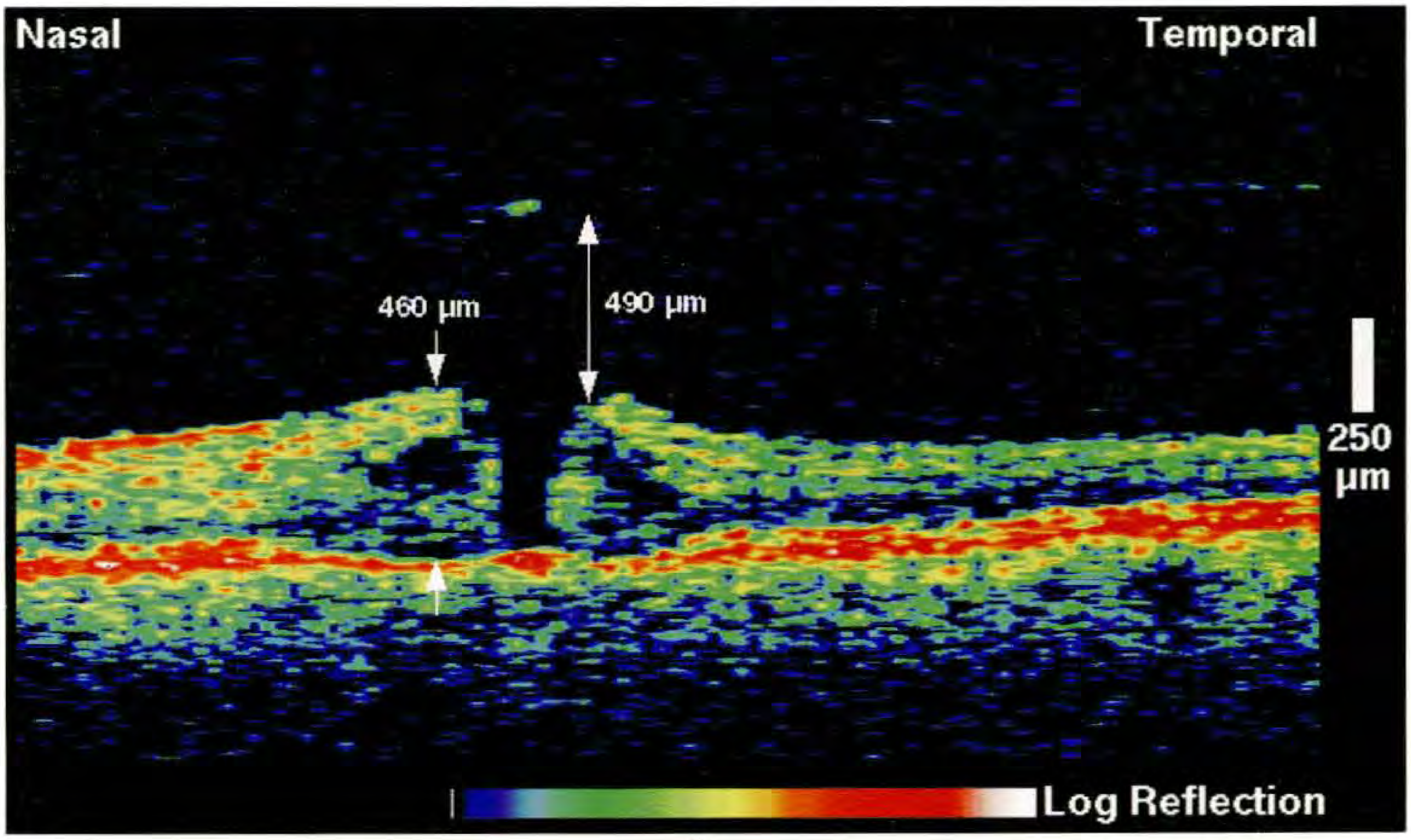

C

Case 3-9 continued

Clinical Summary

Examination of the patient's right eye showed no abnormalities on slit-lamp biomicroscopy (D).

Optical Coherence Tomography

An OCT tomogram (E) obtained through the macula illustrated a normal fovea with a small (approximately 150 µm) detachment of the posterior vitreous. The reflection from the posterior hyaloid was faint just above the fovea, but suggested a complete vitreous detachment and a reduced or negligible risk of hole development in this fellow eye.

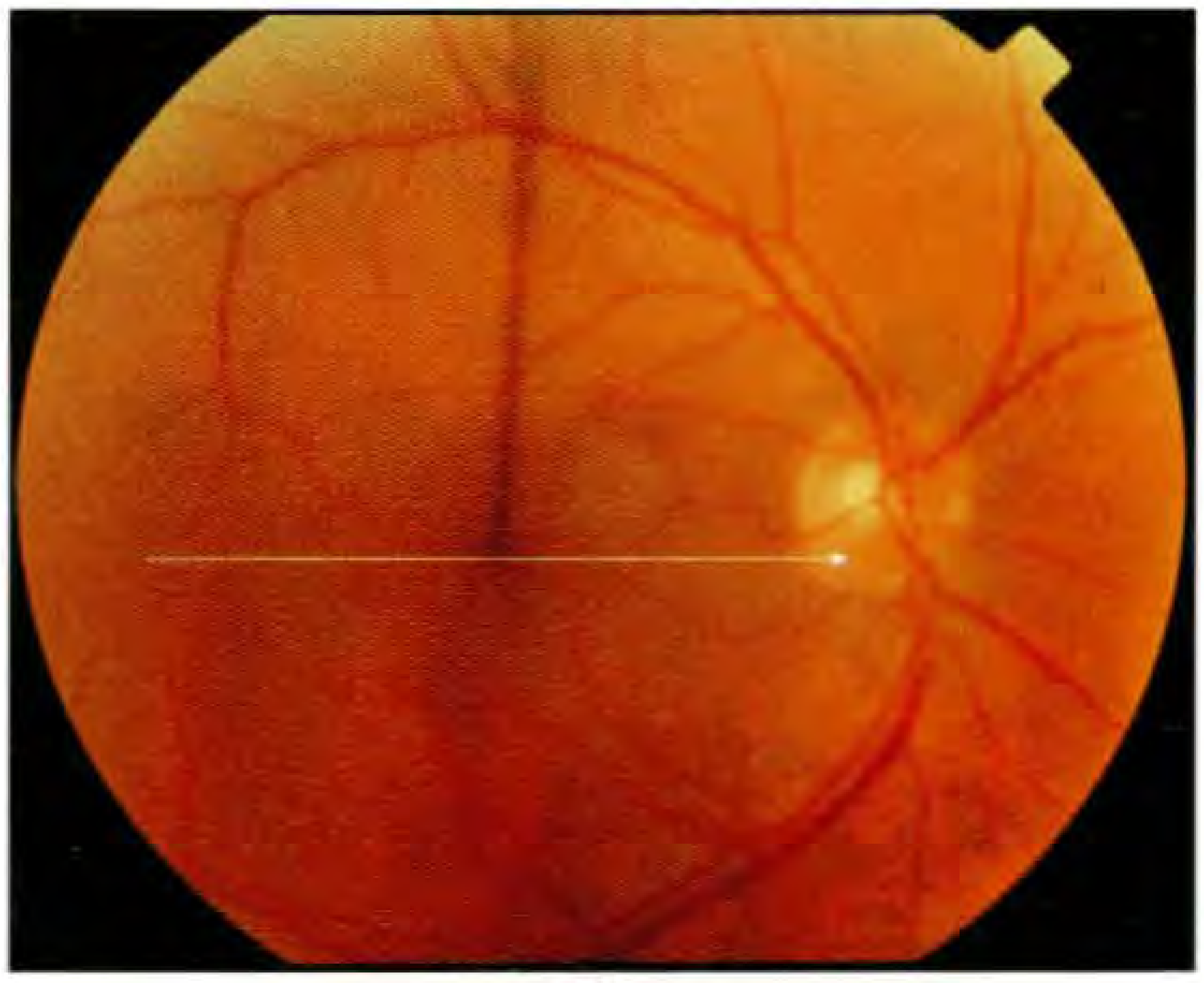

D

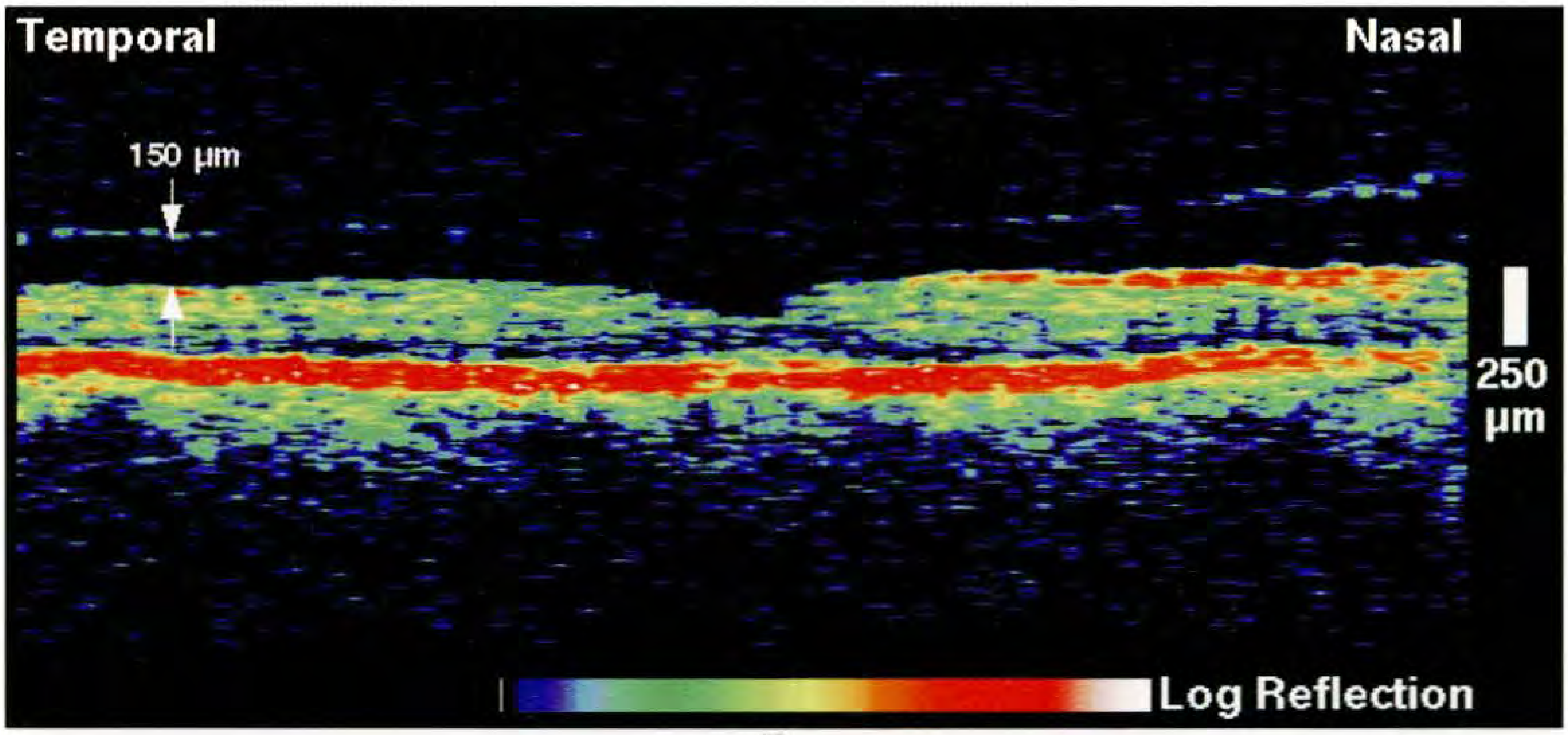

E

A

Case 3-10. Stage 3 Macular Hole with a Pseudo-operculum in the Fellow Eye

Clinical Summary

A 72-year-old woman was examined seven months after undergoing pars plana vitrectomy and membrane peeling for a Stage 3 macular hole. Slit-lamp biomicroscopy (A) revealed that the hole was still patent. Her visual acuity in this eye was 20/400.

Optical Coherence Tomography

A vertical OCT section (B) showed a narrow (approximately 150 µm diameter at its minimum in the image) full-thickness hole with a large surrounding region of retinal edema and detachment. The retinal thickness reached a maximum of 420 µm in the image.

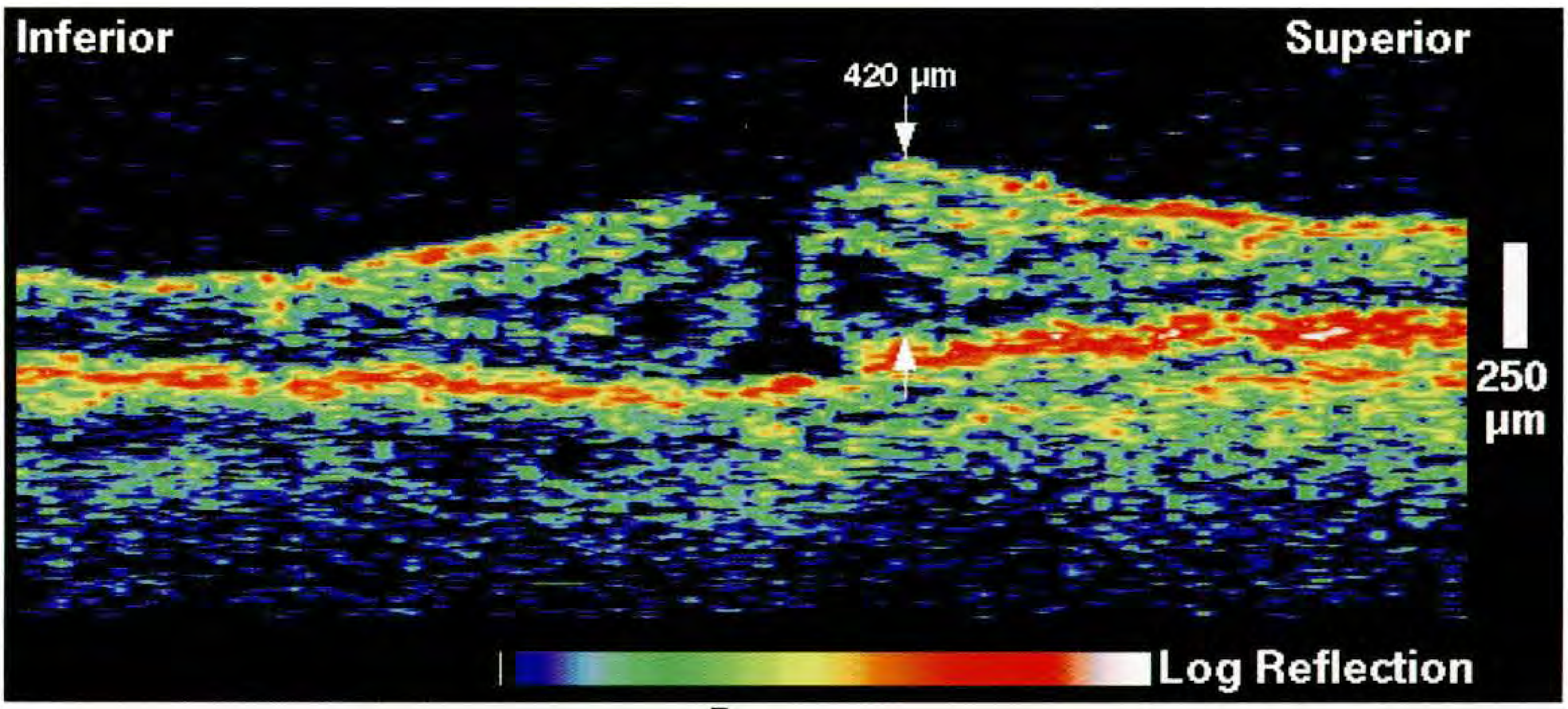

B

Case 3-10 continued

Clinical Summary

Examination of the patient's right eye (C) revealed a pseudo-operculum in front of the fovea. The visual acuity in this eye was 20/25.

Optical Coherence Tomography

An OCT image (D) confirmed the presence of a small piece of tissue situated approximately 720 μm in front of a normal appearing fovea. The posterior hyaloid was barely visible nasally in the image as a thin, minimally reflective band contiguous with the pseudo-operculum and separated from the retina. The finding of a pseudo-operculum suggested an arrested stage of hole development in this fellow eye due to spontaneous vitreofoveal separation, and a minimal associated risk of a full-thickness hole developing in this eye.

C

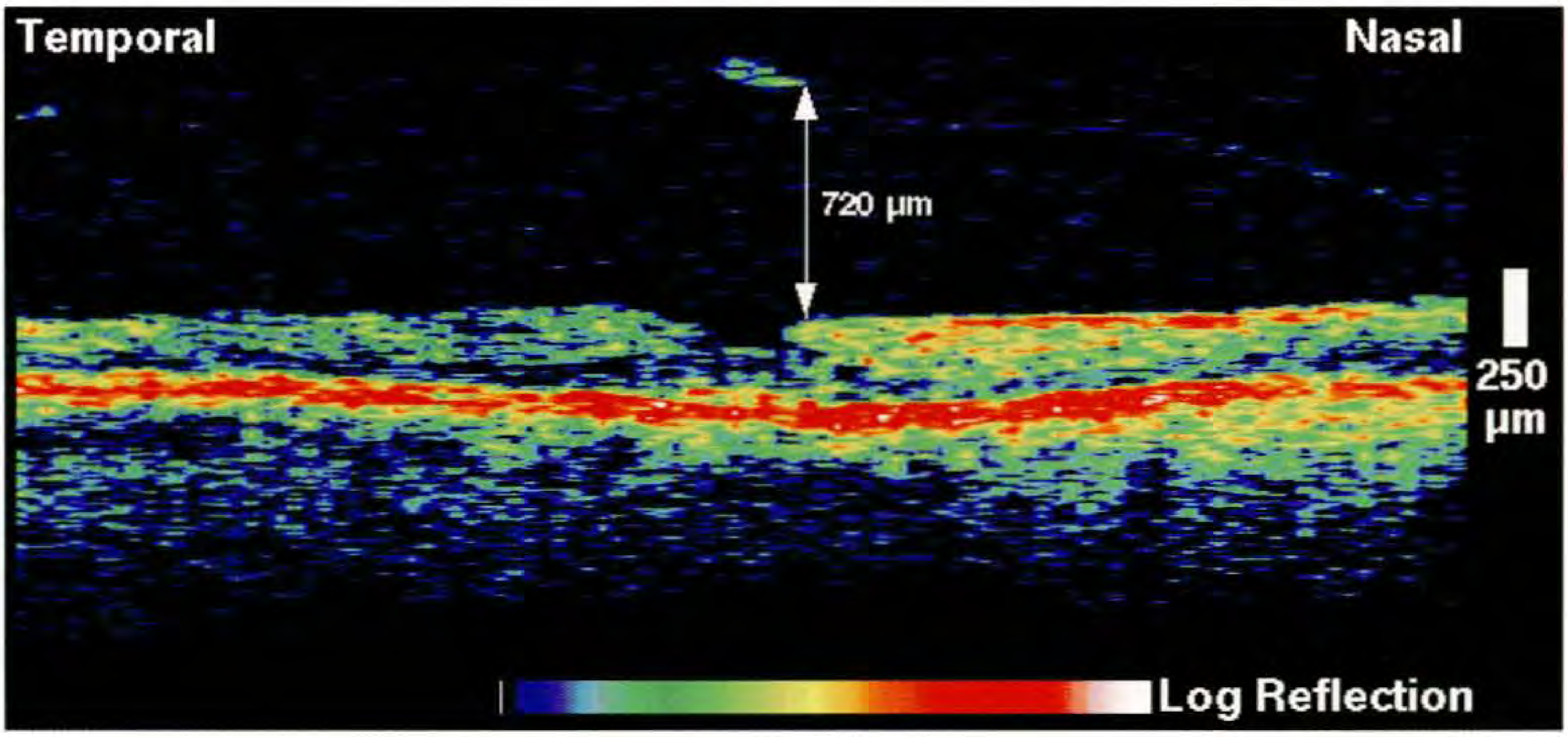

D

A

Case 3-11. Stage 3 Macular Hole with a Macular Pseudohole in the Fellow Eye

Clinical Summary

An 82-year-old woman had an epiretinal macular membrane in both eyes. In her right eye (A), the membrane was associated with a full-thickness macular hole and a visual acuity of 20/100.

Optical Coherence Tomography

OCT (B) demonstrated a Stage 3 hole with moderate surrounding retinal edema. The epiretinal membrane was visible as a thin reflective band just anterior to the inner limiting membrane

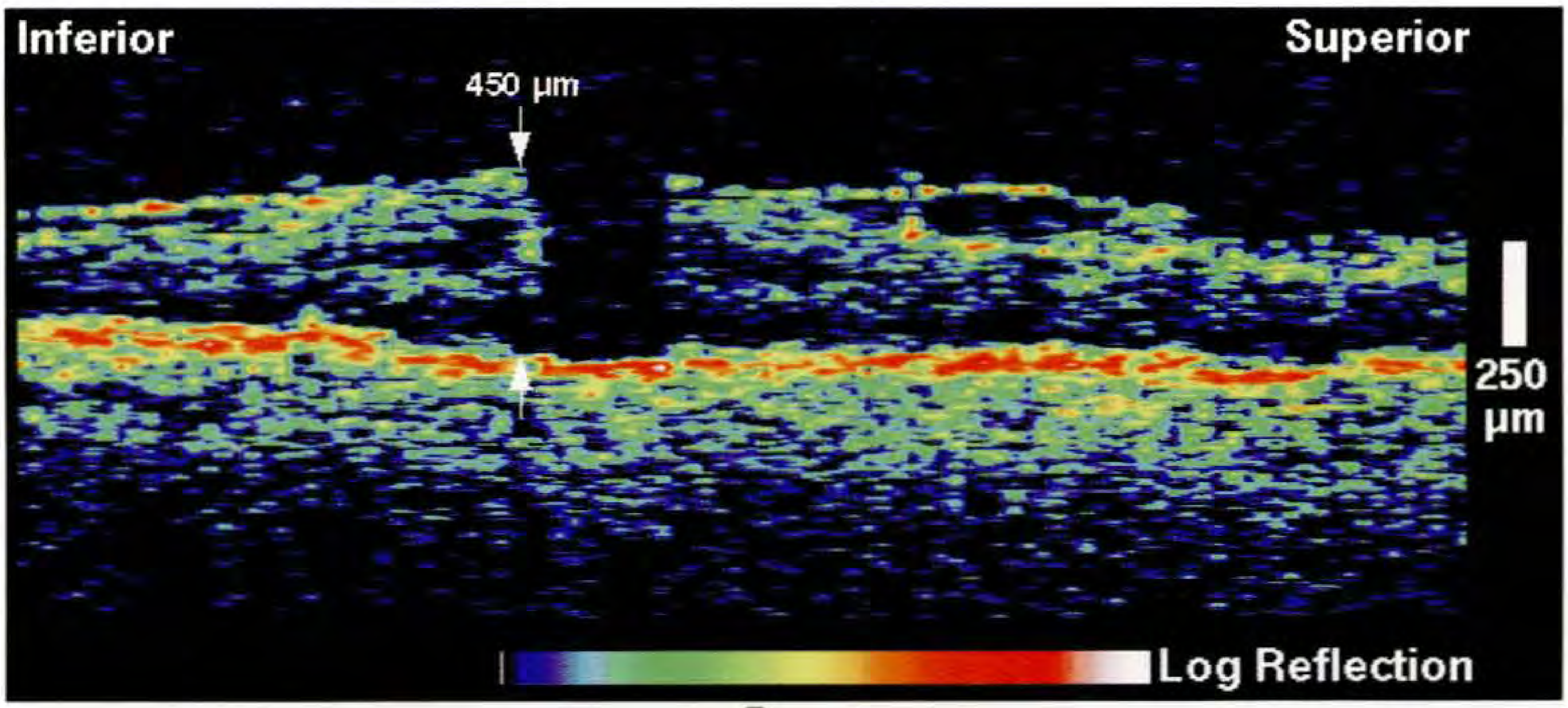

B

Case 3-11 continued

Clinical Summary

In the left eye (C), the epiretinal membrane was associated with a macular pseudohole. The visual acuity in this eye was 20/30.

Optical Coherence Tomography

A horizontal OCT section (D) revealed a steepened foveal pit contour simulating a macular hole. The presence of retinal tissue in the outer foveal layers, however, confirmed the diagnosis of a macular pseudohole. The epiretinal membrane was tightly adherent to the inner retinal surface and only visible where there was a difference in optical reflectivity between the membrane and neurosensory retina (arrow).

C

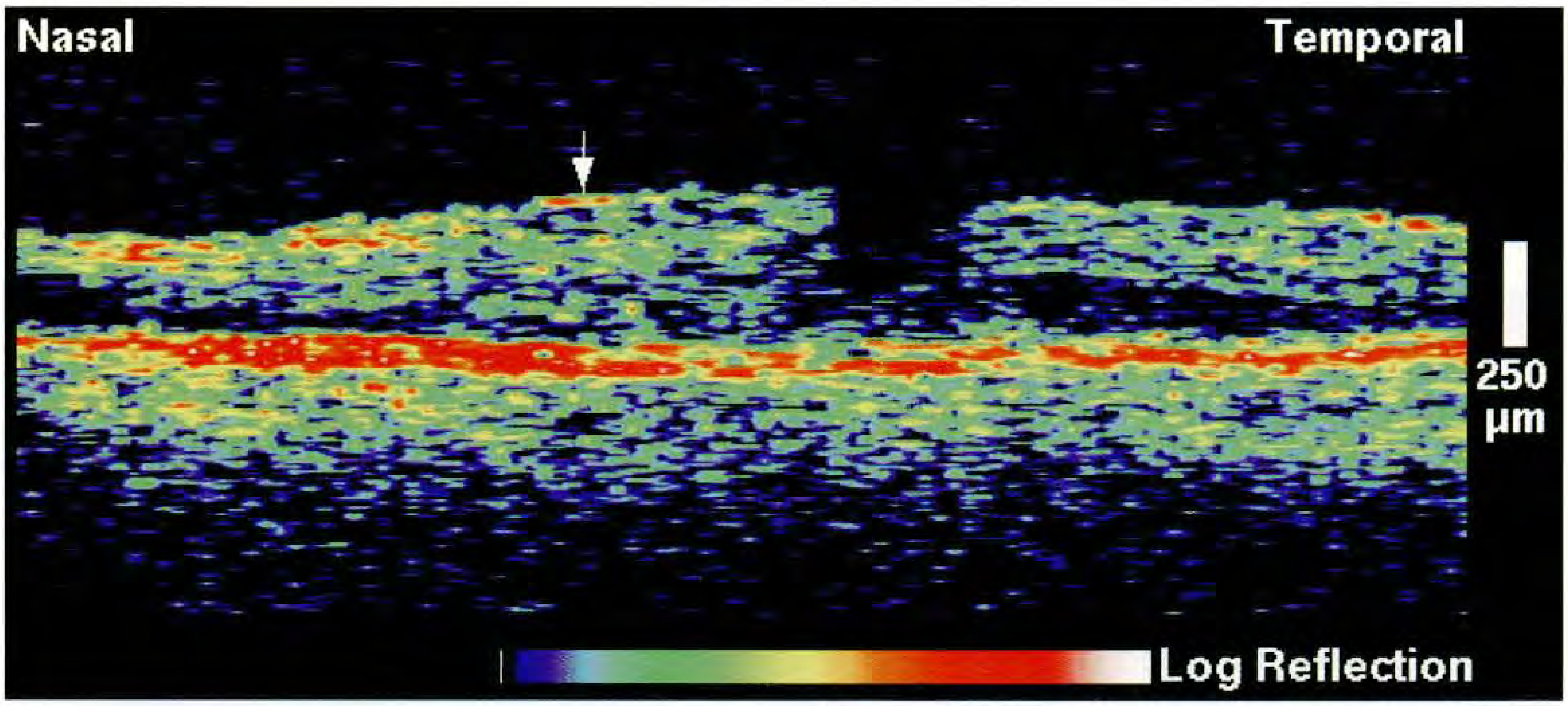

D

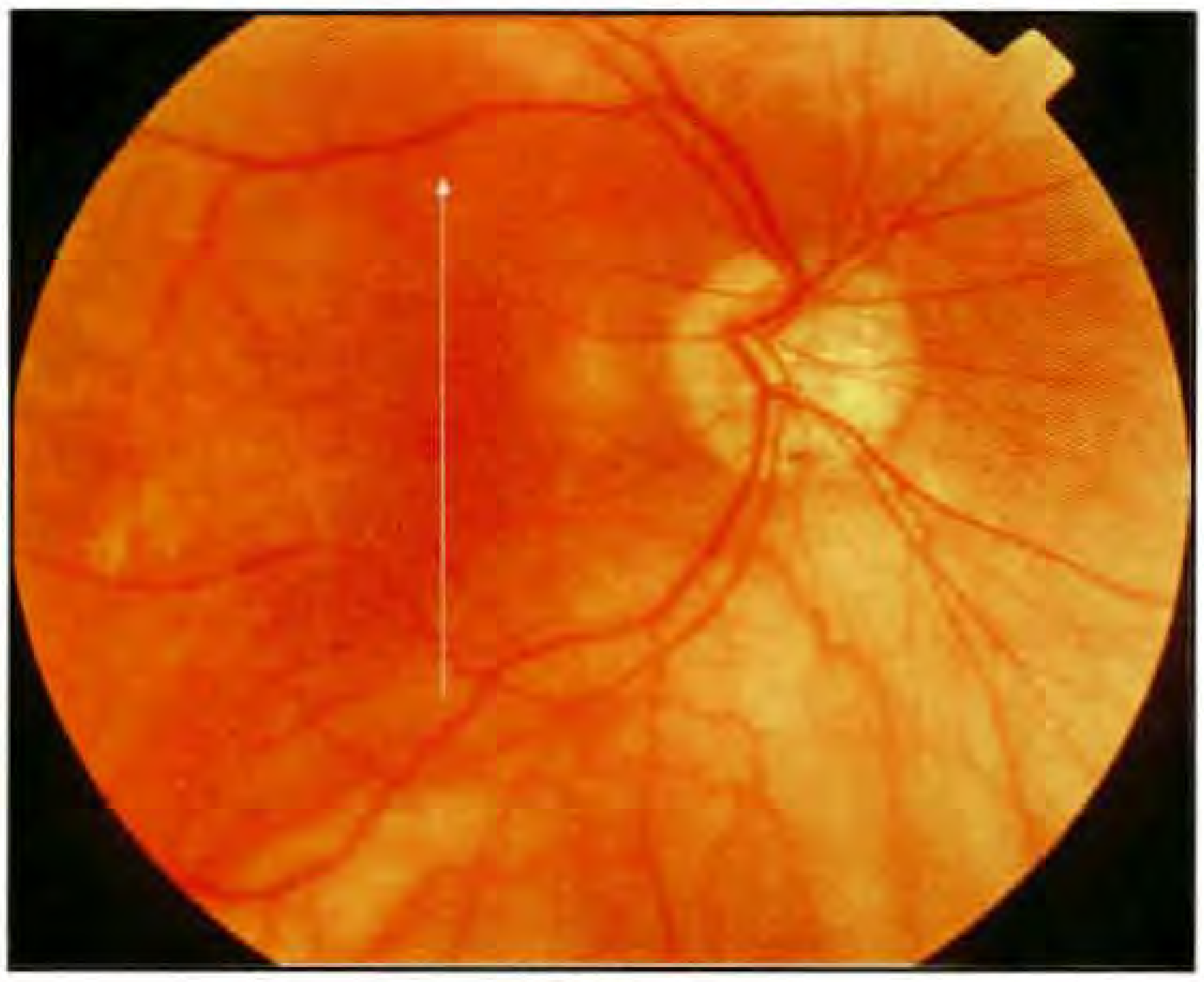

A

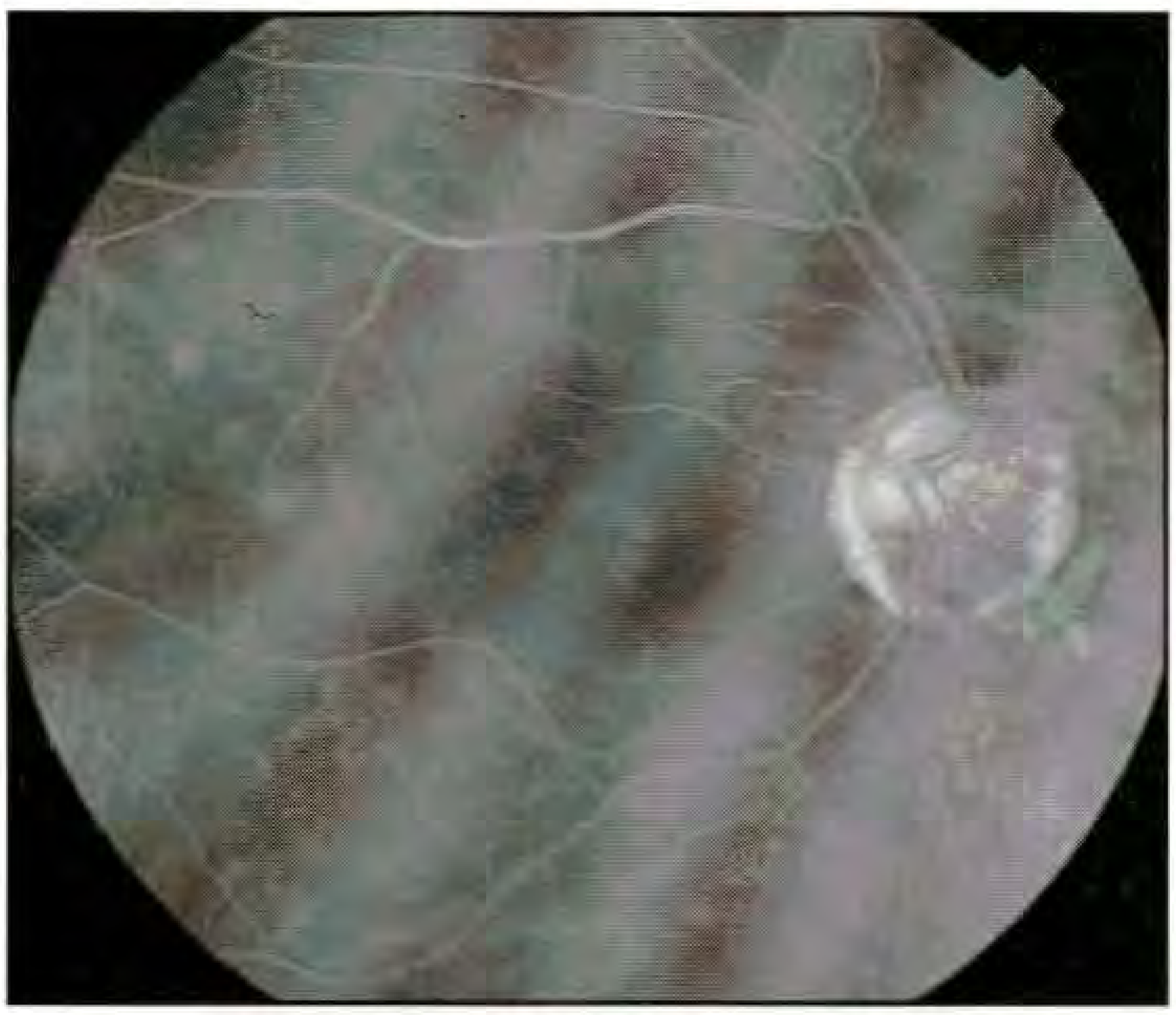

B

Case 3-12. Stage 3 Macular Hole with a Lamellar Hole in the Fellow Eye

Clinical Summary

A 69-year-old woman had a full-thickness macular hole in her right eye associated with a visual acuity of 20/100 (A). Fluorescein angiography (B) showed mild leakage surrounding the fovea consistent with a cuff of subretinal or intraretinal fluid accumulation.

Optical Coherence Tomography

The vertical OCT tomogram (C) exhibited a classic Stage 3 hole with surrounding cystic changes and macular edema. Enhanced backscatter was noted from retinal pigment epithelium beneath the hole consistent with either a lack of probe beam attenuation through retinal tissue, or pigmentary changes.

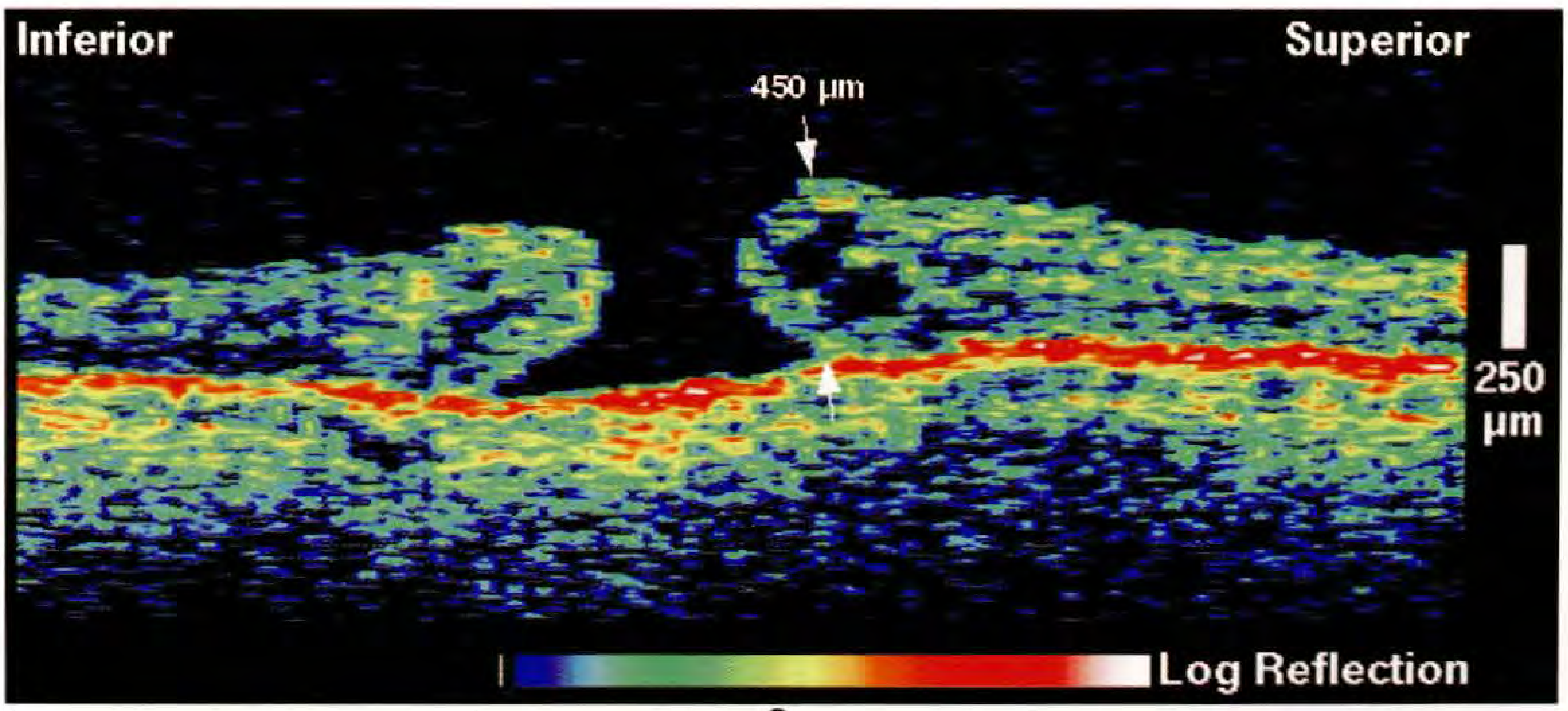

C

Case 3-12 continued

Clinical Summary

The patient had undergone cataract extraction in her fellow eye two years earlier and since then had noted itching and tearing in this eye with blurred vision. Dilated fundus examination (D) showed either a cyst or a hole in the central macula. Fluorescein angiography (E) did not show any leakage in the macular region. The visual acuity in this eye was 20/200.

Optical Coherence Tomography

An OCT image (F) obtained through fixation delineated a partial thickness or lamellar hole with a contour suggesting the rupture of a macular cyst. Optical backscatter was clearly present from the outer retinal layers at the base of the hole. The retina appeared to be dividing at the outer plexiform layer at the inferior margin of the hole.

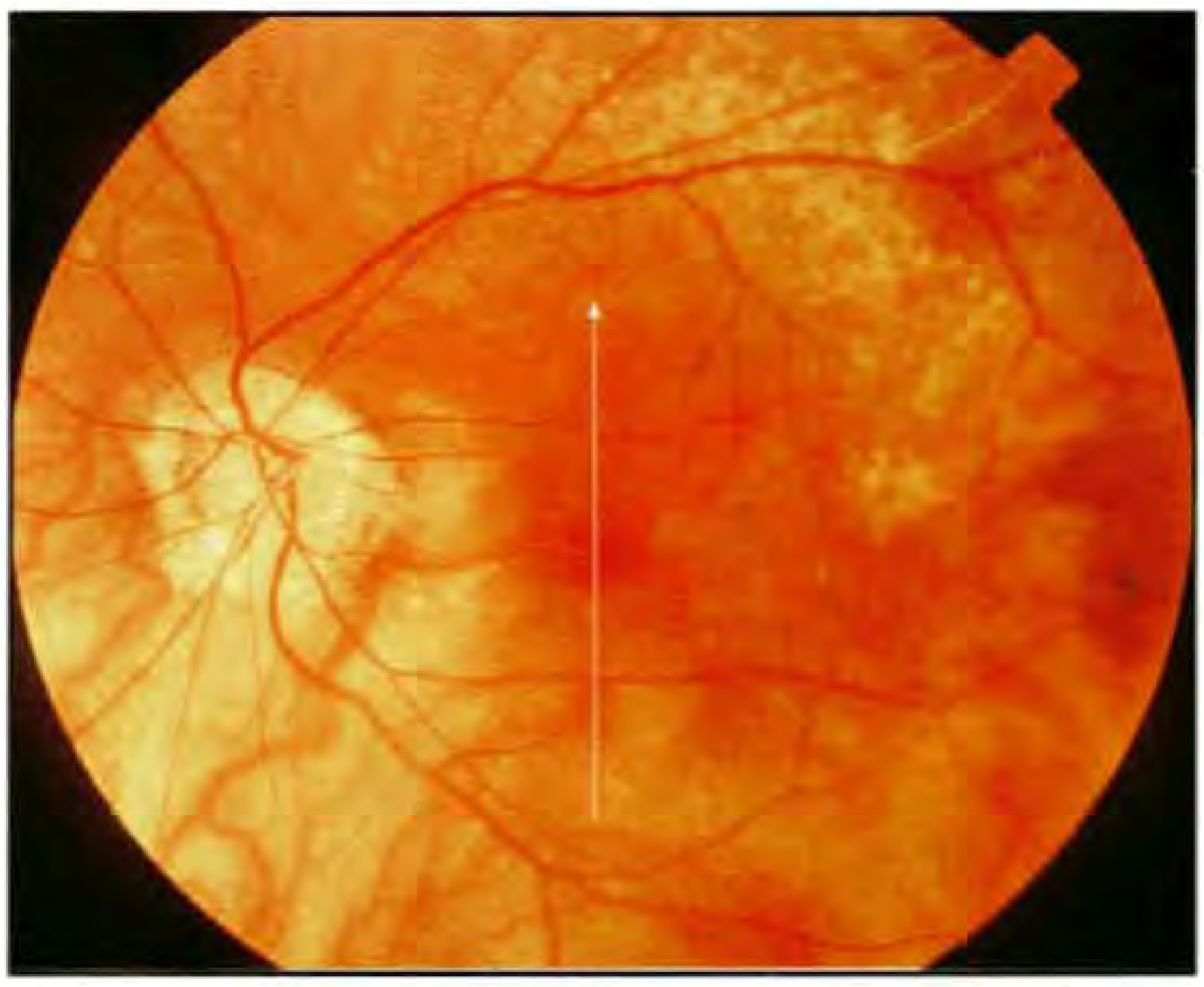

D

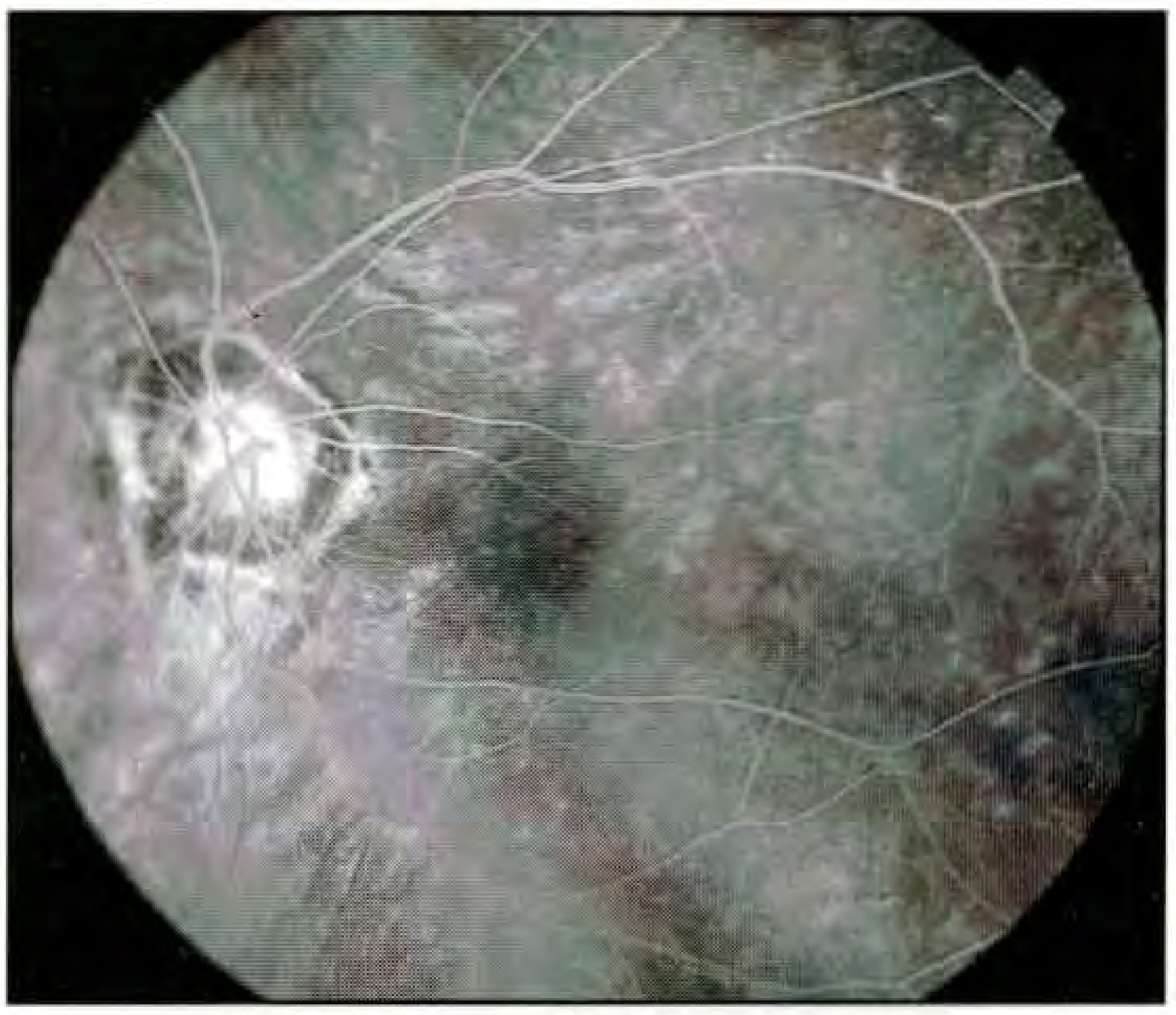

E

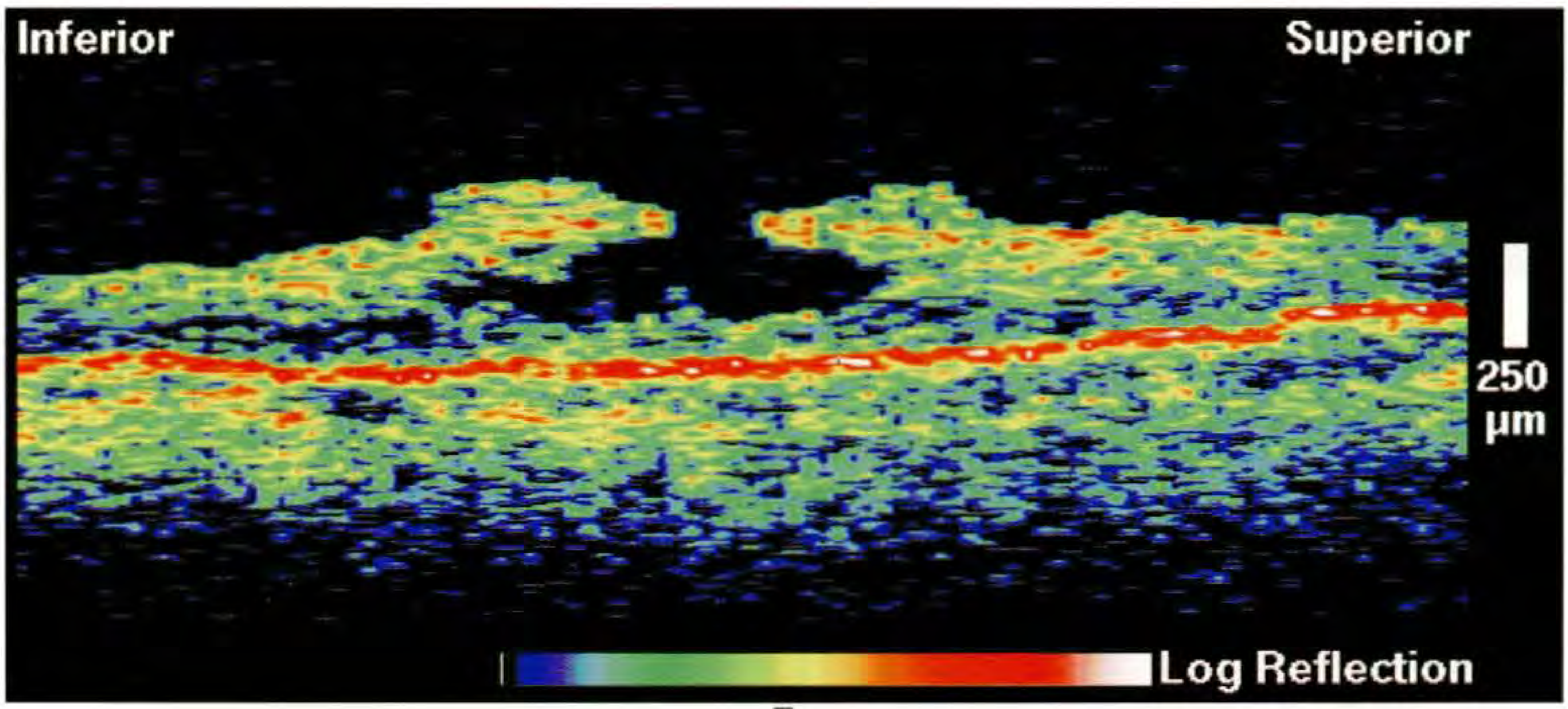

F

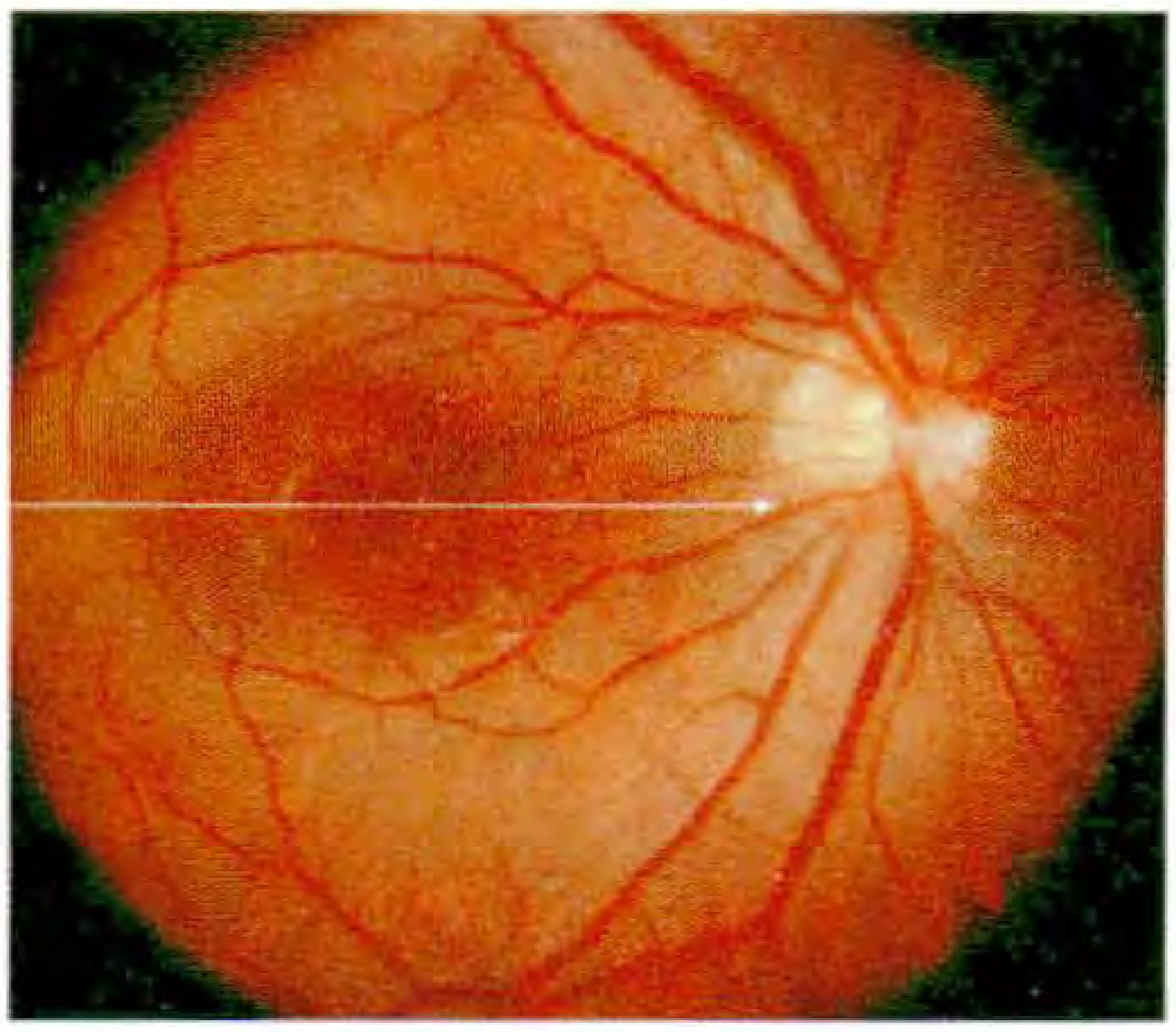

A

Case 3-13. Stage 4 Macular Hole with Vitreomacular Traction in the Fellow Eye

Clinical Summary

A 29-year-old woman had a macular hole in her right eye with a visual acuity of counting fingers (A).

Optical Coherence Tomography

The OCT tomogram (B) showed a characteristic full-thickness loss of retinal tissue in the fovea and surrounding retinal edema. The posterior hyaloid membrane was completely detached from the retina by approximately 400 µm, consistent with a Stage 4 classification. Cystic spaces were observed in the outer retina immediately surrounding the hole.

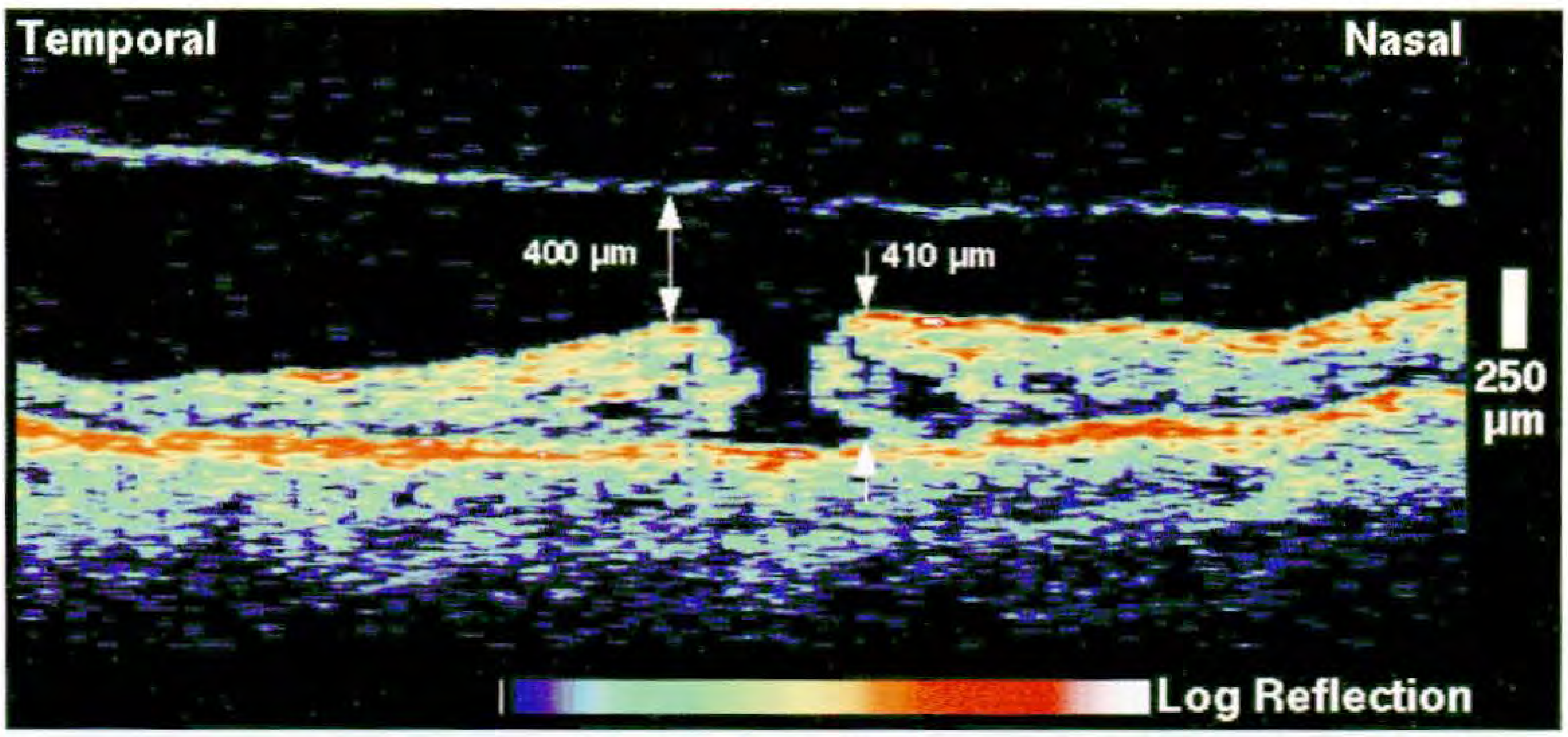

B

Case 3-13 continued

Clinical Summary

Contact lens examination (C) of the patient's left eye revealed fine striae radiating from the central macula. The visual acuity in this eye was 20/20.

Optical Coherence Tomography

An OCT image through fixation (D) demonstrated a perifoveal detachment of the posterior vitreous with significant vitreofoveal traction. The normal structure of the foveal pit was disrupted; however, the traction only appeared to affect the inner retinal layers.

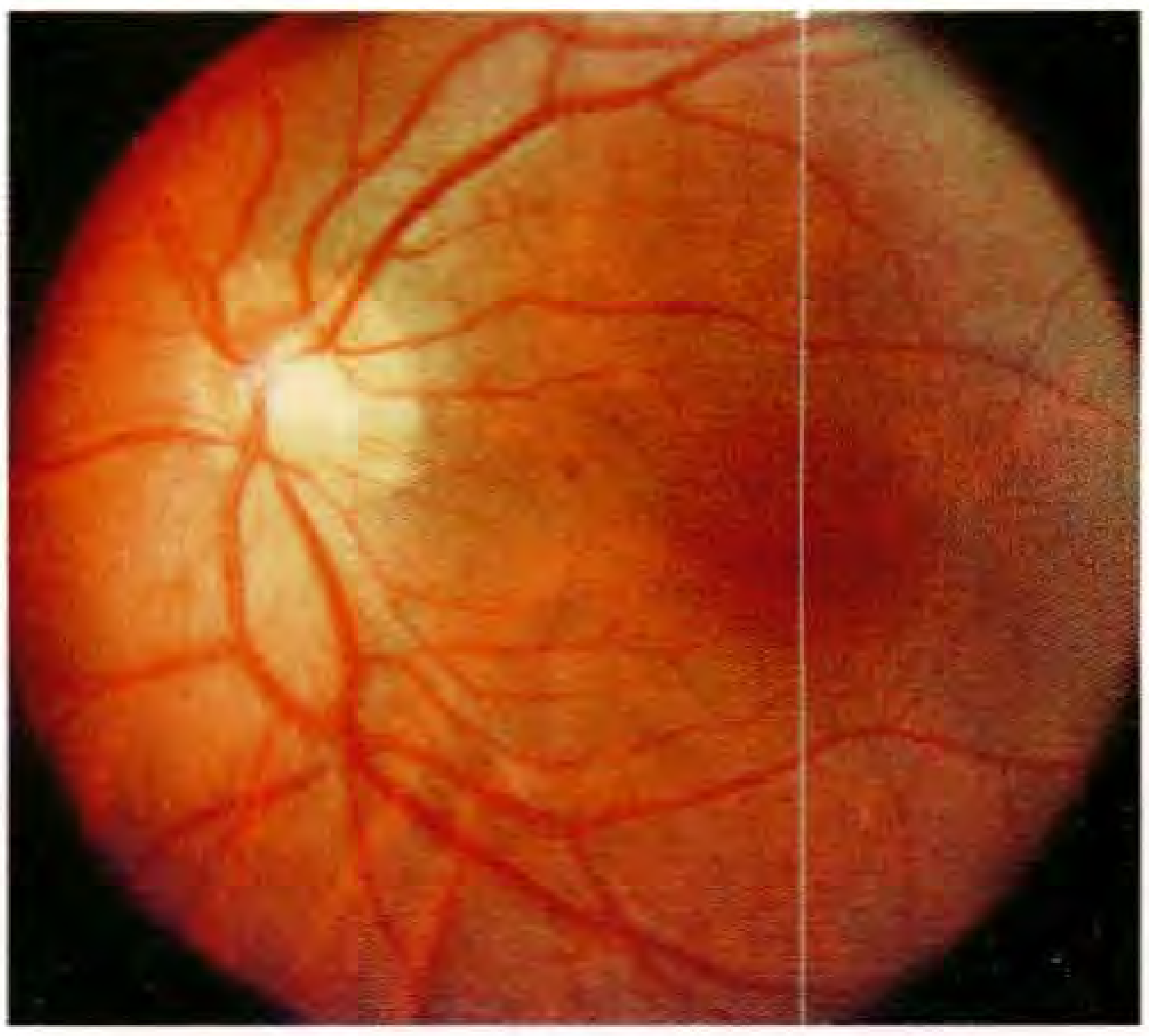

C

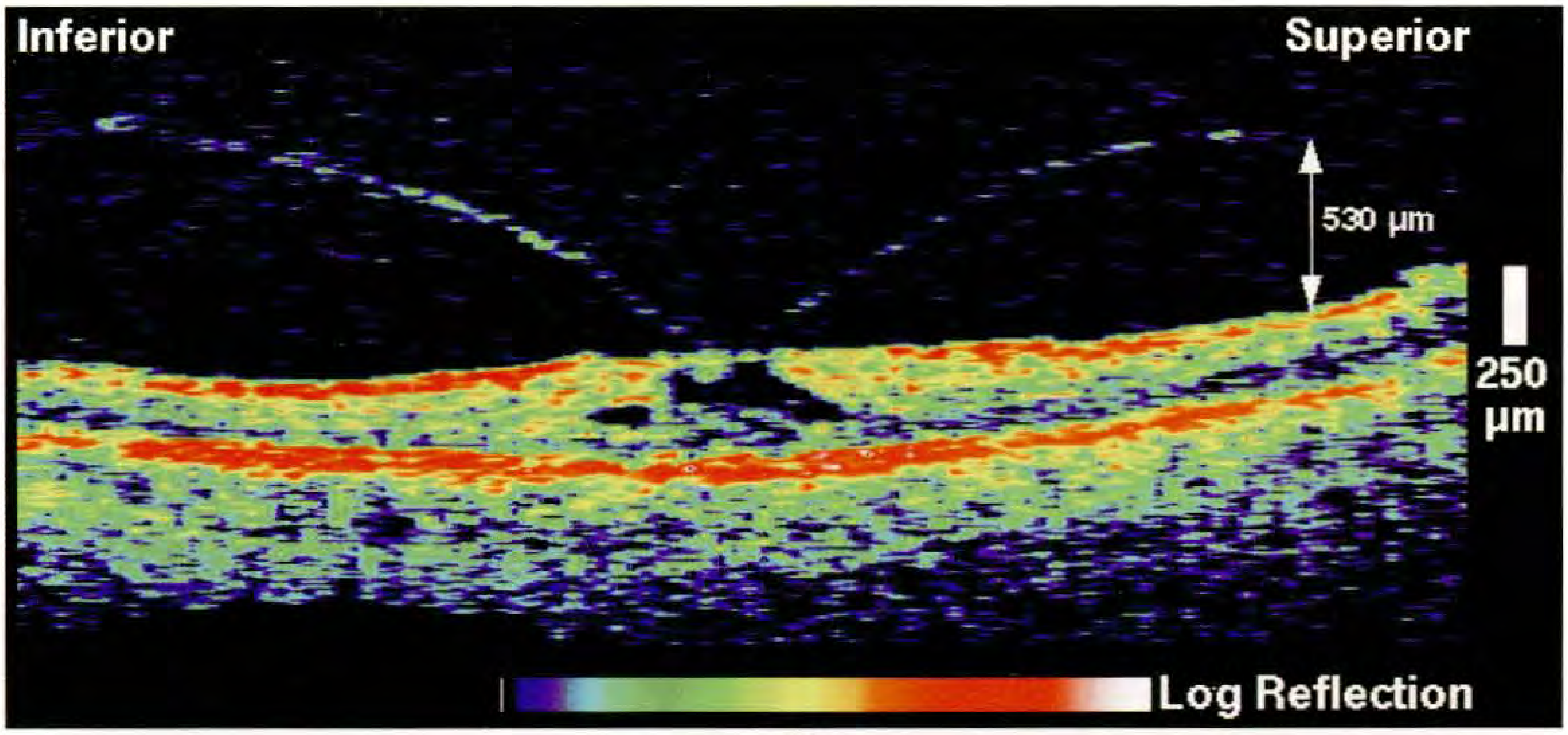

D

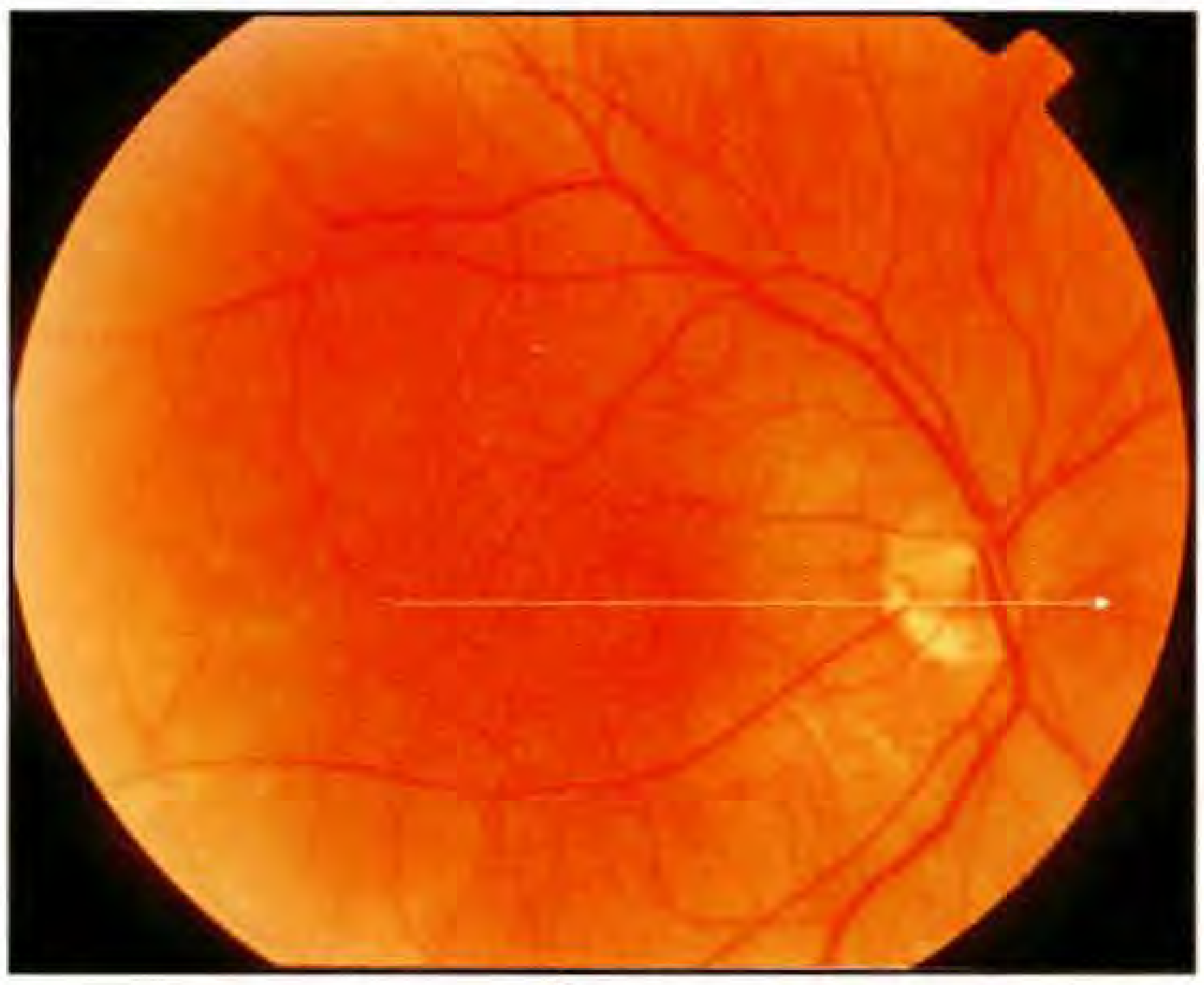

A

B

Case 3-14. Stage 4 Macular Hole with Operculum

Clnical Summary

A 58-year-old woman was evaluated for decreasing vision in her right eye over a period of a year. Her visual acuity in this eye was counting fingers at 7 feet. Slit-lamp biomicroscopy (A) revealed a full-thickness macular hole and a cuff of subretinal fluid. A posterior vitreous detachment was observed and a mild epiretinal membrane was noted surrounding the hole. Fluorescein angiography (B) demonstrated stable hyperfluorescence in the center of the macula consistent with a window defect. A faint rim of hyperfluorescence surrounding the fovea was observed in later views consistent with macular edema.

Optical Coherence Tomography

An OCT image (C) through the macula and optic disc showed a 540 μm diameter full-thickness defect in the neurosensory retina. Reduced optical reflectivity corresponding to fluid accumulation and cystic changes was evident in the outer retinal layers surrounding the hole. The posterior vitreous was separated from both the macula and optic disc by about 300 to 500 μm in the tomogram establishing the diagnosis of a Stage 4 macular hole. A region of increased reflectivity in the posterior hyaloid directly above the fovea most likely represented an operculum.

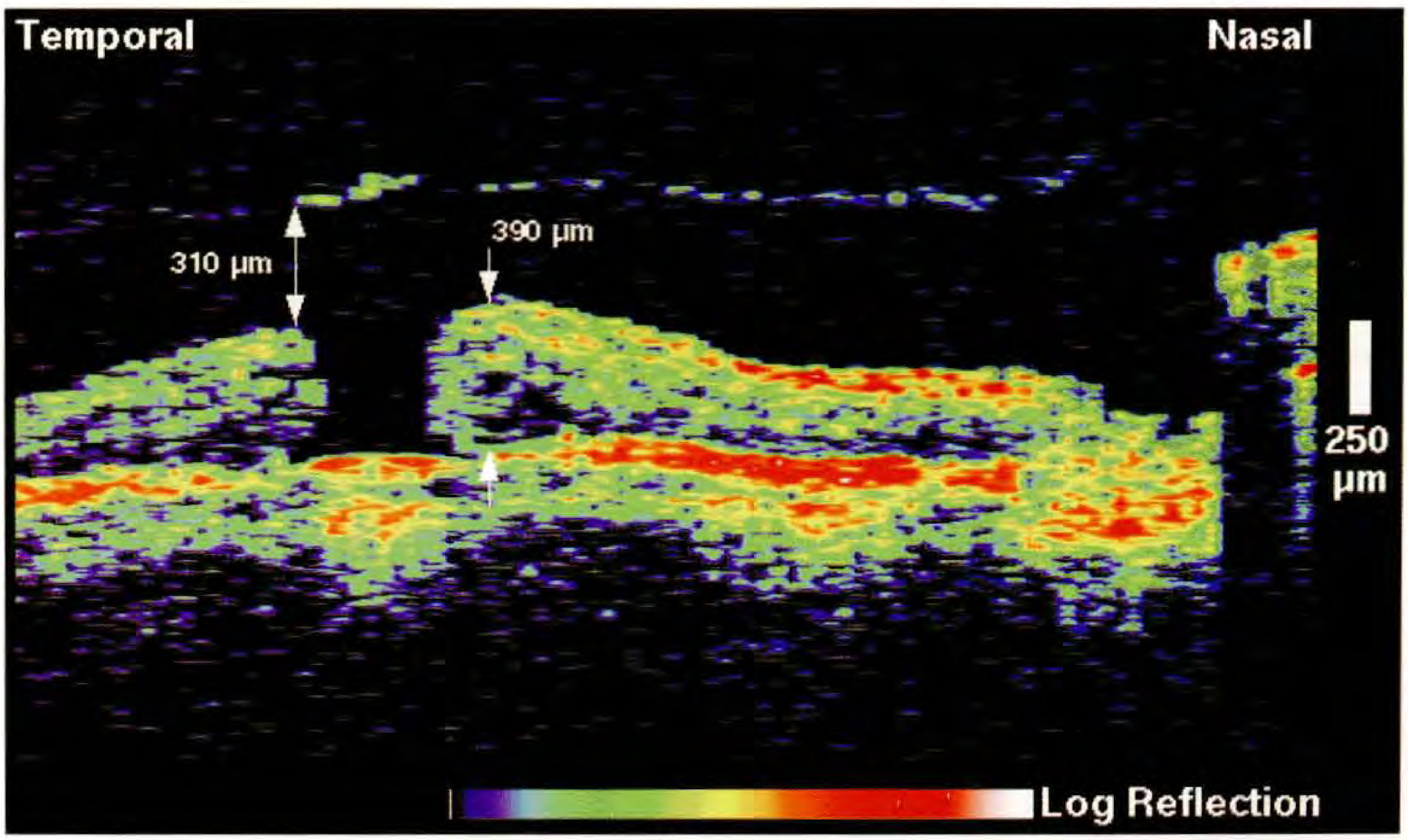

C

Case 3-15. Stage 4 Macular Hole

Clinical Summary

A 73-year-old woman had a full-thickness macular hole in her left eye associated with a visual acuity of counting fingers at 7 feet (A).

Optical Coherence Tomography

The OCT image (B) showed a large full-thickness hole with significant surrounding retinal edema. The retinal thickness at the edge of the hole measured 500 µm. The posterior hyaloid membrane was completely separated from the retina by approximately 350 µm consistent with a Stage 4 classification. The hole diameter was 660 µm at its minimum point in the image.

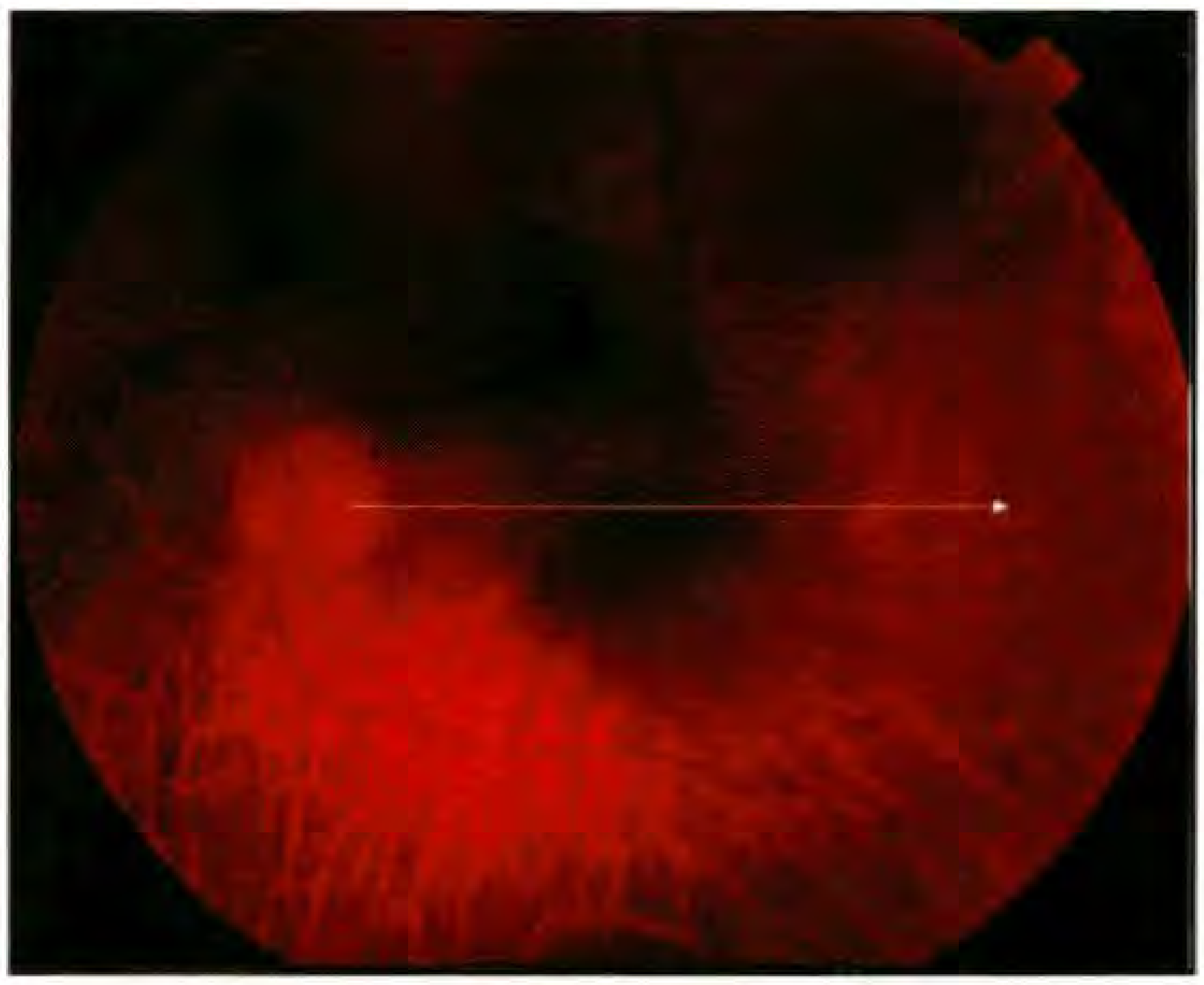

A

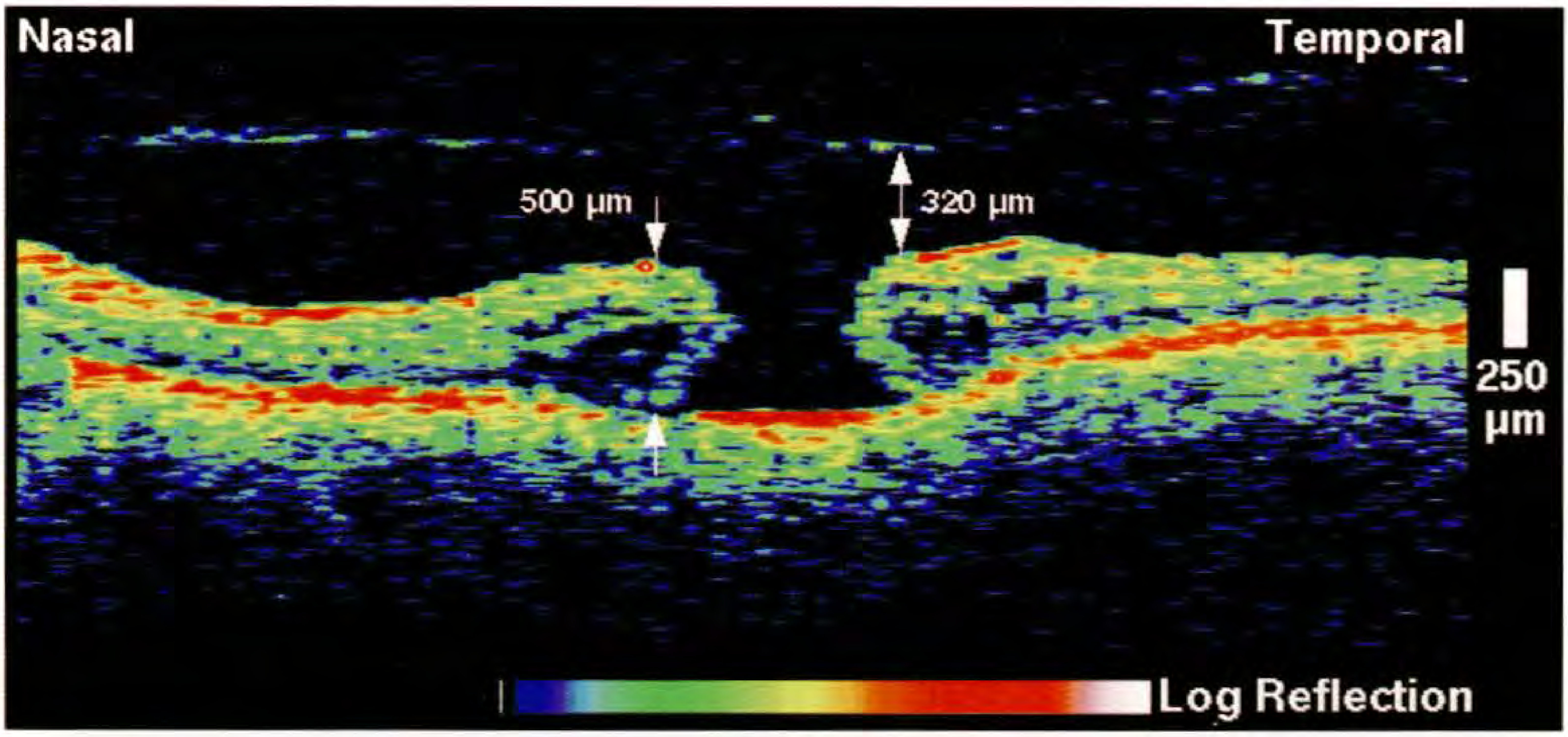

B

A

B

Case 3-16. Macular Hole and Age-Related Macular Degeneration

Clinical Summary

A 72-year-old man with age-related macular degeneration was referred for difficulty reading and worsening visual acuity in the left eye, which was assessed at counting fingers at three feet. Slit-lamp biomicroscopy (A) revealed a fibrovascular scar in the central macula with no evidence of subretinal fluid or hemorrhage. A small, full-thickness macular hole was also observed centrally. Fluorescein angiography (B) demonstrated a hyperfluorescent area in the central macula with late staining but no leakage or pooling, consistent with a disciform scar.

Optical Coherence Tomography

OCT examination (C) confirmed a full-thickness macular hole in the fovea. Retinal atrophy was noted surrounding the hole and the retinal thickness measured at the temporal margin of the hole was 130 μm. The reflective band corresponding to the retinal pigment epithelium and choriocapillaris was thickened in the central macula consistent with a disciform scar.

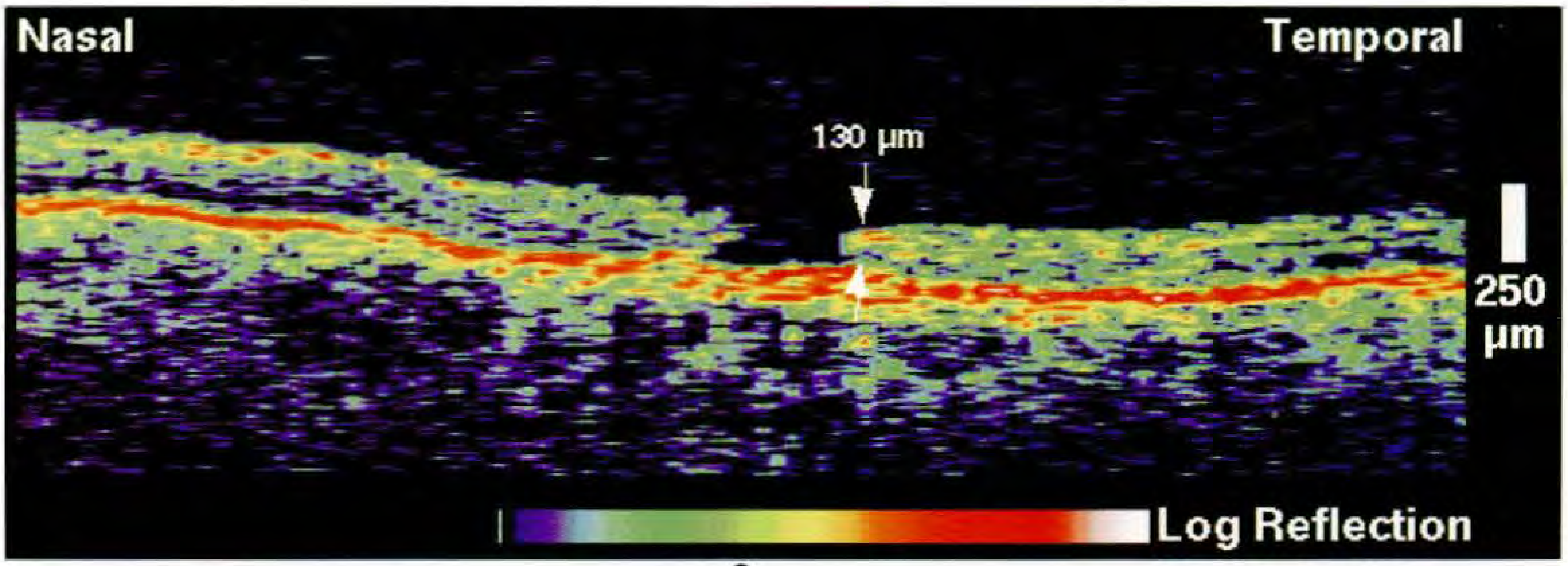

C

Case 3-17. Macular Hole and Atrophic Laser Scar

Clinical Summary

A 75-year-old man with age-related macular degeneration had undergone indocynanine green enhanced diode laser photocoagulation in his right eye eight months earlier for choroidal neovascularization. Slit-lamp biomicroscopy (A) showed an atrophic laser scar in the center of the macula with no subretinal fluid, hemorrhage, or exudate. The visual acuity in this eye was 20/100. Fluorescein angiography (B) showed an area of hypofluorescence in the macula with surrounding hyperfluorescence, and late staining consistent with a fibrovascular scar.

Optical Coherence Tomography

OCT examination (C) delineated a full-thickness loss of retinal tissue in the fovea. The abnormal contour of the hole suggested an atypical development. A large, highly reflective region below the neurosensory retina was evident in the central macula corresponding to the laser scar.

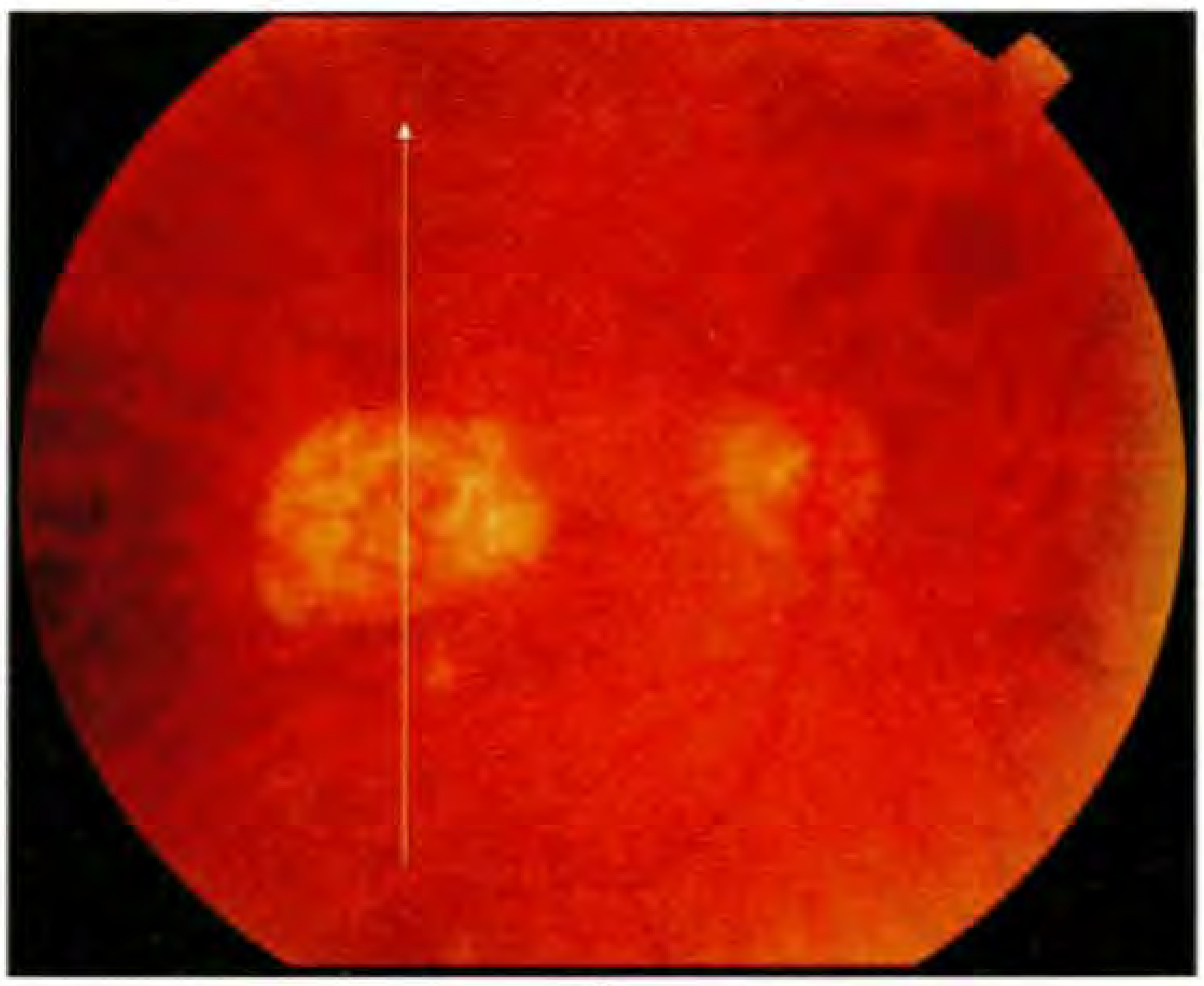

A

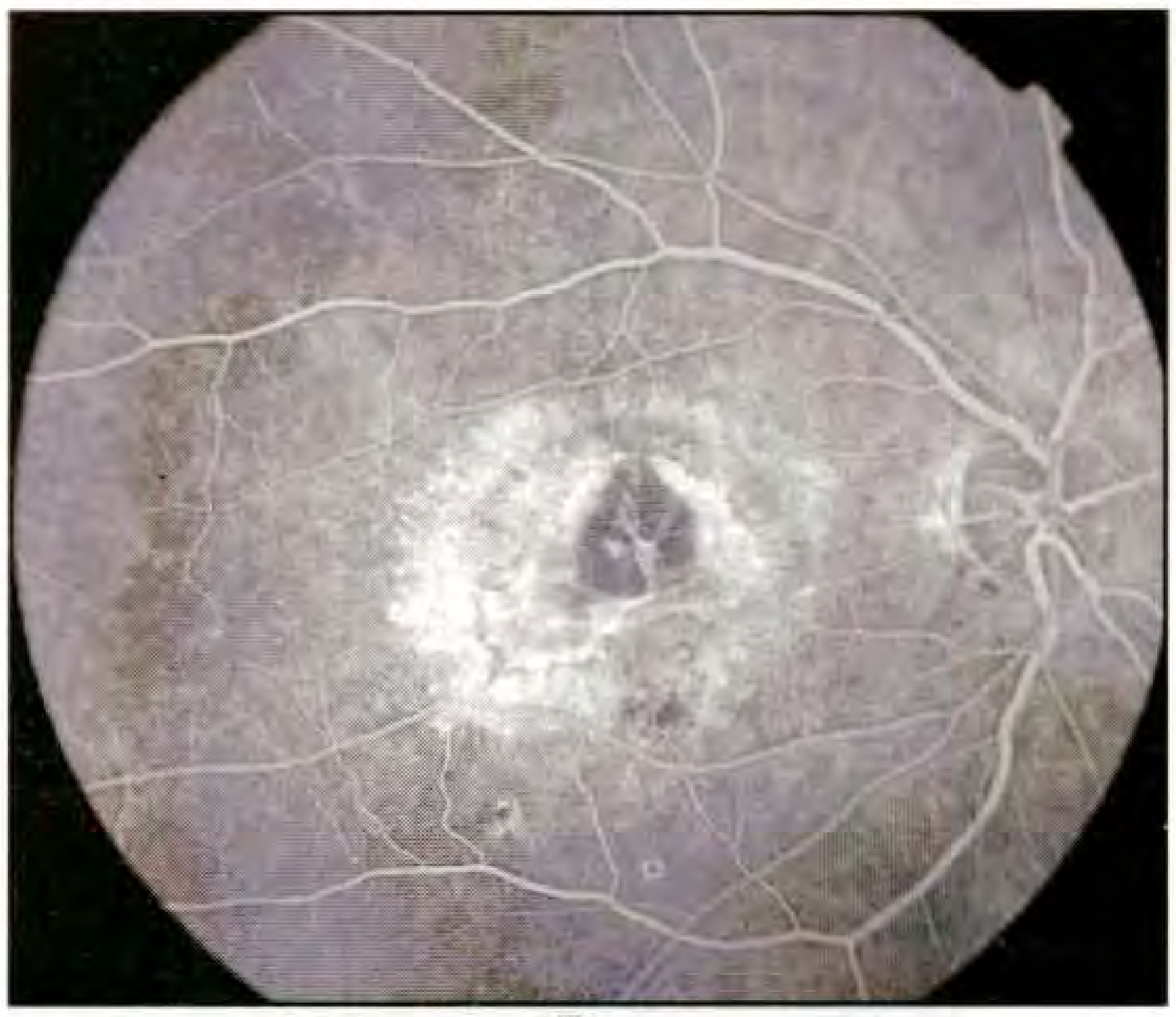

B

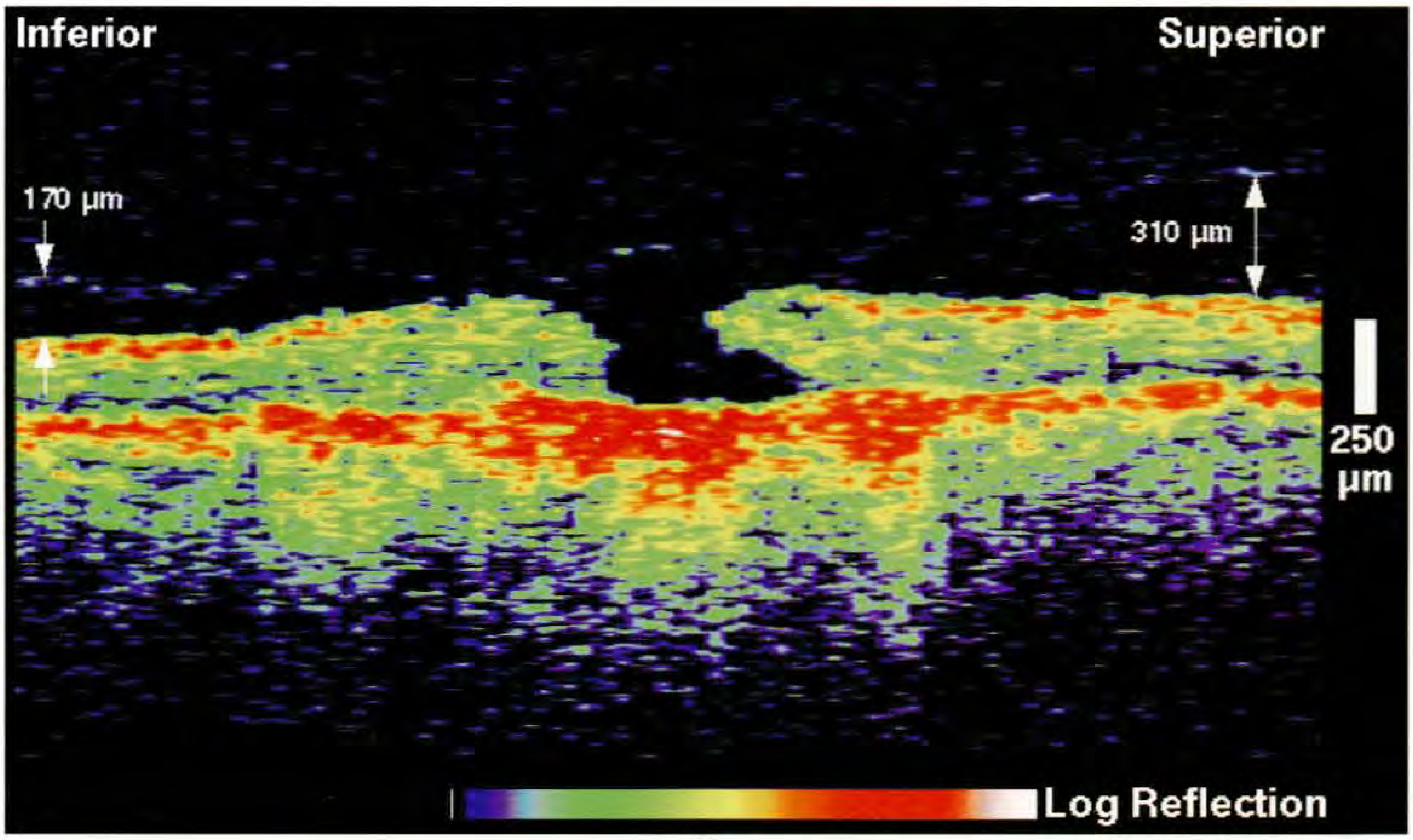

C

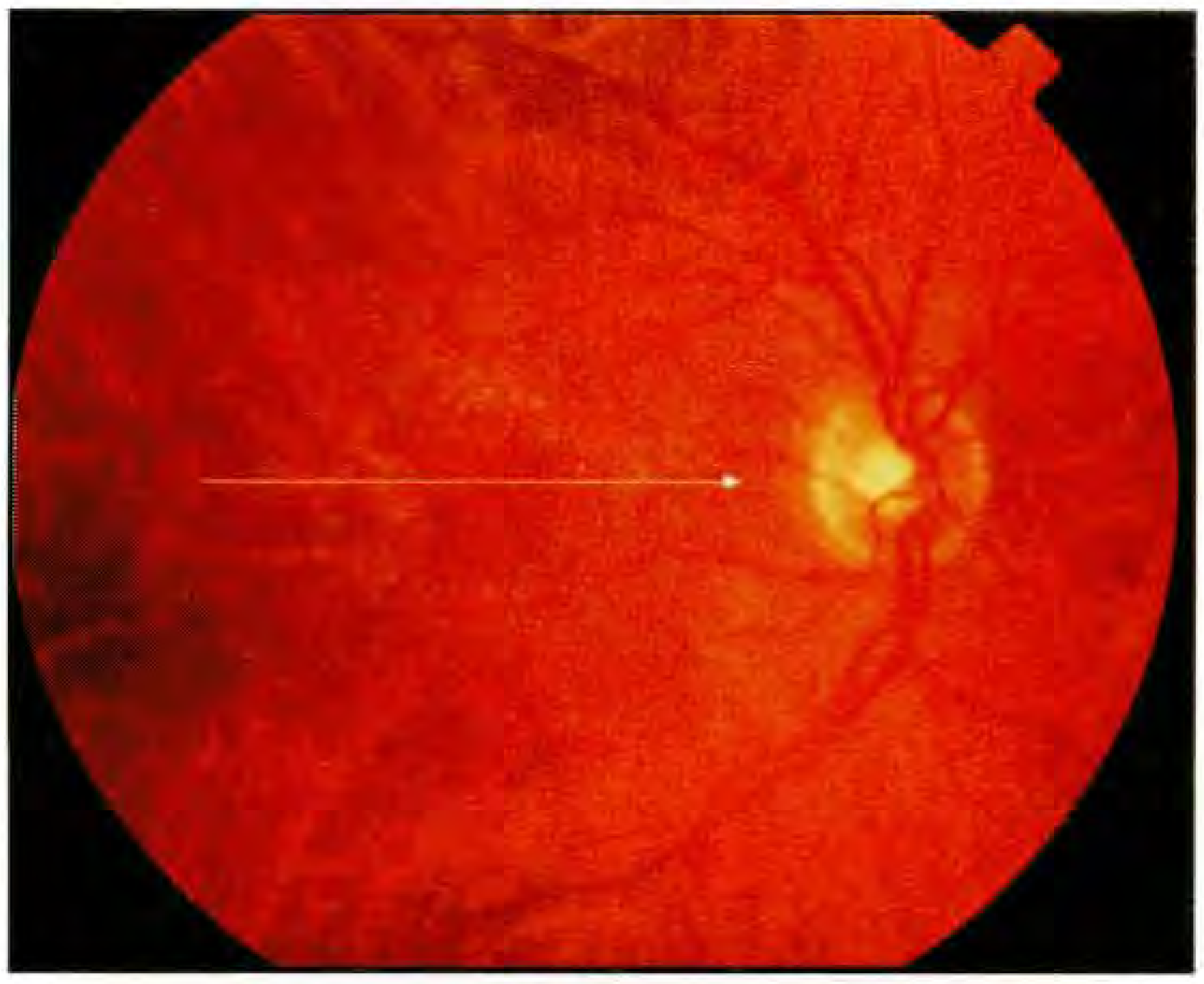

A

Case 3-18. Full-thickness Macular Hole with an Atrophic Scar in the Fellow Eye

Clinical Summary

This patient was a 76-year-old man with age-related macular degeneration and a history of laser photocoagulation treatment in both eyes. Examination of the right eye (A) showed a full-thickness macular hole which was associated with a visual acuity of 20/200.

Optical Coherence Tomography

OCT examination (B) confirmed the presence of a Stage 3 macular hole with minimal surrounding subretinal fluid accumulation. The retinal thickness measured at the margin of the hole was 290 μm and the hole diameter was approximately 530 μm at its minimum in the image. Small, minimally reflective cystic spaces were identified in the macula surrounding the hole.

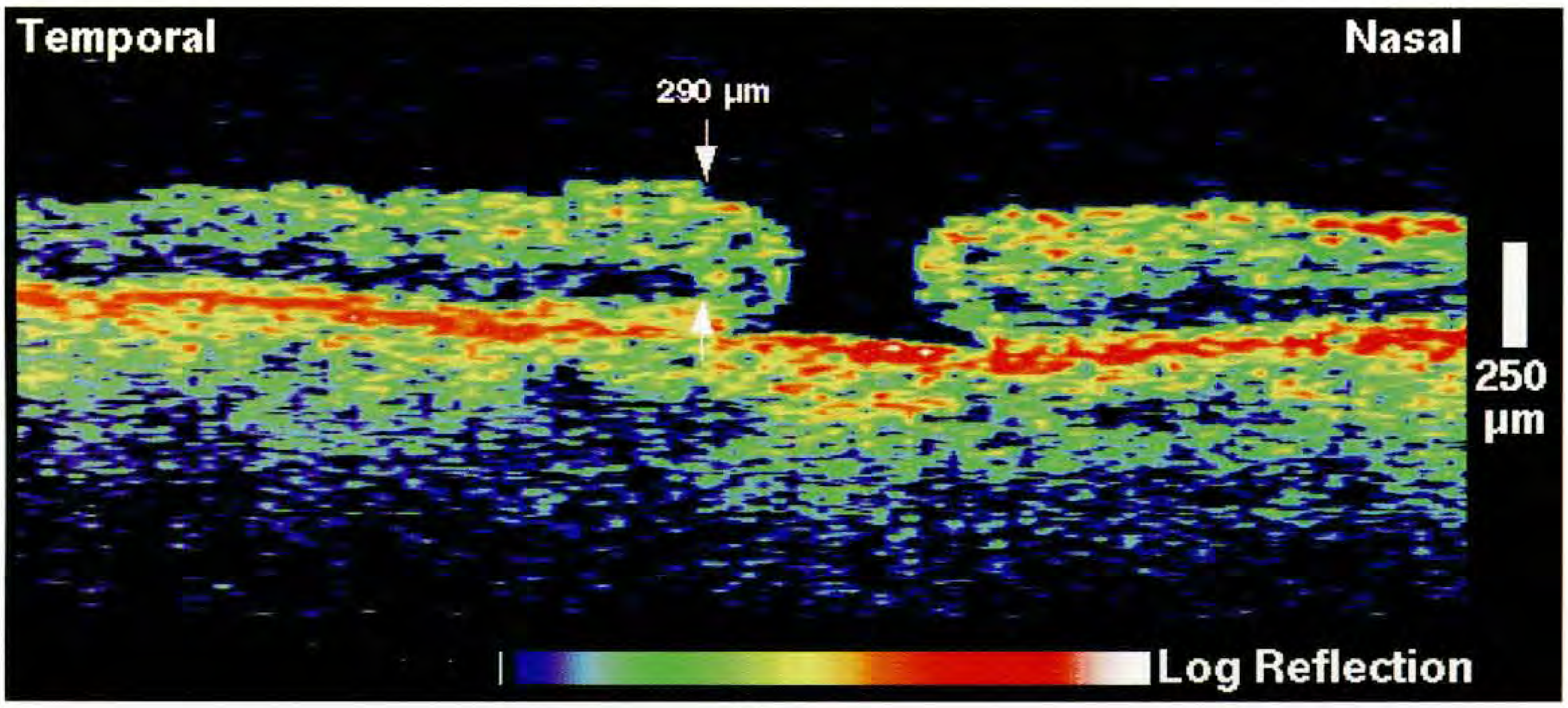

B

Case 3-18 continued

Clinical Summary

The patient's left eye (C) was notable for a large disciform scar in the macula which appeared to form an annulus around the fovea.

Optical Coherence Tomography

A full-thickness macular hole was observed in a horizontal OCT image (D) acquired through the fovea. The contrast in optical reflectivity between the retinal photoreceptors and the retinal pigment epithelium was attenuated. Increased reflectivity from the choroid was observed consistent with both a fibrovascular scar and enhanced penetration of the probe beam through an atrophic pigment epithelium. A faint reflection from the posterior hyaloid membrane spanned the top of the hole.

C

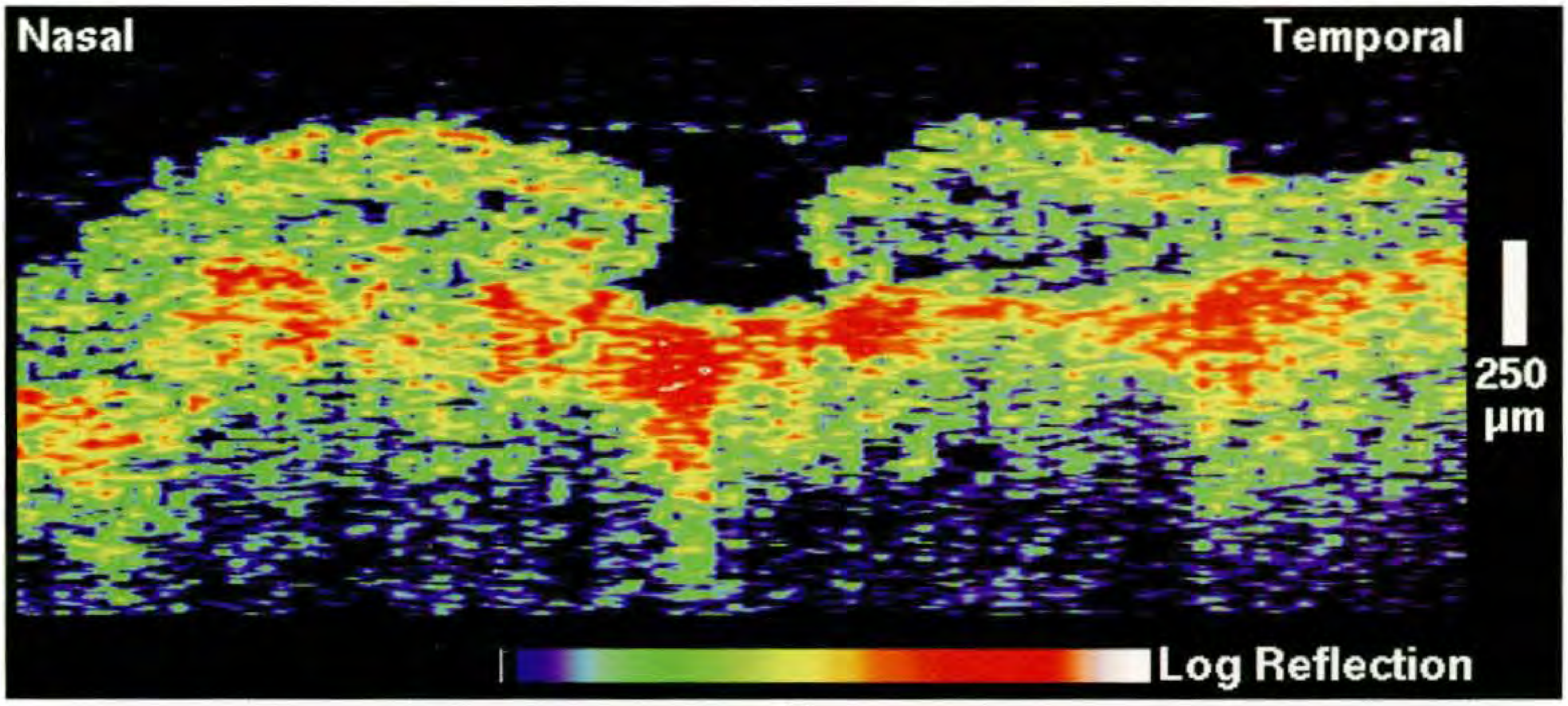

D

A

Case 3-19. Lamellar Macular Hole and Raised Pigment Lesion

Clinical Summary

A 73-year-old man had a visual acuity of 20/200 in his left eye. Slit-lamp biomicroscopy (A) showed microaneurysms consistent with diabetic retinopathy, a faint bullseye pattern in the fovea, and a raised pigmented lesion along the superior arcade.

Optical Coherence Tomography

An OCT image (B; white line on A) through fixation showed a partial-thickness hole in the fovea with an intact outer retinal layer centrally. The pigmented lesion (C; black line on A) appeared as a focal area of enhanced backscatter which shadowed all reflections below. Chorioretinal atrophy surrounded the lesion which was visible as thinning of the neurosensory retina and enhanced choroidal reflectivity due to increased penetration of the probe beam through the reduced pigmentation.

B

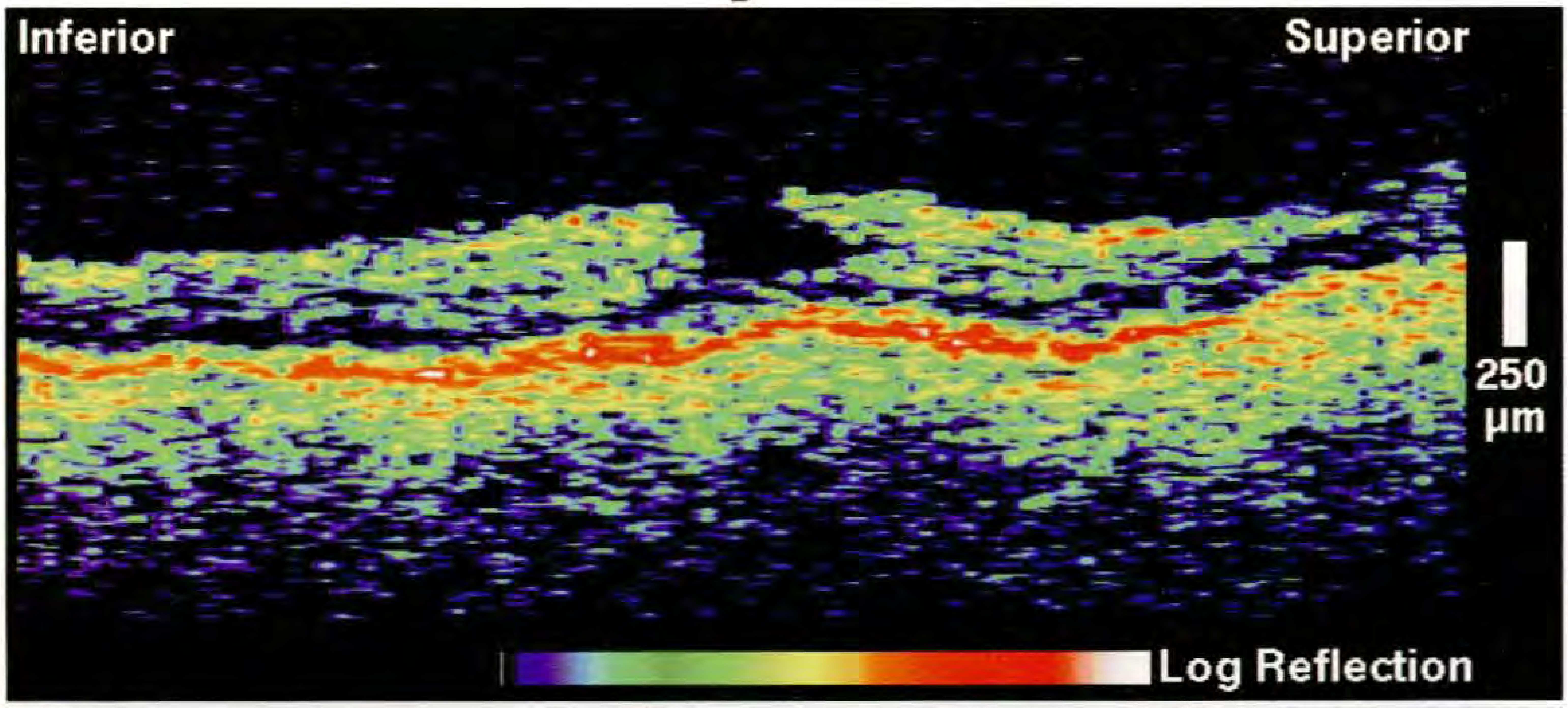

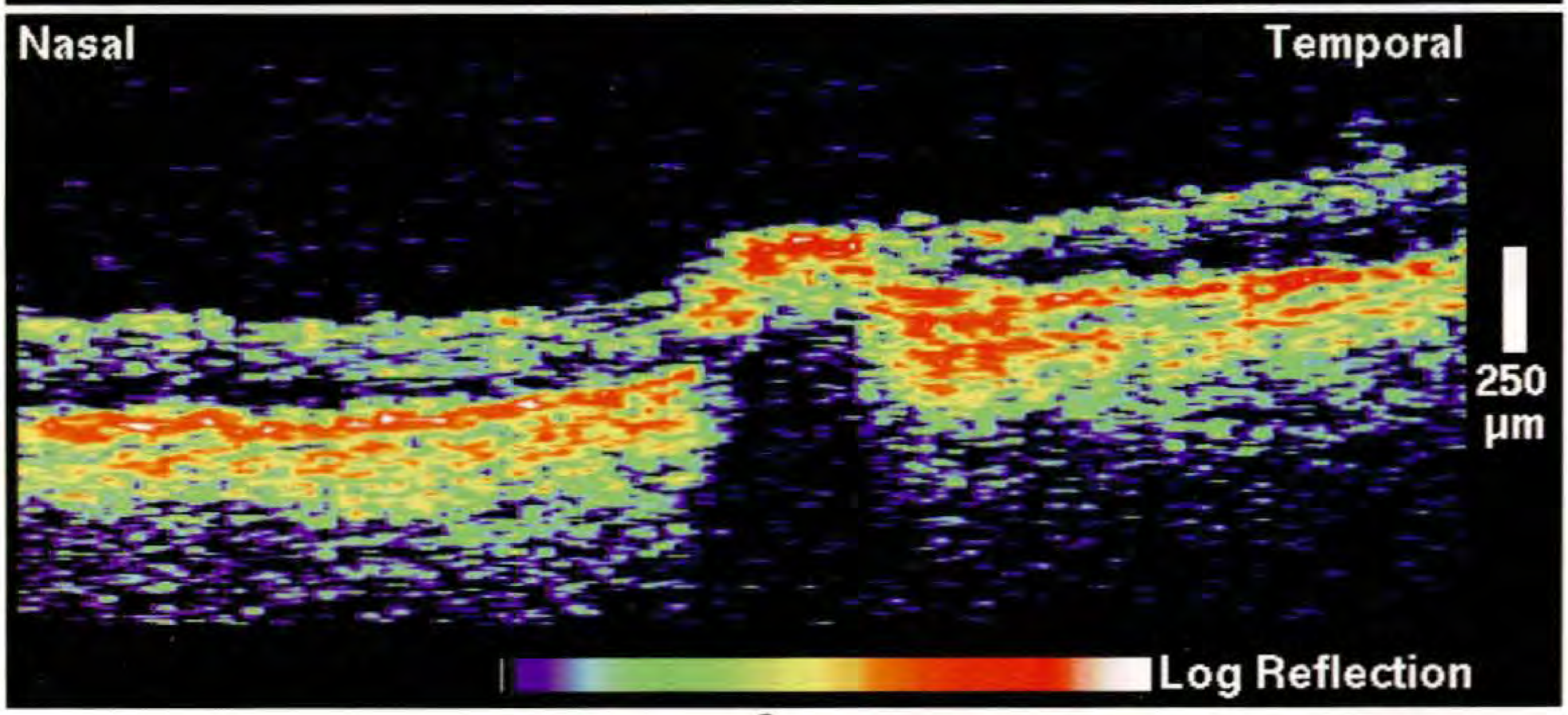

C

Case 3-20. Lamellar Macular Hole

Clinical Summary

A 61-year-old man was referred for evaluation of a possible macular hole in his left eye. He had noted a gradual decline in his vision for approximately two years. On examination, his visual acuity in the this eye was 20/60. Slit-lamp biomicroscopy (A) showed a red spot in the fovea, but no evidence of a full-thickness hole or an epiretinal membrane.

Optical Coherence Tomography

The contour of the foveal pit was altered on OCT imaging (B); however, the presence of retinal tissue at the base of the fovea ruled out the diagnosis of a full-thickness macular hole. The shape of the contour suggested the rupture of a large macular cyst, consistent with a lamellar hole. The retina surrounding the hole was thickened, reaching a maximum of 370 µm in the image.

A

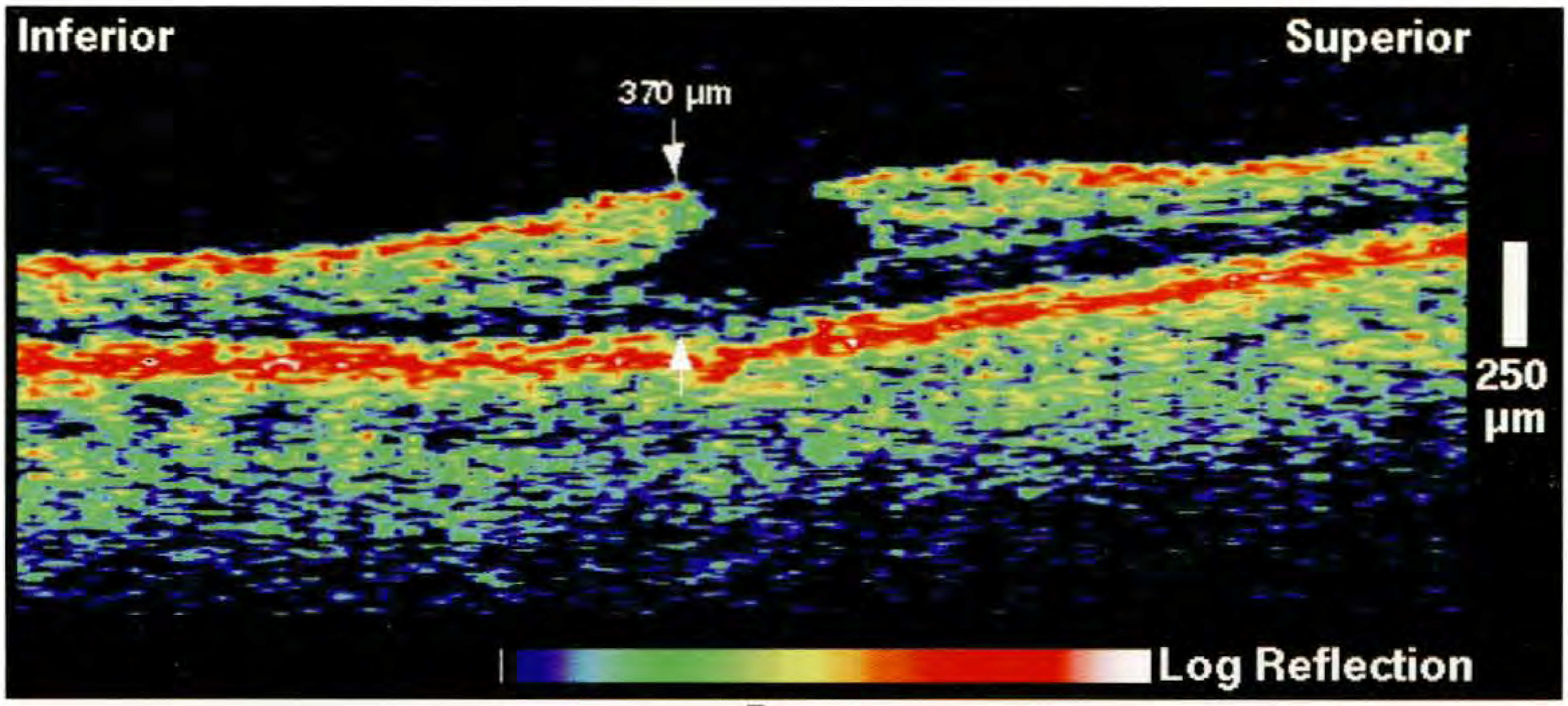

B

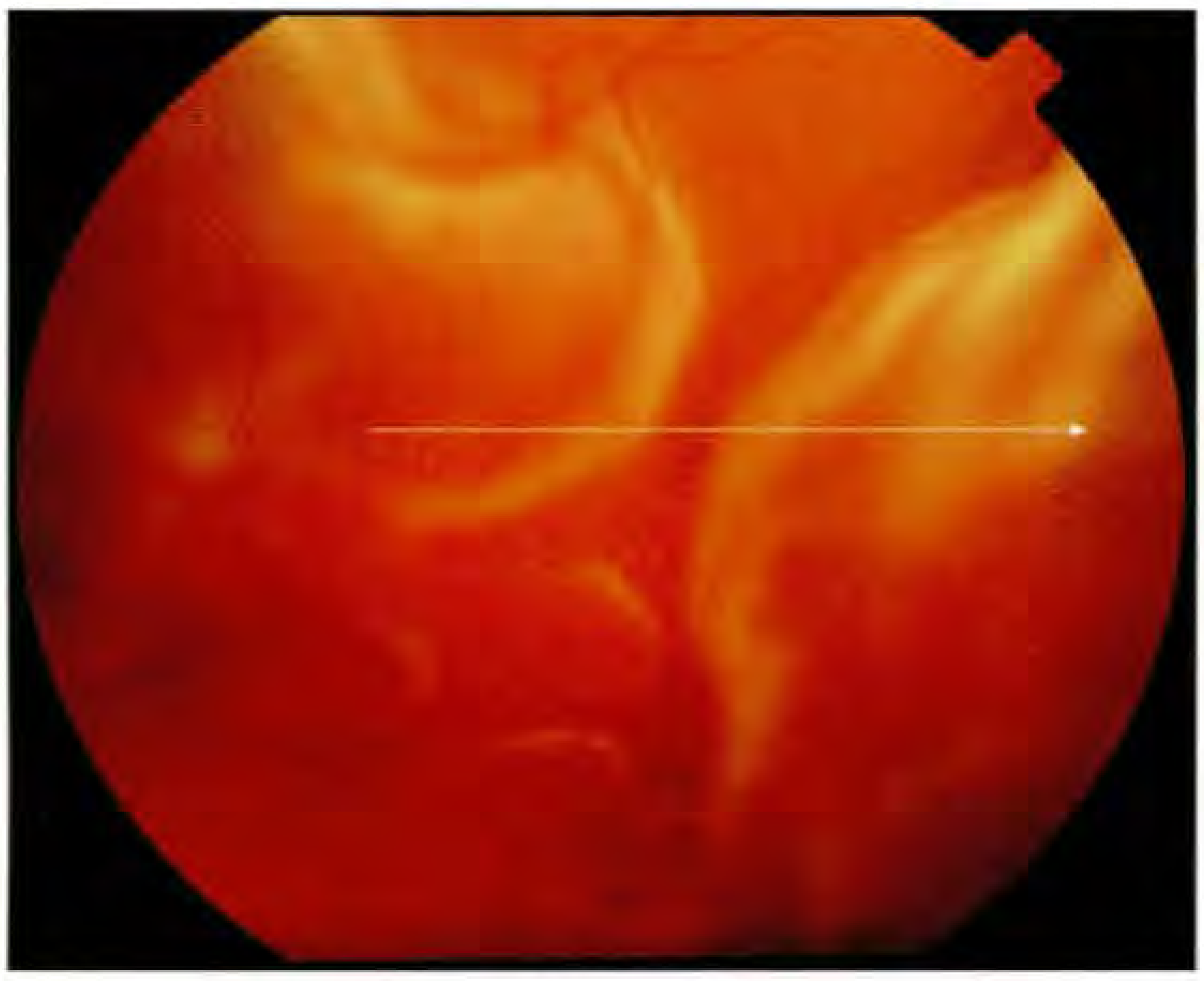

A

Case 3-21. Full-thickness Macular Hole with Retinal Detachment

Clinical Summary

A 71-year-old woman was referred for evaluation of a full-thickness macular hole in her right eye. She reported a decline in the visual acuity in this eye, which was assessed at hand motions only, over the past one and one-half weeks. Indirect ophthalmoscopy (A) showed a full-thickness macular hole and a rhegmatogenous retinal detachment extending from two to ten o'clock and involving the macula. Mild, fixed folds were observed inferiorly.

Optical Coherence Tomography

The OCT scan (B) graphically depicted the separation between the neurosensory retina and retinal pigment epithelium, which seemed to originate nasally and increase temporally in the image. A full-thickness break in the retina was noted, consistent with a macular hole. Small intraretinal cysts were also observed. The optical backscatter signal from the pigment epithelium and choroid was enhanced directly beneath the macular hole due to increased penetration of the incident and reflected probe light through that region.

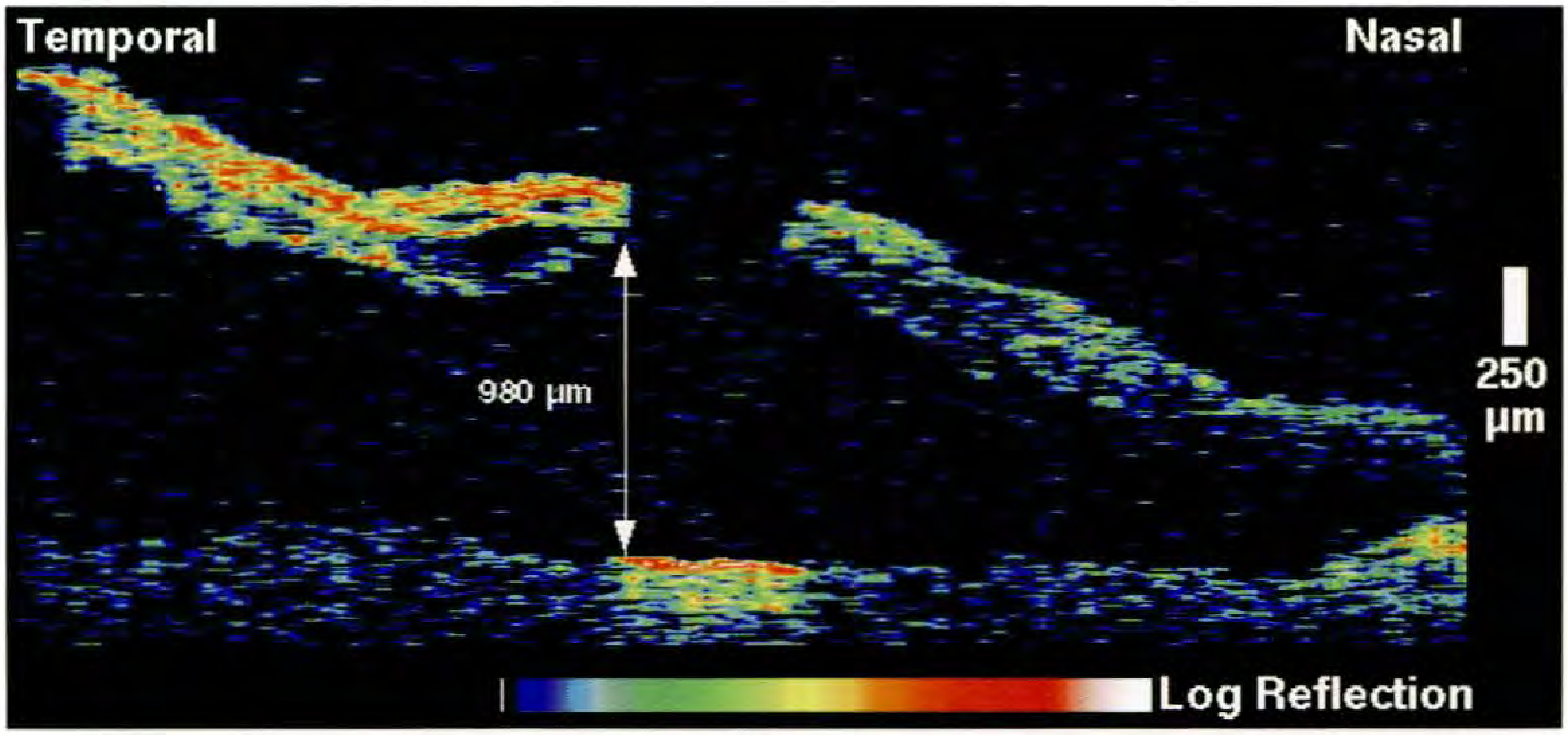

B

Case 3-22. Microhole

Clinical Summary

A 45-year-old man had a visual acuity of 20/30 in his right eye associated with the clinical diagnosis of a macular microhole (A).

Optical Coherence Tomography

A horizontal OCT scan (B) showed a narrow, punched-out loss of retinal tissue. The photoreceptor layer was preserved consistent with a partial thickness hole. The diameter of the hole was 230 μm.

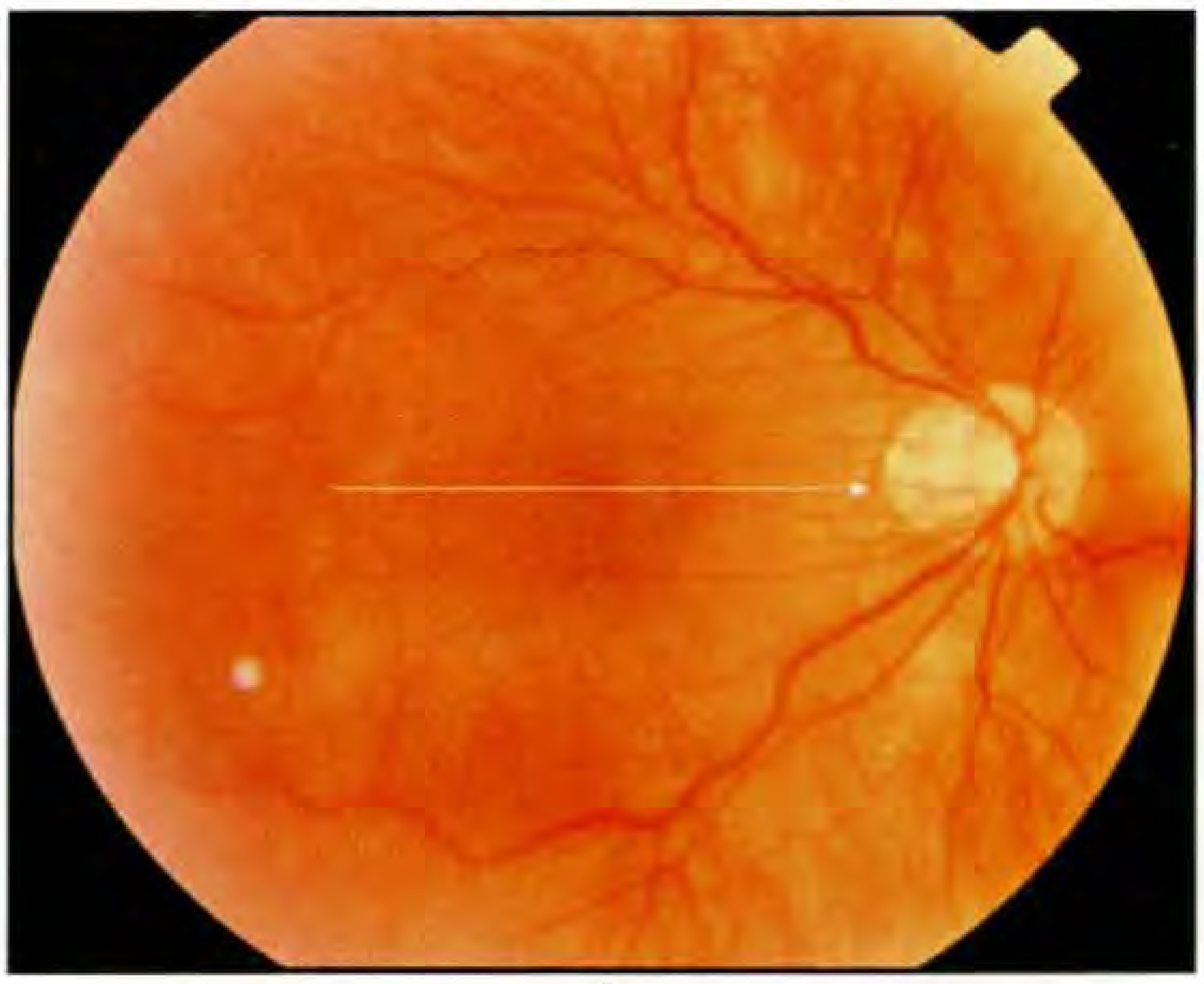

A

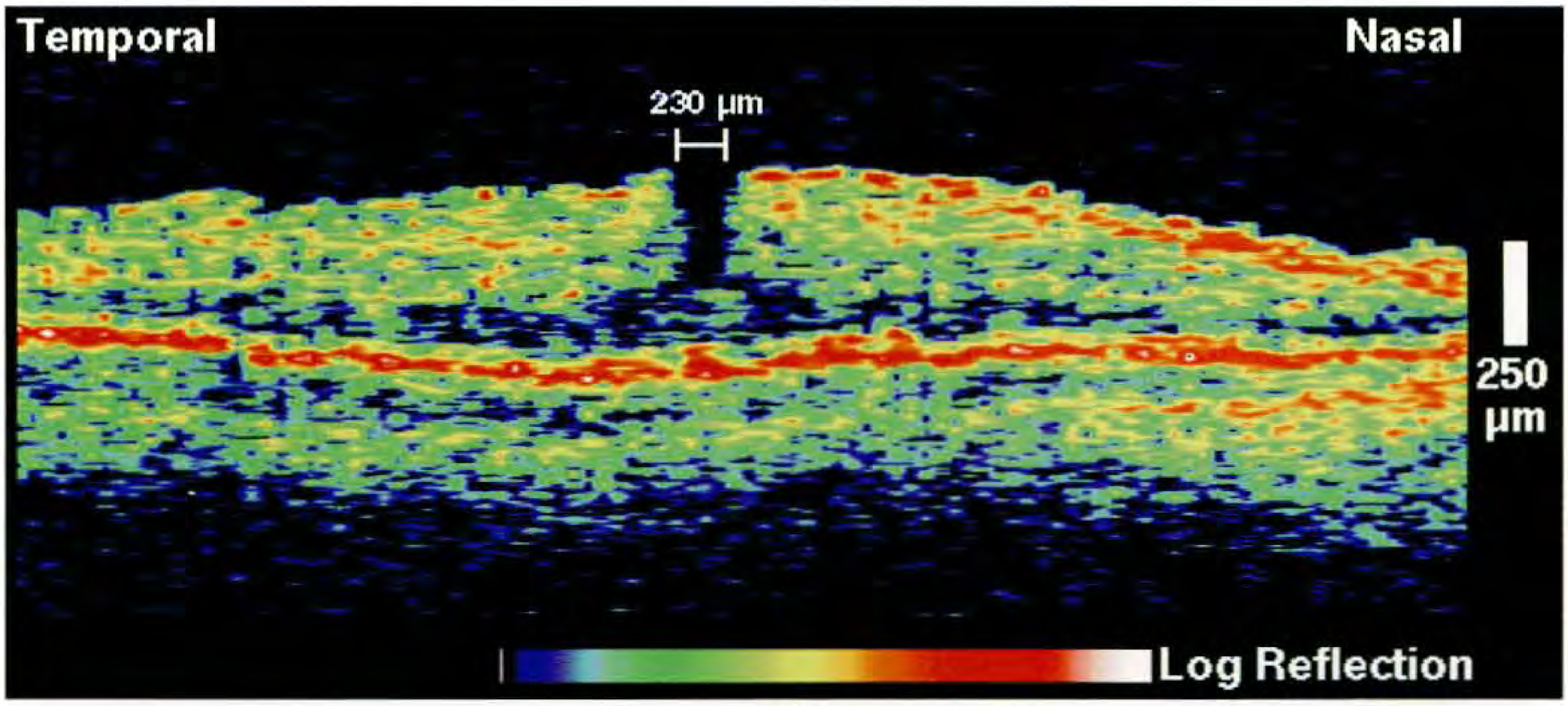

B

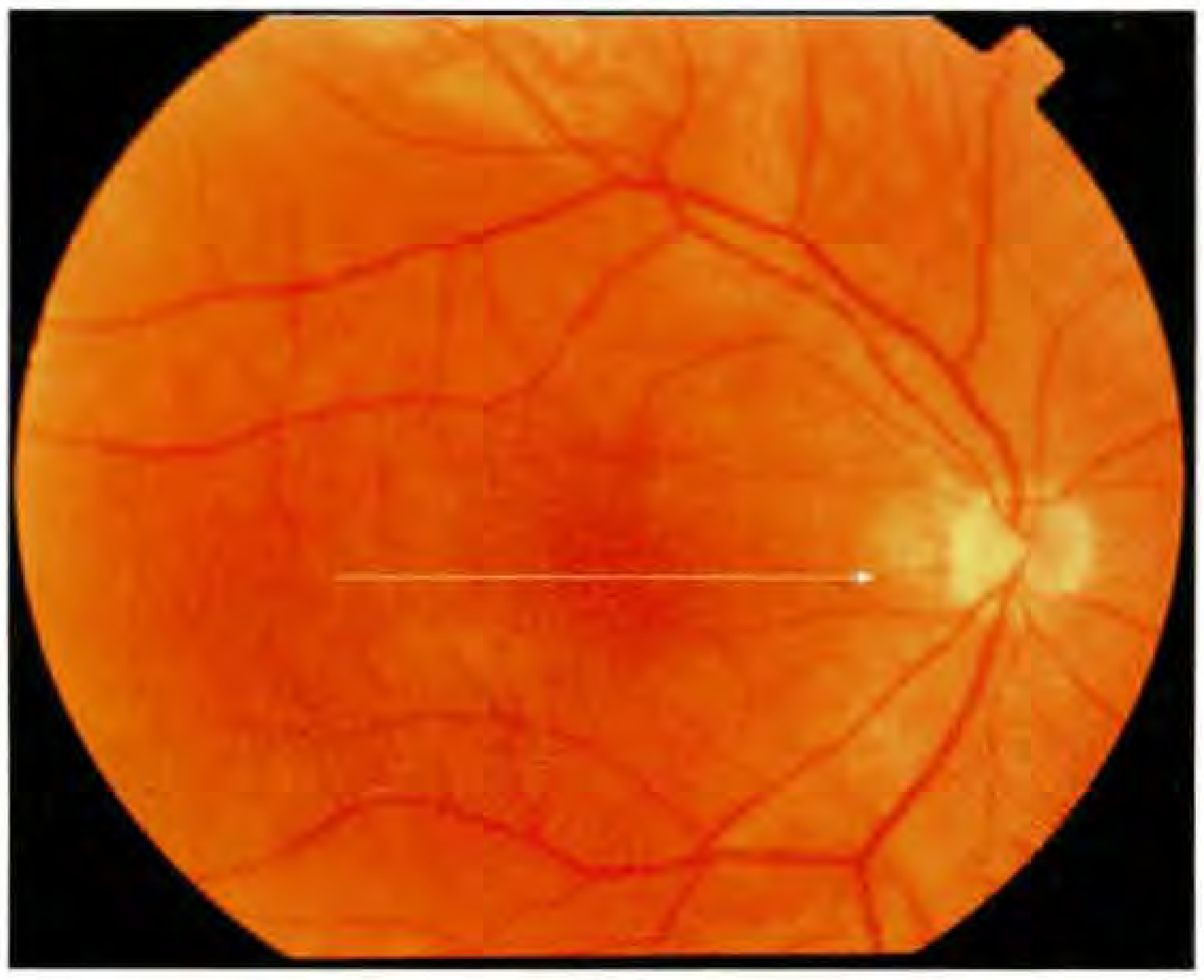

A

Case 3-23. Atypical Full-Thickness Macular Hole

Clinical Summary

A 46-year-old woman had suffered a posterior vitreous separation in her right eye five months earlier. Her vision had remained blurry after her flashes and floaters had resolved. On examination, her visual acuity was 20/70 in this eye. A small full-thickness macular hole was observed on contact lens examination (A).

Optical Coherence Tomography

A horizontal OCT section (B) confirmed a small full-thickness hole with a characteristic anvil shape and mild surrounding macular edema. The minimum width of the hole measured only 140 µm on the image. The finding was of interest since the posterior vitreous detachment definitely preceded the development of the hole.

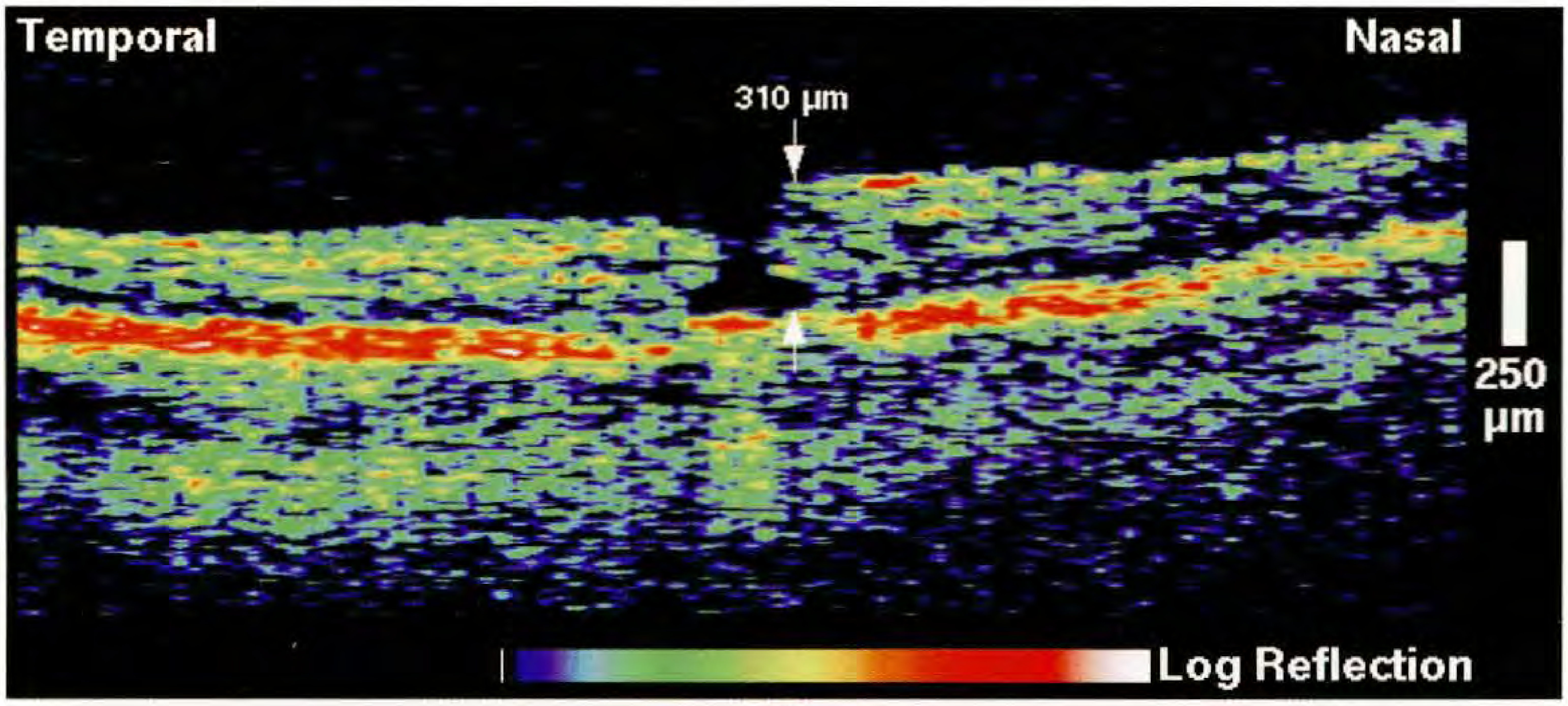

B

Case 3-24. Vitreomacular Traction

Clinical Summary

A 55-year-old woman with a history of panuveitis of undetermined etiology in both eyes reported sharp pains in each eye without aches or photophobia. Slit-lamp examination (A) of the right eye characterized an epiretinal membrane in the macula with a pseudohole or foveal cyst. Hypertrophy of the pigment epithelium was noted in the midperiphery, but there was no vasculitis.

Optical Coherence Tomography

A vertical OCT section (B) through the macula showed a tuft of vitreoretinal traction disrupting the foveal architecture. A weak reflection anterior to the retina corresponded to the posterior hyaloid. A large, optically transparent intraretinal region in the fovea and superior macula indicated cystic fluid accumulation.

A

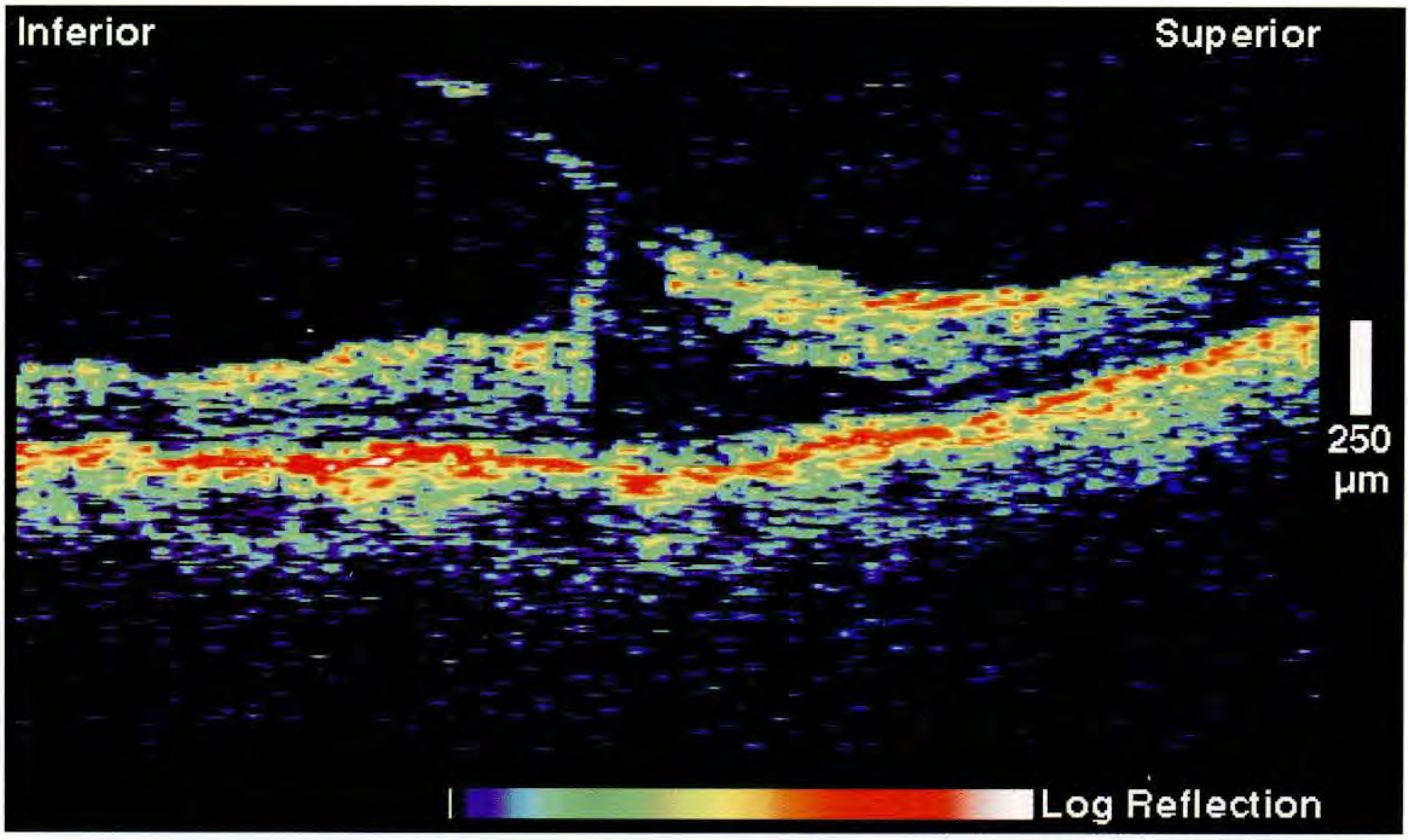

B

A

Case 3-25. Vitreomacular Traction Before and After Vitrectomy

Clinical Summary

An 83-year-old woman was referred for worsening vision in her left eye. Dilated fundus examination (A) revealed a very shallow, incomplete posterior vitrous separation and an area of thickened posterior hyaloid overlying the macula. A small epiretinal membrane was also noted. The patient's visual acuity in this eye was 20/200 which improved to 20/100 through a pinhole. The clinical diagnosis was vitreomacular traction syndrome with epiretinal membrane formation.

Optical Coherence Tomography

A linear OCT tomogram (B) acquired through the macula delineated a foveal disruption associated with an incomplete detachment of the posterior vitreous. The posterior hyaloid membrane appeared as two lightly reflective bands anterior to the retina which exhibited traction on the fovea. A thin membrane on the retinal surface was also observed temporal to the fovea consistent with the epiretinal membrane noted on clinical examination.

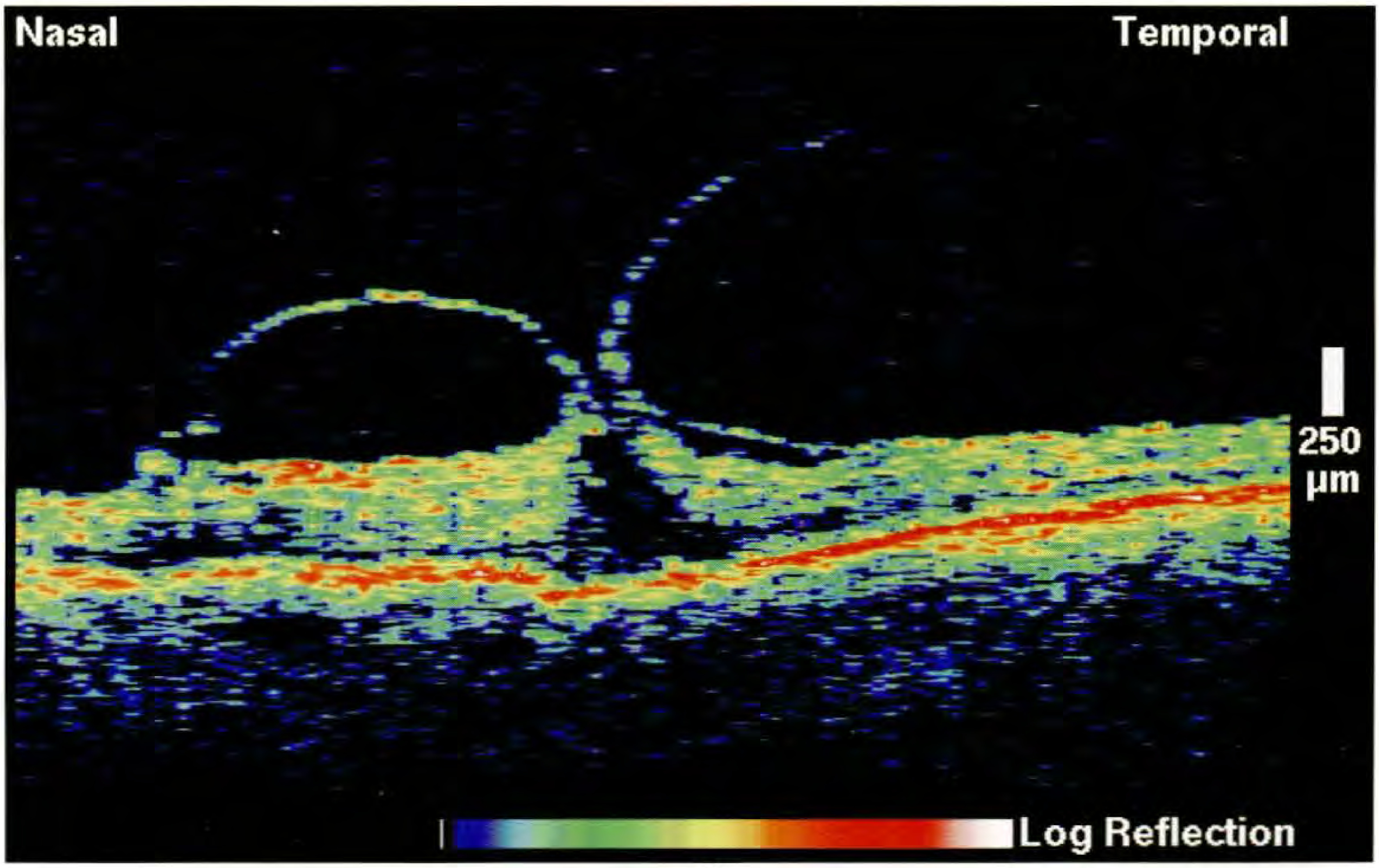

B

Case 3-25 continued

Follow-up Examination

The patient elected to undergo pars plana vitrectomy and membrane peeling in her left eye in attempt to improve vision. On follow-up examination one month after the operation, her visual acuity had declined to 20/250.

Follow-up Optical Coherence Tomography

A repeat OCT examination (C) showed the disappearance of the reflective strands corresponding to the posterior hyaloid membrane as a result of the vitrectomy. The disruption in the fovea, however, persisted and a large, non-reflective region was present in the outer fovea consistent with a retinal cyst. The epiretinal membrane was also still evident just temporal to the fovea where it was slightly separated from the neurosensory retina.

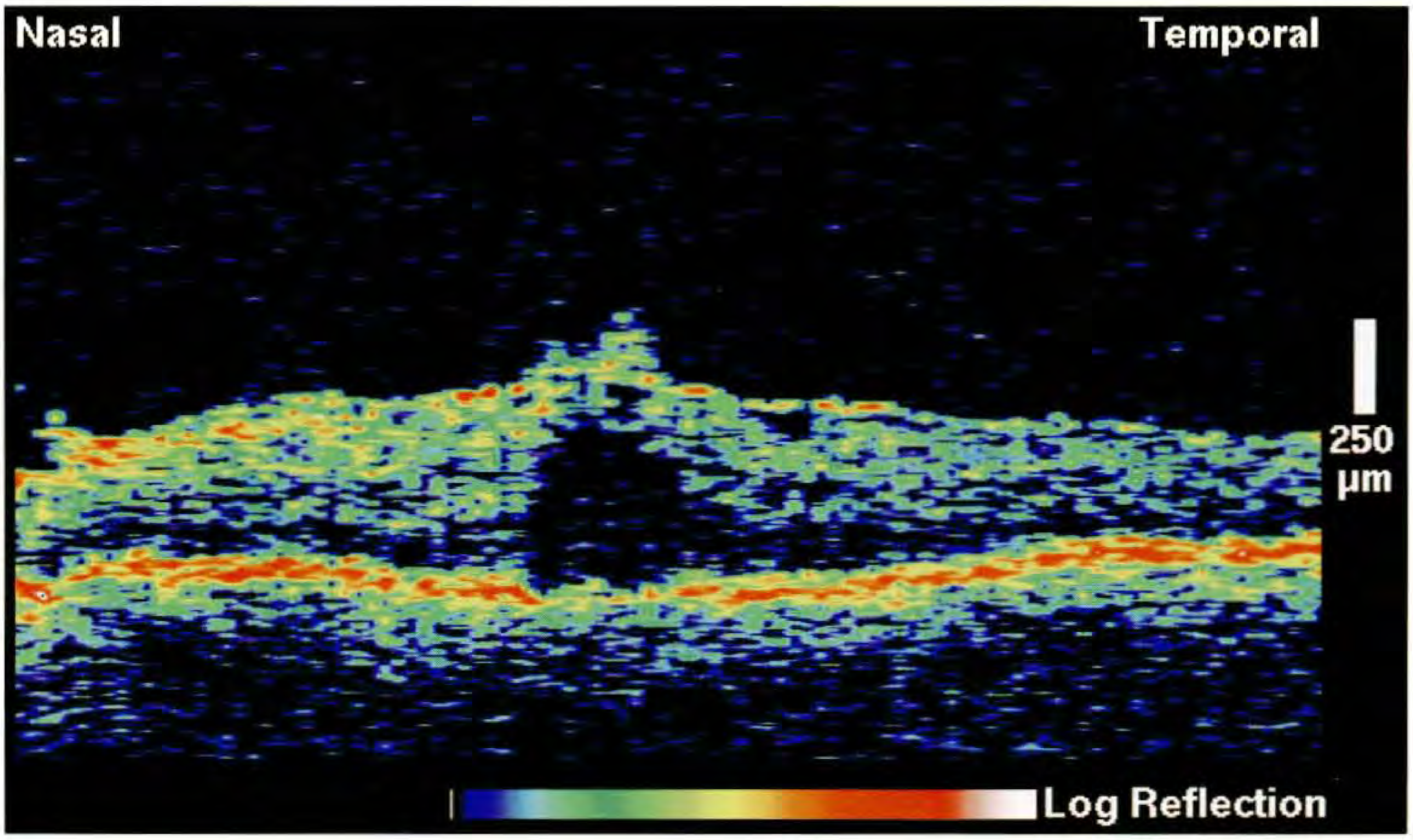

C

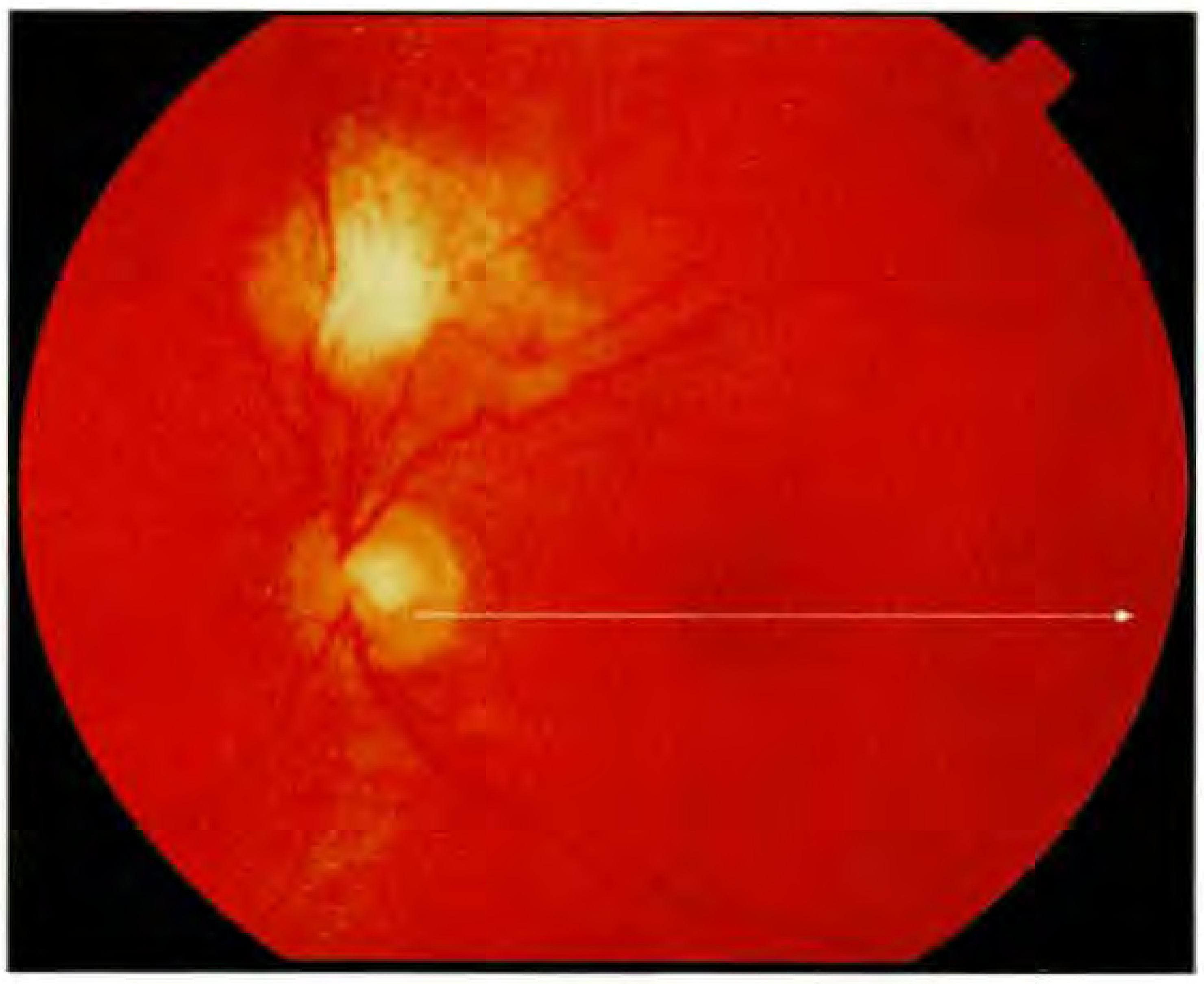

A

Case 3-26. Vitreoretinal Traction and Healed Macular Hole

Clinical Summary

A 83-year-old woman had a history of a macular hole and a total retinal detachment in her left eye that was treated with pars plana vitrectomy, scleral buckling, drainage of subretinal fluid, and fluid-gas exchange. On examination, the visual acuity in this eye was counting fingers. The retina appeared completely flat, the hole was closed, and there were some mild pigmentary changes in the macula (A).

Optical Coherence Tomography

An OCT image (B) through the central macula showed that the contour of the foveal pit was steepened nasally. Increased backscattering was observed from the nominally transparent photoreceptors in the fovea.

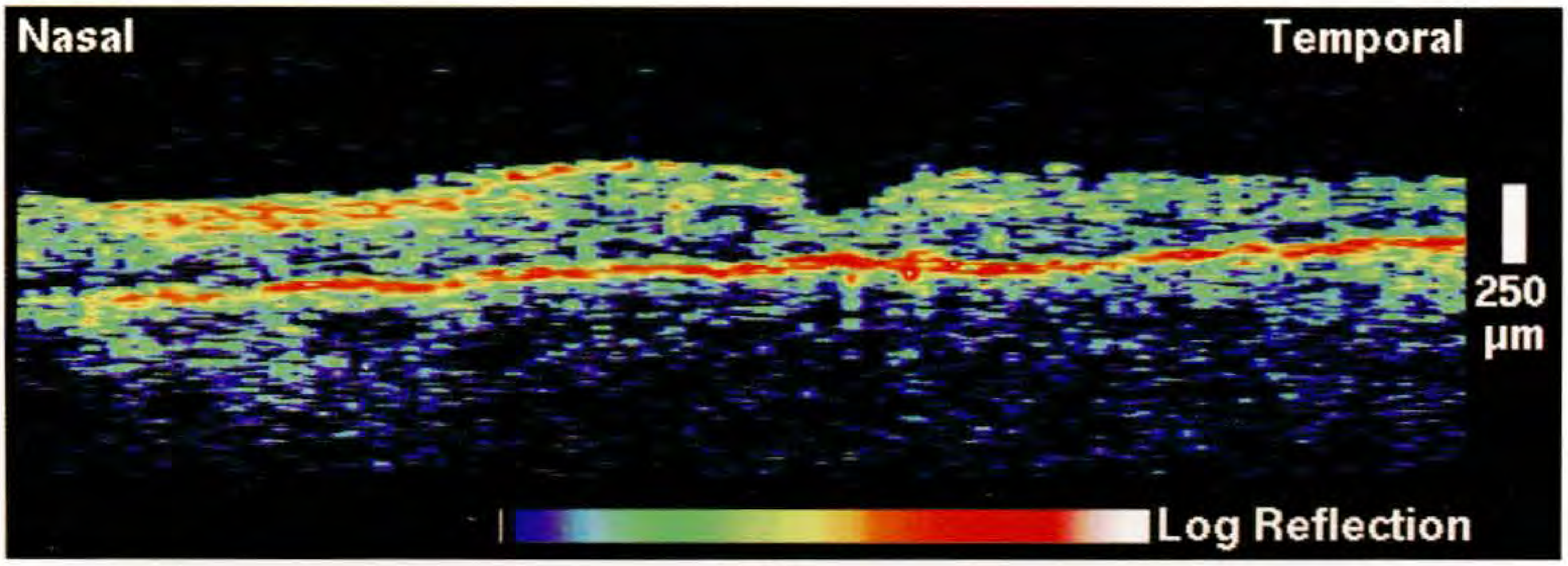

B

Case 3-26 continued

Clinical Summary

The right eye appeared normal on slit-lamp biomicroscopy (C) and no vitreous detachment was noted. The best corrected visual acuity was 20/40.

Optical Coherence Tomography

A horizontal OCT tomogram (D) delineated an extrafoveal detachment of the posterior vitreous and traction by the posterior hyaloid on the macula. The neurosensory retina directly beneath the detached vitreous was significantly thinned.

C

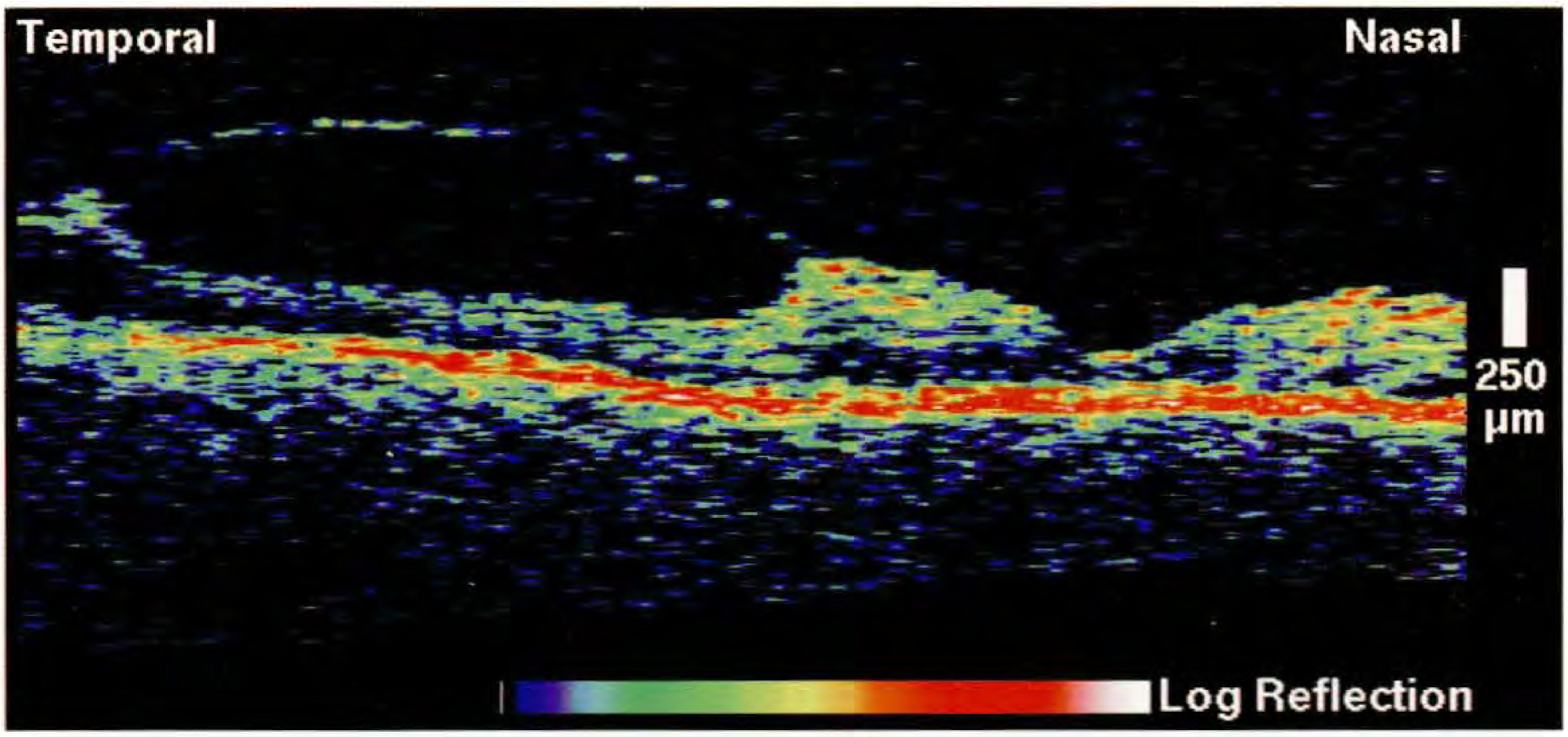

D

A

Case 3-27. Vitreomacular Traction

Clinical Summary

An 87-year-old woman with age-related macular degeneration had a visual acuity of 20/80 in her right eye (A). A partial posterior vitreous detachment was noted with an area of vitreous traction along the superotemporal vascular arcade.

Optical Coherence Tomography

A linear scan (B; white line on A) through the macula displayed retinal thickening and a large cyst in the fovea above an apparently intact photoreceptor layer. A reflective membrane appeared to be exhibiting traction on the superior macula. The high reflectivity of this membrane was more consistent with preretinal fibrosis than the posterior hyaloid. A second vertical tomogram temporal to the fovea (C; black line on A) demonstrated the vitreoretinal traction that was observed clinically.

B

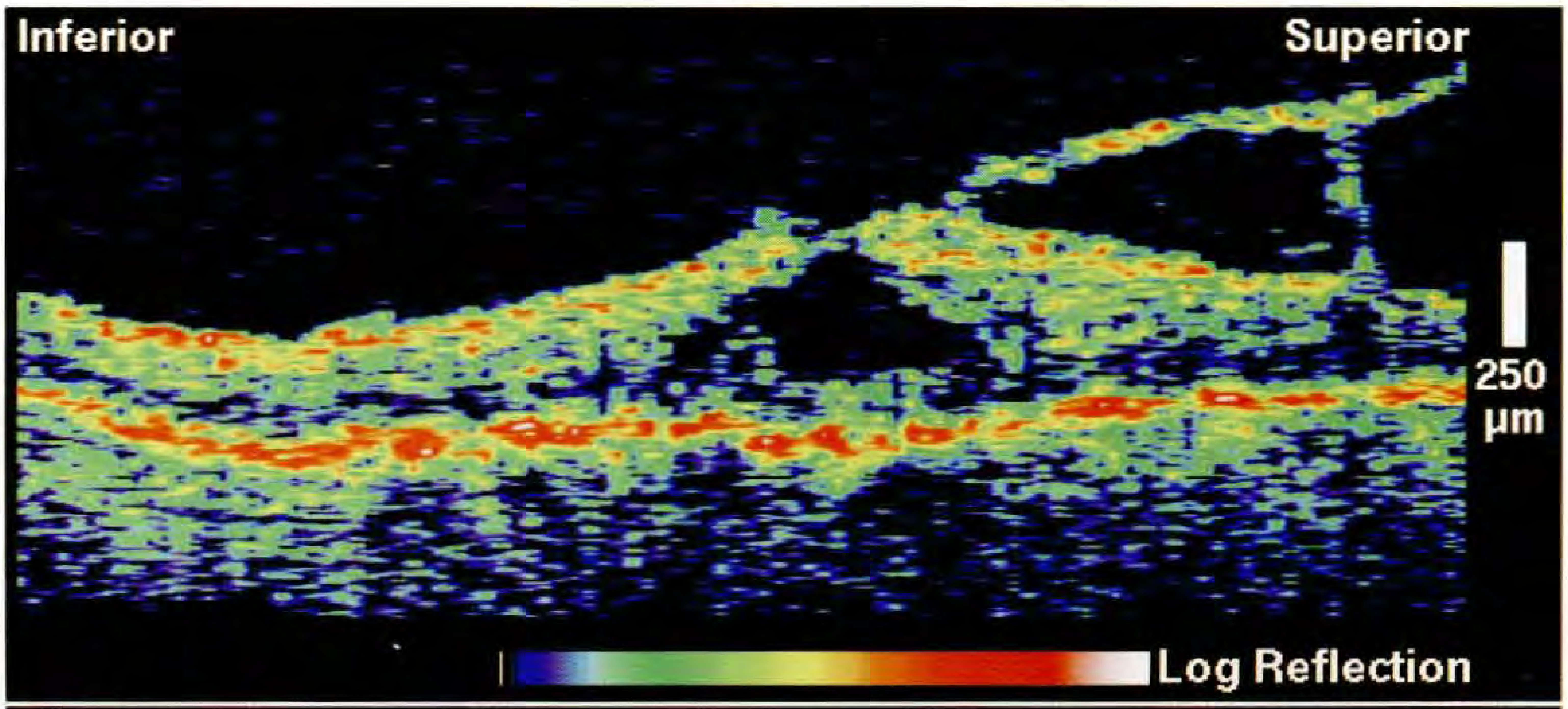

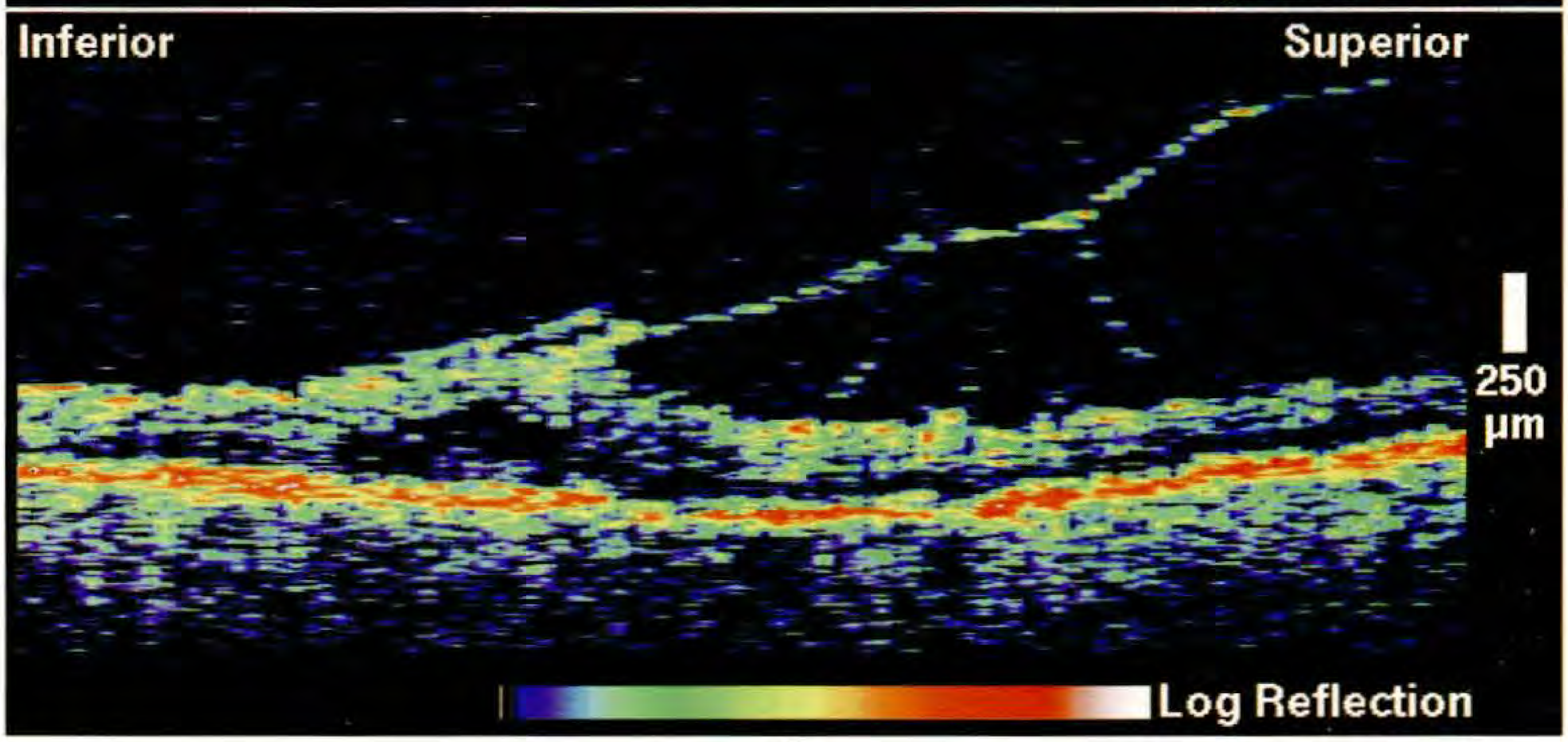

C

CHAPTER 4

Epiretinal Macular Membranes

Macular Pseudohole
Macular Edema
Retinal Traction

Current diagnostic techniques for epiretinal macular membranes include slit-lamp biomicroscopy and fluorescein angiography. OCT images are useful in confirming the diagnosis of faint, diaphanous membranes, and in providing a cross-sectional assessment of factors contributing to vision loss, such as membrane opacity, retinal distortion or tractional detachment, and macular edema. The amount of foveal distortion, detachment, or edema provides an indication of the severity of the membrane. The thickness and reflectivity of the membrane on the OCT tomogram gives information on membrane opacity.

Many studies have attempted to define prognostic indicators, such as membrane thickness or the presence of pre-operative cystoid macular edema, to predict eventual visual outcome after epiretinal membrane surgery [1-3]. OCT provides a means to evaluate the cross-sectional characteristics of an epiretinal membrane, allowing a quantitative measurement of retinal thickness, membrane thickness, and the separation between the membrane and inner retina. Retinal thickness has been shown to be a better correlate of visual acuity than fluorescein leakage in patients with various causes of macular edema [4] and might be a predictor of surgical success in patients with an epiretinal membrane. The adhesiveness of the membrane to the retinal surface might also be a prognostic factor. OCT can image small separations of an epiretinal membrane from the retinal surface with high resolution.

OCT is effective in distinguishing macular pseudoholes from ophthalmoscopically similar lesions such as full-thickness macular holes and macular cysts [5,6]. A macular pseudohole associated with an epimacular membrane displays a steepened foveal pit contour on OCT simulating a full-thickness hole, but with retinal tissue at the base of the hole. The membrane is often tightly adherent to the retinal surface and not readily distinguishable; however, it may exhibit increased backscattering compared to the underlying tissue.

An epiretinal membrane must be distinguished on OCT from a detached posterior face which also appears as a reflective band anterior to the retina. The posterior hyaloid, however, often has a weak, patchy reflection that is usually thinner than the reflection originating from an actual preretinal membrane.

A

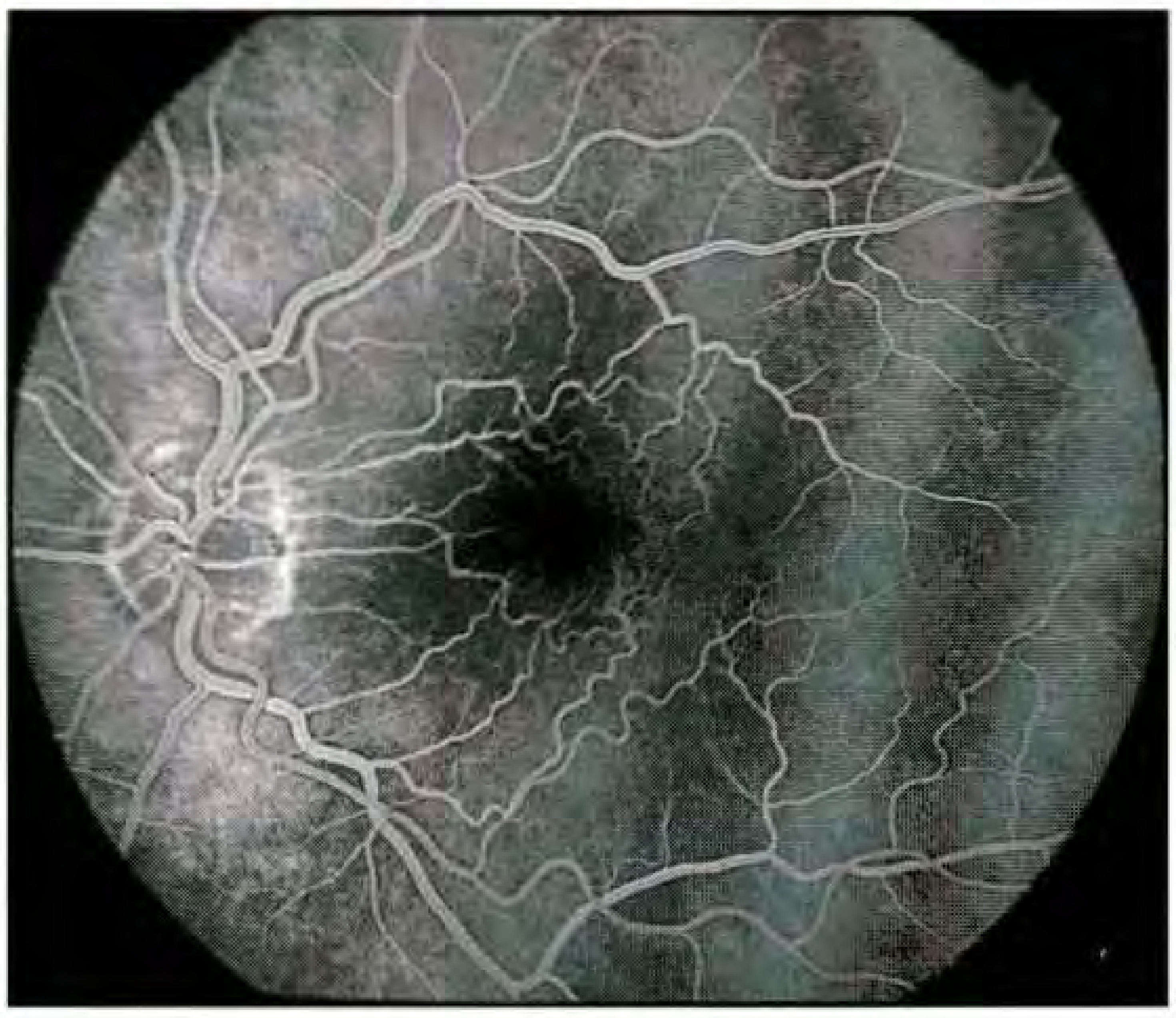

B

Case 4-1. Macular Pseudohole

Clinical Summary

A 75-year-old man was referred for evaluation of a macular abnormality resembling a macular hole in his left eye. He had previously undergone successful cataract surgery in this eye and his visual acuity was 20/25. Dilated fundus examination (A) revealed an oval shaped region in the fovea ophthalmoscopically similar to a hole, a mild epiretinal membrane, and some tortuousity in the papillomacular bundle. Fluorescein angiography (B) was normal except for a small amount of late leakage in the perifoveal area.

Optical Coherence Tomography

OCT examination (C) demonstrated an abnormally steep foveal contour resembling a partial thickness hole with a diameter of approximately 500 µm. The minimally reflective outer retinal layer corresponding to the retinal photoreceptors appeared intact throughout the image, ruling out a full-thickness macular hole. A significant increase in retinal thickness was noted in the macula, reaching a maximum of 570 µm in the tomogram. The epiretinal membrane was not clearly distinct from the neurosensory retina in the OCT image, presumably because of its tight apposition with the inner retina.

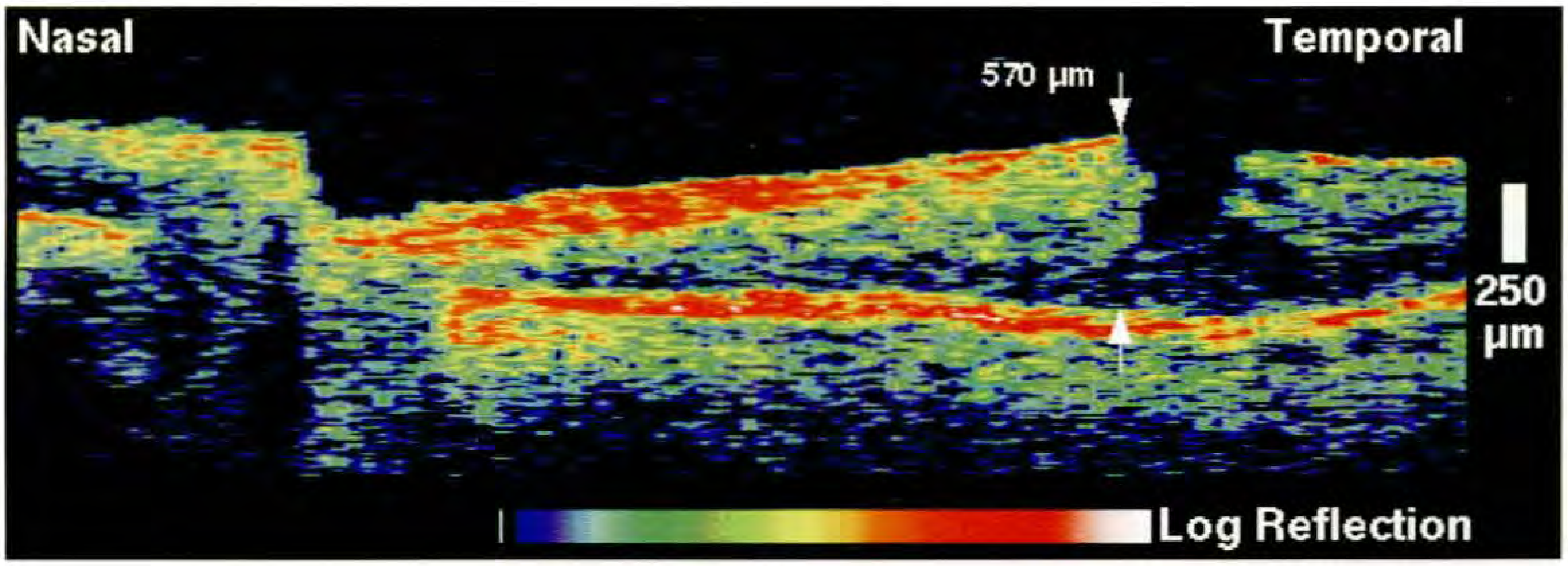

C

Case 4-2. Macular Pseudohole

Clinical Summary

An 82-year-old man had a persistent epiretinal membrane in the right eye, with a visual acuity of 20/80. Five years earlier he had undergone treatment with pars plana vitrectomy and membrane peeling. Dilated ophthalmoscopy (A) showed a reproliferation of the membrane and an associated central defect consistent with a macular pseudohole. Fluorescein angiography (B) demonstrated early hyperfluorescence with fading in the late phase consistent with a window defect.

Optical Coherence Tomography

An OCT tomogram (C) obtained through the pseudohole showed a lesion resembling a macular hole with an inner diameter of approximately 650 µm. The presence of retinal tissue at the base of the hole, however, confirmed the clinical diagnosis of epimacular membrane and an associated pseudohole. The outer neurosensory retinal tissue within the pseudohole appeared condensed, exhibiting reduced thickness and increased backscattering compared to the adjacent photoreceptors. Minimal retinal thickening was observed in the surrounding tissue, which reached a maximum of 470 µm in the image. The epiretinal membrane was not distinctly visible in the tomogram and was most likely tightly adherent to the inner retinal surface.

A

B

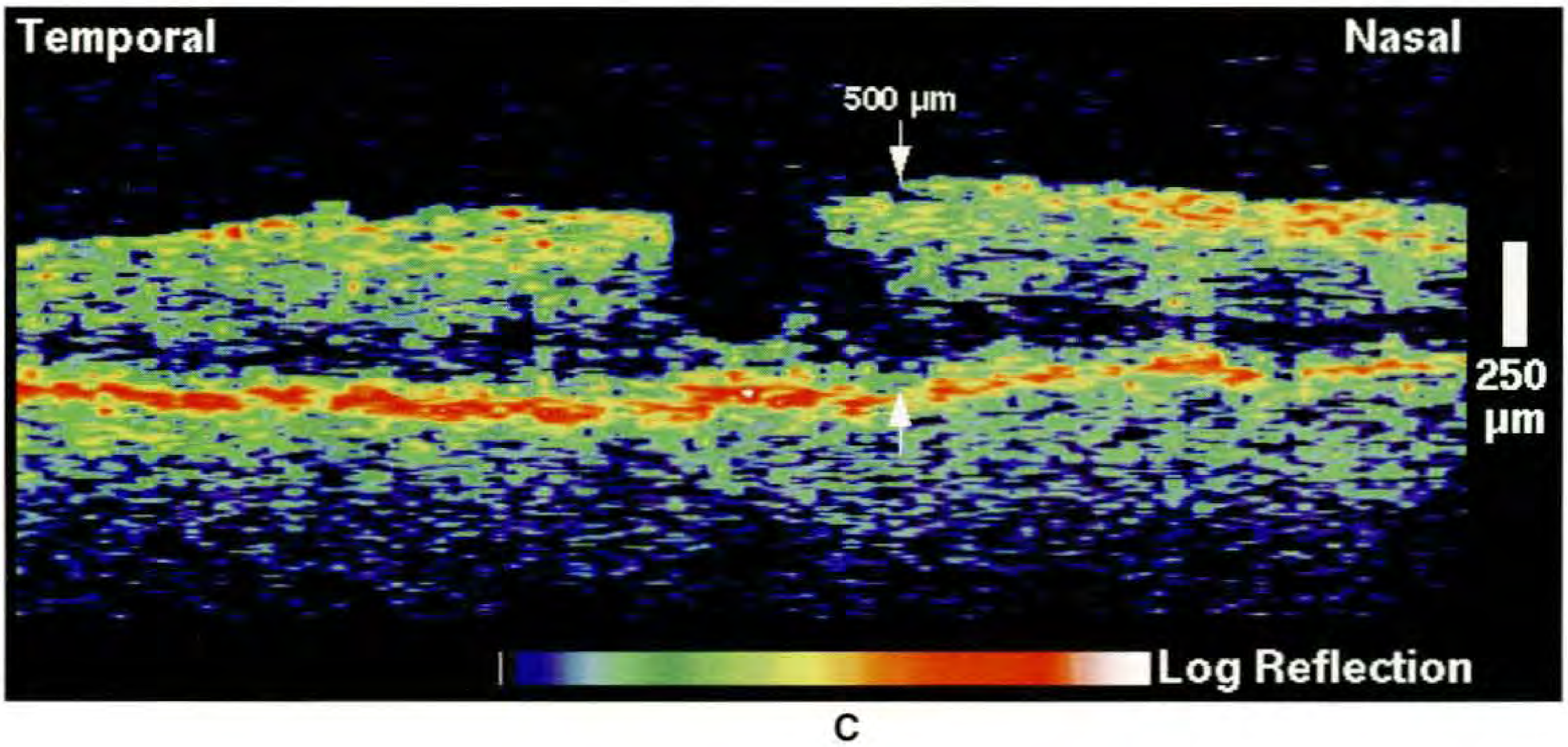

C

A

Case 4-3. Epiretinal Membrane and Macular Pseudohole

Clinical Summary

A 63-year-old man had a retinal lesion resembling a macular hole in his left eye (A). His visual acuity in this eye was 20/60.

Optical Coherence Tomography

A horizontal OCT tomogram (B) was acquired through the fovea. No full-thickness loss of retinal tissue was observed; rather the change in the contour of the foveal pit suggested a macular pseudohole. An epiretinal membrane appeared to be tightly adherent to the retina and was only distinctly visible temporally in the tomogram where it was either separated from the retinal surface or more brightly backscattering than the underlying nerve fiber layer. Diffuse macular thickening was noted.

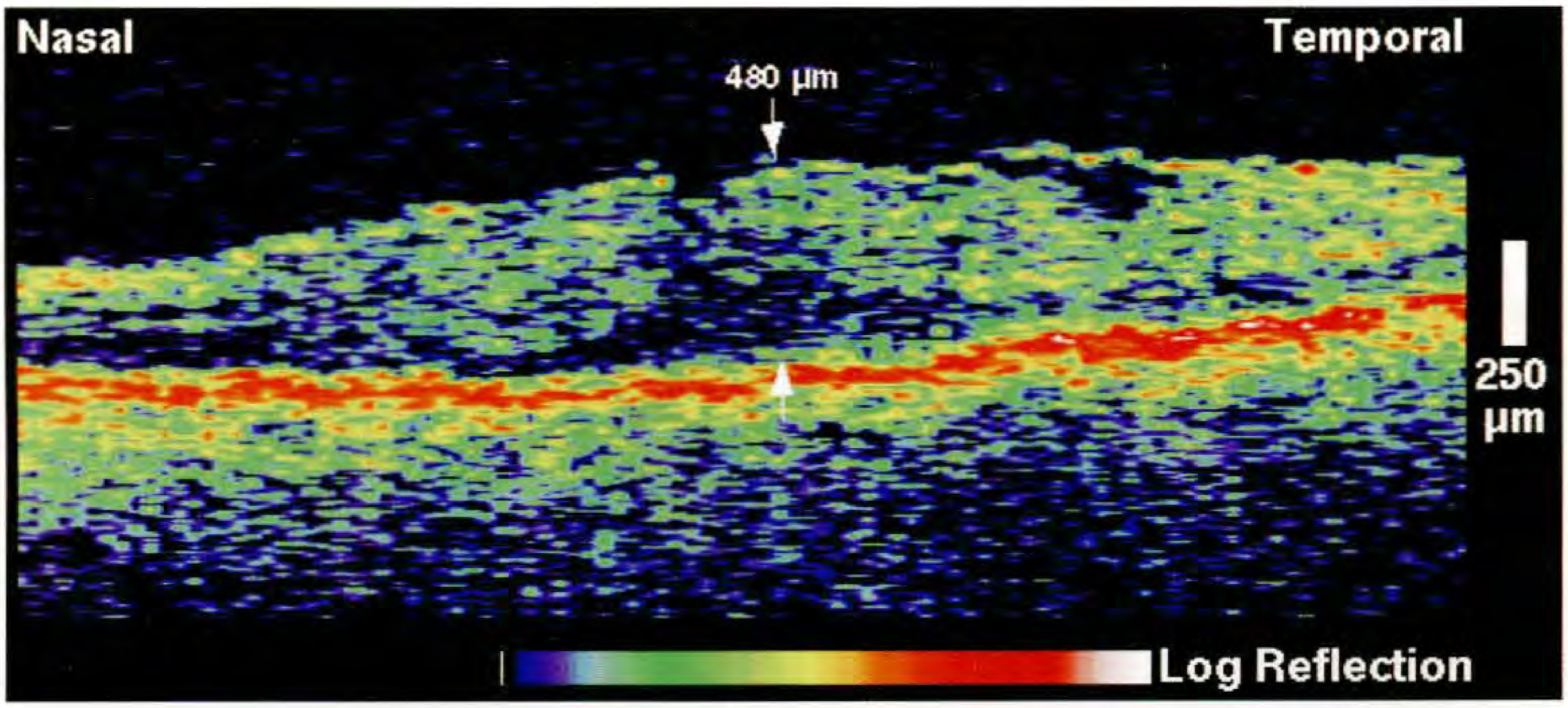

B

Case 4-4. Epiretinal Membrane with Schisis and Macular Pseudohole

Clinical Summary

A 66-year-old woman was evaluated for an epiretinal membrane in her right eye. On examination, her visual acuity in this eye was 20/60 and slit-lamp ophthalmoscopy (A) revealed a deep pseudohole in the central macula. Fluorescein angiography (B) showed increased tortuousity of the retinal vasculature temporally, and straightening of the vessels nasal to the optic disc. Very mild late leakage was noted surrounding the macula.

Optical Coherence Tomography

An OCT image through fixation (C) showed significant retinal thickening due to the development of a schisis cavity within the retina. The epiretinal membrane was visible directly in the fovea (arrows) where it was separated from the contour of the foveal depression. The membrane was also distinguishable from the neurosensory retina temporally in the image where it had higher reflectivity than the underlying retina.

A

B

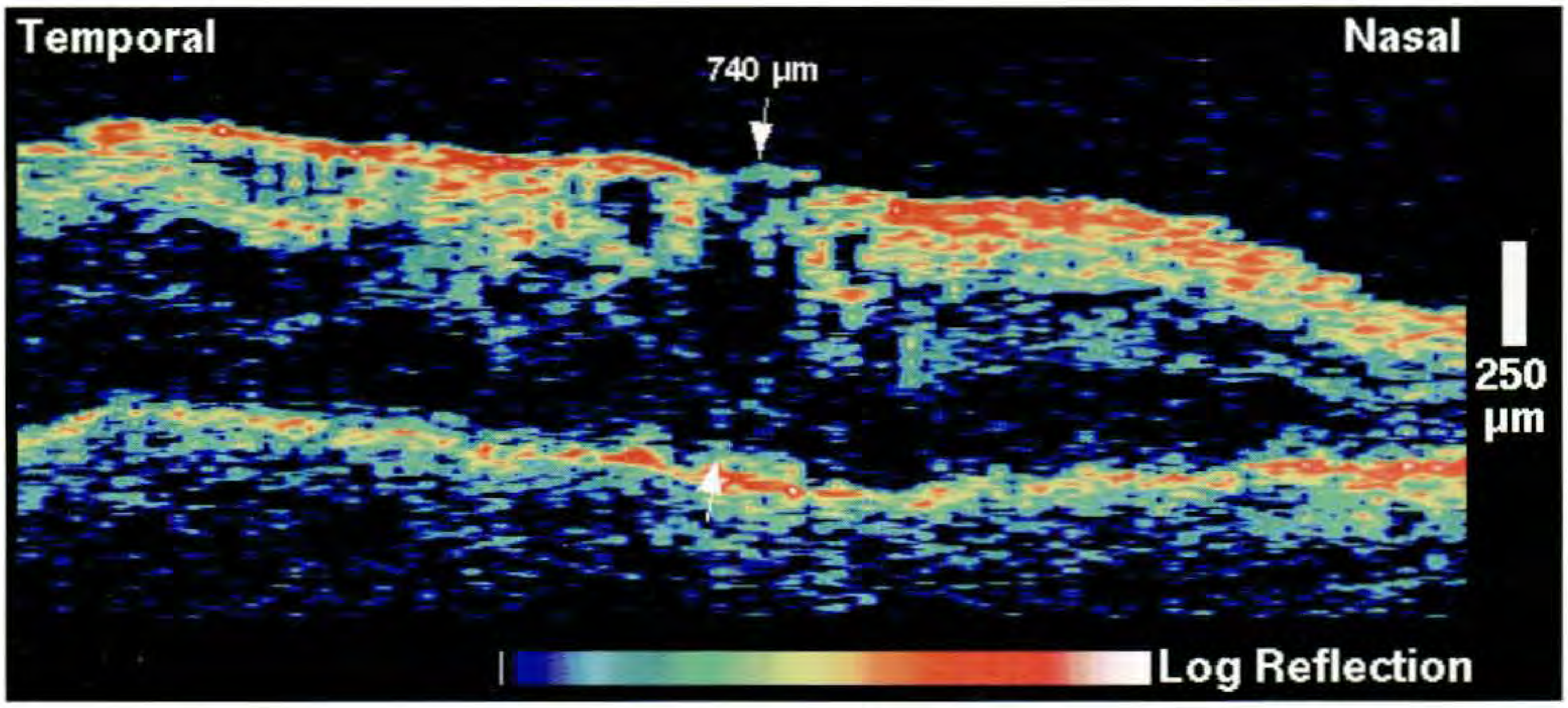

C

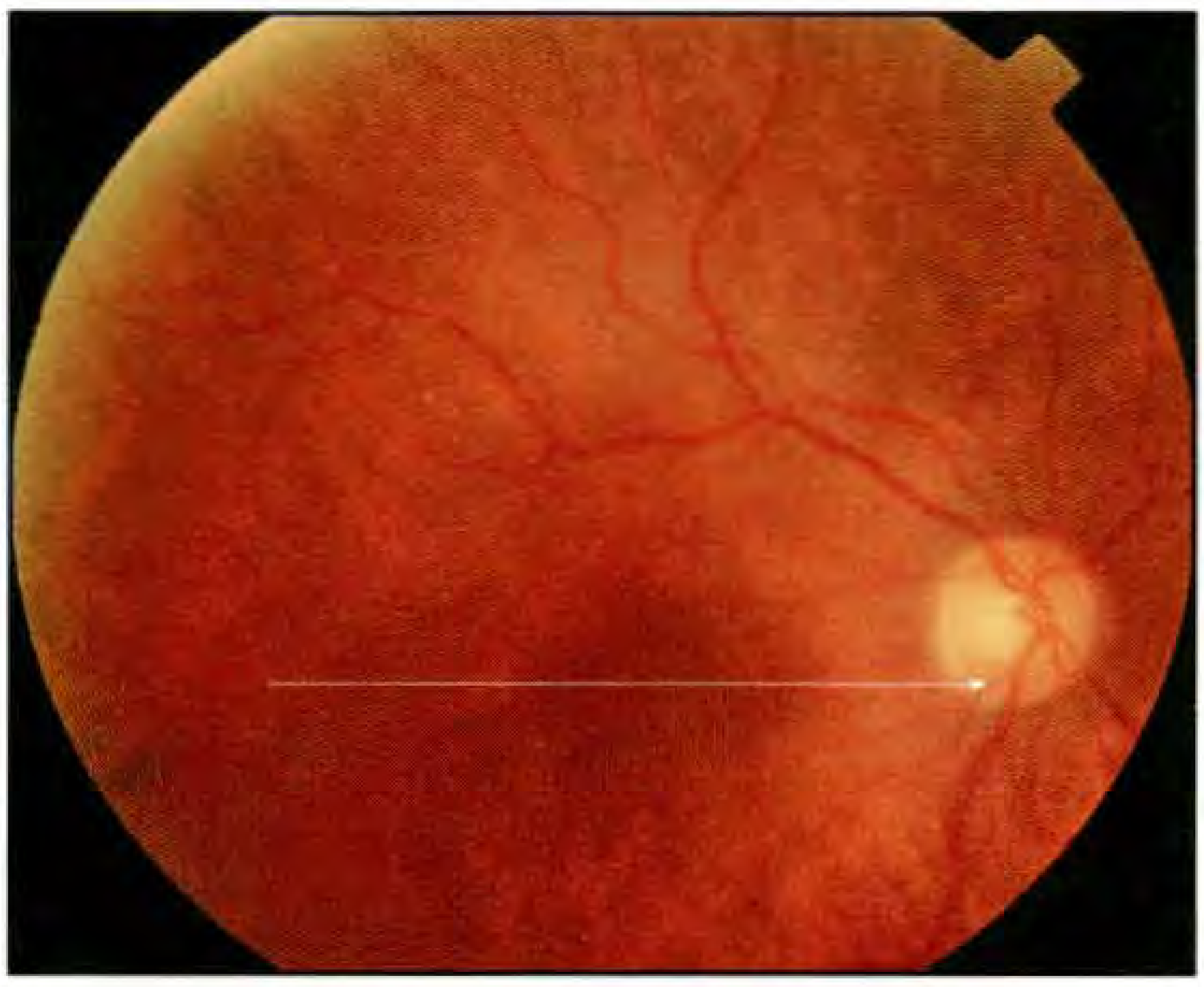

A

Case 4-5. Epiretinal Membrane and Macular Pseudohole

Clinical Summary

A 69-year-old woman noted decreased vision and metamorphopsia in her right eye following a car accident. Her visual acuity in this eye was 20/40. Dilated fundus examination (A) revealed a posterior vitreous separation and a mild epiretinal membrane in the macula with an associated pseudohole.

Optical Coherence Tomography

A horizontal OCT tomogram (B) exhibited an abnormally steep foveal contour with an intact outer retinal layer consistent with a pseudohole. The epiretinal membrane was tightly attached to the retina and visible as a very thin reflection nasal to the fovea (arrow). The surrounding macula was thickened, more nasally than temporally, due to traction by the membrane.

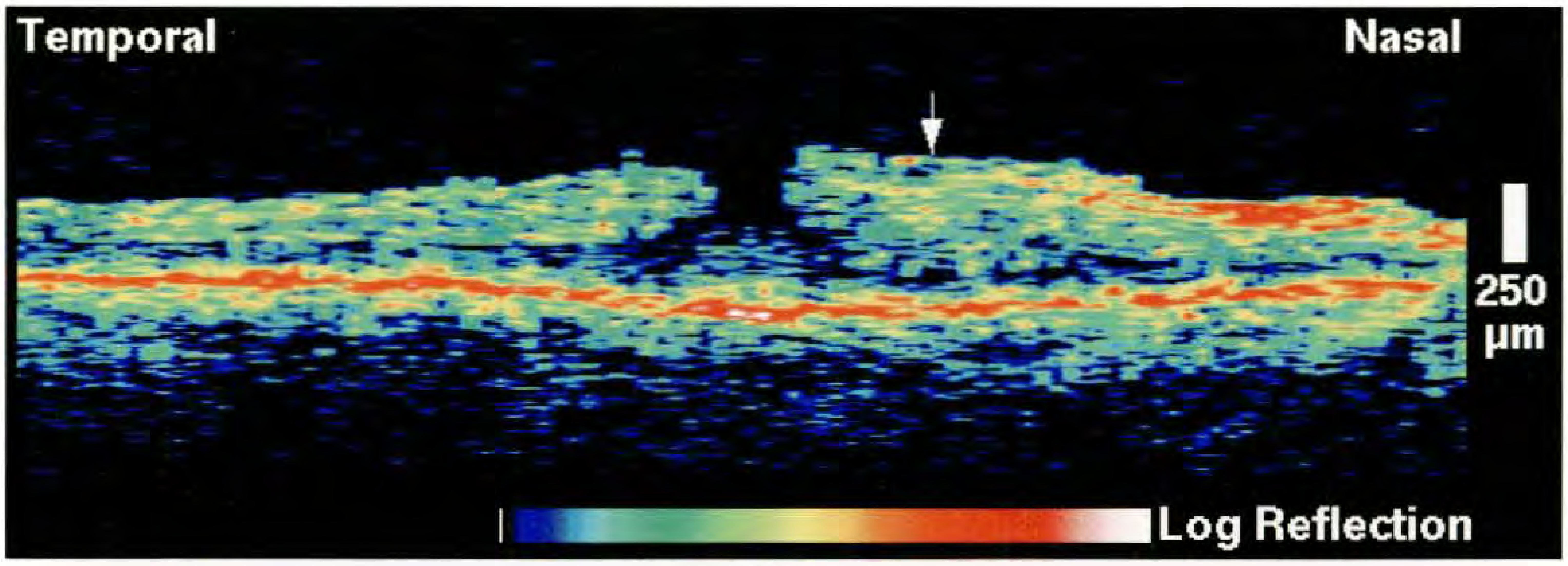

B

Case 4-6. Epiretinal Membrane and Macular Pseudohole

Clinical Summary

A 74-year-old man had an epiretinal membrane and a macular pseudohole in his right eye associated with a visual acuity of 20/40 (A).

Optical Coherence Tomography

OCT (B) showed an altered foveal pit contour and increased retinal thickness; however the membrane was difficult to identify because its reflectivity was indistinguishable from the normal retinal nerve fiber layer. The inner margin of the foveal pit had a well-defined reflective boundary suggesting that the membrane was tightly adherent to Henle's fiber layer in this region.

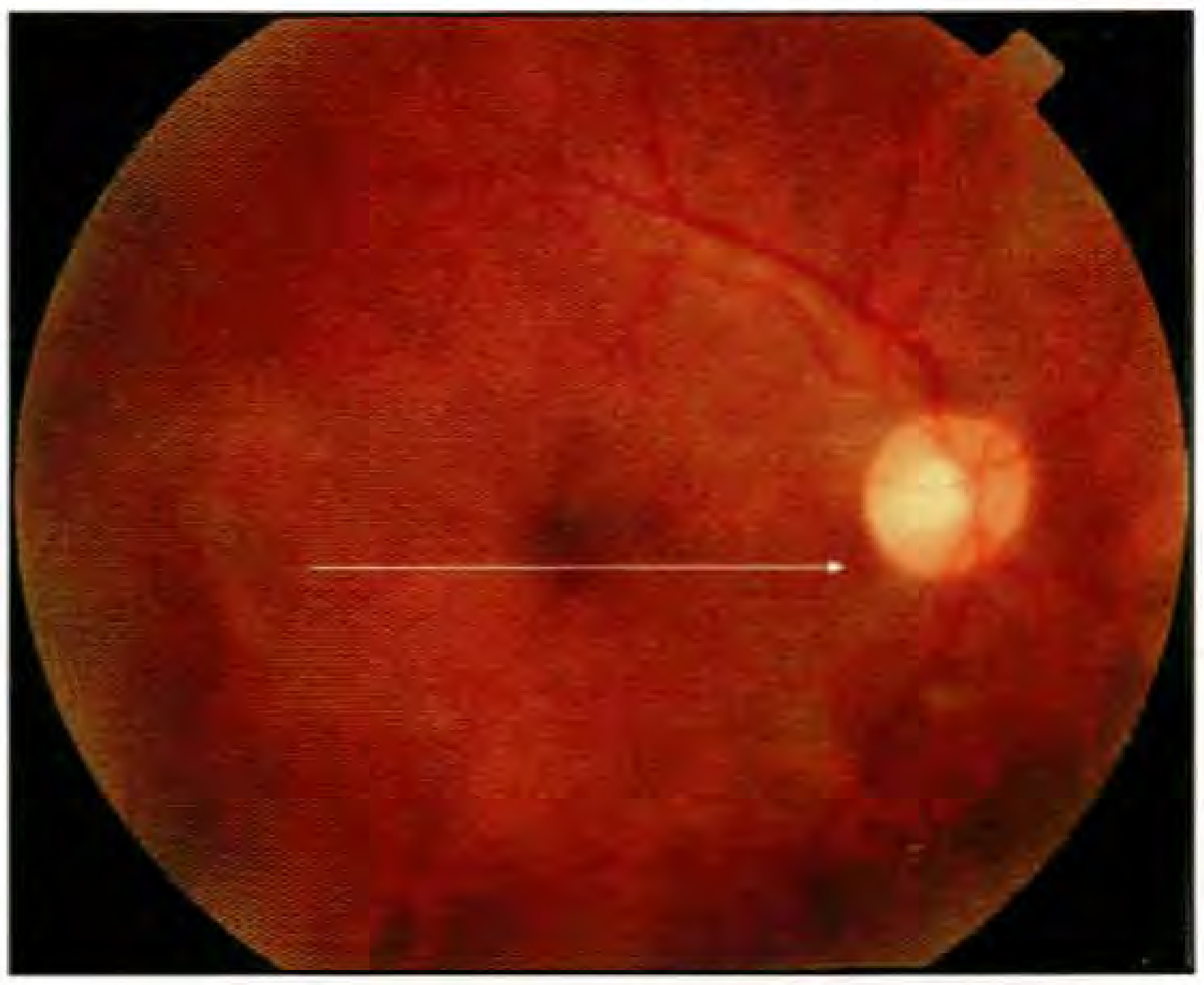

A

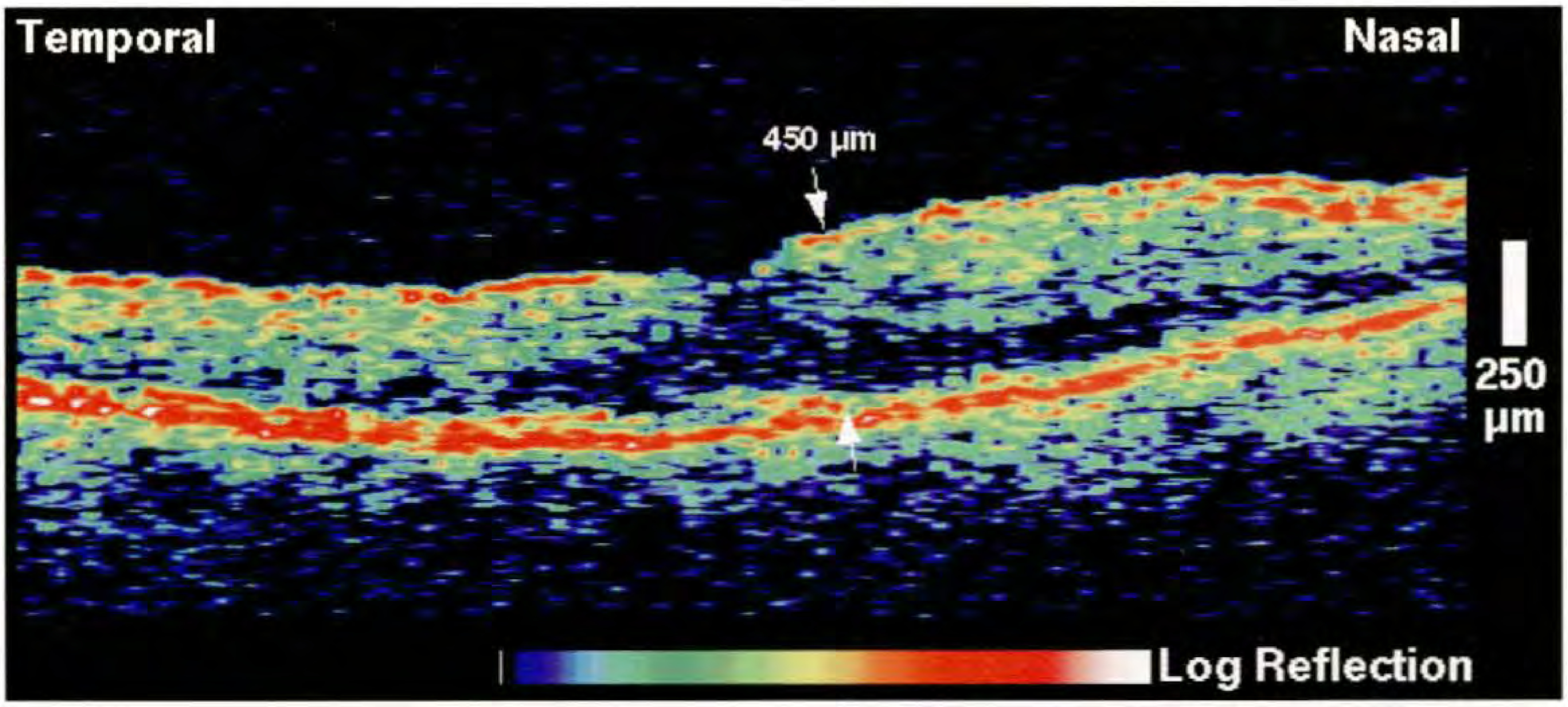

B

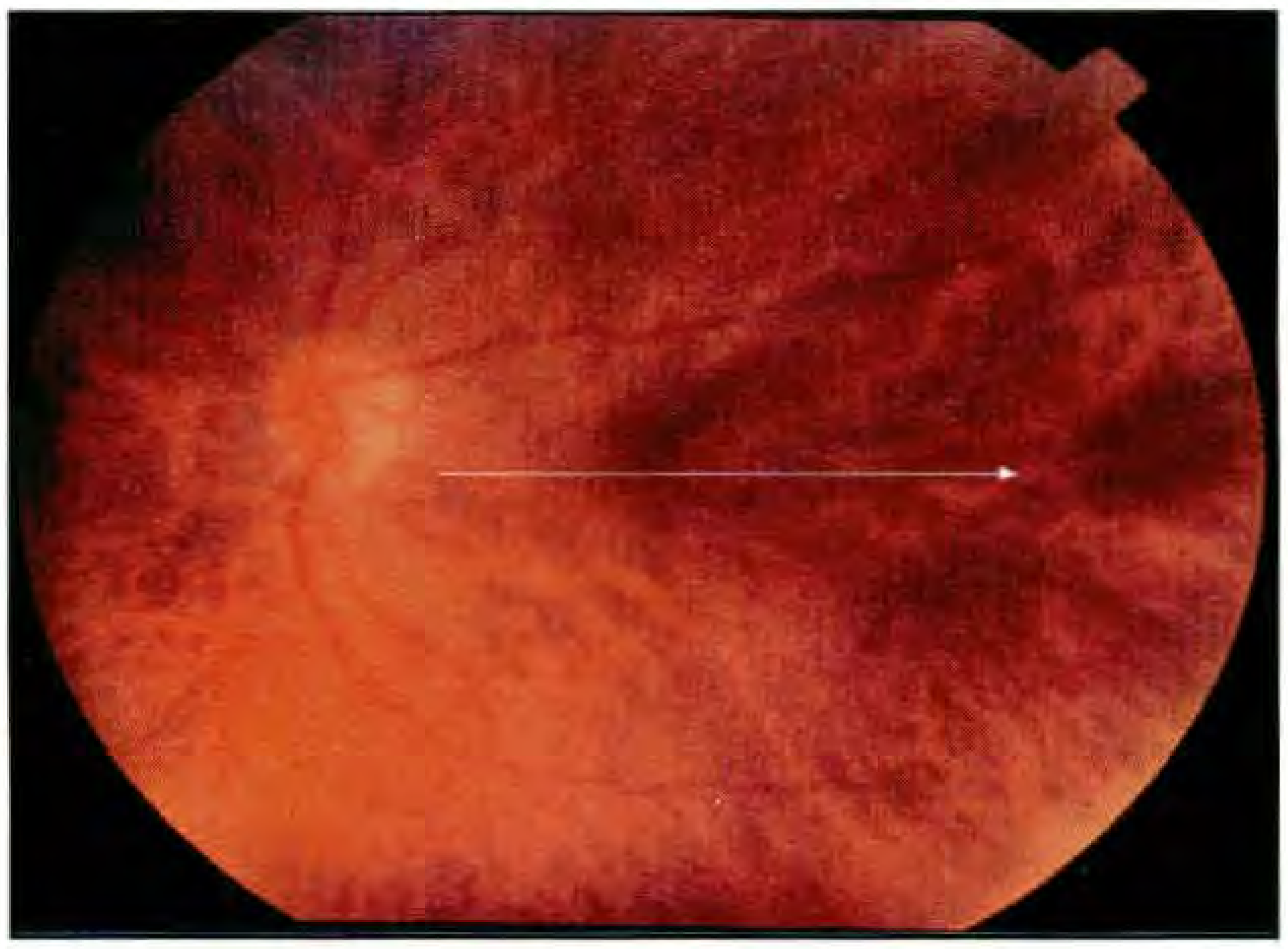

A

Case 4-7. Epiretinal Membrane

Clinical Summary

An 84-year-old man had a visual acuity of 20/200 in his left eye associated with the clinical diagnosis of an epiretinal membrane in the macular area. Dilated ophthalmoscopy (A) showed straightening of the retinal arterioles superior to the fovea.

Optical Coherence Tomography

The OCT scan (B) showed the presence of a highly reflective membrane on the surface of the retina. The neurosensory layer of the fovea appeared to be disrupted, and small areas of minimal backscattering were observed within the neurosensory retina corresponding to macular edema. A vitreal displacement of the choroid and retina was also apparent, either due to the presence of macular edema or traction of the epiretinal membrane on the retina.

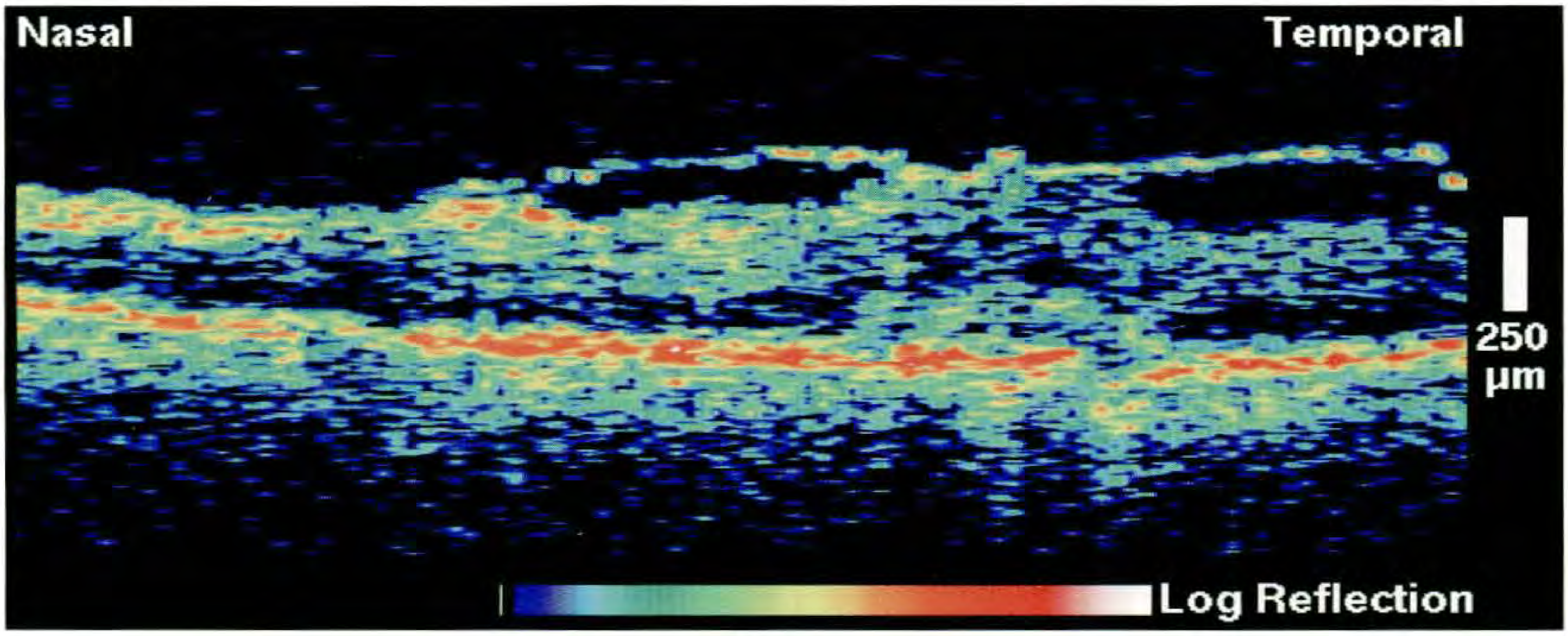

B

Case 4-8. Epiretinal Membrane and Macular Edema

Clinical Summary

A 75-year-old man had macular edema associated with an epiretinal membrane in his right eye (A). His visual acuity was 20/100 through a pinhole.

Optical Coherence Tomography

A vertical OCT tomogram (B) was acquired through the macula. The membrane appears in the image as a thin, reflective band just anterior to the neurosensory retina and attached to the macula. A moderately sized, non-reflective cyst was visible directly in the fovea and a diffuse increase in retinal thickness was noted which reached a maximum of 480 μm in the fovea.

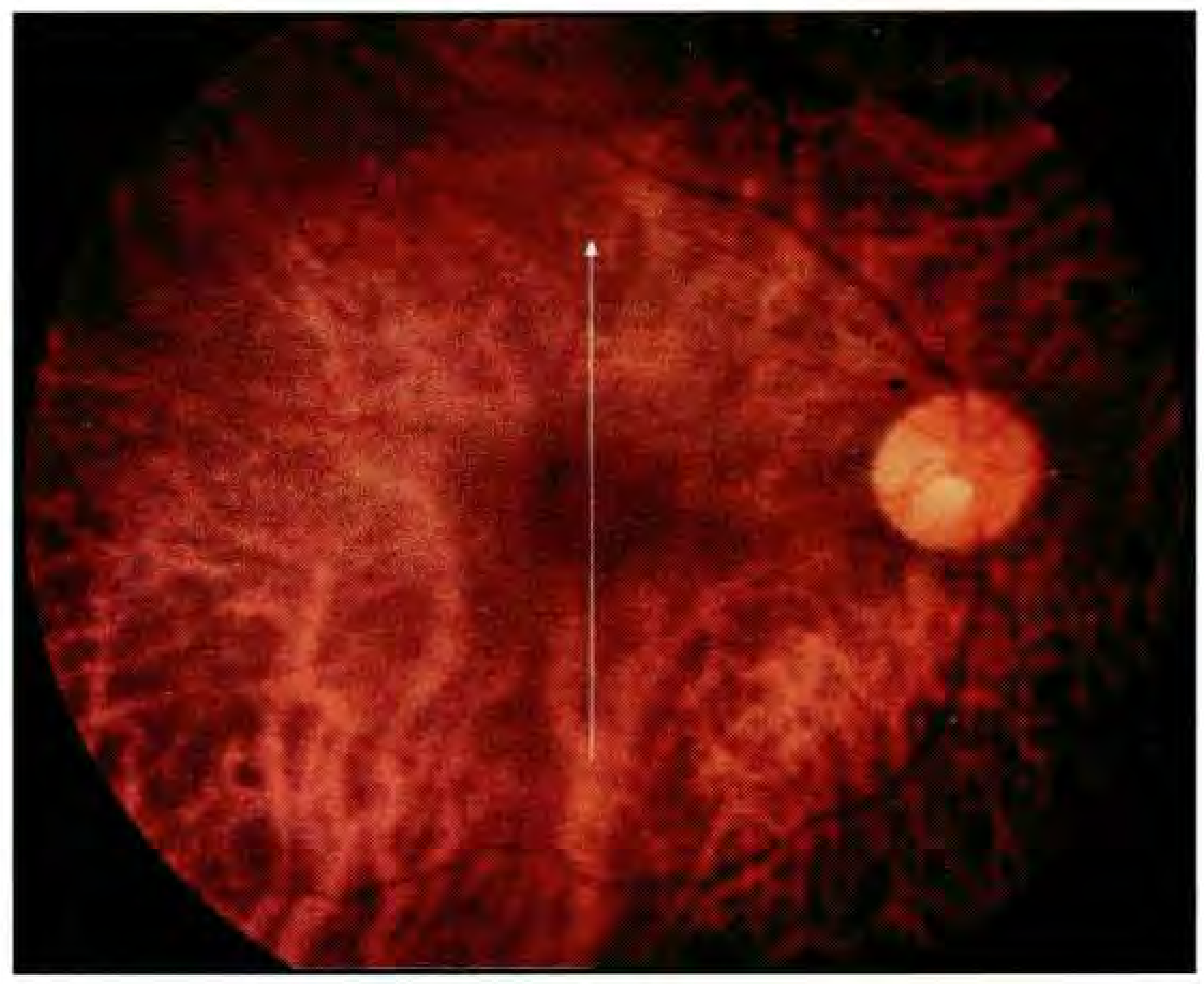

A

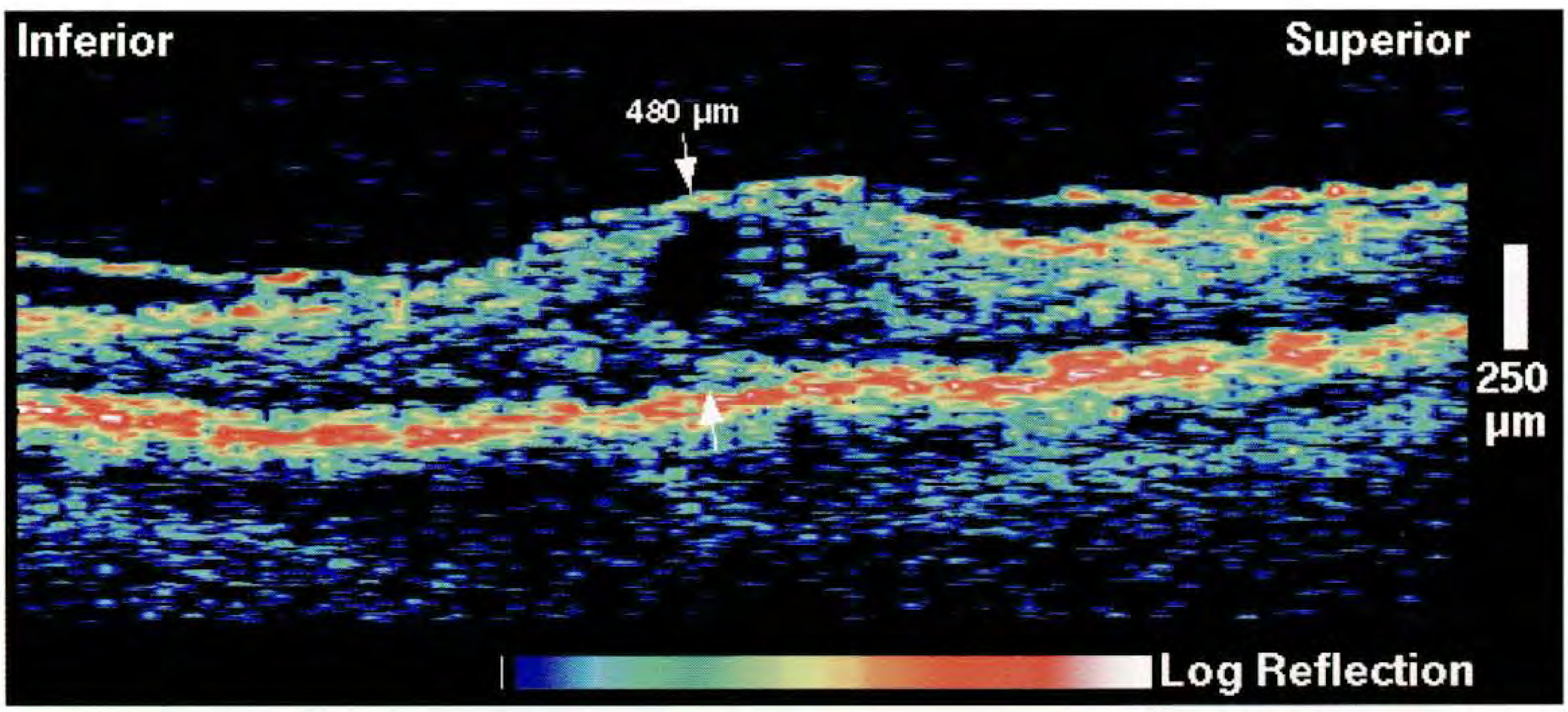

B

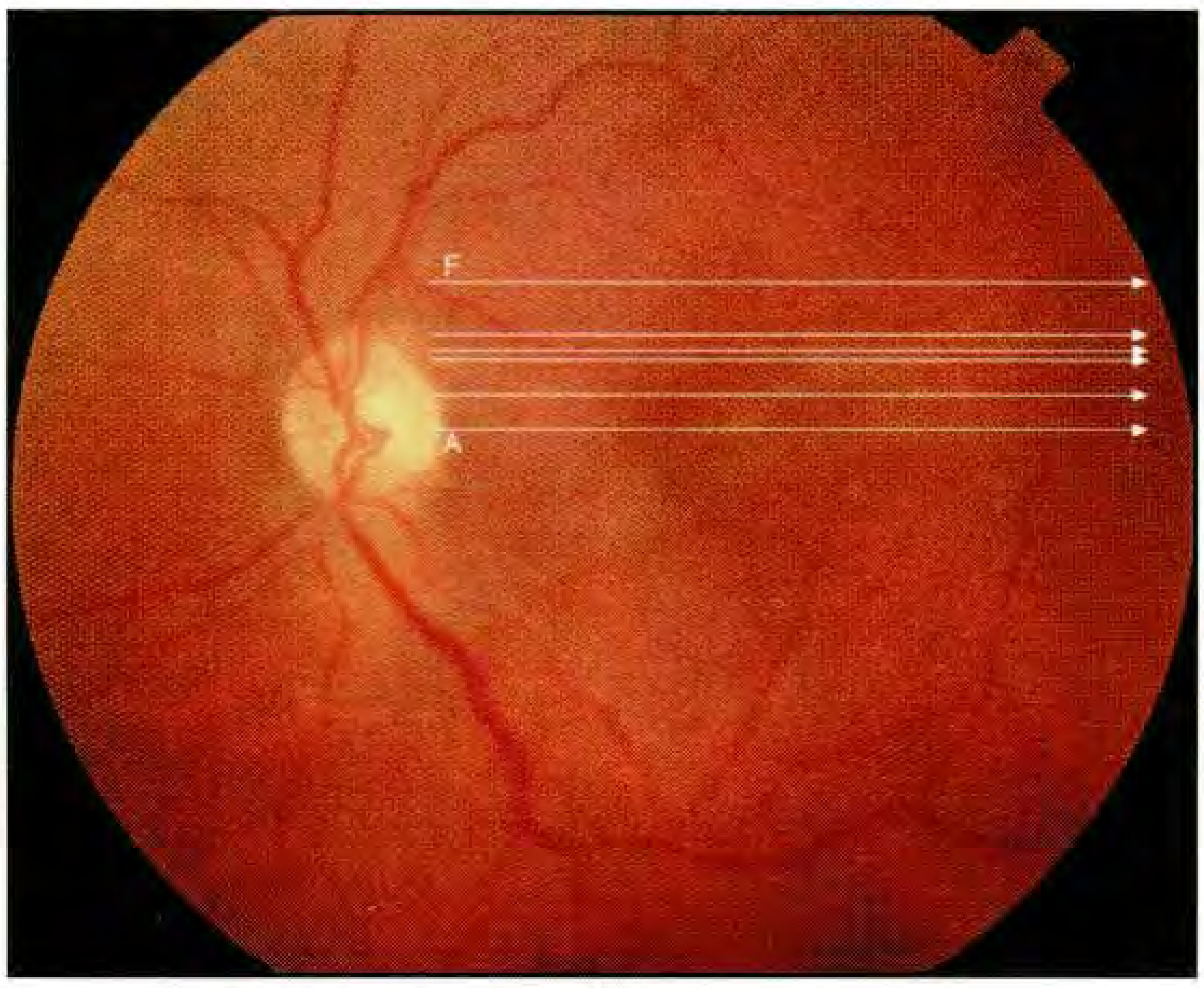

A

B

Case 4-9. Epiretinal Membrane

Clinical Summary

An 85-year-old woman had an epiretinal membrane and edema in the central macula of her left eye associated with a visual acuity of 20/60 (A). Fluorescein angiography (B) displayed straightening of the retinal arterioles inferior to the macula.

Optical Coherence Tomography

A sequence of horizontal tomograms (C) was obtained through the macula. Scan A, taken directly through fixation, showed loss of the normal foveal contour, with a measured central thickness of 520 μm. The epiretinal membrane was tightly adherent to the retina in this region. In the superior tomograms, the membrane was condensed into a thick mass anterior to the retina.

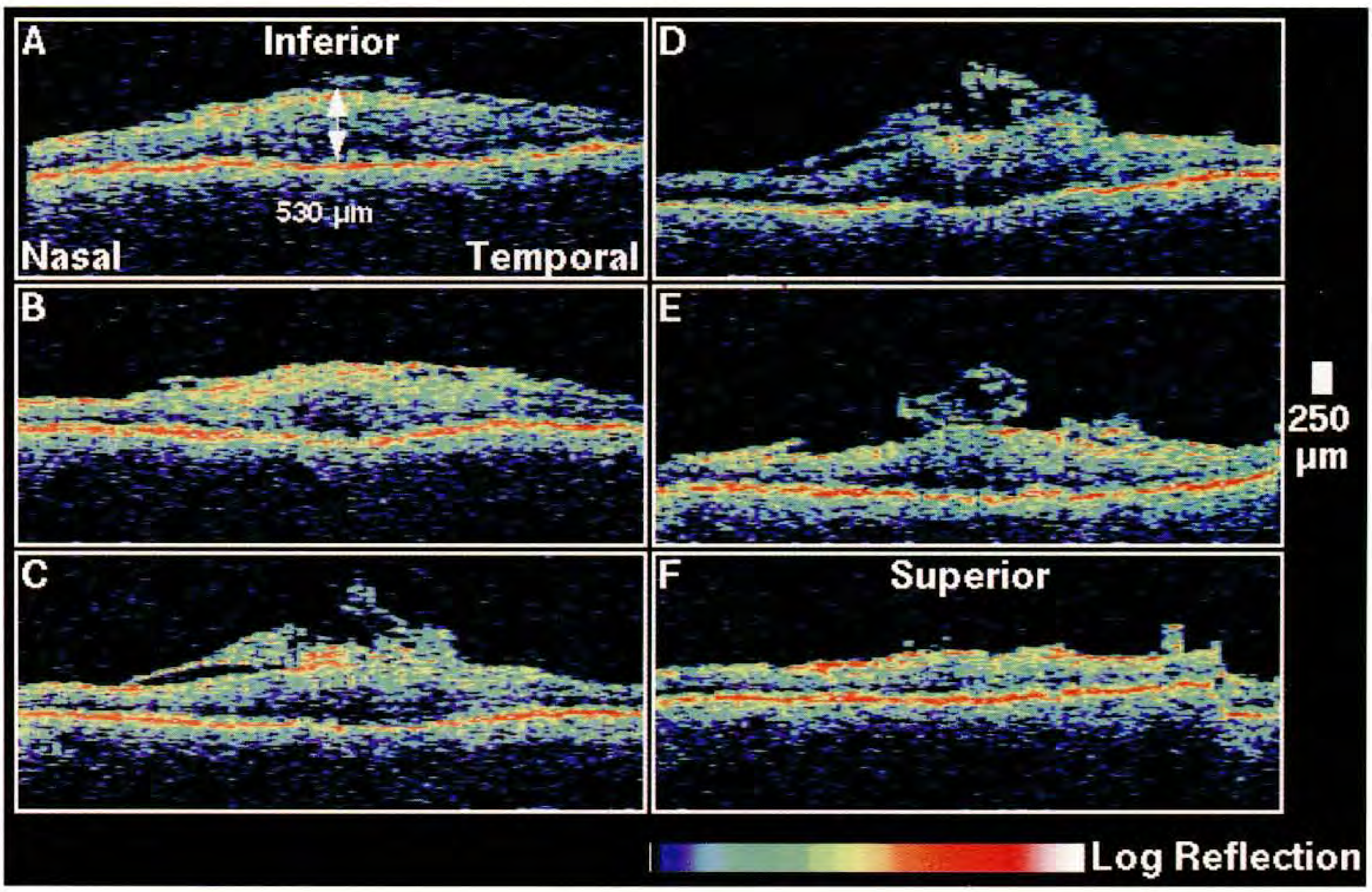

C

Case 4-10. Epiretinal Membrane

Clinical Summary

A 56-year-old man reported a decrease in visual acuity in his right eye over the past three months. On examination, an epiretinal membrane was identified in the central macula without any associated macular edema (A). The visual acuity was 20/30.

Optical Coherence Tomography

OCT (B) delineated a thin, reflective membrane adherent to the retinal surface in the macula. The normal contour of the foveal pit was absent and a non-reflective, cystic space was present in beneath the fovea. The retina was abnormally thickened in the macula, and thinned inferiorly in the image.

A

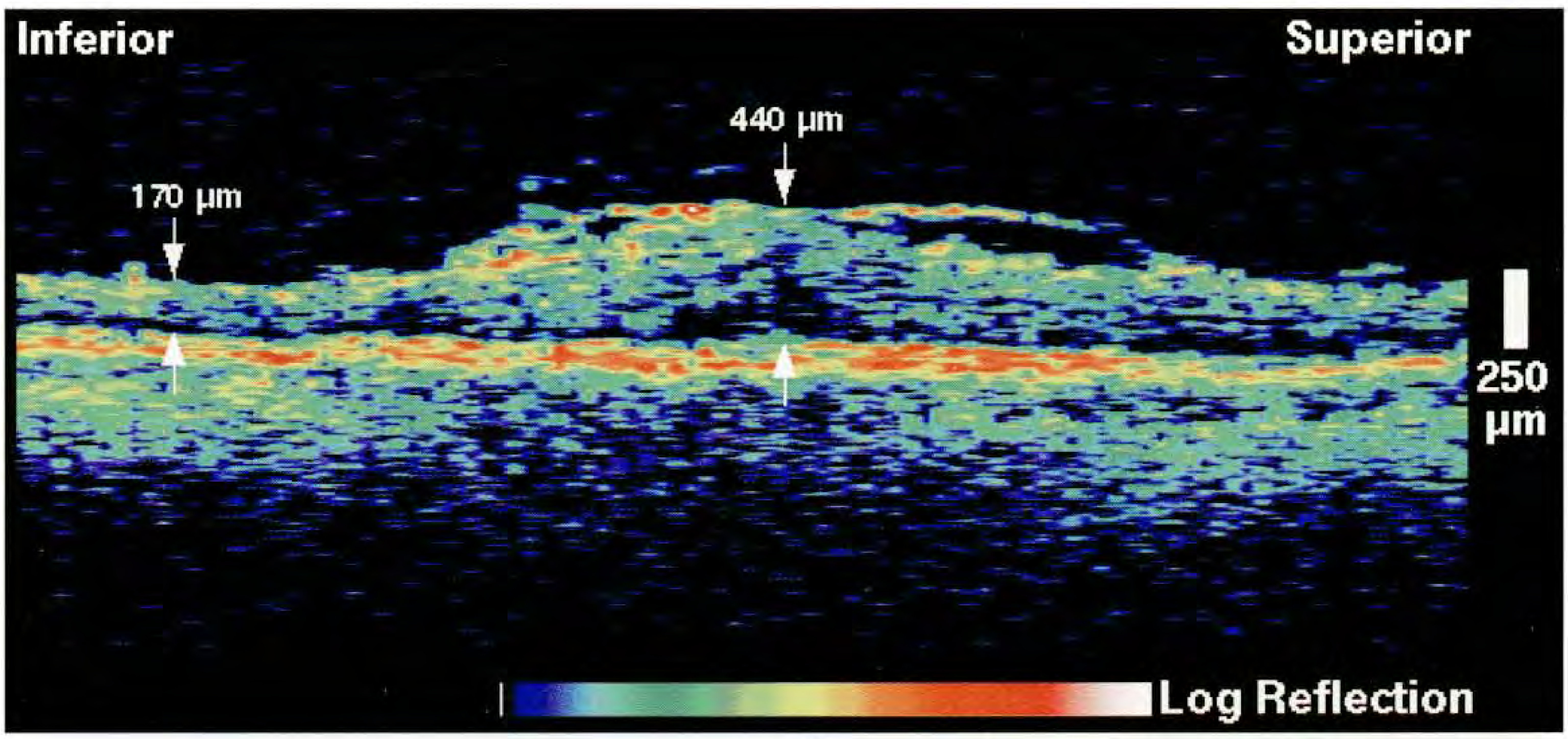

B

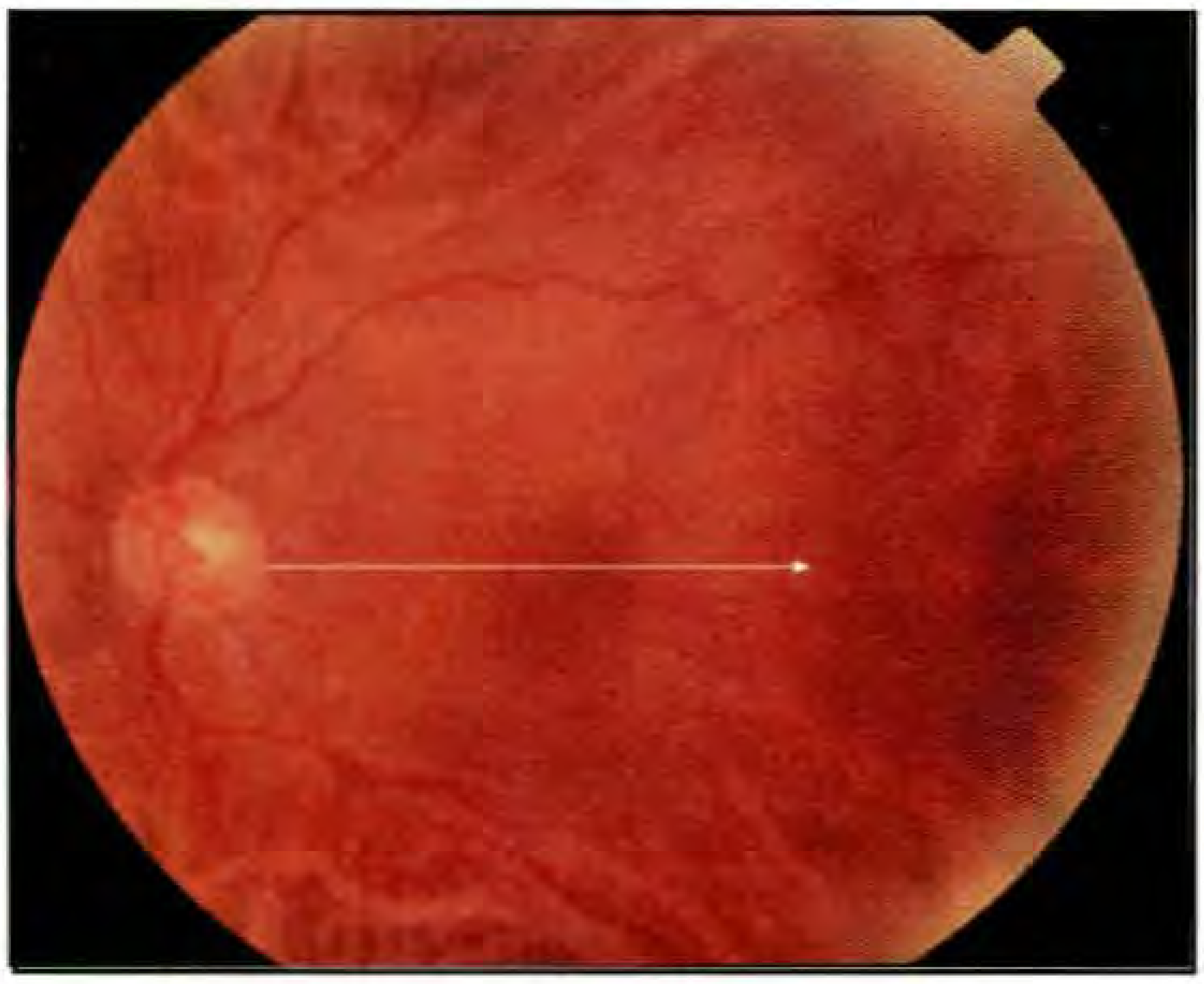

A

Case 4-11. Epiretinal Membrane

Clinical Summary

A 67-year-old man had diabetes mellitus and an epiretinal membrane in his left eye associated with a visual acuity of 20/20 (A).

Optical Coherence Tomography

The membrane appeared in the OCT image (B) as a thin, brightly reflective band tightly adherent to the surface of the retina, and was identifiable by its increased backscattering compared to retinal tissue. There was a loss of the normal foveal contour, consistent with foveal traction or edema.

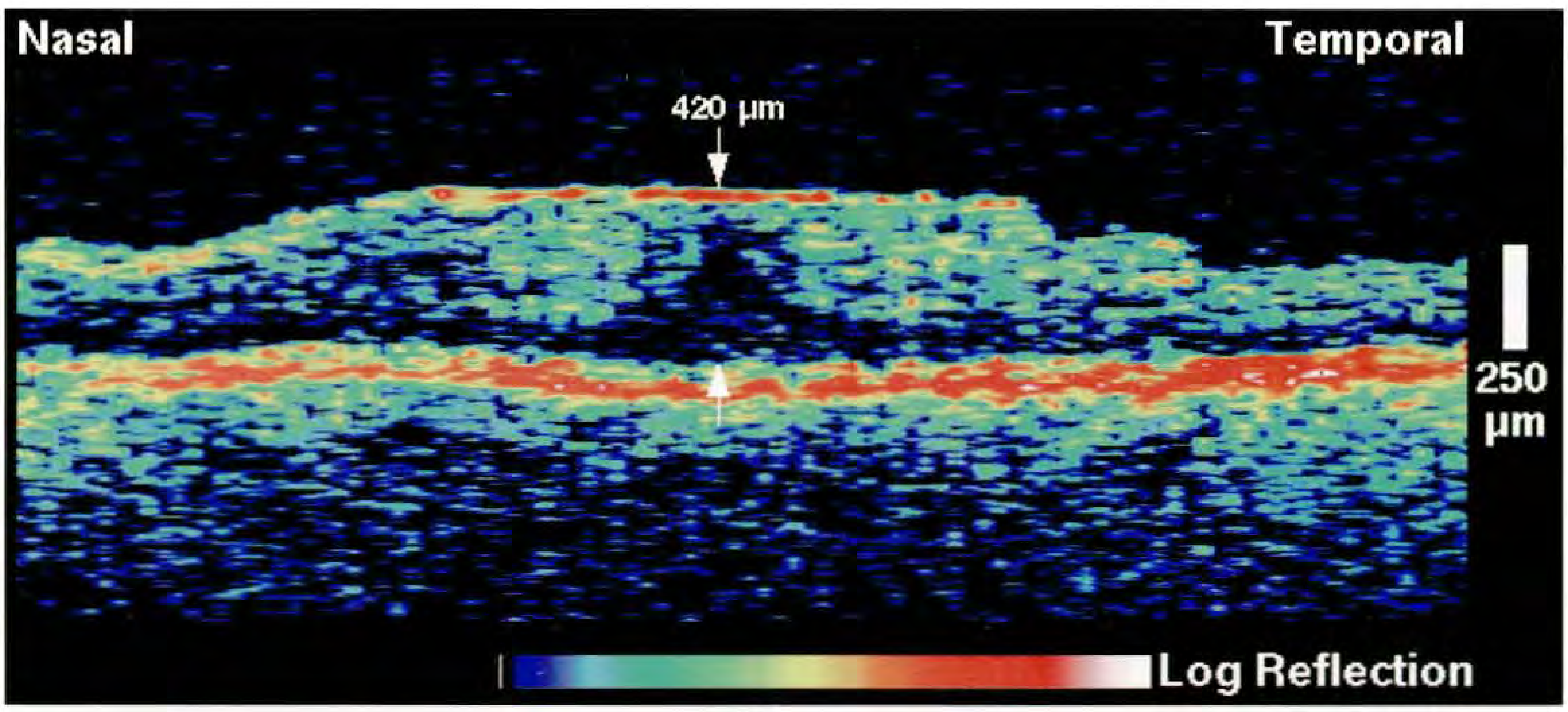

B

Case 4-12. Epiretinal Membrane

Clinical Summary

An epimacular membrane in the right eye of a 71-year-old man was examined (A). His visual acuity in this eye was 20/200.

Optical Coherence Tomography

A vertical OCT tomogram (B; white line on A) was acquired directly through the patient's fixation. The fovea was almost unidentifiable in the middle of the scan (arrows) due to traction by the epiretinal membrane, which appeared as a red, reflective band attached to the inner retina. Small cysts were visualized throughout the macula in the intermediate layers of the retina. A horizontal OCT image (C; black line on A) obtained superior to the fovea showed apparent contraction of the membrane, and elevation of the nasal retina.

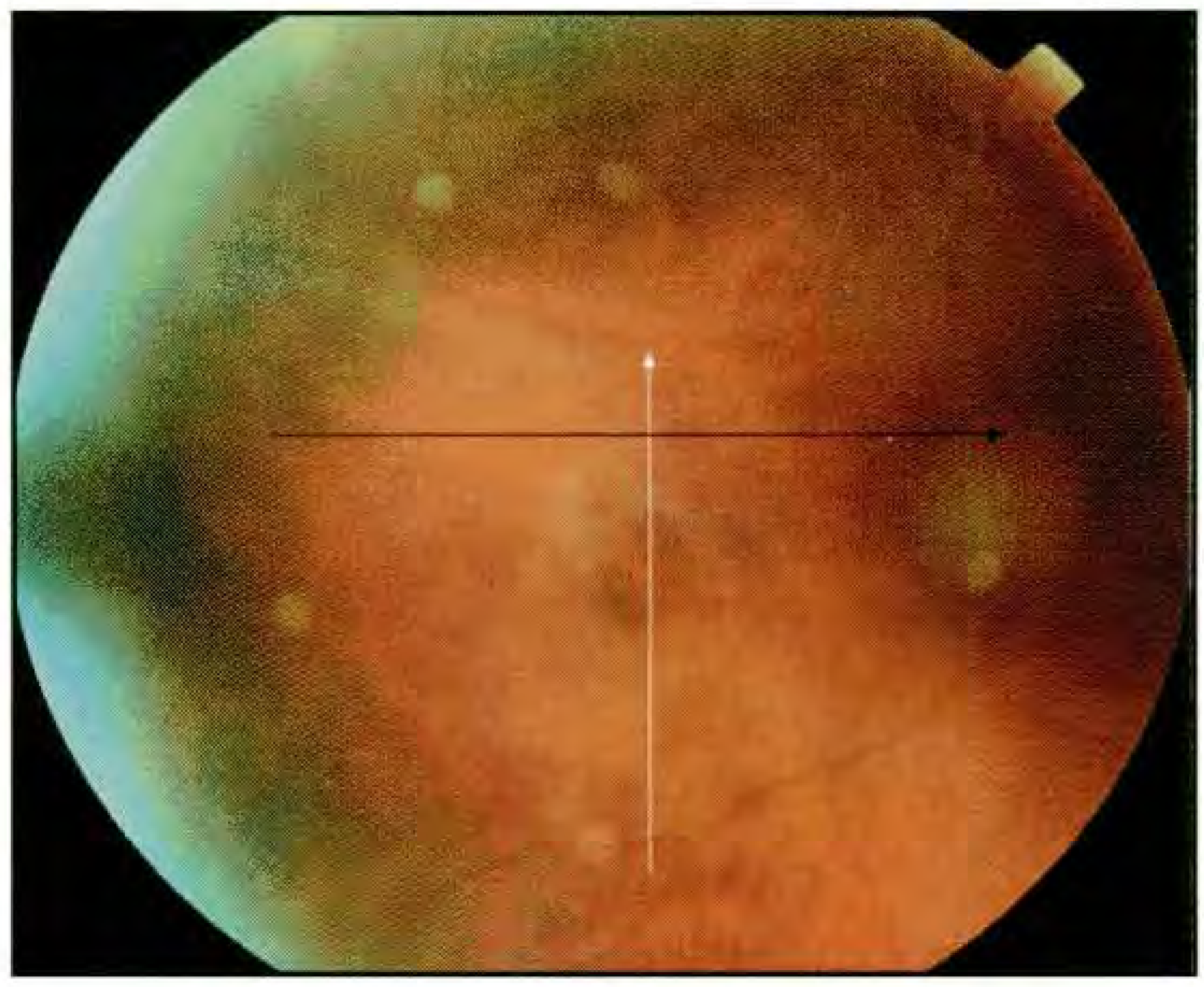

A

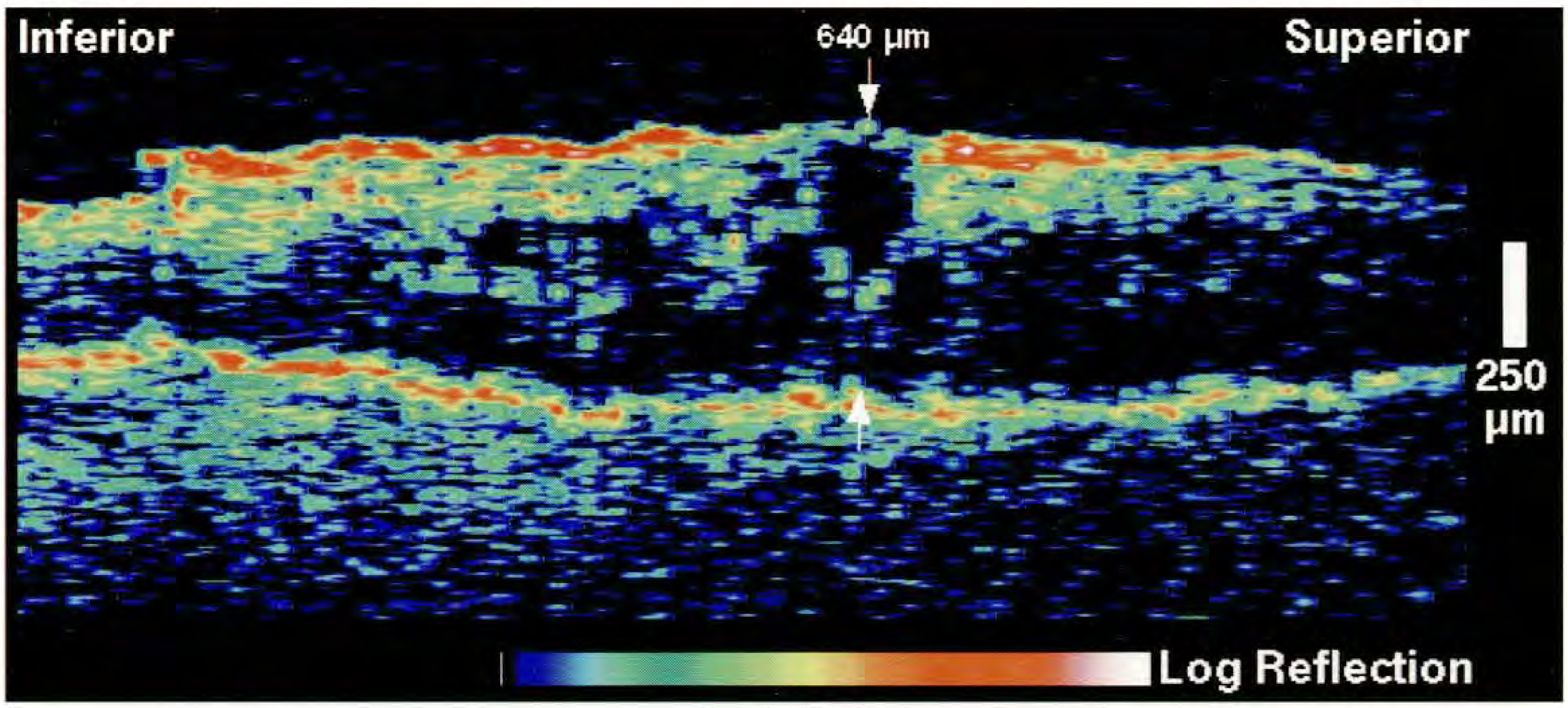

B

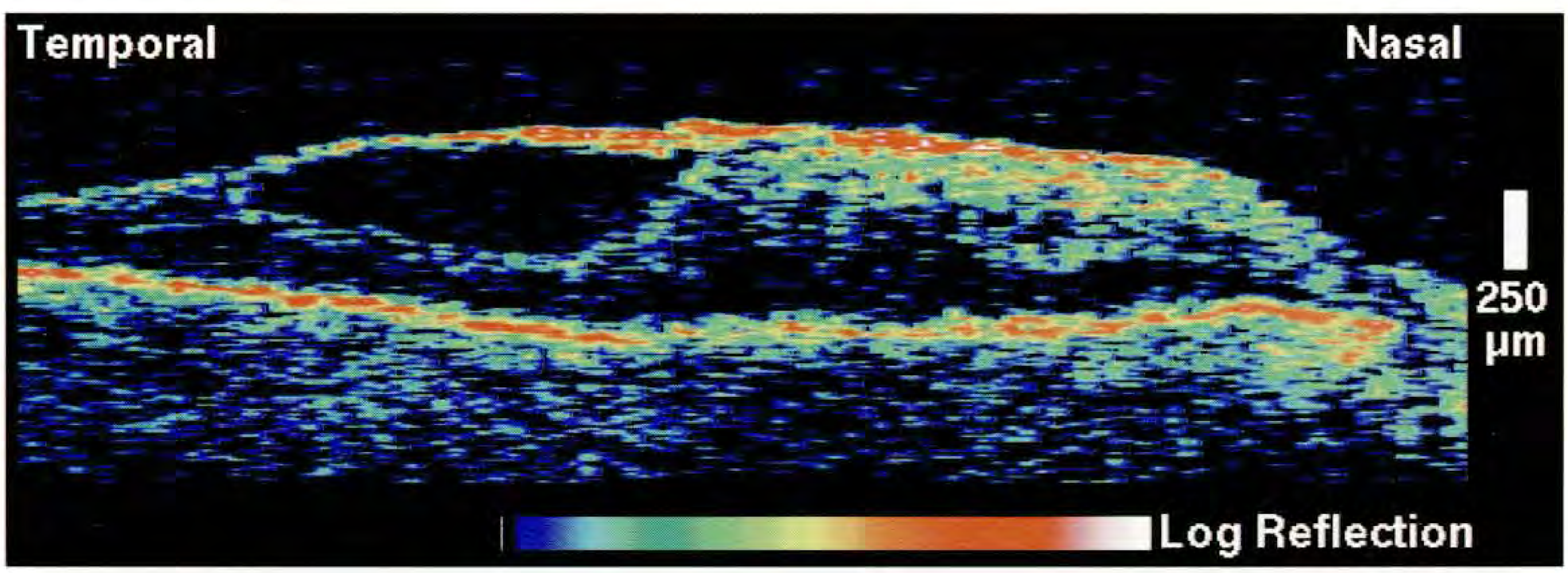

C

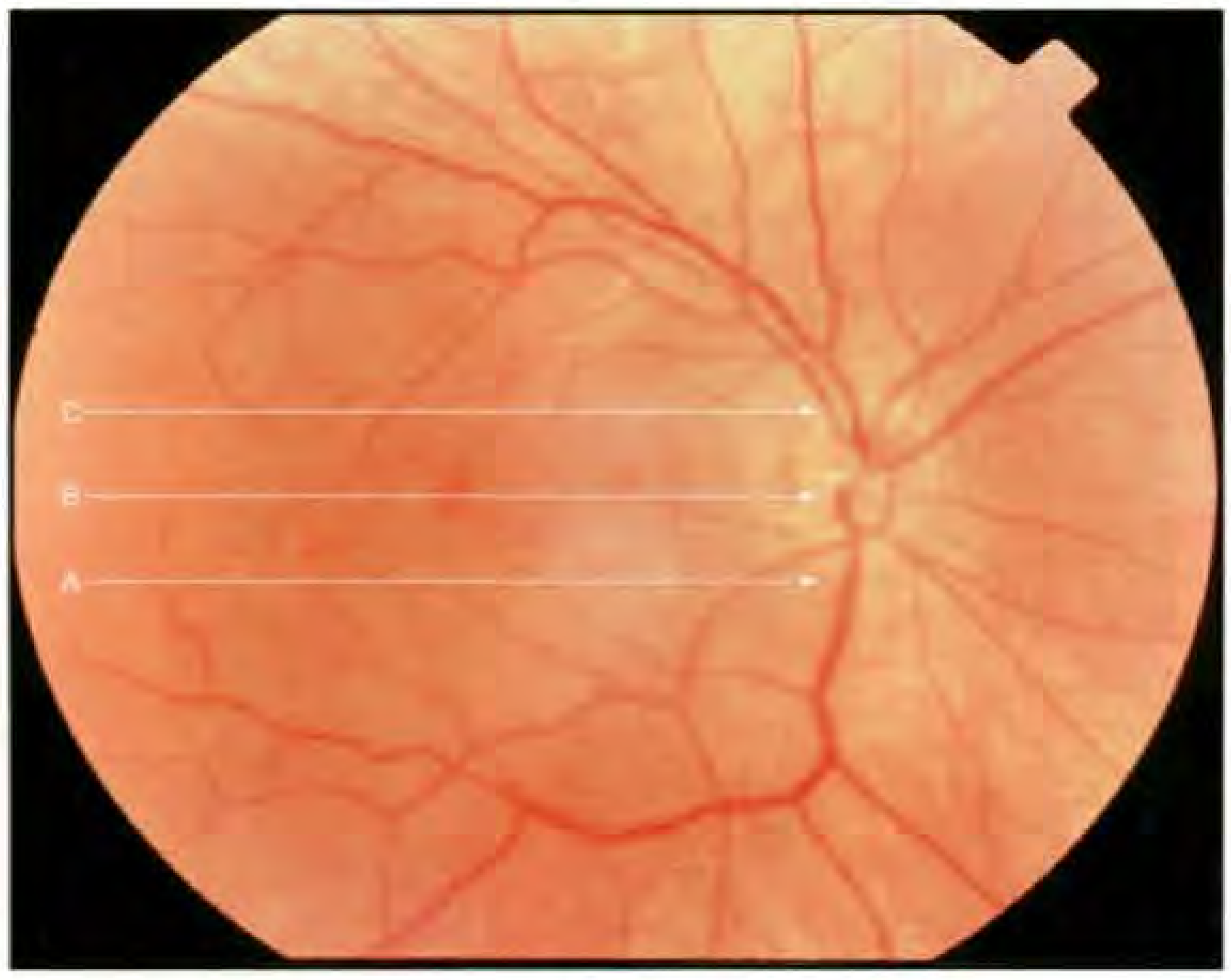

A

Case 4-13. Epiretinal Membrane

Clinical Summary

A 57-year-old man had an epiretinal membrane in his right eye associated with a visual acuity of 20/25 (A).

Optical Coherence Tomography

A series of horizontal OCT scans (B) delineated the membrane as a thin, reflective band contiguous with the retinal surface. Mild tangential traction was apparent where membrane was separated from the retina and in the fovea where the foveal depression was absent (arrow).

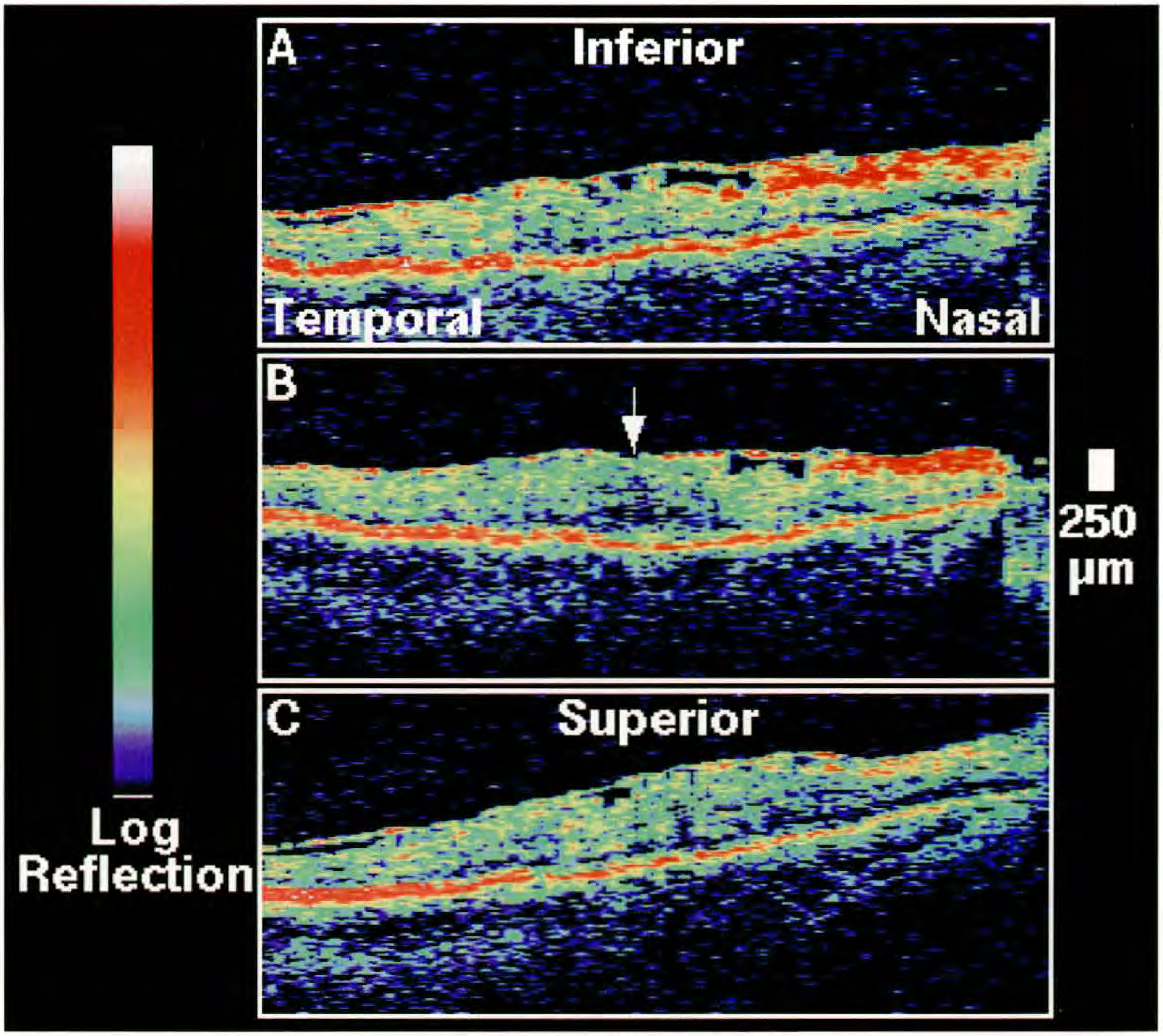

B

Case 4-14. Epiretinal Membrane

Clinical Summary

A 71-year-old woman had recently undergone cataract surgery in her right eye; however, her visual acuity in this eye had not improved beyond 20/100. Slit-lamp examination (A) showed an epiretinal membrane in the macular region and a posterior vitreous detachment.

Optical Coherence Tomography

An OCT scan through fixation (B) demonstrated a region of focal retinal thickening in the central macula due to either traction or macular edema. The foveal depression was absent. An epiretinal membrane was visible as a moderately reflective, thin band adherent to the retinal surface.

A

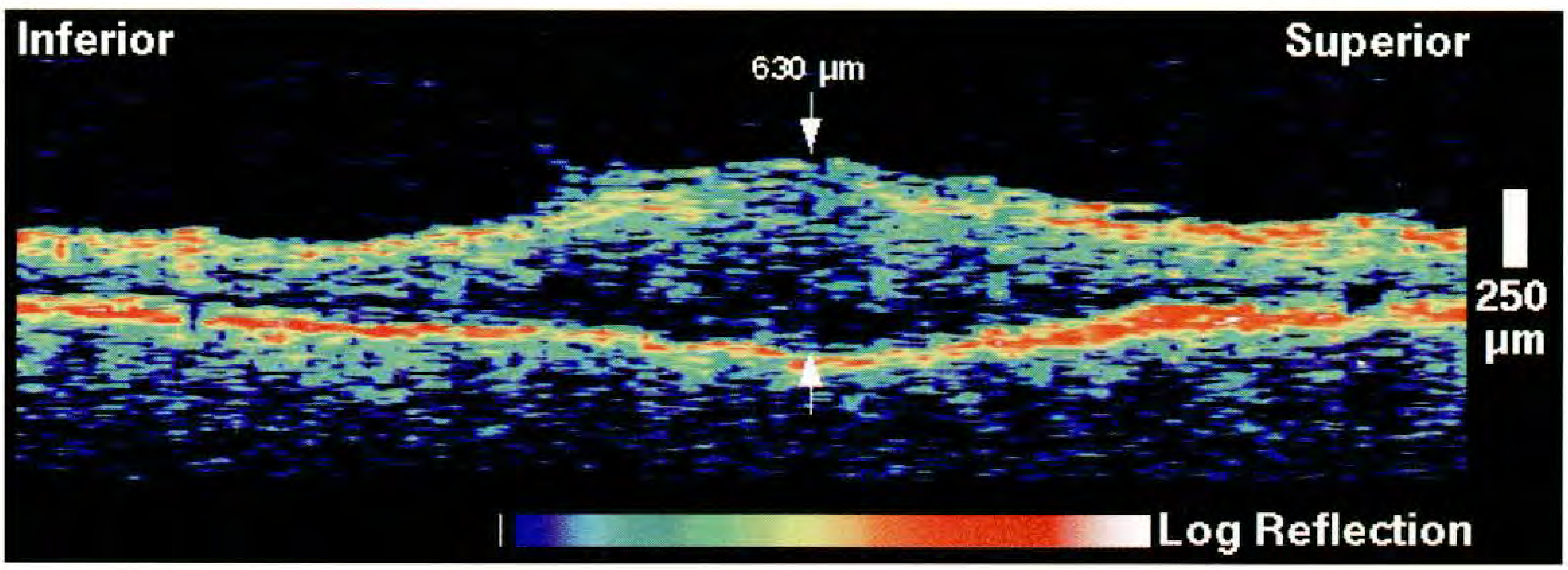

B

CHAPTER 5

Retinal Vascular Occlusion

Branch Retinal Vein Occlusion
Central Retinal Vein Occlusion
Central Retinal Artery Obstruction

Retinal vascular occlusions are common causes of acute vision loss. While the characteristic ophthalmoscopic and fluorescein angiographic findings are typically diagnostic [1-3], in the venous occlusive diseases OCT tomograms are useful in quantitatively monitoring the development of macular edema and resolution of retinal thickening following treatment. Macular thickening may be measured at one or many points on identically placed tomograms to accurately track intraretinal or subretinal fluid accumulation with high resolution [4].

In retinal venous occlusion, the morphological findings visible in OCT cross-section include macular thickening, intraretinal cyst formation, lamellar macular holes, subretinal fluid accumulation, and papilledema. Cases of retinal artery obstruction exhibit acute macular edema followed by retinal atrophy, both of which may be assessed quantitatively on OCT by measurements of retinal thickness. The retinal pallor that often accompanies ischemic retinal injury is visible on the OCT tomograms as enhanced reflectivity from the retinal nerve fiber layer and inner neurosensory retina.

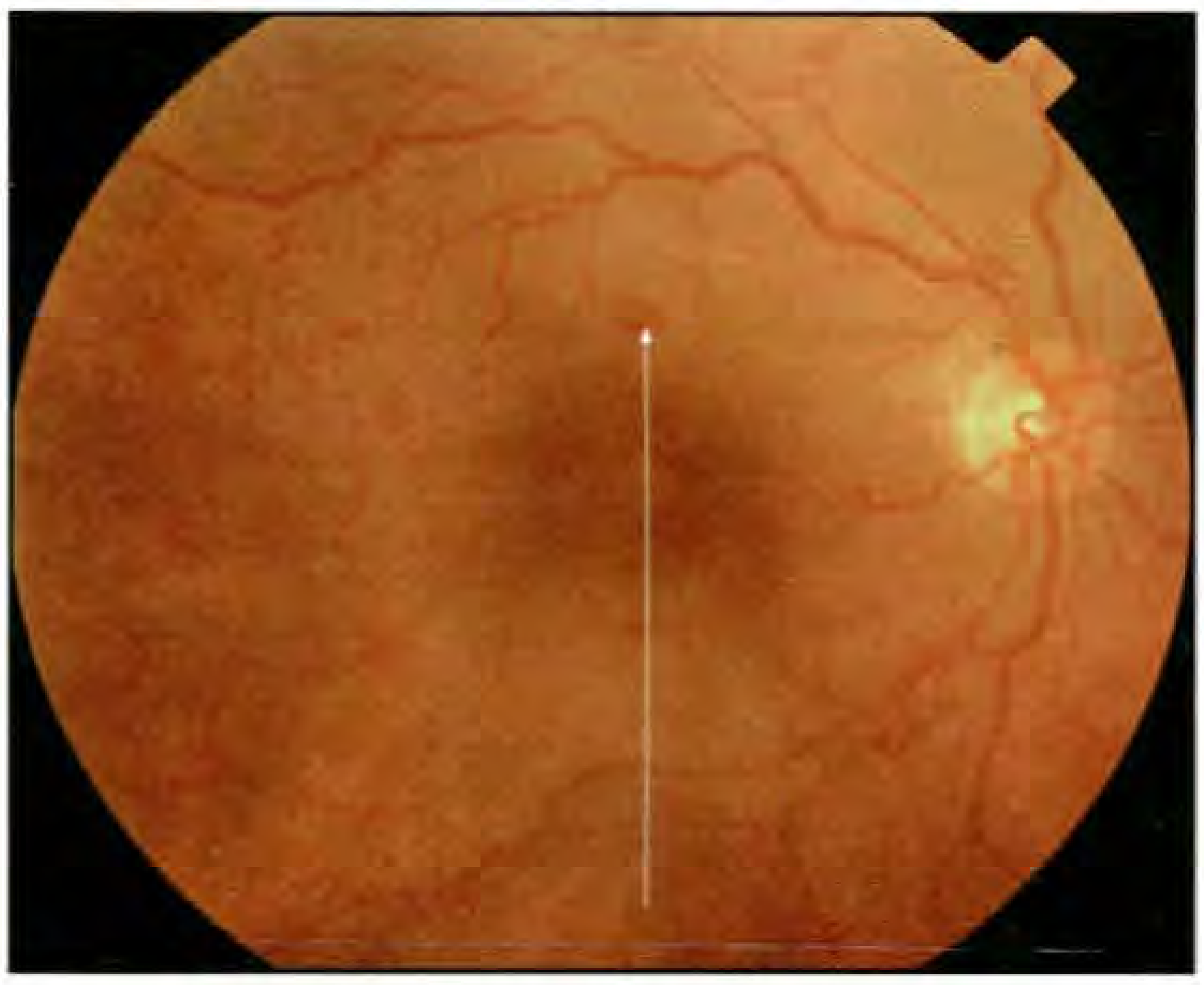

A

B

Case 5-1. Branch Retinal Vein Occlusion and Macular Edema Before and After Treatment

Clinical Summary

A 64-year-old woman with a history of branch retinal vein occlusion four years ago in her right eye was referred for decreasing visual acuity in this eye over a period of four weeks. The visual acuity was 20/50. Indirect ophthalmoscopy (A) showed a narrowing of an inferotemporal branch retinal vein with collateral vessels throughout the macula. Venous dilation, severe arterio-venous nicking, and several blot hemorrhages were also noted. Multiple collateral vessels and late leakage from dilated microvascular segments were observed in the inferior macula on fluorescein angiography (B). A focal constriction was also seen in the inferotemporal branch artery.

Optical Coherence Tomography

A vertical OCT tomogram (C) taken through the fovea showed significant fluid accumulation in the outer retinal layers of the inferior macula. The retinal thickness was measured to be 600 μm at the foveal boundary.

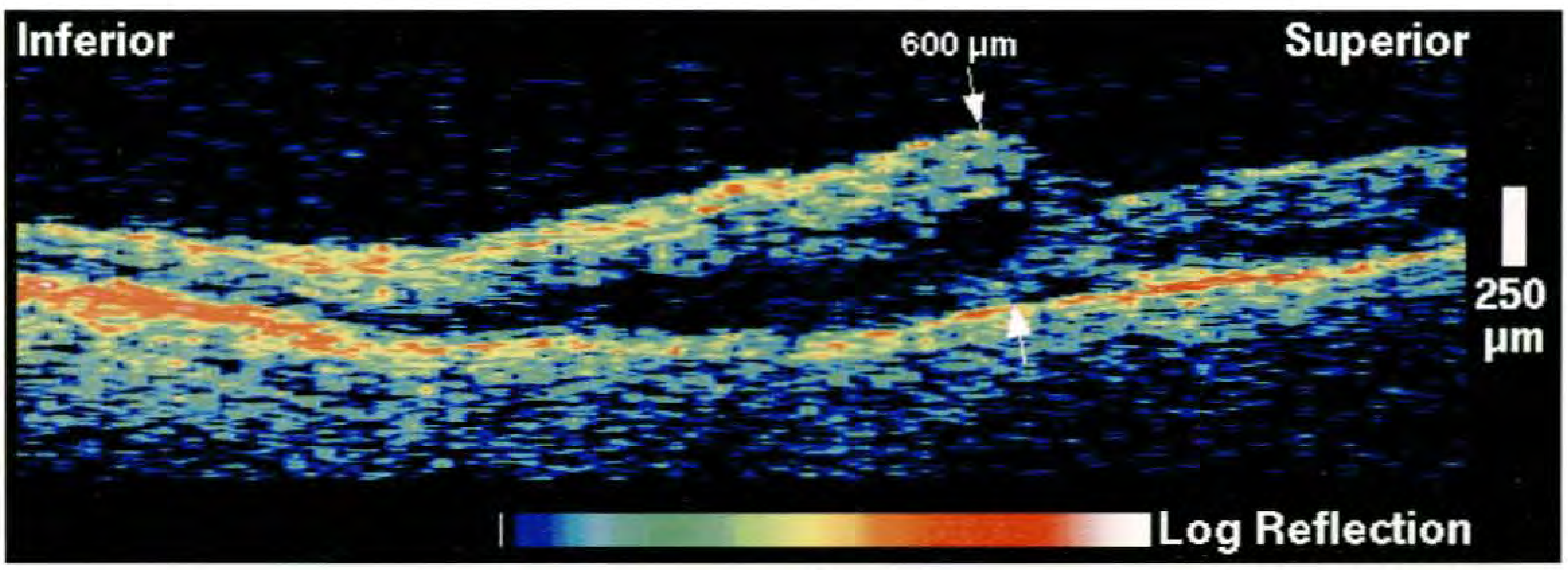

C

Case 5-1 continued

Follow-up Examination

The patient received photocoagulation treatment with a dye yellow laser and returned for a follow-up appointment one month later. A significant decrease in the fluid accumulation was observed on slit-lamp biomicroscopy (D) and her visual acuity had improved to 20/20.

Follow-up Optical Coherence Tomography

A follow-up OCT image (E) confirmed an improvement in the macular edema. The retinal thickness measured at the inferior margin of the fovea had decreased to 350 μm

D

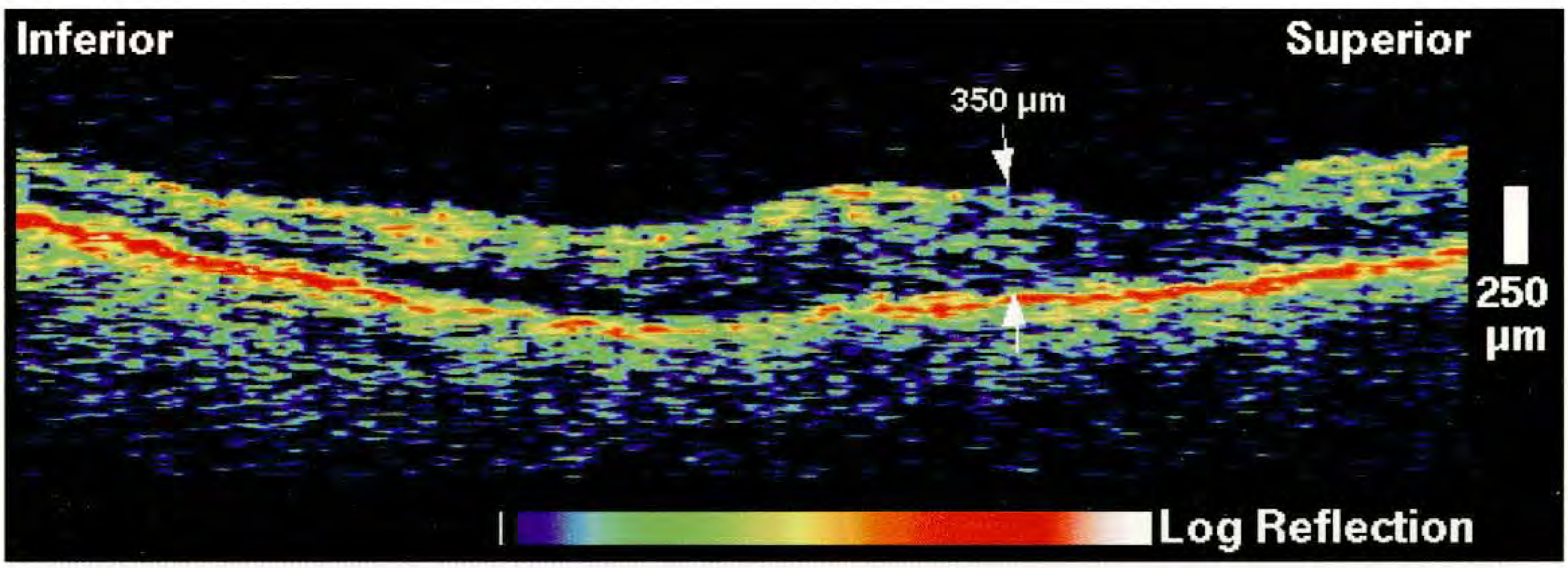

E

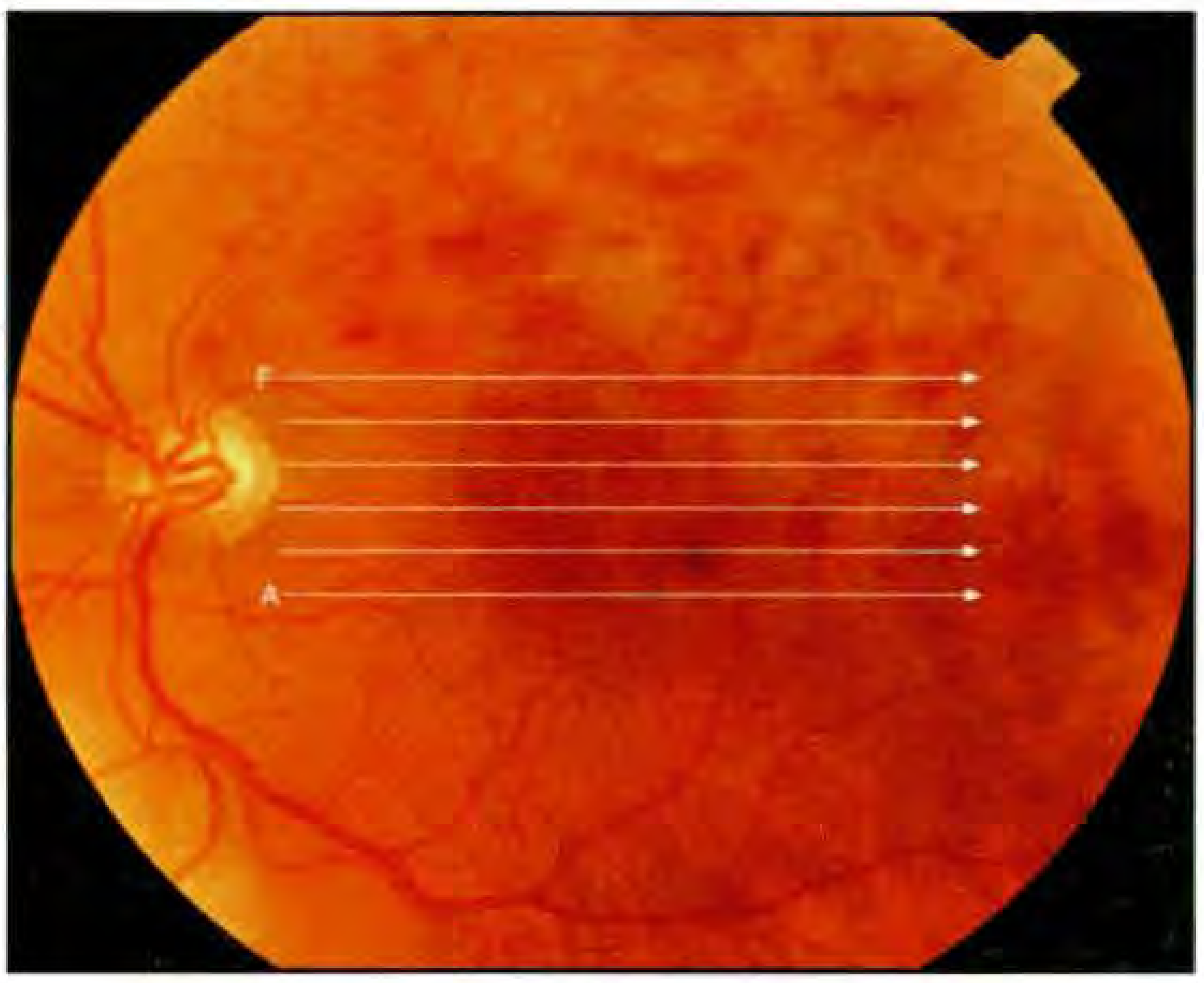

A

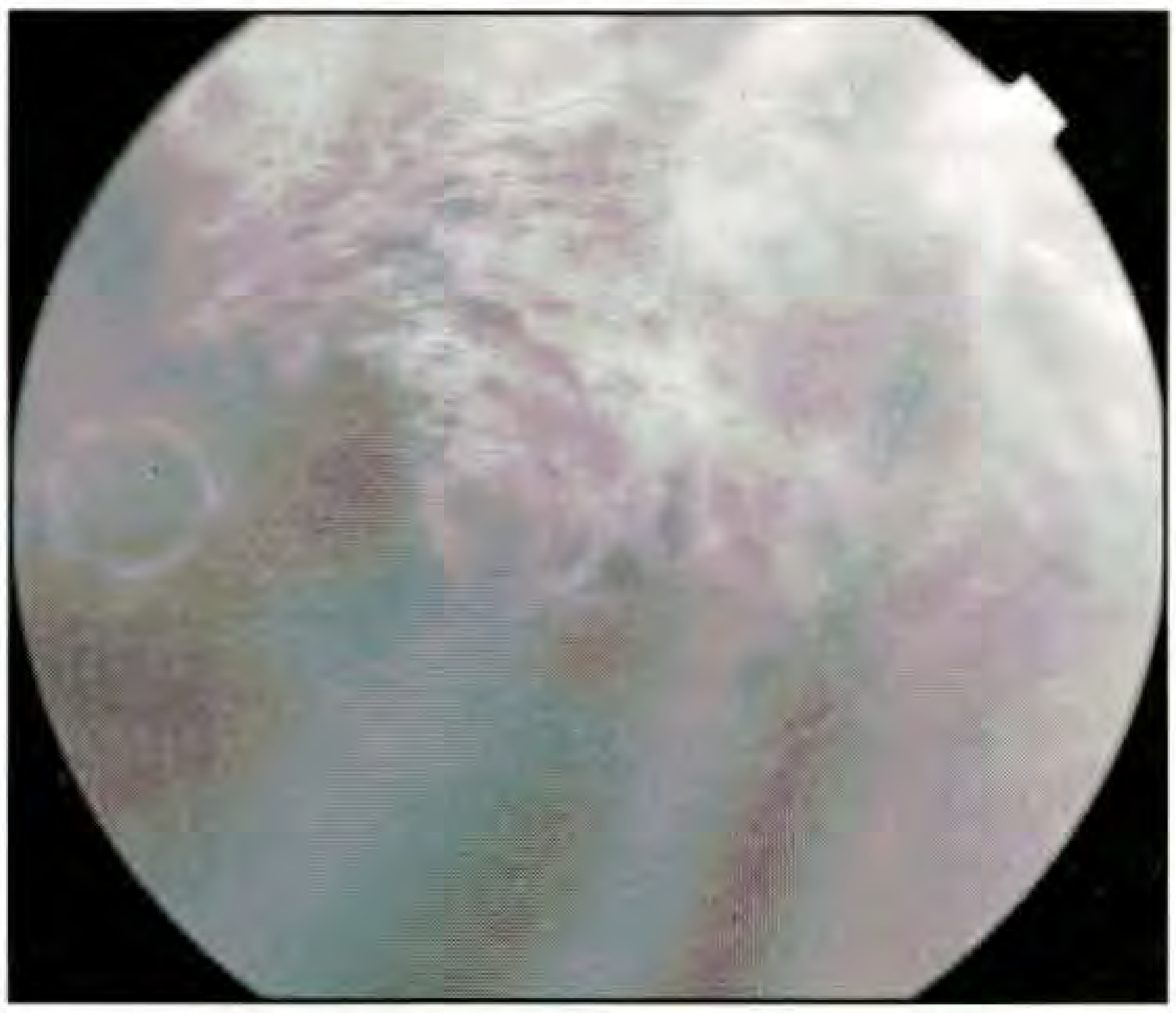

B

Case 5-2. Branch Retinal Vein Occlusion

Clinical Summary

A 66-year-old man had an occlusion of the superior branch retinal vein in his left eye. His visual acuity was 20/70 in this eye. Dilated fundus examination (A) showed a dilated and tortuous superotemporal retinal vein with surrounding intraretinal hemorrhage and significant macular edema. Late leakage of fluorescein dye was observed on angiography (B) and was most prominent in the temporal aspect of the superior hemisphere. Focal laser photocoagulation treatment was performed and the patient was examined one month later.

Optical Coherence Tomography

A sequence of horizontal tomograms (C) delineated increased retinal thickening superotemporal to the fovea, with reduced reflectivity corresponding to serous fluid accumulation preferentially in the outer retinal layers. The retinal thickness directly in the fovea was 320 µm and increased superiorly as expected. Scan B, taken directly through fixation, identified an intraretinal cyst temporal to the center, and a small detachment of the neurosensory retina just beneath the fovea. Intraretinal hemorrhages appeared as focal areas of bright, intraretinal backscattering which partially shadowed the reflections from the retinal pigment epithelium and choriocapillaris below (*e.g.* scan C, arrow).

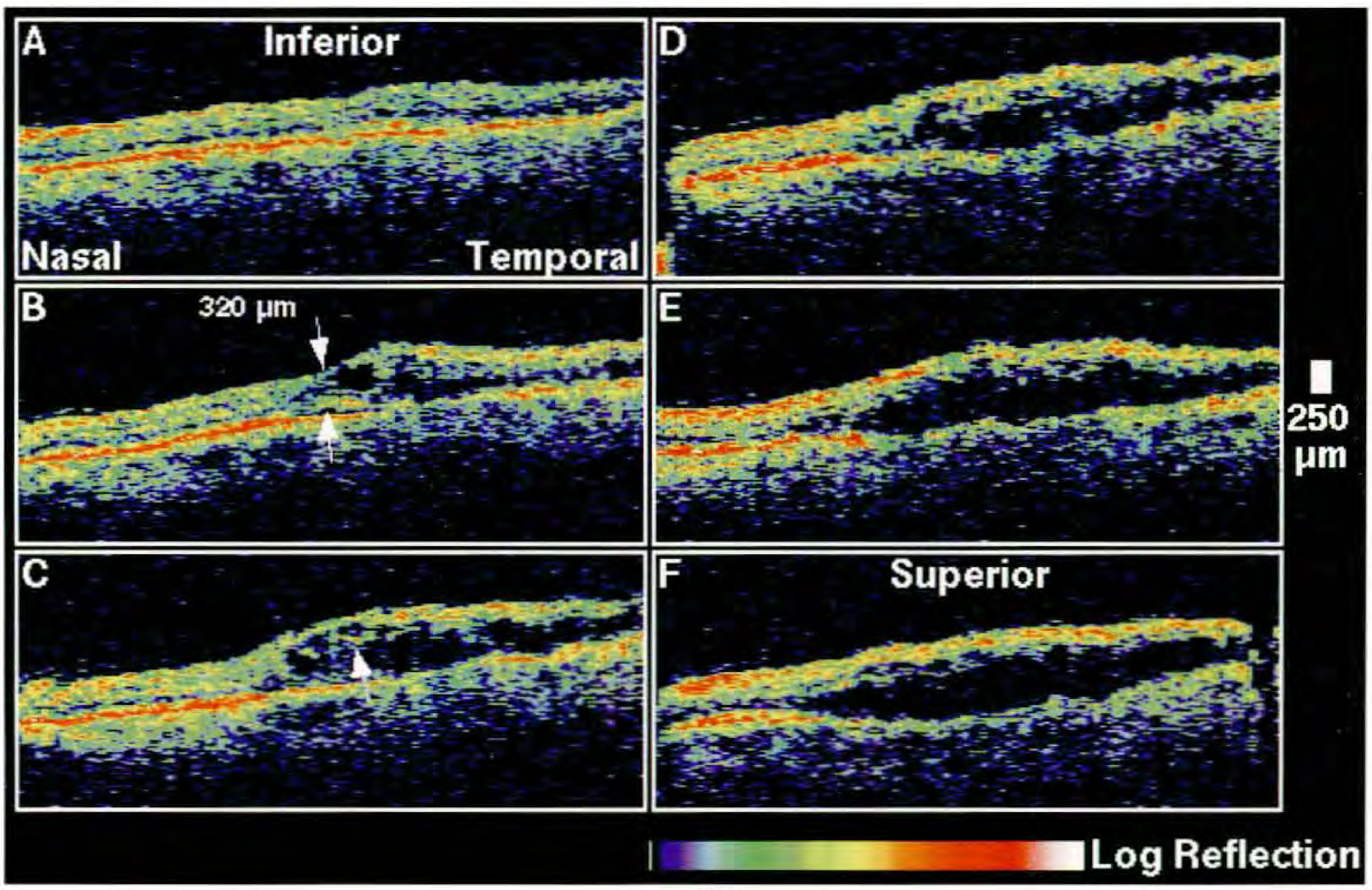

C

Case 5-2 continued

Follow-up Examination

Two months later, a follow-up examination indicated persistence of the macular edema and the patient received additional focal laser photocoagulation in his left eye. The eye was re-evaluated after one additional month. The visual acuity had improved slightly to 20/60. Persistent edema and hemorrhage were noted in the distribution of the superotemporal vein on ophthalmoscopy (D).

Follow-up Optical Coherence Tomography

A follow-up set of OCT images (E) demonstrated a significant reduction in retinal thickening and fluid accumulation superotemporally. Only a mild decrease in macular thickness was observed in the fovea, however, accounting for the lack of significant improvement in visual acuity. The central foveal thickness was 240 μm.

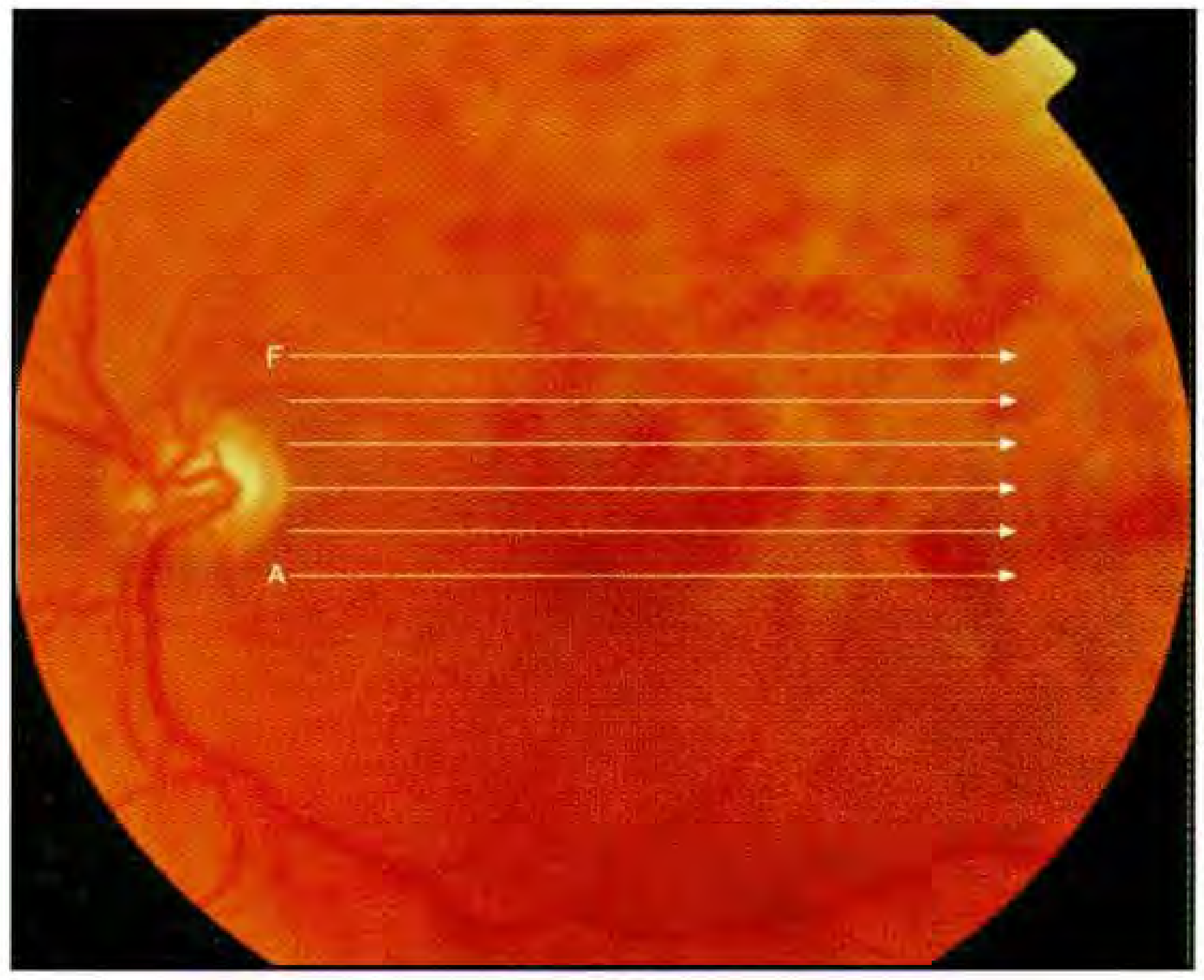

D

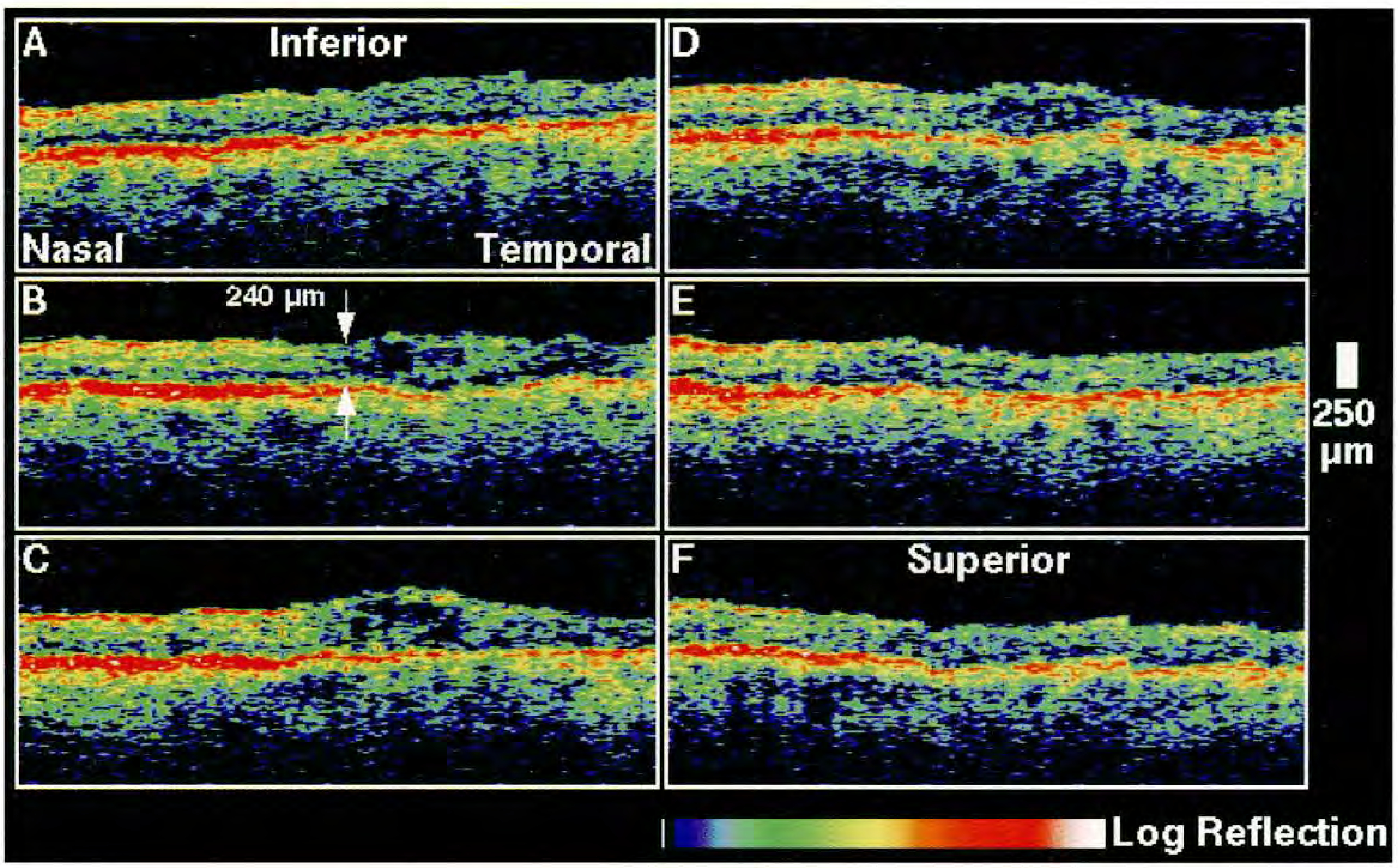

E

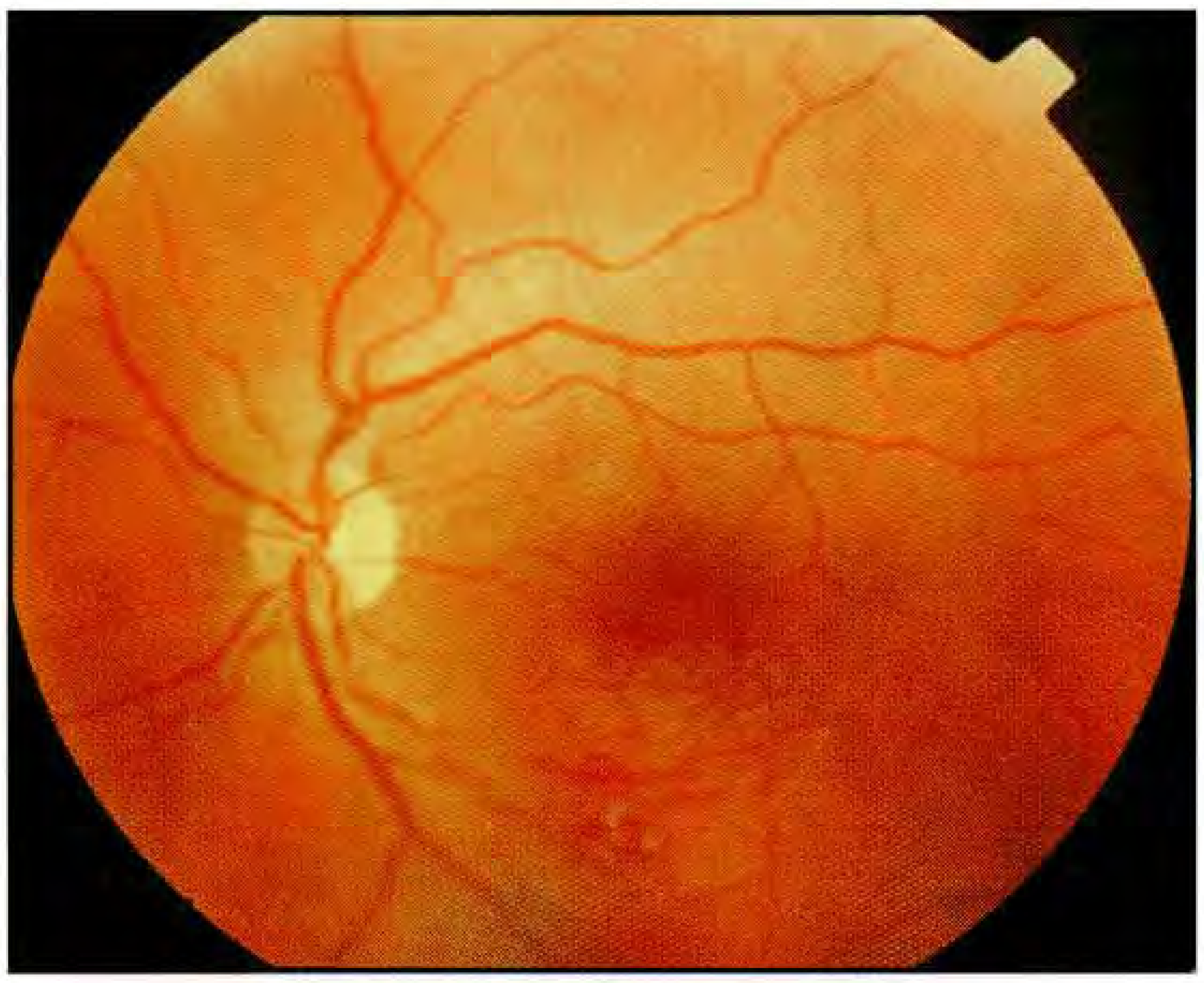

A

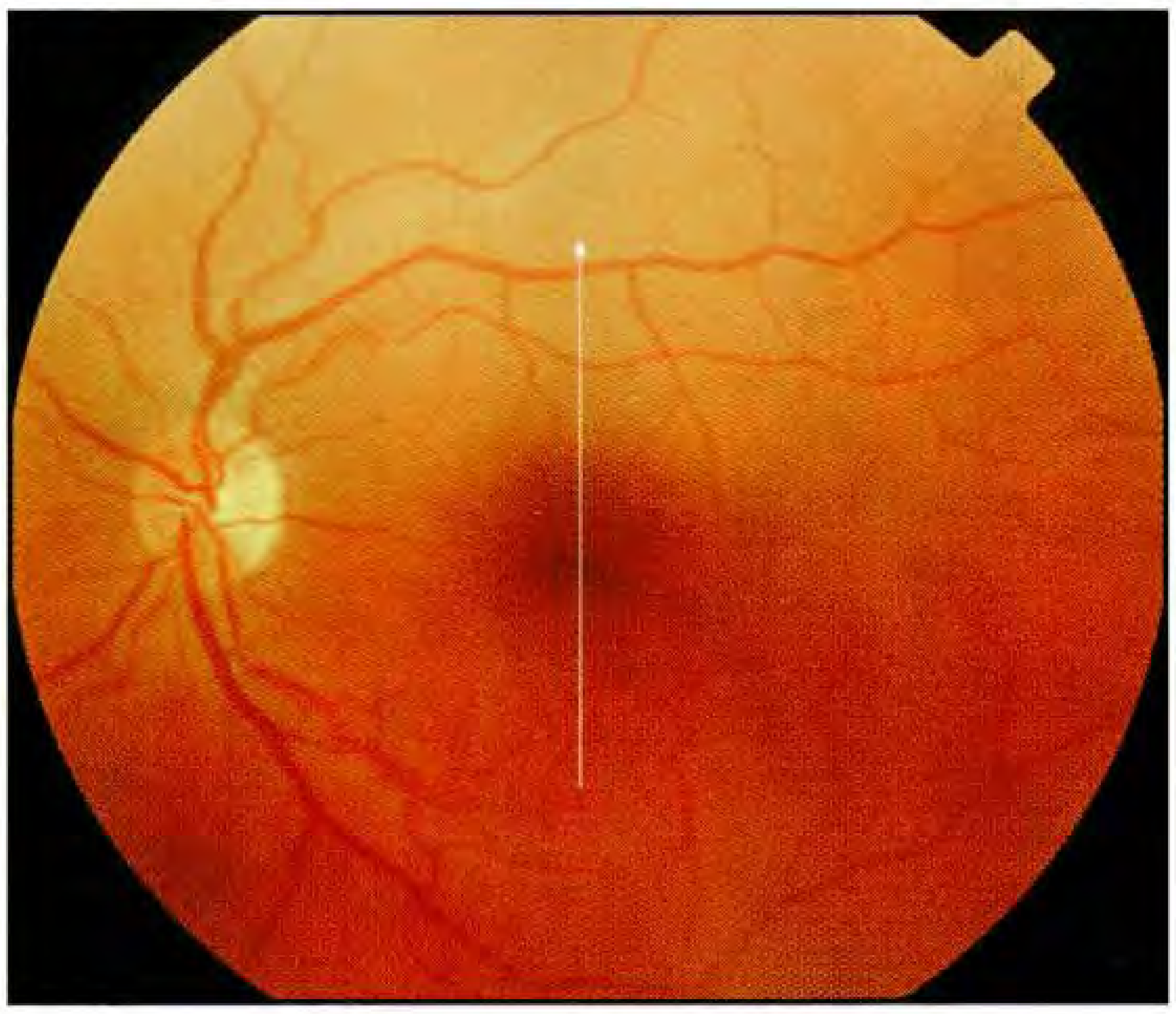

B

Case 5-3. Resolved Branch Retinal Vein Occlusion

Clinical Summary

A 40-year-old man with a history of high blood pressure noted blurry vision in his left eye. On examination (A), he was found to have a resolving inferotemporal branch retinal vein obstruction associated with a mild decrease in visual acuity to 20/30. On a follow-up visit nine months later, there was no evidence of an active vein occlusion. Slit-lamp biomicroscopy (B) showed fine telangiectatic vessels in the macular region, but no macular edema.

Optical Coherence Tomography

A vertical OCT tomogram (C) through fixation disclosed mild macular thickening immediately inferior to but not involving the fovea. The difference between the retinal thickness measured at symmetrical points inferior and superior to the center was 100 μm.

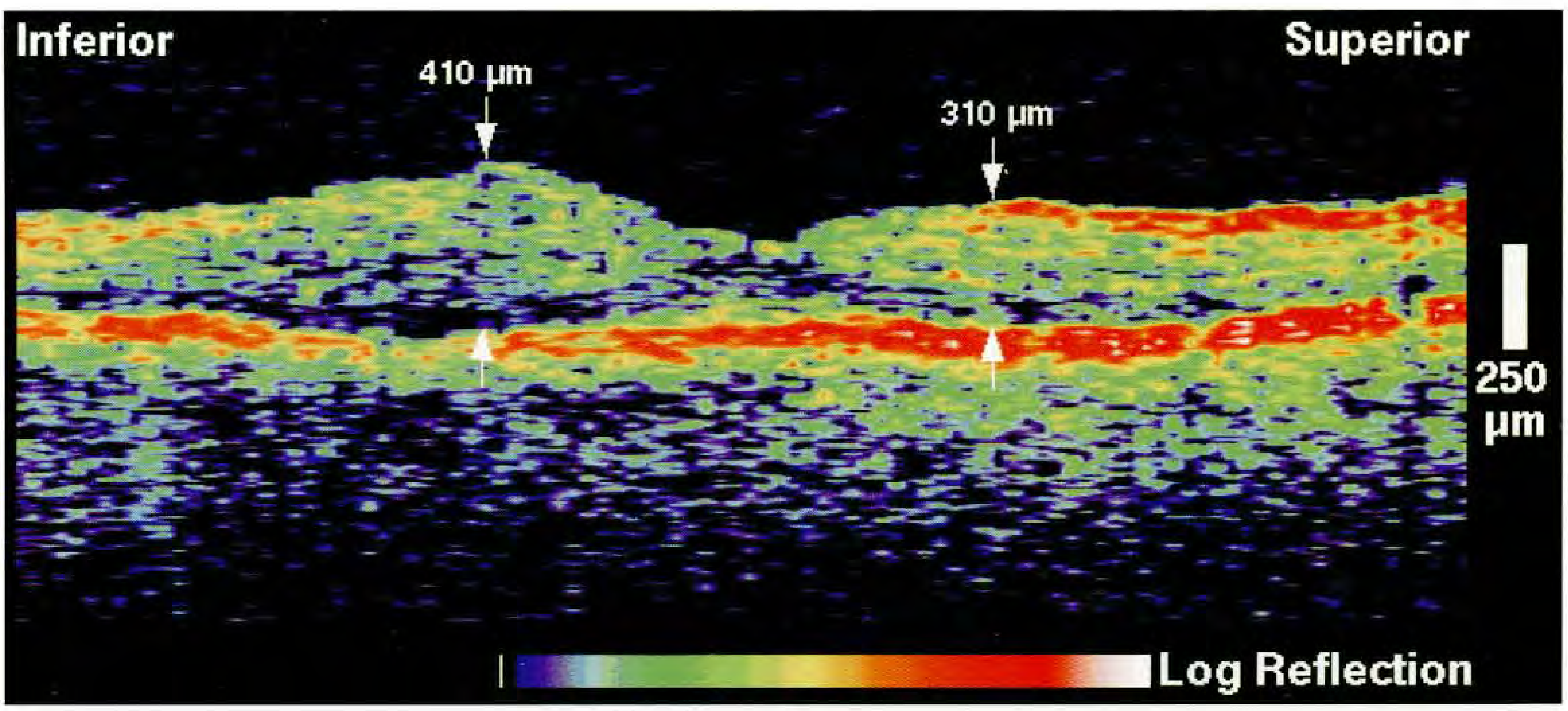

C

Case 5-4. Branch Retinal Vein Occlusion

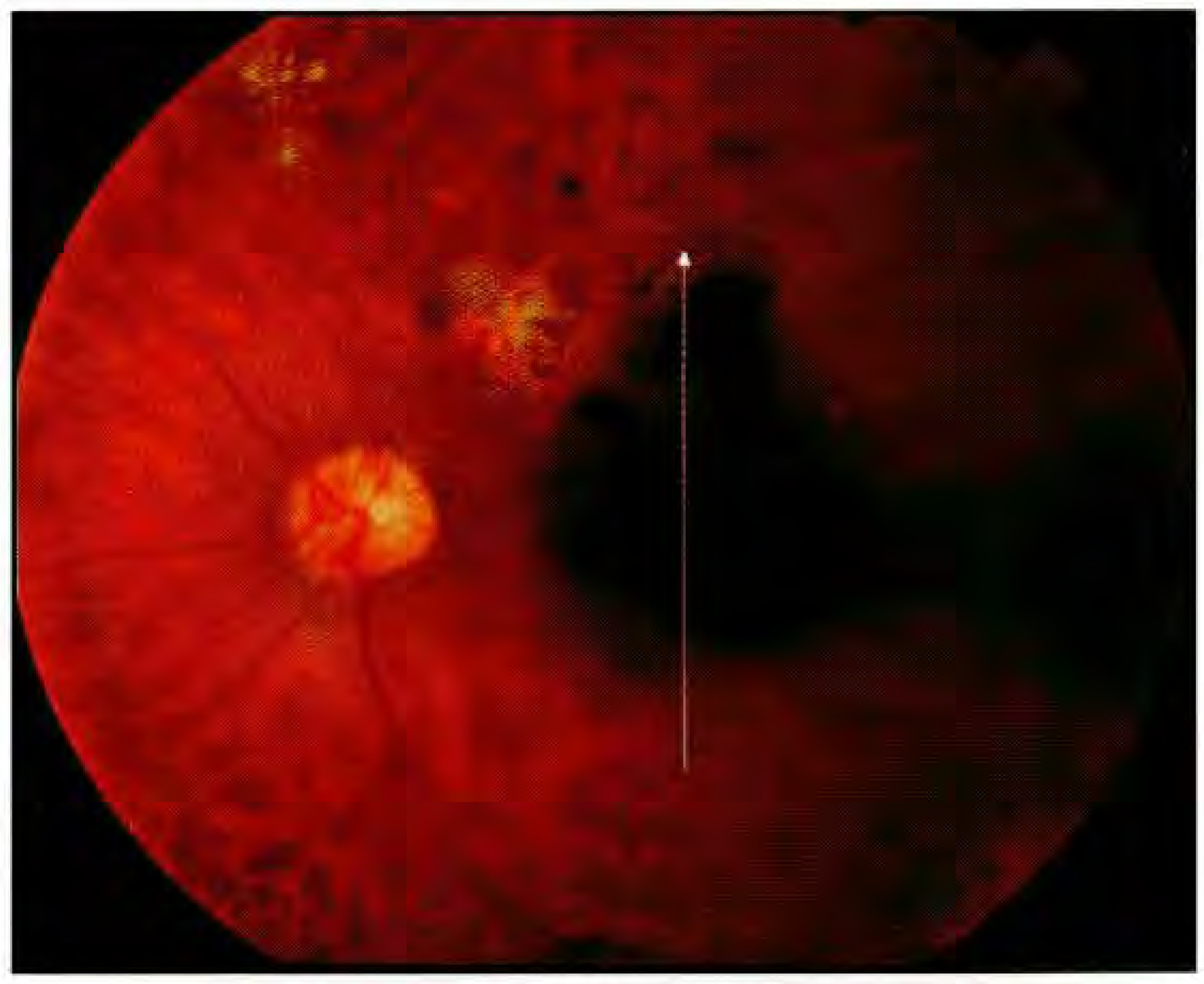

A

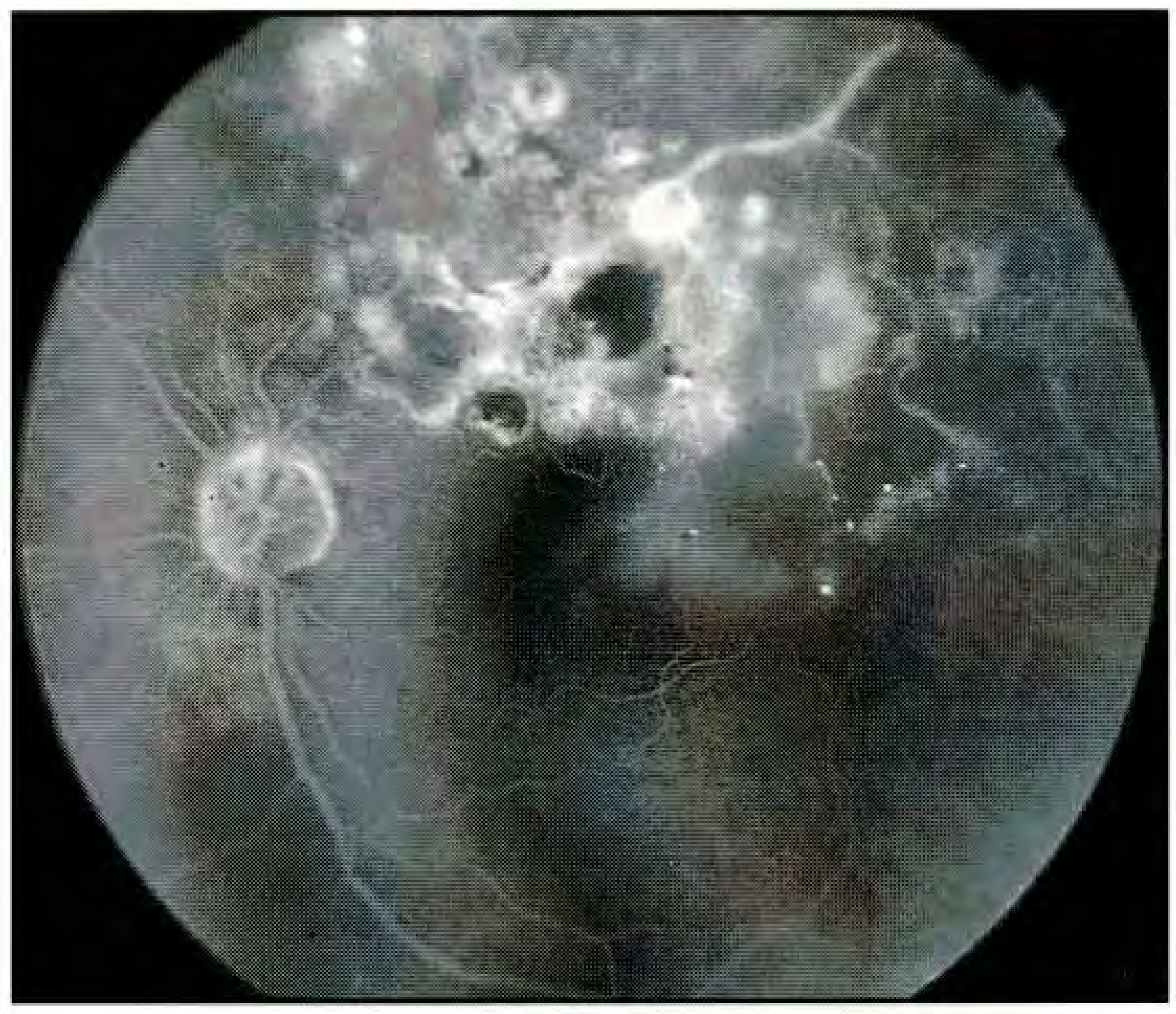

B

Clinical Summary

A 72-year-old man had a longstanding occlusion of the superotemporal branch retinal vein in his left eye. On examination, his visual acuity was 20/40, and dilated ophthalmoscopy (A) showed a foveal cyst with surrounding cystoid macular edema. Laser scars were also identified along the superotemporal arcade. Fluorescein angiography (B) showed hazy hyperfluorescence temporal and superior to the fovea consistent with macular edema, and hypofluorescent areas consistent with previous laser treatment or blood.

Optical Coherence Tomography

A vertical OCT tomogram (C) obtained through fixation delineated a large, optically transparent space in the fovea consistent with an intraretinal cyst. Significant fluid accumulation was seen in the outer retina superior to the fovea. The central macular thickness measured 800 μm. A thin, horizontal band anterior to the retina (arrow) was consistent with a small epiretinal membrane.

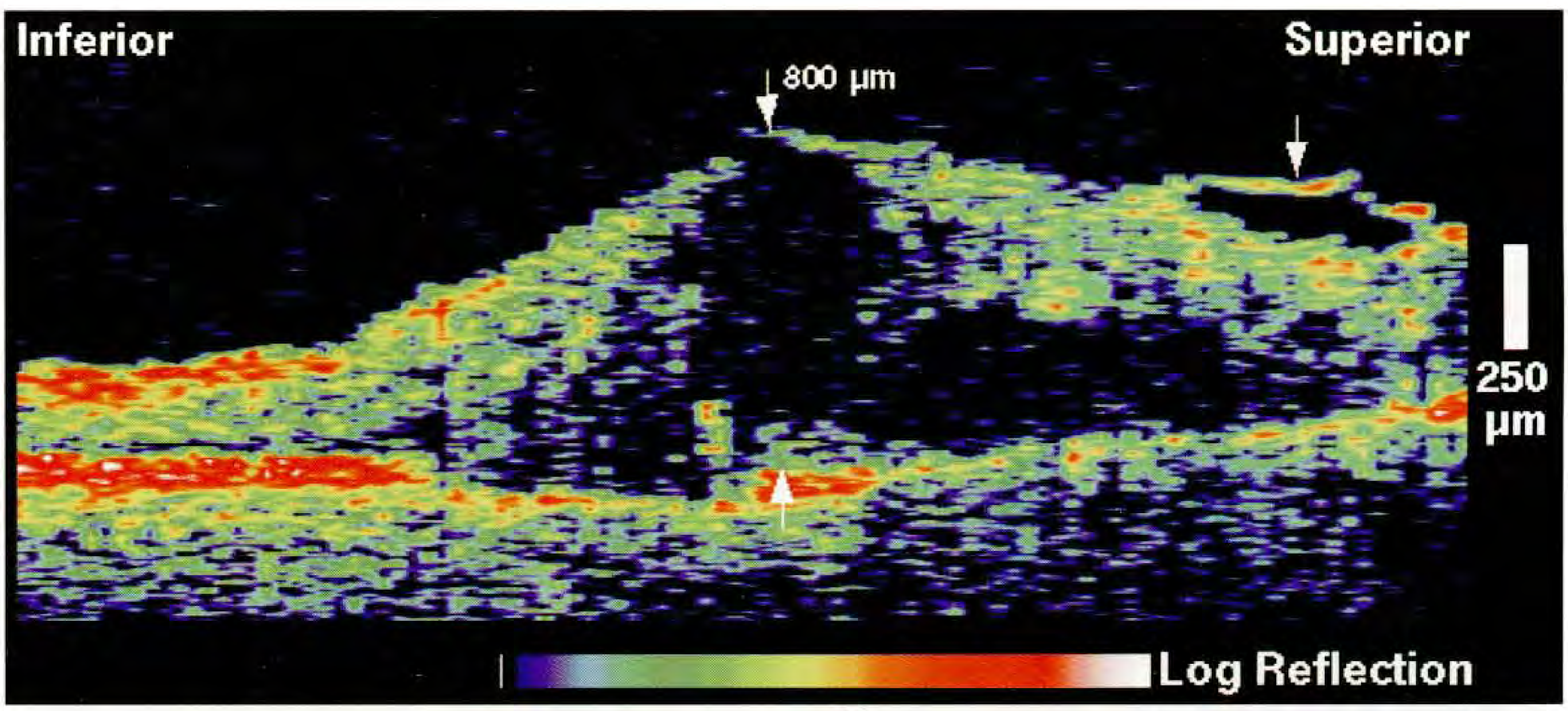

C

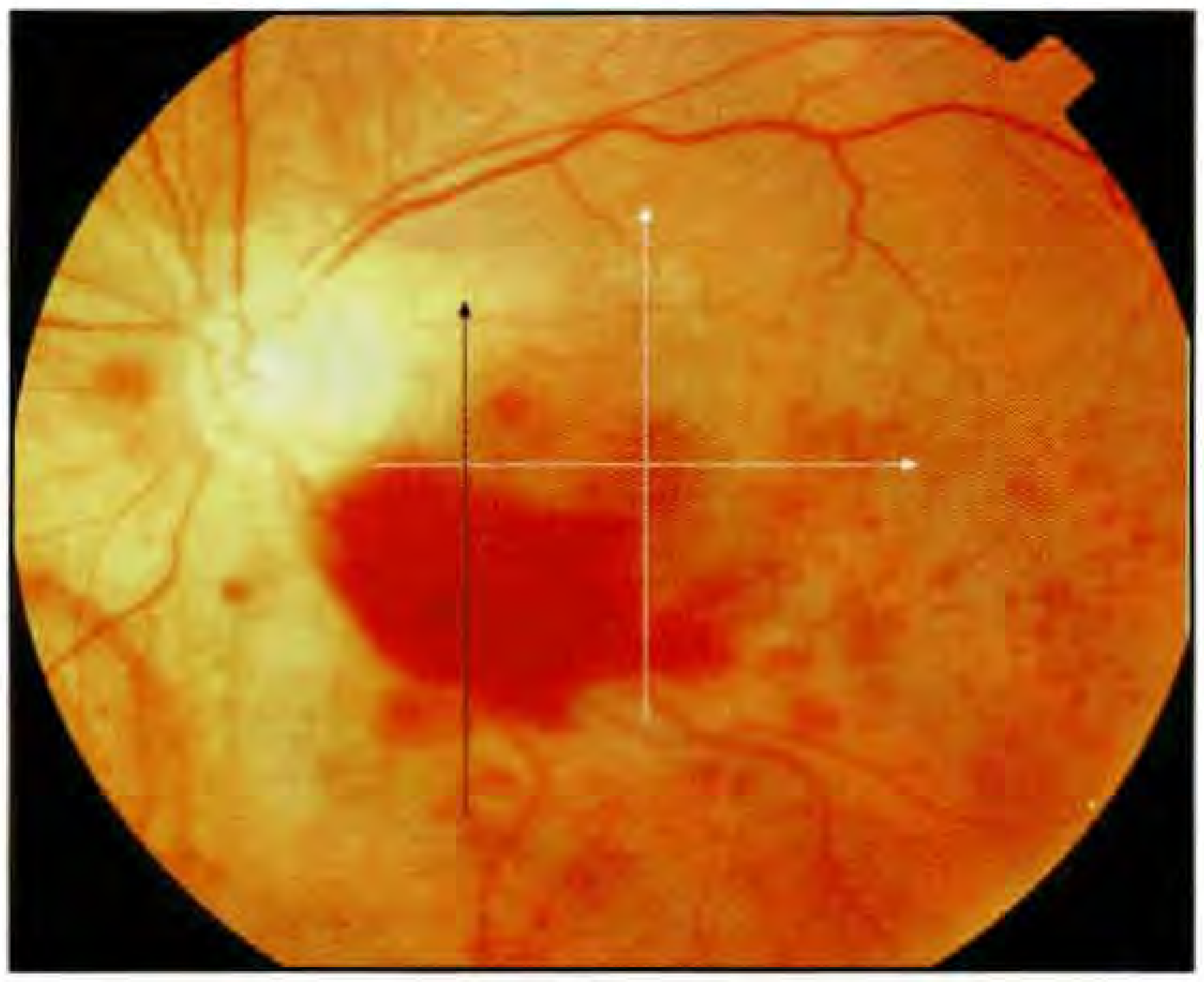

A

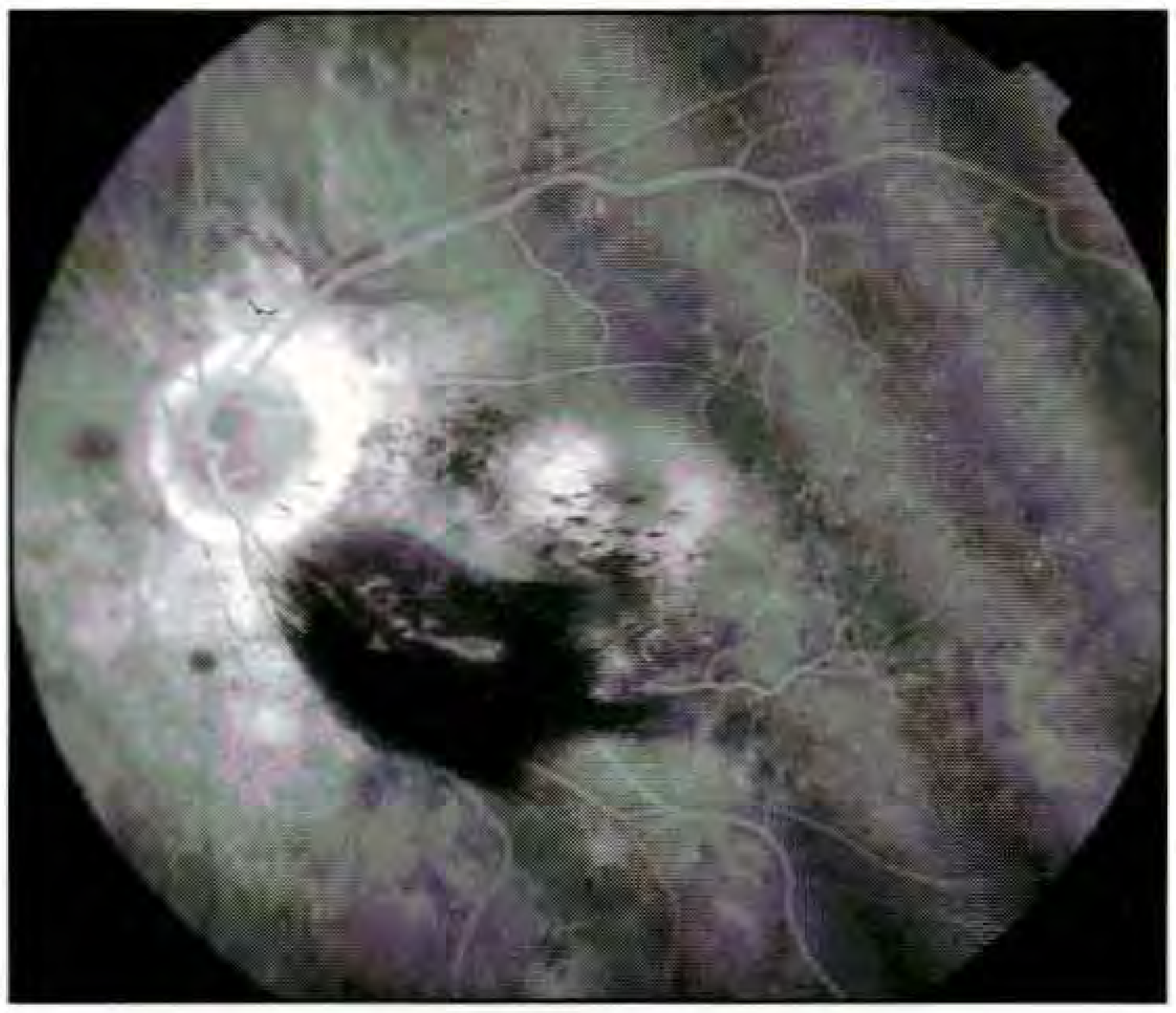

B

Case 5-5. Branch Retinal Vein Occlusion

Clinical Summary

A 85-year-old woman had a visual acuity of 20/200 in her left eye associated with the clinical diagnosis of an inferotemporal branch retinal vein occlusion. Small hemorrhages were observed throughout the inferior retina, with a single large hemorrhage surrounding the inferotemporal retinal vein (A). Fluorescein angiography (B) revealed delayed filling of this vein and late leakage in the macula corresponding to cystoid macular edema.

Optical Coherence Tomography

A horizontal OCT scan (C; horizontal white line on A) obtained through fixation showed increased retinal thickness throughout the macula and most prominently nasal to the center. A large cyst was identified directly in the fovea, with two smaller surrounding cysts consistent with the angiographic leakage pattern. A vertical image (D; vertical white line on A) also acquired through fixation again revealed cystoid macular edema, and retinal thickening inferior to the center. Intraretinal hemorrhage was identified inferiorly by its shadowing of the reflections from the outer retina. The attenuation of the probe beam by the blood was also exemplified in a vertical scan (E; black line on A) taken through the hemorrhage. The blood appeared highly backscattering and almost indistinguishable from the retinal nerve fiber layer, but was identified by the reduced reflections in that area from the retinal pigment epithelium and choroid.

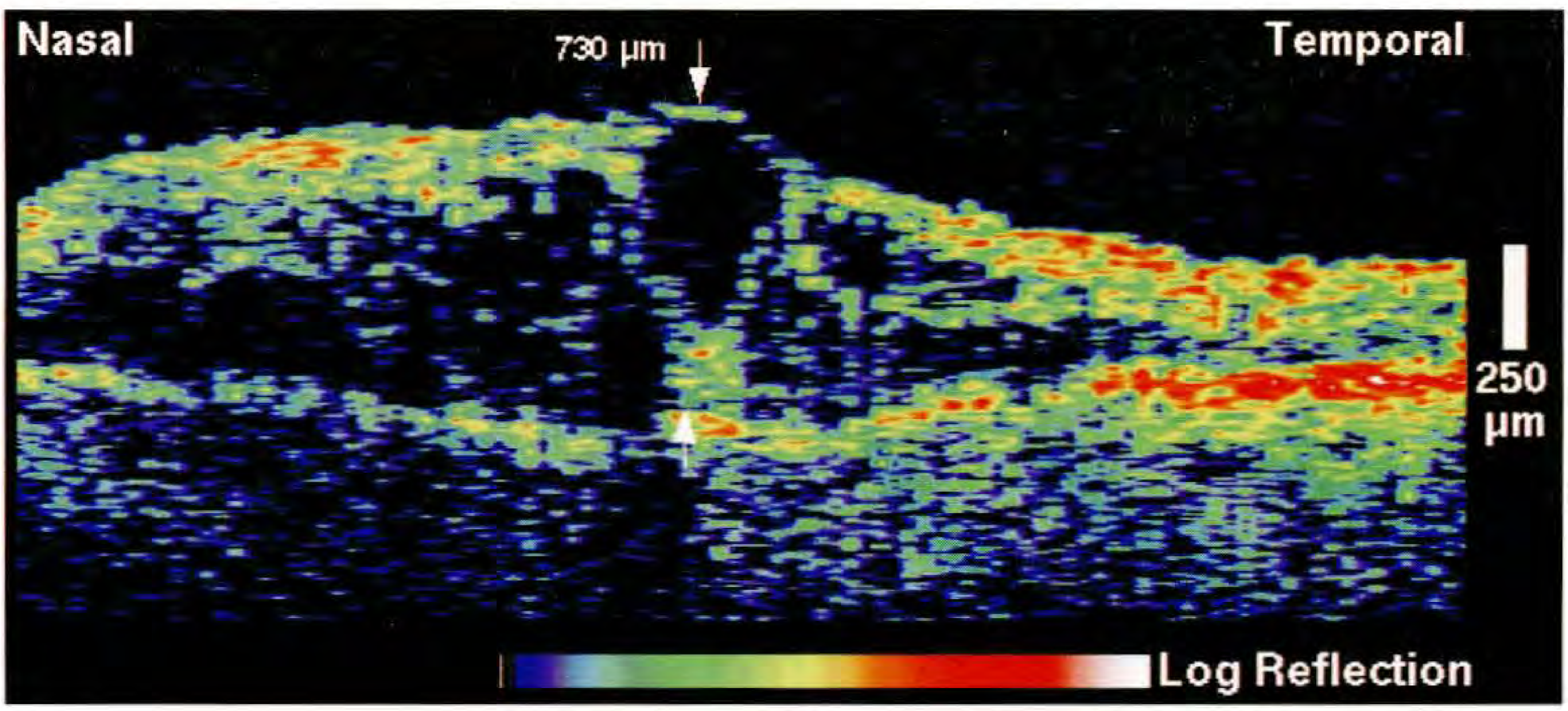

C

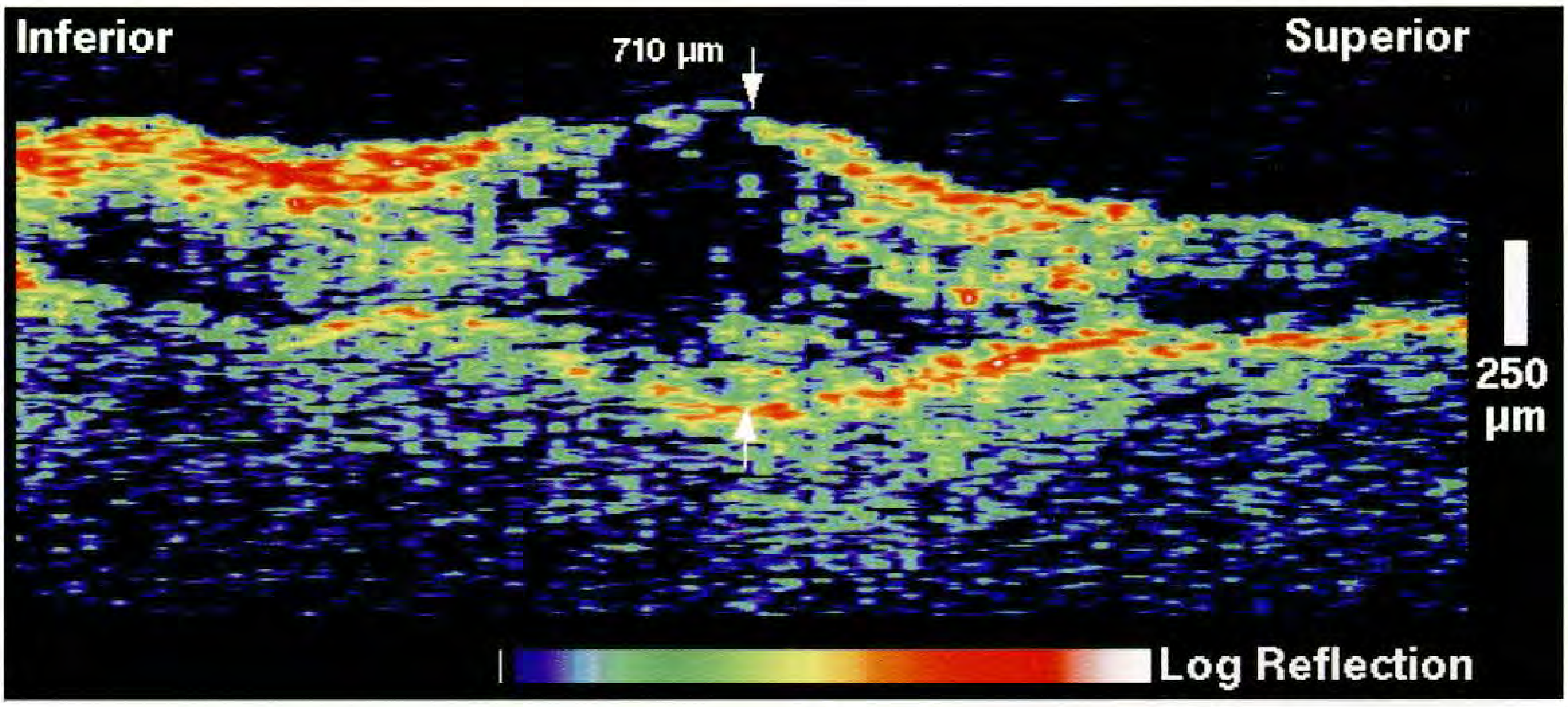
Inferior
710 µm
Superior
250 µm
Log Reflection

D

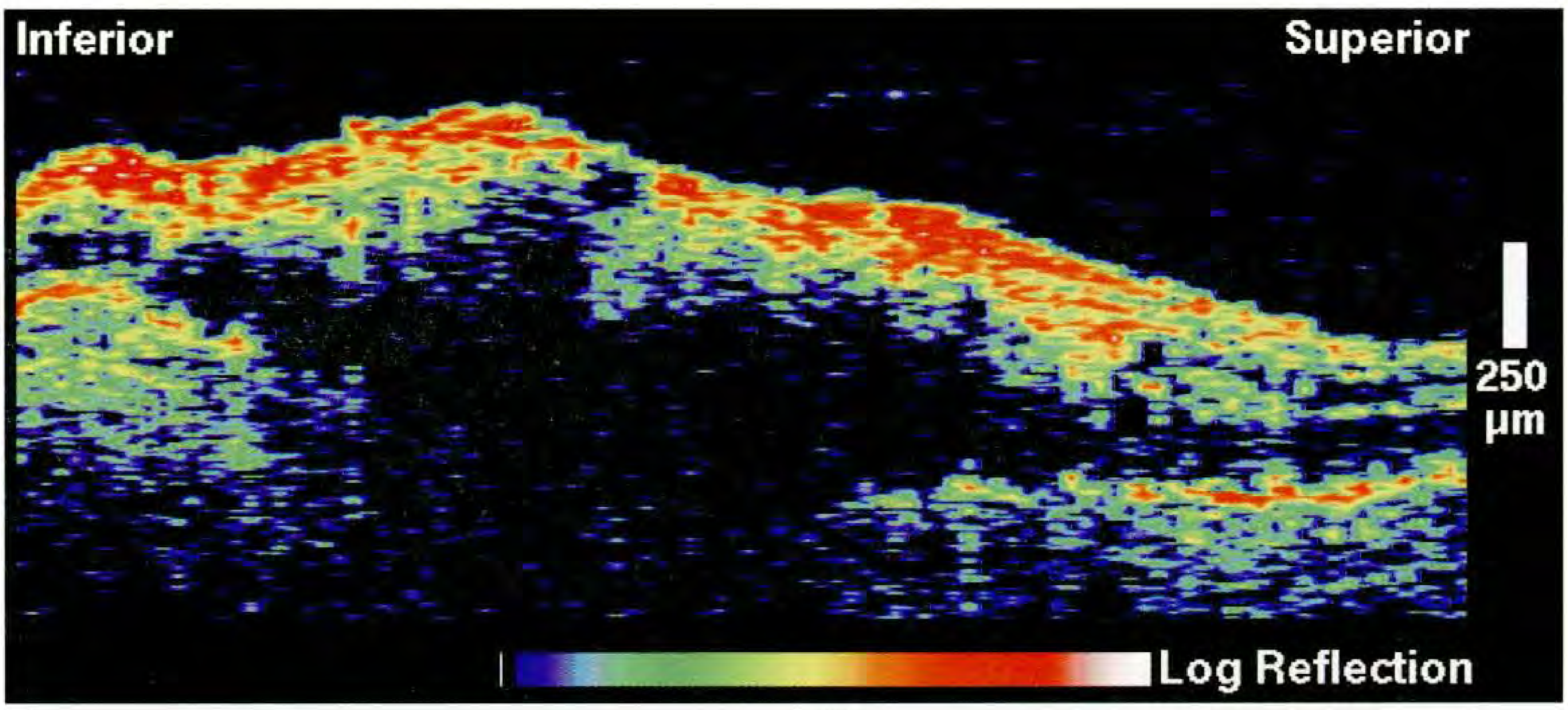
Inferior
Superior
250 µm
Log Reflection

E

A

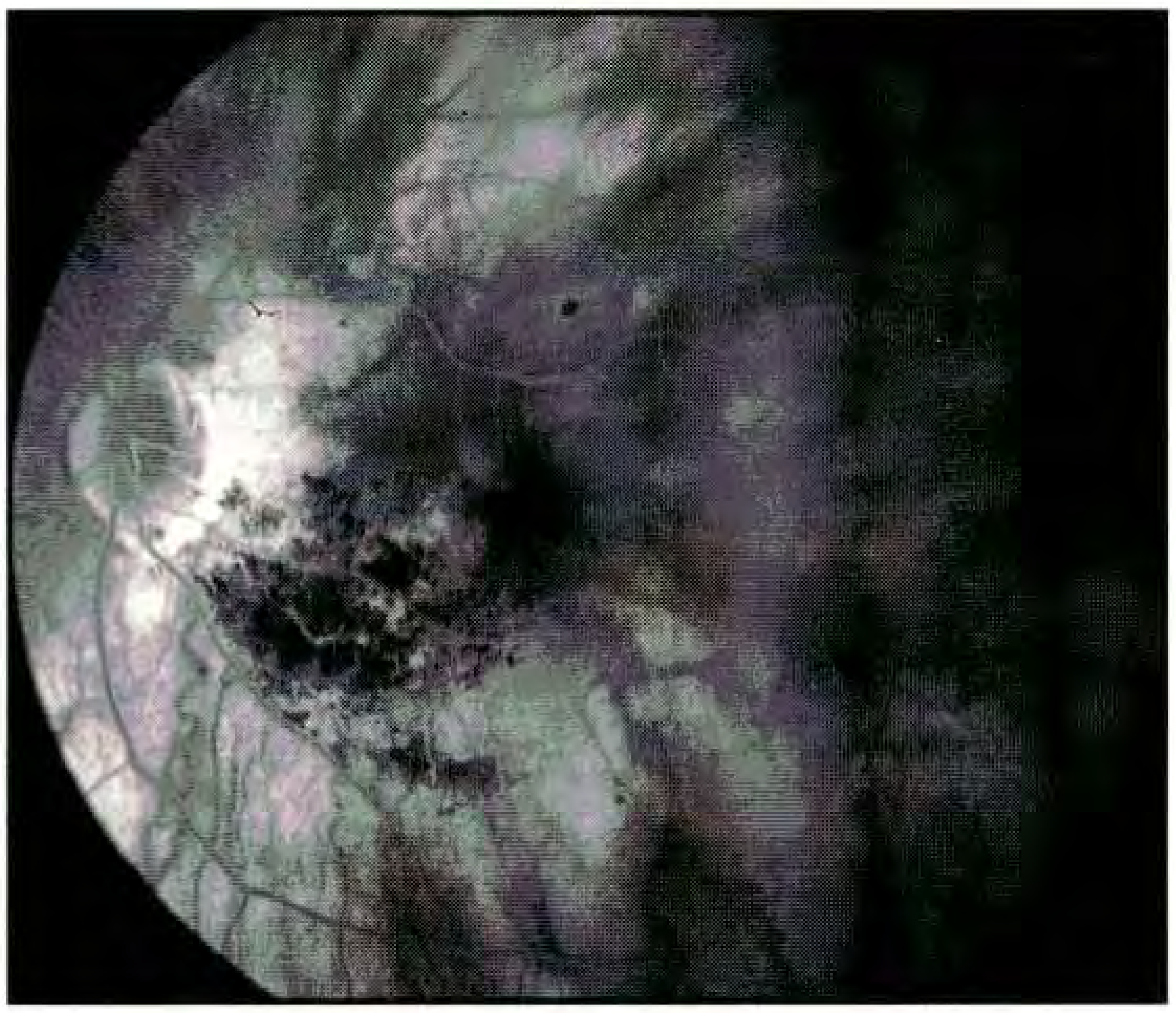

B

Case 5-6. Branch Retinal Vein Occlusion

Clinical Summary

A 79-year-old woman noticed an abrupt loss of vision in her left eye four months earlier. Her past medical history was significant for systemic hypertension, coronary artery disease, and congestive heart failure. On examination, her visual acuity in the left eye was 20/80. Slit-lamp biomicroscopy (A) showed intraretinal hemorrhage nasal to the fovea with moderate retinal thickening that approached the fovea. There was no engorgement or tortuousity of the retinal veins. Fluorescein angiography (B) demonstrated delayed filling of the inferotemporal branch vein, hypofluorescence due to hemorrhage, and mild leakage into the fovea during the late phase.

Optical Coherence Tomography

A horizontal OCT scan through fixation (C) displayed retinal thickening nasal to the center involving the edge of the fovea. The fluid accumulation appeared to specifically involve the outer retinal layers.

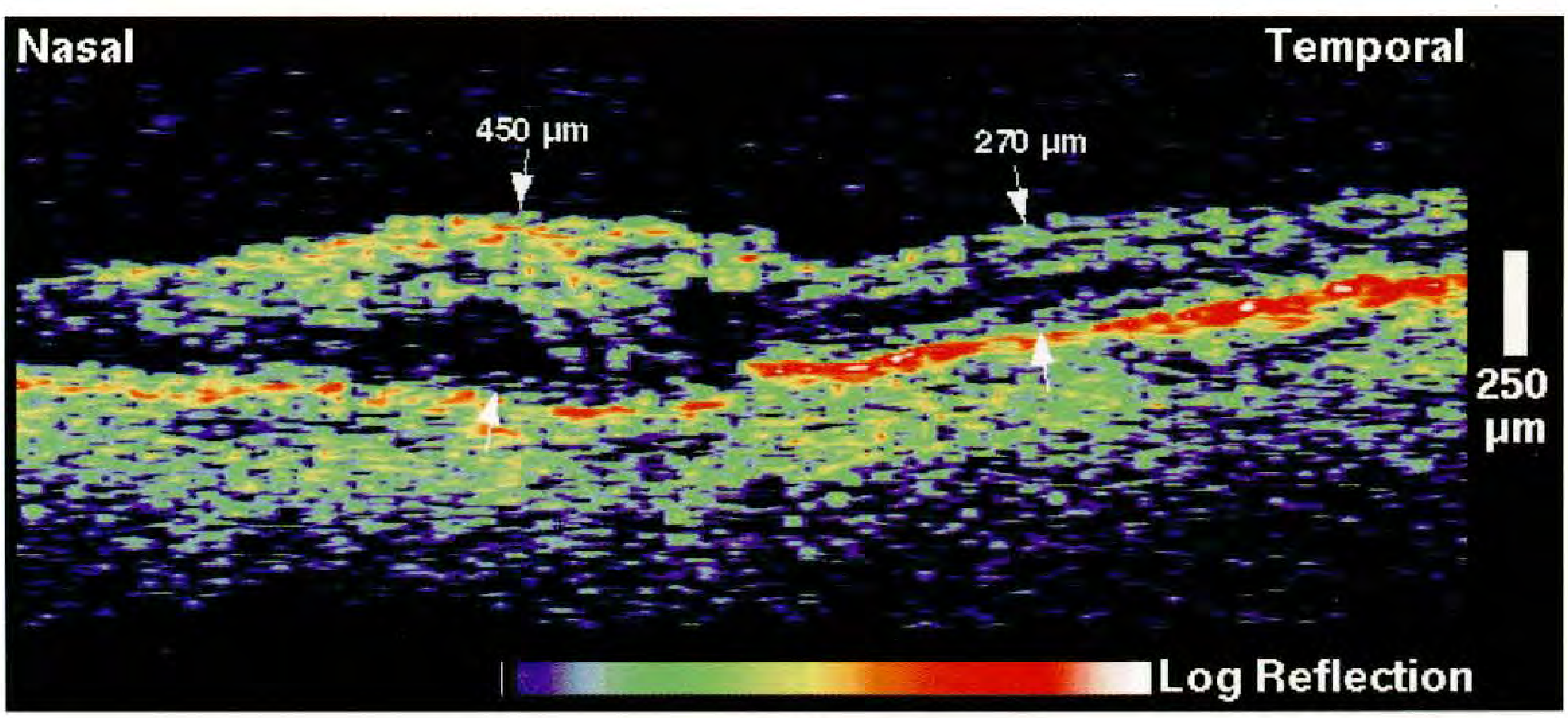

C

Case 5-7. Branch Retinal Vein Occlusion and Lamellar Macular Hole

Clinical Summary

A 65-year-old woman had an inferotemporal branch retinal vein occlusion in her left eye decreasing her visual acuity in this eye to 20/60. Focal laser photocoagulation treatment had been performed one year earlier. The current exam (A) revealed regression of the macular edema, a foveal cyst, and an improved visual acuity to 20/30.

Optical Coherence Tomography

OCT images (B, C) obtained through the fovea showed the persistence of the retinal thickening inferior to the center, with fluid accumulation in the outer retinal layer. The normal contour of the foveal pit was absent, consistent with a lamellar macular hole. Small intraretinal cysts were observed surrounding the hole.

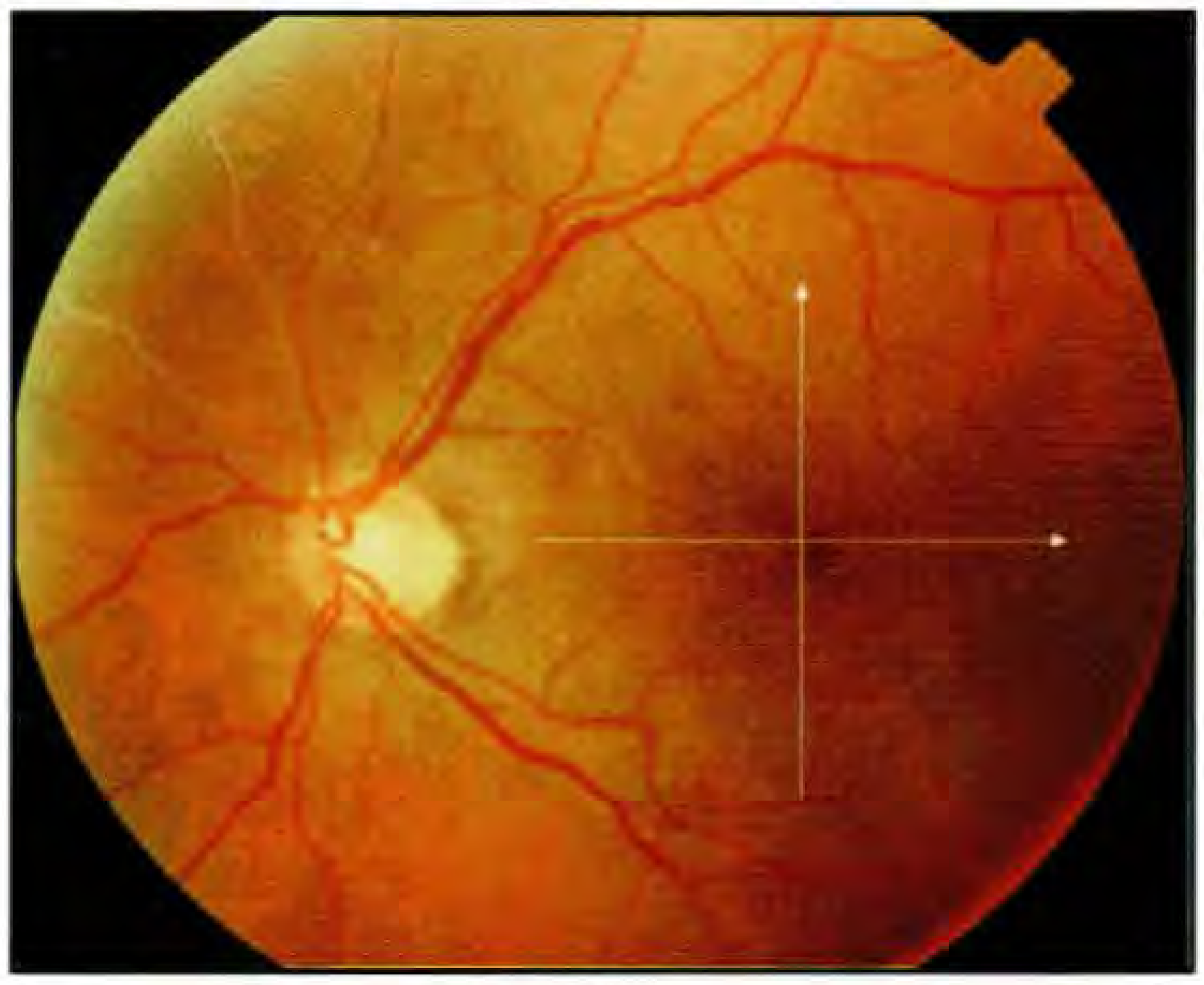

A

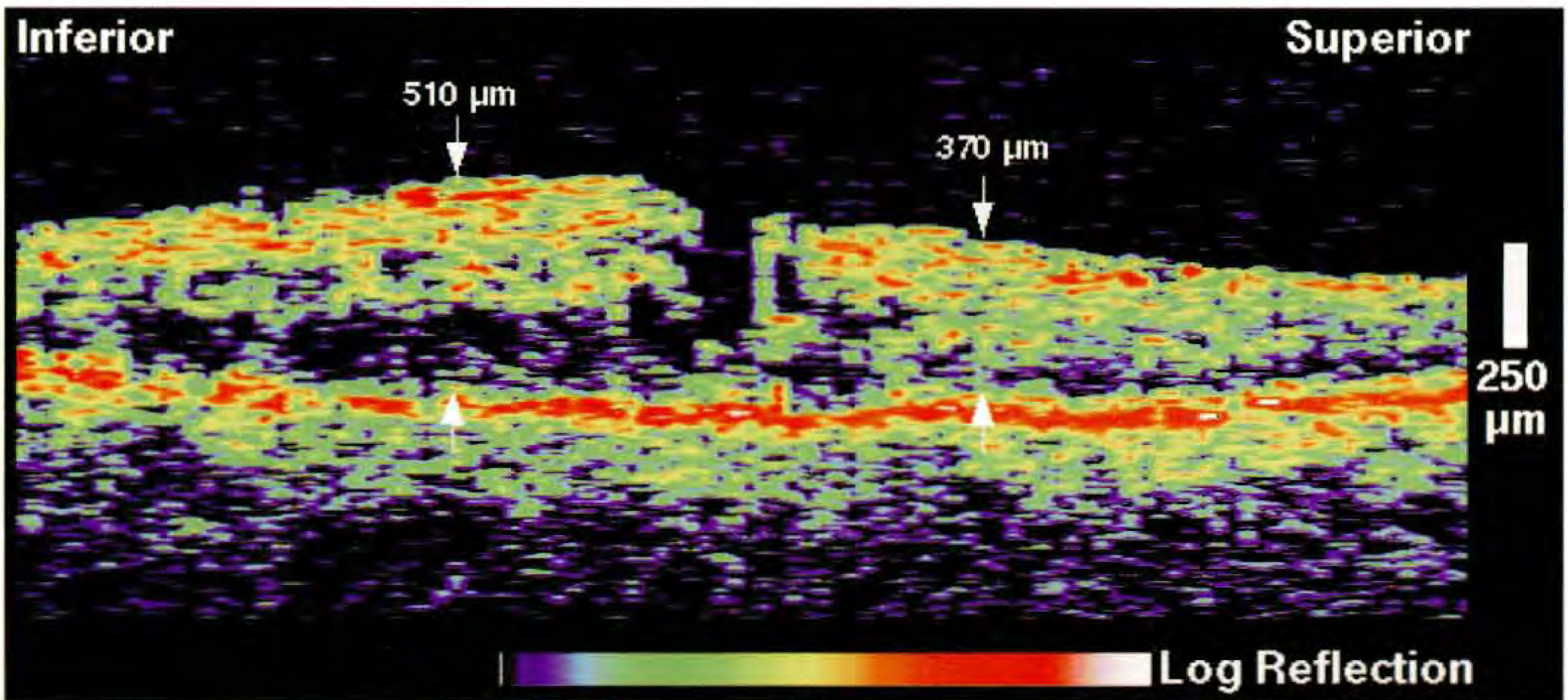

B

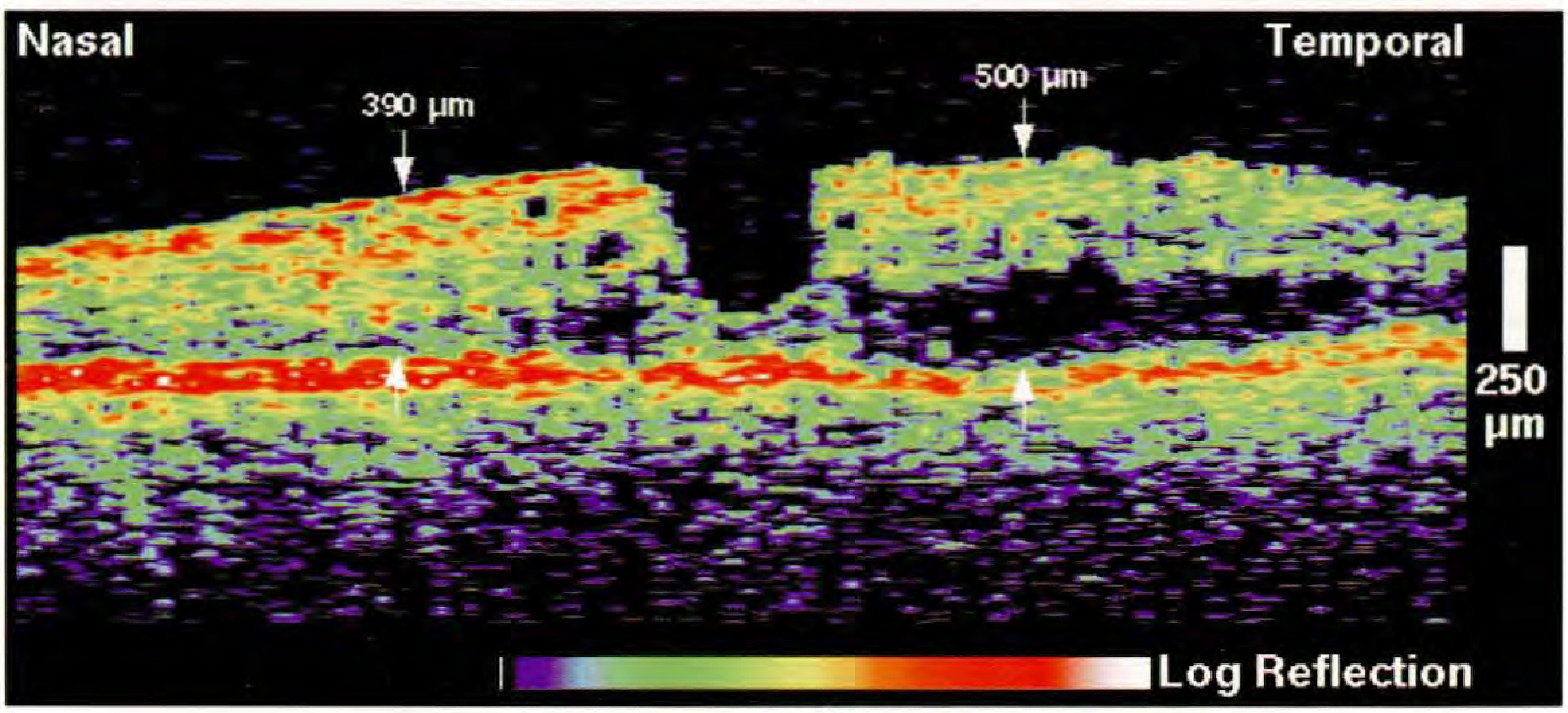

C

A

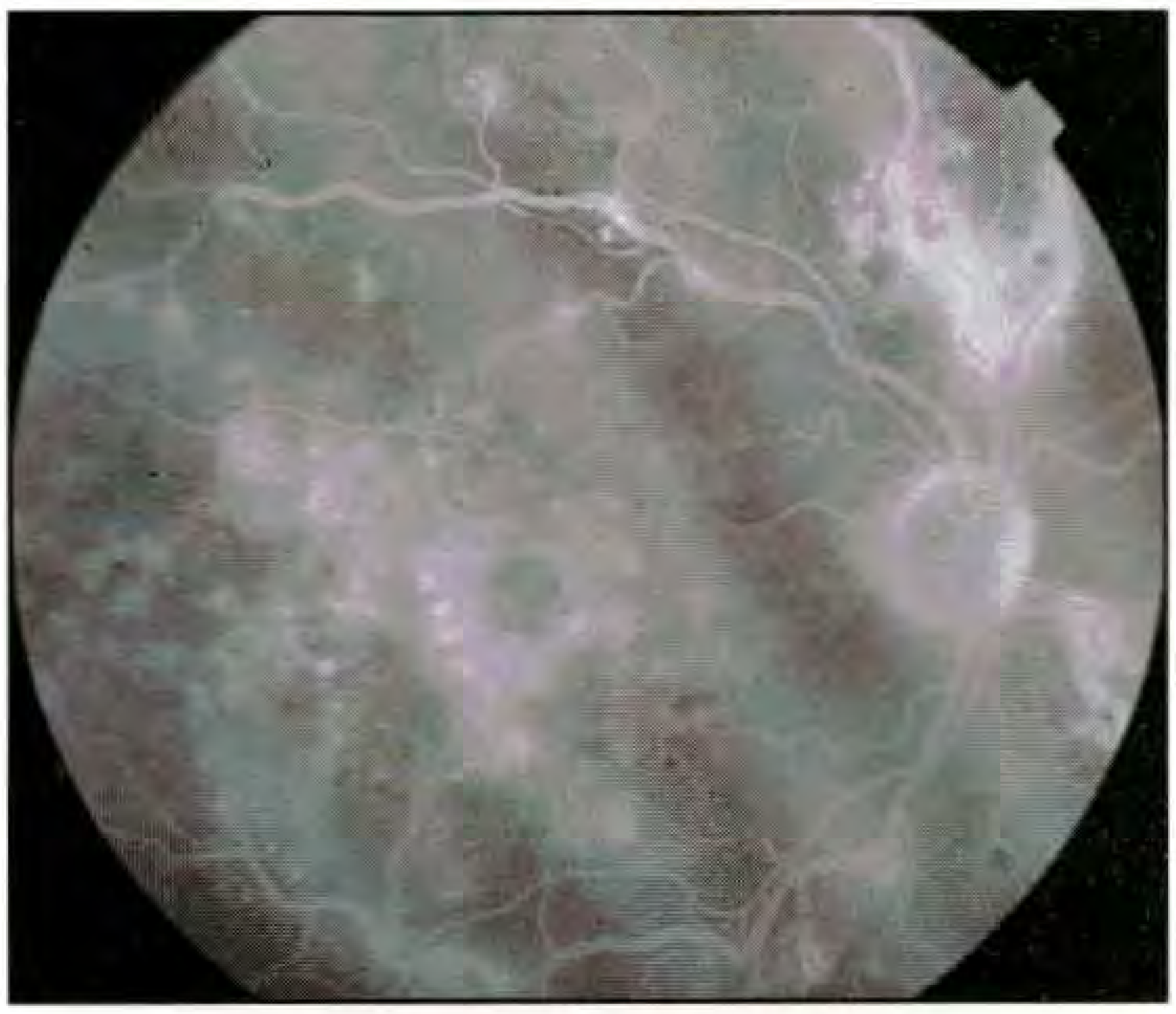

B

Case 5-8. Central Retinal Vein Occlusion with Cystoid Macular Edema and Lamellar Hole

Clinical Summary

An 87-year-old woman with a history of non-ischemic central retinal vein occlusion in both eyes was examined. She had received grid laser photocoagulation in the right eye one month earlier. Slit-lamp biomicroscopy (A) revealed significant cystoid macular edema, engorged retinal veins, and blot and flame-shaped hemorrhages scattered throughout the posterior pole. The visual acuity in this eye was 20/200. Diffuse late leakage was evident on the fluorescein angiogram (B) consistent with cystoid macular edema.

Optical Coherence Tomography

A horizontal OCT tomogram (C) showed an increased retinal thickness of 670 µm in the fovea. The reduced optical backscatter signal observed intraretinally was consistent with cystic fluid accumulation, and a large foveal cyst was observed which extended to the inner limiting membrane.

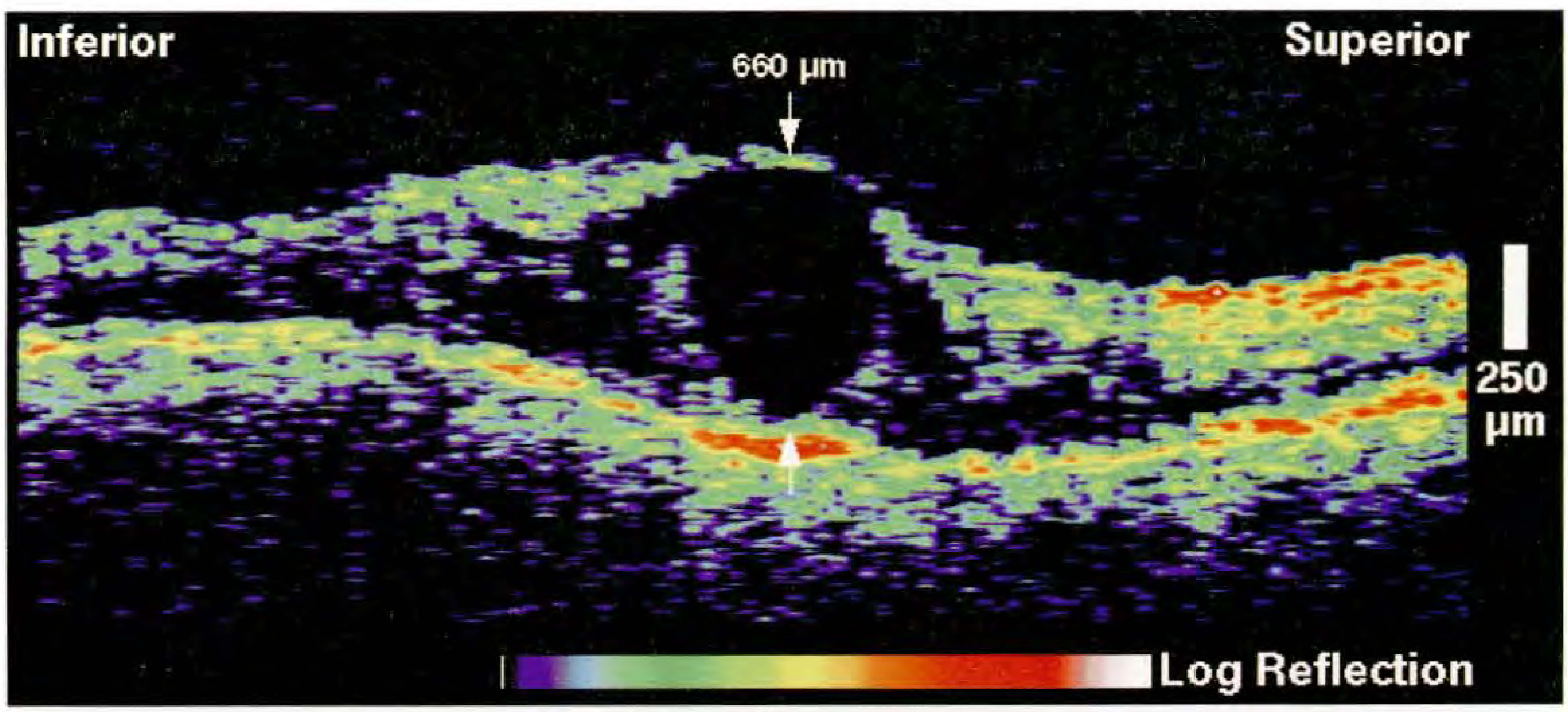

C

Case 5-8 continued

Clinical Summary

The patient's left eye was notable for a large lamellar macular hole, with a visual acuity of counting fingers at five feet (D). Fluorescein angiography (E) displayed a hyperfluorescent ring in the macula consistent with a window defect, and mild late leakage in the perifoveal region.

Optical Coherence Tomography

The OCT image (F), acquired horizontally through the macula, demonstrated a striking partial-thickness hole. The contour of the outer retina suggested the rupture of three large intraretinal cysts.

D

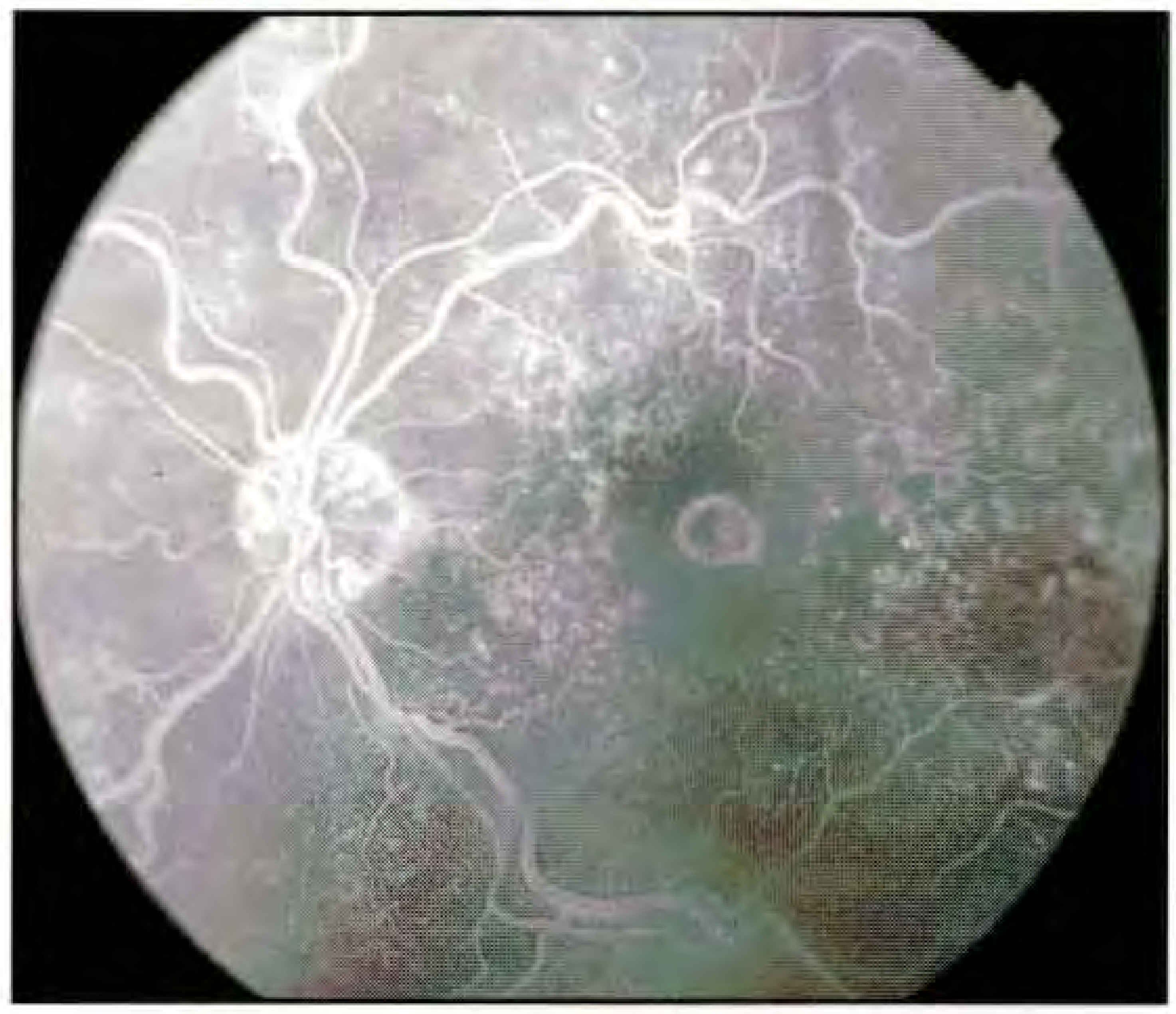

E

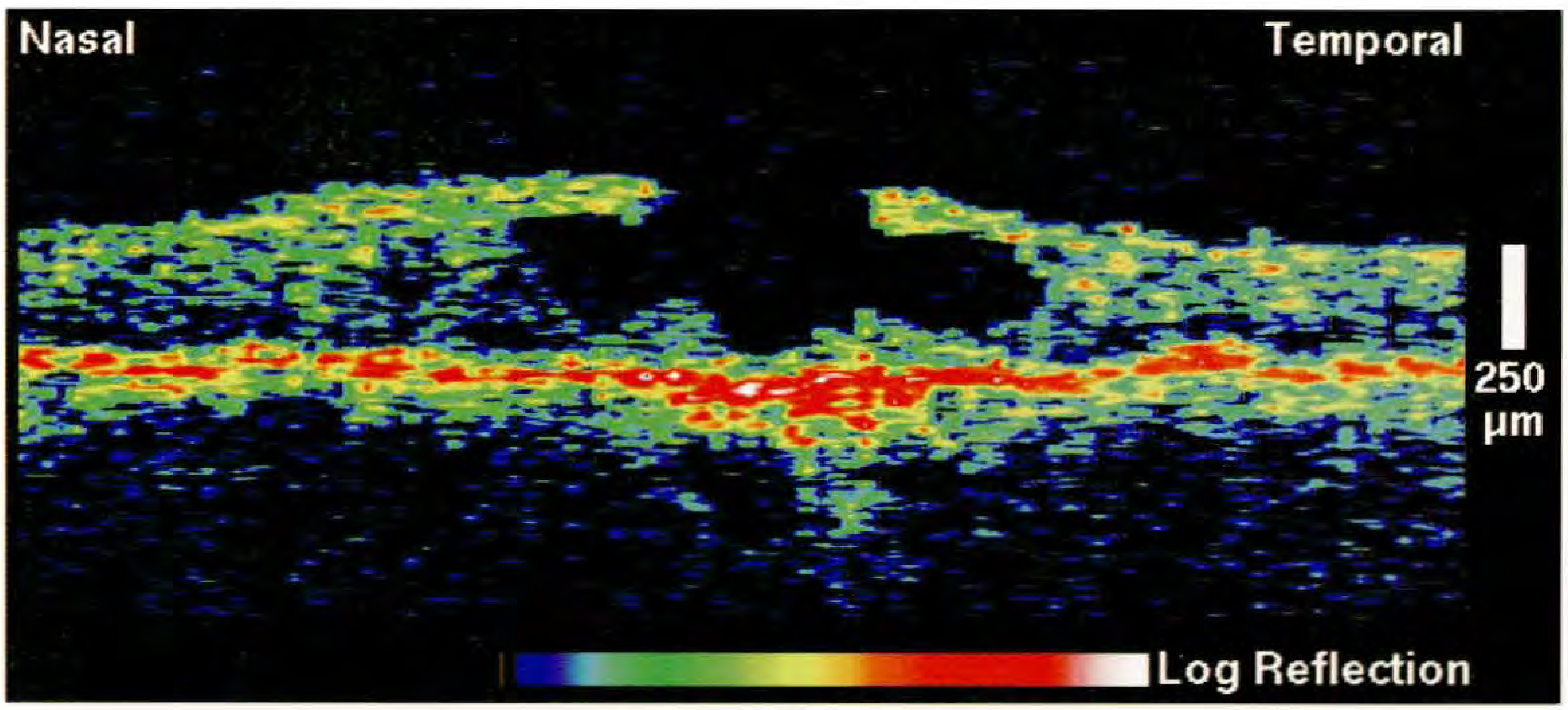

F

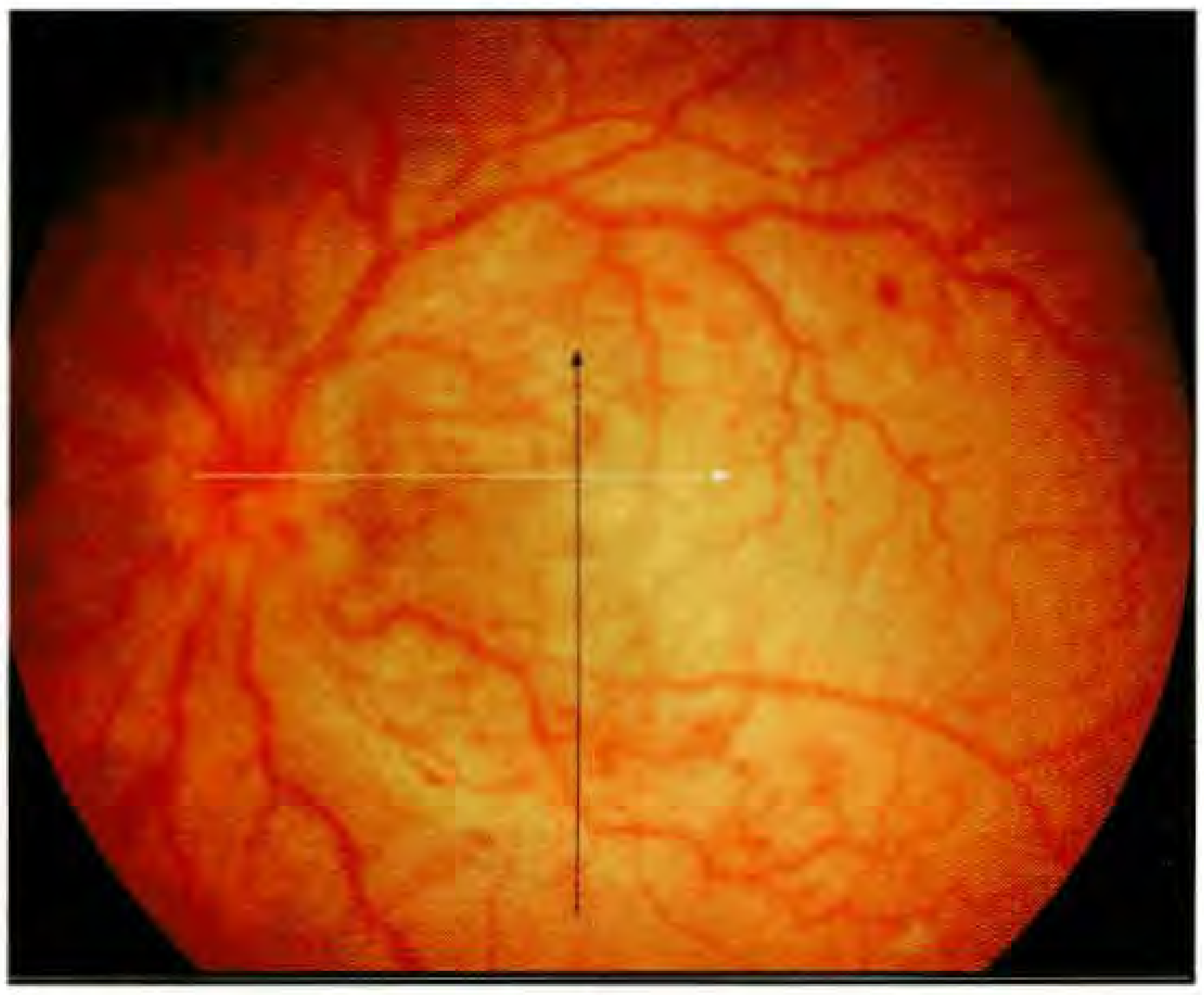

A

B

C

Case 5-9. Central Retinal Vein Occlusion

Clinical Summary

A 20-year-old woman had a central retinal vein occlusion and macular edema in her left eye. The visual acuity in this eye was 20/400. Slit-lamp examination (A) revealed mildly dilated and tortuous veins, retinal hemorrhages, macular thickening, and papilledema. Angiography (B) showed diffuse late leakage of fluorescein dye surrounding the optic disc and the inferotemporal vascular arcade. Hyperfluorescence was also noted superior and nasal to the fovea.

Optical Coherence Tomography

OCT imaging (D; black line on A) demonstrated a diffuse increase in retinal thickness throughout the macula and a disruption of the layers of the retina beneath the fovea consistent with a neurosensory retinal detachment. The outer plexiform layer appeared to be specifically involved consistent with the classically described histopathological findings of macular edema. A linear tomogram (E; white line on A) acquired through the optic disc and macula displayed significant edema of the disc and further delineated the thickening and detachment of the neurosensory retina in the macula.

Follow-up Examination

Seven months later, the patient's visual acuity in this eye had not improved. Dilated fundus examination (C), however, showed that both the optic disc and macula were flat. The retinal venous engorgement and tortuosity had resolved, and no retinal hemorrhages were noted. A subretinal fibrotic scar was evident in the central macula.

Follow-up Optical Coherence Tomography

A follow-up OCT image (F; white line on C) was obtained through the optic disc and macula. Mild disc edema was still present, but the image indicated the disappearance of the macular thickening and the resolution of the neurosensory detachment.

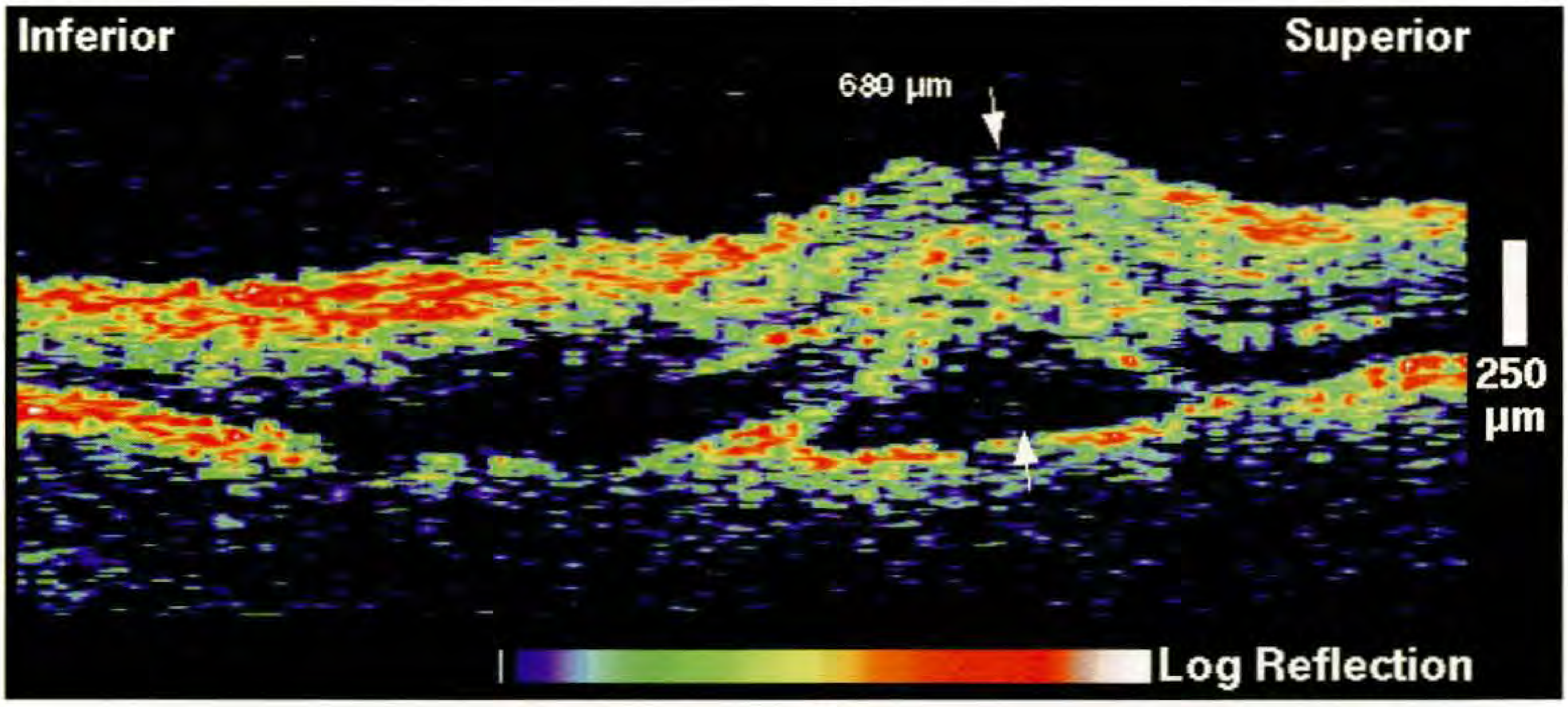
Inferior
Superior
680 μm
250 μm
Log Reflection

D

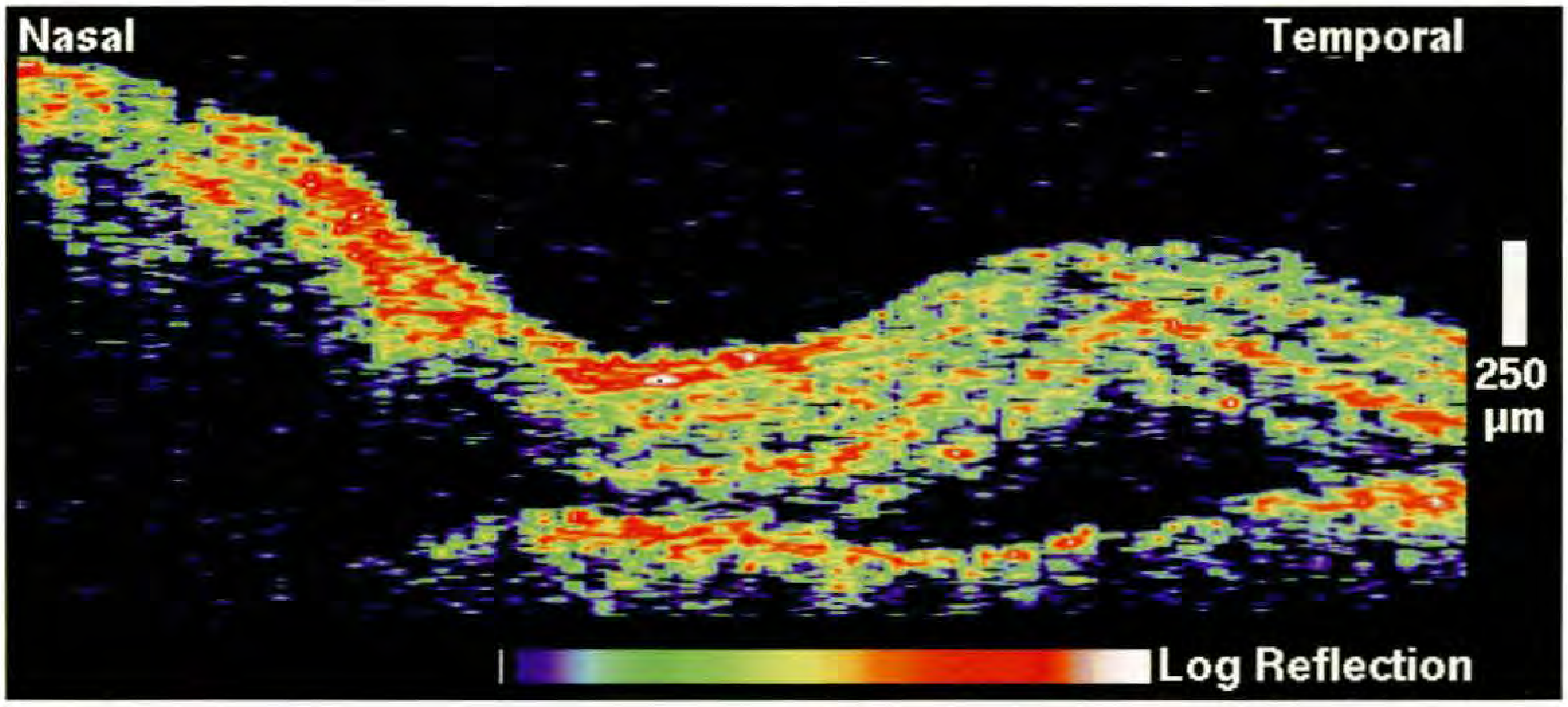
Nasal
Temporal
250 μm
Log Reflection

E

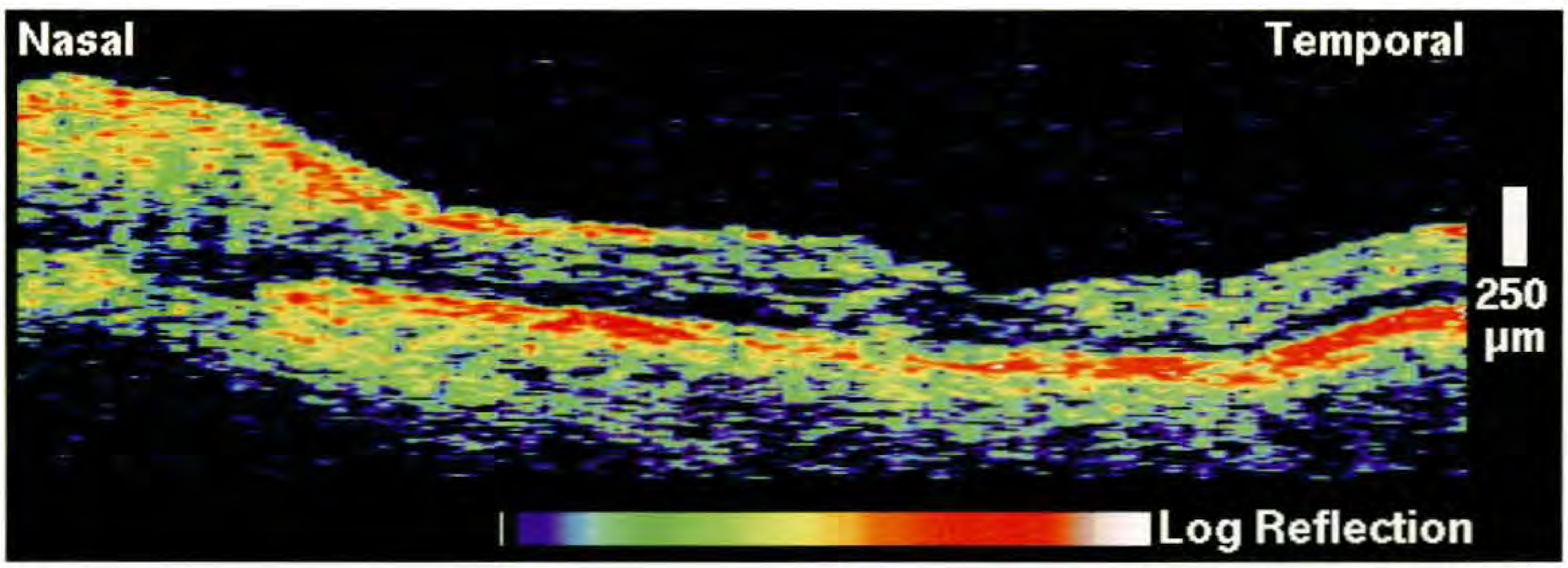
Nasal
Temporal
250 μm
Log Reflection

F

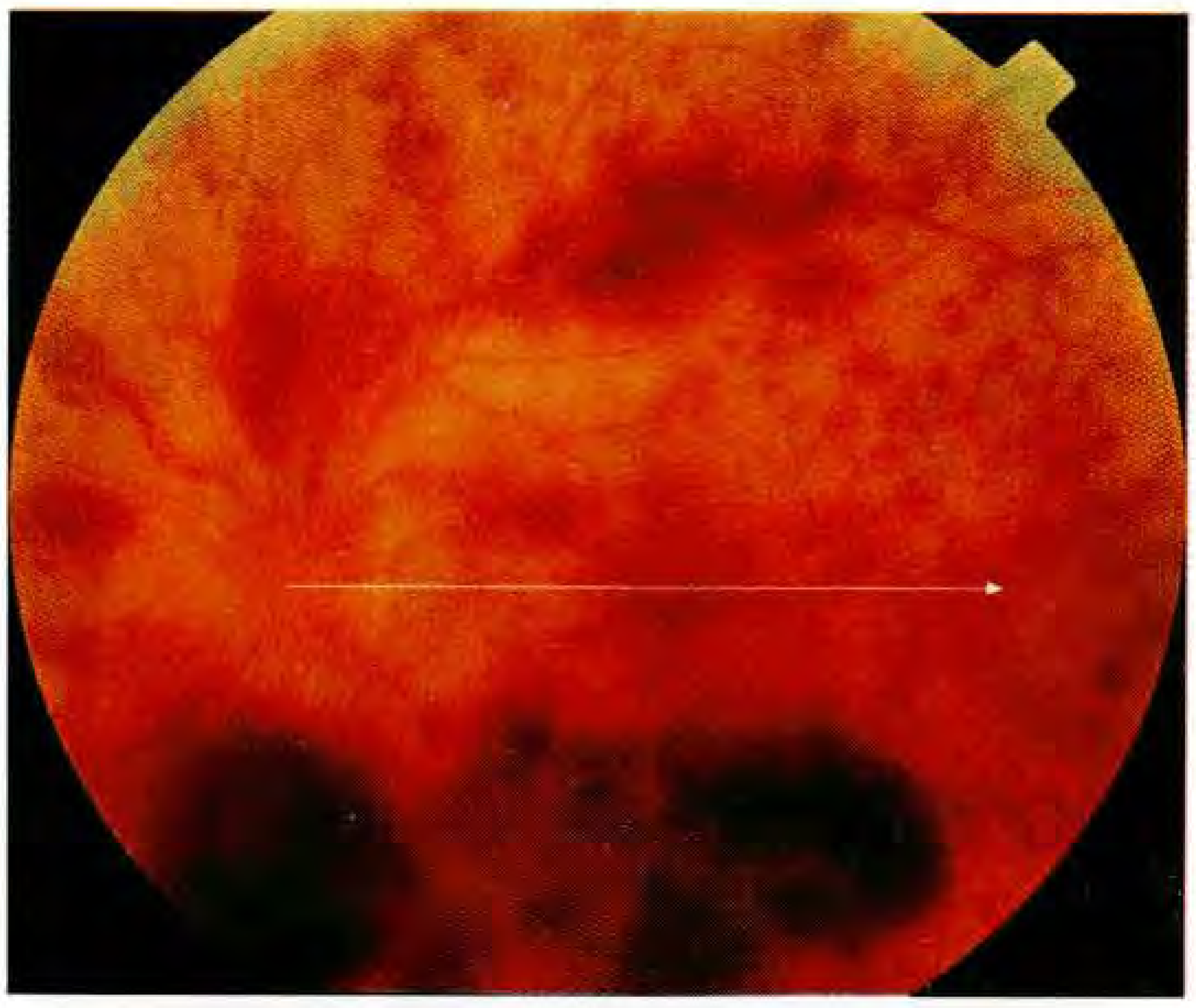

A

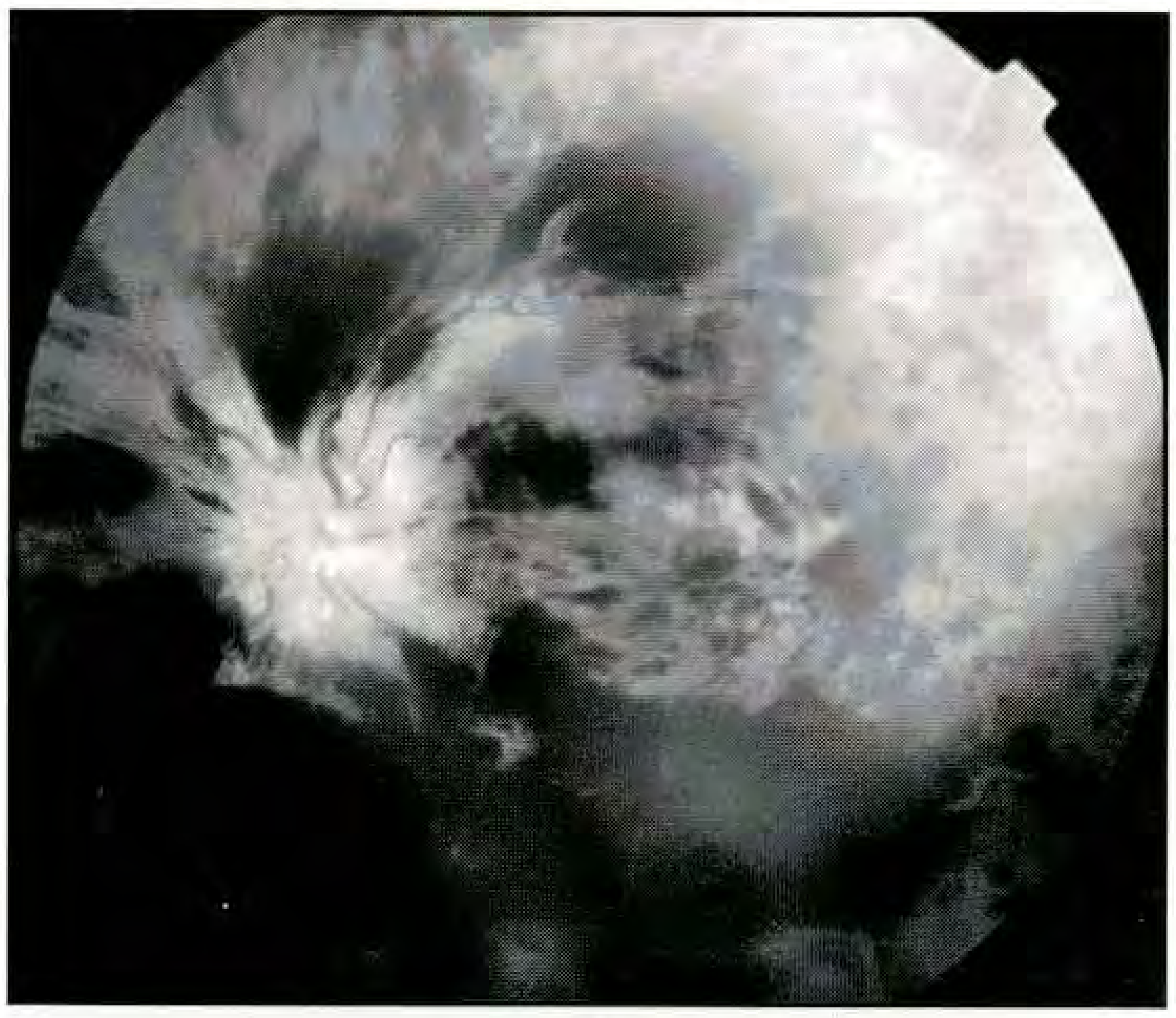

B

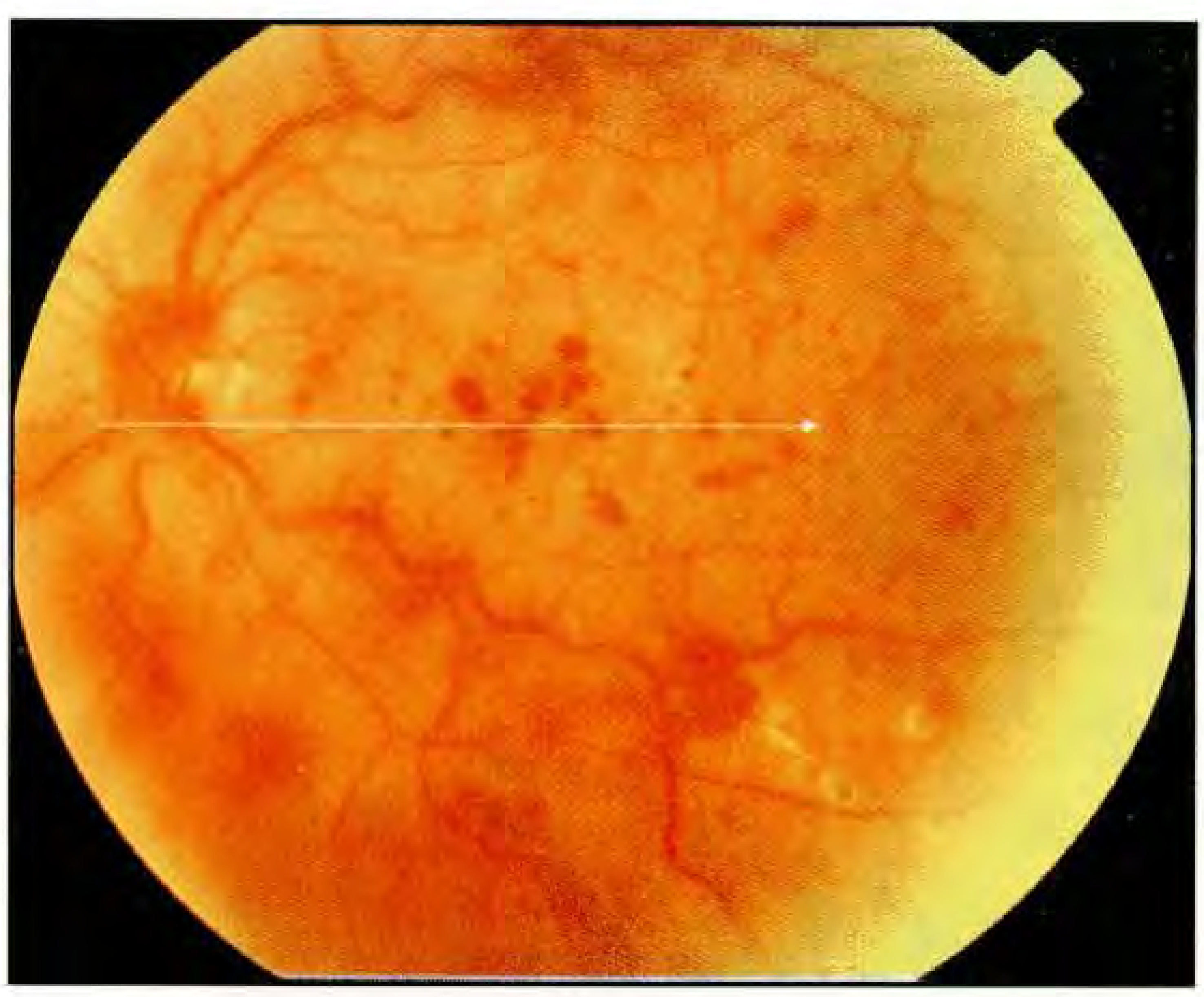

C

Case 5-10. Central Retinal Vein Occlusion

Clinical Summary

A 74-year-old woman with a history of a macular hole in her left eye noticed a sudden decrease in vision in this eye two months earlier. Her systemic work-up was significant for hypertension, transient ischemic attacks, peripheral vascular disease, and atrial fibrillation. On examination, her visual acuity was counting fingers at six inches. Slit-lamp biomicroscopy (A) showed mild edema of the optic disc, dilated and tortuous retinal veins, diffuse macular edema, and significant retinal hemorrhages throughout the macula and periphery consistent with an occlusion of the central retinal vein. No neovascularization was reported. Fluorescein angiography (B) indicated delayed venous filling, diffuse hyperfluorescence of the disc and macula with late leakage consistent with papillary and macular edema, and widespread hypofluorescence due to retinal hemorrhage. The right eye, with a visual acuity of 20/25, was normal on fundus examination except for a posterior vitreous detachment.

Optical Coherence Tomography

OCT examination (D) of the left eye showed a protusion of the disk contour consistent with papilledema. Mild retinal thickening was noted, and was more significant in the nasal compared to the temporal macula. An elevation of the neurosensory retina above an optically lucent space was also observed consistent with a sensory retinal detachment. The right eye (E) was notable for a pseudo-operculum situated approximately 350 μm anterior to the fovea, suggesting an arrested stage of macular hole development in this eye.

Follow-up Examination

Three months later, the patient developed rubeosis iridis, and received panretinal photocoagulation treatment in her left eye with a dye yellow laser. A follow-up examination one month after the procedure showed regressed neovascularization of the iris and significantly reduced retinal hemorrhage (C). The optic disc remained elevated and mild to moderate retinal thickening was still present in the macula. Visual acuity was still counting fingers.

Follow-up Optical Coherence Tomography

A repeat horizontal OCT scan (F) demonstrated a resolution of the sensory retinal detachment observed earlier. The disc edema also was reduced. However, diffuse retinal thickening corresponding to macular edema was still observed, especially nasal to the fovea, and appeared to be slightly increased compared to the previous examination.

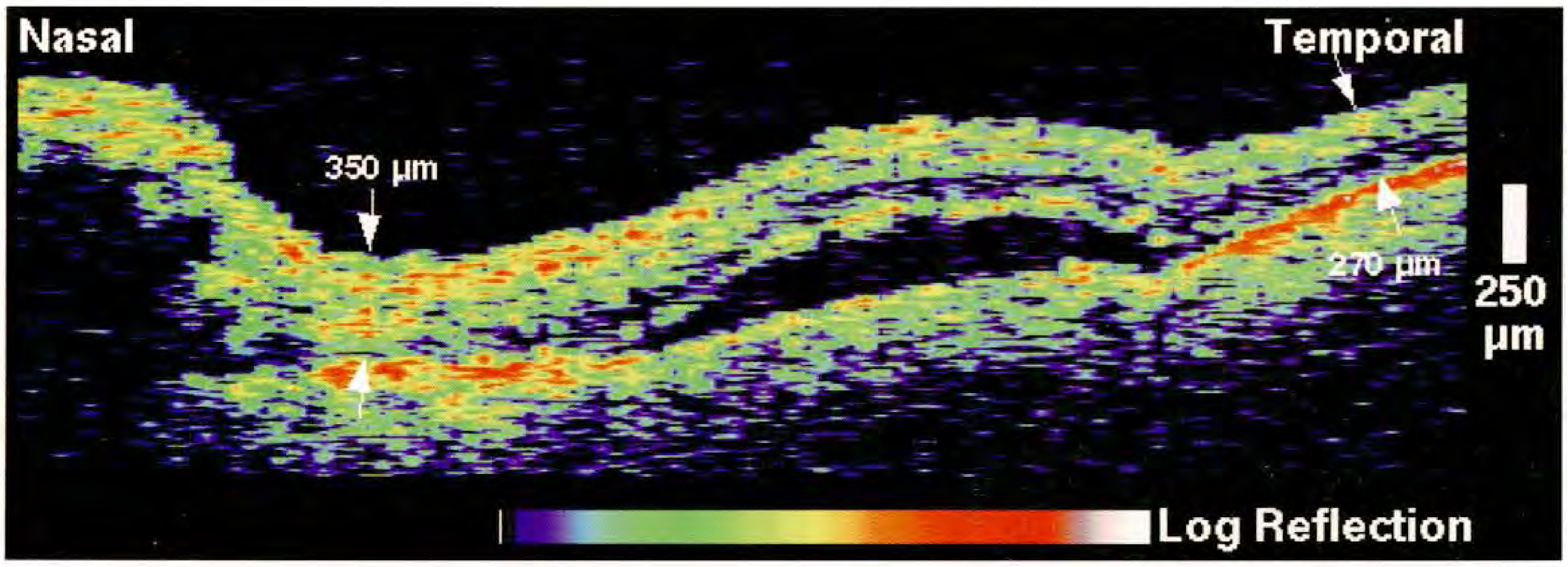
Nasal
Temporal
350 µm
270 µm
250 µm
Log Reflection

D

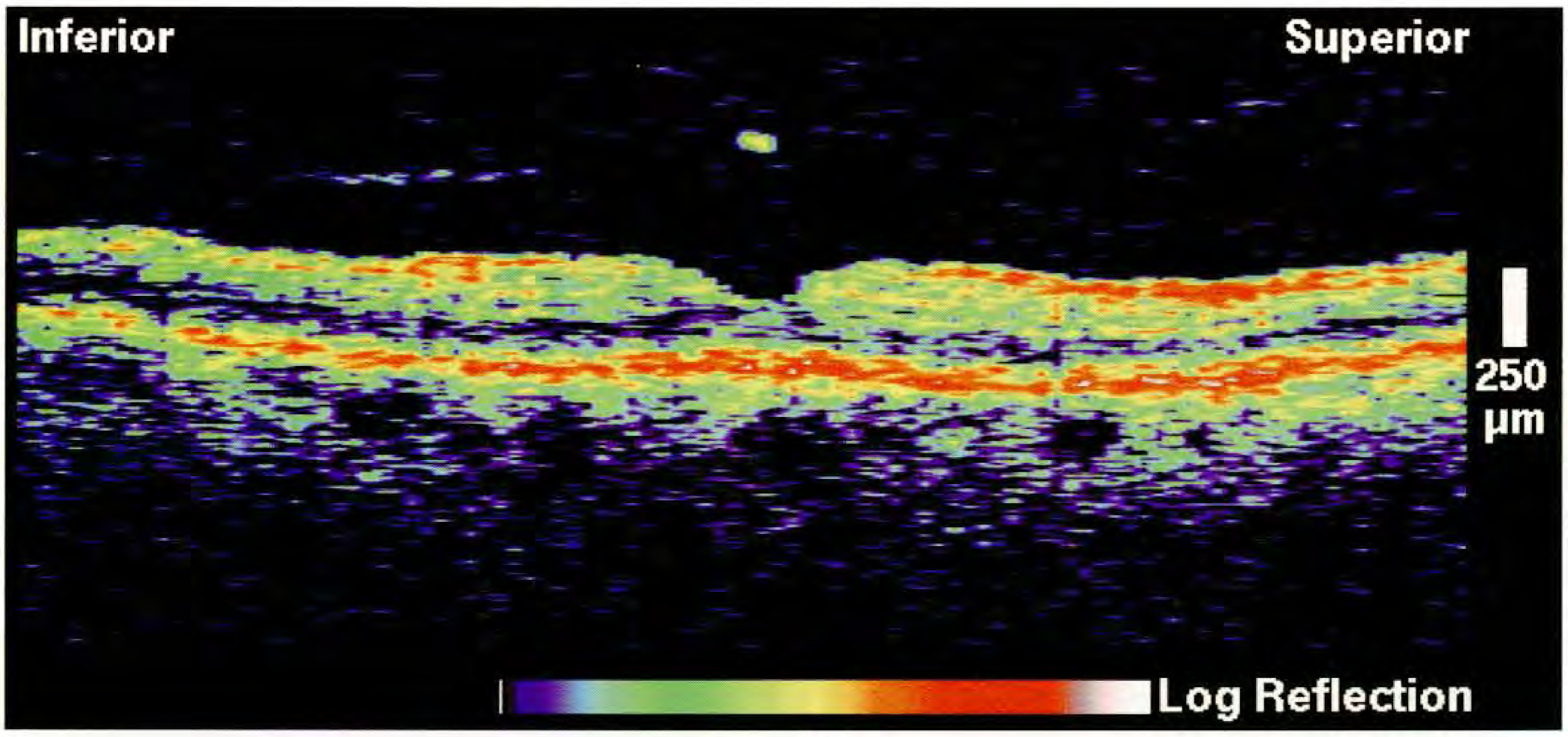
Inferior
Superior
250 µm
Log Reflection

E

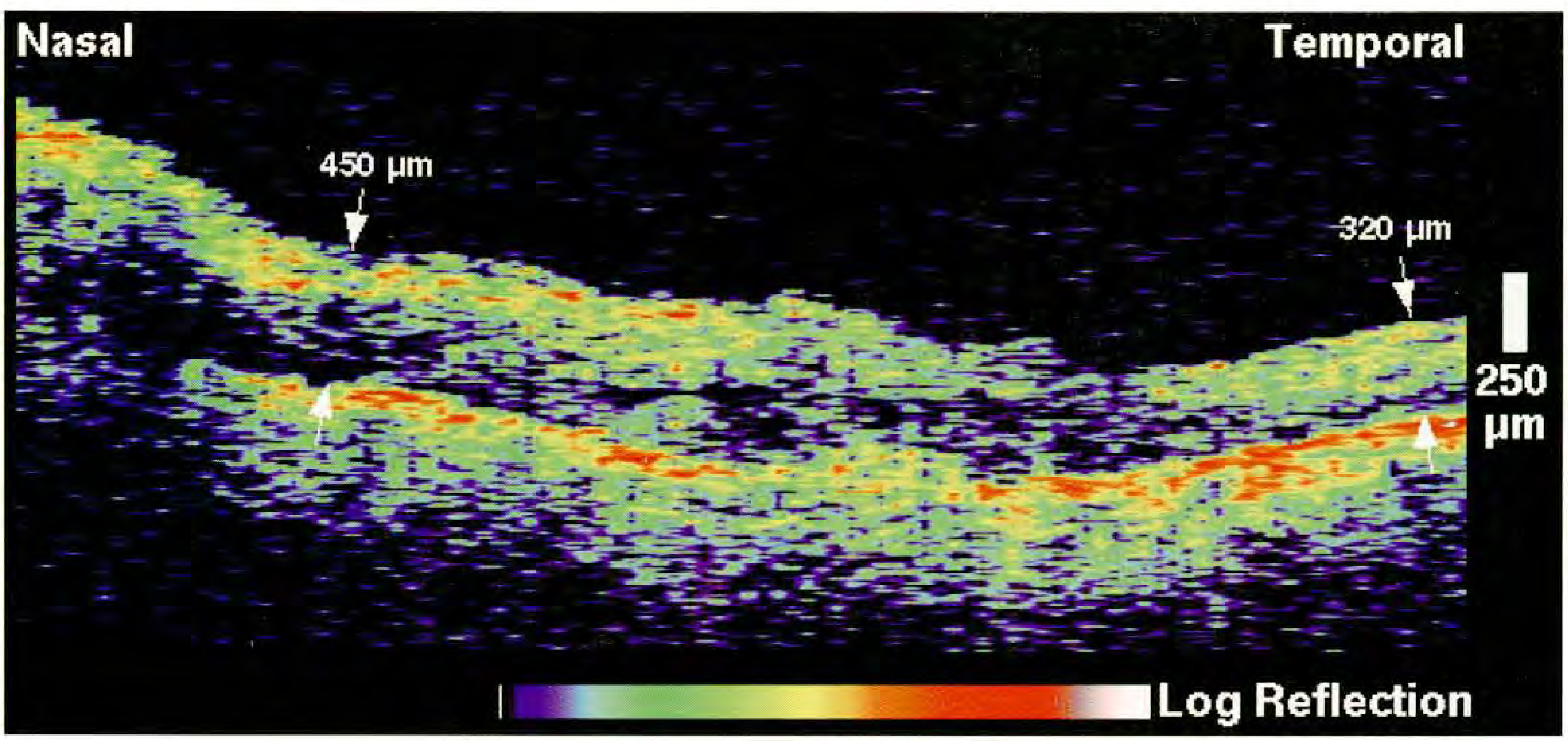
Nasal
Temporal
450 µm
320 µm
250 µm
Log Reflection

F

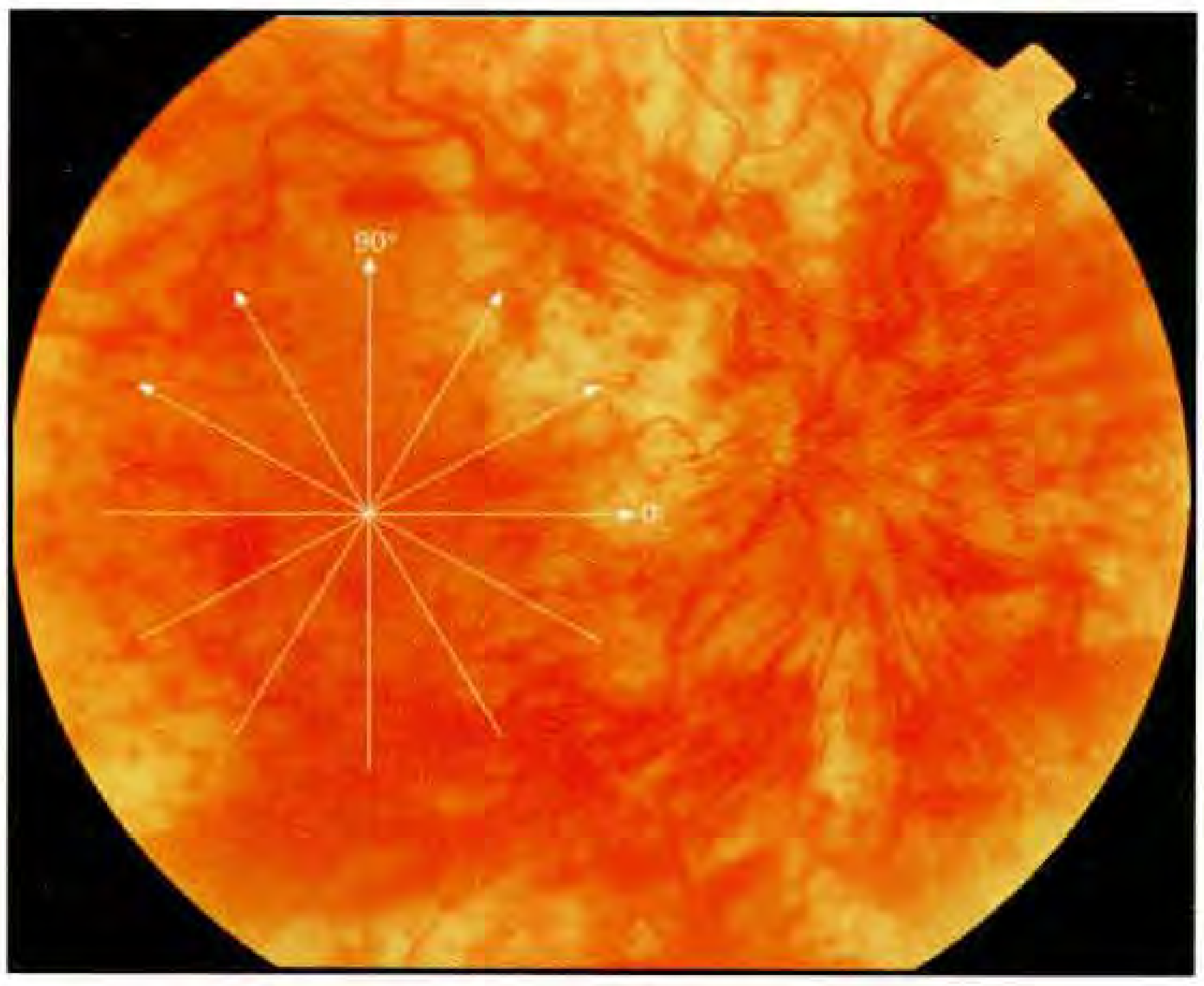

A

Case 5-11. Central Retinal Vein Occlusion

Clinical Summary

An 80-year-old woman had a non-ischemic central retinal vein occlusion in her right eye associated with a visual acuity of 20/300. Slit-lamp biomicroscopy (A) displayed significant hemorrhages throughout the retina, dilated retinal veins, mild swelling of the optic disc, and macular edema.

Optical Coherence Tomography

A series of radial OCT tomograms (B) was obtained through the macula at different angular orientations. Diffuse retinal thickening was observed, and the foveal thickness was increased to 430 μm. The fluid accumulation appeared preferentially in the outer retinal layer with the increased retinal thickness mostly confined to the minimally reflective region just anterior to the retinal pigment epithelium. The nasal retina exhibited significantly more thickening than the temporal retina.

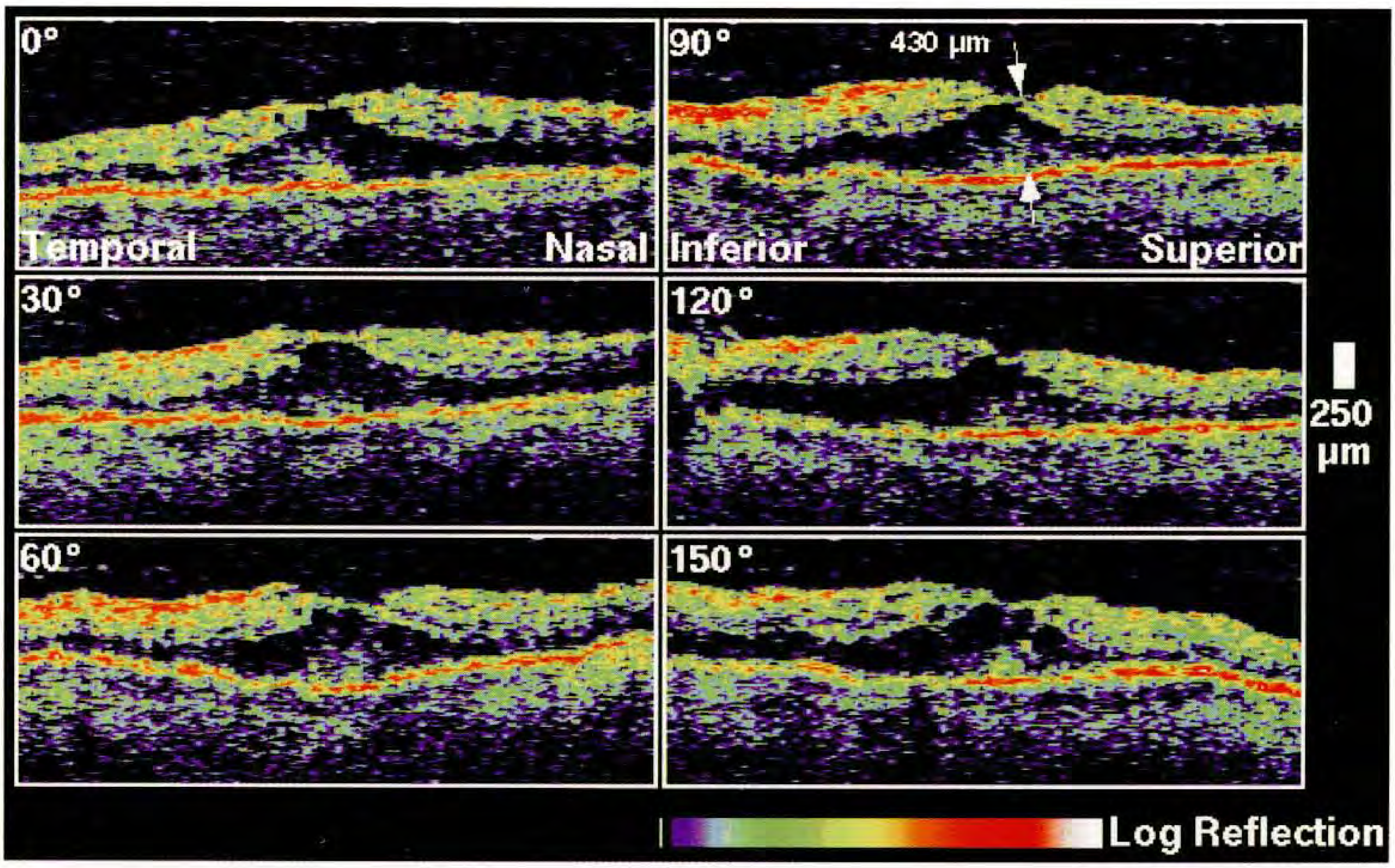

B

Case 5-12. Acute Central Retinal Artery Obstruction

Clinical Summary

A 79-year-old woman experienced profound vision loss in her right eye upon awakening one day earlier. The patient's visual acuity in this eye was counting fingers at two feet and there was no associated pain, photophobia, or floaters. Slit-lamp examination (A) was remarkable for retinal pallor in the macula and a cherry red spot centrally. The inferotemporal retinal arteriole was severely attenuated. Fluorescein angiography (B) confirmed delayed filling of this arteriole. The other retinal arterioles appeared well perfused.

Optical Coherence Tomography

OCT examination (C) showed diffuse thickening of the neurosensory retina throughout the macula with severe elevation directly in the fovea. Reduced optical backscattering from the outer layers of the retina suggested preferential fluid accumulation in this area. Enhanced reflectivity was observed from the inner neurosensory retina, most likely as a result of cellular morphologic changes due to ischemia.

A

B

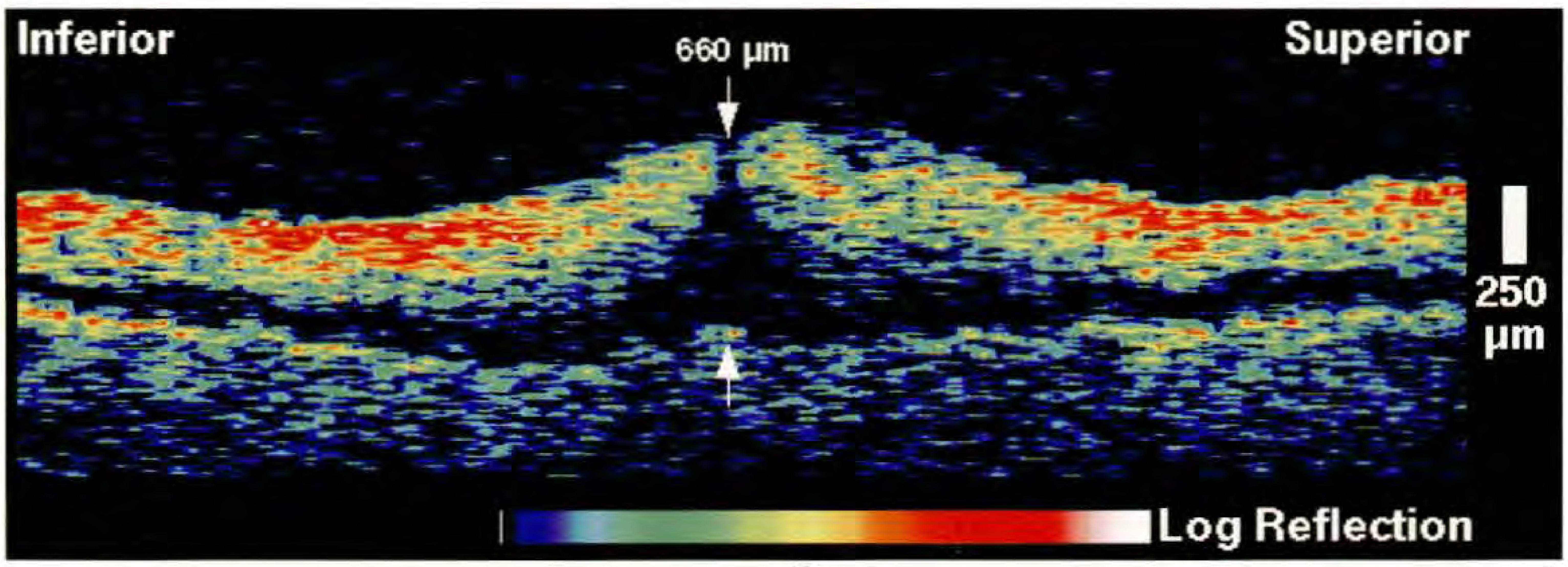

C

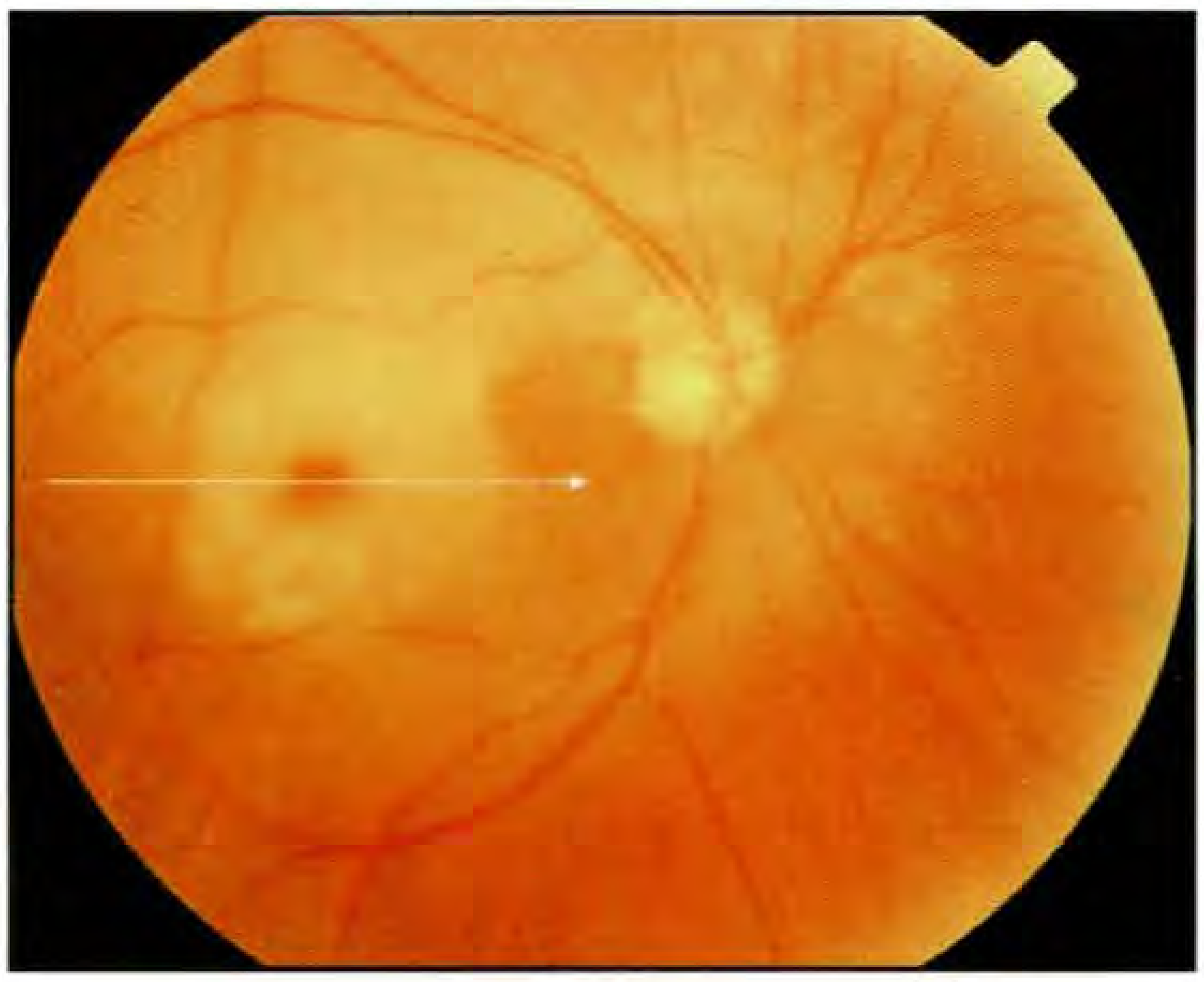

A

Case 5-13. Acute Central Retinal Artery Obstruction

Clinical Summary

An 85-year-old man experienced a sudden loss of vision in his right eye five days earlier. Fundus examination (A) showed a cherry-red spot in the fovea with pale and edematous tissue throughout the macula. The retinal arterioles and venules were markedly attenuated.

Optical Coherence Tomography

A horizontal OCT image (B) through the fovea displayed diffuse thickening of the neurosensory retina. Increased reflectivity was noted from the inner retinal layers corresponding to retinal ischemia, and decreased backscattering was observed from the retinal photoreceptors due to fluid accumulation and retinal edema.

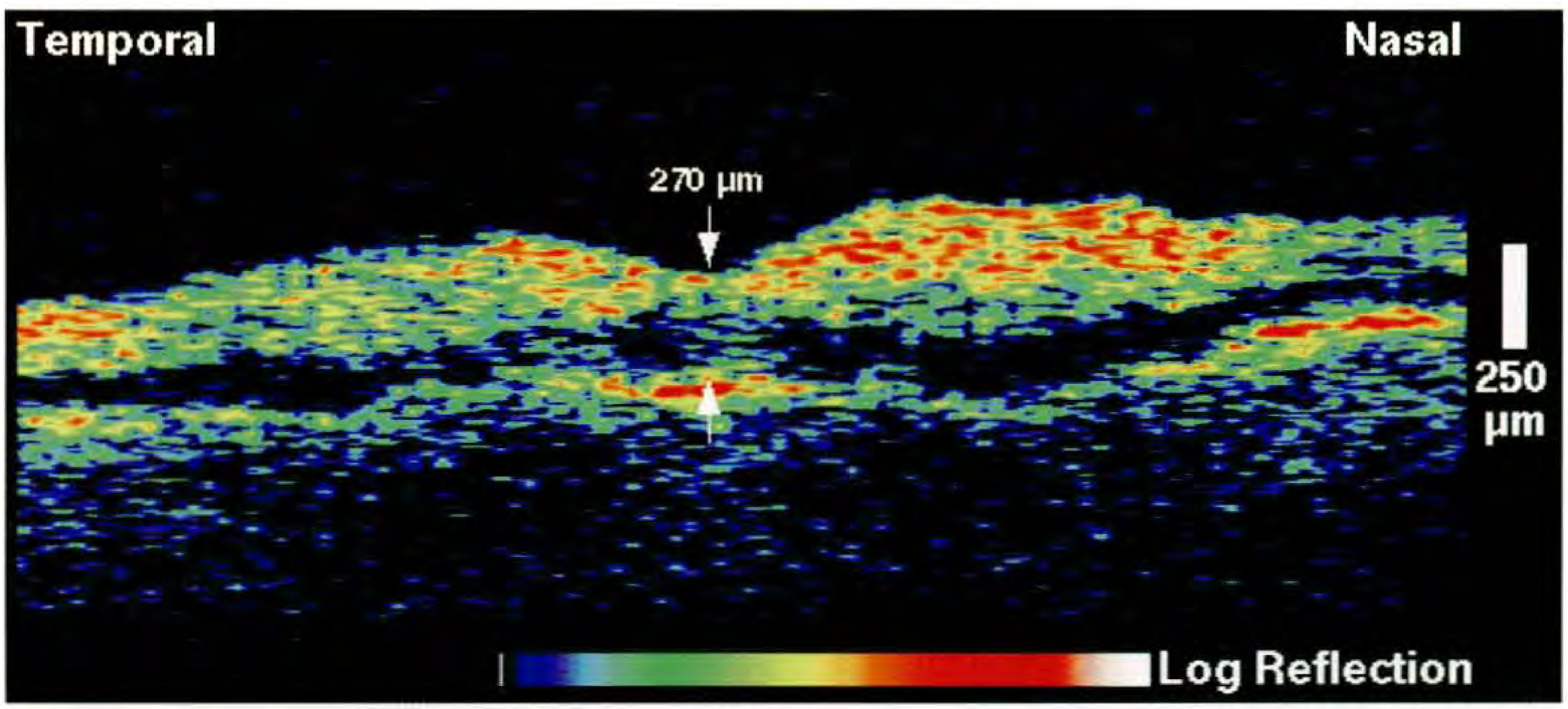

B

Case 5-14. Central Retinal Artery Occlusion with Cilioretinal Artery Perfusion

Clinical Summary

A 67-year-old woman was examined five years after a central retinal artery occlusion in her right eye. Her macula was spared due to perfusion from a cilioretinal artery in the superior macula. Slit-lamp examination (A) revealed a normal macula with attenuated retinal vessels. Her visual acuity in this eye was 20/30.

Optical Coherence Tomography

A vertical OCT image (B) showed severe retinal thinning inferior to the fovea consistent with prolonged retinal ischemia. The retinal thickness in the superior macula appeared normal in the region perfused by the cilioretinal artery.

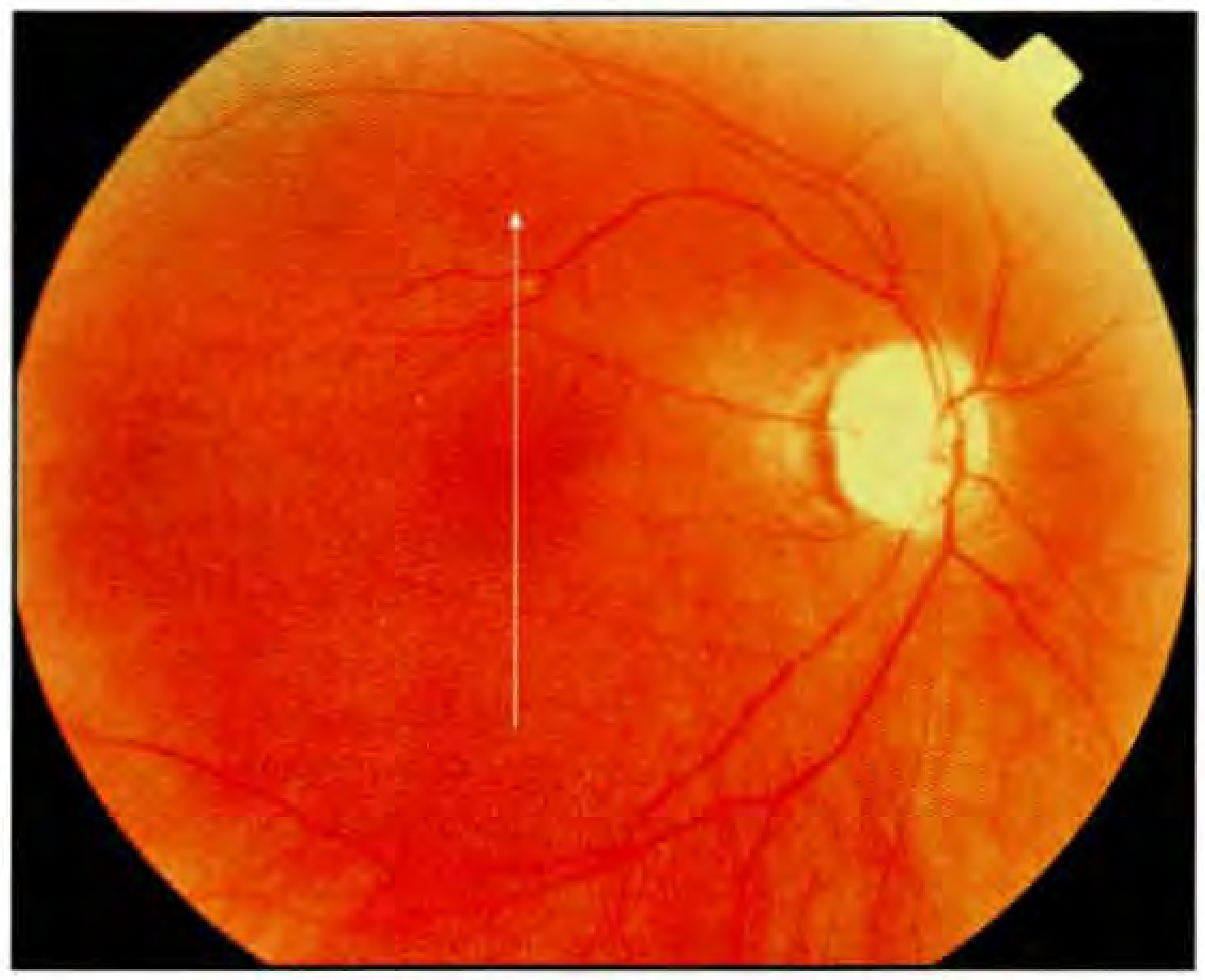

A

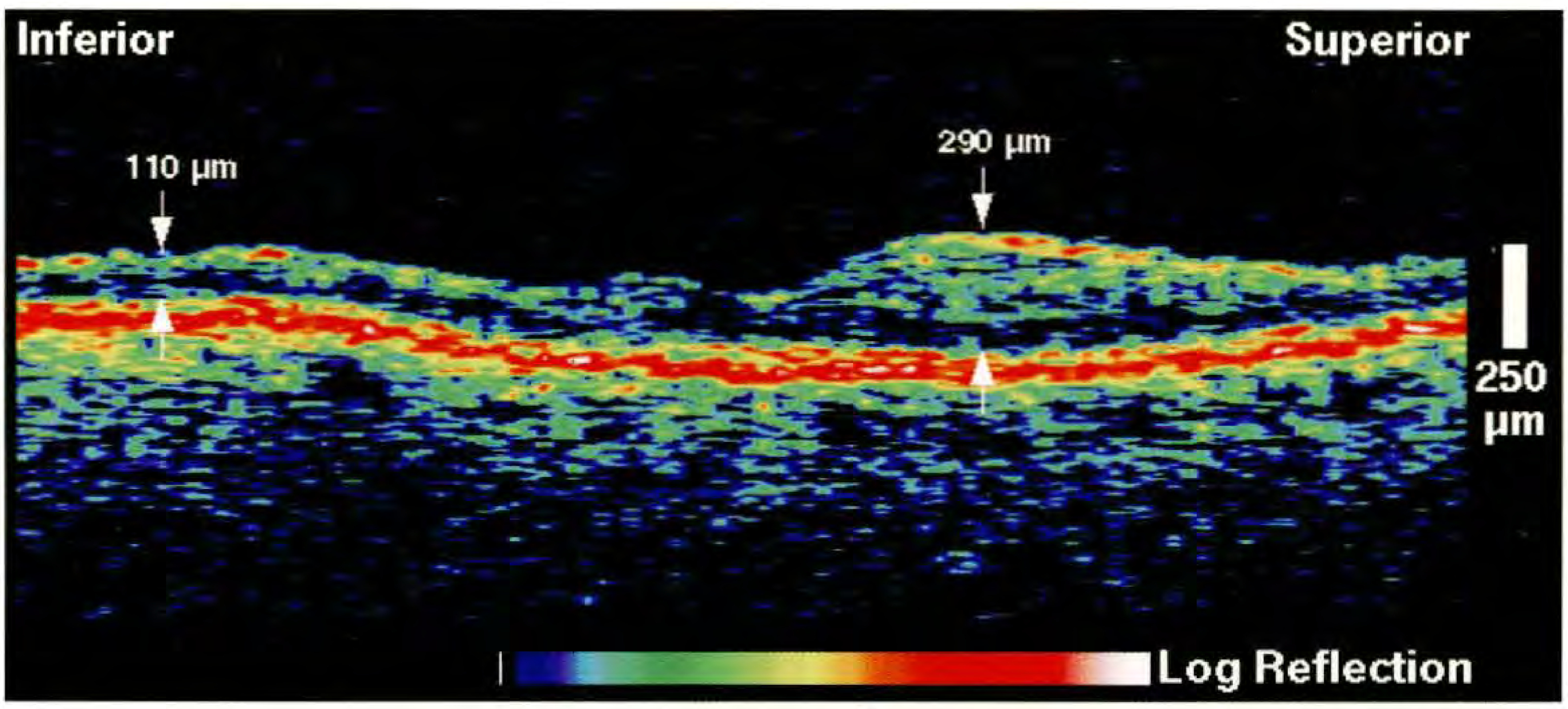

B

CHAPTER 6

Diabetic Retinopathy

Non-Proliferative Diabetic Retinopathy
Proliferative Diabetic Retinopathy

Macular edema is a leading cause of treatable vision loss in patients with diabetic retinopathy [1,2]. The high longitudinal resolution of OCT is effective in quantifying macular thickness due to the well-defined differences in optical reflectivity at the anterior and posterior boundaries of the neurosensory retina. Measurements of central foveal thickness with OCT correlate with visual acuity and can provide an indication of the relative contribution of macular edema, as opposed to other factors such as macular capillary non-perfusion, to vision loss [3]. Retinal thickness has been shown to be better correlated with visual acuity than fluorescein leakage in patients with macular edema [4,5]. Sequential OCT tomograms allow the ophthalmologist to accurately track increases or decreases in retinal thickness with more sensitivity than slit-lamp biomicroscopy [3]. Alternatively, multiple OCT tomograms may be obtained at a series of radial or linear sections through the macula to screen for early retinal thickening throughout the macula [3].

The morphological changes in macular edema visible in diabetic retinopathy include a decreased intraretinal reflectivity corresponding to cystic changes and fluid accumulation. The reduced backscattering is usually most evident in the outer retinal layers, and tomograms of cystoid macular edema closely correspond to classically described histopathologic findings. Chronic cystoid macular edema may lead to the development of a lamellar macular hole, which is evident on OCT as a partial-thickness loss of retinal tissue and an abnormal retinal contour suggesting cystic rupture. Hard exudate appears as a focal area of high intraretinal backscatter which completely shadows the reflection from the neurosensory retina and choroid below the lesion. Hemorrhage also blocks the reflections returning from the deeper retinal layers due to the high scattering and associated high attenuation of light propagating through blood.

Proliferative diabetic retinopathy often leads to neovascularization and preretinal fibrosis. Preretinal membranes are visible in cross-section as thin, reflective bands anterior to the retina. Retinal traction and detachment are often present, and their extent can be directly measured from the OCT tomograms. The distinction between preretinal fibrosis and a detached posterior vitreous is made on the basis of reflectivity. The posterior hyaloid typically has a lower reflectivity than a preretinal membrane due to the optical transparency of the vitreous. Cotton wool spots due to retinal ischemia appear in OCT cross-section as regions of increased reflectivity of the retinal nerve fiber layer and inner neurosensory retina.

A

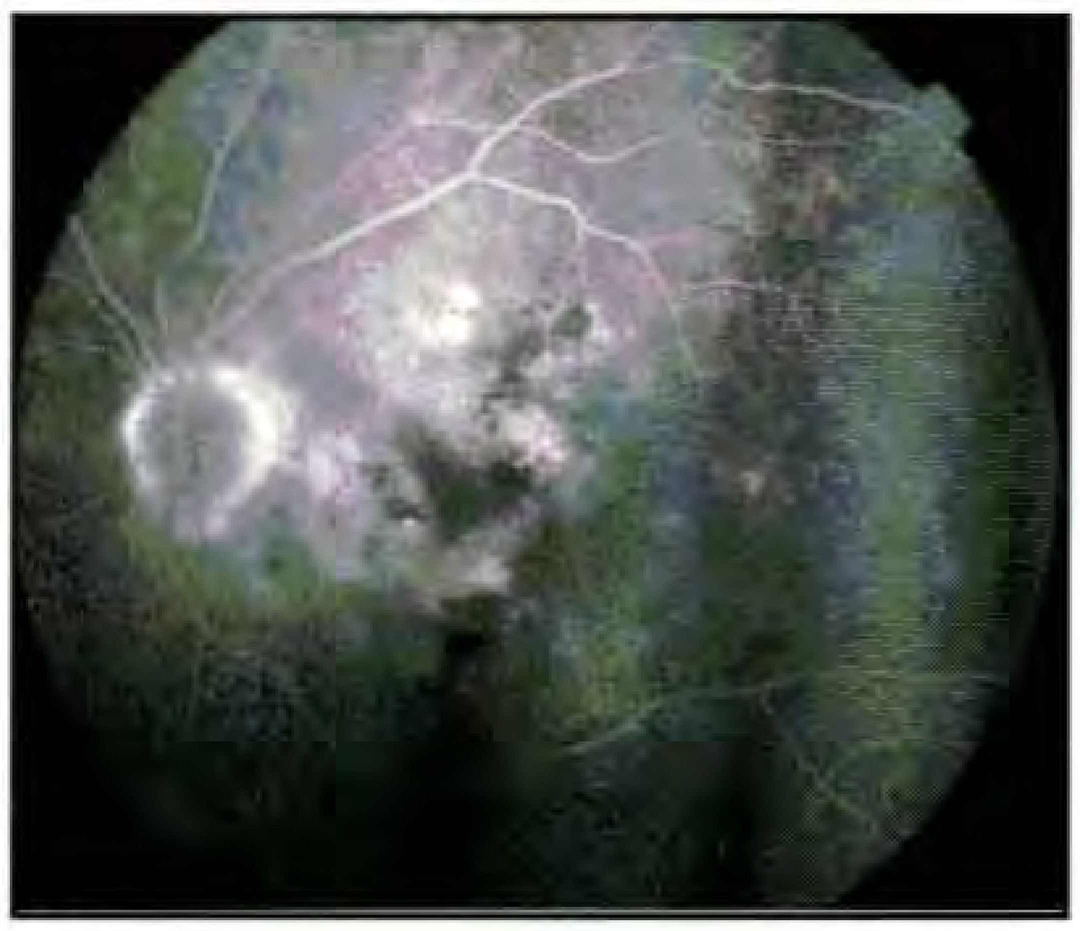

B

Case 6-1. Diabetic Retinopathy

Clinical Summary

A 78-year-old man with non-proliferative diabetic retinopathy in both eyes had received grid laser photocoagulation in his left eye three months earlier for clinically significant macular edema (A). His visual acuity in this eye was 20/125. Fluorescein angiography (B) displayed the previous laser scars, hyperfluorescent spots in the inferior macula and peripapillary region consistent with microaneurysms, and late leakage consistent with macular edema.

Optical Coherence Tomography

A vertical OCT image (C) revealed macular thickening and reduced optical backscatter due to intraretinal fluid accumulation. In a follow-up examination three months later, a repeat OCT image demonstrated that the retinal thickness had decreased from 470 μm to 380 μm at the edge of the fovea (D). The visual acuity, however, exhibited no significant improvement.

C

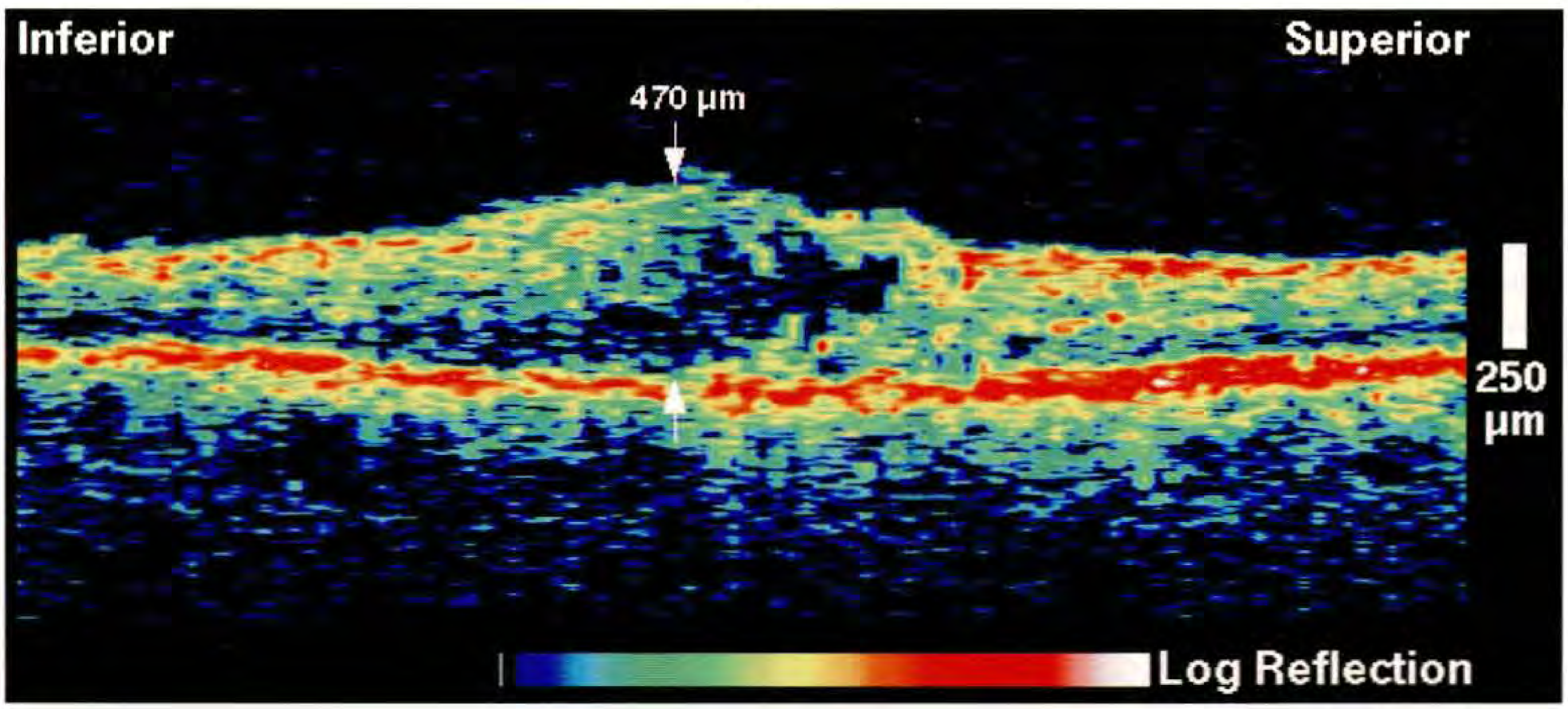

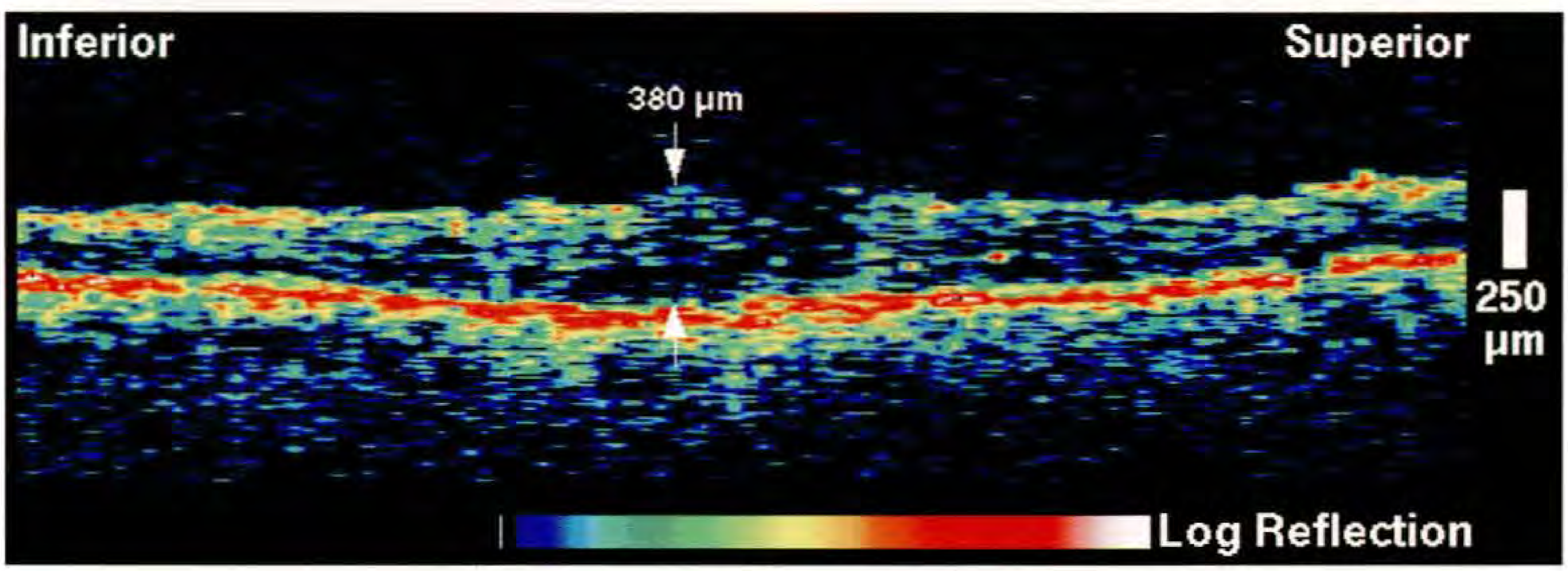

D

Case 6-1 continued

Clinical Summary

Examination of the patient's right eye showed mild blot hemorrhages in the macula, but no clinically significant macular edema (E). Mild late leakage, however, was noted on the fluorescein angiogram (F).

Optical Coherence Tomography

OCT images (G and H) acquired at the three month timepoints showed an increase in retinal thickness from 350 μm to 540 μm nasal to the fovea consistent with the development of macular edema. The patient's visual acuity remained at 20/40 throughout the three month period.

E

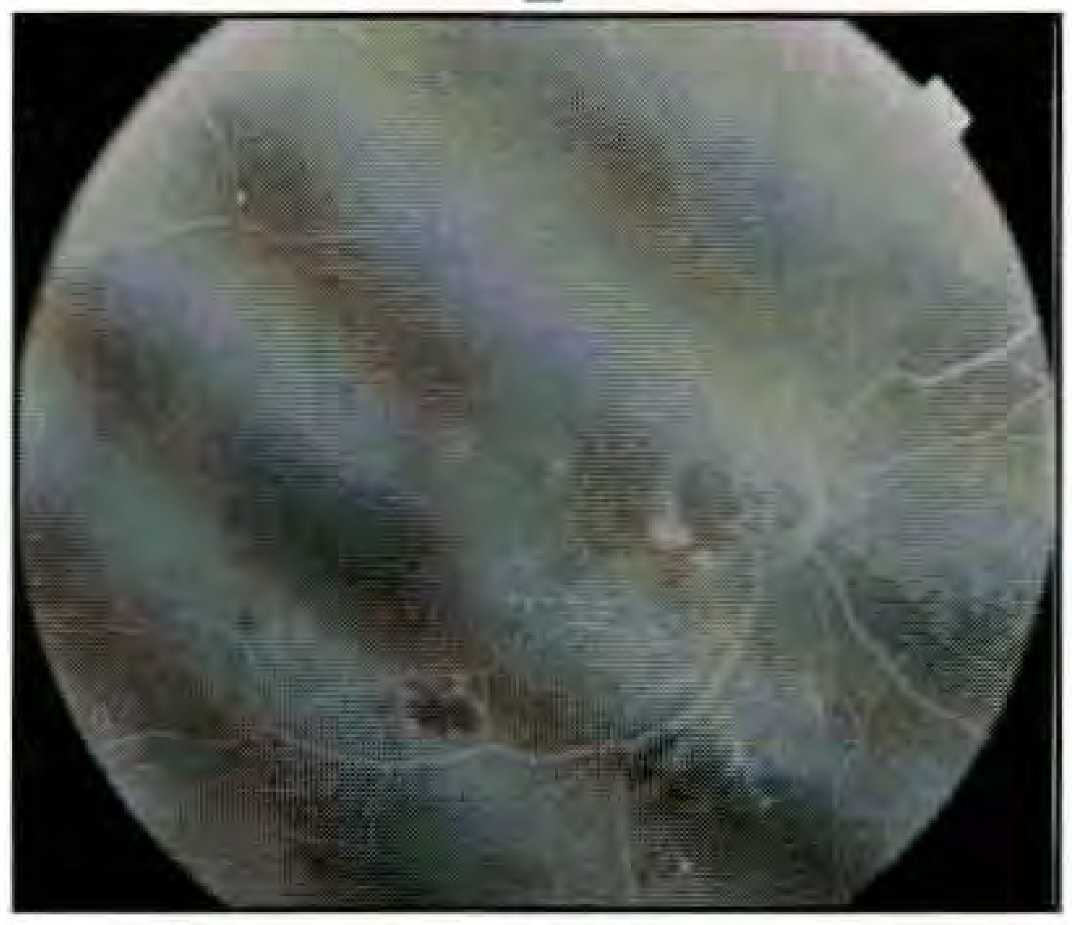

F

G

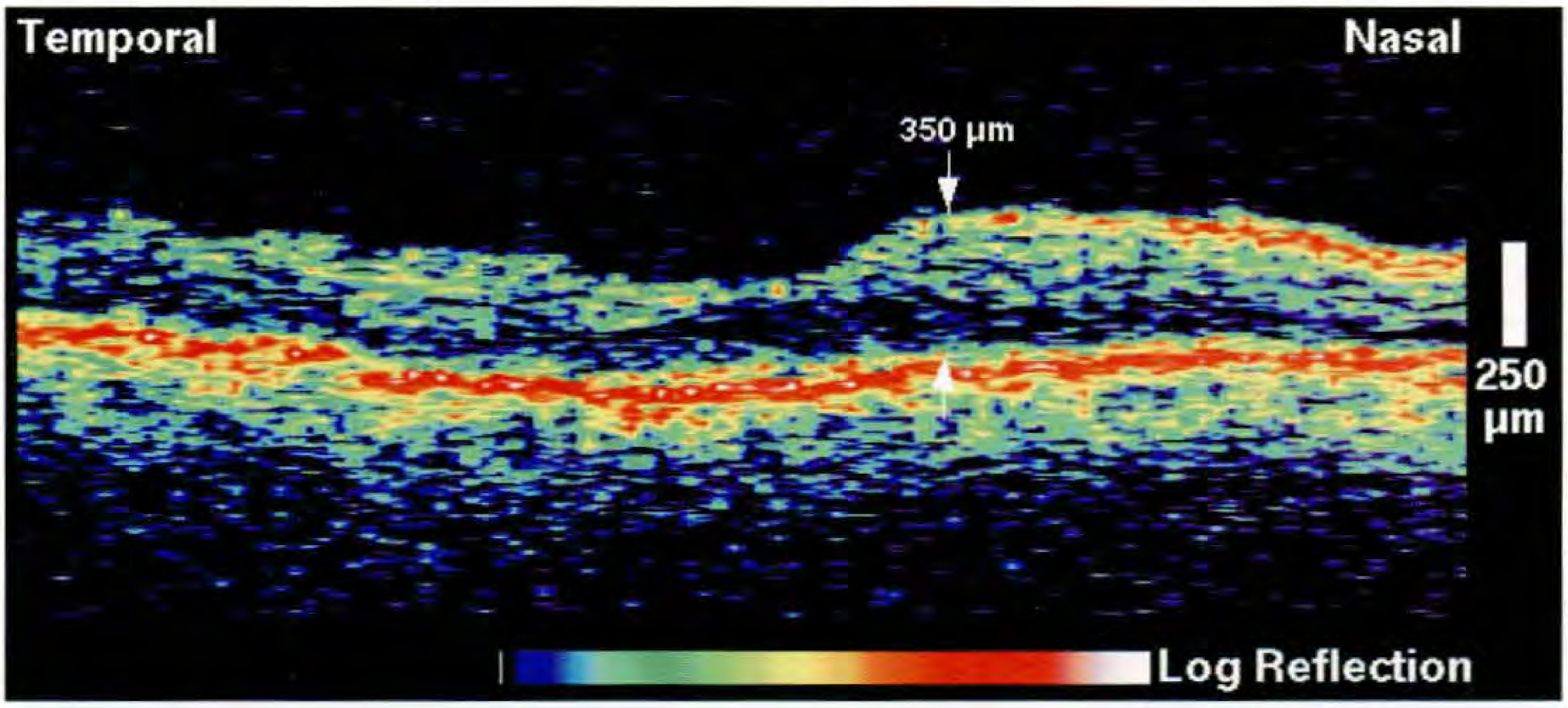

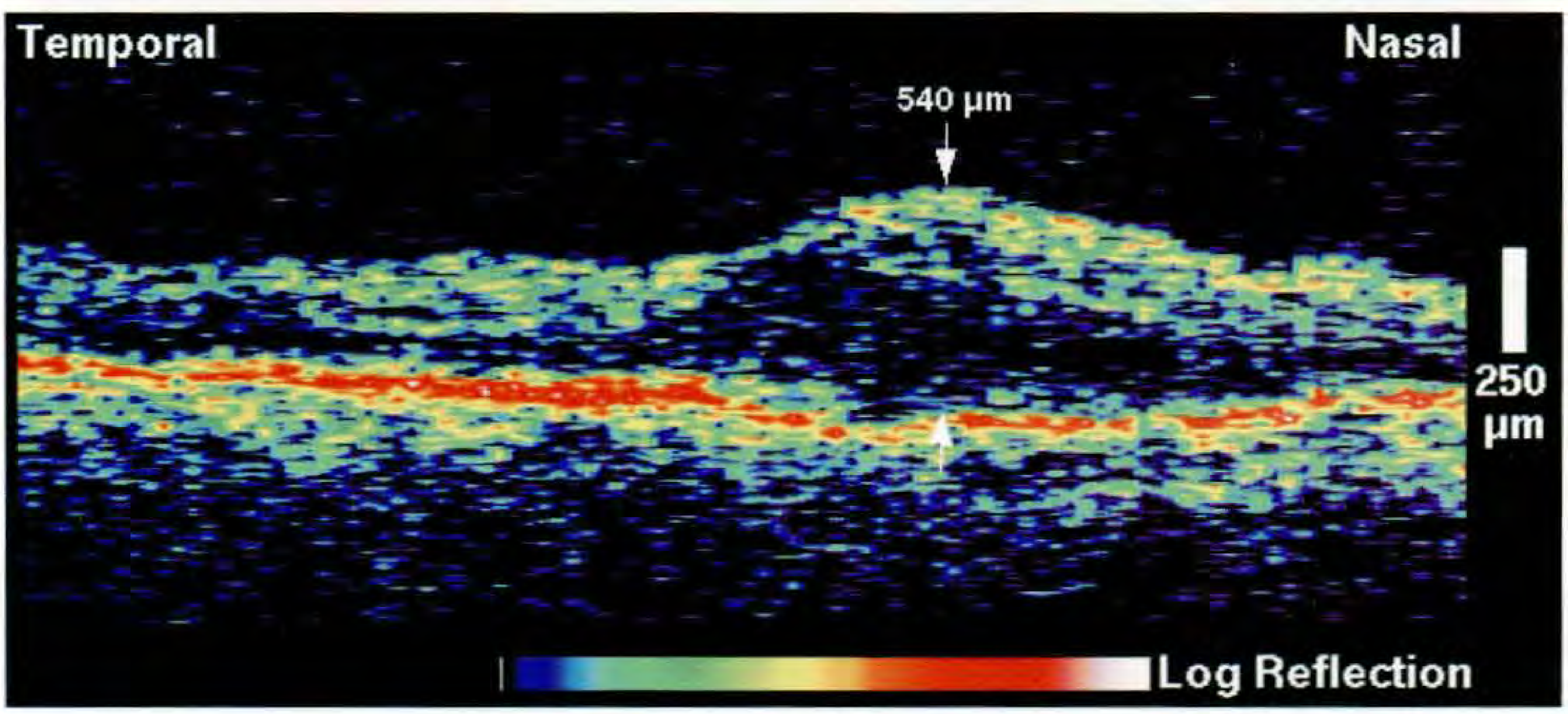

H

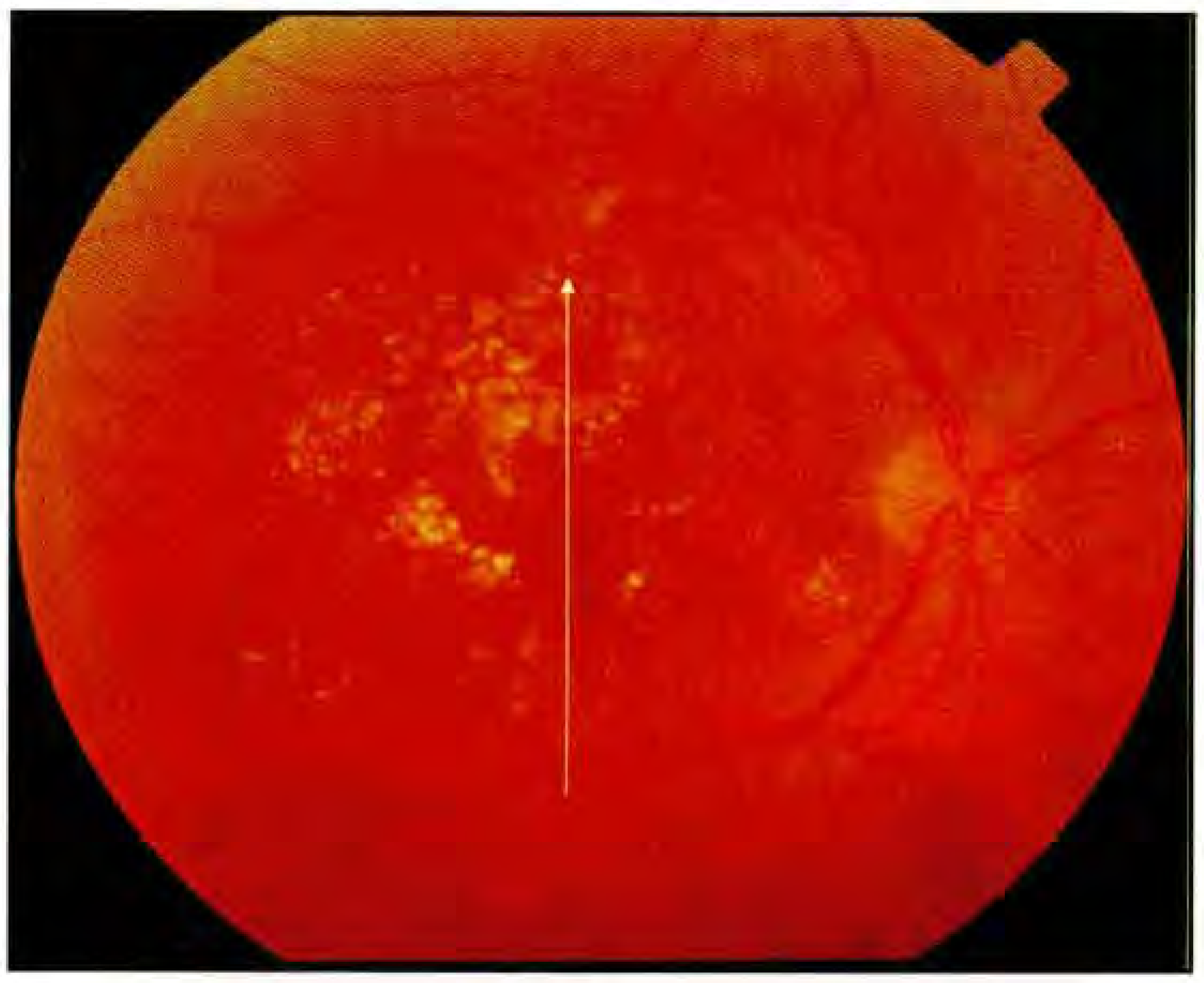

A

Case 6-2. Non-Proliferative Diabetic Retinopathy

Clinical Summary

A 62-year-old man was examined approximately two months after focal laser photocoagulation treatment for background diabetic retinopathy and clinically significant macular edema in both eyes. Fundus examination (A) of his right eye, which had a visual acuity of 20/100, revealed scattered dot and blot hemorrhages throughout the macula, hard exudate, and laser scars.

Optical Coherence Tomography

A vertical OCT image (B) through the macula showed a diffuse increase in retinal thickness and loss of the normal foveal contour consistent with macular edema. The retinal thickness measured in the fovea was 460 µm. A follow-up OCT examination (C) four months later showed a slight reduction in macular thickening to 380 µm. The decreased edema correlated with an improvement in visual acuity to 20/70.

B

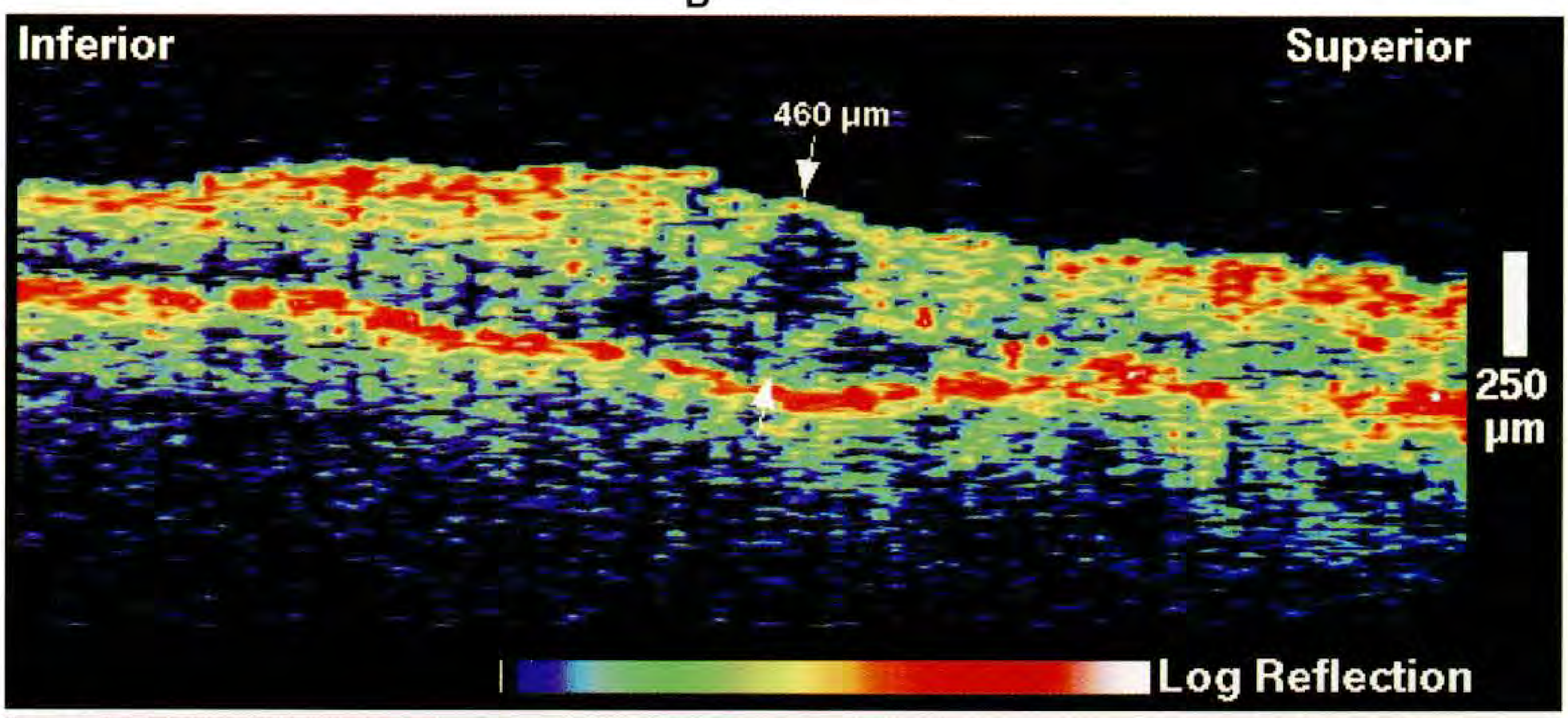

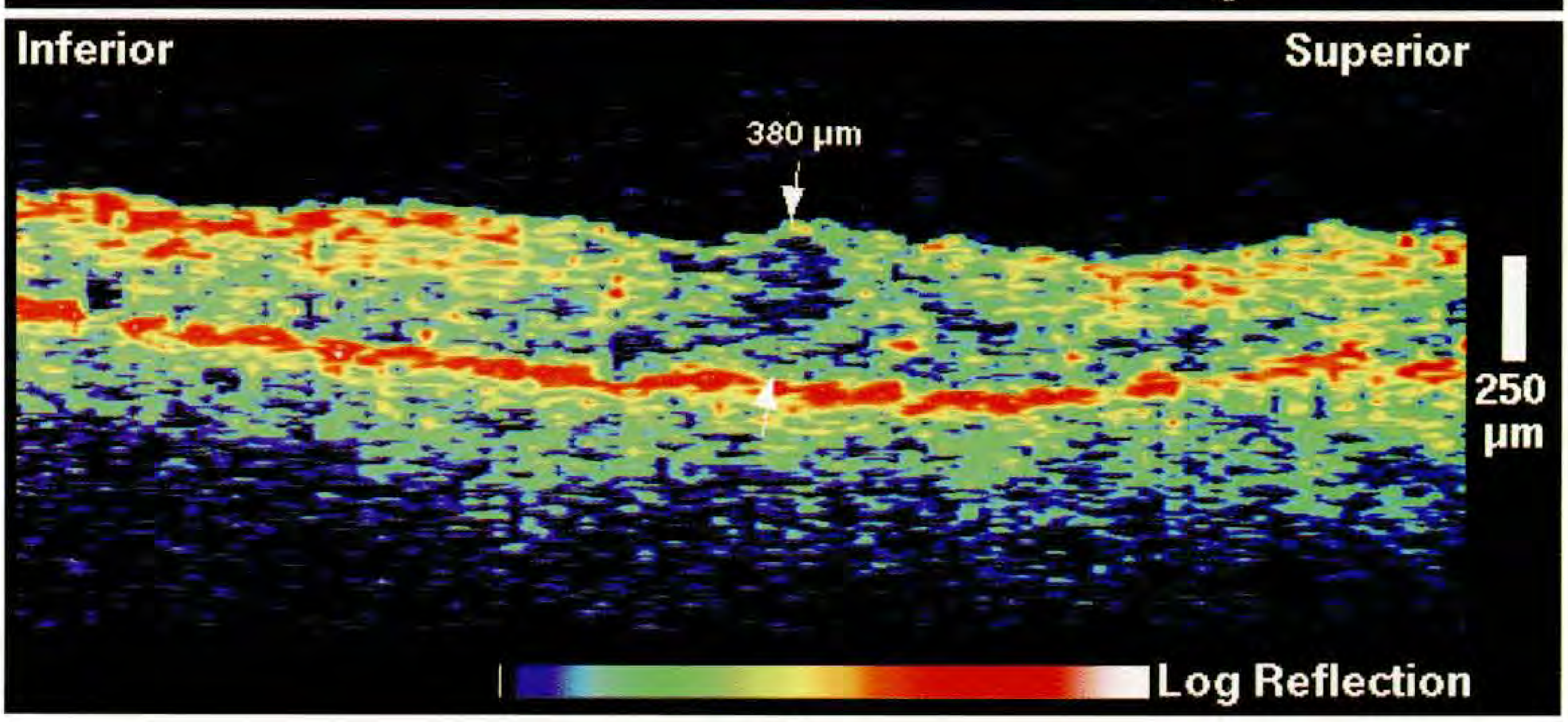

C

Case 6-2 continued

Clinical Summary

Slit-lamp biomicroscopy (D) of the left eye, with a visual acuity of 20/200, also showed scattered dot and blot hemorrhages throughout the posterior pole.

Optical Coherence Tomography

OCT (E) demonstrated macular thickening and reduced optical reflectivity consistent with serous fluid accumulation. The retinal thickness measured directly in the fovea was 280 µm. The patient elected to receive focal argon laser photocoagulation treatment in this eye. Four months later, a follow-up OCT (F) scan showed significantly decreased retinal thickening and increased optical reflectivity from within the neurosensory retina. The central foveal thickness had decreased to 140 µm. The visual acuity in this eye, however, had not improved.

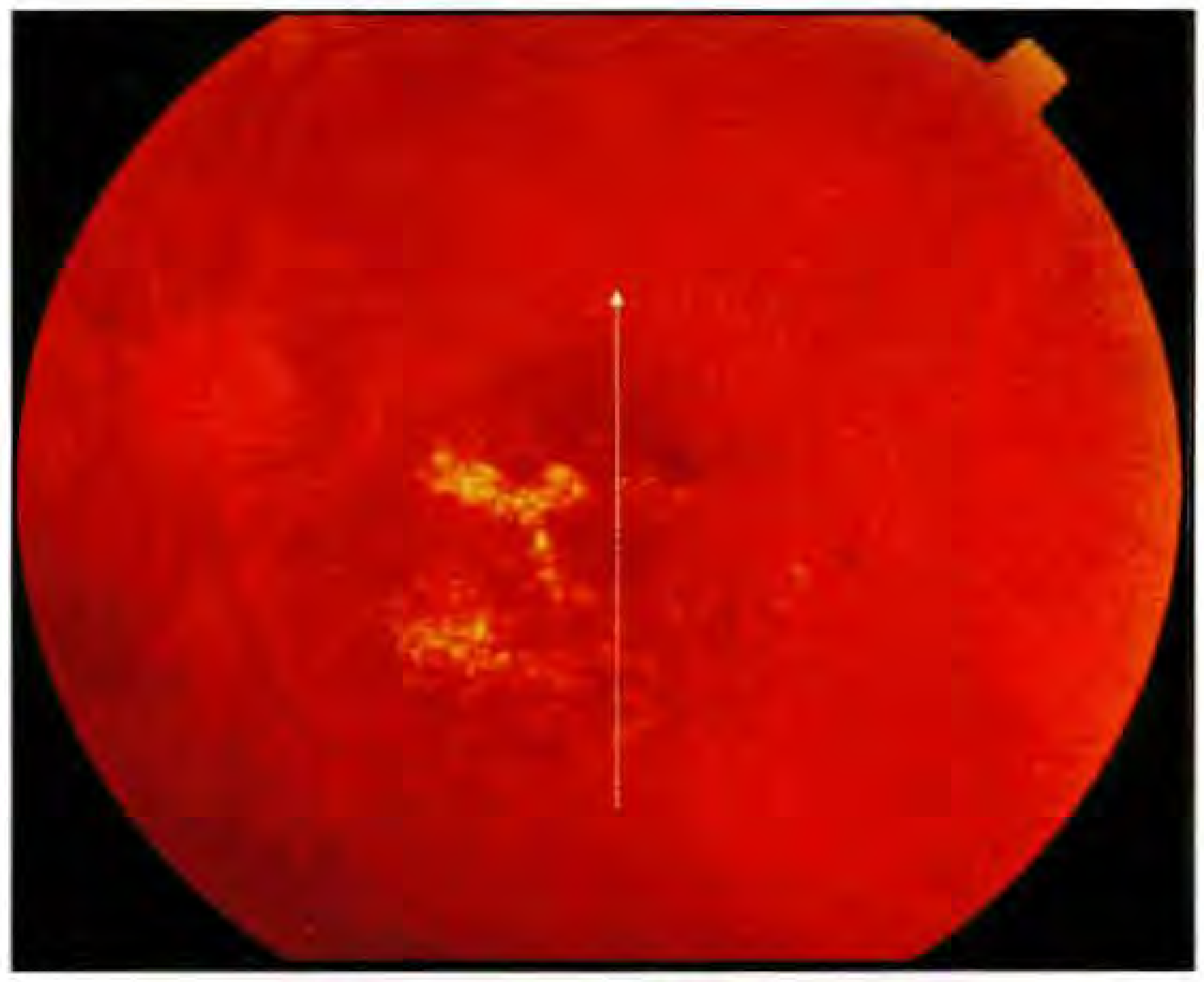

D

E

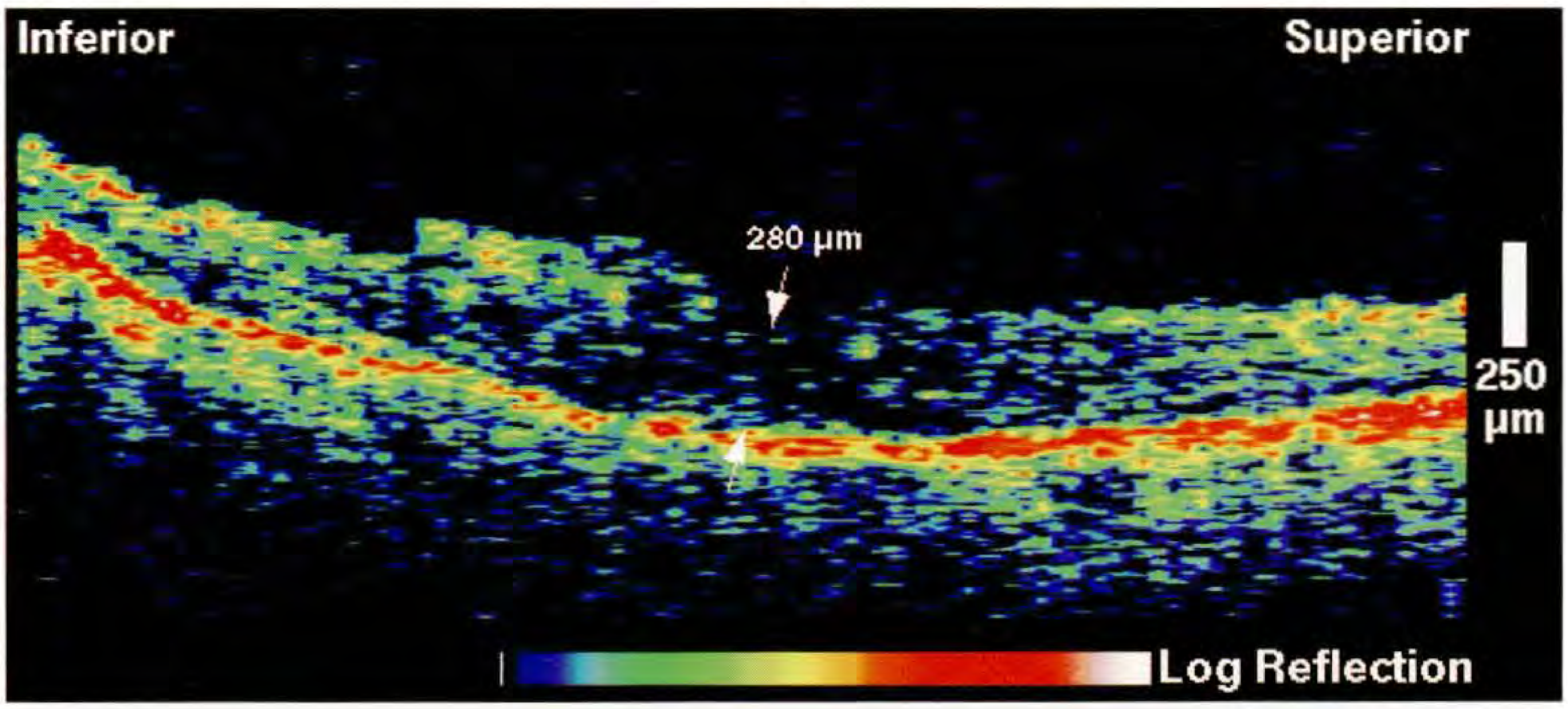

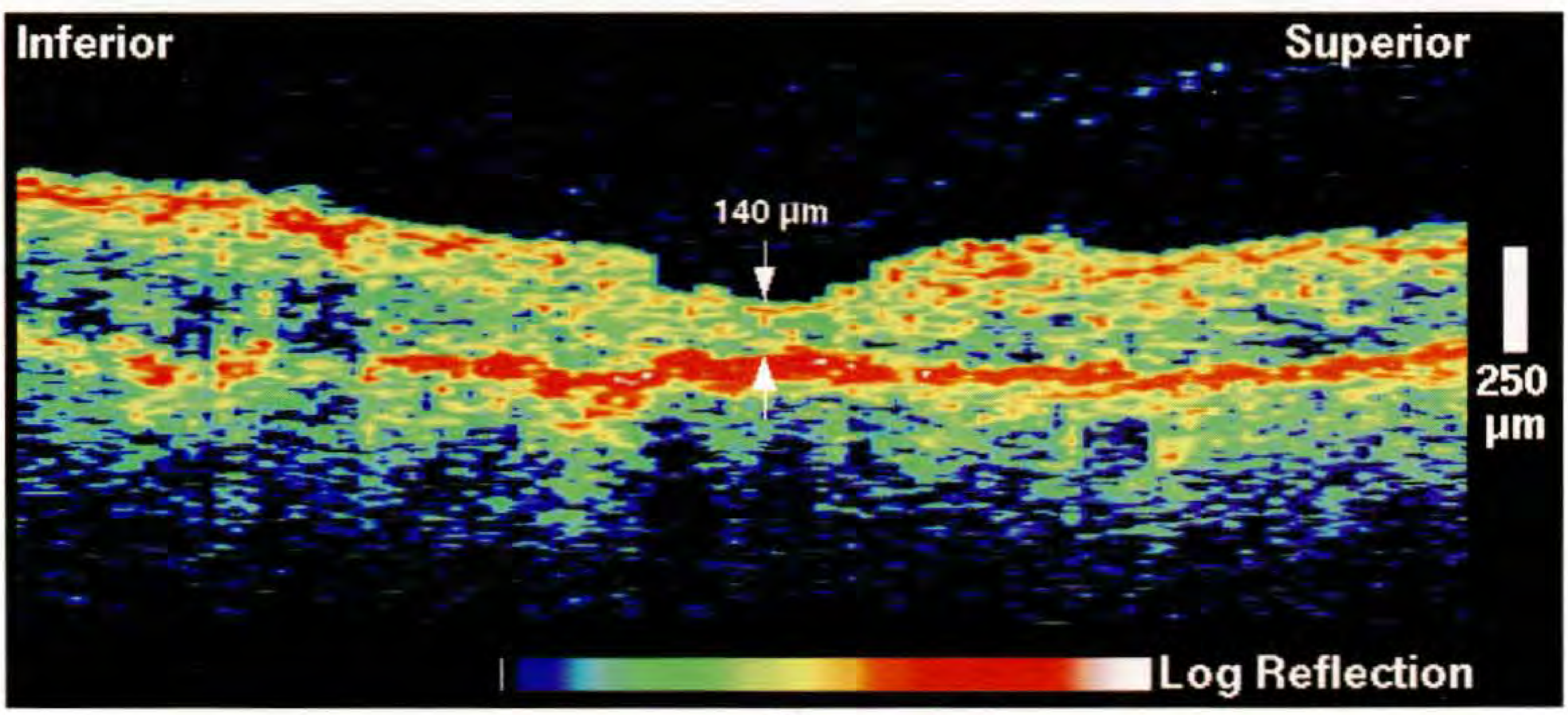

F

A

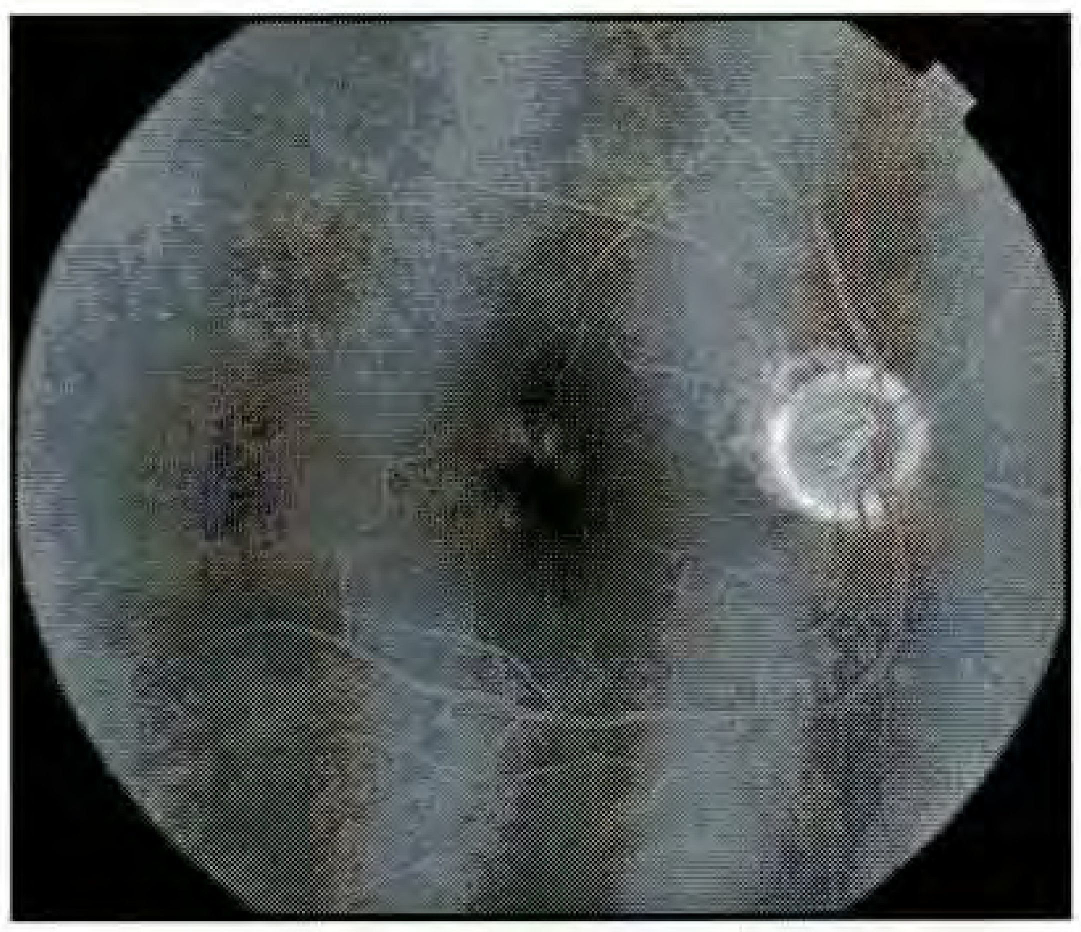

B

Case 6-3. Non-Proliferative Diabetic Retinopathy

Clinical Summary

A 62-year-old man with a 15 year history of adult-onset diabetes mellitus was examined. Dilated ophthalmoscopy (A) showed a small cyst in the fovea with no clinically significant macular thickening. Fluorescein angiography (B) displayed minimal late leakage consistent with macular edema. The patient's visual acuity in this eye was 20/30.

Optical Coherence Tomography

A vertical OCT scan (C) through the fovea showed loss of the normal foveal contour and a focal intraretinal region of minimal optical backscattering consistent with a retinal cyst. The retinal thickness measured directly in the fovea was 350 µm. A follow-up OCT tomogram (D) was obtained two months later and showed the foveal thickness had decreased to 260 µm. However, the visual acuity had dropped to 20/50.

C

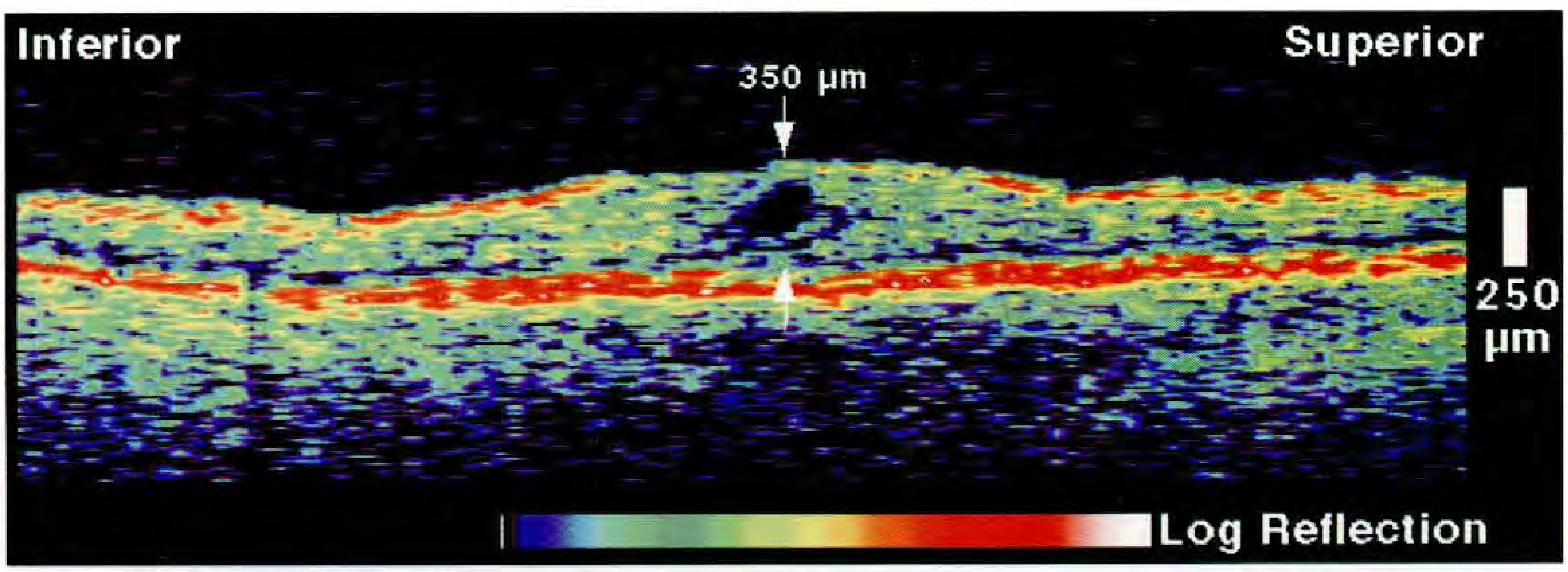

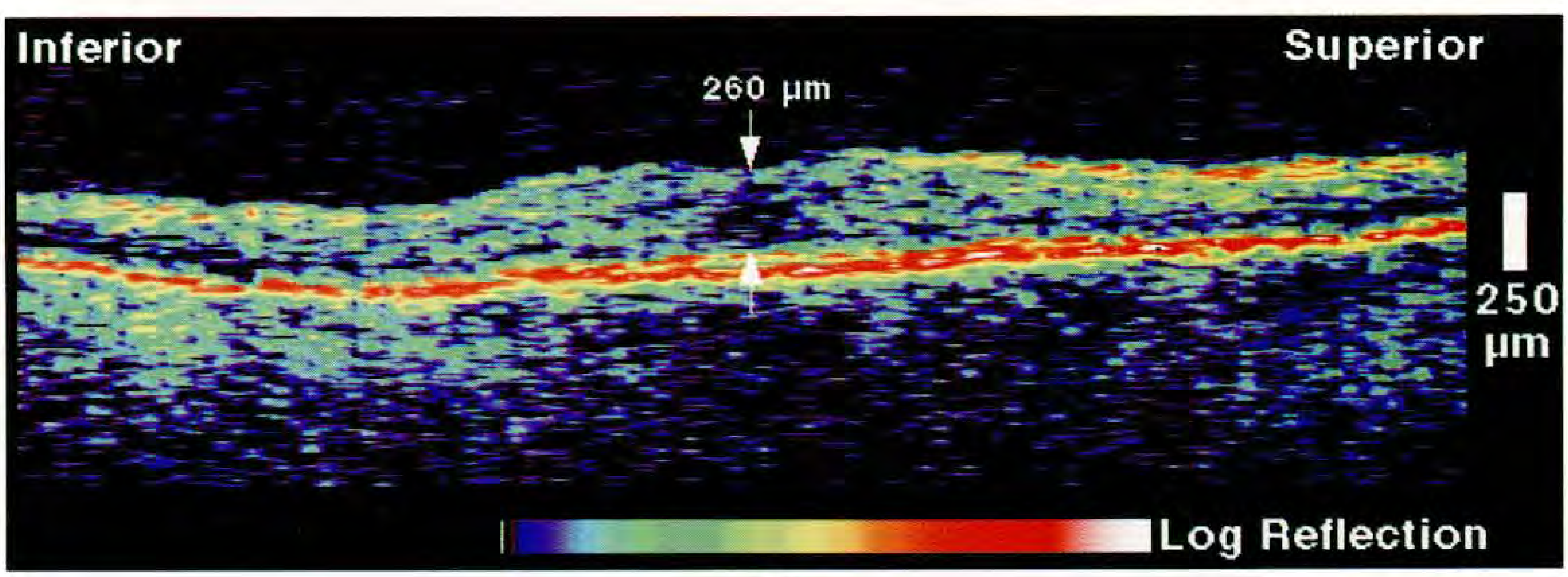

D

Case 6-3 continued

Clinical Summary

Examination of the patient's left eye (E) showed a large foveal cyst and clinically significant macular thickening. Corresponding late leakage of fluorescein dye was observed in the central macula on angiography (F). The visual acuity in this eye was 20/40.

Optical Coherence Tomography

OCT (G) demonstrated macular thickening with a large central cystic space extending to the inner limiting membrane and smaller surrounding cysts. The foveal thickness was 460 µm. Focal laser photocoagulation was performed and the patient returned for a follow-up visit two months later. OCT examination (H) showed that the foveal thickness had significantly decreased to 290 µm and that the retinal cysts had flattened. The patient's visual acuity was 20/50.

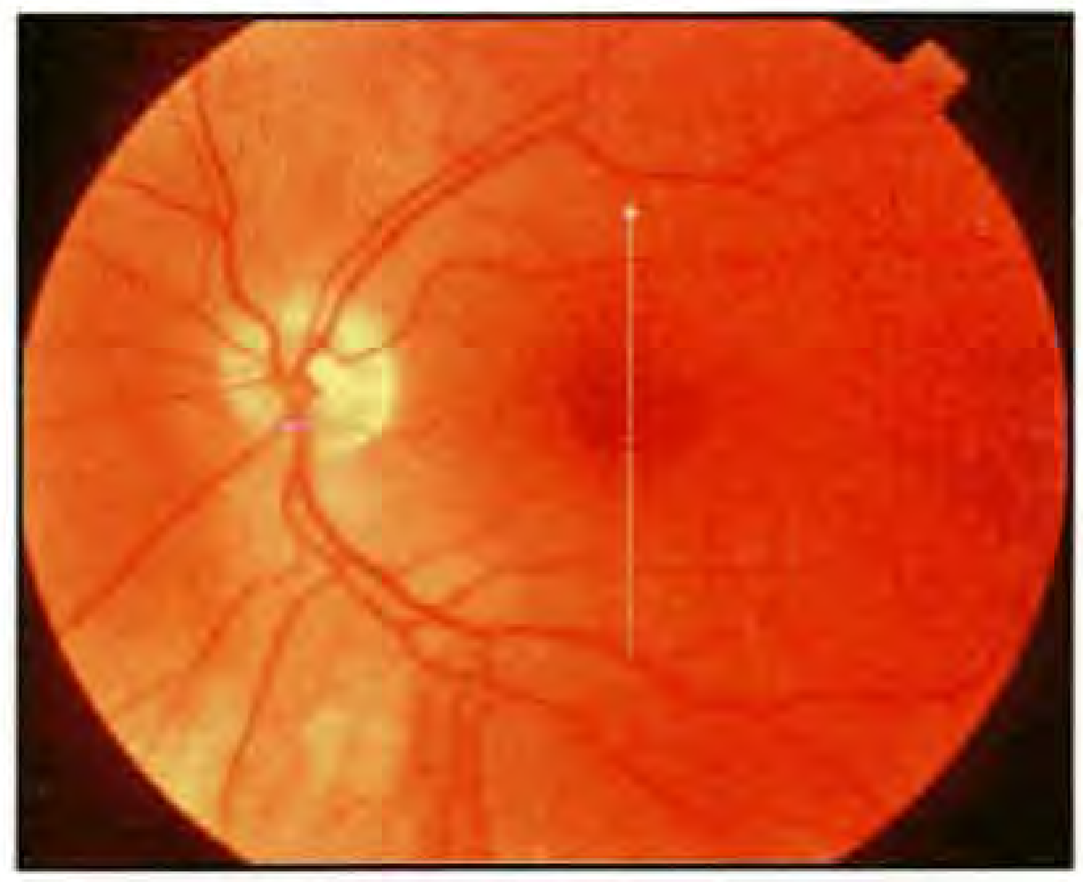

E

F

G

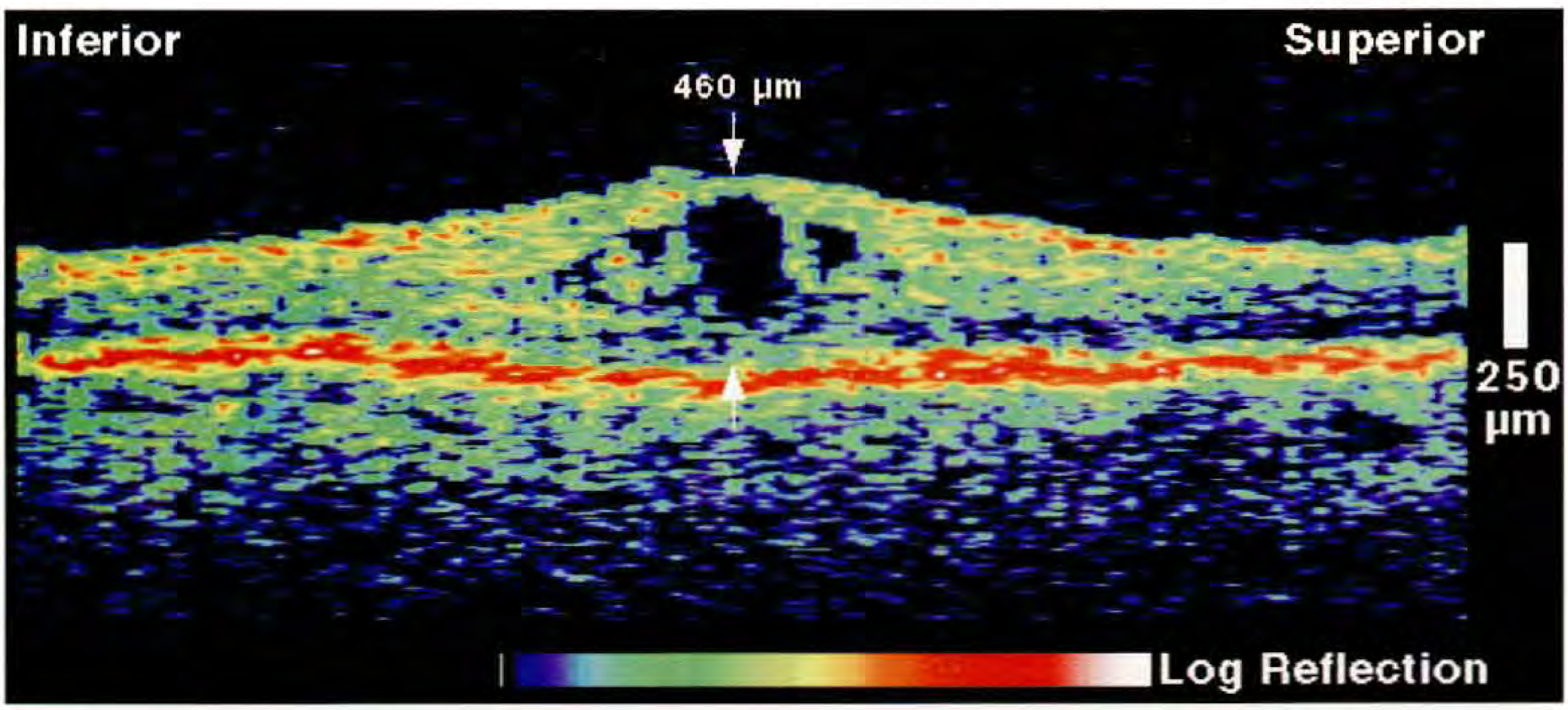

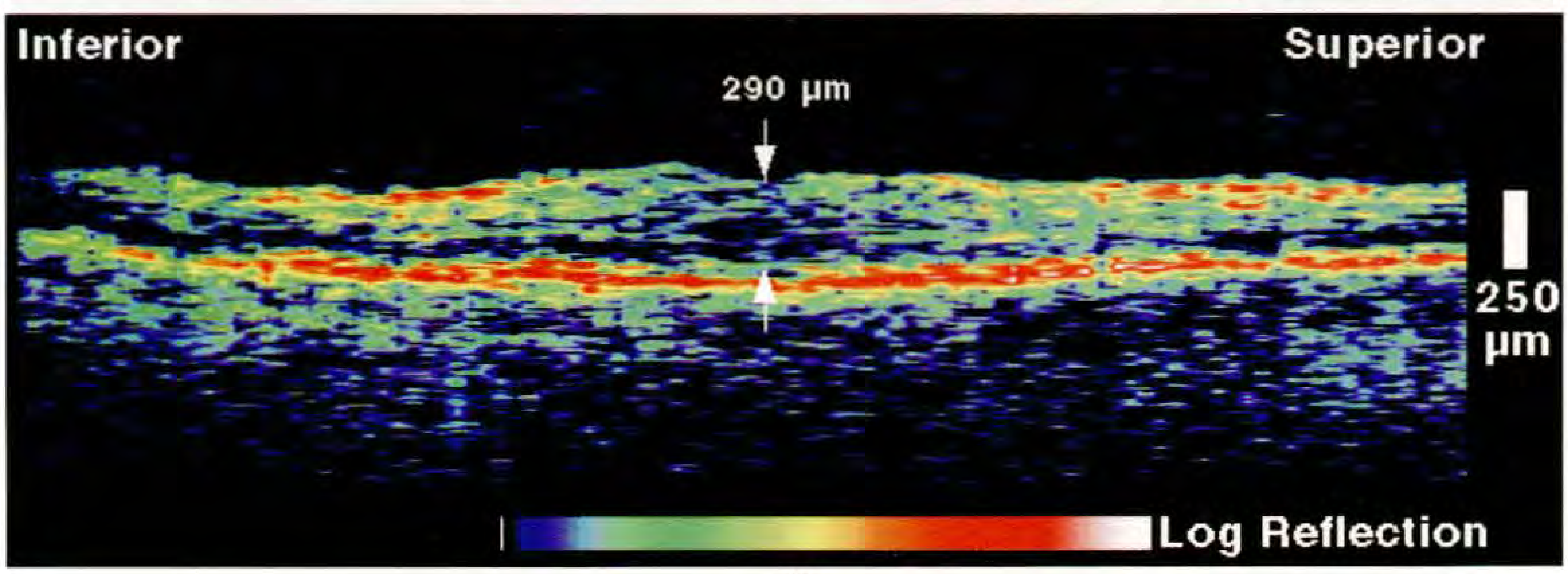

H

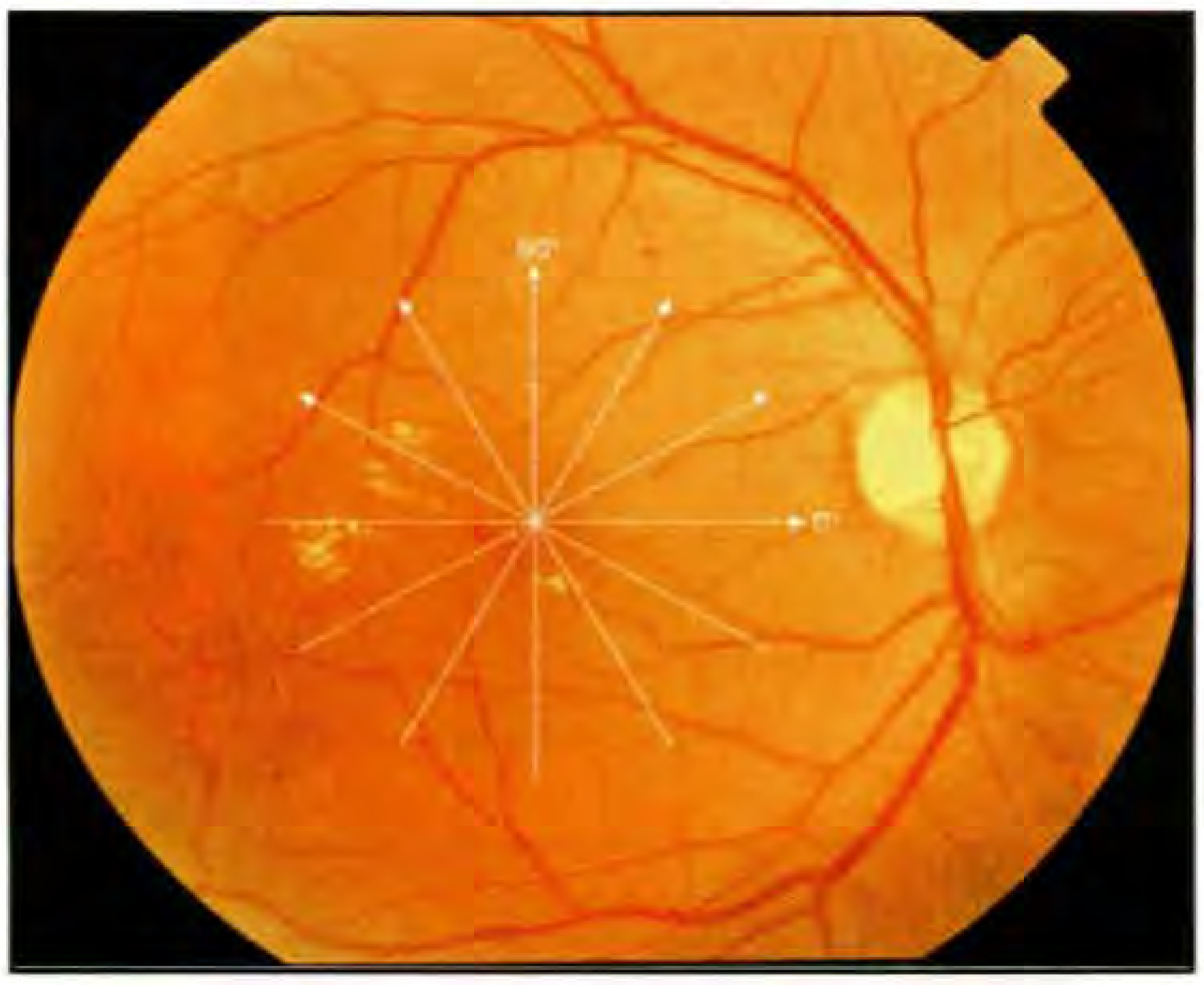

A

Case 6-4. Non-Proliferative Diabetic Retinopathy

Clinical Summary

A 50-year-old man had mild clinically significant macular edema associated with non-proliferative diabetic retinopathy in his right eye (A). His visual acuity in this eye was 20/20.

Optical Coherence Tomography

Radial OCT sections (B) through the fovea were acquired at six equally spaced angular orientations. An absence of the normal contour of the foveal pit was noted along with reduced optical reflectivity in the central macula, consistent with macular edema. The central foveal thickness was 300 µm.

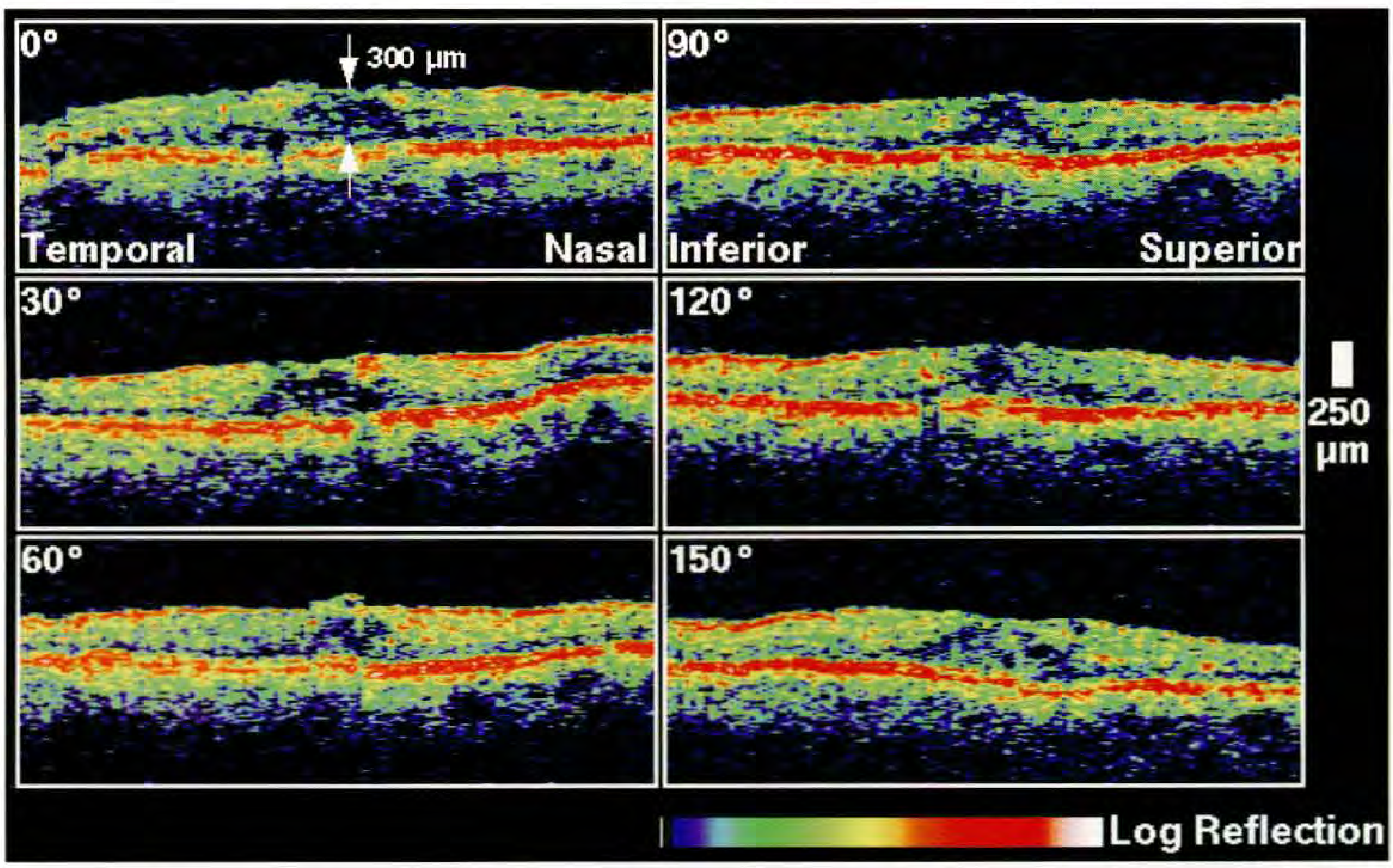

B

Case 6-4 continued

Clinical Summary

The left eye appeared normal on clinical examination, with a visual acuity of 20/20 (C).

Optical Coherence Tomography

OCT (D) also showed a normal macula with no evidence of retinal thickening. The central foveal thickness was 150 μm.

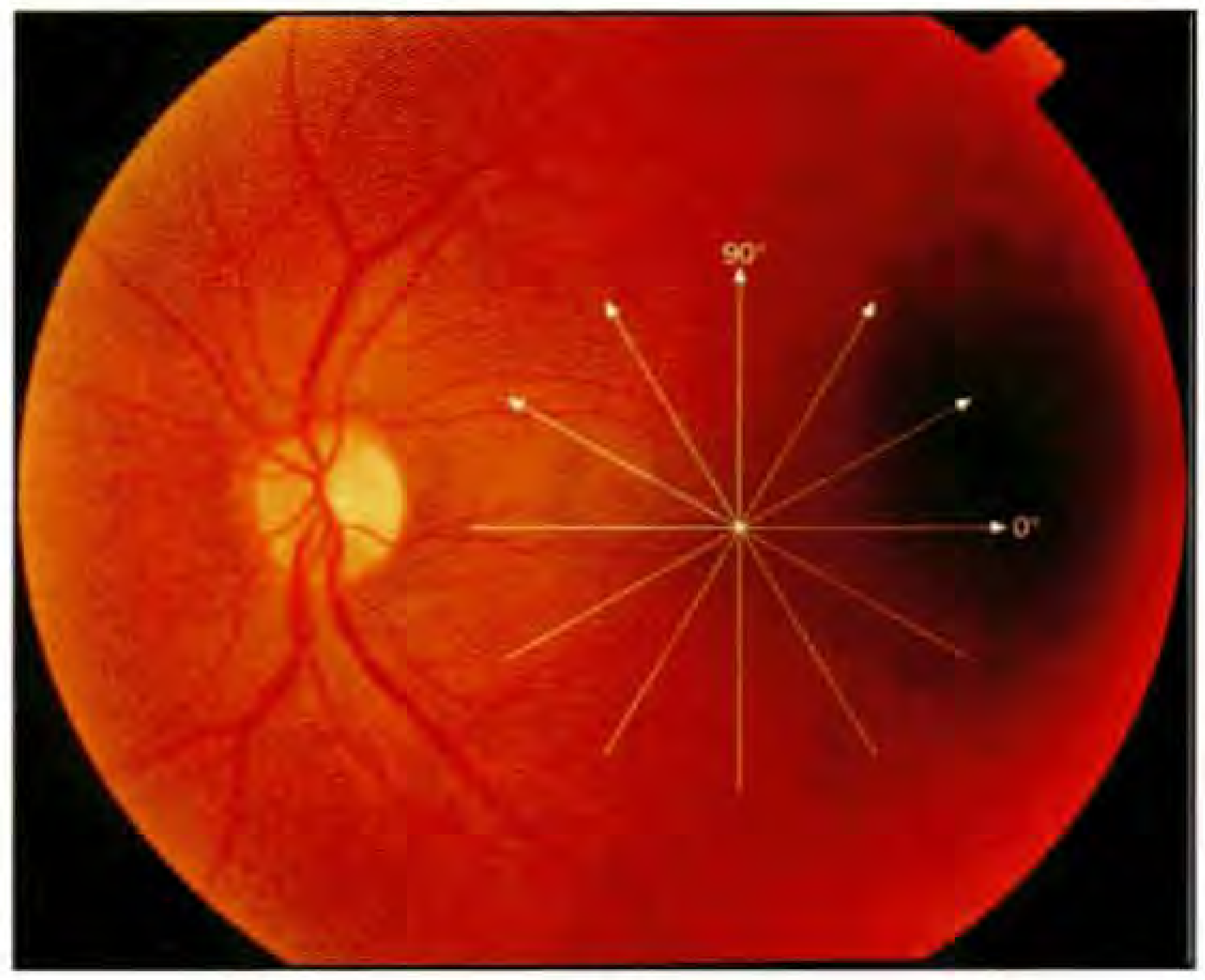

C

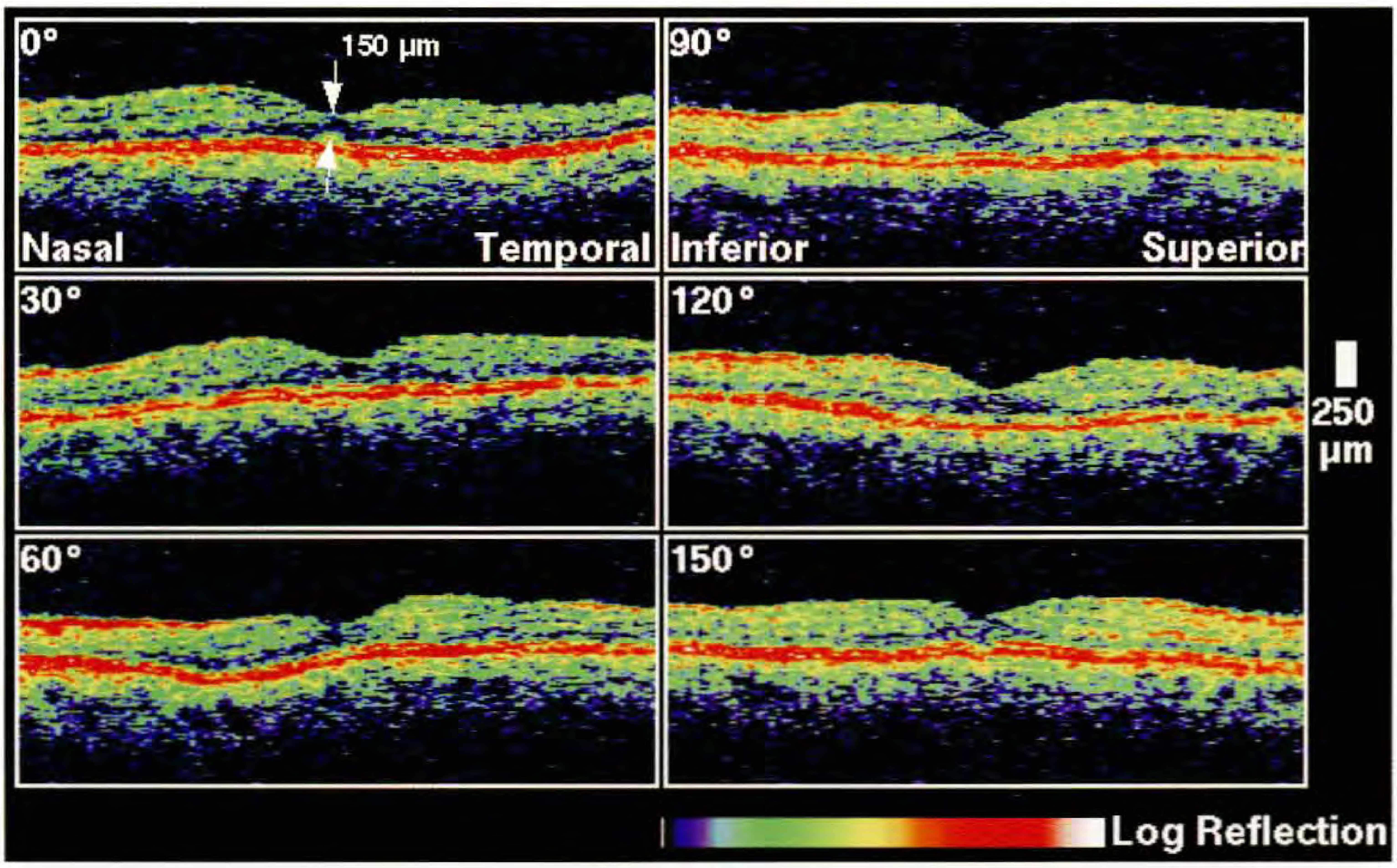

D

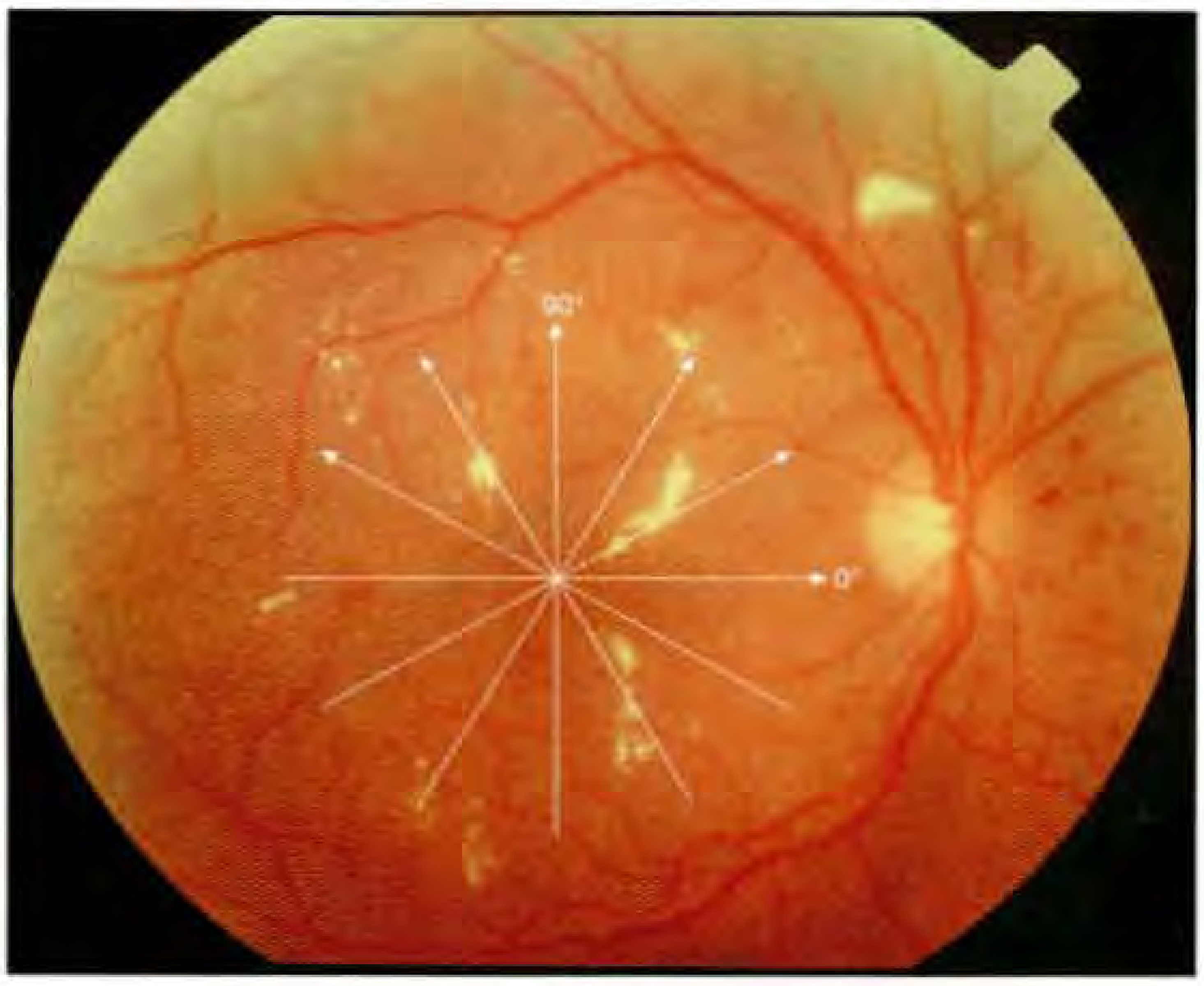

A

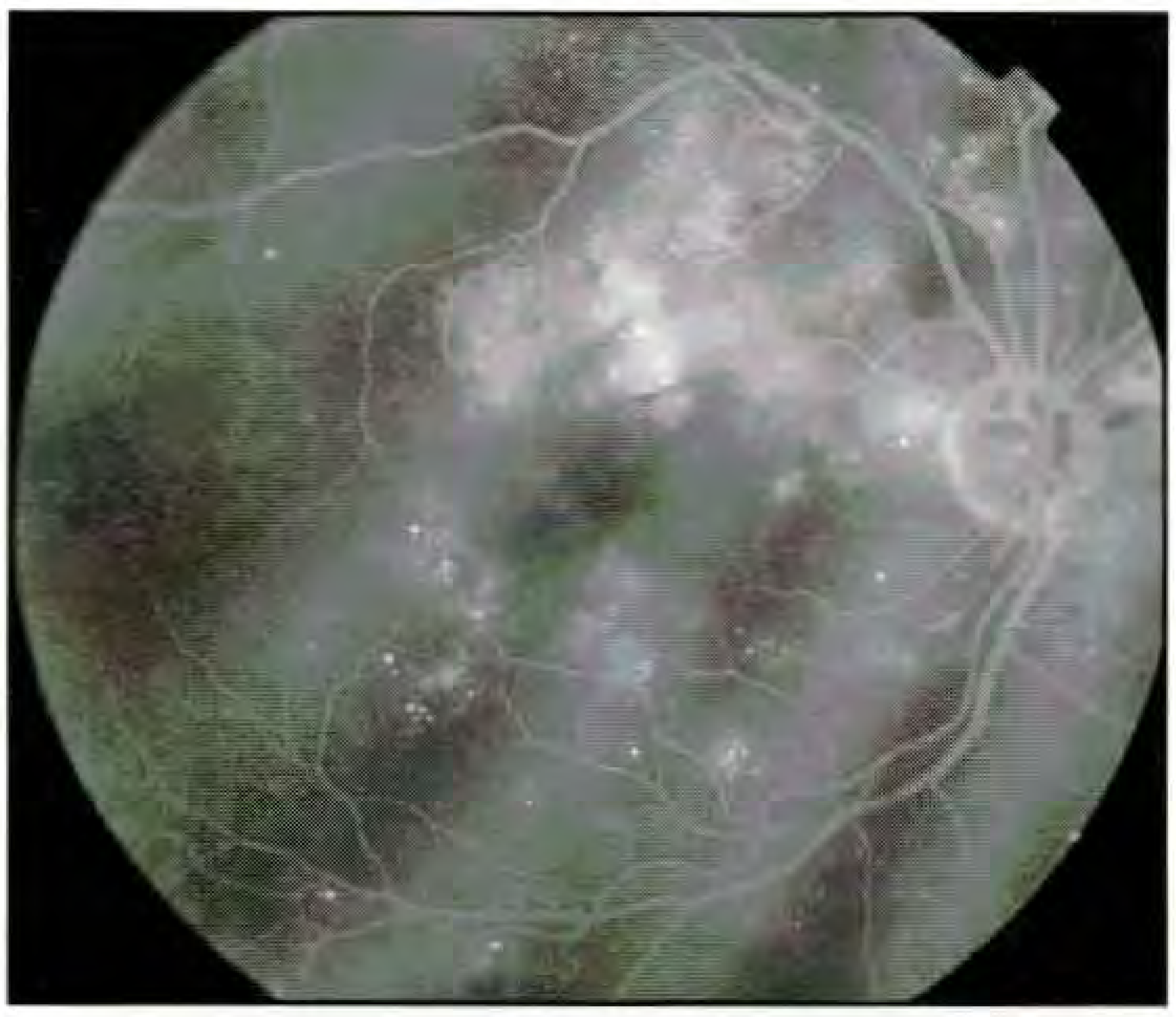

B

Case 6-5. Non-Proliferative Diabetic Retinopathy

Clinical Summary

A 63-year-old man with a visual acuity of 20/200 in his right eye had non-proliferative diabetic retinopathy and macular edema. Scattered dot and blot hemorrhages, microaneurysms, hard exudate, and diffuse macular thickening were noted on dilated fundus examination (A). Angiography revealed focal areas of hyperfluorescence in the macula which demonstrated late leakage of fluorescein dye consistent with microaneurysms (B).

Optical Coherence Tomography

A sequence of radially oriented, linear OCT tomograms (C) was obtained through the macula at different angular orientations. These images showed a diffuse increase in retinal thickness (480 μm in the fovea), minimally reflective spaces corresponding to fluid accumulation in the outer retinal layers, and focal, intraretinal areas of high backscattering corresponding to hard exudate.

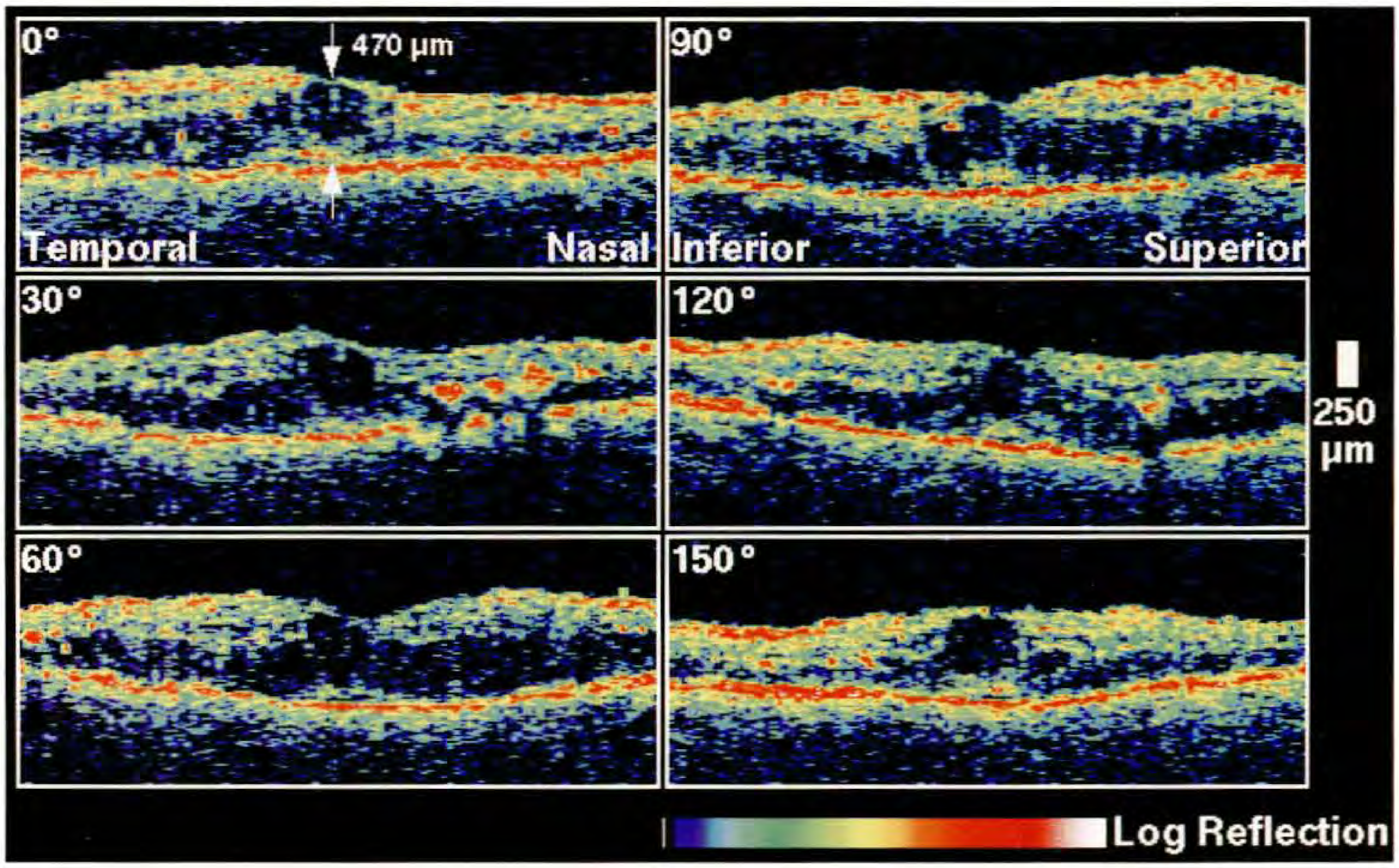

C

Case 6-5 continued

Clinical Summary

Slit-lamp biomicroscopy (D) of the left eye also showed scattered dot and blot hemorrhages and microaneurysms without neovascularization. Punctate hyperfluorescence with late leakage was observed on fluorescein angiography (E) consistent with microaneurysms. The visual acuity was 20/200 in this eye.

Optical Coherence Tomography

Radial OCT sections (F) illustrated diffuse thickening throughout the macula with preferential fluid accumulation in the outer retinal layers. A small detachment of the neurosensory retina with subretinal fluid accumulation was noted just beneath the fovea.

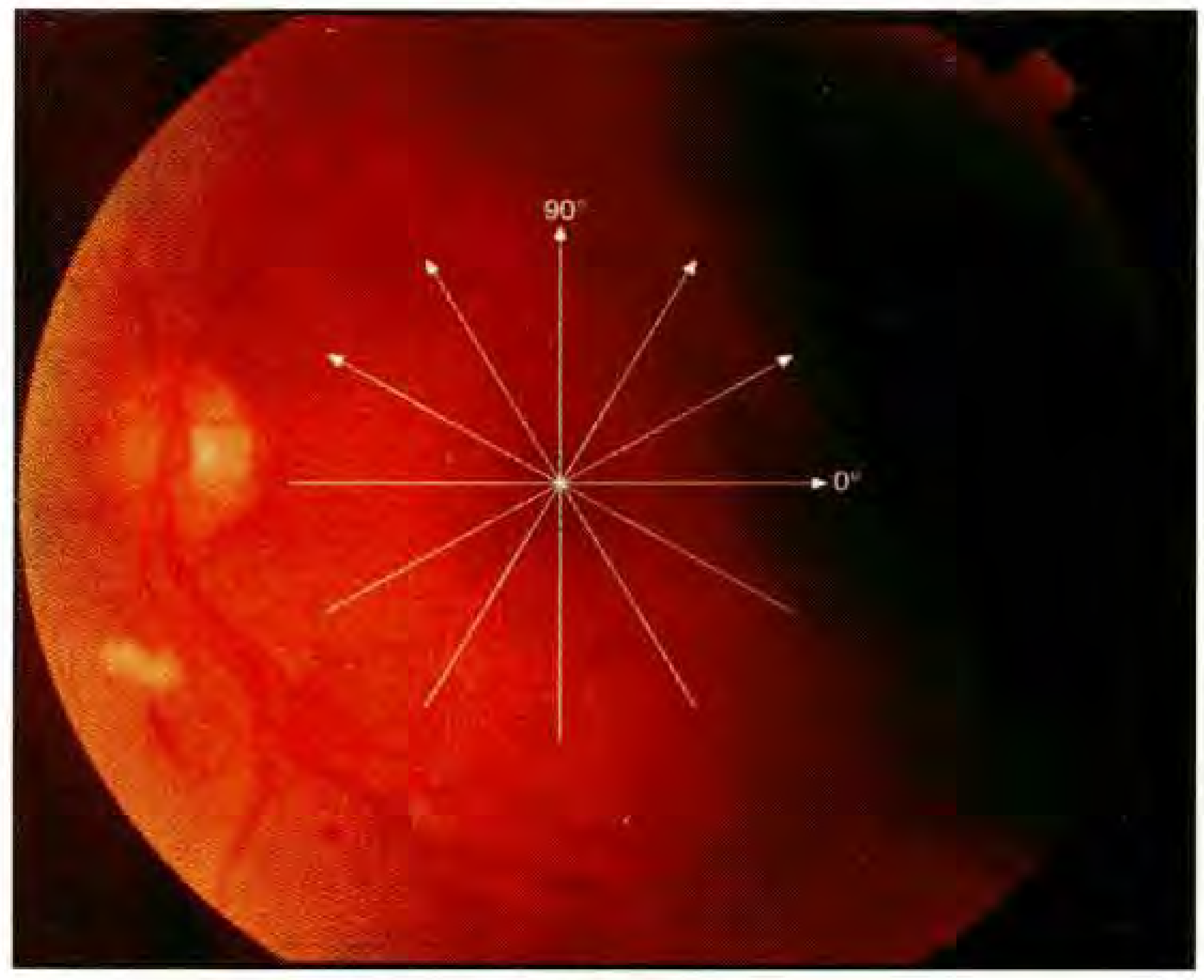

D

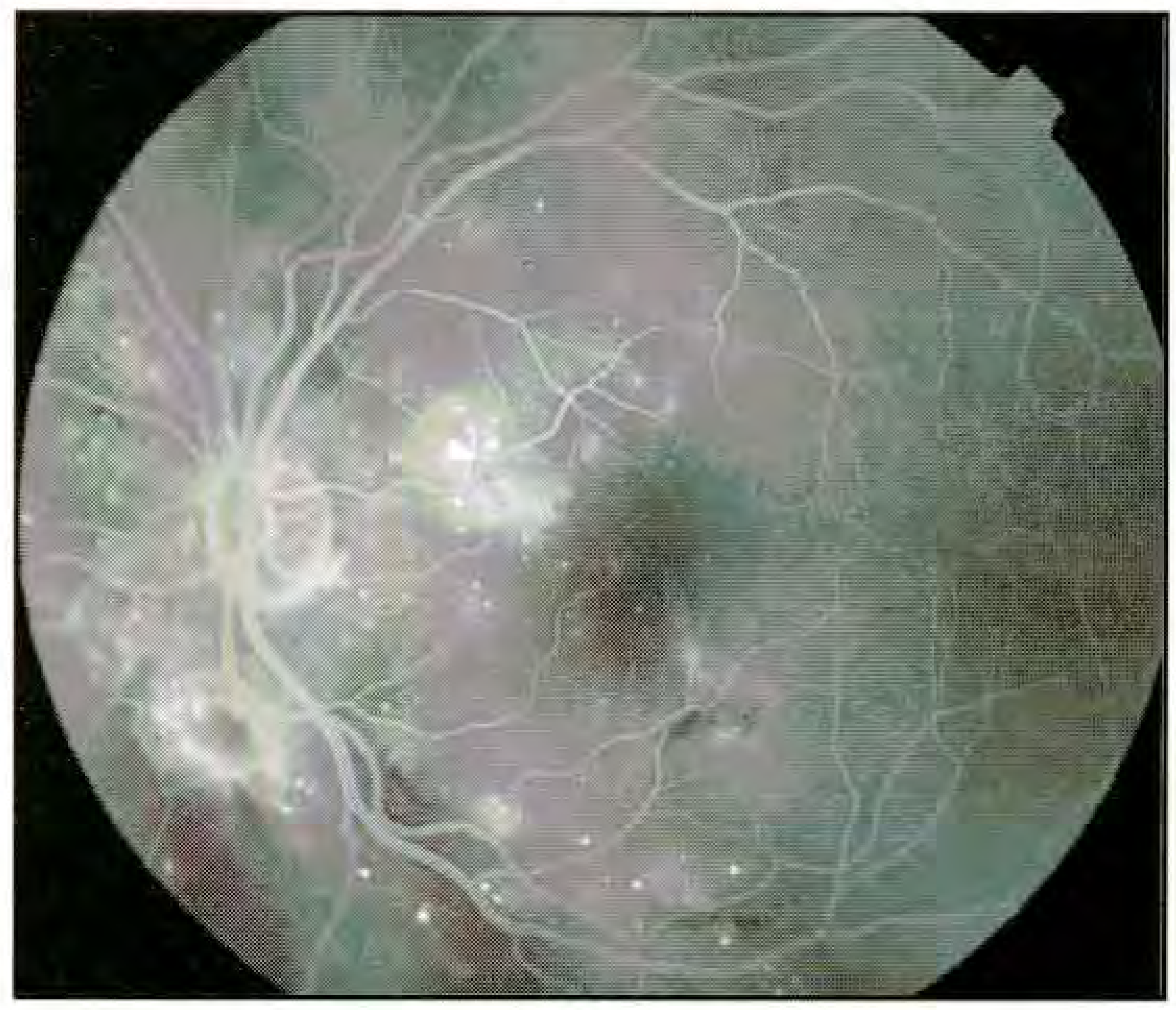

E

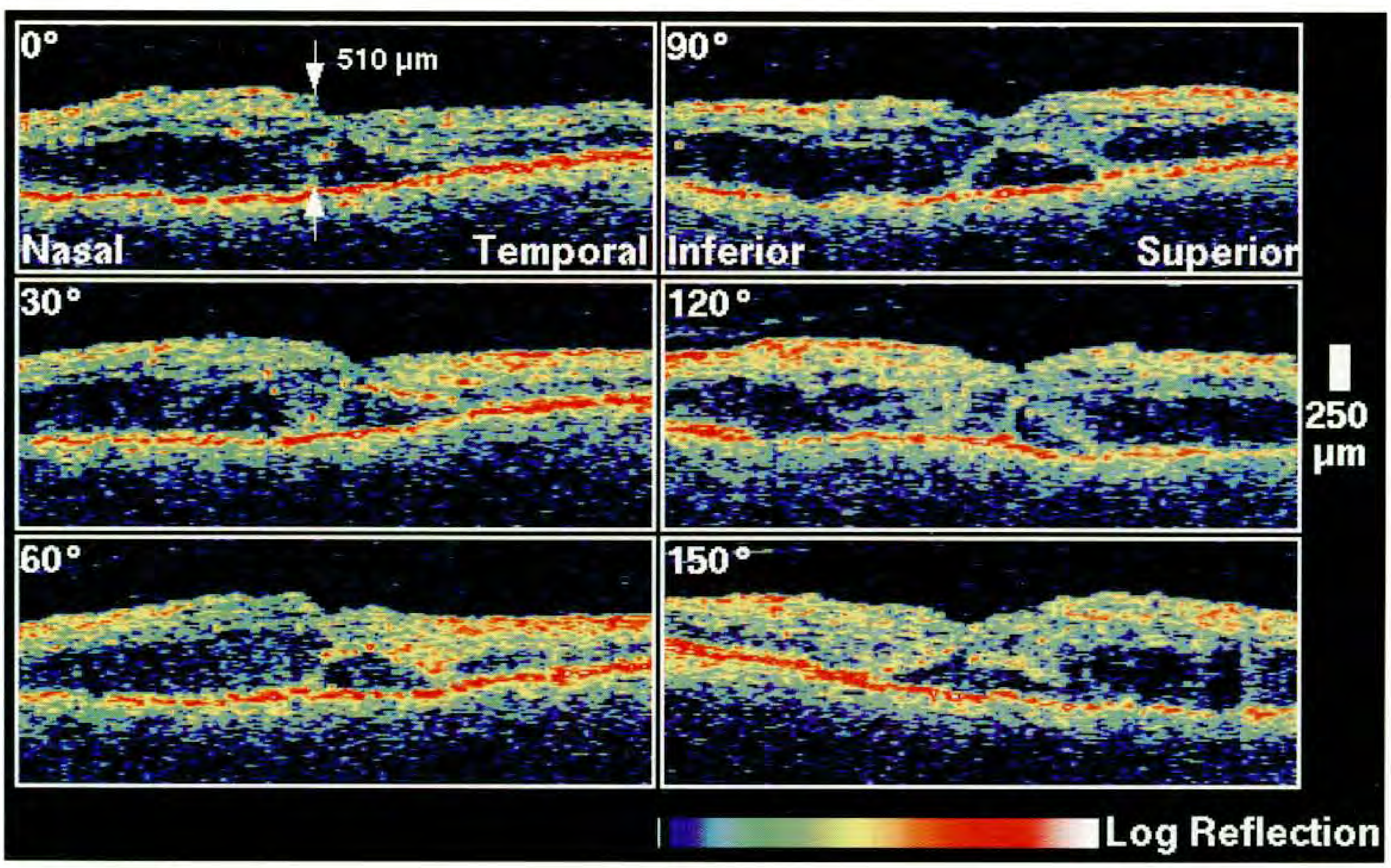

F

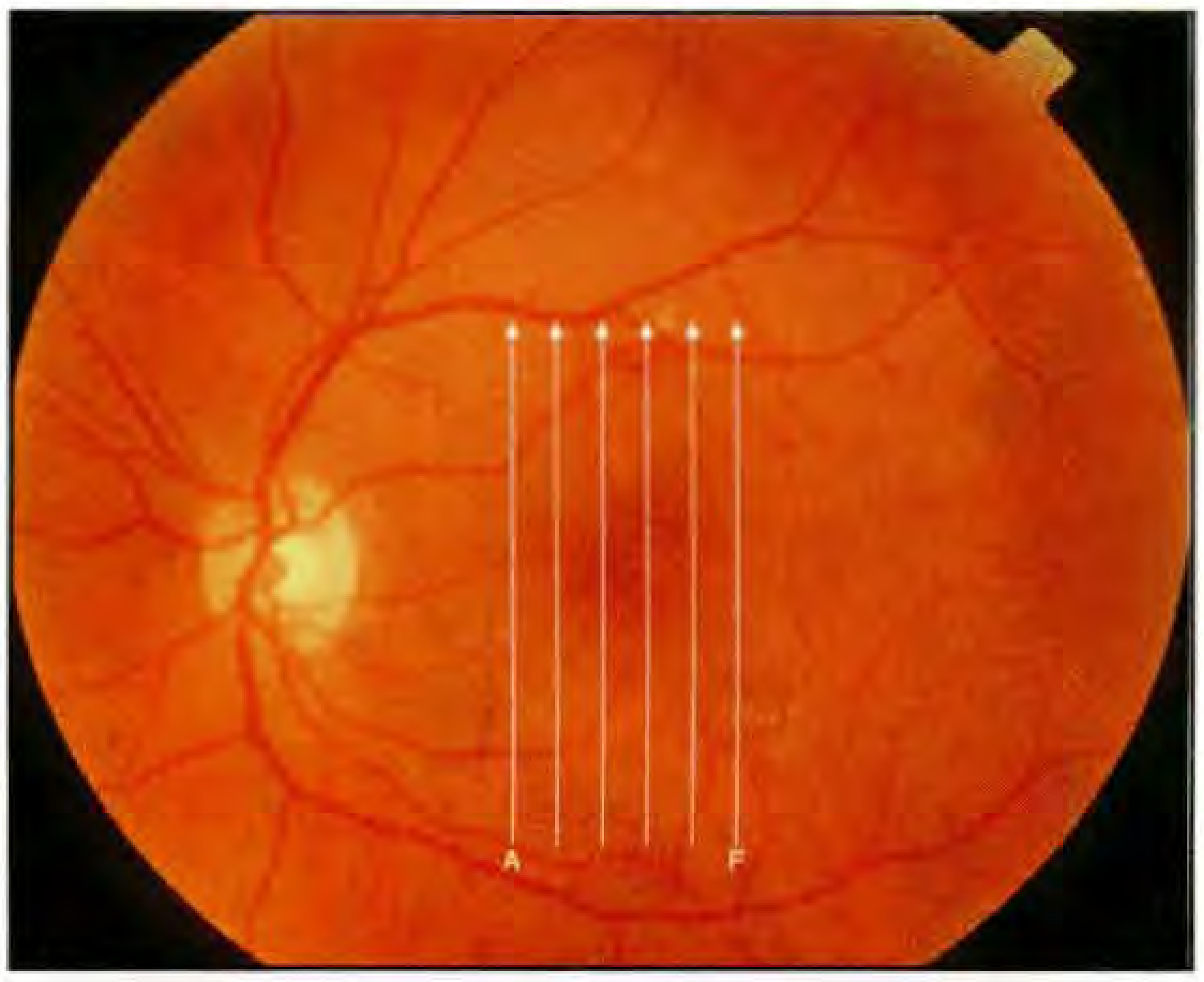

A

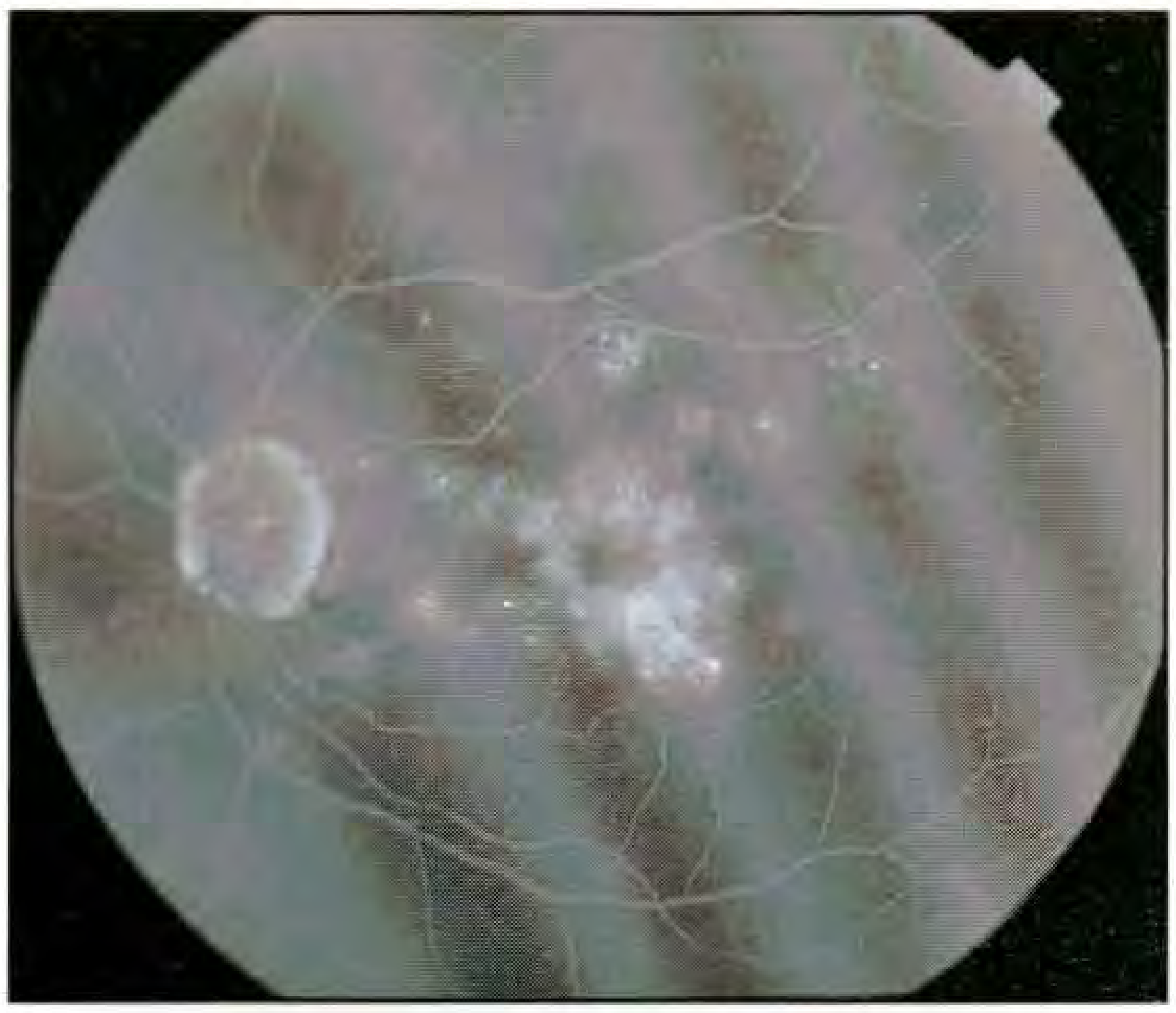

B

Case 6-6. Non-Proliferative Diabetic Retinopathy and Cystoid Macular Edema

Clinical Summary

A 71-year-old woman with a three year history of adult-onset diabetes mellitus was referred for mild non-proliferative diabetic retinopathy and clinically significant macular edema in her left eye. The visual acuity in this eye was 20/70 (A). Fluorescein angiography (B) displayed late leakage in the fovea consistent with cystoid macular edema.

Optical Coherence Tomography

A series of vertical OCT tomograms (C) was obtained through the macula providing three-dimensional information on retinal structure. The retinal thickness was increased in the macula, with large areas of low reflectivity corresponding to intraretinal cysts and fluid accumulation. The retinal thickness measured in scan D, taken directly through the patient's point of fixation, was 650 µm.

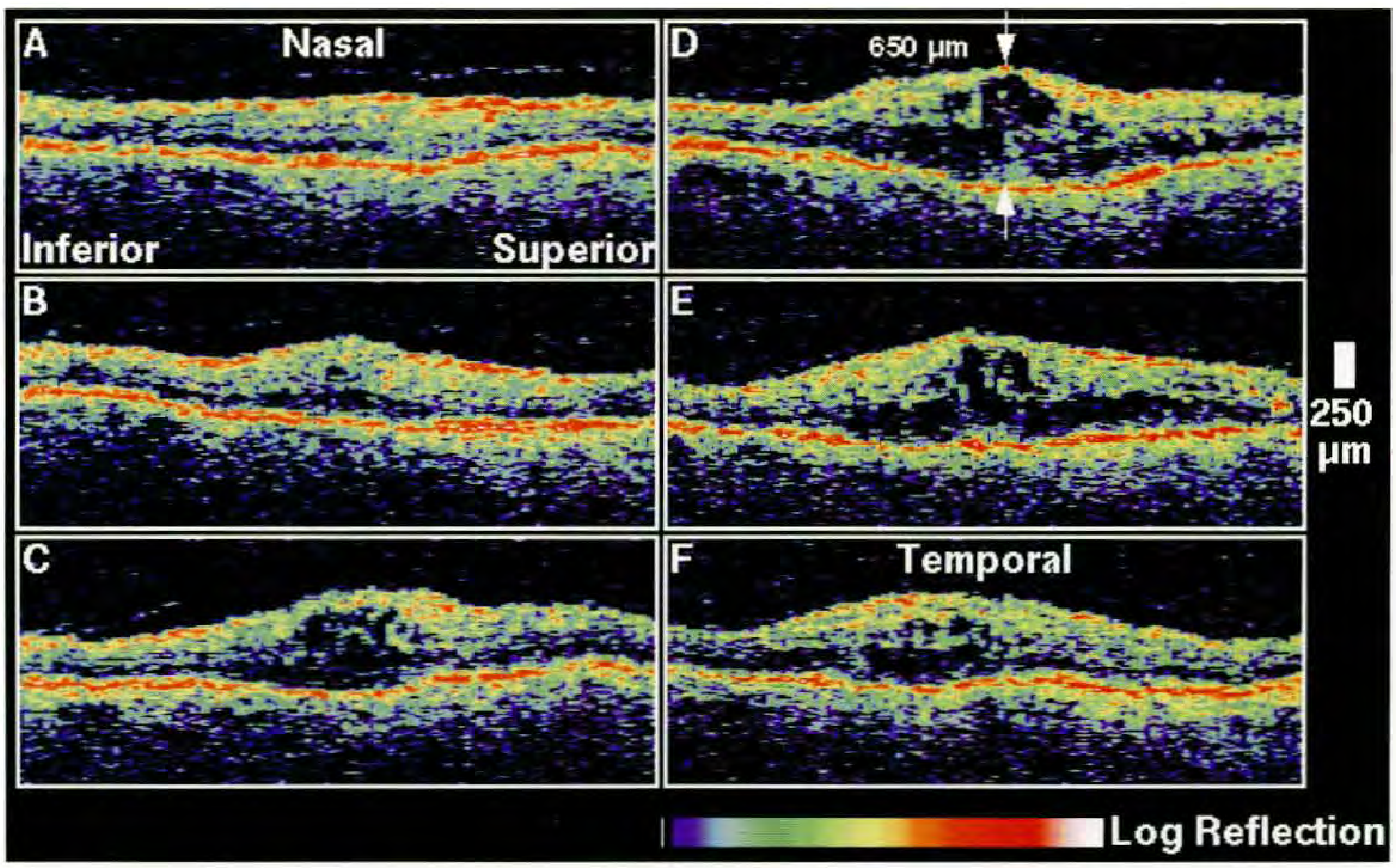

C

Case 6-6 continued

Clinical Summary

Examination of the right eye (D) showed scattered microaneurysms, and dot and blot hemorrhages without clinically significant macular edema or neovascularization. Fluorescein angiography (E) displayed small focal spots of hyperfluorescence with late leakage consistent with microaneurysms. The visual acuity in this eye was 20/25.

Optical Coherence Tomography

Serial vertical images acquired through the macula (F) illustrated moderate retinal thickening in the fovea, with no evidence of cysts or exudate. The retinal thickness measured in Scan D, taken through fixation, was 260 µm.

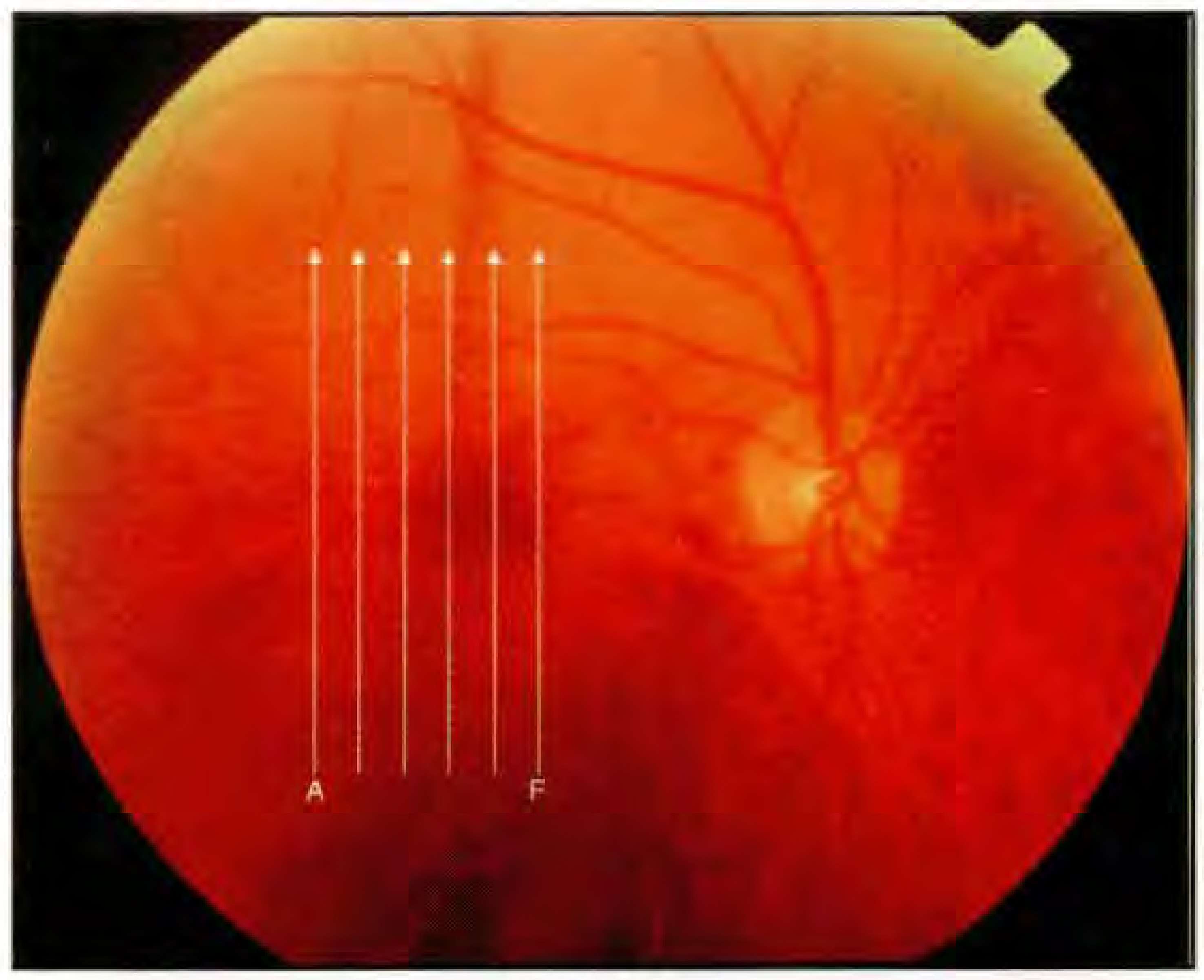

D

E

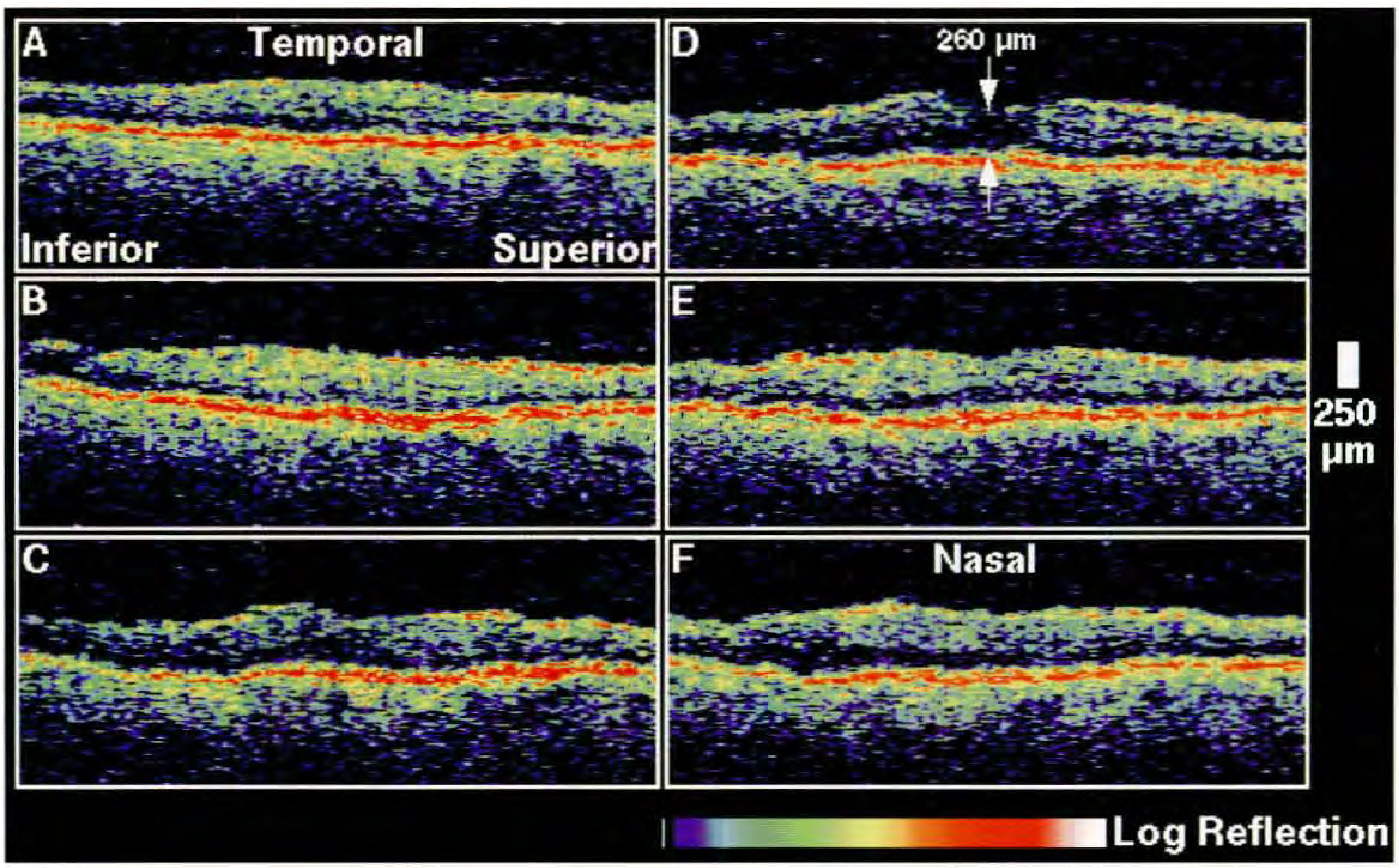

F

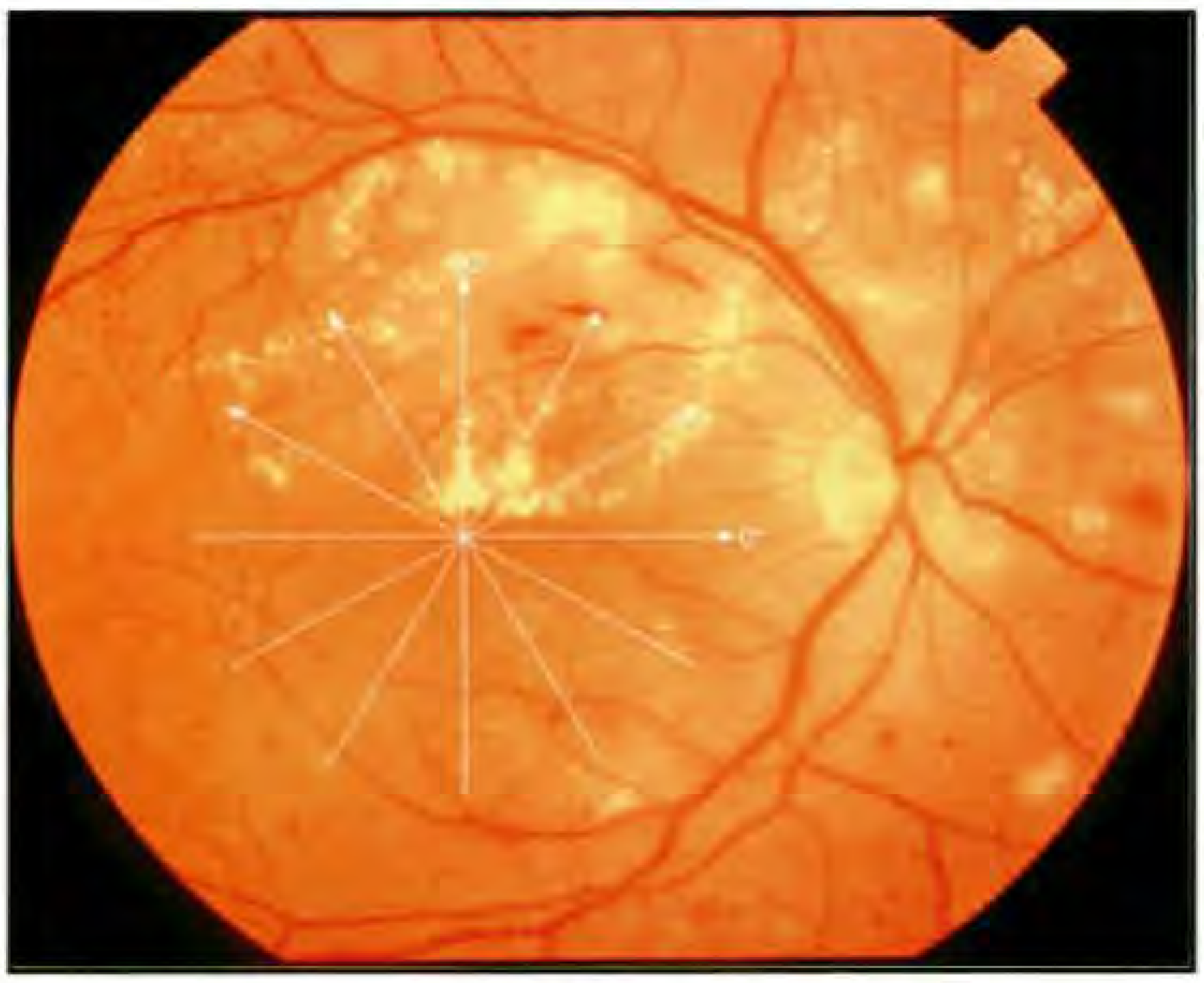

A

Case 6-7. Non-Proliferative Diabetic Retinopathy

Clinical Summary

A 53-year-old diabetic woman had moderately severe macular edema bilaterally. She had previously received focal laser photocoagulation treatment in both eyes approximately four months earlier. Dilated fundus examination (A) of her right eye revealed hard exudate extending from the superotemporal arcade into the macula, blot and flame shaped hemorrhages, and a diffuse increase in retinal thickness. The visual acuity in this eye was 20/30.

Optical Coherence Tomography

A sequence of radial tomograms (B) through the macula confirmed the diffuse thickening in the macula. Large regions of high intraretinal backscattering were observed just superior to the fovea corresponding to hard exudate. The foveal thickness was 270 μm.

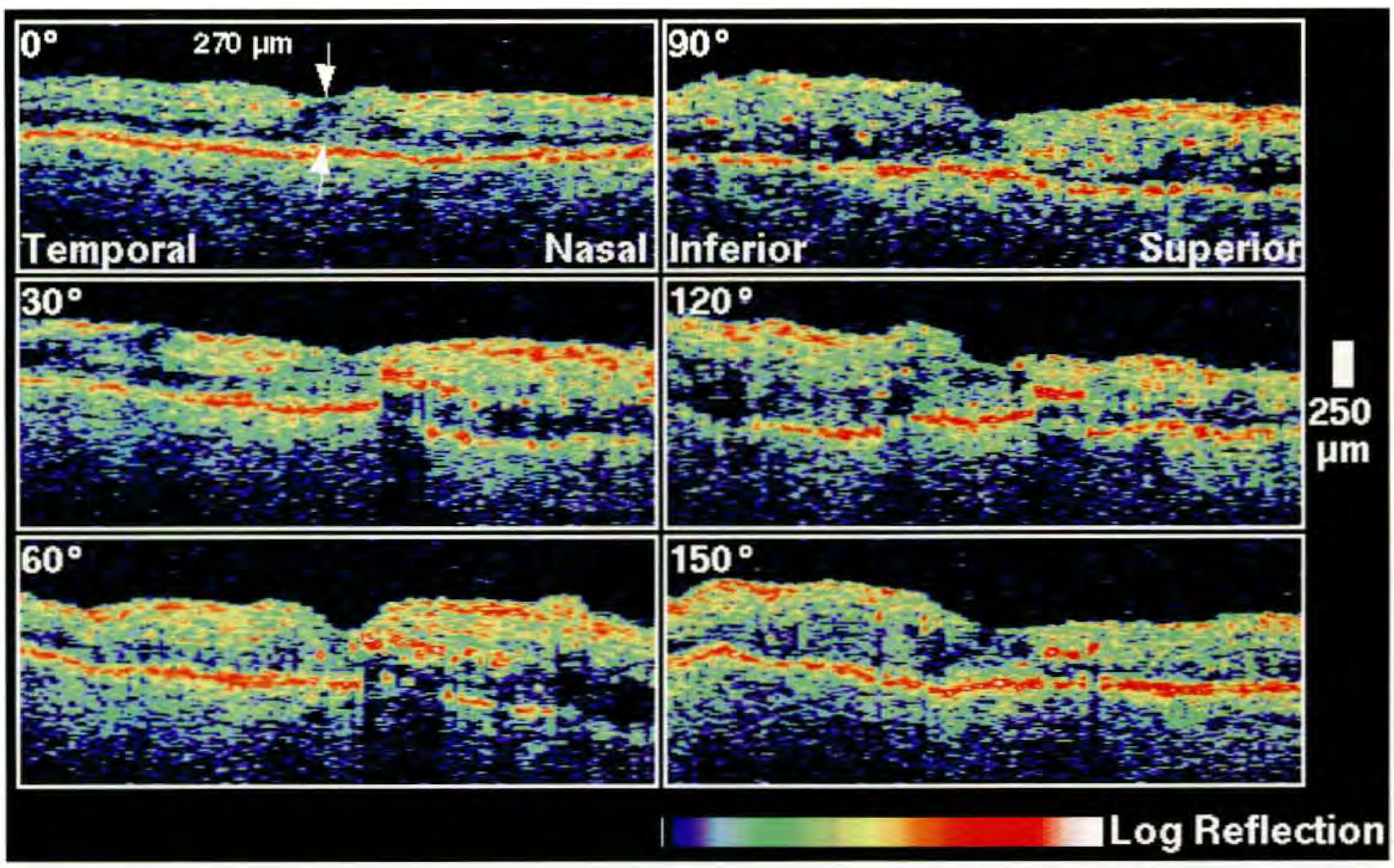

B

Case 6-7 continued

Clinical Summary

The left eye (C) also exhibited significant retinal thickening throughout the macula, and an arcuate region of hard exudate involving the macula. The visual acuity was 20/30.

Optical Coherence Tomography

Radial OCT sections (D) demonstrated diffuse macular thickening, a large cyst directly in the fovea, and significant hard exudate throughout the macula. The central foveal thickness was 300 μm.

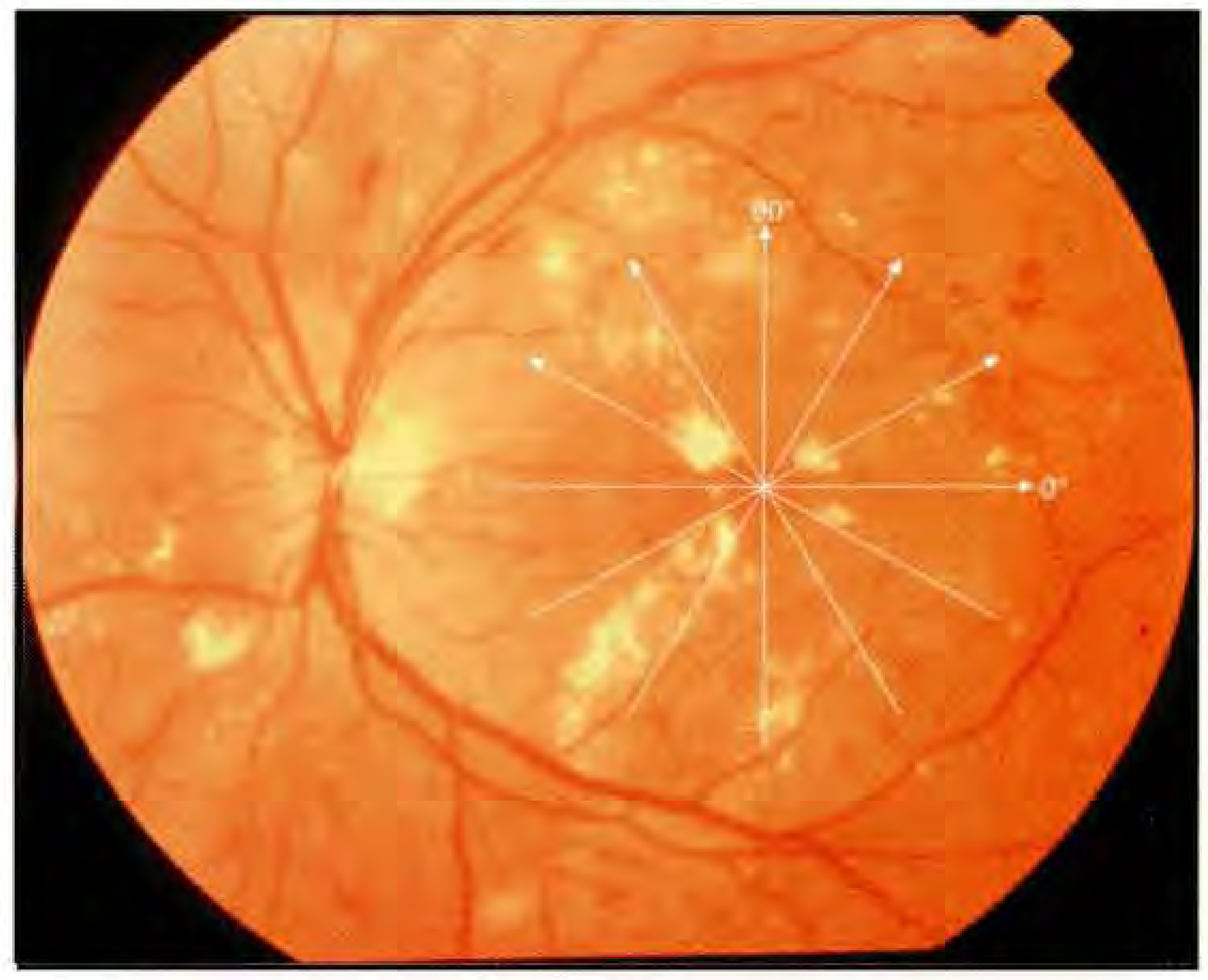

C

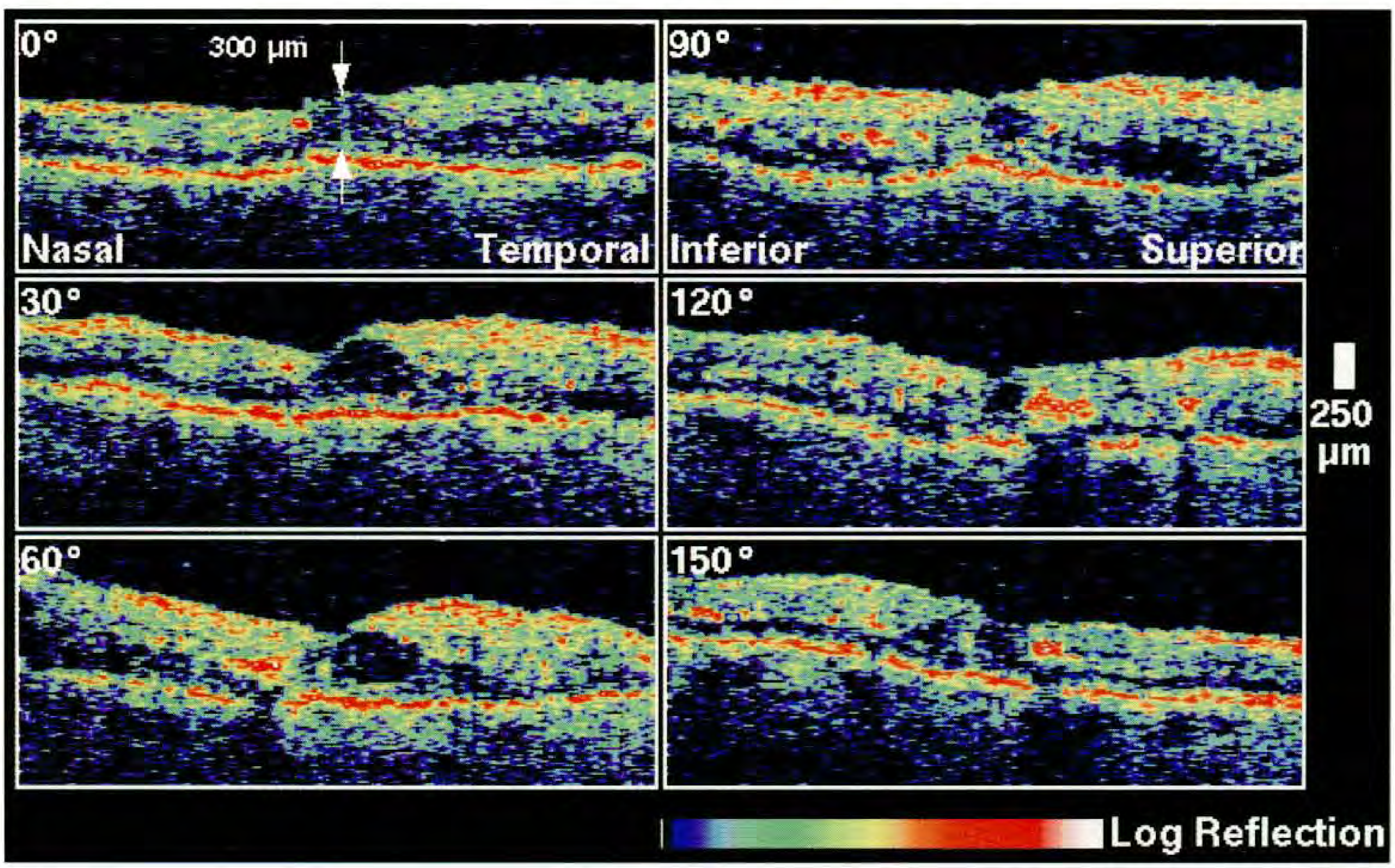

D

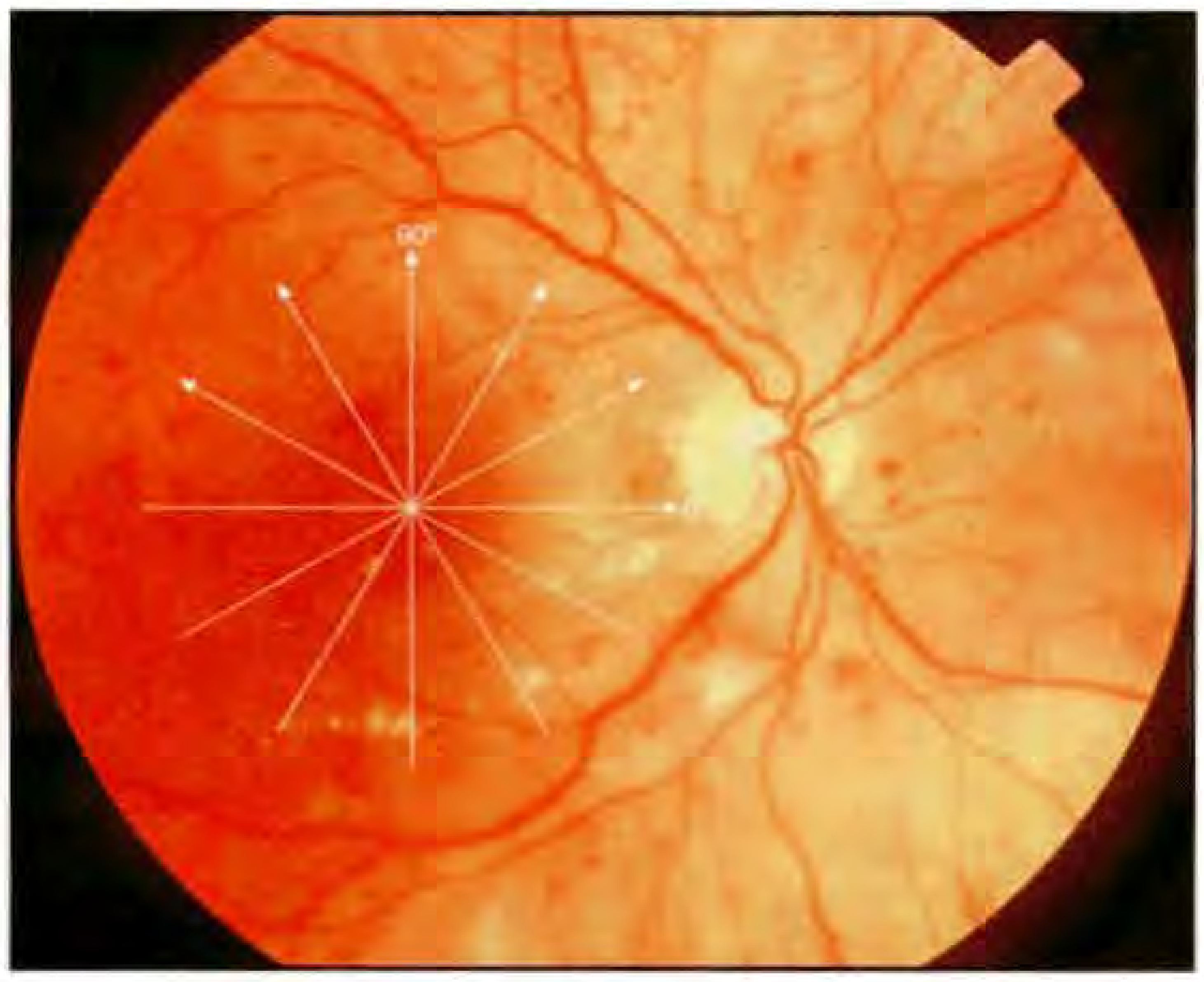

A

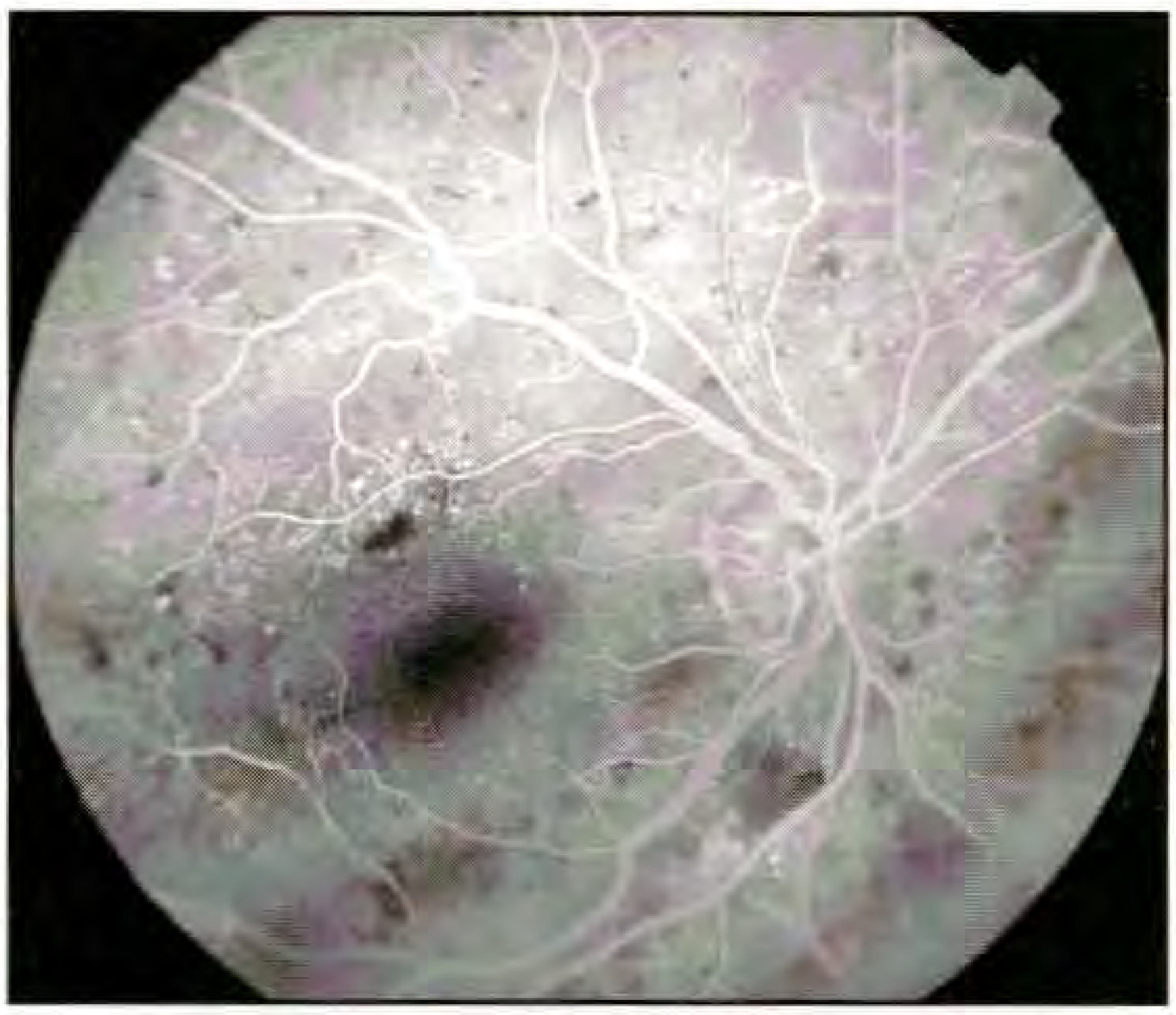

B

Case 6-8. Non-Proliferative Diabetic Retinopathy

Clinical Summary

This patient was a 65-year-old woman with background diabetic retinopathy in both eyes. The visual acuity in the right eye was 20/20. Slit-lamp biomicroscopy of this eye (A) showed dot and blot hemorrhages scattered throughout the posterior pole, retinal exudate along the inferotemporal arcade, and clinically significant macular thickening and cysts. Fluorescein angiography (B) displayed punctate hyperfluorescence with late leakage along the superotemporal arcade consistent with microaneurysms.

Optical Coherence Tomography

A series of radial OCT scans (C) was acquired through the macula at equally spaced angular orientations. The images showed a large cyst directly in the fovea and diffuse macular thickening which was most significant in the superotemporal macula. Focal areas of high intraretinal optical reflectivity were observed consistent with hard exudate. The retinal thickness measured directly in the fovea was 550 μm.

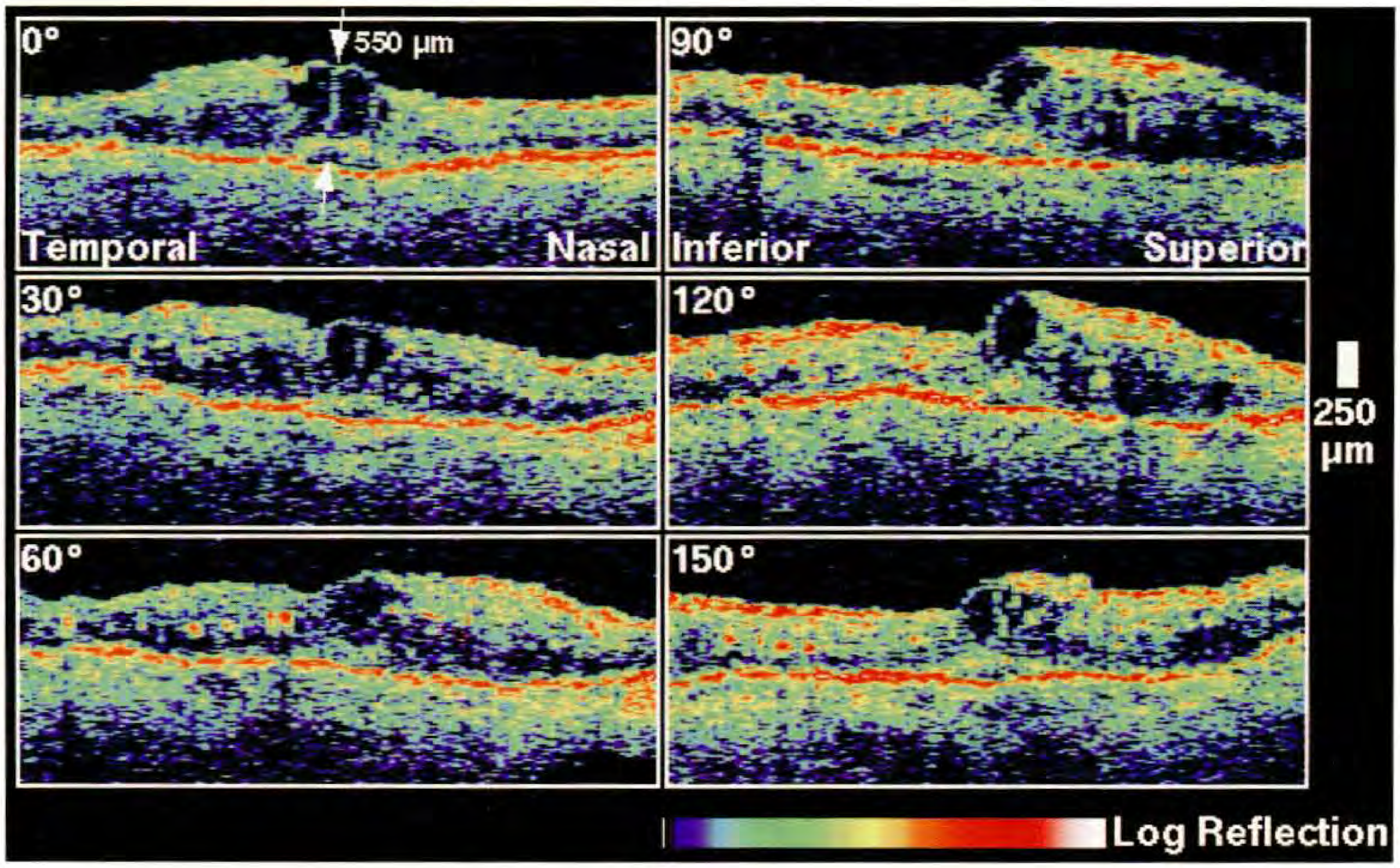

C

Case 6-8 continued

Clinical Summary

In the left eye, dilated fundus examination (D) also displayed significant macular thickening and dot hemorrhages. Visual acuity in this eye, however, was 20/400. Fluorescein angiography (E) demonstrated diffuse late leakage consistent with macular edema.

Optical Coherence Tomography

Radial OCT sections (F) of the left eye revealed a striking cyst in the central macula which occupied the entire thickness of the retina. Several smaller cysts and diffuse macular thickening were noted in the surrounding retina. The foveal thickness was measured to be 720 µm.

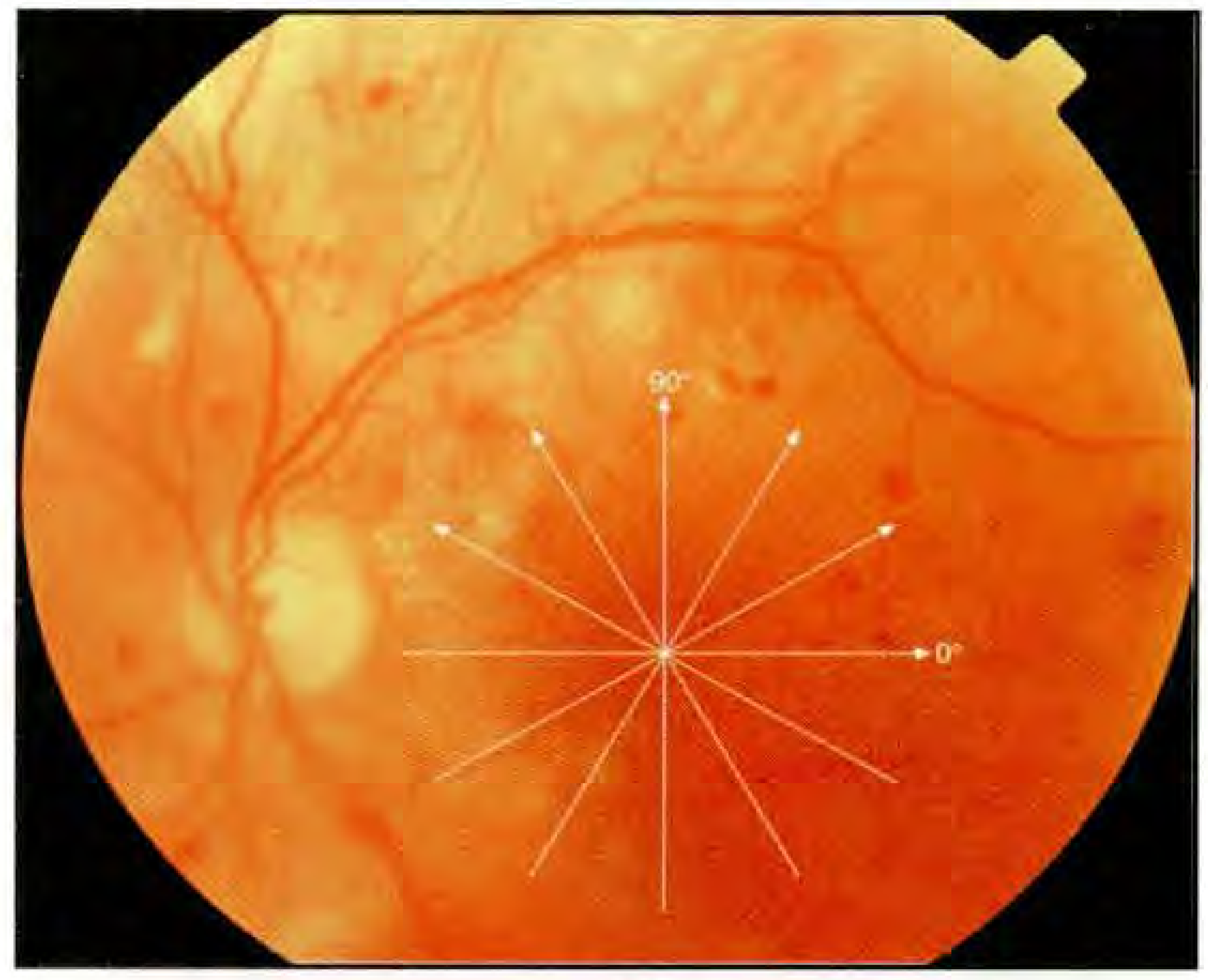

D

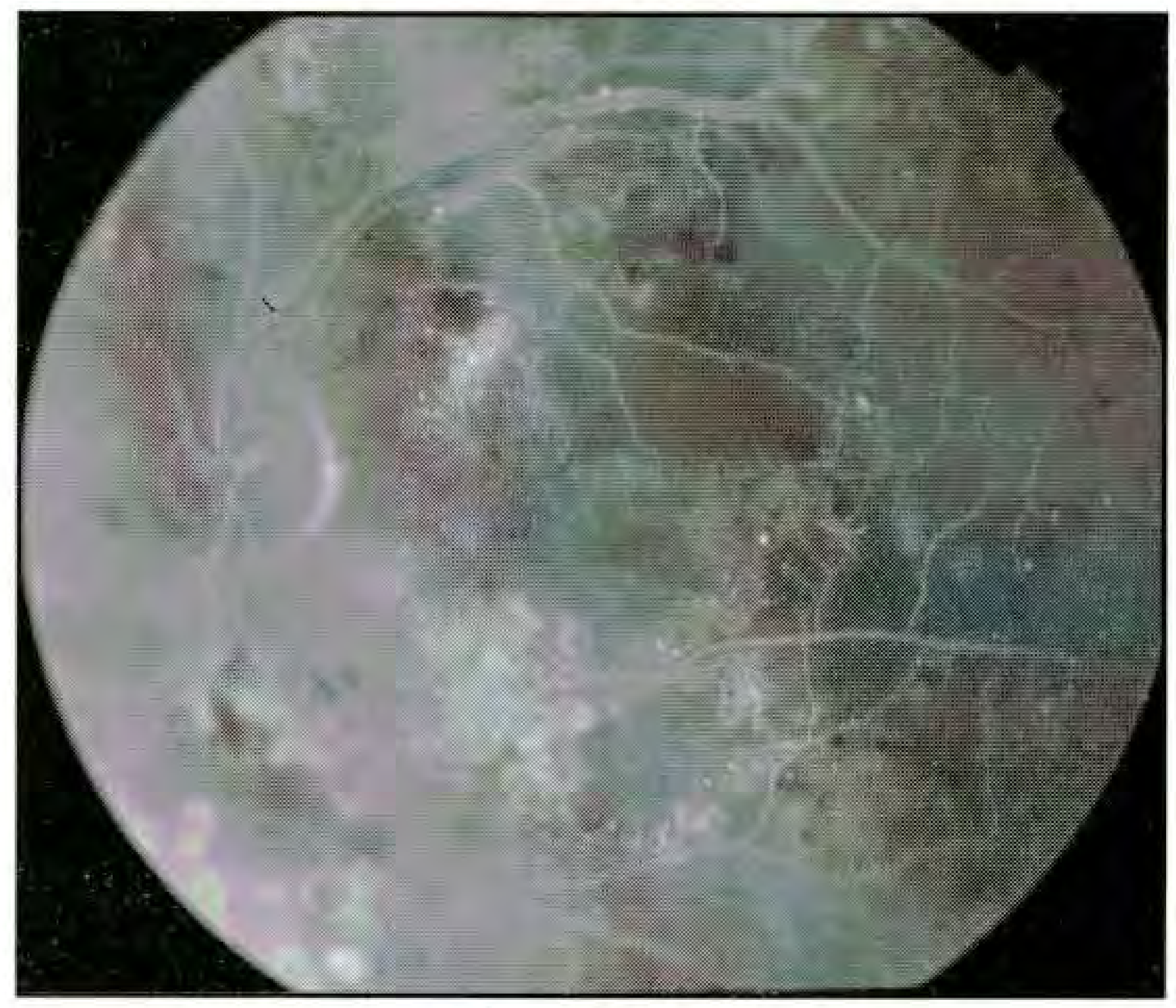

E

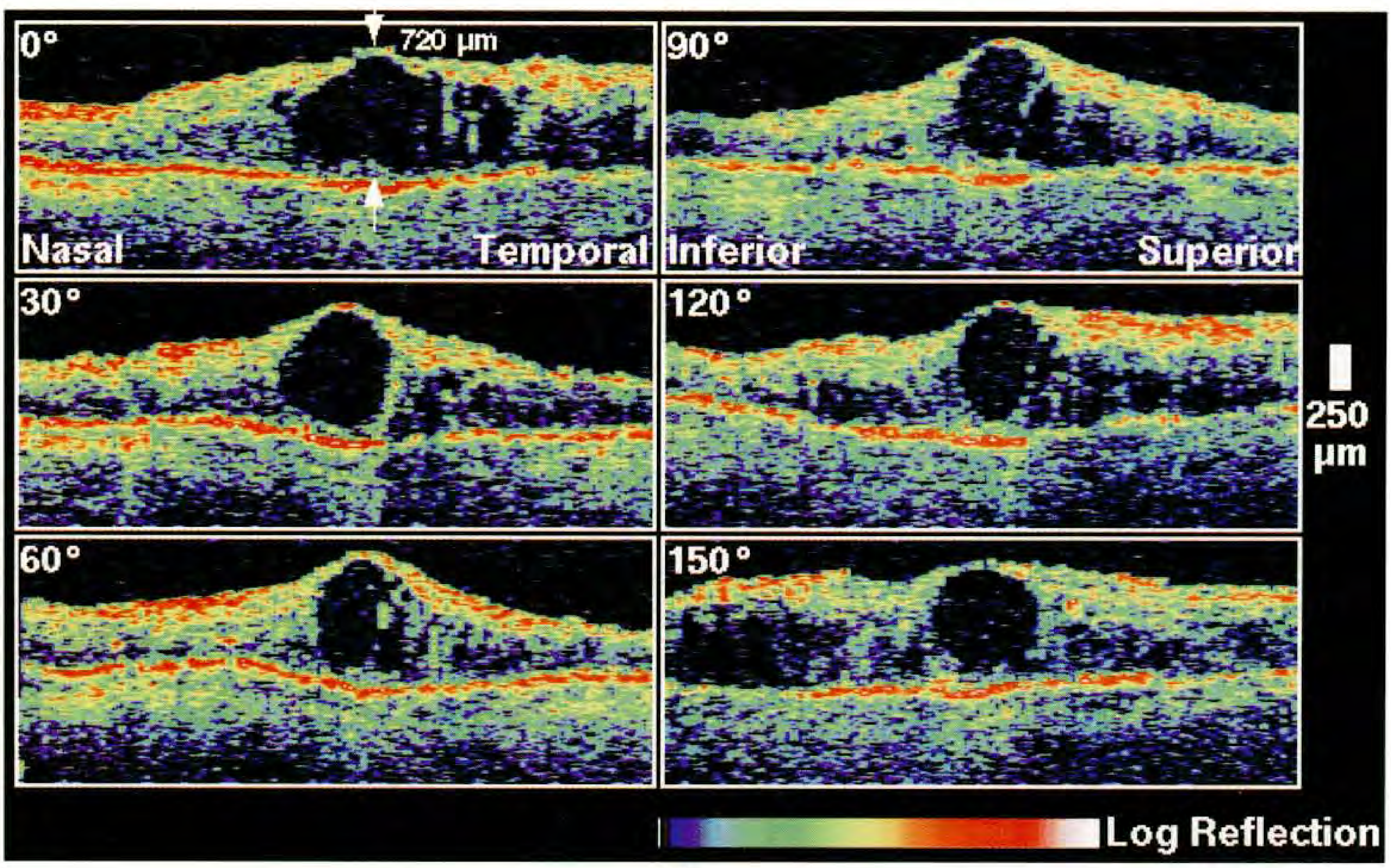

F

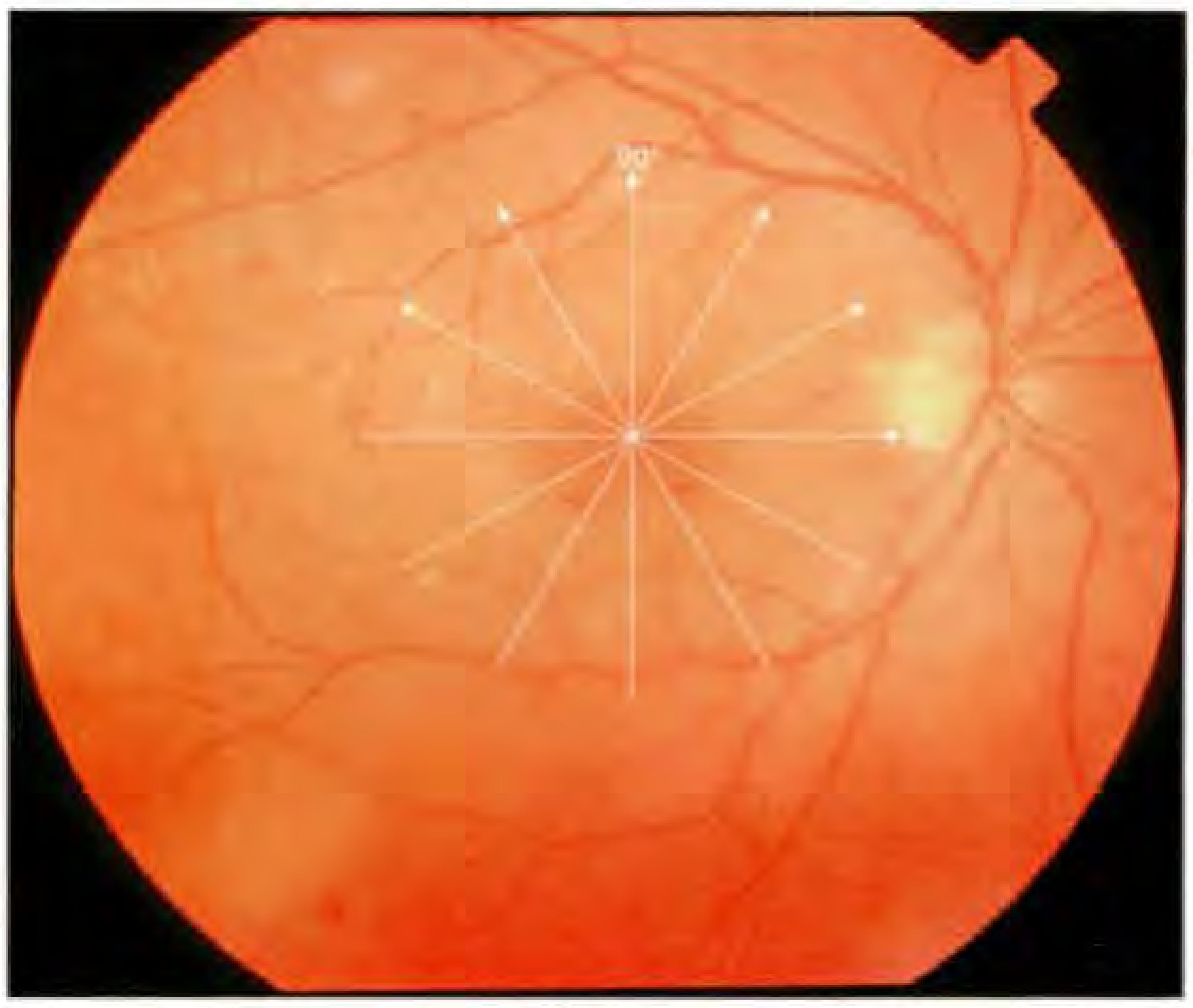

A

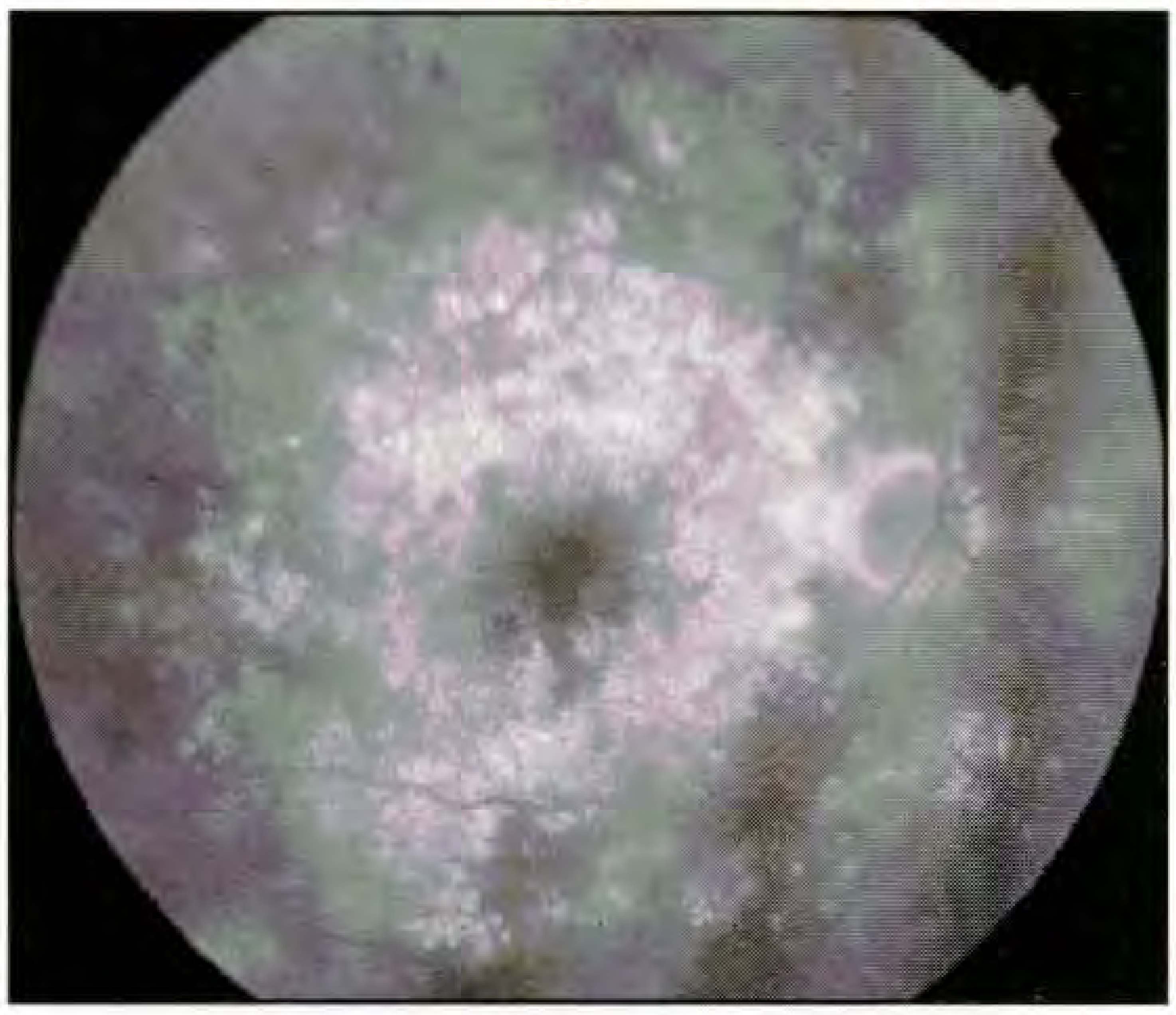

B

Case 6-9. Non-Proliferative Diabetic Retinopathy

Clinical Summary

A 71-year-old woman had received grid laser photocoagulation treatment seven months earlier for background diabetic retinopathy and clinically significant macular edema in her right eye. On examination, her visual acuity in this eye was 20/60 . Residual cystoid macular edema and some scattered microaneurysms were noted on clinical examination (A). Fluorescein angiography (B) displayed some diffuse late staining of the retinal pigment epithelium around the macula consistent with old cystoid macular edema.

Optical Coherence Tomography

Radial OCT sections (C) obtained through the fovea demonstrated the persistence of retinal thickening throughout the macula. The foveal thickness was 270 µm. The contour of the foveal pit appeared steepened and narrowed. A small neurosensory detachment was observed directly beneath the fovea which was not evident clinically.

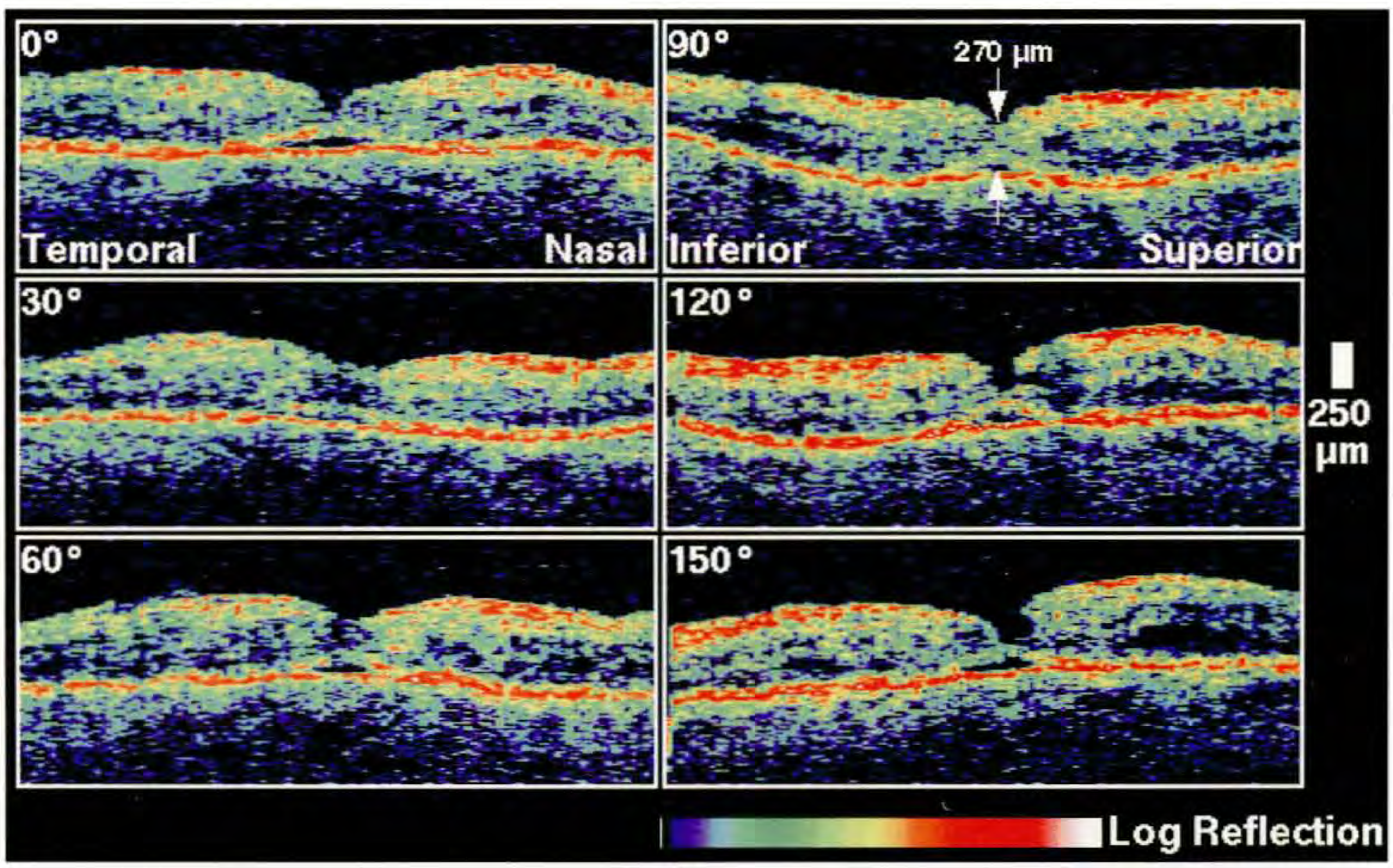

C

Case 6-10. Non-Proliferative Diabetic Retinopathy

Clinical Summary

A 68-year-old woman was referred for worsening visual acuity and macular edema in her right eye. Slit-lamp examination (A) revealed diffuse dot and blot hemorrhages, and microaneurysms consistent with non-proliferative diabetic retinopathy. Two areas of retinal thickening were noted temporal and inferior to the fovea, and hard exudate was identified inferotemporally. The visual acuity was 20/40. Fluorescein angiography (B) confirmed the presence of macular edema and showed late leakage in the inferotemporal macula. Focal laser treatment was performed. Three months later, the visual acuity had improved to 20/30 and follow-up examination revealed only a tiny area of retinal thickening directly in the fovea.

Optical Coherence Tomography

OCT images (C) obtained at the follow-up visit showed the persistence of retinal thickening inferior and temporal to the fovea. Reduced optical backscatter signal from the outer retina suggested preferential fluid accumulation in these areas. The central macular thickness was measured at 250 μm.

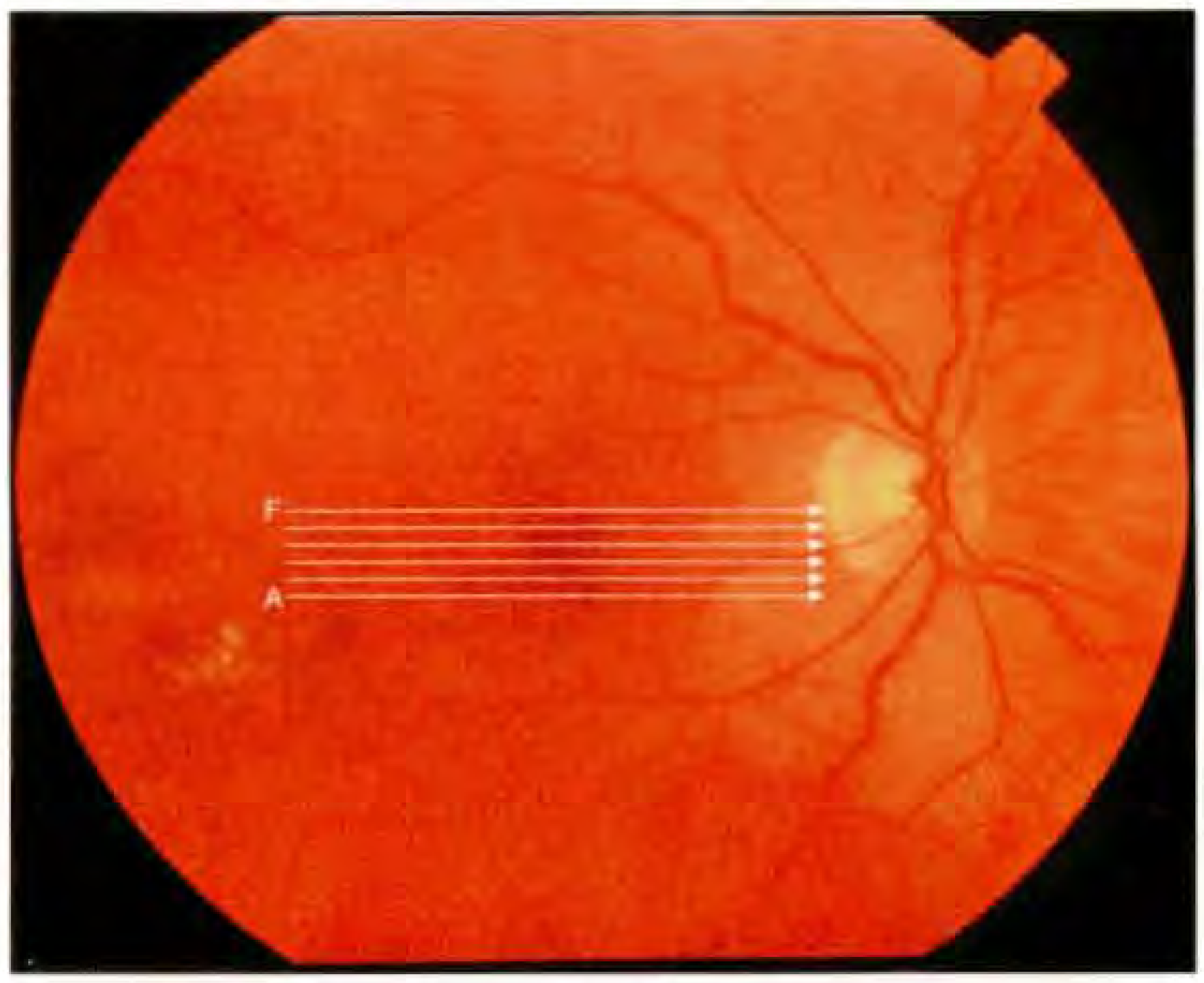

A

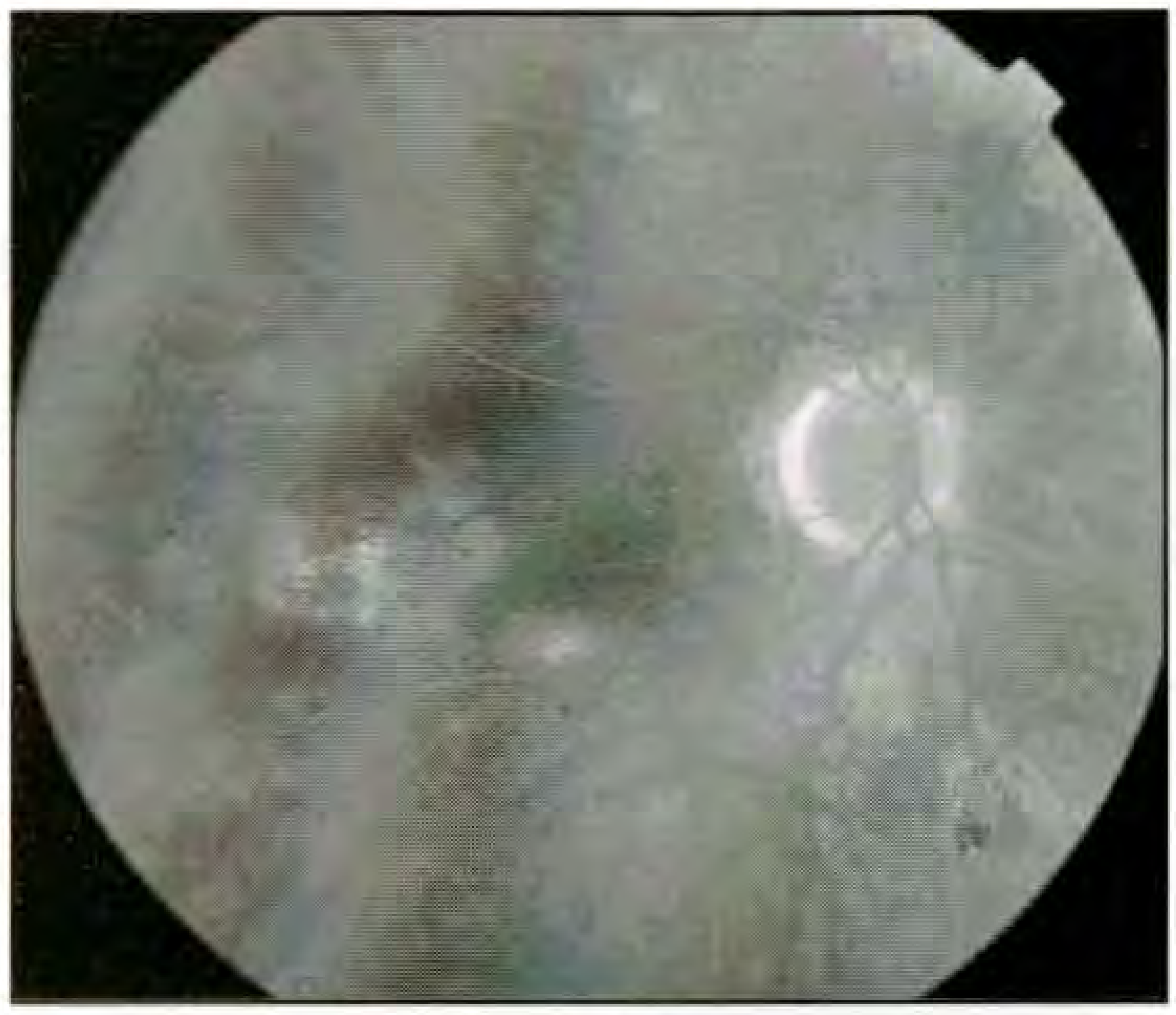

B

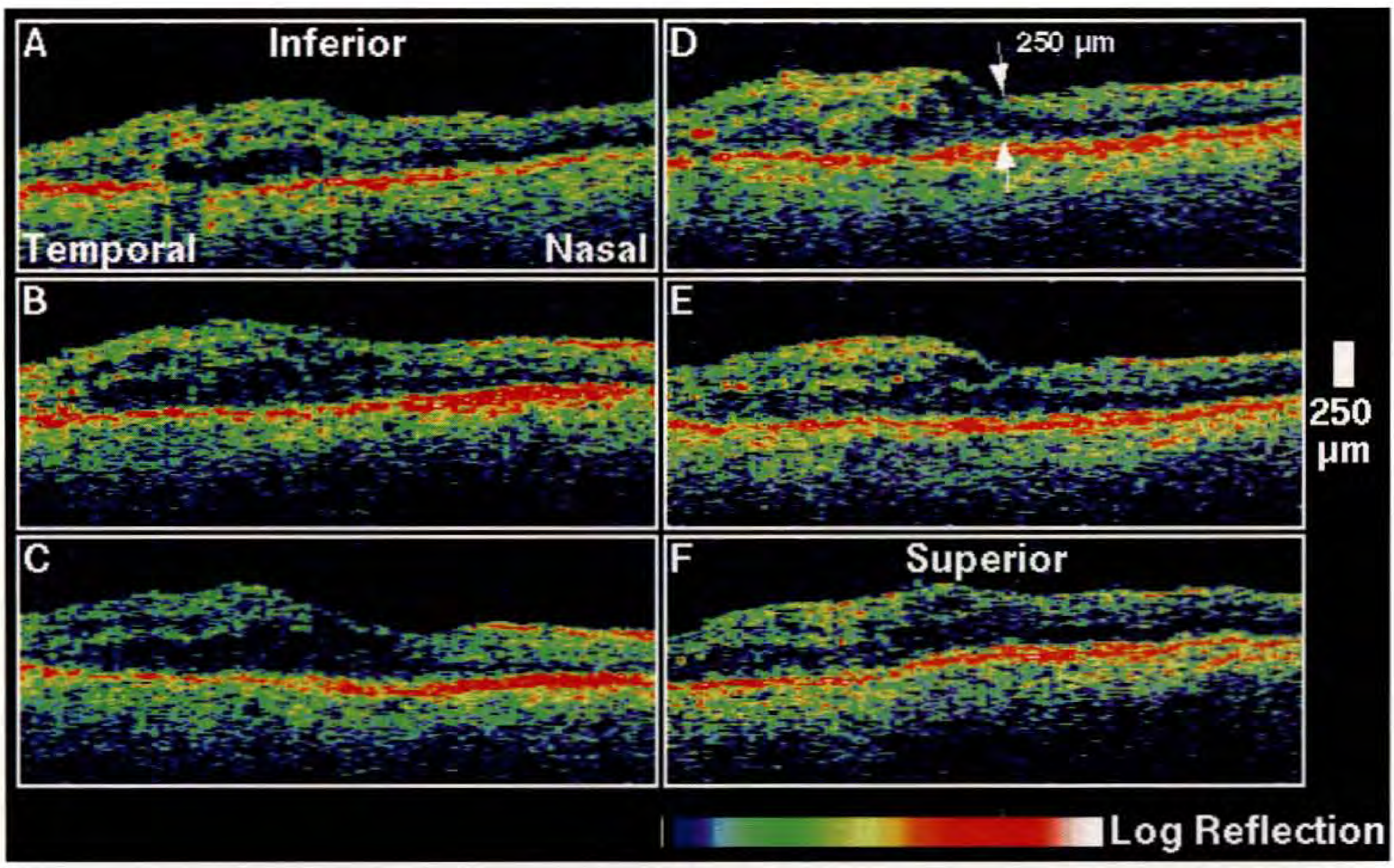

C

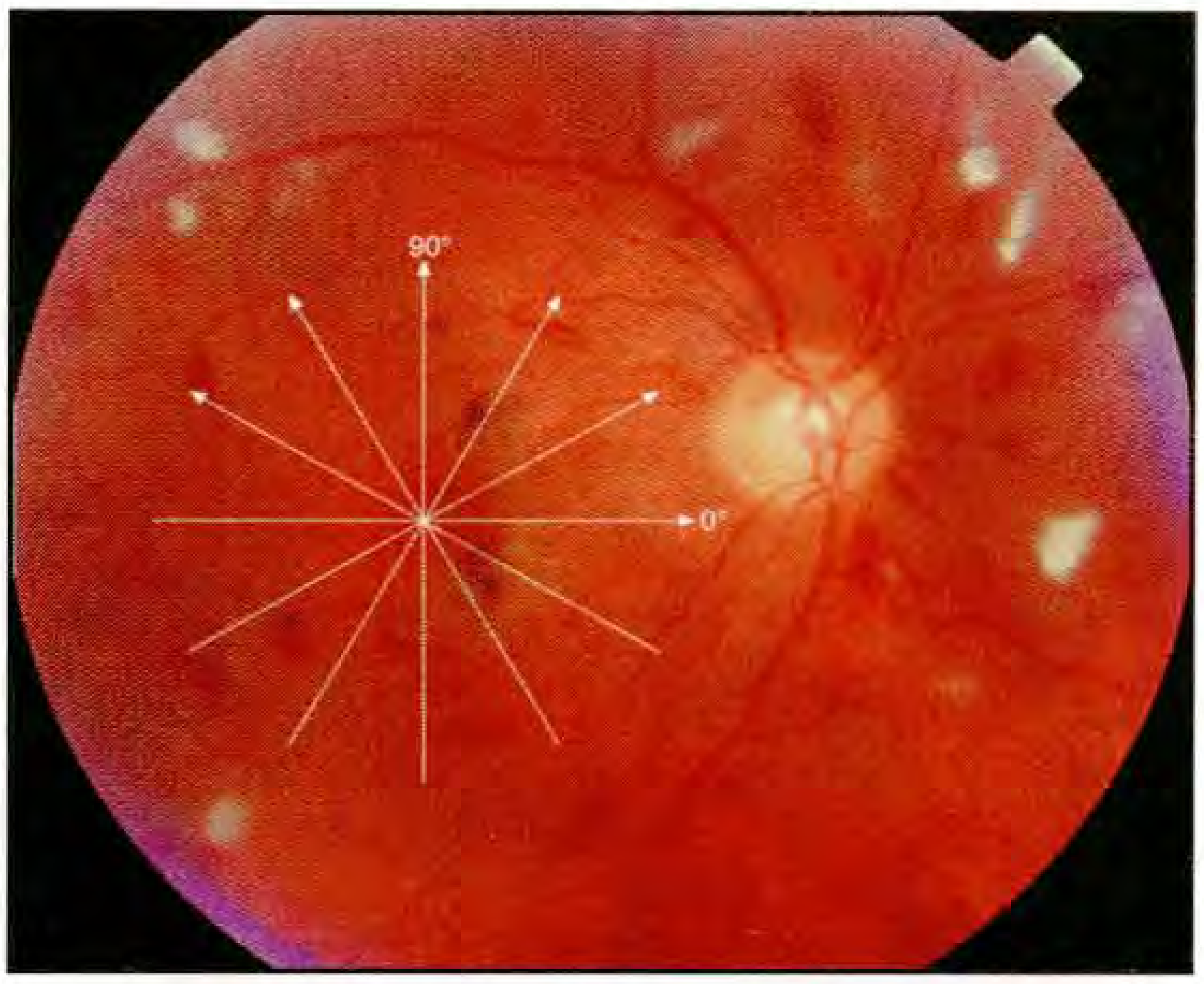

A

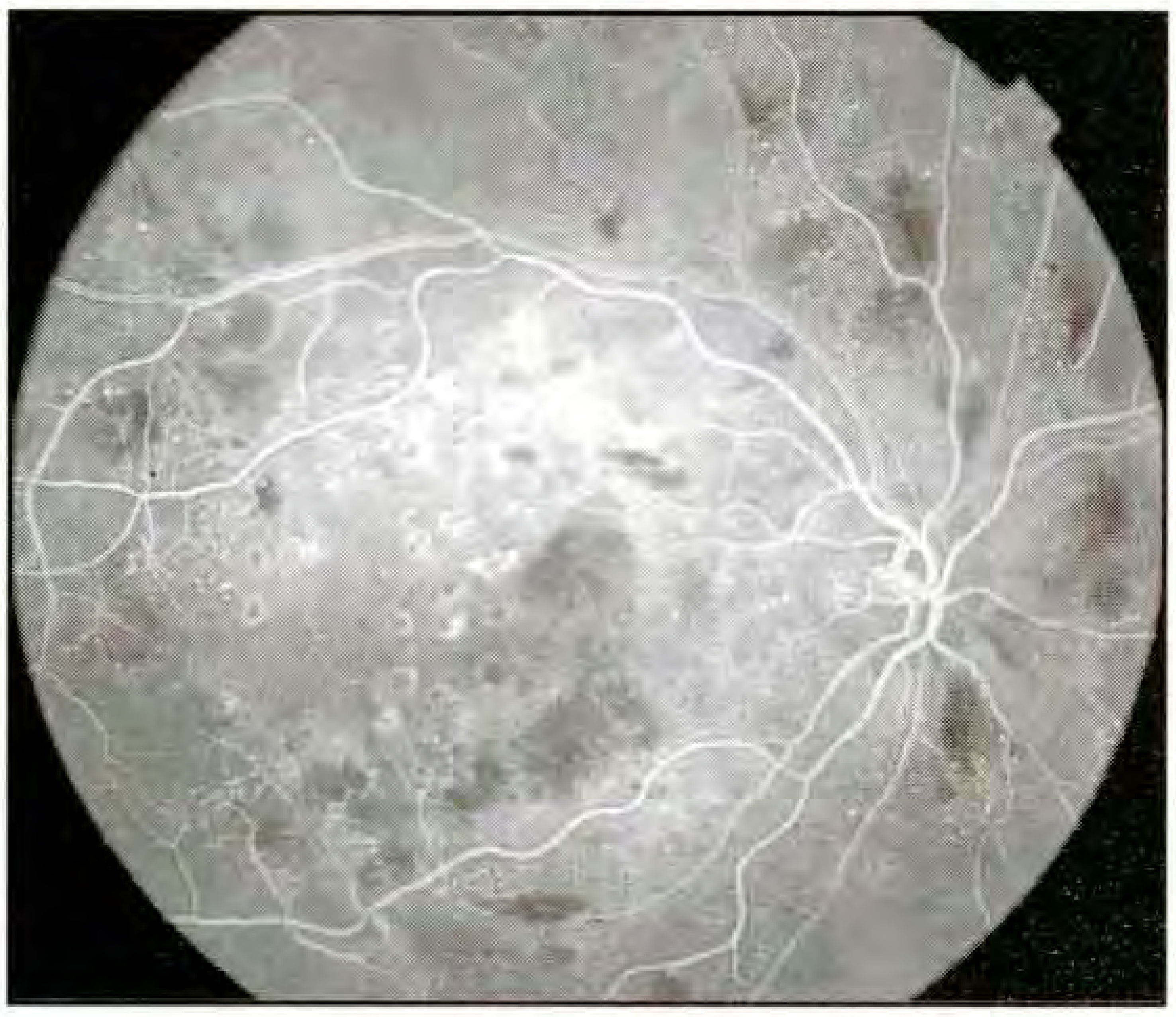

B

Case 6-11. Non-Proliferative and Proliferative Diabetic Retinopathy

Clinical Summary

This patient was a 73-year-old man with diabetic retinopathy who had previously received multiple laser treatments in both eyes. Examination of the right eye (A), with a visual acuity of 20/60, revealed a normal optic disc, multiple cotton wool spots, and moderate to severe non-proliferative diabetic retinopathy. No significant macular thickening was observed. Some macular capillary non-perfusion was identified on fluorescein angiography (B), which also demonstrated an absence of late leakage.

Optical Coherence Tomography

Radial OCT sections (C) through the macula showed no foveal edema and the measured central macular thickness was 150 µm. The reflection from the retinal pigment epithelium and choriocapillaris appeared slightly disrupted in areas of previous focal laser photocoagulation treatment.

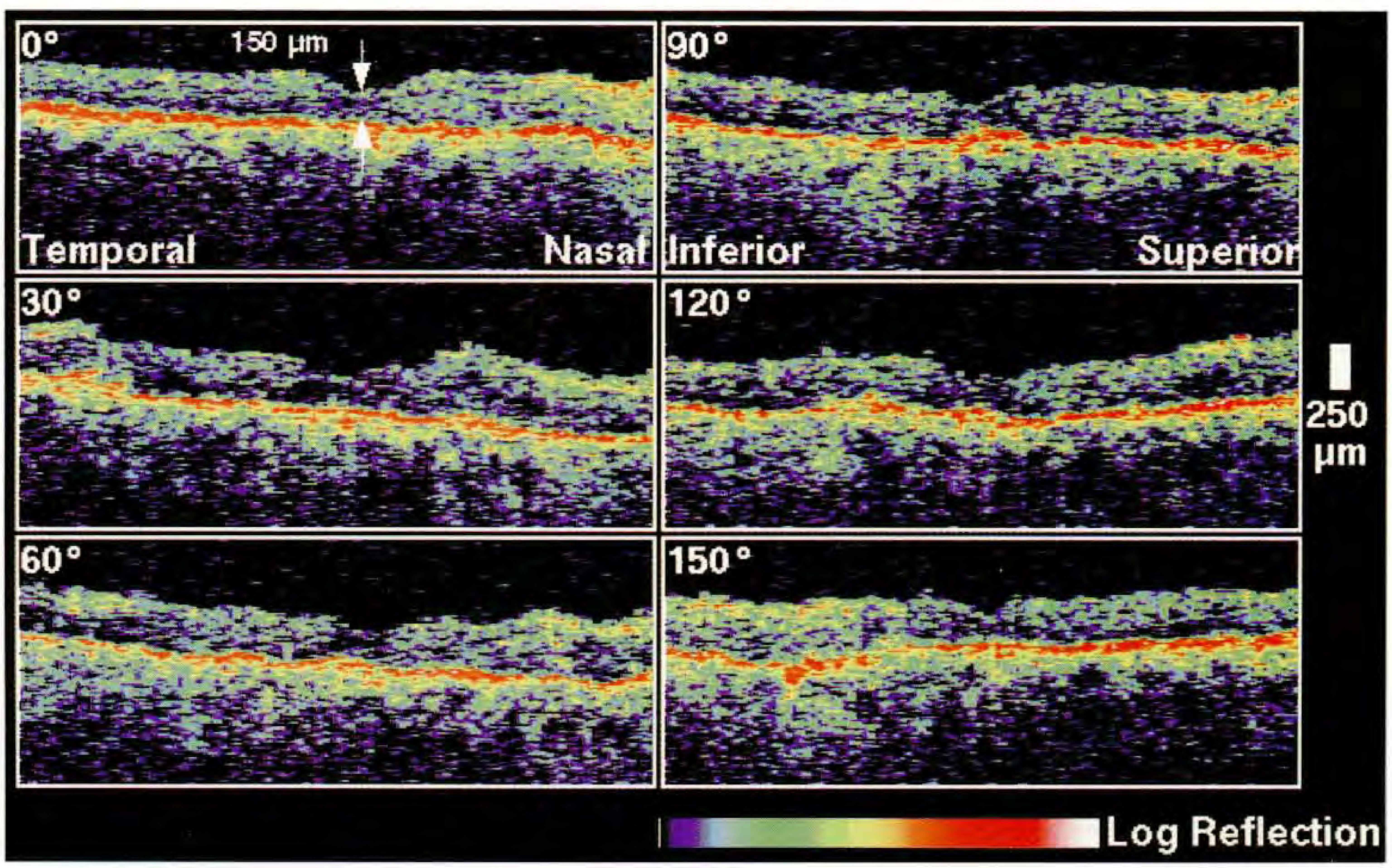

C

Case 6-11 continued

Clinical summary

The patient had a history of a moderate vitreous hemorrhage in his left eye consistent with a diagnosis of proliferative diabetic retinopathy in this eye. The visual acuity in this eye was counting fingers at five feet. Diffuse macular edema was noted on slit-lamp examination (D), which also showed retinal hemorrhage involving the macula and cotton wool spots close to the superior and inferior arcades. Fluorescein angiography (E) showed some macular capillary dropout and diffuse hyperfluorescence surrounding the optic disc and inferior arcade.

Optical Coherence Tomography

A series of radial OCT tomograms (F) was acquired through the fovea. The macula appeared diffusely thickened with large intraretinal areas of no optical backscattering corresponding to macular cysts. The retinal thickness measured directly in the fovea was 510 μm.

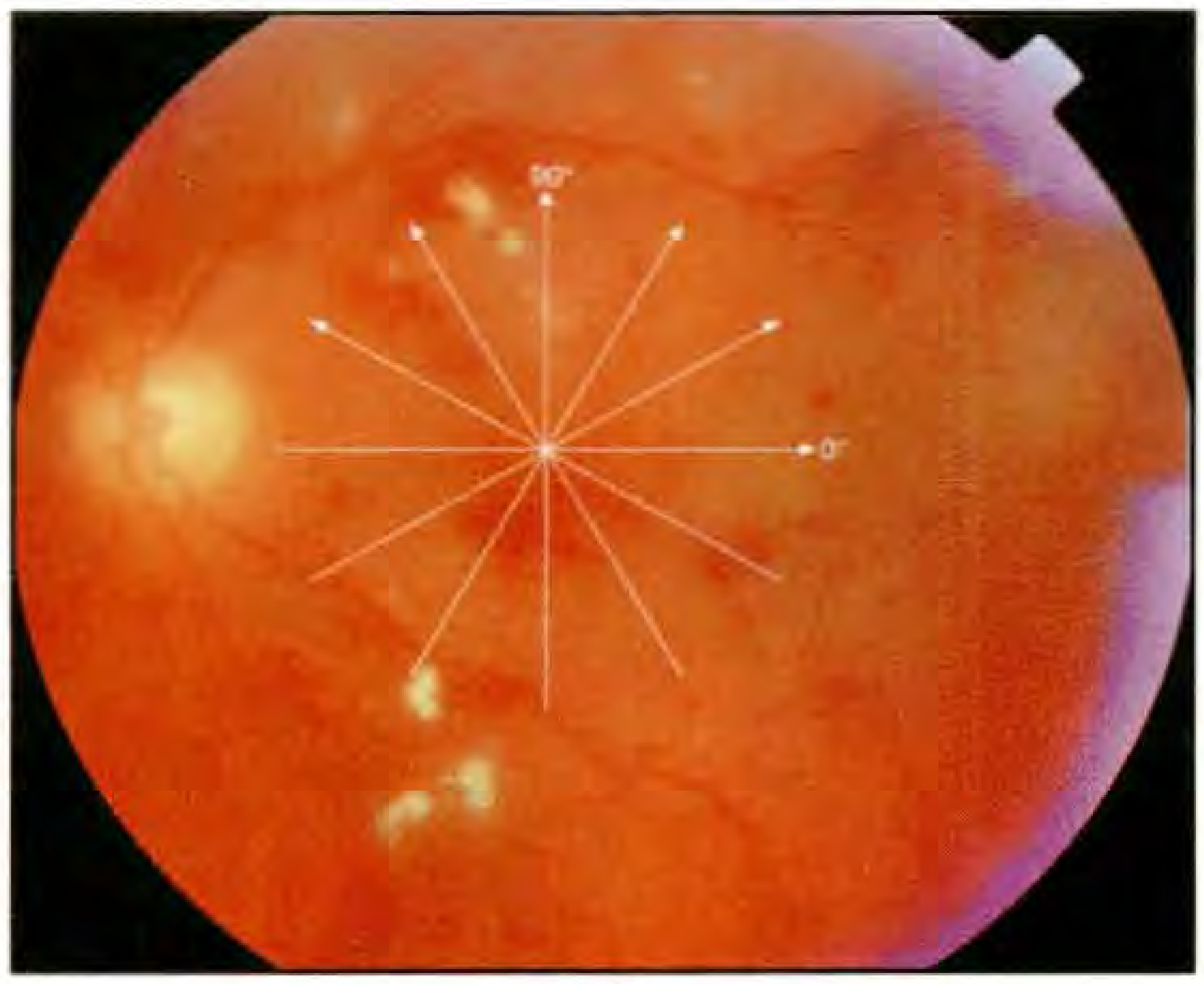

D

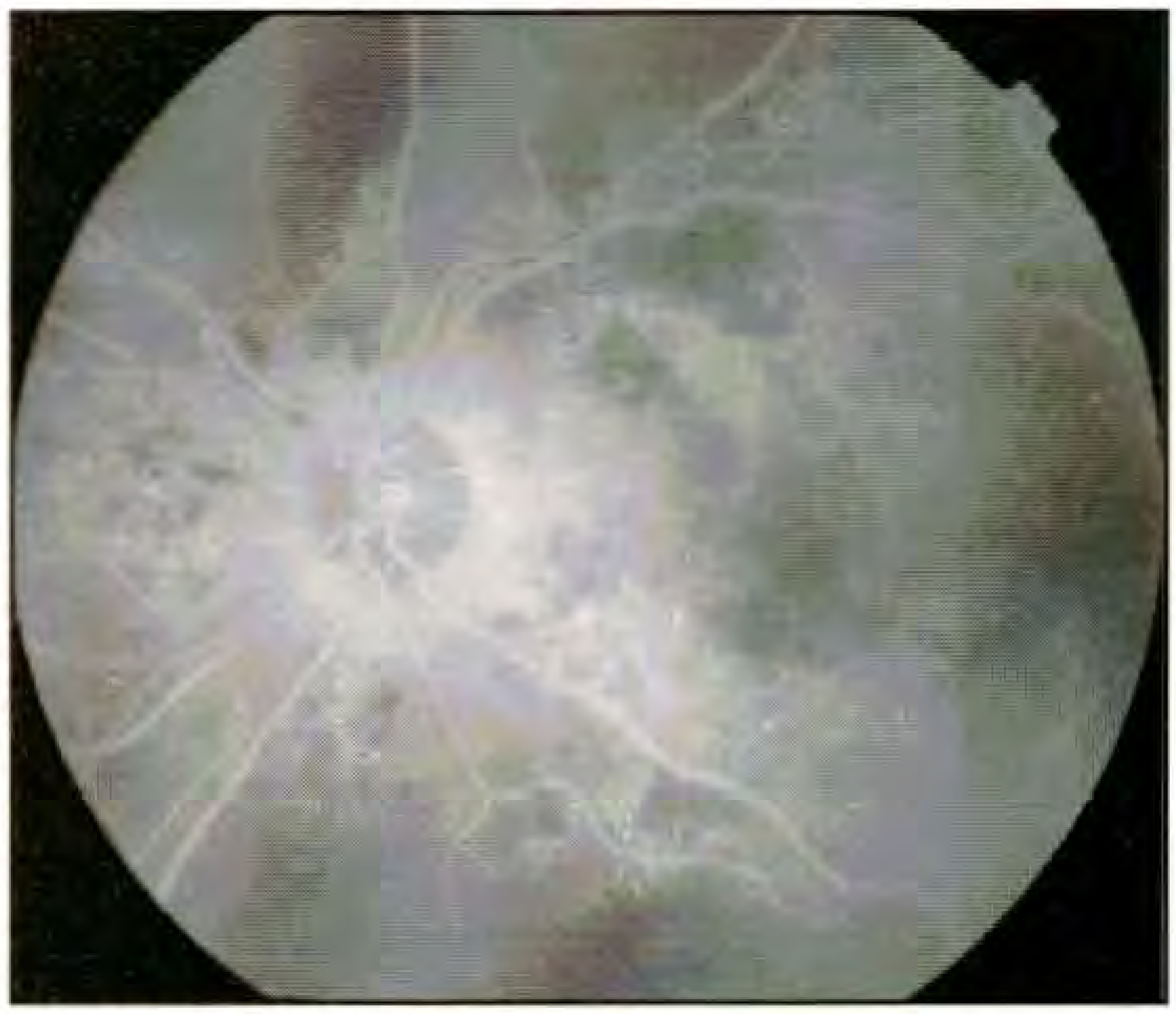

E

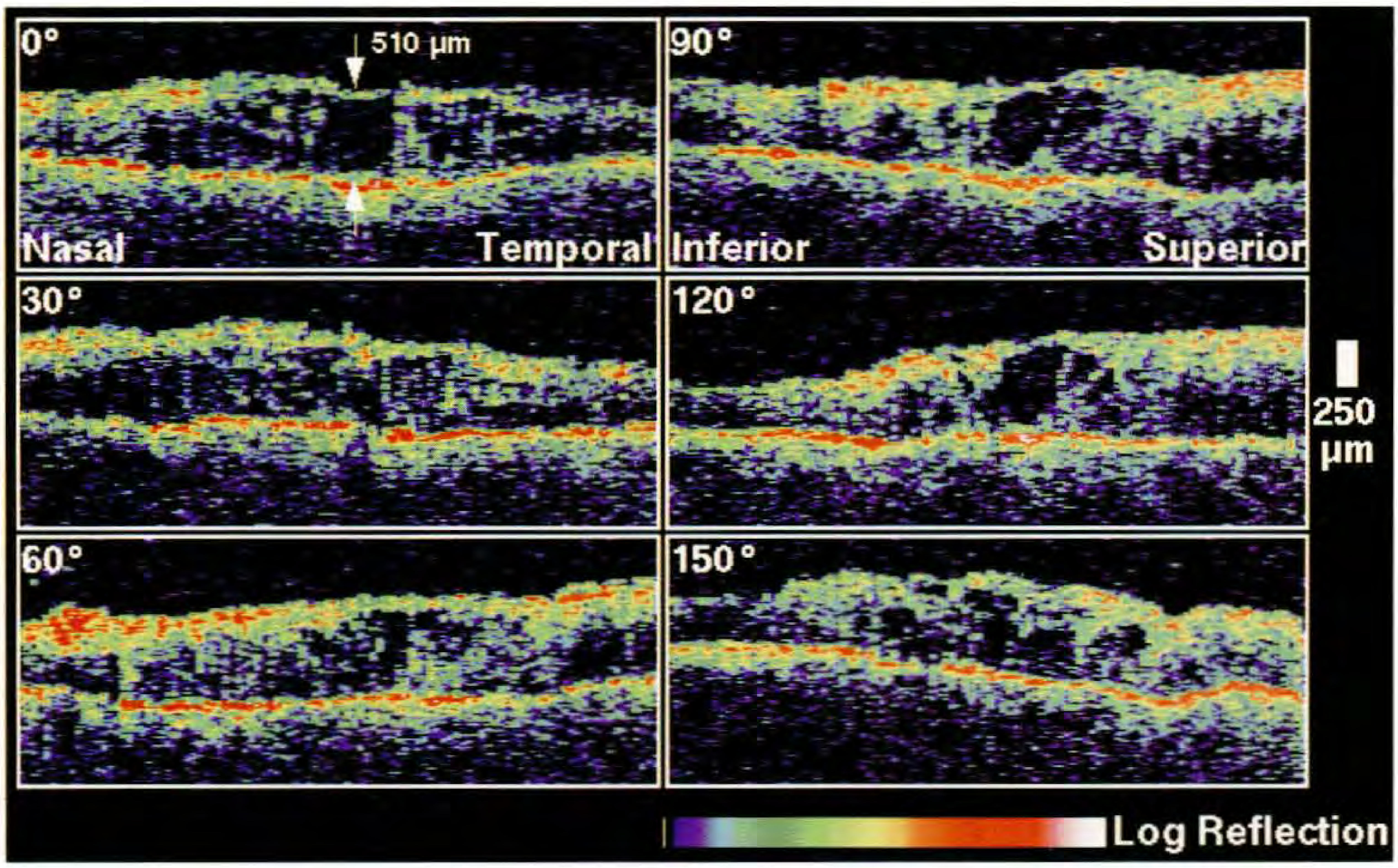

F

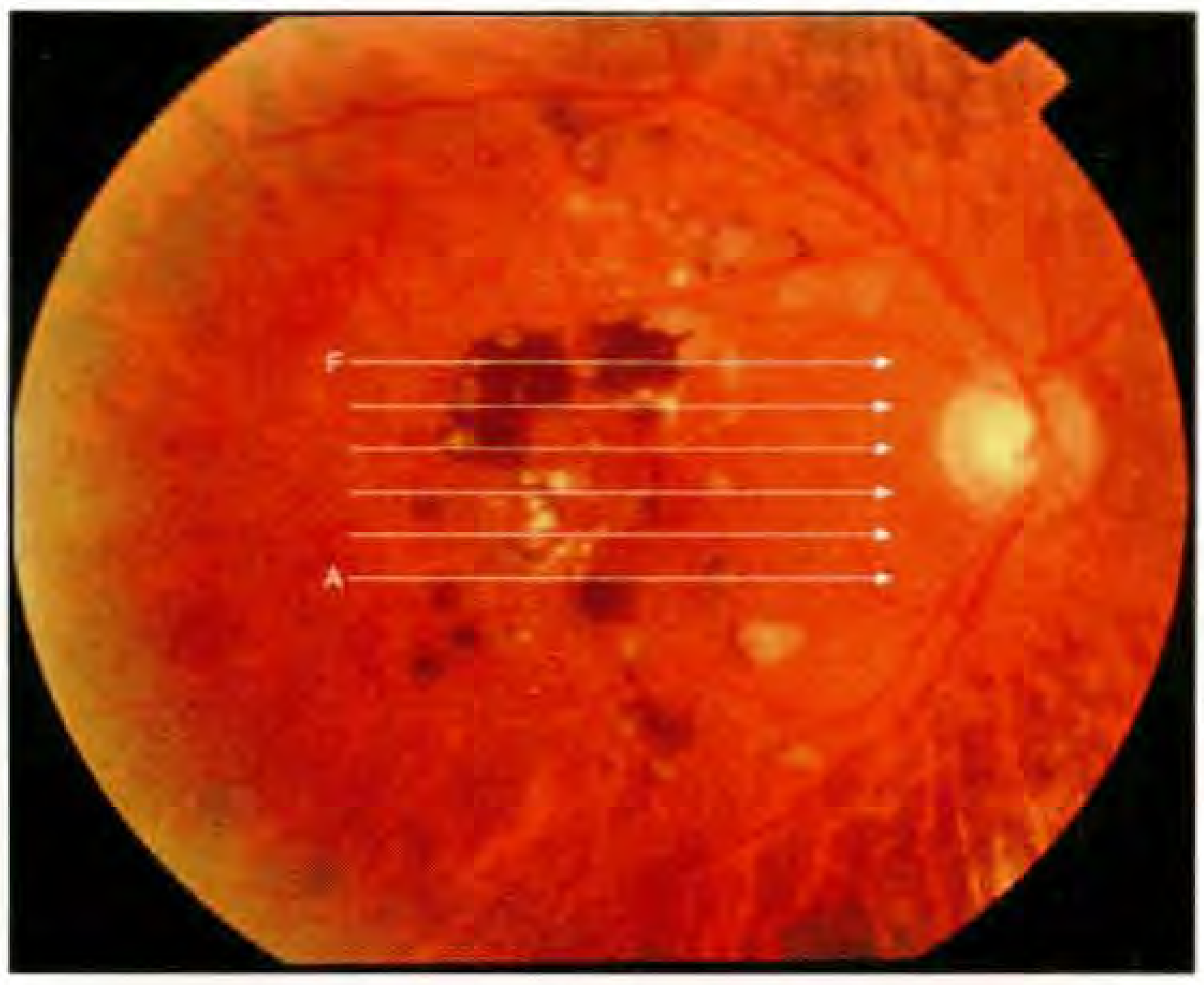

A

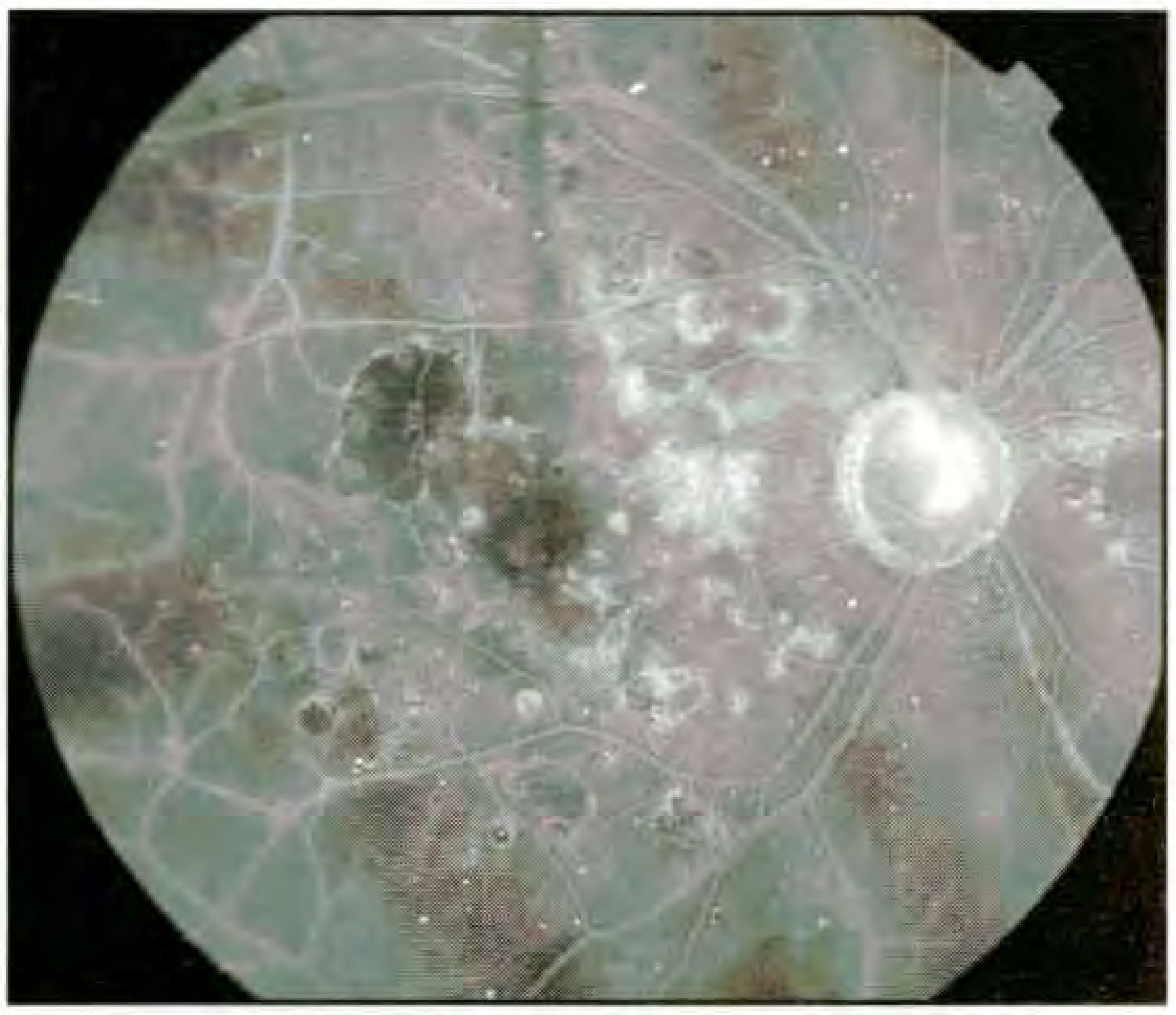

B

Case 6-12. Proliferative Diabetic Retinopathy

Clinical Summary

A 62-year-old man with a history of proliferative diabetic retinopathy and panretinal laser photocoagulation in both eyes was examined. The right eye had a visual acuity of 20/60 with diffuse clinically significant macular edema and panretinal laser scars (A). Fluorescein angiography (B) revealed hypofluorescence consistent with retinal hemorrhage, a slightly enlarged foveal avascular zone, and minimal late leakage.

Optical Coherence Tomography

Sequential horizontal OCT scans (C) delineated diffuse retinal thickening and reduced optical reflectivity consistent with intraretinal fluid accumulation. The foveal thickness was 320 µm. Retinal exudate was identified by small focal areas of high backscattering. The retina appeared atrophic superotemporally (scan F) consistent with the panretinal photocoagulation. The minimum retinal thickness in this region was 140 µm.

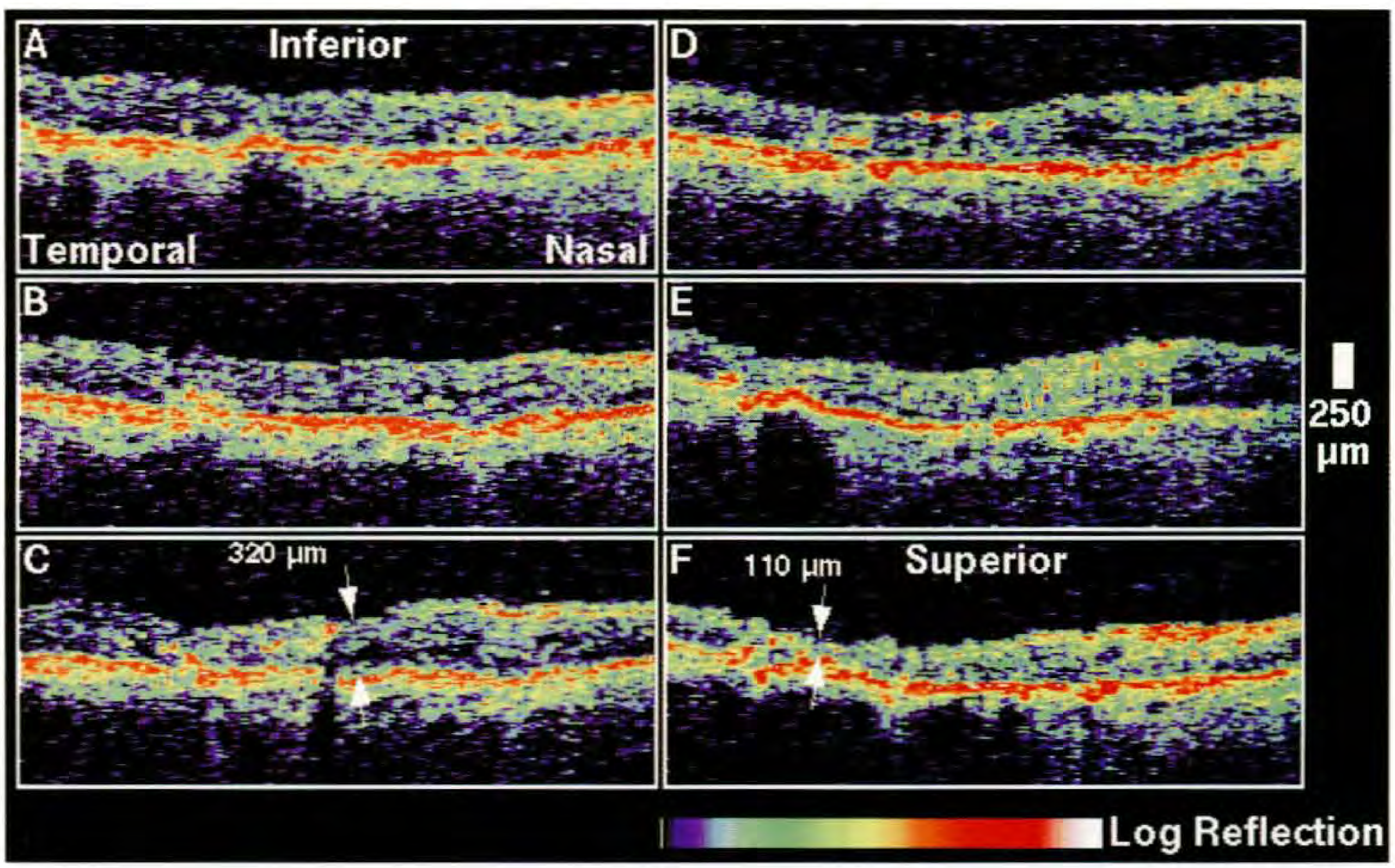

C

Case 6-12 continued

Clinical Summary

The left eye had a visual acuity of 20/80 and also displayed diffuse macular edema and panretinal laser photocoagulation scars (D). Minimal late leakage of fluorescein dye and an enlarged foveal avascular zone were observed on angiography (E).

Optical Coherence Tomography

OCT examination (F) confirmed the diffuse macular thickening and showed a broad depression in the central macula consistent with macular non-perfusion and ischemia (scan D). Intraretinal exudate was also noted. The foveal thickness was measured to be mildly increased at 190 μm.

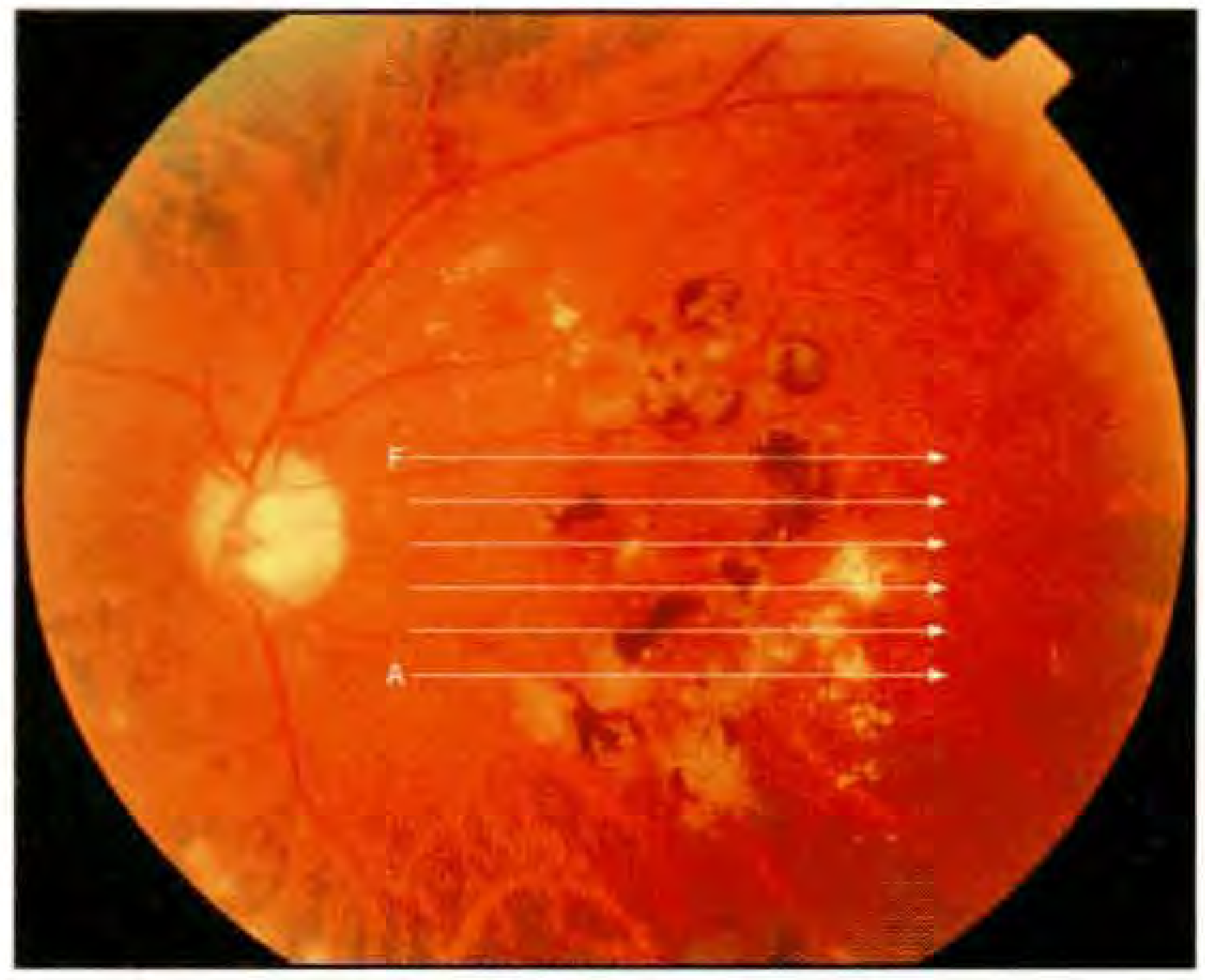

D

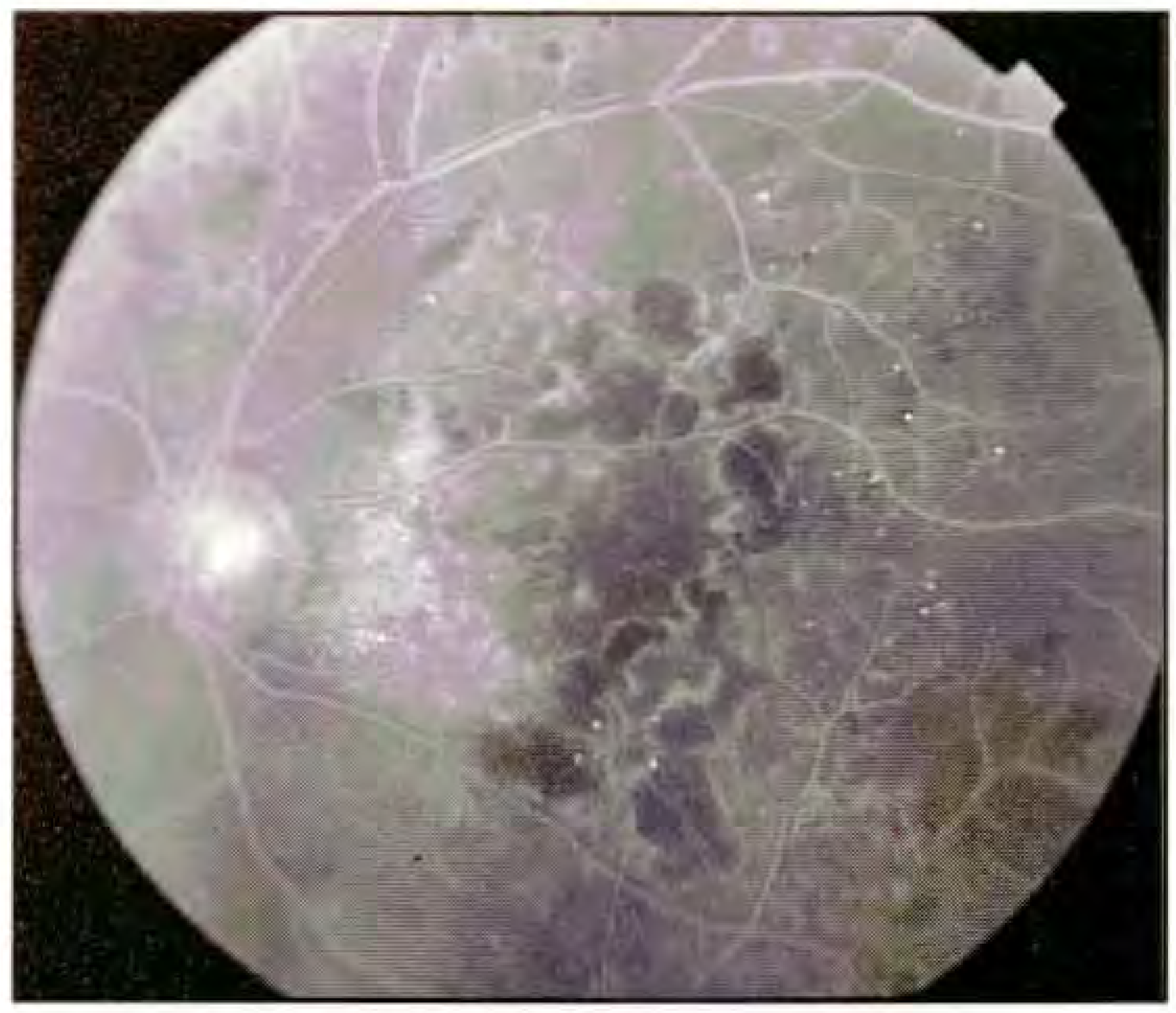
E

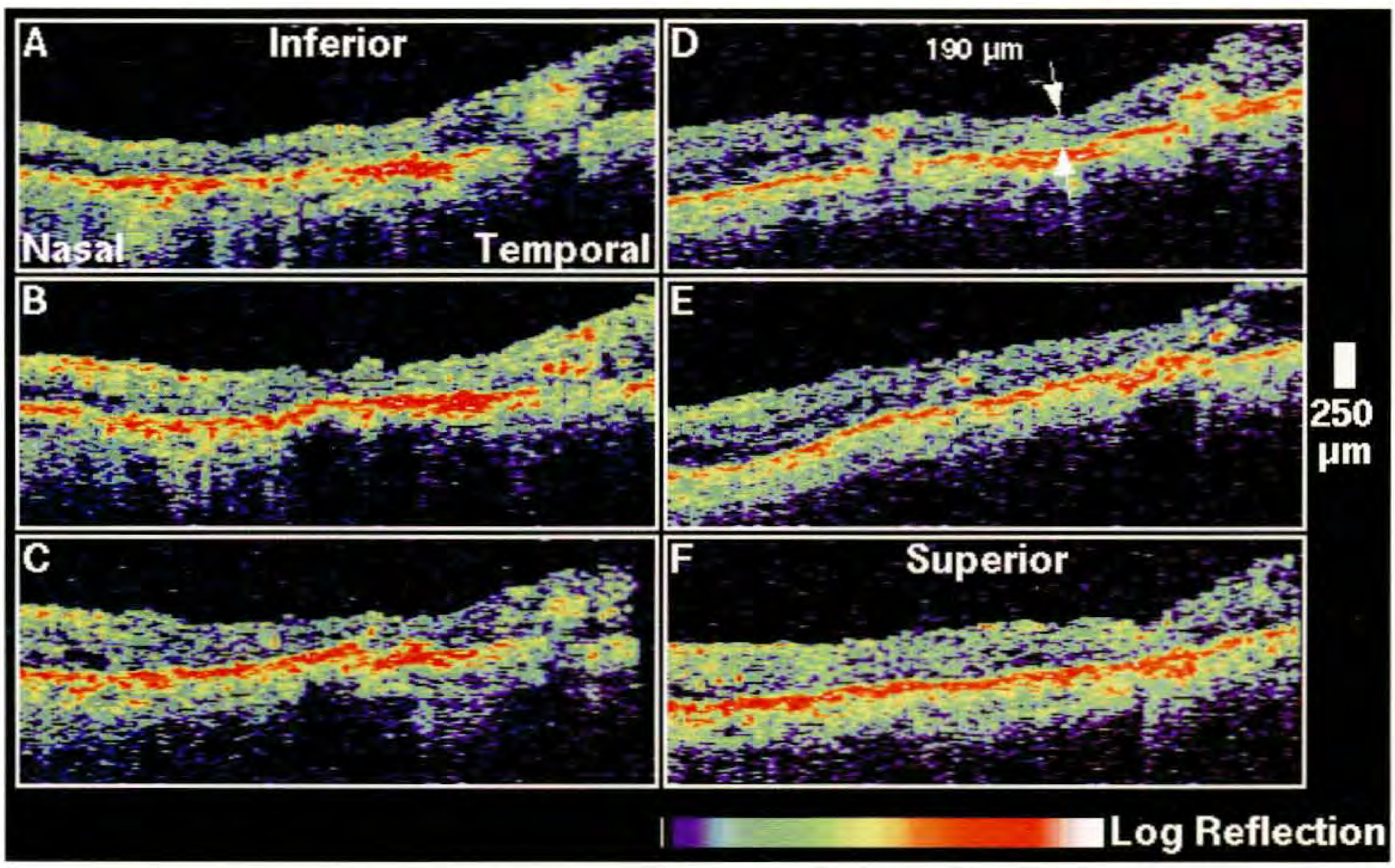

F

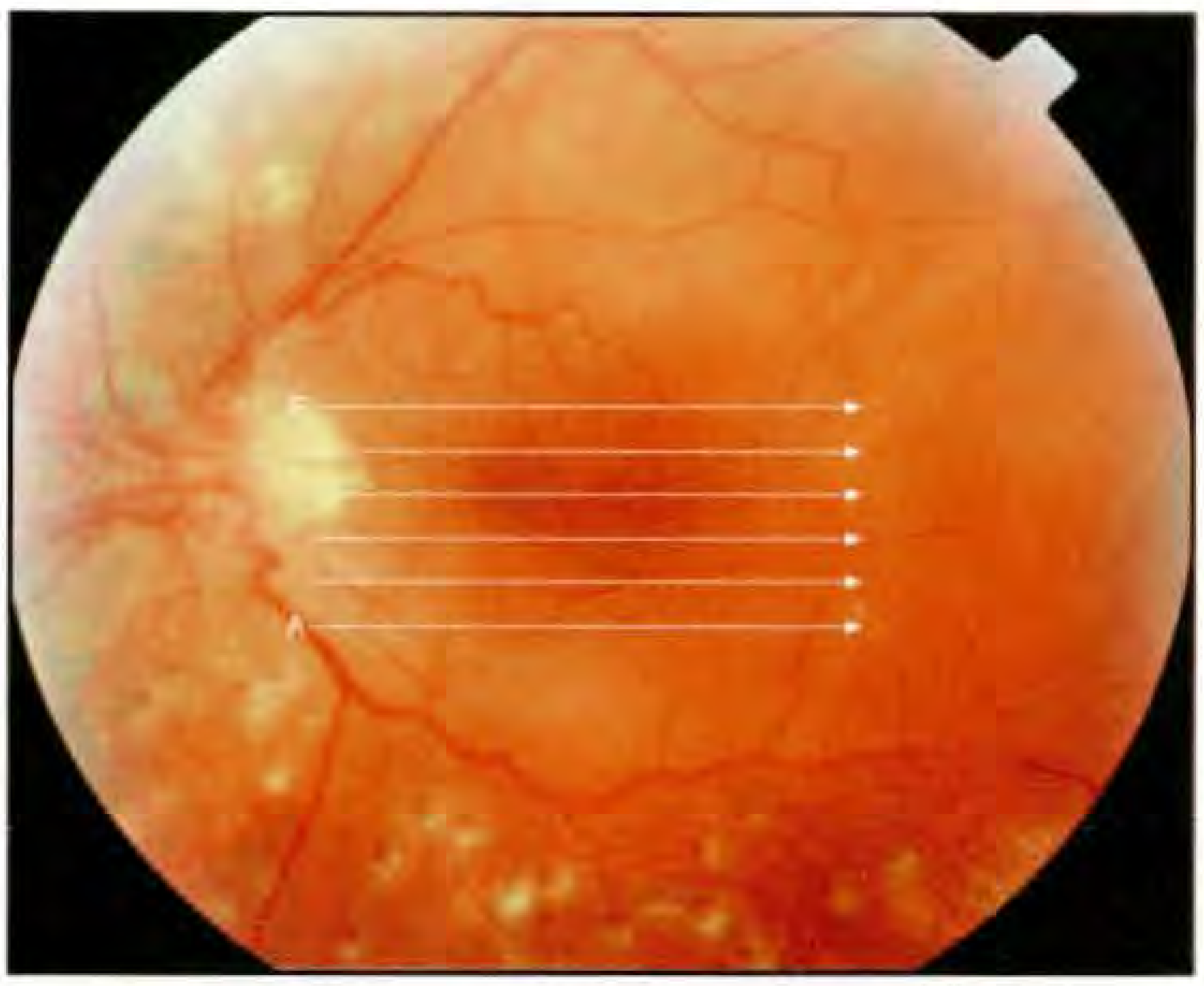

A

Case 6-13. Proliferative Diabetic Retinopathy with Preretinal Fibrosis

Clinical Summary

A 45-year-old woman with proliferative diabetic retinopathy and a visual acuity of 20/50 in her left eye was examined. Dilated indirect ophthalmoscopy (A,C) revealed a large frond of neovascularization extending superonasally and inferonasally from the optic disc which was associated with preretinal fibrosis and mild hemorrhage. The posterior hyaloid was partially detached and appeared to exhibit traction in the nasal macula with associated macular edema.

Optical Coherence Tomography

Horizontal OCT scans (B; white lines on A) obtained through the macula showed increased retinal thickening nasally consistent with traction of the posterior hyaloid membrane on the retina. Scan D, taken through fixation in this eye, demonstrated loss of the normal foveal contour. A sequence of vertical tomograms (D; white lines on C) was also acquired nasal to the optic disc and illustrated the three-dimensional structure of the preretinal membrane. The membrane was thinner nasally, and appeared to be attached to the retina at several focal points of traction suggesting horizontally oriented striae.

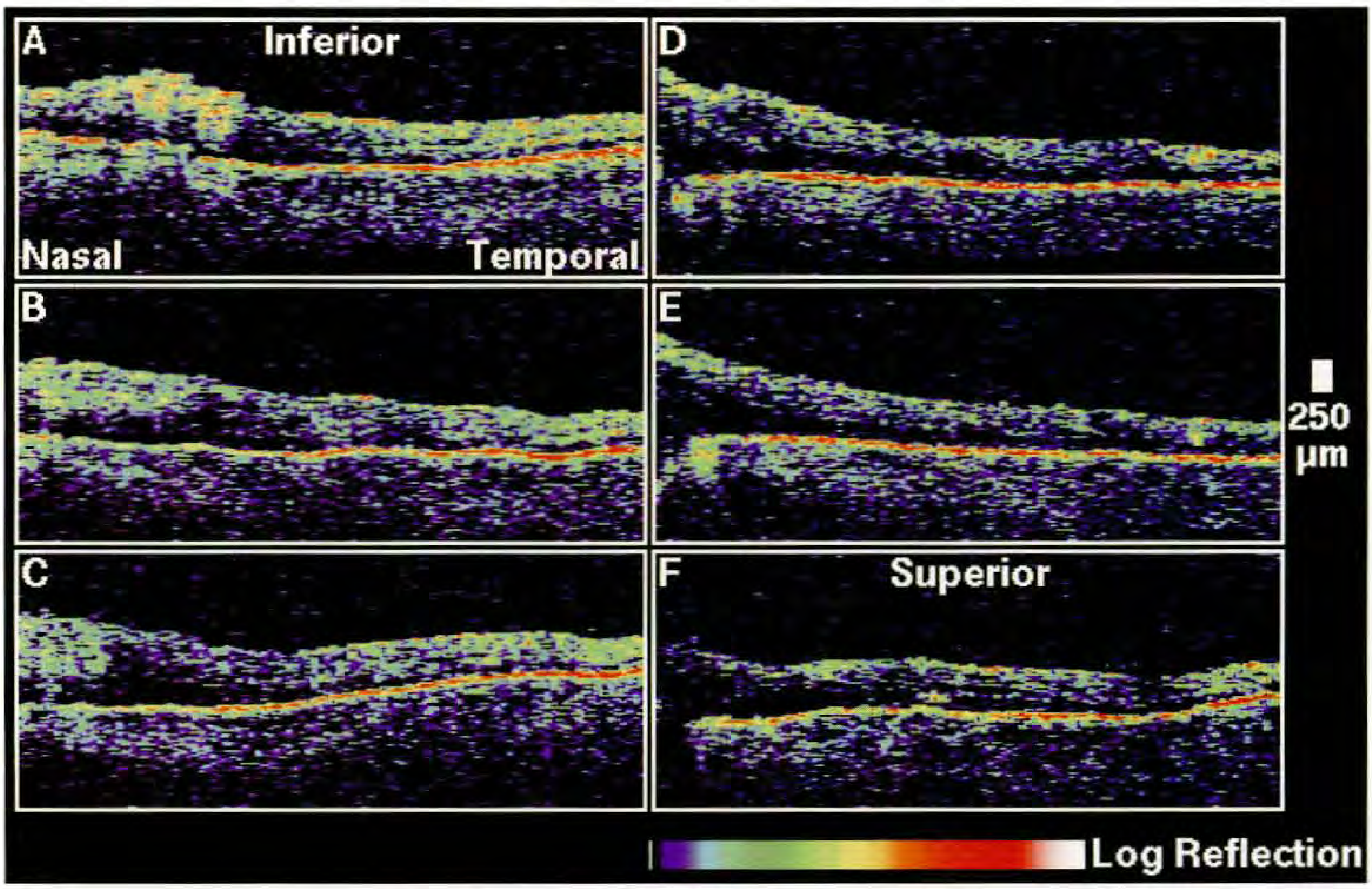

B

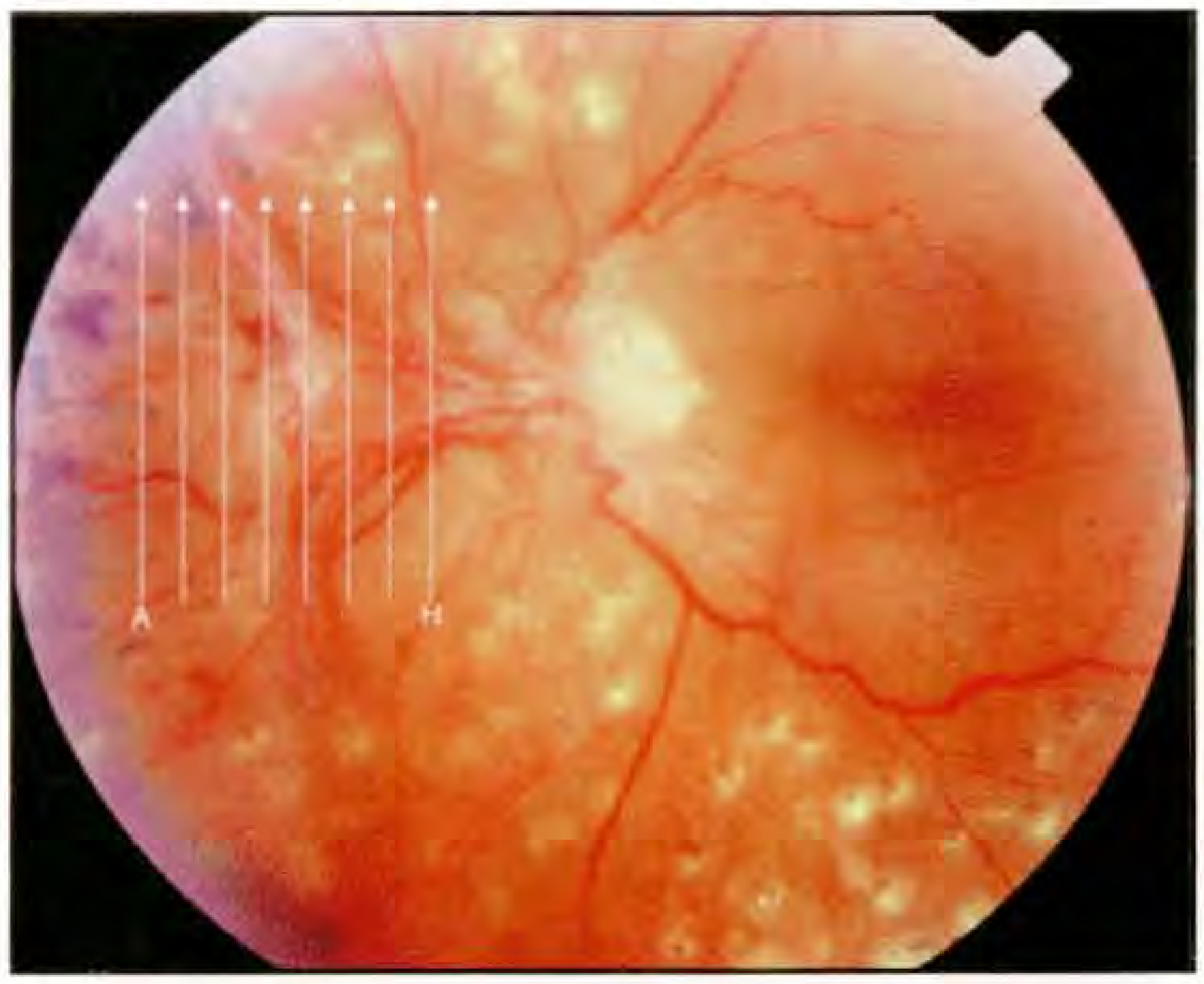

C

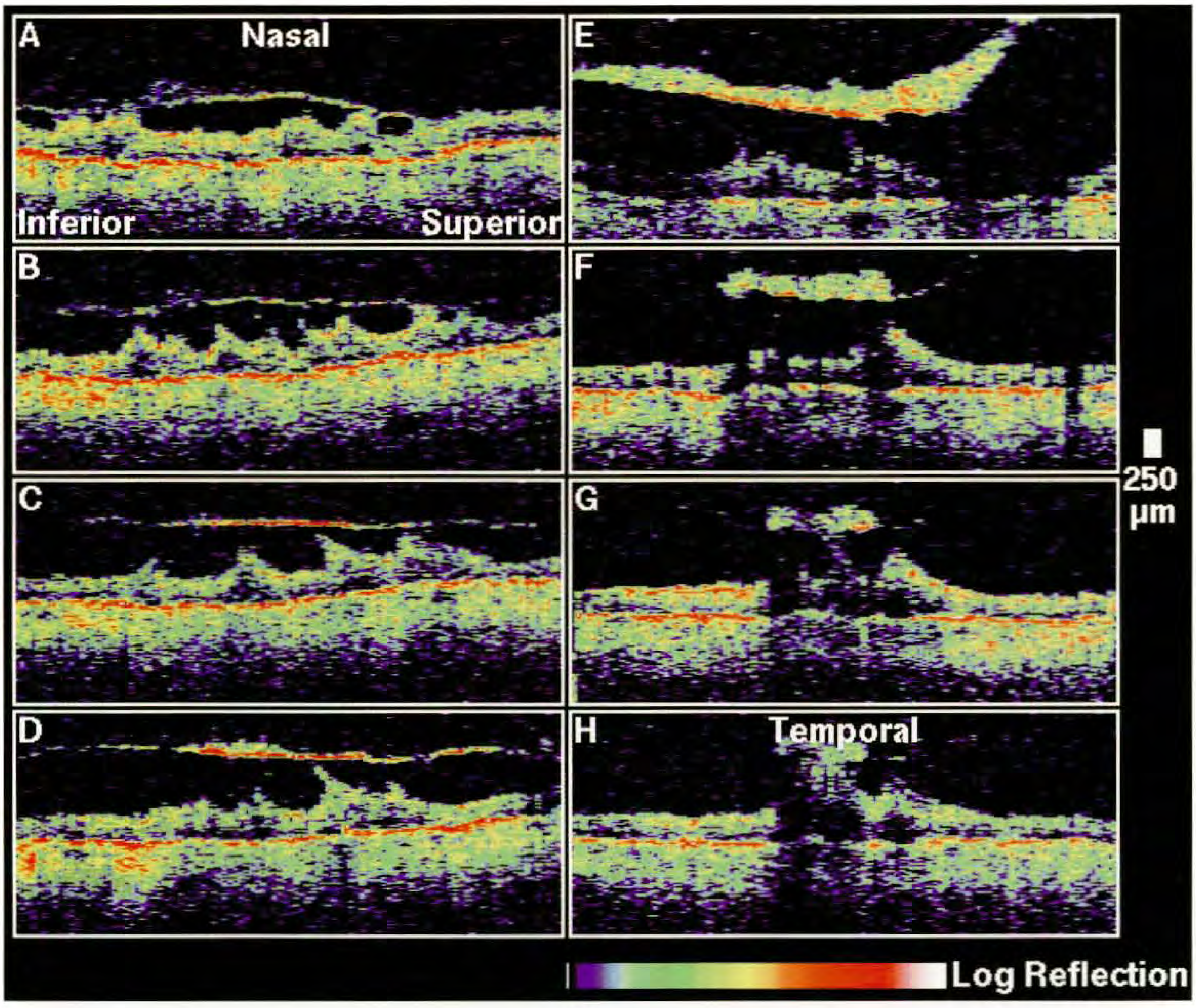
A
Nasal
Inferior
Superior
B
C
D
E
F
G
H
Temporal
250
µm
Log Reflection

D

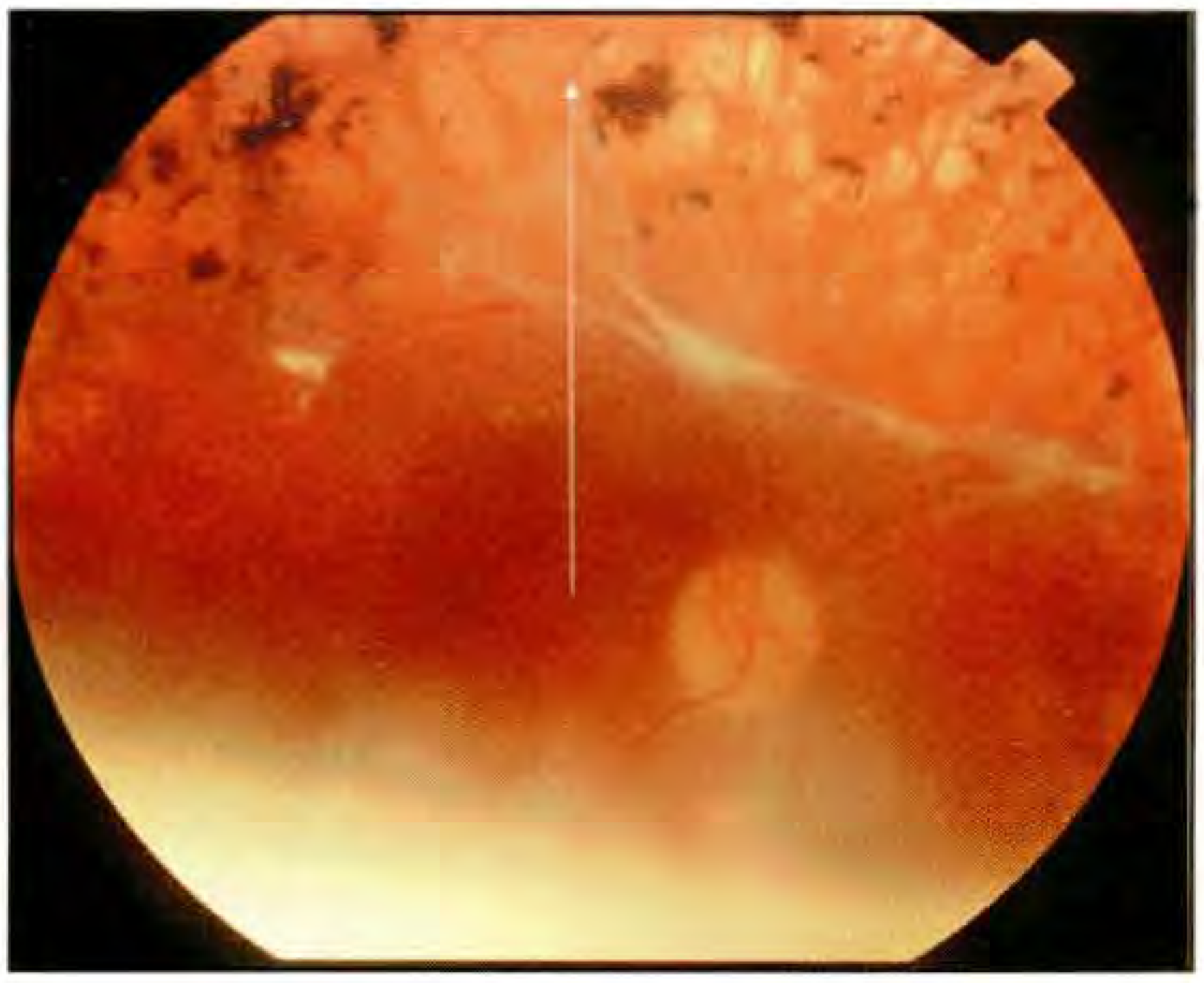

A

Case 6-14. Proliferative Diabetic Retinopathy with Retinal Traction

Clinical Summary

A 37-year-old man with proliferative diabetic retinopathy in both eyes was referred for evaluation of possible traction macular detachments. Examination of the right eye revealed a visual acuity of 20/30 and preretinal fibrosis extending along the superotemporal vascular arcade (A). A localized traction detachment was observed superior to the optic disc and encroaching into the superonasal macula.

Optical Coherence Tomography

An OCT tomogram (B) obtained across the superotemporal arcade showed severe, focal retinal elevation. A region of preretinal fibrosis (arrow) was observed anterior the retina consistent with a traction retinal detachment. The reflections from the choroid were absent below the detachment due to attenuation of the probe beam passing through the overlying lesion. Several scattered vitreous opacities were noted.

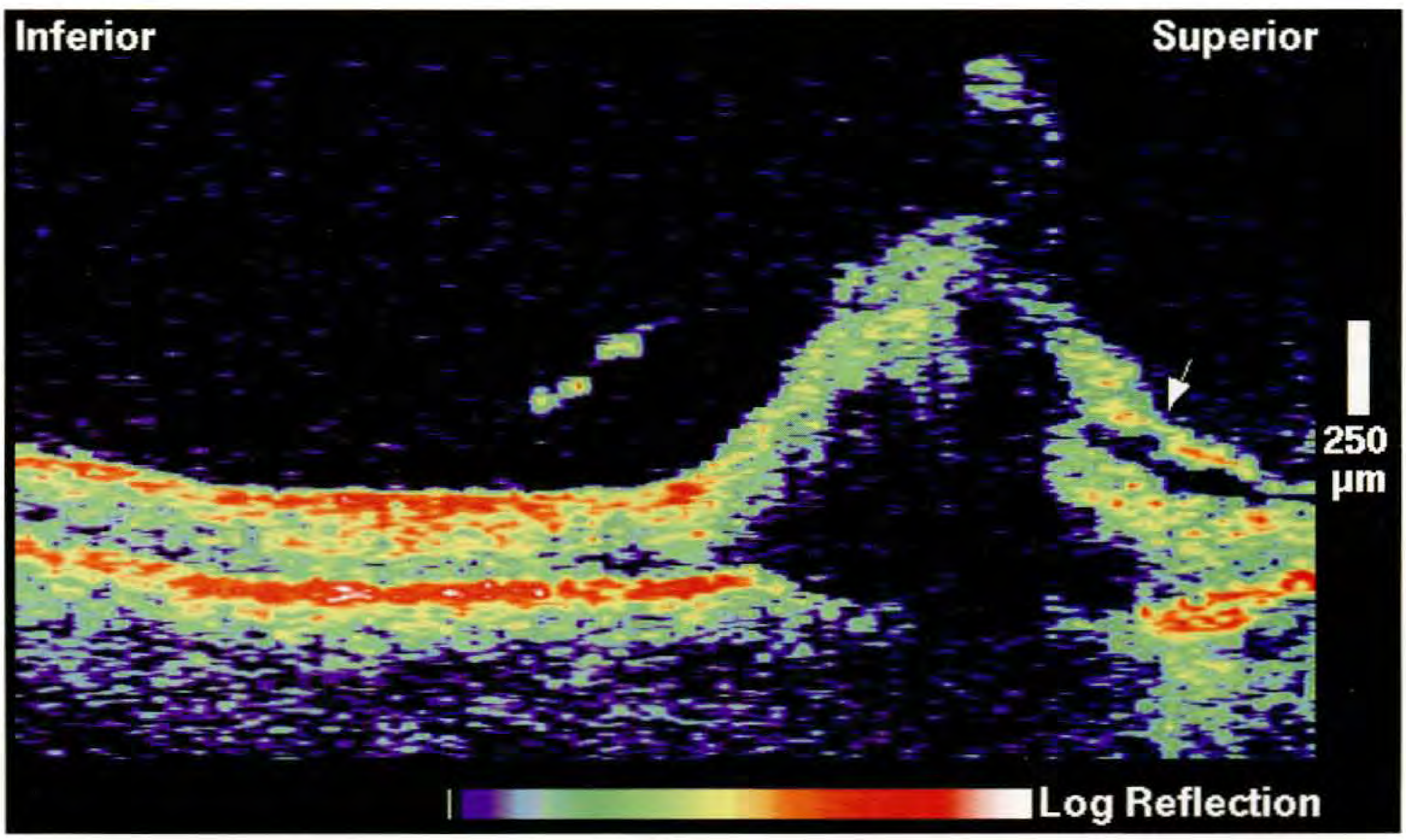

B

Case 6-14 continued

Clinical Summary

The left eye had a visual acuity of 20/60 and was remarkable for extraretinal fibrous proliferation along both the superior and inferior vascular arcades (C). Retinal striae were observed radiating from the inferotemporal arcade to the macula center.

Optical Coherence Tomography

An image (D; white line on C) through fixation showed a large central macular cyst with an associated increase in foveal retinal thickness. A highly reflective preretinal membrane was noted along the superotemporal arcade and appeared to be adherent to the retinal surface (E; black line on C). The retinal thickness in this region was diffusely increased.

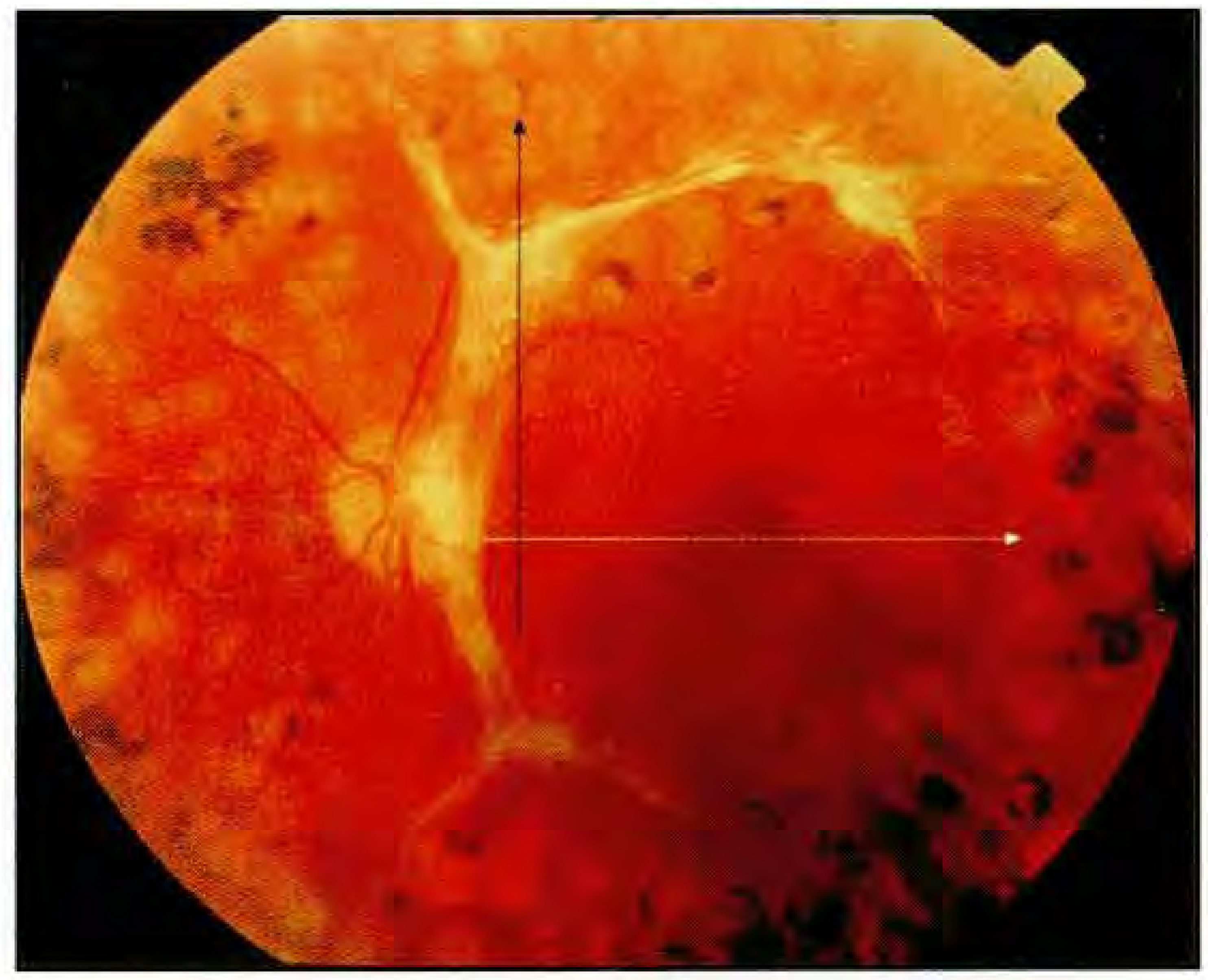

C

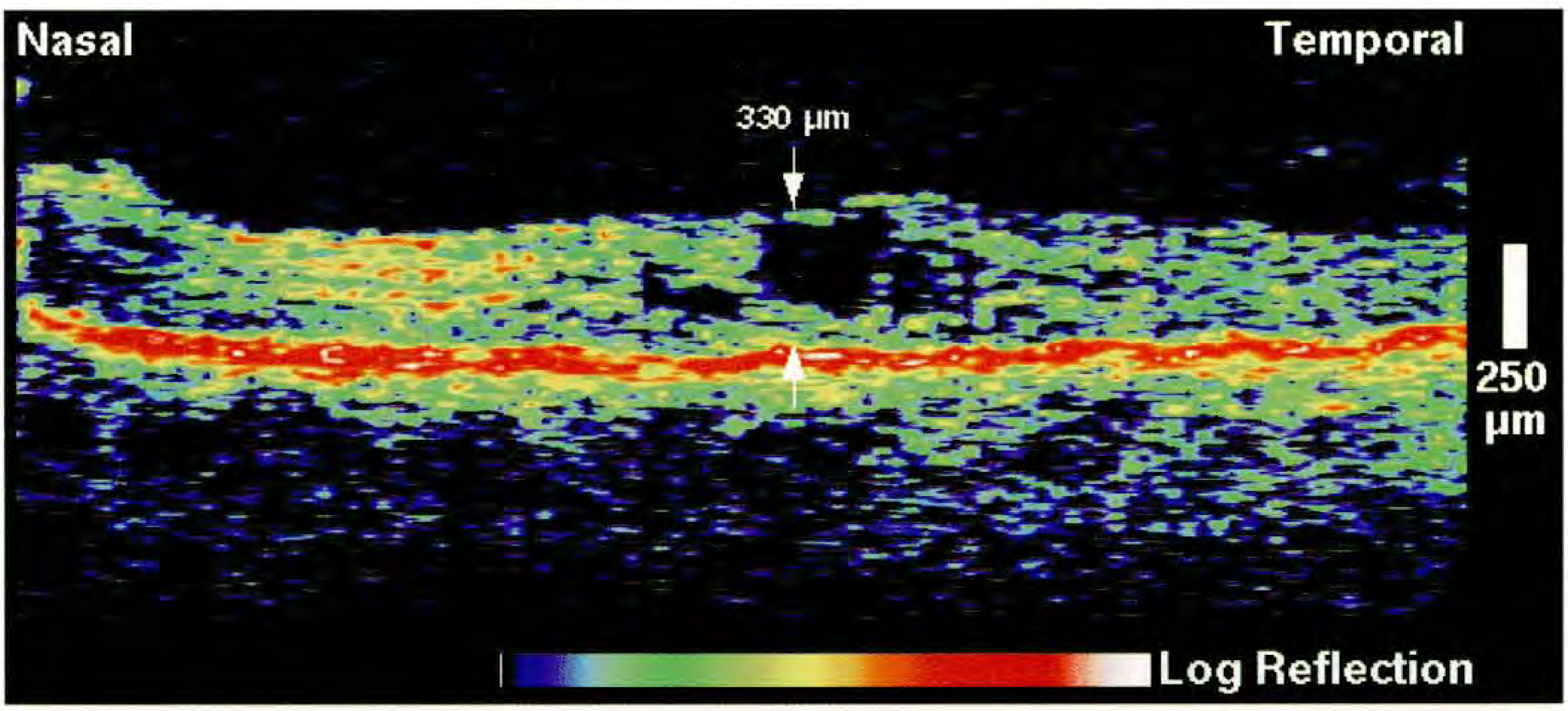

D

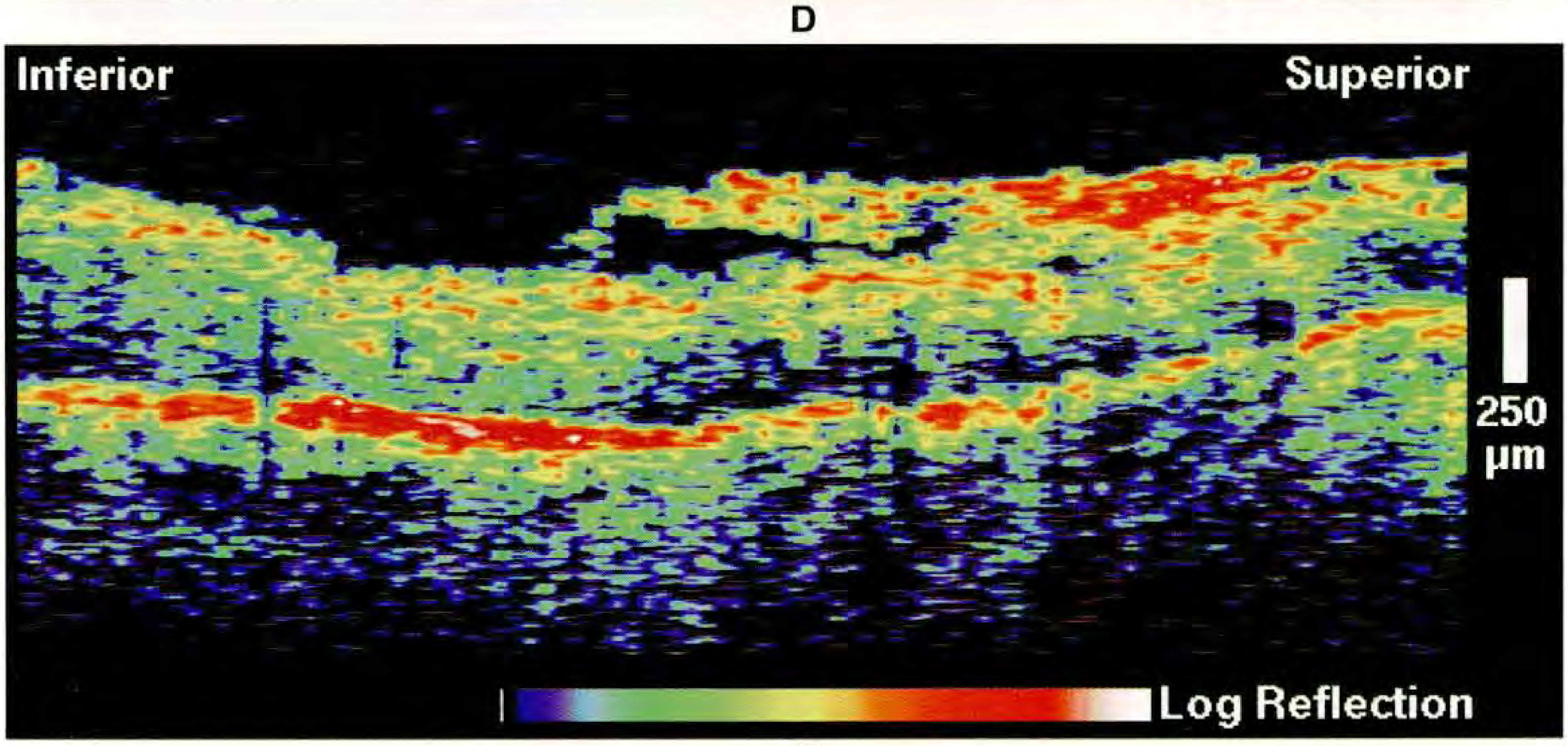

E

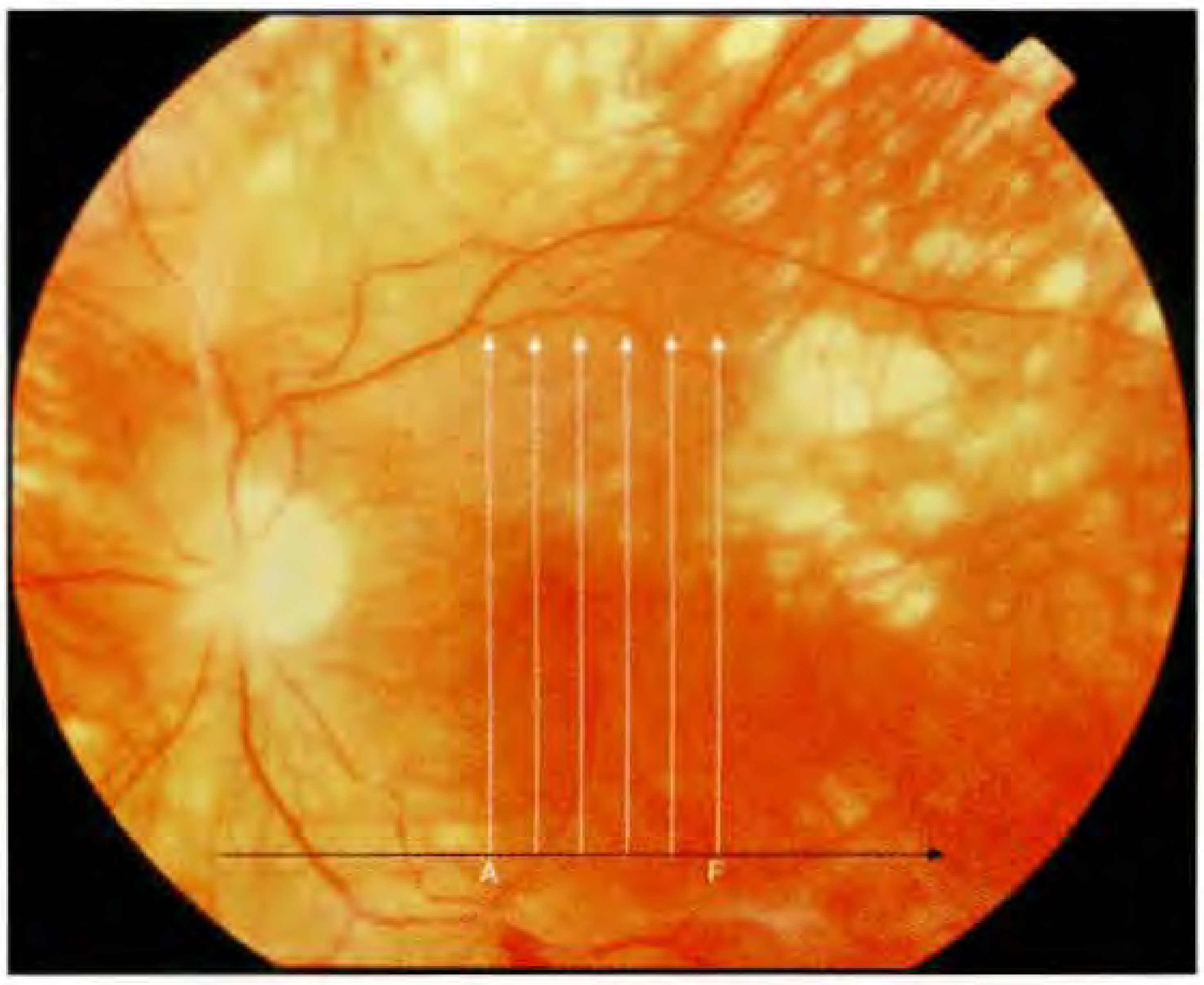

A

Case 6-15. Proliferative Diabetic Retinopathy with Traction Retinal Detachment

Clinical Summary

A 70-year-old man with proliferative diabetic retinopathy was examined one year after pan-retinal laser photocoagulation in his left eye. His visual acuity in this eye was 20/50 with no recent changes. Slit-lamp biomicroscopy (A) showed a regression of previously noted neovascularization of the optic disc. Vitreous condensation and fibrosis were observed in the inferior macula with a new associated region of traction retinal detachment inferotemporal from the fovea. There was no evidence of clinically significant macular edema.

Optical Coherence Tomography

A series of vertical OCT images (B; white lines on A) acquired through the macula displayed elevation of the neurosensory retina above an optically clear space consistent with traction retinal detachment. A thin, reflective band anterior to the retina corresponded to the epiretinal membrane observed clinically. The membrane was tightly adherent to the retina in the temporal images, and separated from the retina nasally. Two reflective bands anterior to the retina were observed in a horizontal OCT tomogram (C; black line on A) obtained through the inferior macula and most likely corresponded to an epiretinal membrane and the posterior hyaloid. Traction by the membrane on the retina was clearly demonstrated temporally in the image.

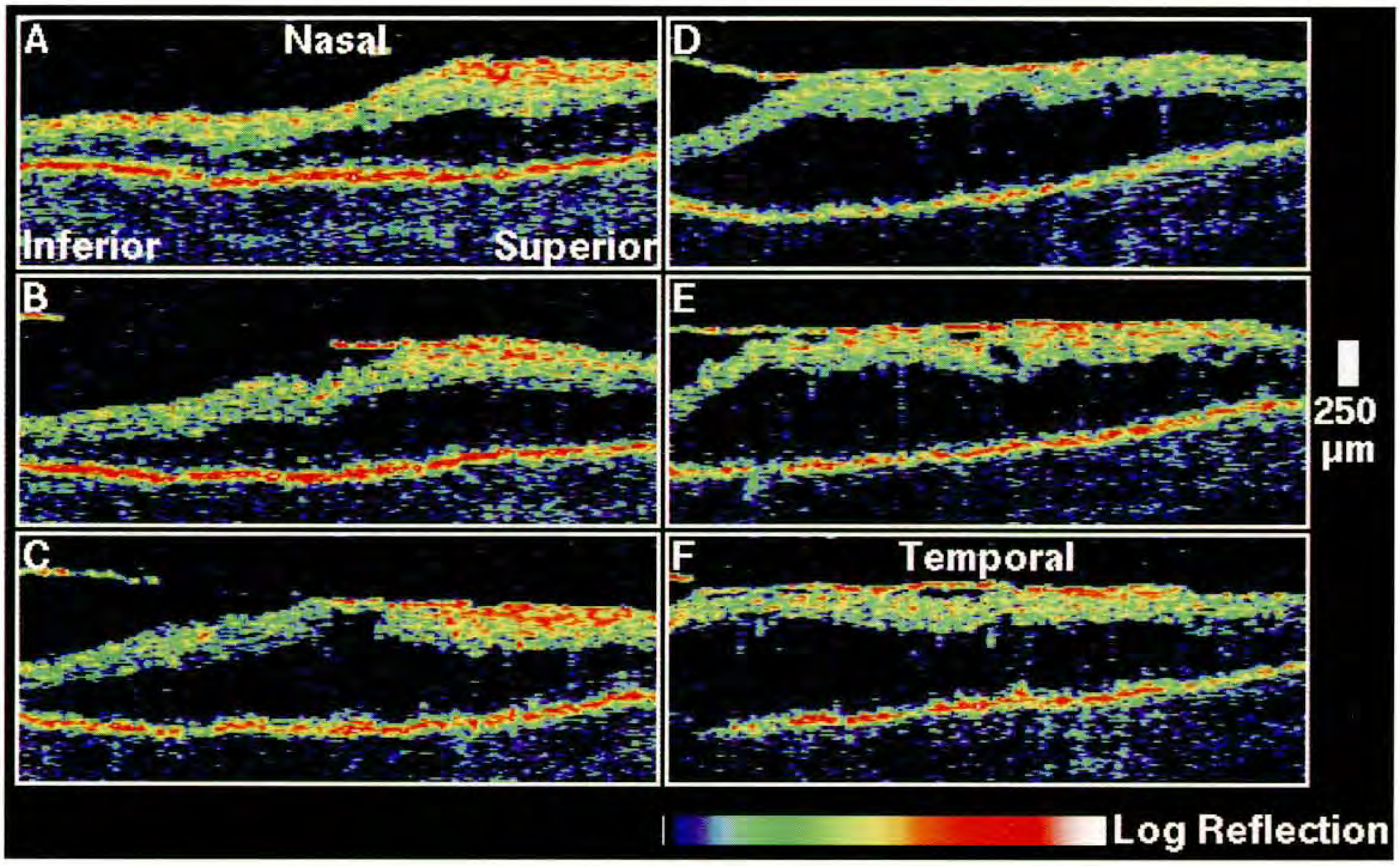
A
Nasal
Inferior
Superior
B
C
D
E
F
Temporal
250
µm
Log Reflection

B

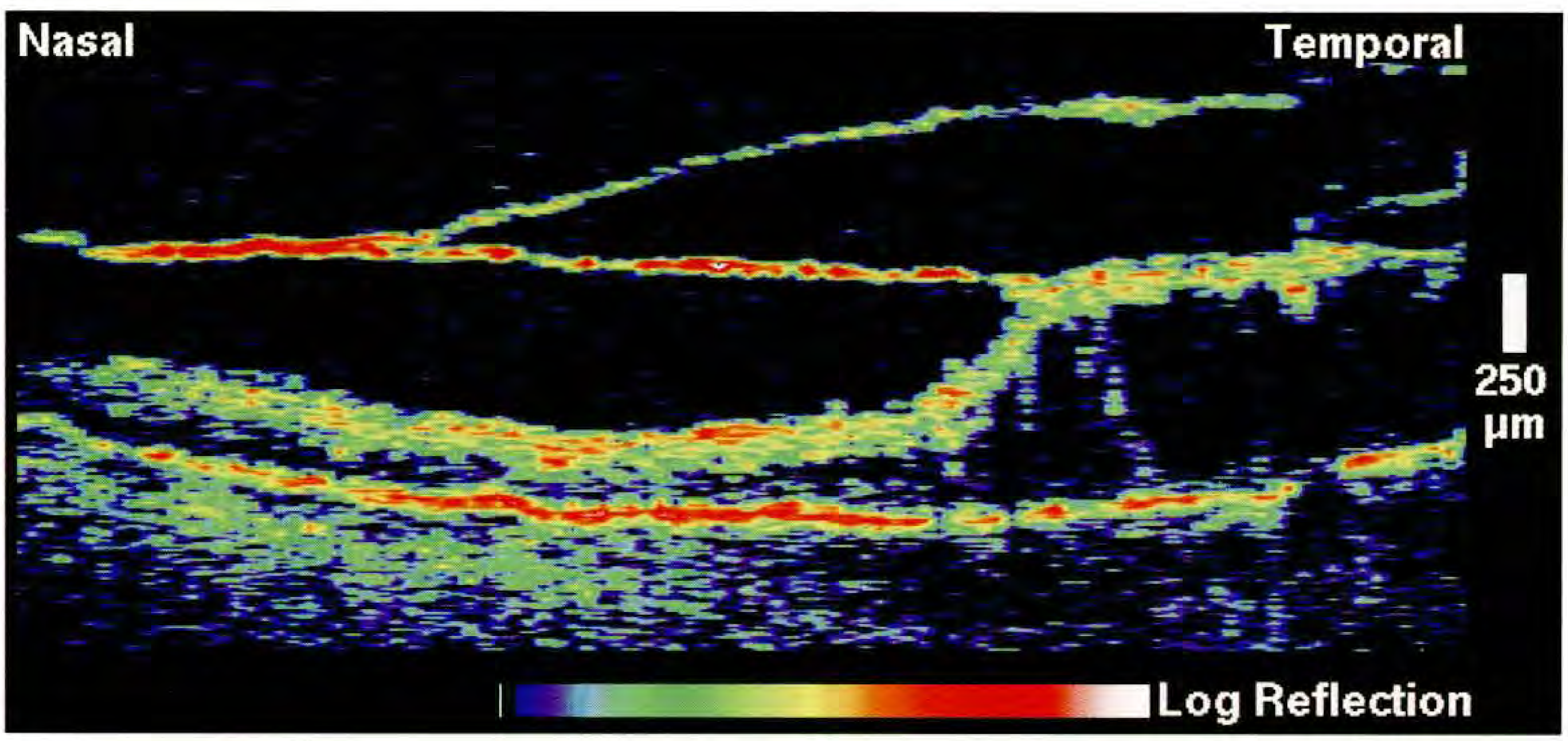
Nasal
Temporal
250
µm
Log Reflection

C

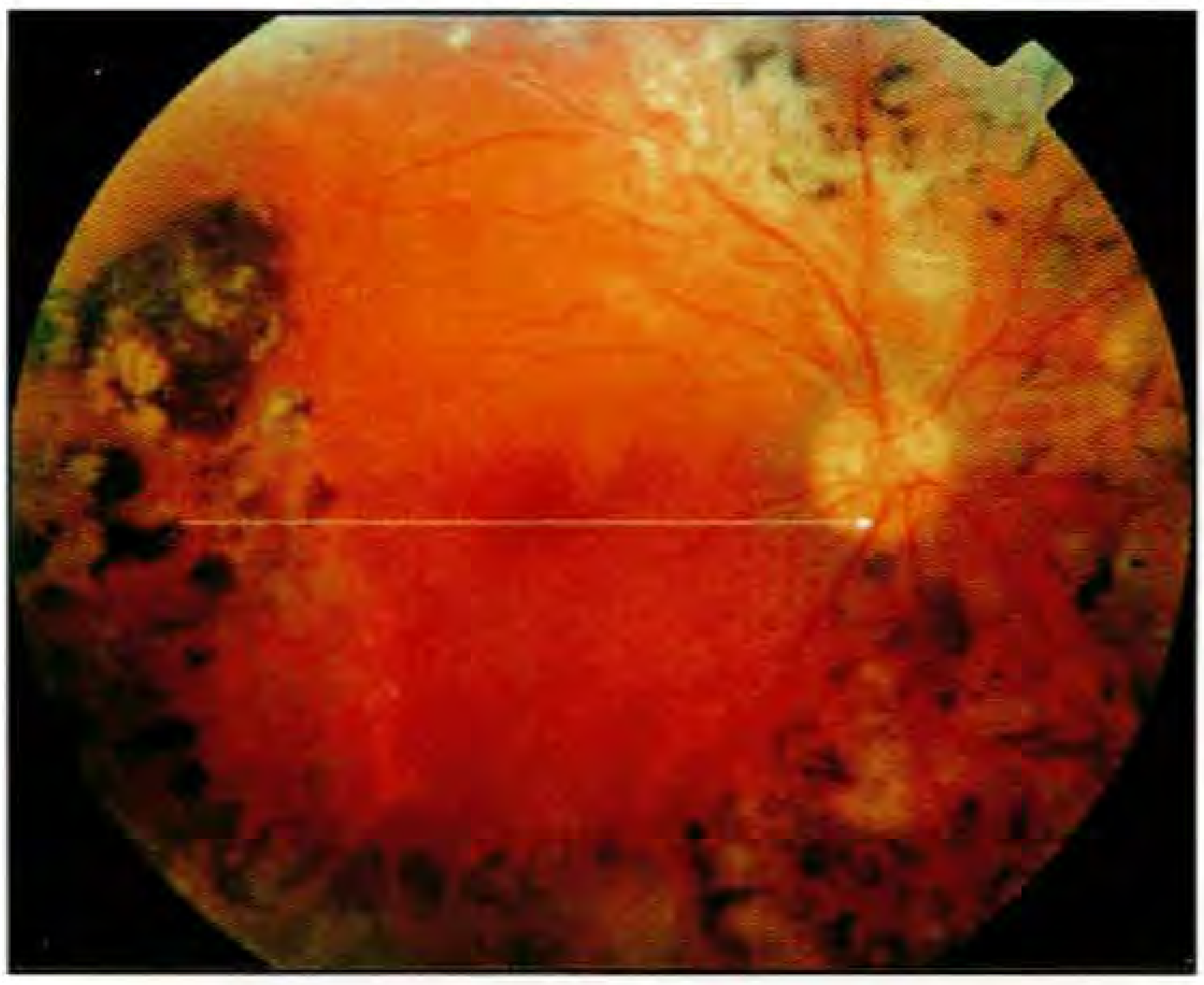

A

Case 6-16. Proliferative Diabetic Retinopathy

Clinical Summary

A 35-year-old man with stable, longstanding proliferative diabetic retinopathy was examined. Indirect ophthalmoscopy (A) of his right eye displayed a mild epiretinal membrane in the macula with no clinically significant macular edema. Panretinal photocoagulation laser scars were evident in the periphery.

Optical Coherence Tomography

A horizontal OCT scan (B) through the fovea illustrated the epiretinal membrane nasally. An abrupt retinal thinning was noted temporally corresponding retinal atrophy in the region of photocoagulation treatment.

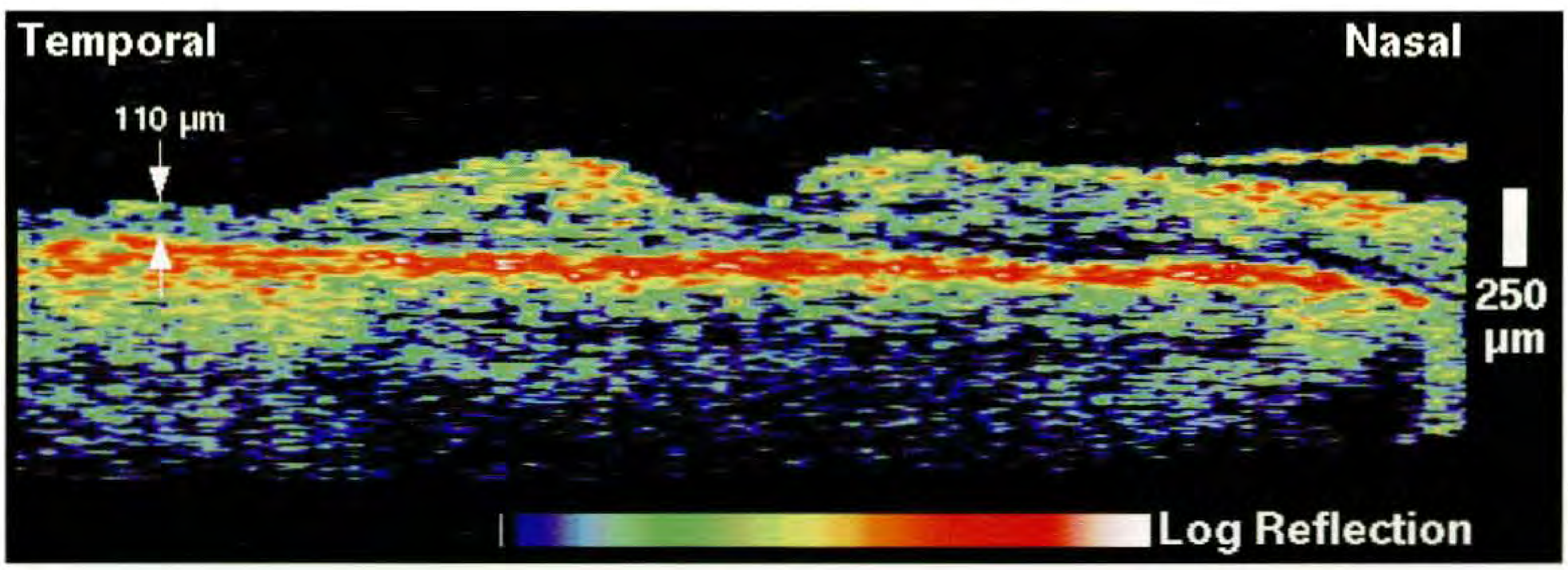

B

Case 6-16 continued

Clinical Summary

Clinical examination of the left eye (C) showed laser photocoagulation scars in the periphery, but no clinically significant macular edema, active neovascularization, or hemorrhage. The visual acuity in this eye was 20/30.

Optical Coherence Tomography

An OCT image (D) taken inferior to the fovea demonstrated a thin brightly backscattering layer anterior to the retina consistent with a thick epiretinal membrane.

C

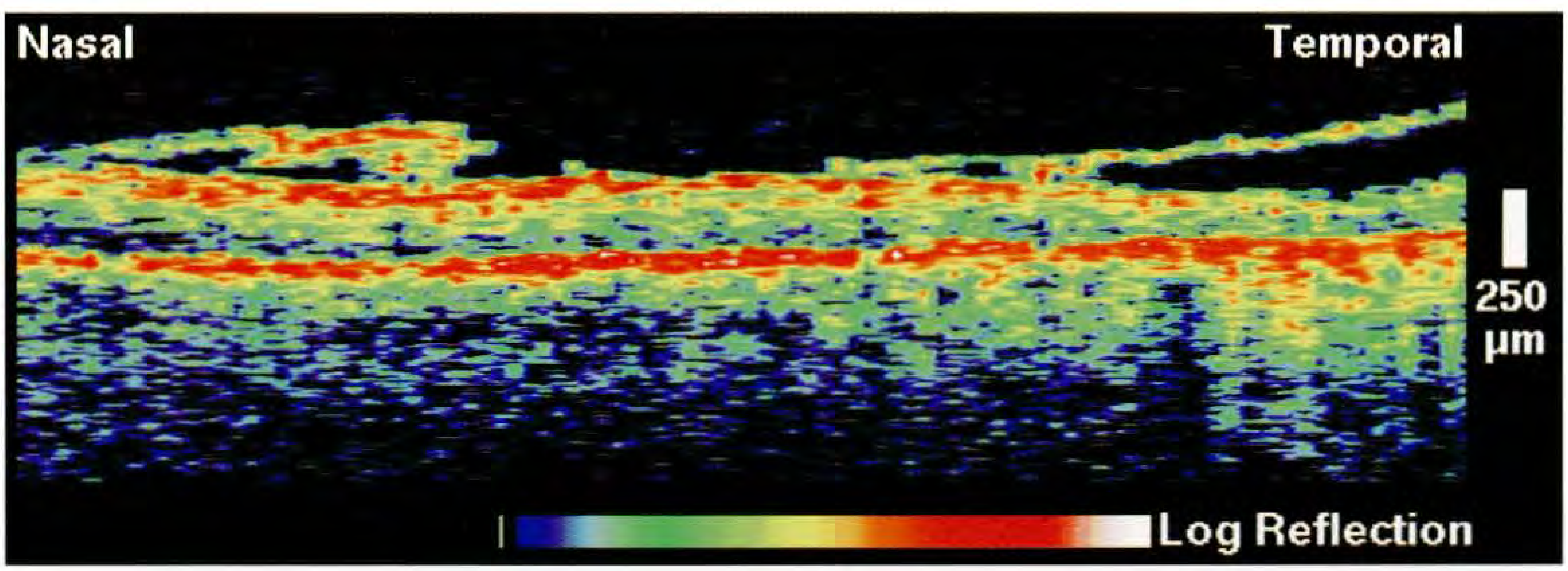

D

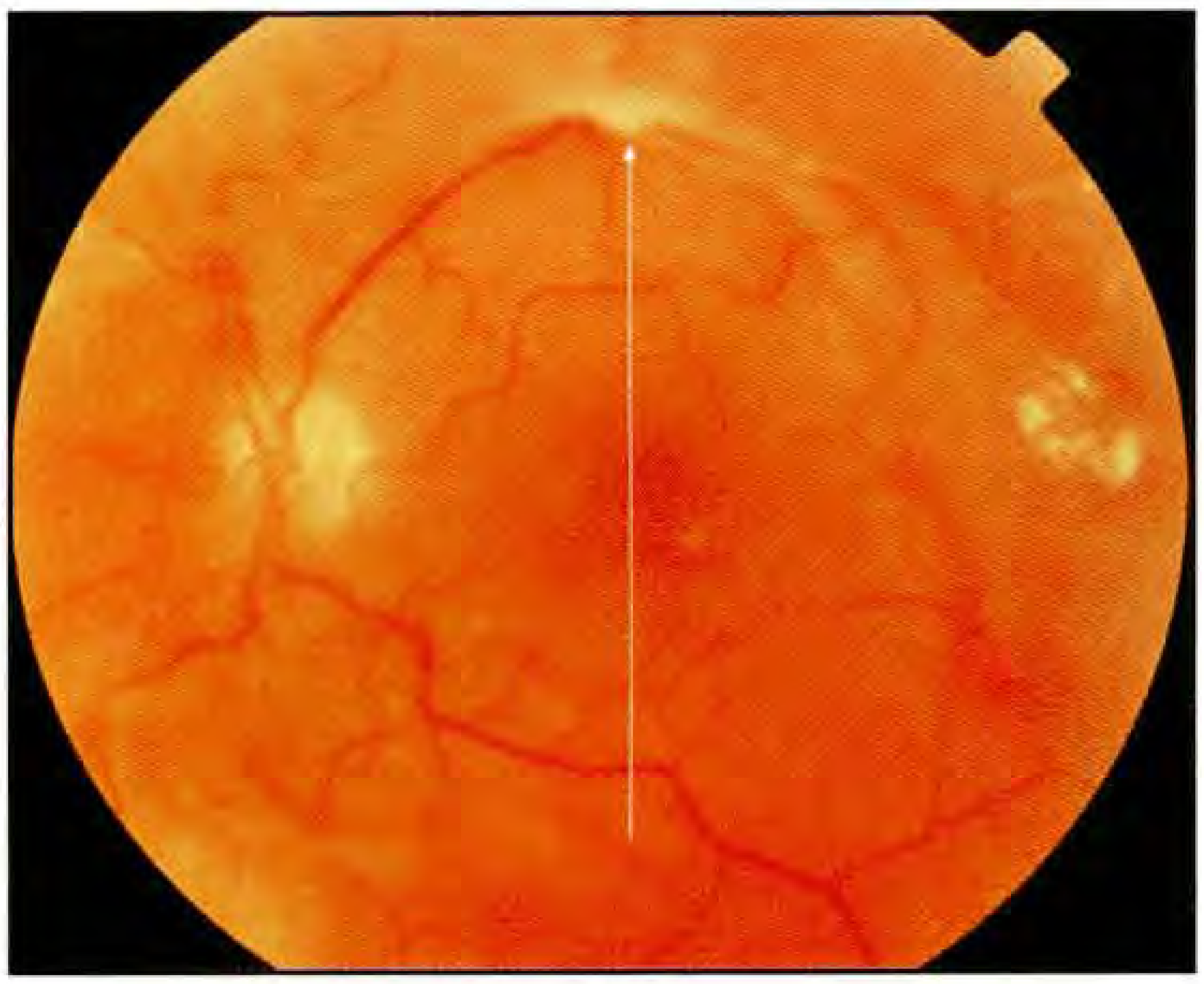

A

Case 6-17. Proliferative Diabetic Retinopathy with Traction Retinal Detachment

Clinical Summary

A 63-year-old woman was evaluated for proliferative diabetic retinopathy in her left eye. On examination, her visual acuity in this eye was 20/60. Dilated ophthalmoscopy (A) revealed neovascularization of the optic disc and traction retinal detachments superotemporally and nasally.

Optical Coherence Tomography

An OCT tomogram (B) was obtained through fixation to assess the whether the traction detachment extended under the fovea. The image showed a large detachment of the neurosensory retina superior to the foveal depression; however, the fovea itself appeared intact. No significant macular thickening was observed.

A separate tomogram (C; scan not shown on A) acquired nasal to the optic disc showed a focal, tractional retinal detachment. Abnormally strong backscatter was observed from a detached posterior hyaloid consistent with epiretinal membrane proliferation along the posterior vitreous face. Membrane strands were observed extending between the posterior hyaloid and the retinal surface. Weak optical backscatter anterior to the retina was noted inferiorly in the image suggesting early fibroblast proliferation.

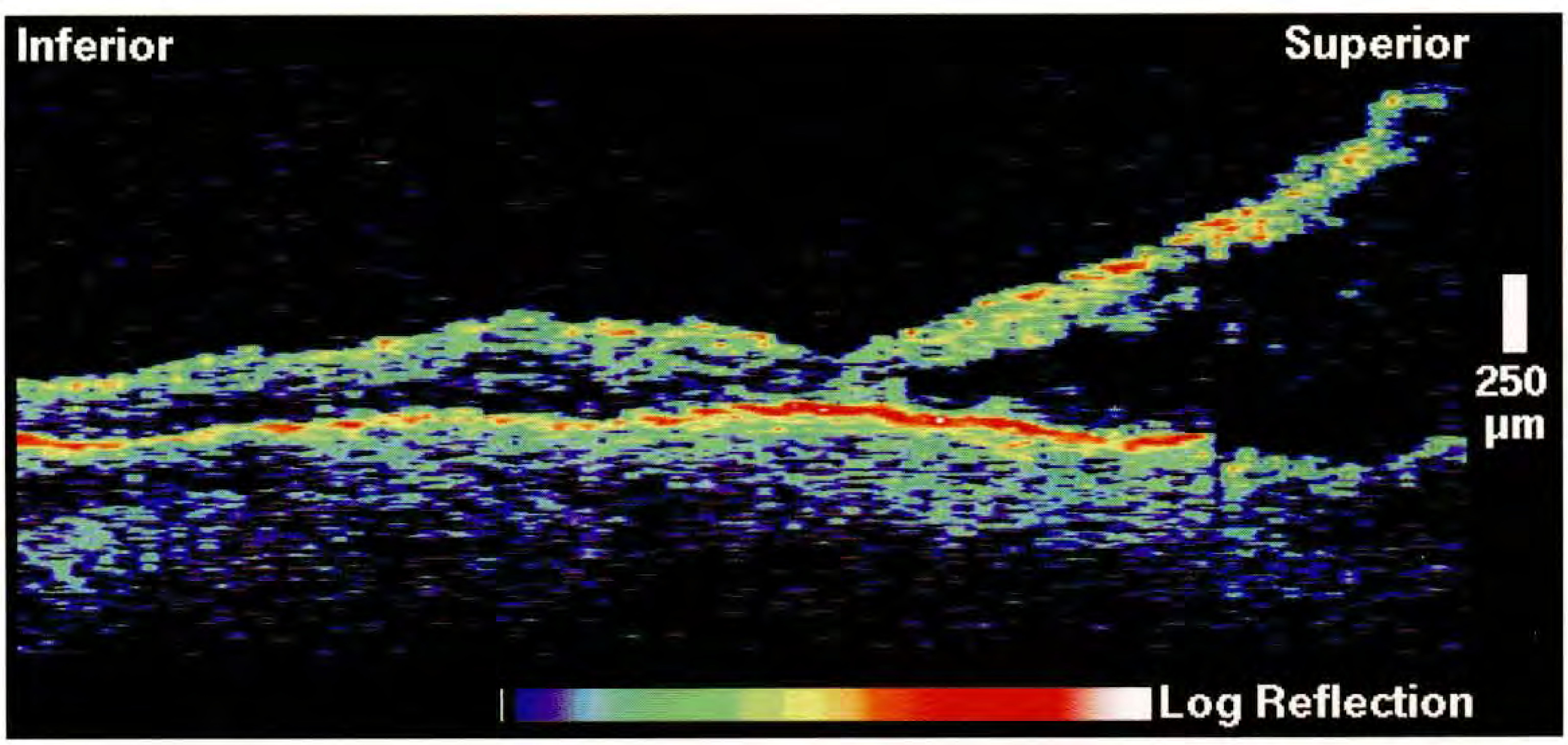

B

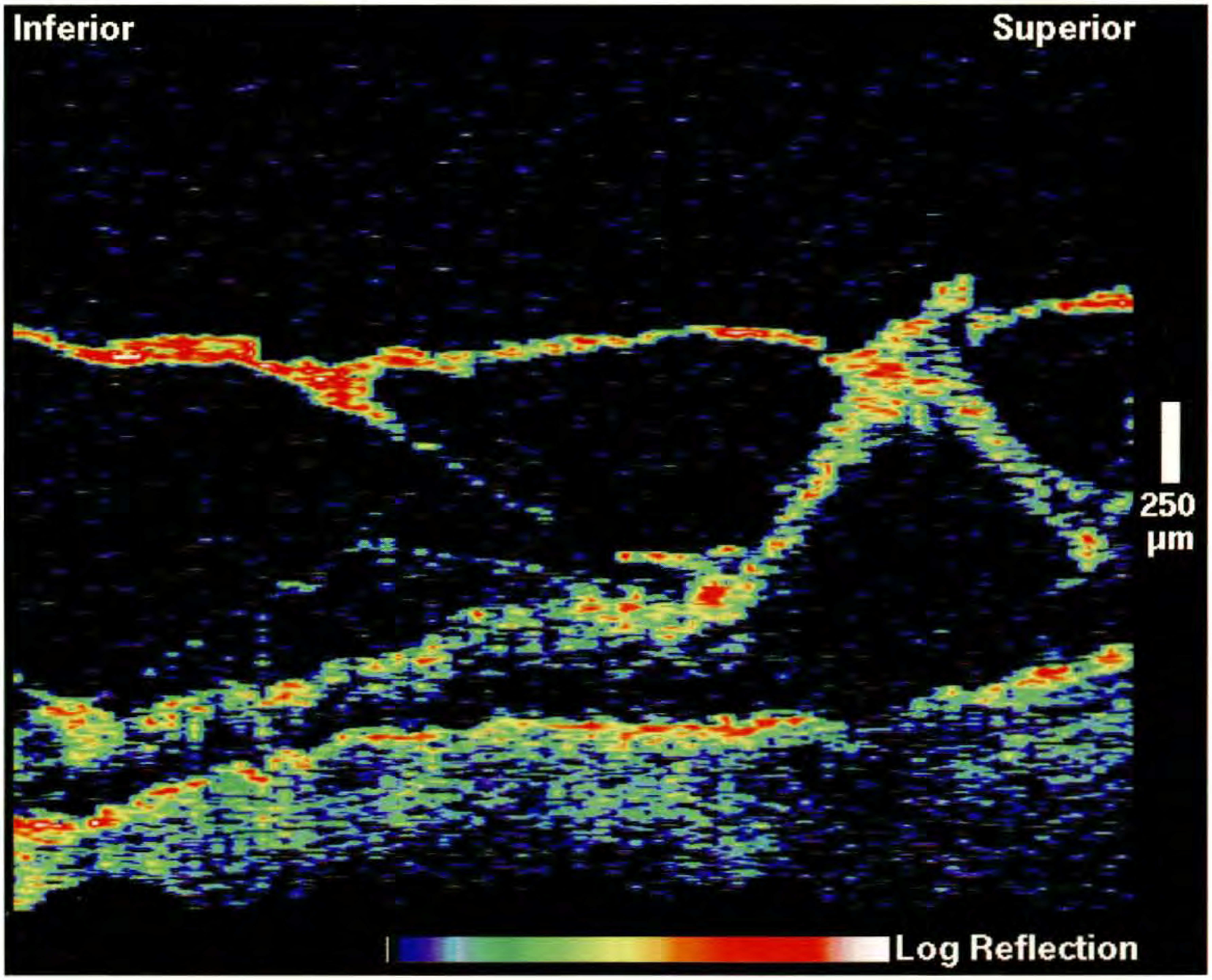

C

CHAPTER 7

Central Serous Chorioretinopathy

OCT offers an objective test for the quantitative evaluation of patients with central serous chorioretinopathy. Longitudinal examinations with OCT are able to track the resolution of the sensory retinal detachment with more sensitivity than slit-lamp biomicroscopy and with a single, permanently recorded measurement [1].

The diagnosis of central serous chorioretinopathy may be difficult in cases where the serous detachment is small. OCT is highly sensitive to small elevations of the neurosensory retina because of the clear difference in optical reflectivity between retinal tissue and serous fluid. Although central serous chorioretinopathy typically affects adults between 20 and 50 years of age, the disease may be mistaken for age-related macular degeneration and subretinal neovascularization in older patients [2]. The occult form of choroidal neovascularization may show a similar angiographic appearance to central serous chorioretinopathy when a focal leakage point is present. OCT can provide additional diagnostic information in these cases by confirming the existence of a neurosensory detachment versus abnormalities in the choriocapillaris or pigment epithelium caused by a neovascular membrane.

The serous retinal detachment of central serous chorioretinopathy may be distinguished from a pigment epithelial detachment on OCT by observation of the reflective layer corresponding to the retinal pigment epithelium (RPE) and choriocapillaris. Elevation of this reflection above an optically clear space occurs when the pigment epithelium is detached. Intense shadowing of the choroidal reflection is also observed due to increased attenuation of light from the detached RPE. In contrast, neurosensory detachments exhibit a well-defined reflection at the fluid-RPE interface. Occasionally, the reflection from the posterior margin of the detached sensory retina may mimic a detached RPE, however, only minimal shadowing of the choroidal reflection occurs.

Fluorescein angiography typically shows one or more focal areas of hyperfluorescence corresponding to leakage at the level of the retinal pigment epithelium [3-7]. OCT tomograms through these leakage areas show a small elevation of a reflective layer corresponding to the pigment epithelium over an optically clear space consistent with a serous pigment epithelial detachment.

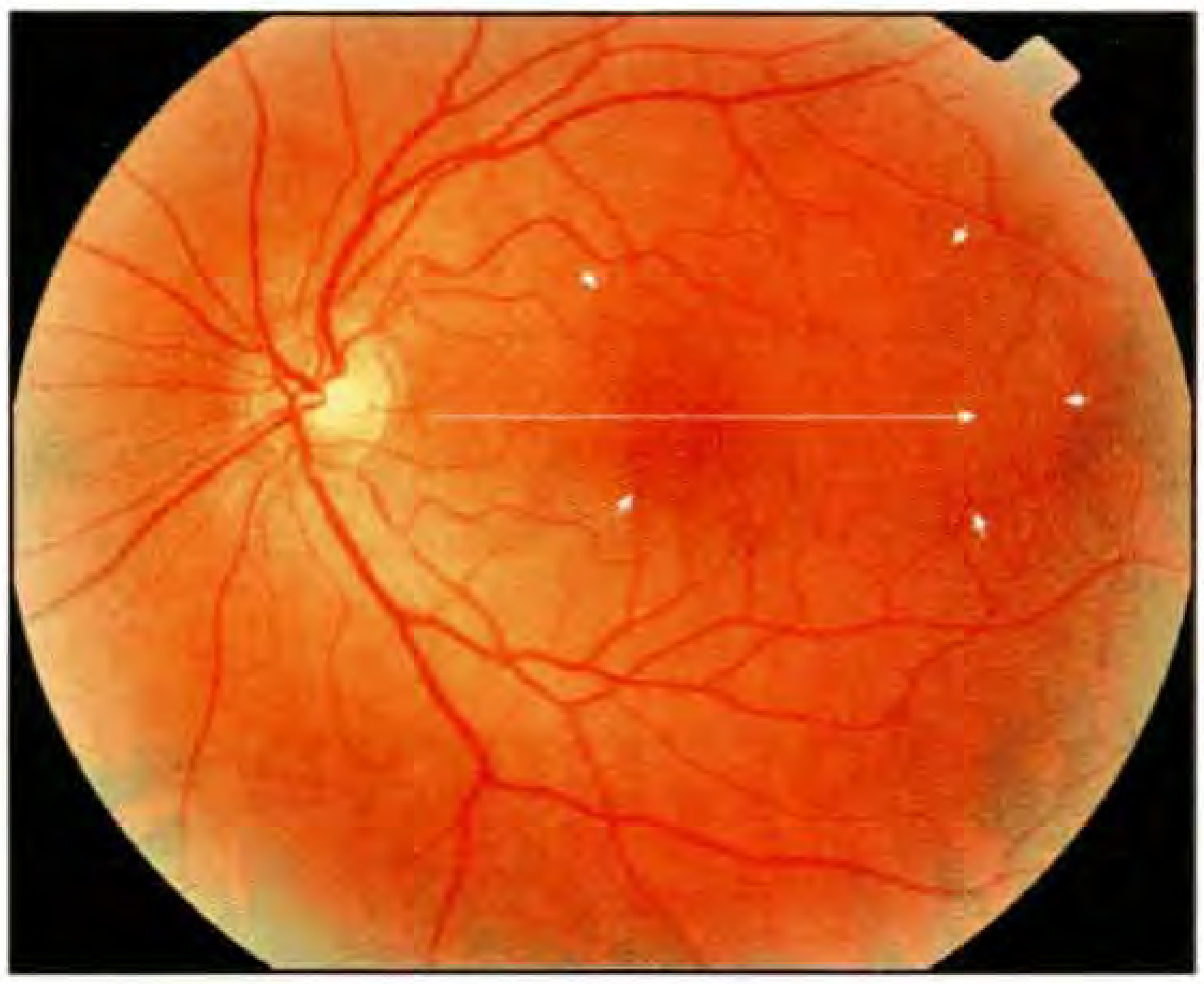

A

B

Case 7-1. Central Serous Chorioretinopathy

Clinical Summary

A 57-year-old man noticed an abrupt onset of visual blurring in his left eye over a period of one day. He described the area as gray with sharply defined borders. Slitlamp biomicroscopy (A) showed a shallow serous elevation of the neurosensory retina in the macula including the fovea. His visual acuity in this eye was 20/25. Fluorescein angiography (B) displayed multiple, focal areas of hyperfluorescence. An area superotemporal to the fovea showed increasing hyperfluorescence with intense late leakage. Two hyperfluorescent spots were also noted superior to the optic disc and nasal to the fovea, consistent with either pigment epithelial detachments or window defects.

Optical Coherence Tomography

A horizontal OCT section (C) acquired directly through the fovea illustrated an elevation of the neurosensory retina above an optically clear space corresponding to a fluid-filled cavity . The height of the detachment directly beneath the fovea as measured directly from the OCT image was 210 µm.

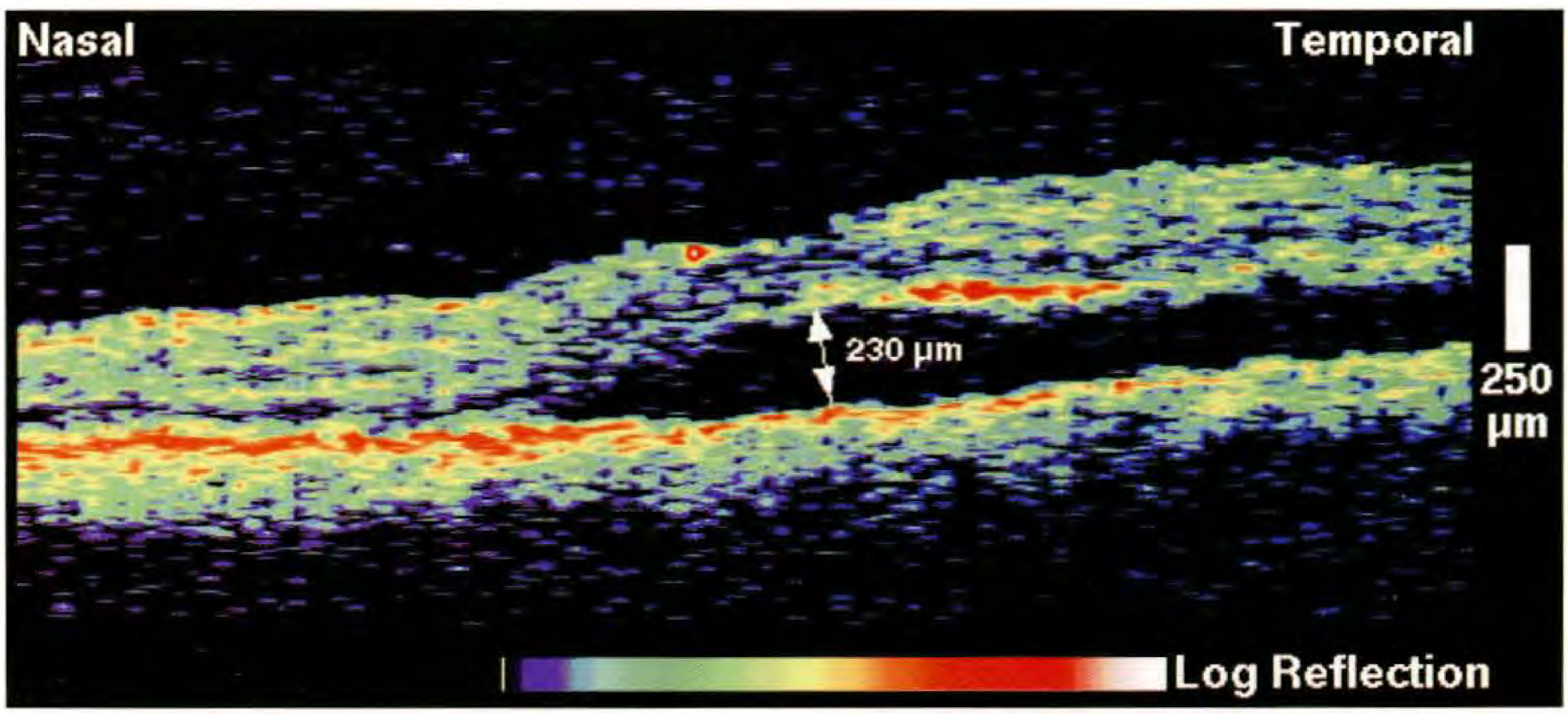

C

Case 7-1 continued

Follow-up Examination

The patient returned for a follow-up visit six weeks later with no improvement in visual acuity. Slit-lamp examination revealed that the serous elevation had decreased since the previous visit. A repeat OCT tomogram (D) taken at this time confirmed the decrease in subretinal fluid accumulation. The height of the detachment was measured to be 120 µm directly beneath the fovea. On follow-up examination another two months later, the patient noted a decrease in the size of the scotoma in his left eye, and his visual acuity had returned to 20/20. No remaining subretinal fluid was observed on indirect ophthalmoscopy. A third horizontal OCT image (E) taken through the fovea showed that the detachment had completely resolved directly beneath the fovea. However, a residual region of fluid accumulation remained temporal to the fovea.

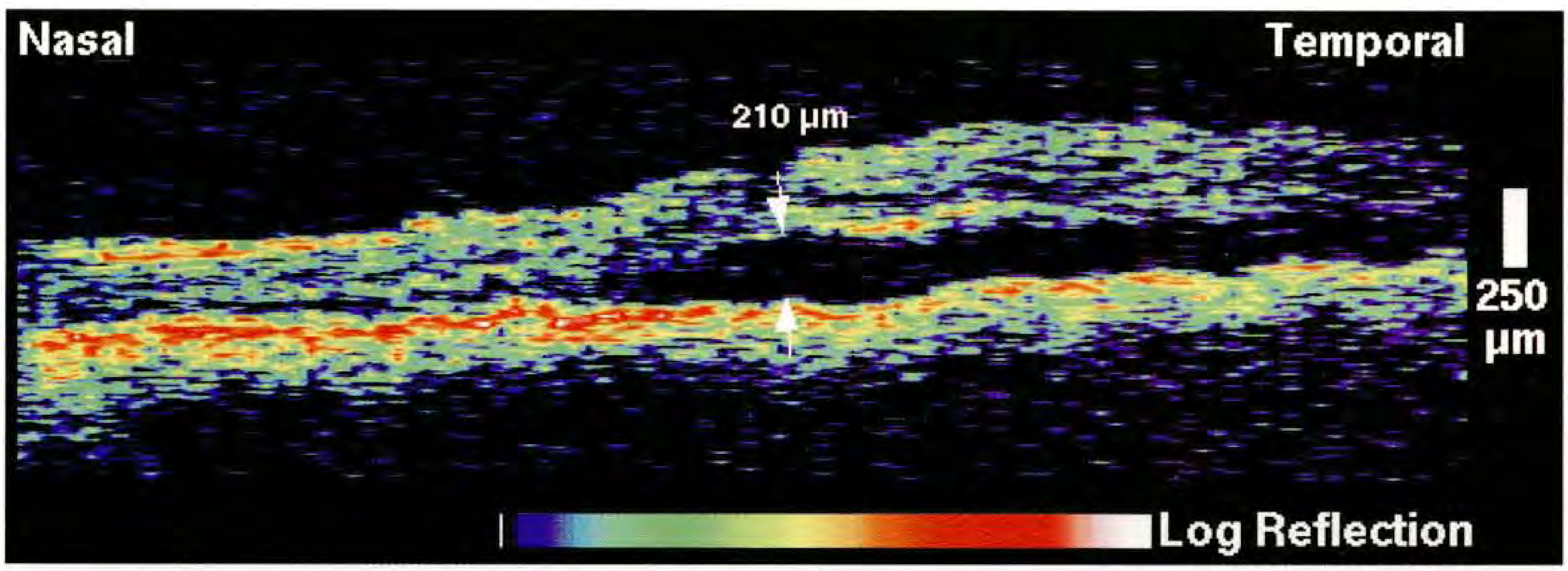

D

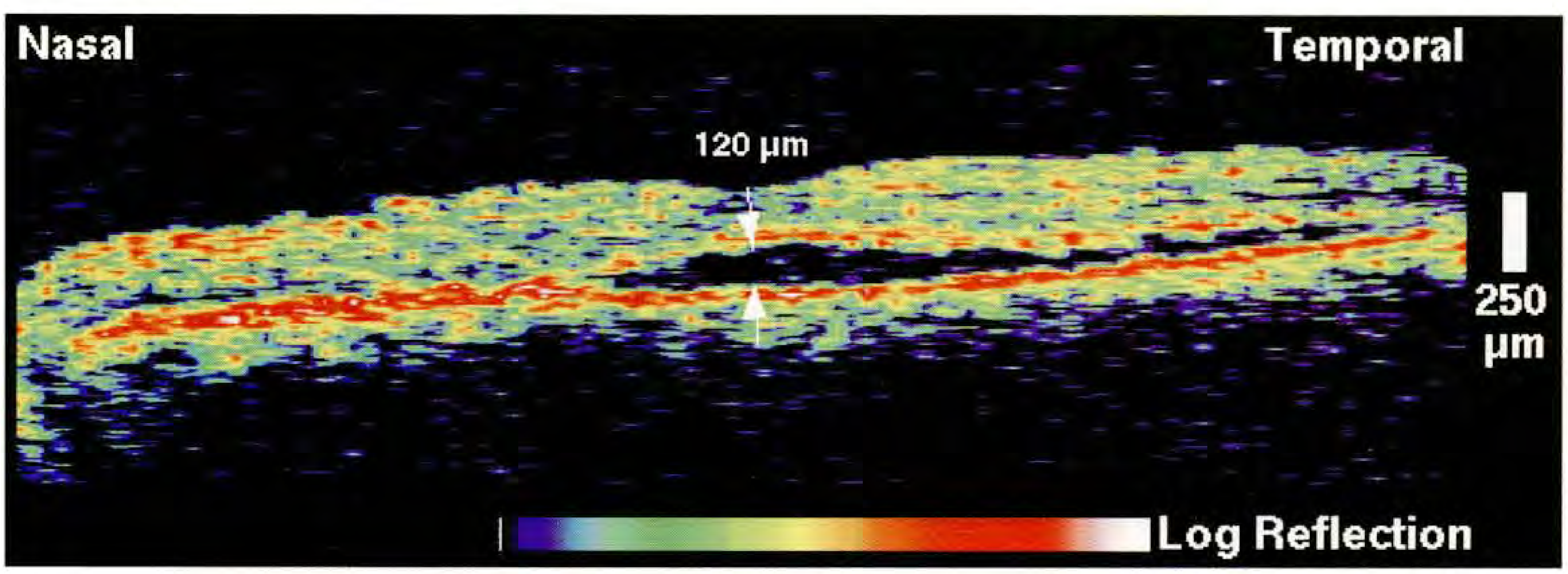

E

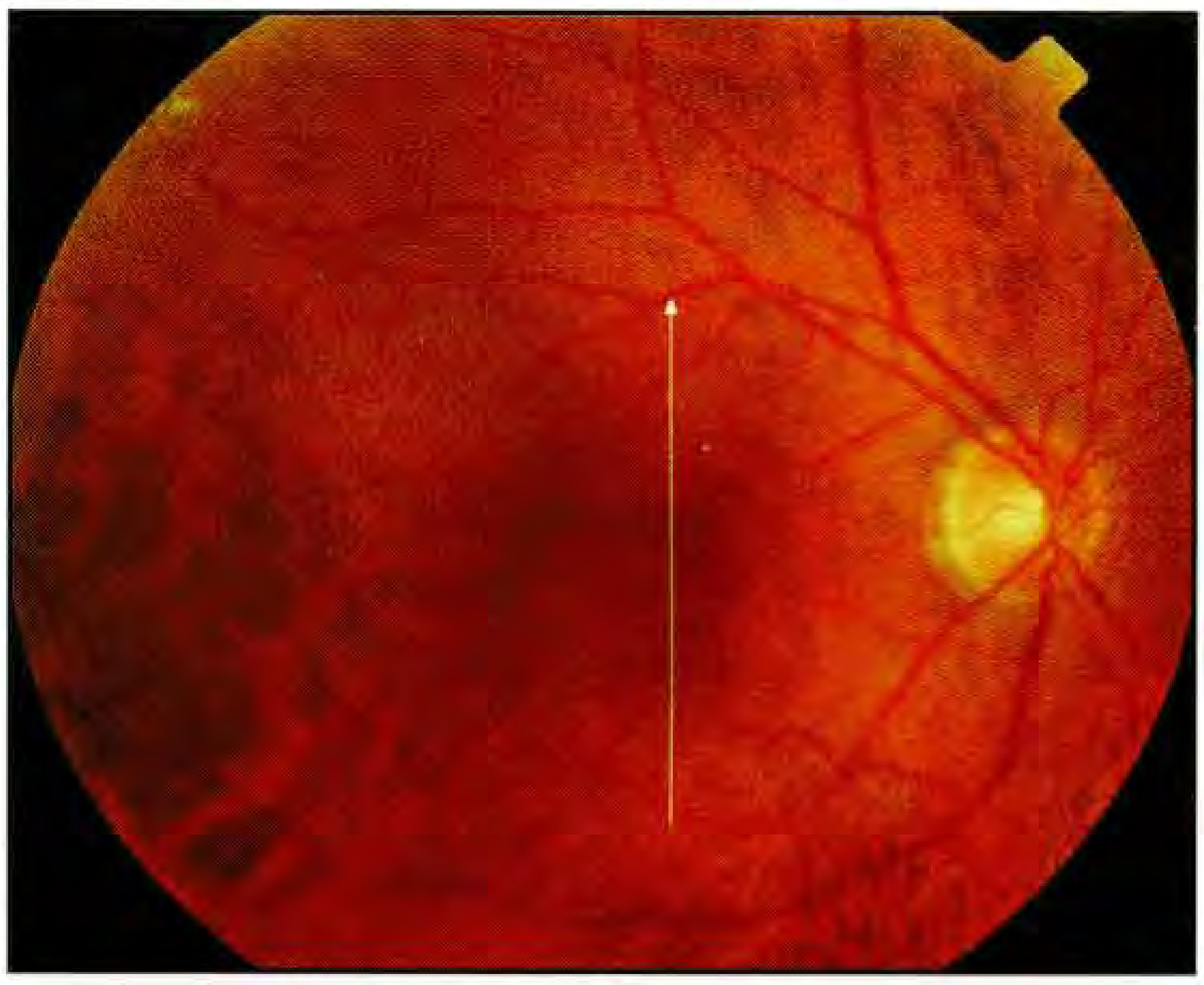

A

B

Case 7-2. Central Serous Chorioretinopathy

Clinical Summary

A 65-year-old man noted decreasing vision in his right eye over the period of one month. On examination, his visual acuity in this eye was 20/50. Dilated ophthalmoscopy (A) showed a serous elevation of the neurosensory retina directly in the macula. A small hyperfluorescent spot with late leakage superior to the fovea was seen on the fluorescein angiogram (B). Mottled hyperfluorescence was also noted further superiorly and superotemporally in the angiogram.

Optical Coherence Tomography

A vertical OCT tomogram (C) was obtained slightly nasal to the fovea through both the neurosensory detachment and the leakage point located superior to the fovea displayed on angiography. The tomogram showed a small serous retinal detachment, with a height of 110 µm at its maximum in the image. The neurosensory retina above the detachment appeared thickened, measuring approximately 300 µm compared with 200 µm at the inferior edge of the image. The optical reflectivity from within the neurosensory retina in this region was reduced, consistent with intraretinal edema and cystic changes. A focal elevation of the reflective band corresponding to the retinal pigment epithelium was noted just superior to the neurosensory detachment on the OCT image, consistent with a small serous detachment of the pigment epithelium (arrow).

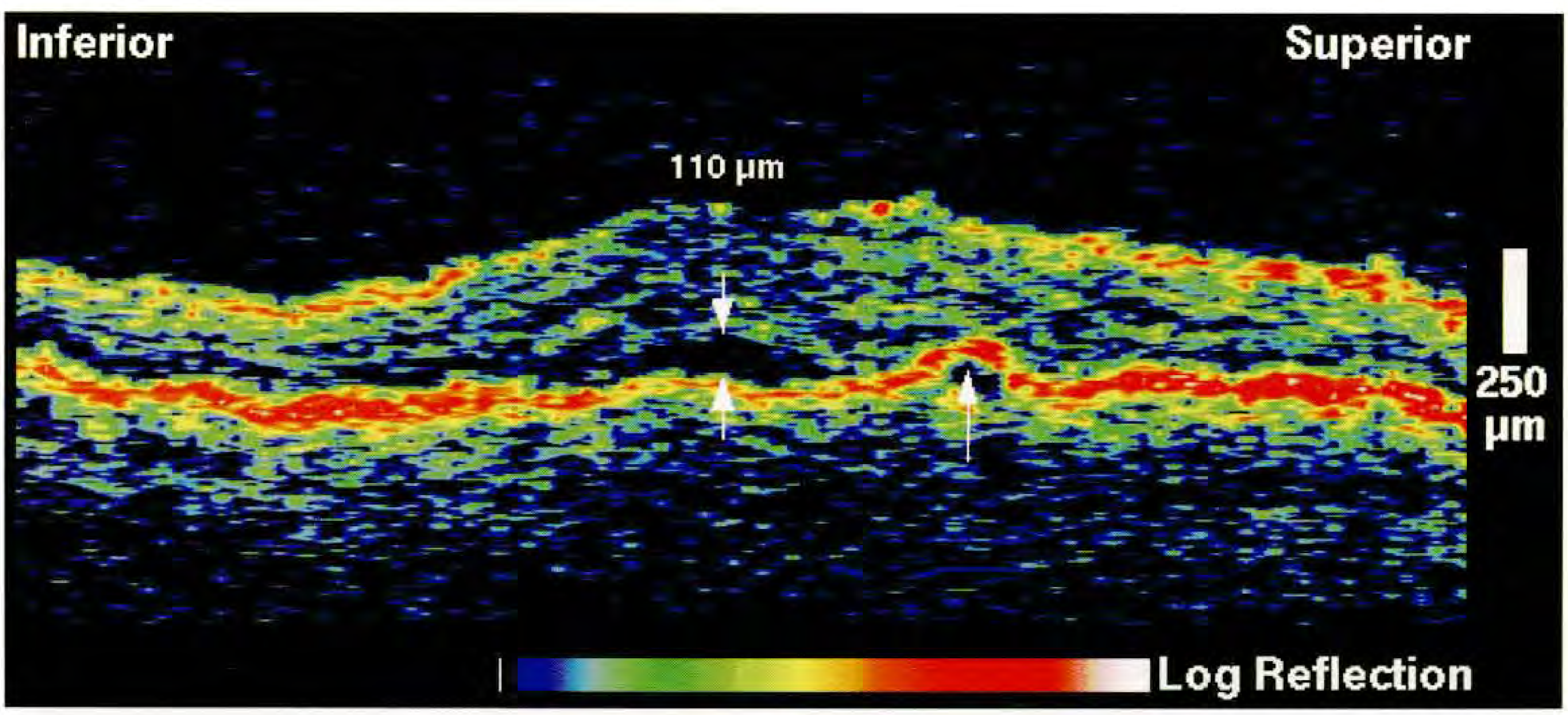

C

Case 7-2 continued

Follow-up Examination

The patient elected to receive argon laser photocoagulation treatment in this eye, applied to the leakage point observed on fluorescein angiography. On follow-up examination one month later, he described greatly improved vision and his acuity had returned to 20/25. Slit-lamp examination (D) showed that the retinal detachment had flattened. Fluorescein angiography (E) displayed hypofluorescence superior to the macula consistent with laser treatment, and mild surrounding hyperfluorescence.

Follow-up Optical Coherence Tomography

A repeat OCT tomogram (F) taken through the same cross-section of the retina confirmed resolution of the serous detachment. Additionally, the thickness of the neurosensory retina above the previous area of detachment had decreased from 300 to 250 μm consistent with the disappearance of the intraretinal edema. A concomitant increase in the optical backscatter signal from this region was also noted. A slight disturbance in the red band corresponding to the retinal pigment epithelium was seen consistent with a laser scar. The reflectivity from the photoreceptors in this area also appeared to be increased.

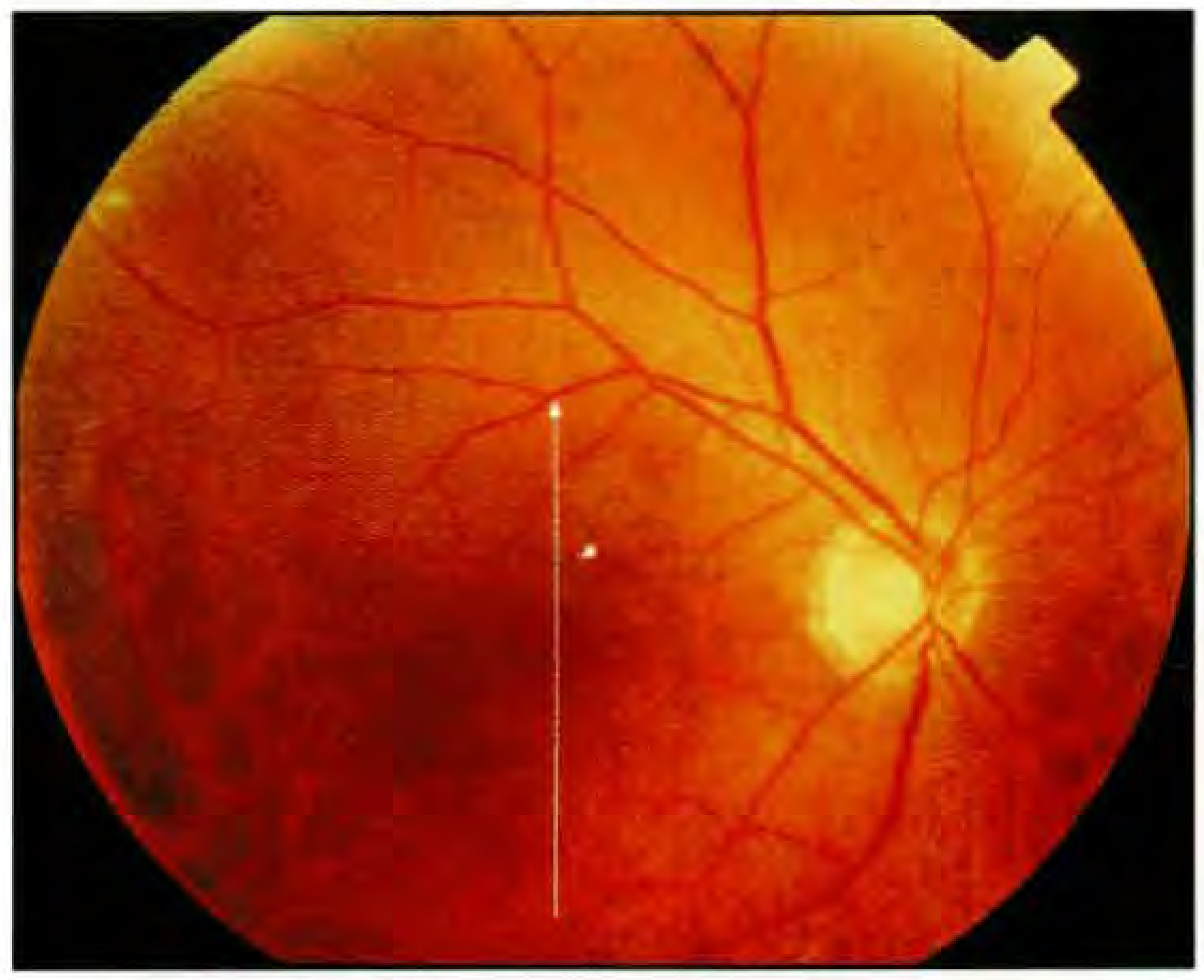

D

E

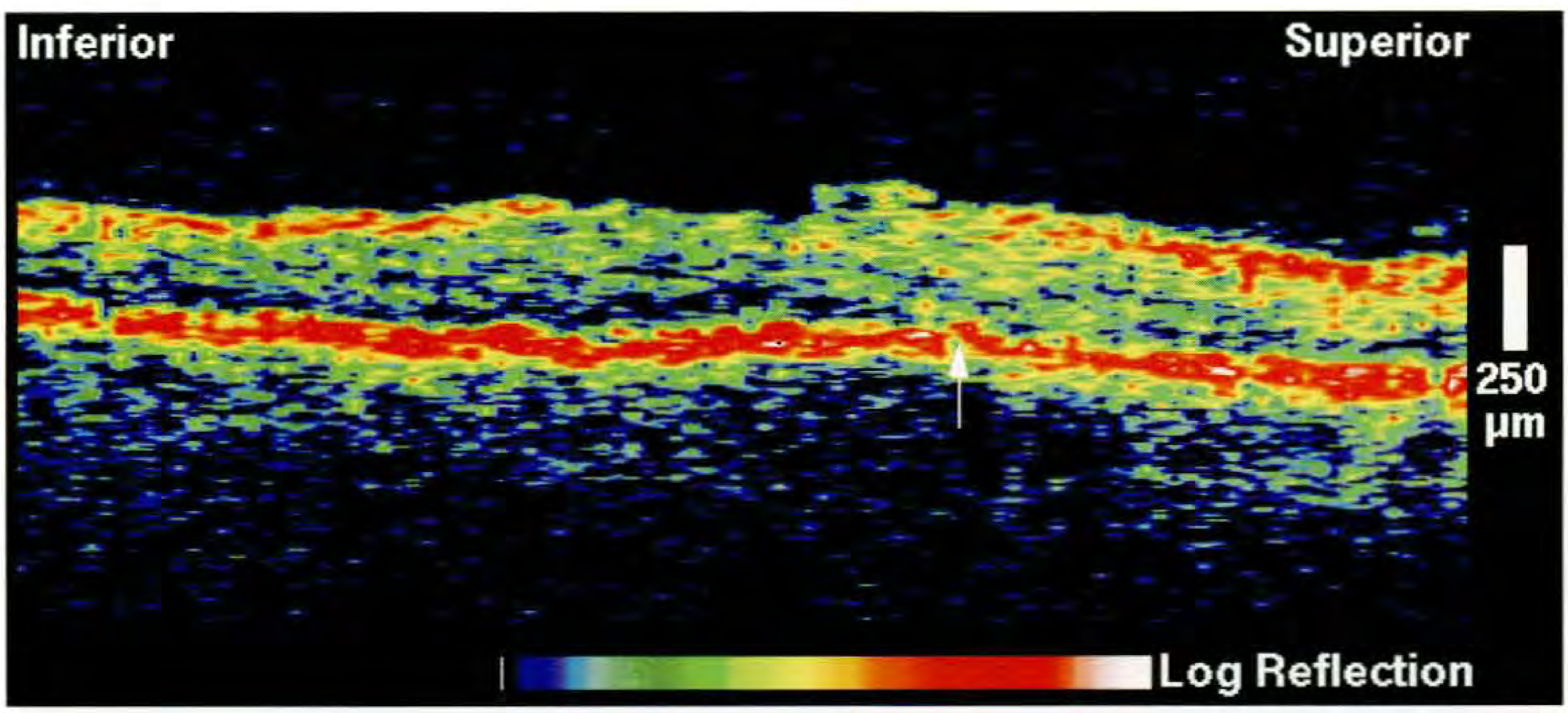

F

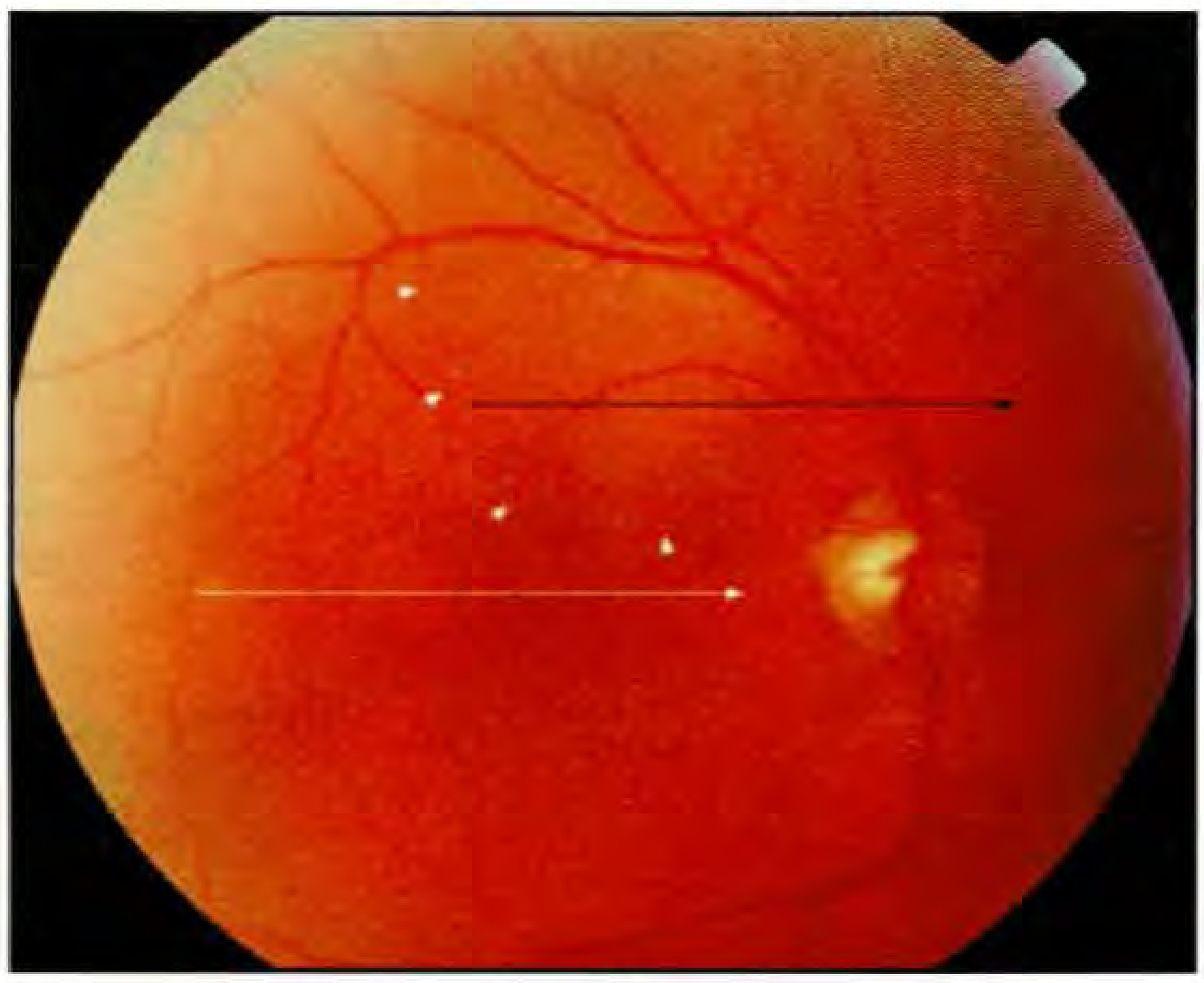

A

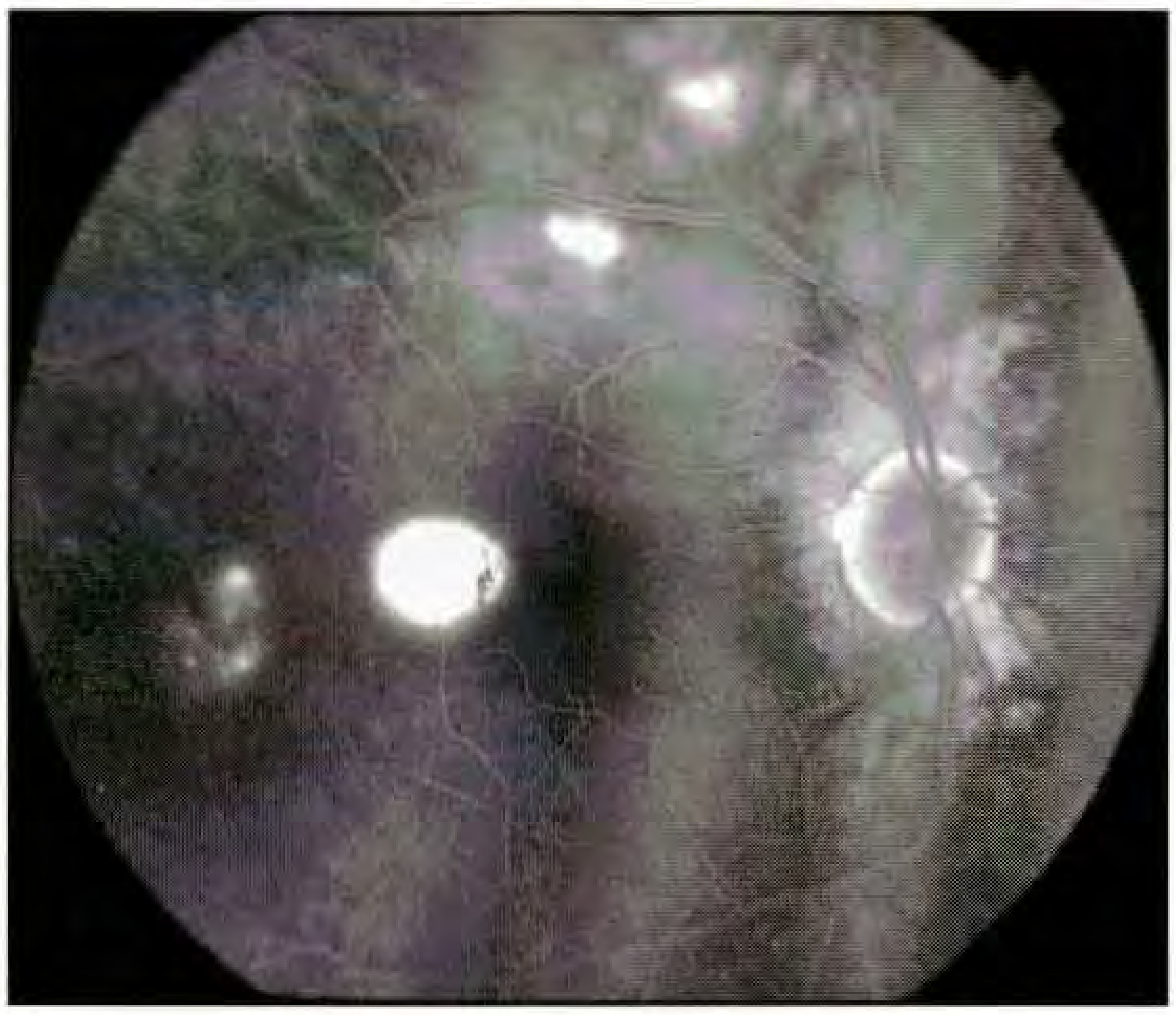

B

Case 7-3. Central Serous Chorioretinopathy

Clinical Summary

A 41-year-old man had both a neurosensory detachment and a retinal pigment epithelial detachment of the macula of his right eye which was associated with the diagnosis of idiopathic central serous chorioretinopathy (A). His visual acuity was 20/40. Fluorescein angiography (B) displayed filling of a small retinal pigment epithelial detachment temporal to the fovea and hyperfluorescence along the superotemporal arcade in the temporal macula consistent with a neurosensory detachment of the retina.

Optical Coherence Tomography

OCT images were obtained through both areas of retinal pathology. A tomogram (C; white line on A) taken through the area of retinal pigment epithelium (RPE) detachment toward the optic disc showed elevation of both the retina and RPE over an optically clear space consistent with serous fluid. The choroidal tissue beneath the detachment was shadowed by the highly backscattering RPE above. The adjacent normal retina in the image showed that the reflective band corresponding to the RPE and choriocapillaris was thicker than the detached RPE alone. An OCT image (E; black line on A) taken through the area of the neurosensory detachment revealed an elevation of the neurosensory retina and a large area of low reflectivity consistent with a fluid-filled space. The reflective band corresponding to RPE and choriocapillaris in this image appeared intact beneath the serous fluid cavity, except where it was shadowed by retinal blood vessels.

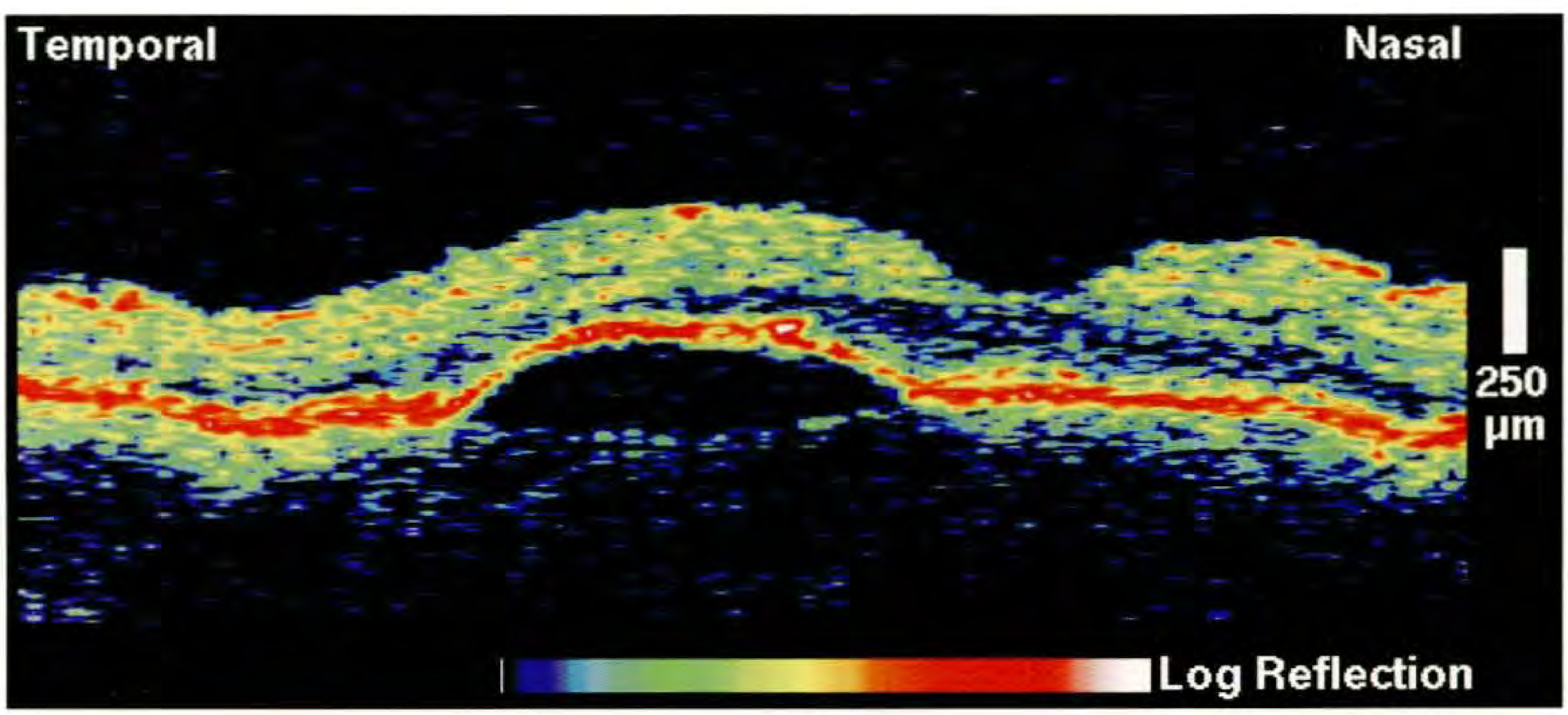

C

Case 7-3 continued

Follow-up Clinical Summary

Four months later, the patient experienced spontaneous resolution of the neurosensory detachment, but persistence of the retinal pigment epithelial detachment in the right eye (D). Fluorescein angiography (not shown) again exhibited filling of a small retinal pigment epithelial detachment temporal to the fovea, but no evidence of the previous neurosensory detachment in the superior macula.

Follow-up Optical Coherence Tomography

An OCT tomogram (F) taken through the area of previous neurosensory detachment showed no evidence of retinal elevation or subretinal fluid accumulation, consistent with the clinical observation of resolution.

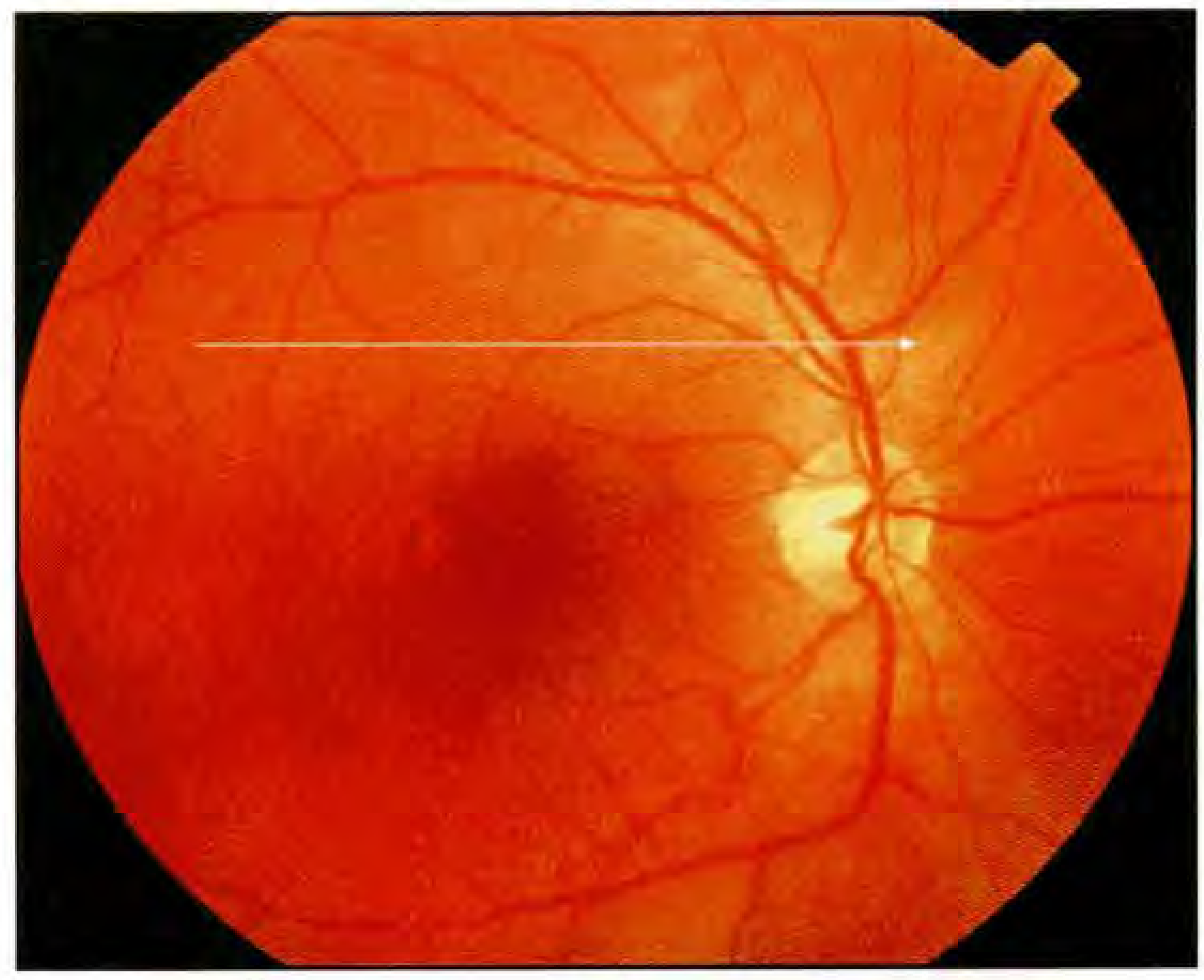

D

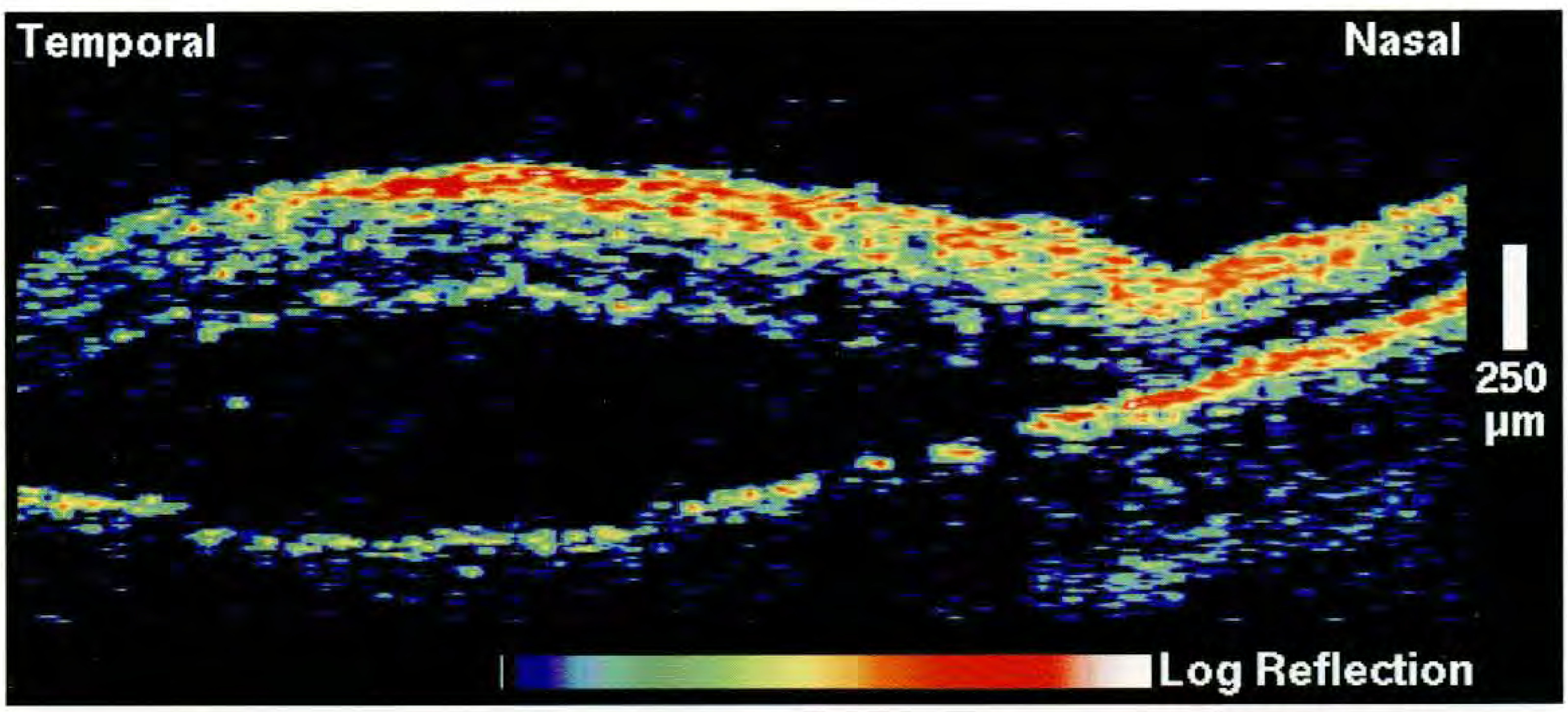

E

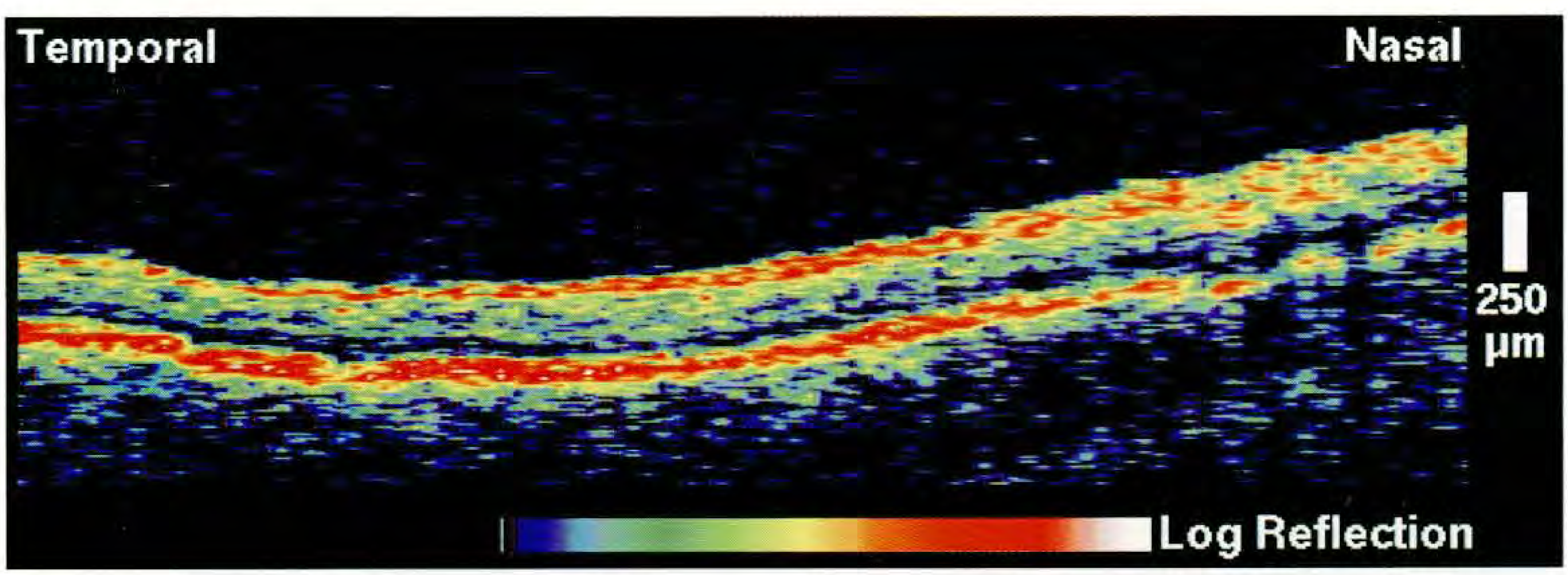

F

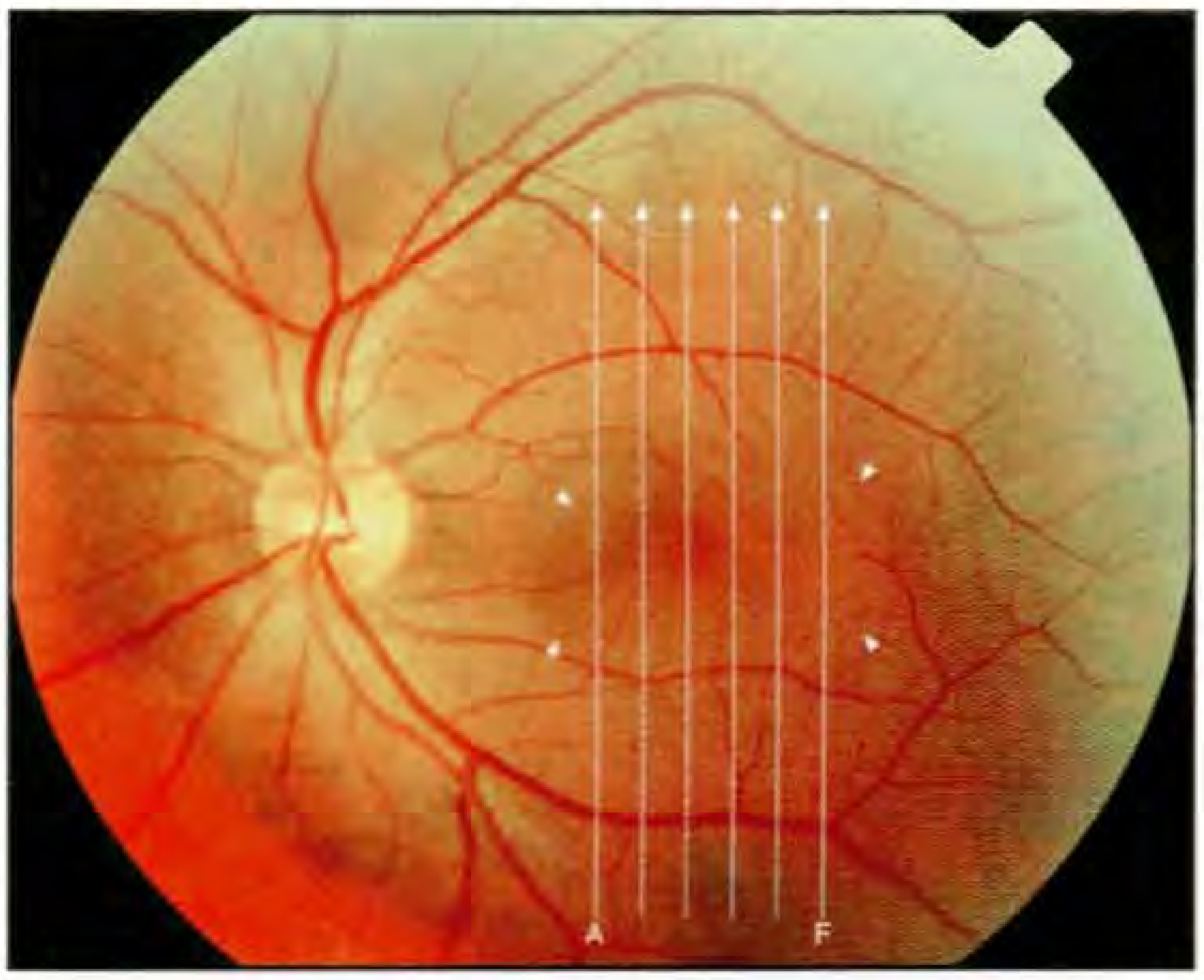

A

B

Case 7-4. Central Serous Chorioretinopathy

Clinical Summary

A 39-year-old man was referred for blurry vision in his left eye and evaluation of possible recurrent central serous chorioretinopathy. He was originally diagnosed eight years earlier and had experienced spontaneous resolution of the serous detachment. In the past few days, however, his visual acuity in this eye had declined to 20/80. Slit-lamp examination (A) confirmed the existence of a neurosensory detachment in the macula. Fluorescein angiography (B) displayed faint patchy hyperfluorescence surrounding the fovea which faded in the late phase of the angiogram consistent with a window defect.

Optical Coherence Tomography

A sequence of vertical OCT tomograms (C) was obtained through the neurosensory detachment, providing three-dimensional information on the extent of the subretinal fluid accumulation. There appeared to be little or no increase in retinal thickness above the detachment, and no decrease in optical backscatter signal from within the neurosensory retina.

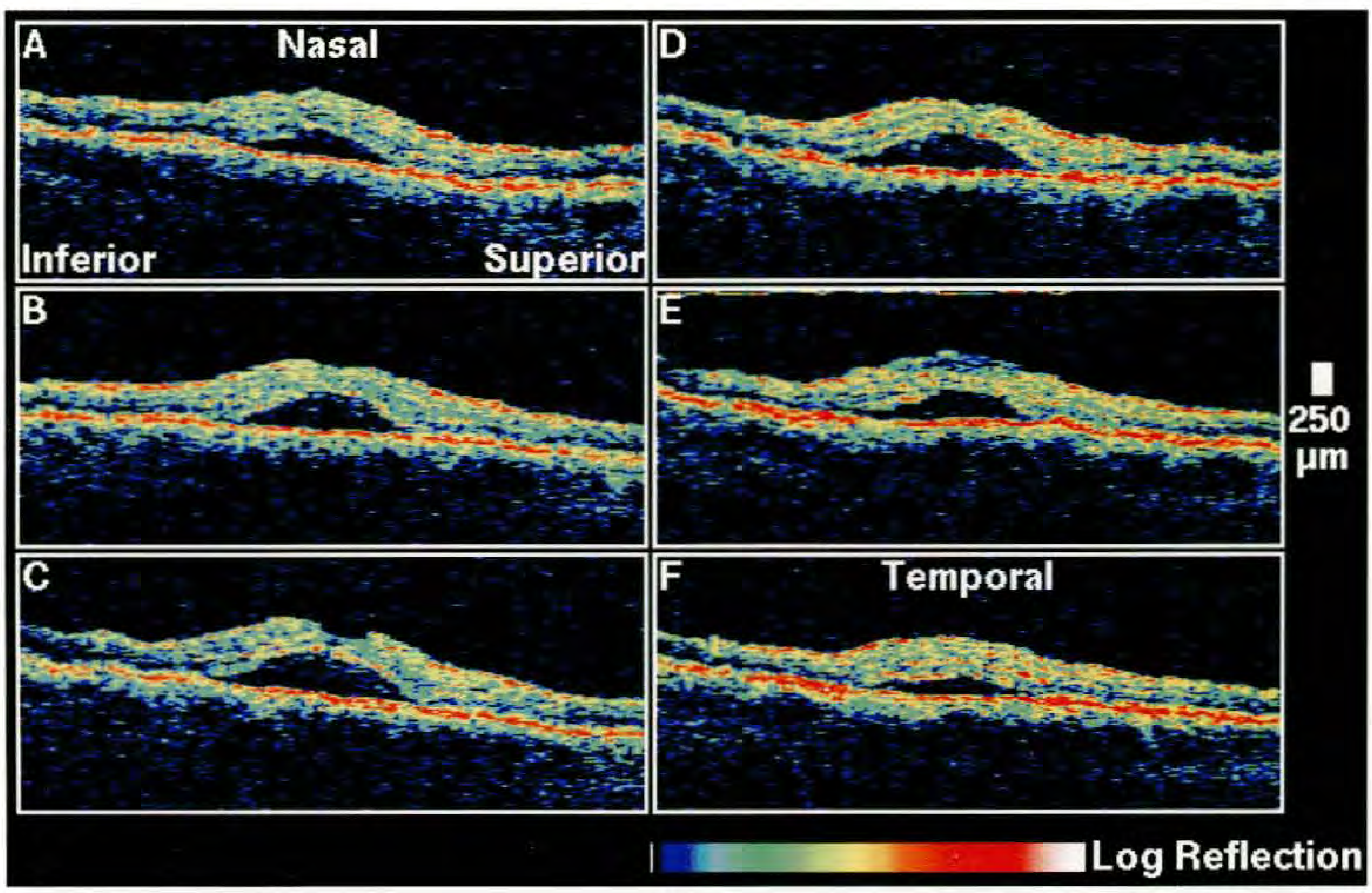

C

Case 7-4 continued

Follow-up Examination

Six weeks later, slit-lamp biomicroscopy (D) indicated that the detachment had resolved. There was a corresponding improvement in visual acuity to 20/40.

Follow-up Optical Coherence Tomography

A repeat sequence of vertical tomograms (E) showed a shallow neurosensory detachment and residual subretinal fluid that was significantly improved since the previous examination.

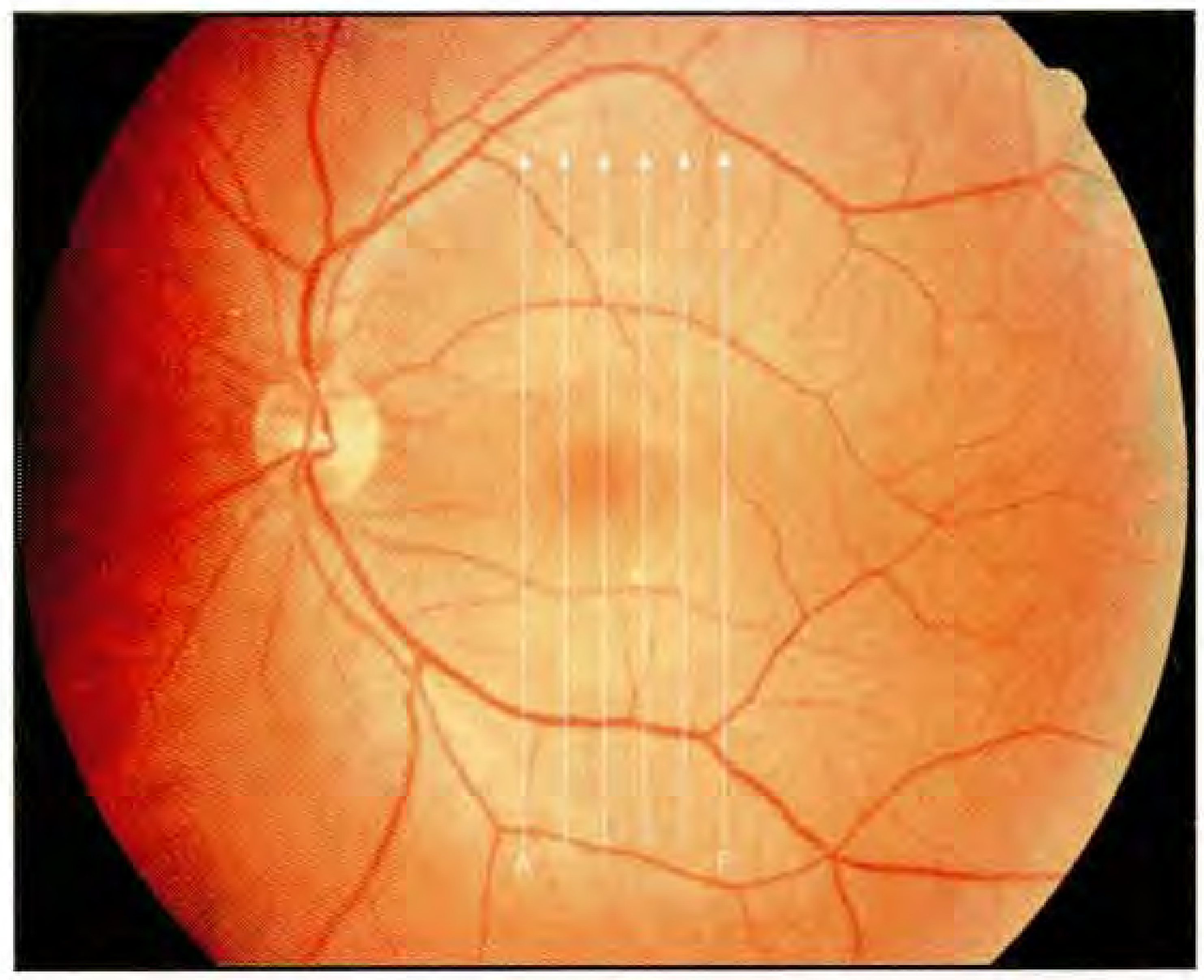

D

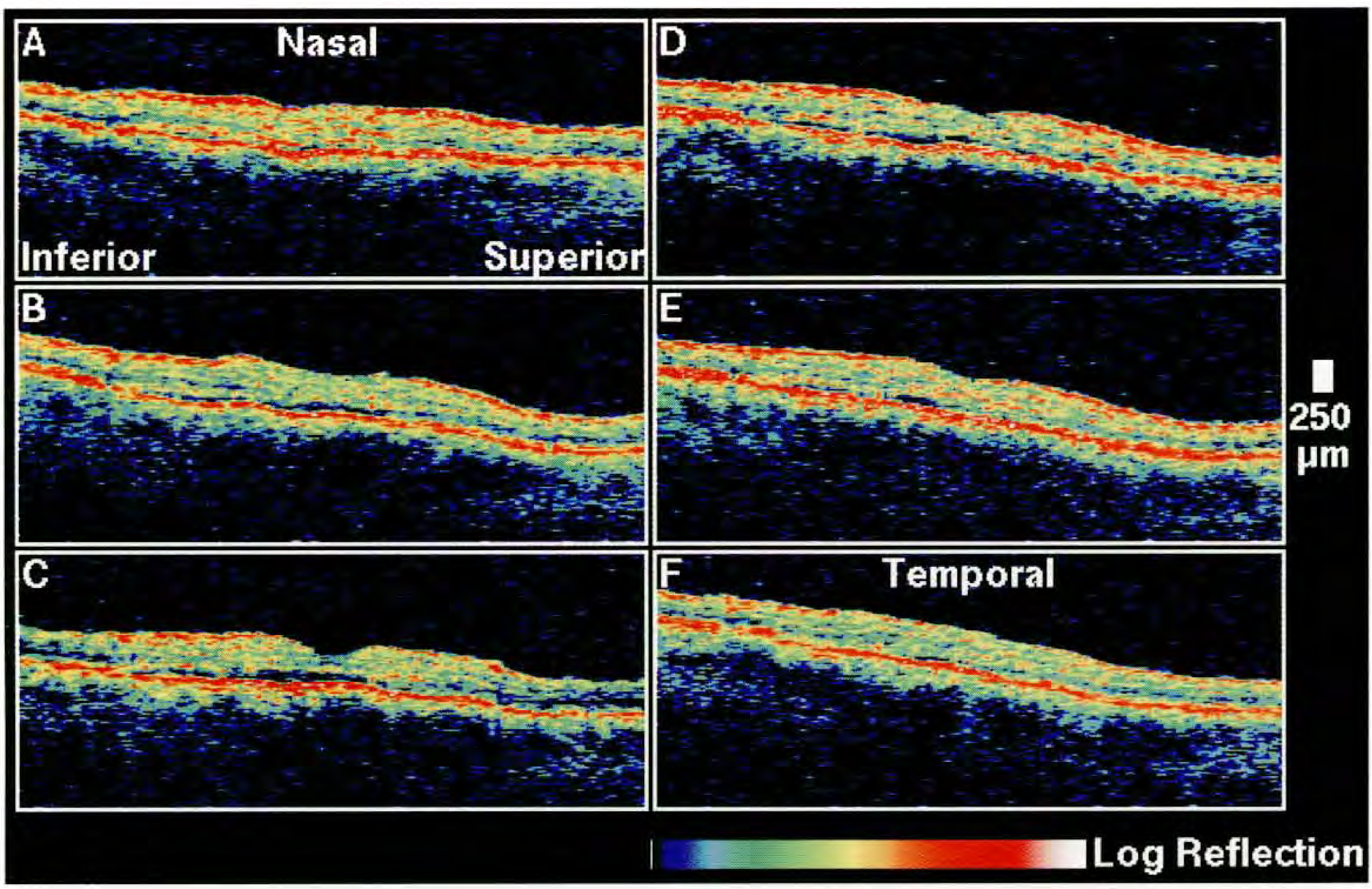

E

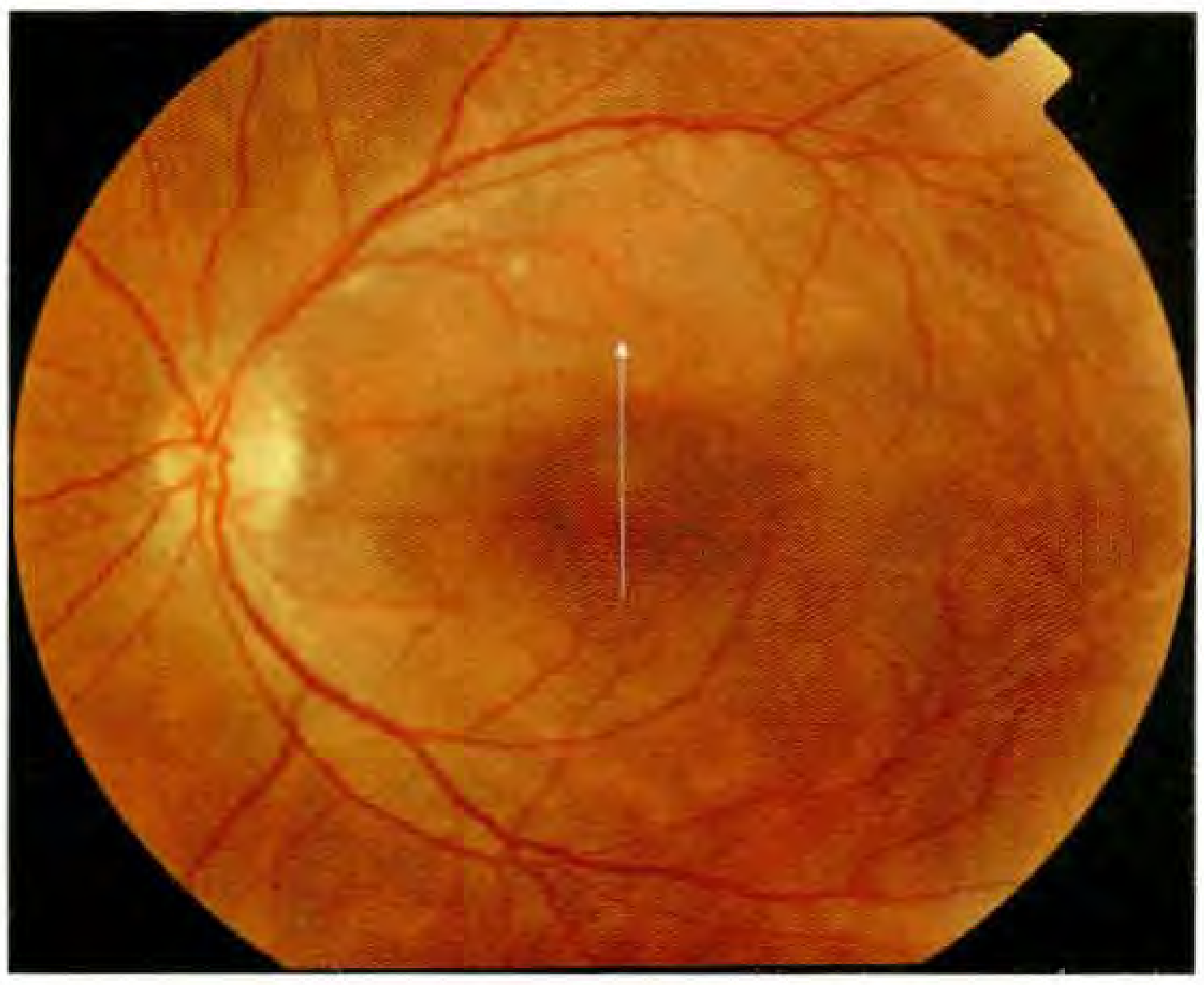

A

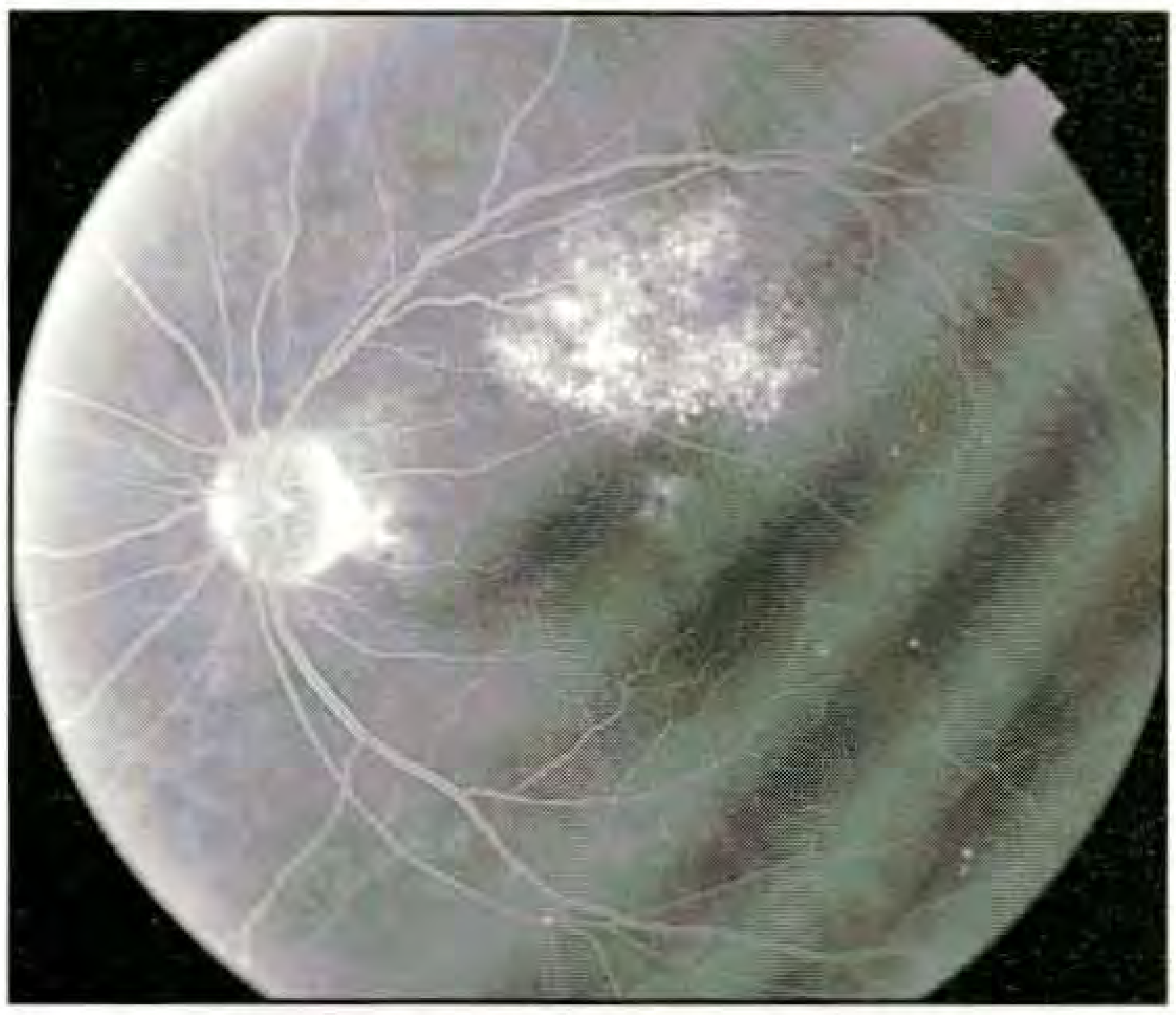

B

Case 7-5. Progression of Central Serous Chorioretinopathy

Clinical Summary

An 87-year-old man had a history of central serous chorioretiopathy in both eyes. The left eye had been treated with argon laser photocoagulation nine years earlier. He had noted a new onset of metamorphopsia in this eye over the past six months. Dilated fundus examination (A) showed a small hyperpigmented scar within a shallow neurosensory detachment superior to the fovea. Fluorescein angiography (B) showed two hyperfluorescent spots just superior to the fovea with no leakage in the late phase. A speckled pattern of hyperfluorescence was noted superior to the macula. The visual acuity was 20/20.

Optical Coherence Tomography

A vertical OCT image (C) taken just temporal to the fovea delineated two small neurosensory detachments with a height of approximately 70 µm. A horizontal tomogram (not shown) acquired directly through fixation showed a normal fovea with no subretinal fluid.

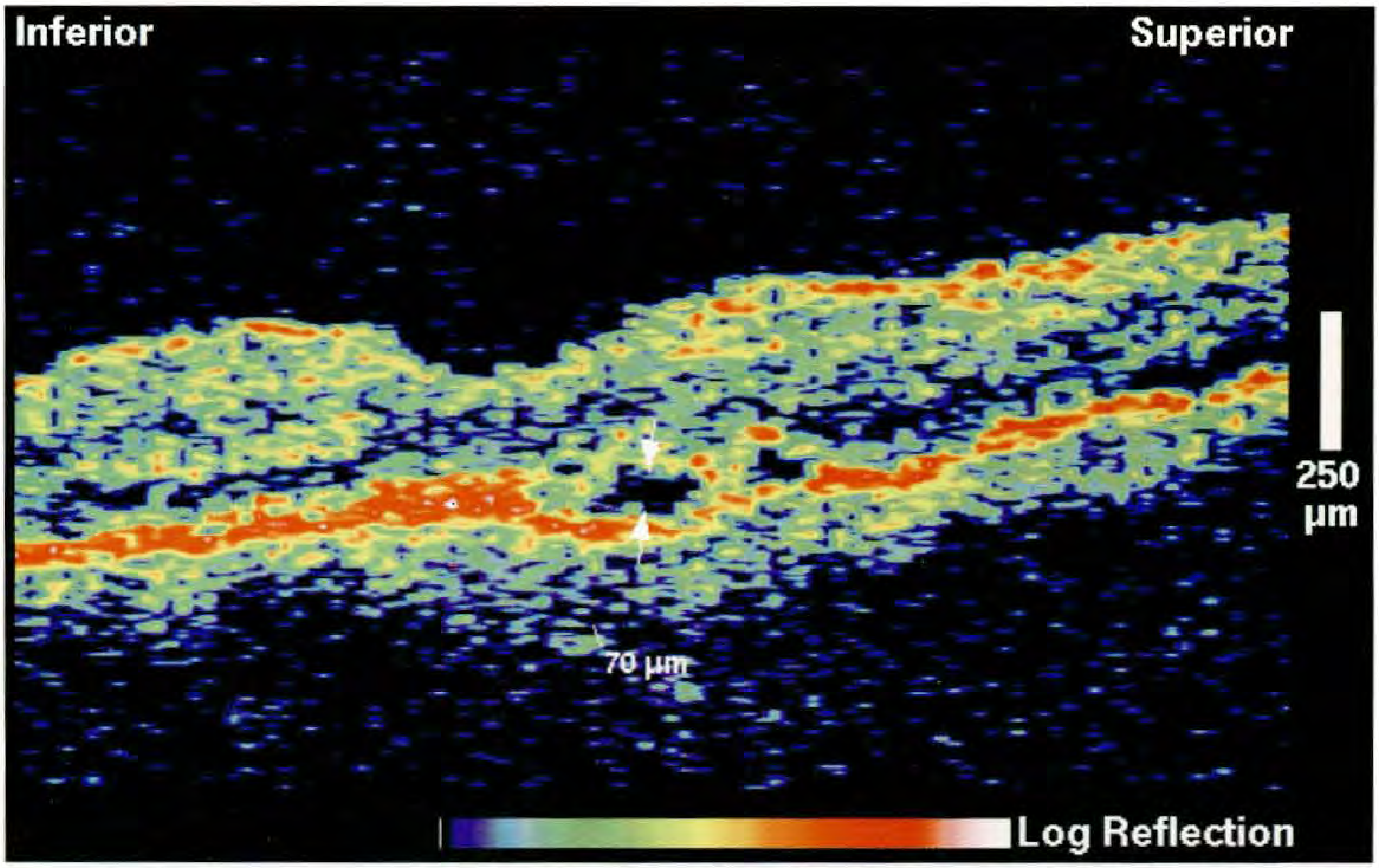

C

Case 7-5 continued

Follow-up Examination

The patient returned approximately five months later and slit-lamp biomicroscopy (D) of the left eye demonstrated increased subretinal fluid in the superotemporal macula involving the fovea. The visual acuity had declined to 20/30.

Optical Coherence Tomography

A repeat vertical tomogram (E; white line on D) taken slightly temporal to the fovea showed that the two previous neurosensory detachments had coalesced and had increased in height to 140 μm. Subretinal fluid was identified beneath the fovea. A horizontal image (F; black line on D) through the macula also displayed subretinal fluid accumulation temporal to and involving the fovea. The reflectivity from the photoreceptors beneath the fovea appeared increased.

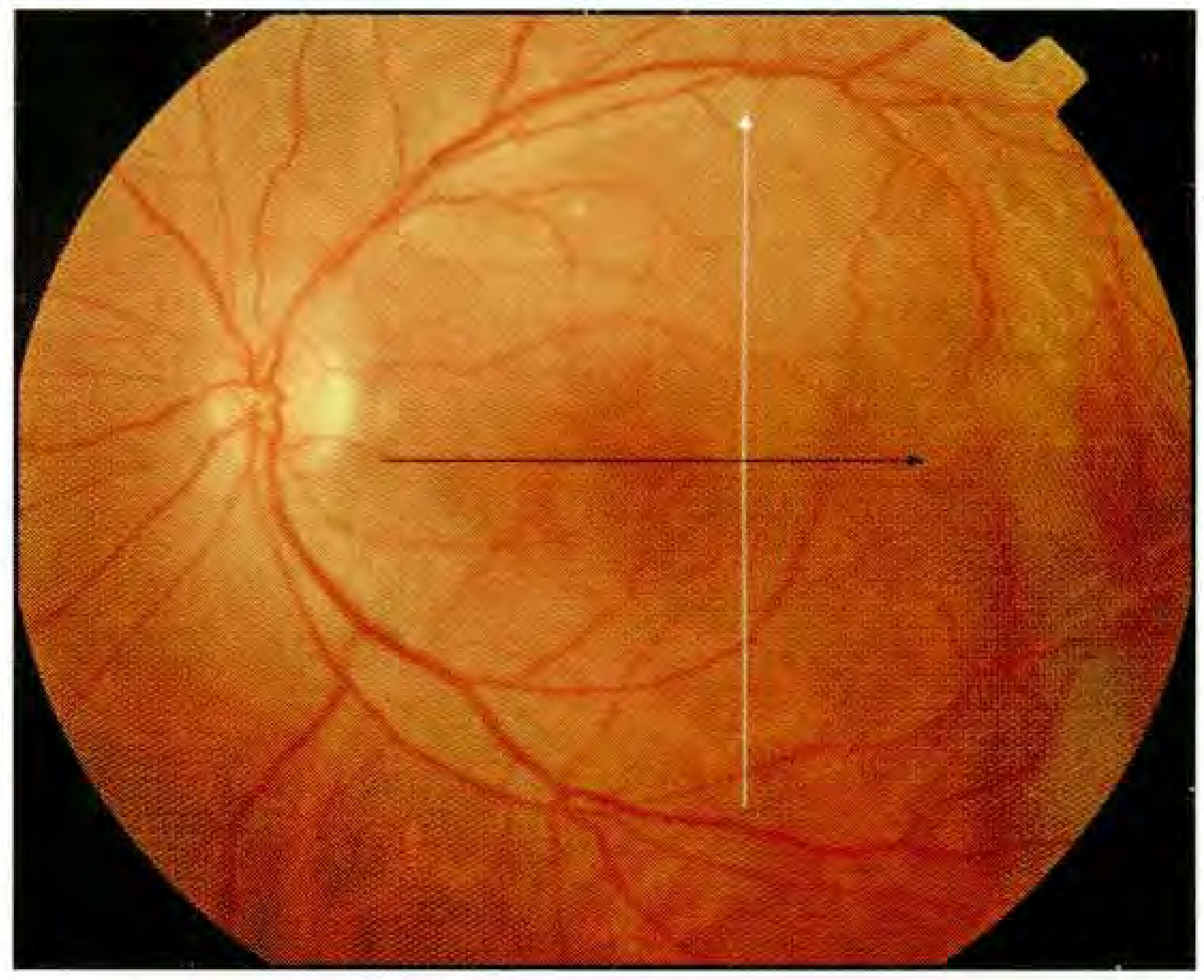

D

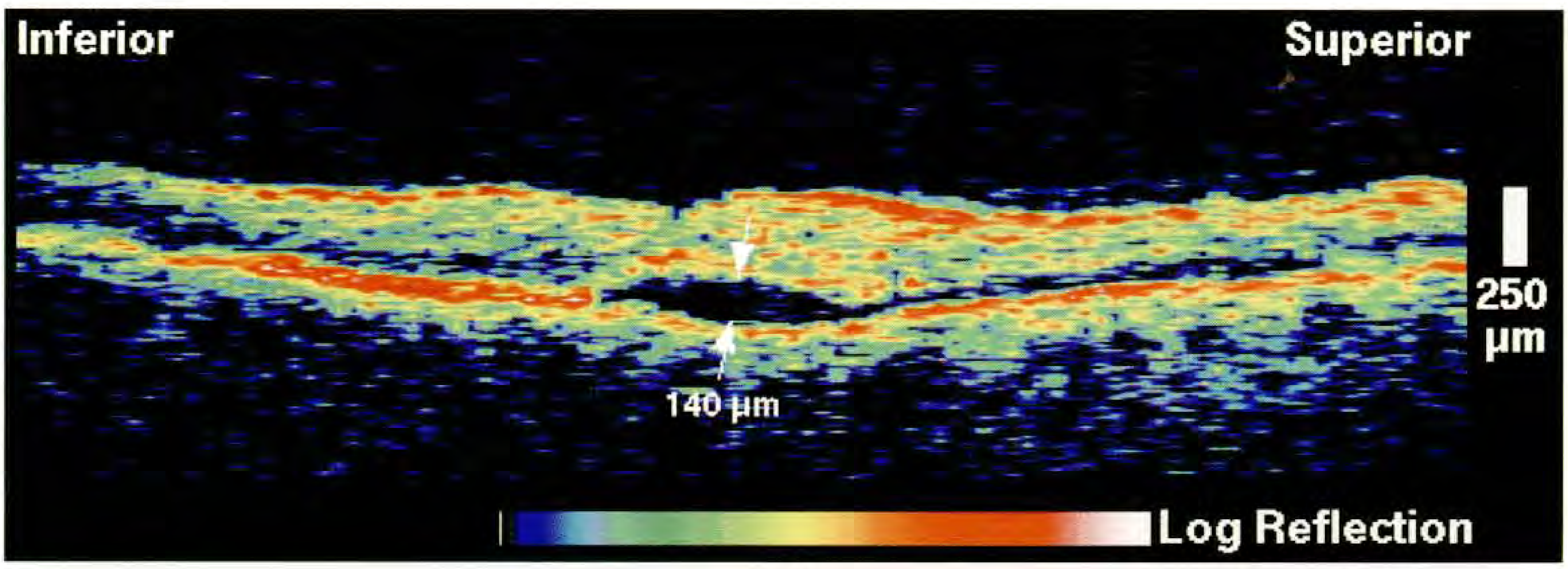

E

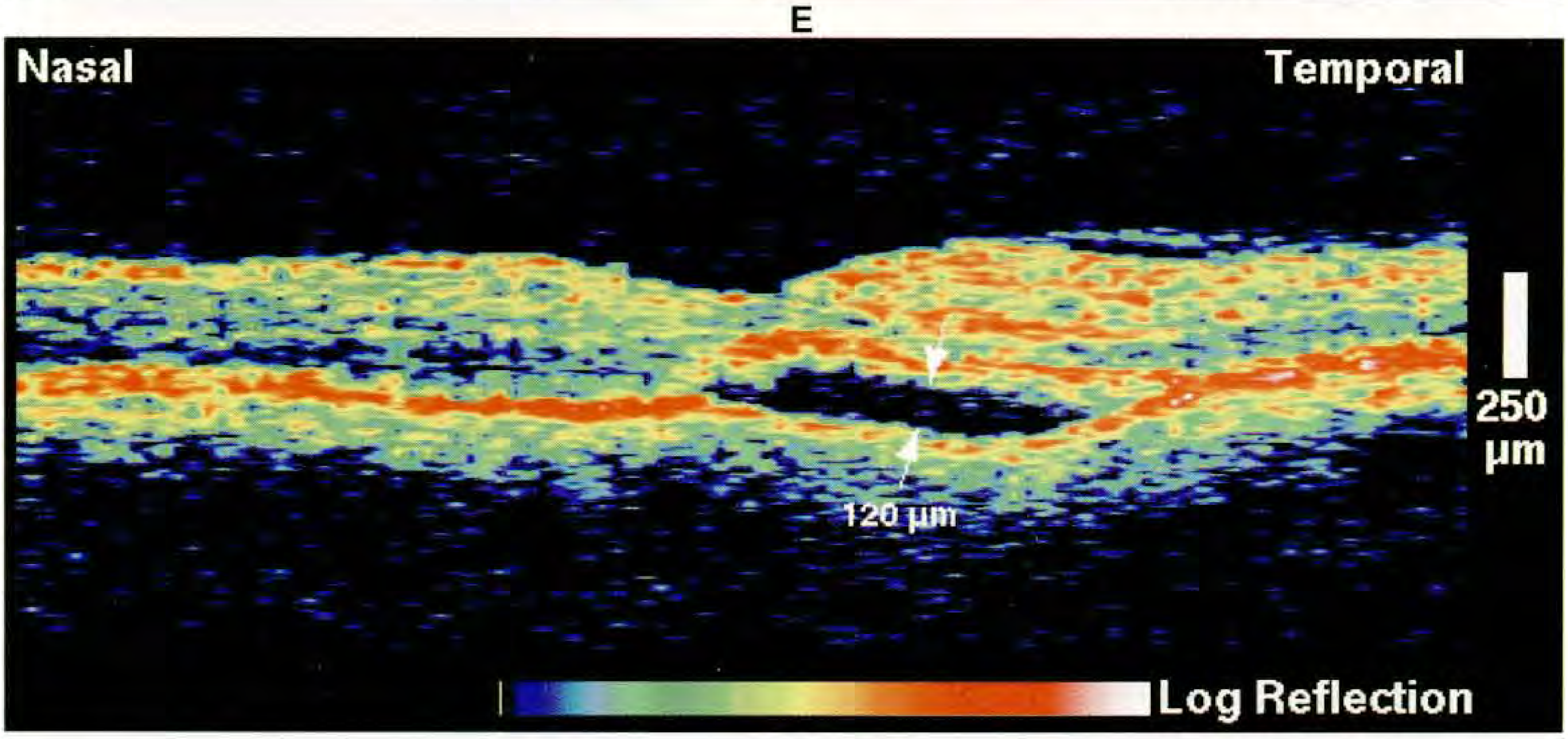

F

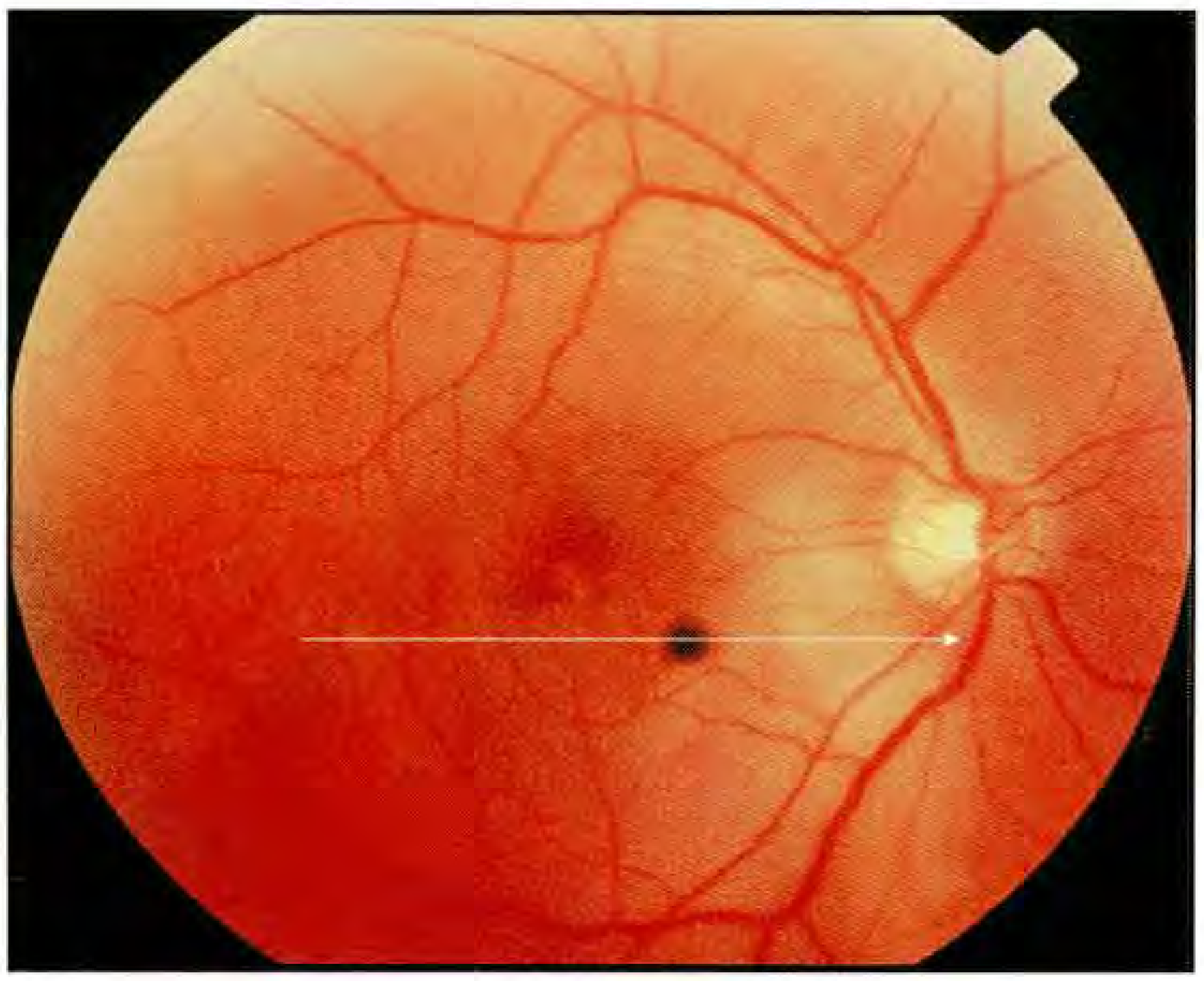

A

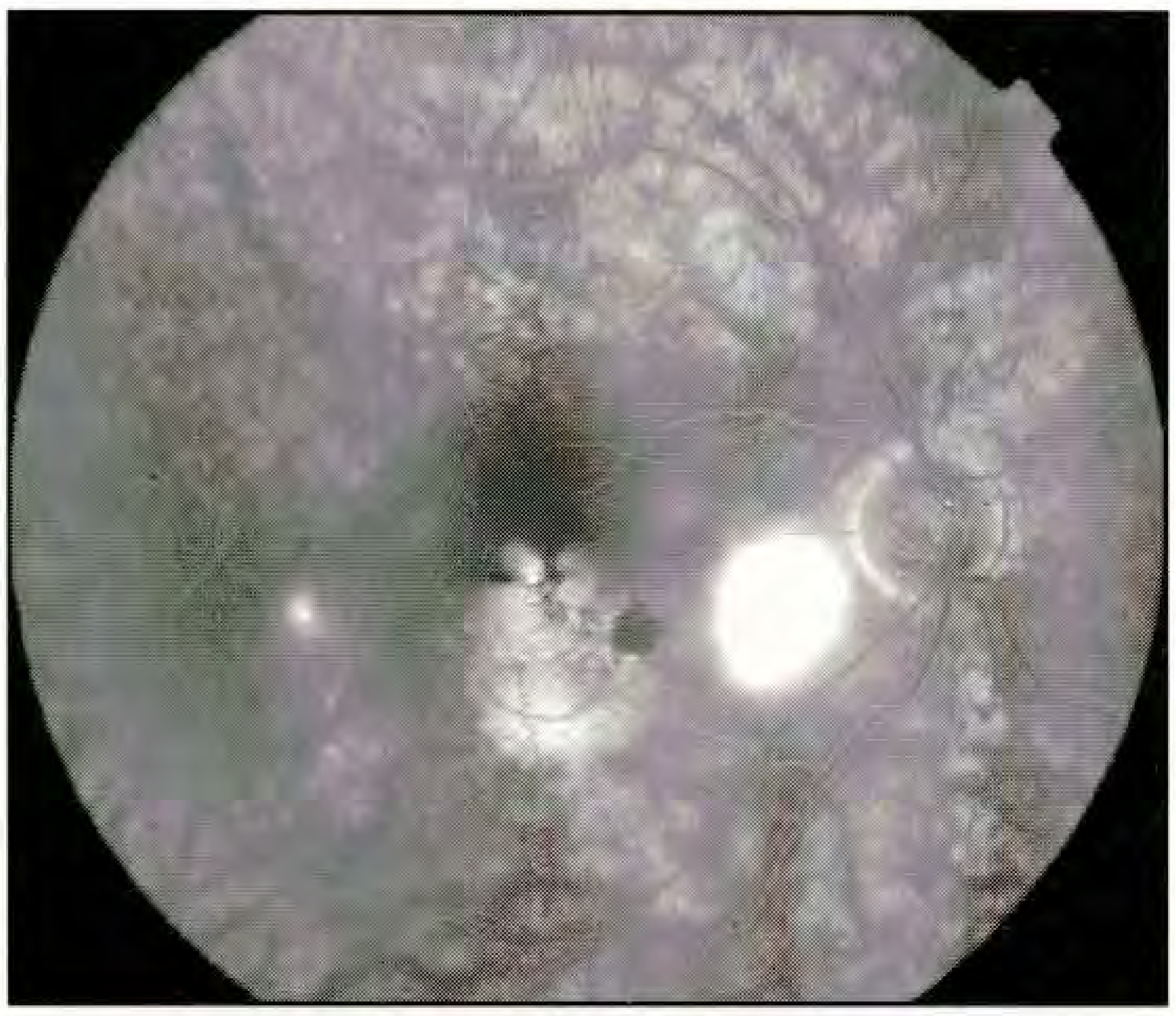

B

Case 7-6. Recurrent Central Serous Chorioretinopathy with Laser Treatment

Clinical Summary

A 45-year-old man with a history of central serous chorioretinopathy in his right eye was evaluated after he noticed increasingly blurred vision in this eye over the previous four weeks. He had received focal laser photocoagulation treatment one year earlier. His visual acuity on examination was 20/50, and indirect ophthalmoscopy (A) showed neurosensory detachments temporal to the optic disc and in the central macula. Mild pigment epithelial mottling was also noted in the central macula, and a focal area of pigment aggregation was described inferonasal to the fovea. Fluorescein angiography (B) showed three pinpoint areas of hyperfluorescence which were temporal to the macula, in the superior macula, and temporal to the disc. The fluorescence increased in size and intensity as the angiogram progressed consistent with central serous chorioretinopathy. The area temporal to the disc displayed significant late leakage. A larger, mild patch of hyperfluroescence was noted in the central macula which increased in intensity but not size during the late phases of the angiogram consistent with a pigment epithelial detachment. A hypofluorescent spot nasal to the macula corresponded to the region of pigment aggregation.

Optical Coherence Tomography

A horizontal tomogam (C) was acquired inferior to the center. A pigment epithelial detachment (3) was noted in the middle of the image. Three neurosensory detachments (1,2,5) were also observed corresponding to the areas of pinpoint hyperfluorescence seen on fluorescein angiography. The area of pigment aggregation (4) appeared as a focal thinning of the neurosensory retina combined with enhanced backscattering from the red band corresponding to the retinal pigment epithelium.

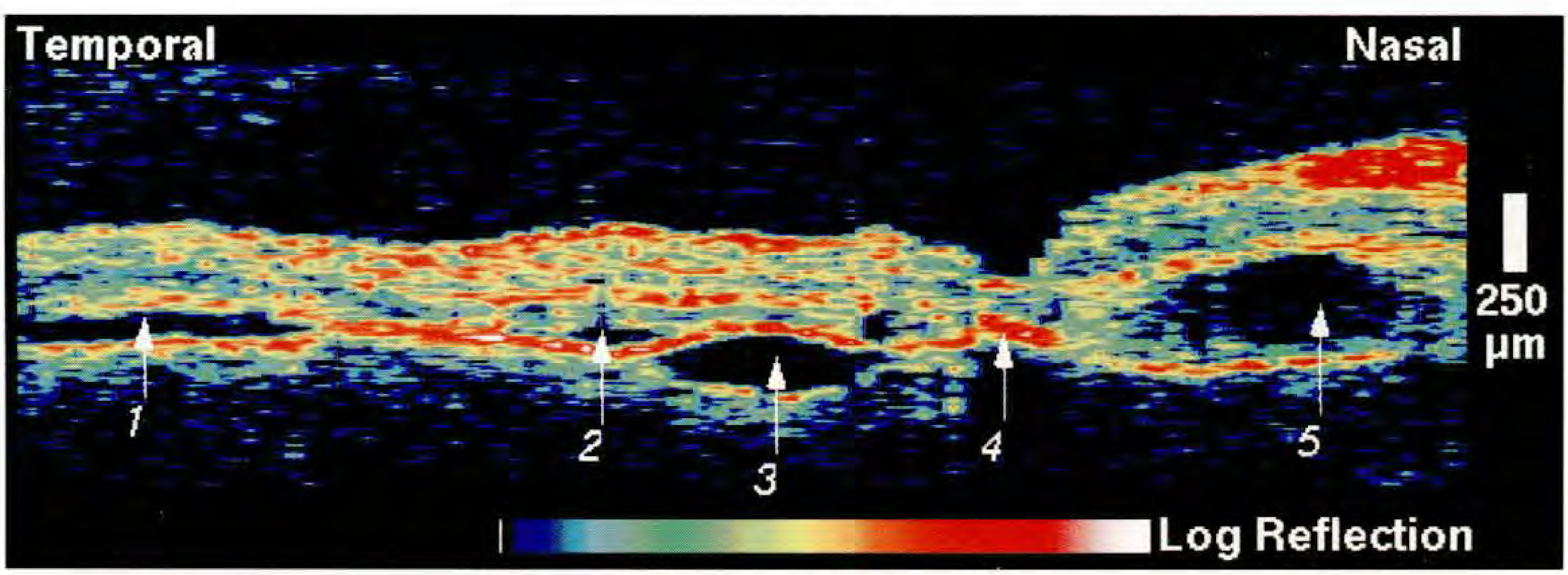

C

Case 7-6 continued

Follow-up Examination

The patient received focal dye yellow laser photocoagulation treatment and was seen in follow-up one month later with an improvement in visual acuity to 20/40. Slit-lamp examination (D) revealed a pigment epithelial detachment in the central macula, but no subretinal fluid temporal to the optic disc could be detected. Fluorescein angiography (E) showed decreased hyperfluorescence compared to the previous exam temporal to the disc and temporal to the macula. The hyperfluorescence in the central macula, however, remained essentially unchanged.

Follow-up Optical Coherence Tomography

A follow-up OCT image (F) demonstrated that all three of the previous neurosensory detachments had resolved in cross-section. The pigment epithelial detachment and region of pigment aggregation were still observed.

D

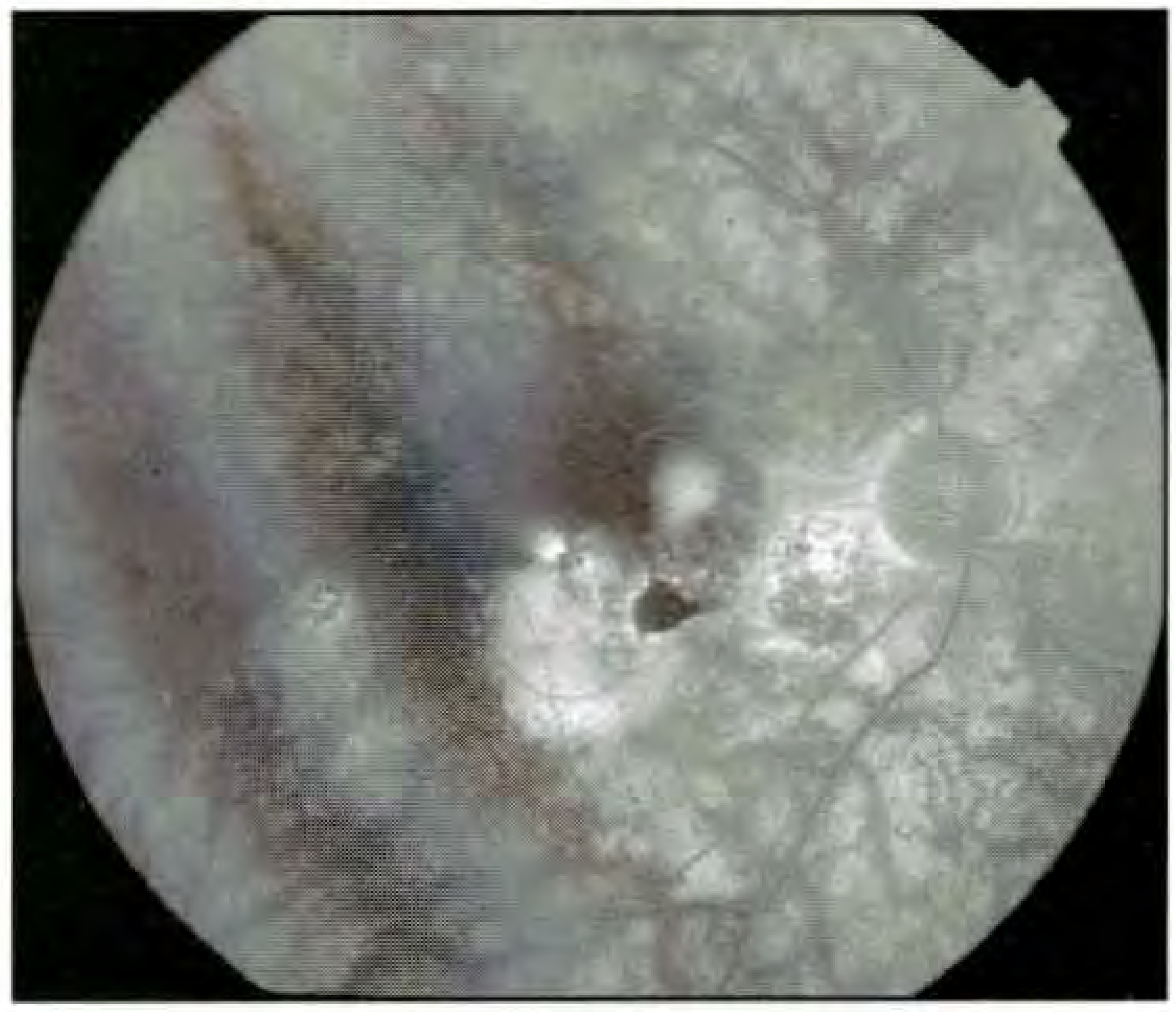

E

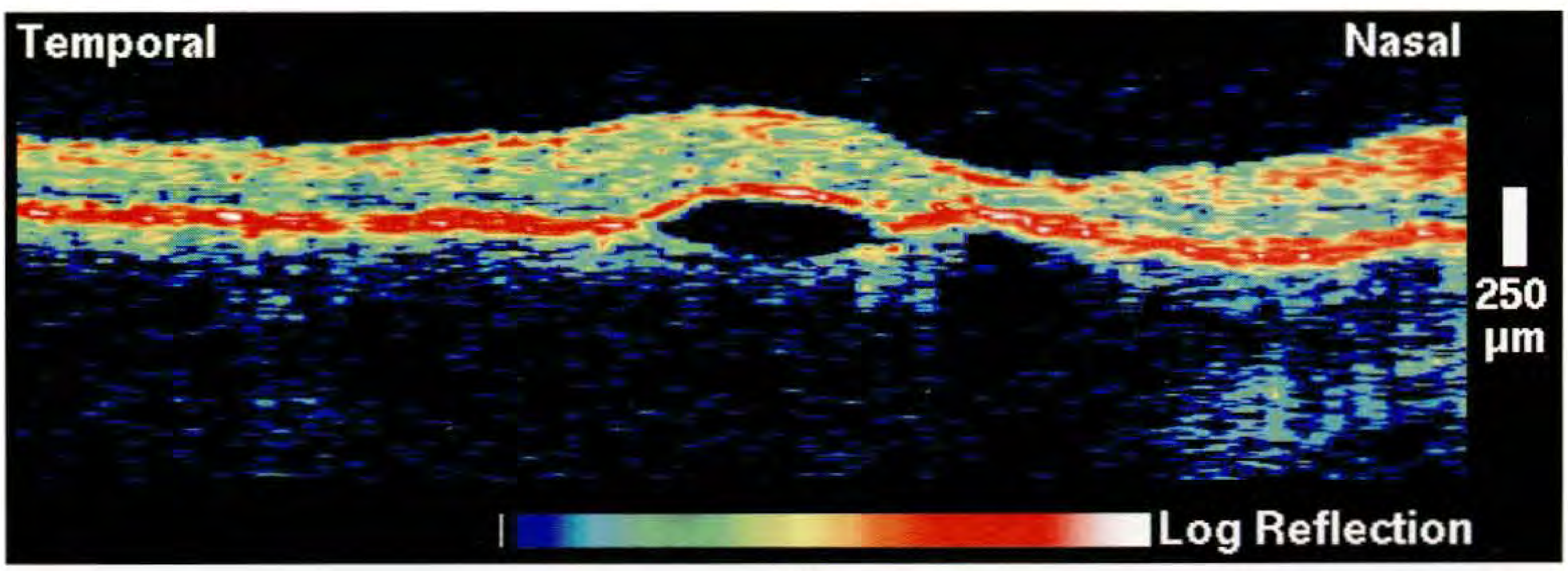

F

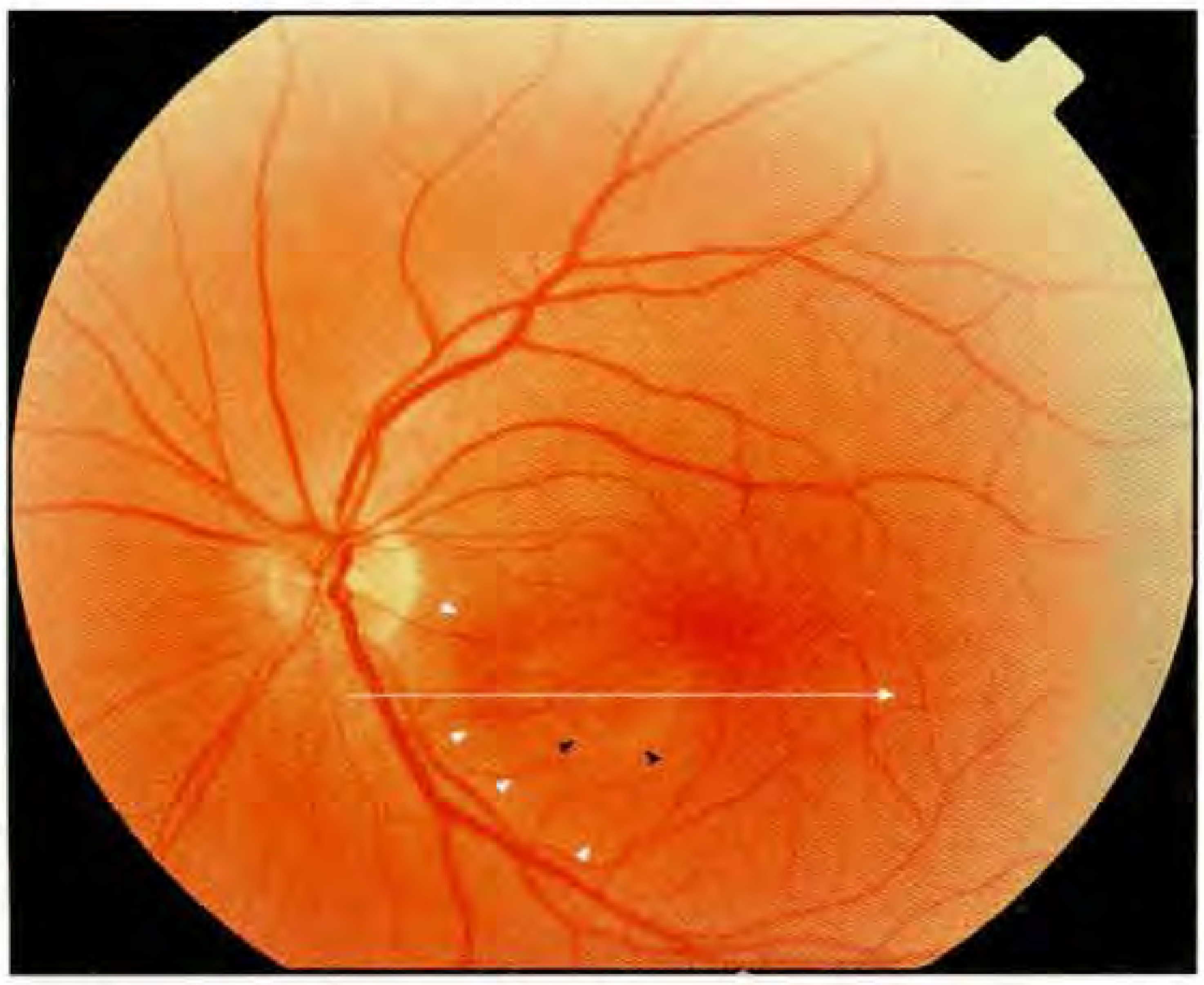

A

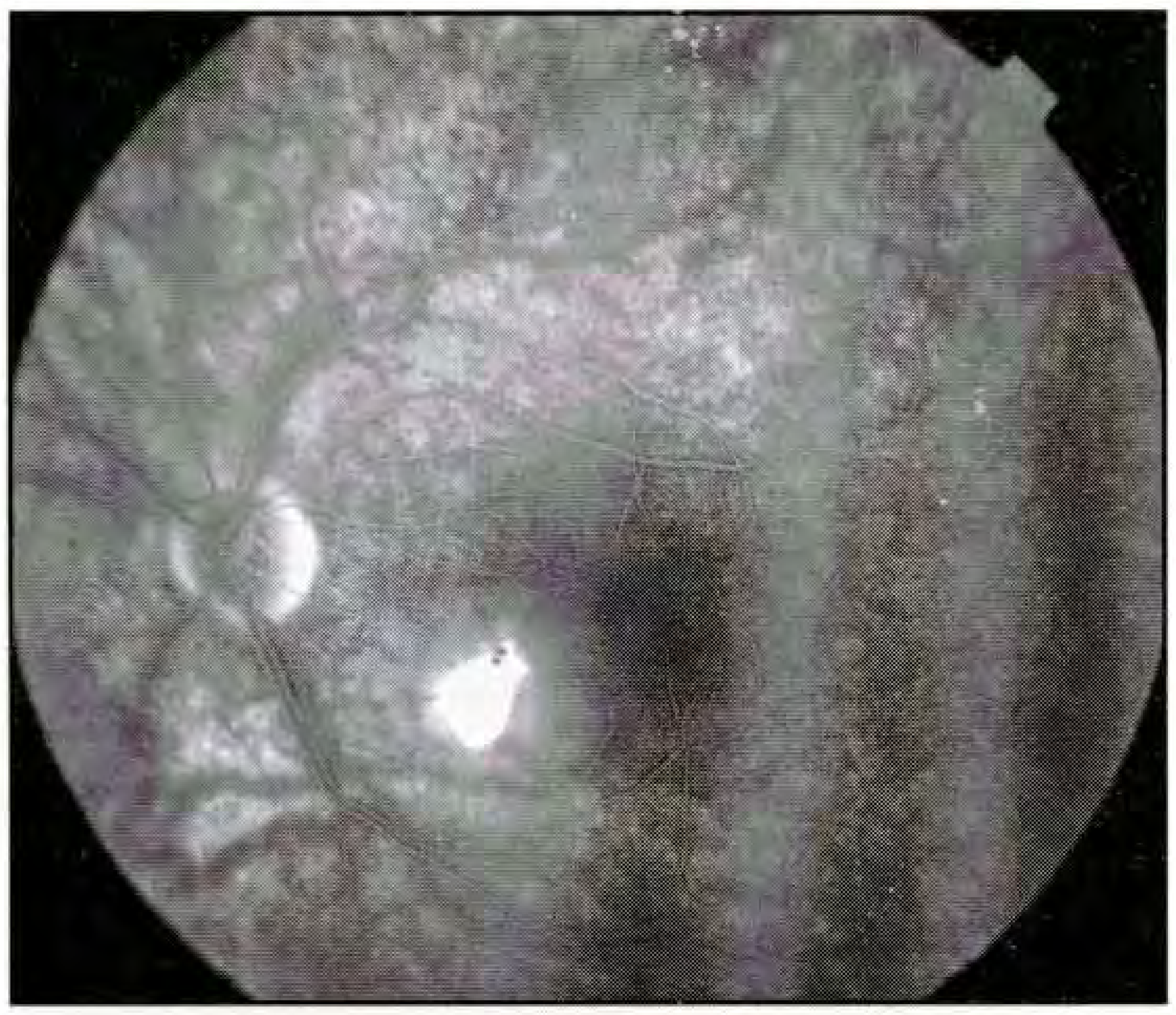

B

Case 7-7. Central Serous Chorioretinopathy

Clinical Summary

A 39-year-old man noticed a brown spot in his left visual field four days earlier which was followed by reduced visual acuity and a brown discoloration in his superior visual field. His visual acuity was 20/50 in the left eye. Dilated fundus examination (A) revealed a pigment epithelial detachment inferonasal to the fovea with a collection of surrounding subretinal fluid. Fluorescein angiography (B) showed a hyperfluorescent region which increased in intensity but not size as the study progressed consistent with a pigment epithelial detachment.

Optical Coherence Tomography

OCT (C) confirmed the presence of broad neurosensory detachment surrounding a localized detachment of the pigment epithelium. As compared to the neurosensory detachment, the detached retinal pigment epithelium more deeply shadowed the reflected signal originating from the choroid below and exhibited sharper margins.

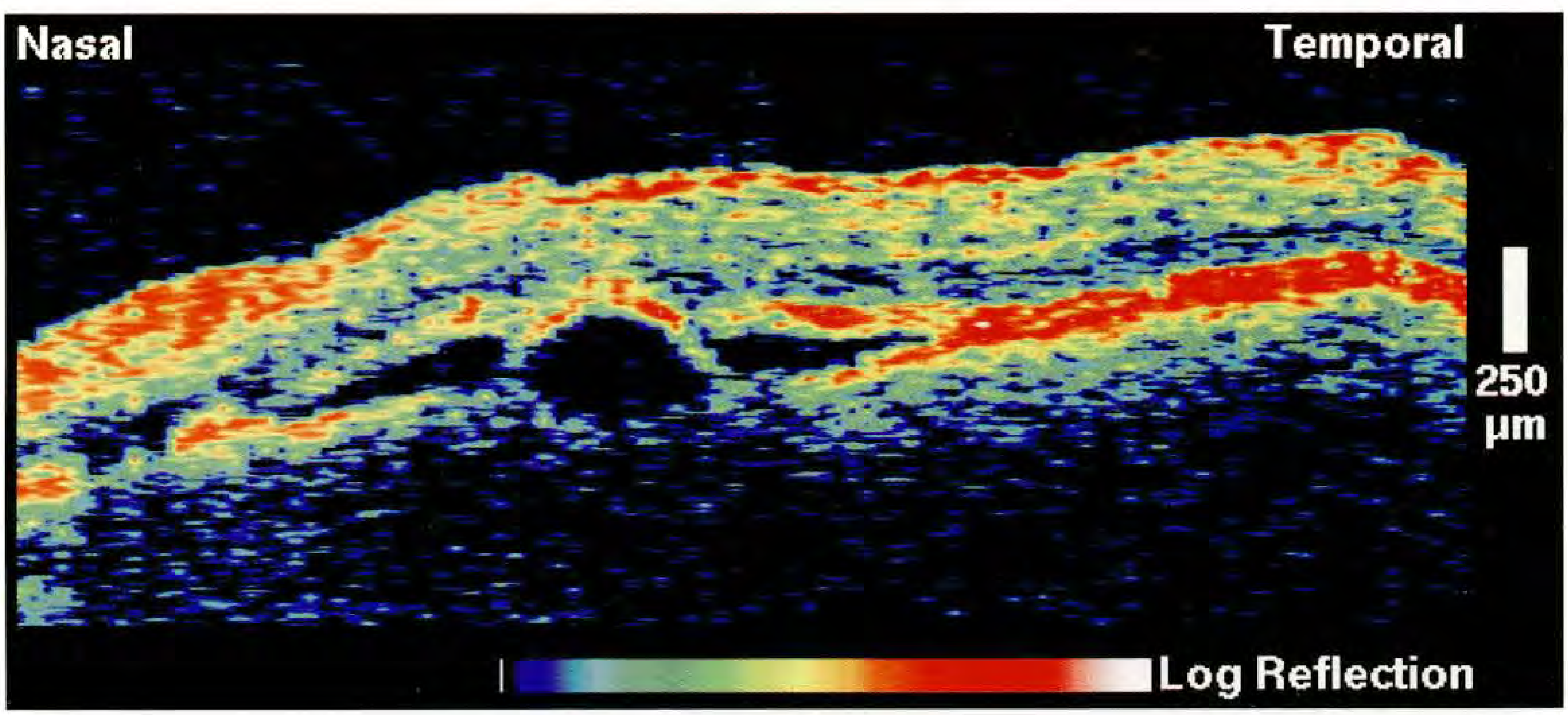

C

Case 7-7 continued

Follow-up Examination

The patient returned five months later and noted no change in his vision. On examination, however, the visual acuity in his left eye had improved from 20/50 to 20/20. Slit-lamp biomicroscopy (D) demonstrated a reduction in the subretinal fluid accumulation surrounding the pigment epithelial detachment.

Follow-up Optical Coherence Tomography

A repeat horizontal tomogram (E) showed that the pigment epithelial detachment had not changed; however, there was a reduction in the neurosensory detachment. Residual subretinal fluid was identified that was not visible on dilated fundus examination.

D

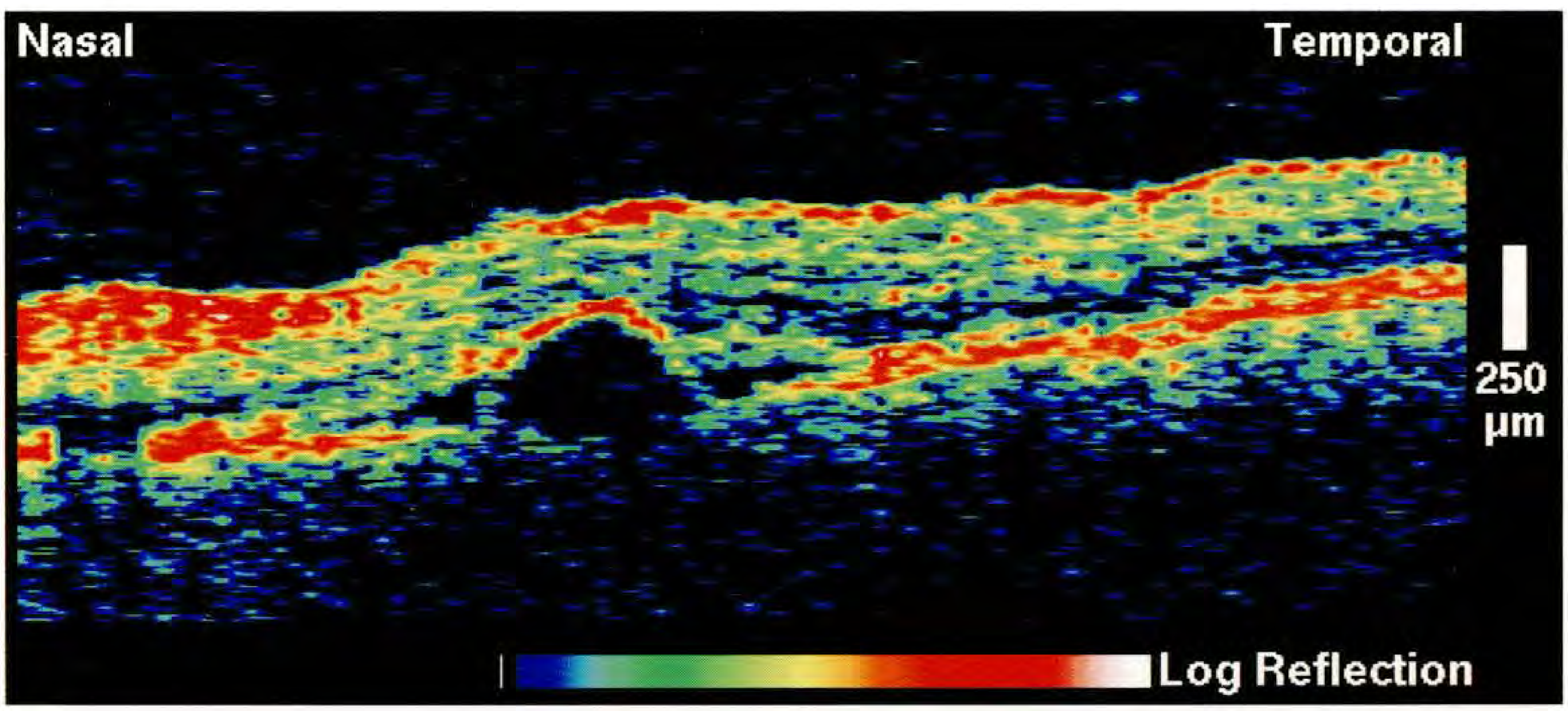

E

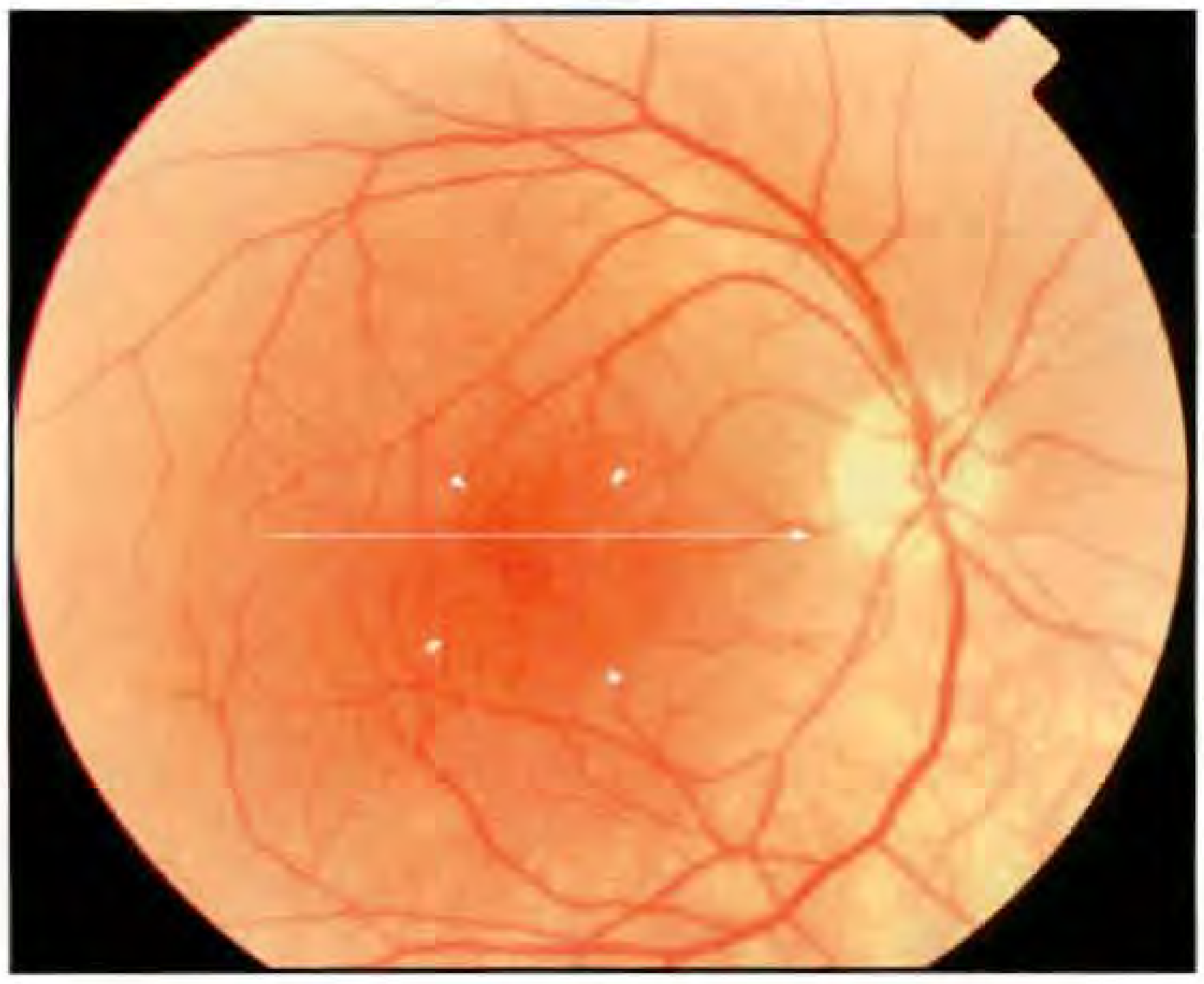

A

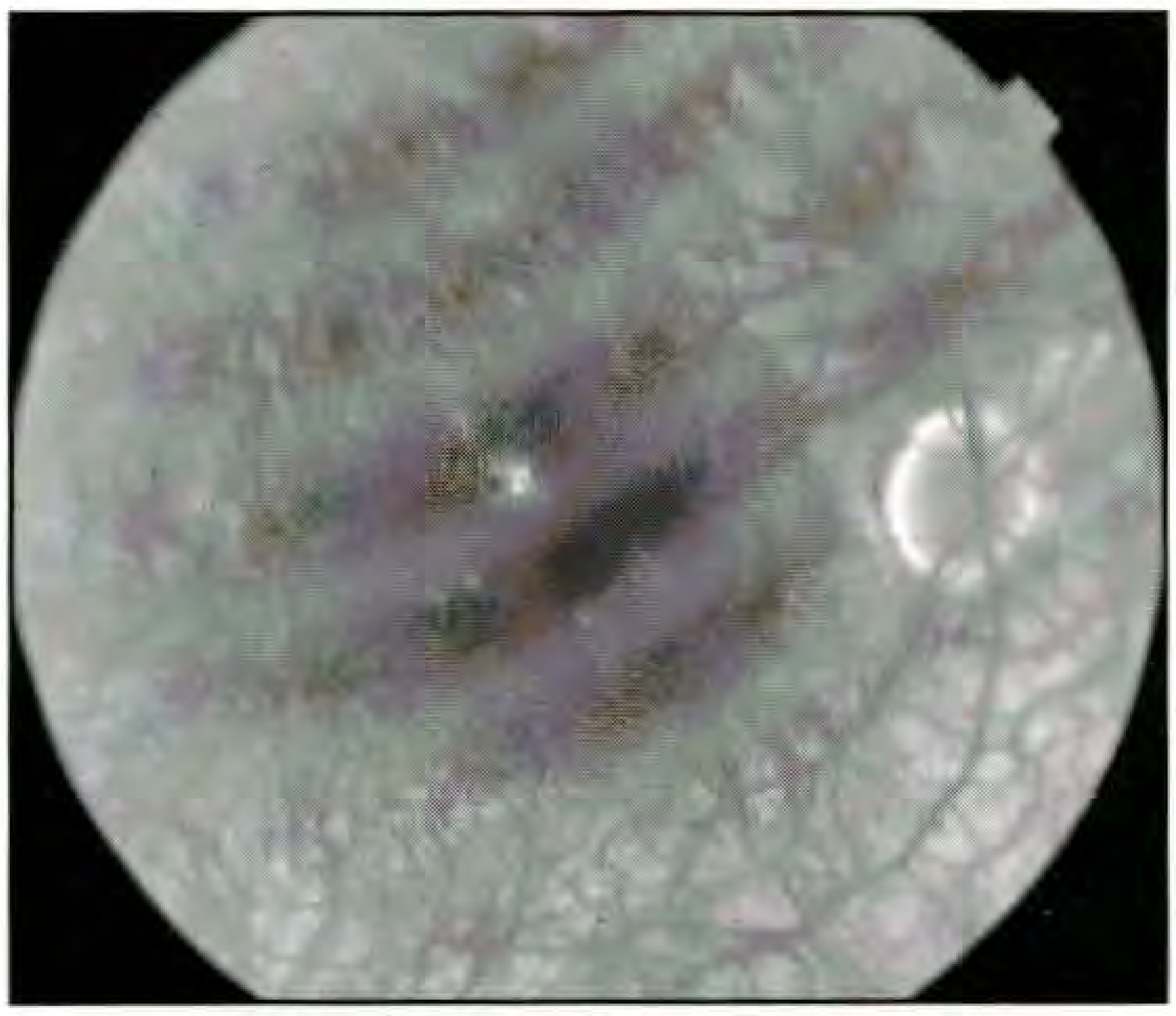

B

Case 7-8. Central Serous Chorioretinopathy and Retinal Cyst

Clinical Summary

A 50-year-old man had experienced a sudden onset of vision loss one week prior to evaluation. On examination, his visual acuity was 20/40 in the right eye and slit-lamp biomicroscopy (A) showed a collection of subretinal fluid in the macula. A hyperfluorescent spot superotemporal to the fovea was identified on fluorescein angiography (B), consistent with central serous chorioretinopathy.

Optical Coherence Tomography

An OCT image (C) obtained superior to the fovea displayed the neurosensory detachment which had a height of 130 µm. A large intraretinal cyst was also visible temporal to the region of subretinal fluid accumulation.

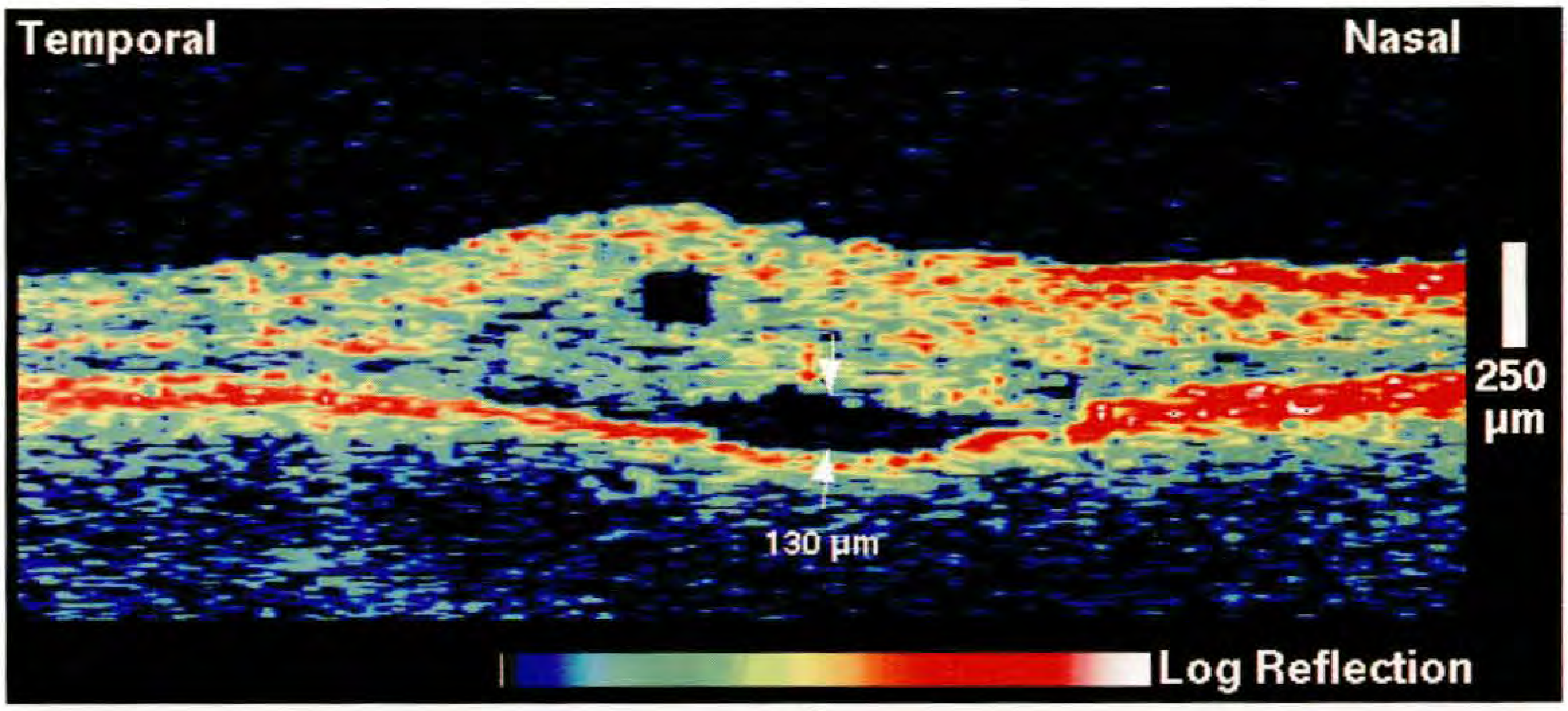

C

Case 7-8 continued

Follow-up Examination

Two months later, the patient's visual acuity in the right eye had improved to 20/25. Fundus examination (D) revealed a substantial decrease in the subretinal fluid.

Optical Coherence Tomography

A repeat OCT tomogram (E) also showed resolution of the neurosensory detachment. A flattening of the intraretinal cyst was also noted.

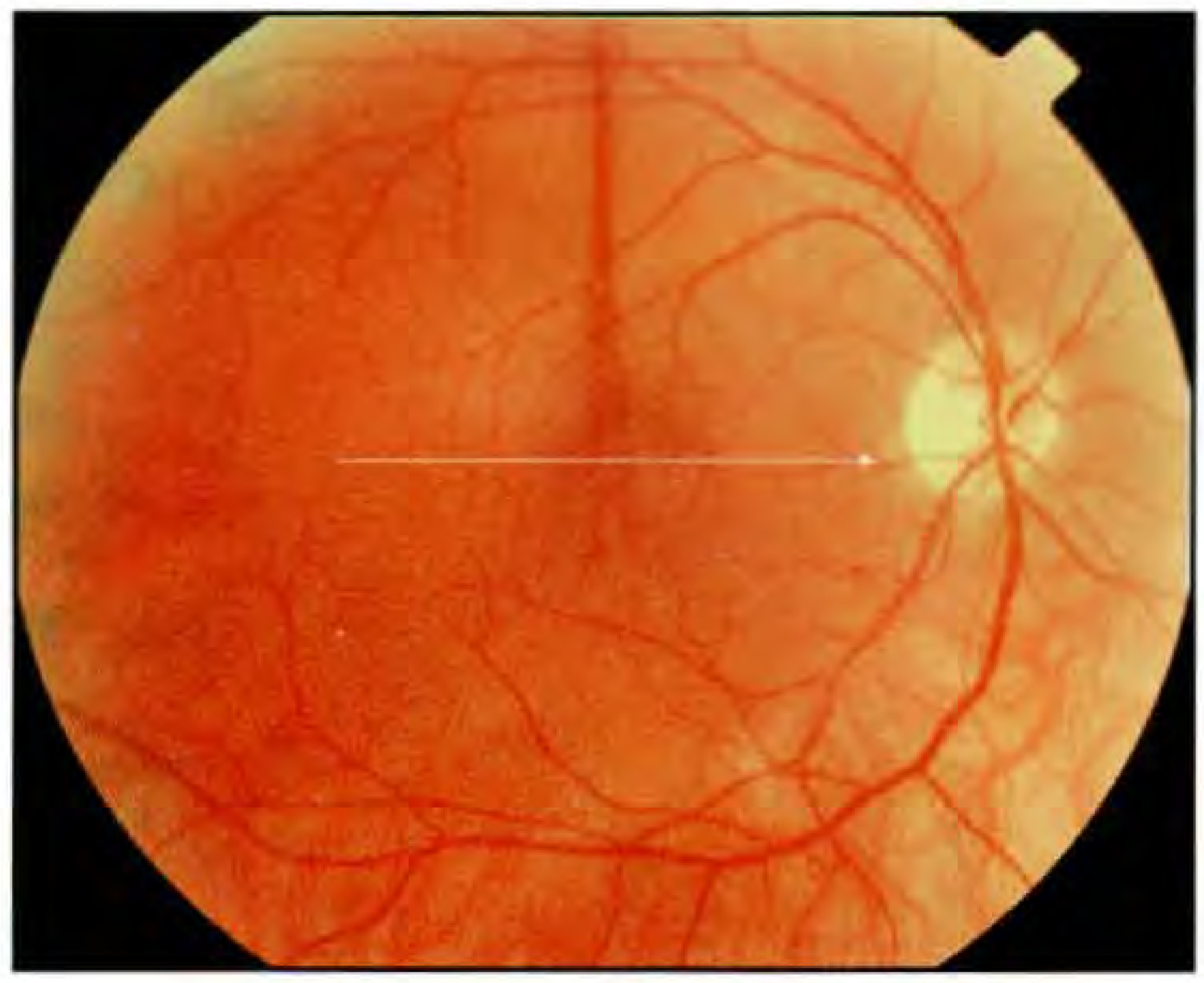

D

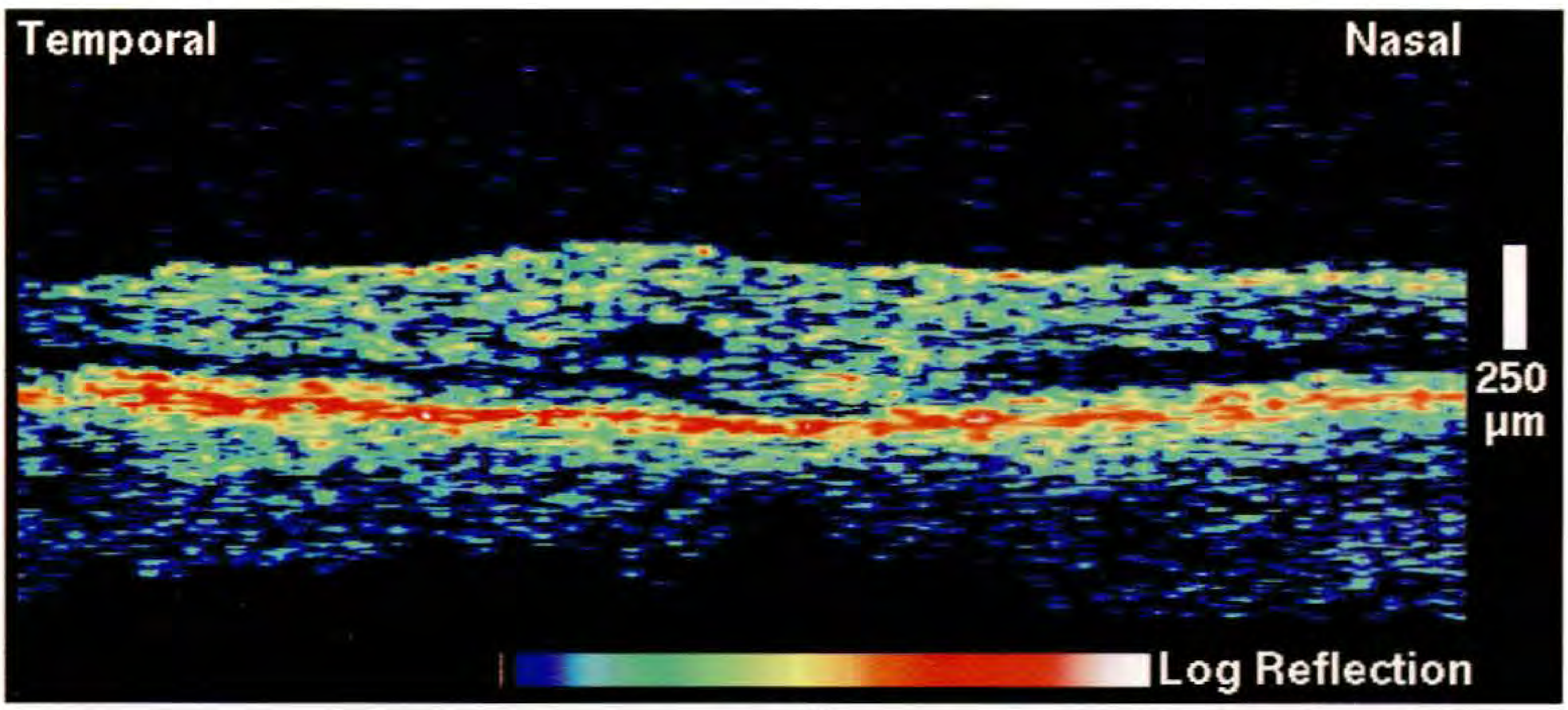

E

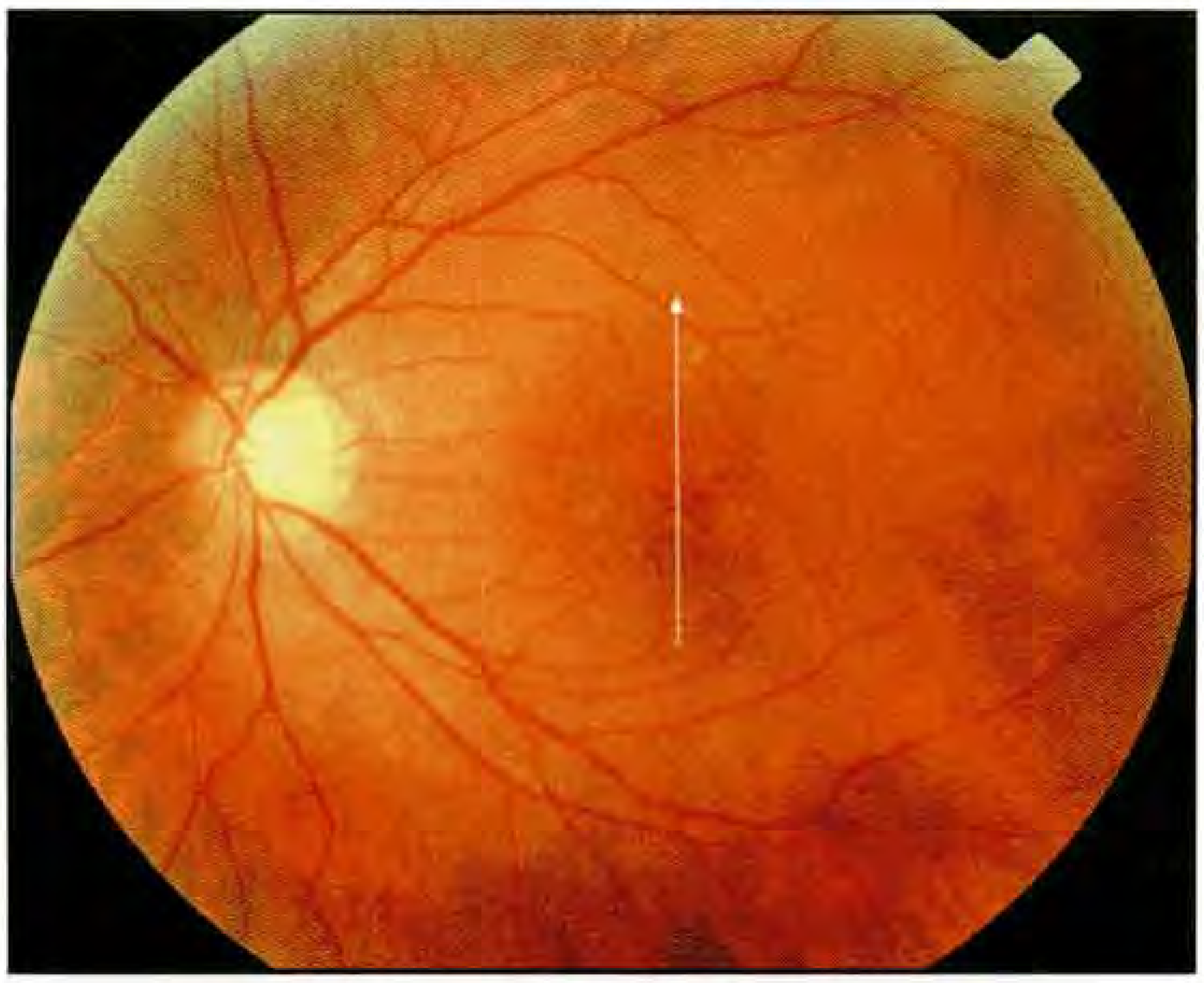

A

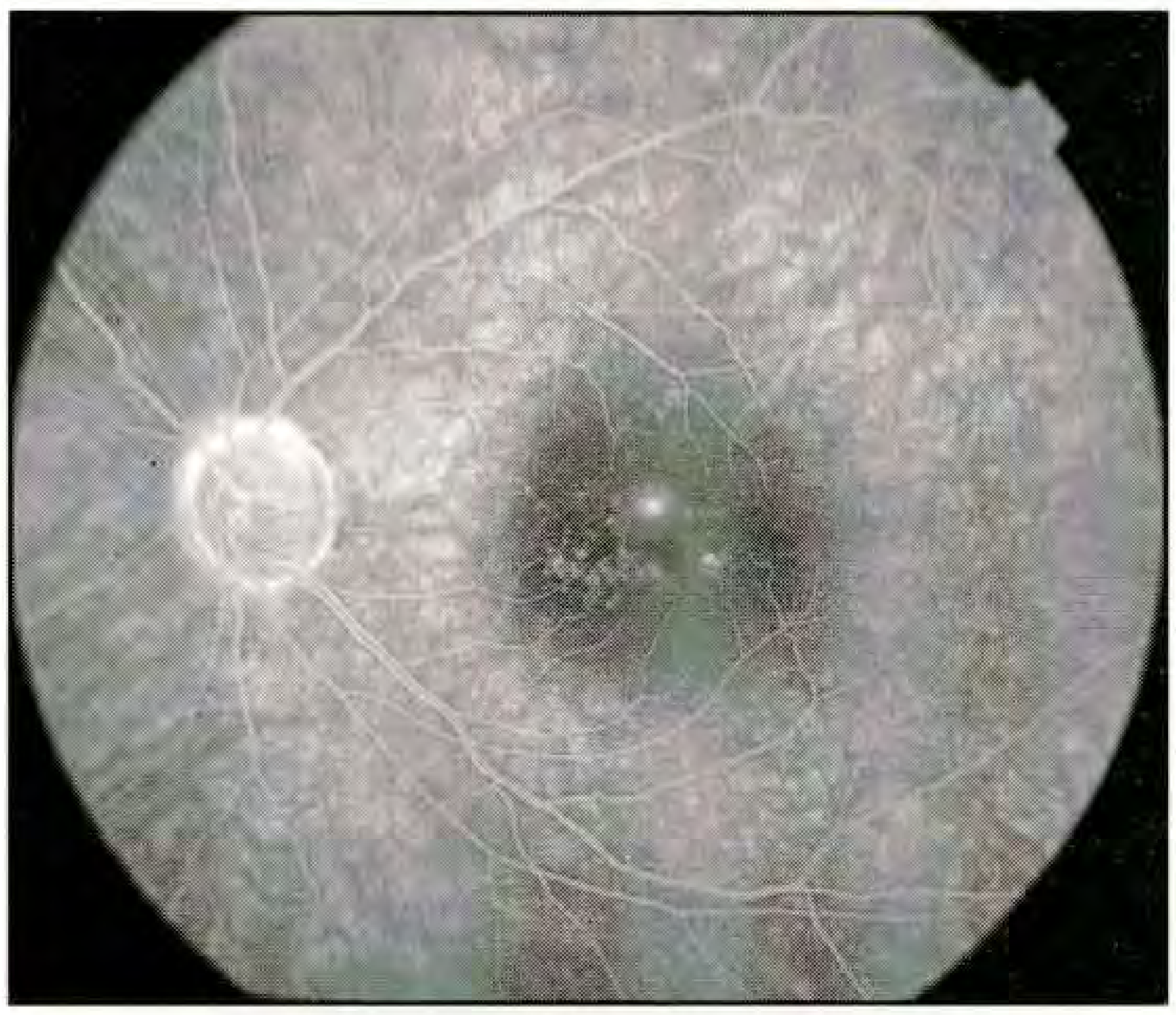

B

Case 7-9. Central Serous Chorioretinopathy

Clinical Summary

A 50-year-old woman was referred for micropsia on Amsler grid testing of her left eye, and mild drusen and pigmentary changes in the macula. The referring ophthalmologist was concerned about possible choroidal neovascularization secondary to age-related macular degeneration. Her visual acuity was 20/20. Slit-lamp biomicroscopy (A) showed a small area of serous retinal elevation just superotemporal to the fovea and pigment epithelial changes within the macula. Two focal hyperfluorescent spots were observed in the macula on fluorescein angiography (B). Faint hyperfluorescence surrounded these two spots on late views consistent with a serous retinal detachment.

Optical Coherence Tomography

A vertical OCT tomogram (C) taken directly through the fovea showed a small, 90 μm elevation of the neurosensory retina with no evidence of intraretinal edema, consistent with a diagnosis of central serous chorioretinopathy. A thickening or disruption of the reflective band corresponding to the retinal pigment epithelium and choriocapillaris was not observed in the image which was evidence against the diagnosis of choroidal neovascularization.

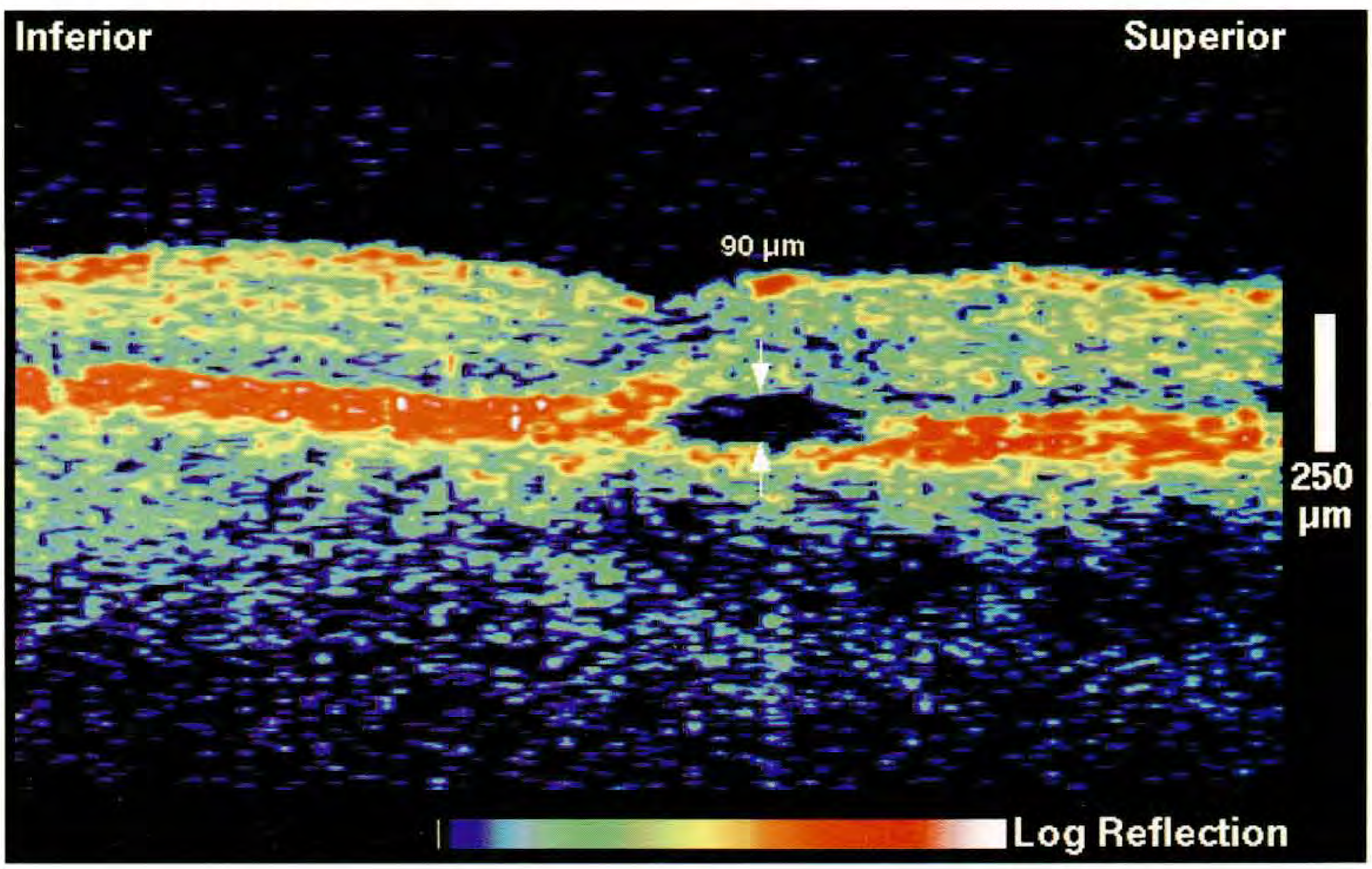

C

Case 7-10. Central Serous Chorioretinopathy

Clinical Summary

A 45-year-old man with a history of recurrent central serous chorioretinopathy had recently noticed a black spot in his left visual field. His visual acuity in the left eye on examination was 20/20; however, slit-lamp biomicroscopy (A) revealed a collection of subretinal fluid temporal to the optic disc. Fluorescein angiography (B) displayed a hyperfluorecent spot temporal to the disc which increased in intensity in late frames. A classic smokestack appearance of leakage was noted superior to this spot in the very late phase consistent with a diagnosis of central serous chorioretinopathy.

Optical Coherence Tomography

A sequence of horizontal tomograms (C) delineated the sensory retinal detachment which reached a maximum of 270 μm in the image. The subretinal fluid did not involve the fovea.

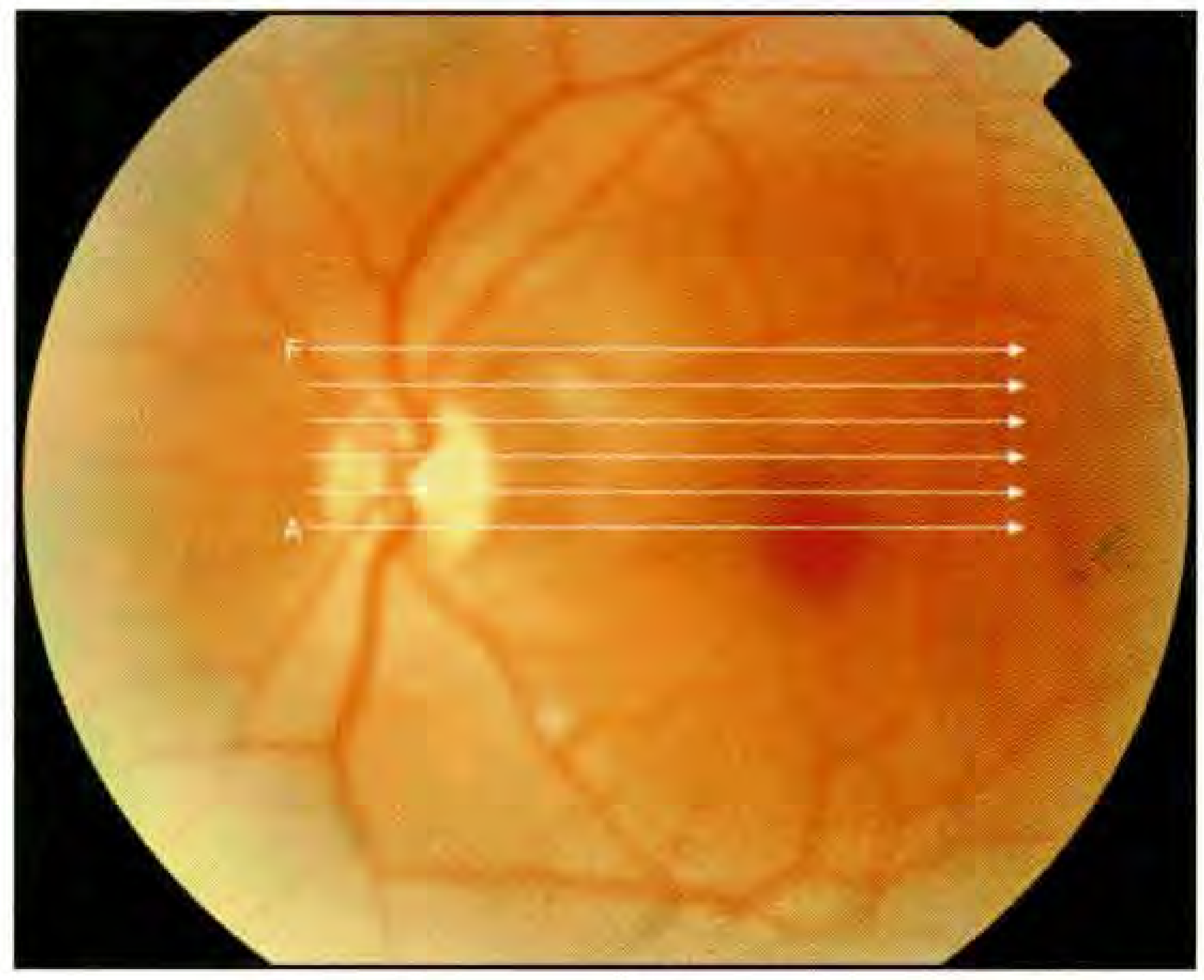

A

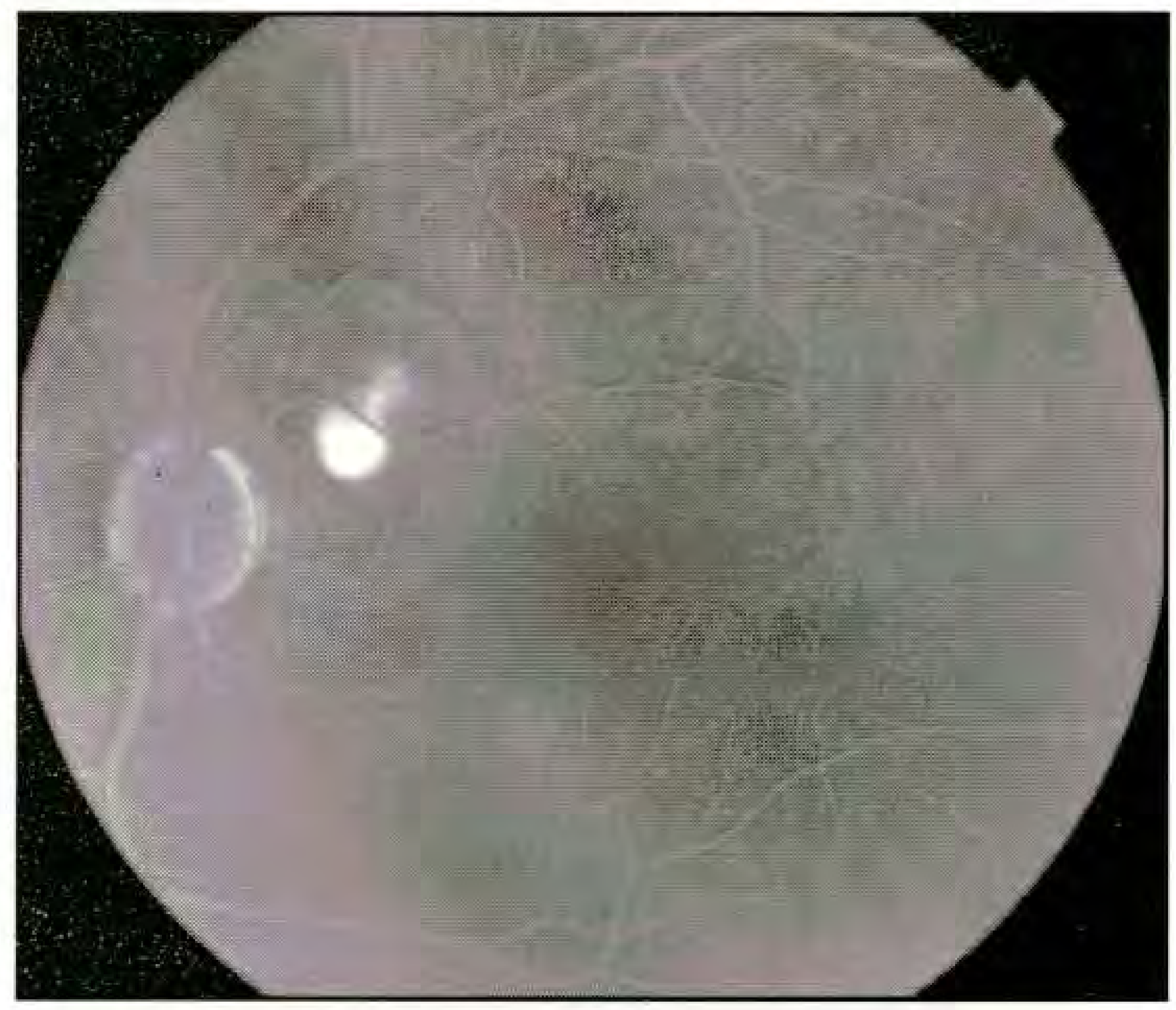

B

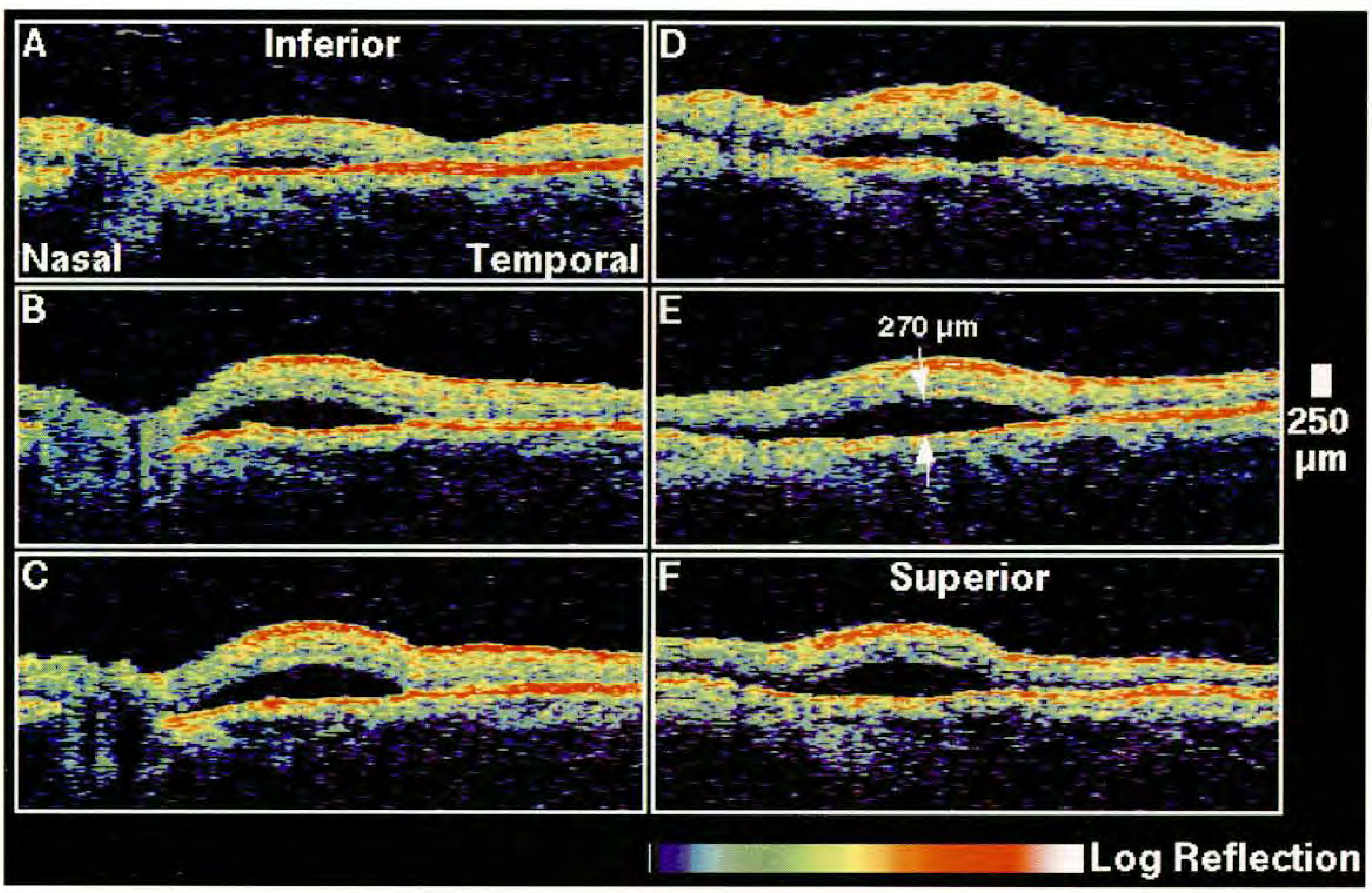

C

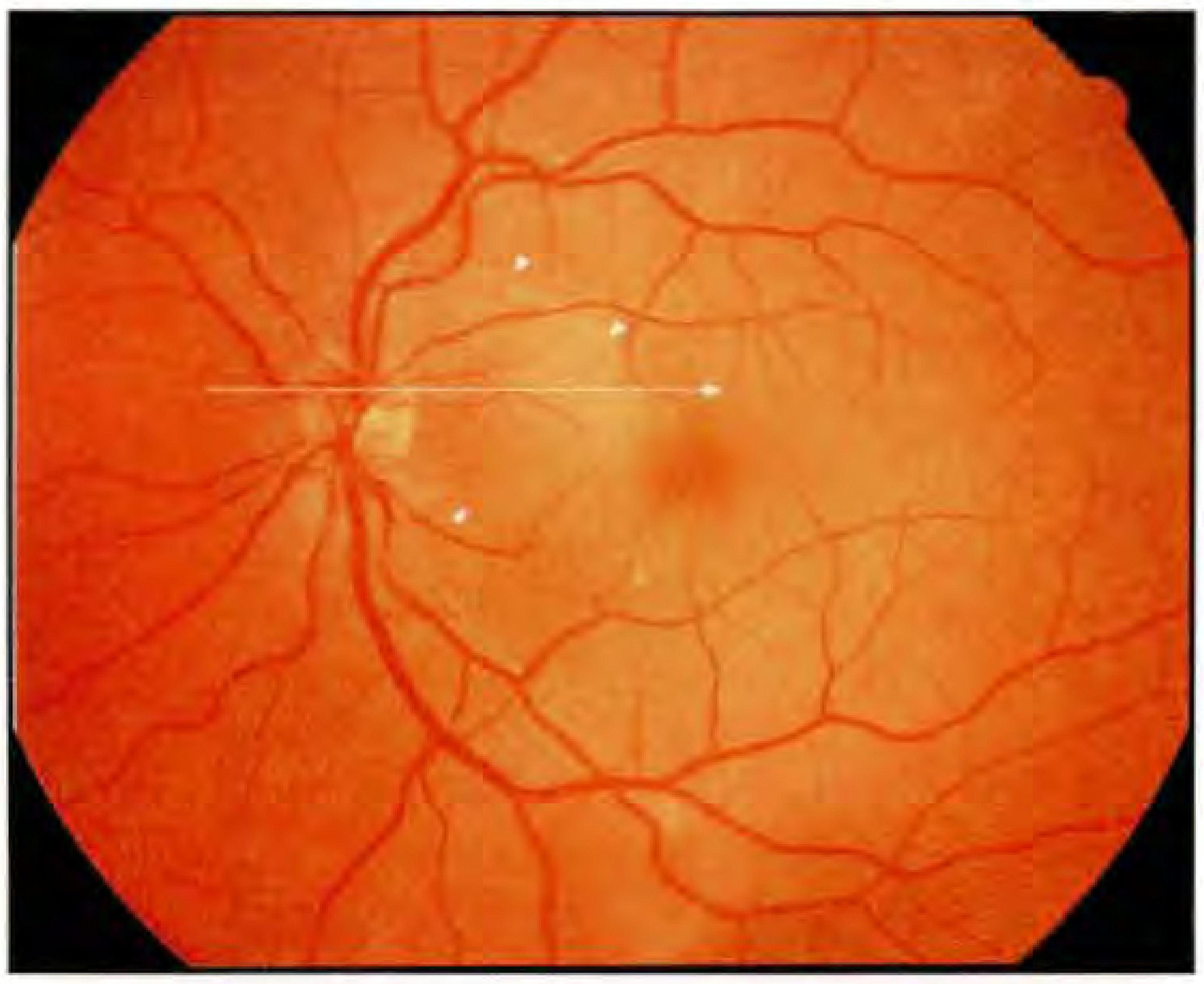

A

Case 7-11. Bilateral Central Serous Chorioretinopathy Associated with Pregnancy

Clinical Summary

A 32-year-old woman described a "bleached-out" area in her visual field which had developed over the past four to five days, and was beginning to compromise her central vision. She was 23 weeks pregnant with no history of pre-eclampsia. Fundus examination (A) of her left eye revealed a serous elevation of the neurosensory retina extending directly into the fovea consistent with a diagnosis of central serous chorioretinopathy. Fluorescein angiography was not performed.

Optical Coherence Tomography

A horizontal OCT tomogram (B) taken through the patient's optic disc and fovea also showed a detachment of the neurosensory retina extending along the papillomacular axis, and beginning to encroach beneath the fovea.

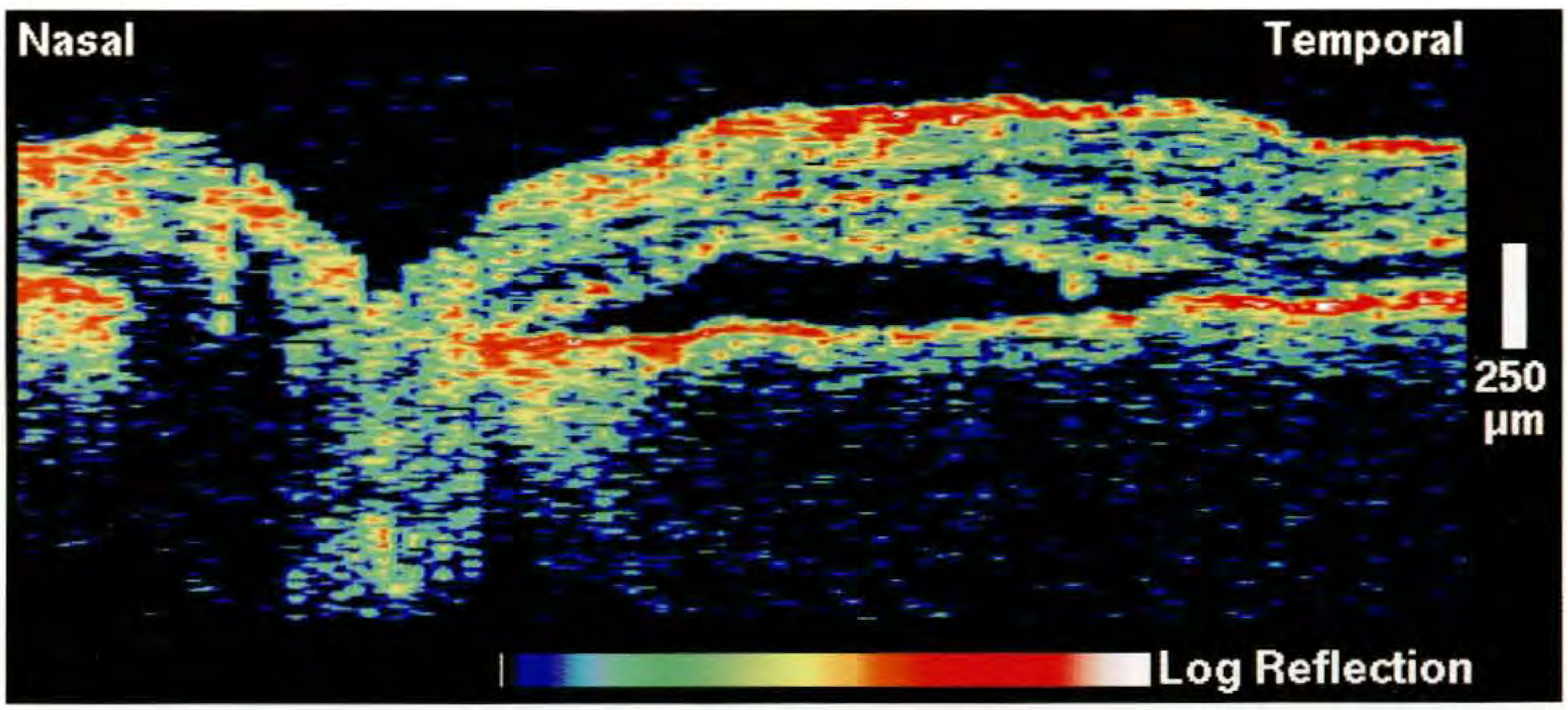

B

Case 7-11 continued

Clinical Summary

Slit-lamp examination also revealed an area of serous elevation superior to the fovea in the patient's right eye (C).

Optical Coherence Tomography

A vertical OCT tomogram (D) showed a shallow detachment of the neurosensory retina superior to the foveal depression. Superiorly in the image, a faintly reflective band was evident just anterior to the retina, most likely representing the posterior hyaloid. The membrane appeared to be separated from the retina inferior to the region of serous retinal detachment, and suggested that vitreoretinal traction may have facilitated the detachment.

C

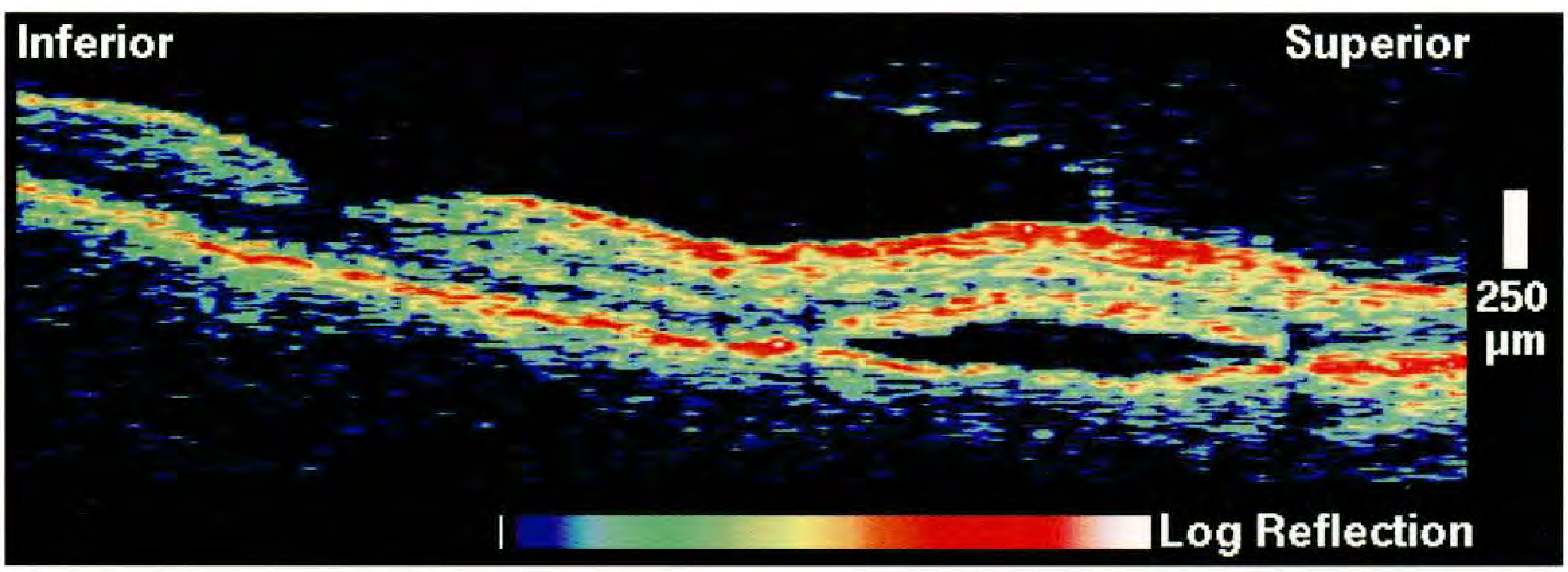

D

CHAPTER 8

Macular Degeneration

Non-exudative Age-related Macular Degeneration
Serous and Hemorrhagic Detachments of the Retina and RPE
Fibrovascular Pigment Epithelial Detachments
Choroidal Neovascularization

OCT can cross-sectionally image the morphological changes in non-exudative age-related macular degeneration. Soft drusen cause a modulation in the highly reflective band defining the posterior boundary of the neurosensory retina consistent with the accumulation of material within or beneath Bruch's membrane [1]. The apparent elevation of the RPE is similar in appearance to a serous pigment epithelial detachment (PED); however, unlike a PED, soft drusen display shallow margins and mild backscatter signal is observed which extends from the RPE into the choroid. Geographic atrophy is highly distinctive on OCT because the overlying retina is thinned and the hypopigmented RPE causes increased penetration of the optical probe beam into the deeper choroid, significantly enhancing the reflections from this layer.

OCT images of exudative macular degeneration and choroidal neovascularization may aid in the diagnosis and management of this pervasive disease. Many eyes with choroidal neovascularization (CNV) lack the fluorescein angiographic features required for treatment eligibility according to the Macular Photocoagulation Study guidelines [2,3]. OCT may represent a new technique for visualizing angiographically occult CNV. OCT is effective in the identification and quantification of subretinal, intraretinal, and sub-RPE fluid, and is particularly useful in evaluating possible foveal involvement of fluid accumulation. Measurements of retinal thickness with OCT provide an objective means of following edema and subretinal fluid in a patient through successive examinations.

Neurosensory detachments appear in cross-section as elevations of the sensory retina above an optically clear space, with well-defined boundaries at the fluid-RPE and fluid-retina interfaces, and shallow margins at the edges of the lesions. In contrast, serous PEDs show an elevation of the reflective band corresponding to the RPE, sharp margins, and shadowing of the reflections returning from the deeper choroid. The shadowing may be due to increased reflectivity and attenuation of the probe light through the decompensated RPE cells. Intraretinal fluid may be localized into non-reflective cysts, or may cause a diffuse increase in retinal thickness and an associated reduction in retinal reflectivity. Hemorrhagic detachments show bright backscatter which corresponds to the level of blood accumulation and results in decreased light penetration and significant attenuation of the choroidal reflection. Hemorrhagic neurosensory detachments may be difficult to distinguish from hemorrhagic PEDs due to the similarity in reflectivity between blood and detached pigment epithelium.

CNV typically presents in one of three manners on OCT imaging. Classic, angiographically well-defined CNV [4] is usually visualized as a localized disruption and fusiform thickening of the RPE / choriocapillaris reflection with definite boundaries (*e.g.* Case 8-33). The concomitant presence of subretinal fluid or retinal edema aids in identification. Fibrovascular PEDs, a form of angiographically occult CNV [4], display a well-defined elevation of the RPE reflection above a mildly backscattering region corresponding to fibrovascular proliferation (*e.g.* Case 8-25). Unlike a serous or hemorrhagic PED and similar to confluent soft drusen, no shadowing of the choroidal reflection is present. Finally, CNV may present as enhanced choroidal reflectivity, possibly a result of increased optical penetration due to RPE changes, that may have less well-defined boundaries and is usually associated with cystic changes in the overlying retina (*e.g.* Case 8-35).

Progression or laser treatment of neovascular membranes leads to disciform or laser scars, respectively, both of which appear on OCT as highly reflective and well-demarcated lesions at the chorioretinal interface.

A

B

Case 8-1. Soft Drusen

Clinical Summary

A 58-year-old woman with the clinical diagnosis of age-related macular degeneration had dense, soft drusen in her right central macula (A). No subretinal fluid, hemorrhage, or exudate were noted on clinical examination. Fluorescein angiography (B) displayed punctate hyperfluorescence without leakage during all phases of the angiogram consistent with the staining of soft drusen.

Optical Coherence Tomography

Small modulations in the contour of the retinal pigment epithelium were noted in a vertical OCT image (C) taken through the fovea. The lack of shadowing below these contour changes, usually a feature of serous detachments of the pigment epithelium, was consistent with the accumulation of soft drusen beneath the neurosensory retina and within Bruch's membrane.

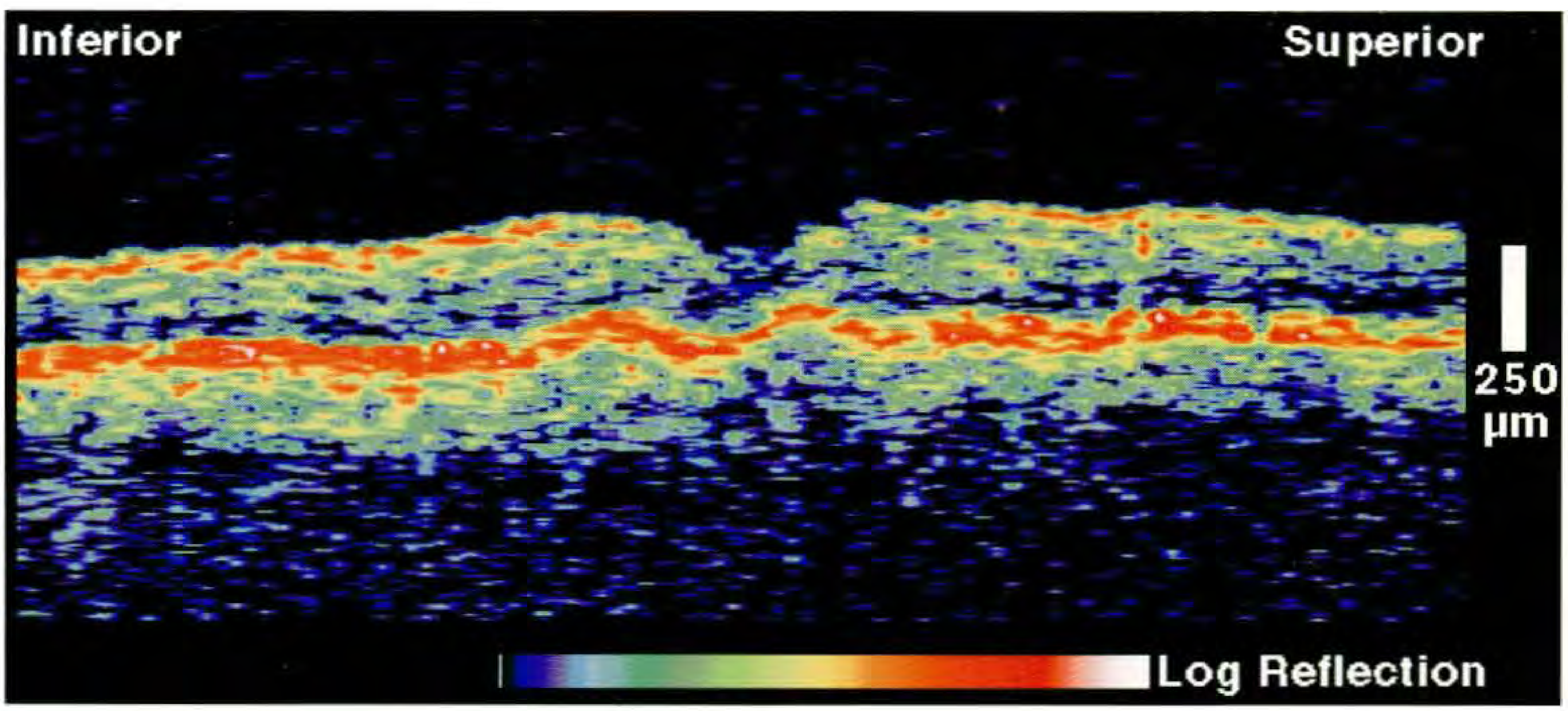

C

Case 8-2. Large Calcified Drusen

Clinical Summary

A 64-year-old woman was referred for a macular lesion nasal to the fovea in her left eye associated with a visual acuity of 20/25. Dilated fundus examination (A) revealed a large area of yellow subretinal material which was identified as a large drusen with dystrophic calcification.

Optical Coherence Tomography

An OCT tomogram (B) taken just superior to the fovea disclosed a focal elevation of the retinal pigment epithelium nasal to the center consistent with the accumulation of sub-retinal pigment epithelial (RPE) material or a diffuse thickening of Bruch's membrane. The overlying sensory retina was mildly thinned in this region, and the elevated RPE did not shadow the reflections from the more outer layers of the retina.

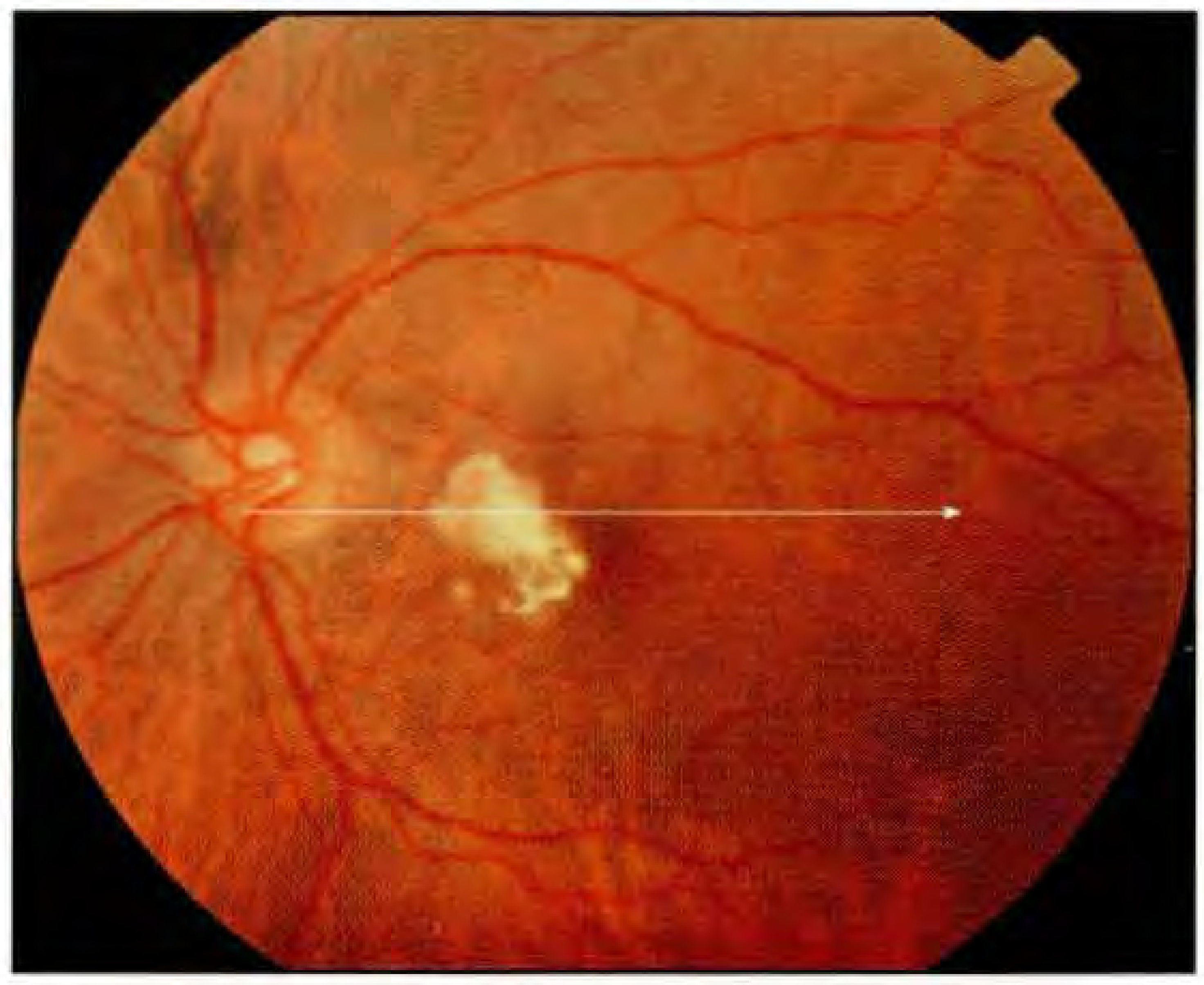

A

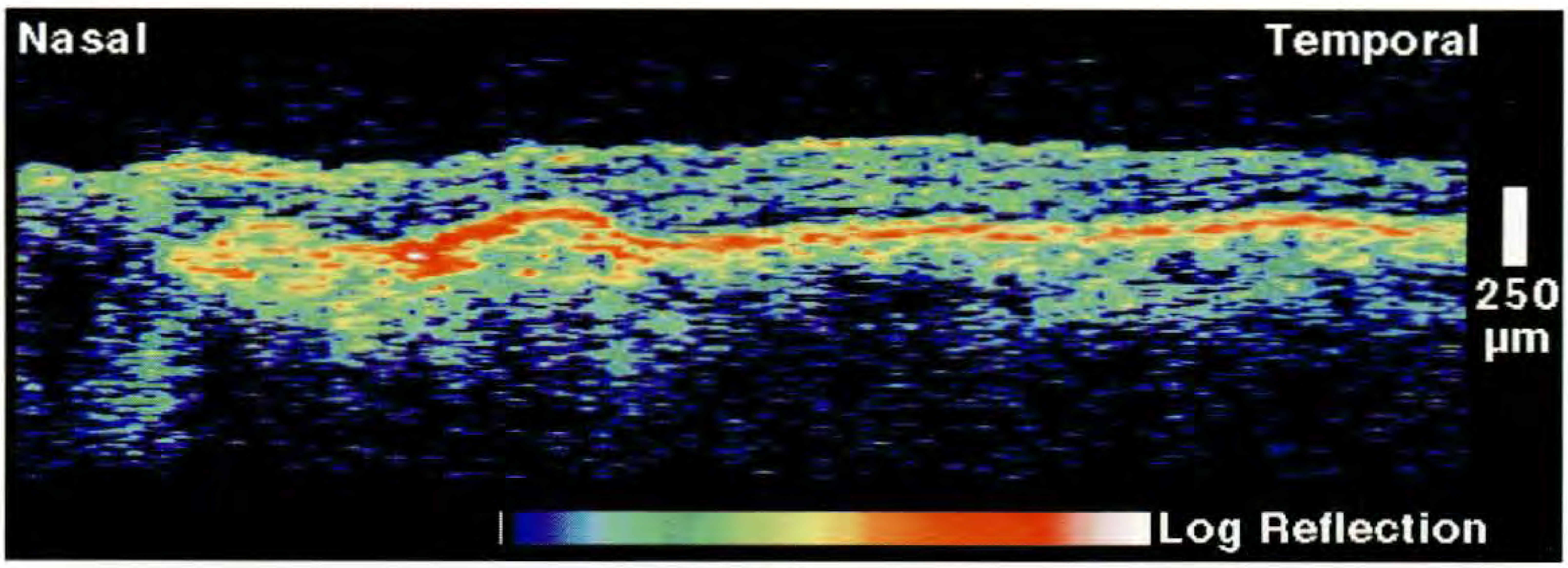

B

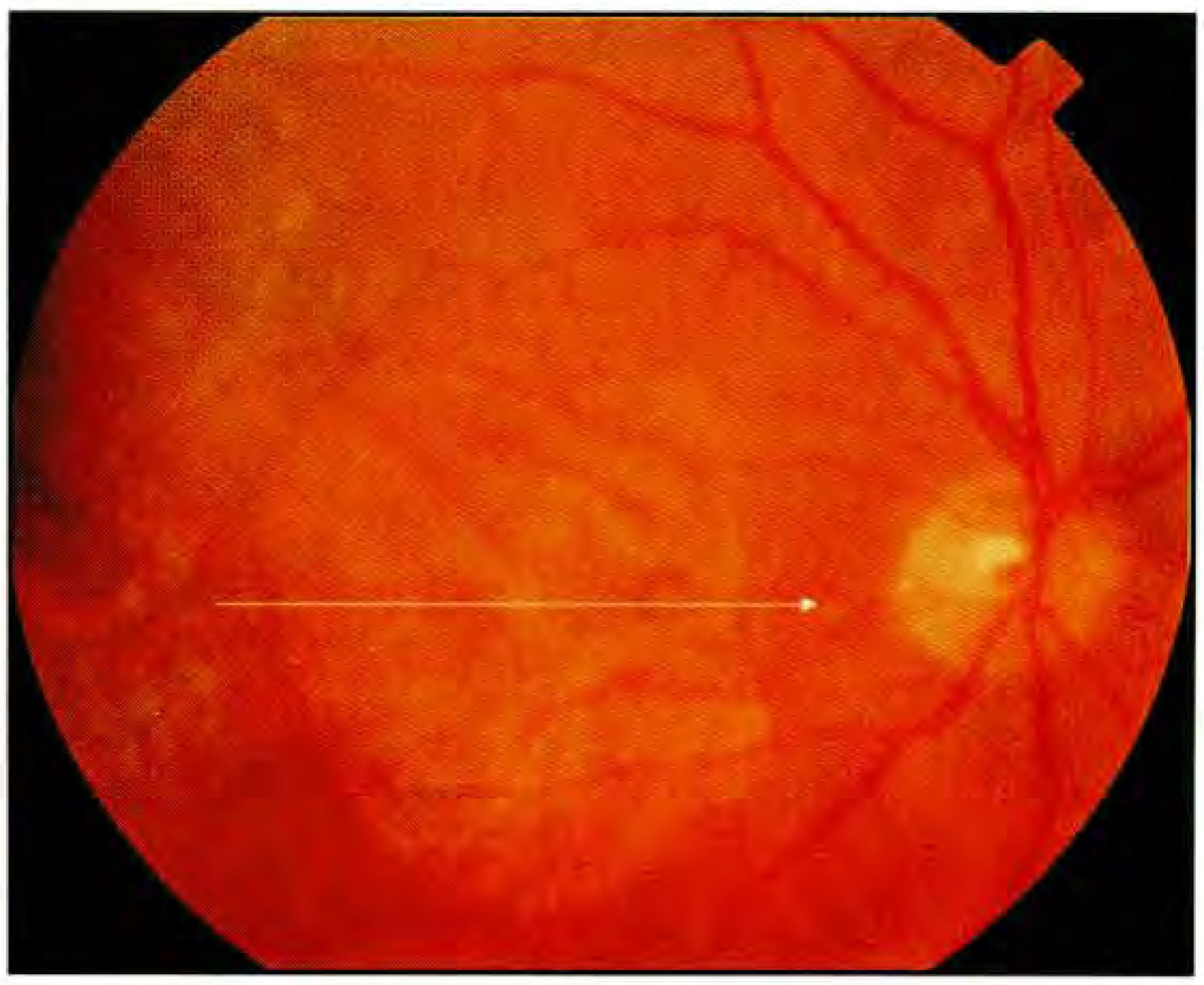

A

Case 8-3. Geographic Atrophy

Clinical Summary

An 85-year-old man with a 10 year history of macular degeneration had a visual acuity of 20/200 in both eyes, which had been stable for the past three years. Slit-lamp examination of his right eye (A) showed geographic atrophy throughout the macula, with no subretinal fluid, hemorrhage, or exudate.

Optical Coherence Tomography

A horizontal OCT scan (B) was obtained through the macula and showed a well-defined region of increased optical reflectivity from the choroid due to increased penetration of both incident and reflected light through the atrophic pigment epithelium. The contour of the foveal depression was altered, and the normal minimally reflective band corresponding to the retinal photoreceptor layer was absent in the image.

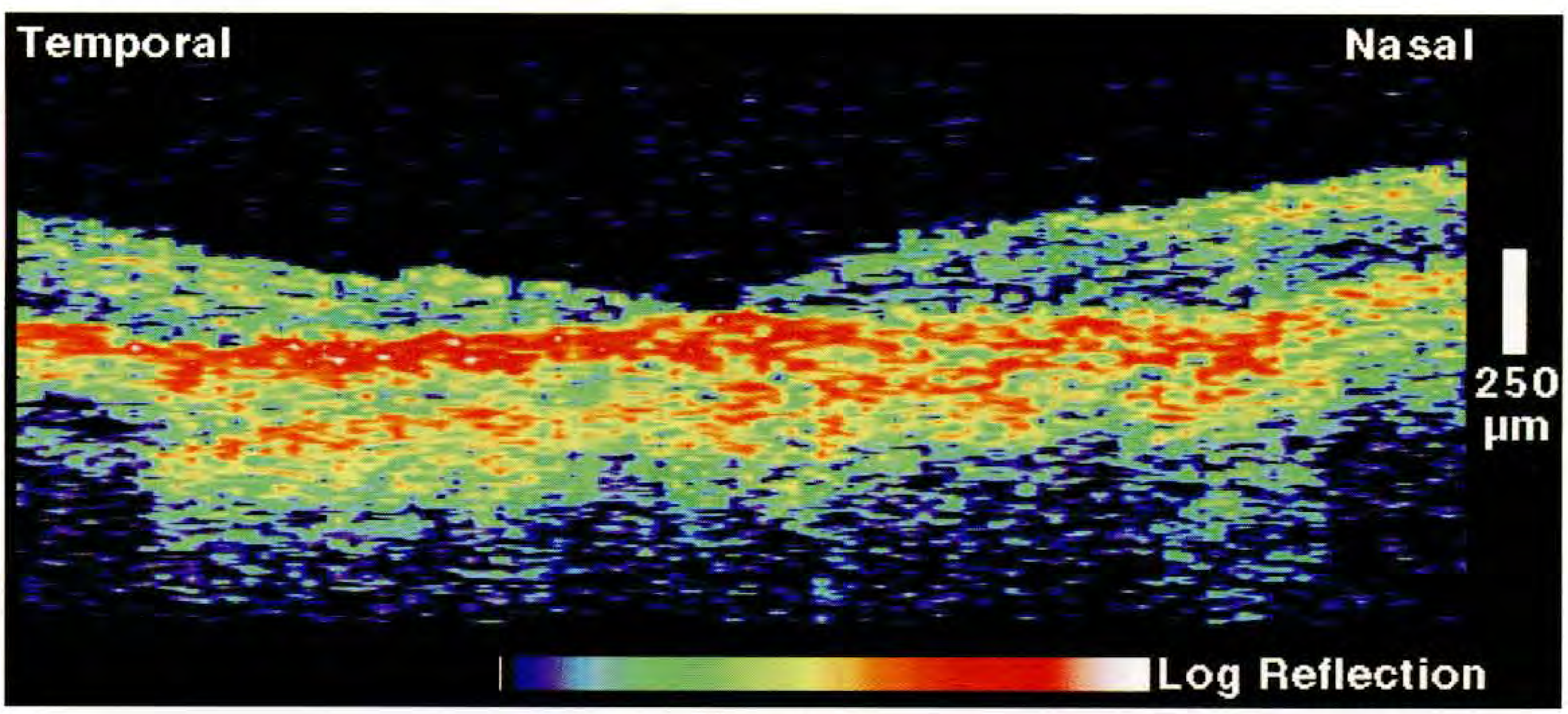

B

Case 8-4. Geographic Atrophy

Clinical Summary

An 85-year-old man with stable age-related macular degeneration had geographic atrophy involving the macula of his left eye without associated subretinal fluid, hemorrhage, or exudate (A). His visual acuity in this eye was counting fingers at four feet.

Optical Coherence Tomography

A sequence of horizontal OCT tomograms (B) demonstrated increased penetration of light through the atrophic region, which was most significant nasal to the fovea, leading to enhanced reflectivity from the choroid. Scan B, taken directly through the fovea, showed thinning of the neurosensory retina in the central macula.

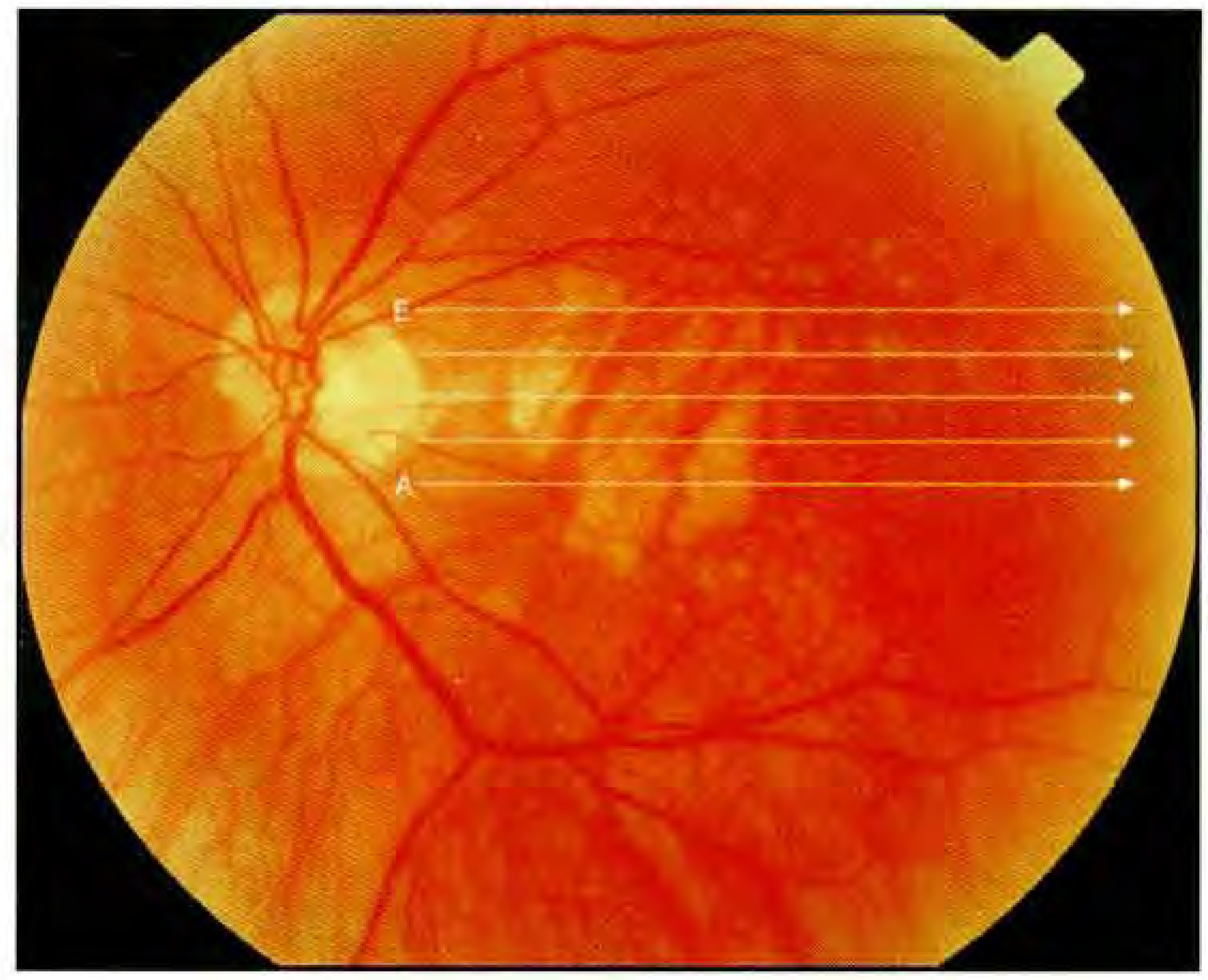

A

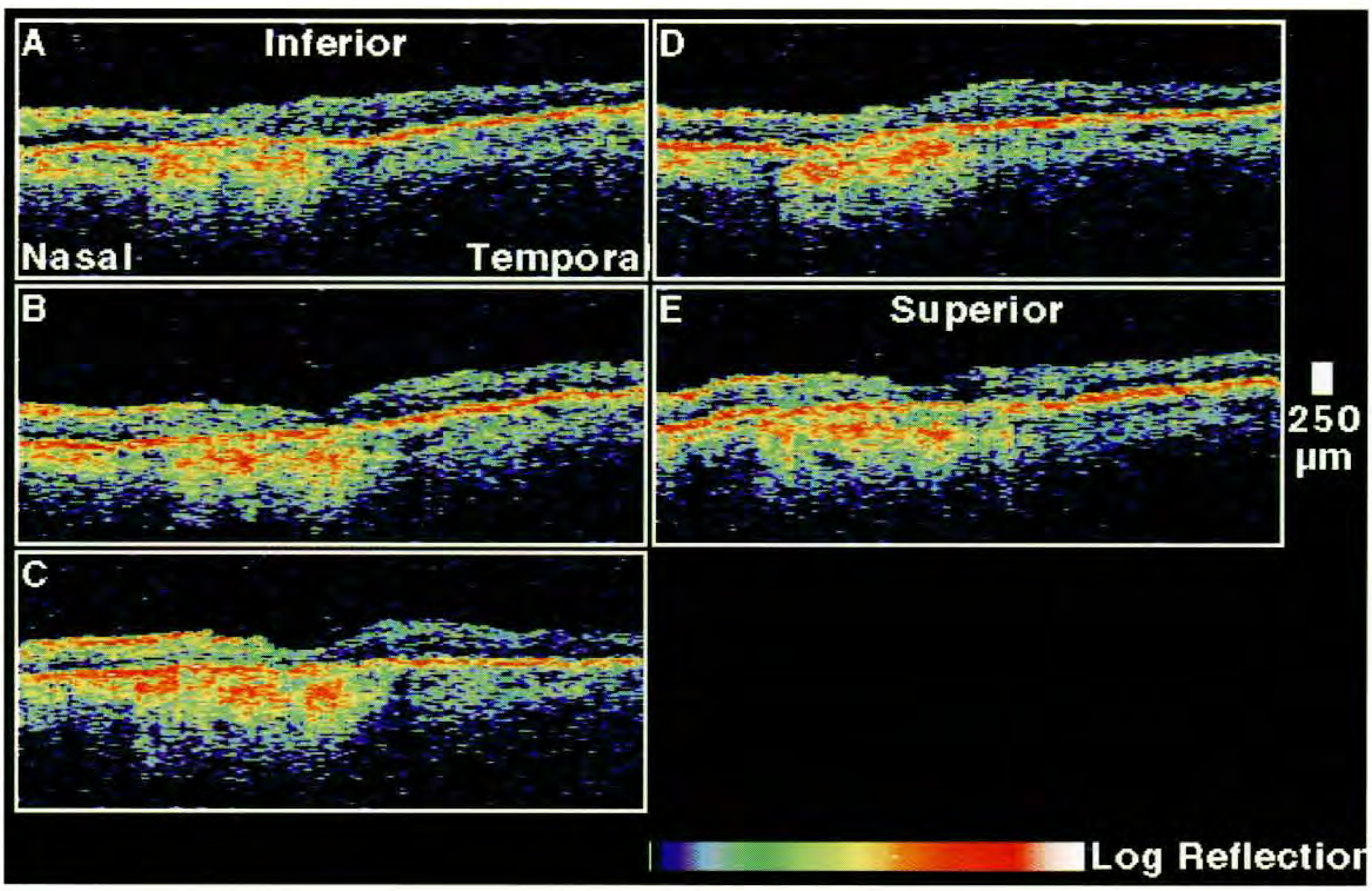

B

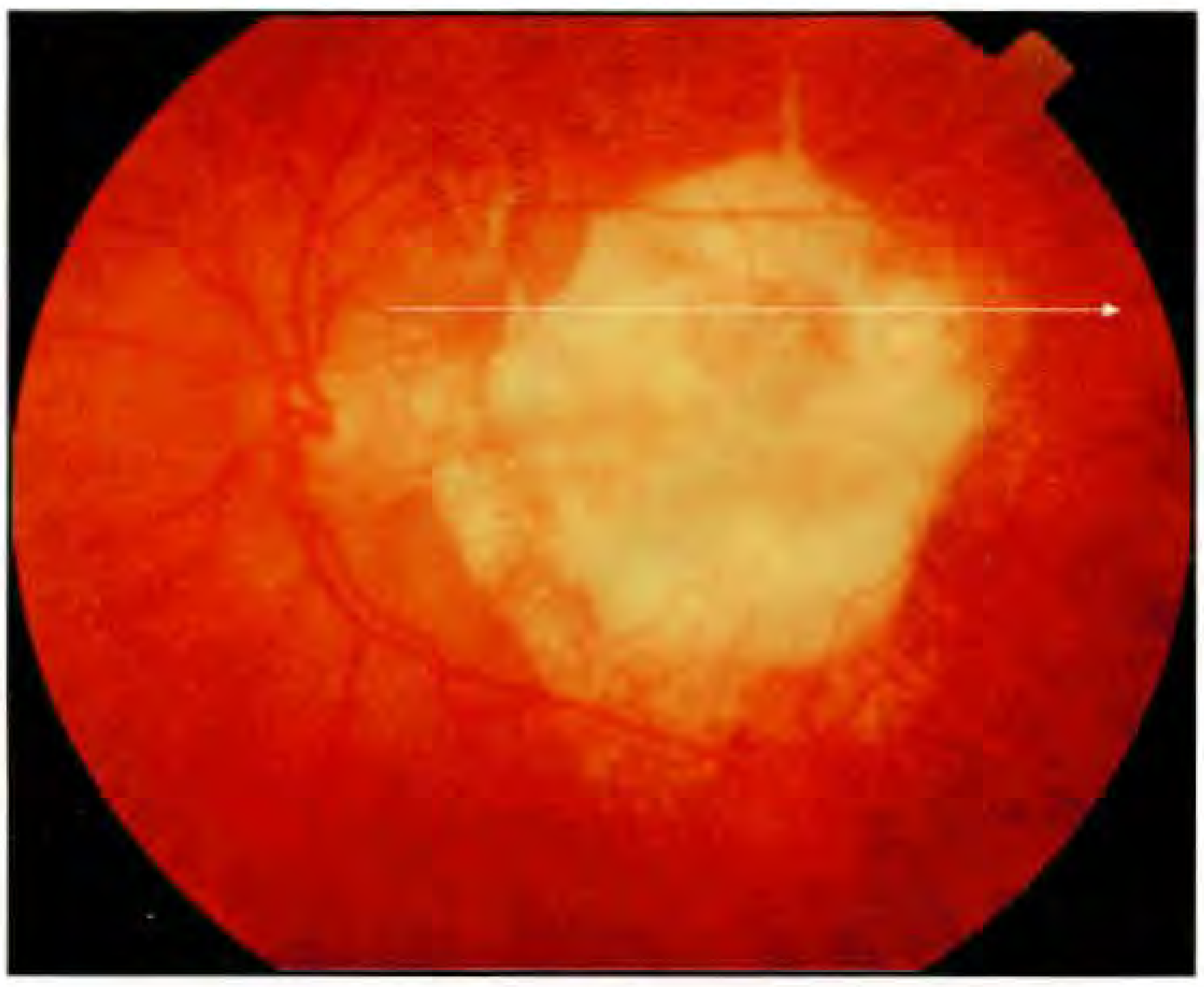

A

Case 8-5. Disciform Scar

Clinical Summary

A 92-year-old woman had age-related macular degeneration and a disciform scar in her left eye (A). Her visual acuity in this eye was 20/400.

Optical Coherence Tomography

The OCT image (B) showed a well-defined region of increased optical reflectivity in the choroid corresponding to the scar. The overlying retina appeared thinned.

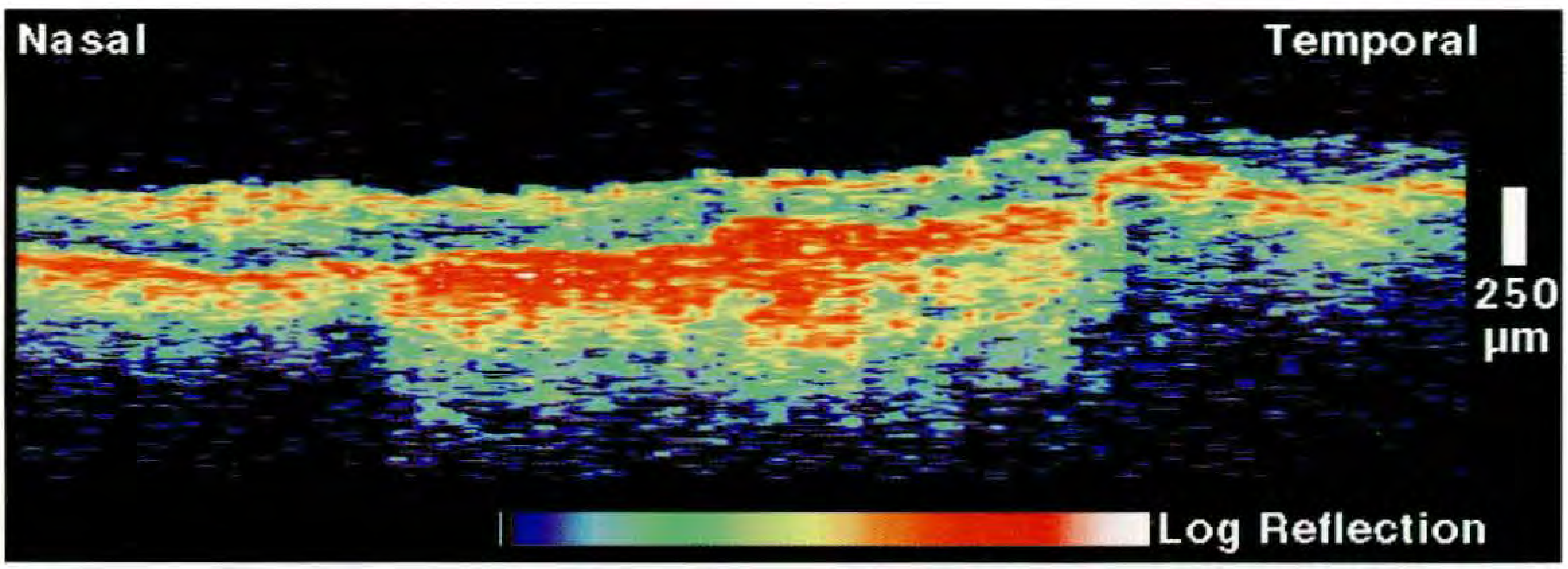

B

Case 8-6. Pigmented Chorioretinal Scar

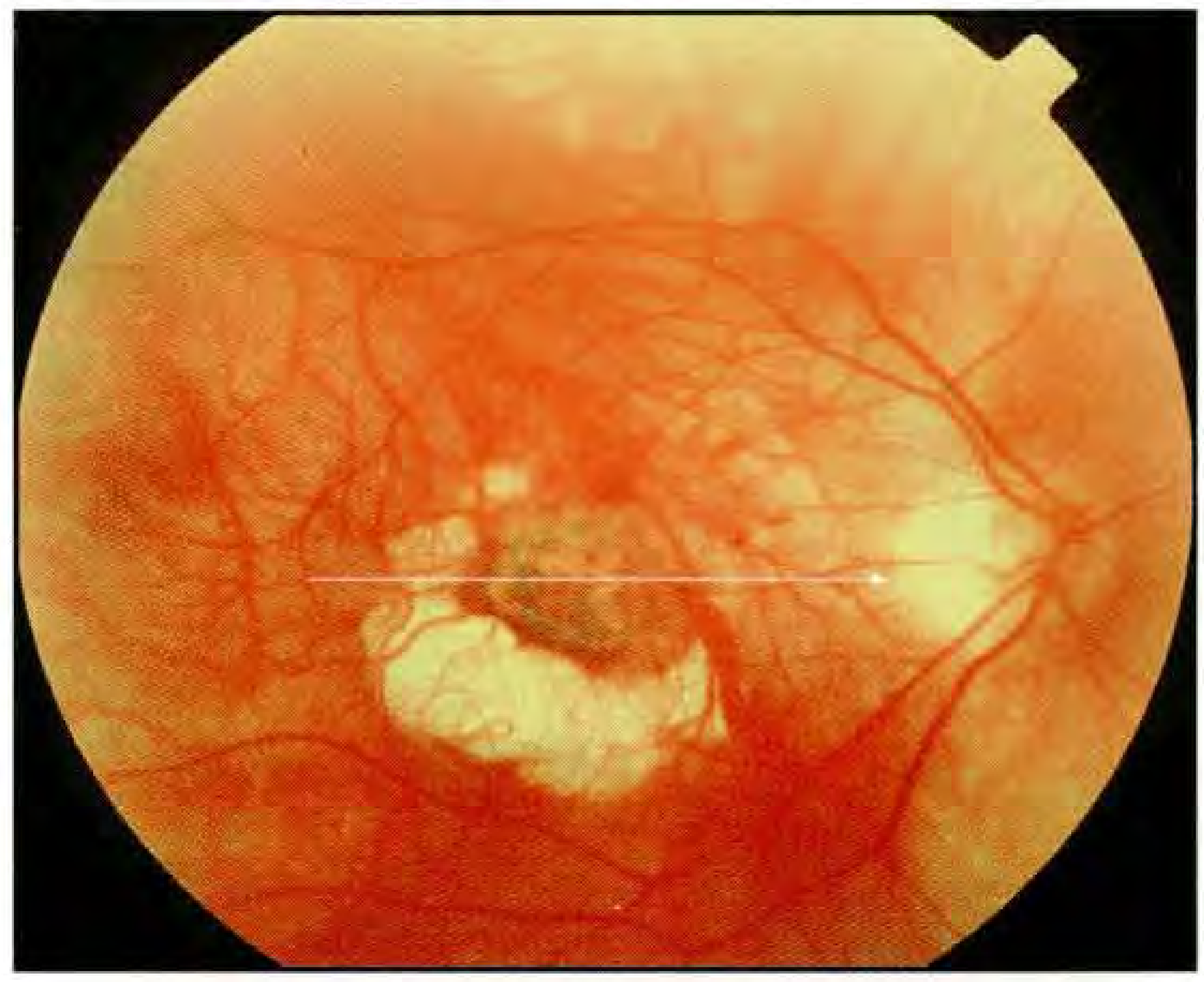

A

Clinical Summary

A 52-year-old man with degenerative myopia experienced a decline in the vision in his right eye two years prior to evaluation. At that time, a choroidal neovascular lesion was diagnosed and treatment was not performed. On the present examination (A), the visual acuity in his right eye was 20/125, and there was a pigmented chorioretinal lesion in the center of the macula. A region of chorioretinal atrophy was noted immediately inferior to the fovea.

Optical Coherence Tomography

A horizontal section (B) disclosed a highly reflective lesion just beneath the fovea. A diffuse increase in choroidal reflectivity temporal and nasal to the lesion was noted consistent with slight pigmentary atrophy. The retina also appeared diffusely thinned. The reflections from the retinal pigment epithelium and choriocapillaris within the lesion shadowed the backscatter signal from the deeper choroid below the lesion consistent with hyperpigmentation and fibrosis.

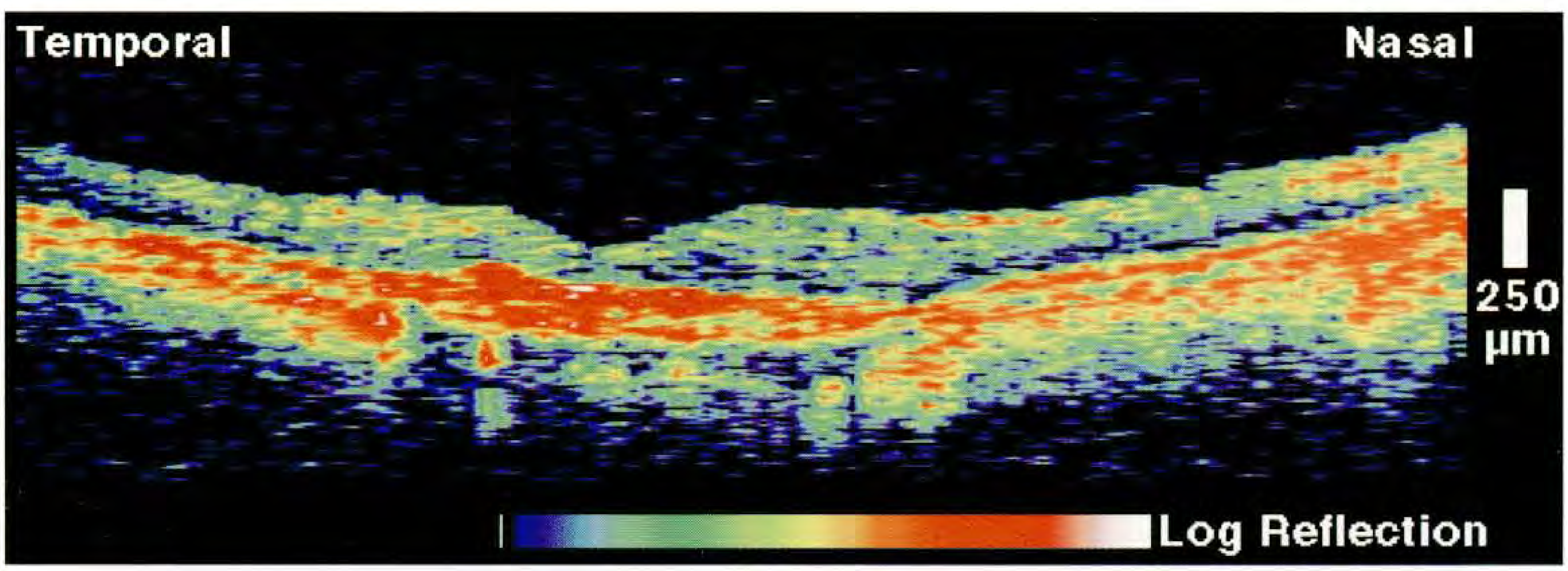

B

Case 8-8. Disciform Scar

Clinical Summary

A 82-year-old woman with age-related macular degeneration had received macular laser photocoagulation in her left eye for choroidal neovascularization 15 months earlier. Her visual acuity in this eye was 20/200. Slit-lamp examination (A) showed the atrophic laser scar inferotemporal to the fovea, with no subretinal fluid, hemorrhage, or exudate.

Optical Coherence Tomography

The laser scar was clearly demarcated as a region of enhanced backscatter, consistent with chorioretinal fibrosis (B). The neurosensory retina was atrophic in the fovea and the minimally reflective band corresponding to the photoreceptor layer was absent.

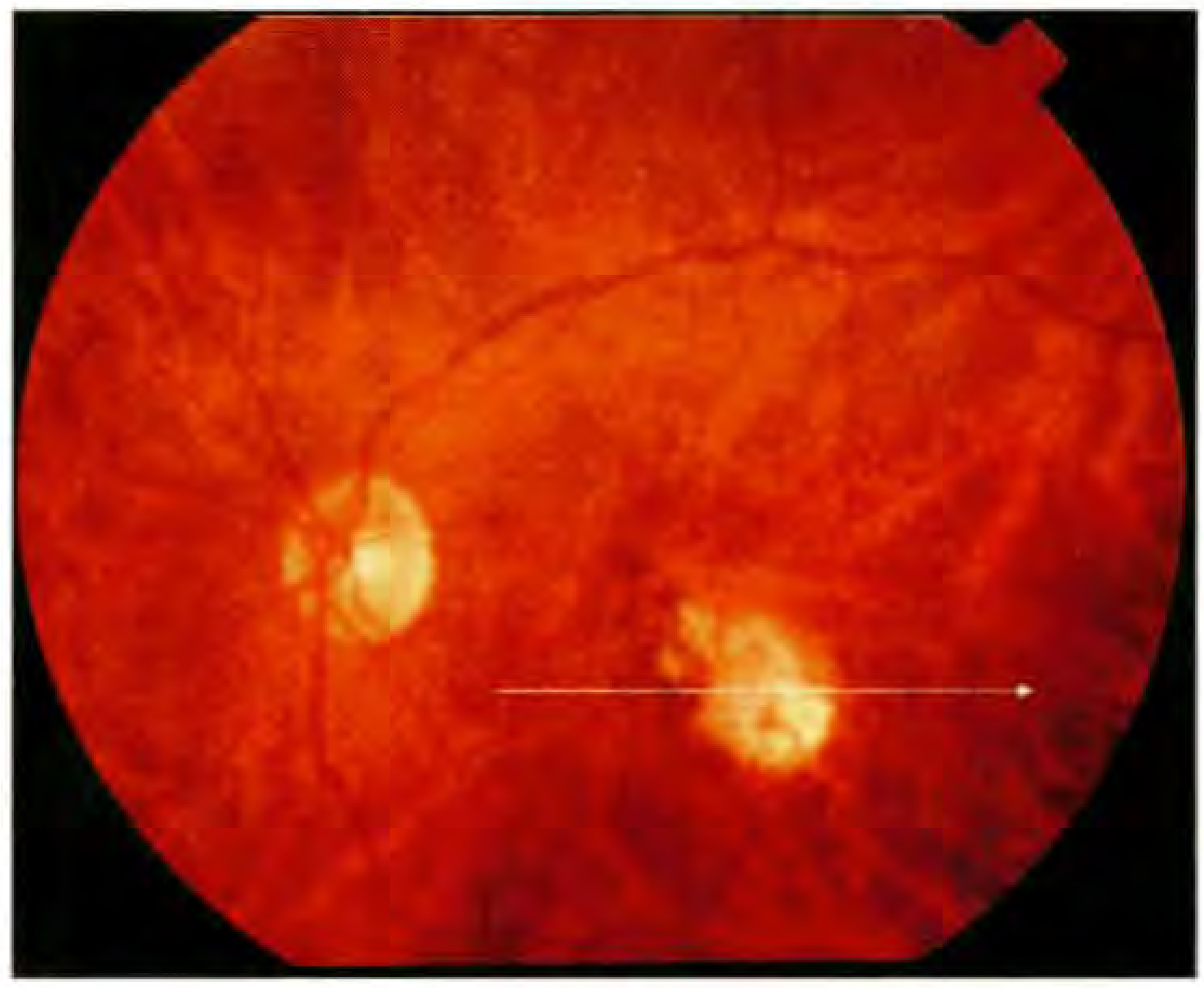

A

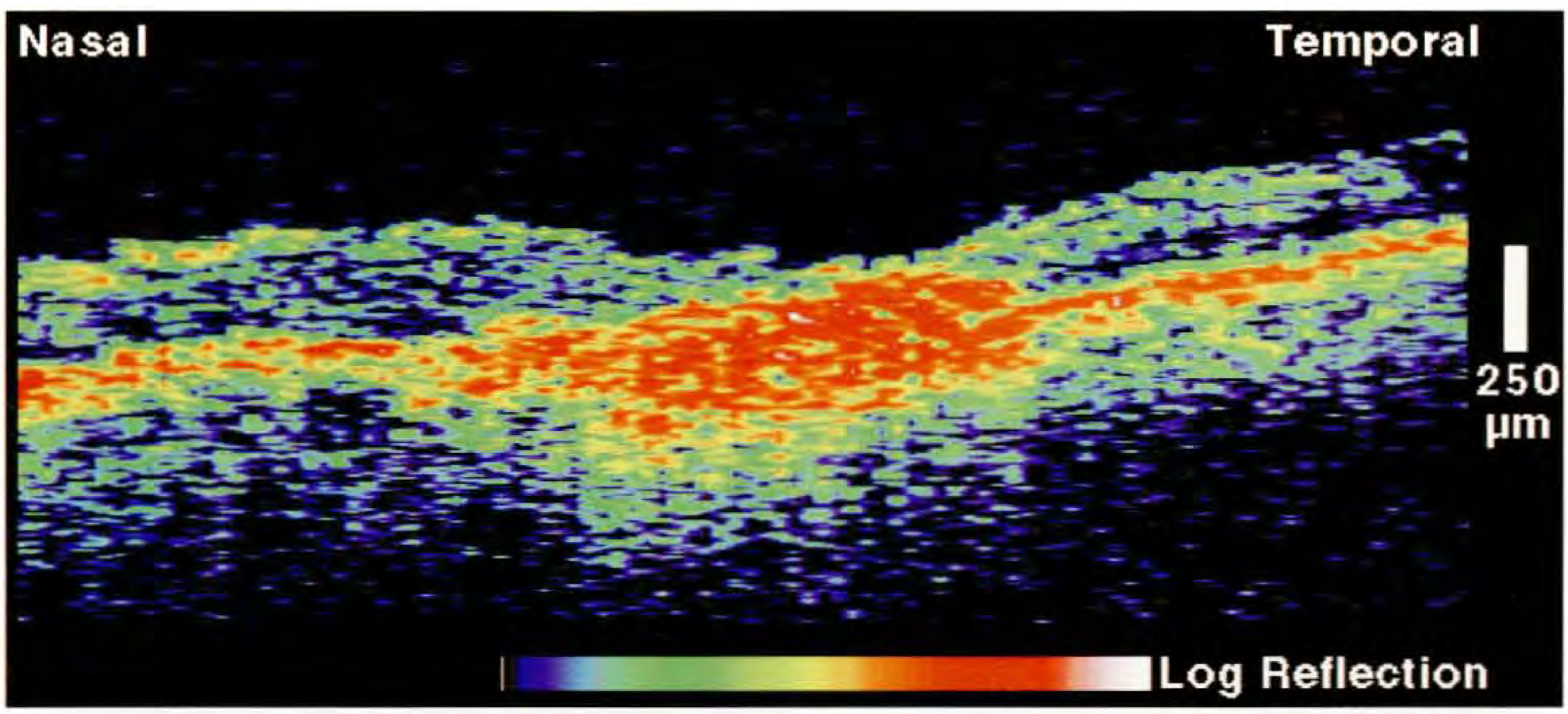

B

Case 8-8. Disciform Scar

Clinical Summary

A 82-year-old woman with age-related macular degeneration had received macular laser photocoagulation in her left eye for choroidal neovascularization 15 months earlier. Her visual acuity in this eye was 20/200. Slit-lamp examination (A) showed the atrophic laser scar inferotemporal to the fovea, with no subretinal fluid, hemorrhage, or exudate.

Optical Coherence Tomography

The laser scar was clearly demarcated as a region of enhanced backscatter, consistent with chorioretinal fibrosis (B). The neurosensory retina was atrophic in the fovea and the minimally reflective band corresponding to the photoreceptor layer was absent.

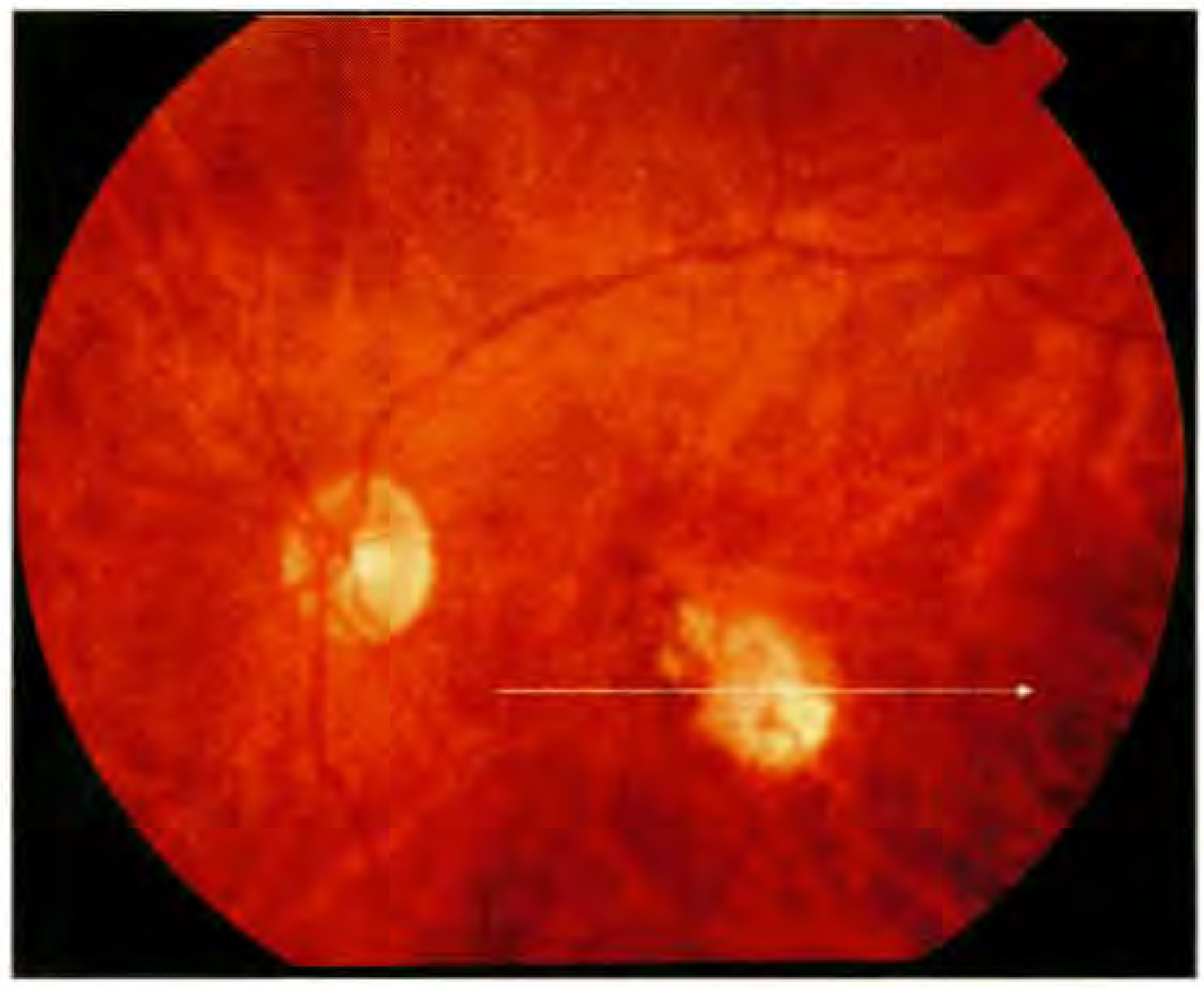

A

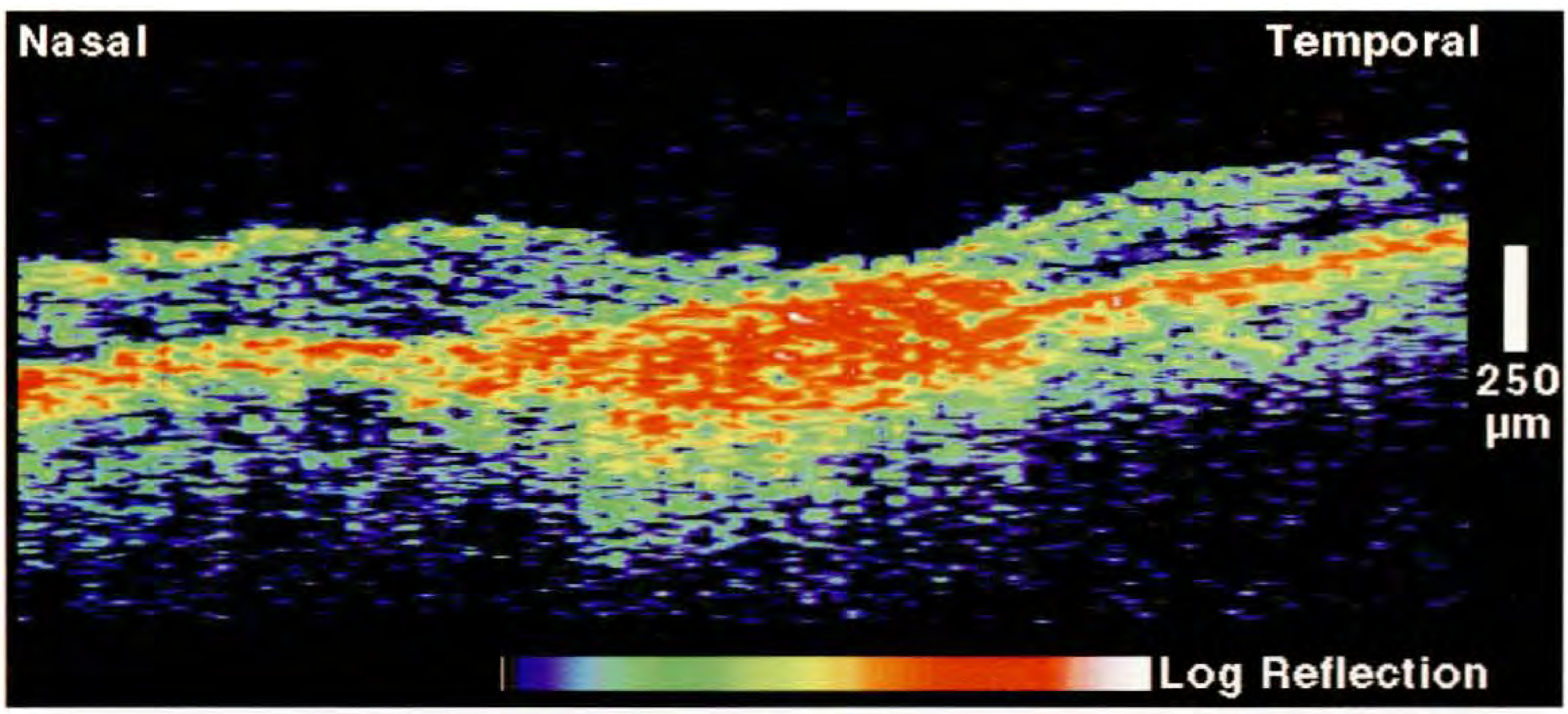

B

A

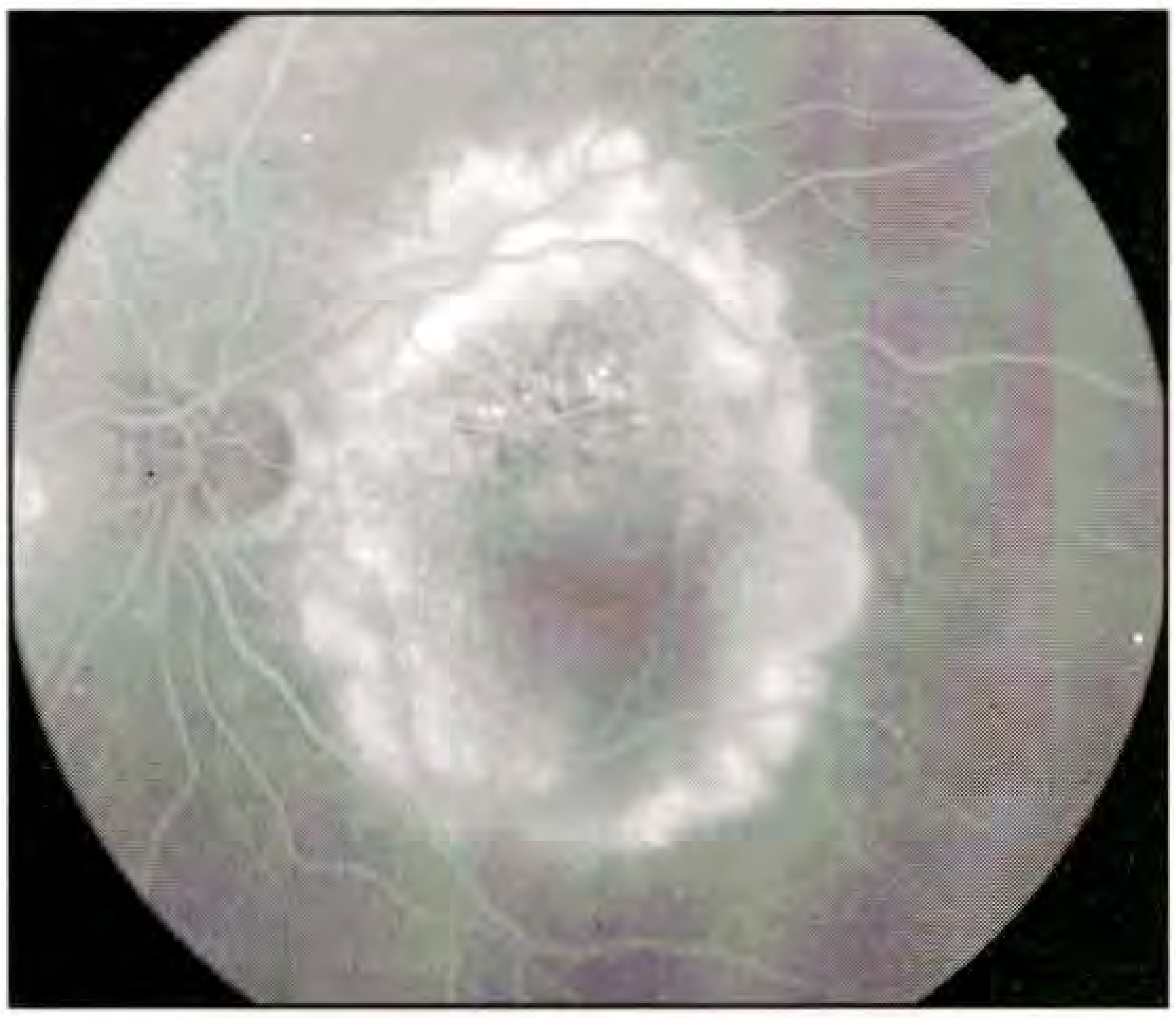

B

Case 8-9. Neurosensory and Pigment Epithelial Retinal Detachment

Clinical Summary

A 70-year-old-man with age-related macular degeneration had probable choroidal neovascularization in his left eye associated with a visual acuity of 20/300. A large neurosensory detachment was observed (A) in the central macula and along the inferior vascular arcade. No hemorrhage was visible and there was minimal exudate. Fluorescein angiography (B) showed mottled hyperfluorescence in the superior macula which increased in intensity as the angiogram progressed. A surrounding hyperfluorescent ring was also observed which demonstrated significant leakage in the late frames.

Optical Coherence Tomography

A horizontal OCT tomogram (C) was acquired through the fovea. A neurosensory detachment was observed directly in the fovea above an optically clear space corresponding to subretinal serous fluid. Two elevations of the retinal pigment epithelium were visible nasal and temporal to the neurosensory detachment, consistent with the hyperfluorescent ring observed on angiography.. The reflective band corresponding to the pigment epithelium appeared intact throughout the image.

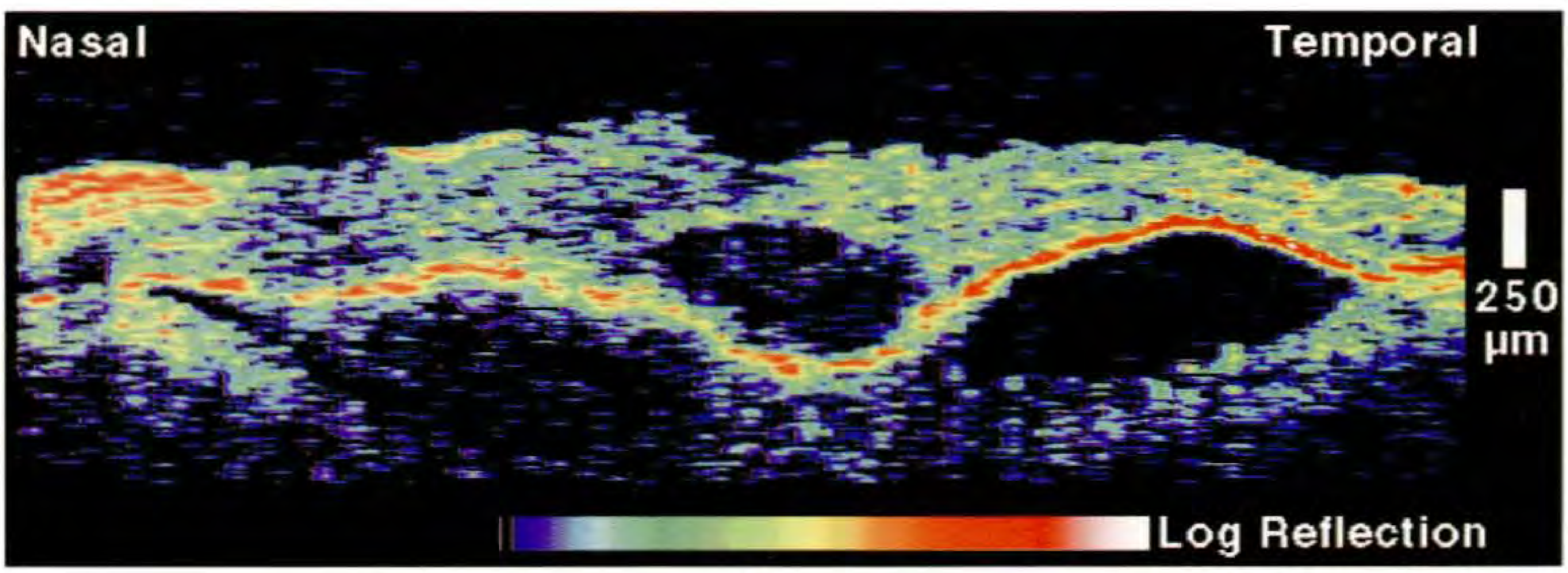

C

Case 8-10. Neurosensory Detachment with Cloudy Subretinal Fluid

Clinical Summary

A 63-year-old man with age-related macular degeneration noted a gradual decrease in vision in his left eye. He had undergone indocyanine green enhanced diode laser photocoagulation 15 months earlier for choroidal neovascularization. On examination, his visual acuity in this eye was 20/160. Slit-lamp biomicroscopy (A) revealed an atrophic chorioretinal scar superonasal to the fovea and a neurosensory detachment extending inferotemporally passing beneath the fovea. The subretinal fluid appeared cloudy with mild subretinal fibrosis.

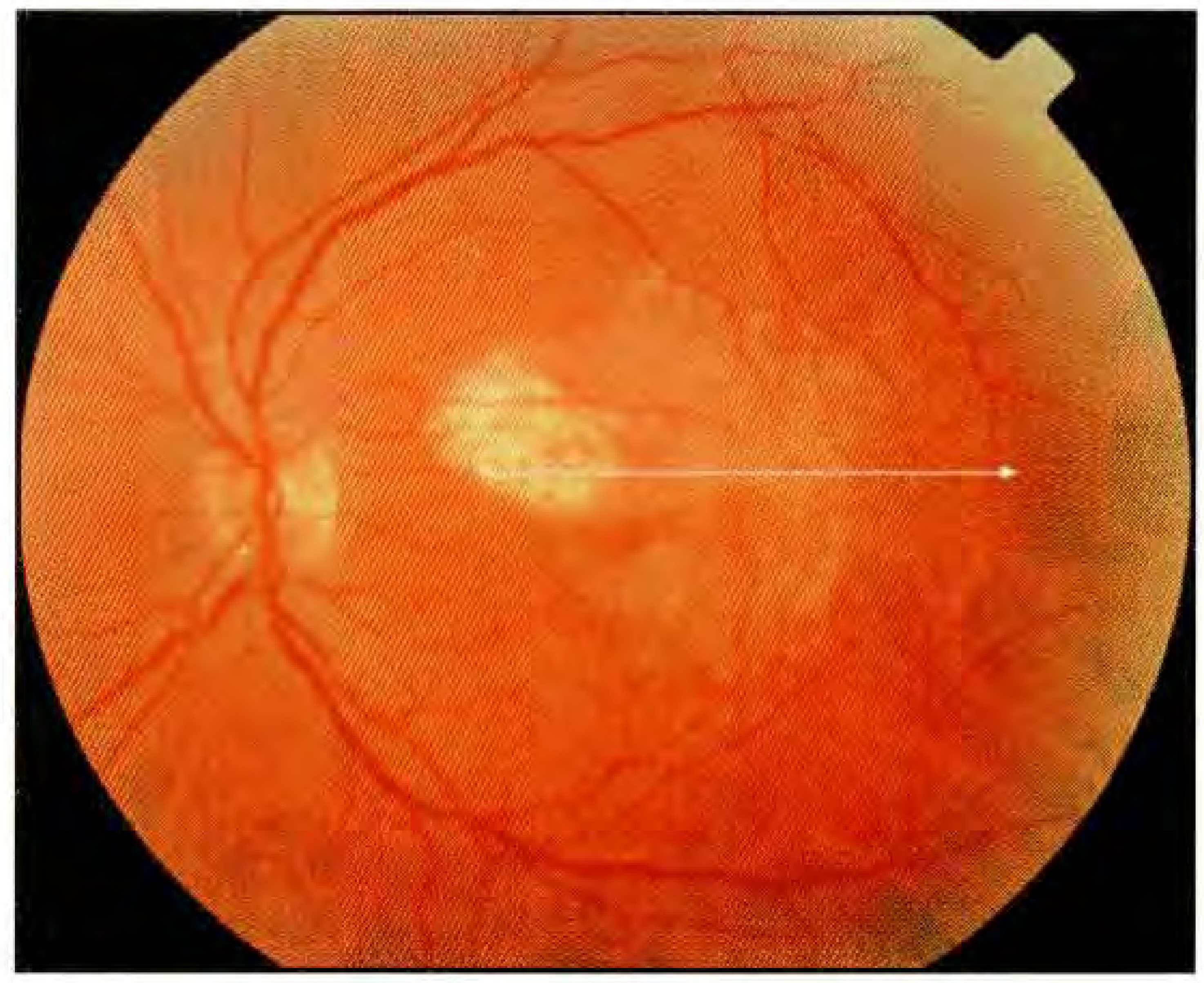

A

Optical Coherence Tomography

On OCT examination (B), the neurosensory retina was elevated over optically transparent regions of serous fluid accumulation and areas of moderate, subretinal backscatter consistent with subretinal fibrosis. The reflection from the pigment epithelium and choriocapillaris was intact below the lesion suggesting the absence of a recurrent neovascular membrane. Enhanced reflectivity was observed beneath the neurosensory retina in the area of the chorioretinal scar.

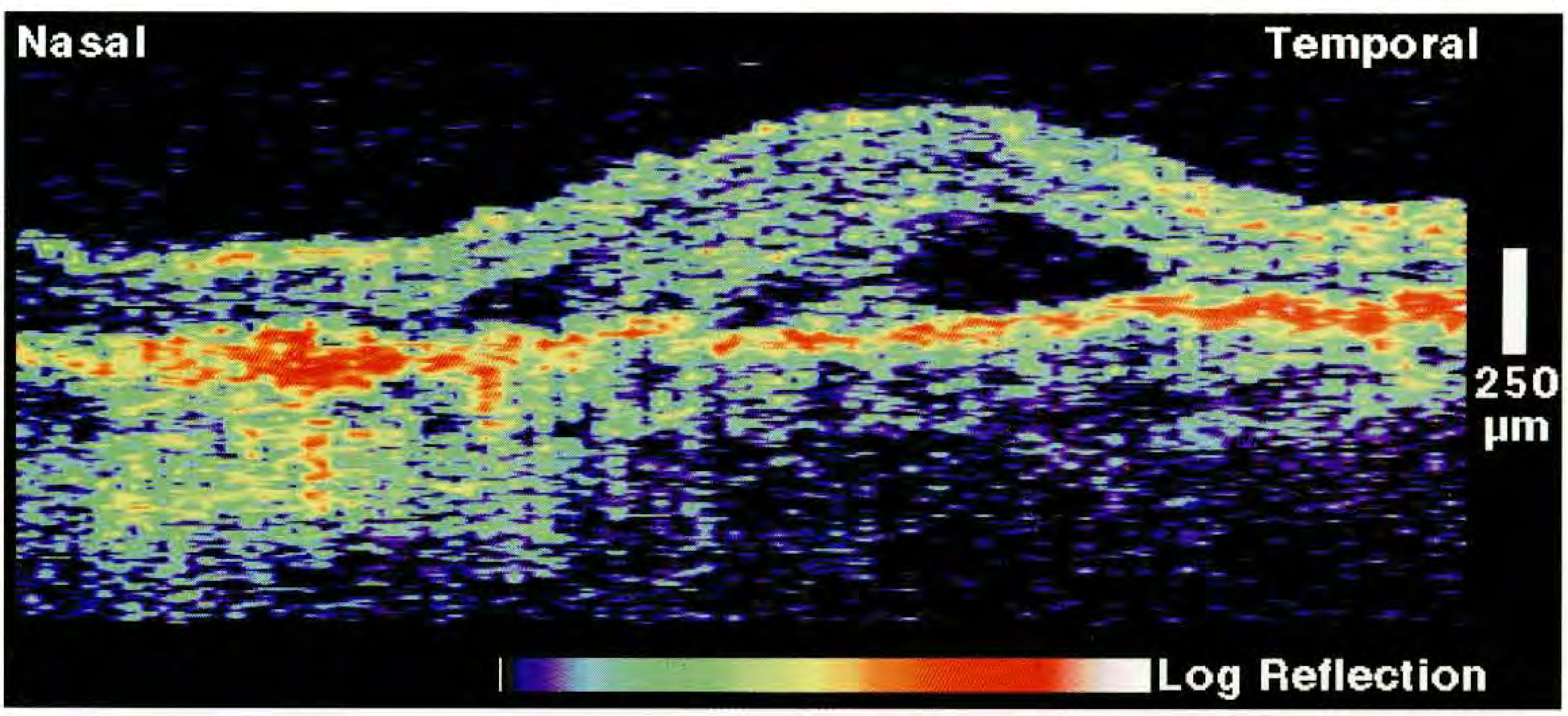

B

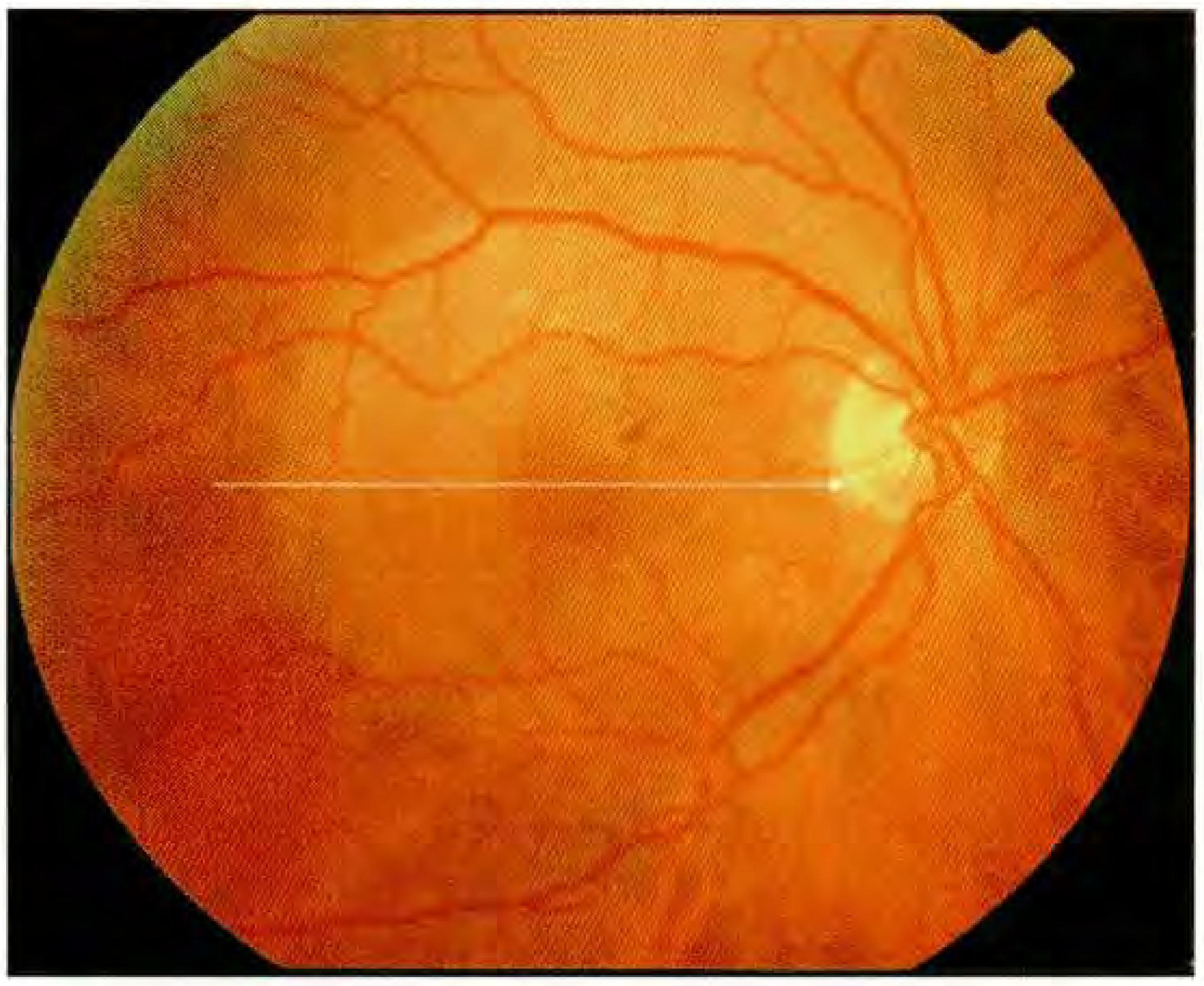

A

B

Case 8-11. Serous Detachment of the Retinal Pigment Epithelium

Clinical Summary

A 70-year-old woman had a large serous detachment of the retinal pigment epithelium in her right eye associated with the clinical diagnosis of age-related macular degeneration (A). Her visual acuity in this eye was 20/400. Fluorescein angiography (B) displayed a plaqoid region of hyperfluorescence nasal to the fovea consistent with a neovascular membrane, and a large area of relative hyperfluorescence involving the macula corresponding to the pigment epithelial detachment.

Optical Coherence Tomography

OCT examination (C) demonstrated a large elevation of the retina and retinal pigment epithelium above an optically clear space. The reflections from the choroid beneath the detachment were attenuated due to shadowing from the highly reflective, detached pigment epithelium. A small pocket of subretinal fluid accumulation was noted temporal to the pigment epithelial detachment. The reflections from the nasal retinal pigment epithelium and choriocapillaris appeared thicker than those at the temporal margin of the image consistent with the leakage pattern of fluorescein dye observed clinically.

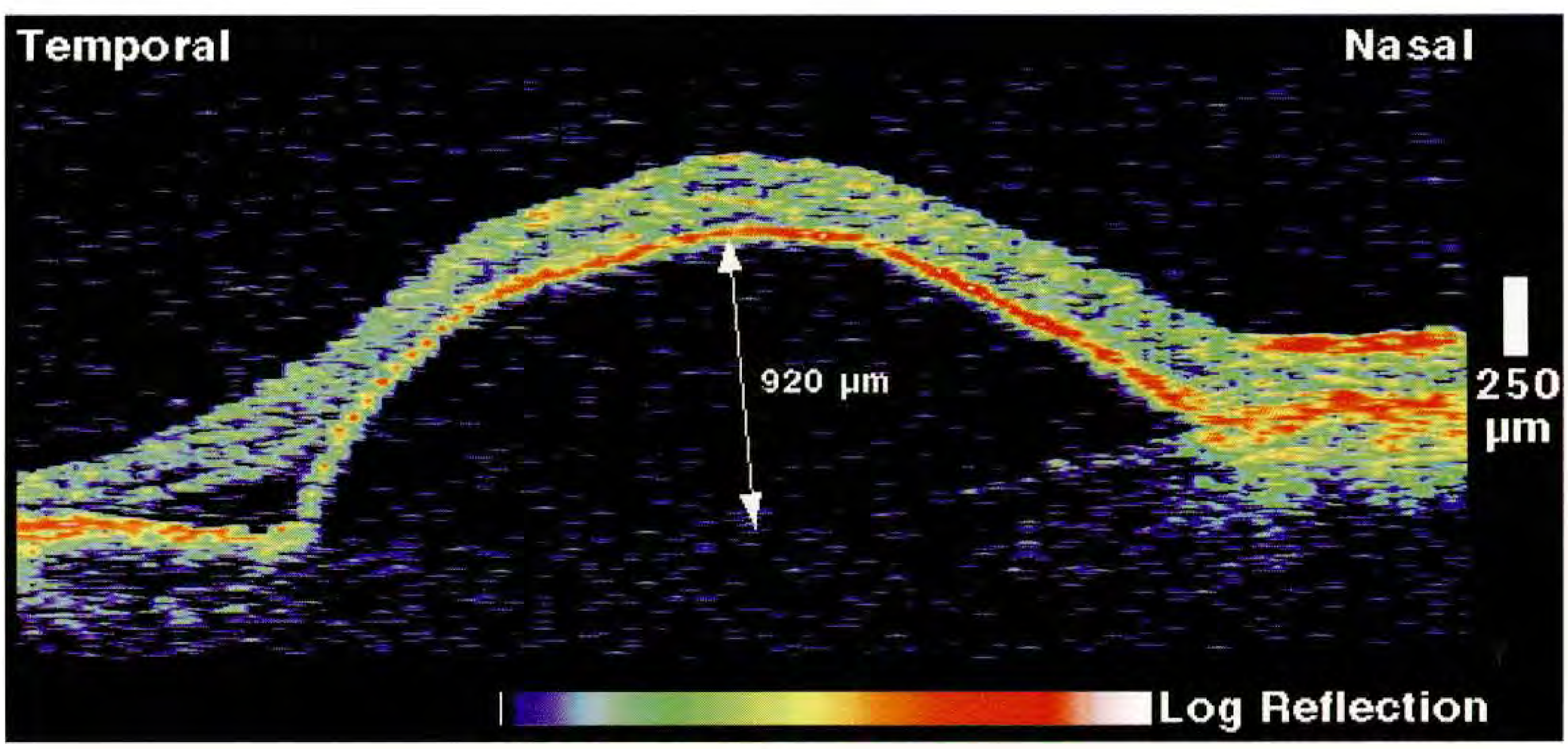

C

Case 8-12. Serous Detachment of the Retinal Pigment Epithelium

Clinical Summary

74-year-old woman with age-related macular degeneration noted a decline in her visual acuity to 20/70 and metamorphopsia in her right eye over the past four to five months. Dilated fundus examination (A) showed a serous pigment epithelial detachment in the central macula. Progressive filling of the detachment was noted on fluorescein angiography (B). Poorly defined hyperfluorescence associated with mild late leakage was also observed inferior and inferotemporal to the fovea.

Optical Coherence Tomography

A vertical OCT tomogram (C) taken through the detachment showed an elevation of the pigment epithelium over an optically clear space corresponding to serous fluid accumulation. The reflection from the choroid below the detachment was attenuated. There was an increase in the thickness of the red band defining the posterior boundary of the neurosensory retina at the inferior margin of the detachment consistent with possible choroidal neovascularization.

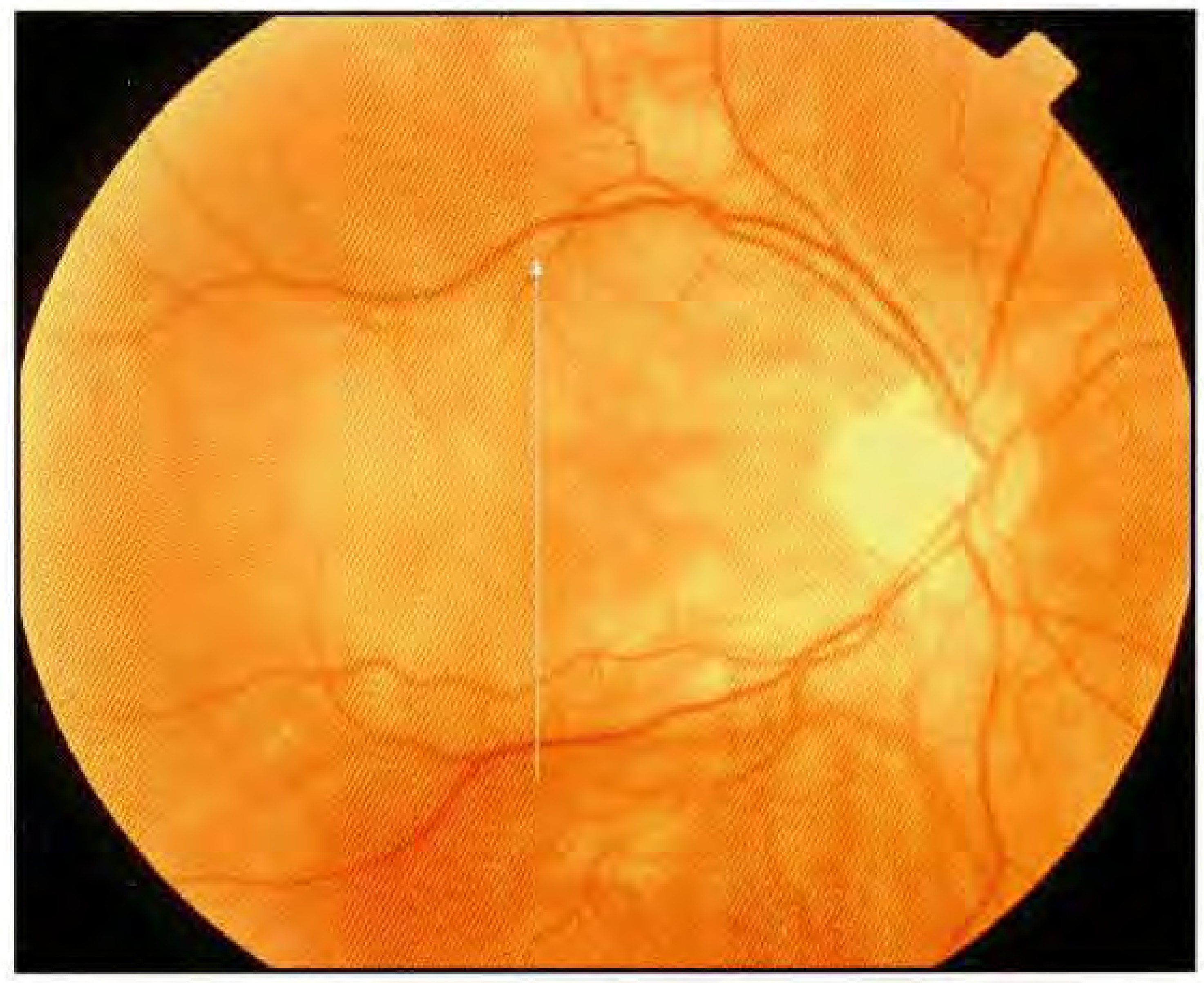

A

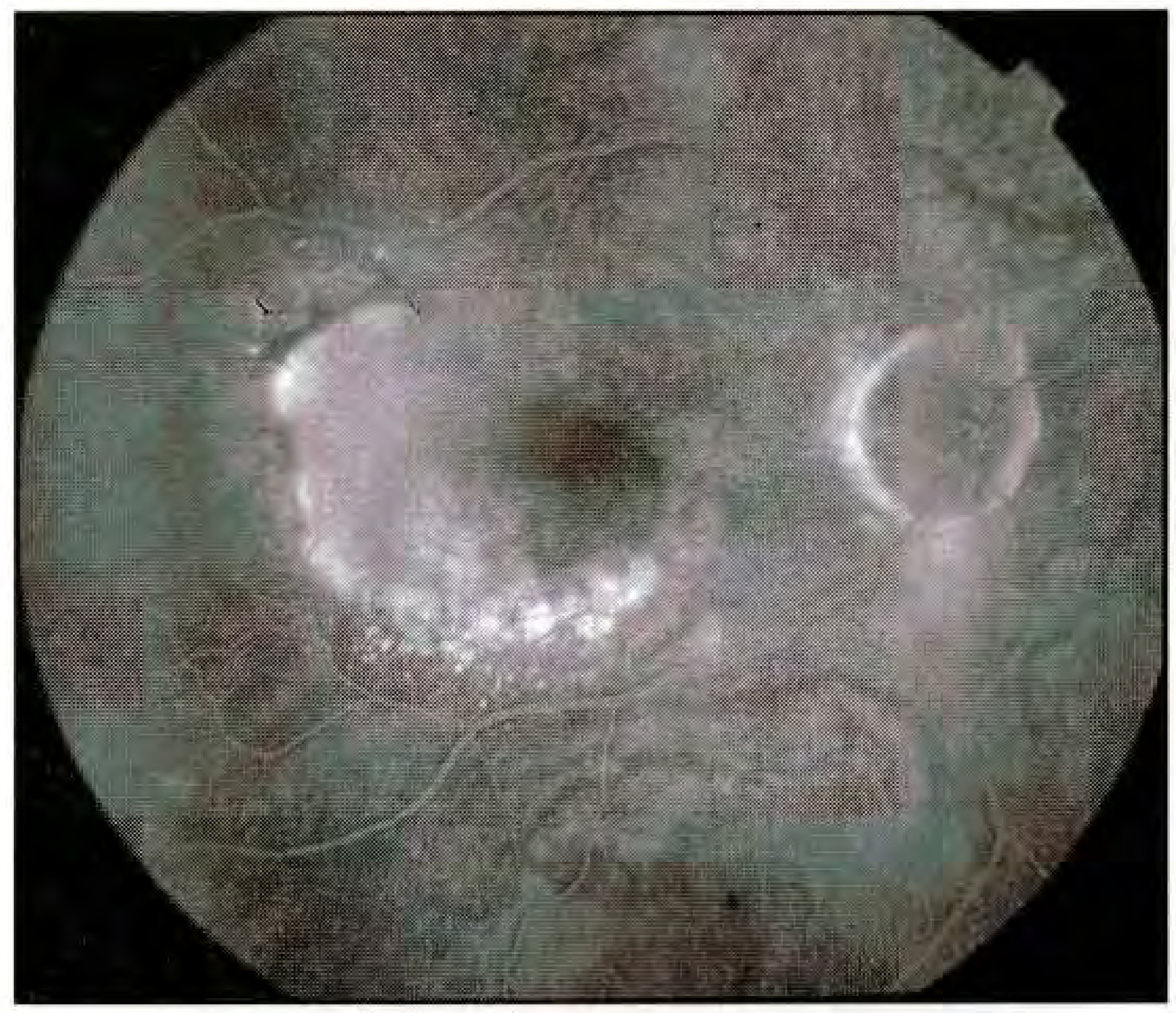

B

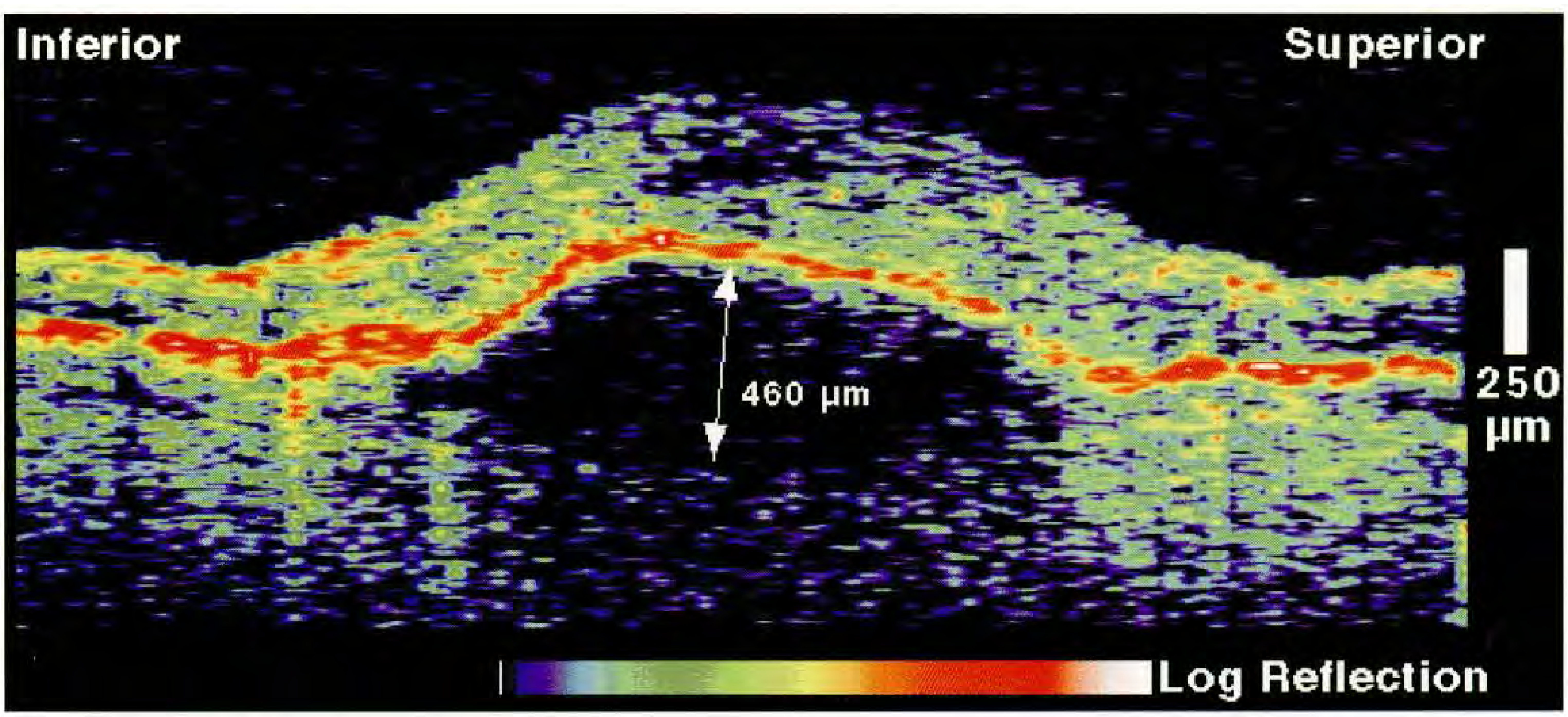

C

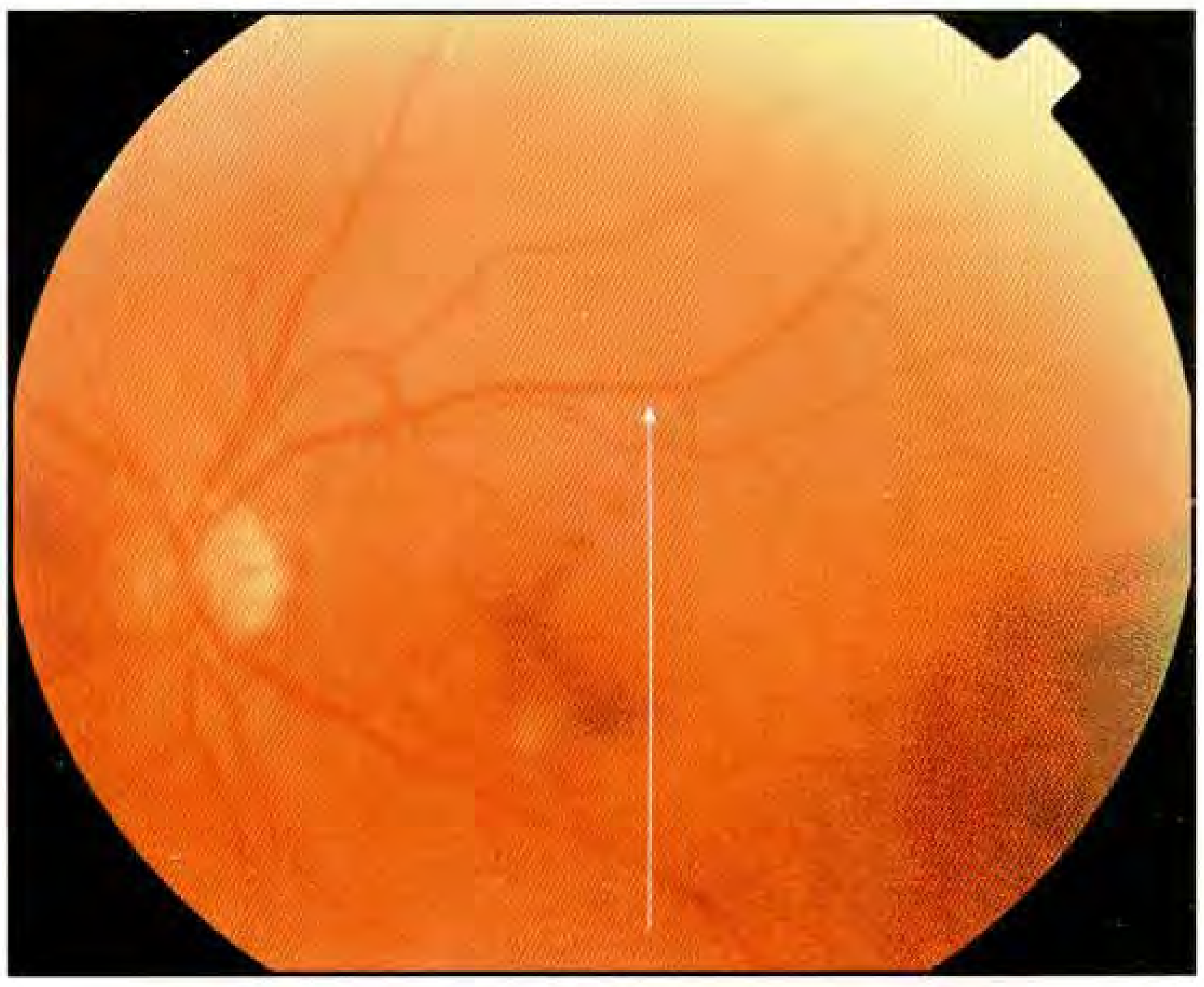

A

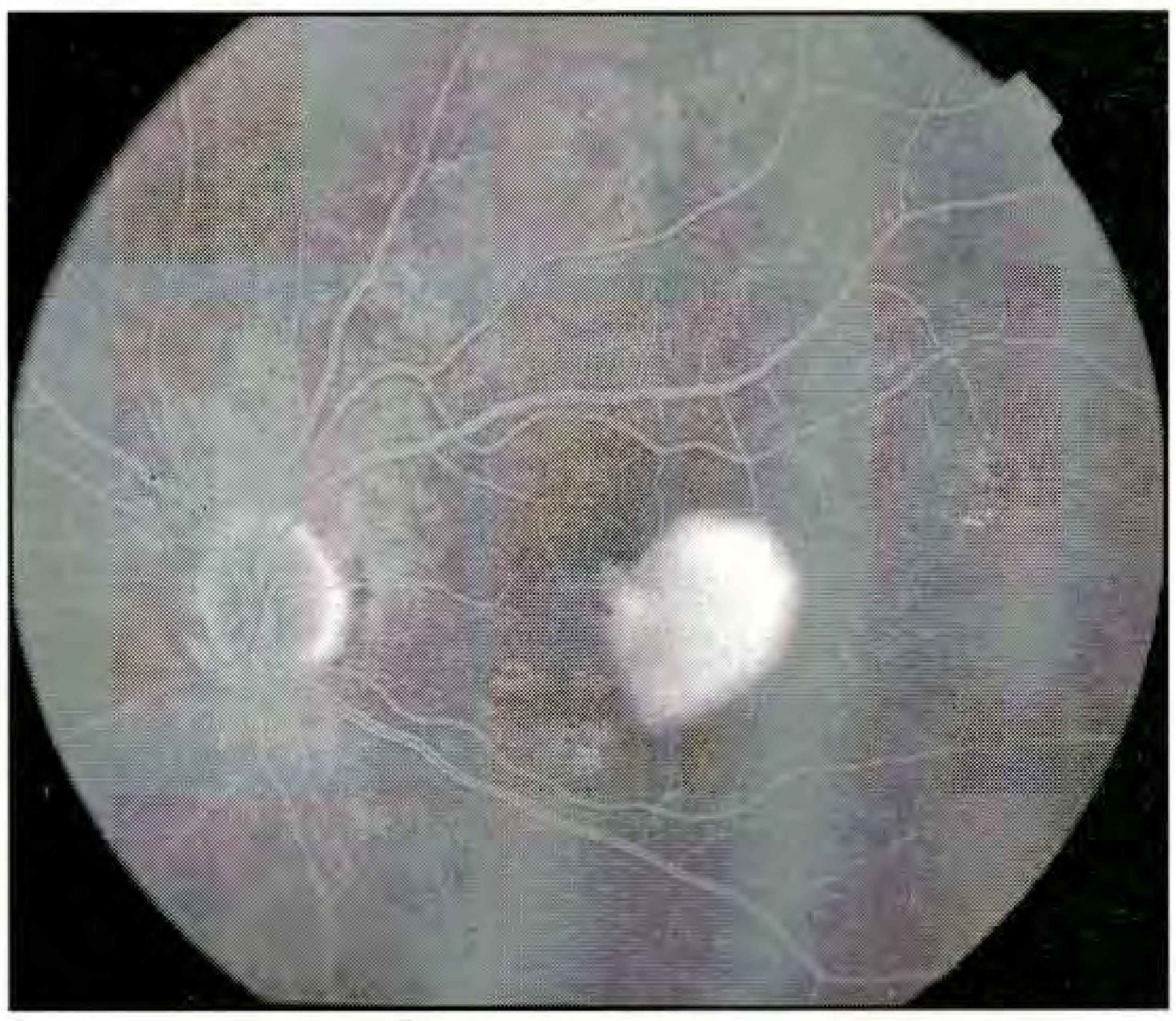

B

Case 8-13. Serous Detachment of the Retinal Pigment Epithelium

Clinical Summary

A 75-year-old woman reported a decline in her reading vision in her left eye over the past seven months. On examination, her visual acuity in this eye was 20/40. An elevated detachment of the retinal pigment epithelium with a small amount of subretinal hemorrhage along the detachment's superonasal border was noted on indirect ophthalmoscopy (A). Fluorescein angiography (B) confirmed filling of the detachment in the central macula.

Optical Coherence Tomography

OCT examination (C) displayed an elevation of the neurosensory retina and retinal pigment epithelium over an optically clear cavity, and shadowing of the reflections from the choroid.

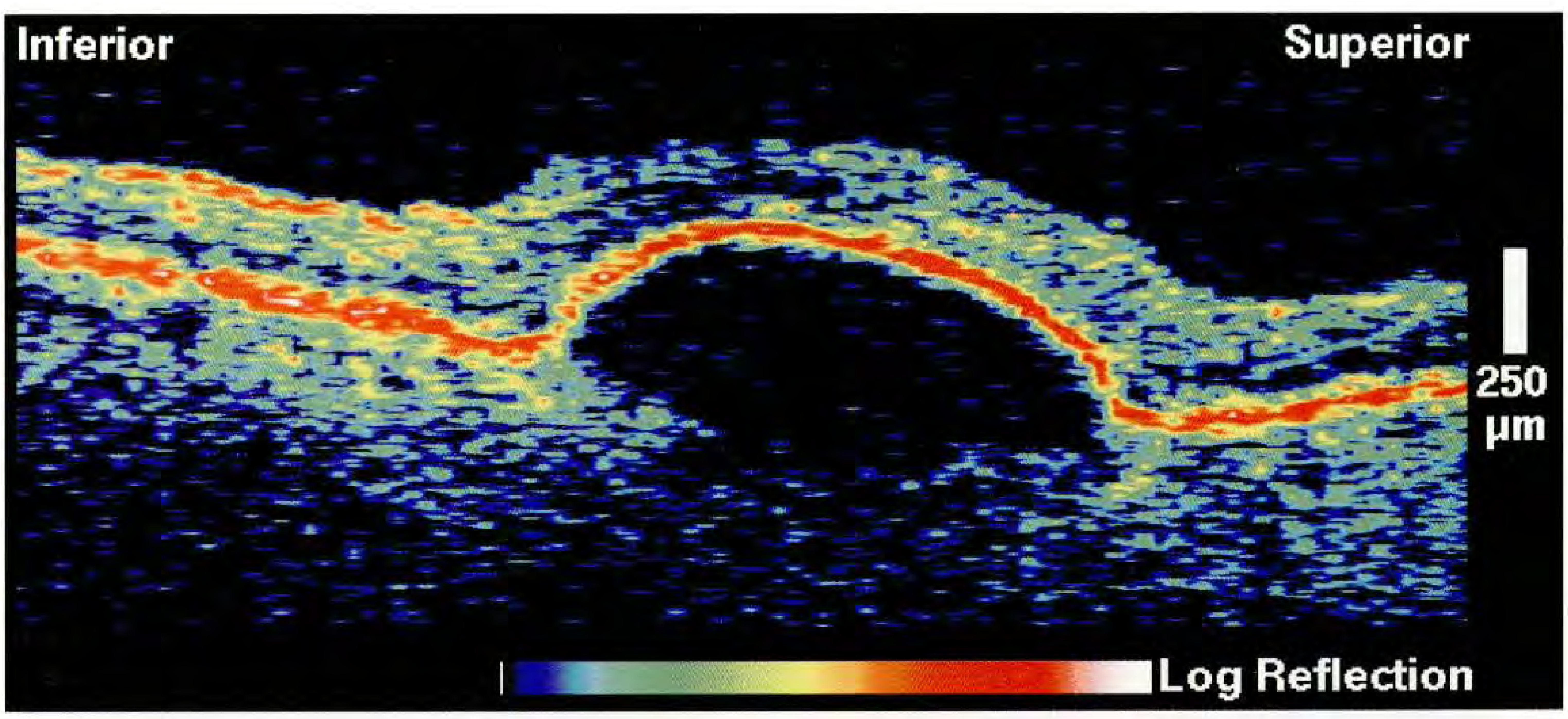

C

Case 8-14. Spontaneous Tear of the Retinal Pigment Epithelium

Clinical Summary

A 69-year-old woman with age-related macular degeneration was evaluated for a decline in the visual acuity of her left eye to 20/200. Fundus examination (A) showed a pigment epithelial detachment with an RPE tear creating an area of retinal pigment epithelial loss along the inferotemporal border. Fluorescein angiography (B) displayed hypofluorescence superonasally and inferotemporally with a well-defined demarcation between these two areas. Increased visualization of the choroidal vasculature and late staining was visible in the inferotemporal region of hyperfluorescence consistent with an absence of the pigment epithelium. The superonasal region of hypofluorescence exhibited a reticular pattern which increased in size and intensity as the angiogram progressed consistent with choroidal neovascularization.

Optical Coherence Tomography

The OCT image (C) exhibited a well-defined elevation of the neurosensory retina and pigment epithelium which shadowed the reflections from the choroid below. Two red reflective layers were visible below the sensory retina in the area of the detachment consistent with a folded, double-layer of pigment epithelium. The choroidal neovascularization below the detachment was not visible due to the lack of optical penetration. A non-reflective region of subretinal fluid was evident superotemporal to the detachment in the image. Enhanced reflectivity and optical penetration of the choroid was noted in this region consistent with the lack of retinal pigment epithelium.

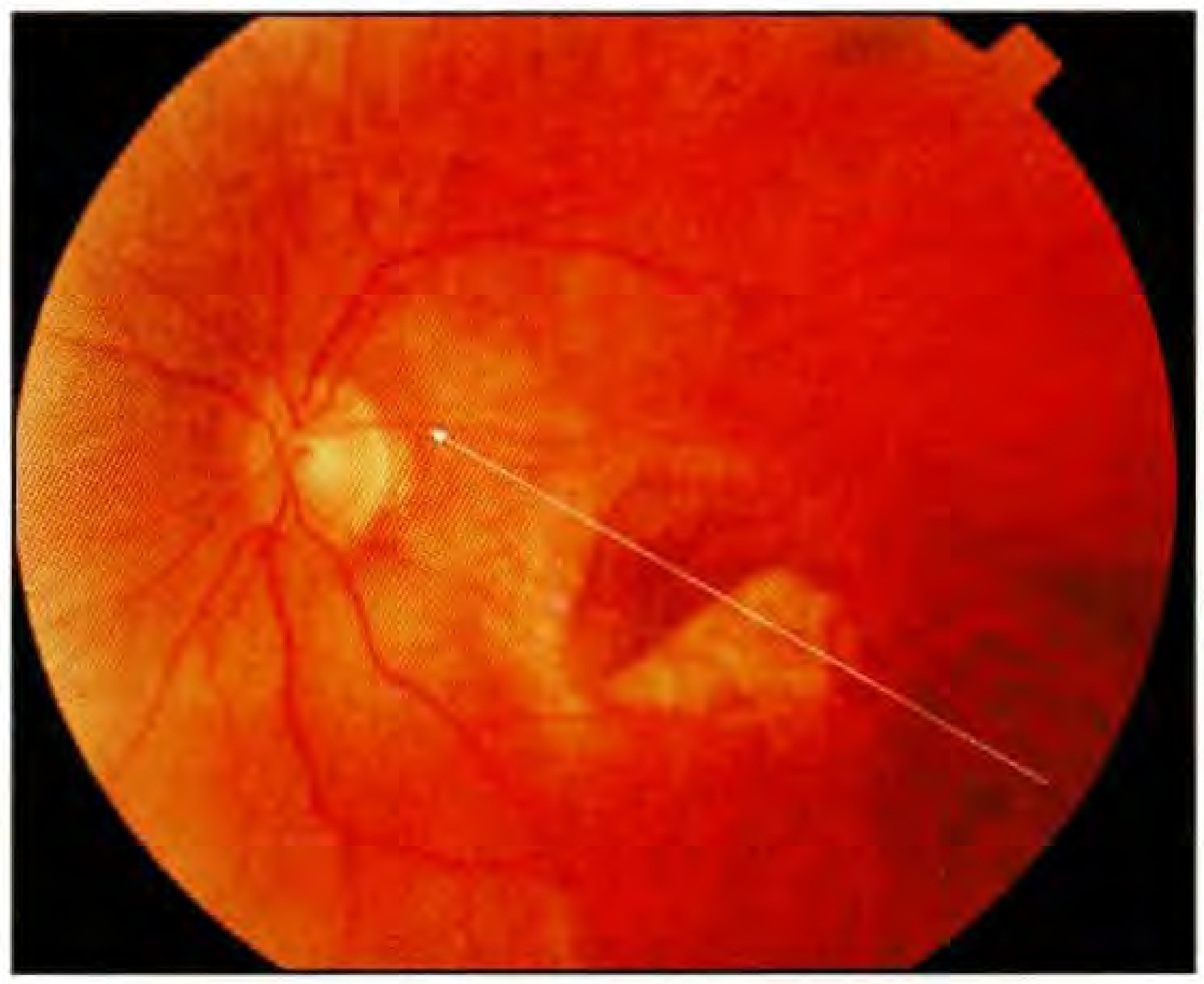

A

B

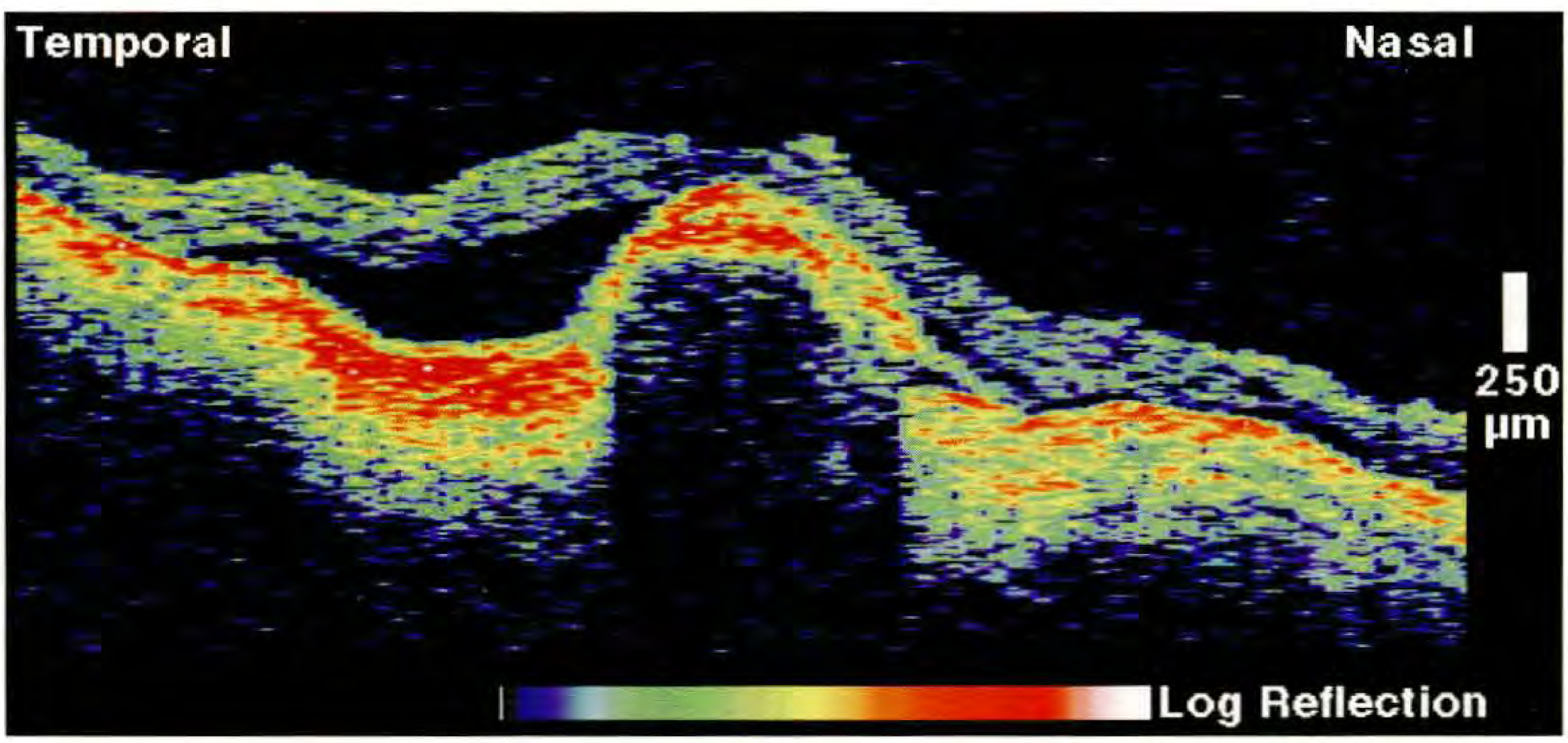

C

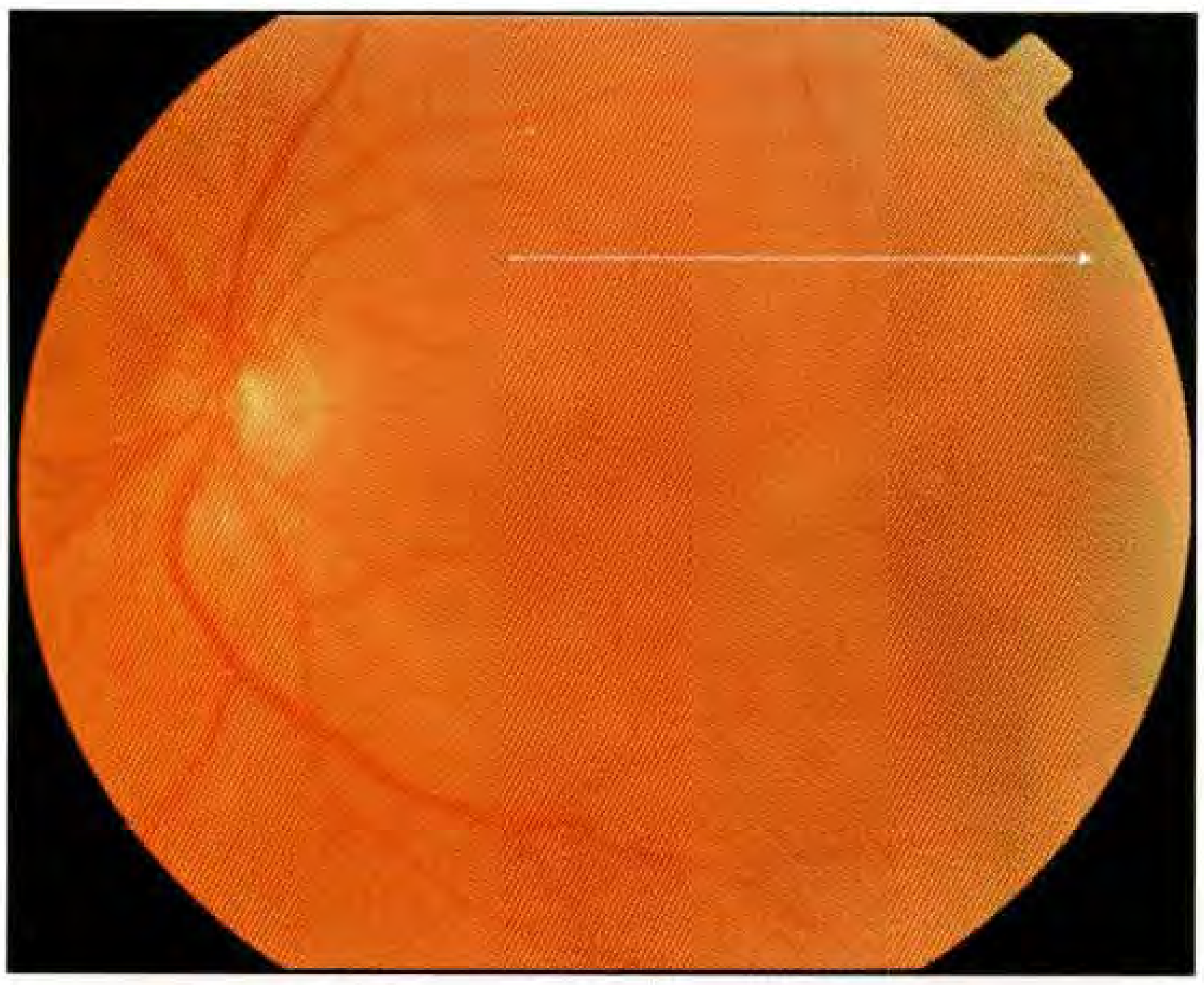

A

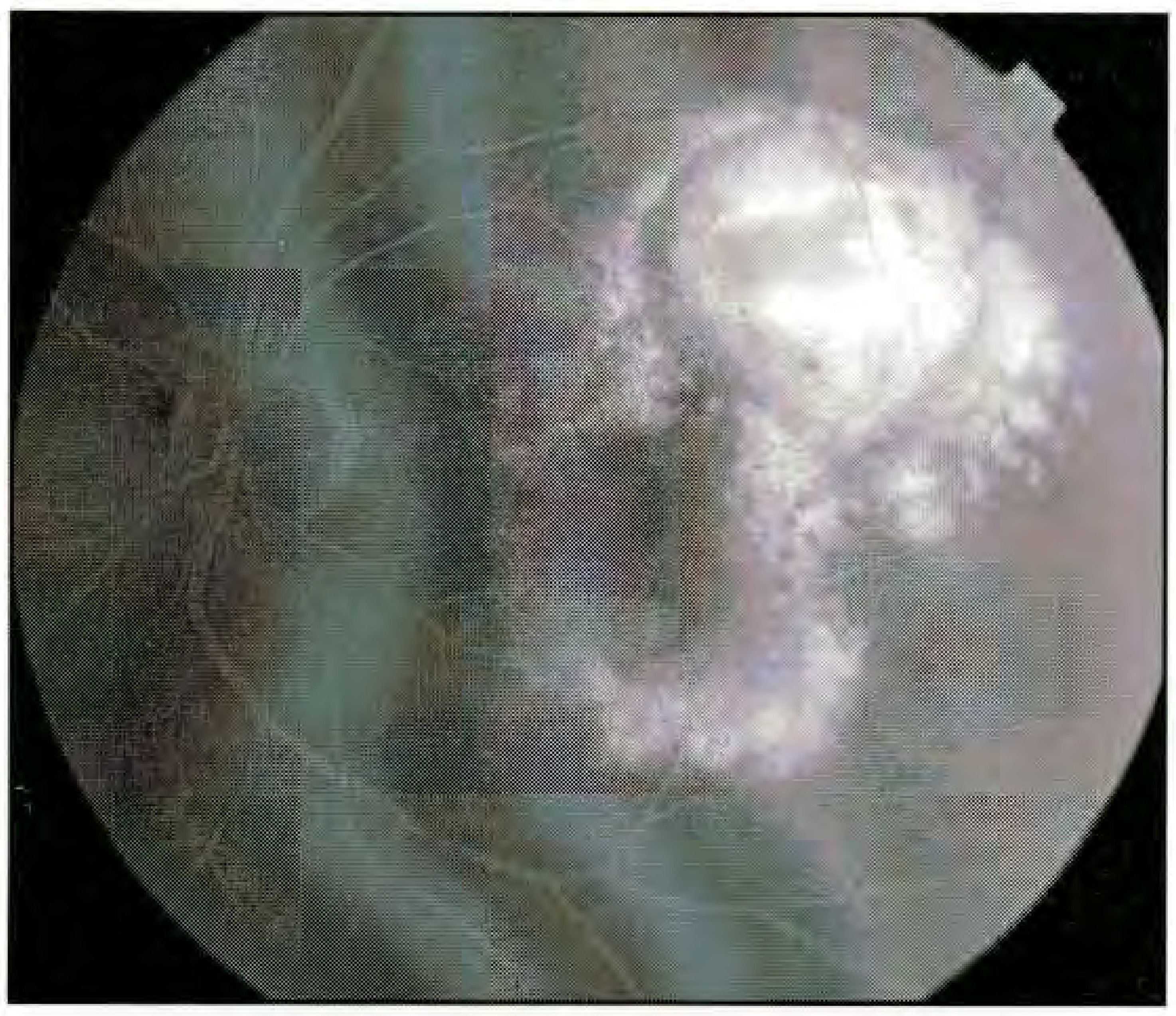

B

Case 8-15. Serous Detachment of the Retinal Pigment Epithelium

Clinical Summary

A 74-year-old woman with a history of bilateral pigment epithelial detachments recently noted a slight decline in the visual acuity in her left eye. Slit-lamp biomicroscopy (A) identified serous detachment of the retinal pigment epithelium immediately superotemporal to the fovea. Fluorescein angiography (B) revealed a bilobed region of hyperfluorescence. The superior portion of the lesion showed late dye pooling consistent with a pigment epithelial detachment.

Optical Coherence Tomography

A horizontal OCT scan (C) acquired through the detachment displayed a large elevation of the retinal pigment epithelium over a non-reflective cavity with shadowing of the choroid below. Two areas of subretinal fluid accumulation were noted adjacent to the detachment on either side.

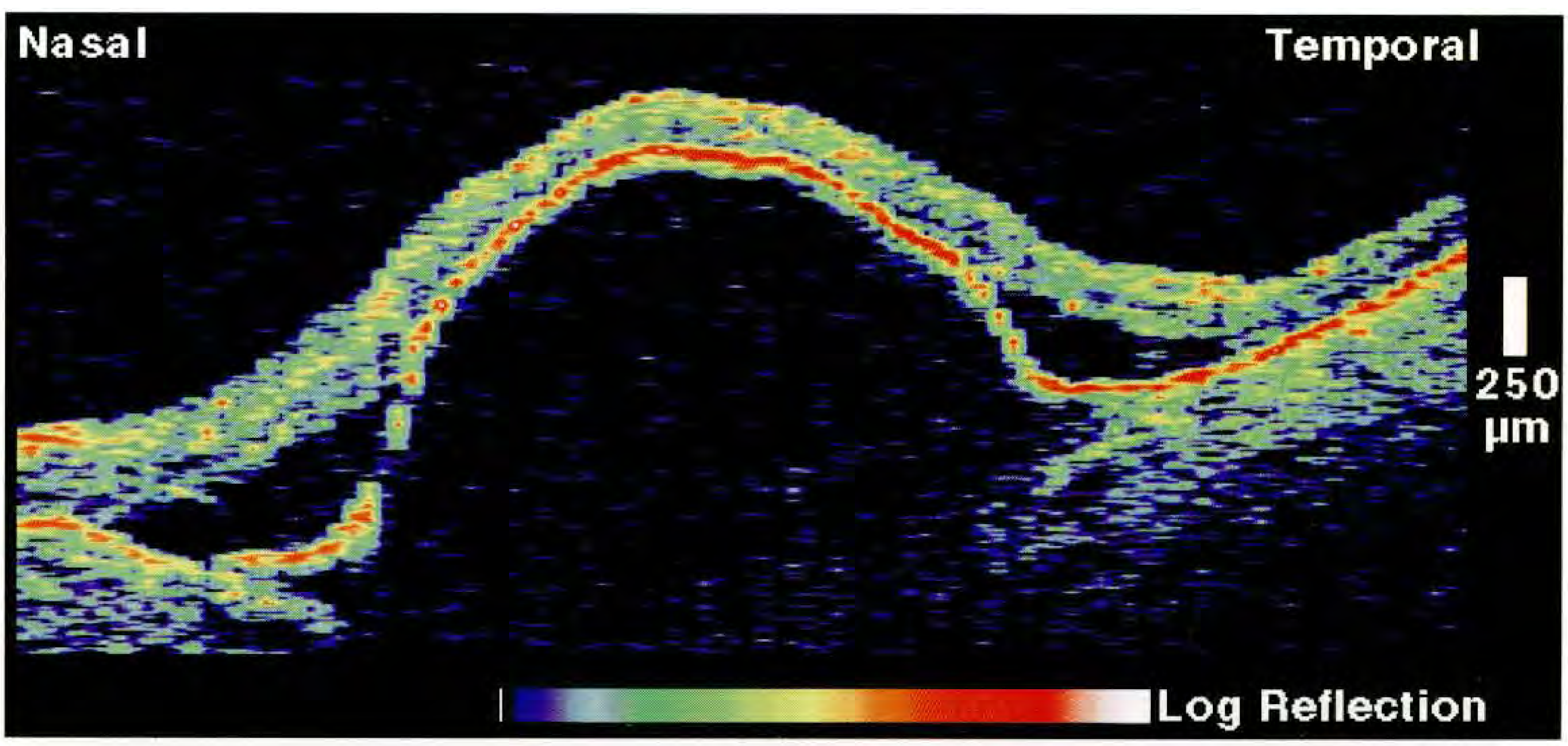

C

Case 8-16. Detachment of the Retinal Pigment Epithelium

A

Clinical Summary

A 72-year-old man with age-related macular degeneration was evaluated for slowly decreasing vision. On examination, the visual acuity in his left eye was 20/50. Dilated ophthalmoscopy (A) revealed a shallow pigment epithelial detachment in the macula with surrounding drusen.

Optical Coherence Tomography

An OCT image (B) taken superior to the fovea showed a slight elevation of the retina and the reflective band corresponding to the retinal pigment epithelium. Low to moderate backscatter was observed beneath the detachment consistent with either a cloudy exudate or fibrovascular proliferation.

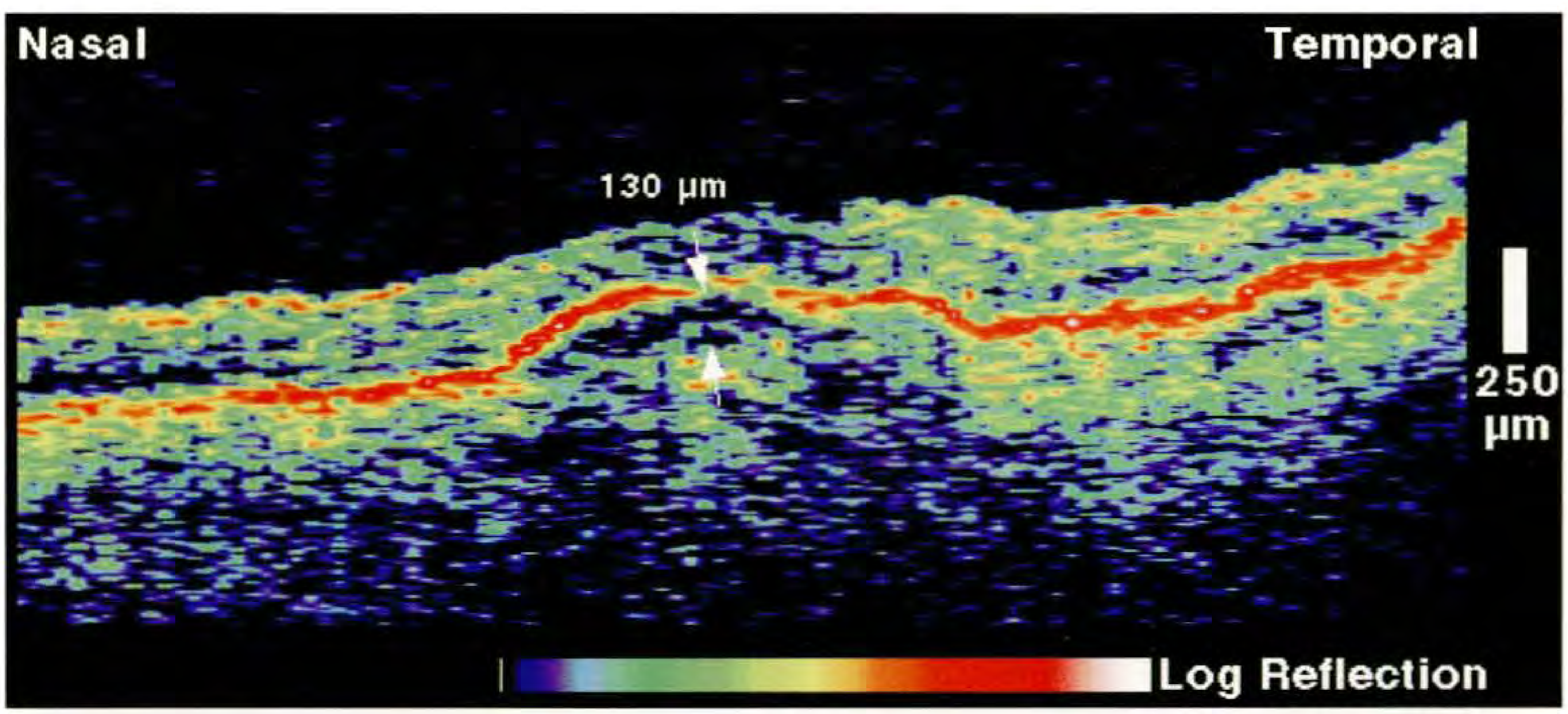

B

A

Case 8-17. Serous Neurosensory and Pigment Epithelial Detachments

Clinical Summary

A 72-year-old woman with exudative age-related macular degeneration was studied. Her visual acuity in the right eye was 20/80. Slit-lamp examination (A) revealed two serous pigment epithelial detachments in the inferior and superior macula.

Optical Coherence Tomography

A vertical OCT section (B) displayed two detachments of the retina and pigment epithelium above optically clear serous fluid cavities. The inferior detachment extended beneath the fovea. The reflections from the choroid were reduced below the detachments consistent with shadowing from the detached pigment epithelium above. A pocket of subretinal fluid was identified between the two pigment epithelial detachments.

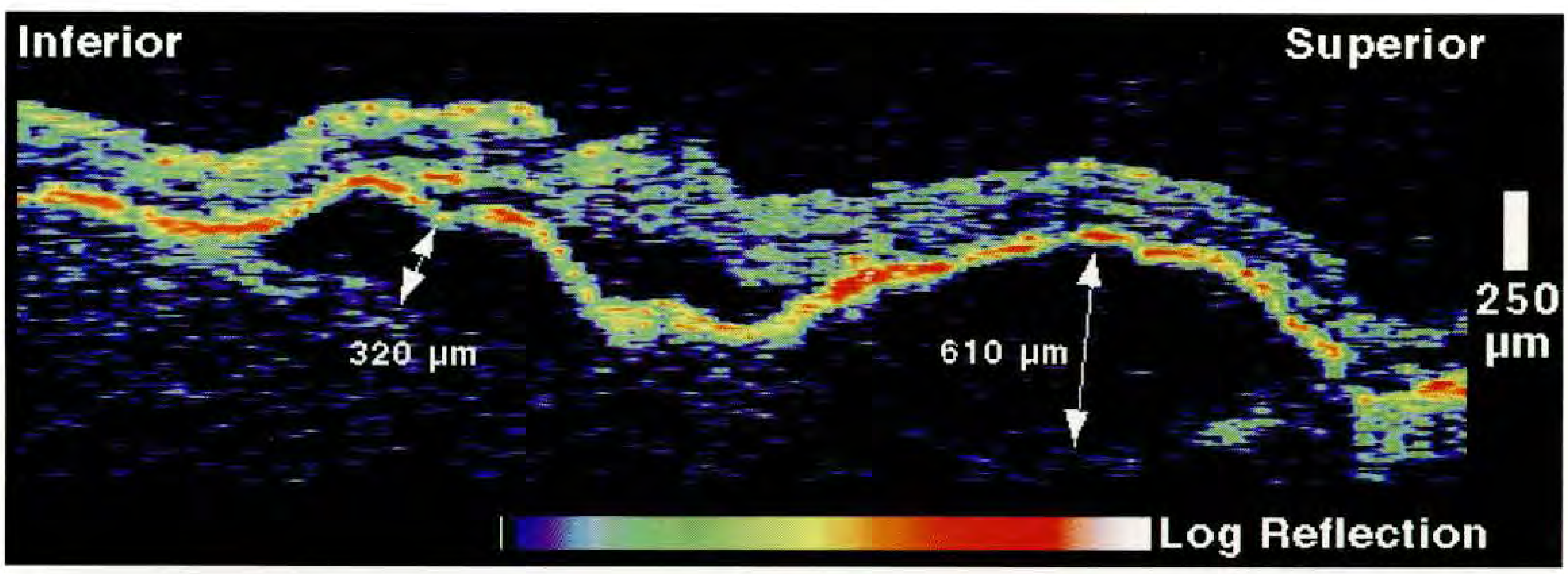

B

Case 8-17 continued

Clinical Summary

The patient's left eye had a visual acuity of counting fingers associated with a serous neurosensory retinal detachment and subretinal neovascularization (C).

Optical Coherence Tomography

OCT (D) showed a large elevation of the retina over an optically clear cavity. The reflection from the choroid was not attenuated beneath the cavity consistent with a neurosensory detachment. The lack of a continuous, highly reflective thin band corresponding to a normal retinal pigment epithelium and choriocapillaris suggested the presence of a choroidal neovascular membrane beneath the detachment.

C

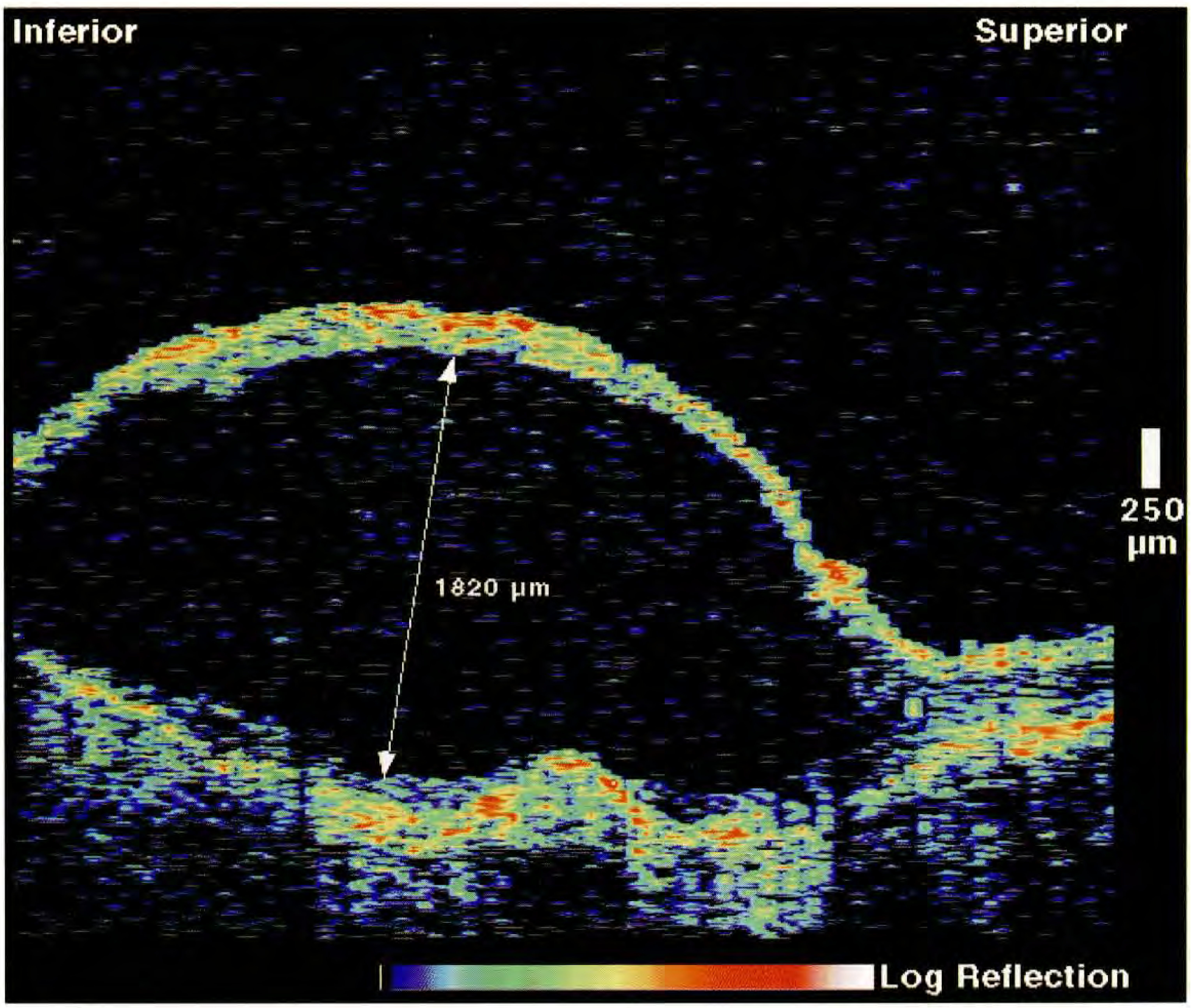

D

A

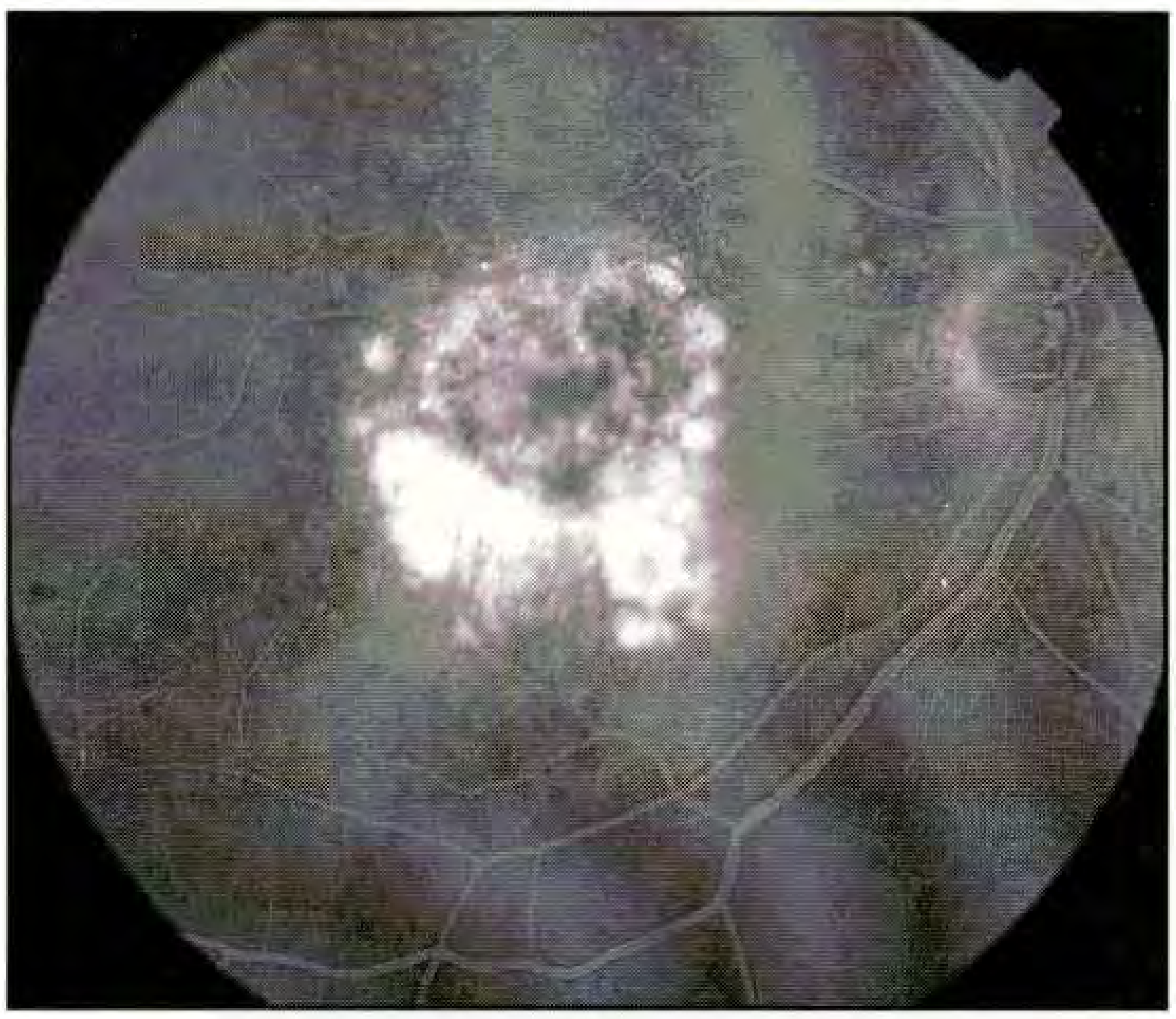

B

Case 8-18. Fibrovascular Pigment Epithelial Detachment and Soft Drusen

Clinical Summary

A 71-year-old man with exudative age-related macular degeneration had a visual acuity of 20/60 in his right eye. Dilated fundus examination (A) of this eye showed a mottled pigment epithelial detachment in the central macula. Fluorescein angiography (B) displayed stippled hyperfluorescence consistent with a fibrovascular pigment epithelial detachment. Late leakage was present along the inferior border of the lesion.

Optical Coherence Tomography

A vertical tomogram (C) delineated an elevation of the neurosensory retina and retinal pigment epithelium (RPE) with moderate optical backscatter below the RPE confirming fibrovascular proliferation. The reflective band corresponding to the RPE and choriocapillaris was thickened and fragmented along the inferior border of the lesion consistent with subretinal neovascularization and corresponding to the area of late leakage observed on angiography.

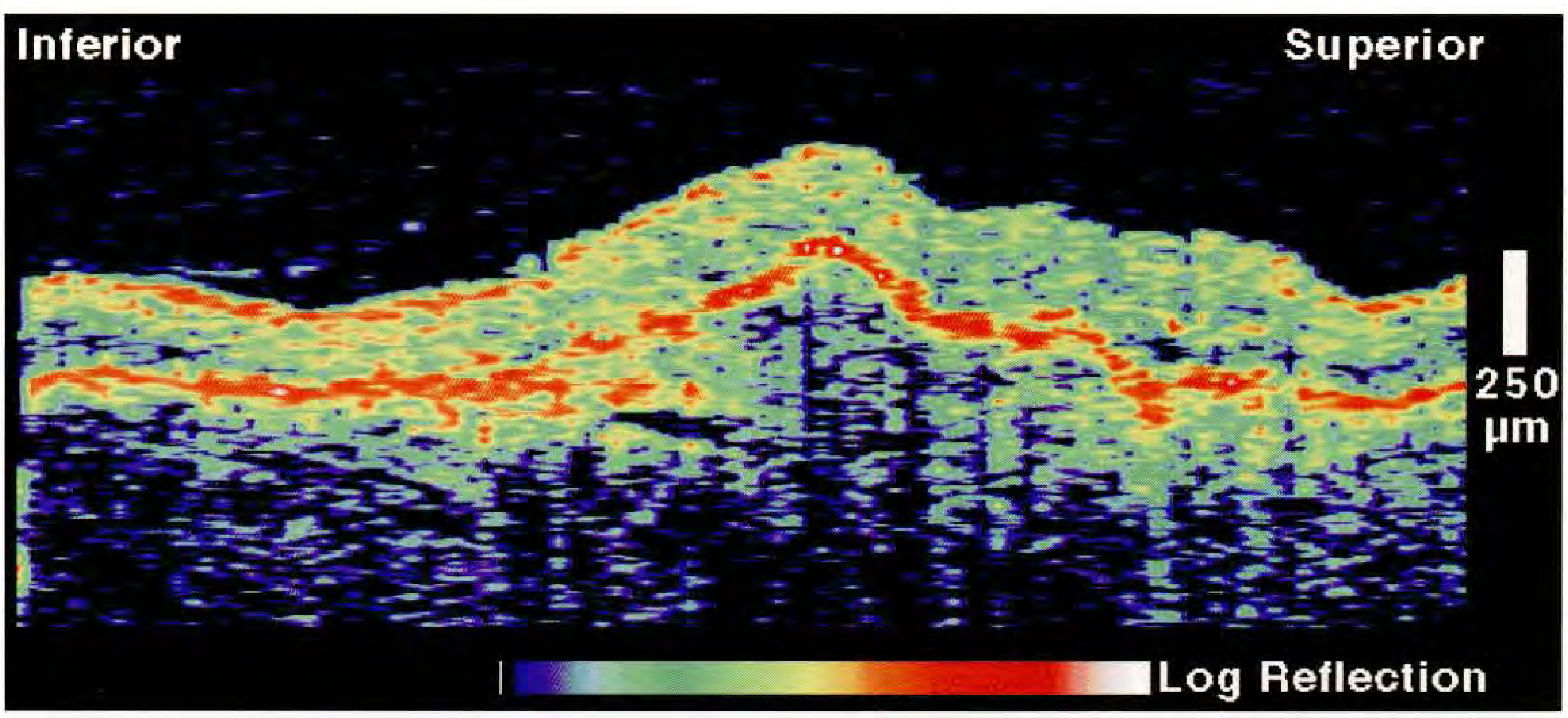

C

Case 8-18 continued

Clinical Summary

The patient's left eye was notable for soft drusen in the central macula associated with a visual acuity of 20/40 (D).

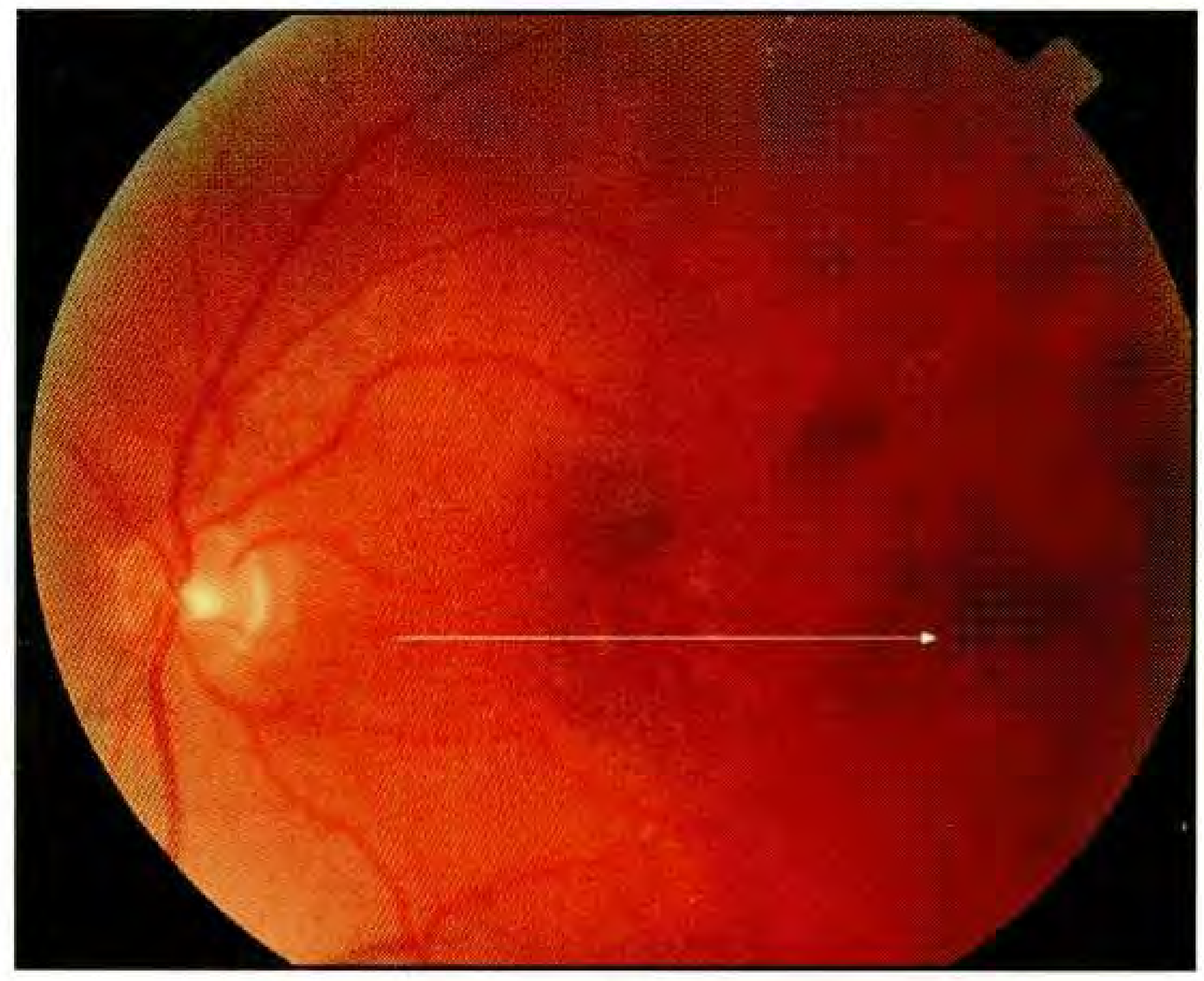

D

Optical Coherence Tomography

OCT (E) demonstrated small modulations in the contour of the RPE with moderate optical reflectivity below the lesions consistent with soft drusen.

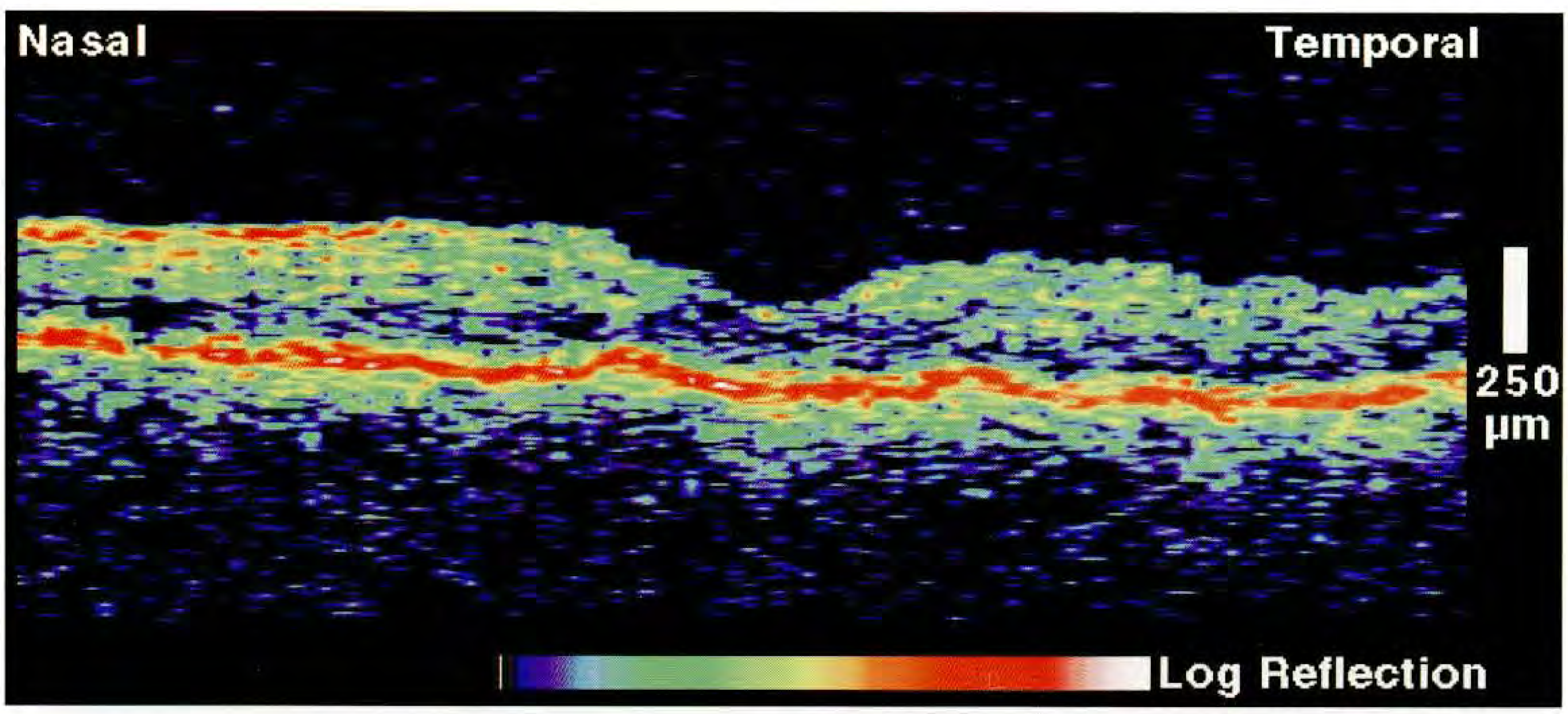

E

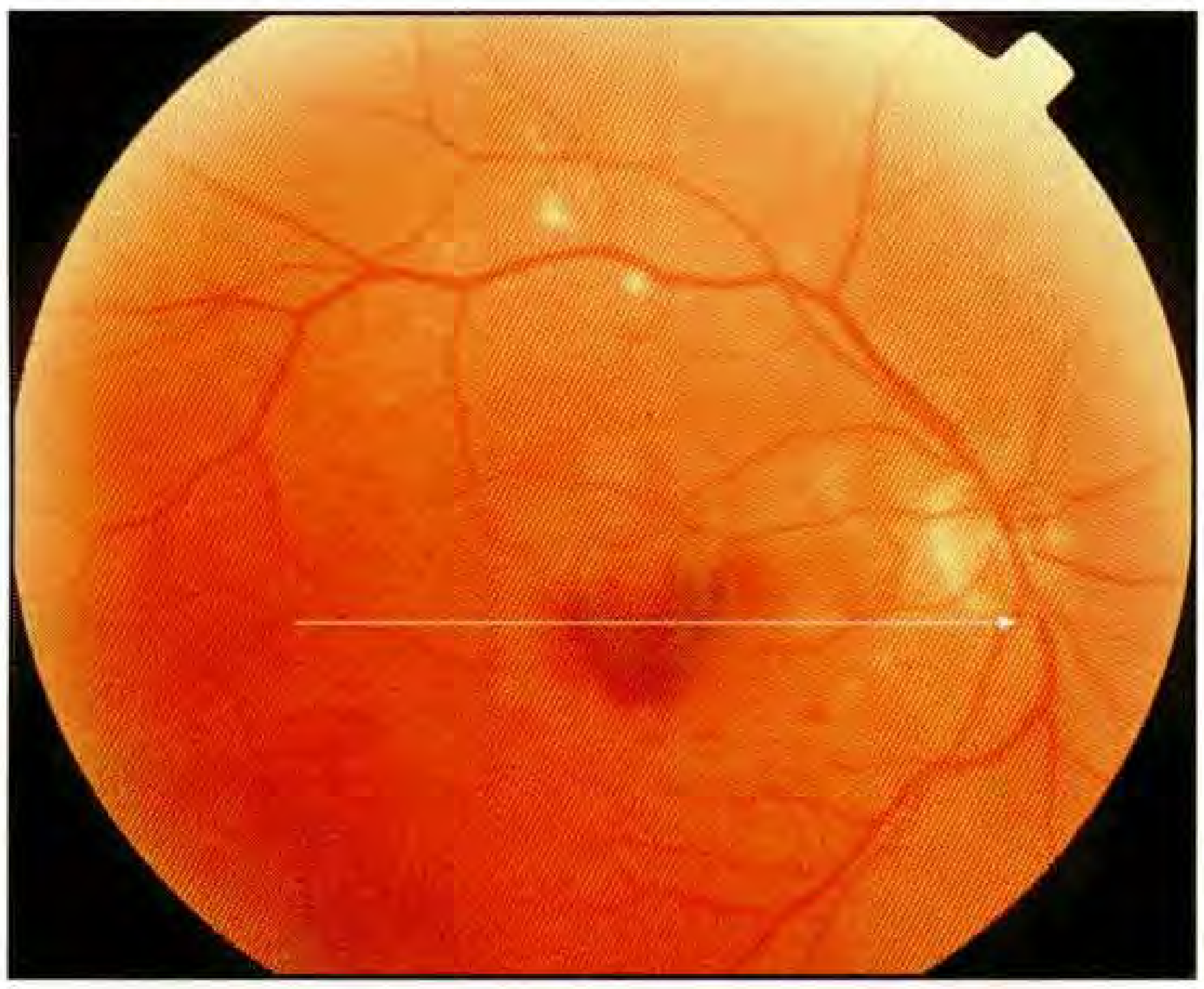

A

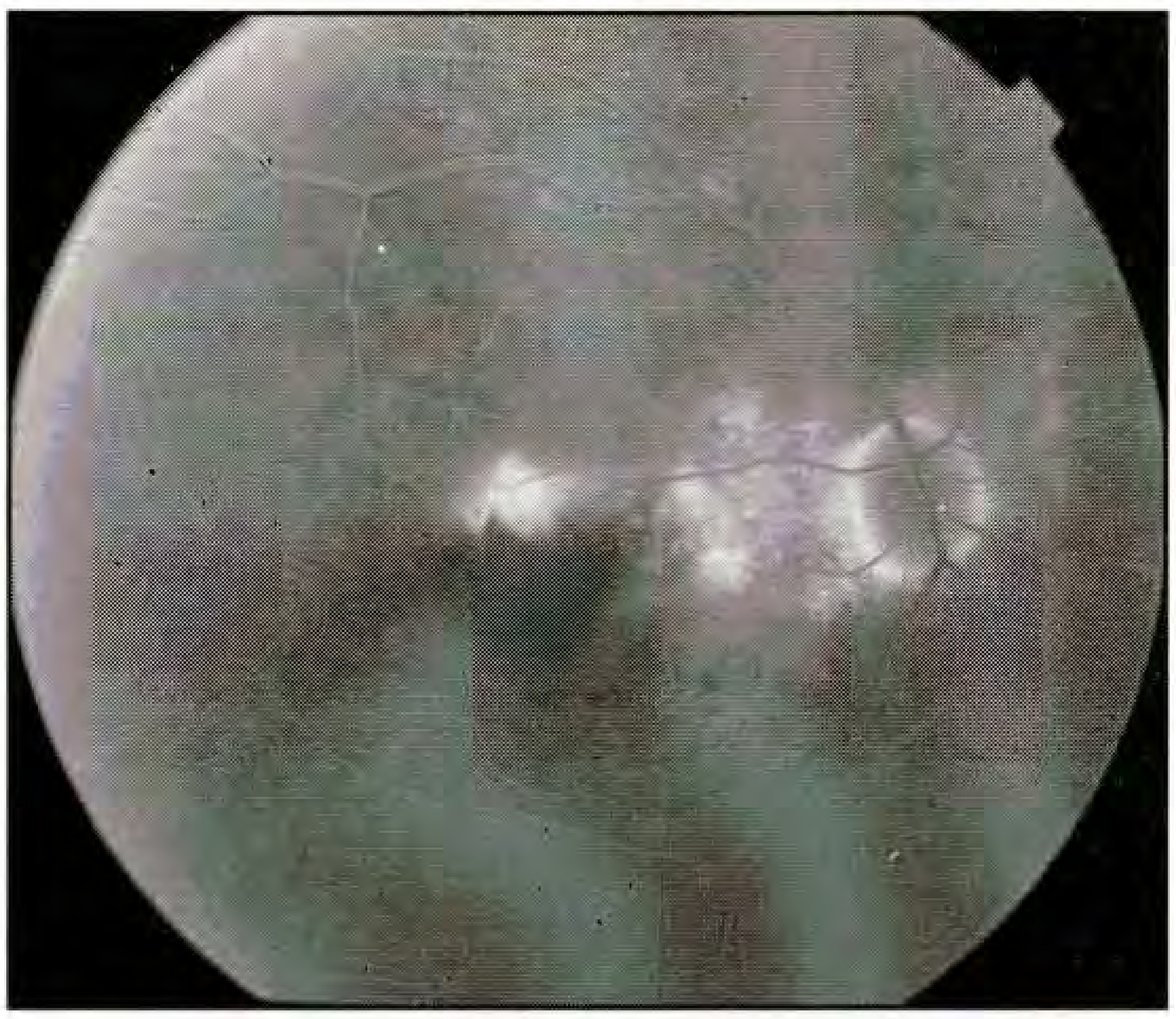

B

Case 8-19. Hemorrhagic Detachment of the Retinal Pigment Epithelium

Clinical Summary

A 78-year-old man with age-related macular degeneration noted decreased vision in his right eye over a period of two months. On examination, his vision was assessed at 20/80. Slit-lamp biomicroscopy (A) showed a central hemorrhagic pigment epithelial detachment with surrounding subretinal fluid. A hypofluorescent lesion on fluorescein angiography (B) confirmed the hemorrhage, and late leakage was noted superior to the fovea. Indocyanine green angiography (not shown) revealed a focal area of hyperfluorescence nasal to the pigment epithelial detachment which was suspicious for choroidal neovascularization.

Optical Coherence Tomography

An OCT image (C) acquired horizontally showed an elevation of both the neurosensory retina and a red band corresponding to the retinal pigment epithelium. The red band appeared thinner in the region of the detachment than in the surrounding retina, where it was indistinguishable from the reflection from the choriocapillaris. Small pockets of minimal reflectivity were noted adjacent to the detachment corresponding to the subretinal fluid observed clinically. The reflections from the pigment epithelium and choriocapillaris appeared thicker in the nasal compared to the temporal aspect of the image, consistent with the putative region of choroidal neovascularization. Moderate backscatter which attenuated quickly with depth was observed beneath the detached RPE consistent with hemorrhage.

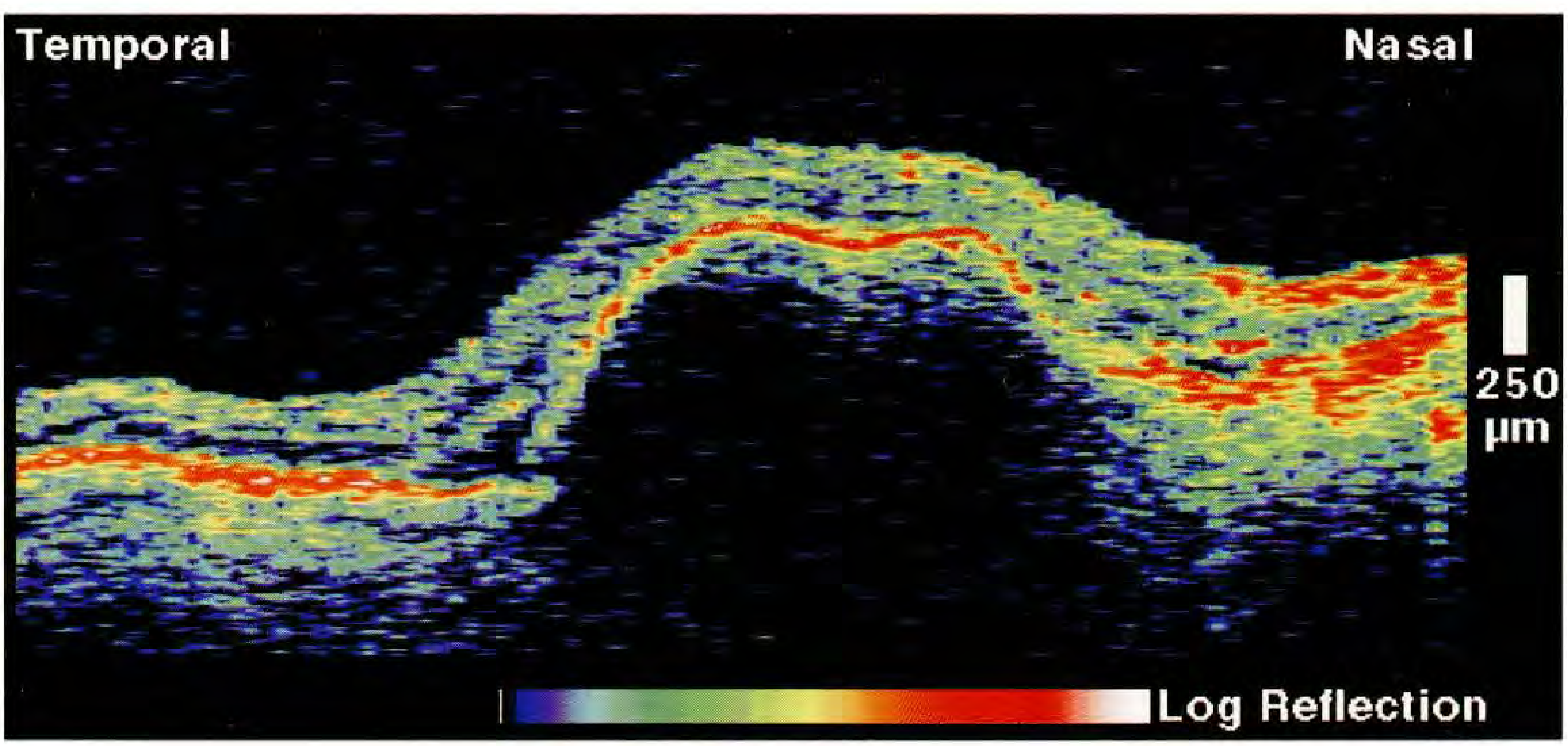

C

Case 8-20. Hemorrhagic Detachment of the Retinal Pigment Epithelium

Clinical Summary

A 65-year-old woman had a hemorrhagic pigment epithelial detachment in her right eye. Slit-lamp examination (A) showed the detachment inferotemporal to the fovea, an additional serous pigment epithelial detachment superotemporal to the macula, and subretinal fluid and cystoid macular edema directly in the fovea. Her visual acuity in this eye was 20/100. Fluorescein angiography (B) revealed a large area of hyperfluorescence consistent with hemorrhage and a hyperfluorescent lesion superotemporal to the fovea consistent with a serous detachment of the retinal pigment epithelium (RPE). Hyperfluorescence was also observed within and nasal to the fovea.

Optical Coherence Tomography

An OCT image (C) obtained through the hemorrhagic detachment of the RPE showed an elevation of the neurosensory retina. The blood filled cavity was highly reflective towards the surface, but significantly attenuated the reflections returning from deeper within the hemorrhage and choroid. The reflective band corresponding to the RPE was indistinguishable from the anterior margin of the hemorrhage.

A

B

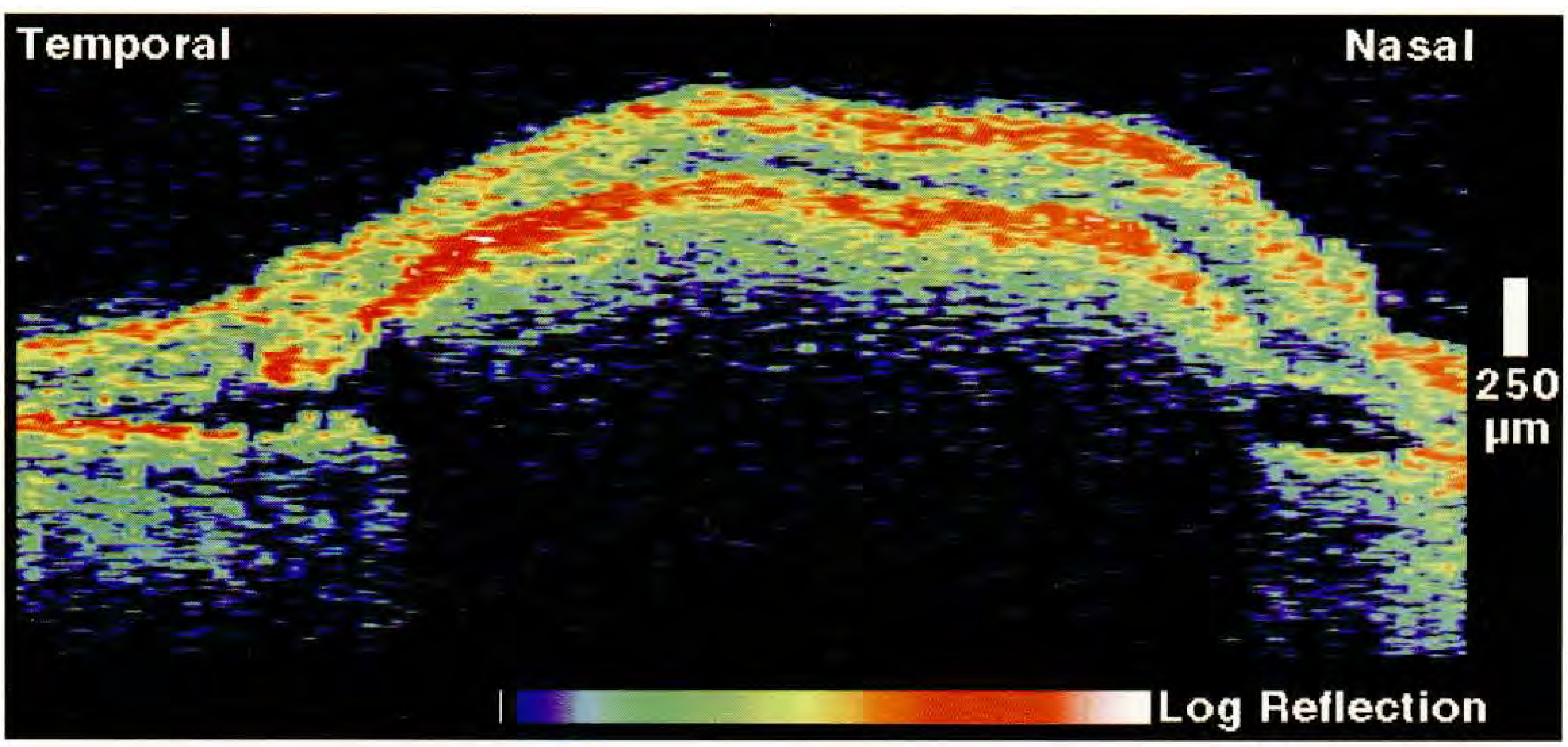

C

A

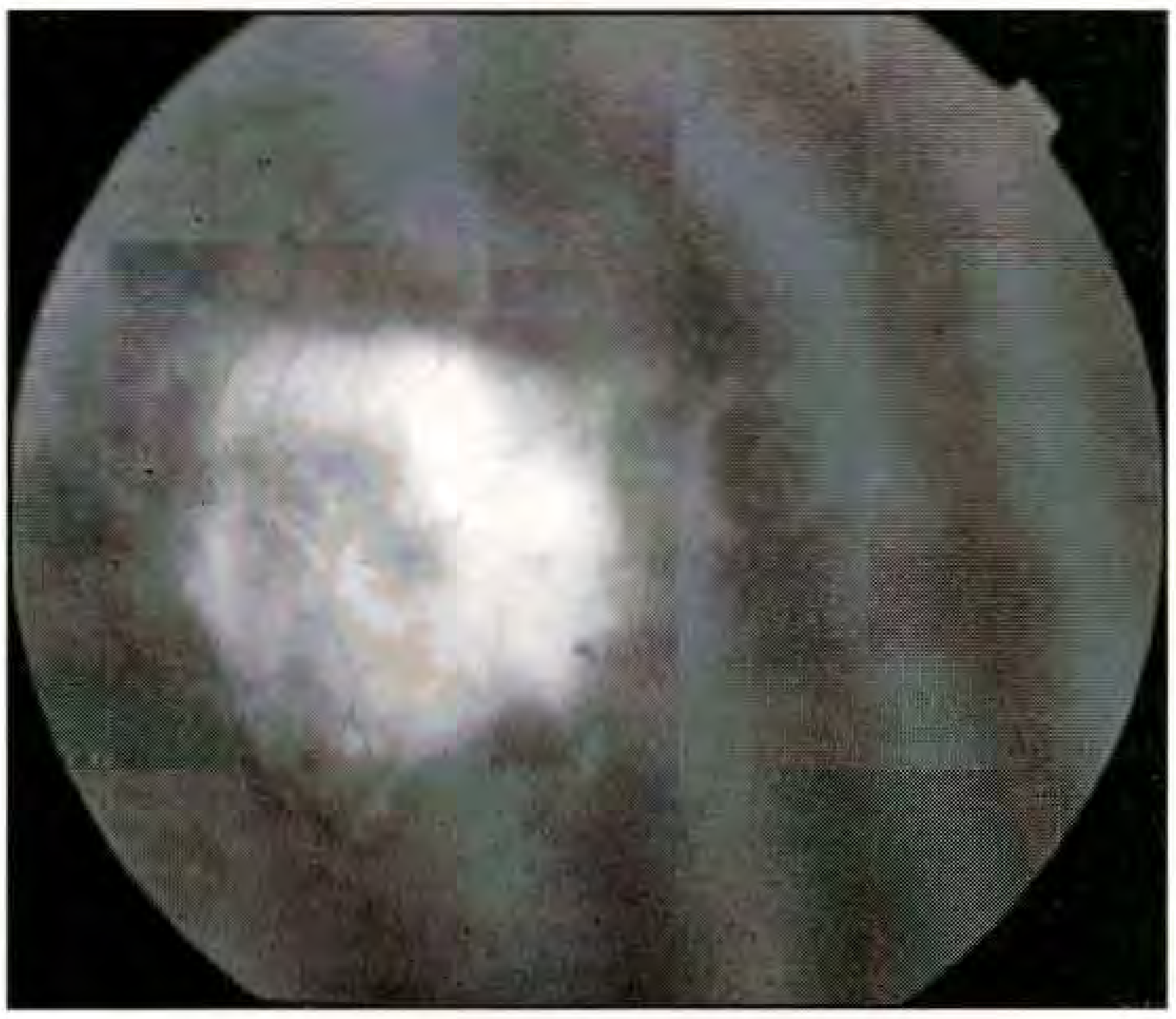

B

Case 8-21. Fibrovascular Pigment Epithelial Detachment and Cystoid Macular Edema

Clinical Summary

An 81-year-old woman reported decreasing vision in her right eye over the past 12 months. Clinical examination revealed a visual acuity of 20/400 associated with a large area of subretinal fluid and overlying cystoid macular edema in the central macula (A). Fluorescein angiography (B) was notable for a large area of hyperfluorescence during the late phase.

Optical Coherence Tomography

OCT (C) revealed thickening of the neurosensory retina and non-reflective spaces within the outer plexiform layer consistent with cystoid macular edema. The reflection from the retinal pigment epithelium (RPE) and choriocapillaris appeared disrupted throughout the temporal aspect of the image consistent with choroidal neovasculariation.

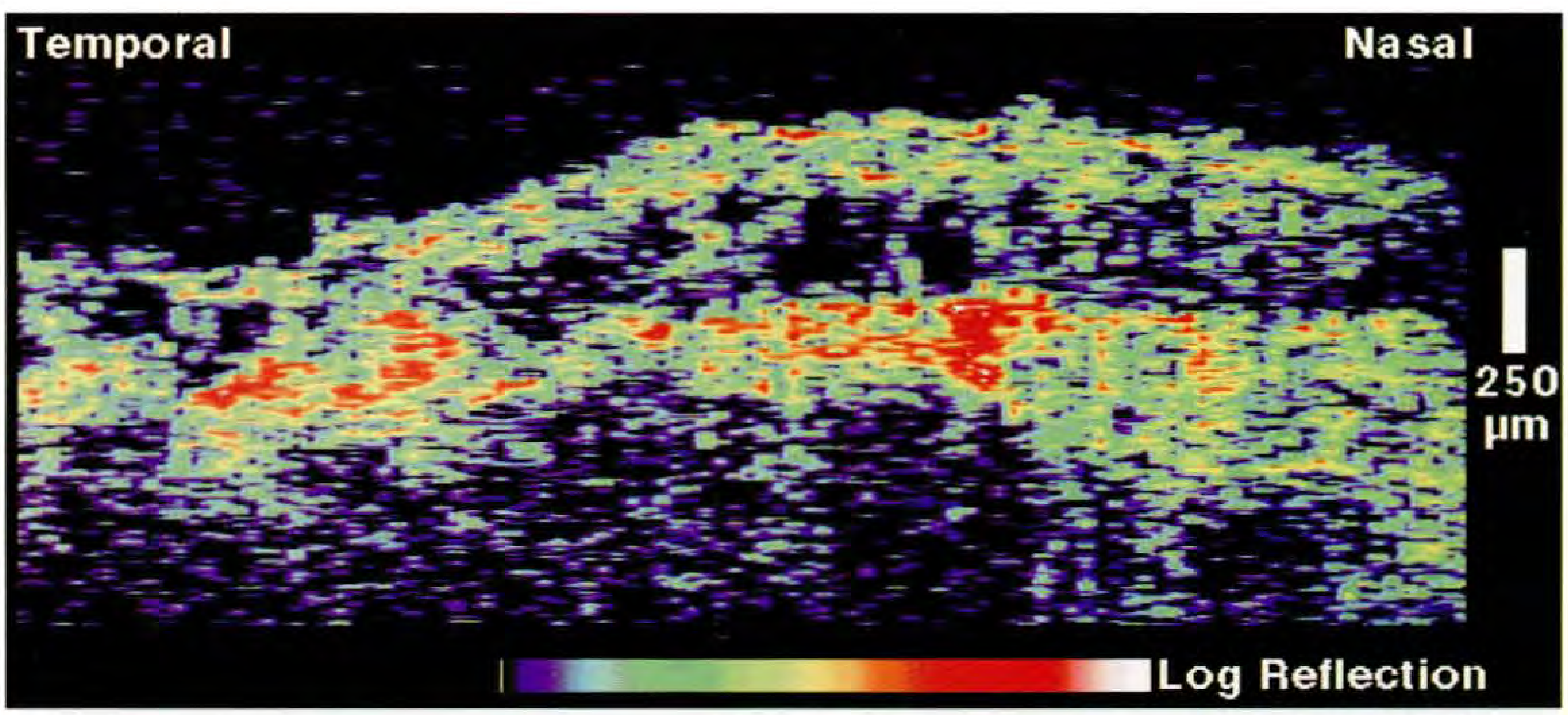

C

Case 8-21 continued

Clinical Summary

The patient experienced an even more rapid decline in vision in her left eye, with her visual acuity in this eye reaching 20/400 over a period of four months. Slit-lamp examination (D) showed a fibrovascular pigment epithelial detachment in the central macula and a serous pigment epithelial detachment superotemporal to the fovea. Neovascularization of the optic disc was also observed associated with evidence of partial occlusion of the superotemporal branch vein. Fluorescein angiography (E) confirmed pooling of dye within the serous pigment epithelial detachment. Several other regions of mild hyperfluorescence were observed surrounding the fovea. The superotemporal branch arteriole and vein exhibited delayed filling.

Optical Coherence Tomography

A vertical OCT image (F) taken through the fibrovascular pigment epithelial detachment showed an elevation of the red band corresponding to the RPE with moderate optical backscatter below consistent with fibrovascular proliferation. The reflection from the RPE was attenuated and fragmented through the inferior margin of the lesion. Non-reflective cystic spaces were identified in the fovea.

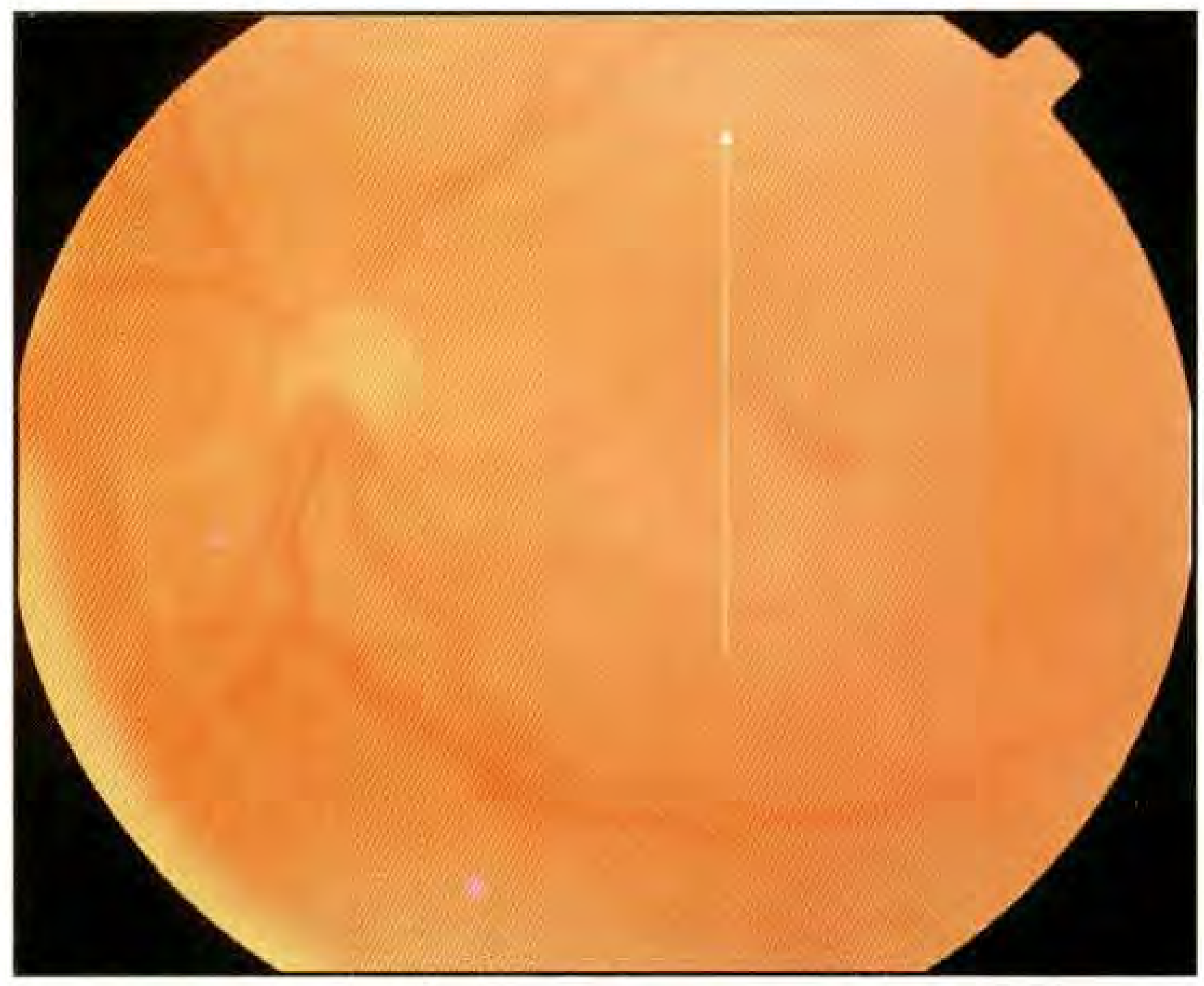

D

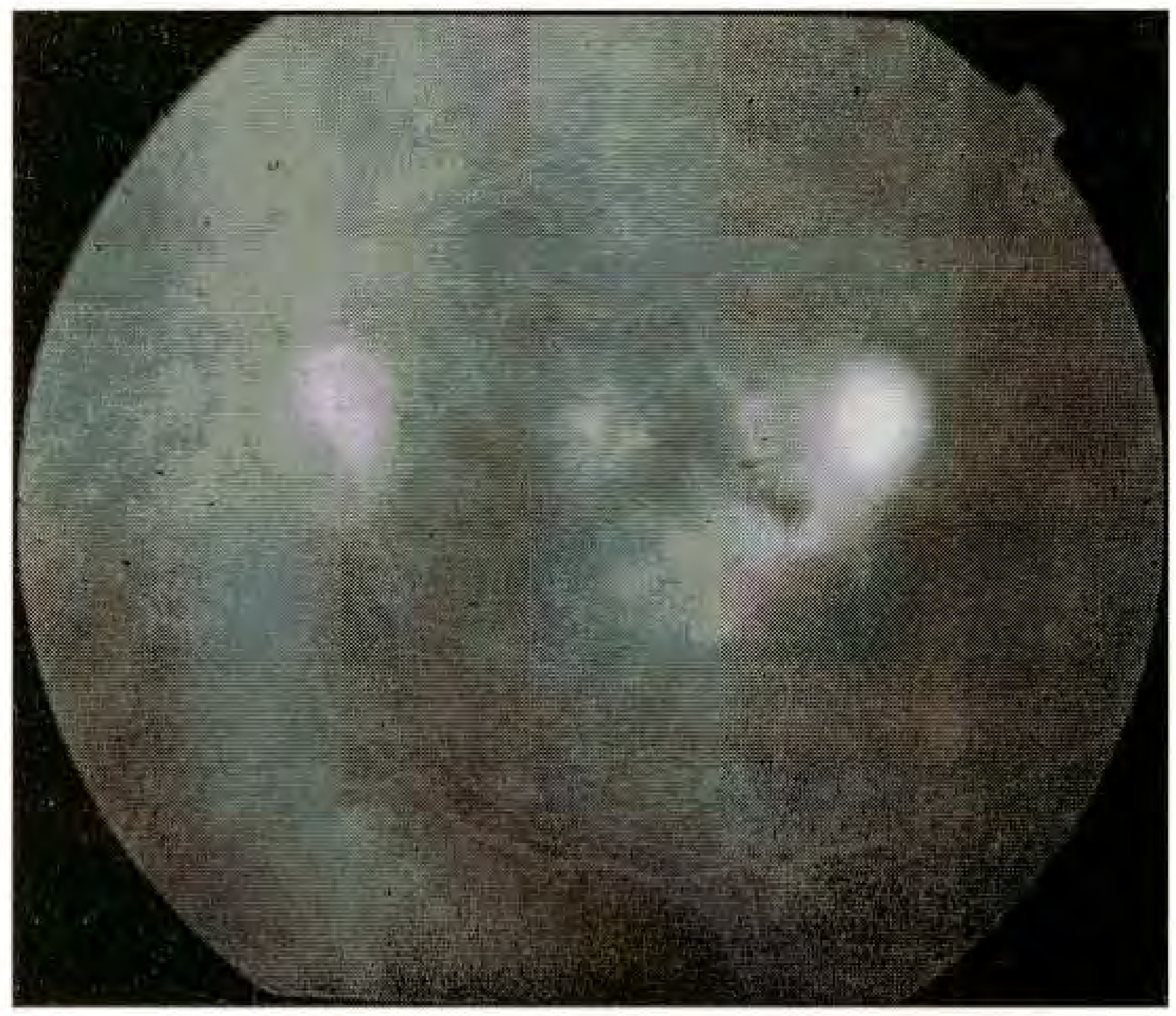

E

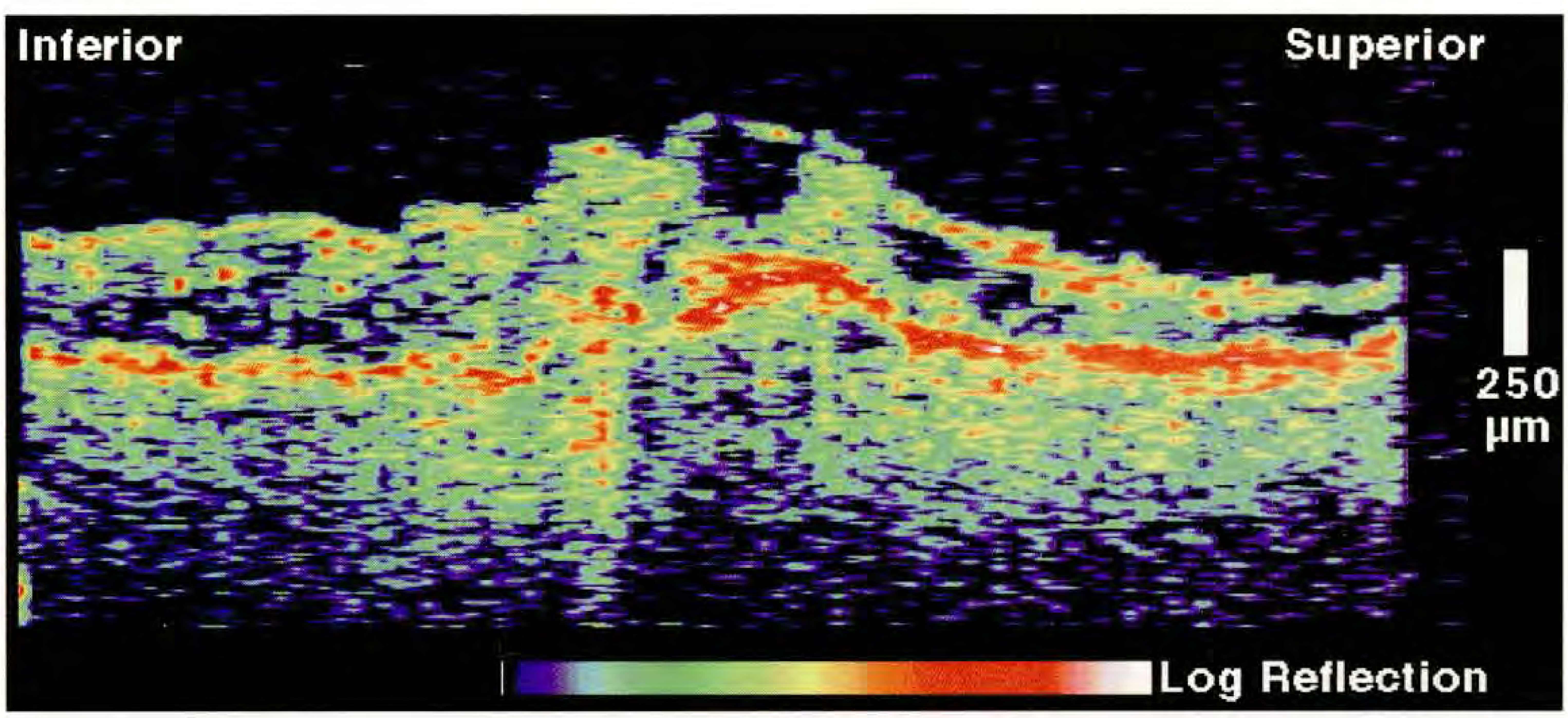

F

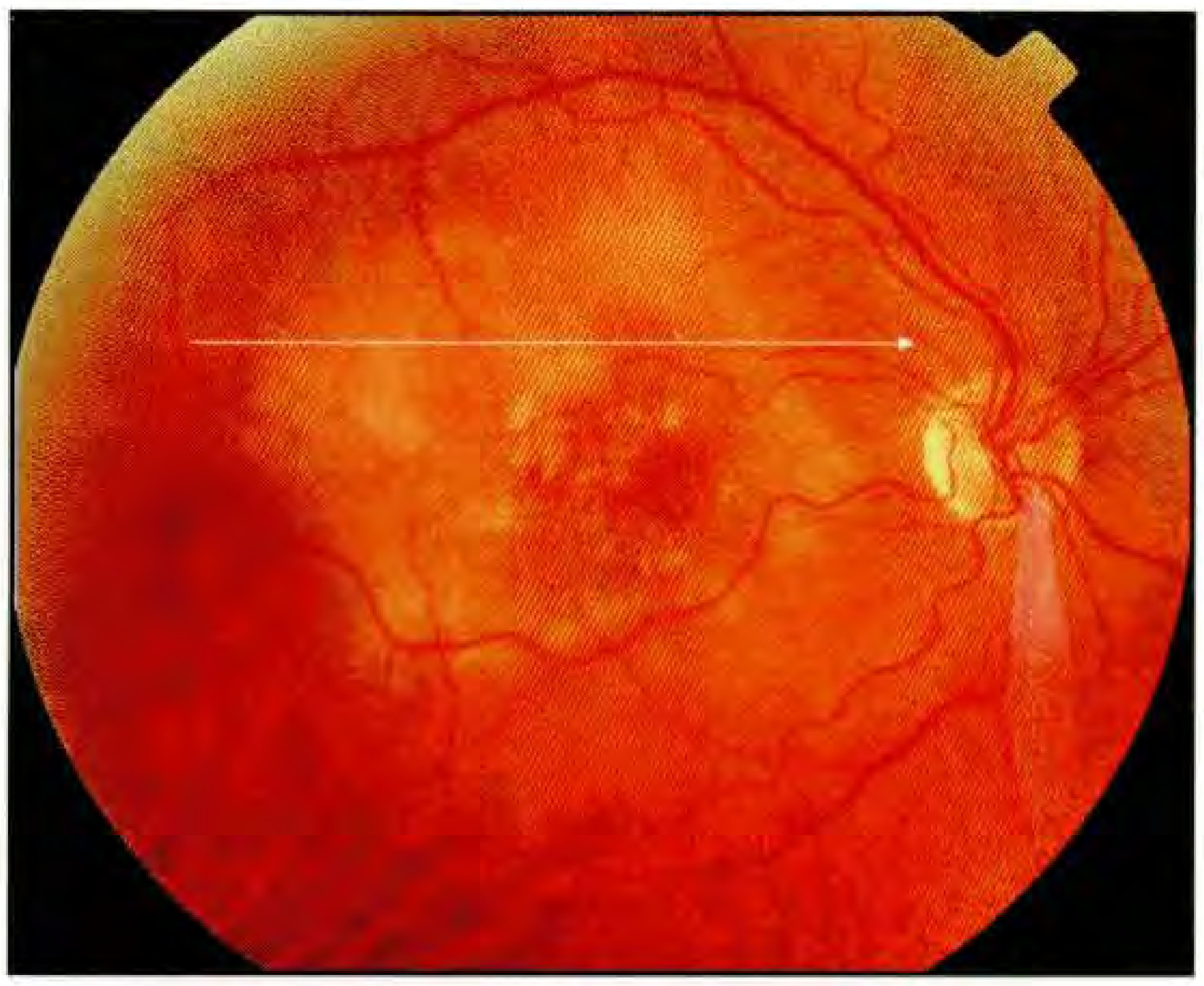

A

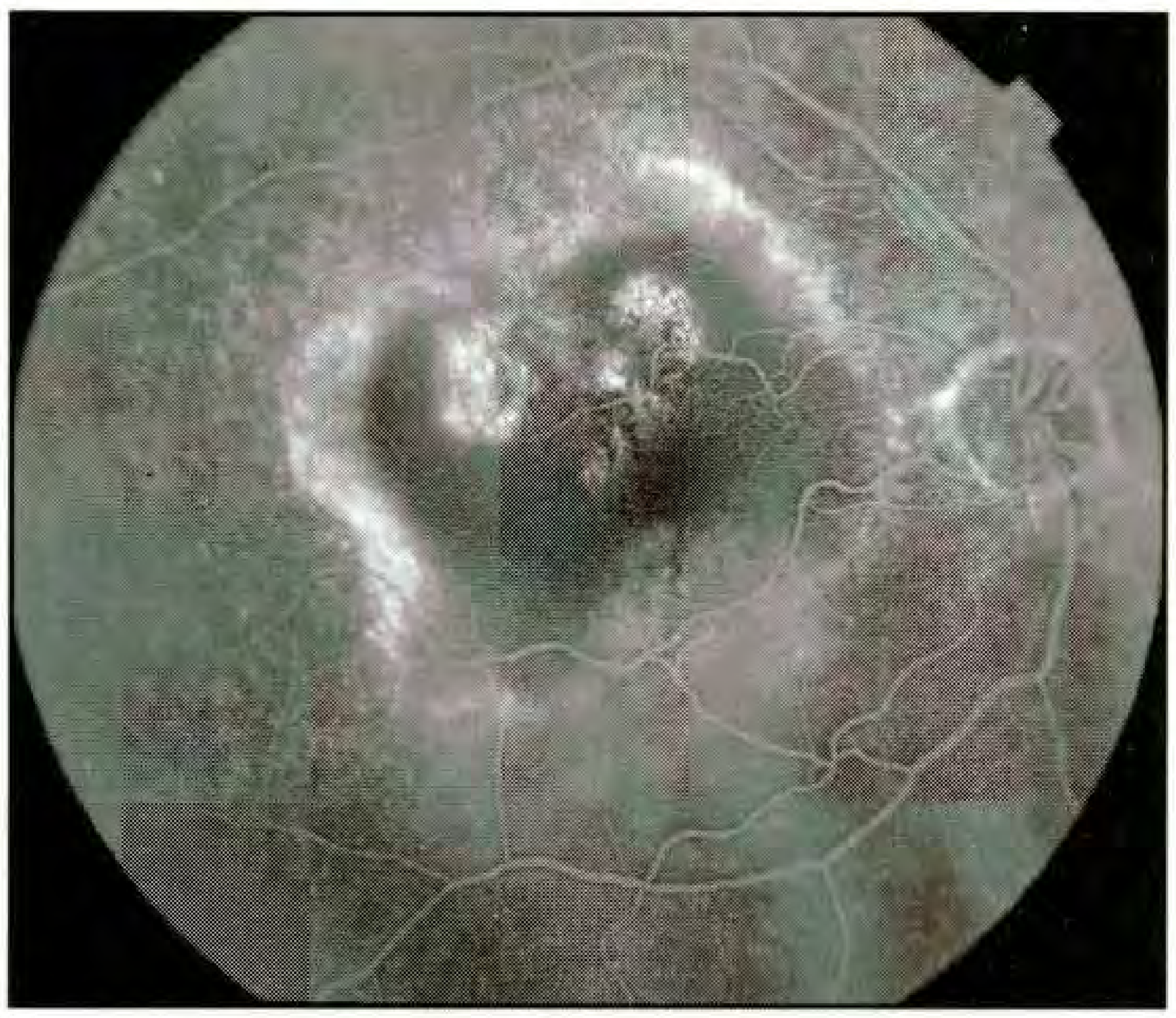

B

Case 8-22. Fibrovascular Pigment Epithelial Detachment

Clinical Summary

A 63-year-old woman with a history of age-related macular degeneration was evaluated for a decline in her reading vision in her right eye over the previous two weeks. Her visual acuity in this eye was 20/400. Dilated fundus examination (A) revealed a pigment epithelial detachment with mottled pigmentation in the central macula surrounded by a large cuff of serous subretinal fluid. Fluorescein angiography (B) showed a bilobed region of hyperfluorescence within a large hypofluorescent lesion. The hyperfluorescent areas increased in intensity and size as the study progressed. A hyperfluorescent rim was noted surrounding the entire lesion.

Optical Coherence Tomography

A linear section (C) superior to the fovea showed two elevations of the retinal pigment epithelium, with mild backscatter persisting beneath both lesions consistent with fibrovascular pigment epithelial detachments. The reflection bounding the posterior neurosensory retina also appeared thicker in the region of the detachments suggesting neovascularization. A small collection of subretinal fluid was observed between the two detachments.

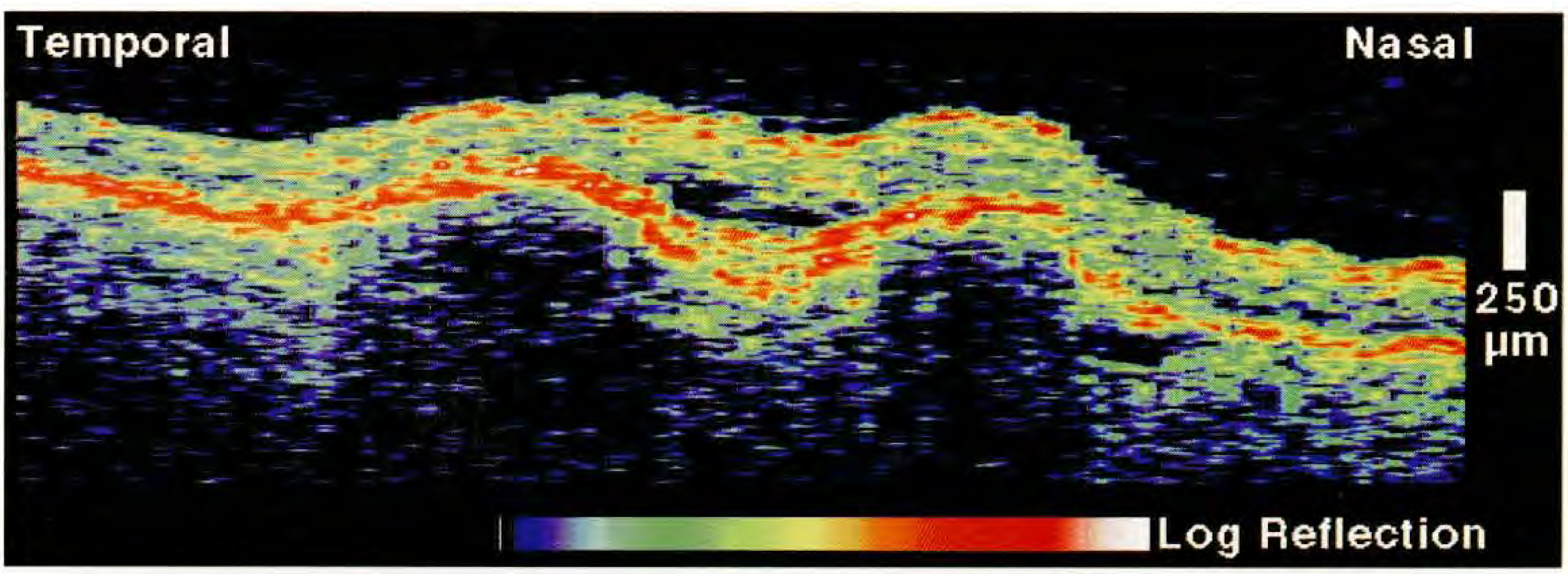

C

Case 8-23. Neurosensory and Fibrovascular Pigment Epithelial Detachment

Clinical Summary

An 82-year-old man had age-related macular degeneration associated with a visual acuity of 20/80 in his left eye. Slit-lamp biomicroscopy (A) was remarkable for cloudy subretinal fluid in the central macula with a small amount of central subretinal hemorrhage. Fluorescein angiography (B) displayed a small, focal hyperfluorescent lesion temporal to the fovea that exhibited poorly defined leakage in the late phase.

Optical Coherence Tomography

A vertical section (C) taken inferotemporal to the fovea showed an elevation of the retinal pigment epithelium (RPE) above a mildly reflective region consistent with a fibrovascular pigment epithelial detachment. A shallow neurosensory detachment which exhibited well-defined retina-fluid and RPE-fluid borders was observed inferior to this lesion.

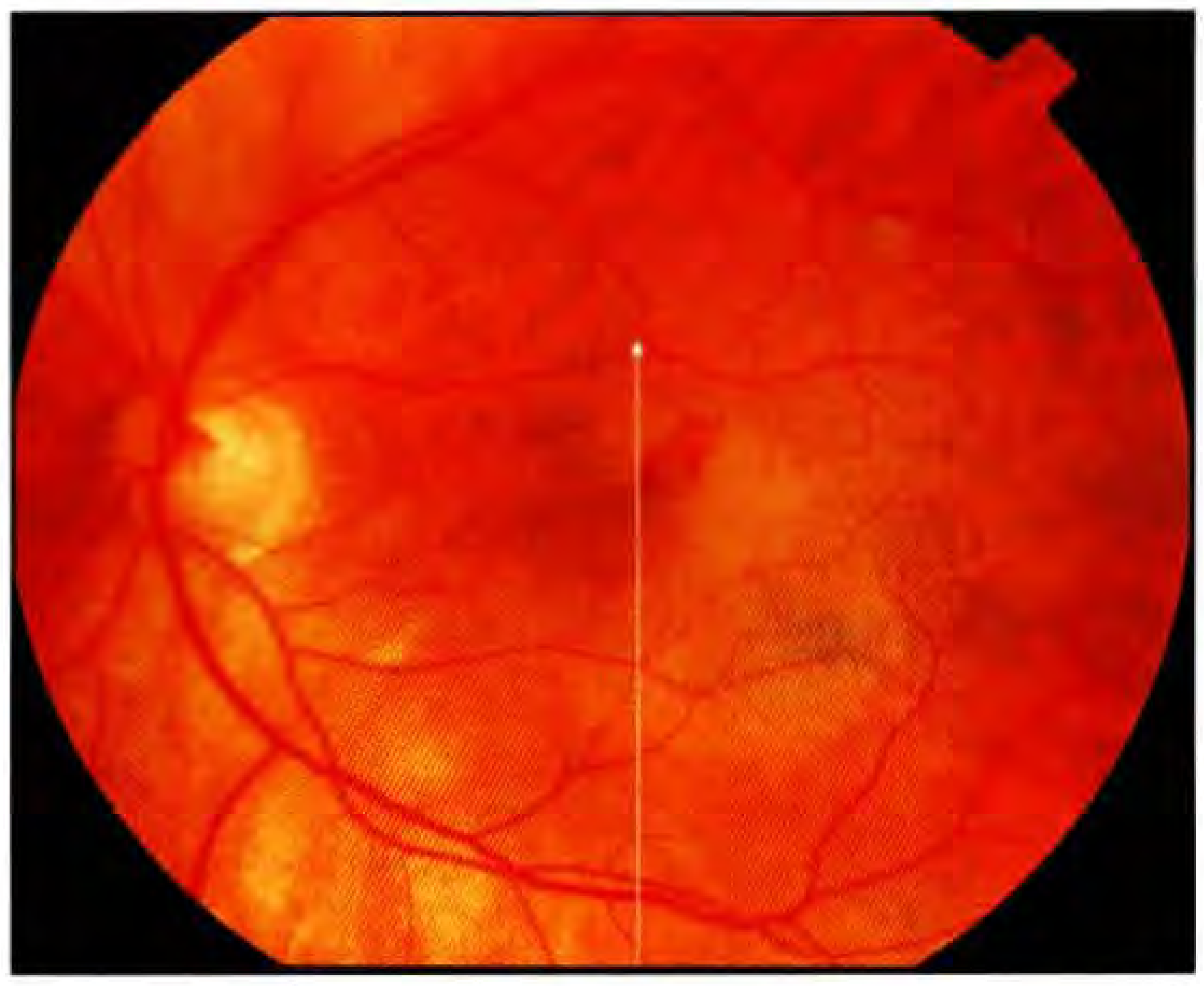

A

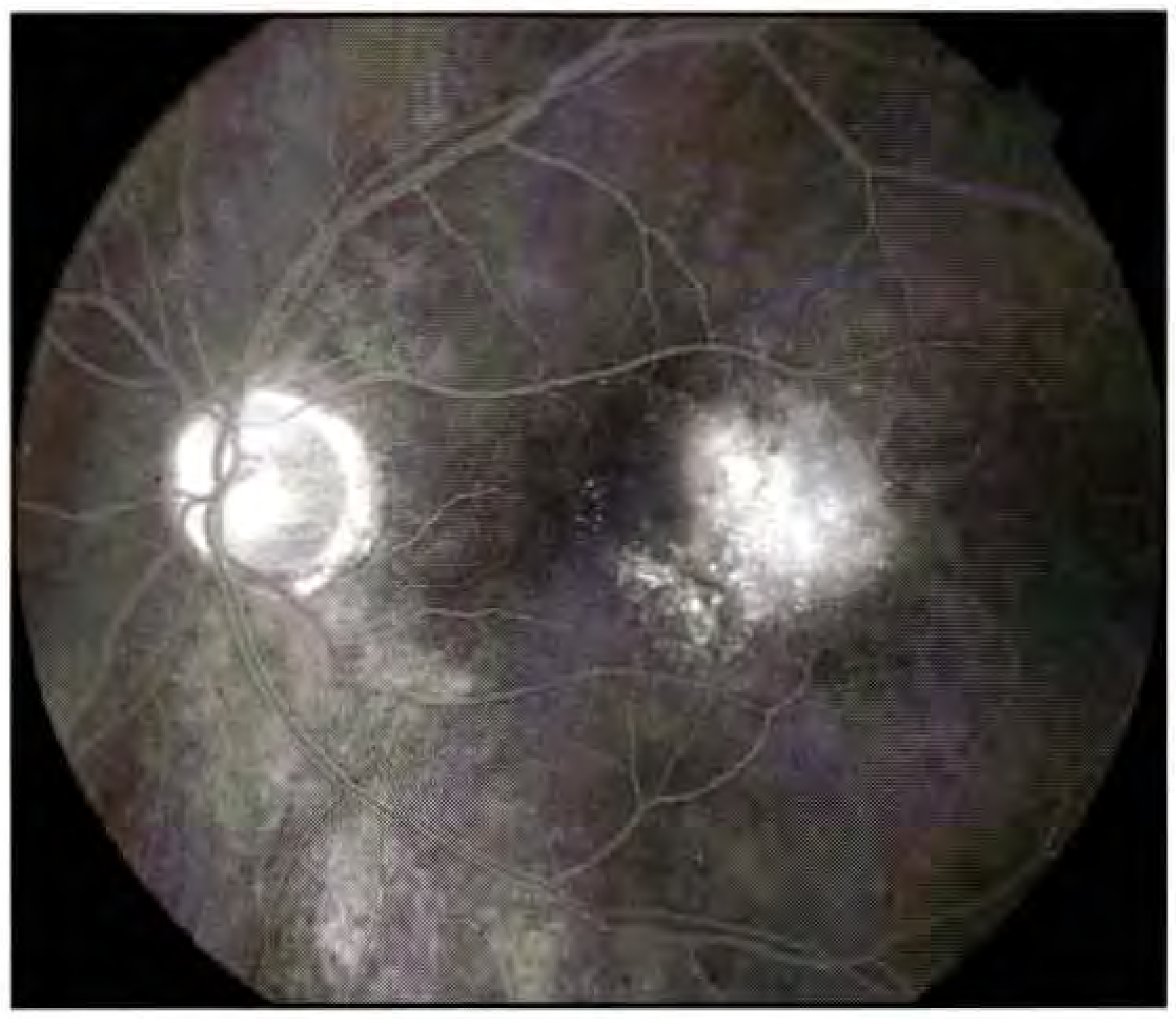

B

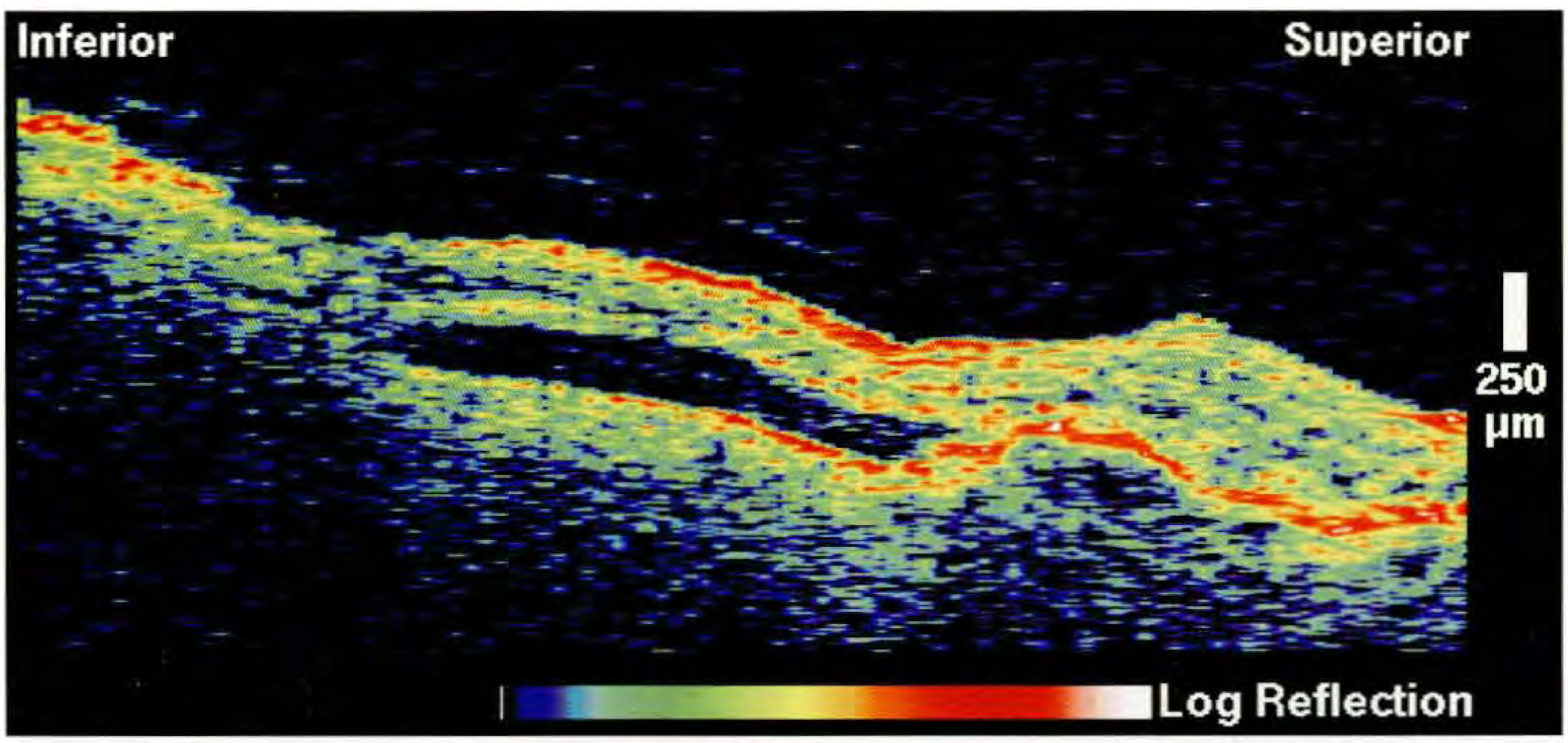

C

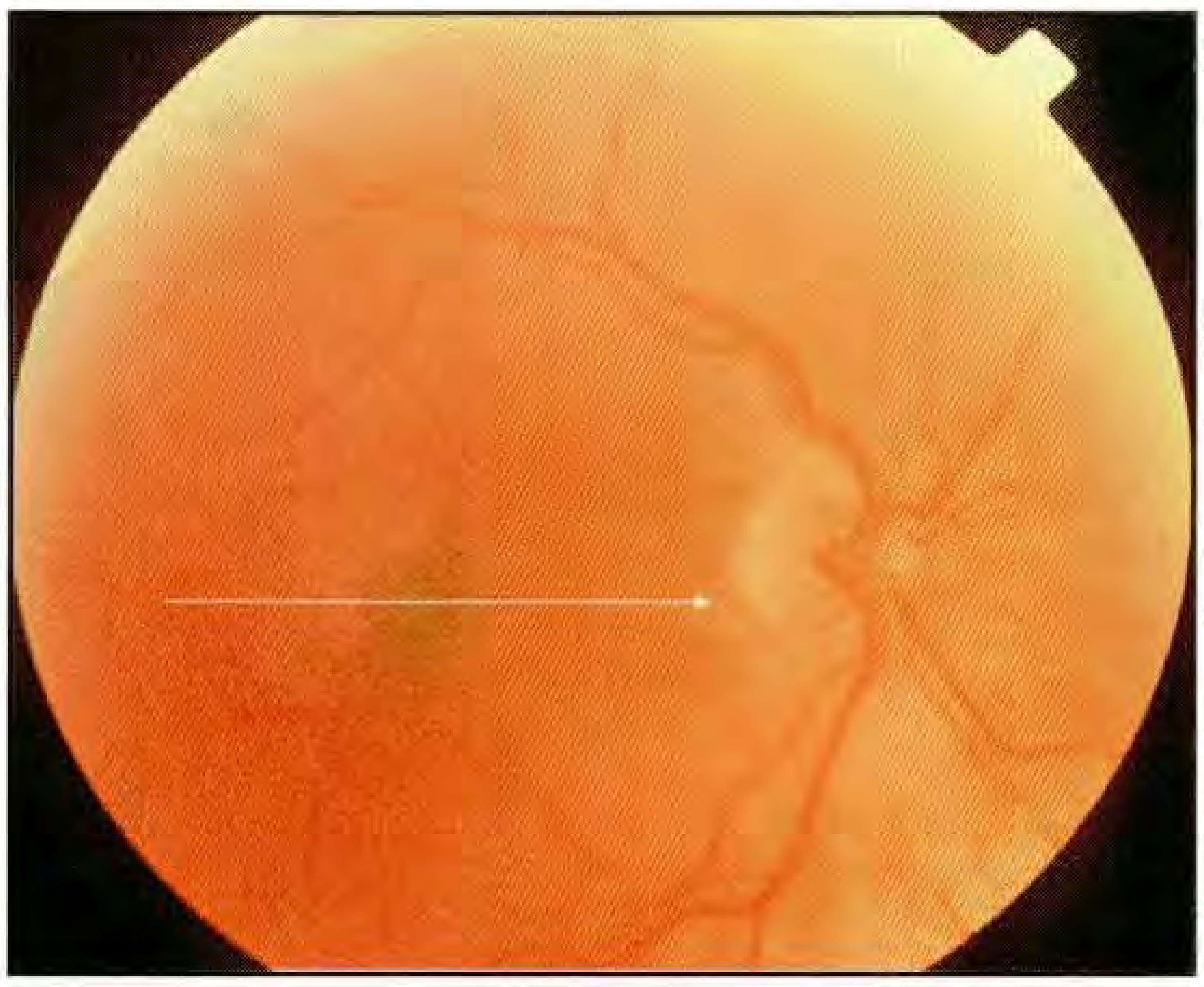

A

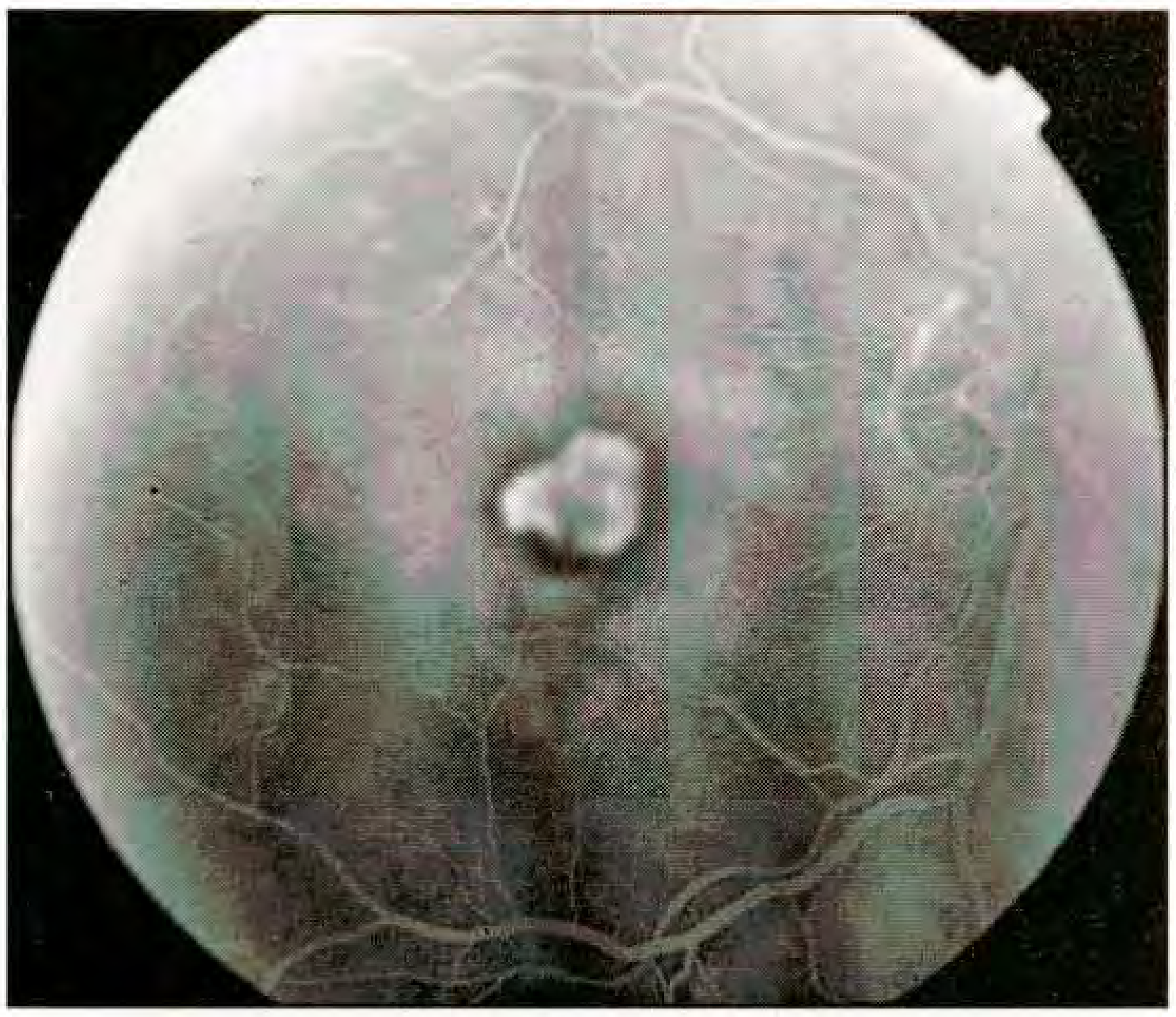

B

Case 8-24. Fibrovascular Pigment Epithelial Detachment

Clinical Summary

A 75-year-old woman had a visual acuity of counting fingers in her right eye associated with age-related macular degeneration. Dilated ophthalmoscopy (A) showed an elevated, moderately pigmented fibrovascular detachment of the retinal pigment epithelium in the central macula. Fluorescein angiography (B) showed a well-defined hyperfluorescent lesion centrally which demonstrated leakage of dye as the angiogram progressed consistent with well-defined choroidal neovascularization.

Optical Coherence Tomography

An elevation of the neurosensory retina and retinal pigment epithelium (RPE) was observed on a horizontal OCT tomogram (C) acquired through the detachment. The reflection from the RPE was abnormally thickened and not well defined beneath the lesion. Moderate optical backscatter was noted extending from the detached RPE into the choroid consistent with fibrovascular proliferation.

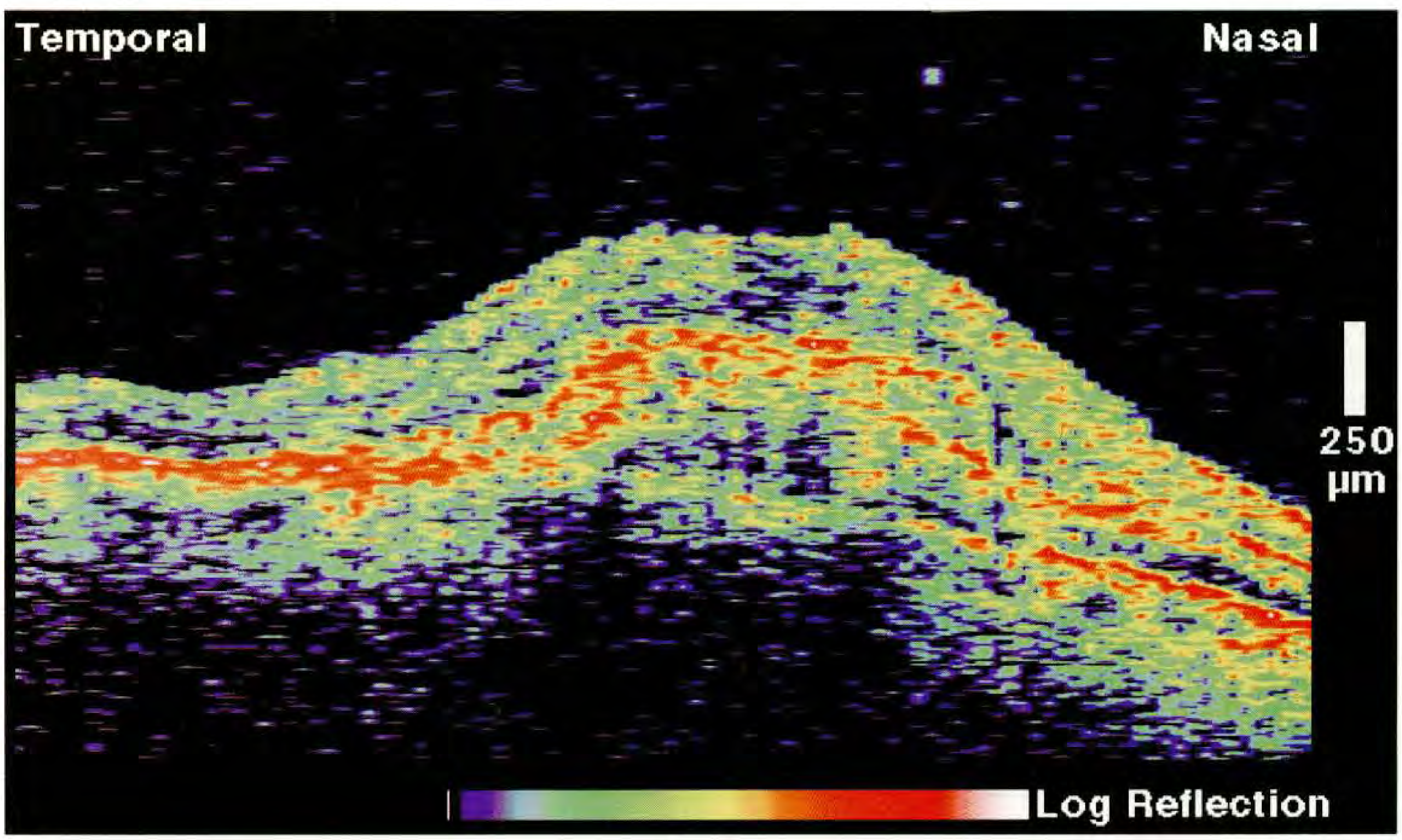

C

Case 8-25. Fibrovascular Pigment Epithelial Detachment

Clinical Summary

An 84-year-old woman experienced an abrupt decline in the vision in her right eye approximately two months prior to examination. She reported that her vision in this eye had been stable since then. On examination, her visual acuity was 20/200. Dilated ophthalmoscopy (A) showed a fibrovascular pigment epithelial detachment in the central macula with mild subretinal fluid and hemorrhage along the inferior border of the lesion. Fluorescein angiography (B) exhibited a well-defined area of hyperfluorescence centrally which demonstrated progressive dye leakage. Irregular hyperfluorescence was noted surrounding the central lesion which also showed mild leakage.

Optical Coherence Tomography

A vertical OCT image (C) through the detachment demonstrated an elevation of the retina and retinal pigment epithelium over a moderately backscattering region consistent with fibrovascular proliferation. A small amount of subretinal fluid was identified superior to the lesion.

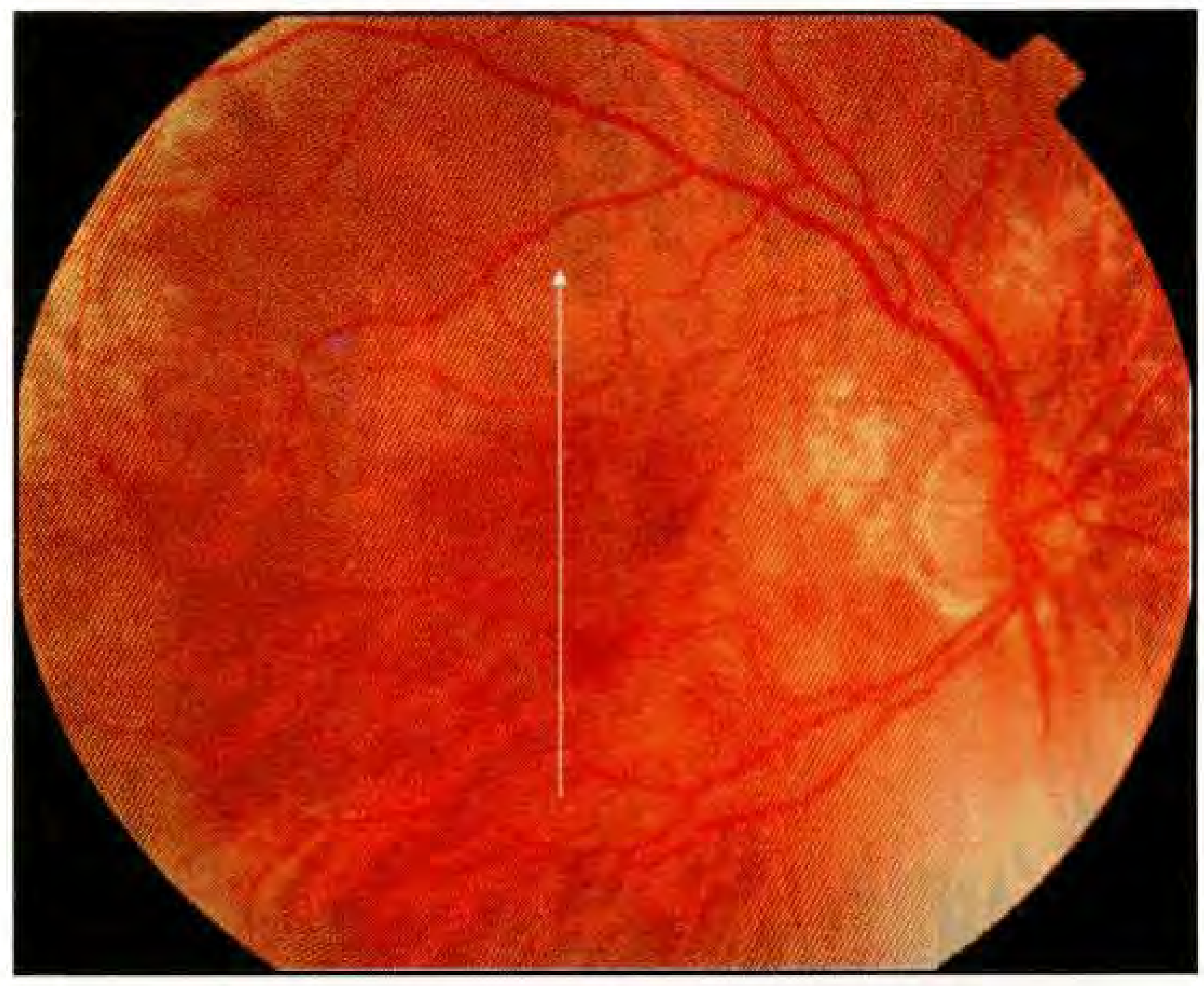

A

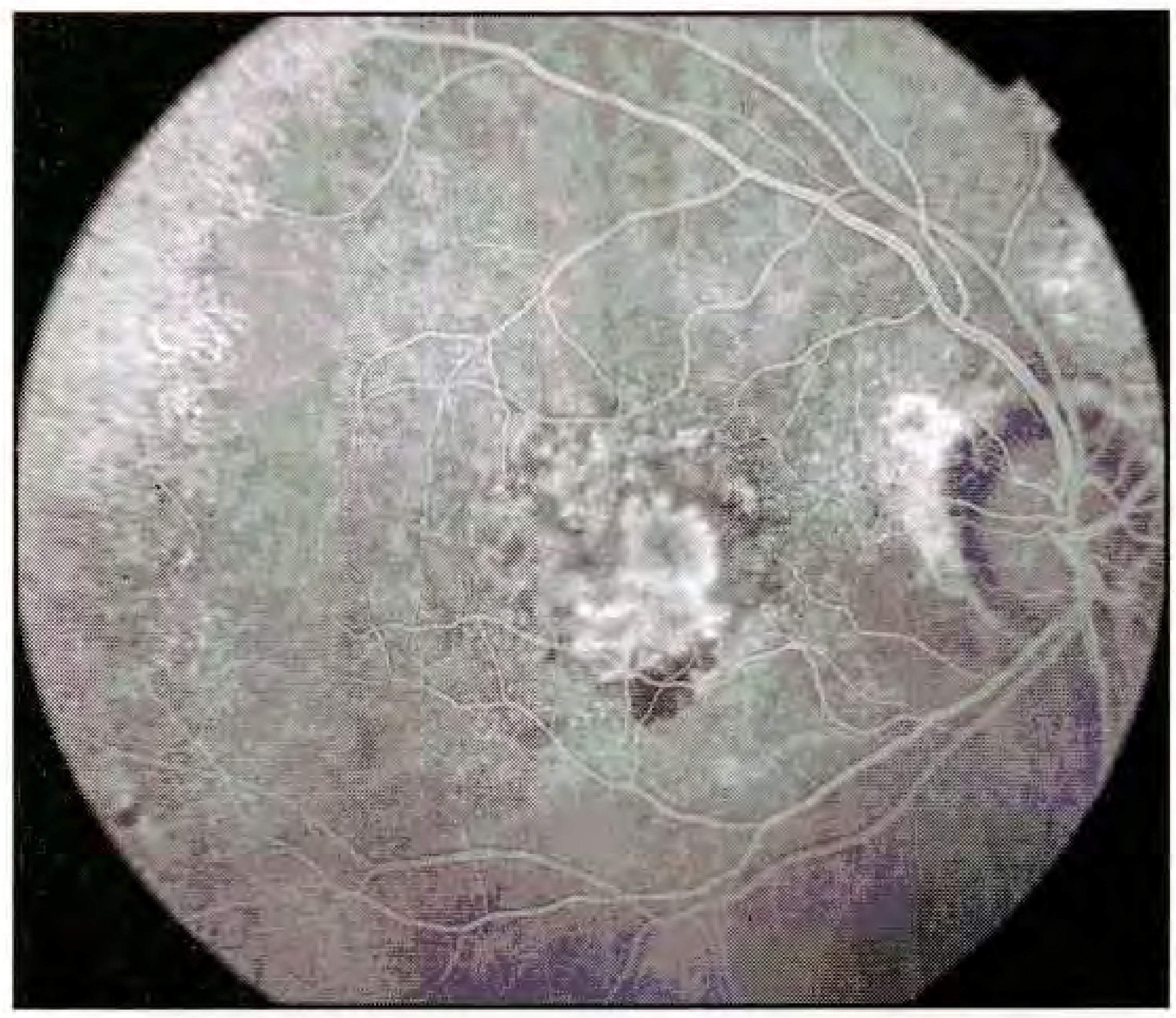

B

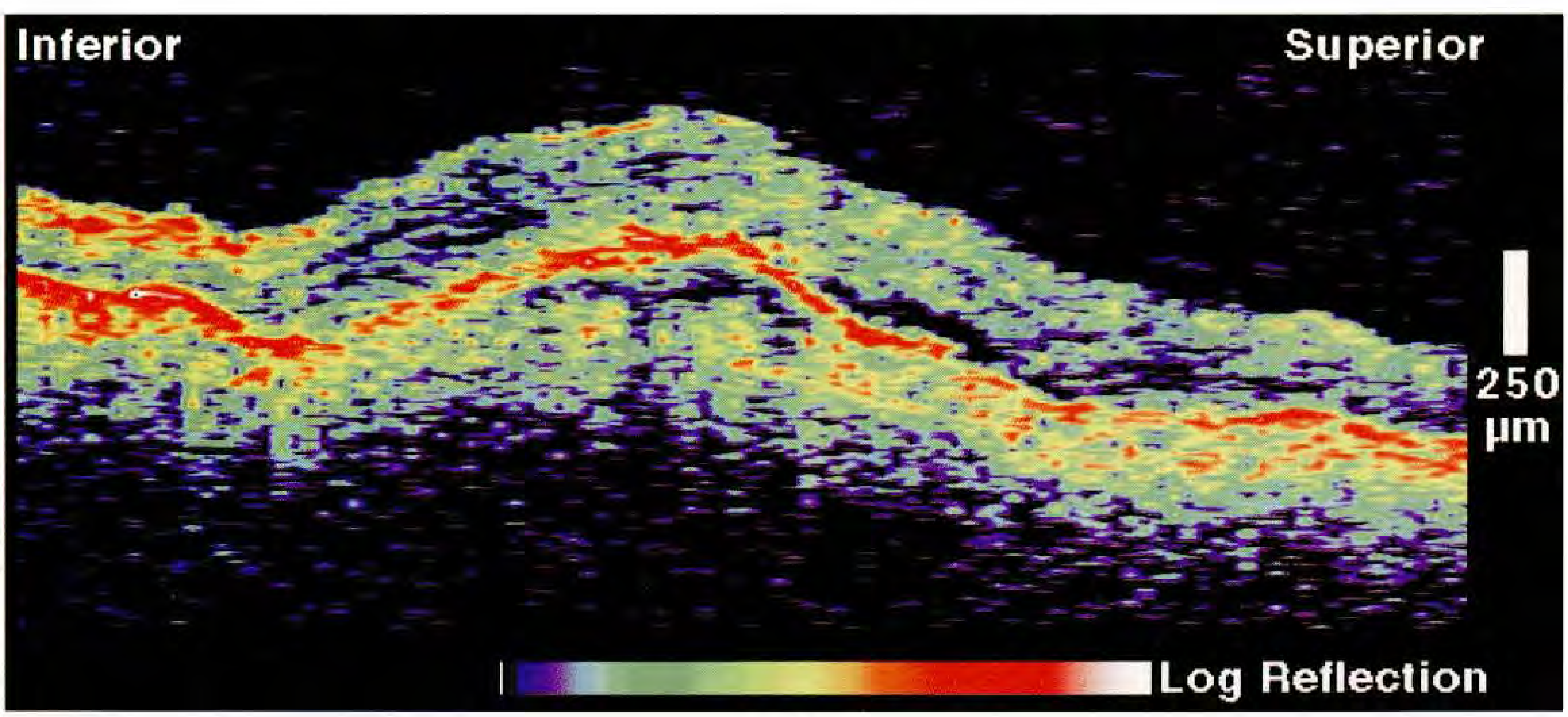

C

A

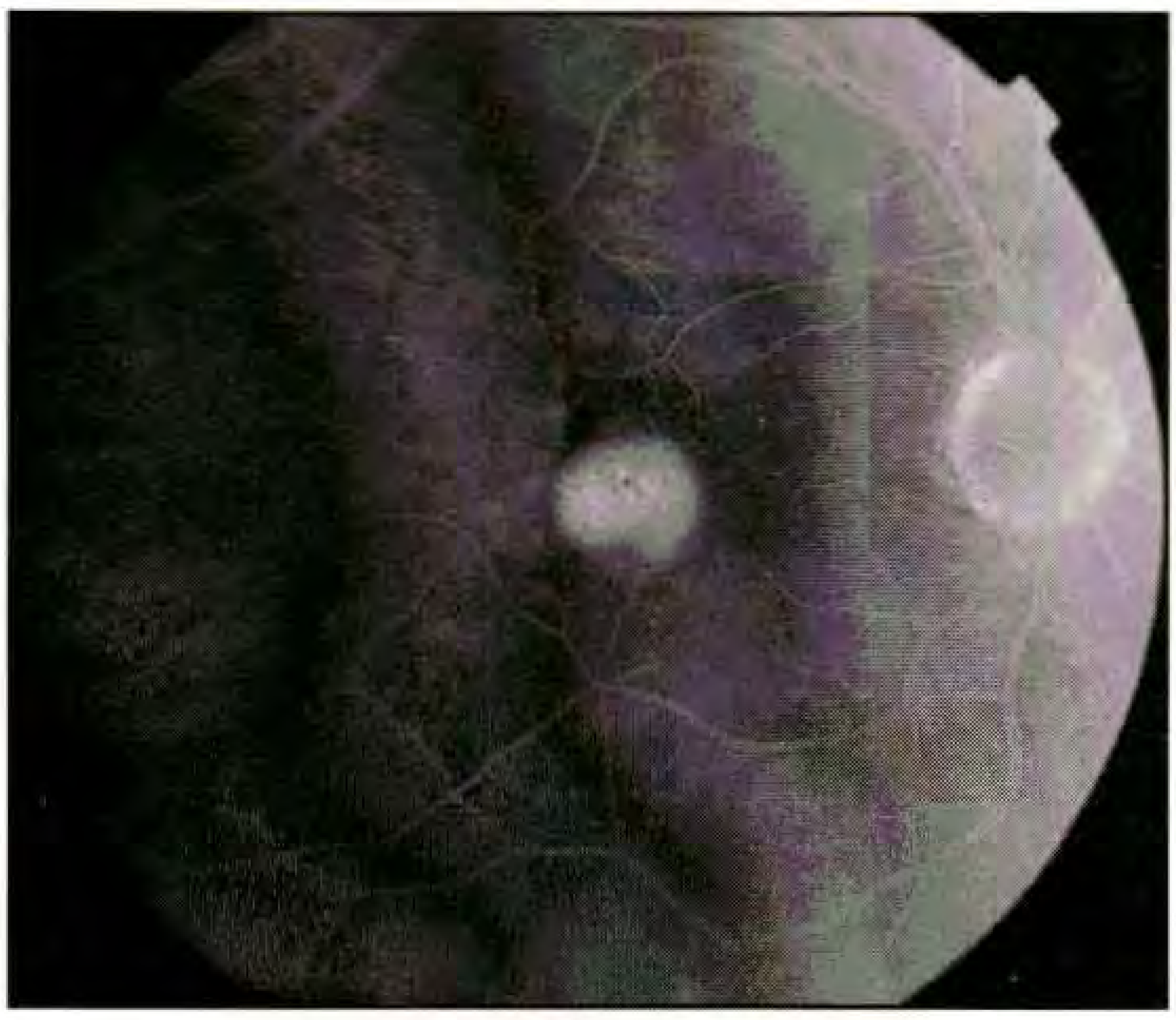

B

Case 8-26. Serous Pigment Epithelial Detachment and Subretinal Neovascularization

Clinical Summary

A 68-year-old man had a visual acuity of 20/40 associated with a serous pigment epithelial detachment in his right eye (A). Fluorescein angiography (B) showed a hyperfluorescent lesion in the central macula which remained homogenous and well-demarcated in the late phase consistent with a serous detachment of the retinal pigment epithelium.

Optical Coherence Tomography

The retina and reflective band corresponding to the retinal pigment epithelium (RPE) were detached over an optically clear cavity, consistent with sub-pigment epithelial serous fluid accumulation (C). The reflection from the choroid was attenuated below the lesion, obscuring the boundary between the choroid and the fluid.

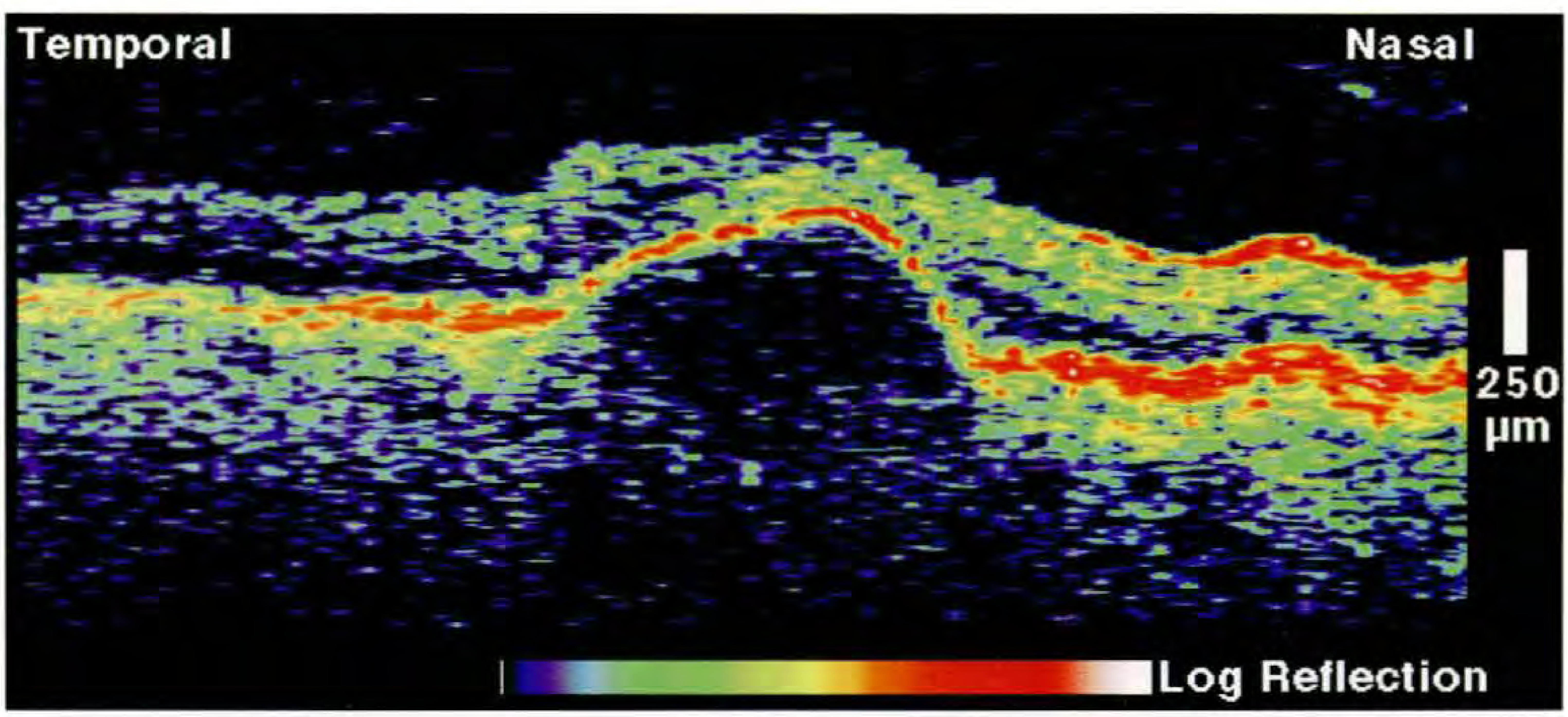

C

Case 8-26 continued

Clinical Summary

The patient's left eye had a visual acuity of 20/80. A pigment epithelial detachment was noted in the central macula with a superonasal region of subretinal hemorrhage (D). Fluorescein angiography (E) displayed a hypofluorescent lesion in the area of subretinal hemorrhage, and hyperfluorescence which increased in intensity, but not size during the late phase consistent with a pigment epithelial detachment. Patchy hyperfluorescence was noted surrounding this detachment without definite late leakage.

Optical Coherence Tomography

A horizontal OCT tomogram (F) disclosed the pigment epithelial detachment and surrounding, optically clear spaces corresponding to subretinal fluid accumulation. The reflections from the choroid below the detachment did not appear attenuated, in contrast to the usual presentation of a serous RPE detachment. Furthermore, faint optical backscatter was observed extending from the choroid into the sub-RPE space suggestive of a neovascular membrane.

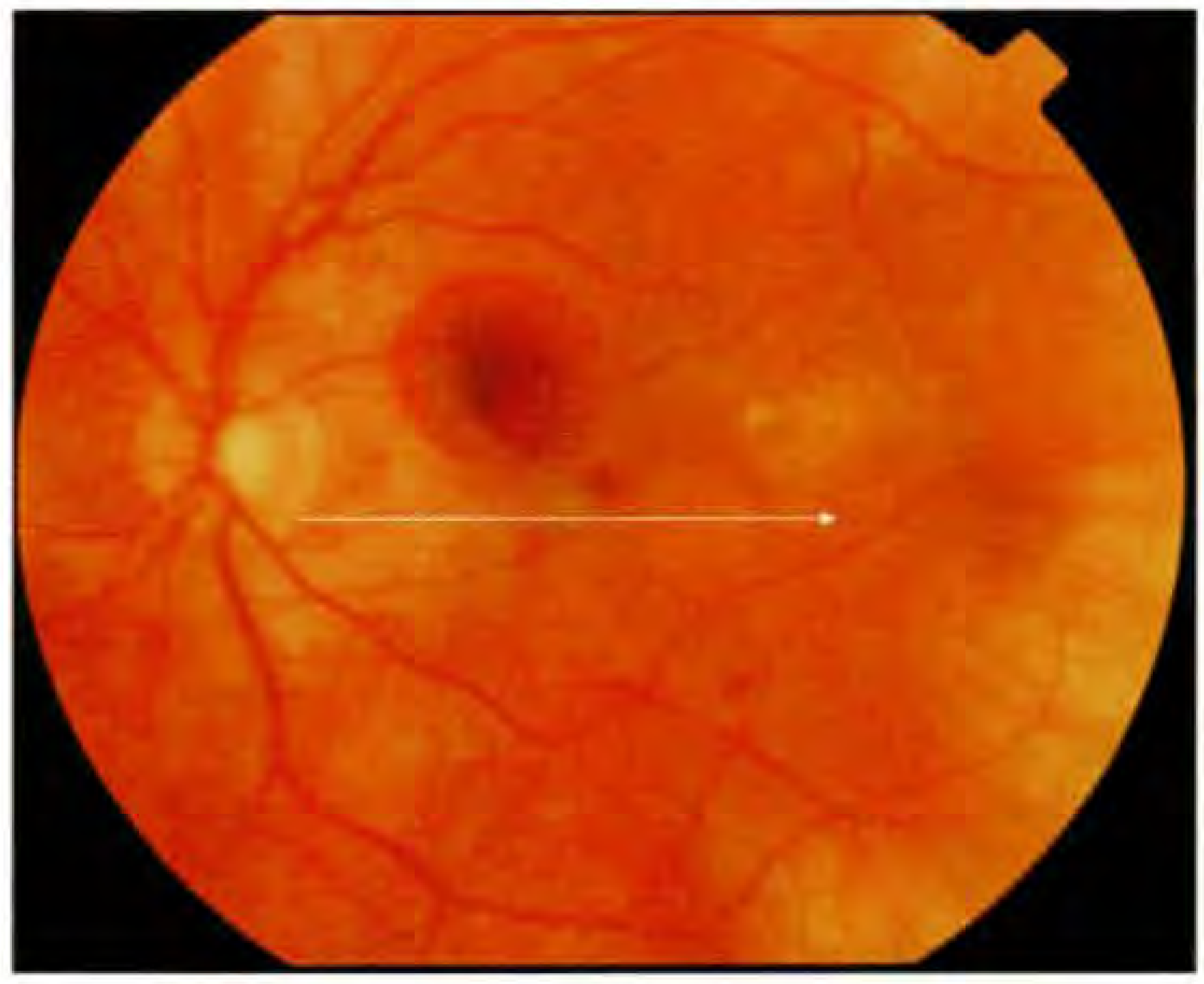

D

E

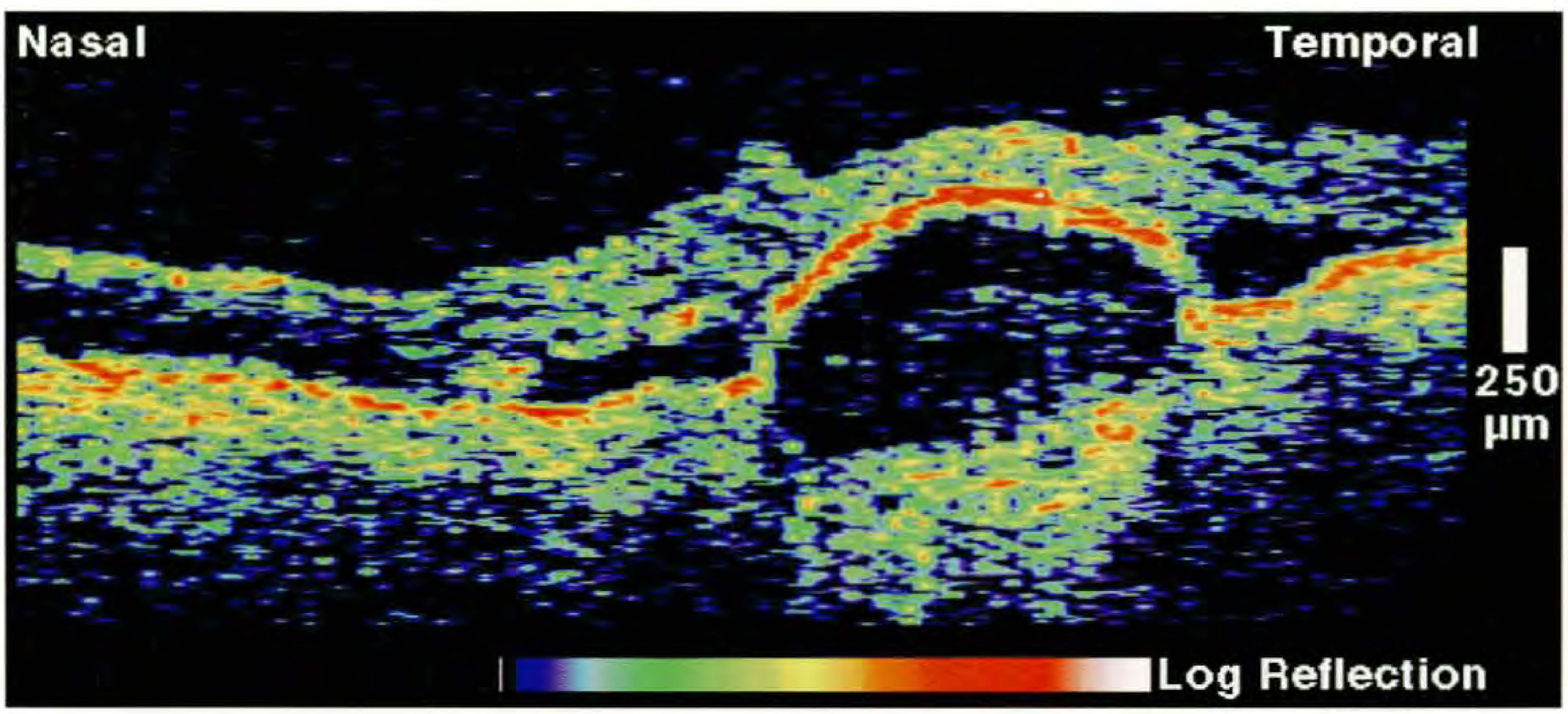

F

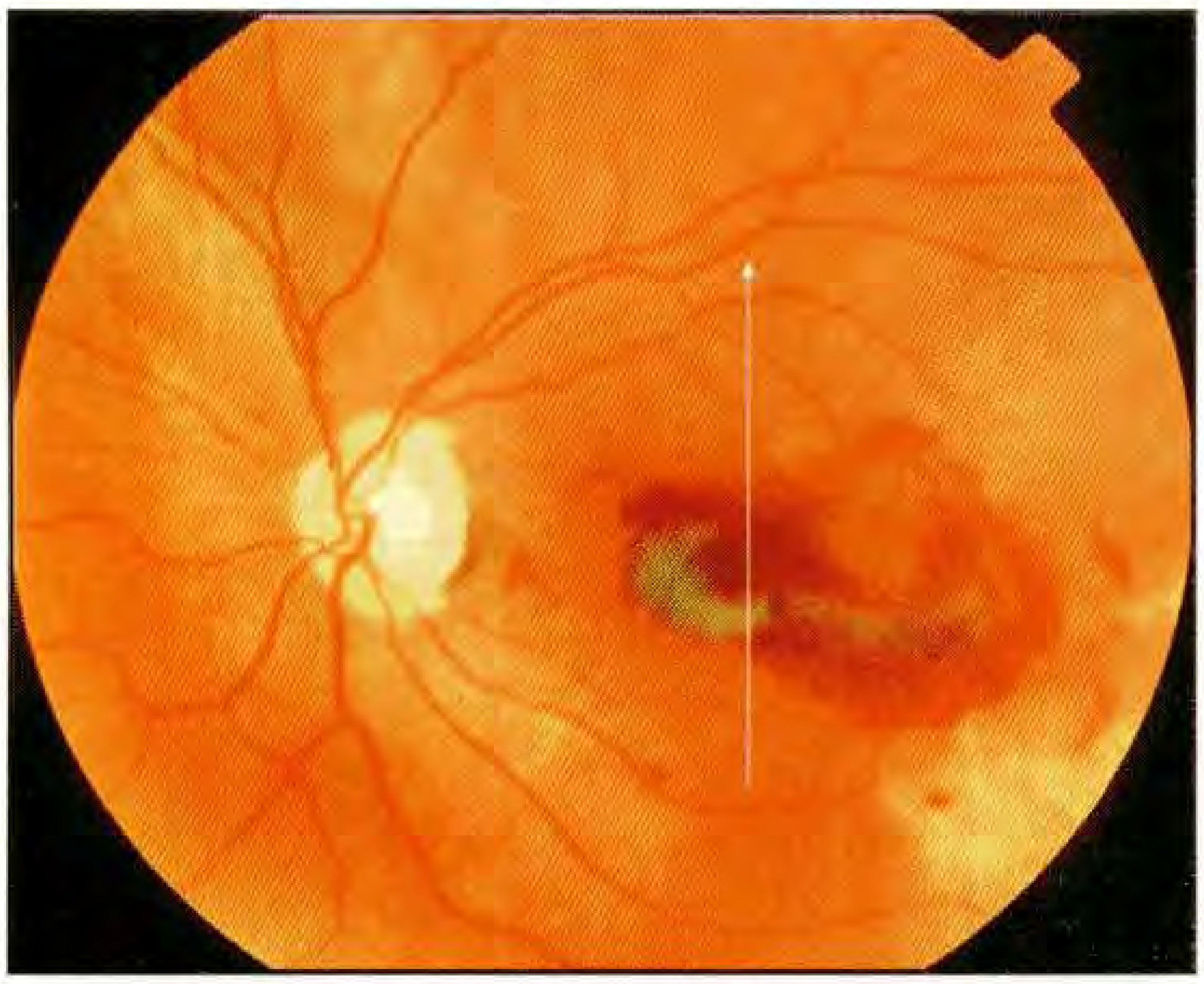

A

B

Case 8-27. Subretinal Hemorrhage and Thrombus

Clinical Summary

A 74-year-old man with the clinical diagnosis of age-related macular degeneration had a sub-macular hemorrhage in his left eye associated with a visual acuity of counting fingers (A). A large hypofluoresecent lesion was present directly in the macula on fluorescein angiography during all phases of the angiogram (B) consistent with hemorrhage. Several areas of relative hyperfluorescence were noted temporal to the fovea.

Optical Coherence Tomography

A vertical tomogram (C) acquired through the fovea showed an elevated macula and a brightly backscattering region directly beneath the fovea. The high reflectivity of this area was consistent with hemorrhage, which attenuated the backscattering signal from the normally bright pigment epithelium and choriocapillaris. An optically clear region of subretinal fluid accumulation was noted immediately inferior to the hemorrhage on the image.

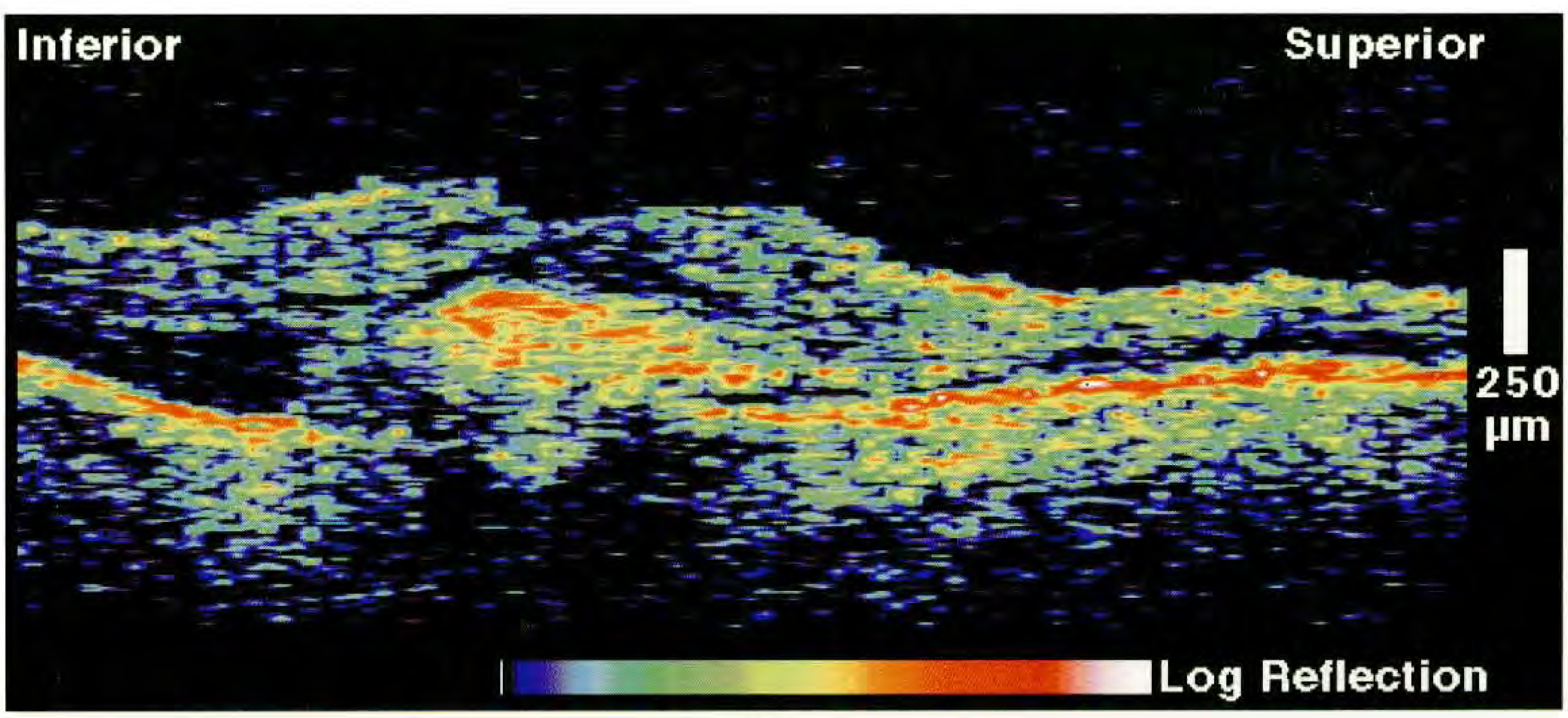

C

Case 8-28. Subretinal Hemorrhage

Clinical Summary

A 78-year-old woman with age-related macular degeneration noted a black spot in her central vision four days earlier. Dilated fundus examination (A) revealed a dense, elevated subretinal hemorrhage in the central and superior macula, and soft drusen temporally.

Optical Coherence Tomography

A horizontal tomogram (B) acquired superior to fixation demonstrated a large area of retinal elevation corresponding to the hemorrhage. Moderate optical backscatter was observed subretinally from the blood and was similar in strength to the reflections from the sensory retinal tissue. Strong attenuation of the incident light shadowed the reflections from the retinal pigment epithelium and choroid below the hemorrhage.

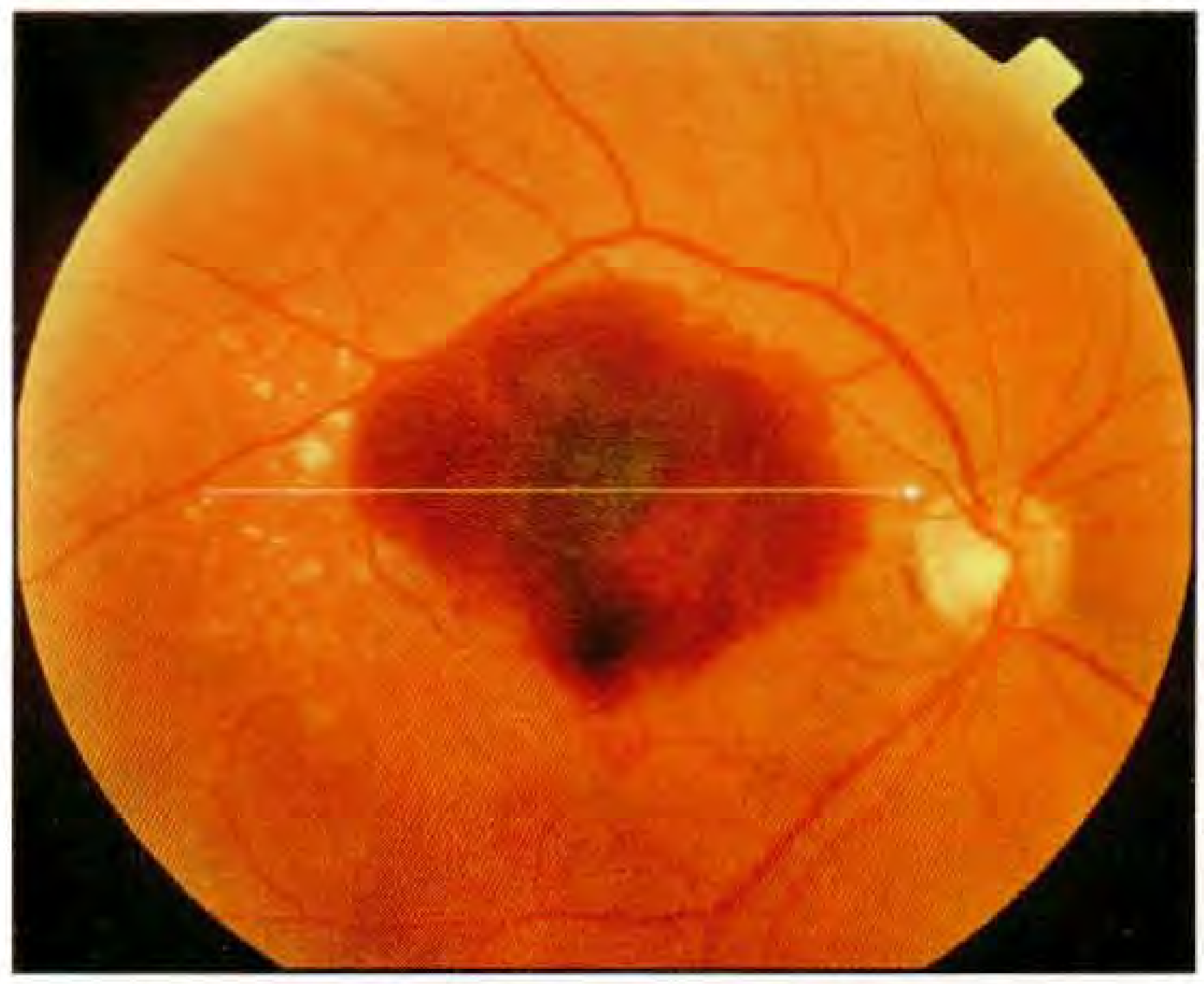

A

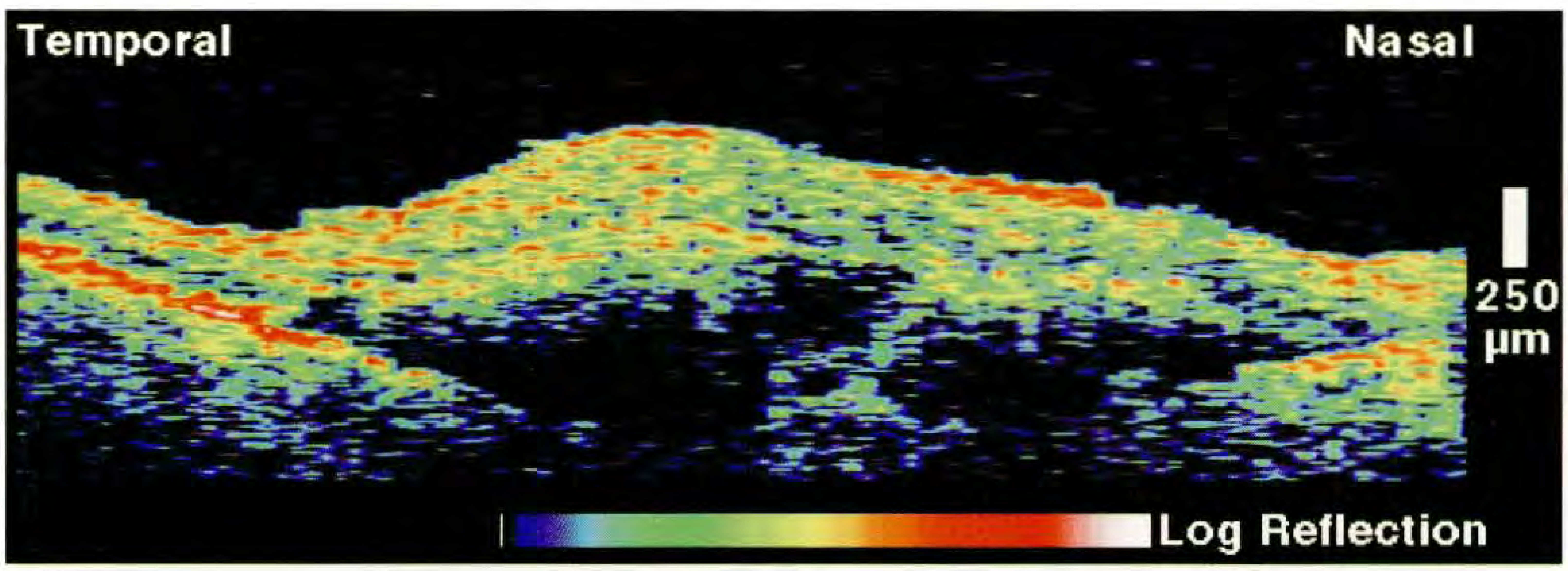

B

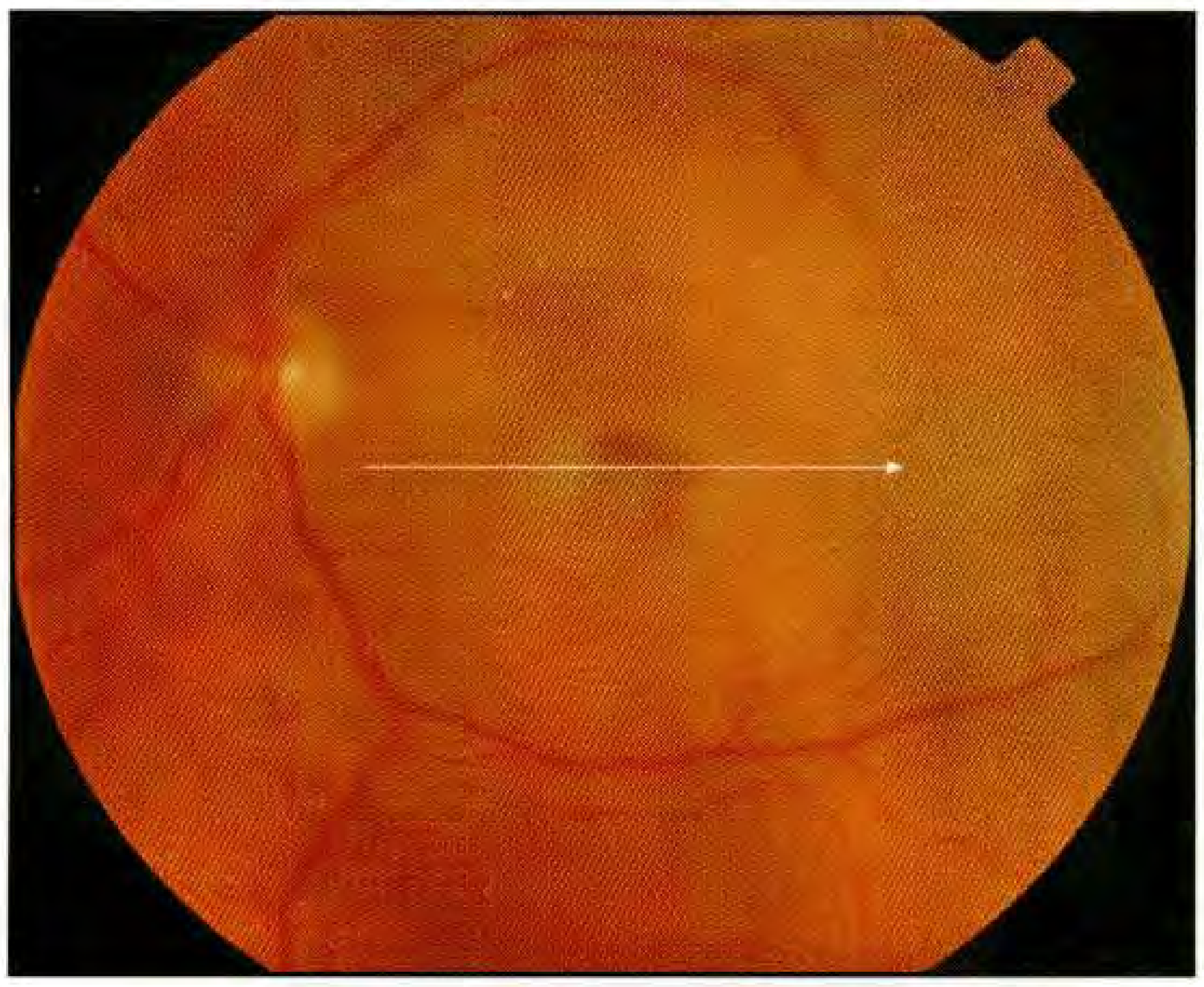

A

B

Case 8-29. Choroidal Neovascularization

Clinical Summary

An 80-year-old man was referred for evaluation of age-related macular degeneration and choroidal neovascularization in his left eye, associated with a visual acuity of counting fingers. A pigment epithelial detachment in the macula with a central area of subretinal hemorrhage was described on slit-lamp examination (A). Fluorescein angiography (B) showed central hypofluorescence corresponding to the hemorrhage with a surrounding border of hyperfluorescence. A small region of hyperfluorescence was evident within this lesion which increased in intensity during later phases of the angiogram consistent with choroidal neovascularization.

Optical Coherence Tomography

An OCT scan (C) taken directly through the fovea demonstrated increased retinal thickness in the macula with reduced optical reflectivity consistent with intraretinal fluid accumulation. The reflective band corresponding to the retinal pigment epithelium and choriocapillaris was thickened in a fusiform manner and disrupted directly beneath the fovea suggesting a well-defined choroidal neovascular membrane in that area.

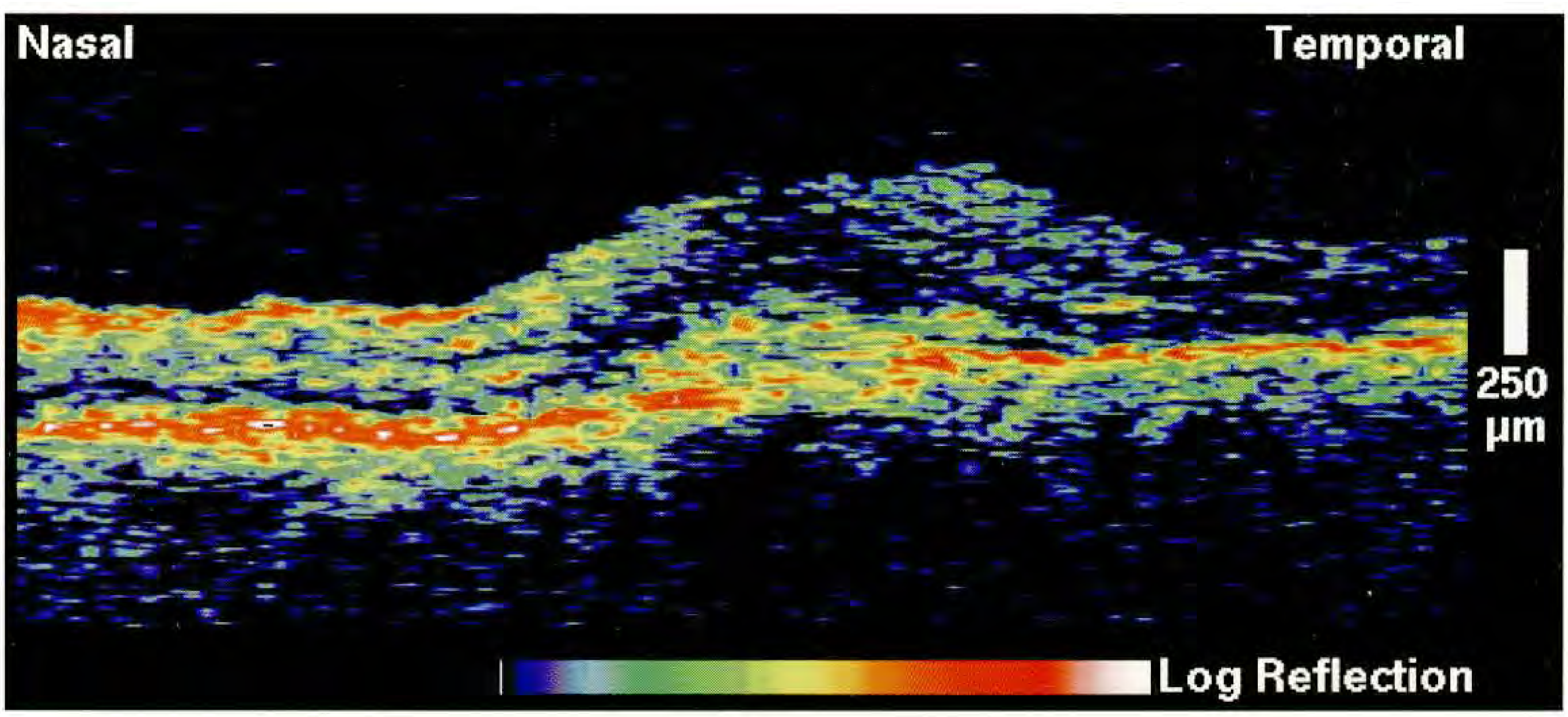

C

Case 8-30. Choroidal Neovascularization

Clinical Summary

A 70-year-old man had a visual acuity of 20/60 in his left eye associated with the clinical diagnosis of age-related macular degeneration with choroidal neovascularization. Subretinal fibrosis was observed temporal to the fovea on slit-lamp examination (A). Fluorescein angiography (B) revealed an area of relative hypofluorescence with a surrounding rim of hyperfluorescence. A small amount of late leakage was noted centrally.

Optical Coherence Tomography

A horizontal OCT image (C) was acquired through the fovea and showed fragmentation and fusiform thickening of the red band corresponding to the retinal pigment epithelium and choriocapillaris, consistent with a small choroidal neovascular membrane. No apparent subretinal fluid or hemorrhage was identified.

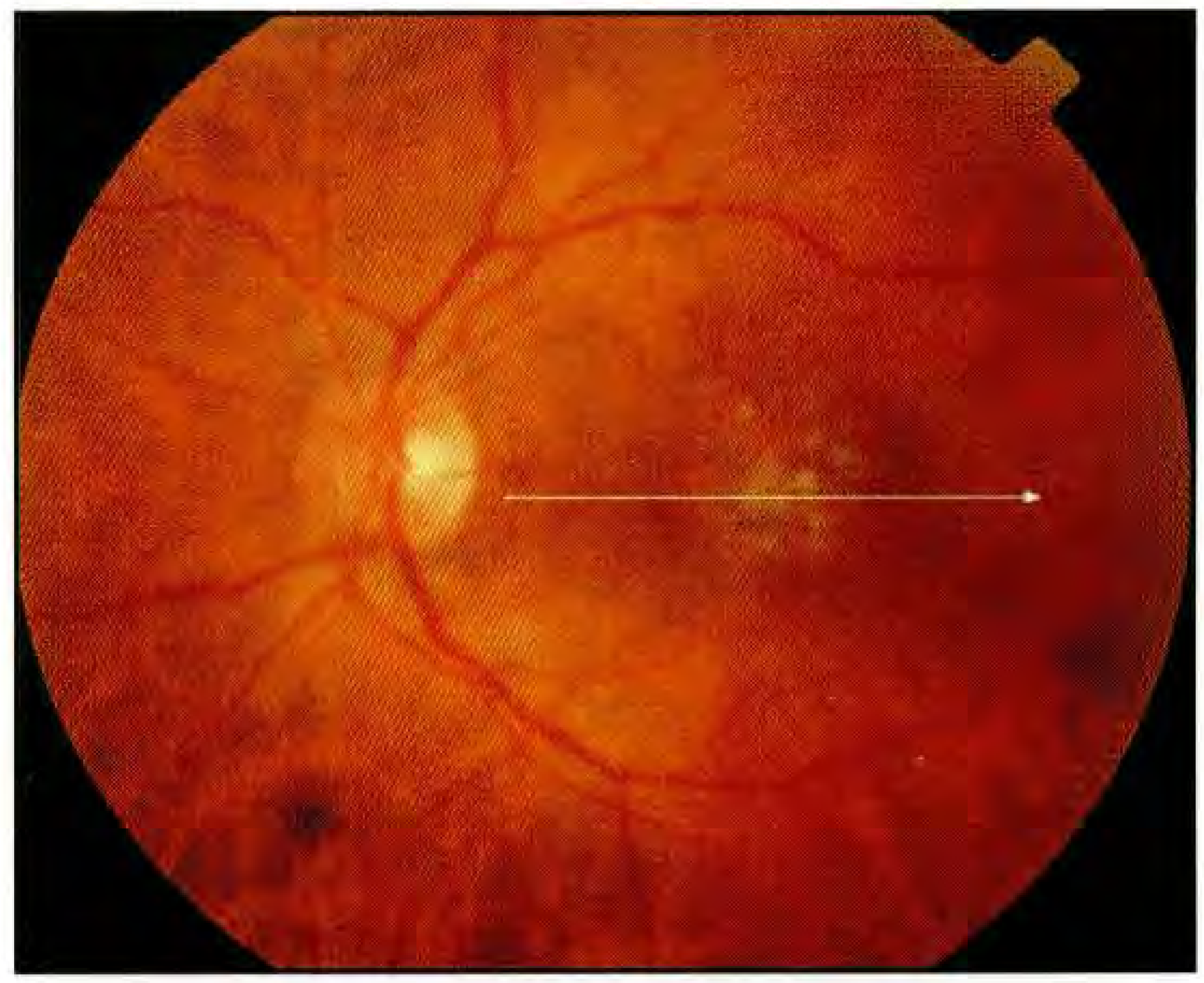

A

B

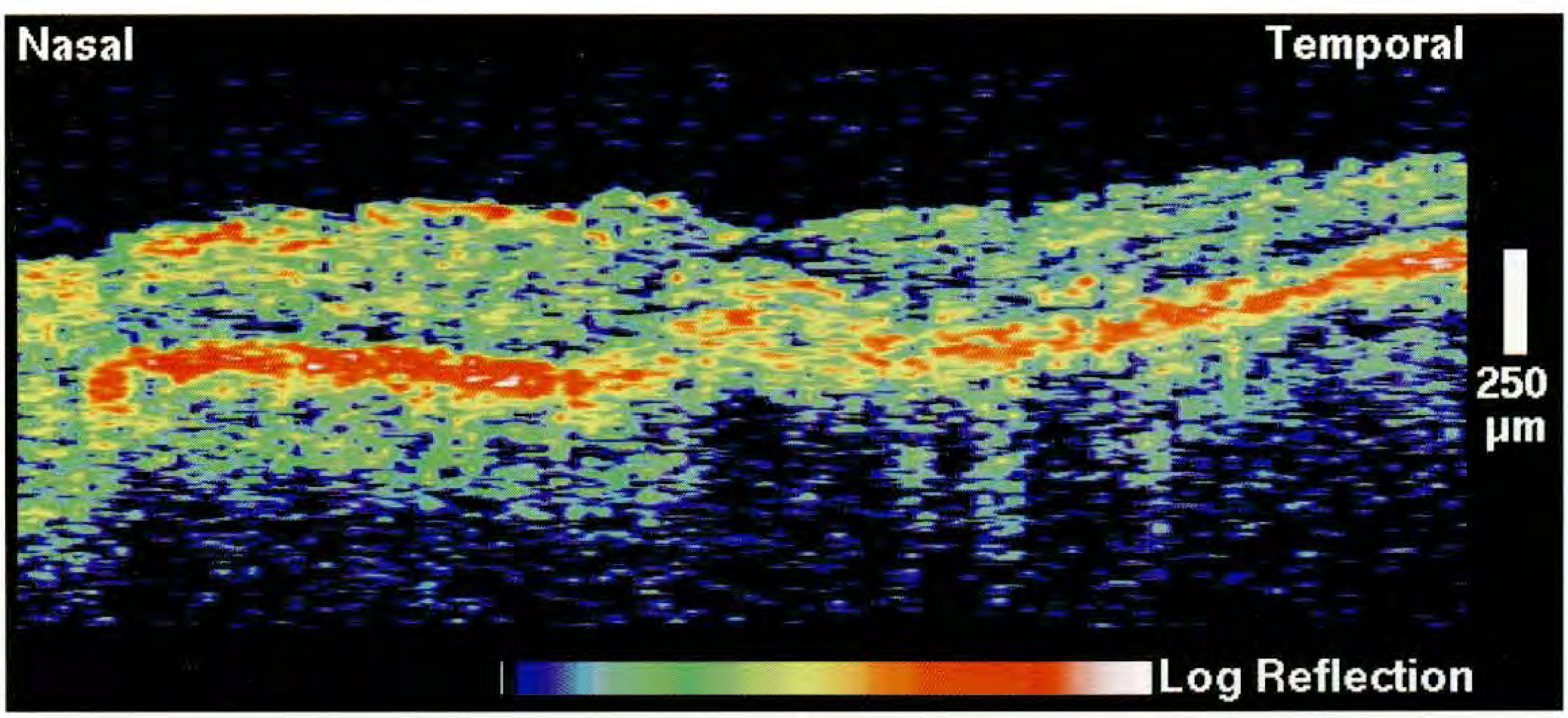

C

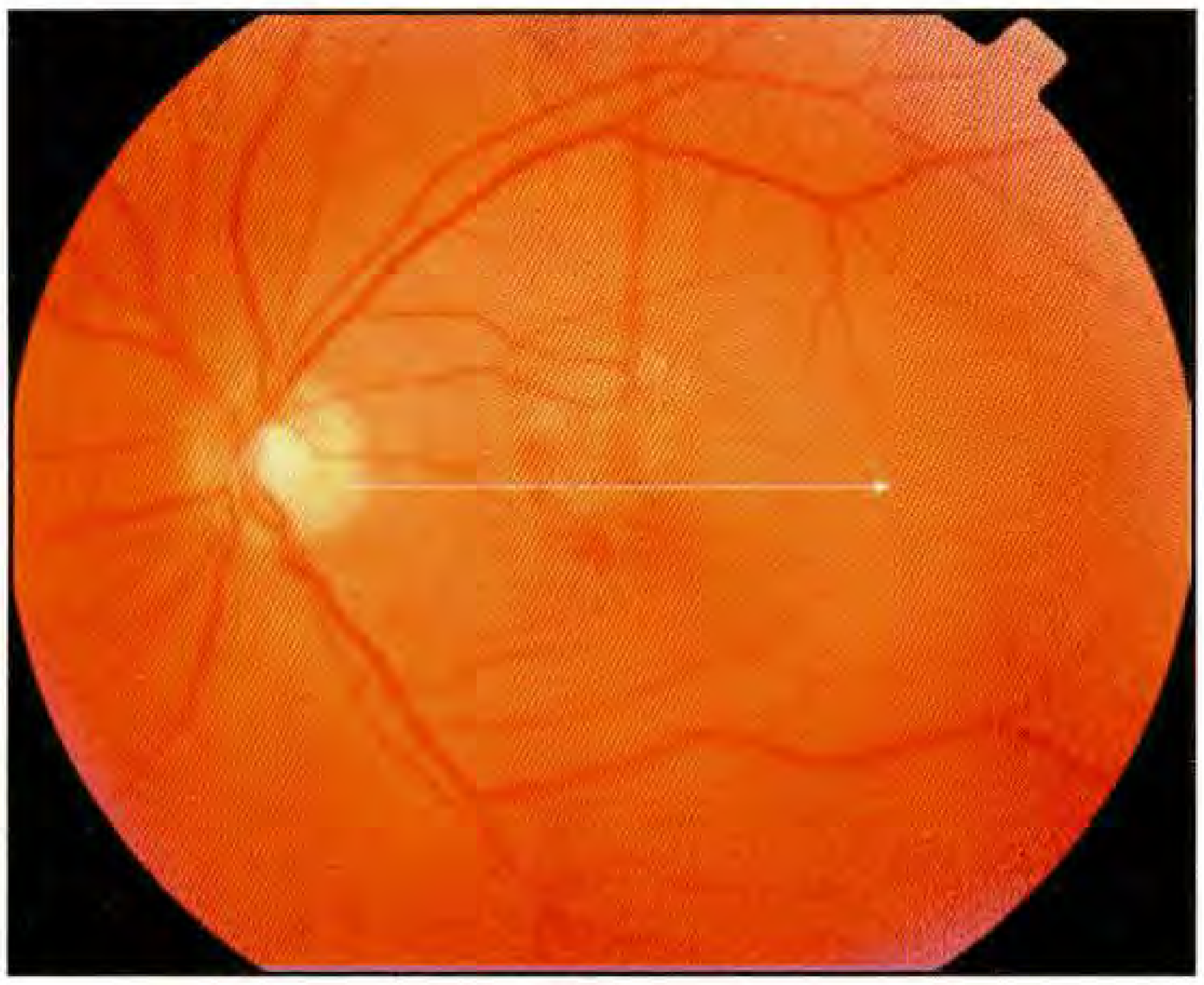

A

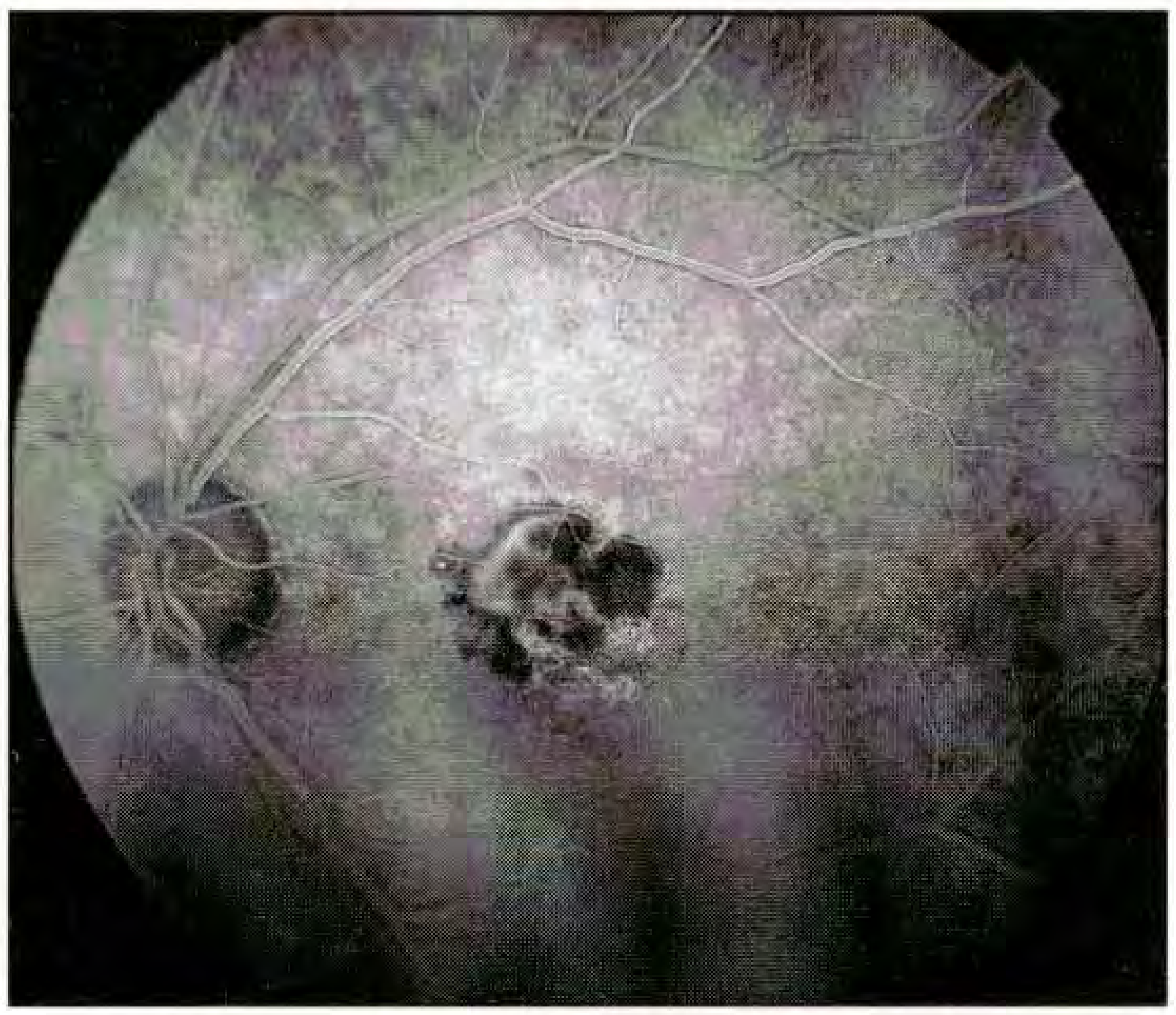

B

Case 8-31. Choroidal Neovascularization

Clinical Summary

A 77-year-old man with age-related macular degeneration had a visual acuity of counting fingers at six inches in his left eye. Slit-lamp examination (A) showed a fibrovascular pigment epithelial detachment in the fovea with surrounding subretinal fluid and hemorrhage. A lacy region of hyperfluorescence within a region of hypofluorescence was seen during the arteriovenous phase of the fluorescein angiogram (B) with late leakage consistent with a choroidal neovascular membrane.

Optical Coherence Tomography

A horizontal OCT scan (C) through the macula revealed a well-defined region of abnormal discontinuities in the retinal pigment epithelium and patchy reflections from the choriocapillaris, consistent with a neovascular membrane. The neurosensory retina above the membrane appeared thickened, and reduced optical reflectivity in this area suggested intraretinal fluid accumulation.

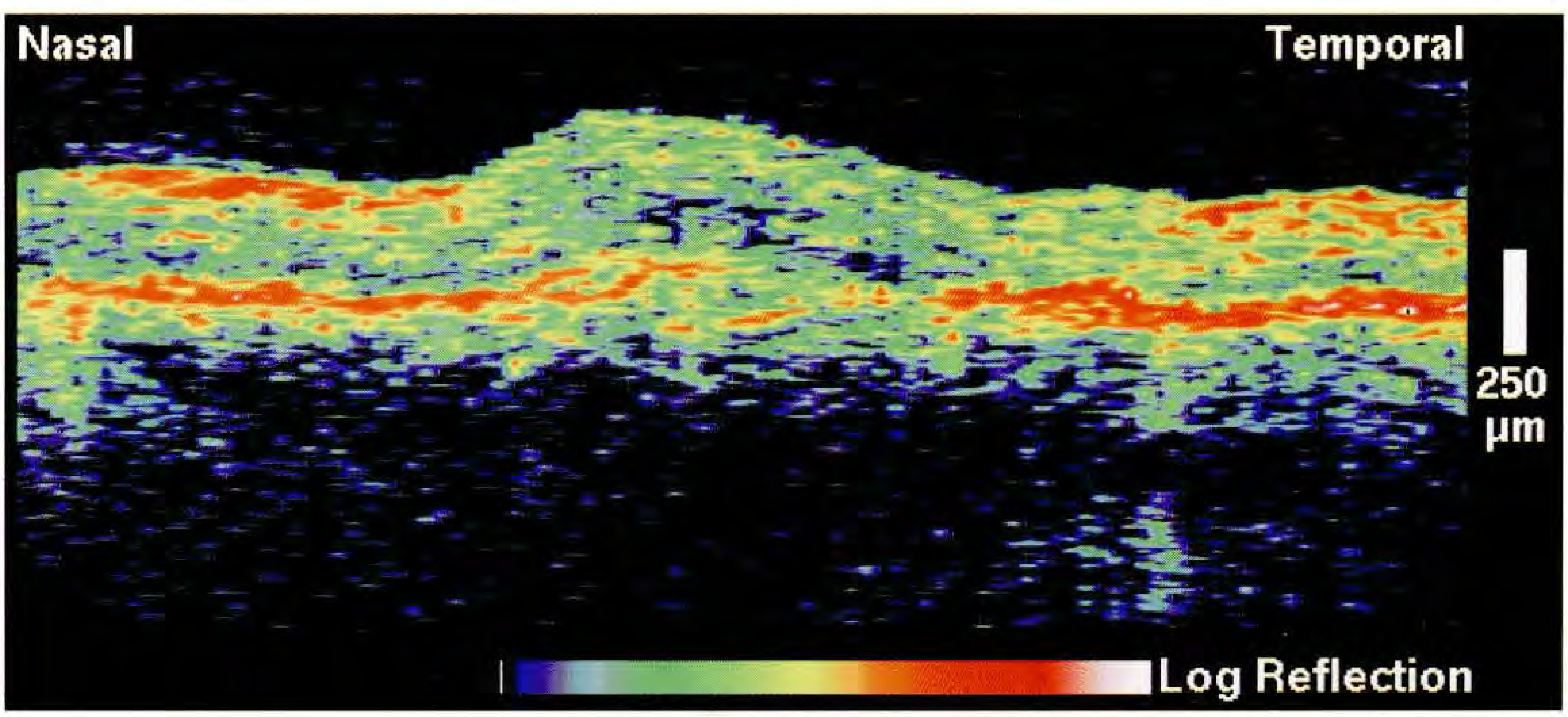

C

Case 8-32. Recurrent Choroidal Neovascularization

Clinical Summary

A 65-year-old man was referred for recurrent choroidal neovascularization in his left macula. He had presented four months earlier for evaluation of a decrease in his vision in his left eye to 20/40. Fundus examination at that time revealed subretinal hemorrhage nasal to the macula. Fluorescein angiography showed paramacular subpigment epithelial neovascularization, and diode laser photocoagulation was performed.

Follow-up slit-lamp examination (A) two weeks later demonstrated persistence of the neovascular membrane in the macula. A lesion in the central macula which was described as either a hemorrhagic pigment epithelial detachment or a subretinal thrombus was observed, with surrounding subretinal fluid, exudate, and trace hemorrhage. The patient's visual acuity had deteriorated to 20/400. Fluorescein angiography (B) displayed a hypofluorescent lesion in the central macula with mild hyperfluorescence along the inferonasal rim. The entire rim of the lesion became hyperfluorescent as the angiogram progressed, and well-defined pooling of dye was observed in the entire region in the late phases.

Optical Coherence Tomography

A vertical OCT tomogram (C) showed what appeared to be a tuft of tissue extending from the choroid into the neurosensory retina, consistent with a neovascular membrane. The reflection from the pigment epithelium was totally absent in this region. The surrounding neurosensory retina was detached, with the accumulation of a minimally backscattering fluid in the subretinal space.

A

B

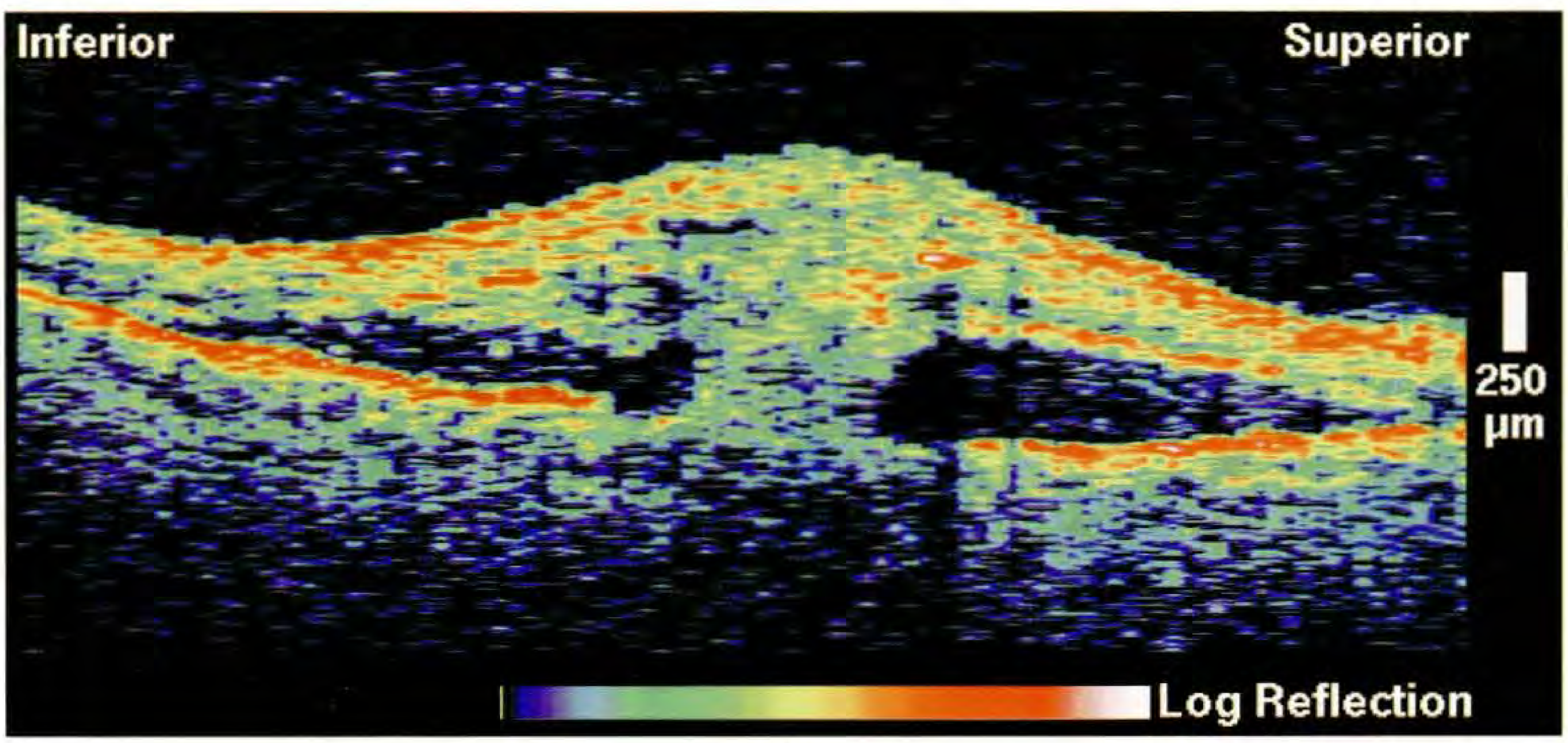

C

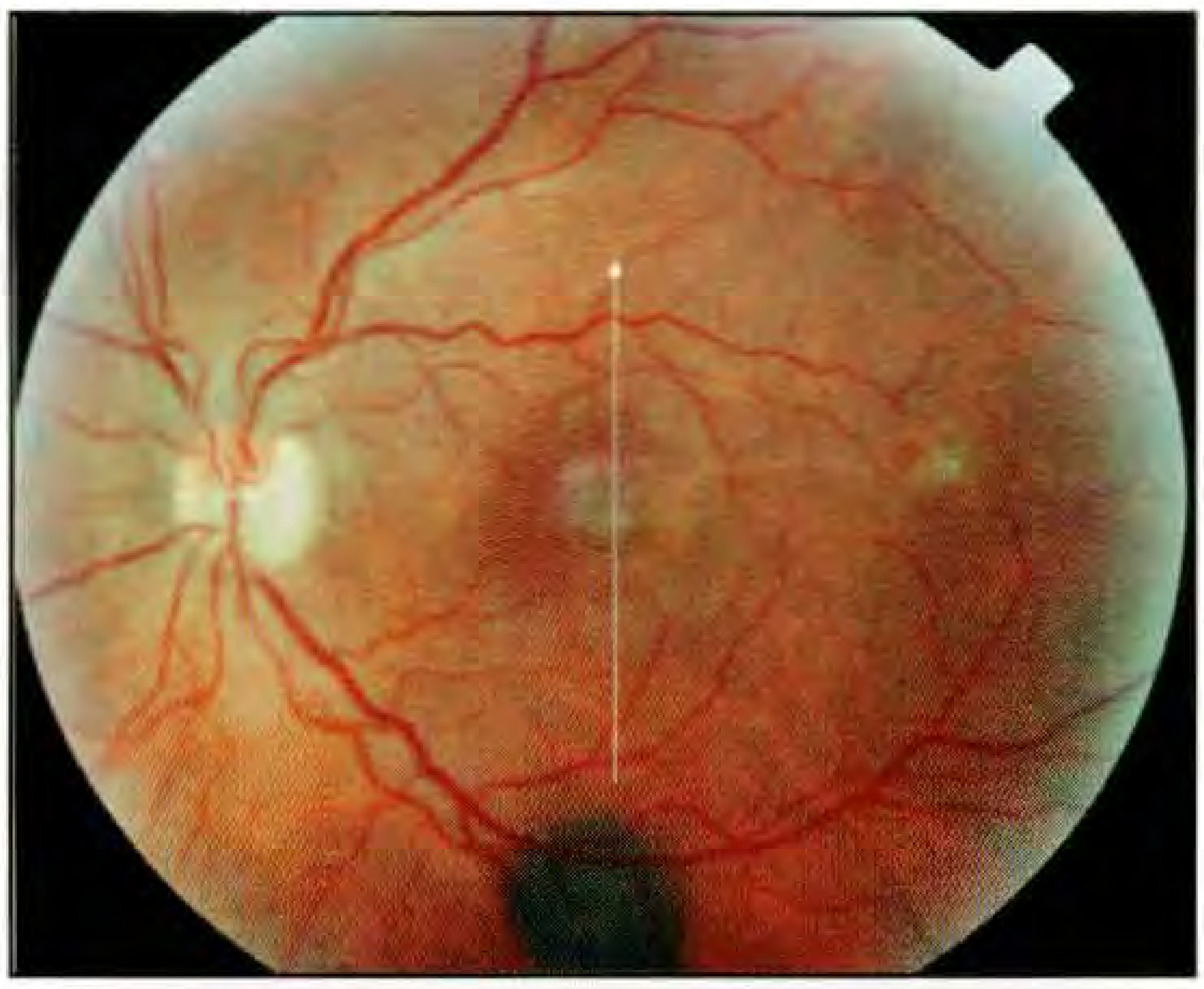

A

B

Case 8-33. Progression of Choroidal Neovascularization

Clinical Summary

A 67-year-old man noticed a central gray spot in his left visual field for two months prior to examination. He reported enlargement of this spot over the most recent two weeks. His visual acuity in this eye was 20/60. Dilated fundus examination (A) revealed a gray, mildly elevated subretinal lesion with a surrounding hypopigmented halo and minimal subretinal fluid. Fluorescein angiography (B) exhibited a well-defined hyperfluorescent lesion centrally which demonstrated leakage in the later phases consistent with subfoveal neovascularization.

Optical Coherence Tomography

A vertical OCT tomogram (C) through fixation showed a small, well-defined region of fusiform thickening in the reflective band representing the retinal pigment epithelium and choriocapillaris. Reduced intraretinal optical reflectivity and loss of the normal foveal contour was noted centrally consistent with macular edema.

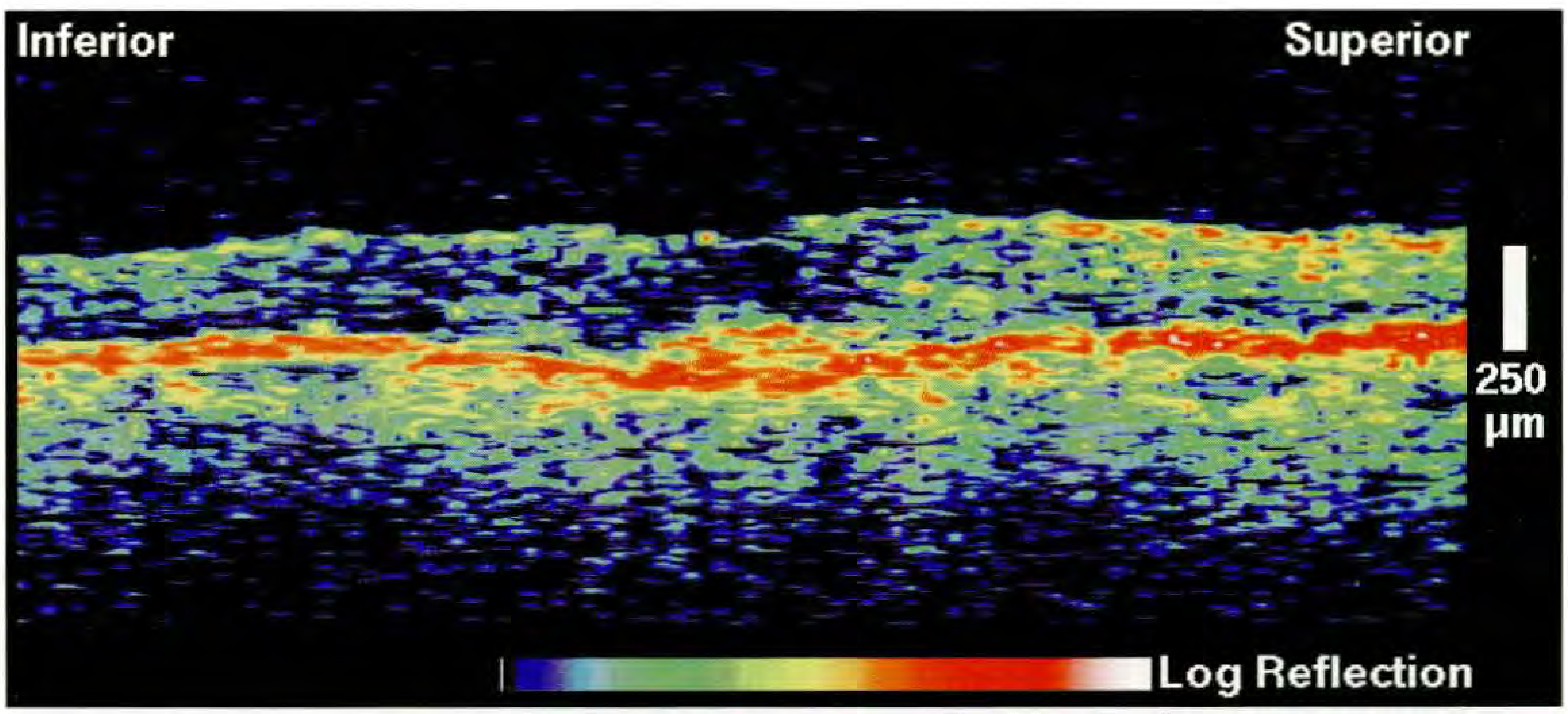

C

Case 8-33 continued

Follow-up Examination

One month later, the patient's visual acuity in the left eye had declined to 20/160. Ophthalmoscopy (D) showed that the central macular lesion had increased in size. A corresponding well-defined region of hyperfluorescence was evident on fluorescein angiography (E). The lesion demonstrated progressive dye leakage consistent with neovascularization.

Follow-up Optical Coherence Tomography

A follow-up OCT tomogram (F) exhibited enlargement of the focal thickening in the reflection corresponding to the pigment epithelium and choriocapillaris. A slight increase in the central macular edema was noted, and a new region of subretinal fluid accumulation was identified superior to the fovea.

D

E

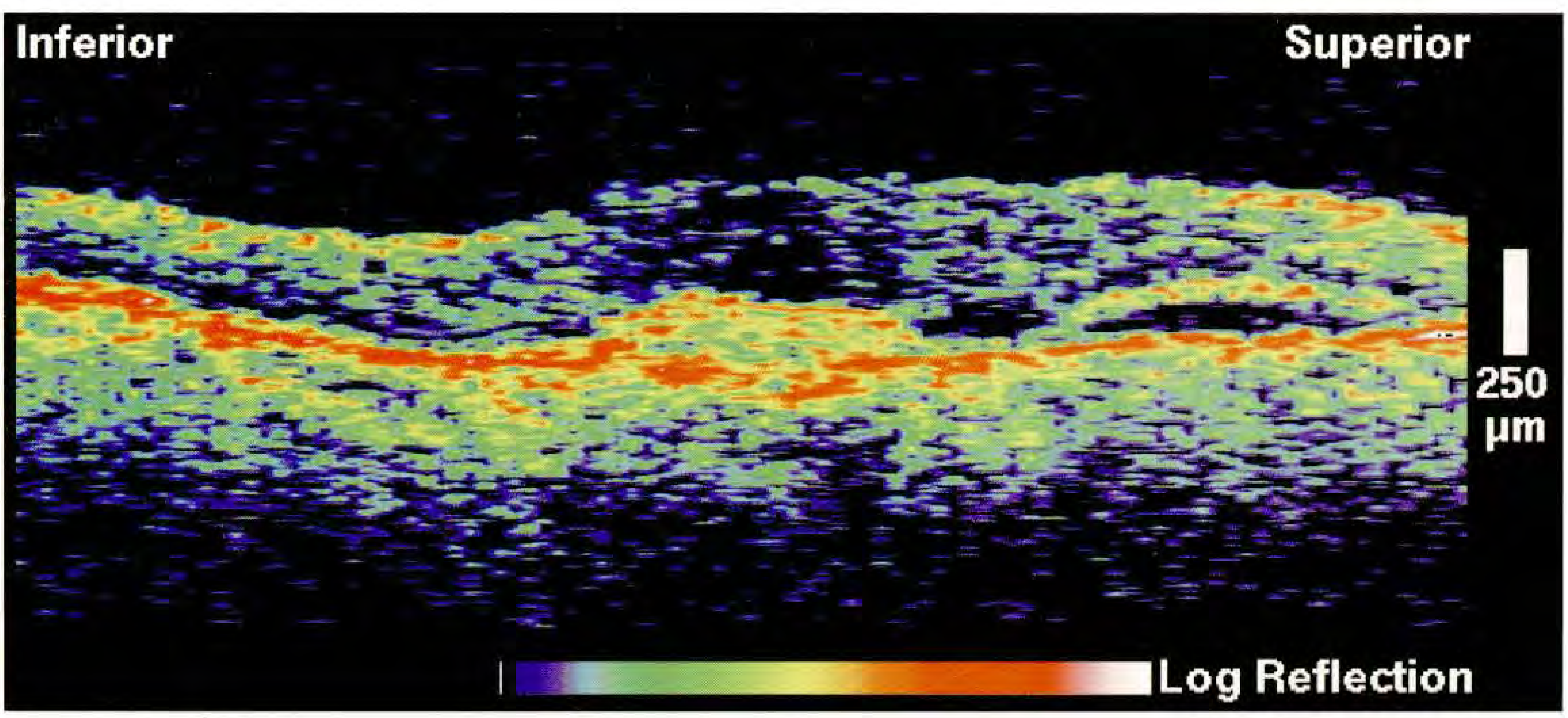

F

A

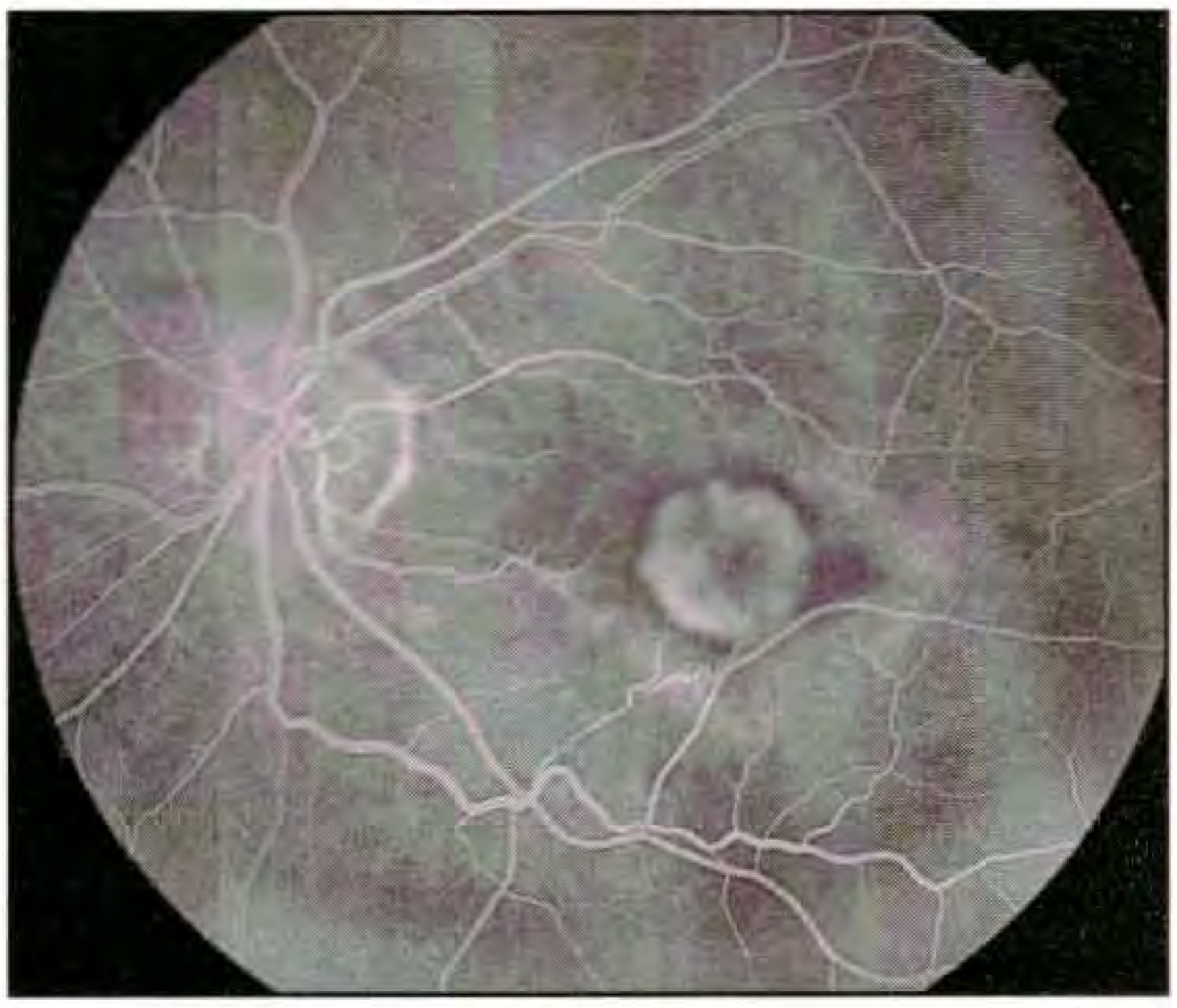

B

Case 8-34. Recurrent Choroidal Neovascularization

Clinical Summary

An 83-year-old woman was referred for evaluation of recurrent choroidal neovascularization in her left eye. She had received laser photocoagulation in this eye two months earlier; however, her visual acuity had not improved from 20/125. Slit-lamp biomicroscopy (A) showed a small pigmented lesion in the central macula with surrounding subretinal fluid and macular edema. A well-defined annulus of hyperfluorescence was evident on fluorescein angiography (B). The annulus increased in intensity in later frames with some late leakage.

Optical Coherence Tomography

A well-defined region of retinal thickening was noted on the OCT scan (C). The reflection from the retinal pigment epithelium and choriocapillaris was diminished in the area of the lesion, and moderate backscatter signal was observed subretinally consistent with a neovascular membrane (arrows). A region of minimal backscattering consistent with subretinal serous fluid accumulation was evident temporal to the lesion. The reflectivity from the subretinal fluid increased in the area just anterior to the membrane.

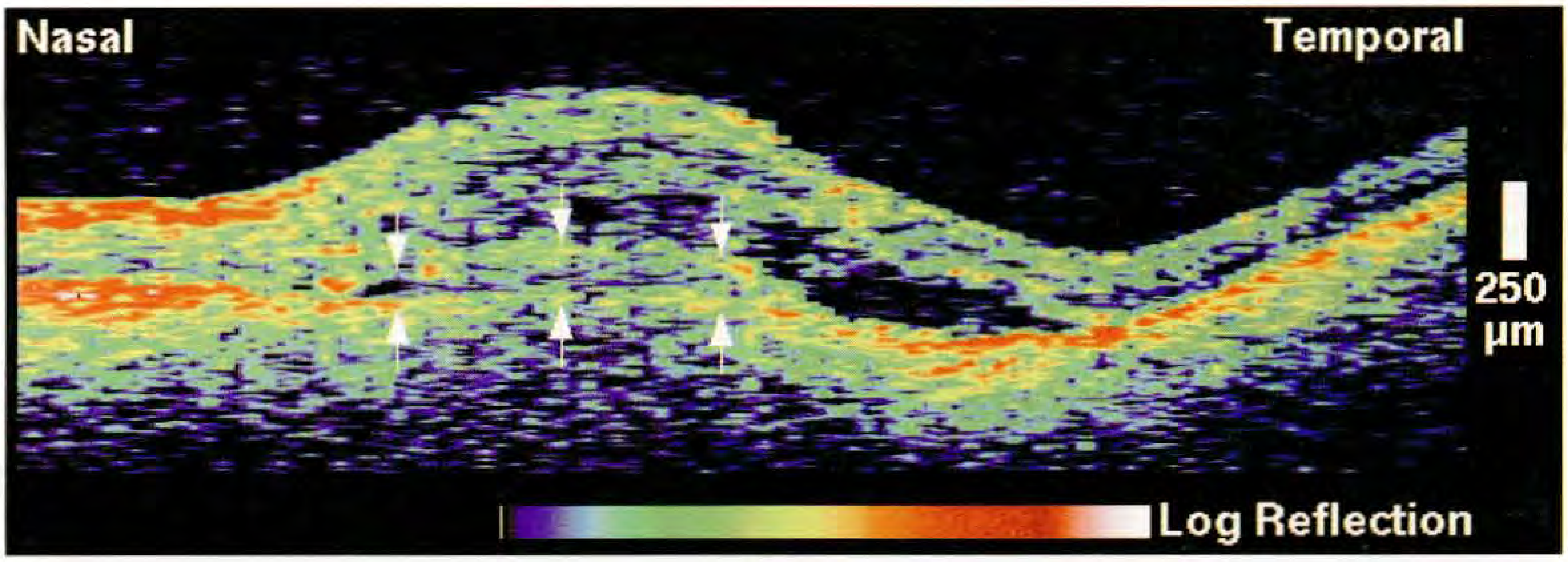

C

Case 8-34 continued

Follow-up Examination

The patient received indocynanine green enhanced diode laser photocoagulation in her left eye and returned one month later for follow-up examination. She reported a new black spot in her central vision and her visual acuity had declined to counting fingers at five feet in this eye. Slit-lamp biomicroscopy (D) showed an atrophic laser scar in the macula with central pigmentation. A corresponding, well-defined region of hypofluorescence was noted in all phases of the fluorescein angiogram (E).

Follow-up Optical Coherence Tomography

The OCT image (F) demonstrated the absence of intraretinal or subretinal fluid accumulation. The reflective band corresponding to the pigment epithelium and choriocapillaris appeared intact throughout the scan, with a slight increase in backscattering in the region of the laser scar.

D

E

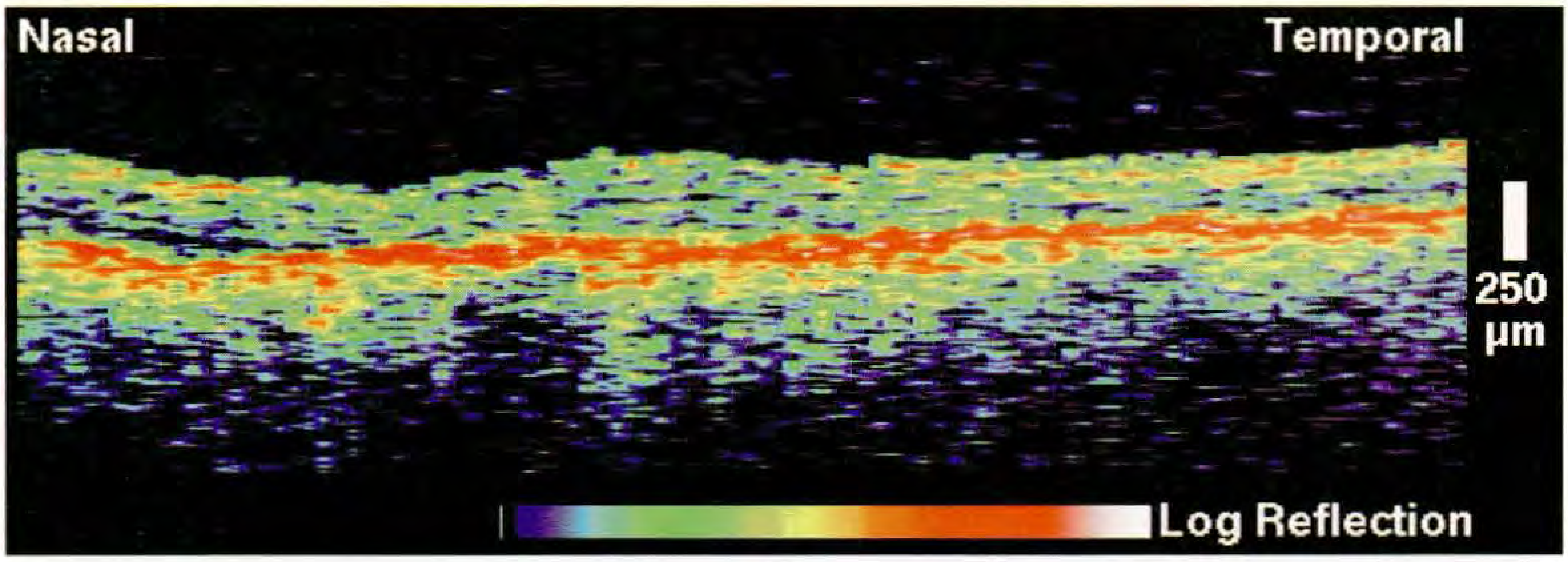

F

A

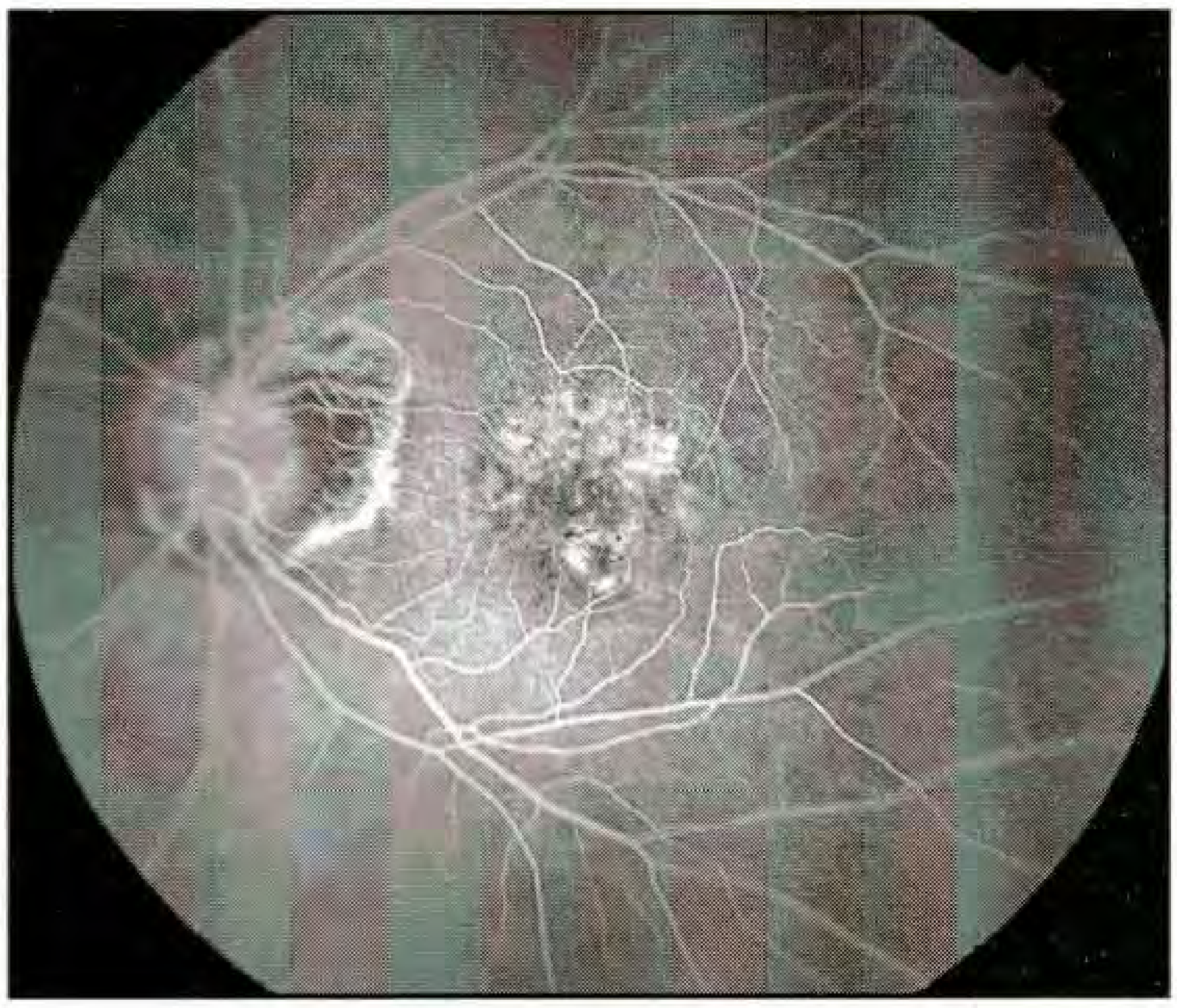

B

Case 8-35. Choroidal Neovascularization and Laser Photocoagulation

Clinical Summary

A 38-year-old woman noted blurred vision in her left eye approximately seven months earlier. Her visual acuity was 20/300 on examination. Slit-lamp biomicroscopy (A) was notable for pigment epithelial atrophy and mottling in the central macula, and subretinal fluid with a small amount of hemorrhage inferior to the fovea. Fluorescein angiography (B) displayed mottled hyperfluorescence superior to the fovea. A focal spot of hypofluorescence surrounded by hyperfluorescence was observed inferiorly consistent with hemorrhage and fluid accumulation. Both lesions increased in intensity with mild leakage during the late phase.

Optical Coherence Tomography

A vertical OCT image (C) displayed a large intraretinal, optically clear space corresponding to a cyst. The retina was mildly thickened surrounding the cyst. Disruption of the reflection from the retinal pigment epithelium and choriocapillaris was present but difficult to observe beneath the cyst because of diffuse, enhanced choroidal reflectivity.

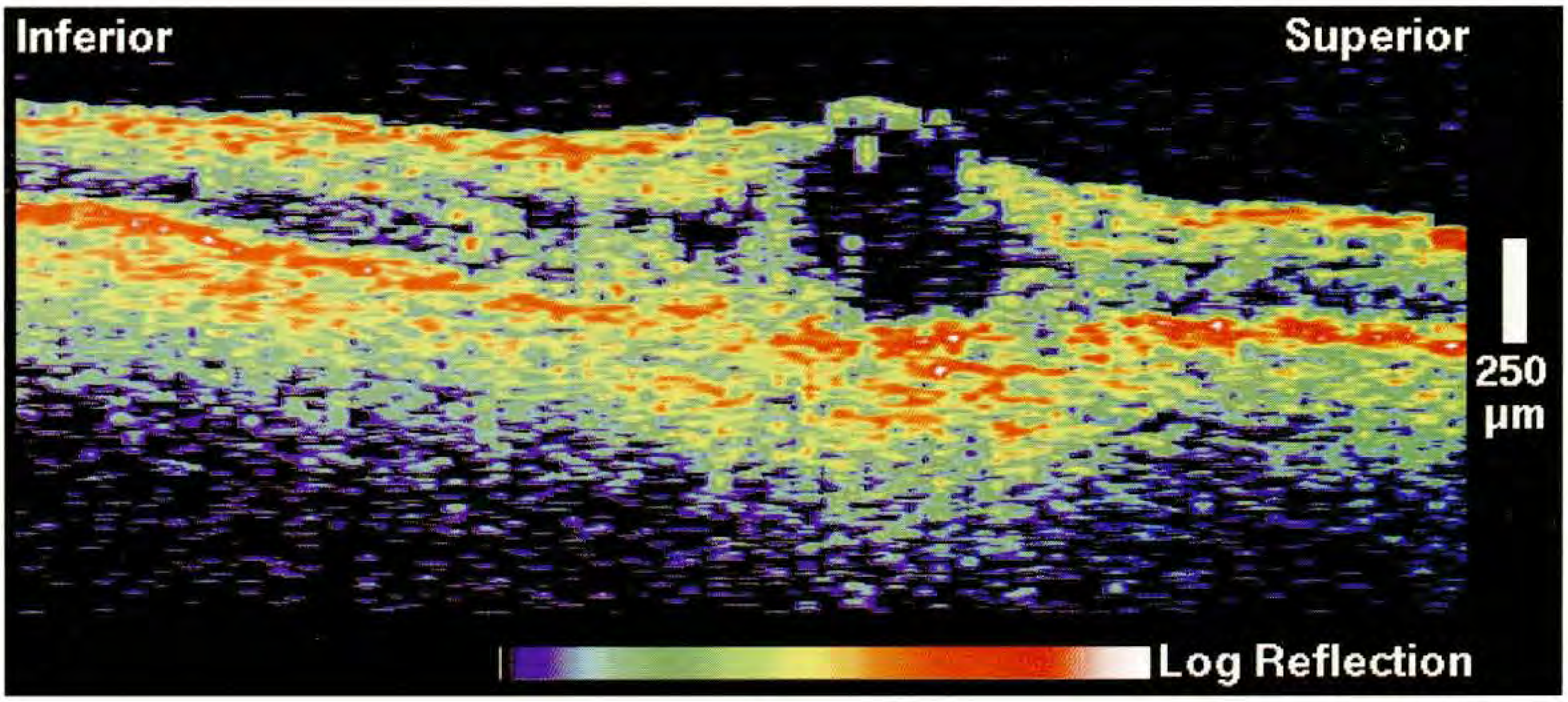

C

Case 8-35 continued

Follow-up Examination

The patient received photocoagulation treatment to the lesion, which was also visualized on indocyanine green angiography, with a dye yellow laser. On follow-up examination three months later, her visual acuity had improved to 20/200. Slit-lamp biomicroscopy (D) showed a pigmented laser scar in the macula with no associated subretinal fluid or hemorrhage. Fluorescein angiography (E) displayed hypofluorescence in the inferior macula with patchy hyperfluorescence superior to this lesion, involving the fovea. Poorly defined late leakage was also observed.

Follow-up Optical Coherence Tomography

OCT (F) revealed resolution of the cystoid macular edema, and a focal region of enhanced choroidal reflectivity and retinal atrophy corresponding to the laser scar.

D

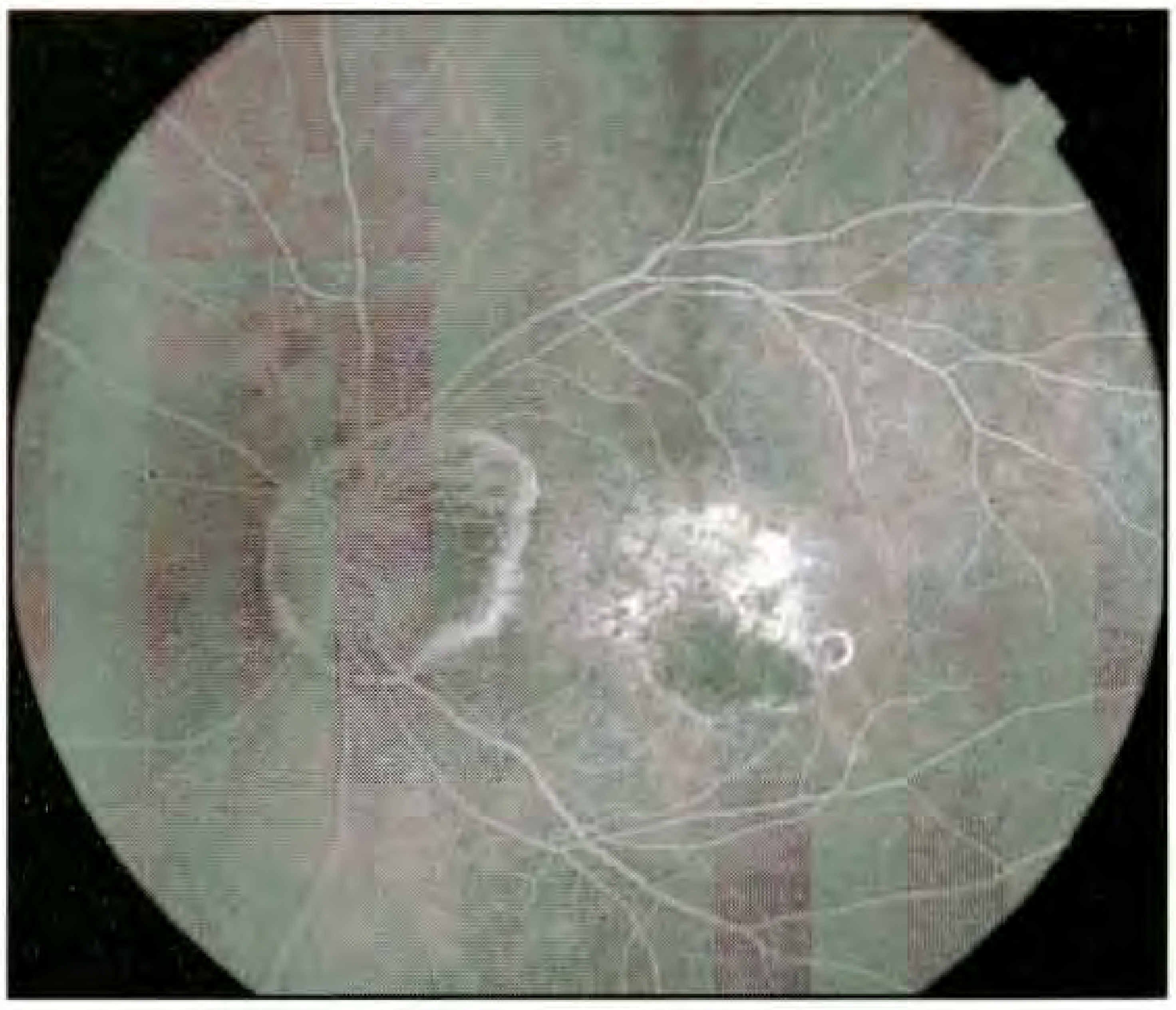

E

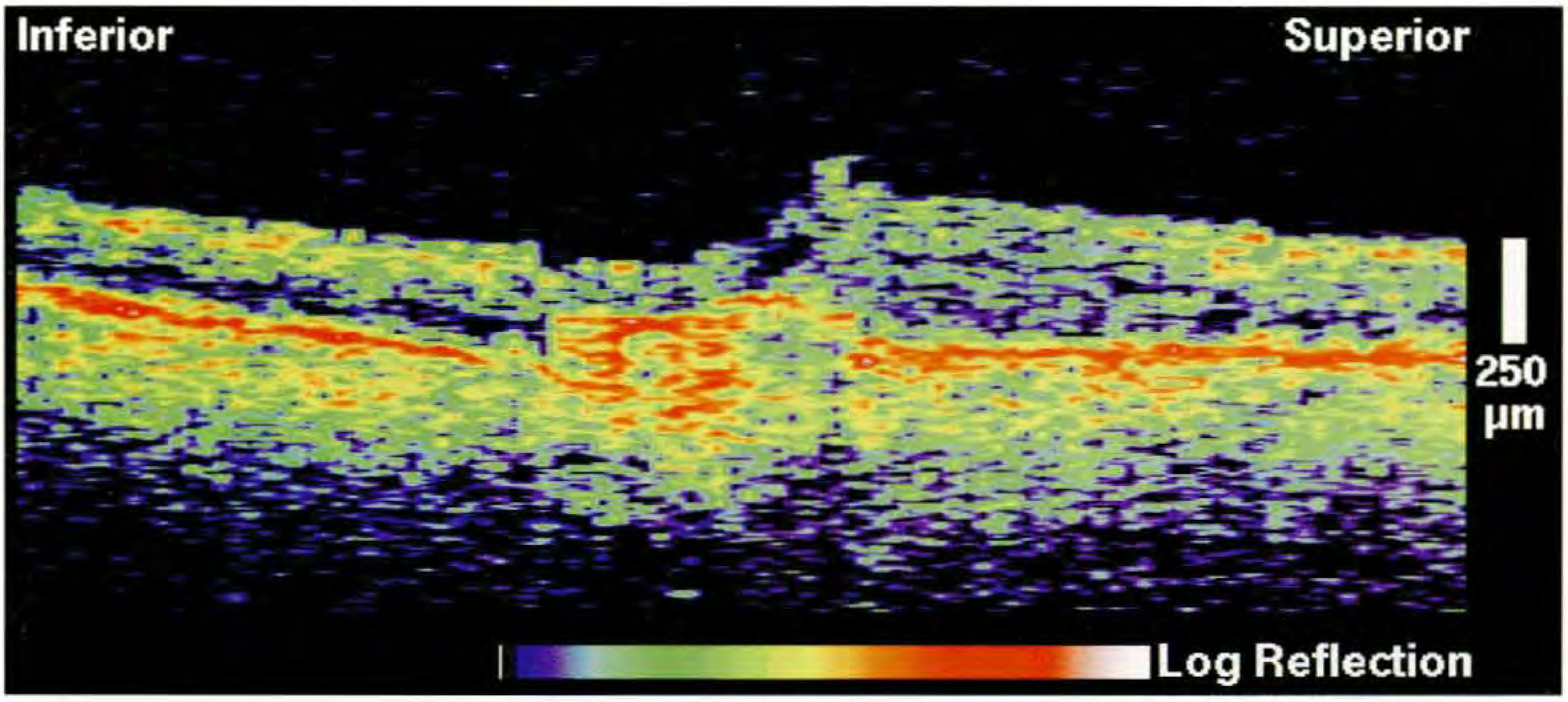

F

Case 8-36. Choroidal Neovascularization

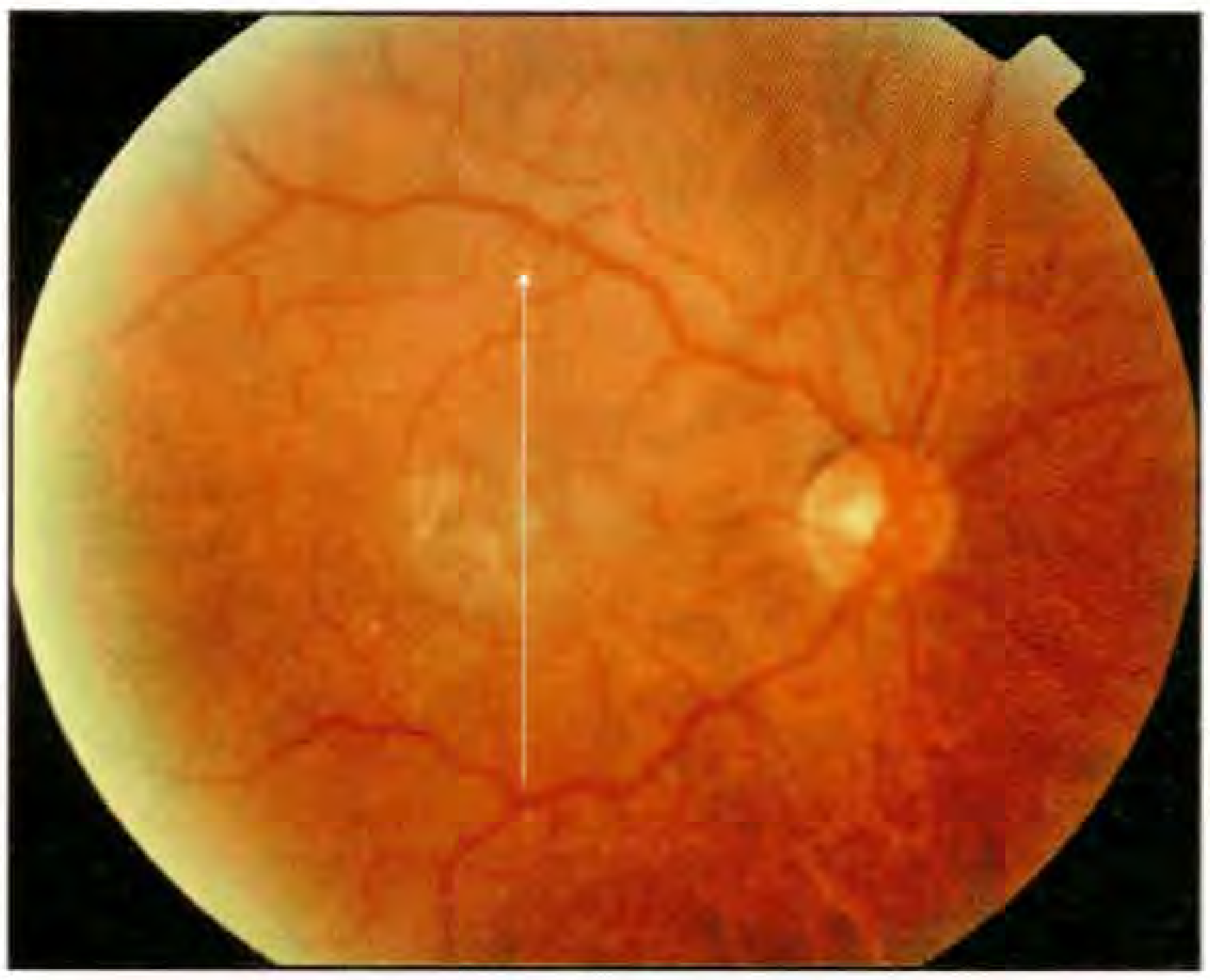

A

B

Clinical Summary

A 74-year-old man with age-related macular degeneration noted gradually decreasing vision in his right eye. His visual acuity in this eye on examination was 20/160, and cloudy subretinal fluid was observed in the central macula on slit-lamp biomicroscopy (A). Two small areas of subretinal hemorrhage were also noted. Fluorescein angiography (B) disclosed patchy hyperfluorescence in the central macula which exhibited late leakage inferiorly consistent with subretinal neovascularization.

Optical Coherence Tomography

A vertical scan (C) through fixation delineated a focal thickening and fragmentation of the reflective band corresponding the retinal pigment epithelium (RPE) and choriocapillaris, suggesting subfoveal choroidal neovascularization. Small non-reflective spaces were observed intraretinally consistent with cysts; however, no significant retinal thickening was noted. A thin line of enhanced backscatter from within the neurosensory retina immediately superior to the lesion was consistent with intraretinal hemorrhage.

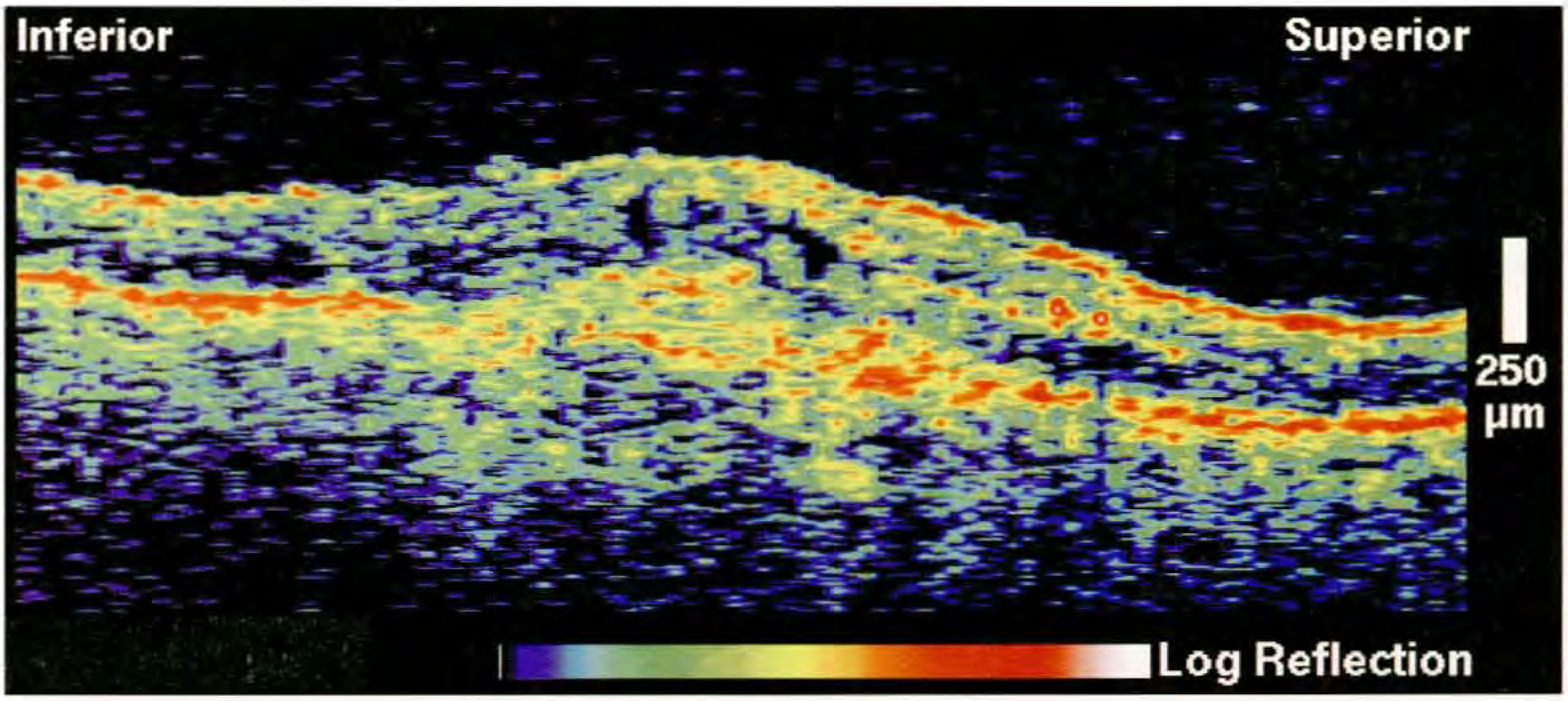

C

Case 8-37. Recurrent Choroidal Neovascularization

Clinical Summary

A 75-year-old man had received multiple laser treatments in his right eye for choroidal neovascularization. He had recently noted a decline in his vision in this eye. On examination (A), he was found to have lightly pigmented laser scars superotemporal and inferior to the fovea which were surrounded by significant subretinal fluid. Patchy subretinal hemorrhage was observed in the superior macula. The visual acuity in this eye was 20/300. Fluorescein angiography (B) showed hypofluorescence superotemporal to the fovea corresponding to the laser scar, and a small area of focal hyperfluorescence centrally which increased in intensity as the angiogram progressed. A well-defined boundary of hyperfluorescence surrounded the entire lesion.

Optical Coherence Tomography

A horizontal image (C) through the fovea showed significant retinal thickening and reduced optical backscatter signifying intraretinal fluid accumulation nasal to the fovea. The reflection from the choroid was reduced below the region of the edema consistent with shadowing. An abnormality in the reflection from the RPE and choriocapillaris was observed directly beneath the fovea (arrows) consistent with a subfoveal neovascular membrane.

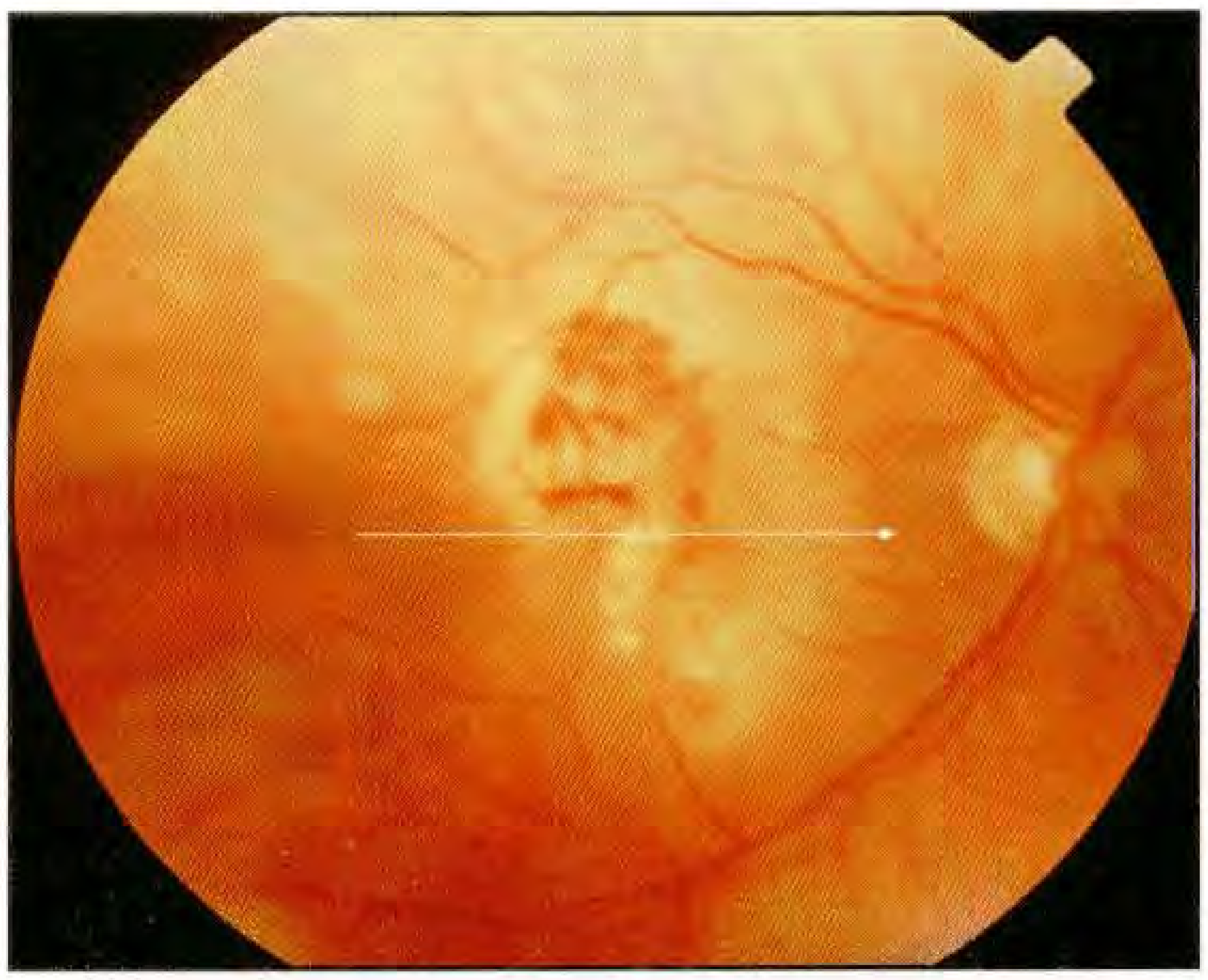

A

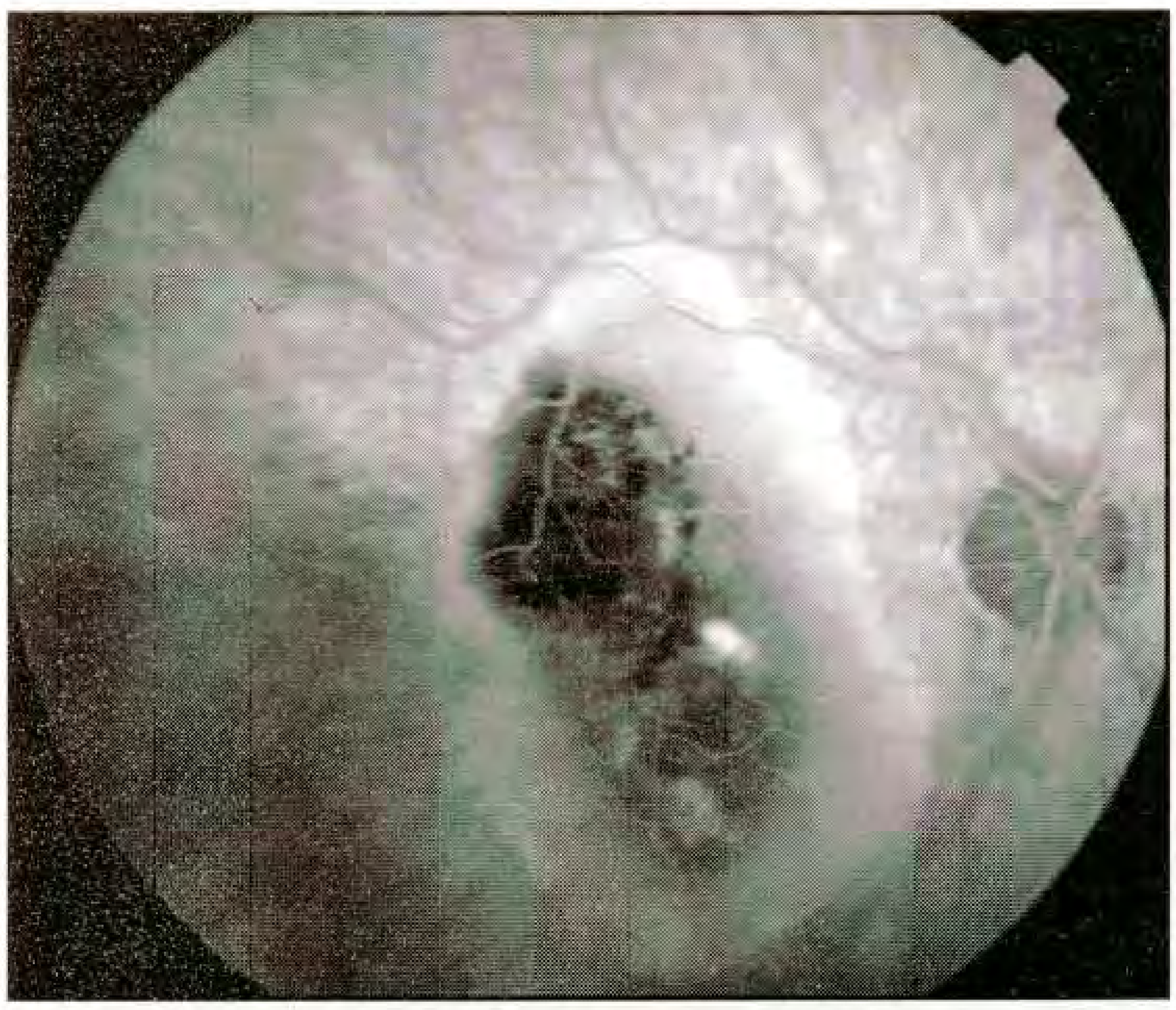

B

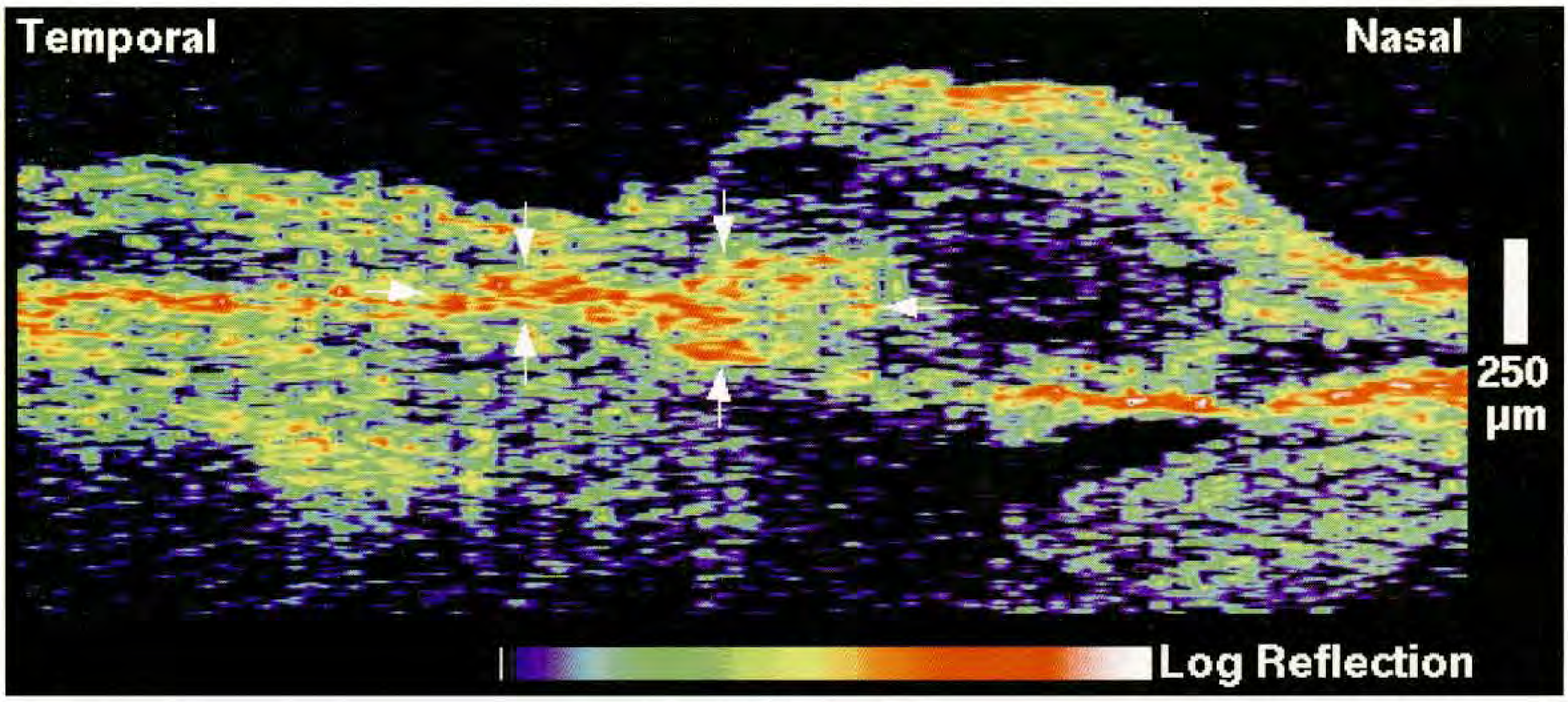

C

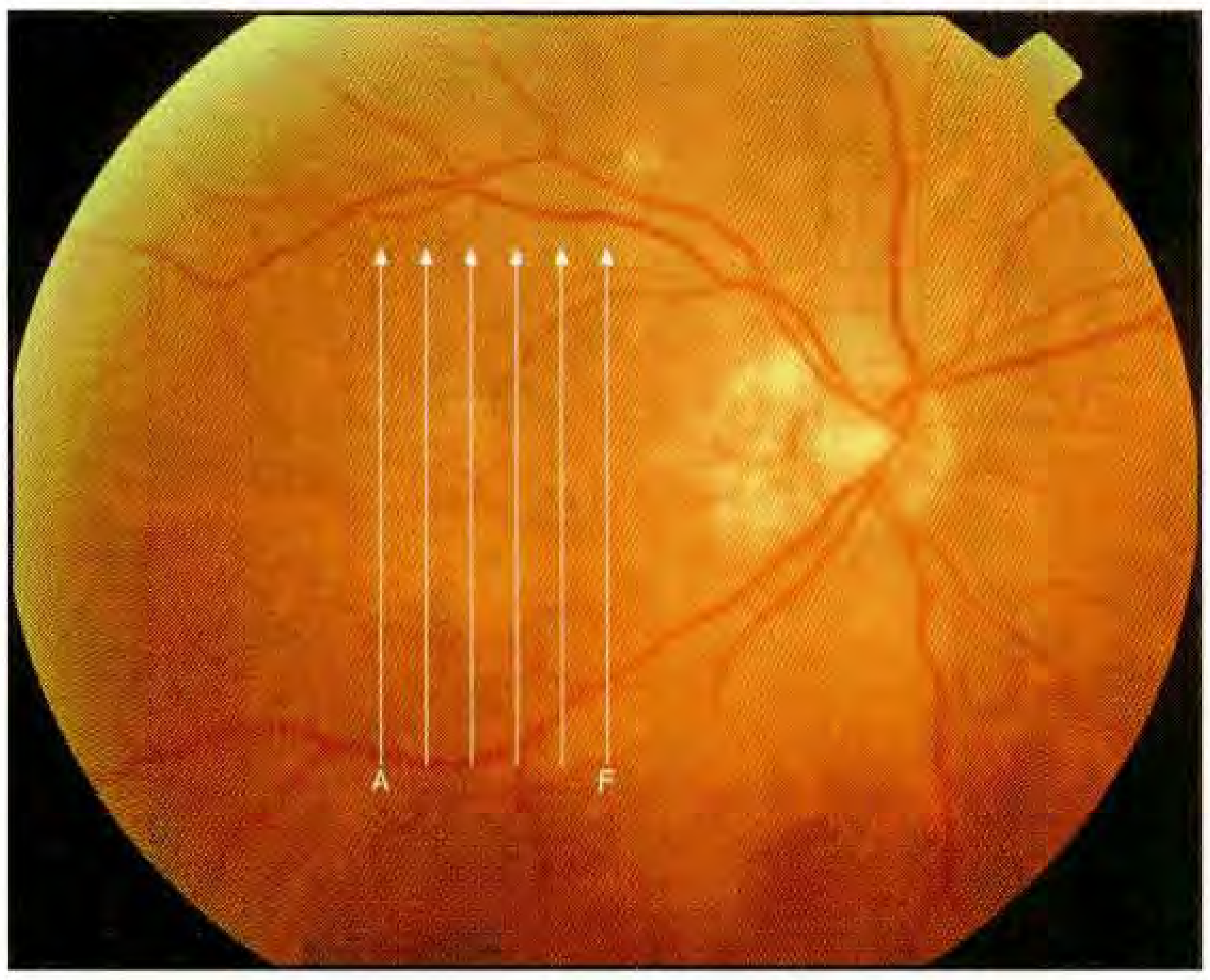

A

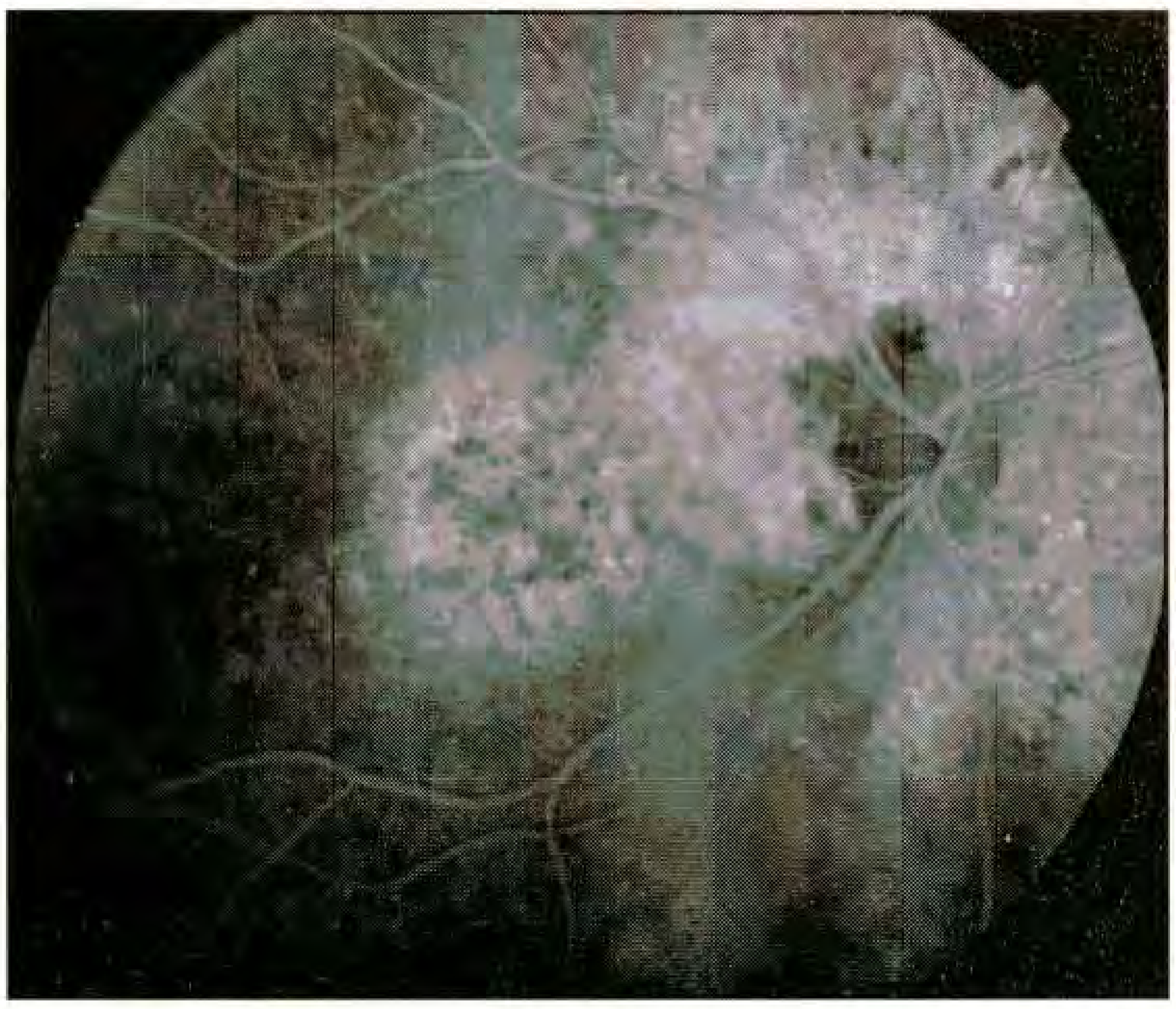

B

Case 8-38. Choroidal Neovascularization and Atrophic Scar

Clinical Summary

An 80-year-old woman with age-related macular degeneration noticed decreasing vision in her right eye over the previous three days. On examination, her visual acuity in this eye was 20/70, and slit-lamp biomicroscopy (A) showed retinal pigment epithelial mottling in the macula and an area of chorioretinal atrophy temporal to the optic disc. Fluorescein angiography (B) displayed mottled hyperfluorescence in the macula and surrounding the optic disc which demonstrated late leakage consistent with a choroidal neovascular membrane.

Optical Coherence Tomography

A sequence of vertical OCT tomograms (C) was obtained through the macula. Slight retinal thickening was observed surrounding the fovea. A well-defined region of increased reflectivity in the inner layers of the neurosensory retina was noted inferior to the fovea and appeared to shadow the reflections from the retinal pigment epithelium and choriocapillaris below. The reflective band corresponding to the pigment epithelium and choriocapillaris was thickened and disrupted in a fairly well-defined region nasal to the fovea (scans D and E) suggesting choroidal neovascularization.

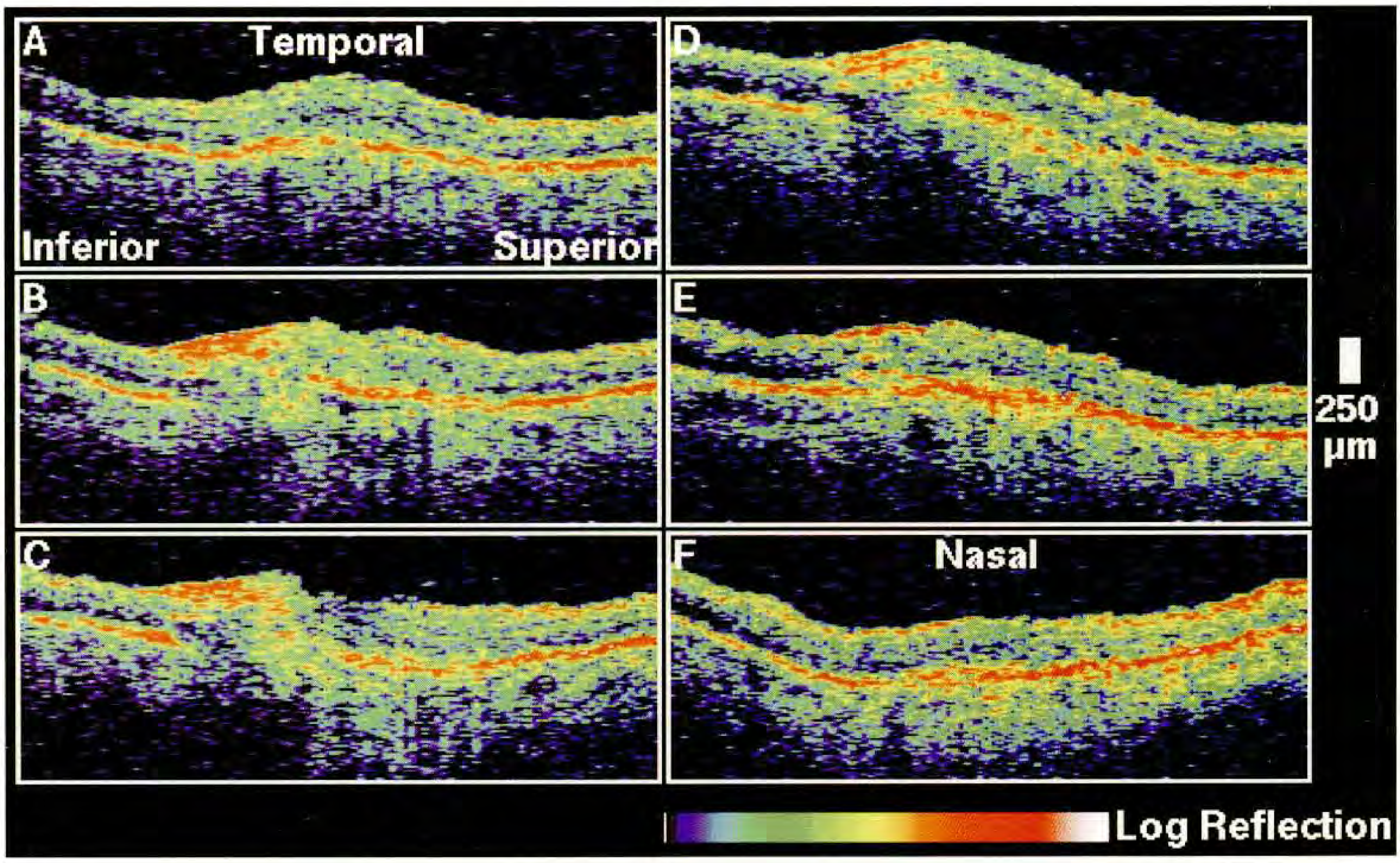

C

Case 8-38 continued

Clinical Summary

In the left eye, the patient had received laser photocoagulation treatment 15 months earlier for a subretinal neovascular membrane. Funduscopic examination of this eye (D) showed a laser scar in the macula nasal to the fovea with subretinal fibrosis and minimal subretinal hemorrhage. A hypofluorescent lesion nasal to the fovea was observed on fluorescein angiography (E). Mottled hyperfluorescence surrounding this lesion exhibited late staining and mild leakage.

Optical Coherence Tomography

A sequence of horizontal OCT images (F) exhibited increased optical reflectivity from the choroid nasal to the fovea consistent with subretinal fibrosis and a laser scar. The neurosensory retina above the lesion was markedly atrophic. Focal intraretinal regions of reduced backscattering observed in scans A and B corresponded to the retinal hemorrhage seen clinically.

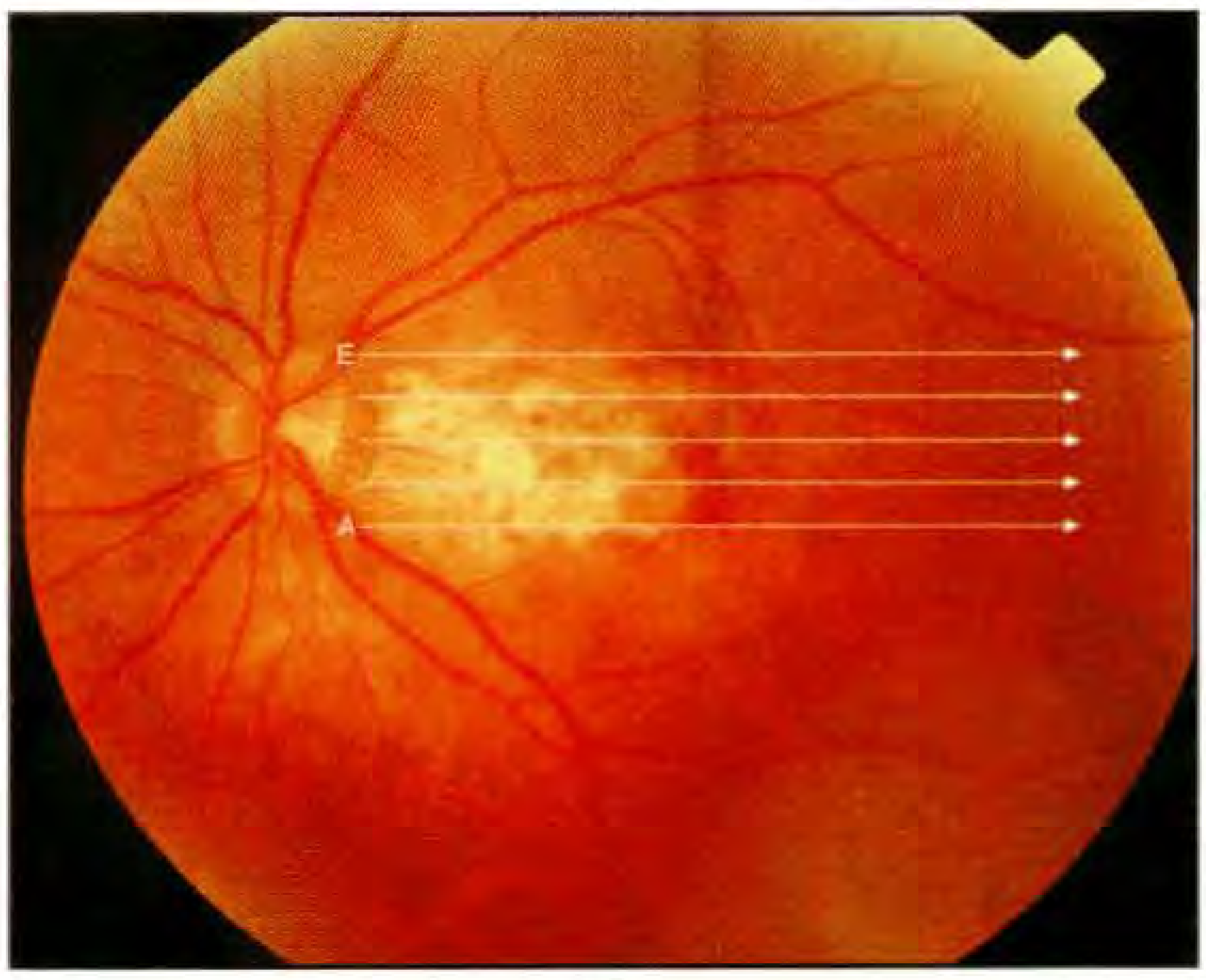

D

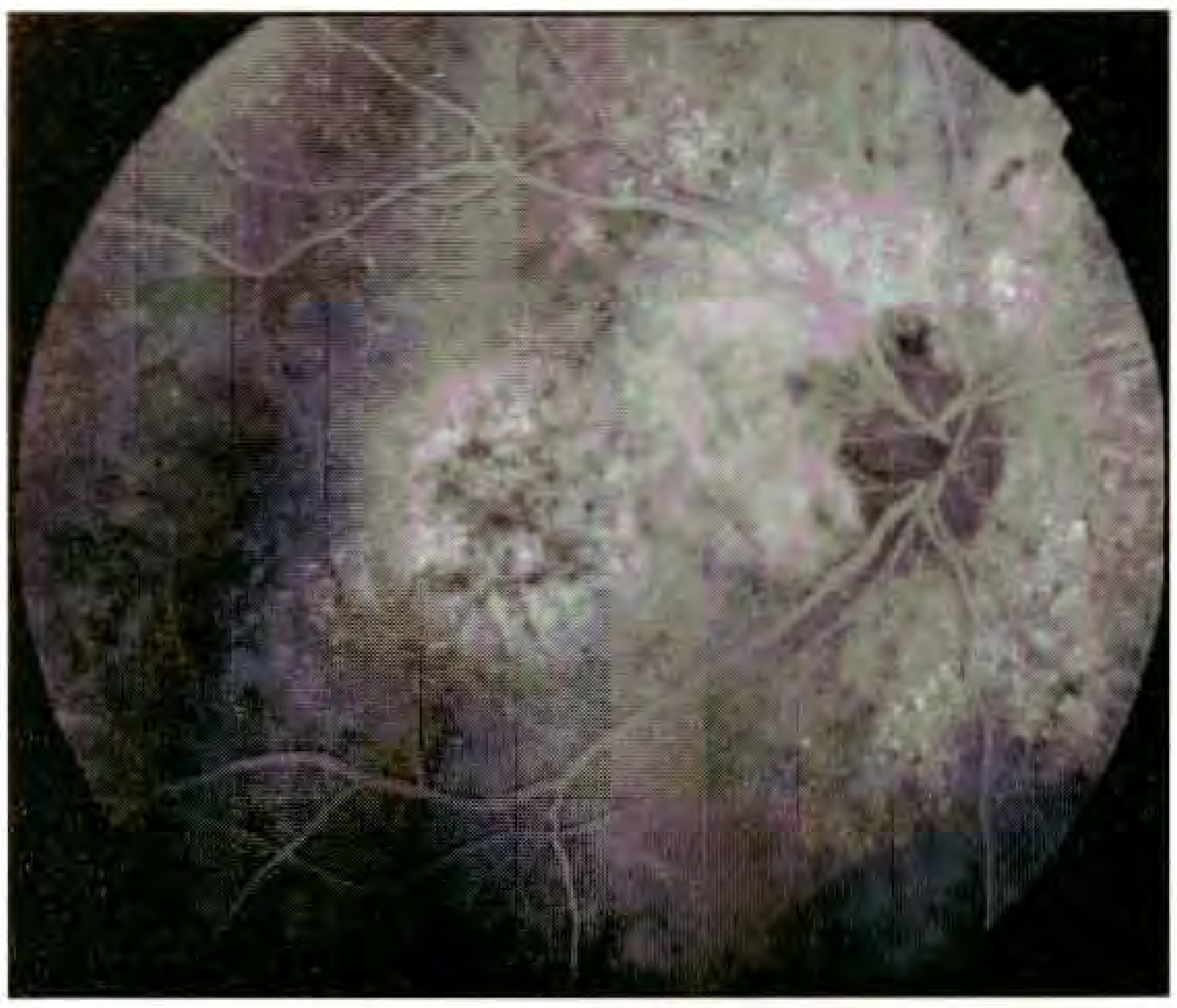

E

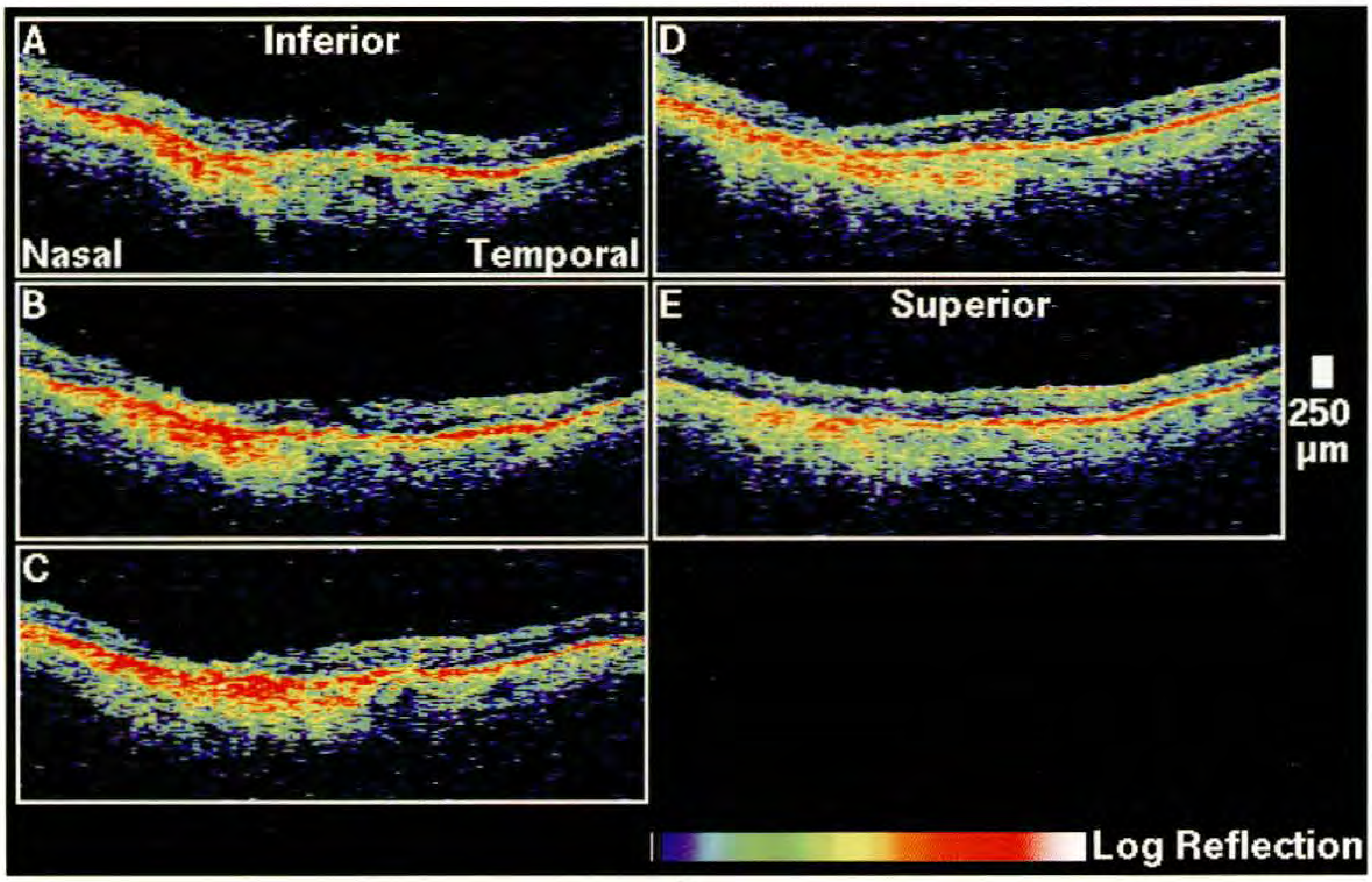

F

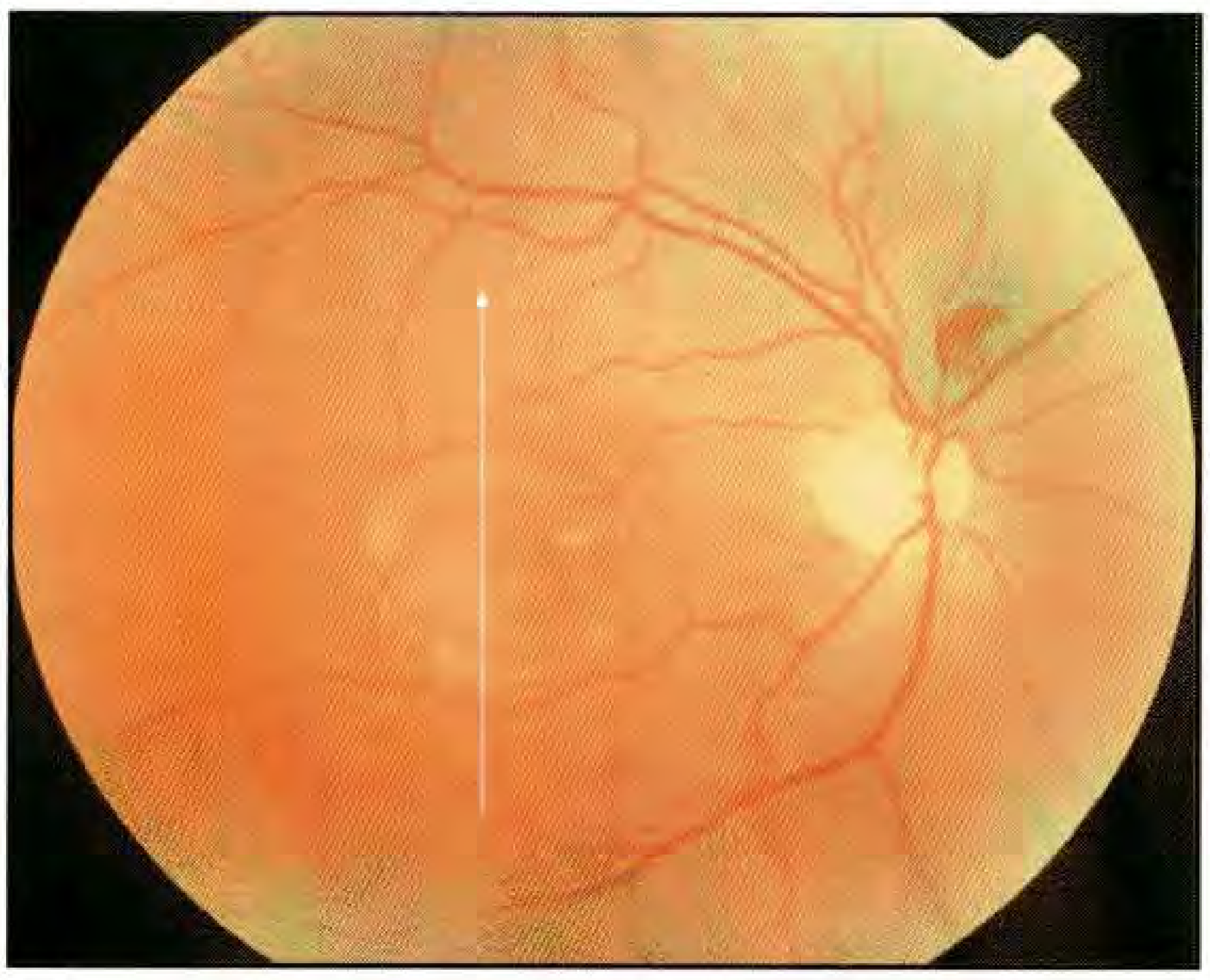

A

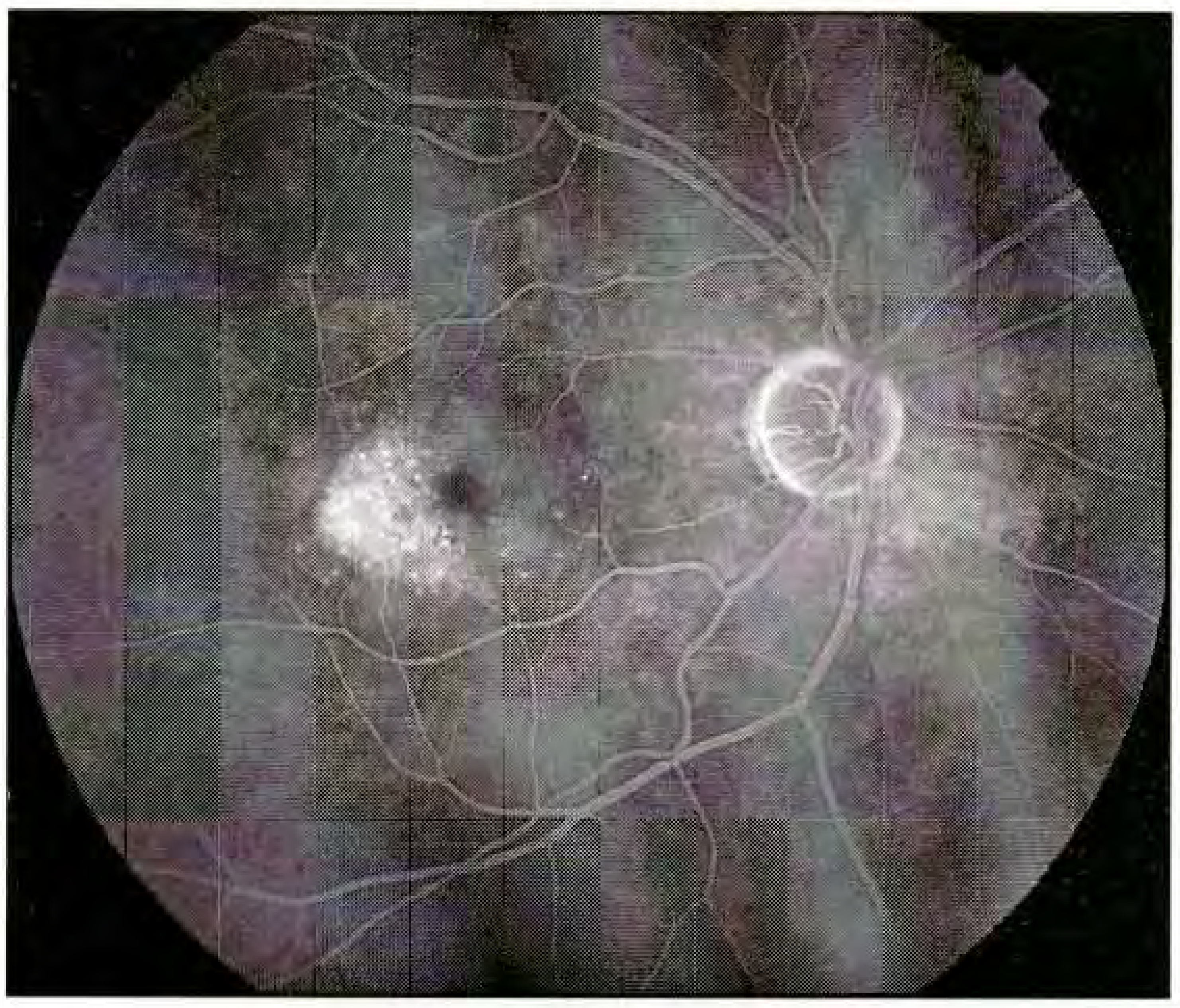

B

Case 8-39. Pigment Epithelial Detachment and Choroidal Neovascularization

Clinical Summary

A 76-year-old woman was evaluated for age-related macular degeneration. Slit-lamp biomicroscopy (A) of her right eye showed a pigment epithelial detachment in the central macula surrounded by a cuff of subretinal fluid. A hyperfluorescent lesion inferotemporal to the fovea was noted on fluorescein angiography (B) which displayed increasing hyperfluorescence and late pooling of dye as the study progressed. The patient's visual acuity was 20/40 in this eye.

Optical Coherence Tomography

A vertical tomogram (C) taken through the detachment showed an elevation of the neurosensory retina and the red band corresponding to the retinal pigment epithelium and choriocapillaris. The reflections from the choroid were attenuated below the detachment. Surrounding regions of neurosensory detachment and subretinal fluid accumulation were noted both inferior and superior to the pigment epithelial detachment.

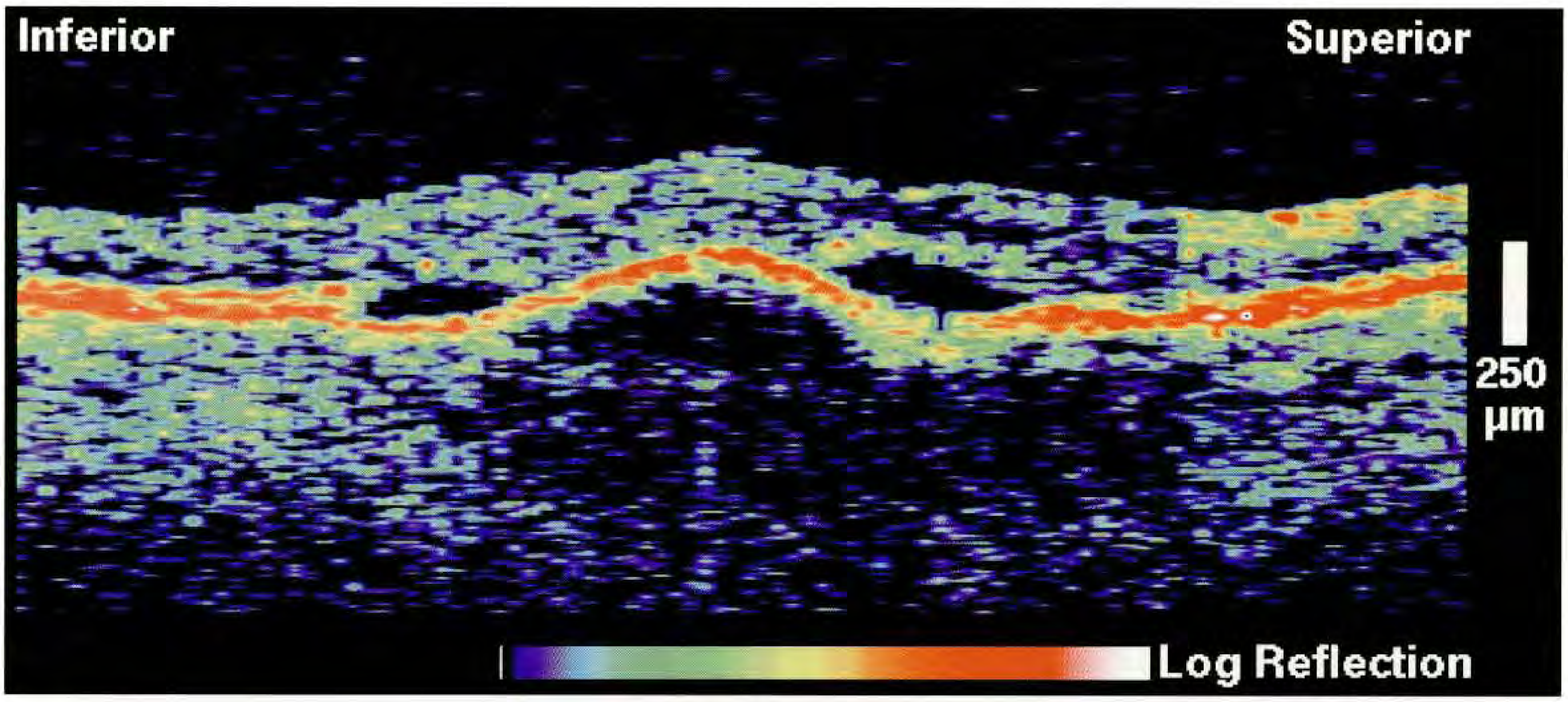

C

Case 8-39 continued

Clinical Summary

Slit-lamp biomicroscopy (D) of the left eye showed soft drusen in the macula with a small elevated retinal tuft in the fovea associated with the clinical diagnosis of a subfoveal neovascular membrane. The visual acuity in this eye was 20/30. Fluorescein angiography (E) showed hyperfluorescence surrounding the fovea consistent with drusen, and mottled hyperfluorescence in a peripapillary distribution.

Optical Coherence Tomography

OCT examination (F) of this eye revealed a small cyst directly in the fovea associated with a focal attachment of the posterior hyaloid membrane. The reflection from the retinal pigment epithelium and choriocapillaris appeared thickened directly beneath the fovea consistent with a subfoveal neovascular membrane.

D

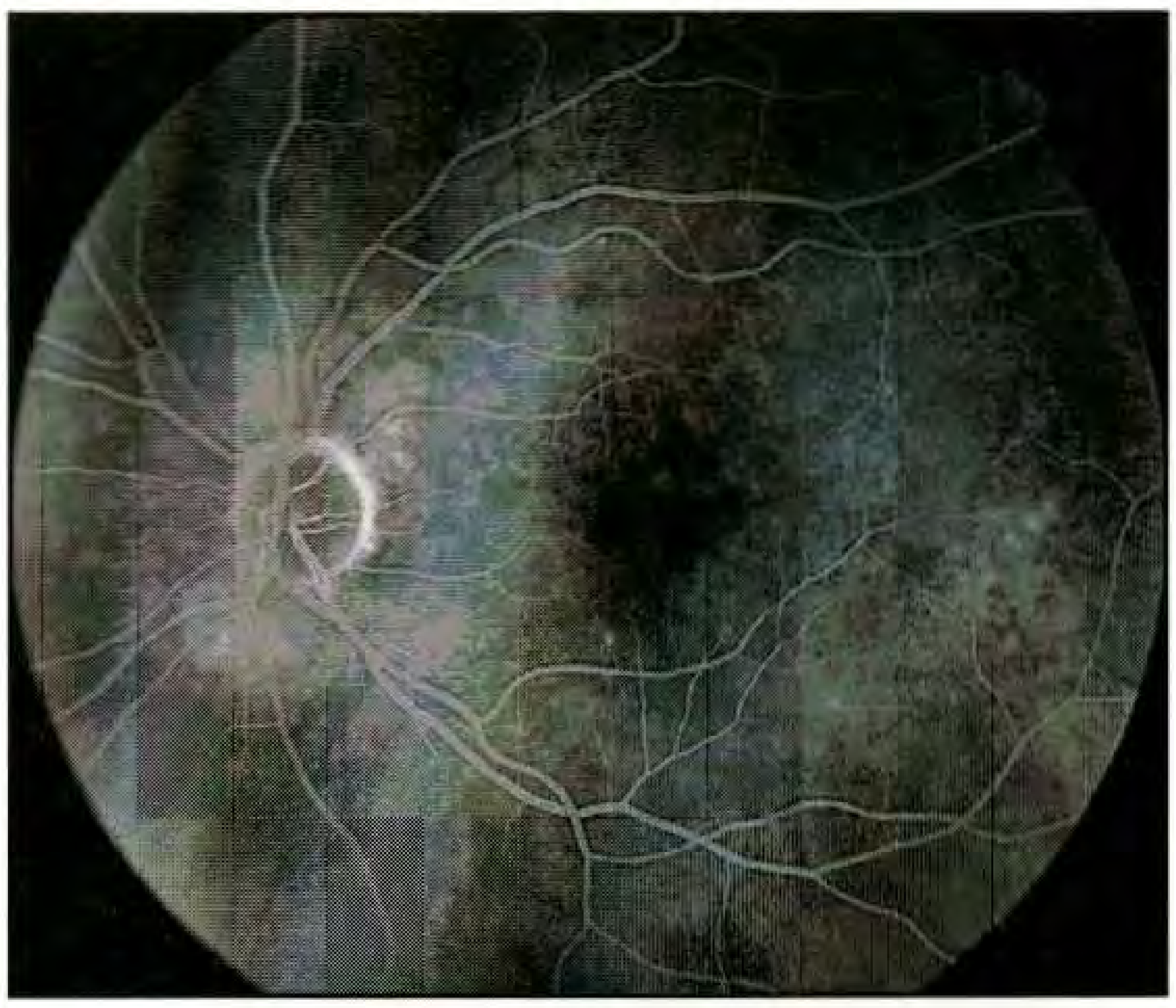

E

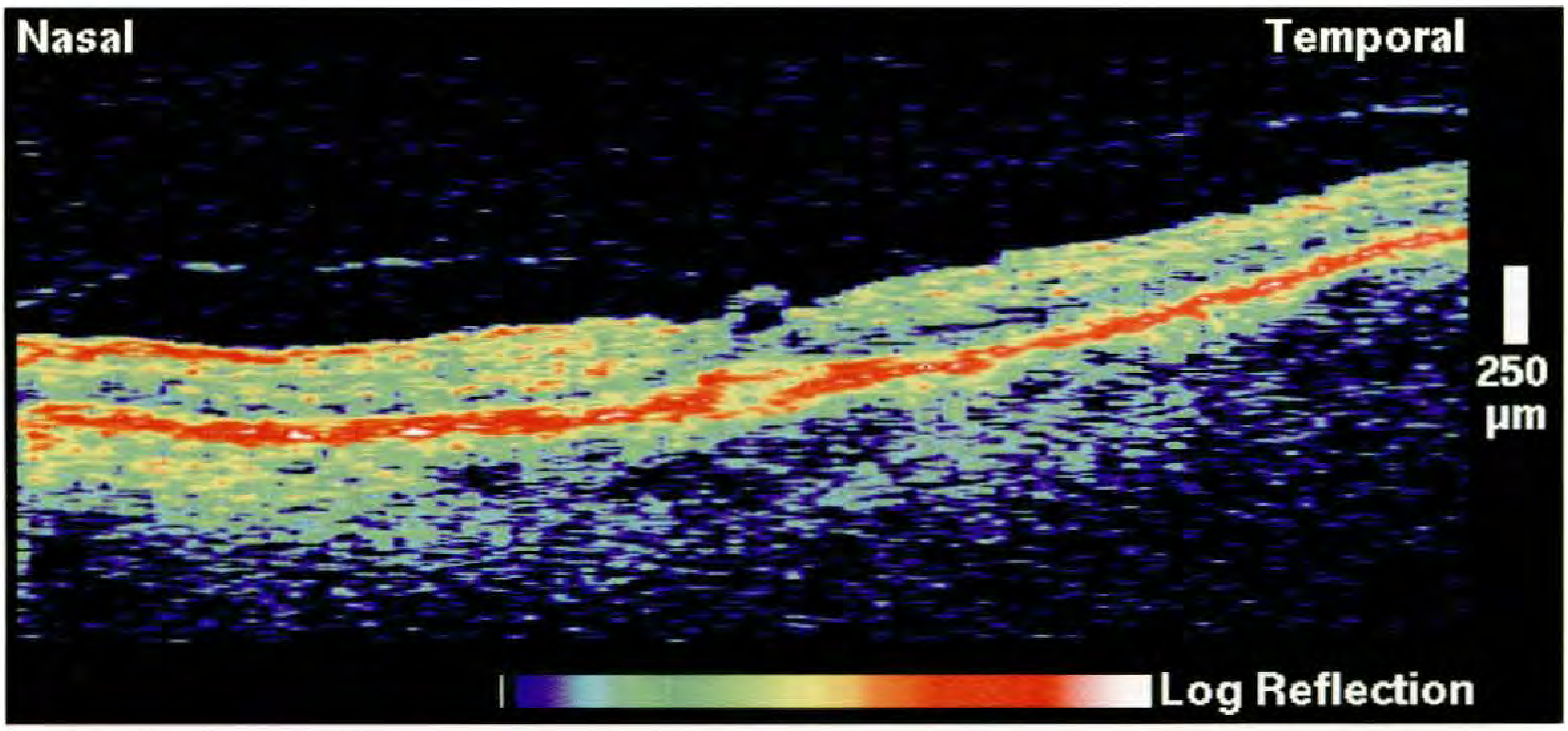

F

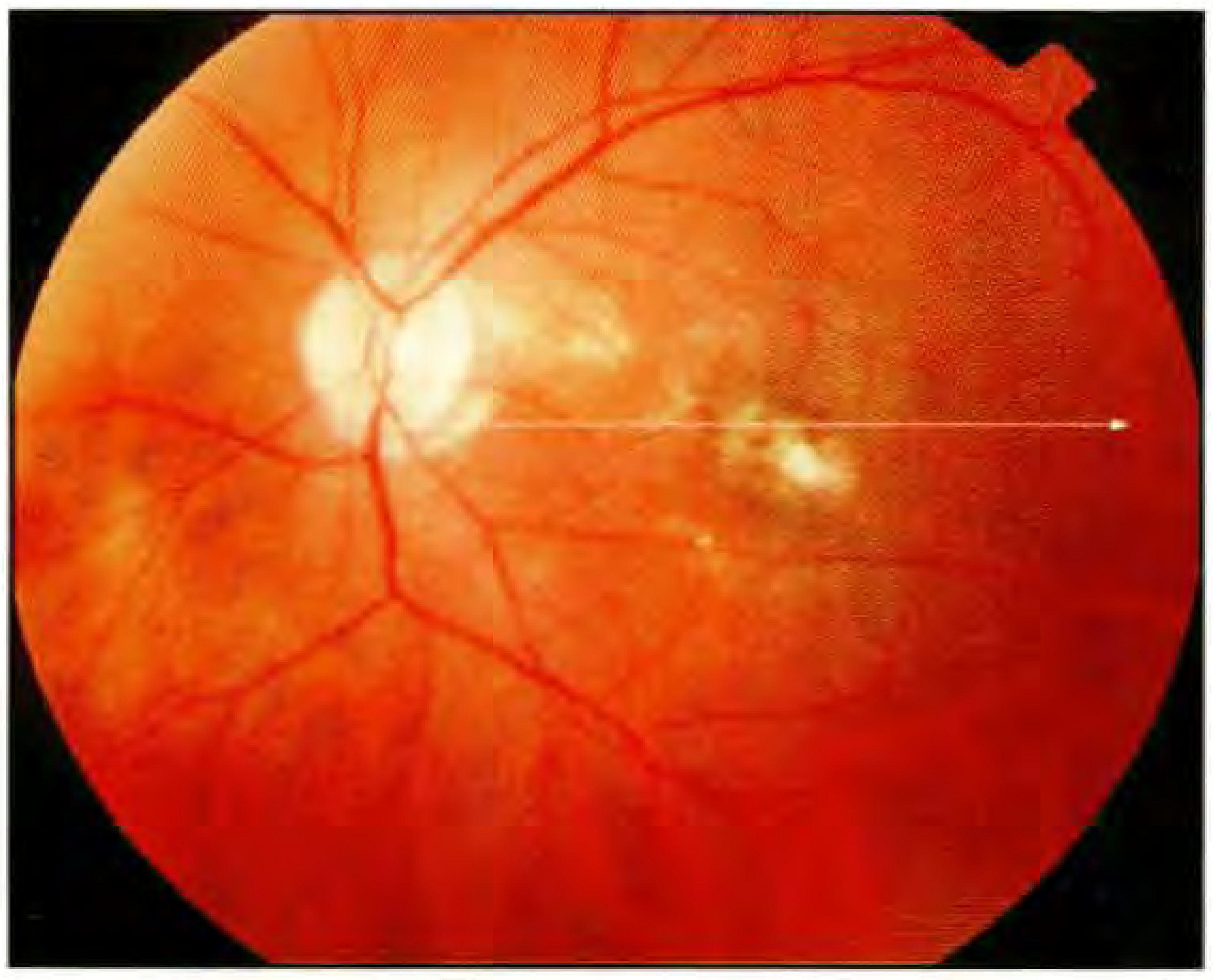

A

Case 8-40. Recurrent Choroidal Neovascular Membrane

Clinical Summary

An 83-year-old woman with age-related macular degeneration complained of worsening vision over the past several months. She had received laser photocoagulation in her left eye three years earlier for choroidal neovascularization. Slit-lamp examination (A) showed subretinal fibrosis in the central macula with surrounding pigment aggregation consistent with an atrophic laser scar.

Optical Coherence Tomography

A horizontal OCT image (B) acquired through the fovea displayed a thickening and disruption of the reflective band corresponding to the retinal pigment epithelium and choriocapillaris, a configuration characteristic of choroidal neovascularization. The absence of very enhanced optical reflectivity from this region was evidence against a laser scar. A focal, intraretinal region of minimal optical reflectivity was observed consistent with a retinal cyst.

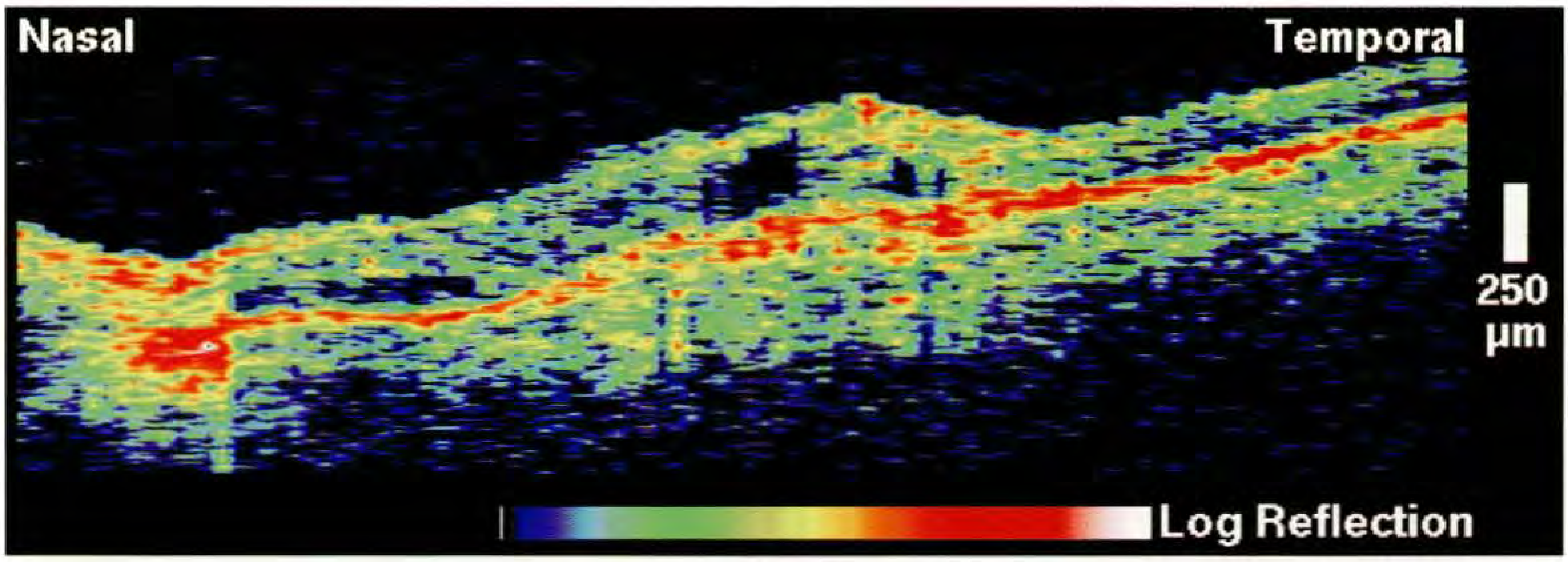

B

Case 8-41. Occult Choroidal Neovascularization

Clinical Summary

A 56-year-man with age-related macular degeneration was referred for evaluation of possible choroidal neovascularization in his left eye. He had noted a decline in vision in this eye to 20/160 over a period of four weeks. Examination of the fundus (A) showed subretinal fluid in the macula with exudate along the inferior border. Spotty areas of hemorrhage were identified just nasal to the fovea. Fluorescein angiography (B) demonstrated irregular hyperfluorescence in the peripapillary region with late leakage and patchy hypofluorescence corresponding to the region of retinal hemorrhage. No well-defined lesions were noted. Indocyanine green angiography (not shown) revealed several small hyperfluorescent lesions in the superior macula and around the optic nerve head consistent with occult choroidal neovascularization.

Optical Coherence Tomography

A horizontal OCT image (C) was acquired through the superior macula. The tomogram showed a region of enhanced optical scatter signal in the choroid which appeared thicker than adjacent reflection from the pigment epithelium and choriocapillaris, consistent with a neovascular membrane. The retina appeared elevated and thickened in the area of the lesion and nasally with reduced optical reflectivity in the outer retina suggesting subretinal fluid accumulation.

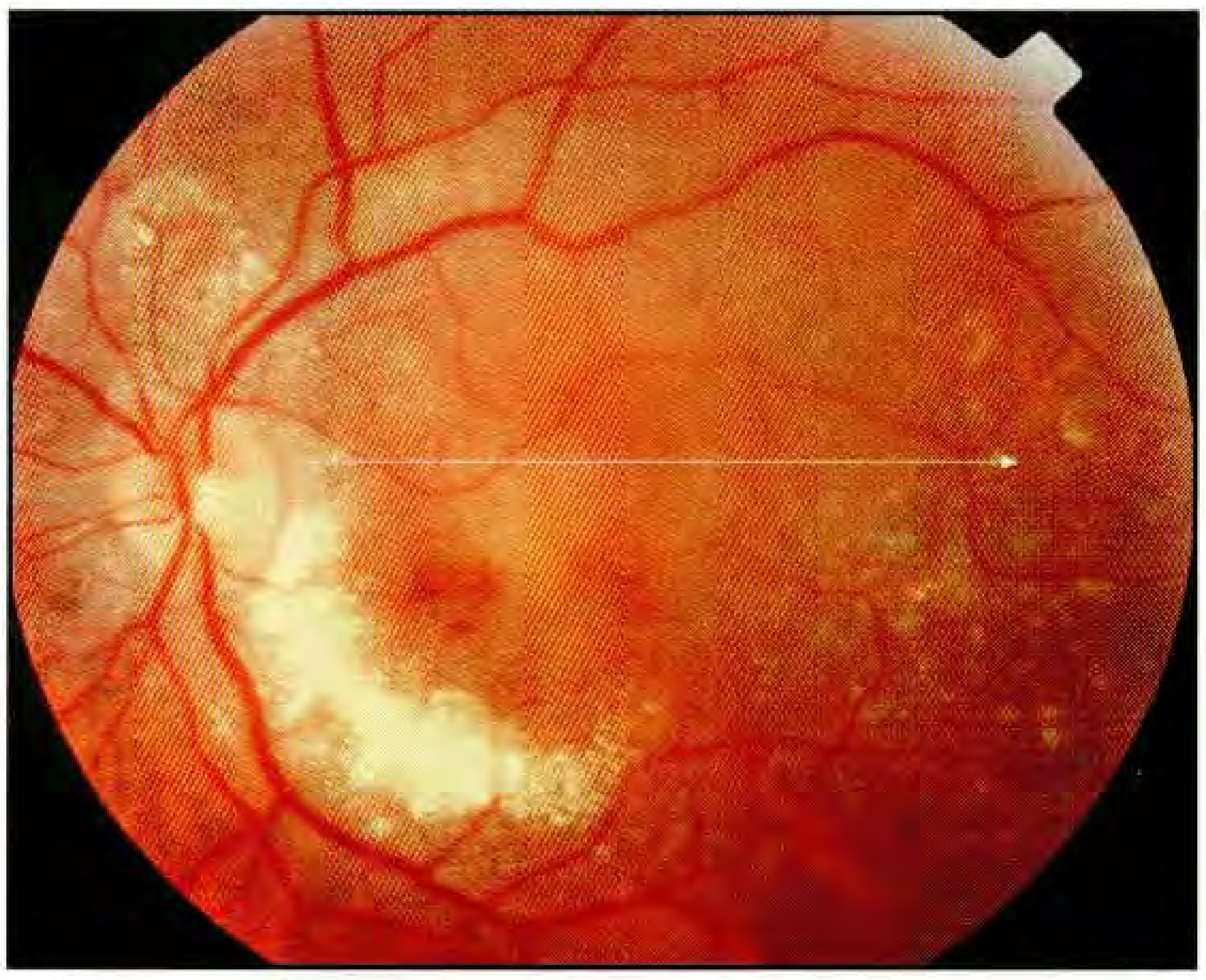

A

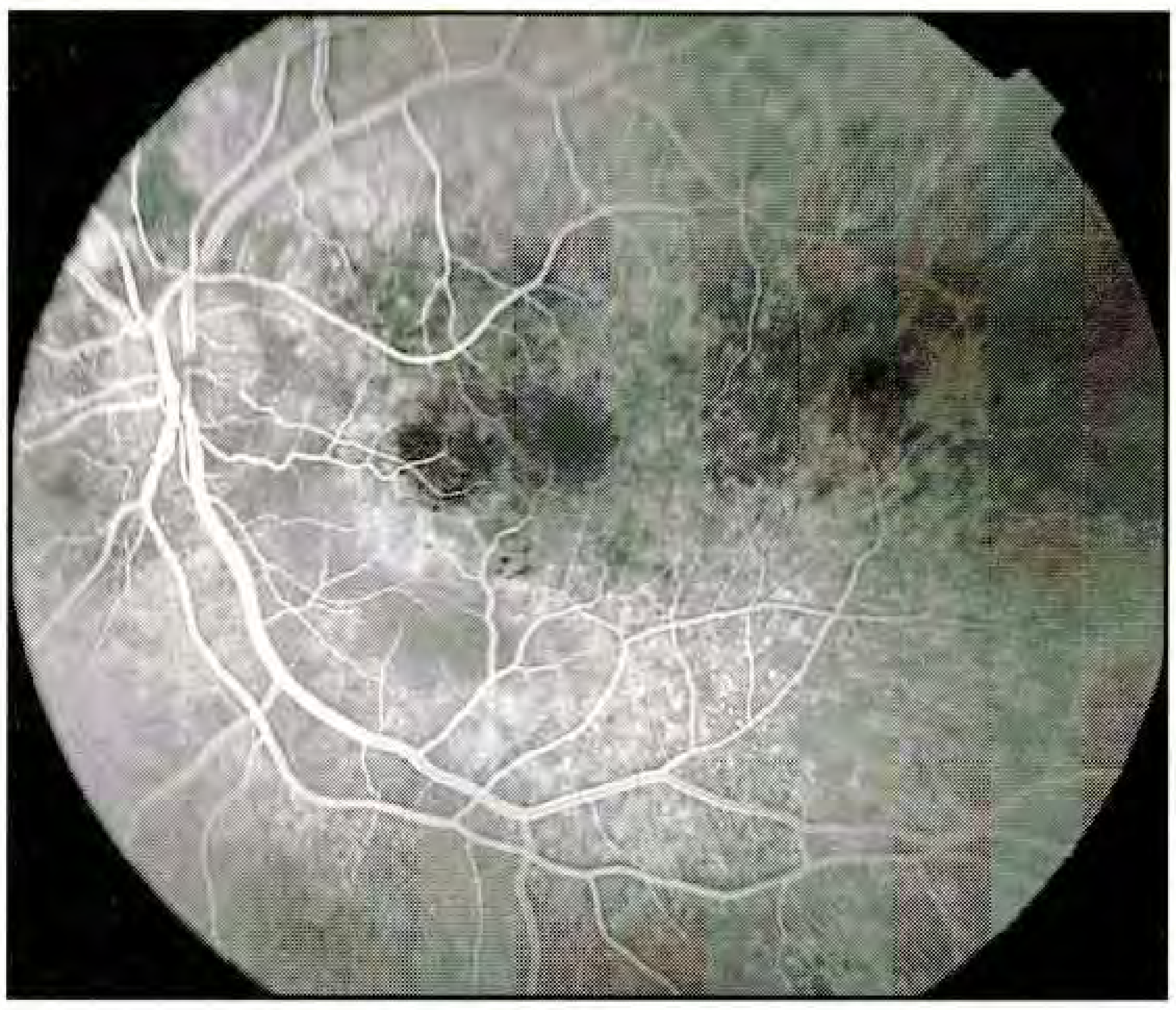

B

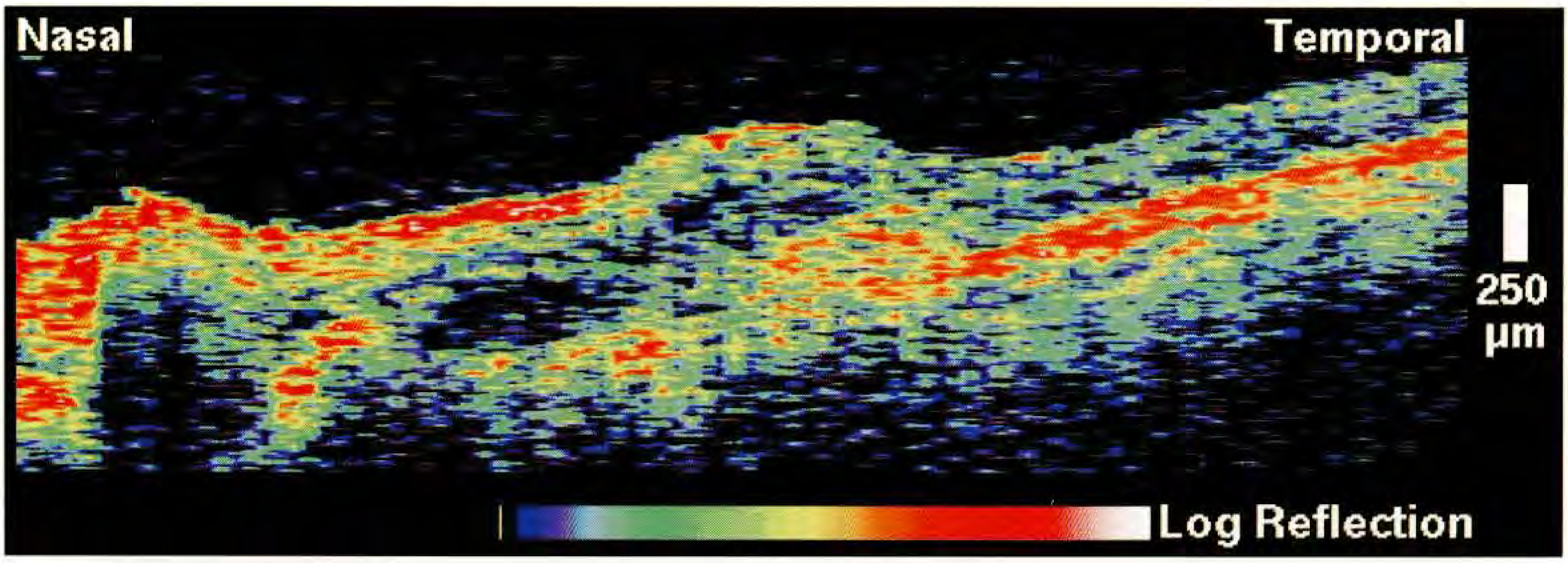

C

A

B

Case 8-42. Choroidal Neovascularization

Clinical Summary

An 83-year-old man with a history of choroidal neovascularization in his right eye complained of new metamorphopsia in his left eye. On examination, his visual acuity in the left eye was 20/100 and slit-lamp biomicroscopy (A) revealed a low, irregular pigment epithelial detachment with no subretinal fluid, hemorrhage, or exudate. Fluorescein angiography (B) showed a poorly defined region of hyperfluorescence in the central macula which increased in intensity as the study progressed.

Optical Coherence Tomography

A vertical OCT image (C) delineated an irregular thickening (arrows) of the reflective layer corresponding to the retinal pigment epithelium and choriocapillaris directly beneath the fovea consistent with subretinal neovascularization. An optically clear space of subretinal fluid accumulation was observed immediately inferior this lesion. There was minimal thickening of the overlying neurosensory retina.

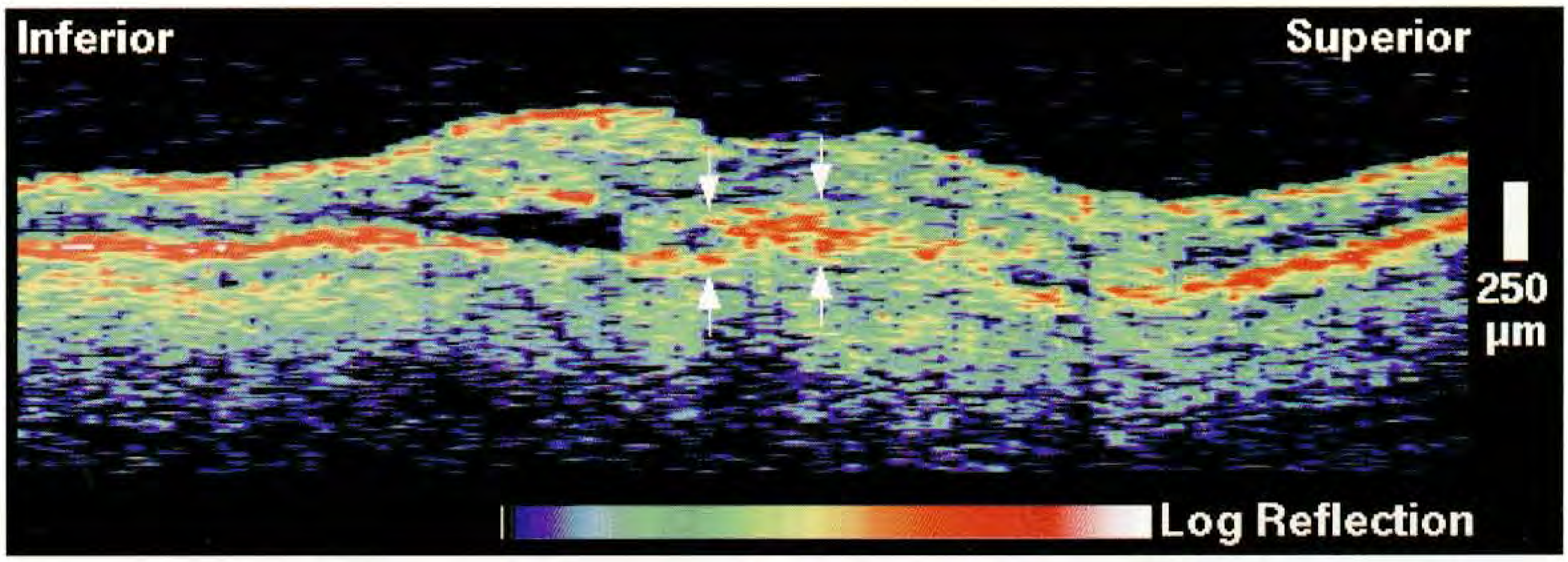

C

Case 8-43. Choroidal Neovascularization

Clinical Summary

A 70-year-old man was referred for evaluation of choroidal neovascularization and a visual acuity of counting fingers in his left eye. Slit-lamp biomicroscopy (A) showed subretinal fluid in the central macula with mild subretinal fibrosis along the inferior border. A hemorrhagic pigment epithelial detachment was present superior to the fovea. Fluorescein angiography (B) displayed a large, well-defined region of patchy hyperfluorescence in the central macula that exhibited leakage during the late phase. A hypofluorescent region superior to the fovea corresponded to the hemorrhagic pigment epithelial detachment.

Optical Coherence Tomography

A vertical OCT image (C) demonstrated a large optically clear space signifying intraretinal fluid accumulation and cystic changes. The reflection from the choroid beneath the lesion was enhanced, consistent with either neovascularization or enhanced penetration of probe beam through the non-reflective intraretinal fluid. A small area of shallow subretinal fluid was noted inferiorly in the image. Superiorly, the retinal pigment epithelium (RPE) and sensory retina were elevated with backscatter signal extending into the sub-RPE space consistent with a hemorrhagic RPE detachment.

A

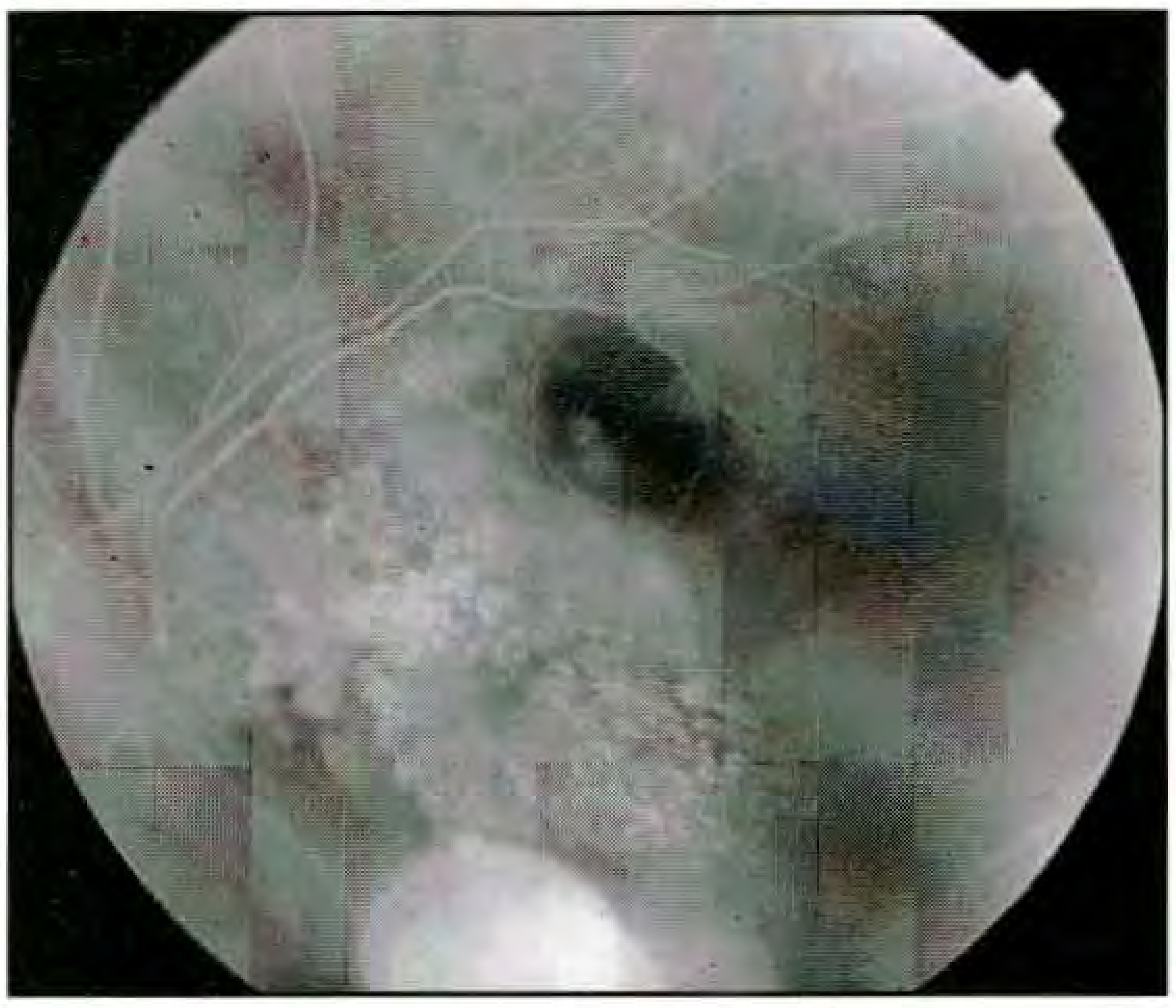

B

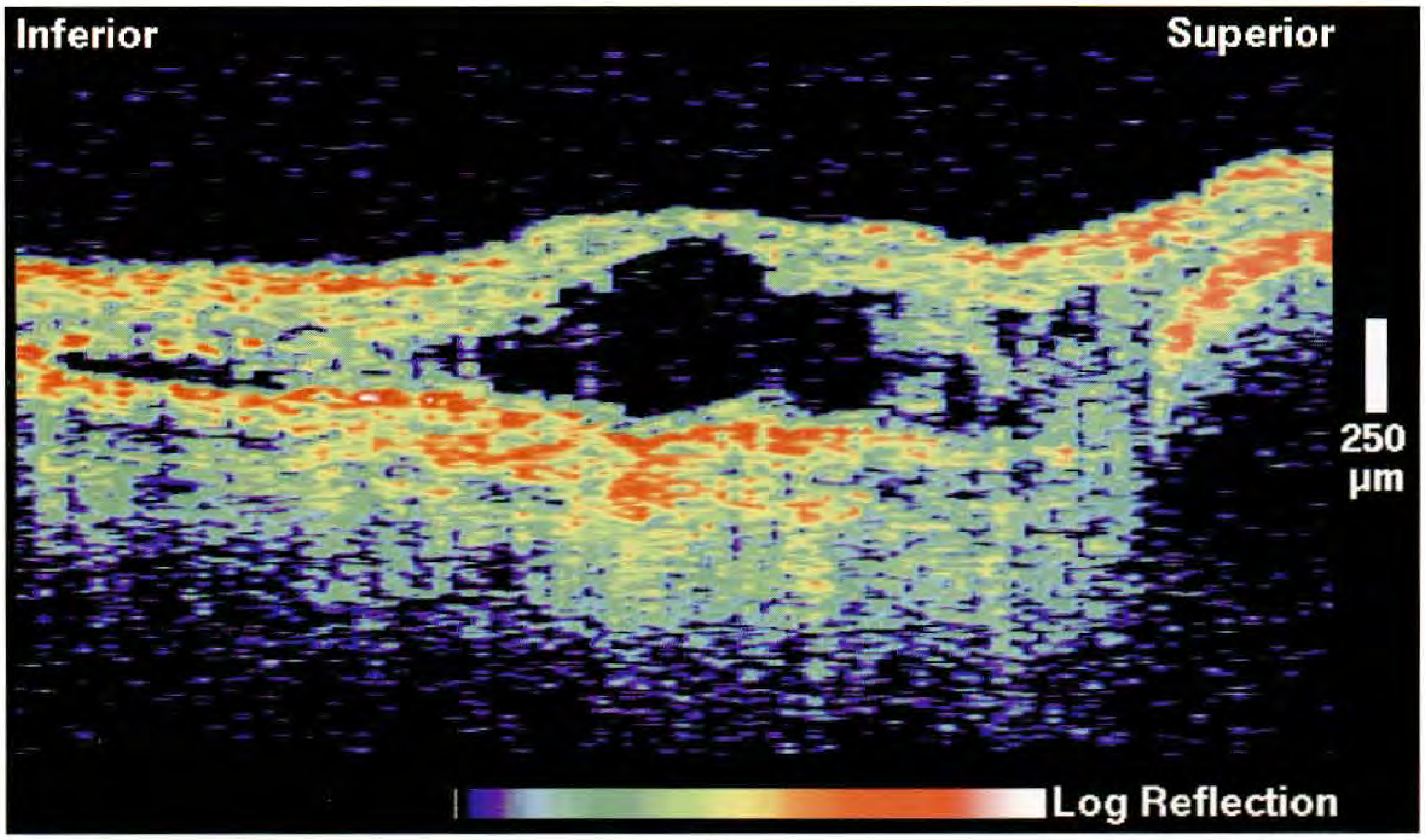

C

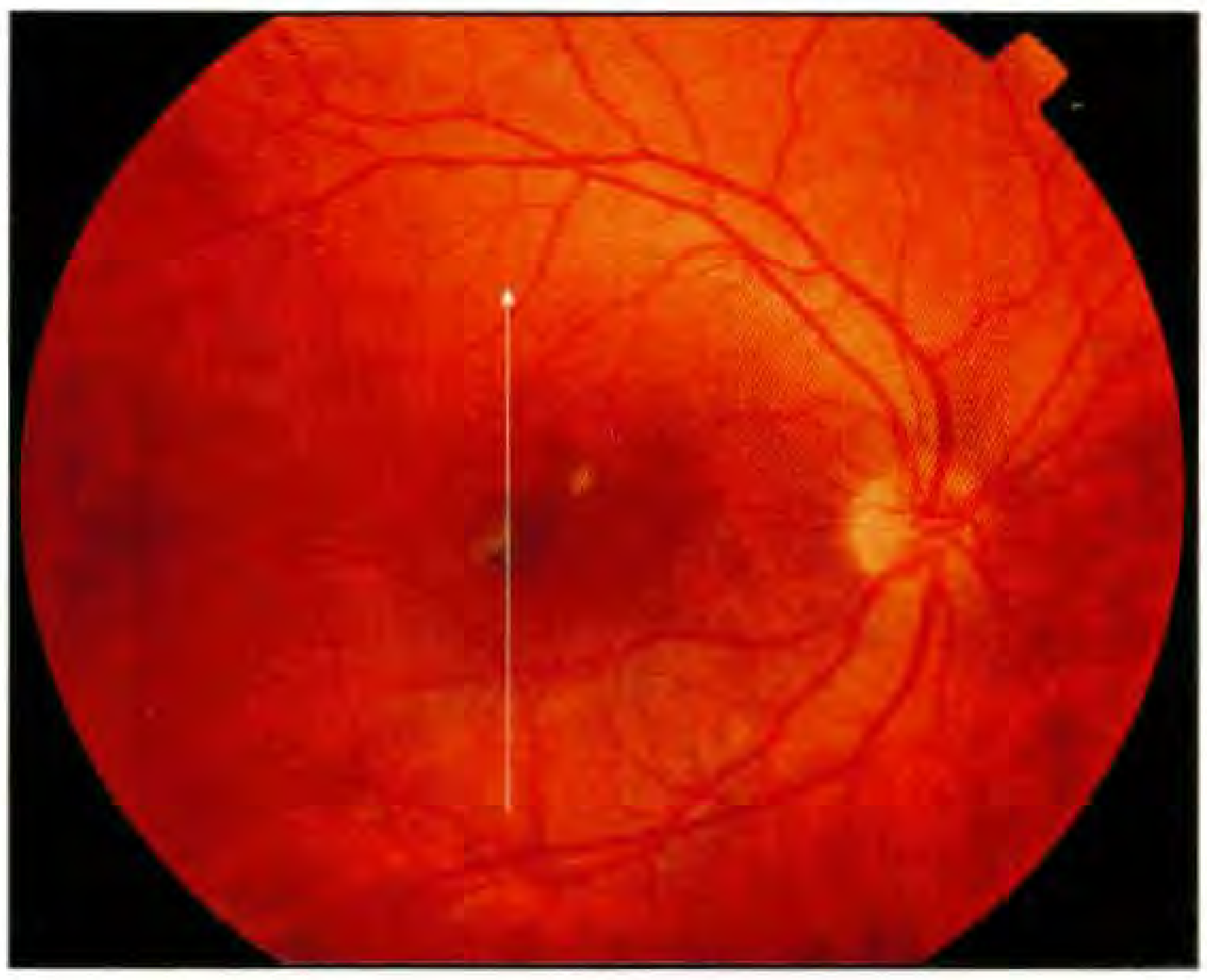

A

B

Case 8-44. Choroidal Neovascularization Secondary to Central Serous Chorioretinopathy

Clinical Summary

A 28-year-old woman had a visual acuity of 20/100 in her left eye associated with a choroidal neovascular membrane secondary to old central serous chorioretinopathy. Examination (A) showed two separate grey-green membranes located within the macula, and an overlying serous detachment of the neurosensory retina. Staining of the membrane was observed on fluorescein angiography (B), with moderate lake leakage of dye.

Optical Coherence Tomography

OCT (C) demonstrated thickening of the neurosensory retina above an area of enhanced backscatter signal corresponding to the neovascular membrane. The boundaries of the membrane were well-defined, and the retinal pigment epithelium appeared to be intact just anterior the membrane. A small amount of subretinal fluid was also observed.

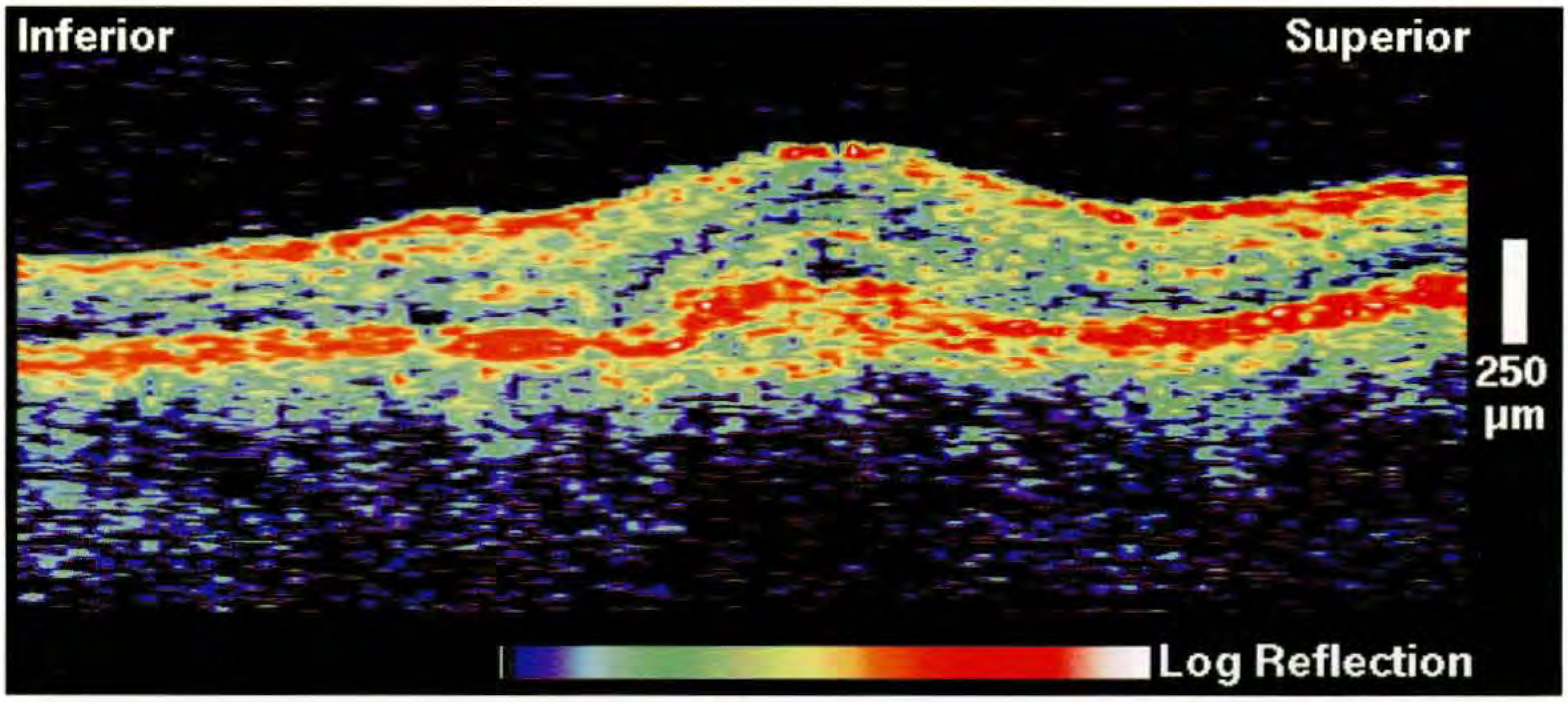

C

Case 8-45. Choroidal Neovascularization

Clinical Summary

A 53-year-old woman had an idiopathic choroidal neovascular membrane in her left eye associated with a visual acuity of counting fingers. Slit-lamp examination (A) showed subretinal fibrosis directly in the fovea. Fluorescein angiography (B) revealed a well-defined focal region of hyperfluorescence just superior to the fovea in the arteriovenous phase which increased in intensity during later phases of the angiogram.

Optical Coherence Tomography

OCT (C) demonstrated a focal thickening of the reflective layer corresponding to the pigment epithelium and choriocapillaris consistent with the neovascularization observed clinically. There appeared to be no significant retinal thickening or intraretinal fluid accumulation.

A

B

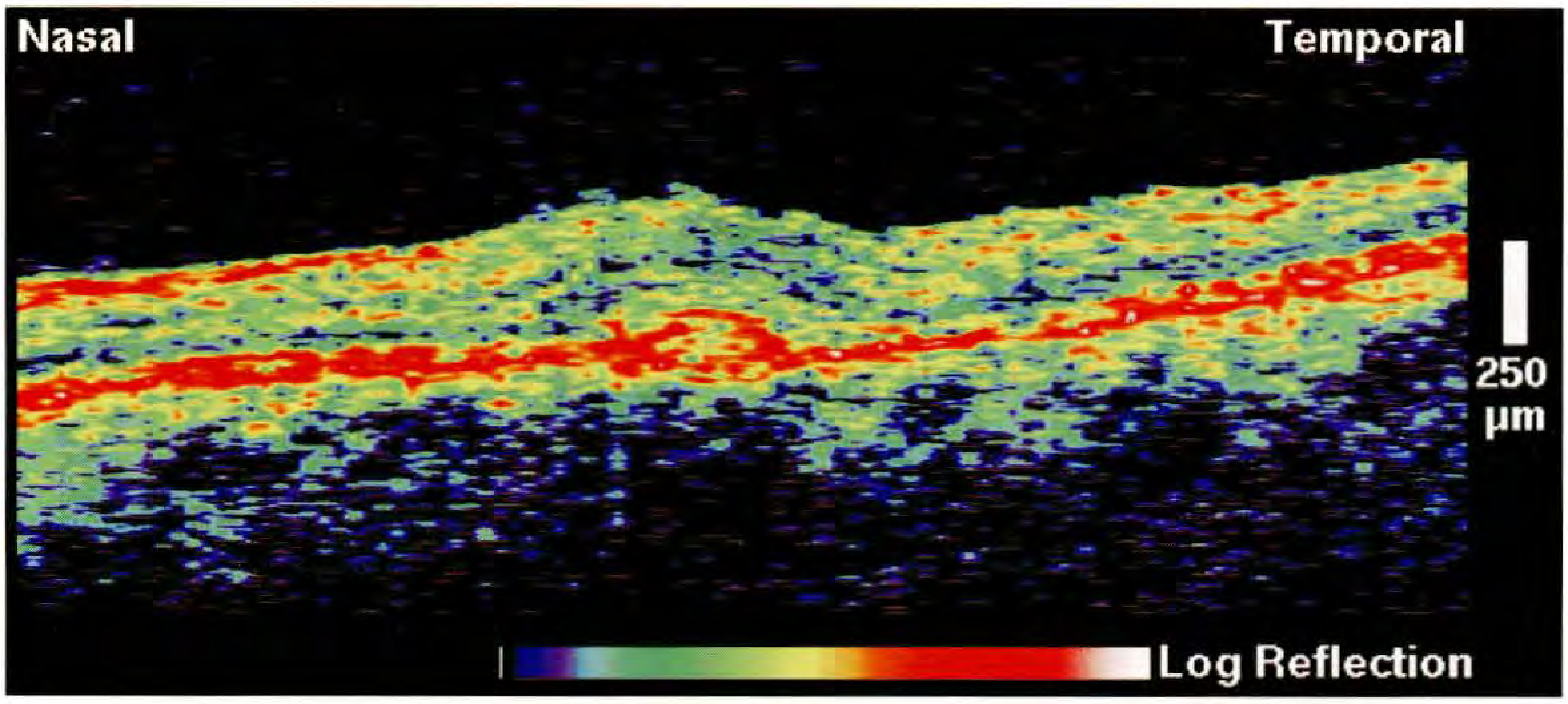

C

A

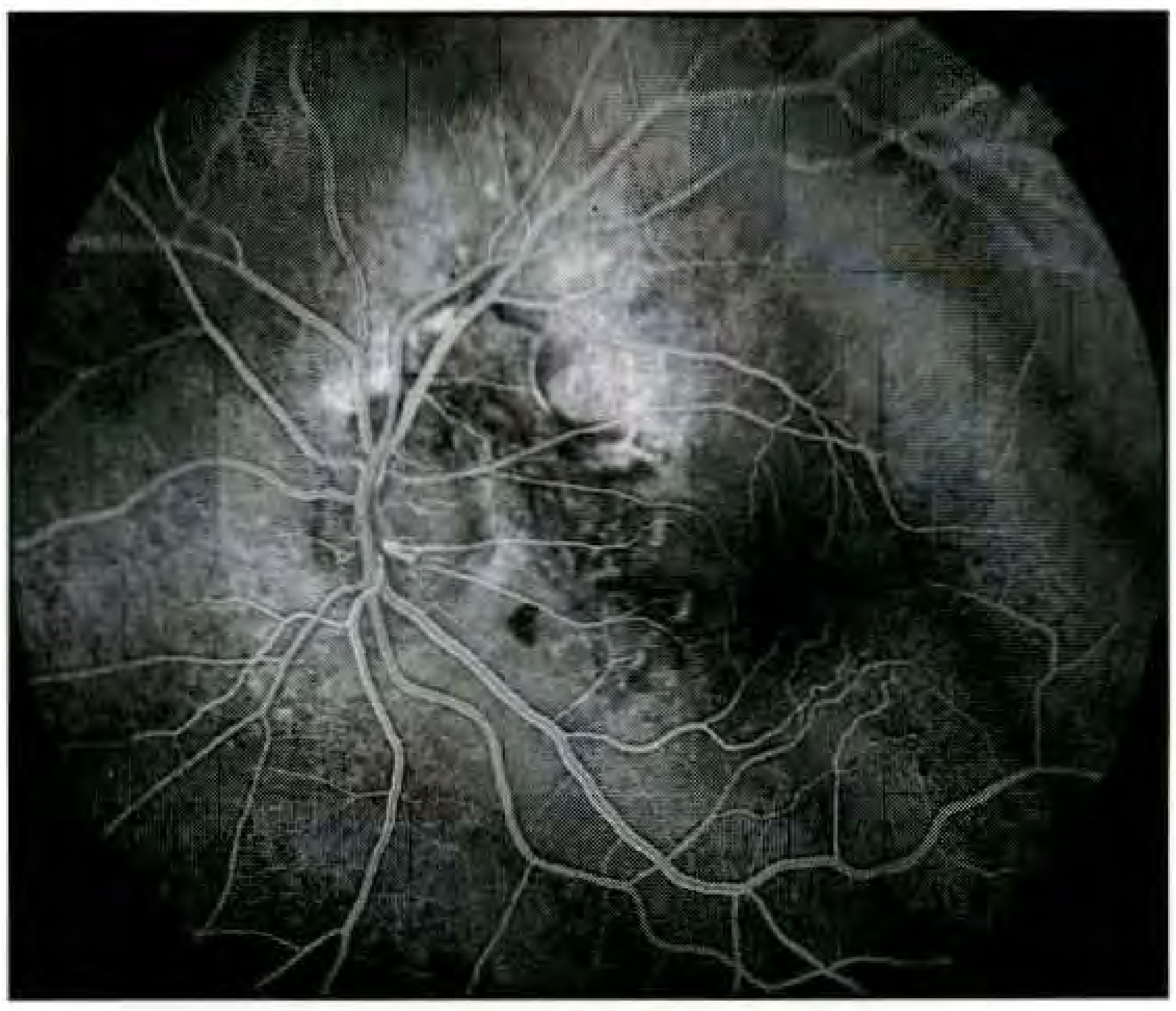

B

Case 8-46. Juxtapapillary Choroidal Neovascularization and Macular Pseudohole

Clinical Summary

A 63-year-old man with a history of uveitis was evaluated for a temporal visual field defect in his left eye. His visual acuity in that eye was 20/20. Slit-lamp ophthalmoscopy (A) indicated a well-defined region of gray discoloration and mild retinal elevation temporal to the optic disc consistent with subretinal neovascularization. A focal spot of subretinal hemorrhage was also seen inferotemporal to the disc. The discoloration and thickening did not involve the foveal center; however, a macular pseudohole was noted in the fovea. Fluorescein angiography (B) revealed an irregular, hyperfluorescent lesion temporal to the disc which gradually increased in intensity in the later phases of the study. Mild late leakage of dye from the lesion was also visible

Optical Coherence Tomography

A horizontal OCT tomogram (C; white line on A) obtained through the optic disc displayed a well-defined, juxtapapillary region of enhanced backscatter signal in the posterior retina corresponding to the neovascularization observed clinically. A vertical image (D; black line on A) was also acquired through the macula. The contour of the foveal pit was steepened consistent with an epiretinal membrane and an associated macular pseudohole. The epiretinal membrane was visible only where it was separated from the neurosensory retina (arrow).

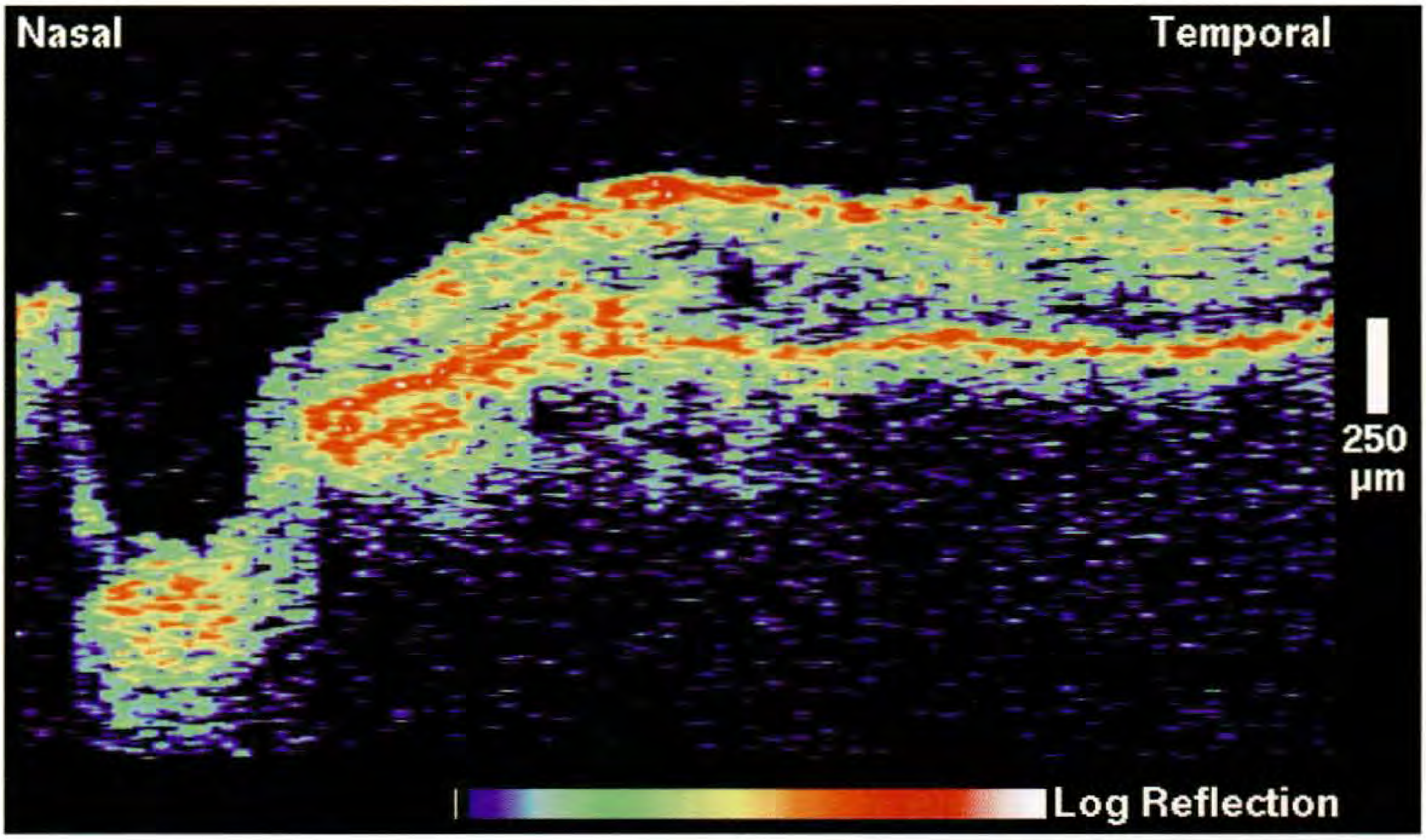
Nasal
Temporal
250 µm
Log Reflection

C

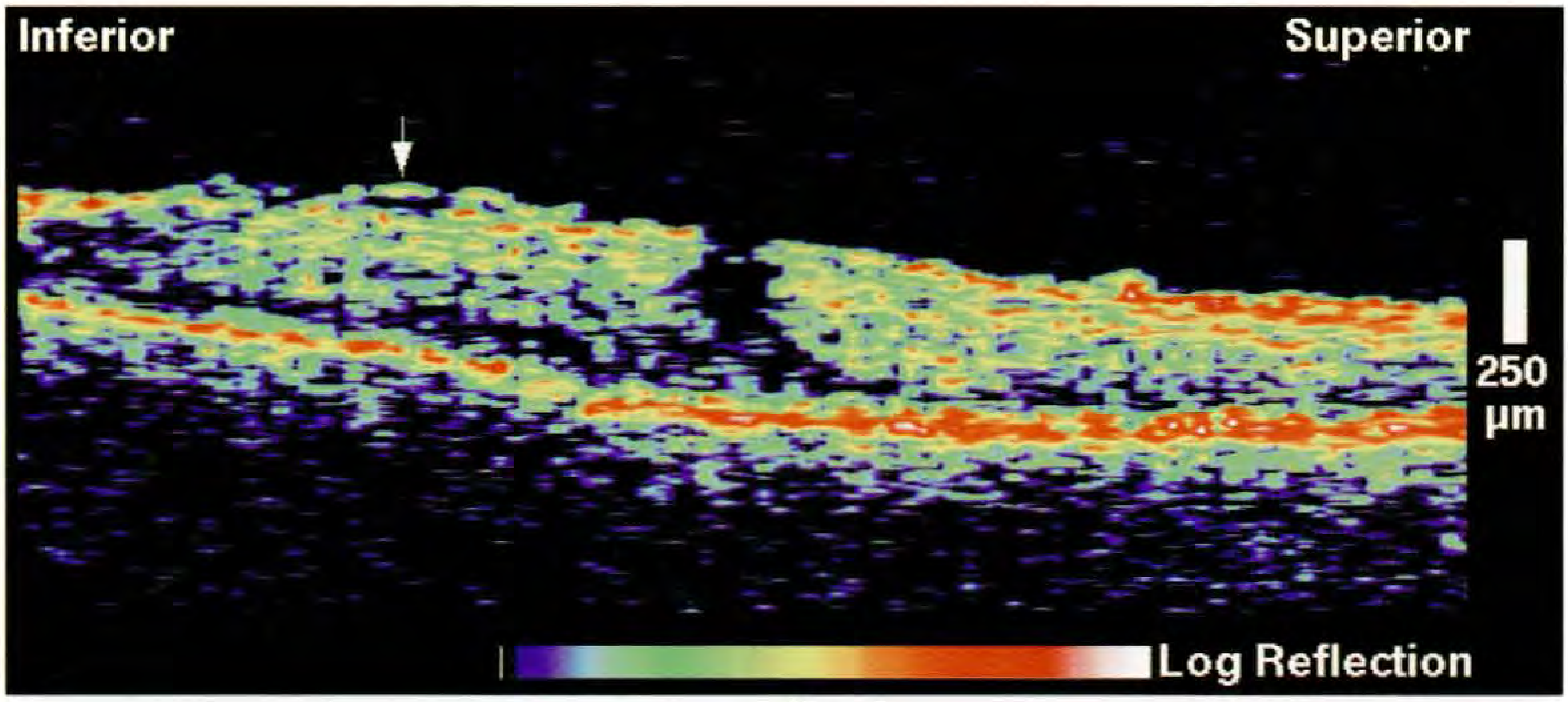
Inferior
Superior
250 µm
Log Reflection

D

A

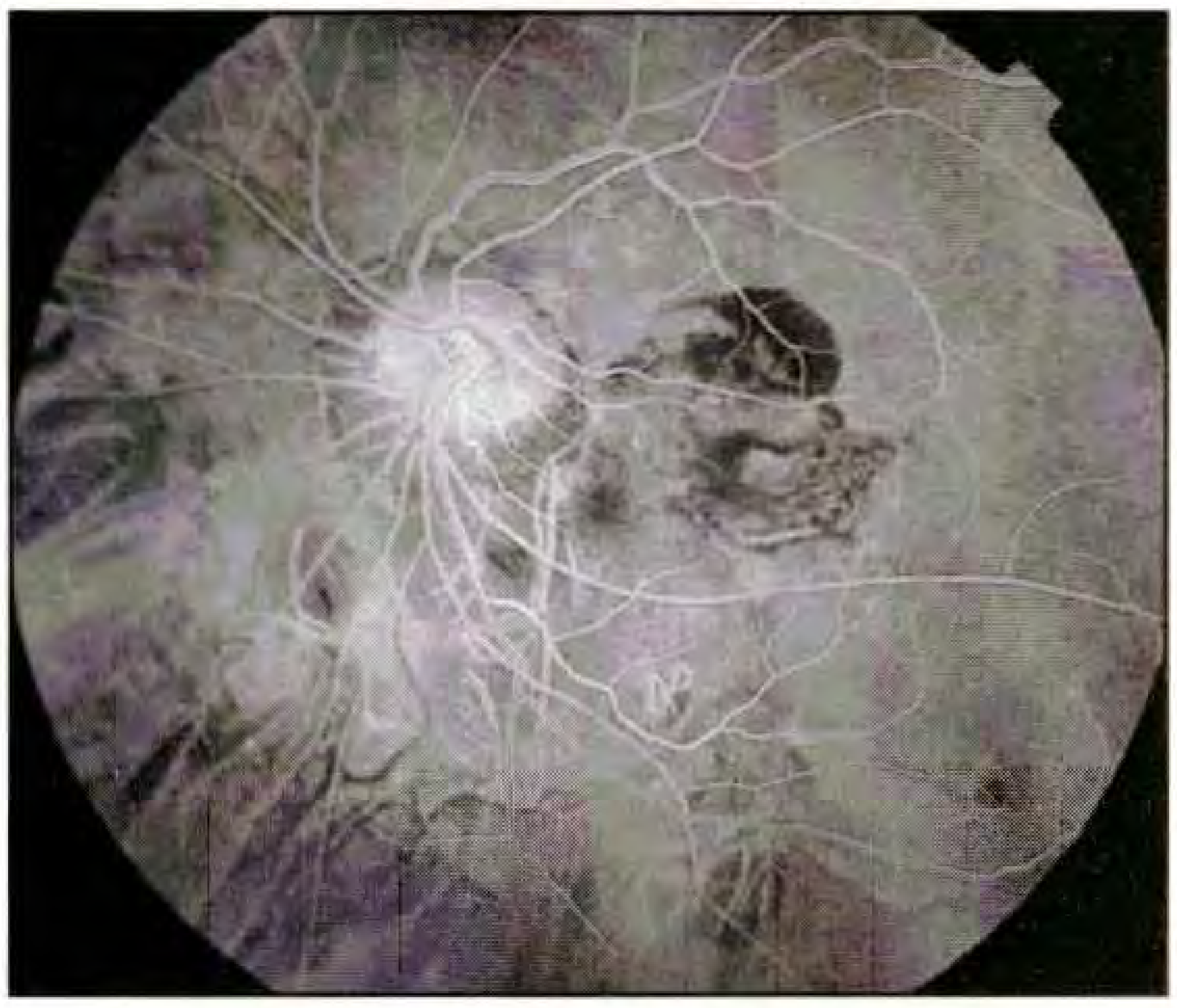

B

Case 8-47. Choroidal Neovascularization

Clinical Summary

A 50-year-old-man with a history of myopic degeneration had a visual acuity of 20/150 in his left eye associated with subfoveal choroidal neovascularization. Indirect ophthalmoscopy (A) demonstrated a pigmented lesion in the macula with hemorrhage along the superior border. A tilted optic disc with peripapillary atrophy and areas of chorioretinal atrophy along the nasal border was also noted. A lacy network of fluorescence consistent with a neovascular membrane was visible centrally within the macula on fluorescein angiography (B), which also showed hypofluorescence in the superior macula due to blockage by hemorrhage.

Optical Coherence Tomography

A well-defined region of enhanced optical reflectivity from the outer layers of the retina was observed in the OCT image (C). The increased backscatter signal was contiguous with the reflection from the retinal pigment epithelium and choriocapillaris consistent with a the presence of a neovascular membrane.

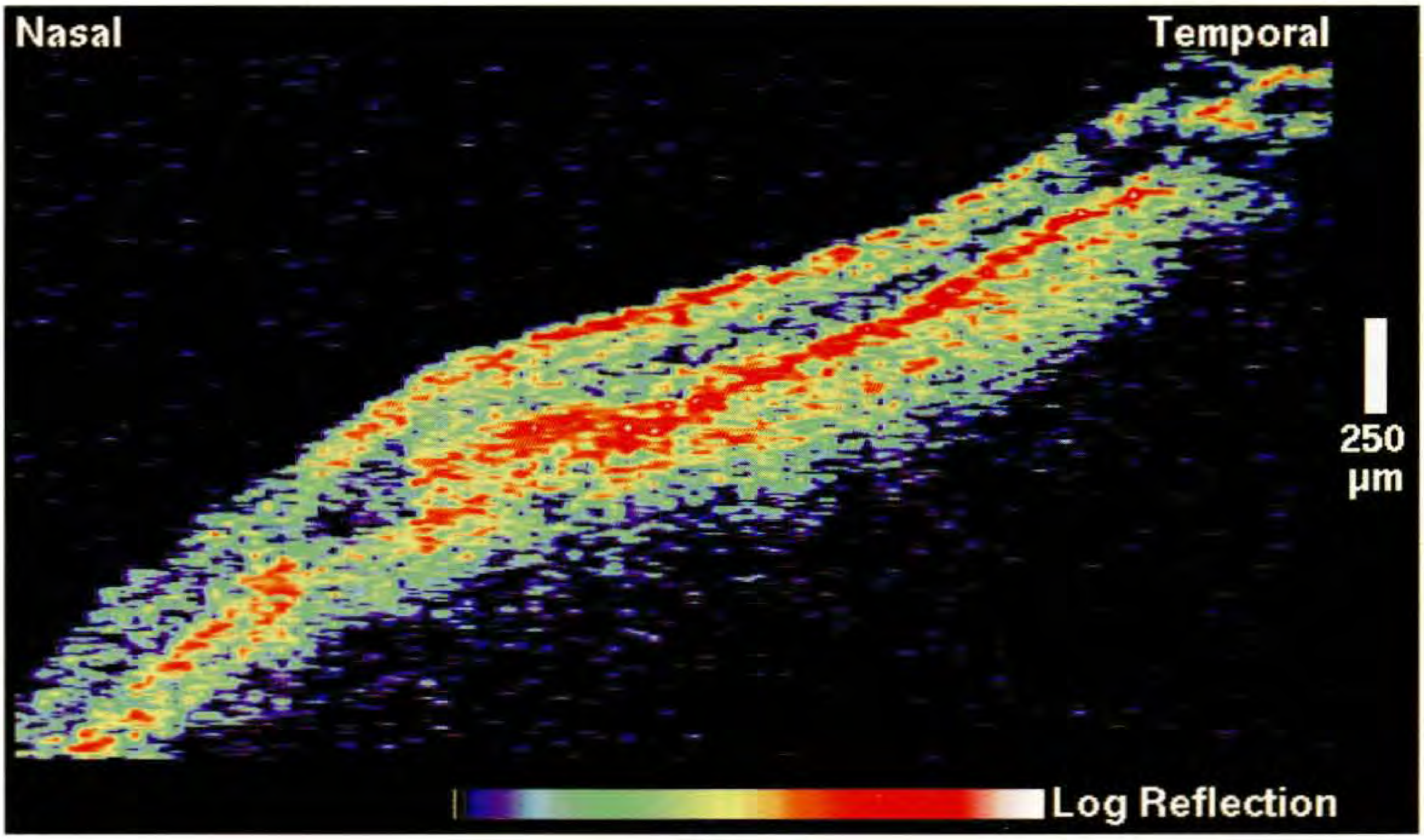

C

Case 8-48. Idiopathic Choroidal Neovascularization

A

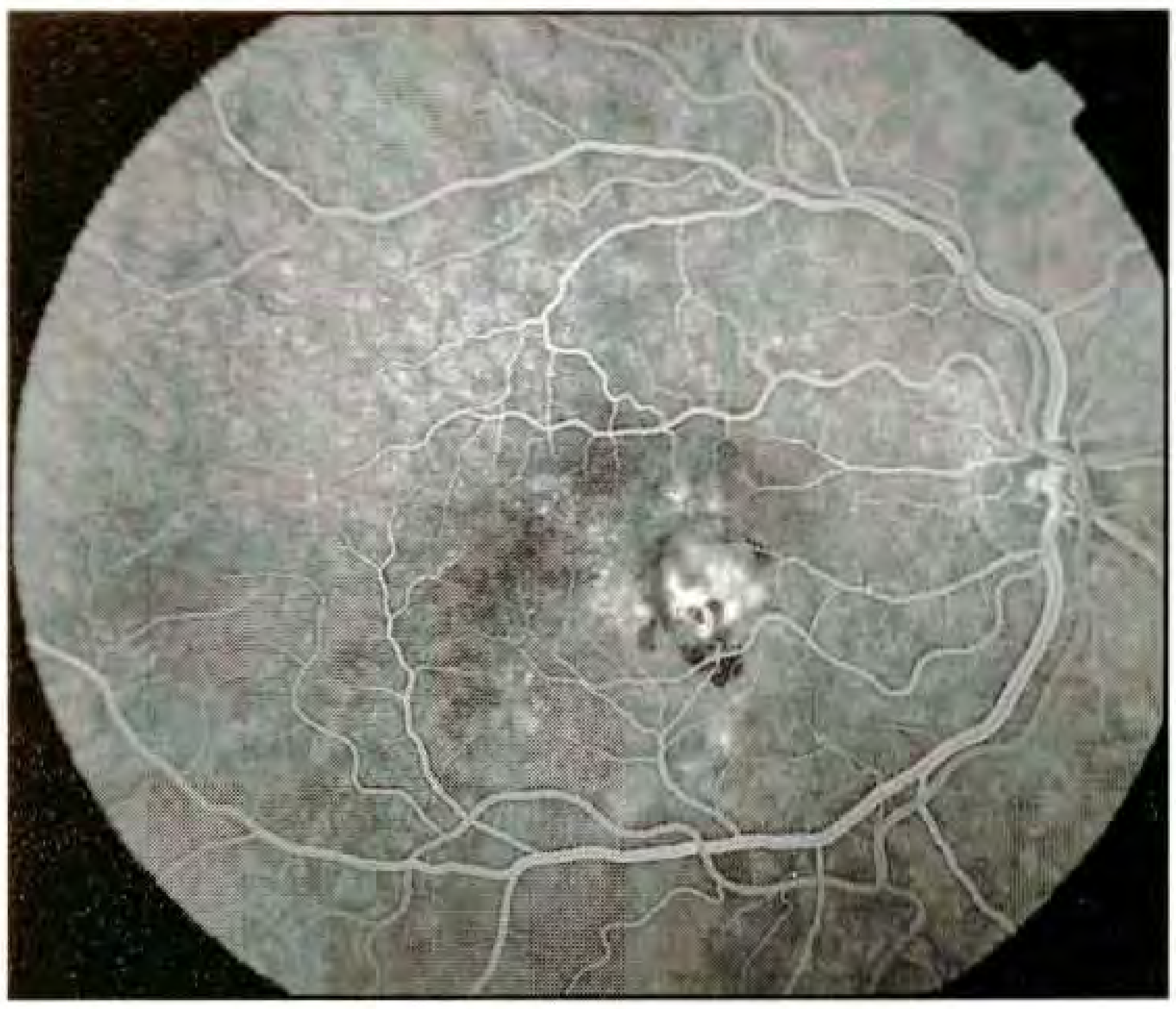

B

Clinical Summary

A 38-year-old man reported a five year history of decreased vision in his right eye with a significant reduction in vision in this eye occuring during the last 12 months. Slit-lamp biomicroscopy (A) disclosed an area of pigment epithelial detachment inferonasal to the fovea within a larger area of serous retinal elevation which extended inferotemporally. Mild subretinal hemorrhage was also noted within the macula. Fluorescein angiography (B) revealed an area of hyperfluorescence inferonasal to the center which showed late leakage. A hypofluorescent border temporally was consistent with hemorrhage.

Optical Coherence Tomography

A horiziontal OCT scan (C) through fixation demonstrated a region of increased retinal thickness and enhanced backscatter from the outer retina most likely corresponding to subretinal neovascularization. The lesion was observed to encroach beneath the fovea (arrow) from the nasal retina. The reflection from the RPE and choriocapillaris was clearly identifiable below the lesion and only appeared to be mildy disrupted.

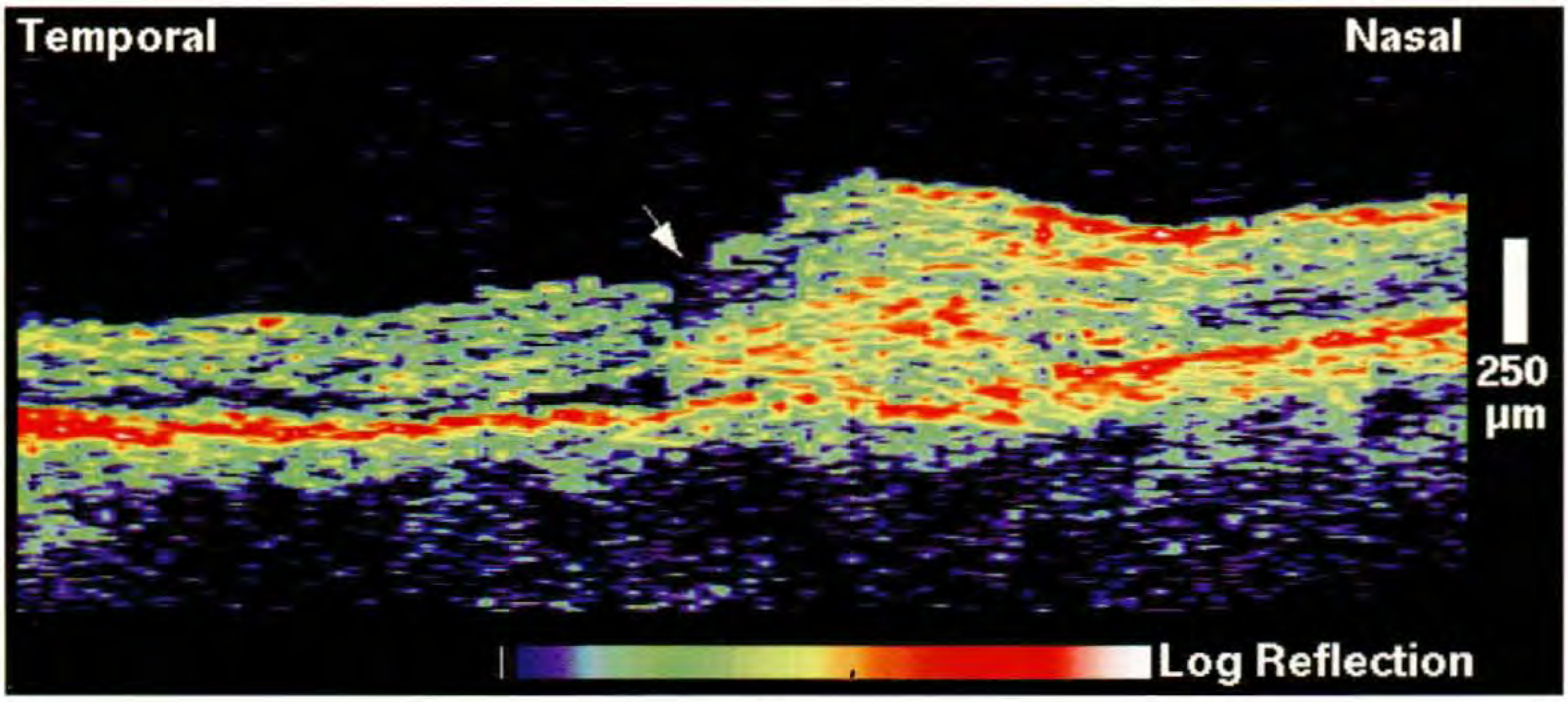

C

CHAPTER 9

Chorioretinal Inflammatory Diseases

Intermediate Uveitis
Presumed Ocular Histoplasmosis Syndrome
Toxoplasmosis Retinitis
Progressive Outer Retinal Necrosis
Cytomegalovirus Retinitis
Human Immunodeficiency Virus Retinopathy

Inflammation as a general rule increases the optical reflectivity from within affected tissue because the migration of inflammatory cells into the retina or vitreous increases the concentration of optical scatterers. OCT can provide dynamic images of the inflammatory process, localizing the infiltrate to specific retinal layers and providing a means to track the extent of inflammation following treatment. The intensity and size of the lesion correlate with the density and extent of the infiltrate, respectively. OCT is also useful in evaluating morphological changes secondary to acute or chronic inflammation, such as retinal edema, fibrosis, and atrophy.

Vision loss due to uveitis is commonly caused by macular edema which may be quantitatively assessed as retinal thickening on the OCT tomogram. Serial follow-up OCT images through the fovea allow the accurate evaluation of macular fluid accumulation and provide an objective means of assessing the efficacy of pharmacological treatment [1].

Many ocular diseases cause chorioretinal inflammation [2]. OCT provides an effective means of quantifying the reflectivity, location, and extent of these inflammatory lesions in cross-section. The typical "punched-out" lesion found in the presumed ocular histoplasmosis syndrome [3] appears on OCT as a focal region of elevated reflectivity in the deeper choroid. Choroidal neovascularization in this disease can also be diagnosed and localized by a disruption and fragmentation of the reflective band corresponding to the retinal pigment epithelium and choriocapillaris on the OCT images.

In contrast, acute toxoplasmosis retinitis [4] or cytomegalovirus lesions [5] exhibit enhanced backscatter due to inflammation primarily affecting the neurosensory retina. Chronic lesions progress to retinal atrophy and fibrosis, which are evident on OCT as increased retinal reflectivity, marked retinal thinning, and increased penetration of the probe light into the choroid.

HIV retinopathy [5] is often manifested by cotton wool spots, probably associated with focal ischemic injury and swollen nerve fiber axons. OCT images demonstrate a corresponding lesion displaying enhanced reflectivity from only the inner retinal layers. In contrast, diseases such as progressive outer retinal necrosis [6] show lesions developing in the outer retinal layers.

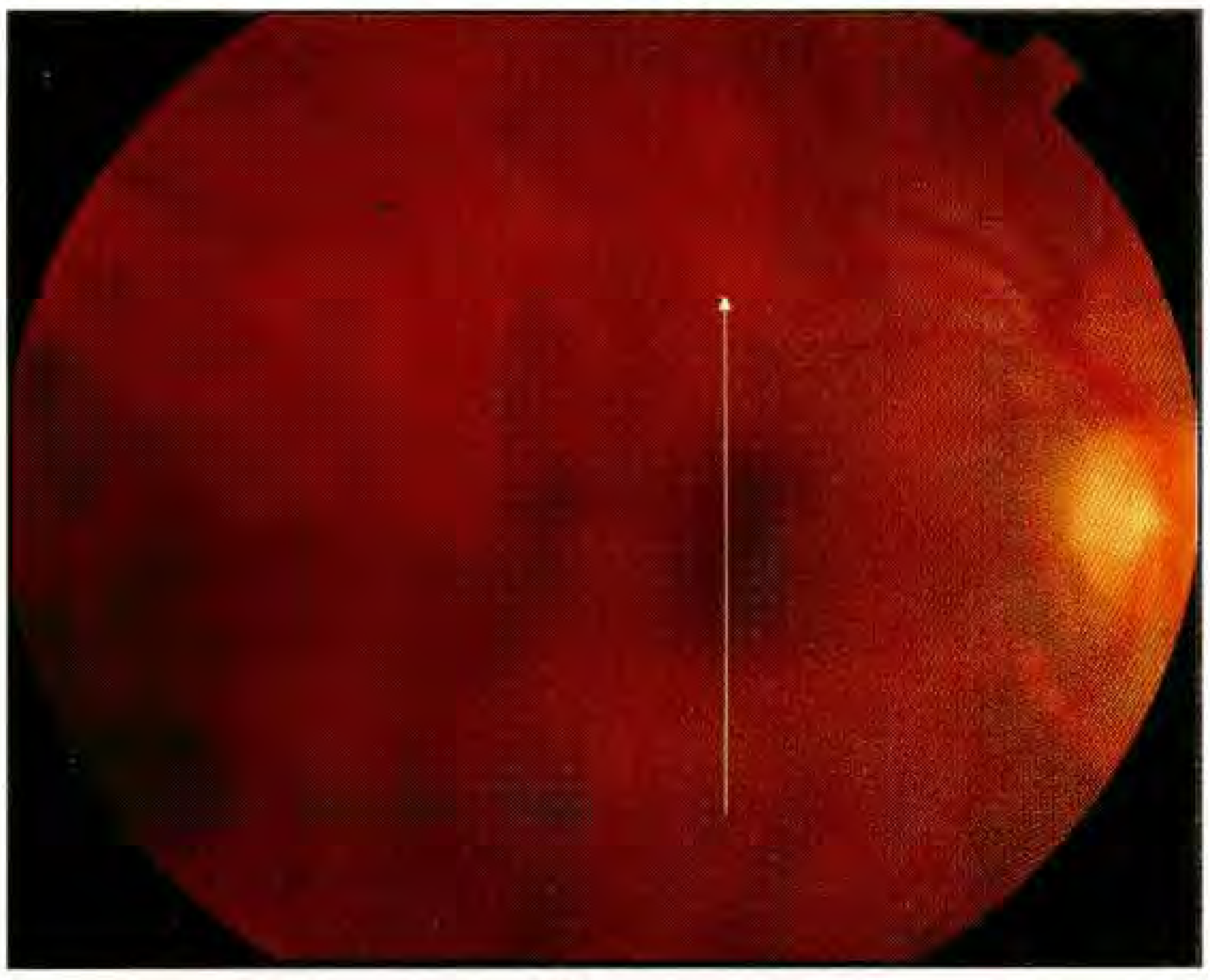

A

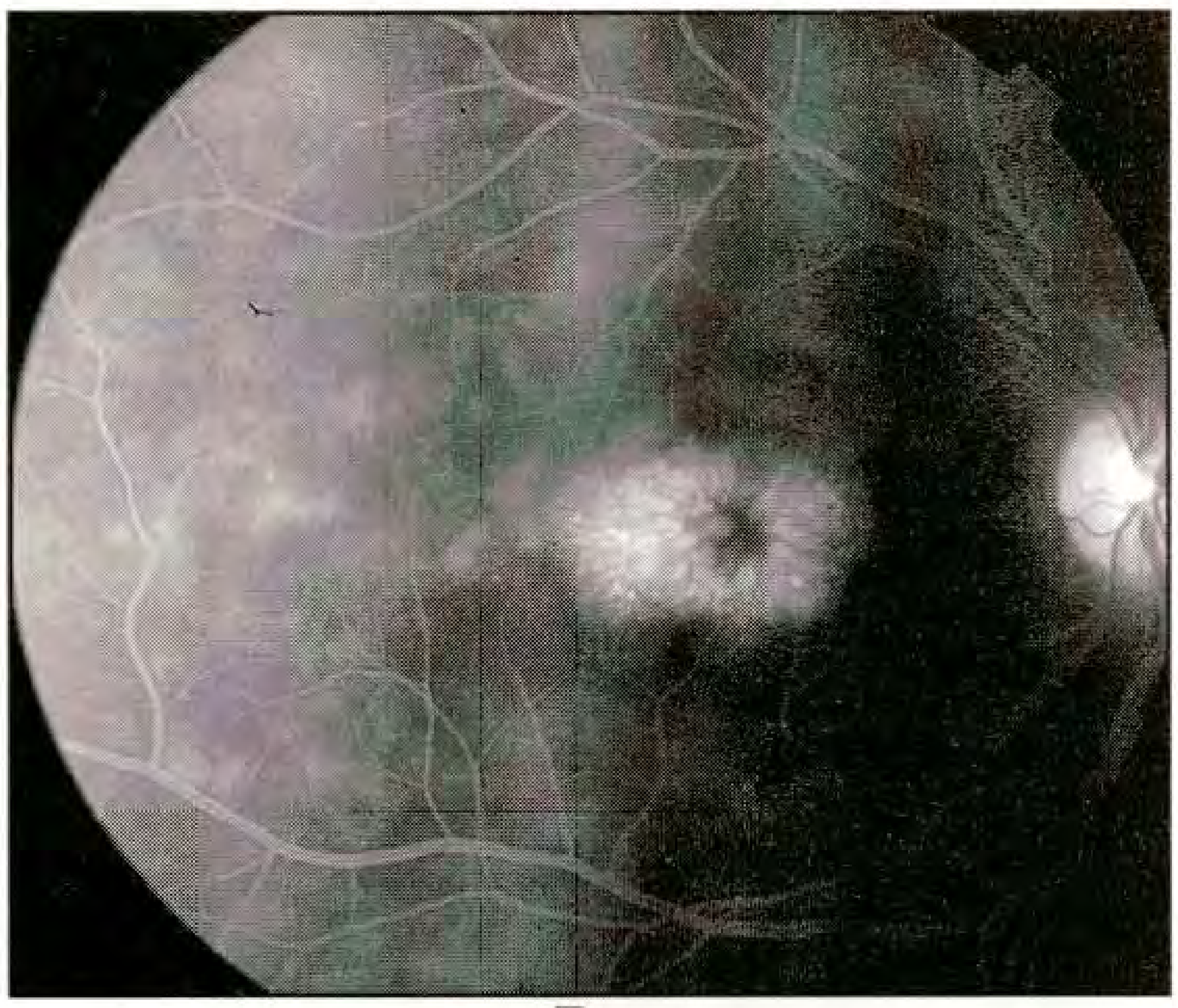

B

Case 9-1. Intermediate Uveitis

Clinical Summary

A 46-year-old man had intermediate uveitis in both eyes. The right eye, with a visual acuity of 20/60, showed cystoid macular edema on fundus examination (A) and late leakage on fluorescein angiography (B).

Optical Coherence Tomography

The OCT tomogram (C) revealed diffuse thickening of the neurosensory retina and reduced optical reflectivity throughout the retinal layers consistent with cystic changes. A neurosensory detachment was observed directly beneath the fovea. The retinal thickness measured centrally was 450 μm.

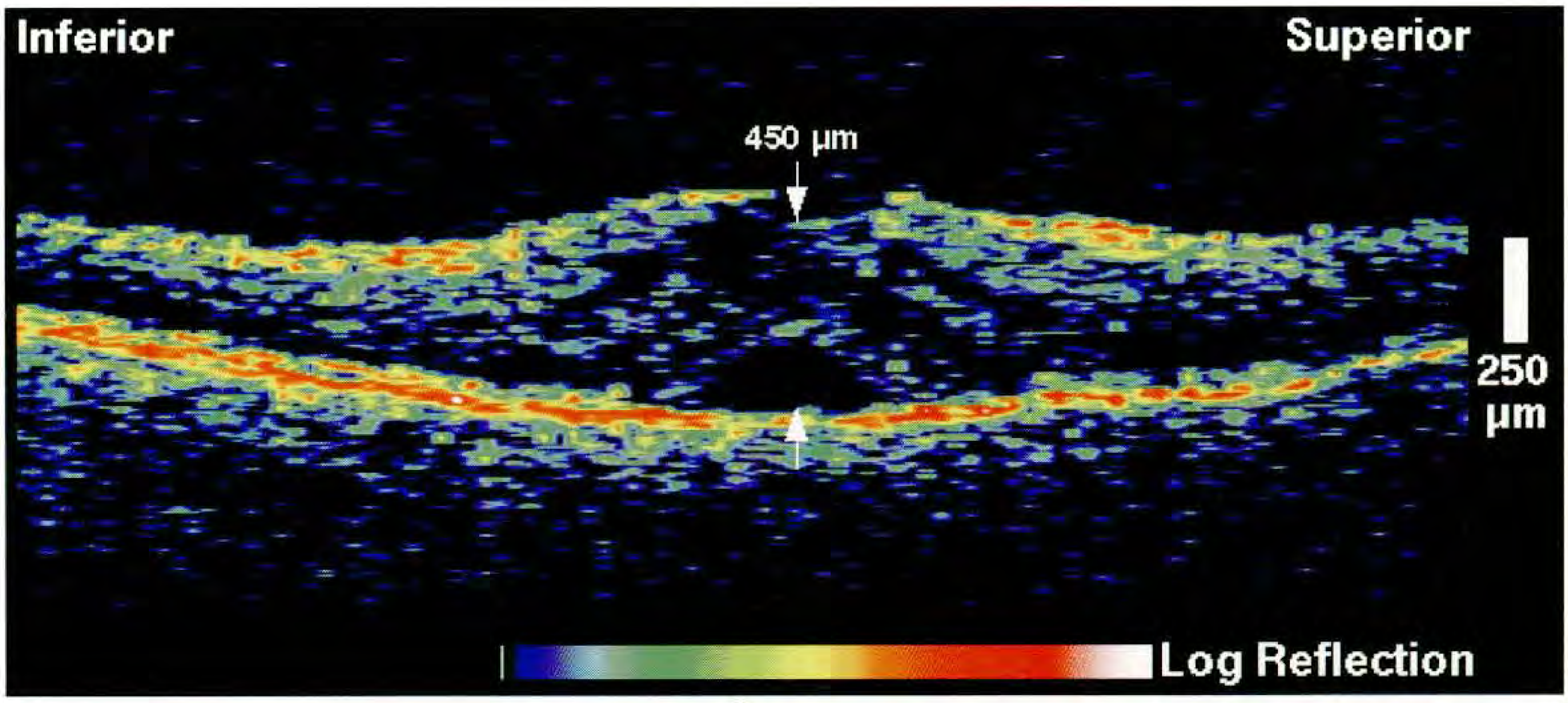

C

Case 9-1 continued

Clinical Summary

The left eye also had cystoid macular edema (D) associated with a visual acuity of 20/80, improving to 20/60 through a pinhole. Pars plana exudate was observed in a snow-bank configuration on slit-lamp examination. Fluorescein angiography (E) showed late leakage in the central macula consistent with cystoid macular edema.

Optical Coherence Tomography

A vertical OCT image (F) through fixation demonstrated a collection of subretinal fluid just beneath the fovea. A large cyst was noted inferior to the center which involved only the outer retinal layers. The high reflectivity observed from the superficial retinal layers suggested preferential fluid accumulation in the deeper retinal tissue. The retinal thickness in the fovea was 480 μm.

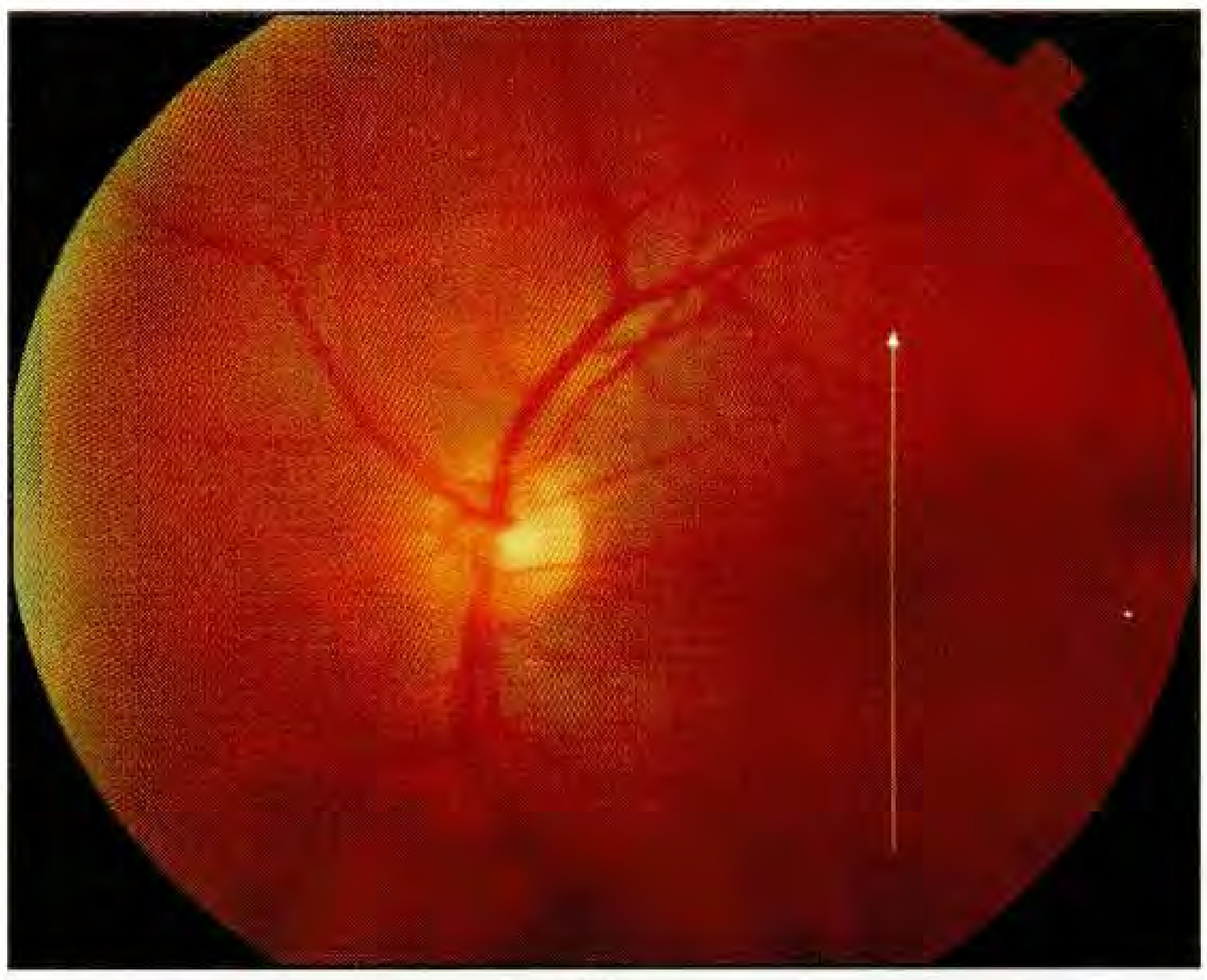

D

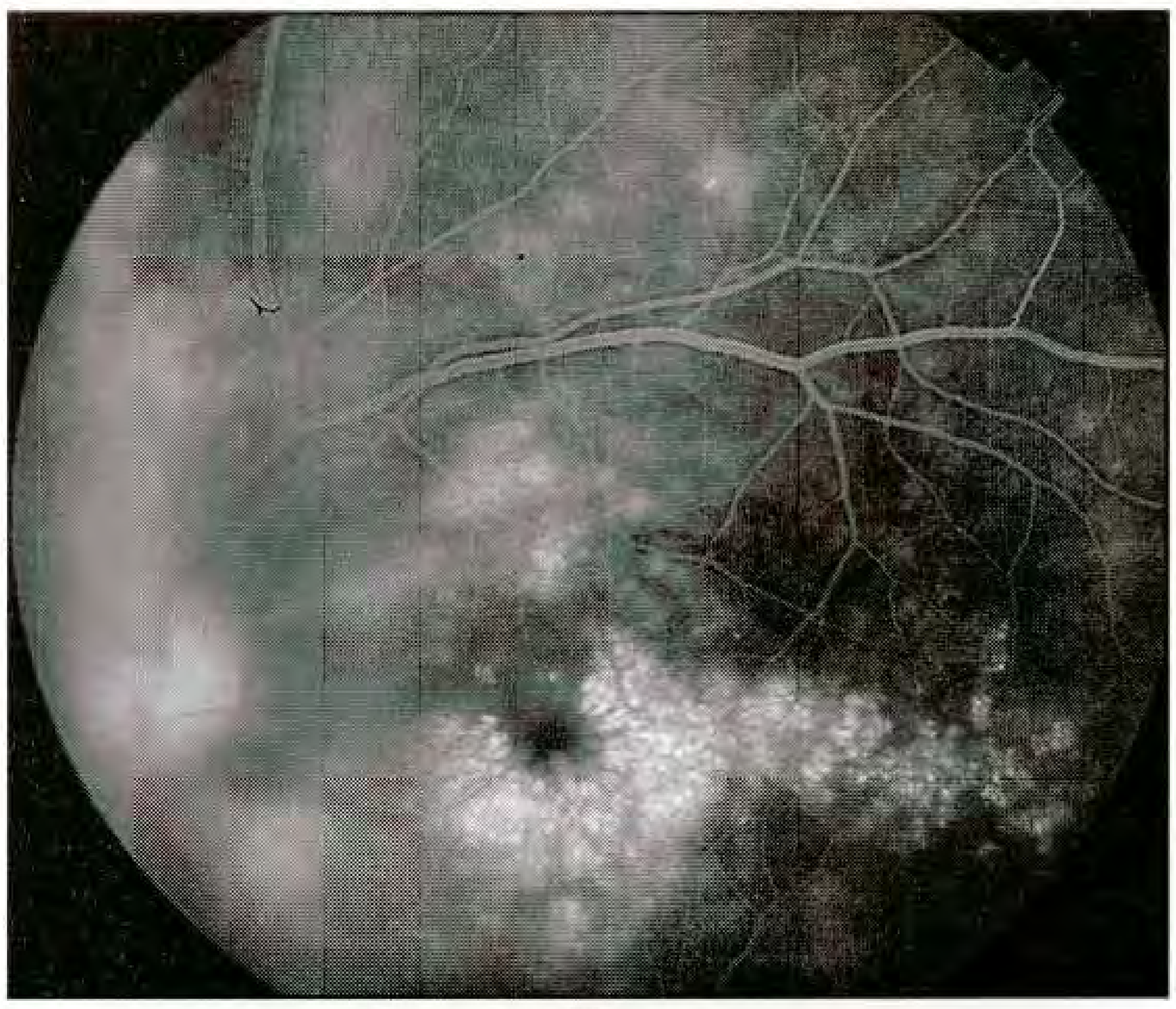

E

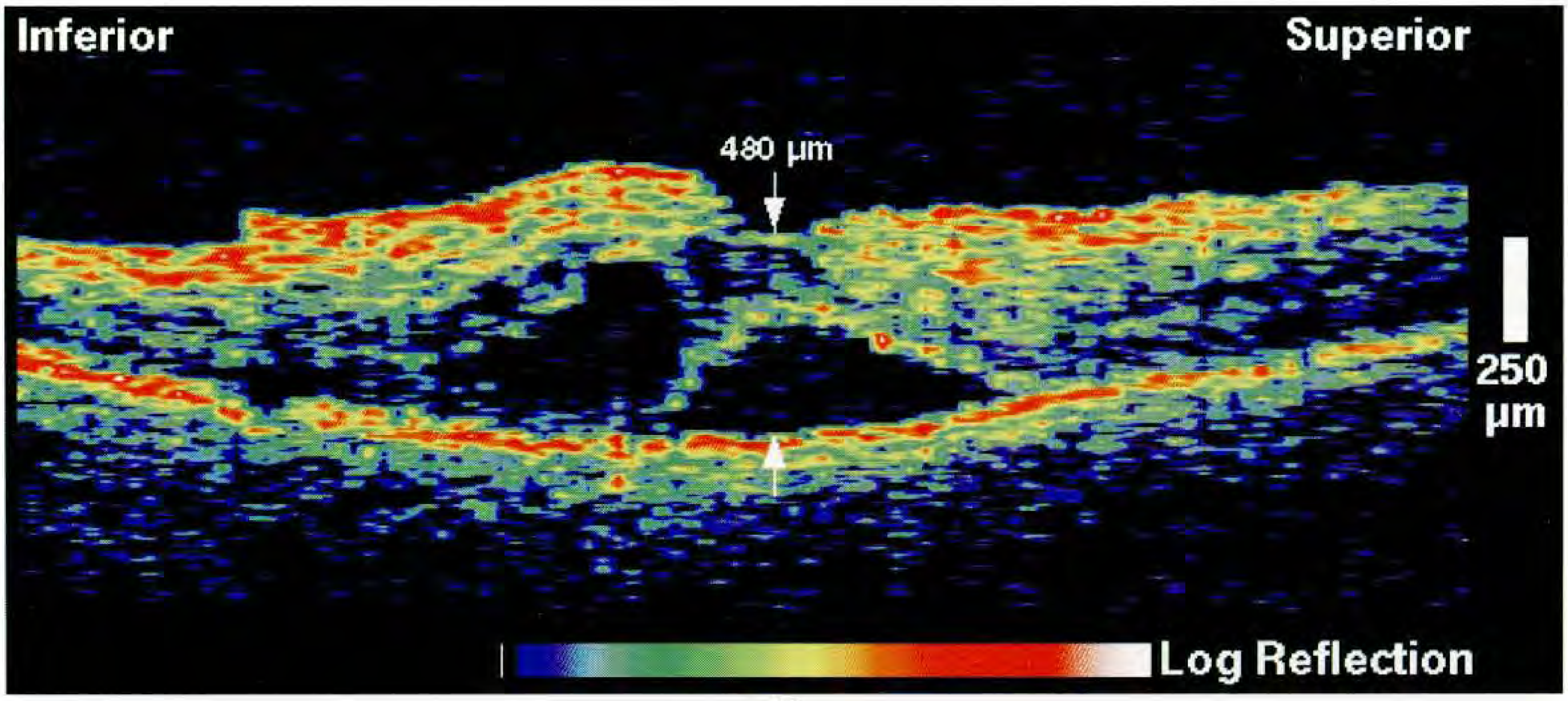

F

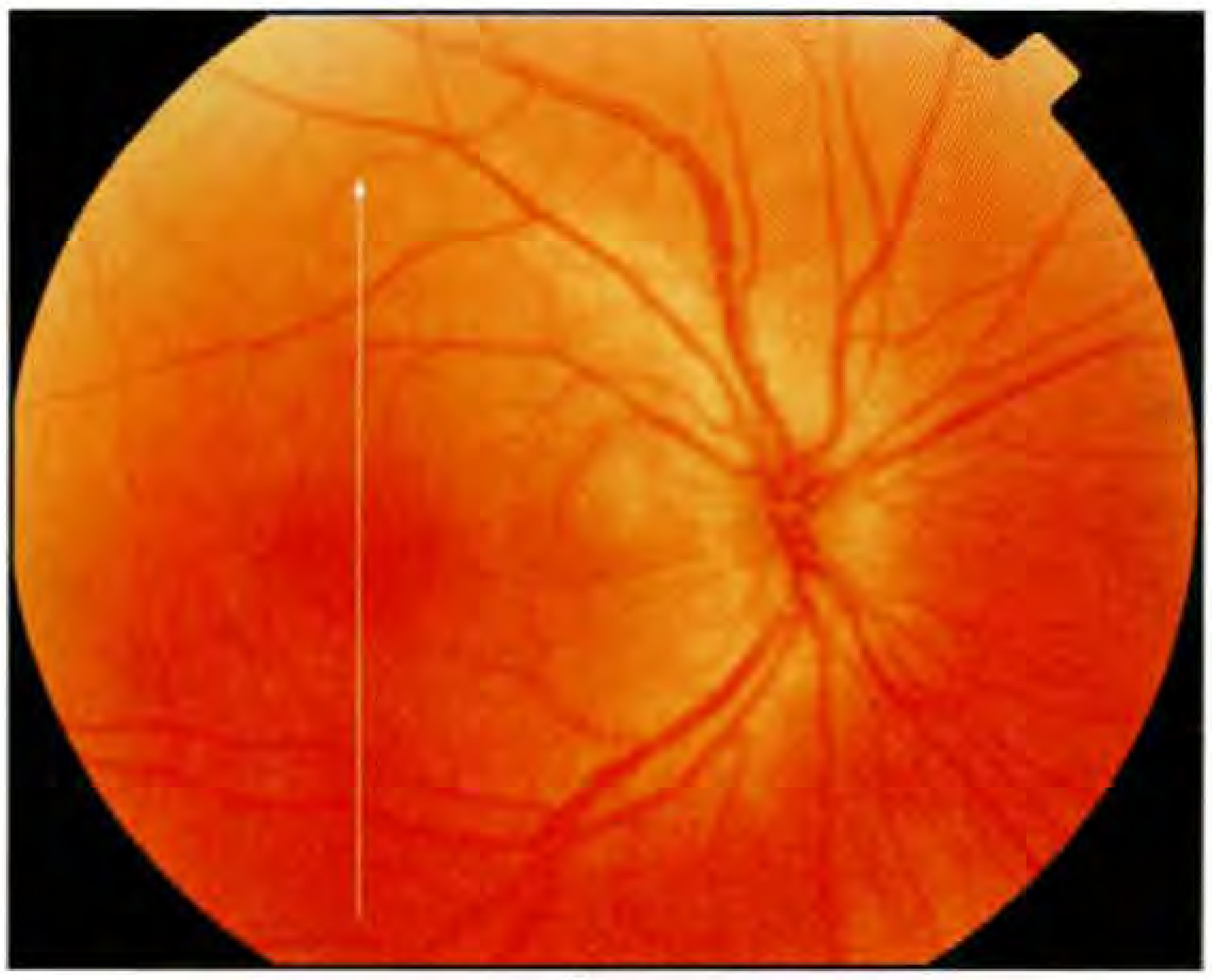

A

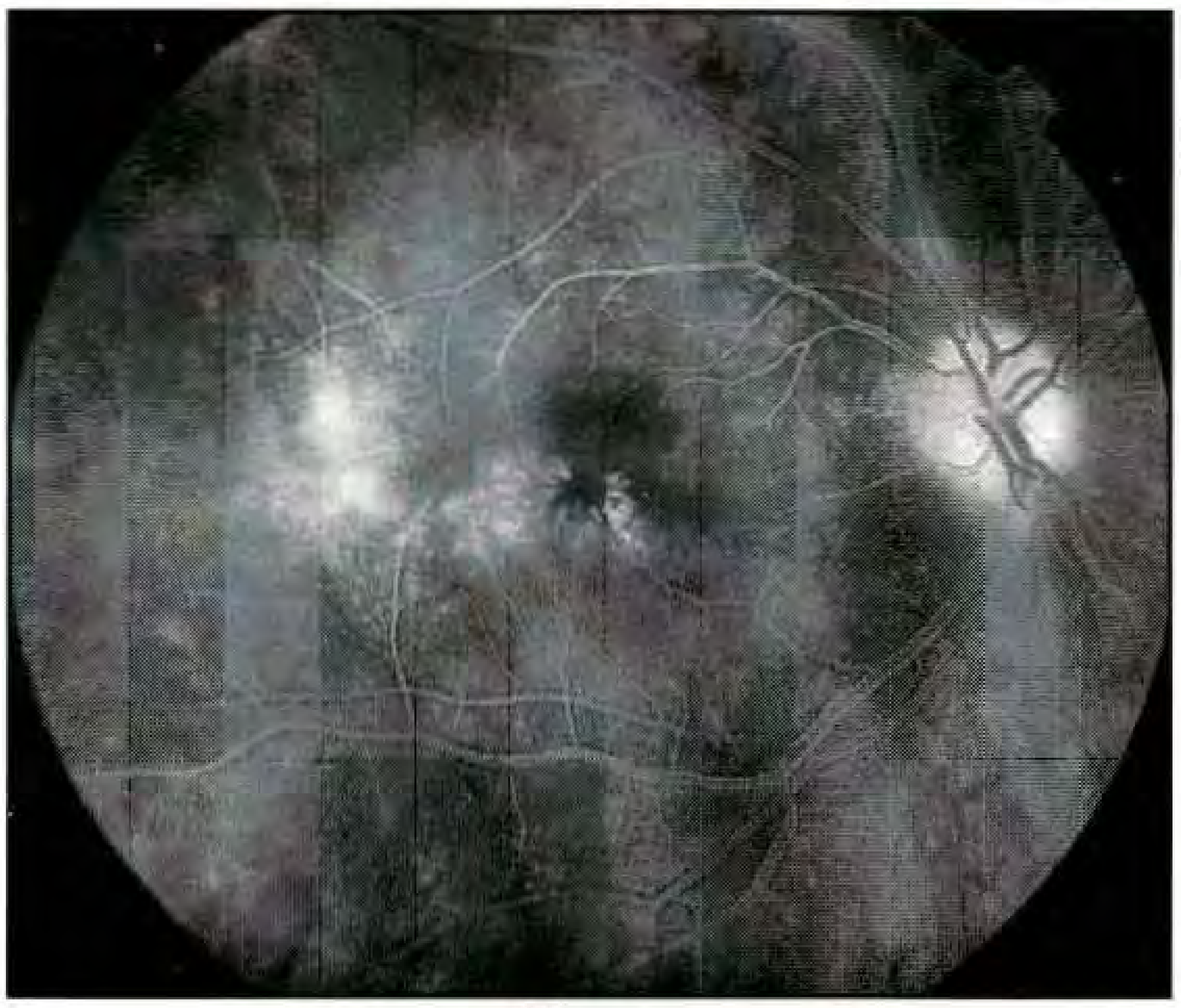

B

Case 9-2. Intermediate Uveitis

Clinical Summary

A 24-year-old woman complained of blurry vision in her right eye beginning nine months earlier associated with the clinical diagnosis of intermediate uveitis. On examination, her uncorrected visual acuity in this eye was 20/30. Fundus examination (A) showed trace cystoid macular edema and a mildy hyperemic optic disc. The retinal vasculature appeared normal, with no sheathing. Fluorescein angiography (B) confirmed mild late leakage surrounding the fovea consistent with macular edema.

Optical Coherence Tomography

A vertical tomogram (C) through fixation demonstrated loss of the normal contour of the fovea and a small cyst directly in the central macula. The foveal thickness was 310 μm.

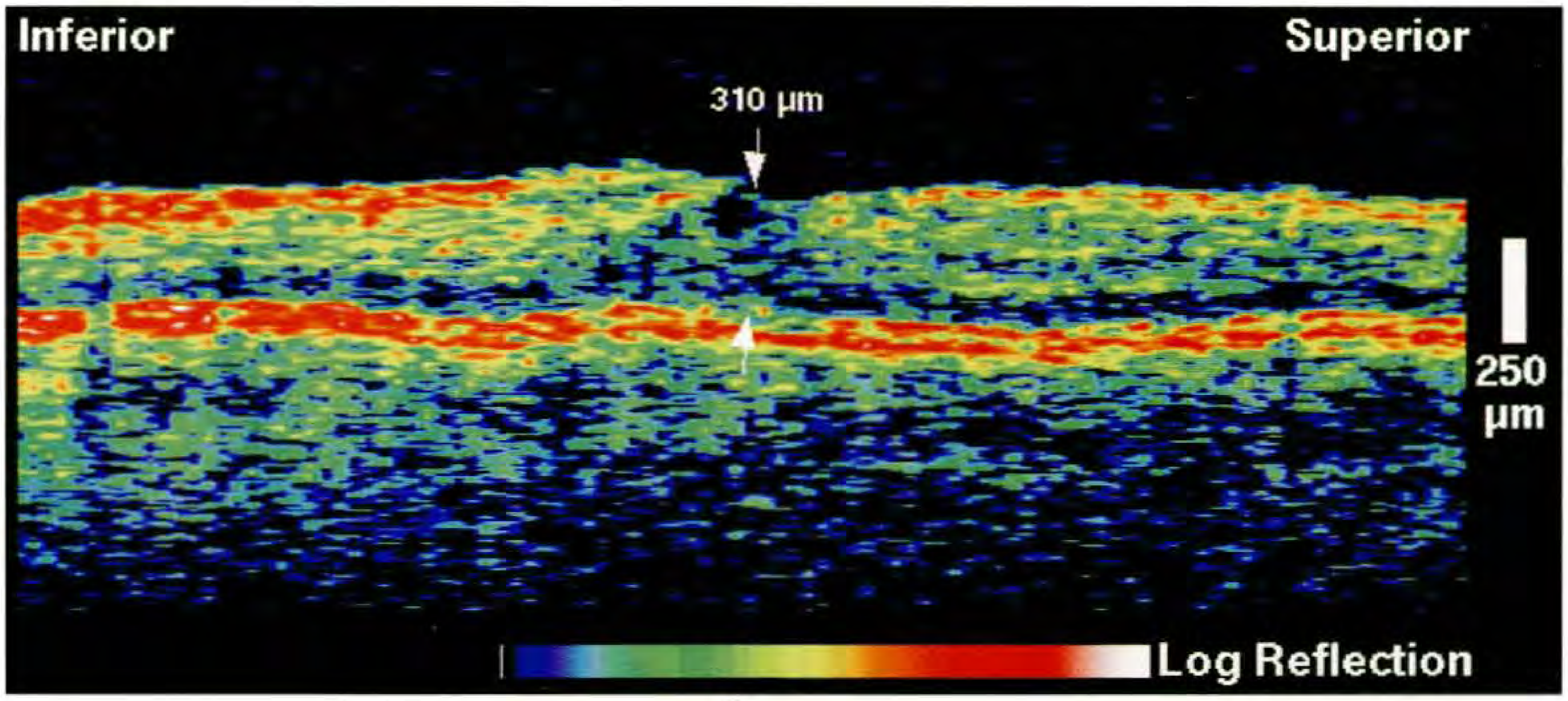

C

Case 9-3. Intermediate Uveitis

Clinical Summary

A 35-year-old woman had a visual acuity of 20/100 in her right eye associated with the clinical diagnosis of panuveitis and cystoid macular edema (A).

Optical Coherence Tomography

The OCT image (B) demonstrated a solitary cyst in the macula and a loss of the foveal depression. The central macular thickness was 350 µm.

A

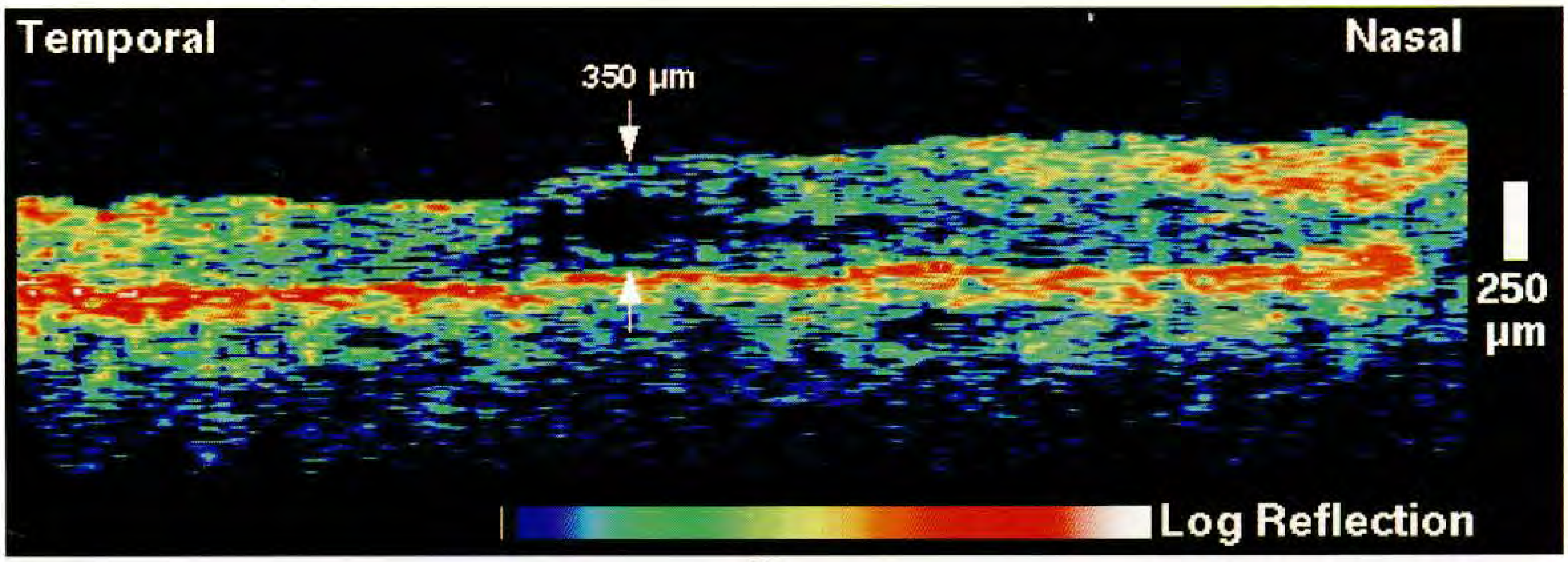

B

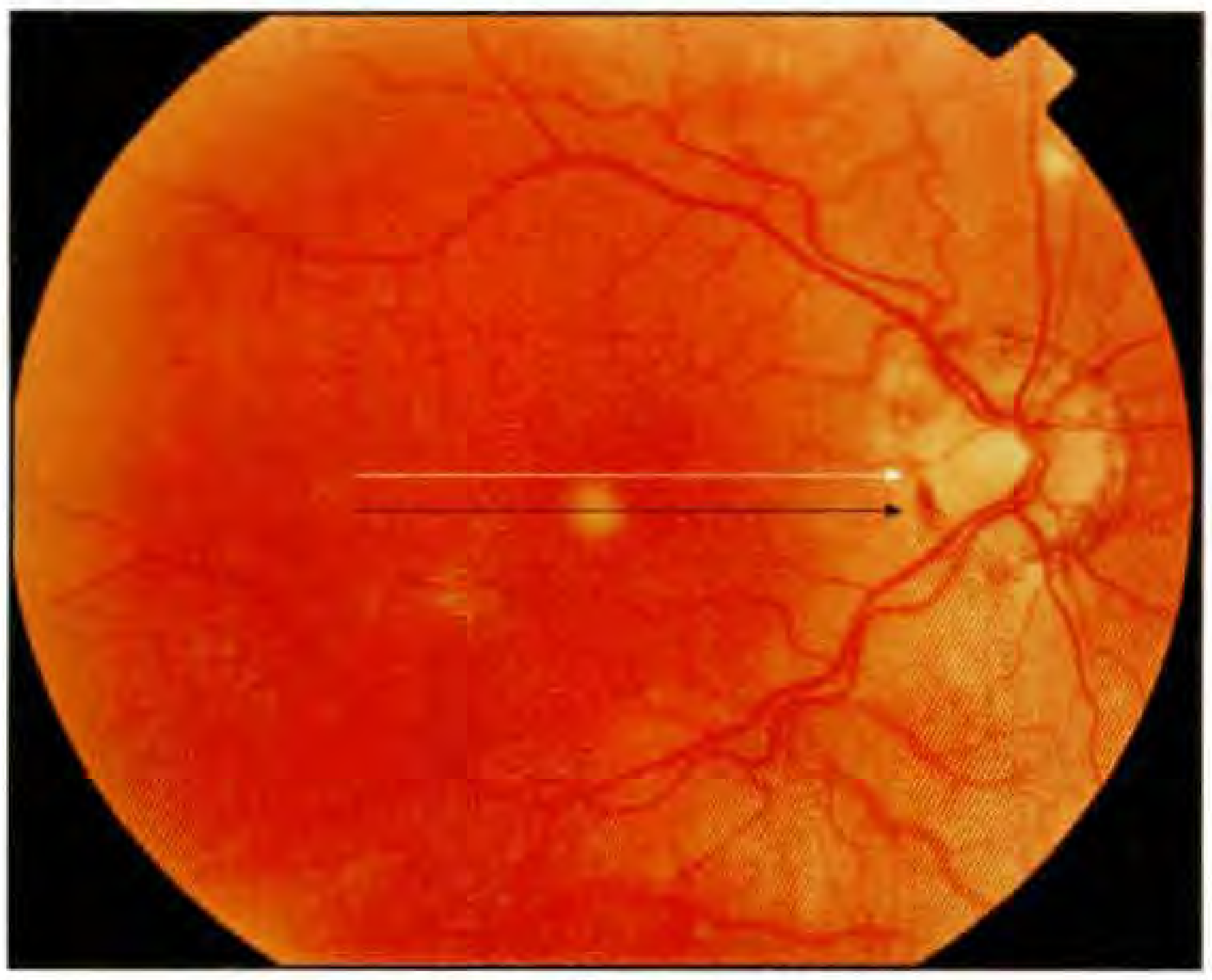

A

B

Case 9-4. Presumed Ocular Histoplasmosis Syndrome

Clinical Summary

A 54-year-old woman reported a three day history of a gray spot in her right central vision. Her visual acuity in this eye was 20/60. Slit-lamp examination (A) revealed mild peripapillary atrophy, punched out chorioretinal lesions in the mid-periphery, and a single atrophic lesion in the central macula consistent with a clinical diagnosis of presumed ocular histoplasmosis syndrome. There was no evidence of subretinal fluid or exudate. Fluorescein angiography (B) displayed a well circumscribed hyperfluorescent lesion in the central macula with a reticular pattern of mild surrounding hyperfluorescence.

Optical Coherence Tomography

A horizontal scan (C) directly through fixation showed loss of the normal contour of the foveal pit and mild subfoveal fluid accumulation. The subretinal fluid appeared mildly backscattering, in contrast to transparent serous fluid. An image (D) acquired through the central atrophic lesion displayed a well-defined region of decreased reflectivity from the retinal pigment epithelium (RPE), and an associated increase in backscattering from the choroid below, consistent with a chorioretinal lesion. The inner retinal layers appeared elevated and compressed above the lesion.

Follow-up Optical Coherence Tomography

The patient started oral prednisone therapy and returned two months later with an improvement in visual acuity to 20/20. A repeat scan (E) through the fovea showed that the subretinal fluid had resolved. A significant improvement in the chorioretinal lesion was also noted on OCT (F), which demonstrated reduced disruption of the retinal layers and RPE in this area. Only a slight increase in the choroidal reflectivity remained.

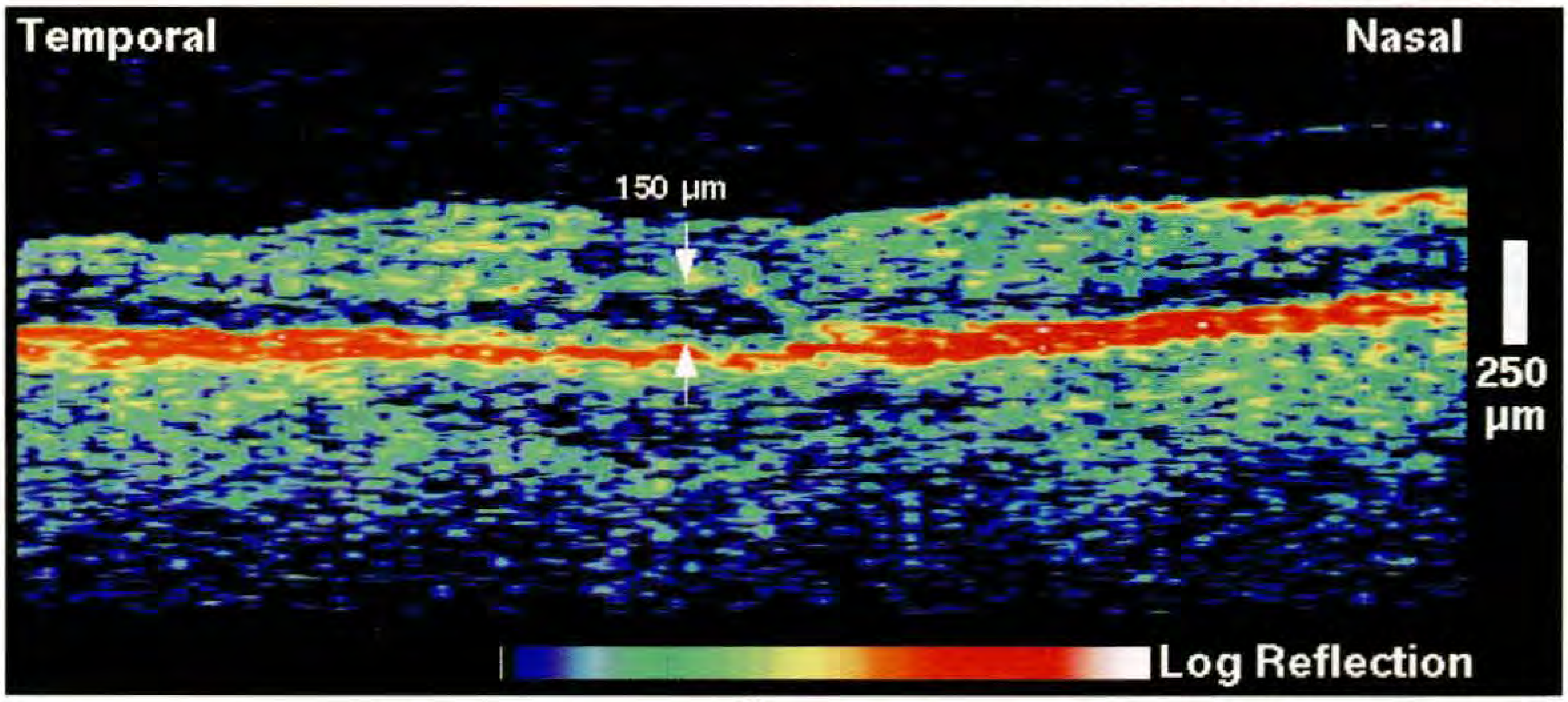

C

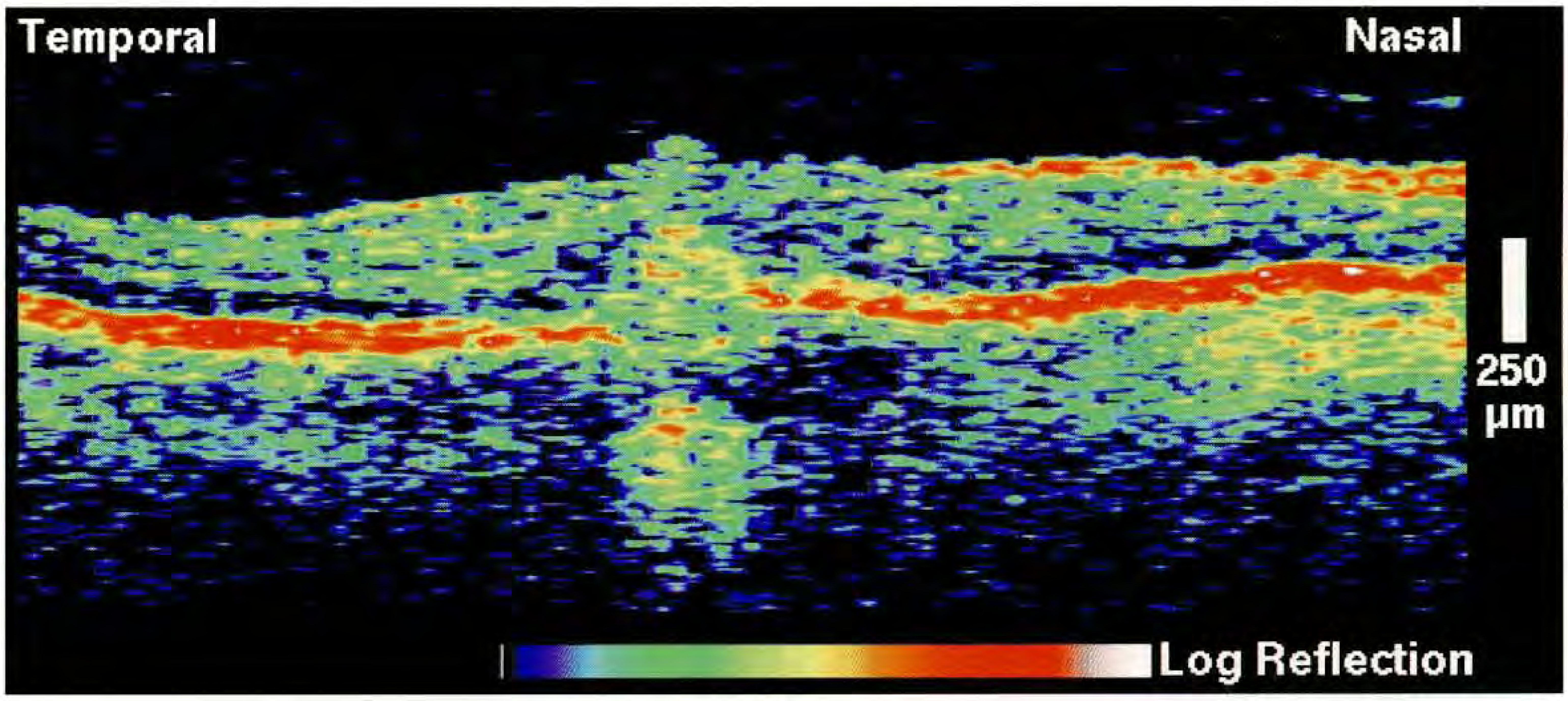
Temporal
Nasal
250 µm
Log Reflection

D

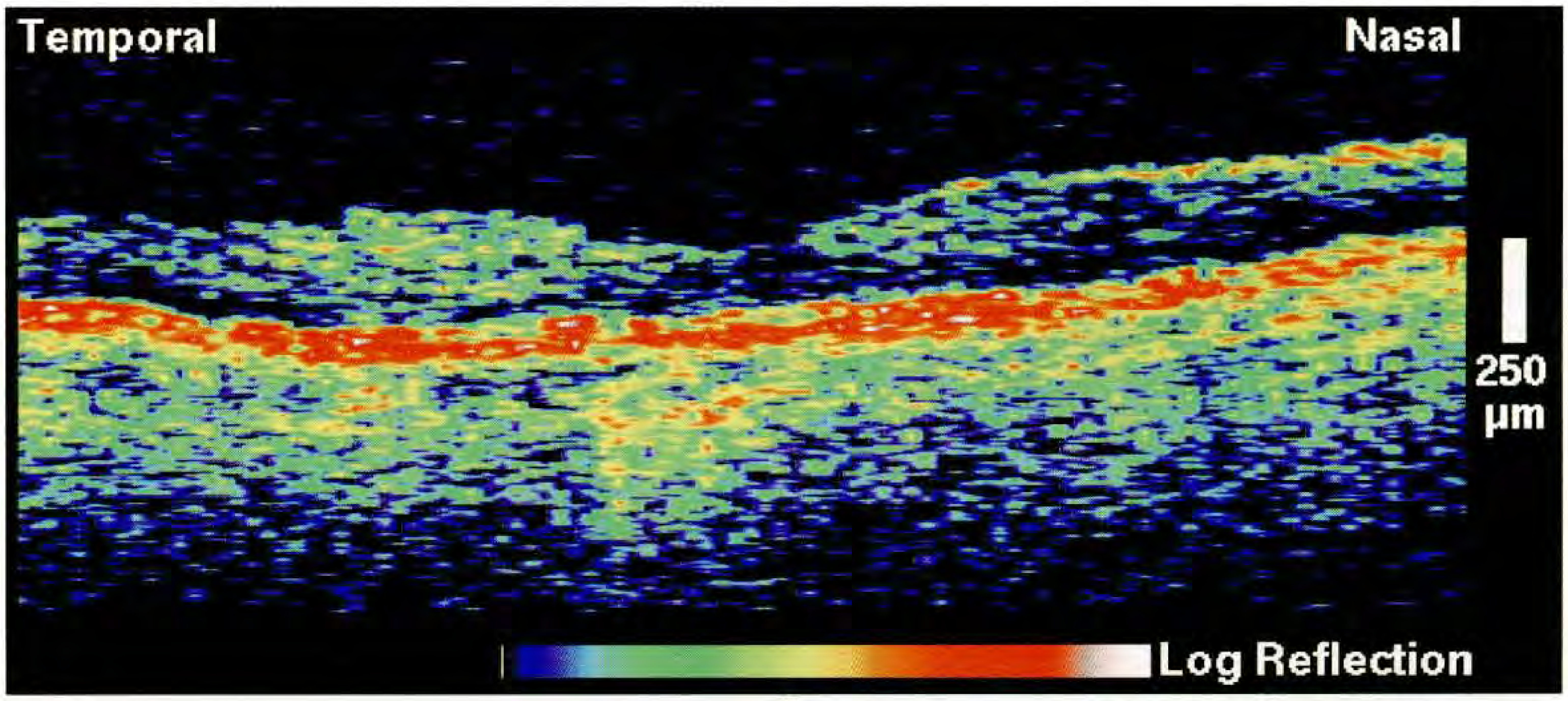
Temporal
Nasal
250 µm
Log Reflection

E

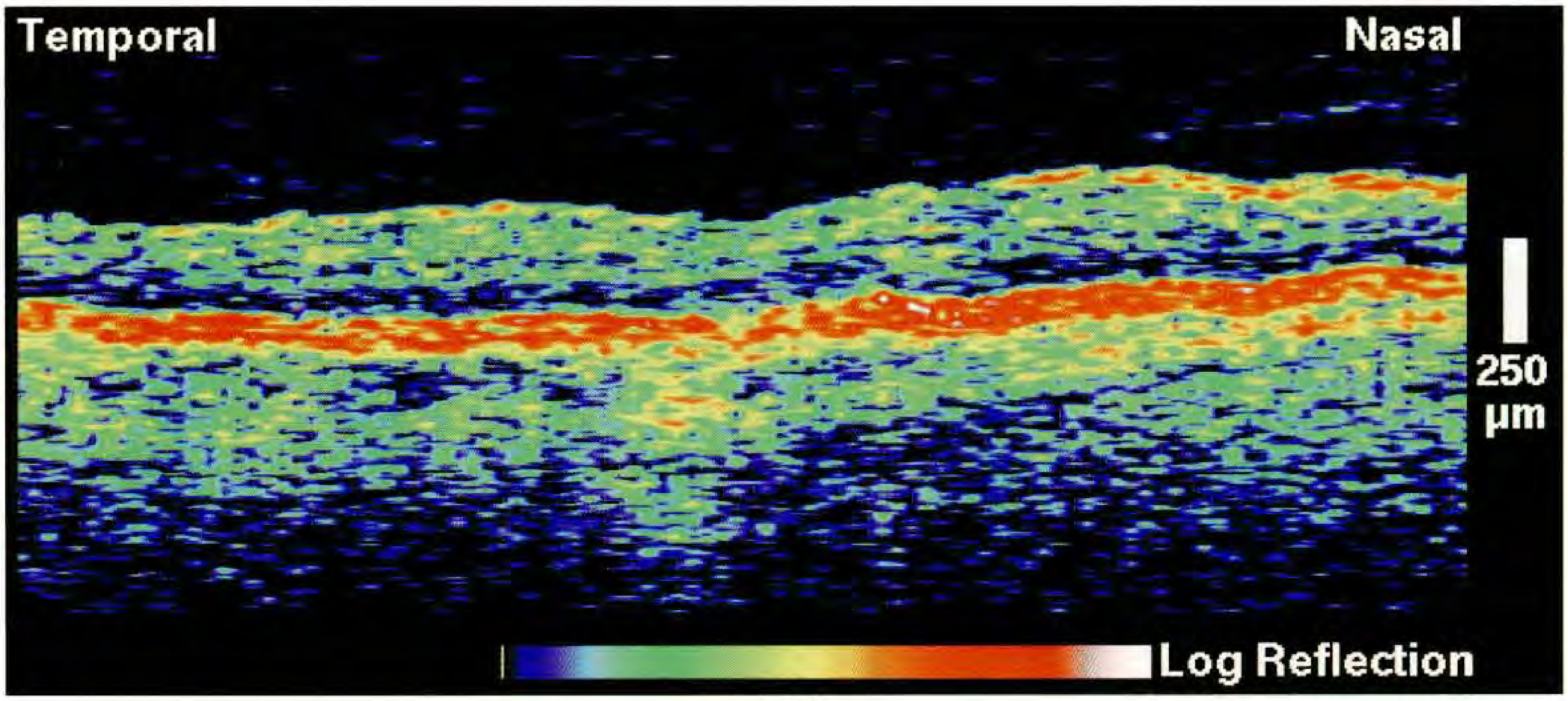
Temporal
Nasal
250 µm
Log Reflection

F

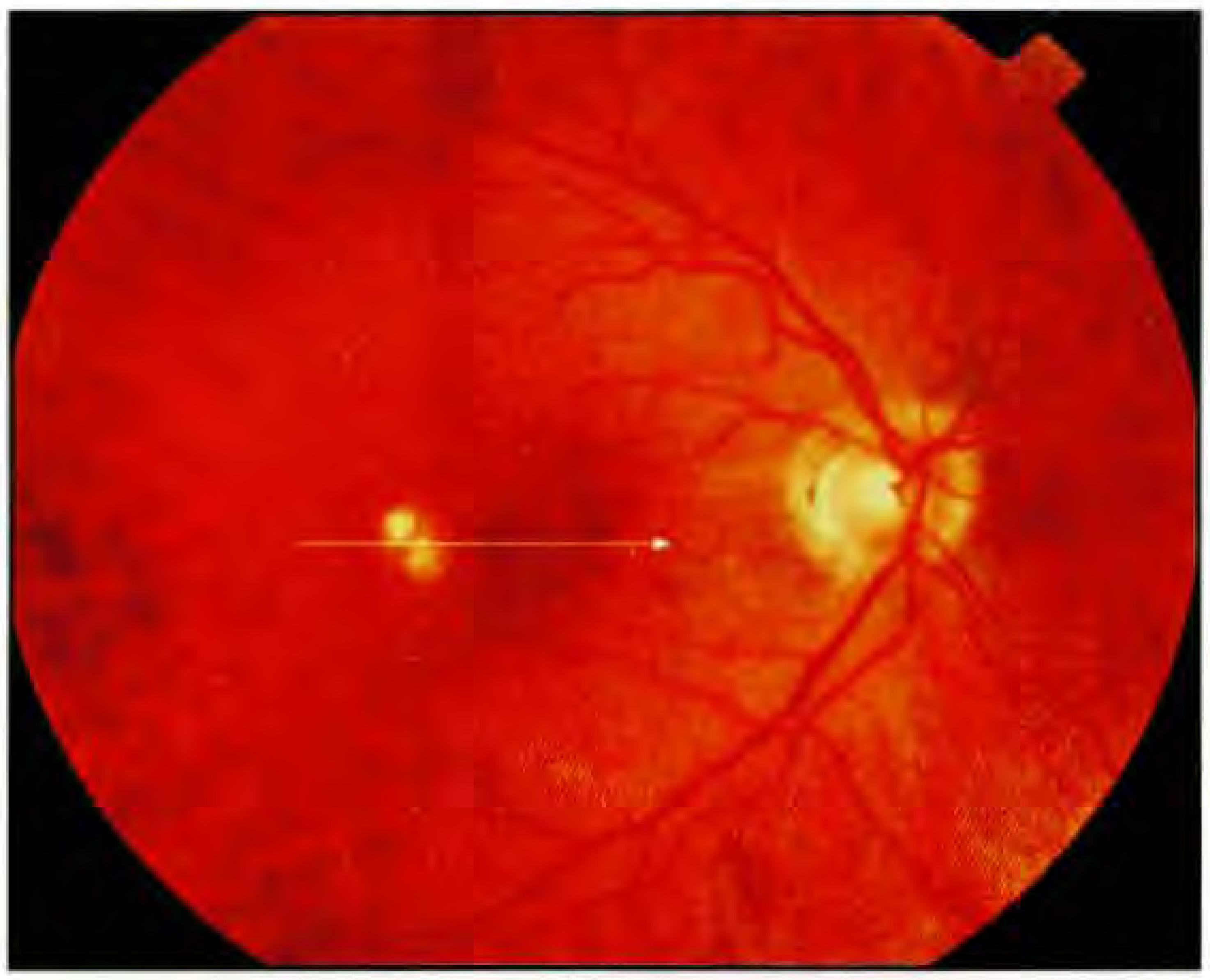

A

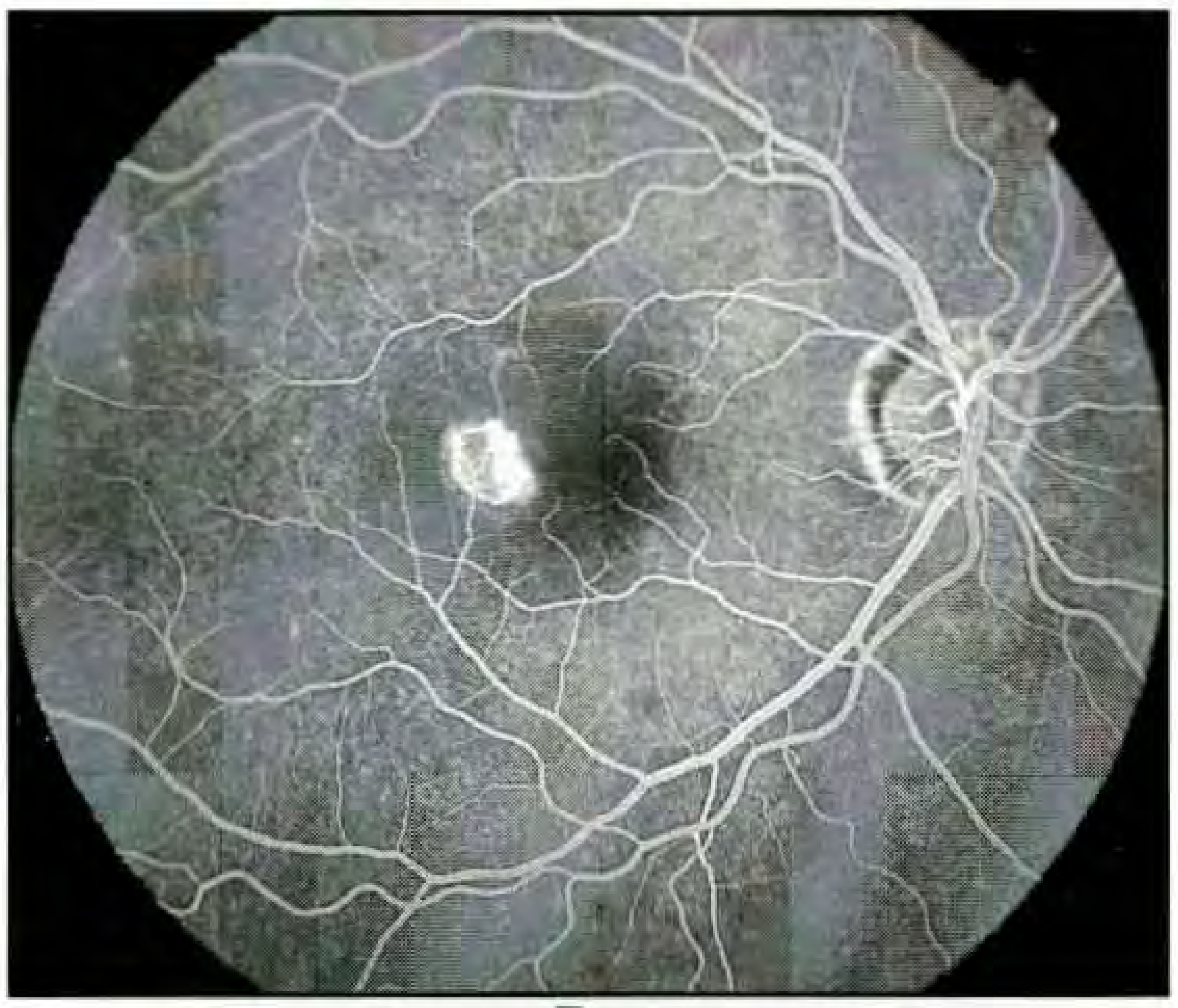

B

Case 9-5. Presumed Ocular Histoplasmosis Syndrome

Clinical Summary

A 41-year-old man receiving oral prednisone therapy for presumed ocular histoplasmosis had a visual acuity of 20/40 in his right eye associated with a juxtafoveal choroidal neovascular membrane. Slit-lamp biomicroscopy (A) showed mild peripapillary atrophy and a punched out chorioretinal scar temporal to the fovea. Fluorescein angiography (B) revealed two contiguous hyperfluorescent areas temporal to the center with the farthest temporal area corresponding to the laser scar. The hyperfluorescent region between the scar and fovea demonstrated late leakage consistent with a neovascular membrane.

Optical Coherence Tomography

A horizontal OCT image (C) demonstrated a focal region of enhanced backscatter within the choroid corresponding to the chorioretinal scar. Just nasal to this lesion, the reflective band consisting of the retinal pigment epithelium (RPE) and choriocapillaris was thickened and disrupted consistent with a neovascular membrane. The retinal layers above the membrane were elevated, and increased retinal thickness in this region was consistent with intraretinal fluid accumulation.

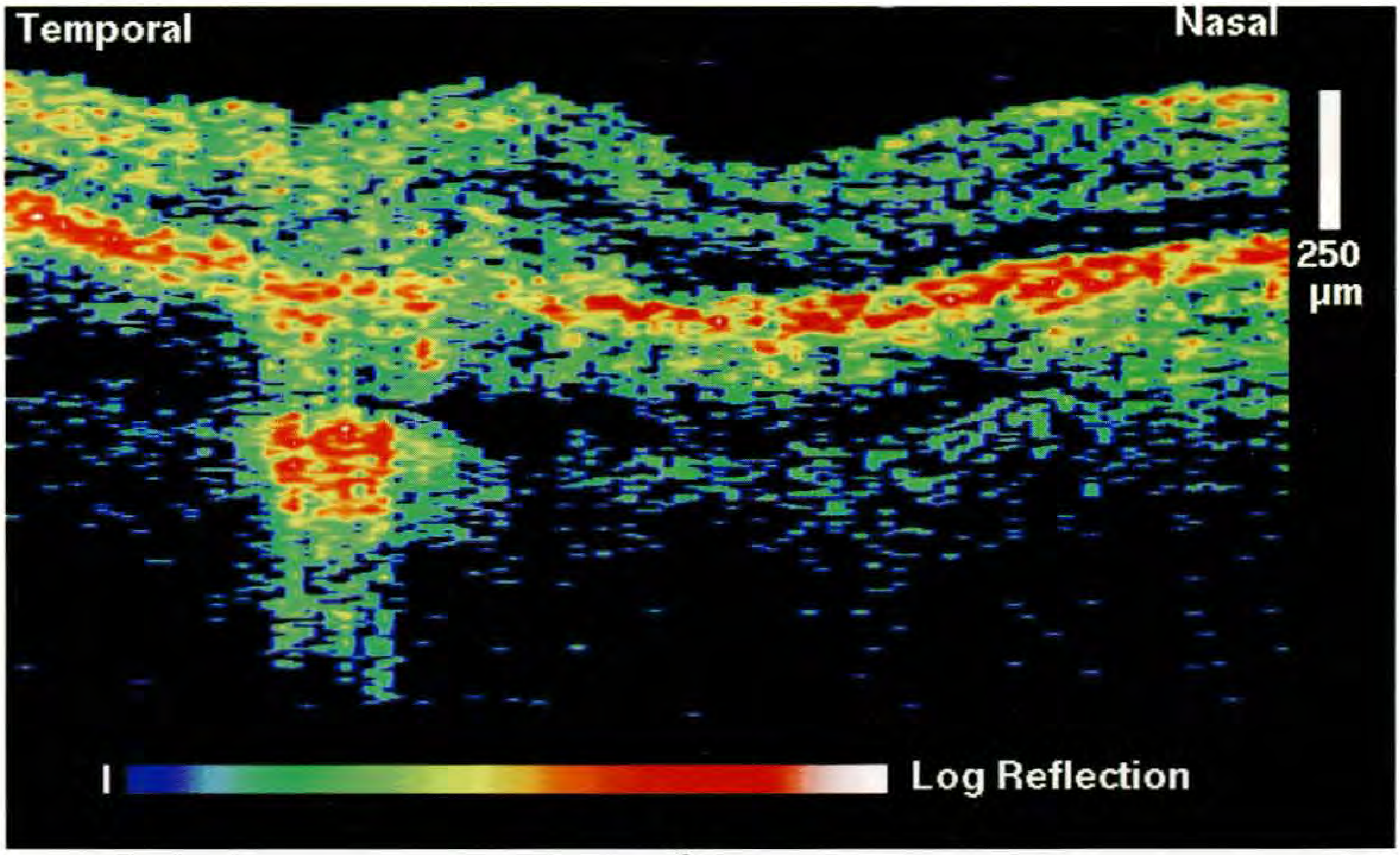

C

Case 9-6. Presumed Ocular Histoplasmosis Syndrome

Clinical Summary

A 45-year-old man with a history of presumed ocular histoplasmosis reported mild distortion and blurring in his left eye since his most recent laser treatment. His visual acuity was assessed at 20/60. Dilated fundus examination (A) revealed a dry laser scar inferior to fixation, multiple punched-out chorioretinal scars throughout the posterior pole, and very mild peripapillary atrophy. A thin subretinal hemorrhage was noted in the central macula. A small depigmented area that appeared to be choroidal neovascularization was observed just superior to the fovea. Fluorescein angiography (B) showed a crescent of hyperfluorescence inferior to the center consistent with previous laser treatment. A small, well-demarcated area of hyperfluorescence superior to the fovea exhibited increasing intensity as the angiogram progressed consistent with a neovascular membrane.

Optical Coherence Tomography

A vertical OCT image (C) through fixation displayed the contour of the foveal pit. Inferior to the center, there was increased backscattering from the layers below the retinal pigment epithelium (RPE) consistent with a laser scar. The reflection from the RPE and choriocapillaris adjacent to the scar immediately superior to the fovea appeared to be fragmented corresponding to the neovascular membrane observed clinically.

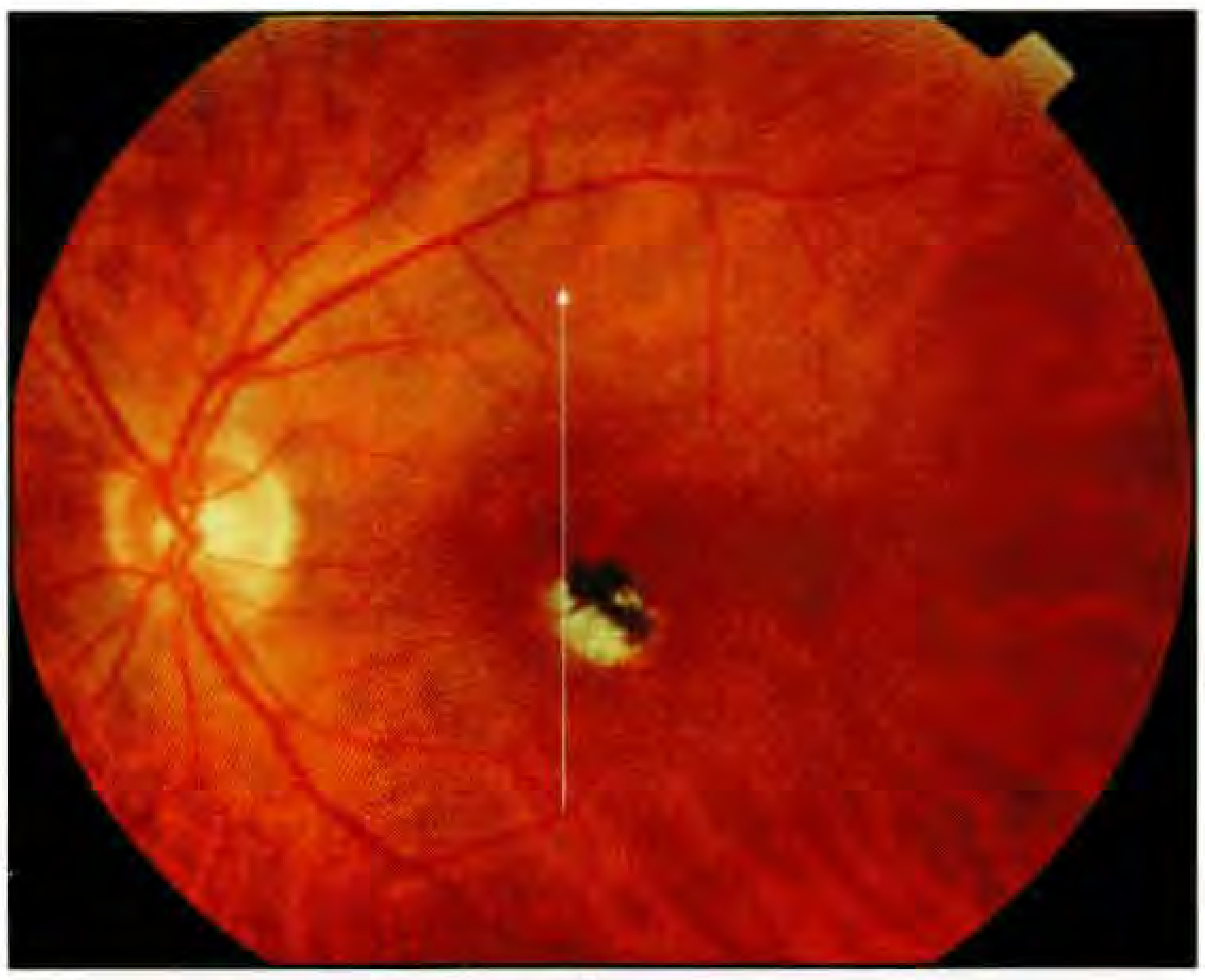

A

B

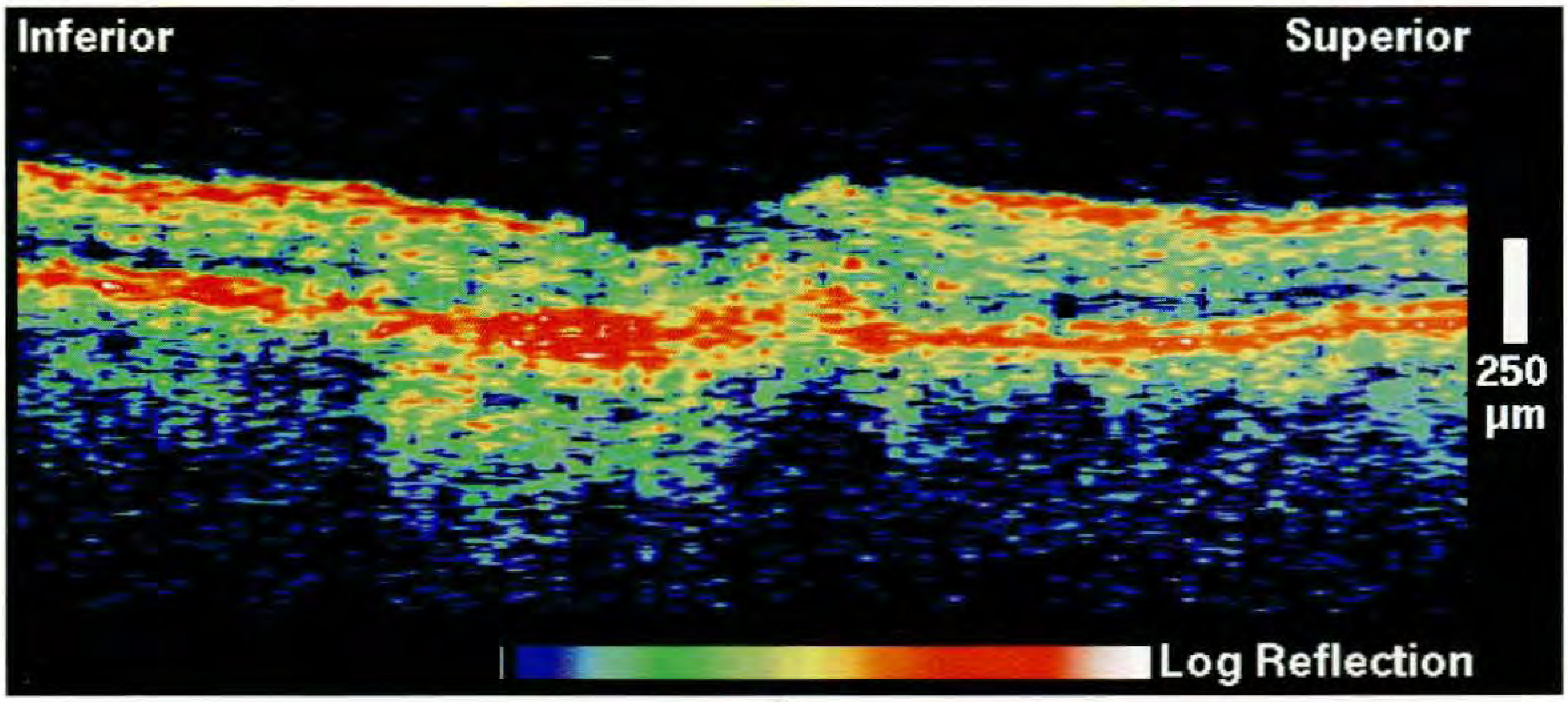

C

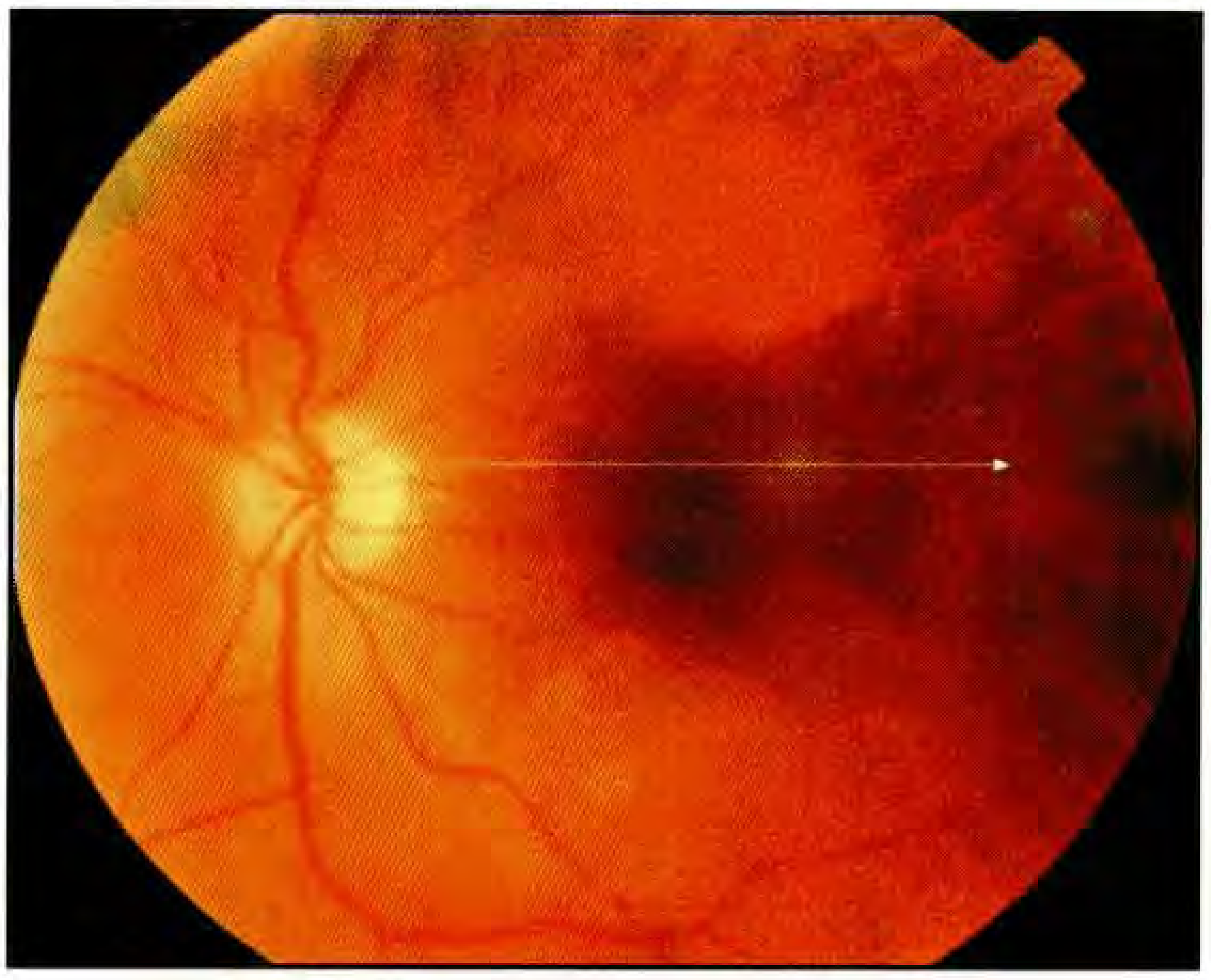

A

Case 9-7. Acute Toxoplasmosis Chorioretinitis

Clinical Summary

A 69-year-old man had noticed a blurry spot in his left eye over the three weeks prior to evaluation. On examination, his visual acuity was 20/50. Slit-lamp biomicroscopy (A) revealed mild posterior vitreous cells and debris, and an area of outer retinal whitening just superior to and involving the fovea. A presumptive clinical diagnosis of toxoplasmosis retinitis was made.

Optical Coherence Tomography

A horizontal tomogram (B) acquired through the superior fovea and lesion demonstrated a focal area of increased intraretinal backscattering corresponding to the retinitis observed on biomicroscopy. The retina was slightly thinned in this area. The superficial layers of the retina appeared to be preferentially involved consistent with the propensity of toxoplasmosis tissue cysts to develop in these layers.

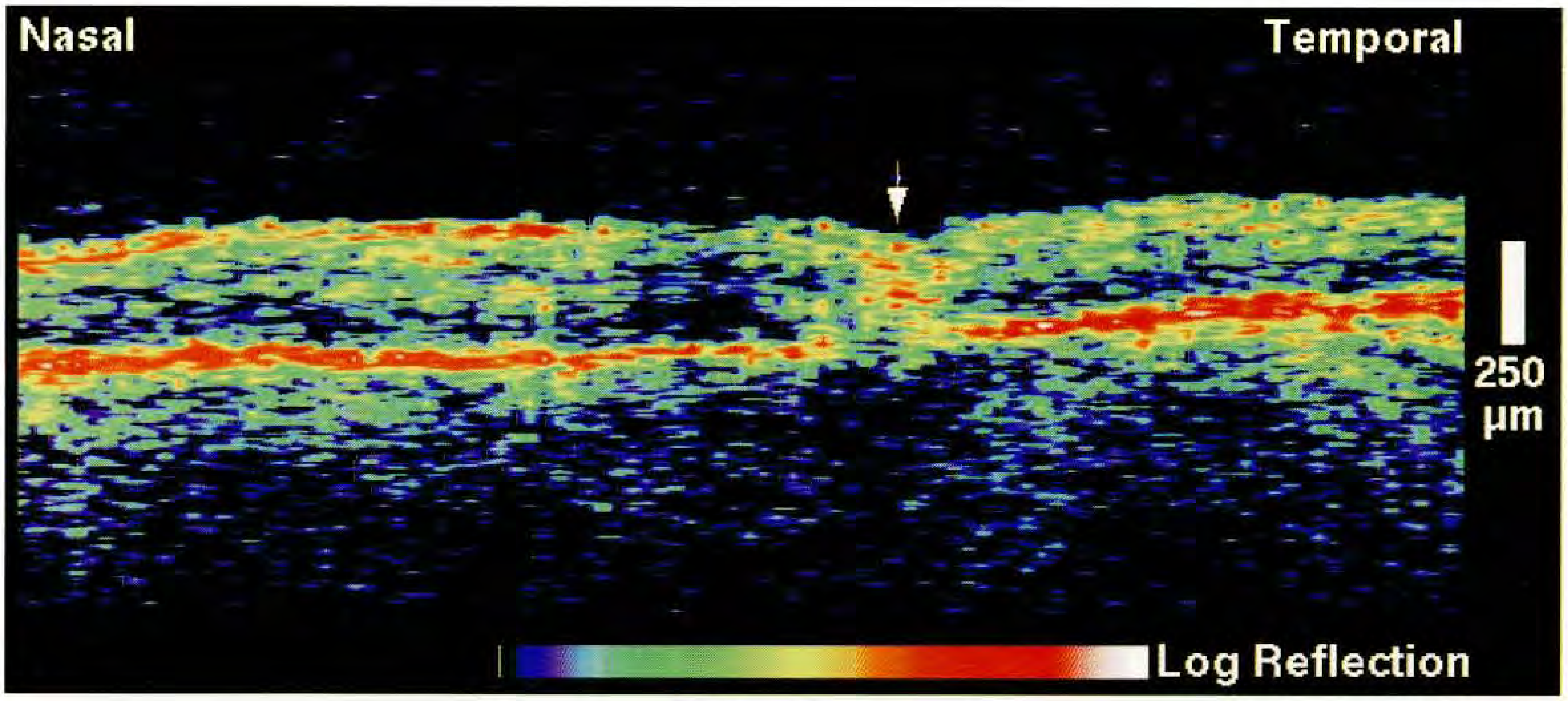

B

Case 9-8. Reactivation of Toxoplasmosis Retinitis

Clinical Summary

A 20-year-old man with a history of toxoplasmosis complained of blurry vision and floaters in his left eye for a week prior to examination. His visual acuity was 20/15 in this eye. Ophthalmoscopy (A) showed a gray retinal lesion immediately above the superotemporal arcade, and an older chorioretinal scar superior to this lesion.

Optical Coherence Tomography

OCT (B; white line on A) through the recent lesion delineated a region of enhanced reflectivity within the neurosensory retina corresponding to the retinal inflammation. Within the lesion, focal areas of fragmentation were observed in the reflective band corresponding to the retinal pigment epithelium (RPE), most likely a result of RPE proliferation and hyperpigmentation. A horizontal image (C; black line on A) through the older chorioretinal scar showed a well-defined region of increased backscatter from the choroid consistent with pigmentary atrophy and increased penetration of the probe beam into the deeper retina. The neural retina was thinned in this region.

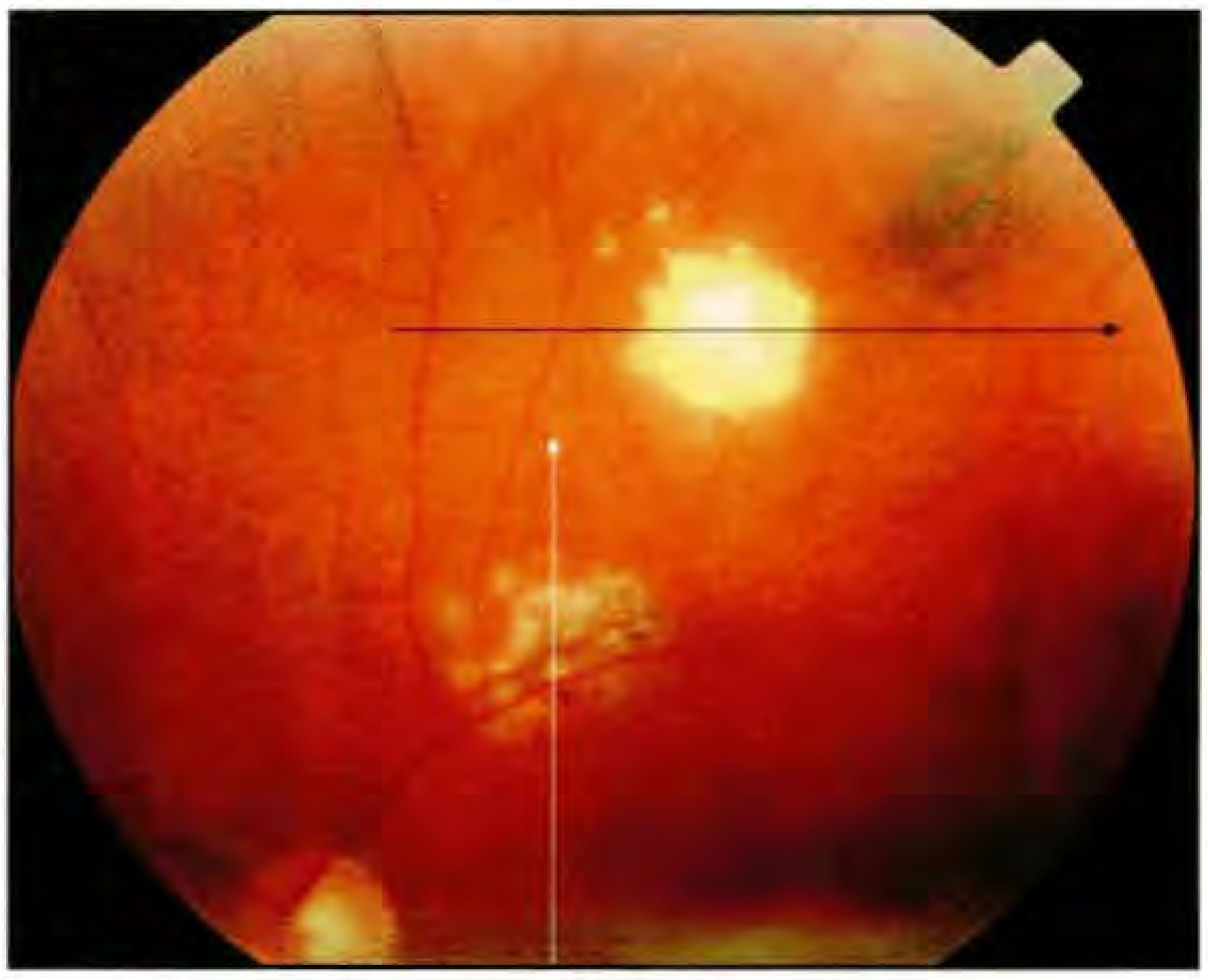

A

B

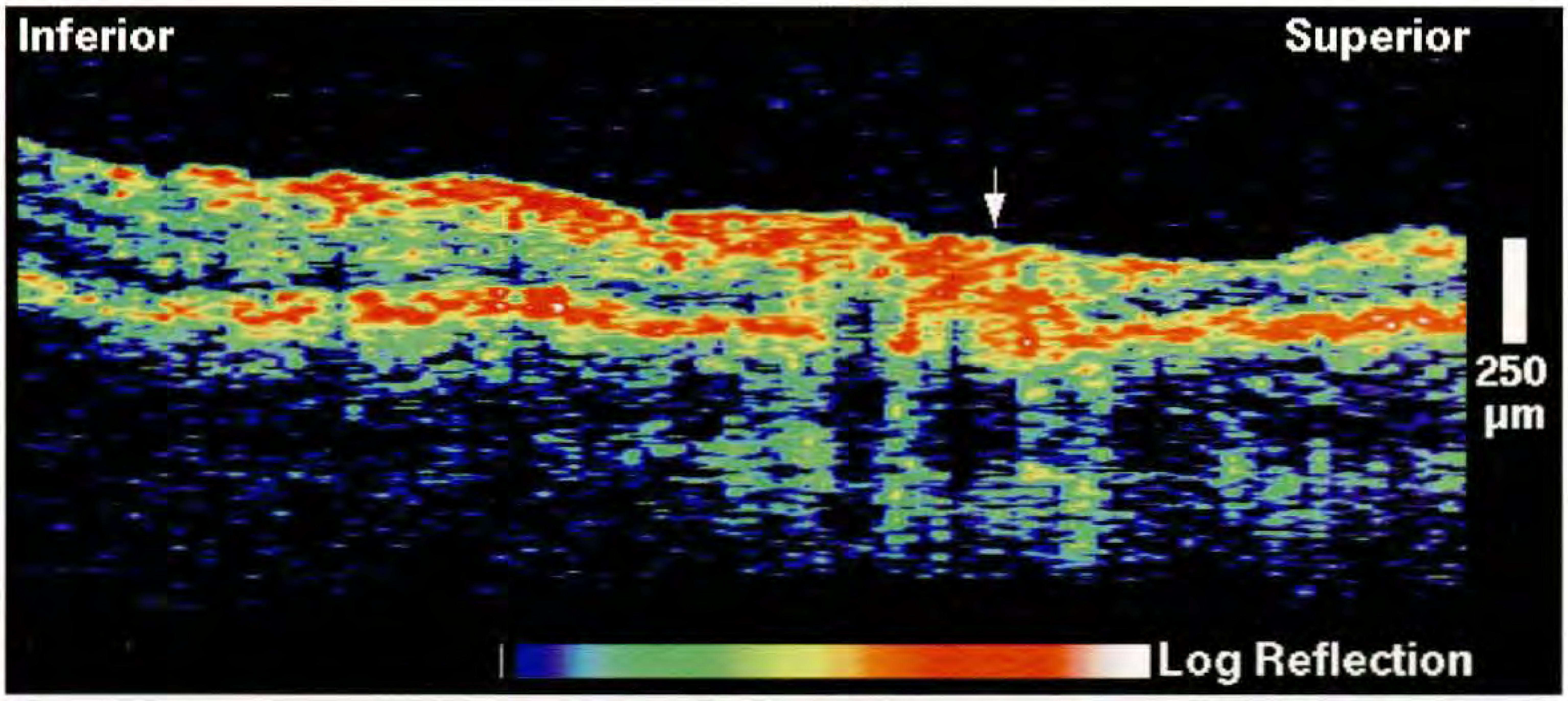

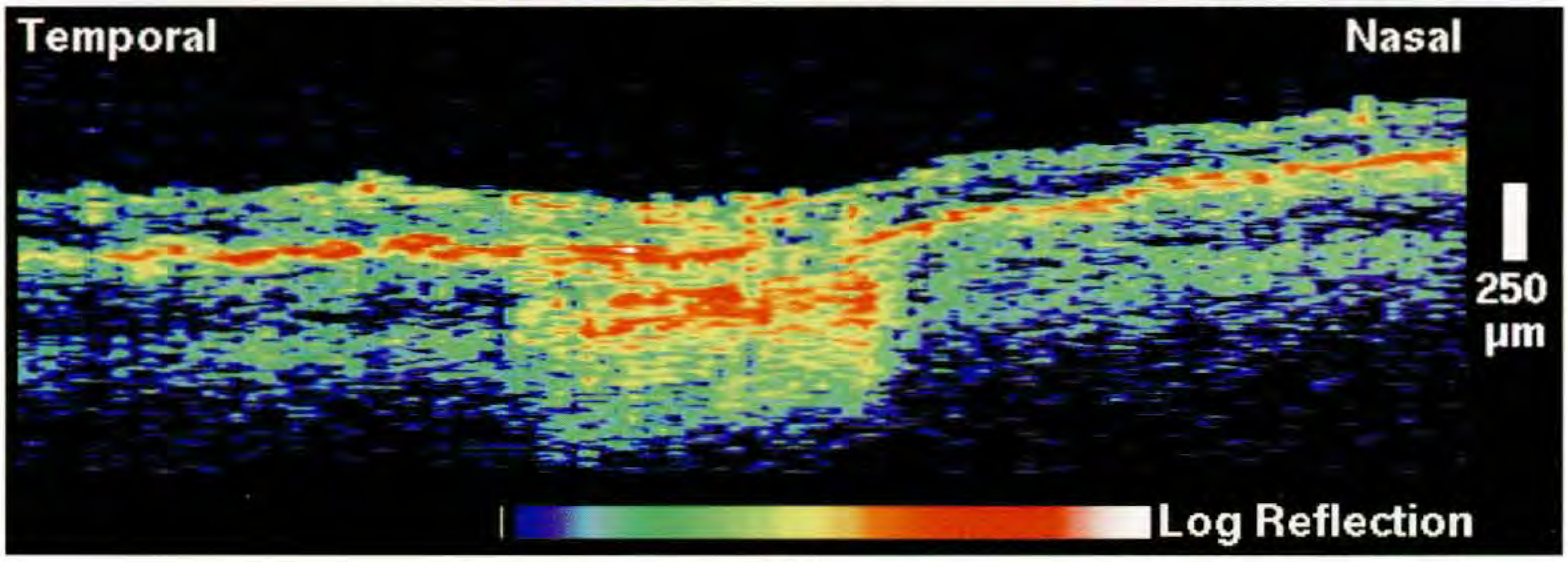

C

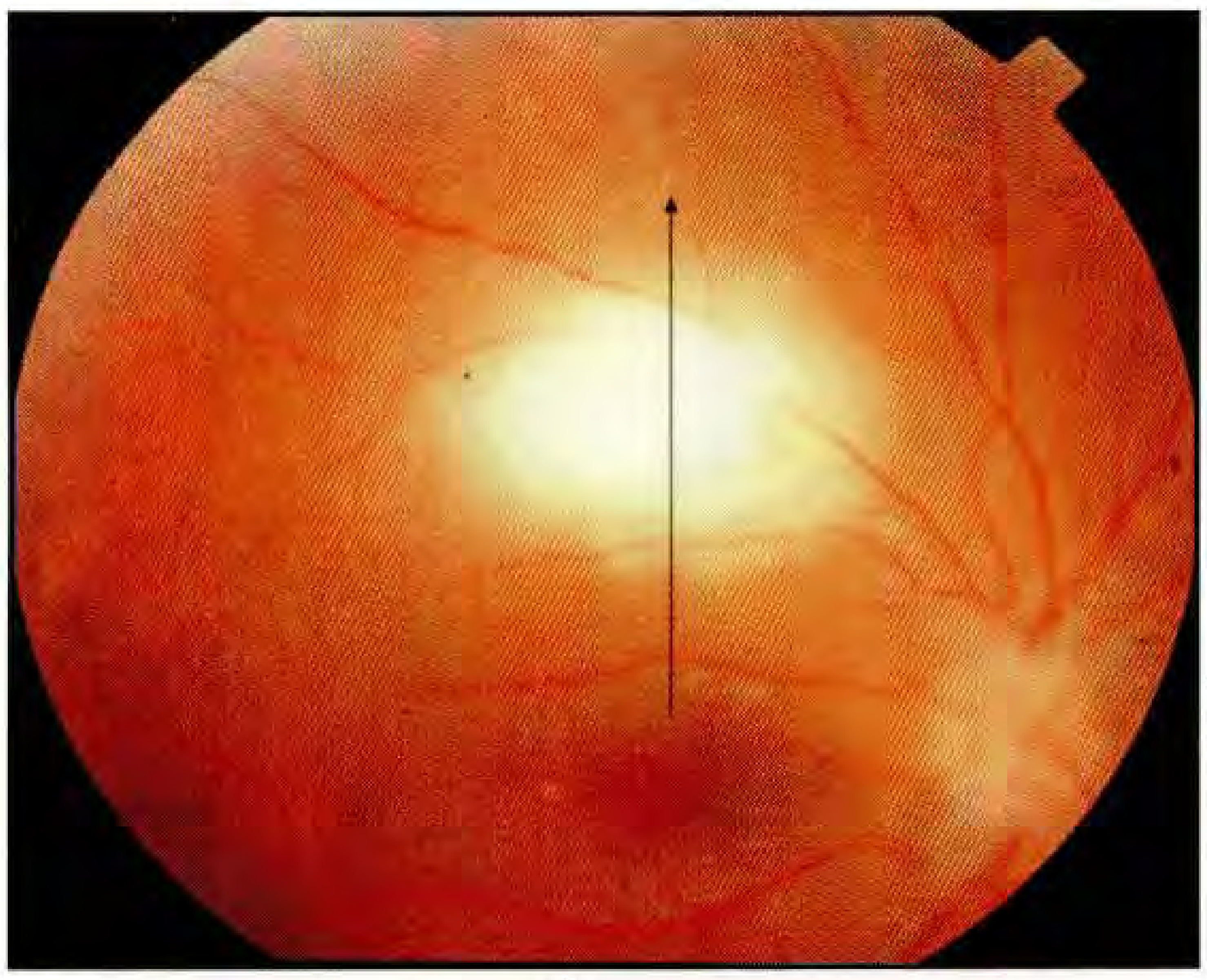

A

B

Case 9-9. Acute Toxoplasmosis Chorioretinitis

Clinical Summary

A 19-year-old woman had right eye pain with bluriness and floaters for two weeks. On examination, her vision in this eye was 20/60. Slit-lamp biomicroscopy (A) revealed a large, white-yellow lesion just beneath the superotemporal arcade, and swelling of the optic nerve. Fluorescein angiography (B) showed late leakage from the disc and the lesion consistent with papillitis and active inflammatory changes along the retinal venules, respectively. A presumptive diagnosis of toxoplasmosis retinitis was made.

Optical Coherence Tomography

A vertical scan (C) through the lesion exhibited a well-demarcated region of enhanced backscattering from the superficial retina consistent with inflammation in the inner retinal layers. The increased reflectivity from these layers shadowed the backscatter signal from the deeper retina and choroid. The involvement of the neurosensory retina was consistent with the predilection of toxoplasmosis for neural tissue. The retina appeared thickened throughout the lesion, although the retinal pigment epithelium could not be directly visualized in the image. Significant backscatter was also observed anterior to the retina, indicative of the migration of inflammatory cells into the vitreous. A partial detachment of the posterior vitreous face was noted throughout the inferior aspect of the lesion.

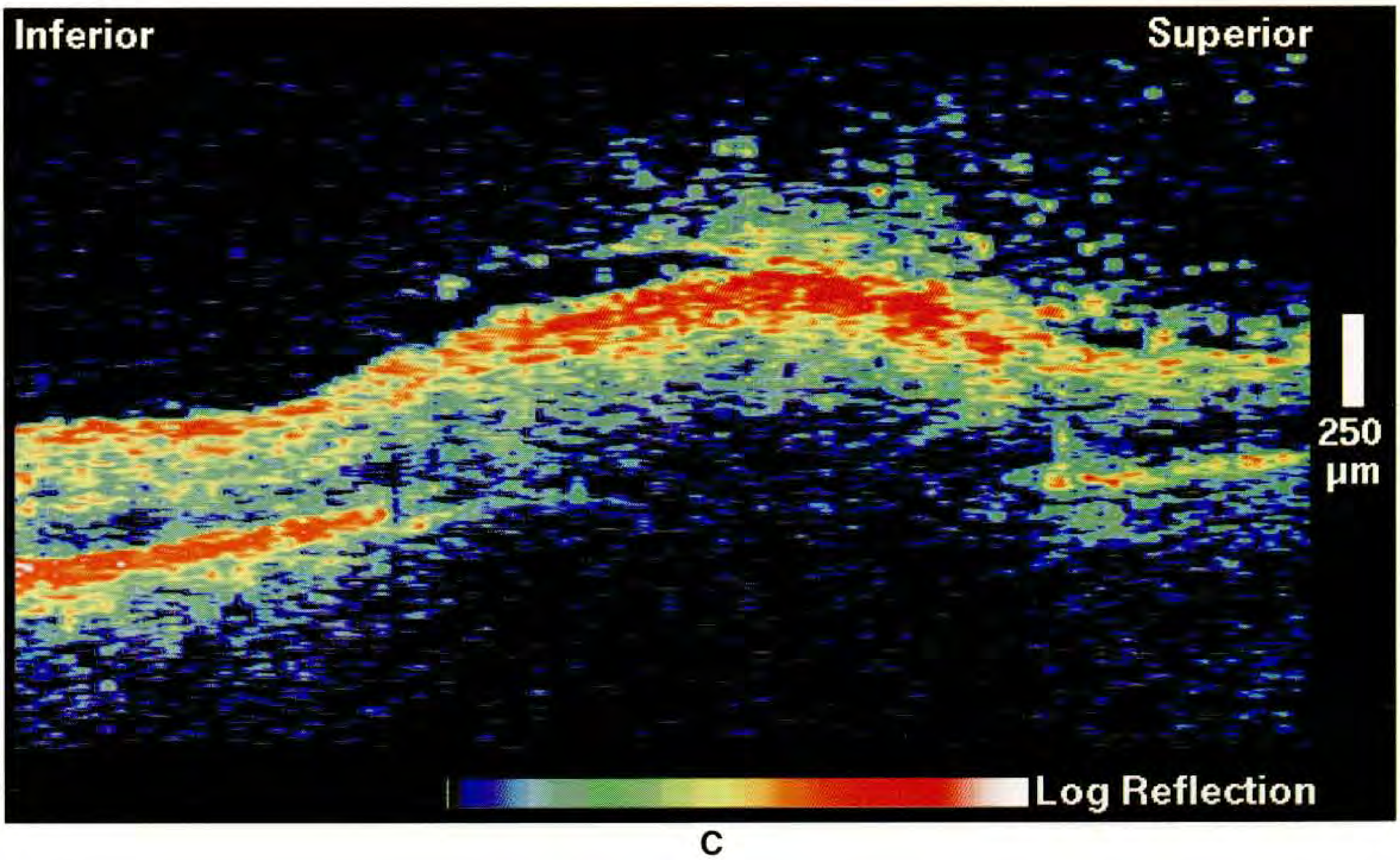

C

Case 9-10. Progressive Outer Retinal Necrosis

Clinical Summary

A 42-year-old man with human immunodeficiency virus (HIV) was referred for decreasing vision, flashes, and floaters in his right eye over the past month. On examination, the visual acuity in this eye was 20/100. Slit-lamp biomicroscopy (A) showed mild macular edema and a yellow subretinal lesion involving the fovea. Several other chorioretinal lesions were identified in the mid-periphery. A clinical diagnosis of progressive outer retinal necrosis was established.

Optical Coherence Tomography

Macular thickening and subretinal fluid accumulation were identified on OCT (B). The tomogram also delineated a focal area of enhanced backscattering from the outer retinal layers directly beneath the fovea. The reflection from the retinal pigment epithelium (RPE) appeared to be reduced in this area, due to either primary involvement of the RPE cells, or shadowing from the lesion above.

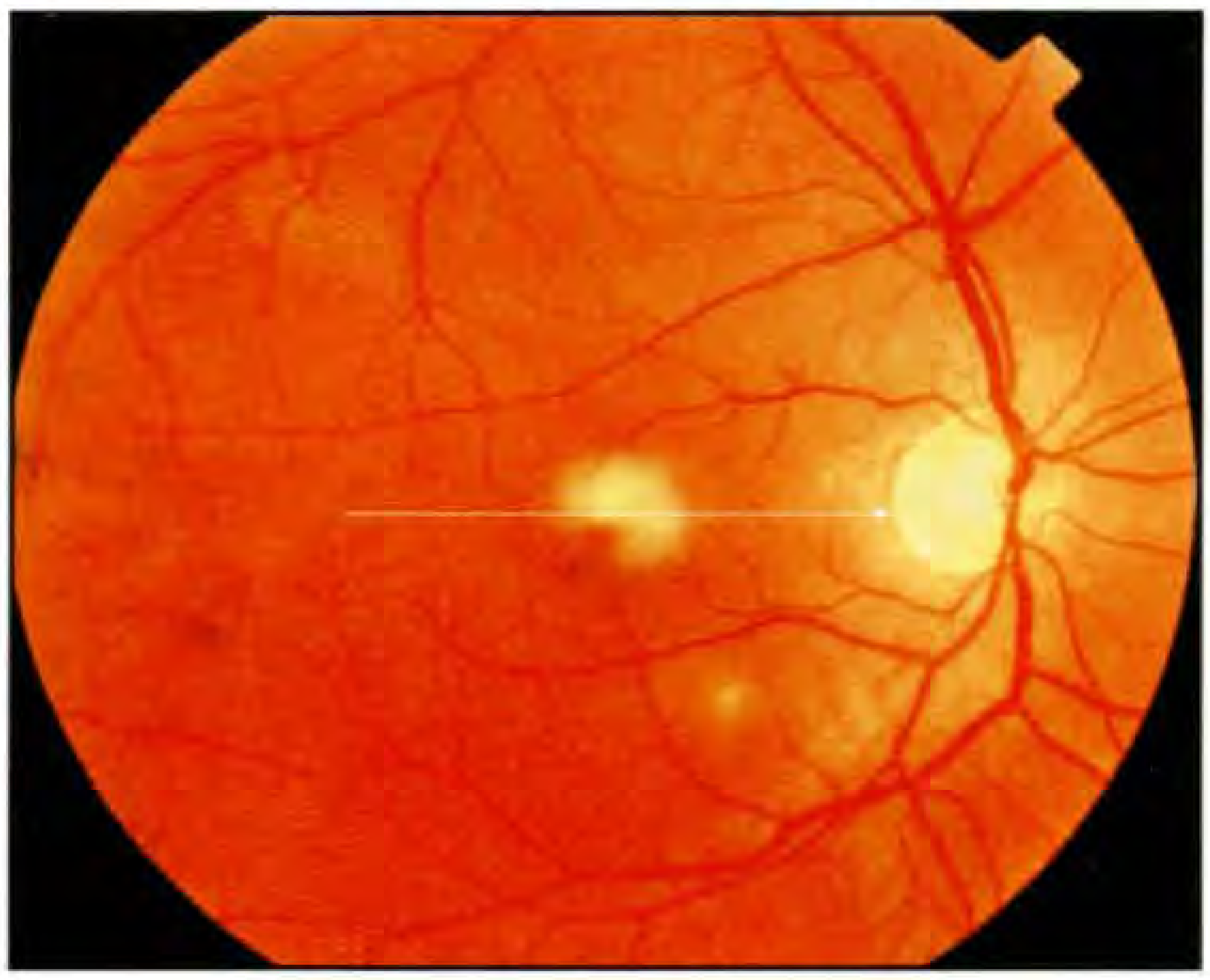

A

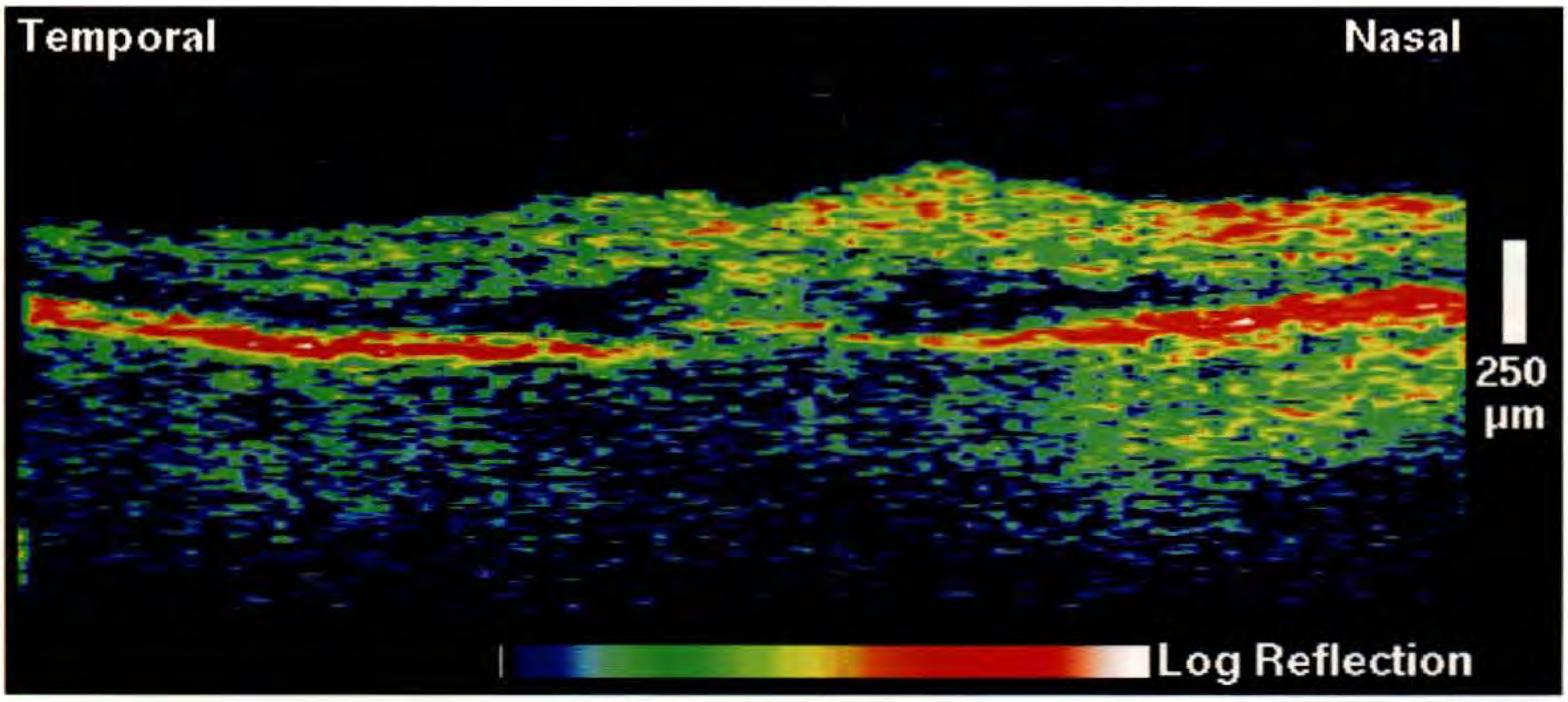

B

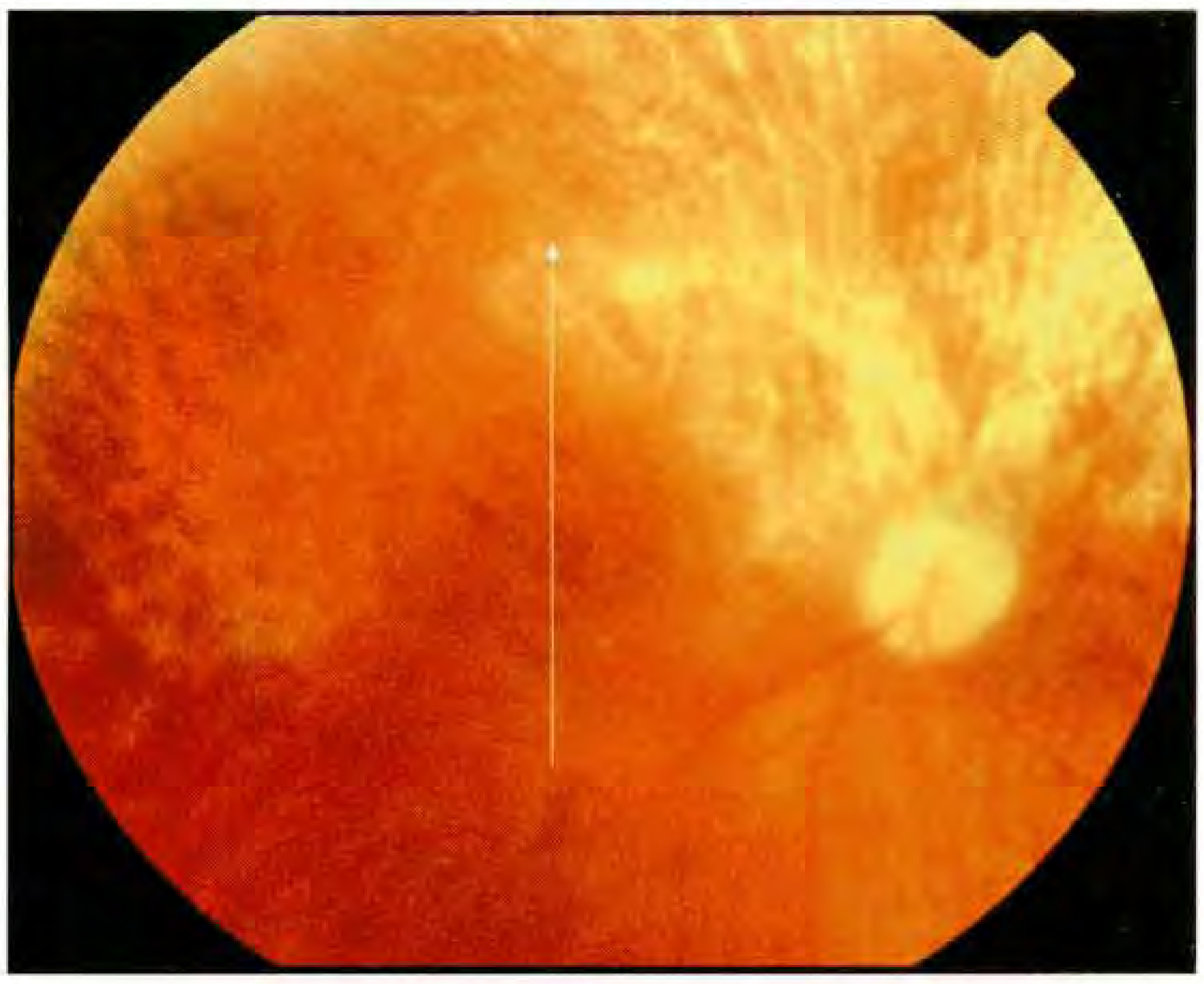

A

Case 9-11. Healed Cytomegalovirus Retini

Clinical Summary

A 36-year-old HIV+ man with a history of cytom lovirus (CMV) retinitis over the past two years notic continued loss of his peripheral vision in the right eye several months prior to examination. His best corre visual acuity on examination was 20/60. Dilated fur examination (A) of this eye showed healed CMV reti superiorly affecting almost half the retina.

Optical Coherence Tomography

A vertical OCT image (B) through fixation der strated a well-defined region of retinal atrophy sup to the center. The retina was severly thinned in this and increased reflectivity was observed in the choroid to fibrosis and scarring, and enhanced penetration o probe beam through the overlying retina. The normal tour of the fovea was absent.

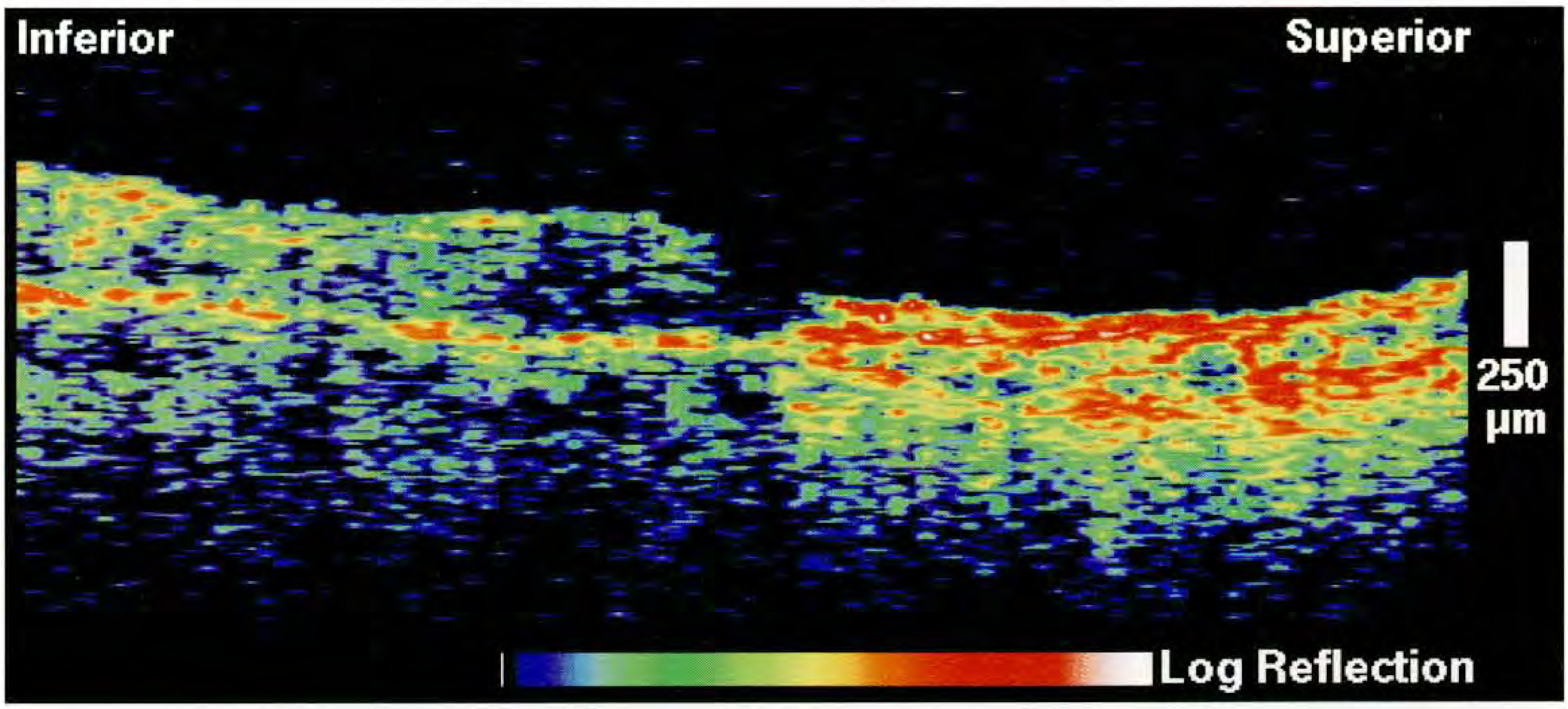

B

Case 9-12. Chorioretinal Scar from Previous Toxoplasmosis

Clinical Summary

A 23-year-old man had a history of toxoplasmosis in both eyes. The left eye (A) was notable for an atrophic and hyperpigmented chorioretinal scar involving the central macula. The visual acuity in this eye was 20/80.

Optical Coherence Tomography

An OCT image (B) taken through the scar displayed a complete loss of neurosensory retinal tissue consistent with an old, focal necrotizing retinitis. Increased reflectivity was observed from the retinal pigment epithelium (RPE) and choroid corresponding to epithelial hyperpigmentation and alteration of the choroidal architecture. The reflection from the choroid was fragmented due to shadowing by the hyperpigmented RPE.

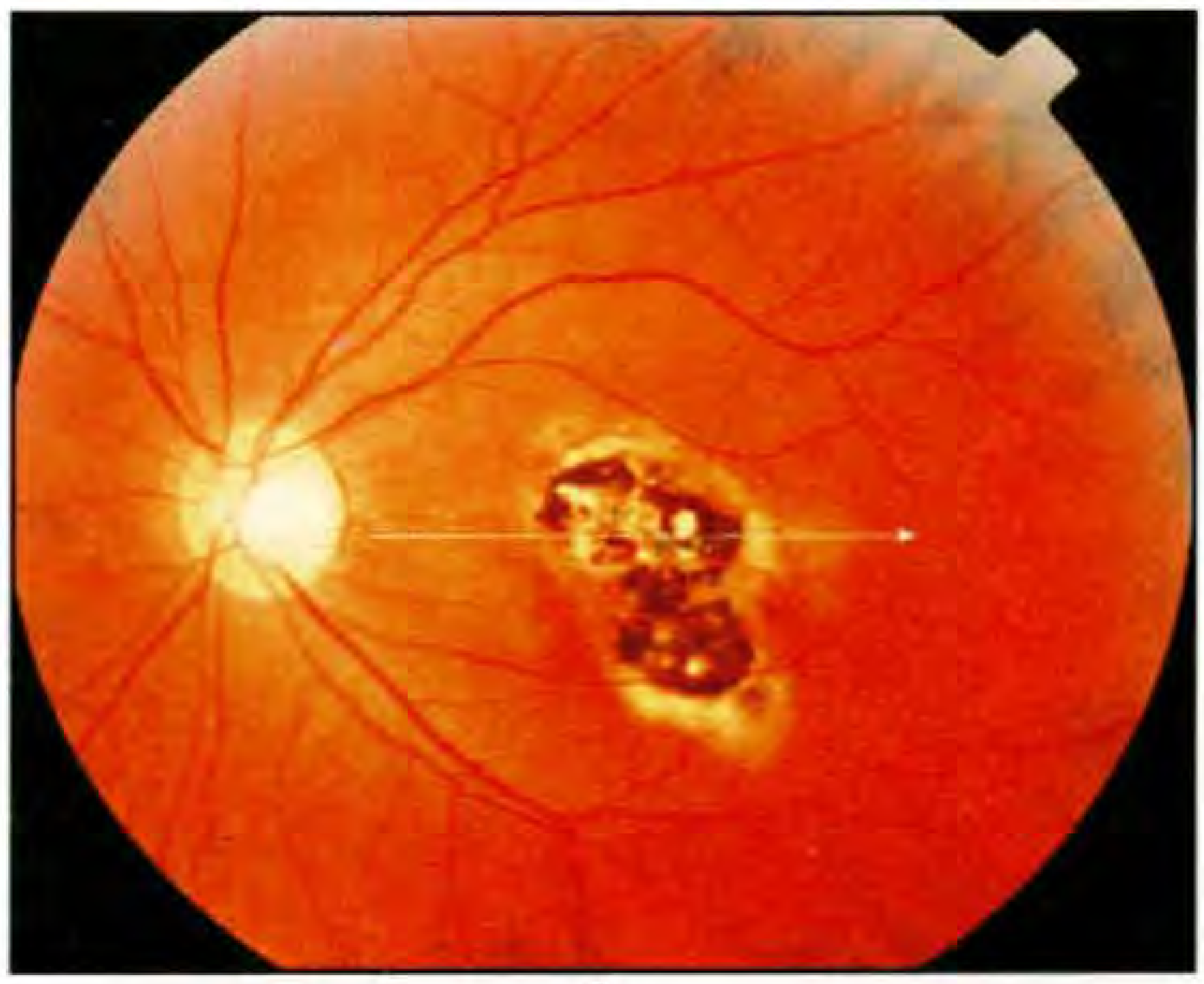

A

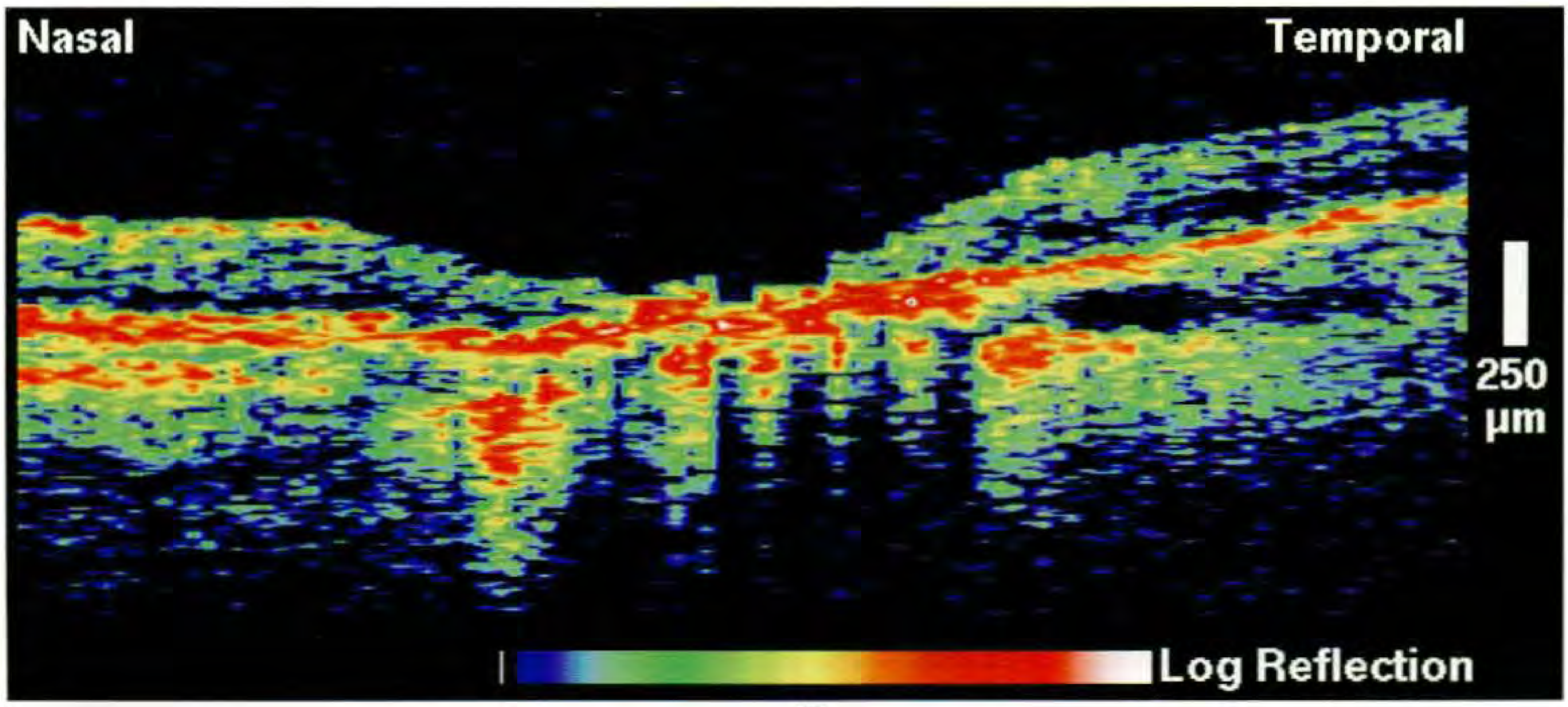

B

A

Case 9-13. HIV Retinopathy and Cotton Wool Spots

Clinical Summary

A 33-year-old man presented with a visual acuity of 20/30 in his right eye associated with the clinical diagnosis of HIV retinopathy. Dilated fundus examination (A) showed a cotton wool spot superior to the fovea and one temporal to the optic disc in the peripapillary region.

Optical Coherence Tomography

A vertical tomogram (B) through fixation demonstrated a focal region of enhanced backscattering (arrow) from within the neurosensory retina corresponding to the cotton wool spot. The outer retina appeared unaffected suggesting that the dominant effect of the ischemia was manifested in the retinal nerve fiber layer.

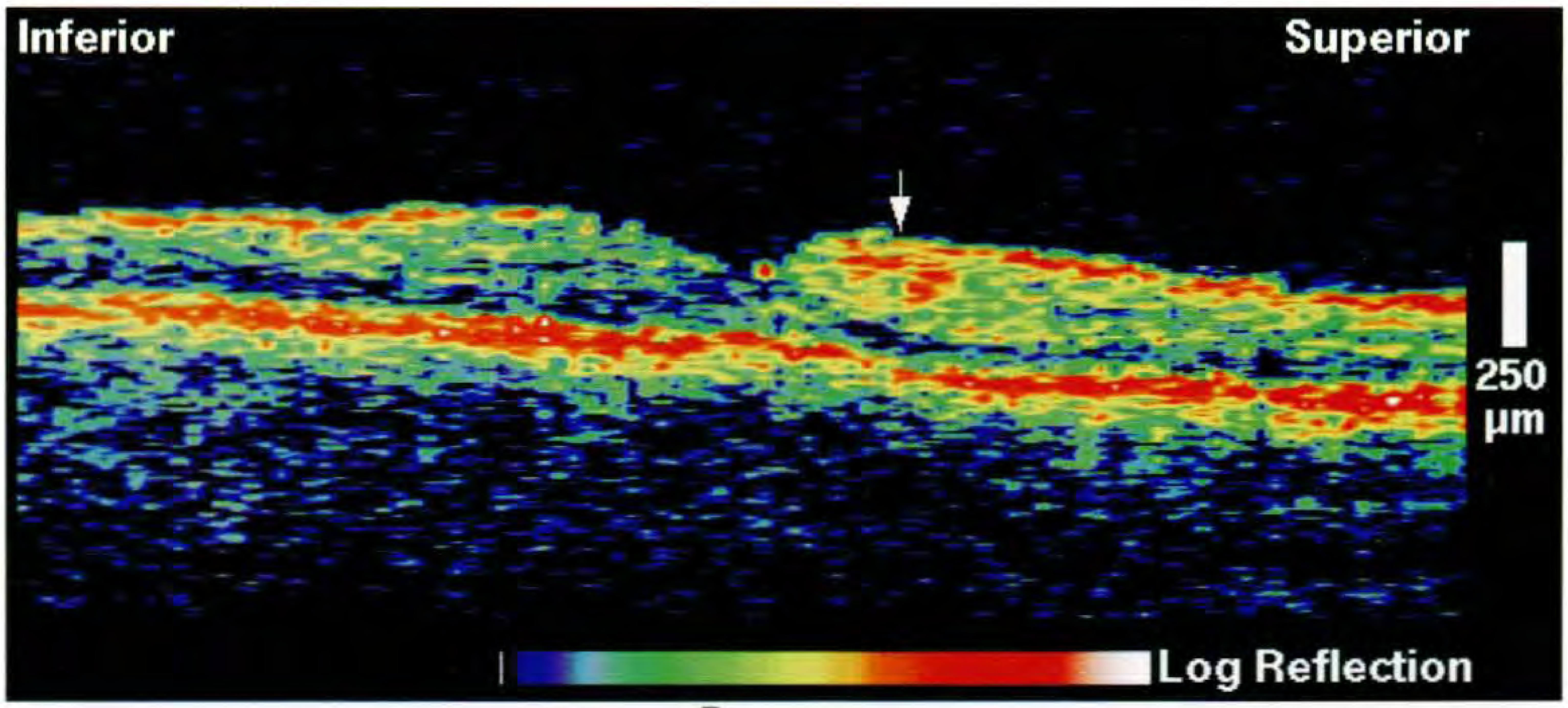

B

Case 9-14. HIV Retinopathy

Clinical Summary

A 24-year-old man with HIV retinopathy noticed decreasing visual acuity in his left eye. On examination, his visual acuity was 20/30. Slit-lamp biomicroscopy (A) revealed multiple cotton wool spots distributed along the inferotemporal and superotemporal arcades, mild edema of the optic disc attributed to neuroretinitis, and a star pattern of exudate directly in the fovea.

Optical Coherence Tomography

A horizontal OCT tomogram (B) through fixation delineated an abnormal band of increased backscatter directly within the fovea compatible with the exudate observed clinically. Significant retinal edema was noted nasal to the center approaching the optic disc. The fluid appeared to be concentrated in the outer neurosensory retina and exhibited minimal reflectivity.

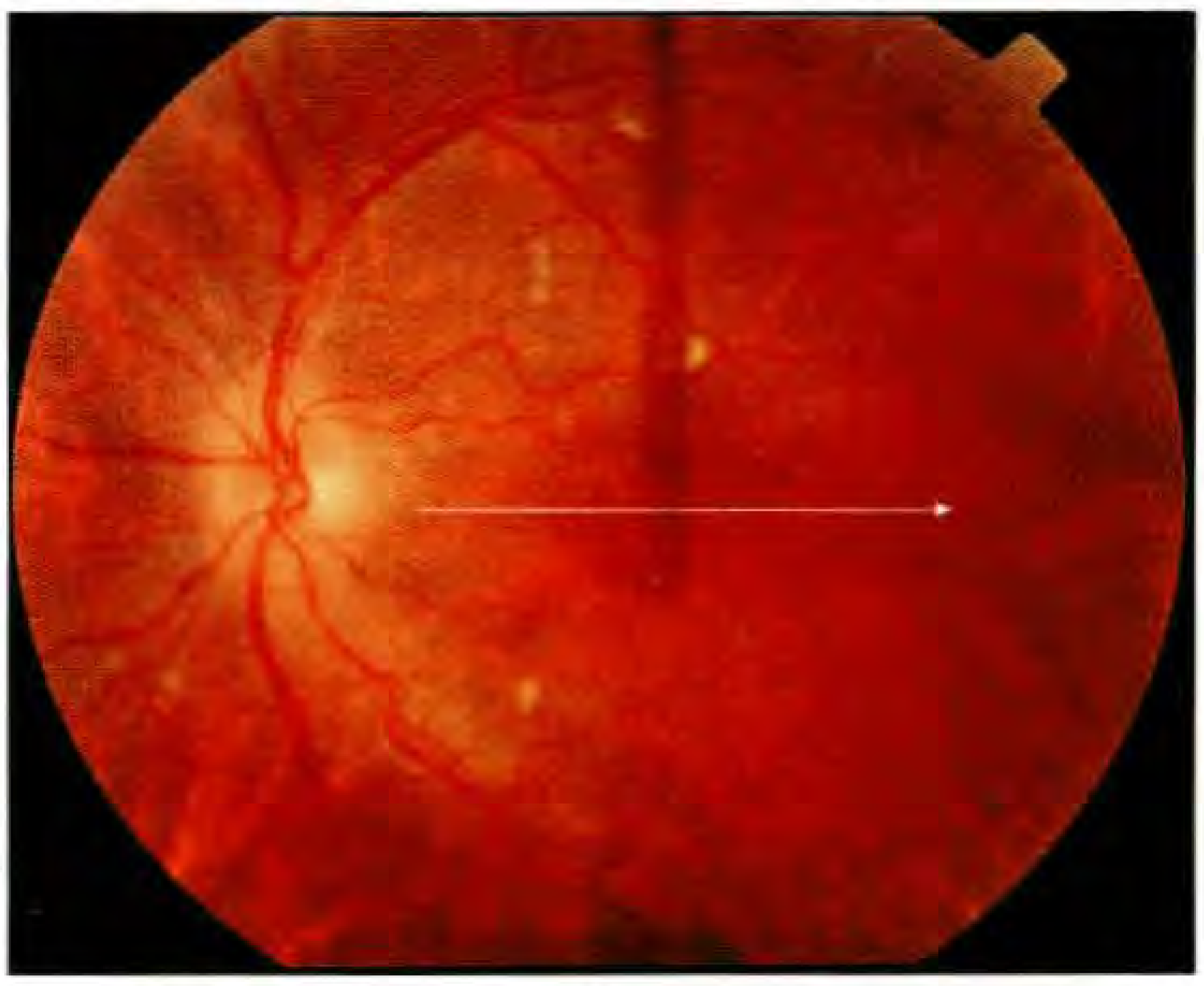

A

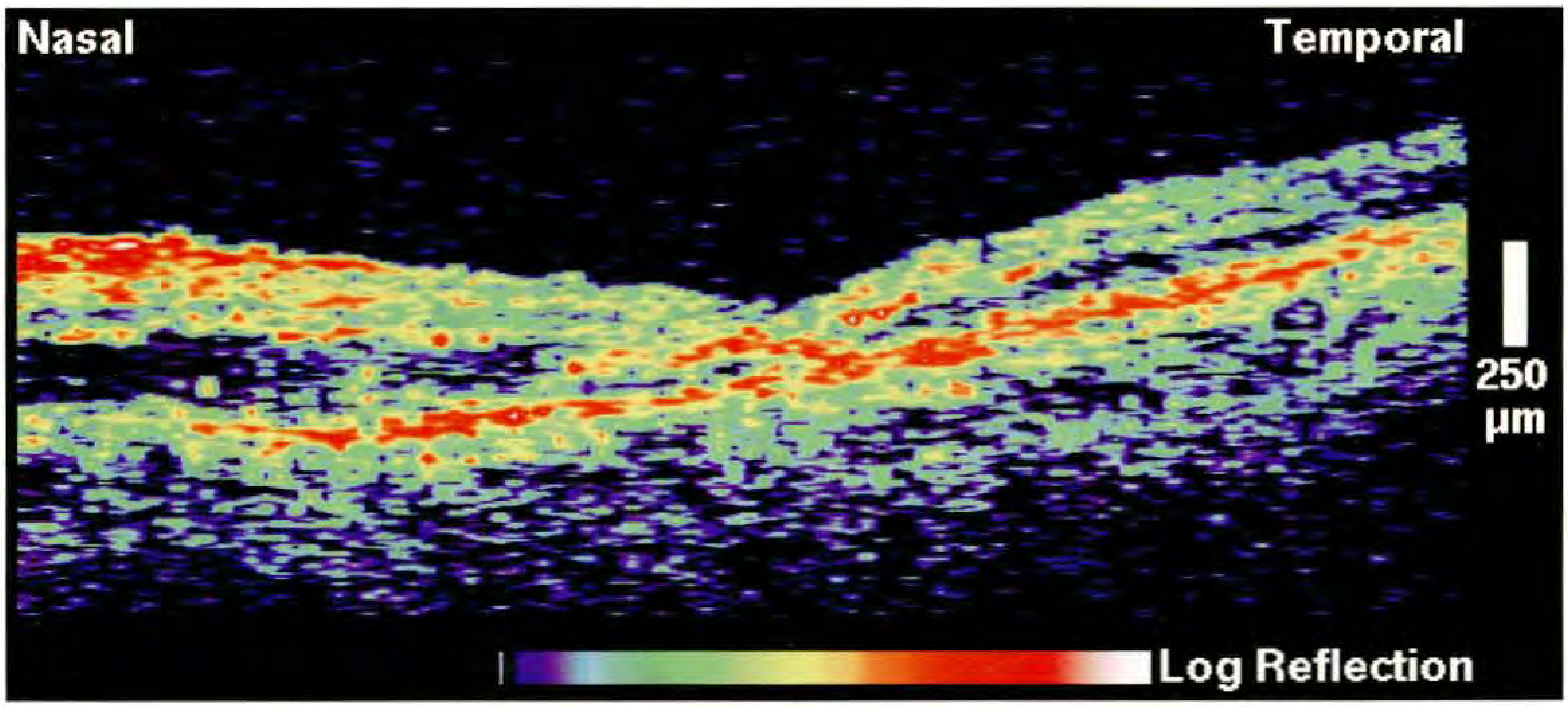

B

CHAPTER 10

Retinal Dystrophies

Adult Vitelliform Macular Dystrophy
Retinoschisis

OCT provides an *in vivo* alternative to histopathologic techniques for the study of hereditary and acquired retinal degenerations. In eyes with adult-onset vitelliform macular dystrophy [1,2], for example, OCT images show a moderately backscattering, subretinal lesion which is distinct from a serous detachment. The neurosensory retina is elevated overlying the lesion and exhibits an apparently compressed photoreceptor layer most likely accounting for the metamorphopsia typically occurring in these patients. Affected eyes may also demonstrate a focal loss of photoreceptors and pigmentary atrophy directly in the fovea [2] which appears on OCT as an abnormal foveal pit contour with increased light penetration into the choroid.

OCT images of retinoschisis reveal a splitting of the neural retina consistent with the classically described histopathological findings [3].

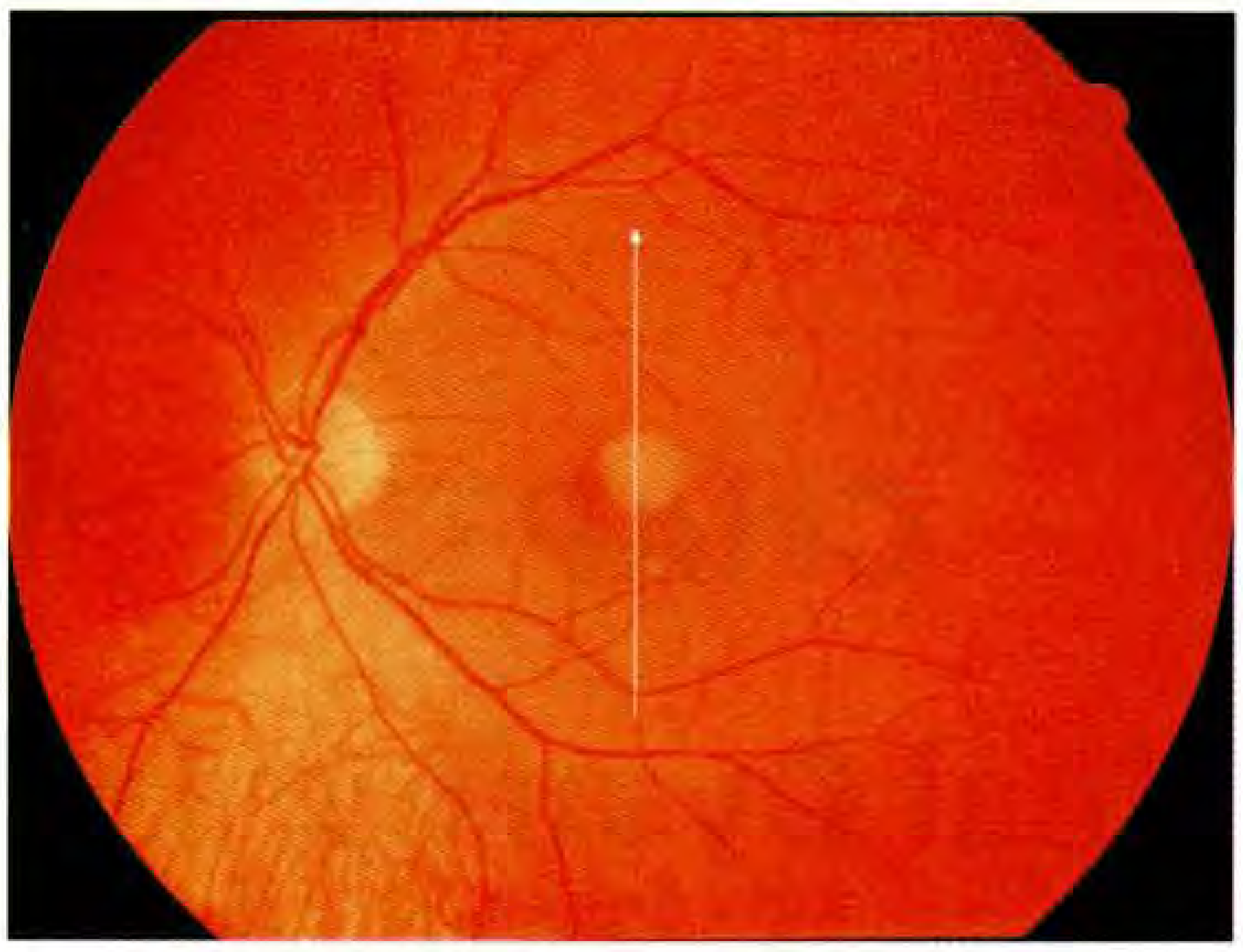

A

Case 10-1. Adult Pseudovitelliform Macular Dystrophy

Clinical Summary

A 56-year-old man had pseudovitelliform macular dystrophy. In the left eye, his visual acuity was 20/30. Examination of the fundus (A) showed a yellow vitelliform lesion in the central macula.

Optical Coherence Tomography

A vertical image acquired through fixation (B) demonstrated a well-circumscribed elevation of the retinal pigment epithelium above a moderately reflective region that appeared to have a defined posterior boundary. The foveal contour was altered due to the displacement of photoreceptors by the lesion.

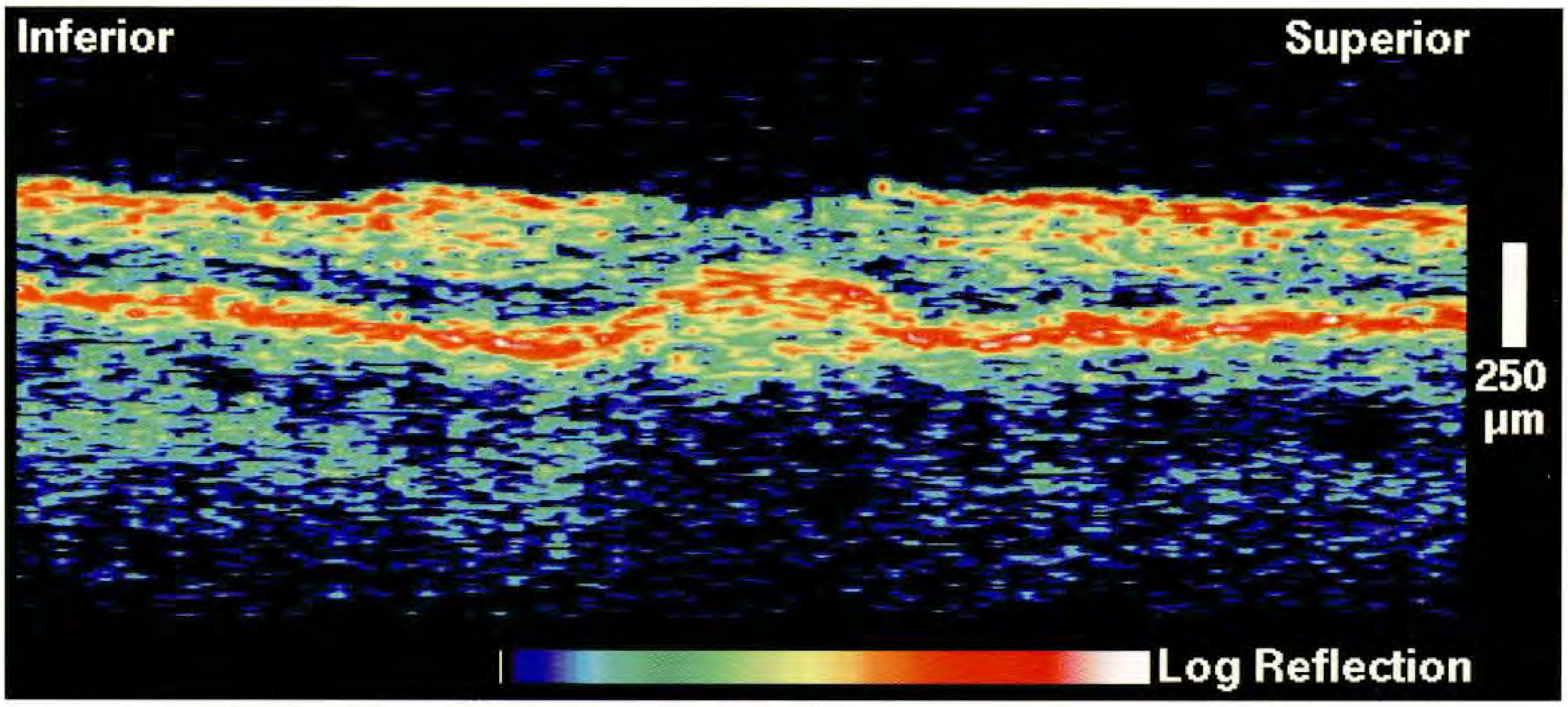

B

Case 10-1 continued

Clinical Summary

The right eye was remarkable for a punched-out region of chorioretinal atrophy in the central macula (C). The visual acuity in this eye was 20/200.

Optical Coherence Tomography

The OCT image (D) showed focal loss of photoreceptors in the fovea, and increased penetration of the probe beam into the choroid consistent with hypopigmentation of the retinal pigment epithelium and a window defect.

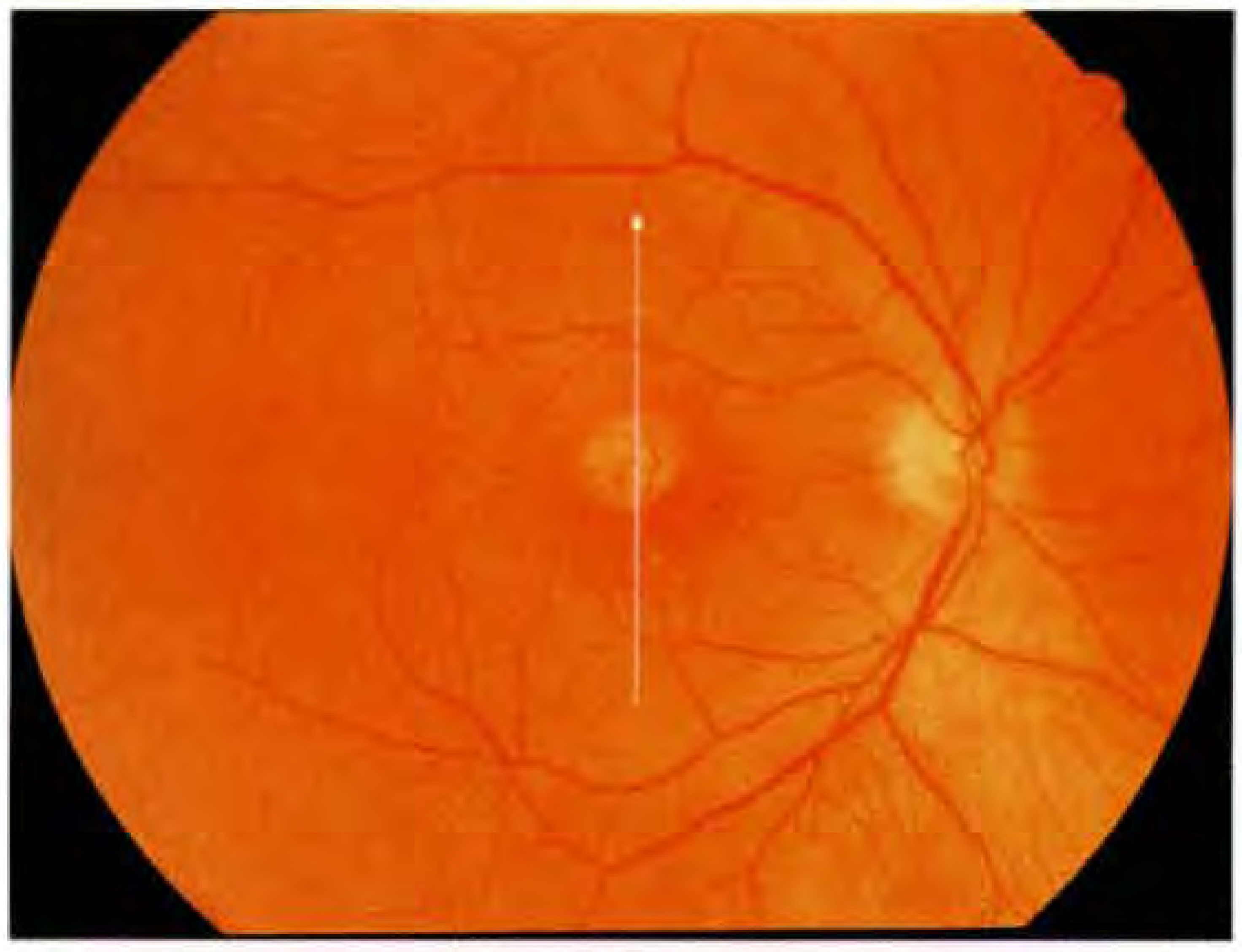

C

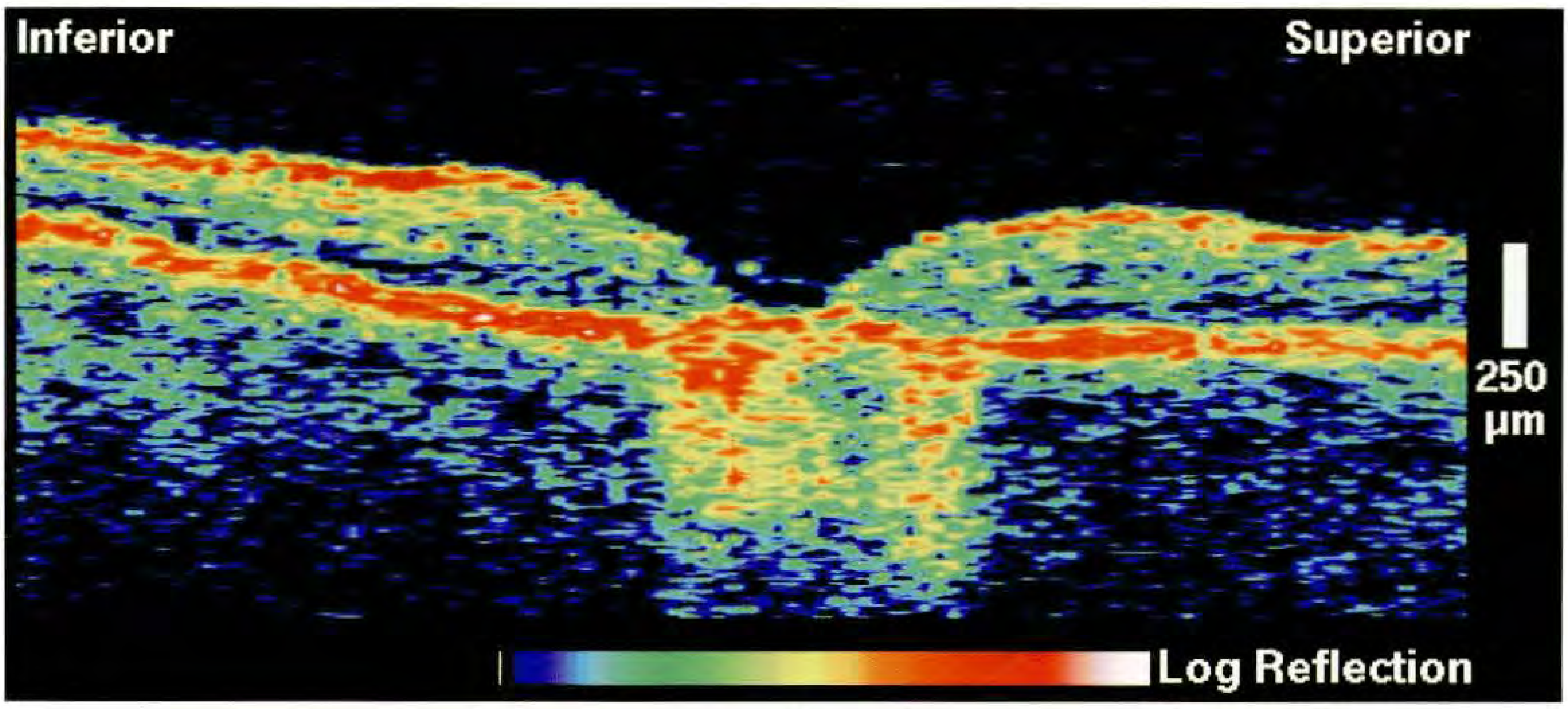

D

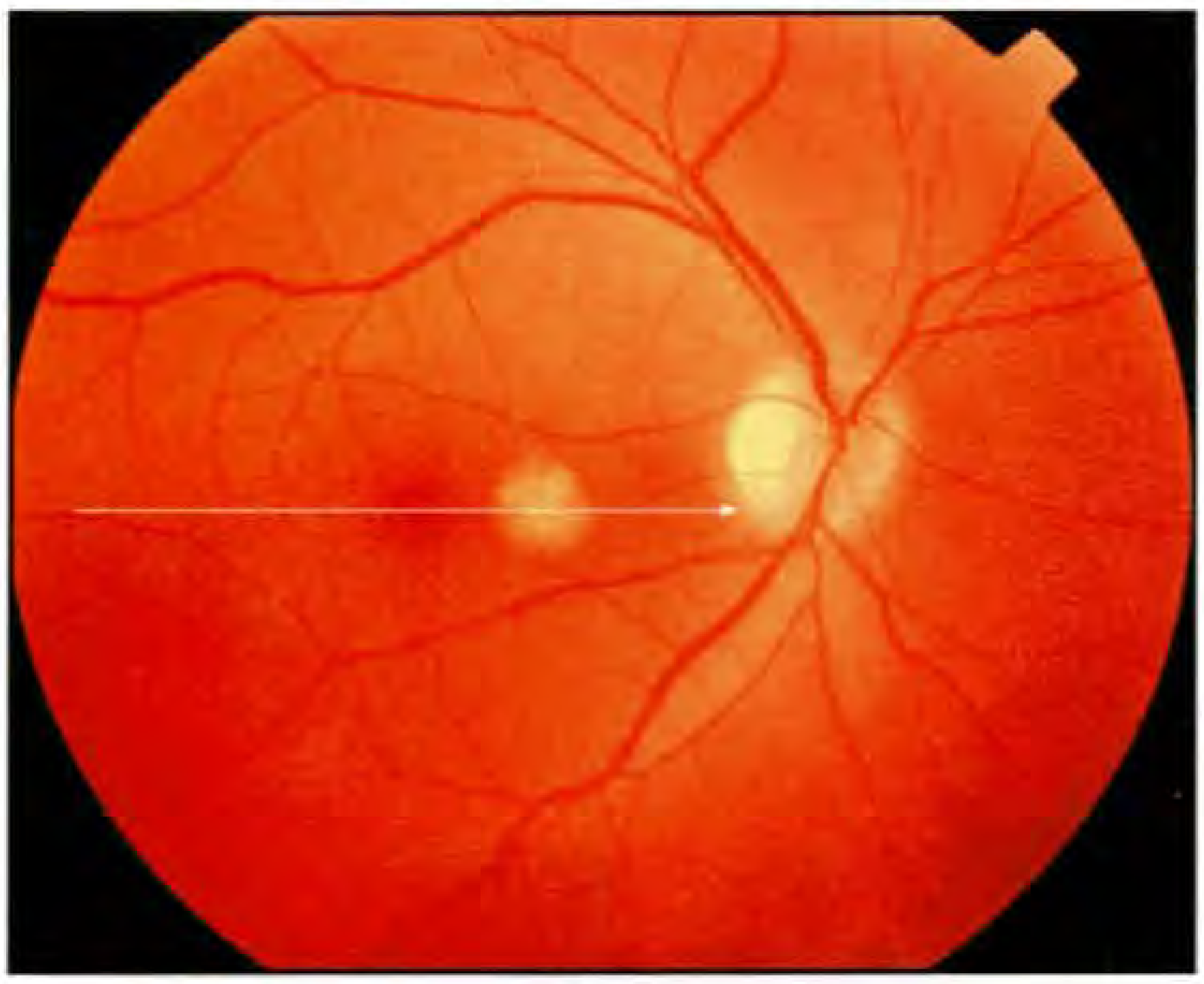

A

Case 10-2. Adult Pseudovitelliform Macular Dystrophy

Clinical Summary

A 58-year-old man with a history of adult vitelliform macular dystrophy was examined. His right eye showed a round, focal elevation of the retina and retinal pigment epithelium over a cream colored lesion just nasal to the fovea (A). The visual acuity in this eye was 20/25.

Optical Coherence Tomography

OCT examination (B) showed an elevation of the reflective band corresponding to the retinal pigment epithelium (RPE) nasal to fixation. The space below the RPE was moderately reflective and not appreciably shadowed by the RPE above, in contrast to the presentation of a serous pigment epithelial detachment. The retinal layers above the lesion appeared compressed.

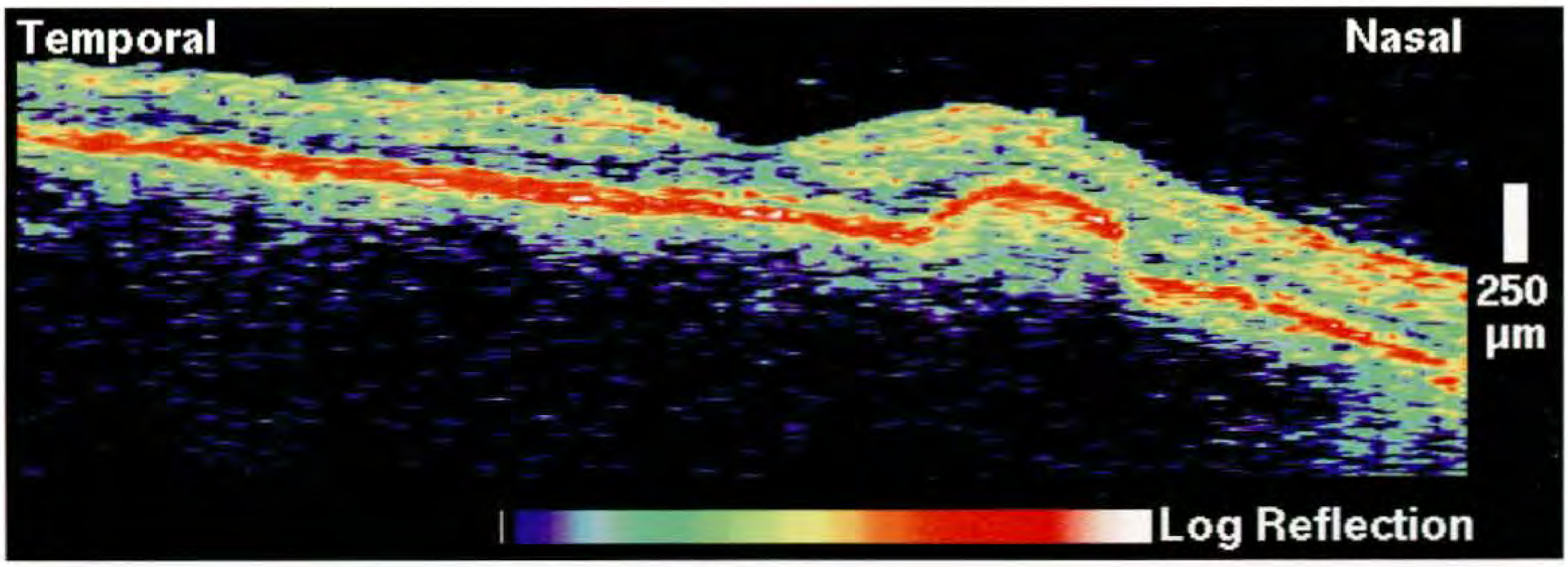

B

Case 10-2 continued

Clinical Summary

The left eye (C) revealed a similar, but slightly larger and more transparent lesion nasal to and involving the fovea. The visual acuity in this eye was correspondingly worse at 20/40.

Optical Coherence Tomography

OCT (D) again delineated the elevation of the RPE, which extended beneath the foveal pit. Comparatively less backscattering signal was observed beneath the RPE in this eye, consistent with the clinical examination. The lesion differed from a classic serous pigmental epithelial detachment because no shadowing of the choroidal reflections was noted.

C

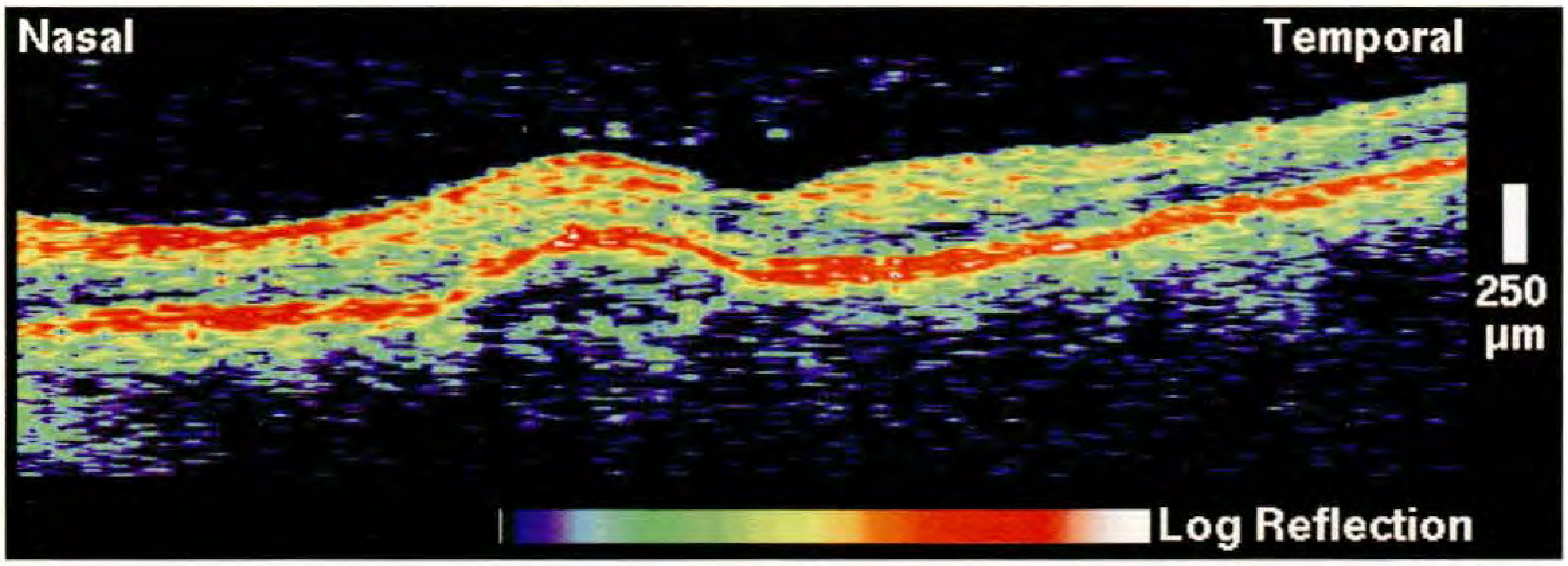

D

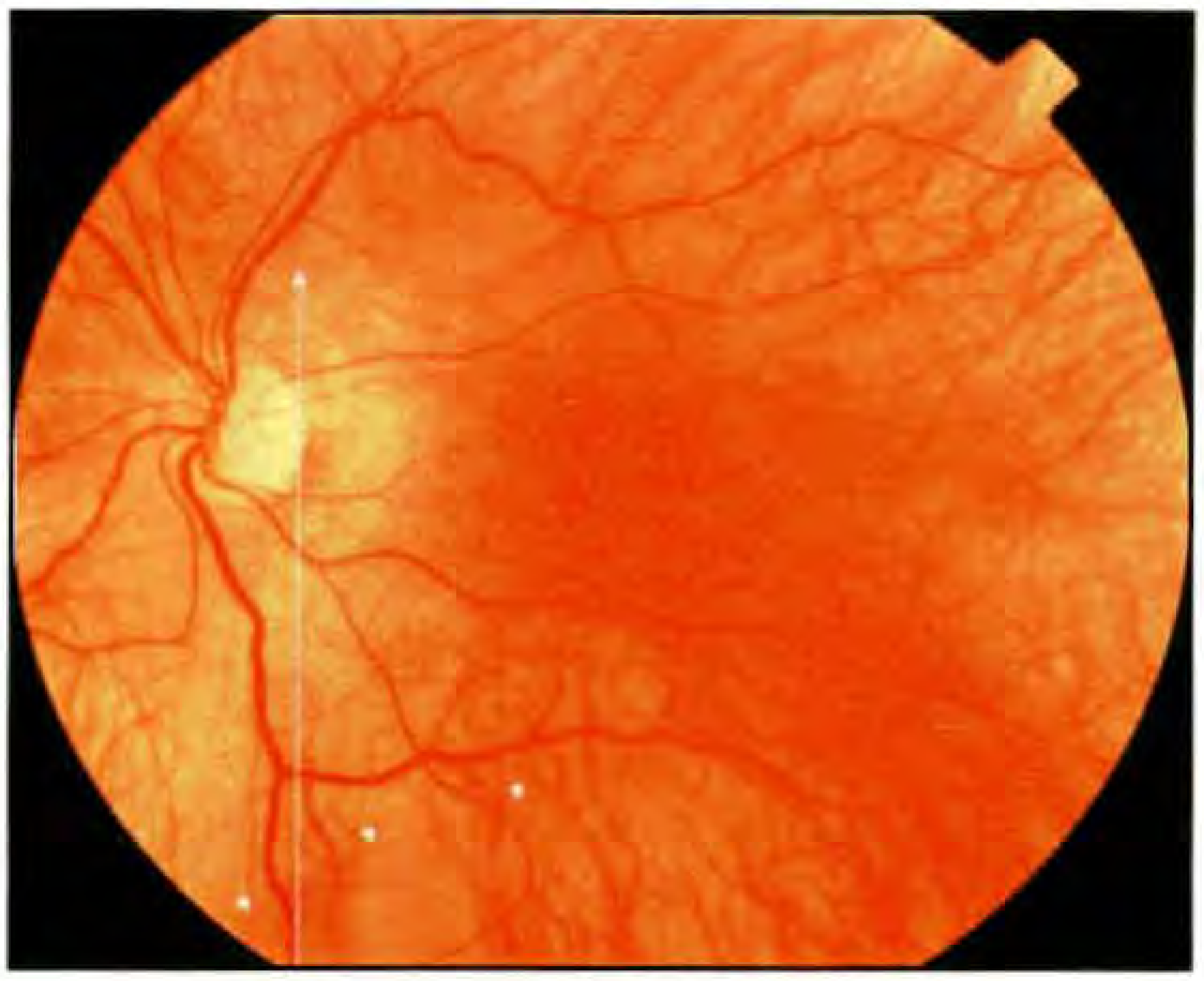

A

Case 10-3. Retinoschisis

Clinical Summary

A 48-year-old woman with acquired retinoschisis was evaluated (A). The schisis cavity was noted inferiorly and extended to within three disc diameters from the optic disc.

Optical Coherence Tomography

A vertical OCT image (B) demonstrated the upper edge of the schisis cavity, which contained an optically transparent space. The separation occured between the outer retinal layers. No bridging retinal elements were observed.

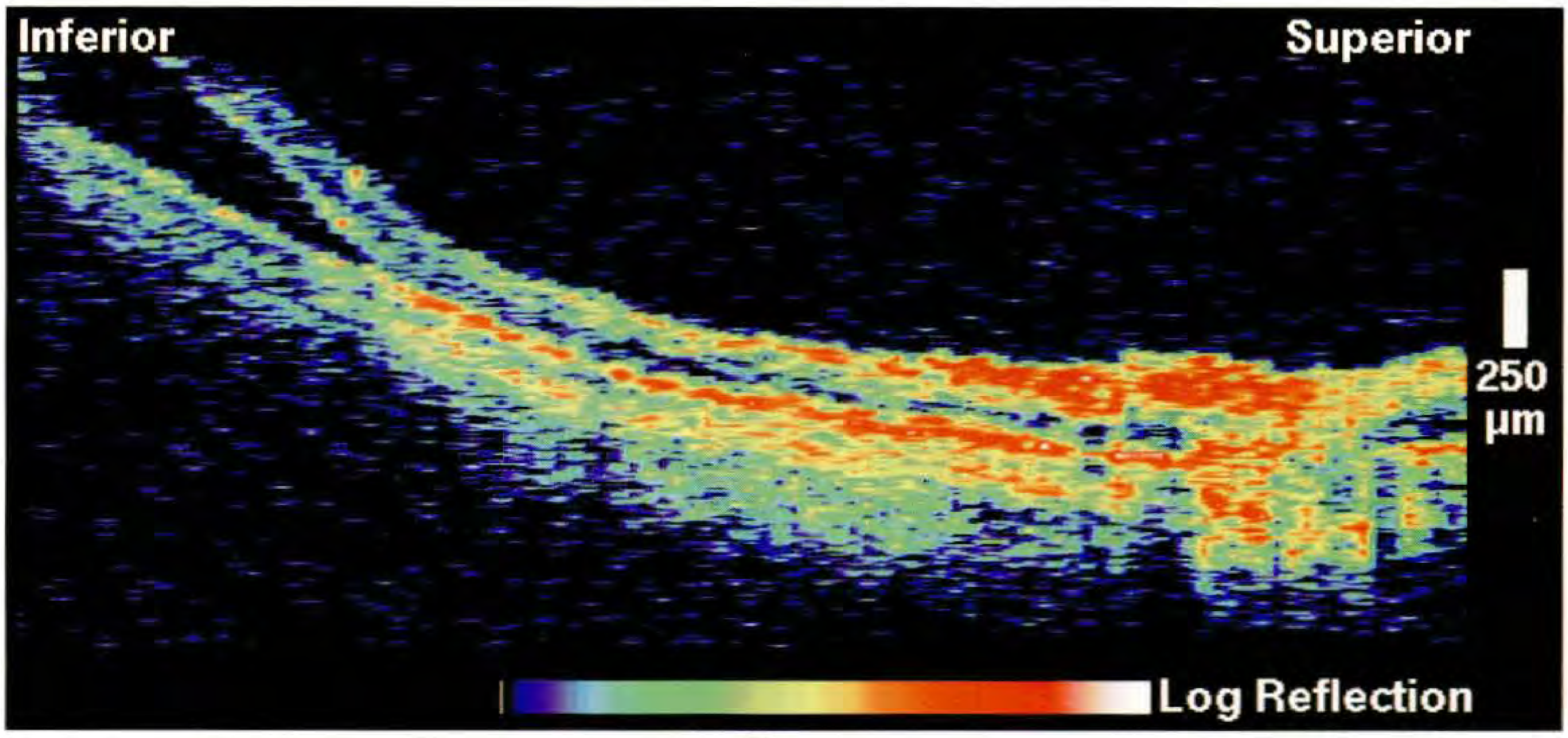

B

CHAPTER 11

Retinal Trauma

Valsalva Retinopathy
Laser Injury
Papilledema
Commotio Retinae
Intraocular Foreign Body
Traumatic Macular Hole

Non-penetrating ocular trauma can cause chorioretinal injury. OCT is particularly useful in evaluating small retinal changes, such as a traumatic macular hole, that are difficult to observe by ophthalmoscopy. OCT also may be effective when the direct or indirect view of the retina is obscured, because only part of the pupil aperture is necessary for OCT imaging [1]. Since OCT is non-contact and uses mostly infrared illumination, it is generally more comfortable to the traumatized patient than other examination techniques, such as contact lens biomicroscopy, fluorescein angiography, and ultrasound B-scan.

Hemorrhage is a common component of trauma. Blood is highly scattering [2], resulting in an intense reflectivity on OCT imaging that quickly attenuates the OCT probe beam and shadows the reflections from the deeper retinal layers. The magnitude of the reflectivity and shadowing depends on the concentration of scatterers with dense infiltrate causing higher reflectivity and reduced penetration of the OCT probe light. The appearance of a severe vitreous hemorrhage on OCT is demonstrated by a case of Valsalva retinopathy [3]. Changes in intraretinal reflectivity result from changes in tissue microstructure, which may be affected for example by edema, inflammatory infiltrate, or photothermal injury.

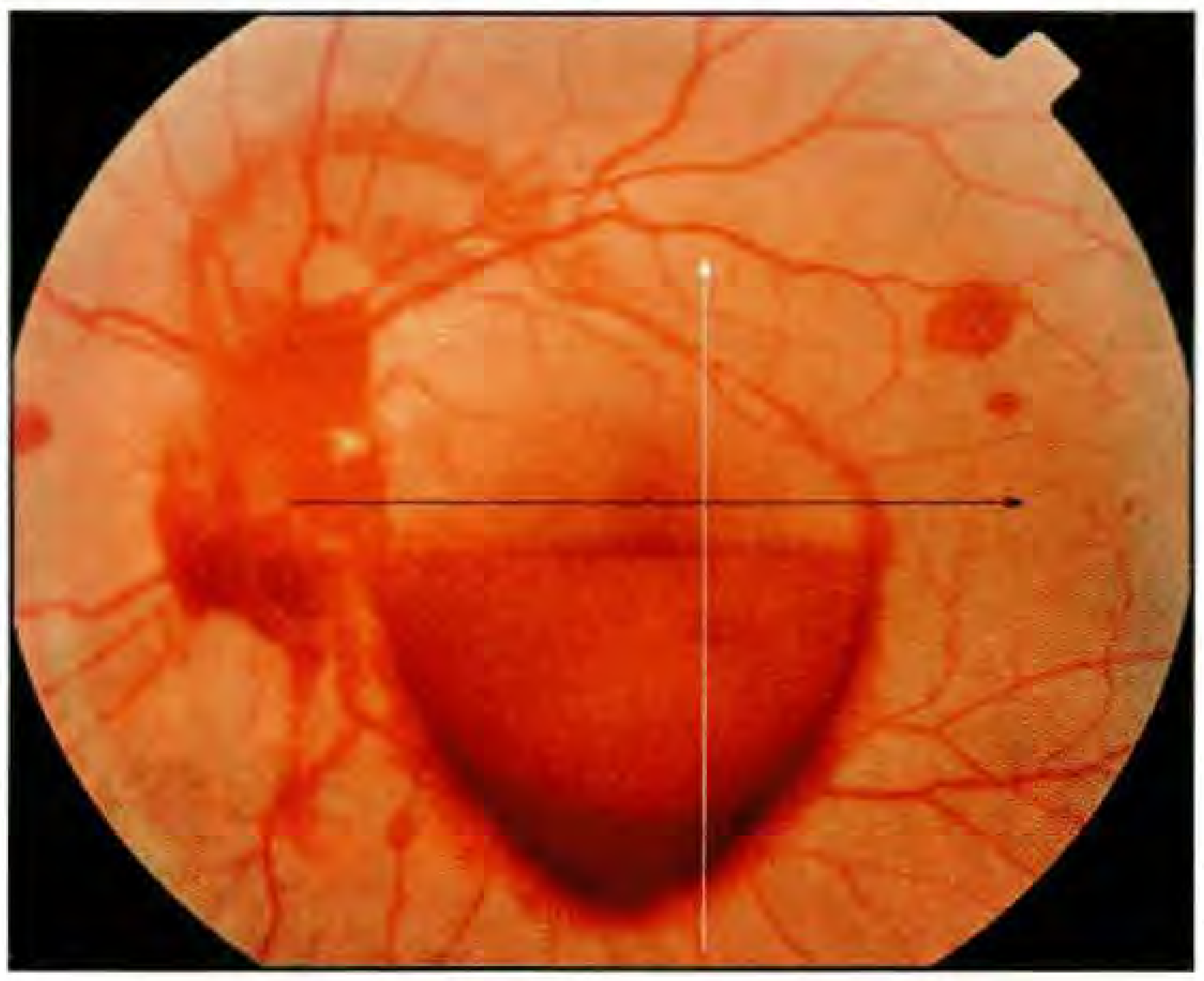

A

Case 11-1. Valsalva Retinopathy

Clinical Summary

A 38-year-old man with a recent episode of bronchitis presented to the emergency room after he noticed floaters and blurred vision in his left eye following a coughing episode. On examination, his visual acuity in this eye was 20/40. Indirect ophthalmoscopy (A) revealed a large, elevated subhyaloid hemorrhage in the inferior macula, mild peripapillary vitreous hemorrhage, and multiple blot hemorrhages around the optic nerve and midperiphery.

B

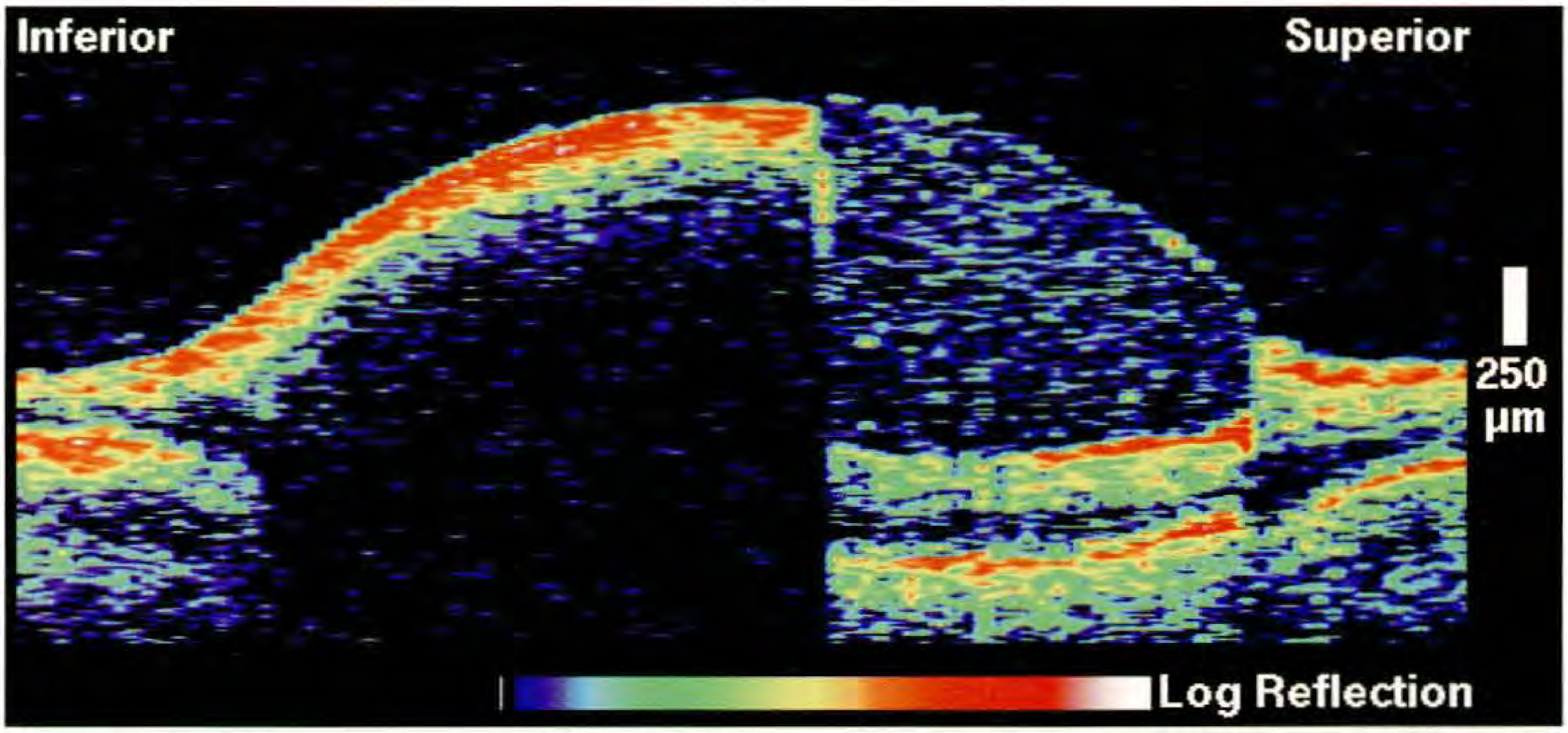

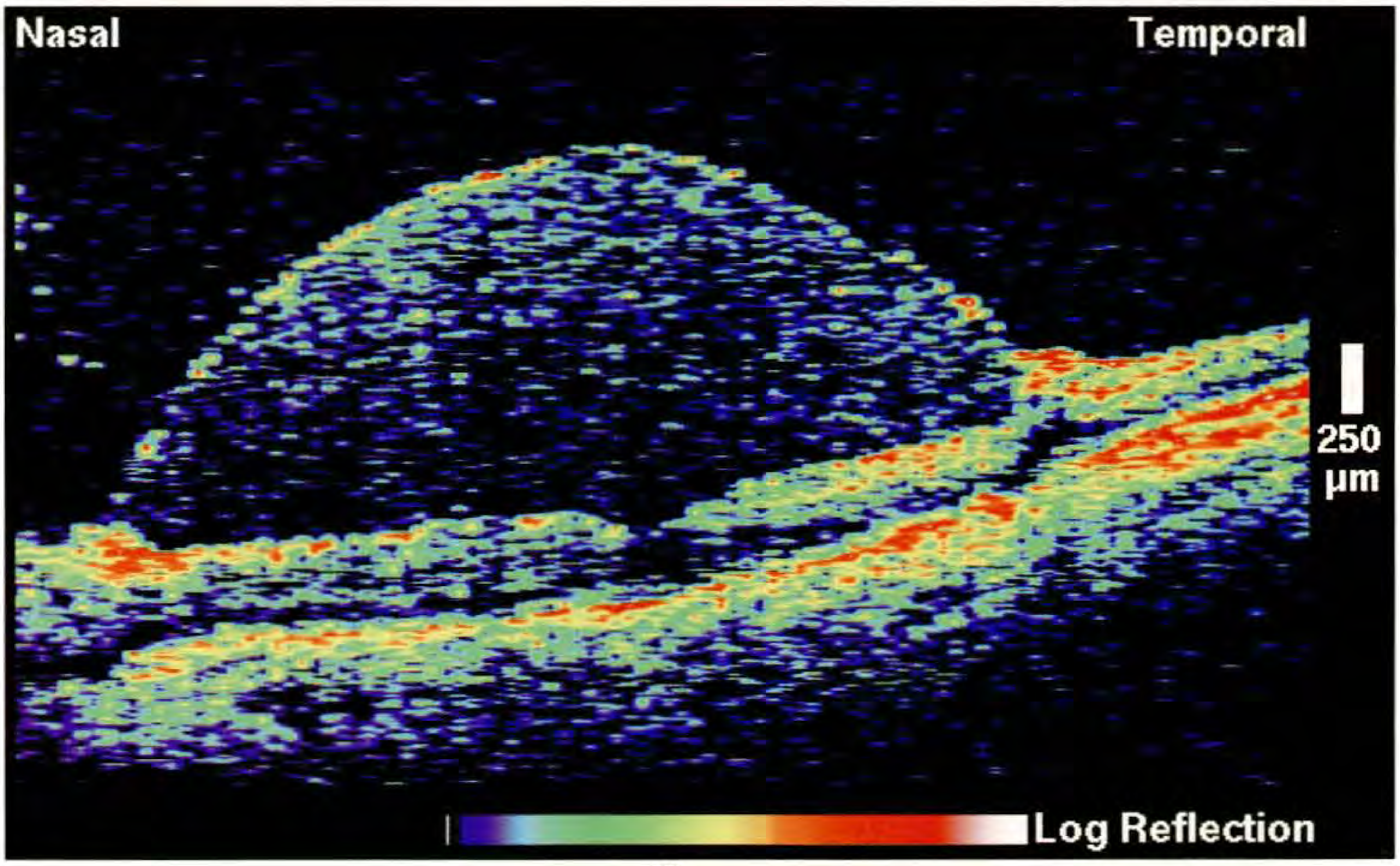

C

Case 11-1 continued

Optical Coherence Tomography

A vertical tomogram (B; white line on A) was divided into two well-defined regions. In the superior region, moderate backscattering was observed between the retina and the posterior hyaloid, which appeared to be exerting traction on the retina. The inferior portion of the image showed a brightly reflective band just beneath the detached posterior hyaloid that shadowed the retina below, consistent with subhyaloid hemorrhage.

A horizontal tomogram (C; black line on A) through fixation depicted slight retinal thickening directly in the fovea, and moderate subhyaloid backscattering signal anterior to the retina. The scattering seemed to be more intense close the vitreous, with the signal decaying slightly towards the retina.

Follow-up Examination

A single ND:YAG laser pulse was applied that day to open the posterior hyaloid and facilitate clearing of the hemorrhage. The patient returned for a follow-up examination one month later with no improvement in visual acuity and continued floaters in his vision. Slit-lamp biomicroscopy (D) displayed old, gray subhyaloid hemorrhage in the inferior macula and trace epiretinal membrane centrally.

Follow-up Optical Coherence Tomography

OCT examination (E) depicted a thin, highly reflective band anterior to the retina, representing either the posterior hyaloid, or an epiretinal membrane contiguous with the posterior hyaloid. The foveal pit appeared slightly narrowed, and mild retinal thickening was observed in the center.

D

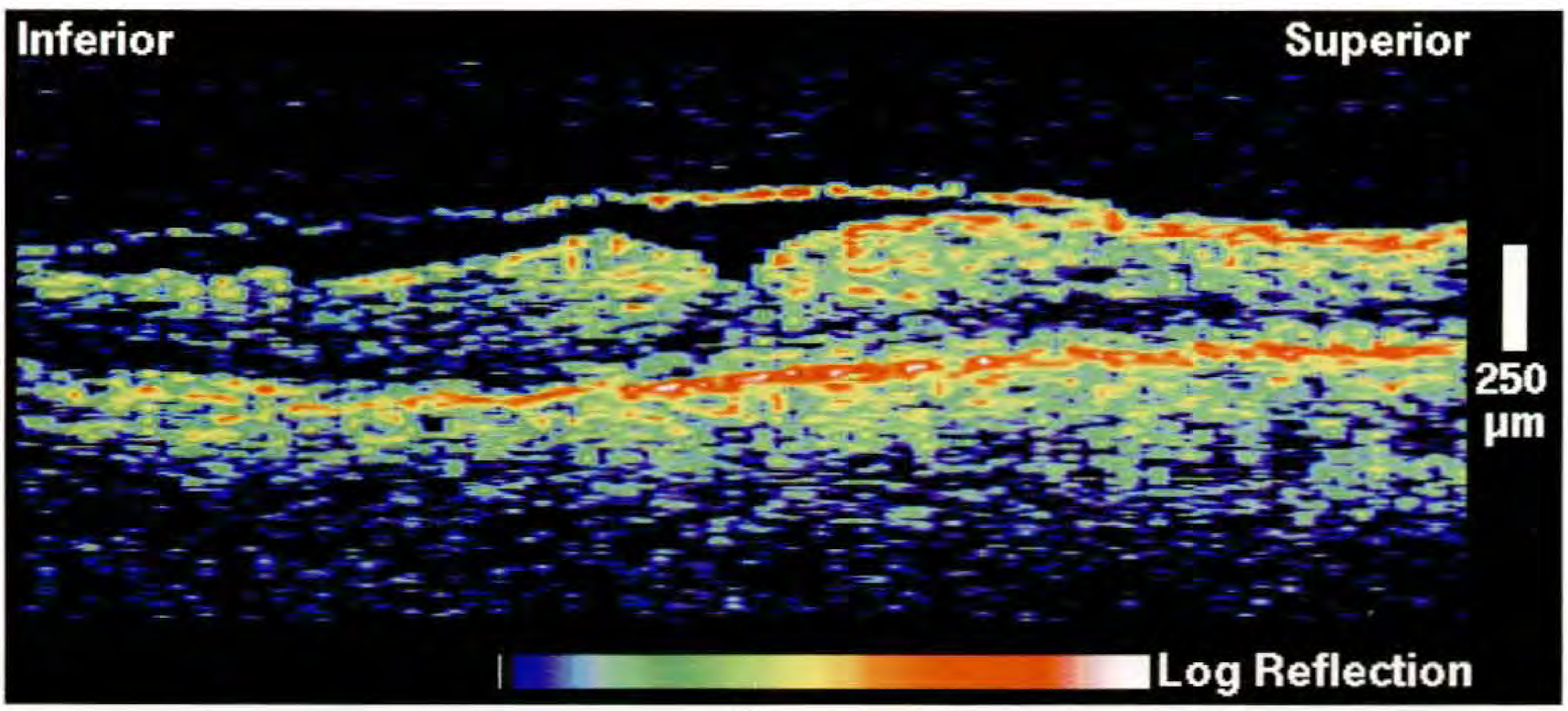

E

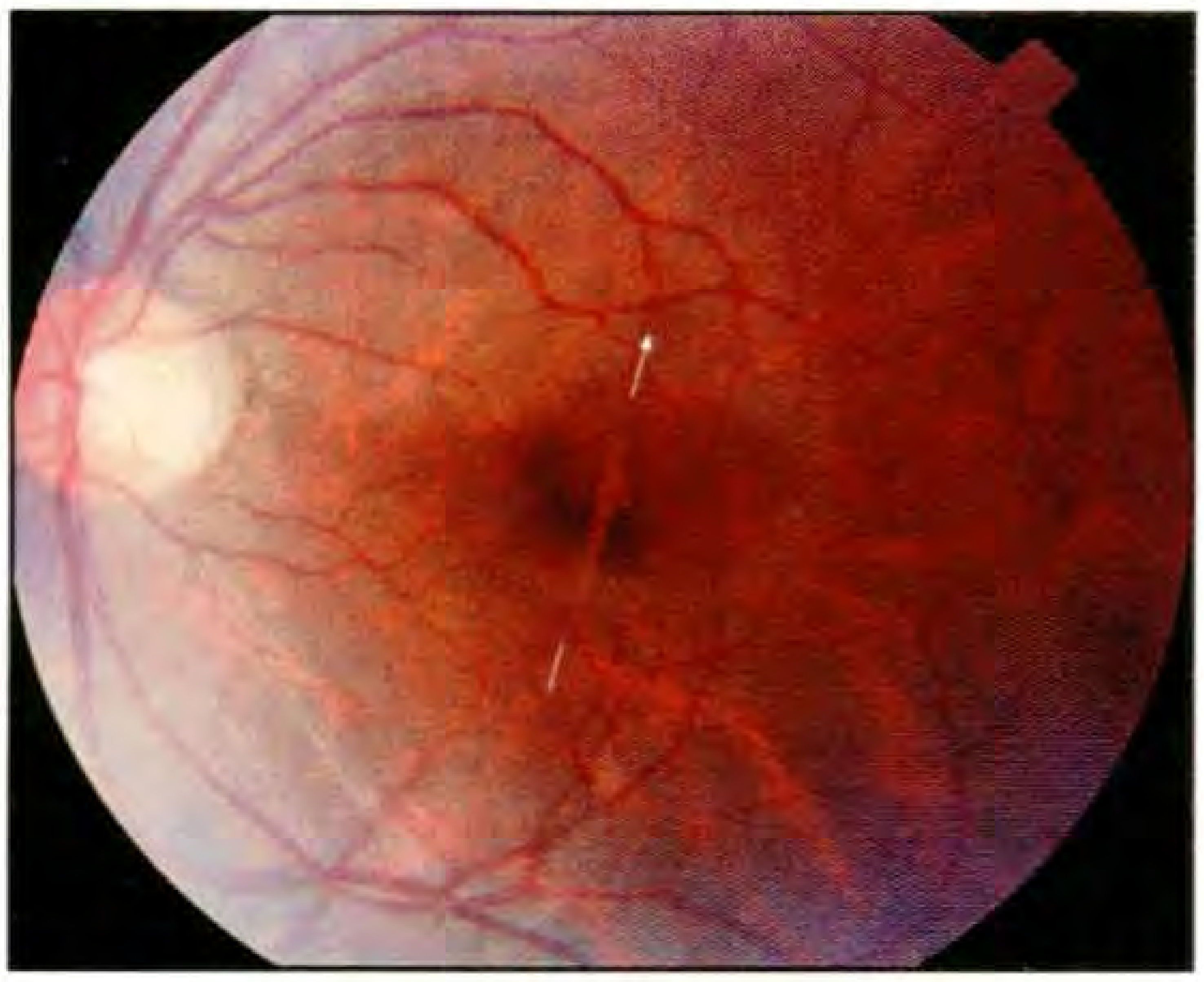

A

Case 11-2. Laser Injury

Clinical Summary

A 28-year-old graduate student accidently gazed into a pulsed titanium:sapphire laser with his left eye while in the laboratory. The laser was operating at 840 nm, with 500 μJ pulses stretched to 1 ps at a 1 kHz repetition rate. The exposure to the eye was less than 1 second off of a 10% reflector. Dilated fundus examination (A) two days later revealed a spindle-shaped, hypopigmented lesion bisecting the fovea. No clear abnormality was visualized on fluorescein angiography (not shown). The visual acuity was 20/25.

Optical Coherence Tomography

An OCT tomogram (B) acquired coincident with the burn showed a mild disturbance in the retinal pigment epithelium and some enhanced reflectivity in the photoreceptor layer, but otherwise no morphological damage.

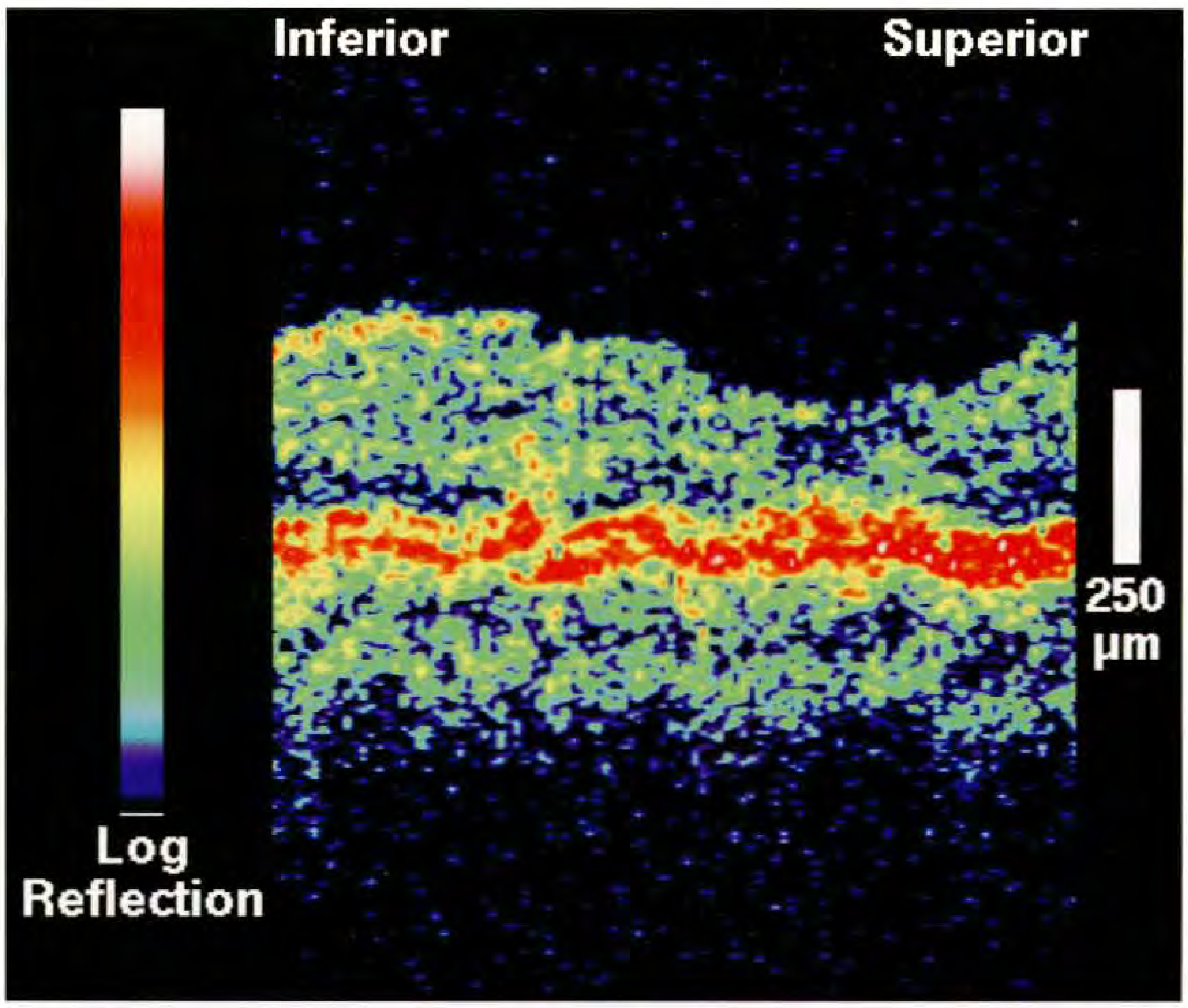

B

Case 11-3. Motor Vehicle Accident

Clinical Summary

A 25-year-old man was examined three weeks after a motor vehicle accident in which he sustained an injury to the left side of his head above the orbit. On examination, the visual acuity was 20/30 and the patient reported seeing several "lint-like" floaters. Ophthalmoscopy (A) revealed optic nerve head swelling, but no macular abnormalities or subretinal fluid. There was a negative Watzke sign.

A

Optical Coherence Tomography

A vertical image through the optic disc (B; white line on A) demonstrated protrusion of the disc contour consistent with papilledema. A partial separation of the posterior vitreous was noted immediately inferior to the disc. A scan (C; black line on A) was also acquired through fixation to evaluate the possible presence of a macular hole. OCT showed an intact fovea with an abnormally wide foveal pit, and an incomplete detachment of the posterior vitreous nasal to the center (arrow).

B

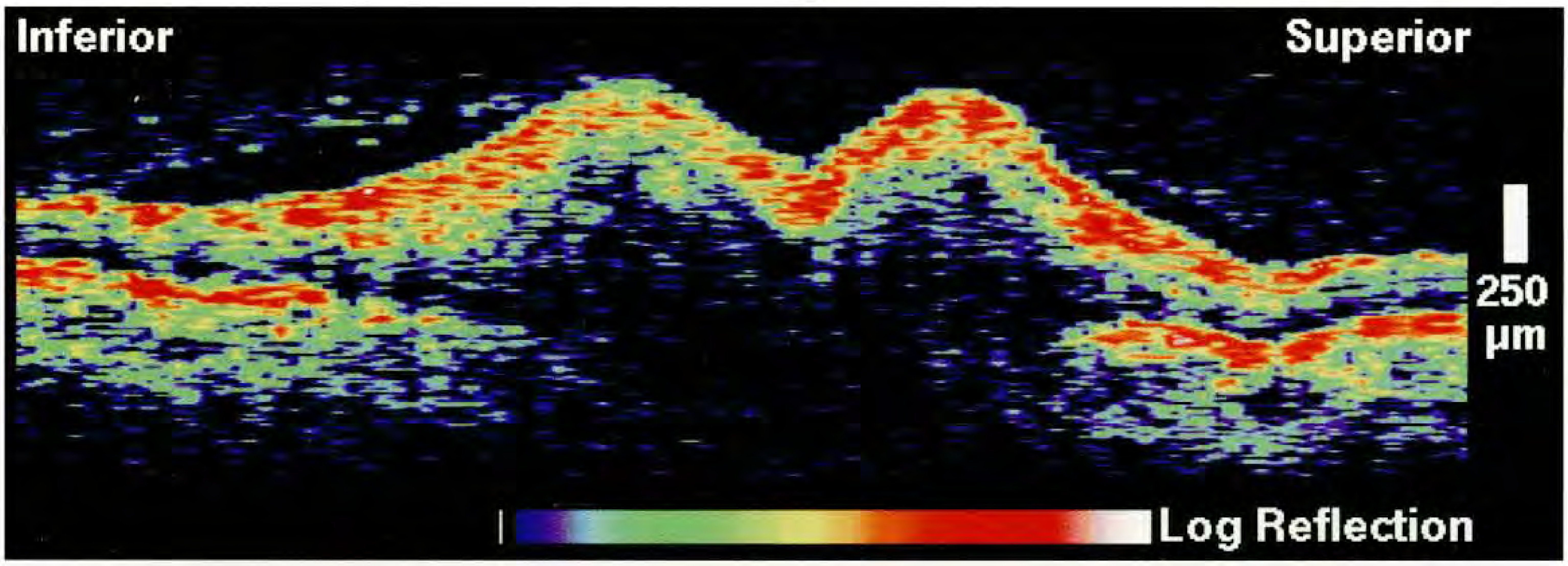

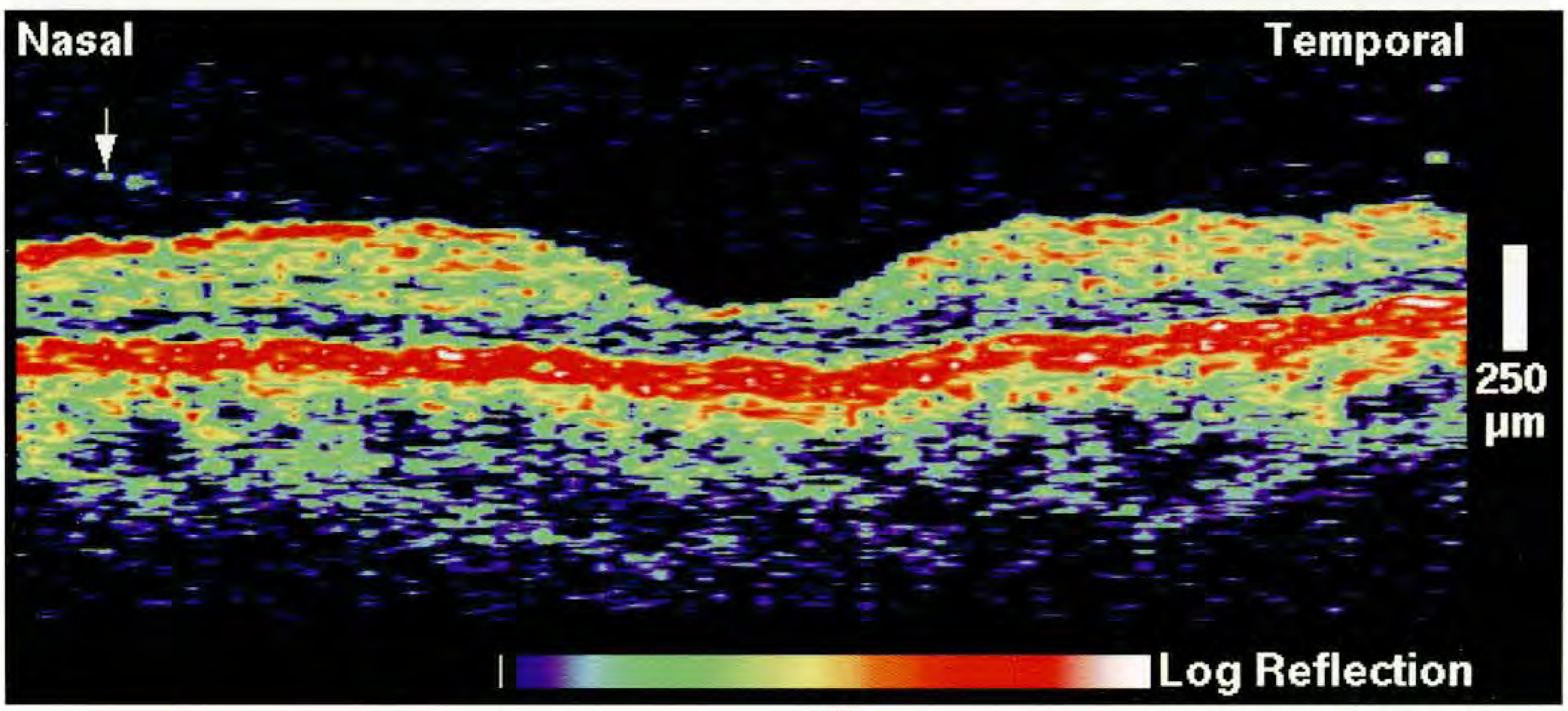

C

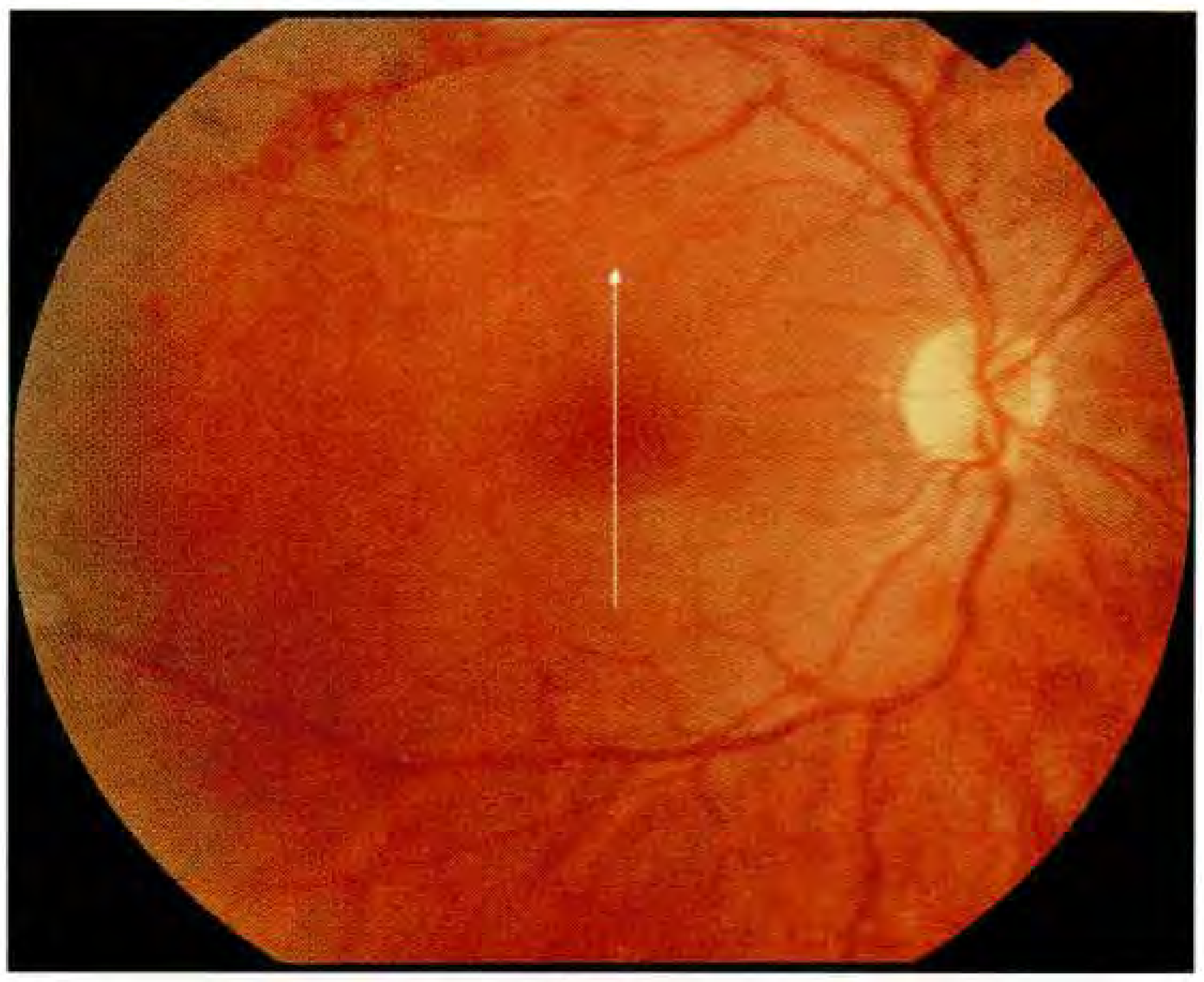

A

Case 11-4. Blunt Trauma

Clinical Summary

A 16-year-old male was examined four days after experiencing blunt trauma to his right eye. His visual acuity in this eye was 20/400. Dilated fundus examination (A) revealed a small hemorrhage directly in the fovea.

Optical Coherence Tomography

An OCT tomogram through the fovea (B) displayed an abnormal foveal contour consistent with the loss of photoreceptors in the foveal pit. A focal region of enhanced backscatter immediately anterior to the retinal pigment epithelium was noted, compatible with the clinical observation of a small subretinal hemorrhage.

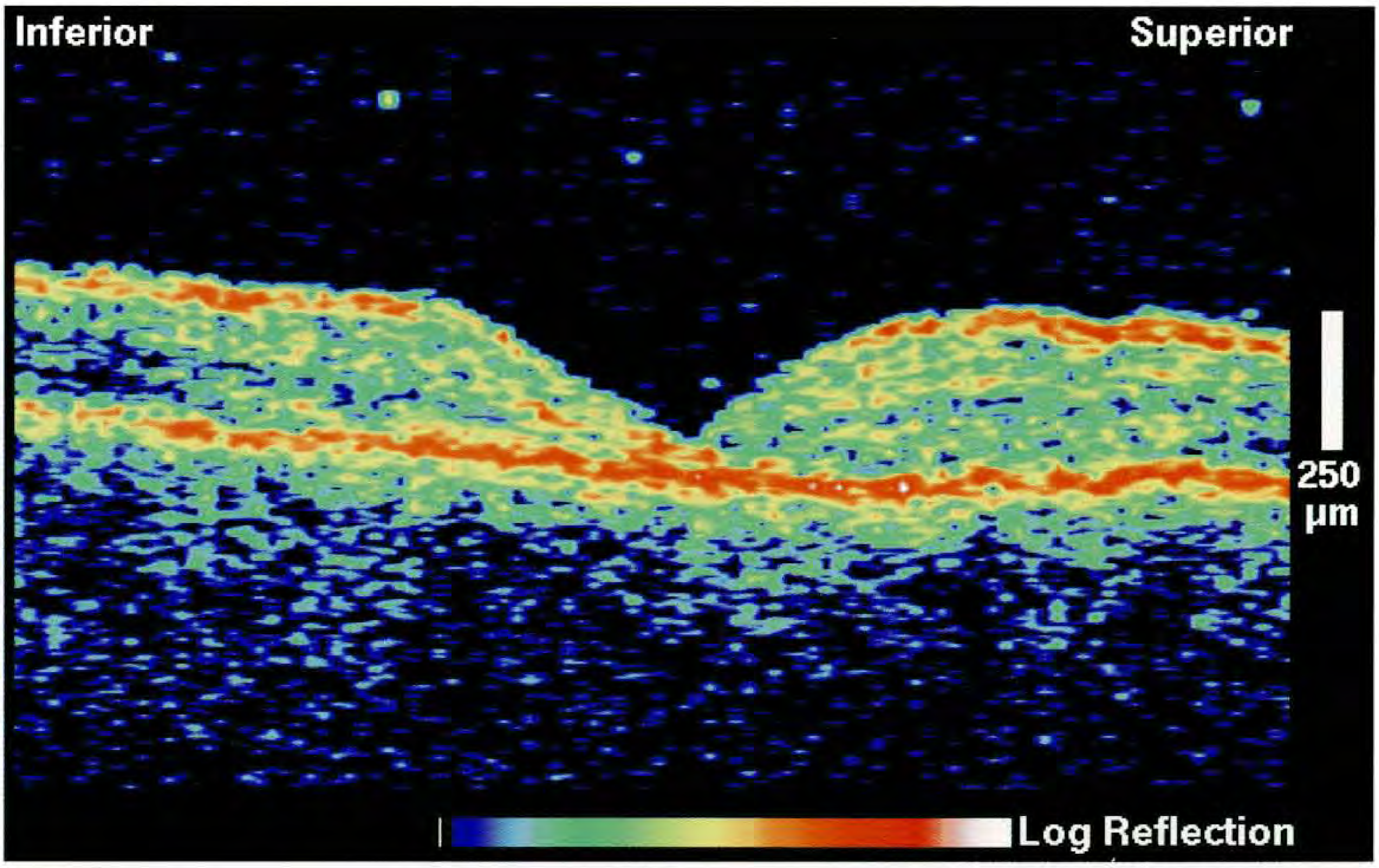

B

Case 11-5. Blunt Trauma

Clinical Summary

A 37-year-old man was examined one month after he sustained blunt trauma to his left orbit due to contact with a brick. The patient described a cloud over his central vision. On examination, his visual acuity in the left eye was 20/200. Slit-lamp biomicroscopy (A) revealed a pigmented scar in the central macula and retinal whitening superior and inferior to the fovea attributed to commotio retinae.

Optica Coherence Tomography

A horizontal OCT image (B) demonstrated complete atrophy of retinal tissue in the fovea. Enhanced reflectivity from the retinal pigment epithelium and choriocapillaris was observed beneath and nasal to the fovea consistent with a pigmented scar.

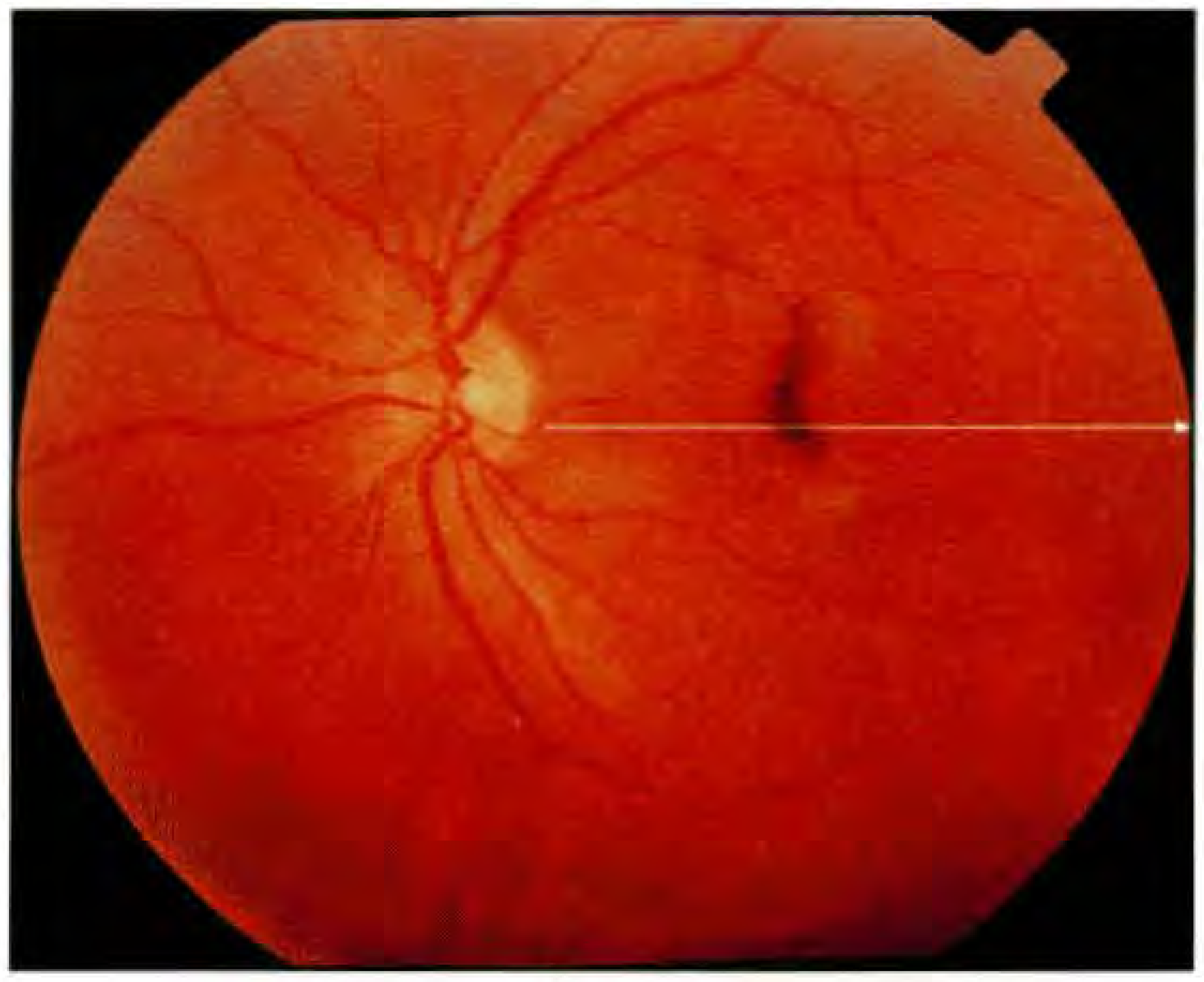

A

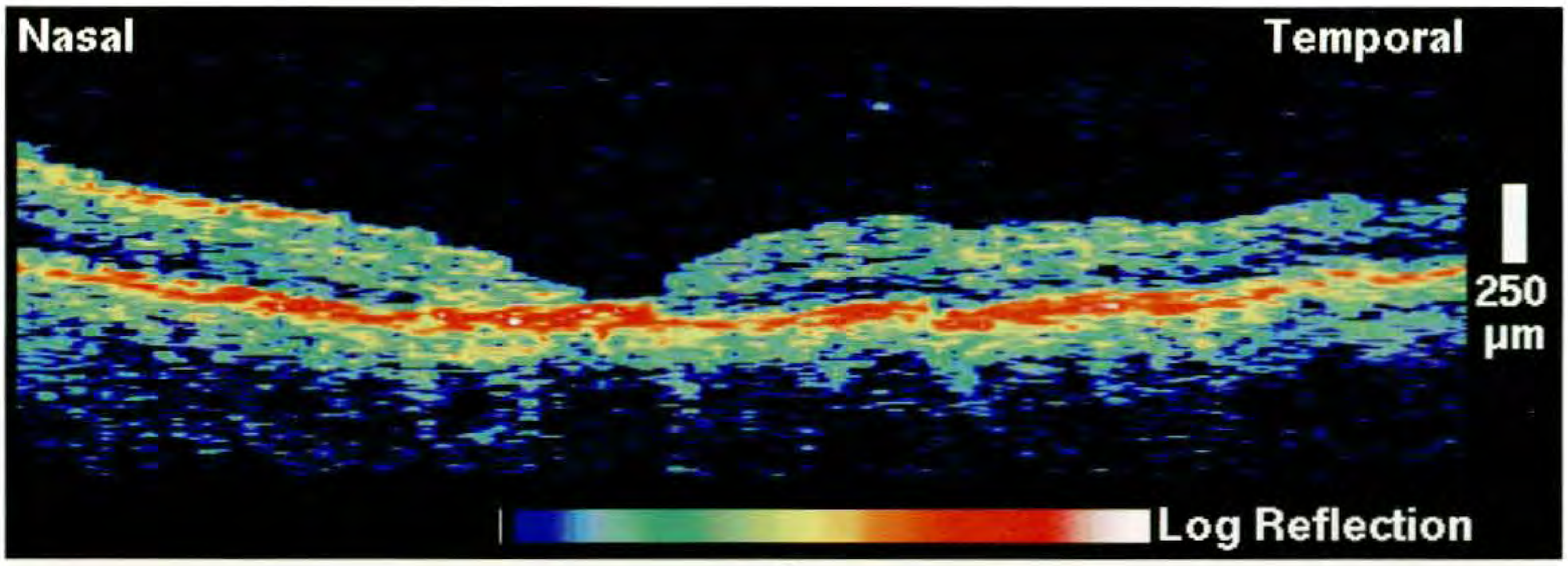

B

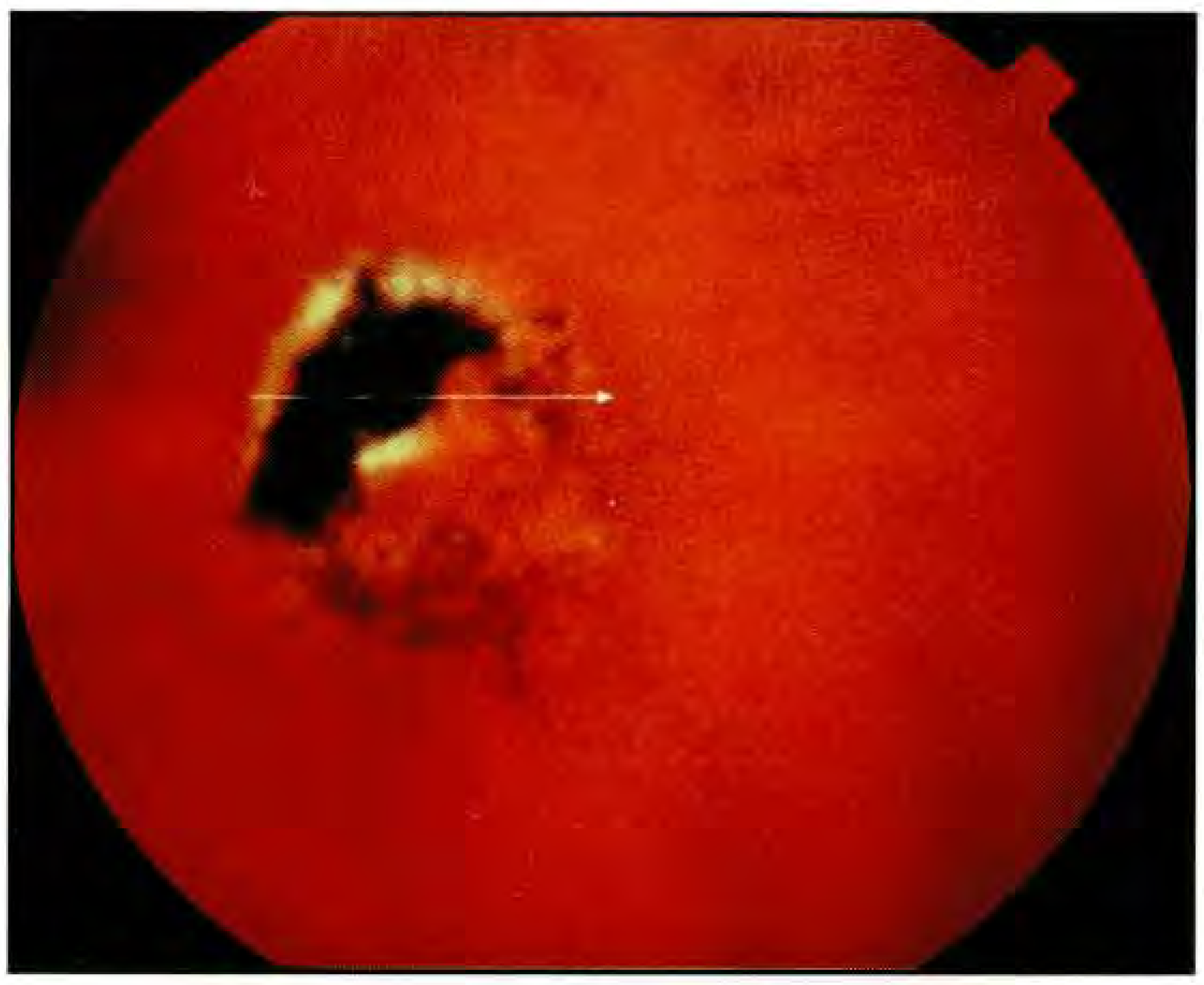

A

Case 11-6. Intraocular Foreign Body

Clinical Summary

A 33-year-old man had a metal intraocular foreign body embedded in his left eye following an unsuccessful attempt to remove the body seven years earlier. His visual acuity in this eye was 20/20 through a pinhole. Ophthalmoscopy (A) revealed a heavily pigmented chorioretinal scar in the inferotemporal macula with surrounding pigmentary dispersion.

Optical Coherence Tomography

A horizontal OCT image (B) showed an elevation of the retina over the foreign body. The reflective band corresponding to the retinal pigment epithelium was thickened and highly backscattering in this region consistent with pigment aggregation. The temporal margin of the lesion demonstrated complete atrophy of the overlying sensory retina. A backscattering band of tissue was observed anterior to the retina and temporal to the lesion, and was compatible with the dispersed pigmented viewed on ophthalmoscopy.

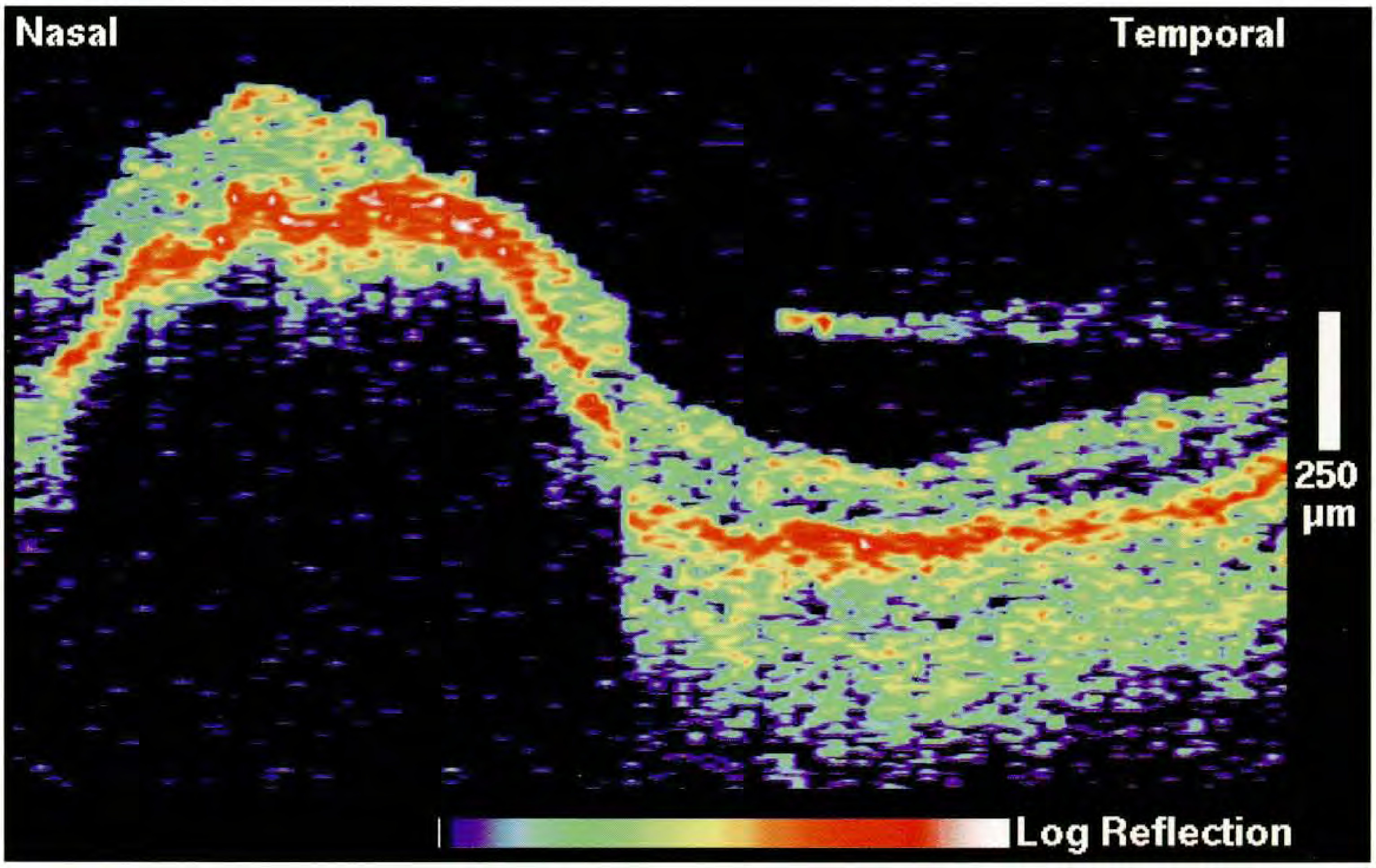

B

Case 11-7. Traumatic Macular Hole

Clinical Summary

A 20-year-old man was evaluated four weeks after blunt trauma to his right eye from an electrical explosion. The day of the examination, he complained of an abrupt loss in visual acuity in this eye, which was assessed at hand motions only. No clinical photographs were obtained due to the poor view of the fundus.

Optical Coherence Tomography

OCT was performed (A) and demonstrated a full-thickness macular hole. The asymmetric contour of the hole was consistent with a traumatic rather than an idiopathic etiology. Reduced reflected signal was observed throughout the image due to the hazy view and resolving vitreous hemorrhage

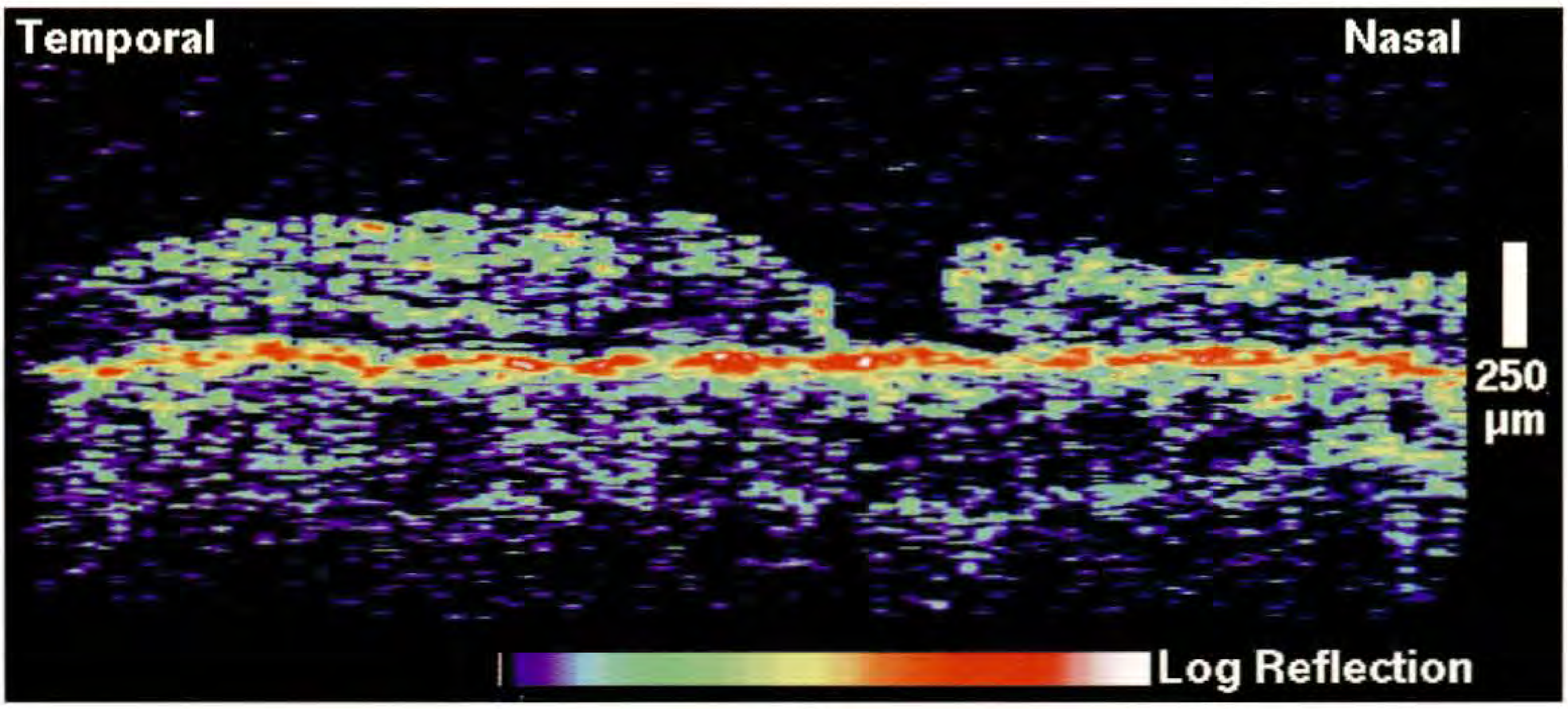

A

Section III

Glaucoma and Diseases of the Optic Nerve

CHAPTER 12

Glaucoma

Normal Nerve Fiber Layer
Normal Nerve Fiber Layer with Visual Field Loss
Glaucoma
Glaucomatous Progression

Measurements of retinal nerve fiber layer (NFL) thickness with OCT are potentially useful in the early diagnosis of glaucoma and the early detection of glaucomatous progression [1,2]. Standard clinical techniques for assessing glaucomatous changes, such as optic nerve head and NFL examination or visual field testing, lack sensitivity and reproducibility. Visual evaluation of the optic nerve head by direct examination or by stereoscopic fundus photography is subjective, and the variability among experienced observers is often great [3]. Small changes in the appearance of the nerve head, such as notches and other local abnormalities, are often difficult to detect. Visual field testing depends on patient cooperation and may also be influenced by non-glaucomatous vision loss. Additionally, significant retinal nerve fiber layer loss may precede both the development of visual field defects and identifiable cupping [4].

The high longitudinal resolution of OCT enables direct measurement of nerve fiber layer thickness with micron-scale resolution. The NFL is highly backscattering and therefore is contrasted from the intermediate retinal layers because the nerve axons are oriented perpendicularly to the OCT probe beam. Several types of scanning patterns are useful in evaluating the optic nerve head and NFL. Radial OCT tomograms acquired directly through the optic disc provide cross-sectional information on cupping and neuroretinal rim area. Three-dimensional information on disc parameters may be obtained from multiple radial tomograms acquired at different angular orientations, or from a series of parallel tomograms offset at various distances from the center of the disc.

A single circular scan around optic nerve head allows the variations in NFL thickness in different regions around the disc to be assessed and compared. A circular tomogram evaluates the cross-sectional structure of the NFL in a cylindrical section surrounding the optic disc, and may be displayed "unwrapped" as a flat image on the page. In more advanced cases of glaucoma, areas of NFL thinning around the disc, as measured by OCT, correlate with visual field defects and losses in the neuroretinal rim [2]. In the earlier stages of glaucoma, NFL thinning may occur out of proportion to visual field loss or cupping. Direct measurement of NFL thinning with OCT may enable earlier detection of glaucomatous changes.

Computer image processing techniques may be applied to the circular OCT tomograms in order to automatically identify the reflective boundaries at the vitreoretinal interface, the retinal pigment epithelium, and the NFL. NFL or retinal thickness may be computed automatically from these boundaries and can be displayed as averaged over quadrant (superior, inferior, temporal, nasal), or over clock hour, or individually for each A-scan comprising the OCT image. These quantitative measurements may then be compared with standard normal values or values obtained from previous examinations to assess glaucomatous progression [2]. The direct measurement of NFL thickness provided by OCT combined with automated image analysis allows a completely objective assessment of glaucoma onset and progression.

A

B

Case 12-1. Normal Optic Nerve and Visual Field

Clinical Summary

A 55-year-old white man was referred for evaluation of asymmetric cupping. Examination of his left eye (A, B) revealed a visual acuity of 20/20, an intraocular pressure of 17 mm Hg, and a normal optic nerve. The Humphrey visual field (D) was full; the patient did not have glaucoma.

Optical Coherence Tomography

A horizontal and vertical tomogram (C) were acquired through the optic disc. Measurements of nerve fiber layer thickness and cup diameter were obtained at two points from each image defined by the termination of the choroid at the lamina cribosa. The cup diameter was assessed at a point 140 μm below the disc diameter. Neuroretinal rim area was calculated from the cup and disc diameters.

A 3.4 mm diameter circular tomogram (E) obtained around the optic disc demonstrated high reflectivity from the nerve fiber layer and normal variations in nerve fiber layer (NFL) thickness consistent with thicker NFL superotemporally and inferotemporally. A computer algorithm was used to estimate the location of the boundaries at the anterior retinal surface (white), the posterior margin of the nerve fiber layer (blue), and the retinal pigment epithelium (blue). Nerve fiber layer thickness was computed automatically and displayed as averaged over quadrant and clock hour. Normal variation in NFL thickness was seen in the circular OCT, with the thickest measurements obtained superotemporally and inferotemporally.

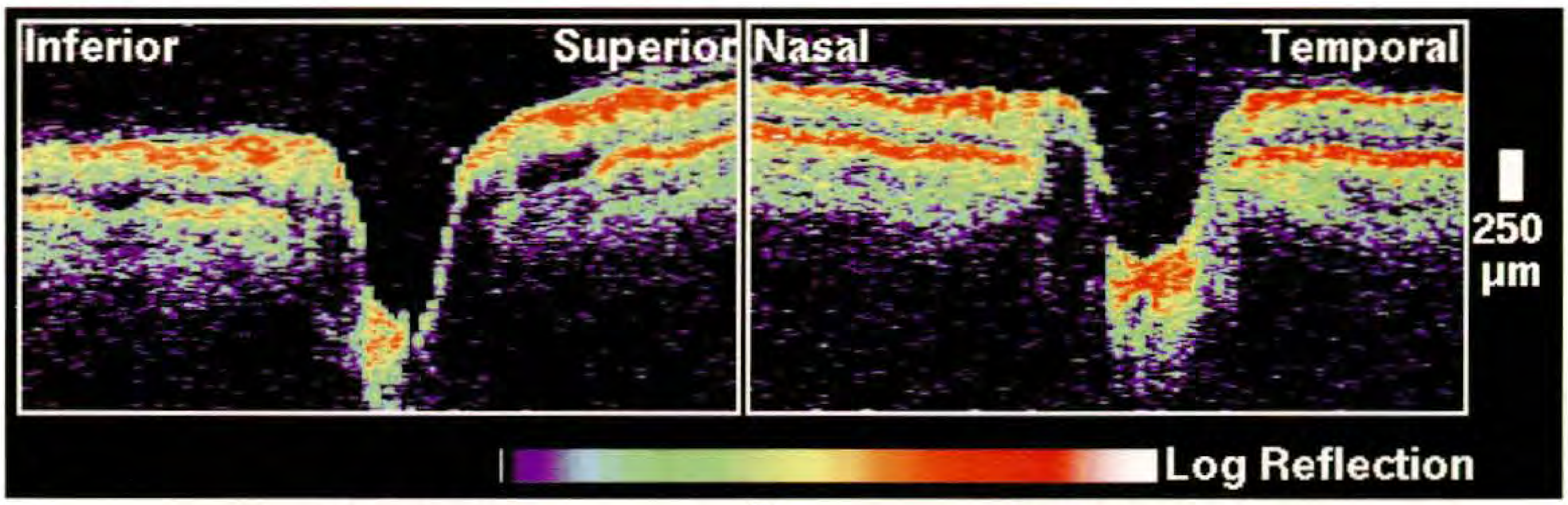

C

VERTICAL		*HORIZONTAL*	
Cup Diameter	**1.05 mm**	**Cup Diameter**	**1.19 mm**
Disc Diameter	**1.44 mm**	**Disc Diameter**	**1.86 mm**
C/D Ratio	**0.73**	**C/D Ratio**	**0.64**
NR Rim Area	**0.76 mm²**		
Inferior NFL	**230 μm**	**Nasal NFL**	**200 μm**
Superior NFL	**170 μm**	**Temporal NFL**	**180 μm**

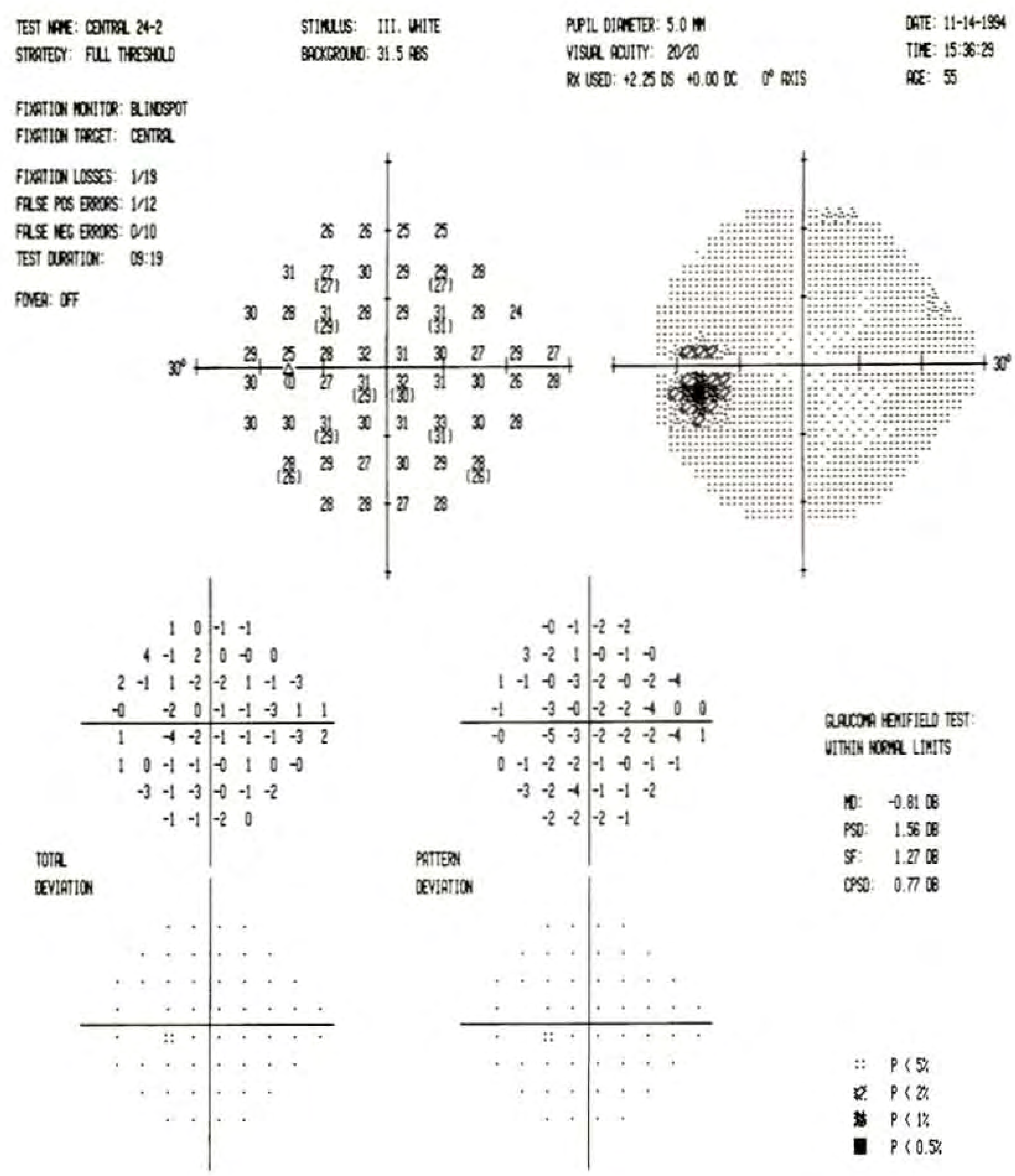
TEST NAME: CENTRAL 24-2
STRATEGY: FULL THRESHOLD
STIMULUS: III, WHITE
BACKGROUND: 31.5 ABS
PUPIL DIAMETER: 5.0 MM
VISUAL ACUITY: 20/20
RX USED: +2.25 DS +0.00 DC 0° AXIS
DATE: 11-14-1994
TIME: 15:36:29
AGE: 55
FIXATION MONITOR: BLINDSPOT
FIXATION TARGET: CENTRAL
FIXATION LOSSES: 1/19
FALSE POS ERRORS: 1/12
FALSE NEG ERRORS: 0/10
TEST DURATION: 09:19
FOVEA: OFF
30°
30°
TOTAL DEVIATION
PATTERN DEVIATION
GLAUCOMA HEMIFIELD TEST: WITHIN NORMAL LIMITS
MD: -0.81 DB
PSD: 1.56 DB
SF: 1.27 DB
CPSD: 0.77 DB
P < 5%
P < 2%
P < 1%
P < 0.5%

D

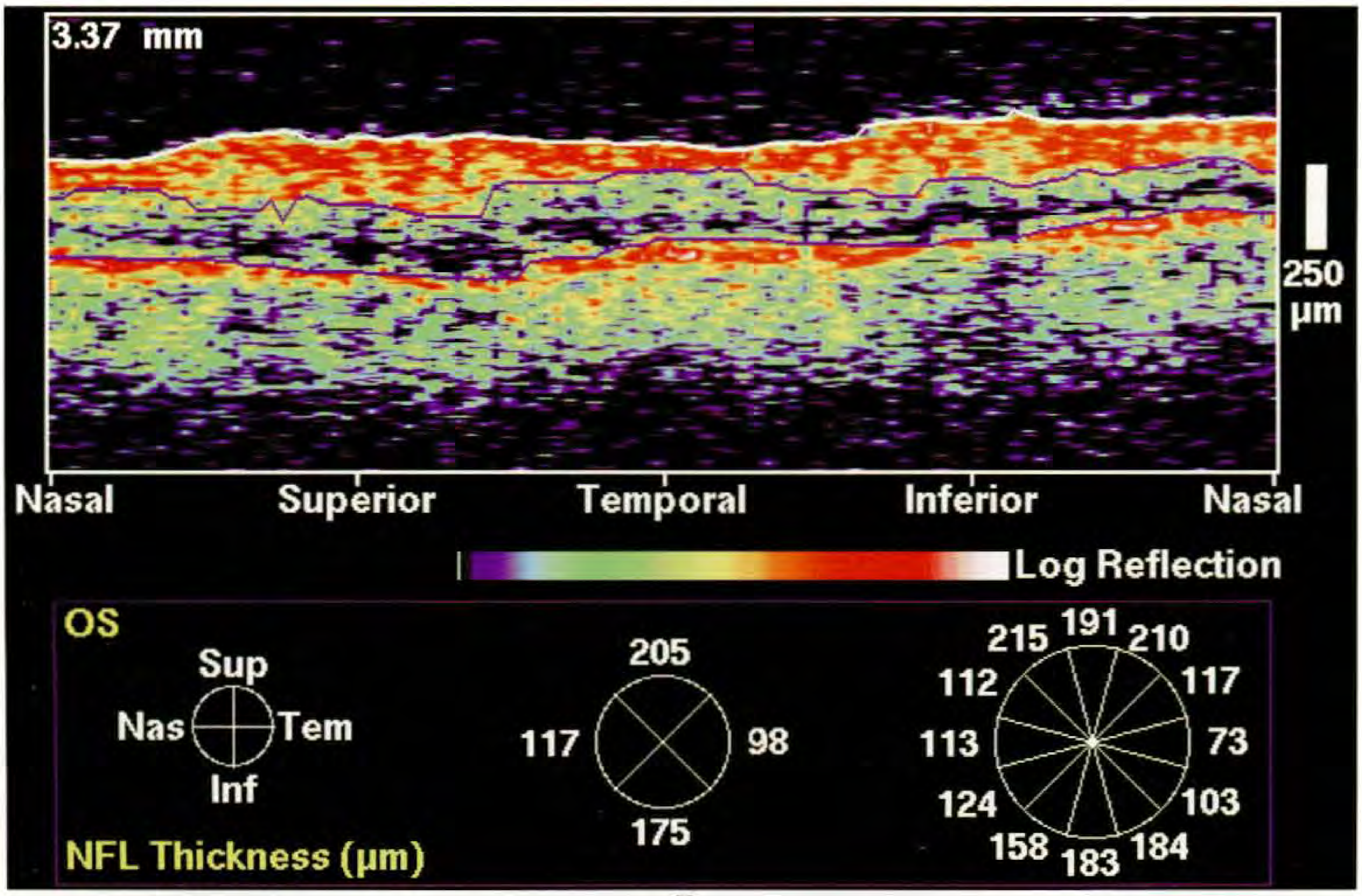
3.37 mm
250 µm
Nasal
Superior
Temporal
Inferior
Nasal
Log Reflection
OS
Sup
Nas
Tem
Inf
NFL Thickness (µm)
205
117
98
175
215
191
210
112
117
113
73
124
103
158
183
184

E

A

B

Case 12-2. Normal Optic Nerve and Visual Field

Clinical Summary

A 41-year-old white female with early glaucoma was taking levobunolol 0.5% twice daily. Examination of her right eye (A, B) showed a normal optic nerve with an intraocular pressure (IOP) of 17 mm Hg. A Humphrey visual field (D) was normal.

Optical Coherence Tomography

Horizontal and linear scans (C) through the optic disc revealed a healthy nerve fiber layer (NFL). NFL thickness was measured from the images at the lamina cribosa as the height of the superficial, red reflective layer. The disc diameter was also assessed between points on the retinal surface perpendicular to the edge of the choroid. The cup diameter was assumed to lie 140 µm below the disc diameter. Neuroretinal rim area was calculated from these measurements.

A circular scan (E) around the disc in the peripapillary region was acquired at a diameter of 3.4 mm. The NFL reached its thickest points superotemporally and inferotemporally. NFL thickness was estimated using a computer algorithm and reported as averaged over quadrant and clock hour.

Comment

This patient's early glaucoma was controlled with levobunolol 0.5% twice daily. When not on medication, her IOP was 30 mm Hg or higher. Her optic nerve heads showed little cupping, and her visual field was full. OCT demonstrated that glaucomatous damage, if any, was minimal. Her NFL thickness was in the normal range.

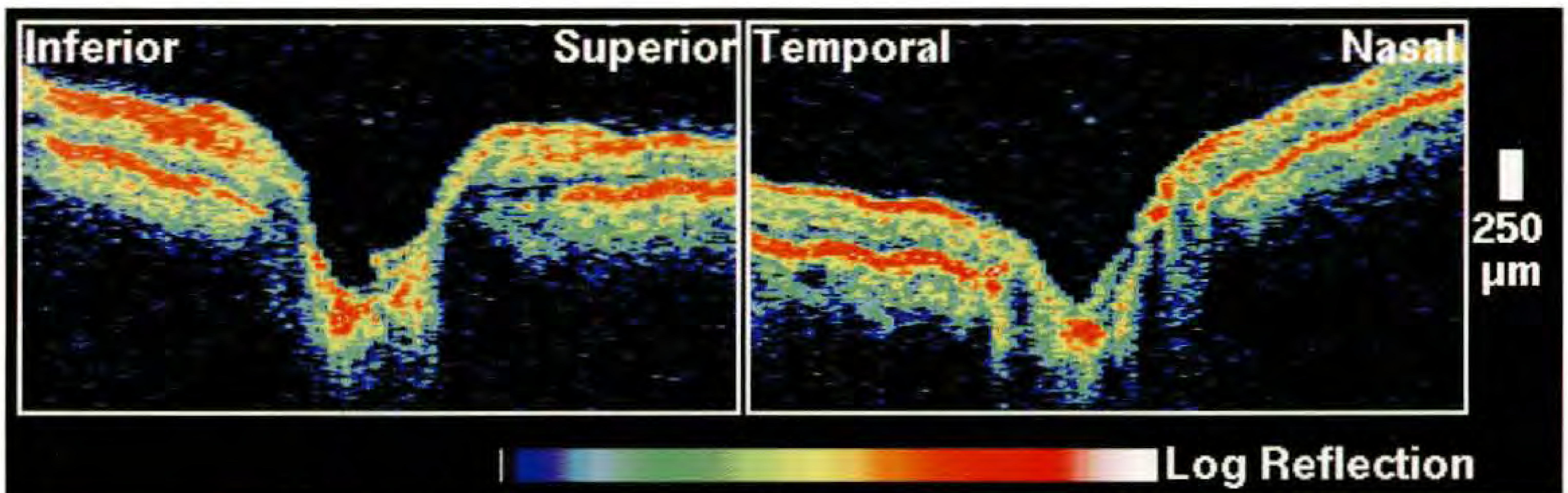

VERTICAL C *HORIZONTAL*

Cup Diameter	**1.35 mm**	**Cup Diameter**	**0.79 mm**
Disc Diameter	**1.95 mm**	**Disc Diameter**	**1.22 mm**
C/D Ratio	**0.69**	**C/D Ratio**	**0.65**
NR Rim Area	**1.56 mm^2**		
Inferior NFL	**180 µm**	**Nasal NFL**	**180 µm**
Superior NFL	**240 µm**	**Temporal NFL**	**210 µm**

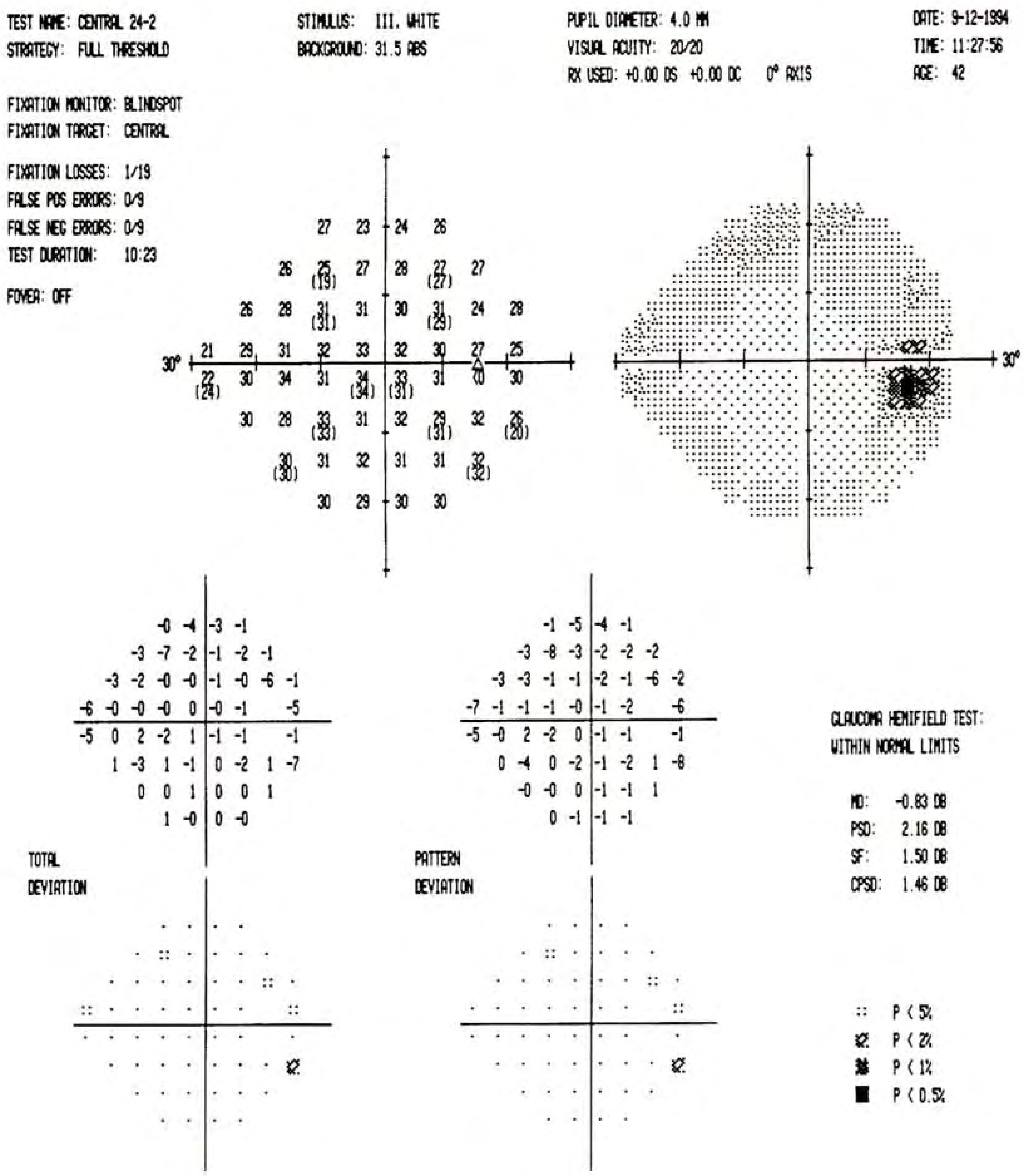
TEST NAME: CENTRAL 24-2
STRATEGY: FULL THRESHOLD
STIMULUS: III, WHITE
BACKGROUND: 31.5 ABS
PUPIL DIAMETER: 4.0 MM
VISUAL ACUITY: 20/20
RX USED: +0.00 DS +0.00 DC 0° AXIS
DATE: 9-12-1994
TIME: 11:27:56
AGE: 42
FIXATION MONITOR: BLINDSPOT
FIXATION TARGET: CENTRAL
FIXATION LOSSES: 1/19
FALSE POS ERRORS: 0/9
FALSE NEG ERRORS: 0/9
TEST DURATION: 10:23
FOVEA: OFF
30°
TOTAL DEVIATION
PATTERN DEVIATION
GLAUCOMA HEMIFIELD TEST:
WITHIN NORMAL LIMITS
MD: -0.83 DB
PSD: 2.16 DB
SF: 1.50 DB
CPSD: 1.46 DB
P < 5%
P < 2%
P < 1%
P < 0.5%

D

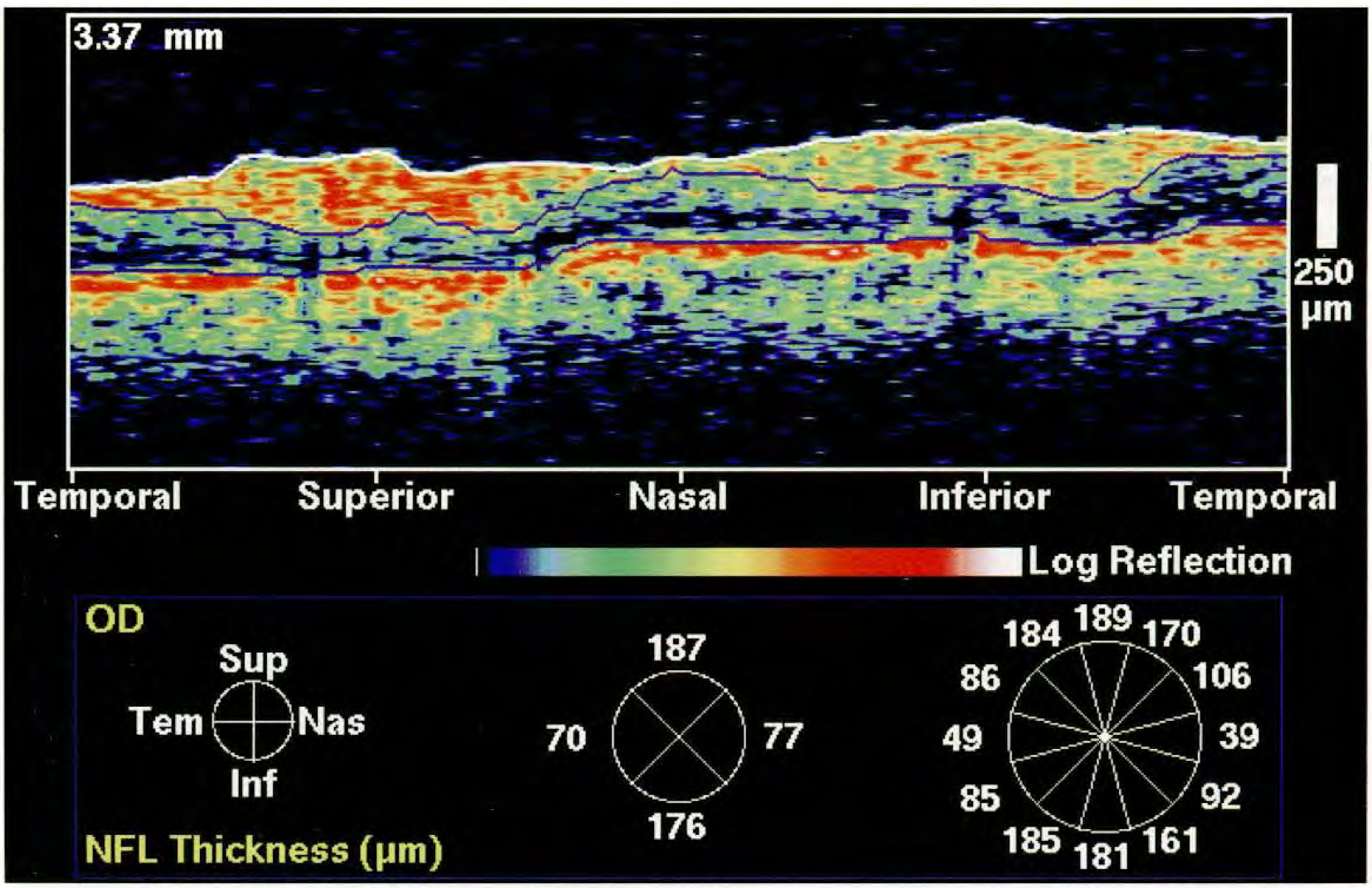
3.37 mm
250 µm
Temporal
Superior
Nasal
Inferior
Temporal
Log Reflection
OD
Sup
Tem
Nas
Inf
NFL Thickness (µm)
187
70
77
176
184 189 170
86
106
49
39
85
92
185 181 161

E

A

B

Case 12-3. Normal Visual Fields with Nerve Fiber Layer Thinning

Clinical Summary

A 43-year-old white man had asymmetric primary open-angle glaucoma which affected the right eye more than the left. Examination of the left eye revealed a visual acuity of 20/20 and an intraocular pressure of 10 mm Hg . Both slit-lamp examination and gonioscopy were unremarkable. Ophthalmoscopy (A, B) showed moderate cupping of the optic disc with mild attenuation of the neuroretinal rim superotemporally. The Humphrey visual field (D) in this eye was full.

Optical Coherence Tomography

A circular tomogram around the disc (E) revealed early thinning of the nerve fiber layer both superiorly and inferiorly. The thinning was consistent with the optic nerve head appearance, but out of proportion to the visual field, indicating that OCT was sensitive to optic nerve changes preceding significant visual field loss. The linear OCTs through the optic nerve head (C) indicated enlargment of the cup in the vertical dimension consistent with his early glaucoma.

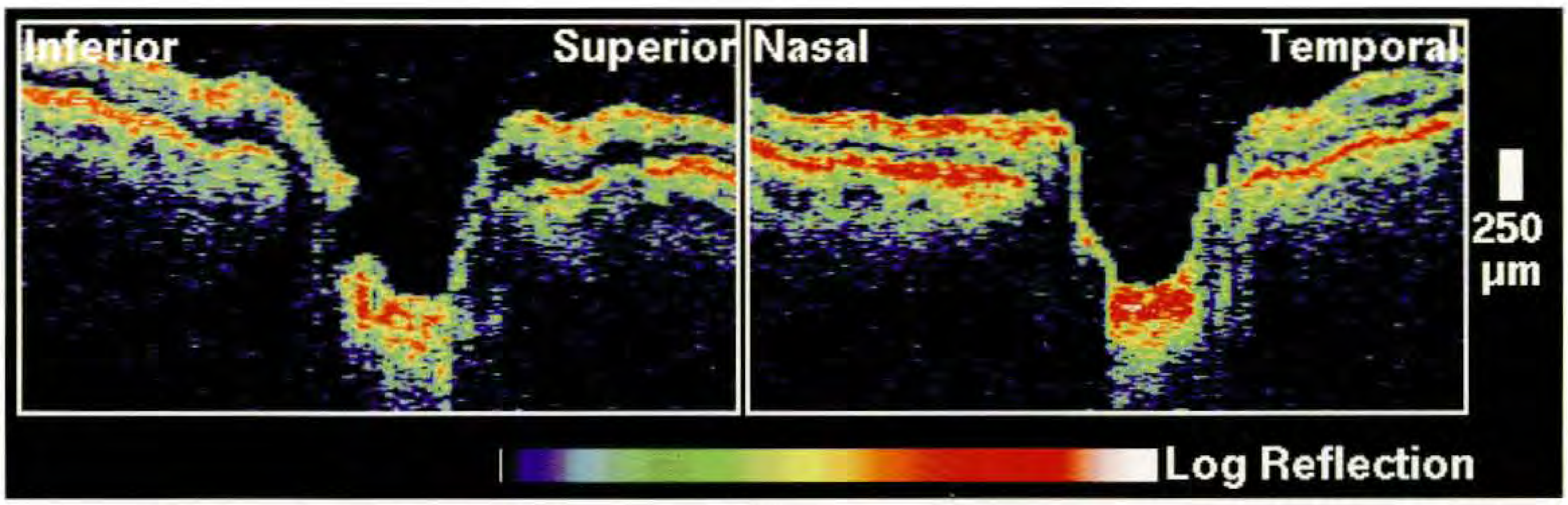

C

VERTICAL		*HORIZONTAL*	
Cup Diameter	1.39 mm	Cup Diameter	0.79 mm
Disc Diameter	1.80 mm	Disc Diameter	1.22 mm
C/D Ratio	0.77	C/D Ratio	0.65
NR Rim Area	1.03 mm^2		
Inferior NFL	160 µm	Nasal NFL	160 µm
Superior NFL	130 µm	Temporal NFL	150 µm

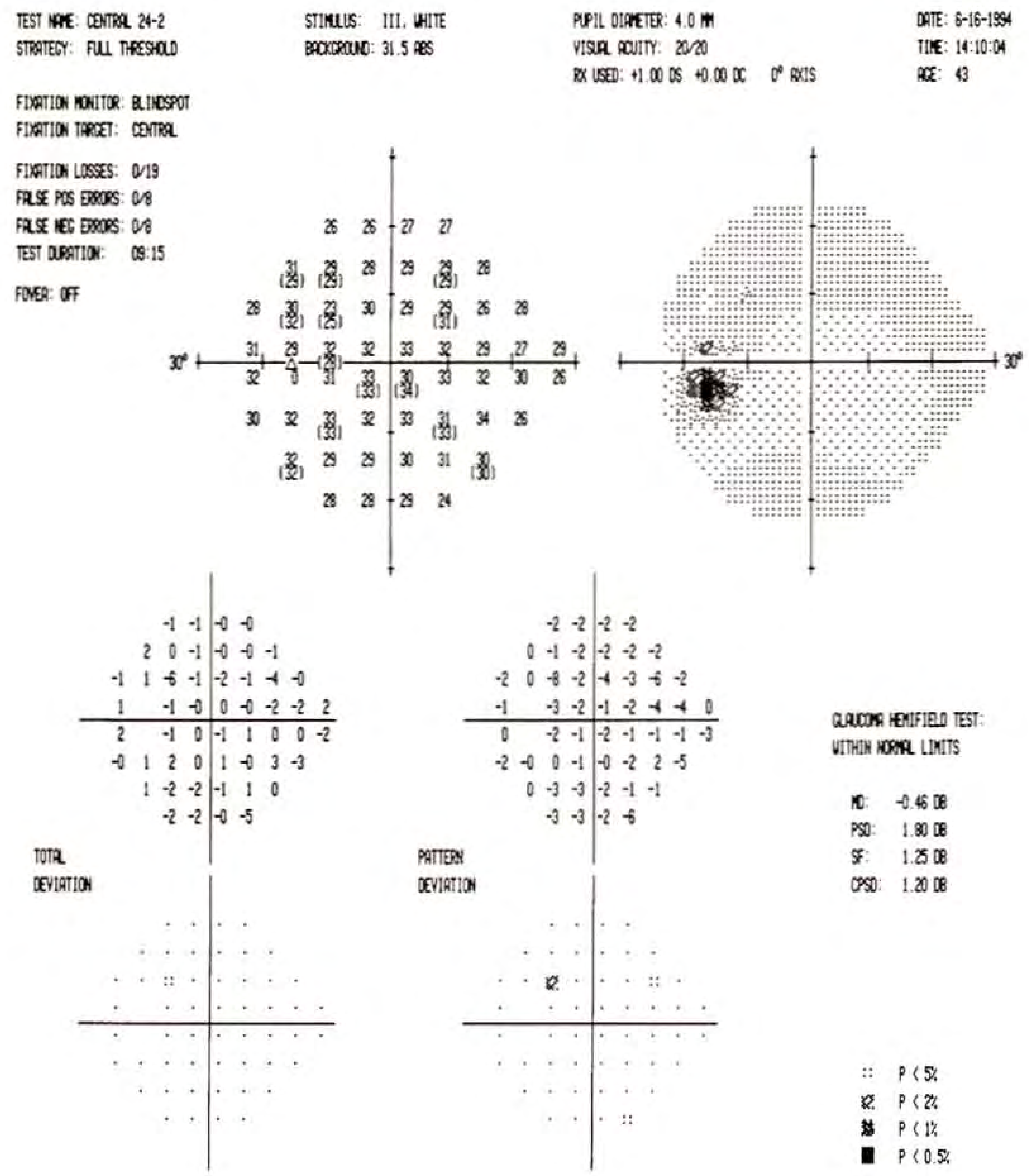
TEST NAME: CENTRAL 24-2
STRATEGY: FULL THRESHOLD
STIMULUS: III, WHITE
BACKGROUND: 31.5 ABS
PUPIL DIAMETER: 4.0 MM
VISUAL ACUITY: 20/20
RX USED: +1.00 DS +0.00 DC 0° AXIS
DATE: 6-16-1994
TIME: 14:10:04
AGE: 43
FIXATION MONITOR: BLINDSPOT
FIXATION TARGET: CENTRAL
FIXATION LOSSES: 0/19
FALSE POS ERRORS: 0/8
FALSE NEG ERRORS: 0/8
TEST DURATION: 09:15
FOVEA: OFF
30°
30°
TOTAL DEVIATION
PATTERN DEVIATION
GLAUCOMA HEMIFIELD TEST: WITHIN NORMAL LIMITS
MD: -0.46 DB
PSD: 1.80 DB
SF: 1.25 DB
CPSD: 1.20 DB
P < 5%
P < 2%
P < 1%
P < 0.5%

D

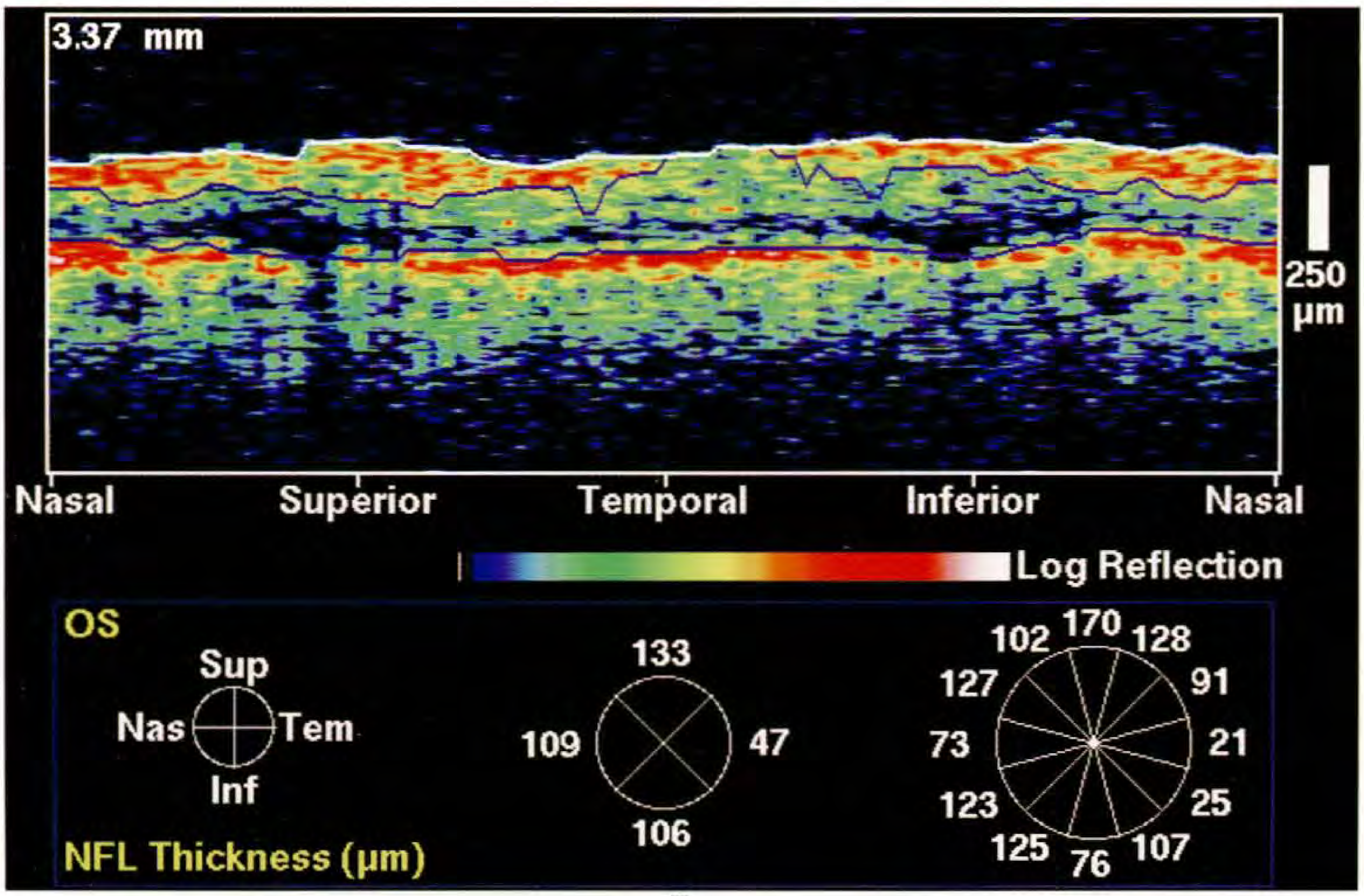
3.37 mm
250 µm
Nasal
Superior
Temporal
Inferior
Nasal
Log Reflection
OS
Sup
Nas
Tem
Inf
NFL Thickness (µm)
133
109
47
106
102
170
128
127
91
73
21
123
25
125
76
107

E

A

B

Case 12-4. Superior Nasal Step

Clinical Summary

A 62-year-old white woman with primary open-angle glaucoma had an intraocular pressure on examination of 19 mm Hg in her right eye while taking levobunolol twice a day and pilocarpine 4% four times daily. Her visual acuity was 20/20, and a Humphrey visual field (D) showed a superior nasal step. Dilated fundus examination (A,B) revealed a moderately cupped disc with thinning of the neuroretinal rim inferotemporally.

Optical Coherence Tomography

A 3.4 mm diameter scan (E) taken in a clockwise circle around the optic disc showed marked attenuation of the inferotemporal nerve fiber layer from 7:00 to 8:00, consistent with the superonasal visual field defect.

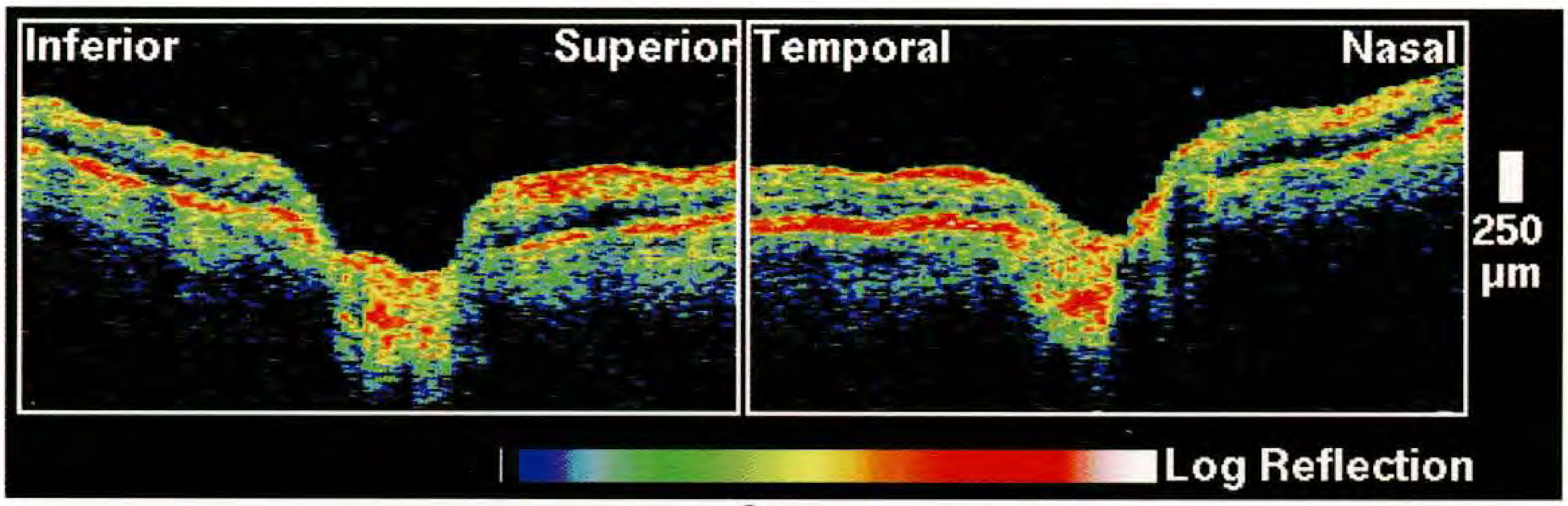

C

VERTICAL		*HORIZONTAL*	
Cup Diameter	1.39 mm	Cup Diameter	0.79 mm
Disc Diameter	1.80 mm	Disc Diameter	1.22 mm
C/D Ratio	0.77	C/D Ratio	0.65
NR Rim Area	1.03 mm^2		
Inferior NFL	160 μm	Nasal NFL	160 μm
Superior NFL	130 μm	Temporal NFL	150 μm

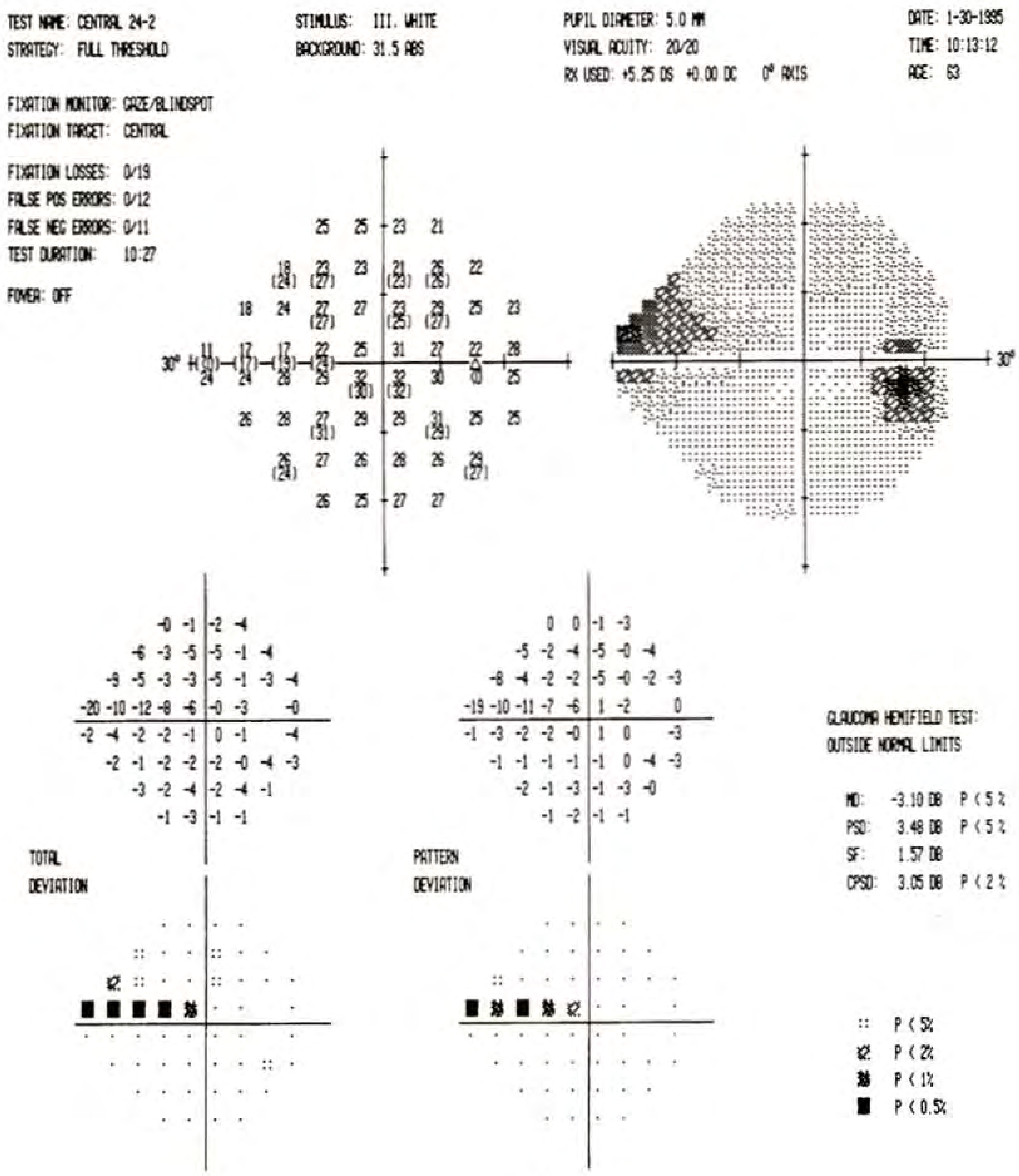

TEST NAME: CENTRAL 24-2
STRATEGY: FULL THRESHOLD
STIMULUS: III, WHITE
BACKGROUND: 31.5 ASB
PUPIL DIAMETER: 5.0 MM
VISUAL ACUITY: 20/20
RX USED: +5.25 DS +0.00 DC 0° AXIS
DATE: 1-30-1995
TIME: 10:13:12
AGE: 63
FIXATION MONITOR: GAZE/BLINDSPOT
FIXATION TARGET: CENTRAL
FIXATION LOSSES: 0/19
FALSE POS ERRORS: 0/12
FALSE NEG ERRORS: 0/11
TEST DURATION: 10:27
FOVEA: OFF
30°
30°
TOTAL DEVIATION
PATTERN DEVIATION
GLAUCOMA HEMIFIELD TEST: OUTSIDE NORMAL LIMITS
MD: -3.10 DB P < 5 %
PSD: 3.48 DB P < 5 %
SF: 1.57 DB
CPSD: 3.05 DB P < 2 %
P < 5%
P < 2%
P < 1%
P < 0.5%

D

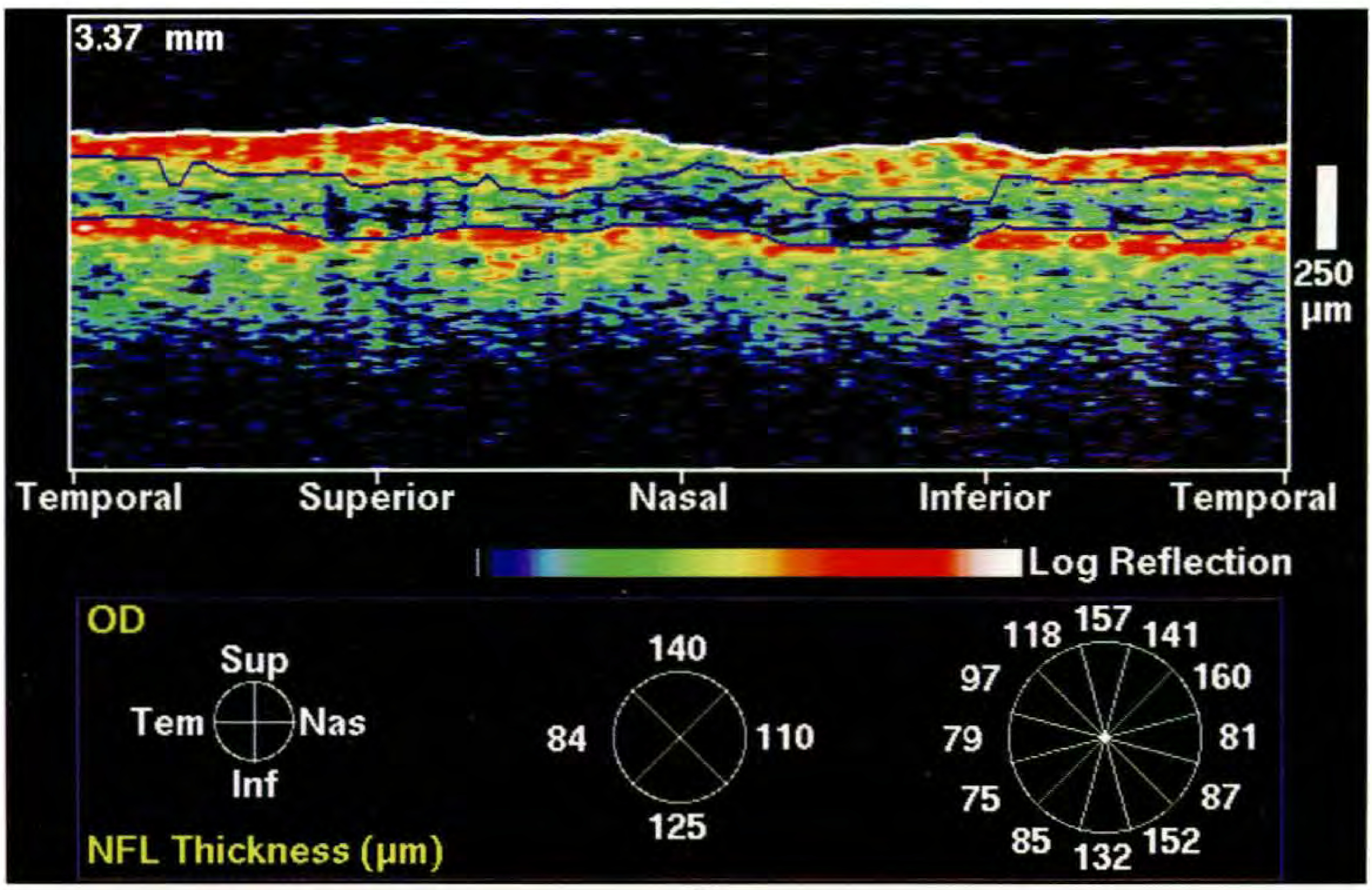

3.37 mm
250 µm
Temporal
Superior
Nasal
Inferior
Temporal
Log Reflection
OD
Sup
Tem
Nas
Inf
NFL Thickness (µm)
140
84
110
125
118
157
141
97
160
79
81
75
87
85
132
152

E

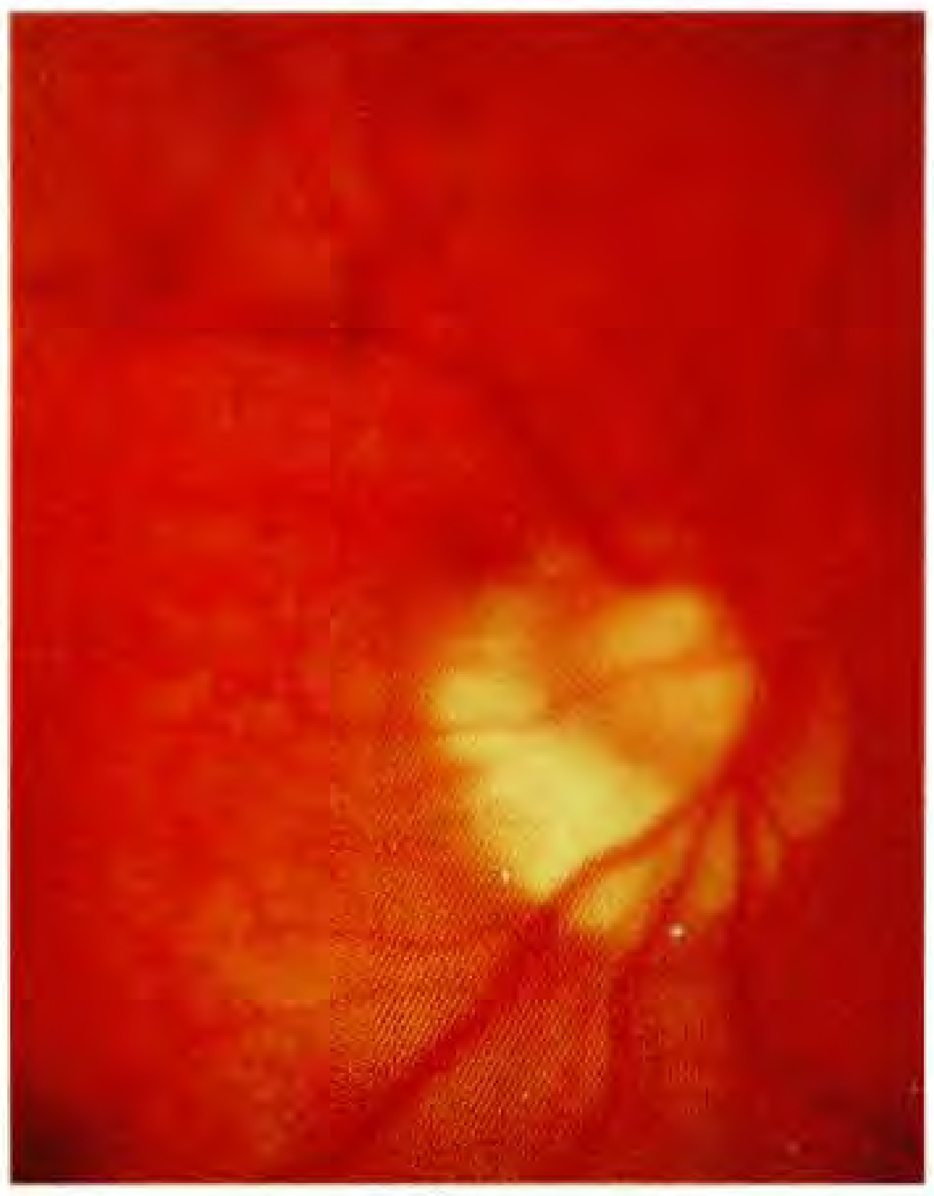

A

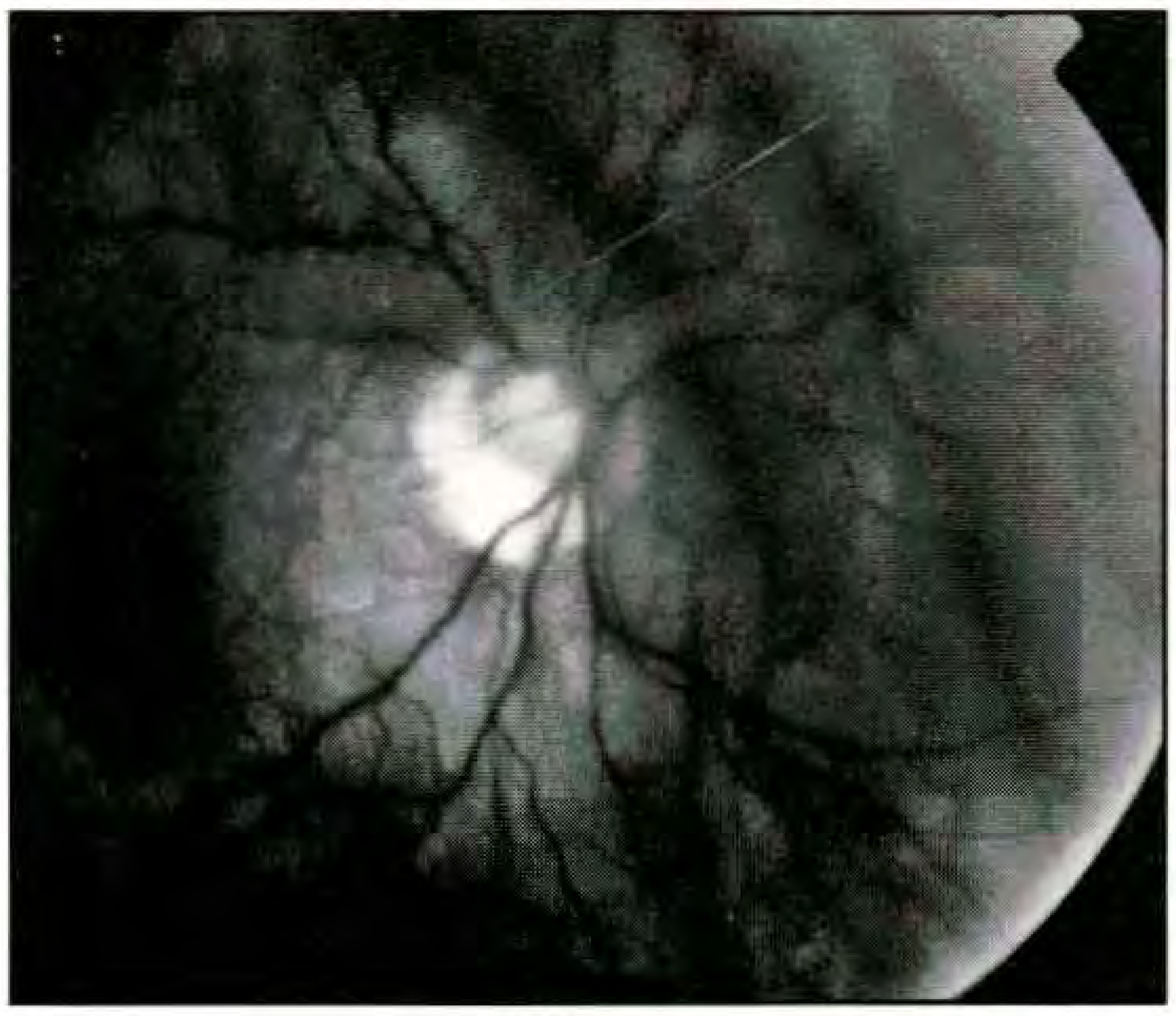

B

Case 12-5. Superior Nasal Step

Clinical Summary

A 50-year-old white man had uncontrolled primary open-angle glaucoma despite a medical regimen of timolol 0.5% and pilocarpine 4% both twice daily. In the right eye, his visual acuity was 20/160 and the intraocular pressure was 24 mm Hg. Slit-lamp examination and gonioscopy were normal and the angle was fully open to the ciliary body band. The right eye showed marked cupping and there was loss of the neuroretinal rim from approximately 6:00 to 9:00 (A, B). A localized superior nasal step was observed on a Humphrey visual field (D).

Optical Coherence Tomography

A circular tomogram (E) around the optic disc at a diameter of 3.4 mm demonstrated marked thinning of the nerve fiber layer from 6:00 to 9:00, consistent with the lack of neuroretinal rim in that region. The nerve fiber layer thinning was greater than that predicted by the visual field defect alone.

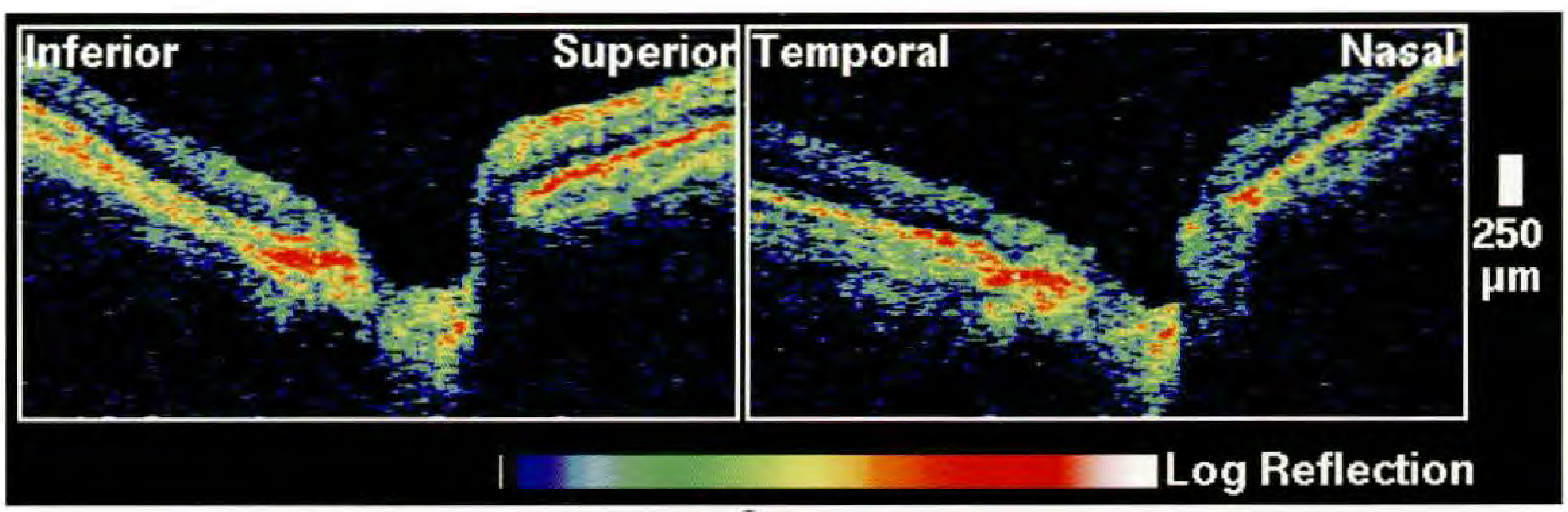

C

VERTICAL		*HORIZONTAL*	
Cup Diameter	**1.18 mm**	**Cup Diameter**	**0.60 mm**
Disc Diameter	**1.61 mm**	**Disc Diameter**	**1.12 mm**
C/D Ratio	**0.73**	**C/D Ratio**	**0.54**
NR Rim Area	**0.94 mm²**		
Inferior NFL	**60 µm**	**Temporal NFL**	**60 µm**
Superior NFL	**180 µm**	**Nasal NFL**	**0 µm**

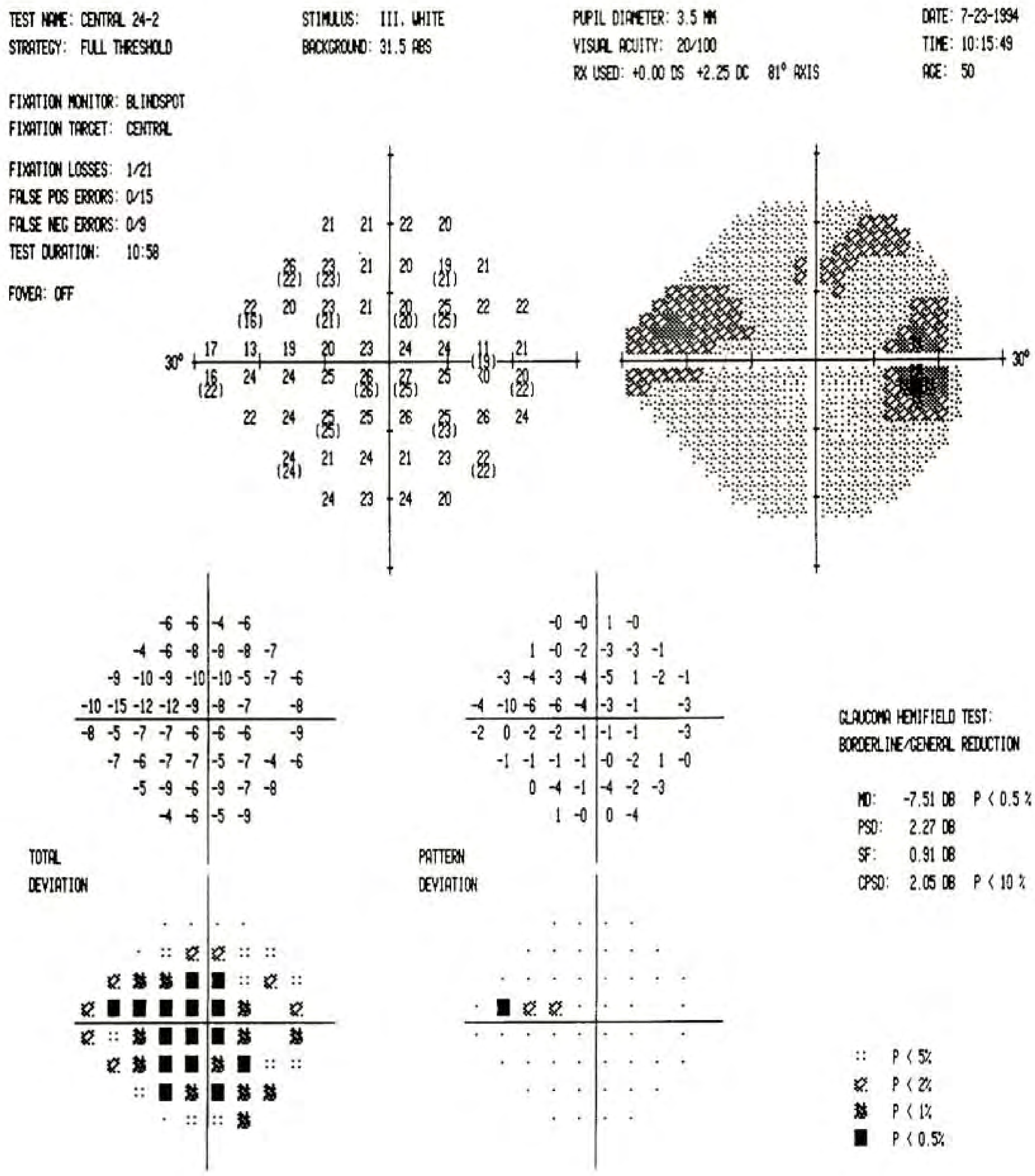

TEST NAME: CENTRAL 24-2
STRATEGY: FULL THRESHOLD
STIMULUS: III, WHITE
BACKGROUND: 31.5 ABS
PUPIL DIAMETER: 3.5 MM
VISUAL ACUITY: 20/100
RX USED: +0.00 DS +2.25 DC 81° AXIS
DATE: 7-23-1994
TIME: 10:15:49
AGE: 50
FIXATION MONITOR: BLINDSPOT
FIXATION TARGET: CENTRAL
FIXATION LOSSES: 1/21
FALSE POS ERRORS: 0/15
FALSE NEG ERRORS: 0/9
TEST DURATION: 10:58
FOVEA: OFF
30°
TOTAL DEVIATION
PATTERN DEVIATION
GLAUCOMA HEMIFIELD TEST:
BORDERLINE/GENERAL REDUCTION
MD: -7.51 DB P < 0.5 %
PSD: 2.27 DB
SF: 0.91 DB
CPSD: 2.05 DB P < 10 %
P < 5%
P < 2%
P < 1%
P < 0.5%

D

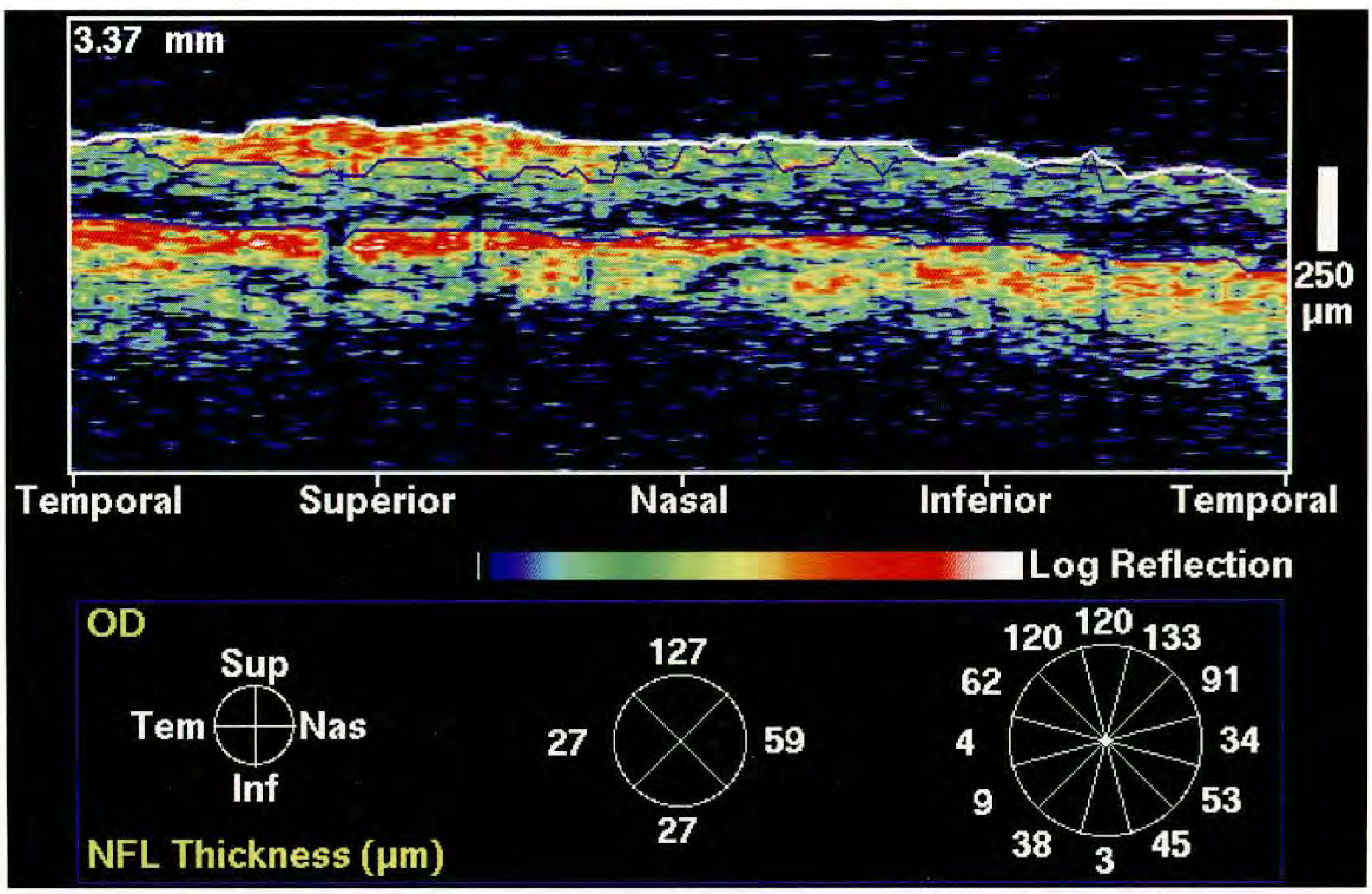

3.37 mm
250 µm
Temporal
Superior
Nasal
Inferior
Temporal
Log Reflection
OD
Sup
Tem
Nas
Inf
NFL Thickness (µm)
127
27
59
27
120
120
133
62
91
4
34
9
53
38
3
45

E

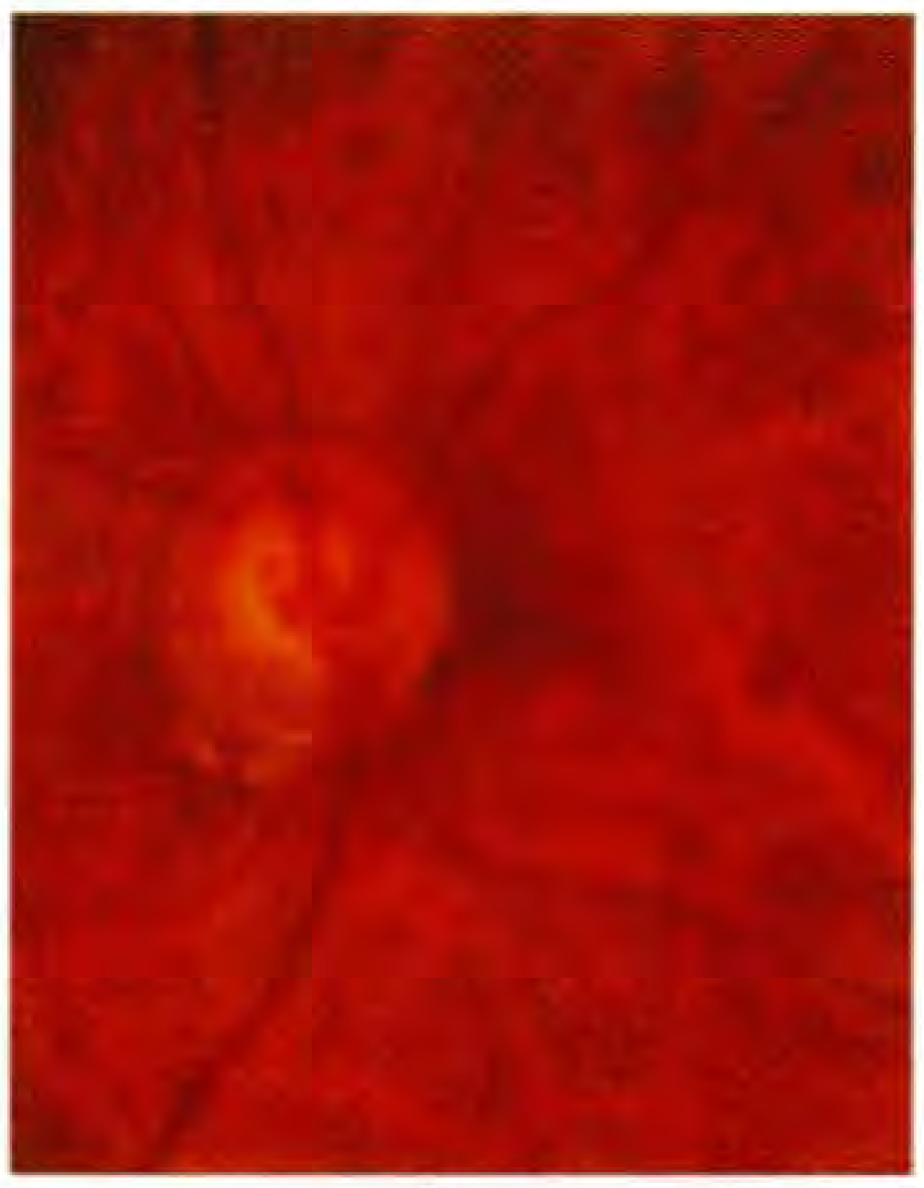

A

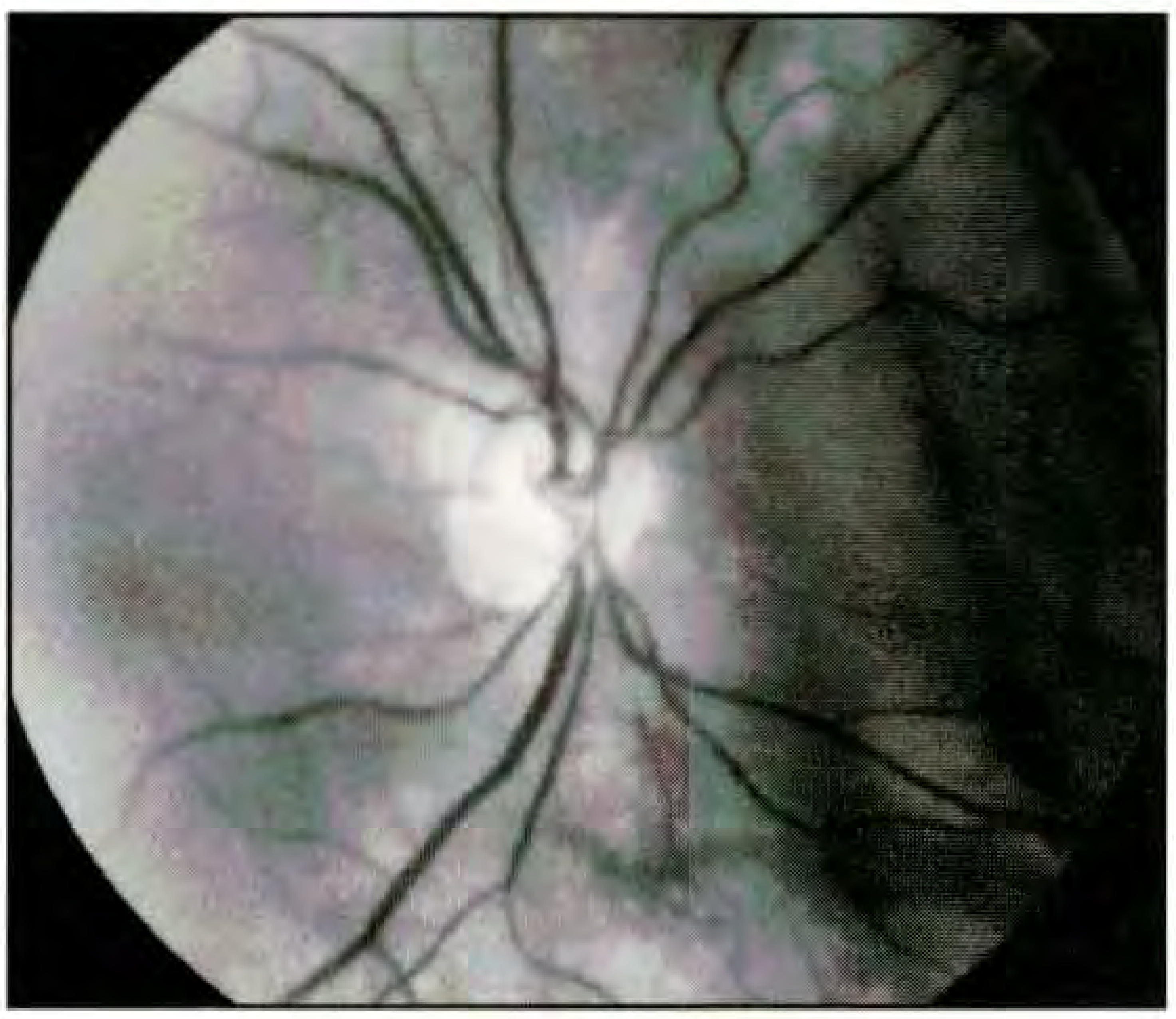

B

Case 12-6. Superior Nasal Step

Clinical Summary

A 67-year-old white woman with primary open-angle glaucoma maintained an intraocular pressure of 23 mm Hg in her right eye. Her ocular medications included timolol 0.5% twice daily and pilocarpine 4% four times a day. Dilated fundus examination (A,B) of the right eye revealed advanced cupping with absence of the neuroretinal rim from 6:00 to 9:00. A Humphrey visual field (D) showed an advanced nasal step.

Optical Coherence Tomography

A circular tomogram (E) around the optic nerve head at a diameter of 3.4 mm showed marked thinning of the nerve fiber layer from 6:00 to 9:00 corresponding to the loss of neuroretinal rim and the superior portion of the nasal step observed clinically. Moderate thinning of the superotemporal nerve fiber layer was also noted in the image consistent with the inferior area of scotoma.

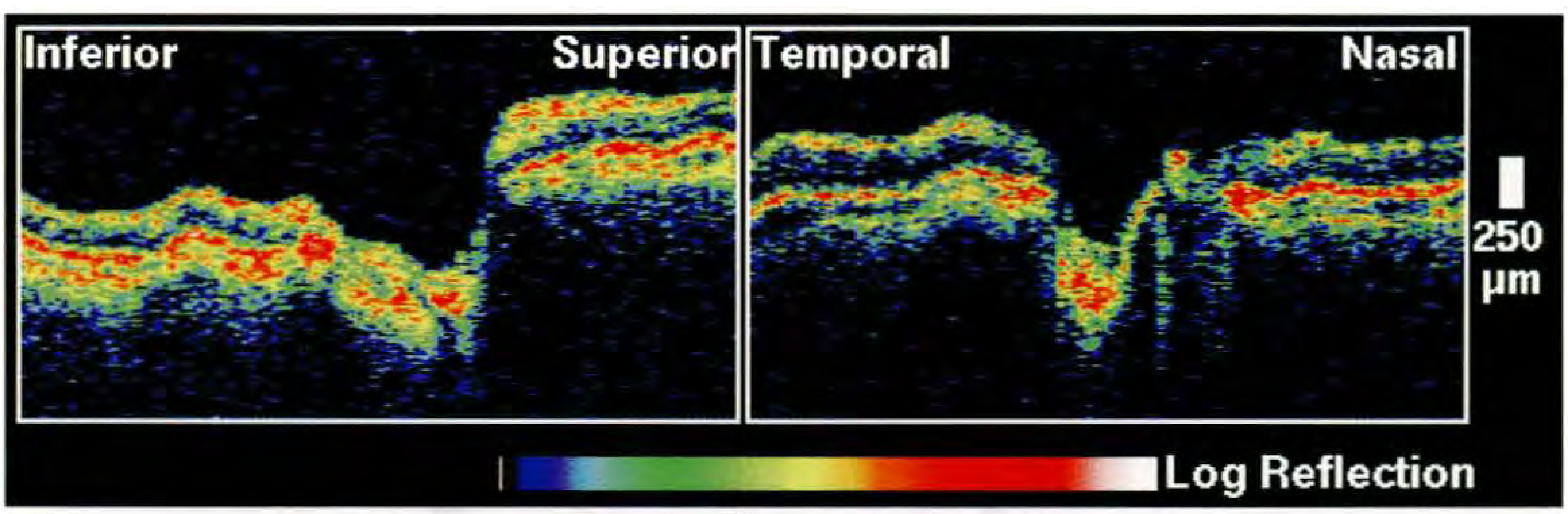

C

VERTICAL		HORIZONTAL	
Cup Diameter	1.20 mm	Cup Diameter	0.77 mm
Disc Diameter	1.48 mm	Disc Diameter	0.83 mm
C/D Ratio	0.81	C/D Ratio	0.93
NR Rim Area	0.59 mm^2		
Inferior NFL	90 µm	Temporal NFL	140 µm
Superior NFL	120 µm	Nasal NFL	90 µm

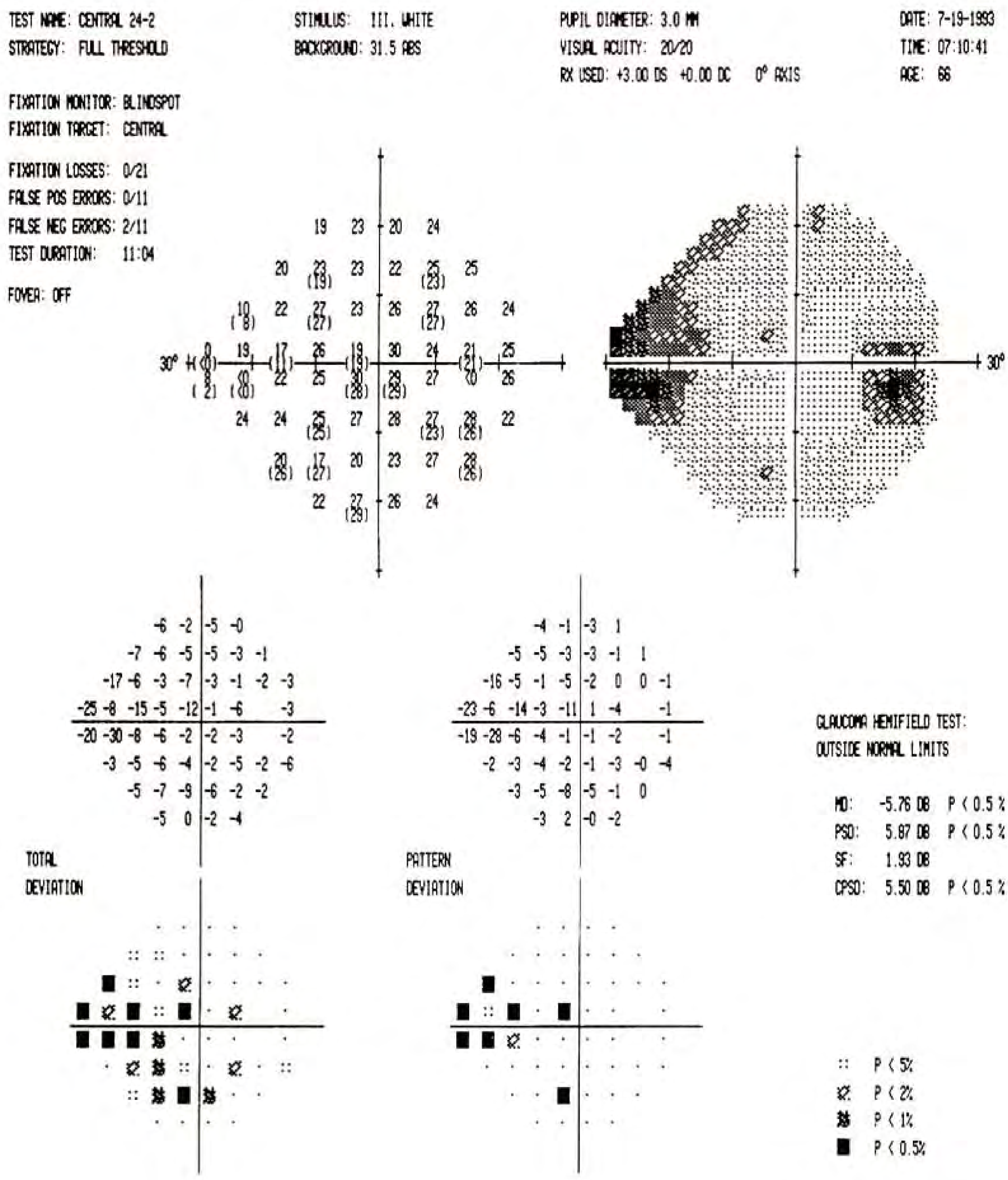

TEST NAME: CENTRAL 24-2
STRATEGY: FULL THRESHOLD
STIMULUS: III, WHITE
BACKGROUND: 31.5 ABS
PUPIL DIAMETER: 3.0 MM
VISUAL ACUITY: 20/20
RX USED: +3.00 DS +0.00 DC 0° AXIS
DATE: 7-19-1993
TIME: 07:10:41
AGE: 66
FIXATION MONITOR: BLINDSPOT
FIXATION TARGET: CENTRAL
FIXATION LOSSES: 0/21
FALSE POS ERRORS: 0/11
FALSE NEG ERRORS: 2/11
TEST DURATION: 11:04
FOVEA: OFF
30°
30°
TOTAL
DEVIATION
PATTERN
DEVIATION
GLAUCOMA HEMIFIELD TEST:
OUTSIDE NORMAL LIMITS
MD: -5.76 DB P < 0.5 %
PSD: 5.87 DB P < 0.5 %
SF: 1.93 DB
CPSD: 5.50 DB P < 0.5 %
P < 5%
P < 2%
P < 1%
P < 0.5%

D

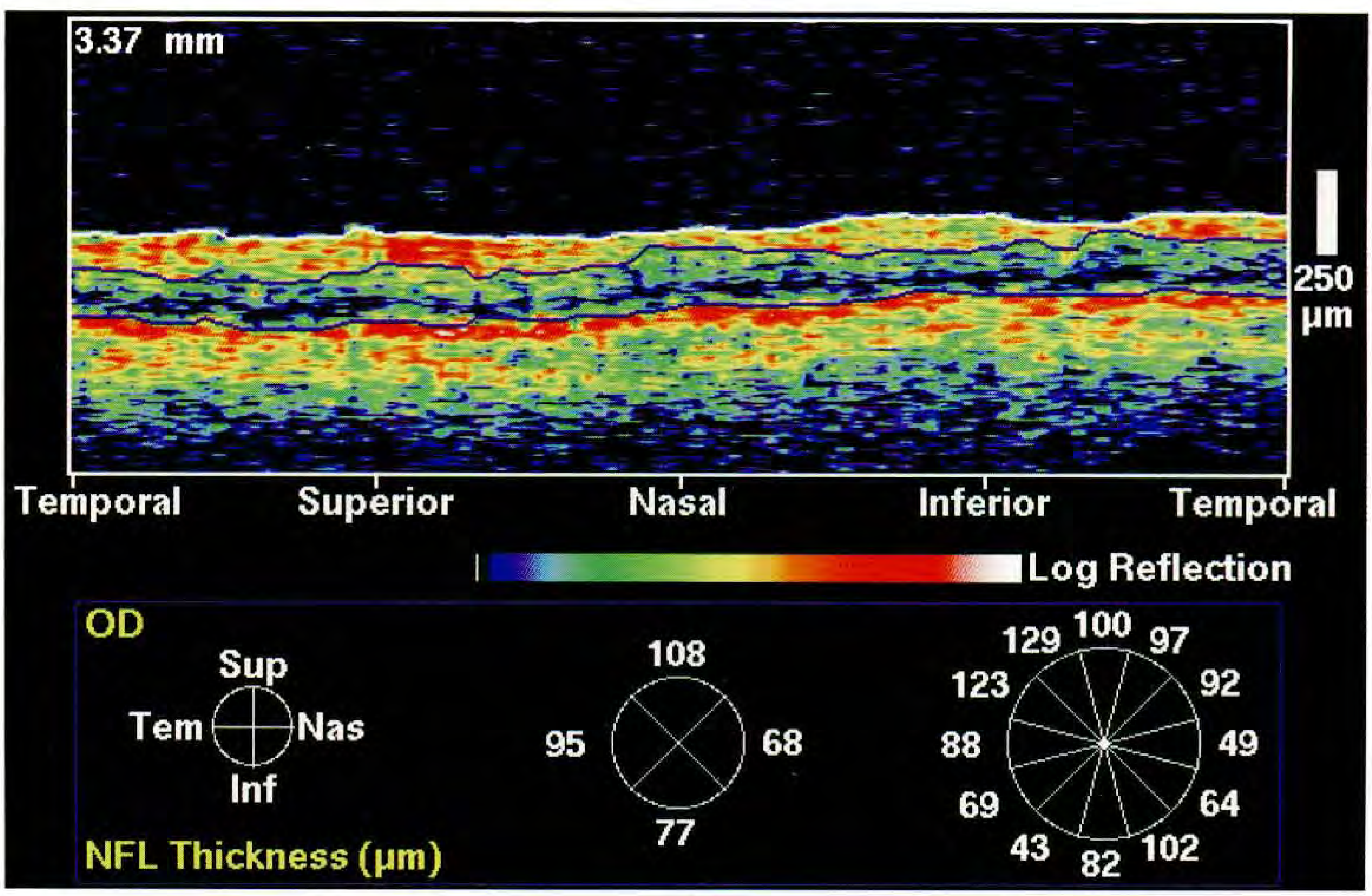

3.37 mm
250 µm
Temporal
Superior
Nasal
Inferior
Temporal
Log Reflection
OD
Sup
Tem
Nas
Inf
NFL Thickness (µm)
108
95
68
77
129
100
97
123
92
88
49
69
64
43
82
102

E

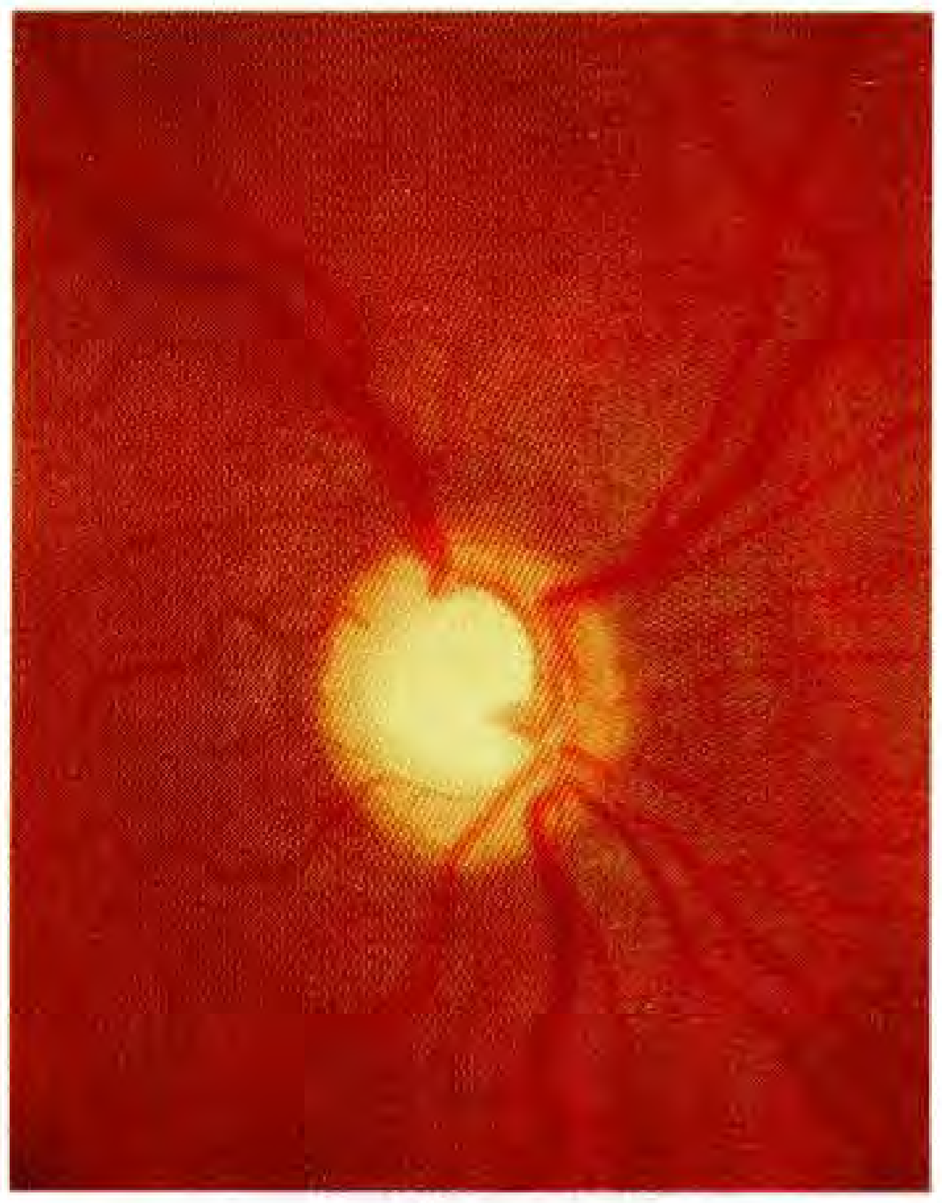

A

B

Case 12-7. Superior and Inferior Nasal Step

Clinical Summary

A 43-year-old white man was referred for a second opinion regarding his diagnosis of glaucoma. He was taking betaxolol 0.25% and dipivefrin 0.1%, each twice daily, and pilocarpine 0.1%, four times a day in the right eye. On examination, the visual acuity was 20/20 in this eye and the intraocular pressure was 26 mm Hg. Slit-lamp examination was normal. Gonioscopy revealed that the angle was open to the ciliary body band except between 10:00 and 2:00, where only the posterior trabecular meshwork was visible. Ophthalmoscopy (A,B) showed marked disc cupping with a severely attenuated neuroretinal rim between approximately 5:00 and 12:00. An advanced superior nasal step with an early inferior nasal step was identified on a Humphrey visual field (D).

Optical Coherence Tomography

The circular OCT section (E) revealed diffuse nerve fiber layer thinning throughout the image, which was considerably worse inferiorly than superiorly. Only a local area of nerve fibers remained within the 12:00 hour, corresponding to the inferonasal area of relative visual preservation.

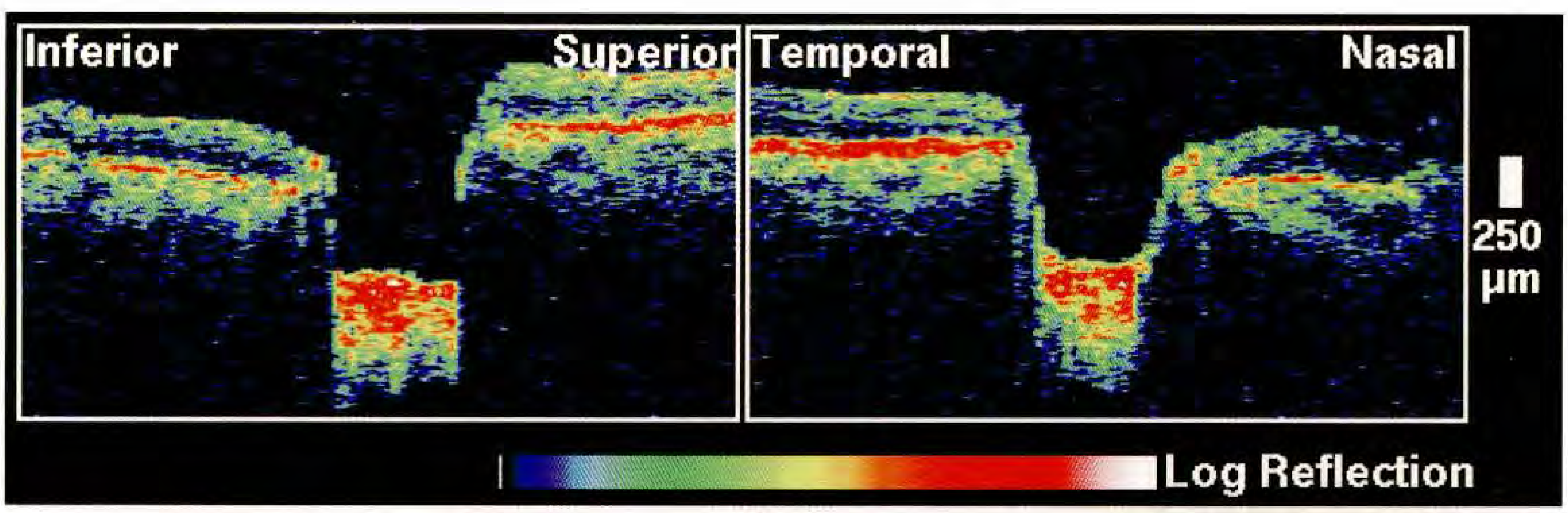

C

VERTICAL		HORIZONTAL	
Cup Diameter	1.22 mm	Cup Diameter	1.31 mm
Disc Diameter	1.55 mm	Disc Diameter	1.44 mm
C/D Ratio	0.79	C/D Ratio	0.91
NR Rim Area	0.72 mm^2		
Inferior NFL	120 µm	Temporal NFL	70 µm
Superior NFL	130 µm	Nasal NFL	90 µm

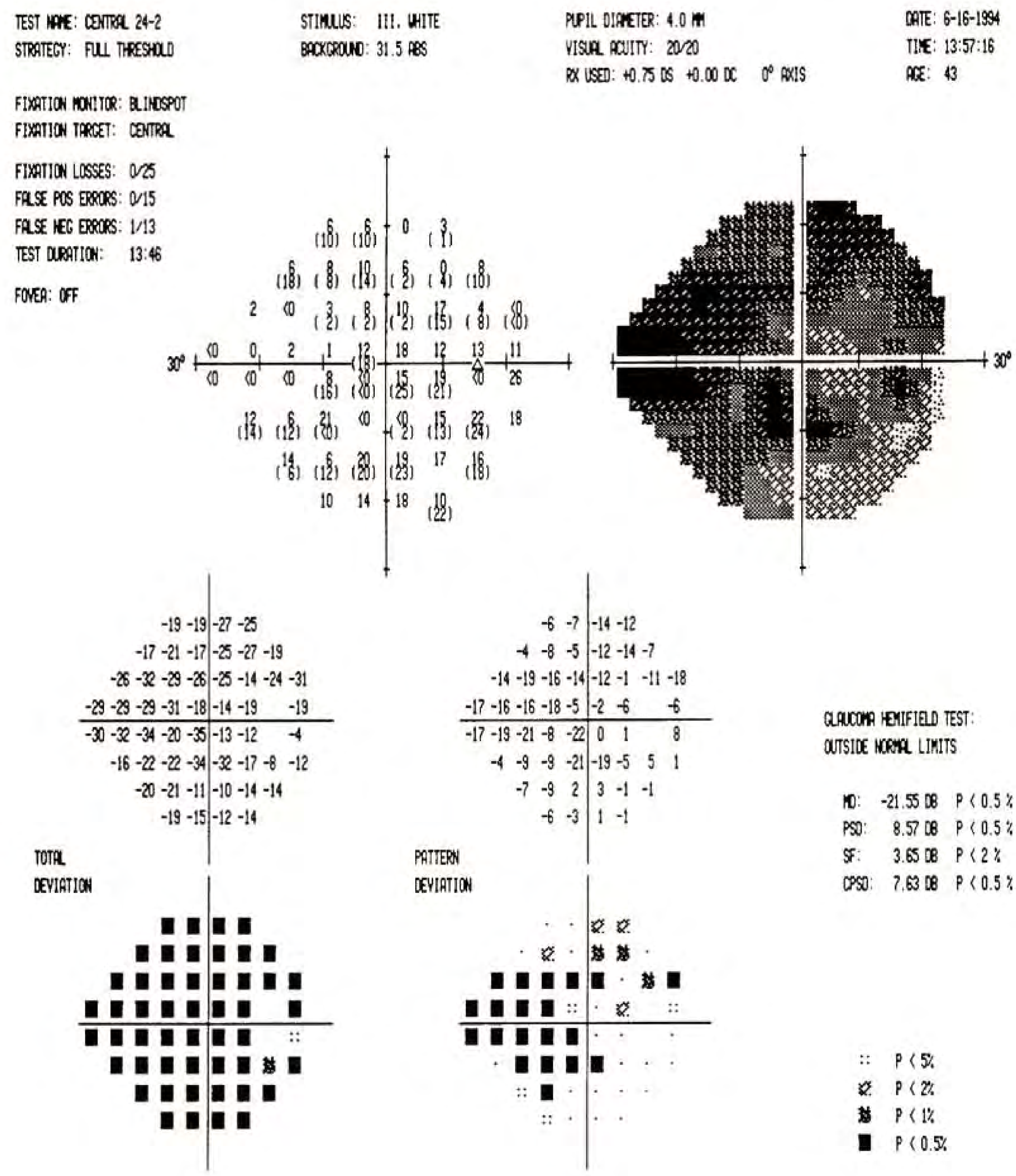
TEST NAME: CENTRAL 24-2
STRATEGY: FULL THRESHOLD
STIMULUS: III, WHITE
BACKGROUND: 31.5 ASB
PUPIL DIAMETER: 4.0 MM
VISUAL ACUITY: 20/20
RX USED: +0.75 DS +0.00 DC 0° AXIS
DATE: 6-16-1994
TIME: 13:57:16
AGE: 43
FIXATION MONITOR: BLINDSPOT
FIXATION TARGET: CENTRAL
FIXATION LOSSES: 0/25
FALSE POS ERRORS: 0/15
FALSE NEG ERRORS: 1/13
TEST DURATION: 13:46
FOVEA: OFF
30°
30°
TOTAL DEVIATION
PATTERN DEVIATION
GLAUCOMA HEMIFIELD TEST: OUTSIDE NORMAL LIMITS
MD: -21.55 DB P < 0.5%
PSD: 8.57 DB P < 0.5%
SF: 3.65 DB P < 2%
CPSD: 7.63 DB P < 0.5%
P < 5%
P < 2%
P < 1%
P < 0.5%

D

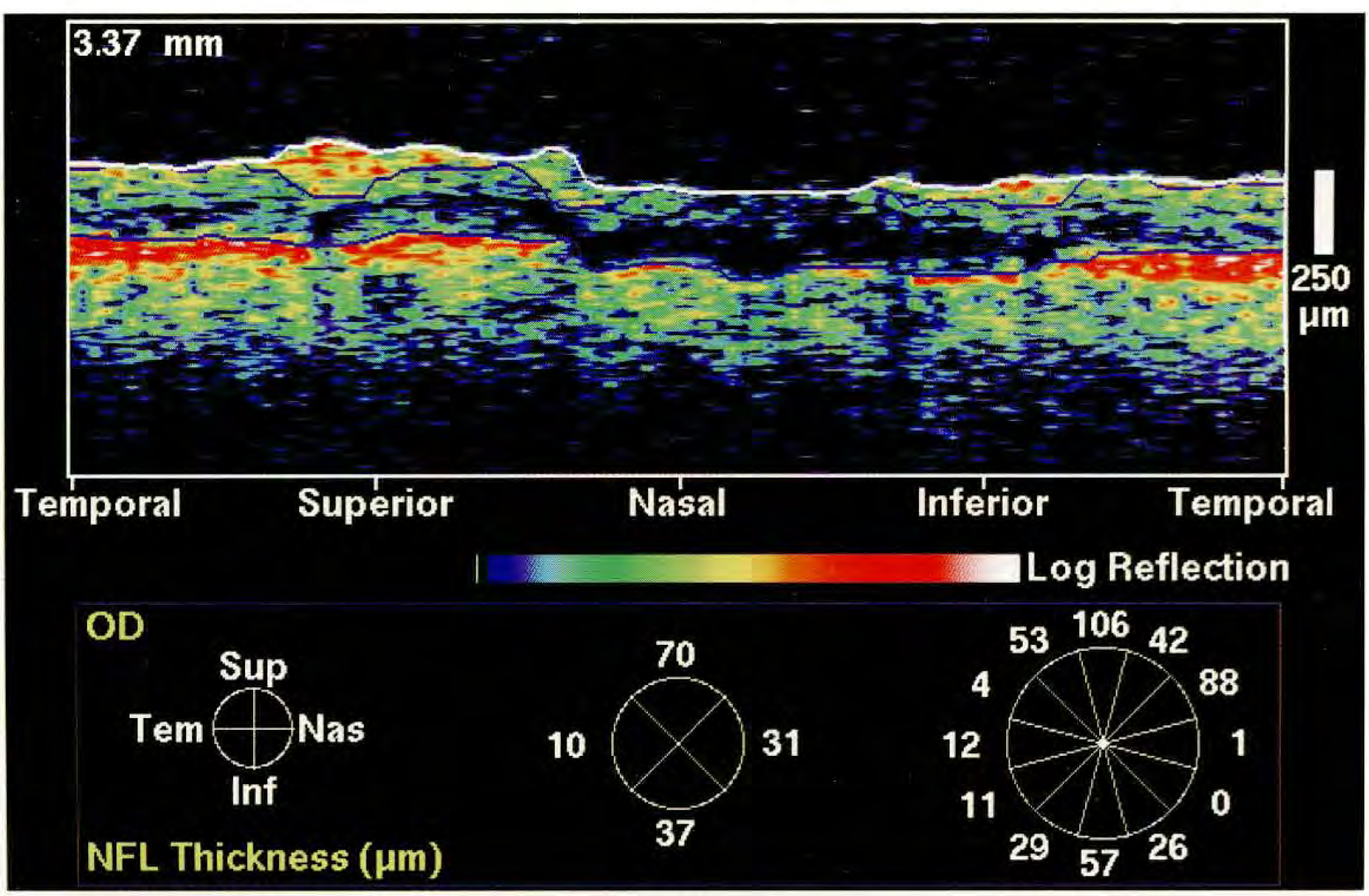
3.37 mm
250 µm
Temporal
Superior
Nasal
Inferior
Temporal
Log Reflection
OD
Sup
Tem
Nas
Inf
NFL Thickness (µm)
70
10
31
37
53
106
42
4
88
12
1
11
0
29
57
26

E

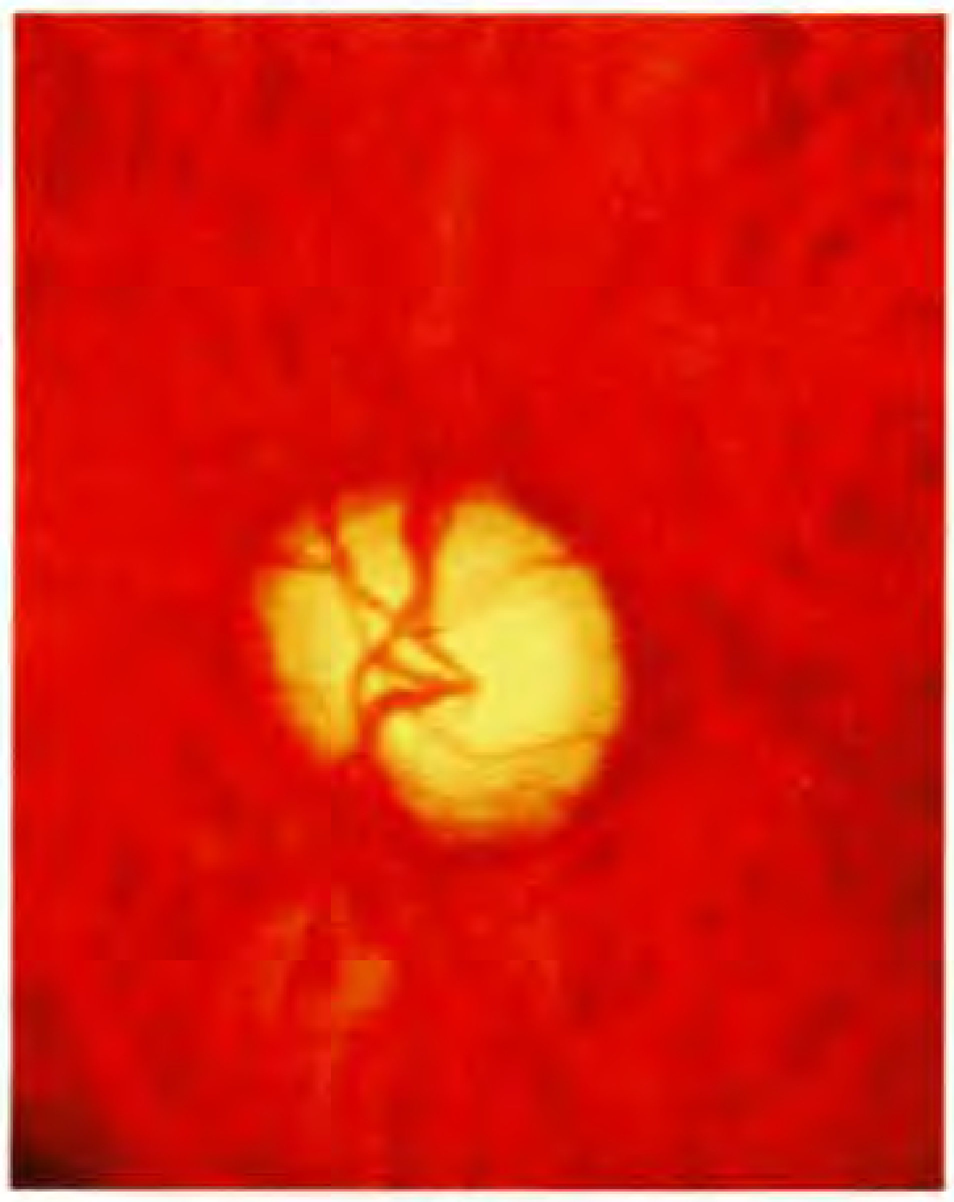

A

B

Case 12-8. Superior and Inferior Nasal Step

Clinical Summary

A 40-year-old white man had undergone trabeculectomy with mitomycin C in his left eye two years earlier. On examination, the intraocular pressure in this eye was 11 mm Hg and had been stable since the surgery. Visual acuity was 20/20. Anterior segment examination was unremarkable. Dilated fundus examination (A,B) revealed marked cupping with loss of the neuroretinal rim between 1:00 and 6:00. An intermediate superior nasal step and an earlier inferior nasal step were identified on the Humphrey visual field (D).

Optical Coherence Tomography

A 3.4 mm diameter circular OCT (E) revealed significant thinning of the nerve fiber layer, greater inferiorly than superiorly, consistent with the visual field defect.

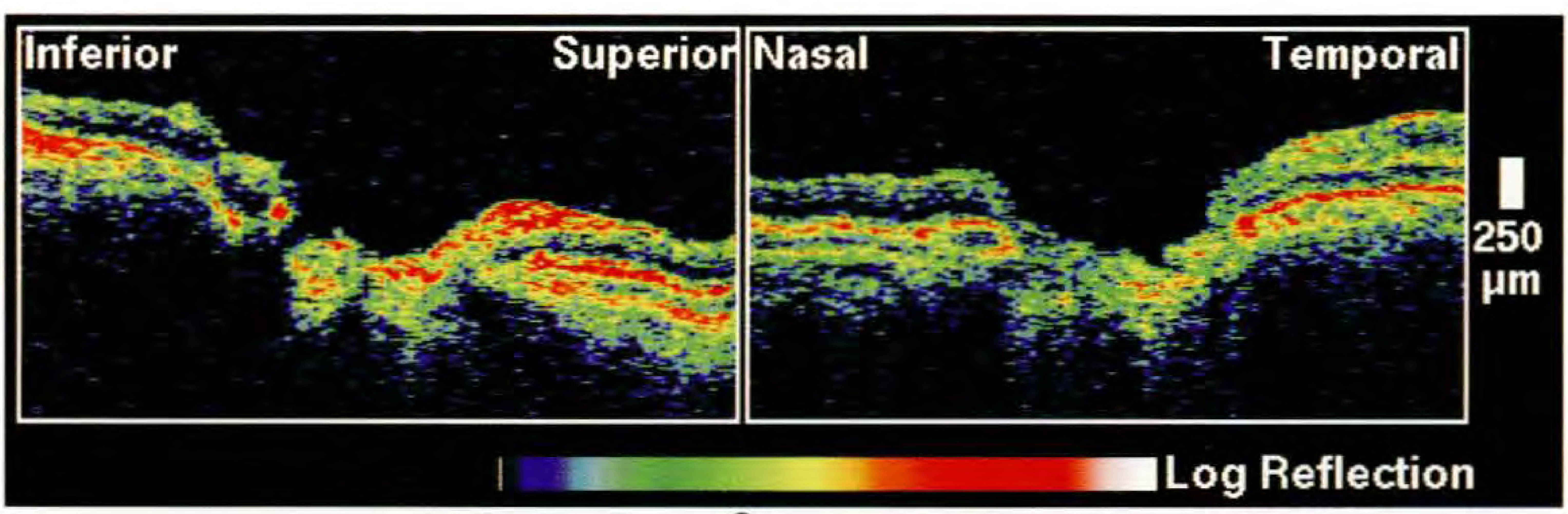

C

VERTICAL		*HORIZONTAL*	
Cup Diameter	**1.39 mm**	**Cup Diameter**	**1.38 mm**
Disc Diameter	**1.84 mm**	**Disc Diameter**	**1.90 mm**
C/D Ratio	**0.76**	**C/D Ratio**	**0.73**
NR Rim Area	**1.14 mm^2**		
Inferior NFL	**180 µm**	**Nasal NFL**	**100 µm**
Superior NFL	**160 µm**	**Temporal NFL**	**40 µm**

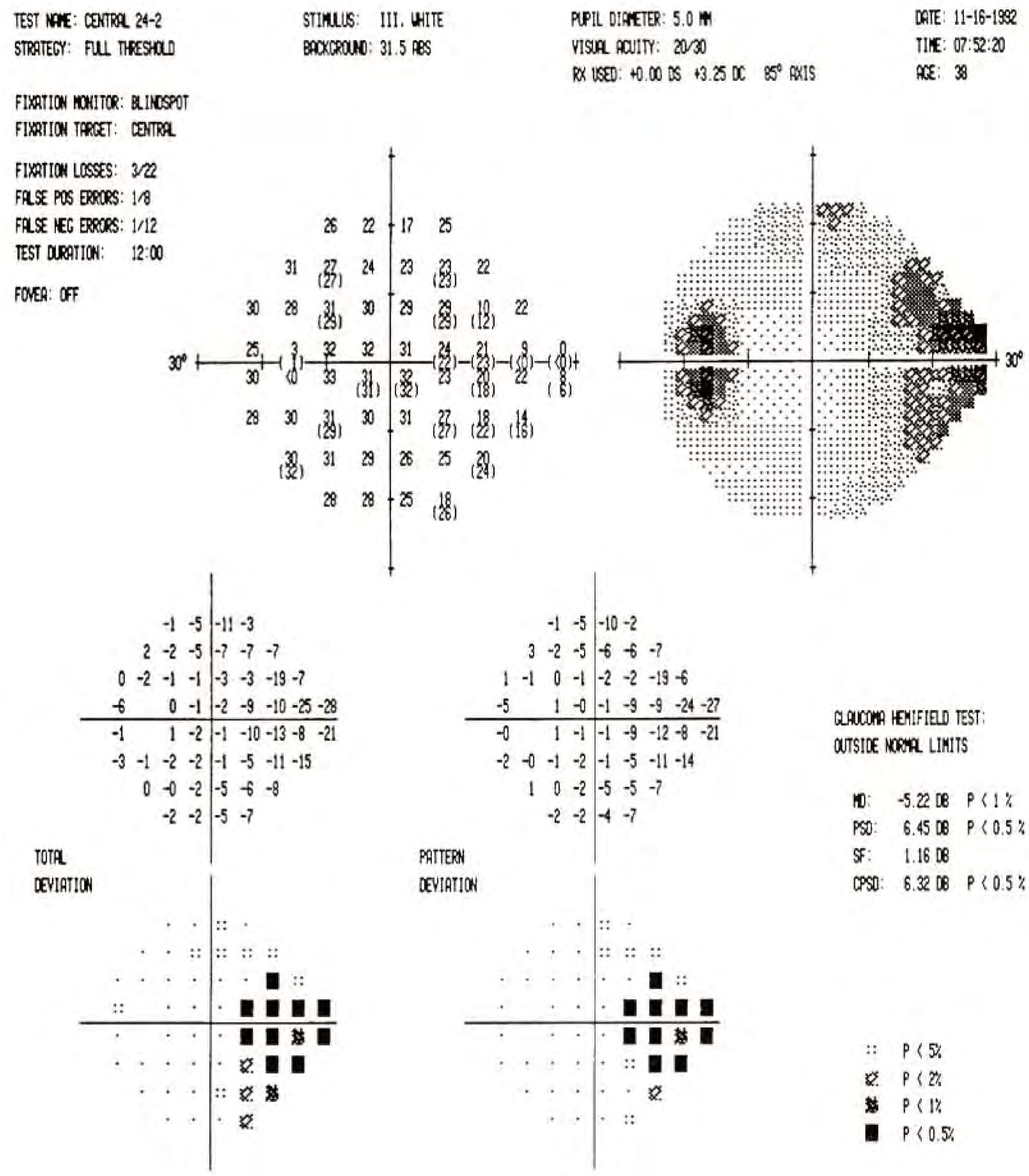

TEST NAME: CENTRAL 24-2
STRATEGY: FULL THRESHOLD
STIMULUS: III, WHITE
BACKGROUND: 31.5 ABS
PUPIL DIAMETER: 5.0 MM
VISUAL ACUITY: 20/30
RX USED: +0.00 DS +3.25 DC 85° AXIS
DATE: 11-16-1992
TIME: 07:52:20
AGE: 38
FIXATION MONITOR: BLINDSPOT
FIXATION TARGET: CENTRAL
FIXATION LOSSES: 3/22
FALSE POS ERRORS: 1/8
FALSE NEG ERRORS: 1/12
TEST DURATION: 12:00
FOVEA: OFF
30°
TOTAL DEVIATION
PATTERN DEVIATION
GLAUCOMA HEMIFIELD TEST:
OUTSIDE NORMAL LIMITS
MD: -5.22 DB P < 1 %
PSD: 6.45 DB P < 0.5 %
SF: 1.16 DB
CPSD: 6.32 DB P < 0.5 %
P < 5%
P < 2%
P < 1%
P < 0.5%

D

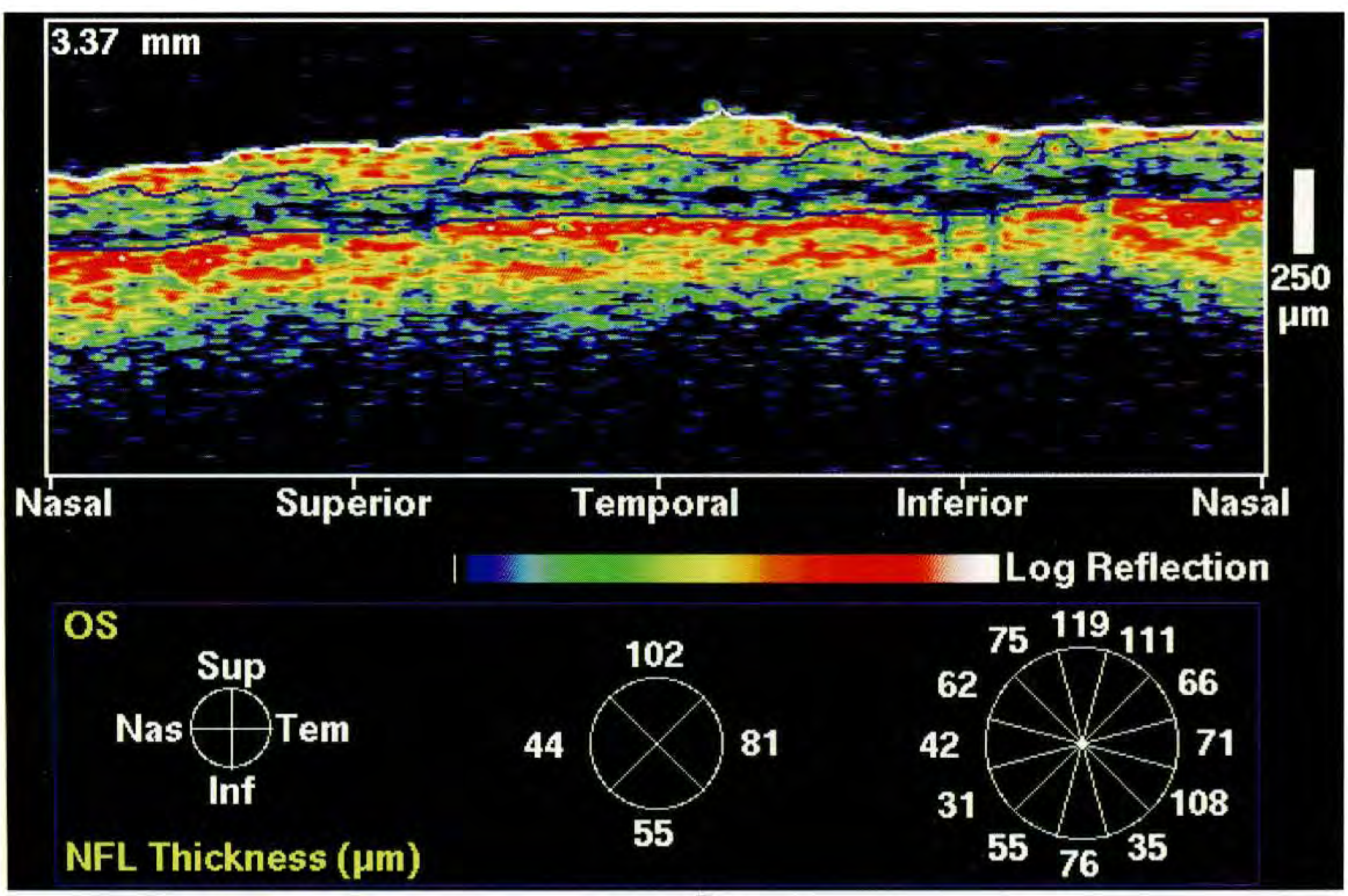

3.37 mm
250 µm
Nasal
Superior
Temporal
Inferior
Nasal
Log Reflection
OS
Sup
Nas
Tem
Inf
NFL Thickness (µm)
102
44
81
55
75
119
111
62
66
42
71
31
108
55
76
35

E

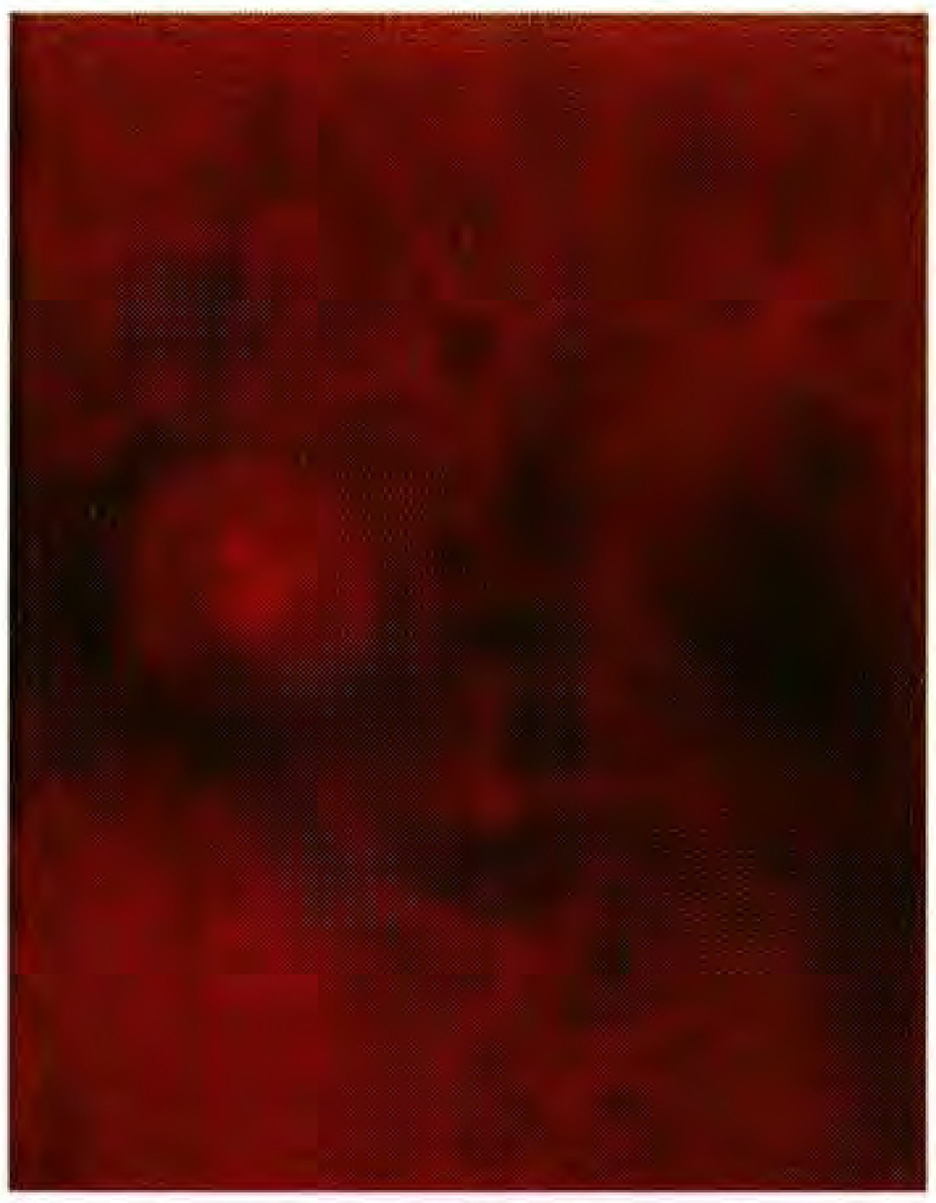

A

Case 12-9. Inferior Nasal Step

Clinical Summary

A 87-year-old white man had glaucoma in his left eye associated with an intraocular pressure of 28 mm Hg and a visual acuity of 20/40. He had been taking carteolol 1% twice daily in this eye. Slit-lamp examination revealed evidence of pseudoexfoliation and 2-3+ nuclear sclerosis of the crystalline lens. Dilated ophthalmoscopy (A) showed a moderately cupped disc with thinning of the neuroretinal rim superotemporally. A Humphrey visual field (C) showed an advanced inferior nasal step.

Optical Coherence Tomography

The circular OCT image (D) showed a diffuse decrease in nerve fiber layer thickness throughout the image, with a focal area of thinning superotemporally. Within the superotemporal bundle, the nerve fiber layer thickness averaged at 1:00 was thinner than the 12:00 and 2:00 hours. In contrast, the thickness at 5:00 was greater than in the surrounding clock hours within the inferotemporal bundle.

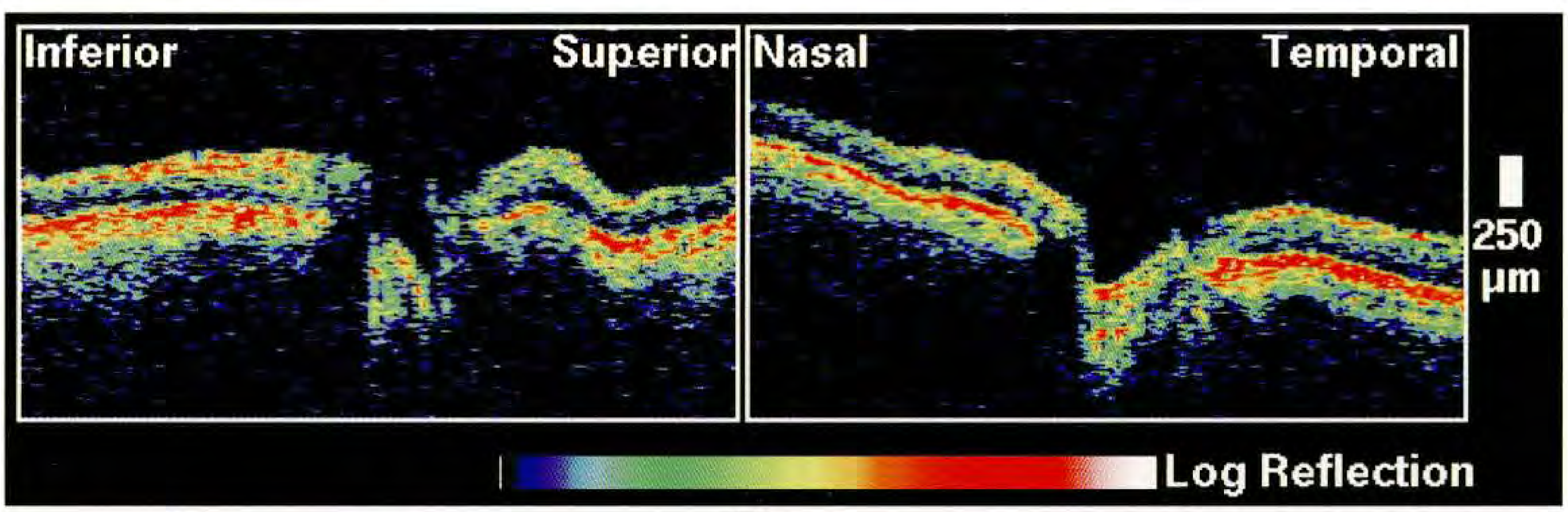

B

VERTICAL		HORIZONTAL	
Cup Diameter	0.61 mm	Cup Diameter	0.85 mm
Disc Diameter	0.89 mm	Disc Diameter	1.46 mm
C/D Ratio	0.69	C/D Ratio	0.58
NR Rim Area	1.33 mm^2		
Inferior NFL	240 μm	Nasal NFL	120 μm
Superior NFL	110 μm	Temporal NFL	80 μm

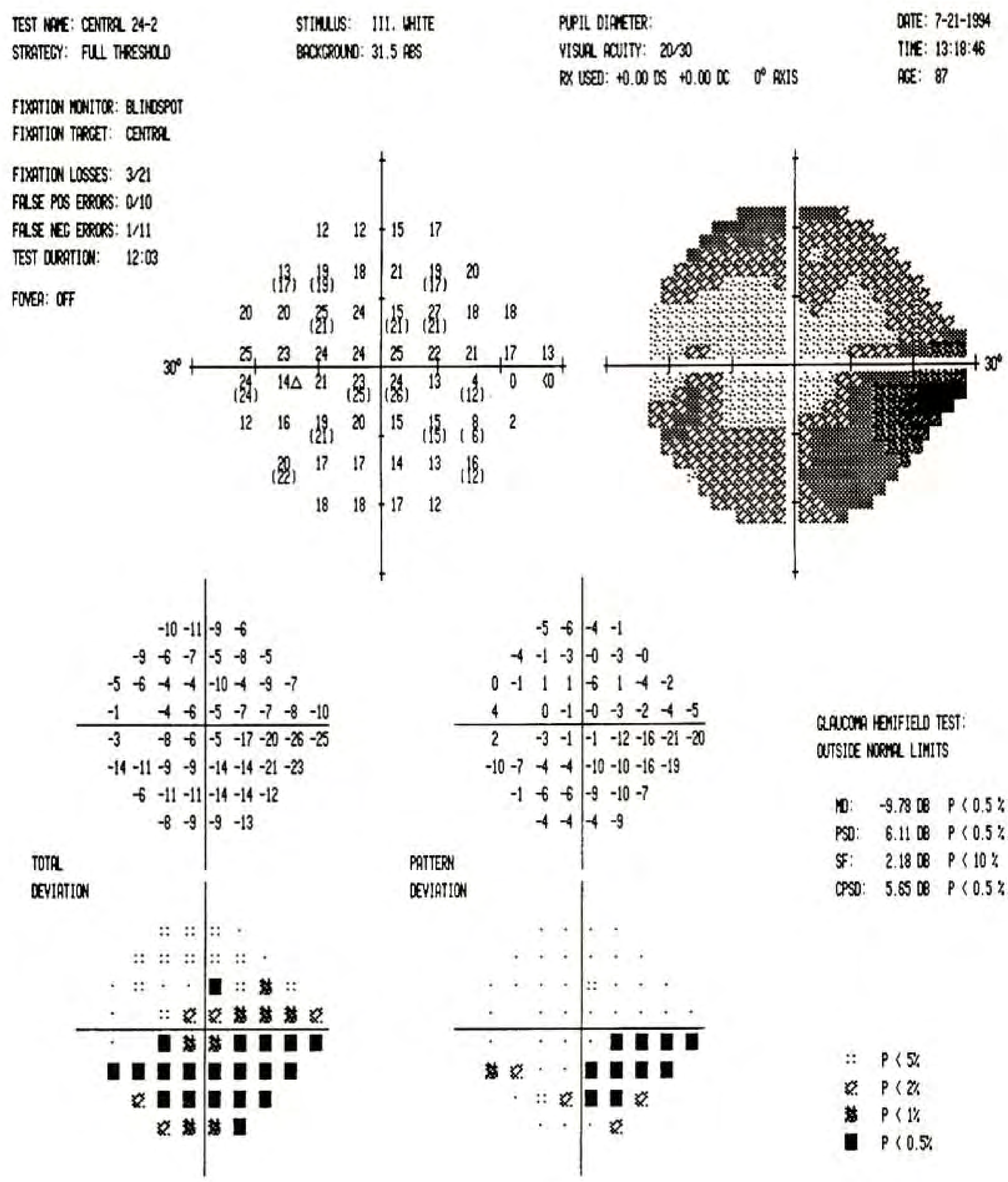
TEST NAME: CENTRAL 24-2
STRATEGY: FULL THRESHOLD
STIMULUS: III, WHITE
BACKGROUND: 31.5 ABS
PUPIL DIAMETER:
VISUAL ACUITY: 20/30
RX USED: +0.00 DS +0.00 DC 0° AXIS
DATE: 7-21-1994
TIME: 13:18:46
AGE: 87
FIXATION MONITOR: BLINDSPOT
FIXATION TARGET: CENTRAL
FIXATION LOSSES: 3/21
FALSE POS ERRORS: 0/10
FALSE NEG ERRORS: 1/11
TEST DURATION: 12:03
FOVEA: OFF
30°
30°
TOTAL DEVIATION
PATTERN DEVIATION
GLAUCOMA HEMIFIELD TEST: OUTSIDE NORMAL LIMITS
MD: -9.78 DB P < 0.5 %
PSD: 6.11 DB P < 0.5 %
SF: 2.18 DB P < 10 %
CPSD: 5.65 DB P < 0.5 %
P < 5%
P < 2%
P < 1%
P < 0.5%

C

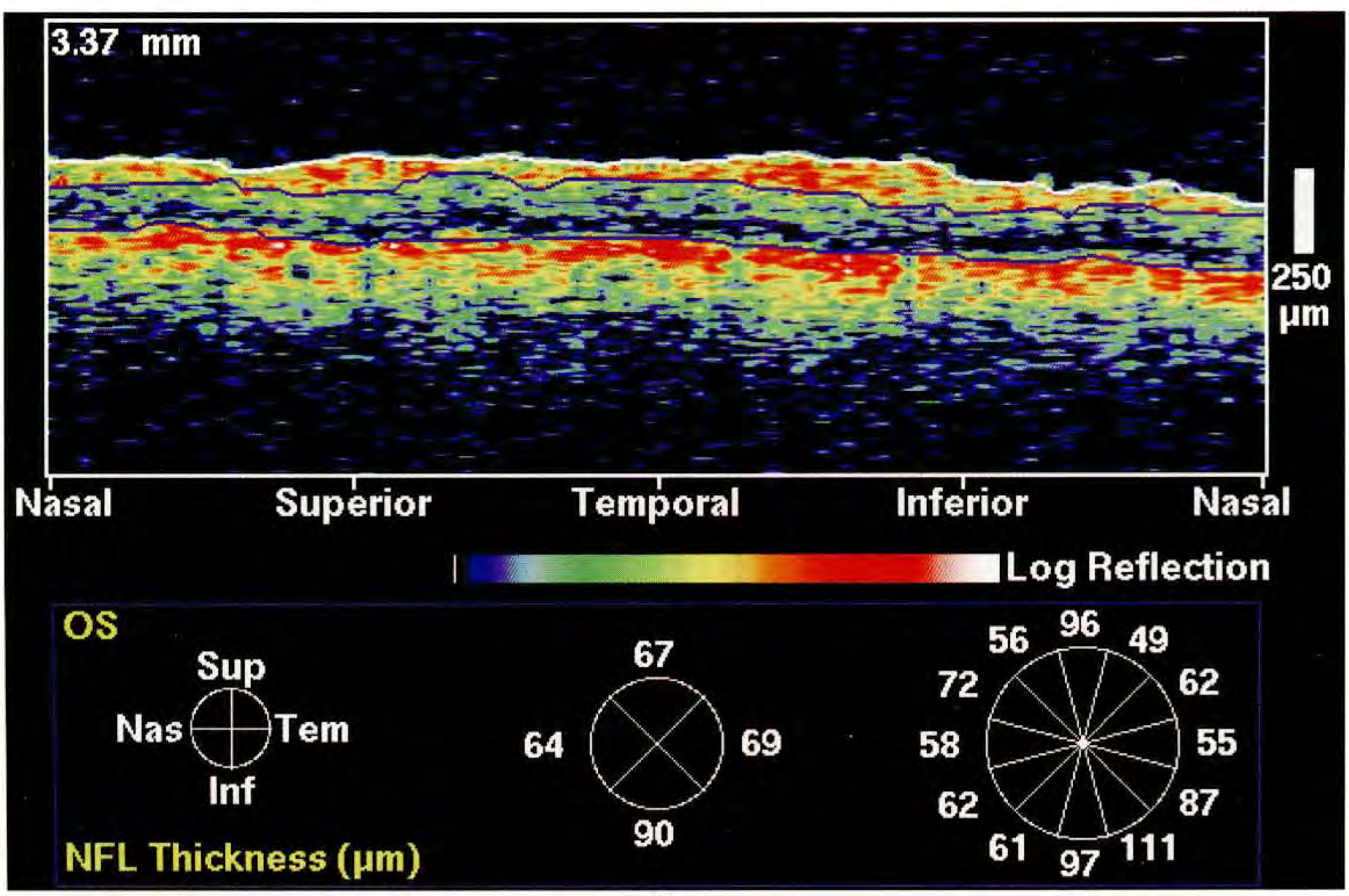
3.37 mm
250 µm
Nasal
Superior
Temporal
Inferior
Nasal
Log Reflection
OS
Sup
Nas
Tem
Inf
NFL Thickness (µm)
67
64
69
90
56
96
49
72
62
58
55
62
87
61
97
111

D

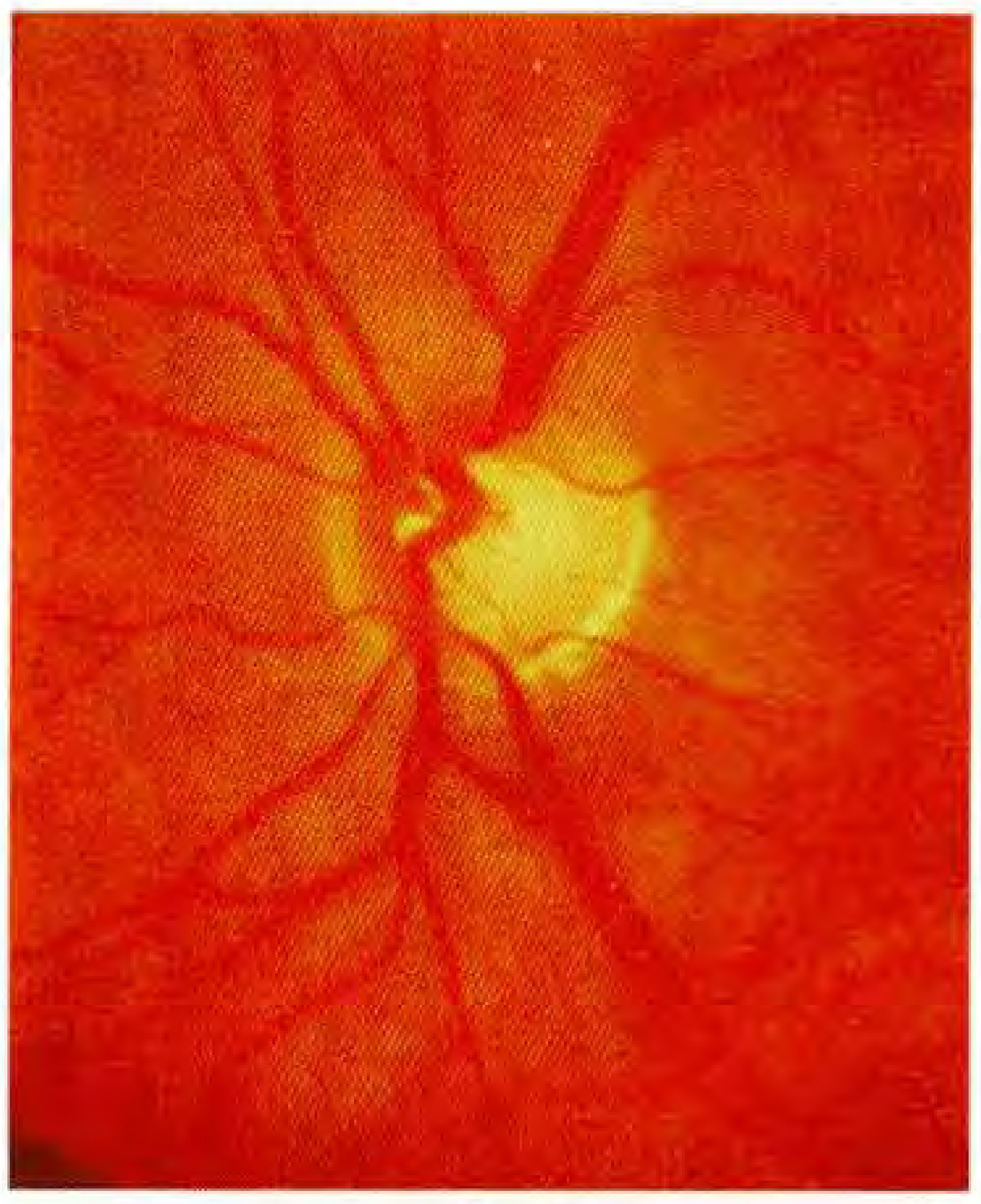

A

B

Case 12-10. Paracentral Scotoma

Clinical Summary

A 50-year-old white woman had an intraocular pressure of 16 mm Hg in her left eye and a visual acuity of 20/20 associated with the diagnosis of normal tension glaucoma. She was being treated with timolol 0.5% twice daily and apraclonidine 0.5% three times a day. Slit-lamp examination and gonioscopy were normal, with visualization of the ciliary body band throughout 360°. Ophthalmoscopy (A,B) revealed marked cupping of the disc and attenuation of the neuroretinal rim from 3:00 to 6:00. A superior paracentral scotoma was evident on the Humphrey visual field (D).

Optical Coherence Tomography

The overall nerve fiber layer thickness was slightly attenuated throughout a 3.4 mm diameter circular tomogram around the disc (E). A focal area of almost total nerve fiber layer drop-out was identified inferotemporally at 5:00, corresponding to the visual field defect.

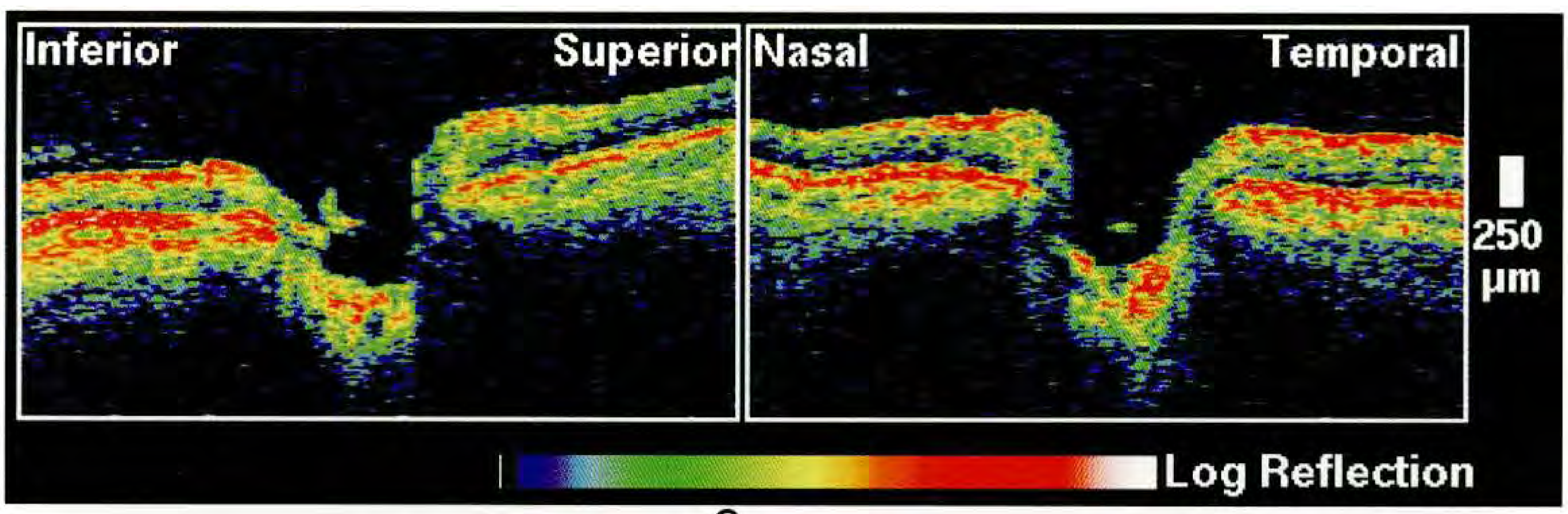

C

VERTICAL		HORIZONTAL	
Cup Diameter	0.97 mm	Cup Diameter	0.93 mm
Disc Diameter	1.44 mm	Disc Diameter	1.23 mm
C/D Ratio	0.67	C/D Ratio	0.76
NR Rim Area	0.89 mm^2		
Inferior NFL	100 µm	Nasal NFL	160 µm
Superior NFL	140 µm	Temporal NFL	160 µm

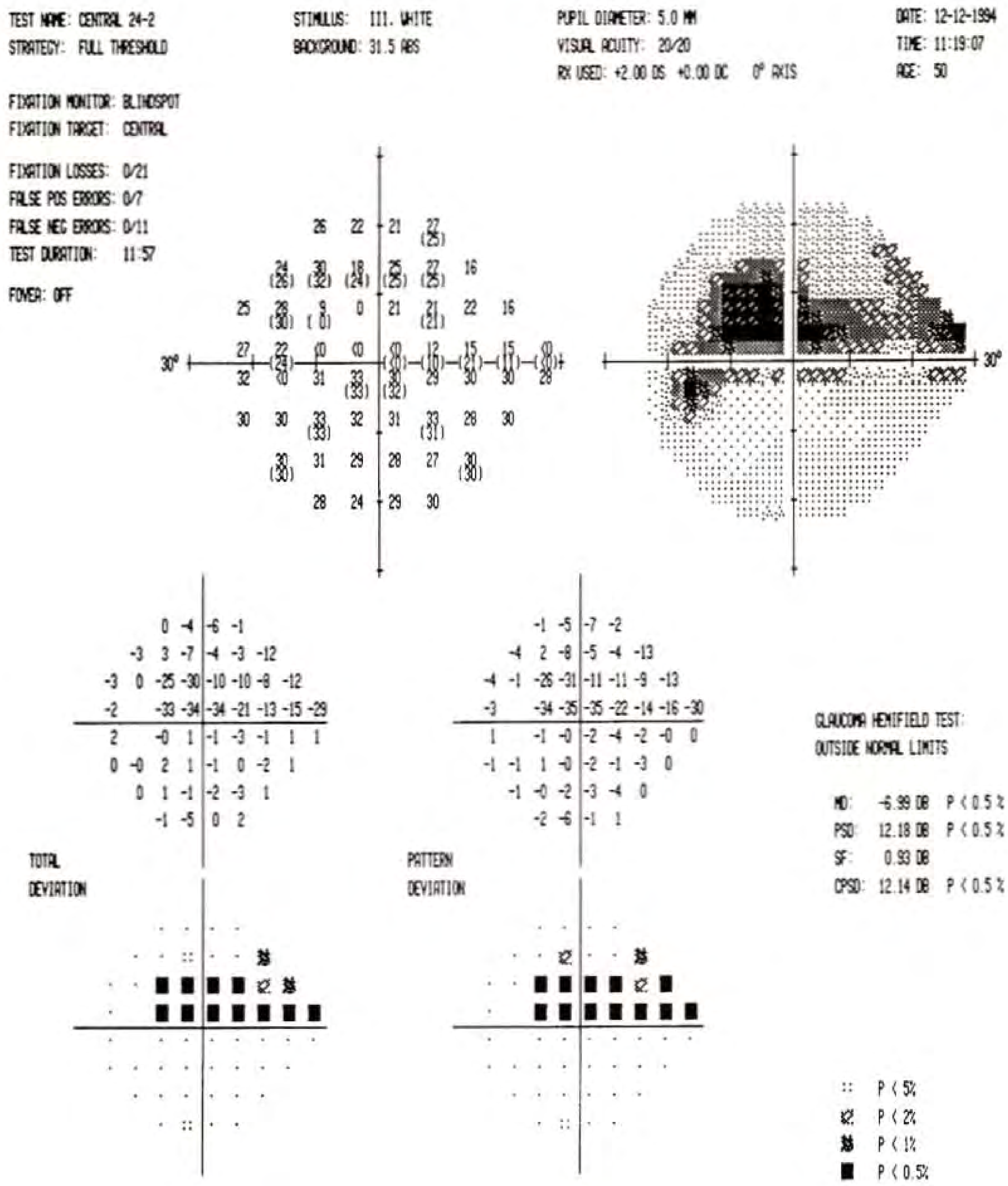
TEST NAME: CENTRAL 24-2
STRATEGY: FULL THRESHOLD
STIMULUS: III, WHITE
BACKGROUND: 31.5 ASB
PUPIL DIAMETER: 5.0 MM
VISUAL ACUITY: 20/20
RX USED: +2.00 DS +0.00 DC 0° AXIS
DATE: 12-12-1994
TIME: 11:19:07
AGE: 50
FIXATION MONITOR: BLINDSPOT
FIXATION TARGET: CENTRAL
FIXATION LOSSES: 0/21
FALSE POS ERRORS: 0/7
FALSE NEG ERRORS: 0/11
TEST DURATION: 11:57
FOVEA: OFF
30°
30°
TOTAL DEVIATION
PATTERN DEVIATION
GLAUCOMA HEMIFIELD TEST:
OUTSIDE NORMAL LIMITS
MD: -6.99 DB P < 0.5 %
PSD: 12.18 DB P < 0.5 %
SF: 0.93 DB
CPSD: 12.14 DB P < 0.5 %
P < 5%
P < 2%
P < 1%
P < 0.5%

D

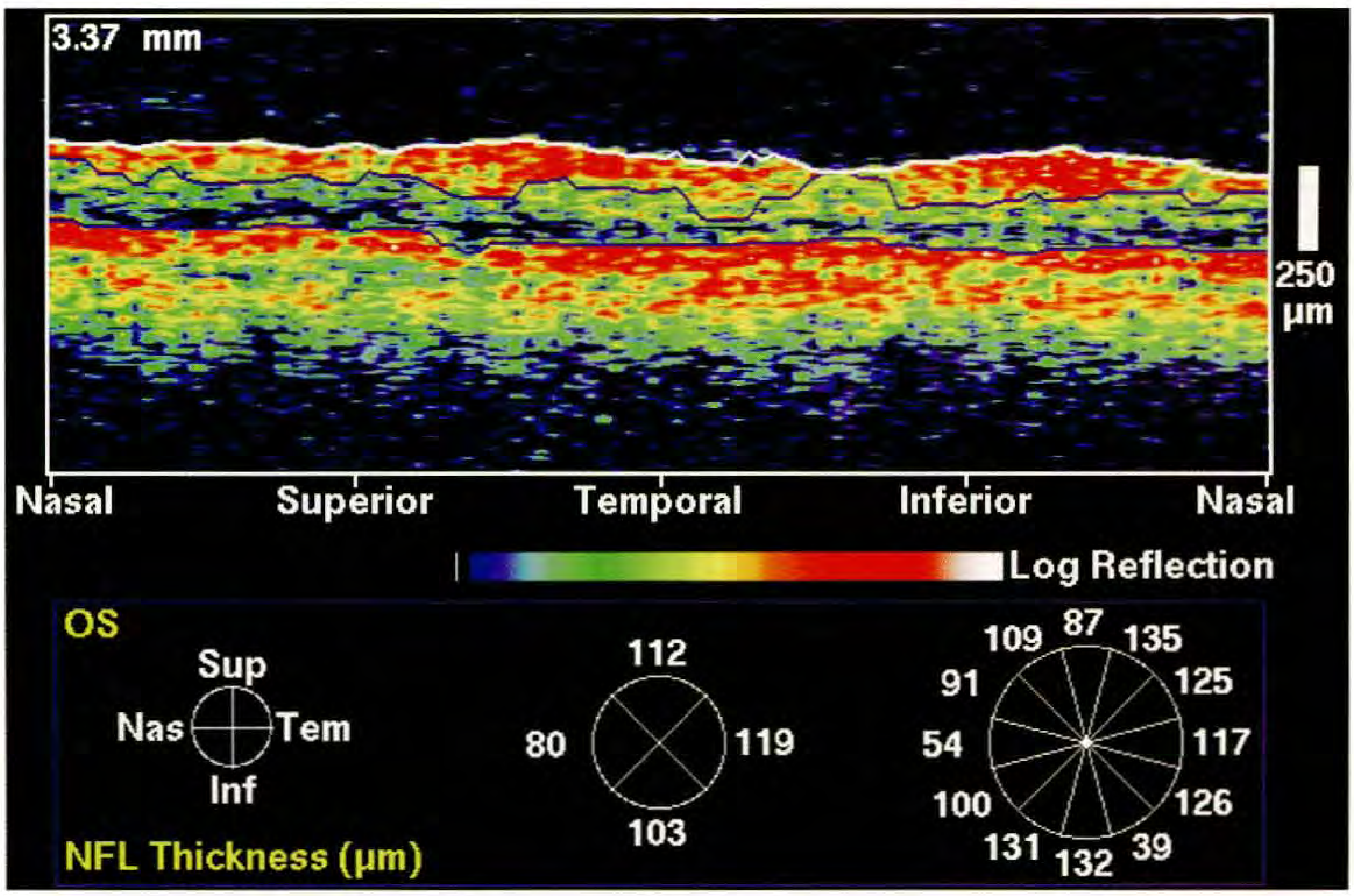
3.37 mm
250 µm
Nasal
Superior
Temporal
Inferior
Nasal
Log Reflection
OS
Sup
Nas
Tem
Inf
NFL Thickness (µm)
112
80
119
103
109
87
135
91
125
54
117
100
126
131
132
39

E

A

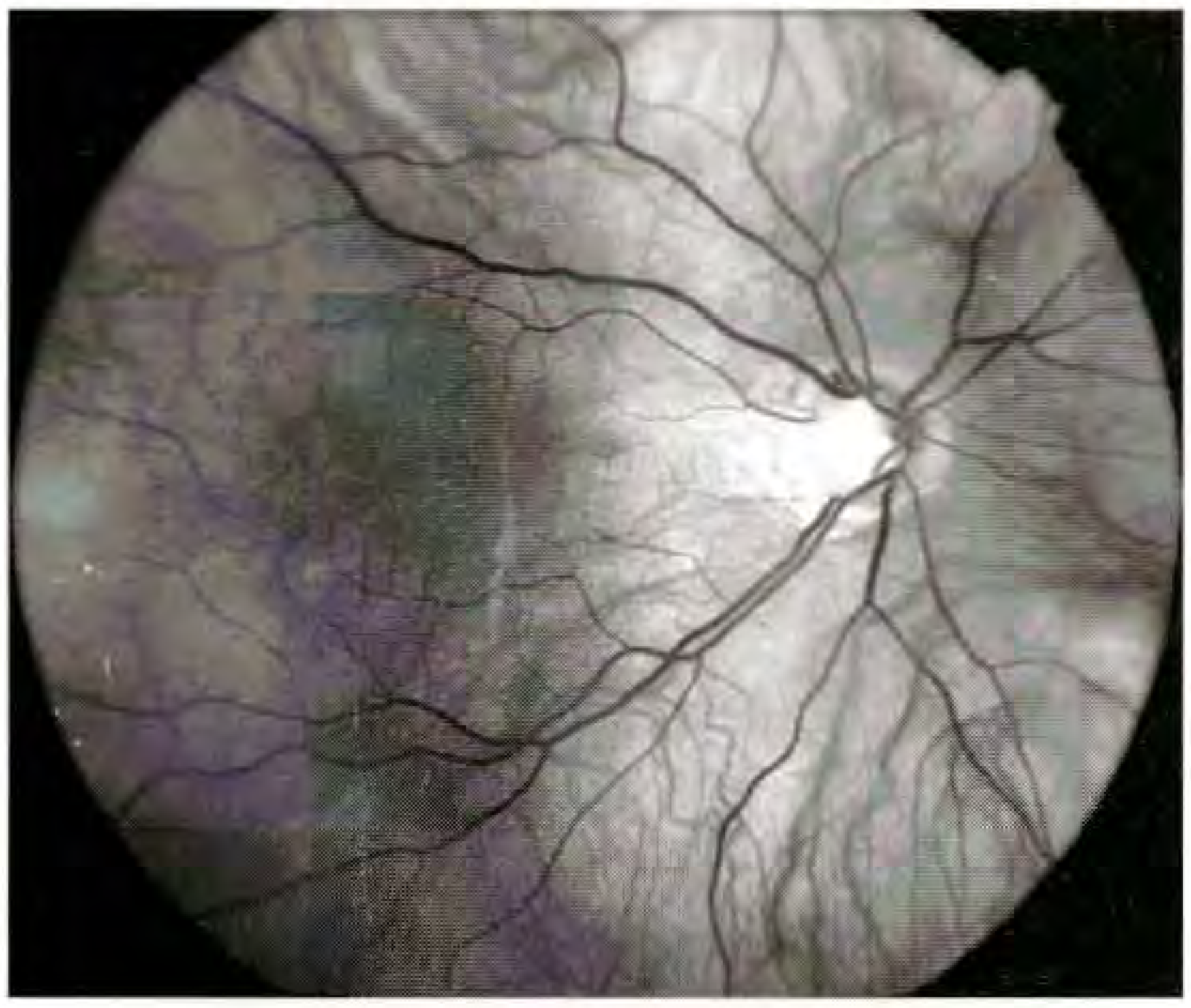

B

Case 12-11. Paracentral Scotoma

Clinical Summary

A 66-year-old white woman had been under treatment for normal tension glaucoma for the past four years. Her current ocular medications included betaxolol 0.5% twice a day and carbachol three times daily. On examination of her right eye, the visual acuity was 20/20 and the intraocular pressure was 18 mm Hg. Slit-lamp examination and gonioscopy were both unremarkable, with visualization of the ciliary body band throughout 360°. Dilated ophthalmoscopy (A,B) showed marked cupping of the optic disc and loss of the neuroretinal rim from approximately 7:00 to 10:00. A disc hemorrhage was present at approximately the 1:00 position. A Humphrey visual field (D) revealed a superior paracentral scotoma extending to the blind spot.

Optical Coherence Tomography

A 3.4 mm diameter circular OCT tomogram (E) around the optic disc showed generalized thinning of the nerve fiber layer throughout the image. The most severe thinning occured between 7:00 and 9:00, consistent with both the loss of neuretinal rim in that region and the superior paracentral scotoma. The nerve fiber layer thickness exhibited a broad depression that reached a minimum of 20 µm in this region.

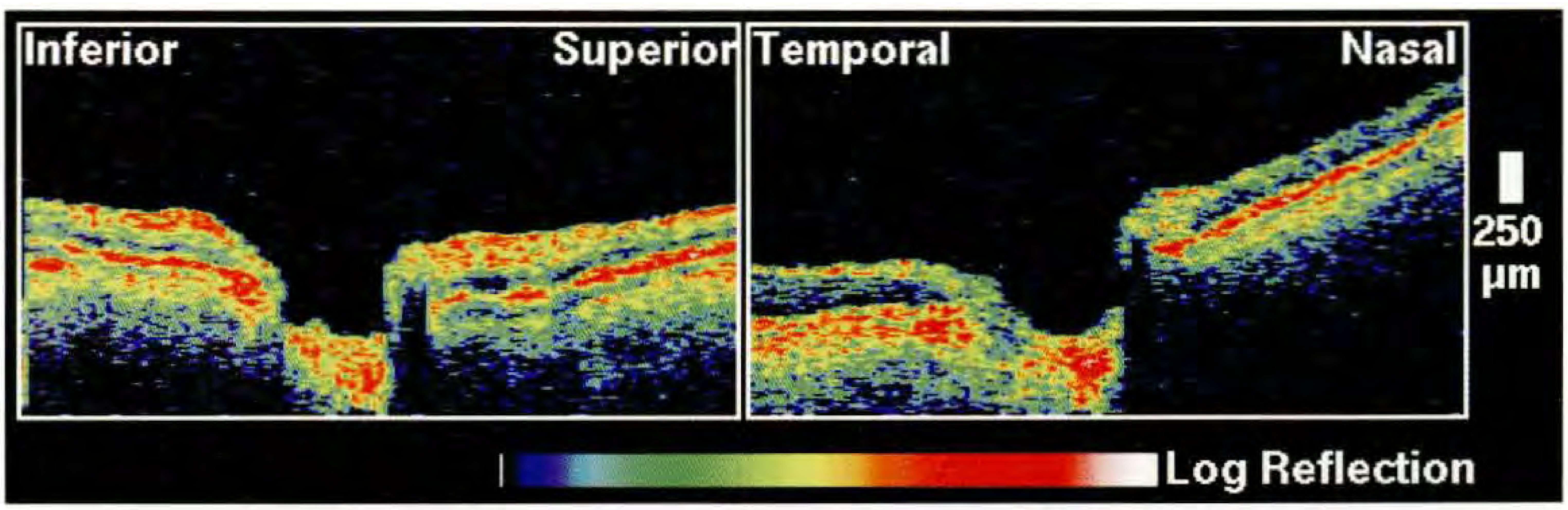

C

VERTICAL		HORIZONTAL	
Cup Diameter	0.90 mm	Cup Diameter	1.04 mm
Disc Diameter	0.99 mm	Disc Diameter	1.28 mm
C/D Ratio	0.91	C/D Ratio	0.81
NR Rim Area	0.13 mm^2		
Inferior NFL	60 µm	Temporal NFL	20 µm
Superior NFL	100 µm	Nasal NFL	100 µm

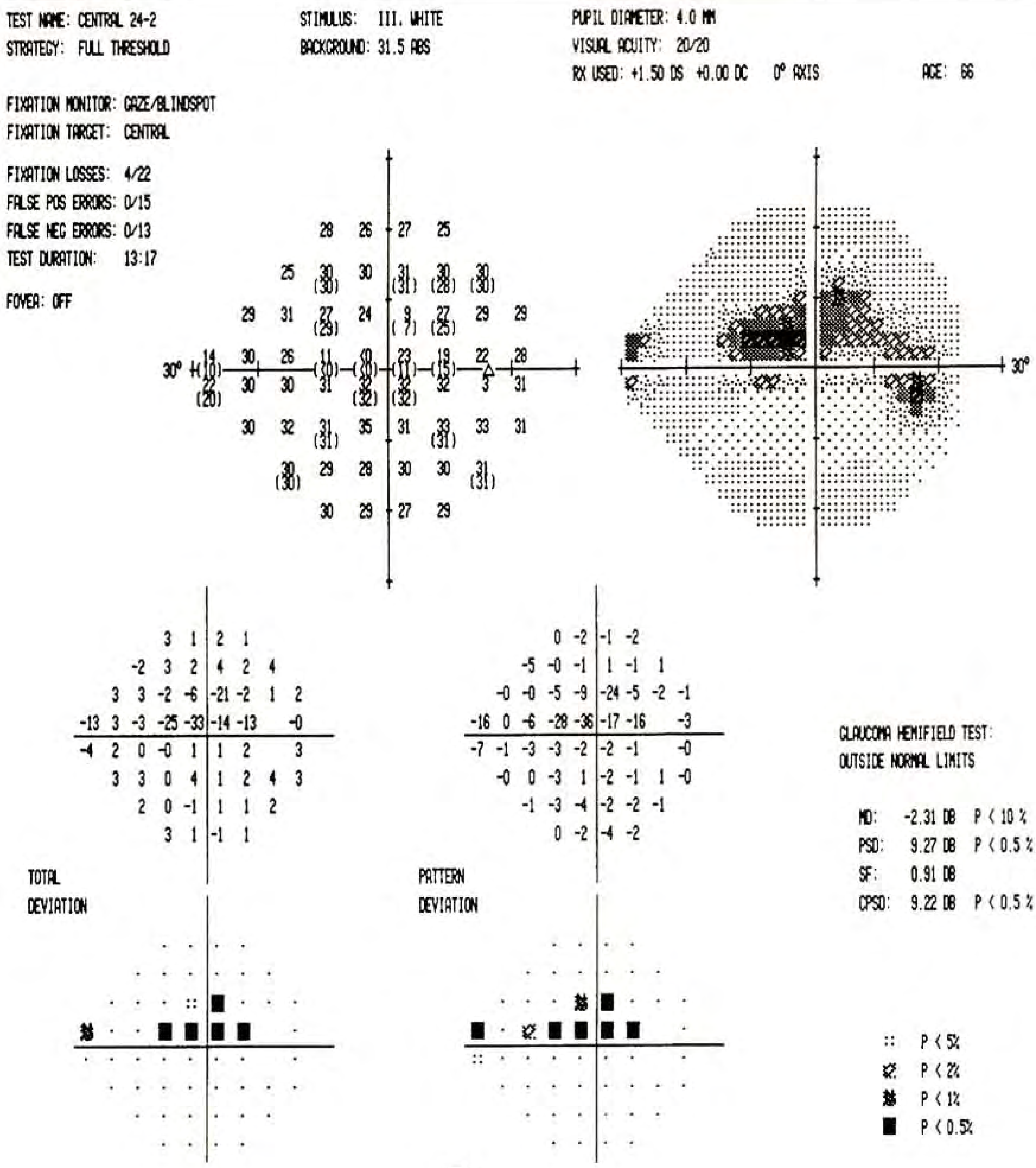
TEST NAME: CENTRAL 24-2
STRATEGY: FULL THRESHOLD
STIMULUS: III, WHITE
BACKGROUND: 31.5 ABS
PUPIL DIAMETER: 4.0 MM
VISUAL ACUITY: 20/20
RX USED: +1.50 DS +0.00 DC 0° AXIS
AGE: 66
FIXATION MONITOR: GAZE/BLINDSPOT
FIXATION TARGET: CENTRAL
FIXATION LOSSES: 4/22
FALSE POS ERRORS: 0/15
FALSE NEG ERRORS: 0/13
TEST DURATION: 13:17
FOVEA: OFF
30°
30°
TOTAL
DEVIATION
PATTERN
DEVIATION
GLAUCOMA HEMIFIELD TEST:
OUTSIDE NORMAL LIMITS
MD: -2.31 DB P < 10 %
PSD: 9.27 DB P < 0.5 %
SF: 0.91 DB
CPSD: 9.22 DB P < 0.5 %
P < 5%
P < 2%
P < 1%
P < 0.5%

D

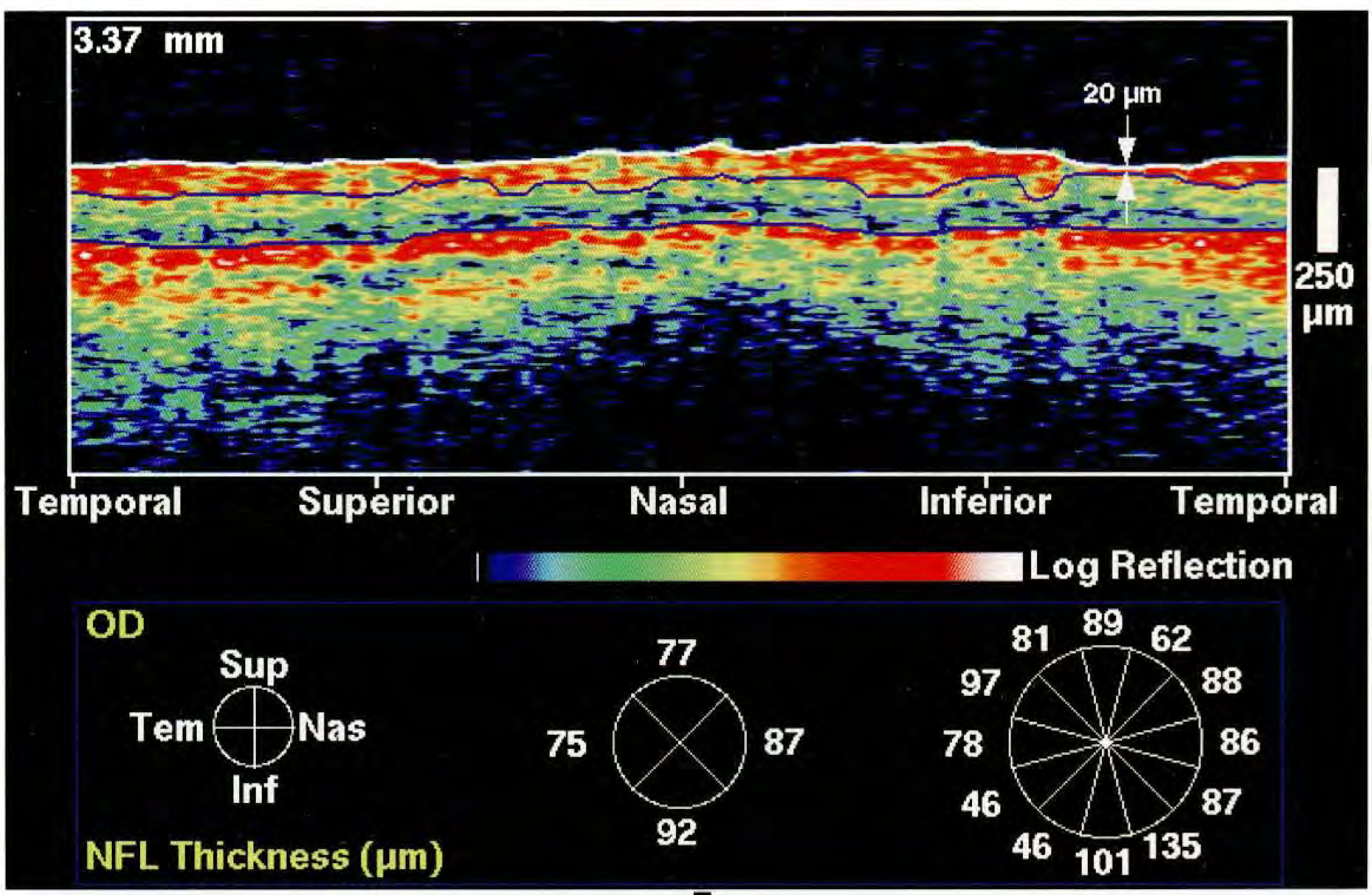
3.37 mm
20 µm
250 µm
Temporal
Superior
Nasal
Inferior
Temporal
Log Reflection
OD
Sup
Tem
Nas
Inf
NFL Thickness (µm)
77
75
87
92
81
89
62
97
88
78
86
46
87
46
101
135

E

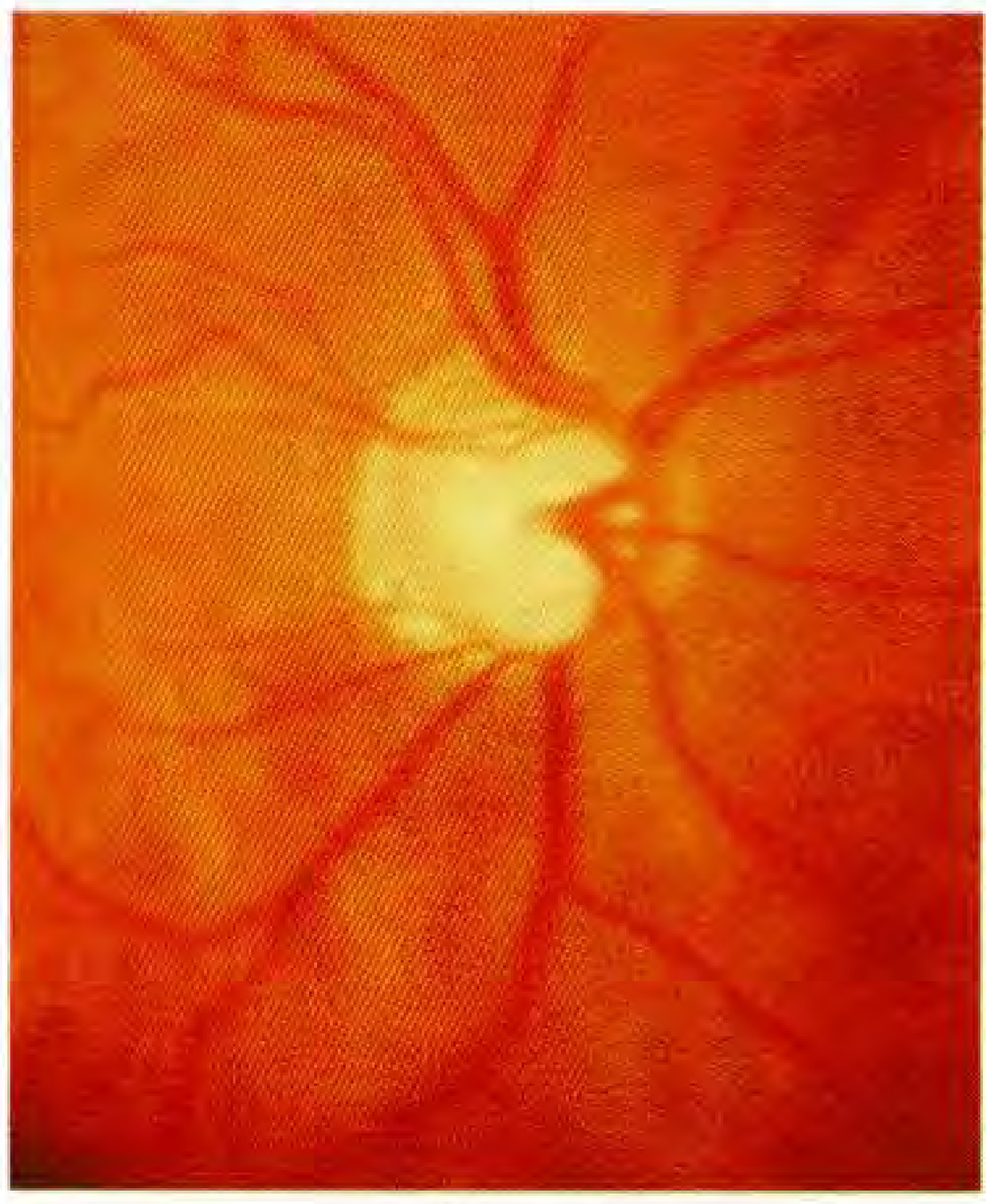

A

B

Case 12-12. Superior Arcuate Scotoma

Clinical Summary

A 50-year-old white woman with normal tension glaucoma was being treated with timolol 0.5% twice daily and apraclonidine 0.5% in both eyes three times a day. On examination of her right eye, the intraocular pressure was 15 mm Hg and the visual acuity was 20/20. Slit-lamp examination was unremarkable and gonioscopy revealed the angles to be open to the ciliary body band. Fundus examination (A,B) displayed marked cupping with loss of the neuroretinal rim from approximately 6:00 to 9:00. A Humphrey visual field (D) revealed a dense superior arcuate scotoma splitting fixation.

Optical Coherence Tomography

A 3.4 mm diameter circular tomogram (E) around the optic disc was notable for extreme, diffuse attenuation of the inferior nerve fiber layer. There was relative preservation of the superior nerve fiber layer.

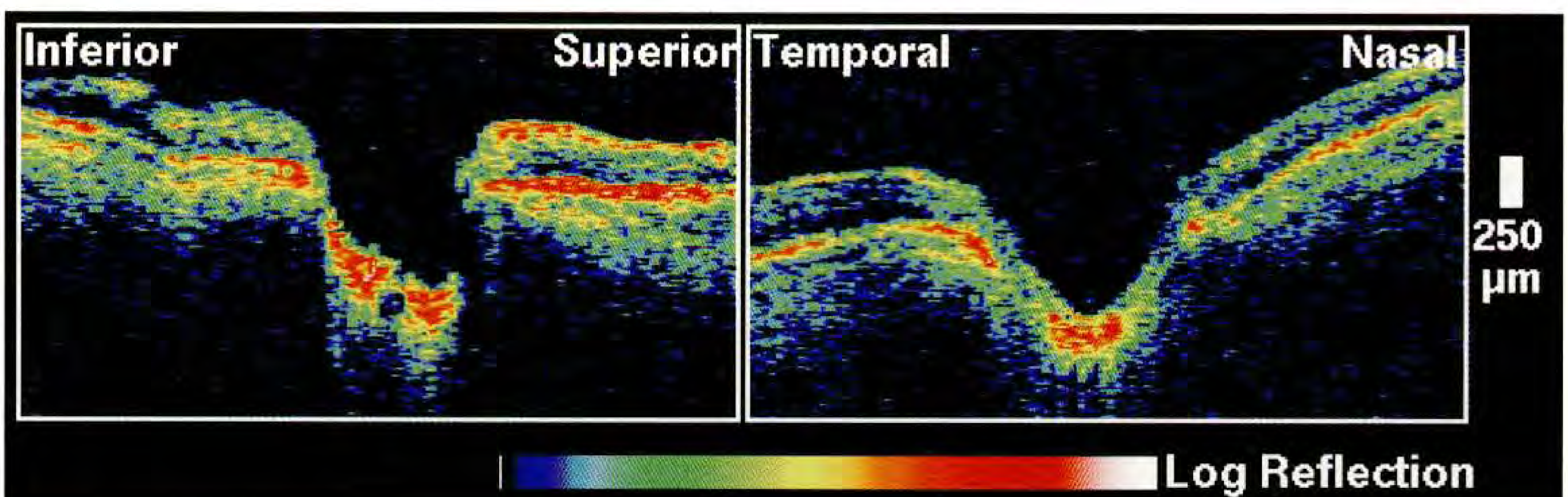

C

VERTICAL		*HORIZONTAL*	
Cup Diameter	**1.18 mm**	**Cup Diameter**	**1.10 mm**
Disc Diameter	**1.46 mm**	**Disc Diameter**	**1.43 mm**
C/D Ratio	**0.81**	**C/D Ratio**	**0.77**
NR Rim Area	**0.58 mm^2**		
Inferior NFL	**100 µm**	**Temporal NFL**	**110 µm**
Superior NFL	**120 µm**	**Nasal NFL**	**130 µm**

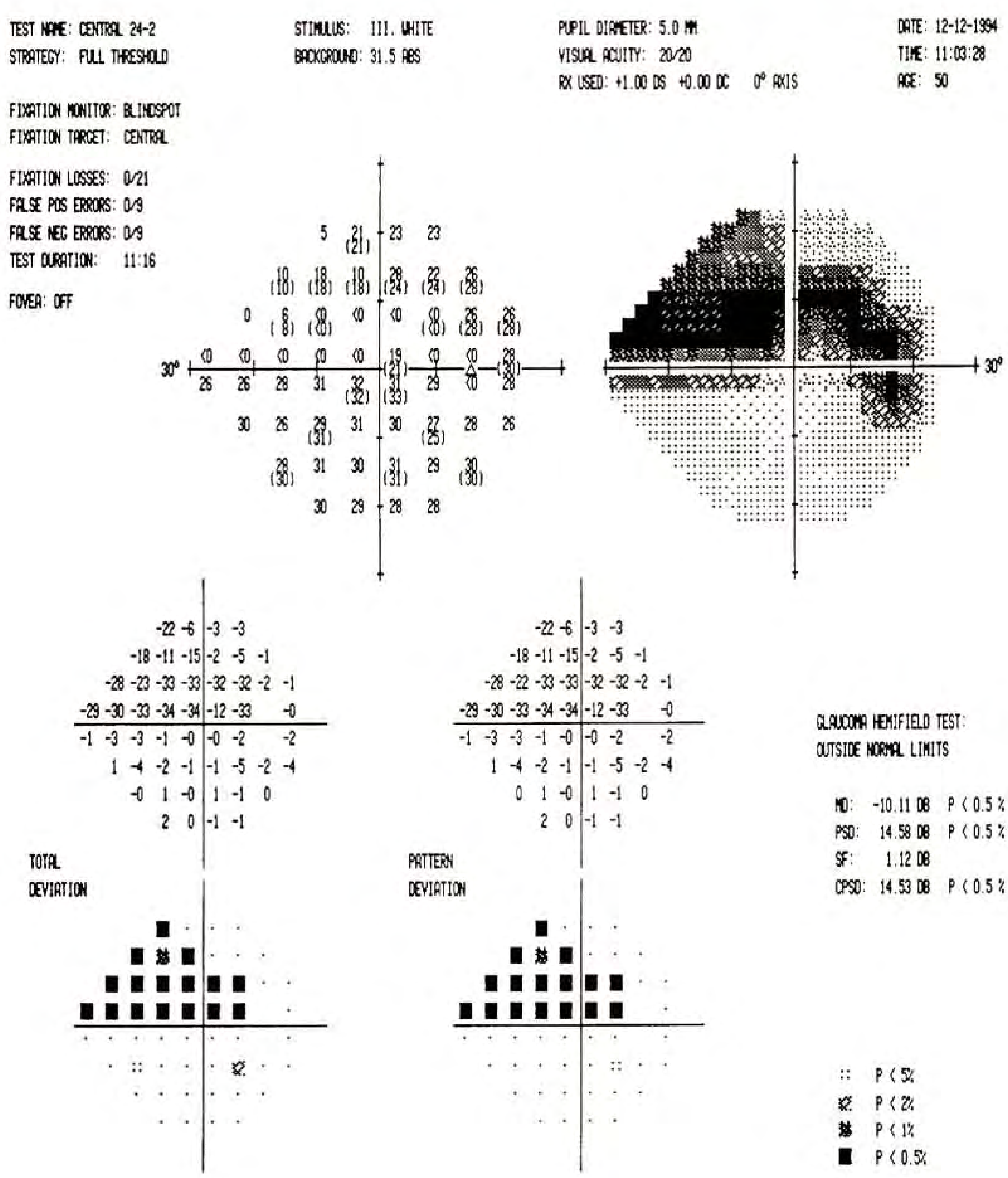
TEST NAME: CENTRAL 24-2
STRATEGY: FULL THRESHOLD
STIMULUS: III, WHITE
BACKGROUND: 31.5 ASB
PUPIL DIAMETER: 5.0 MM
VISUAL ACUITY: 20/20
RX USED: +1.00 DS +0.00 DC 0° AXIS
DATE: 12-12-1994
TIME: 11:03:28
AGE: 50
FIXATION MONITOR: BLINDSPOT
FIXATION TARGET: CENTRAL
FIXATION LOSSES: 0/21
FALSE POS ERRORS: 0/9
FALSE NEG ERRORS: 0/9
TEST DURATION: 11:16
FOVEA: OFF
30°
30°
TOTAL DEVIATION
PATTERN DEVIATION
GLAUCOMA HEMIFIELD TEST: OUTSIDE NORMAL LIMITS
MD: -10.11 DB P < 0.5 %
PSD: 14.58 DB P < 0.5 %
SF: 1.12 DB
CPSD: 14.53 DB P < 0.5 %
P < 5%
P < 2%
P < 1%
P < 0.5%

D

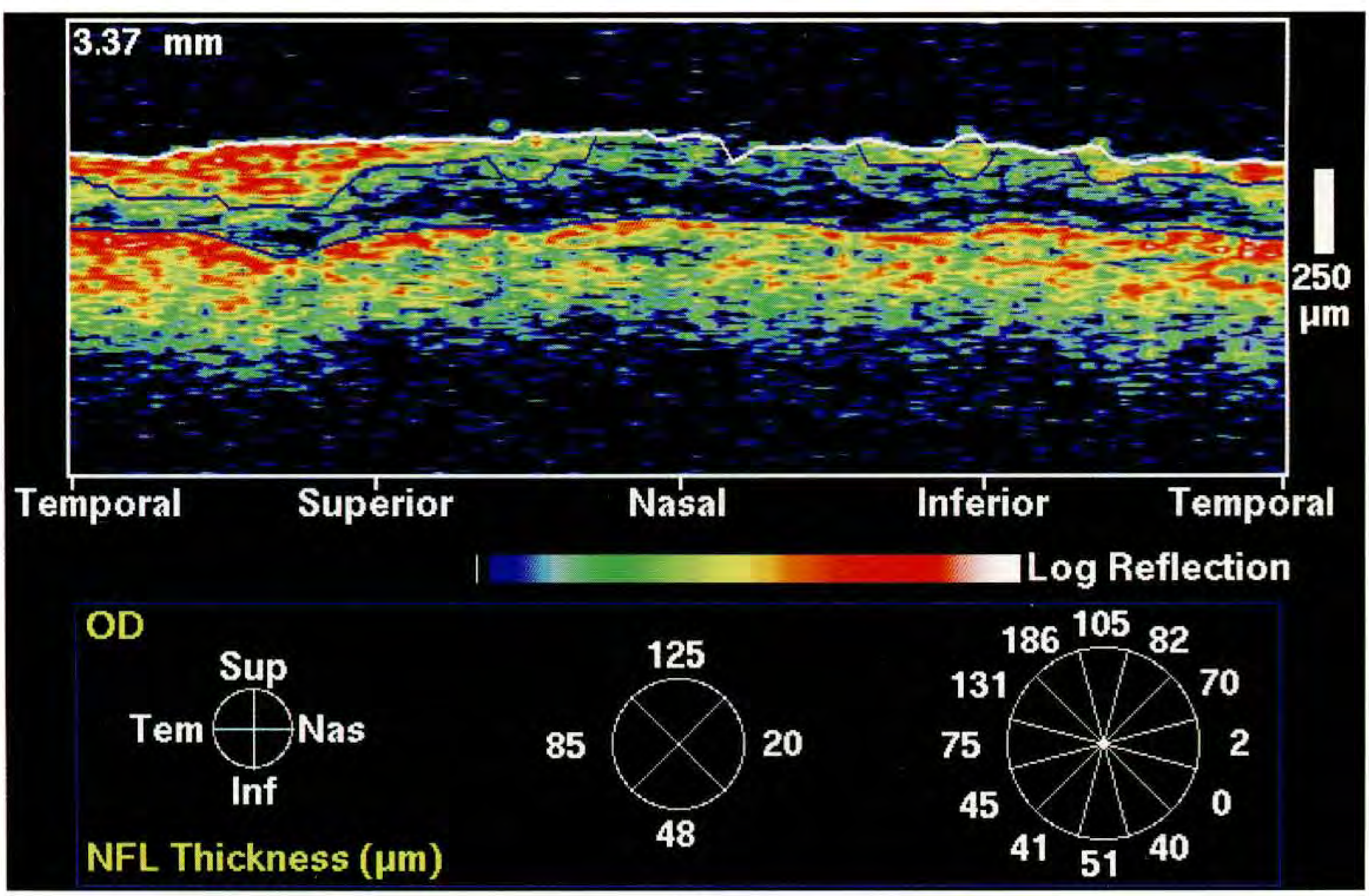
3.37 mm
250 µm
Temporal
Superior
Nasal
Inferior
Temporal
Log Reflection
OD
Sup
Tem
Nas
Inf
NFL Thickness (µm)
125
85
20
48
186
105
82
131
70
75
2
45
0
41
51
40

E

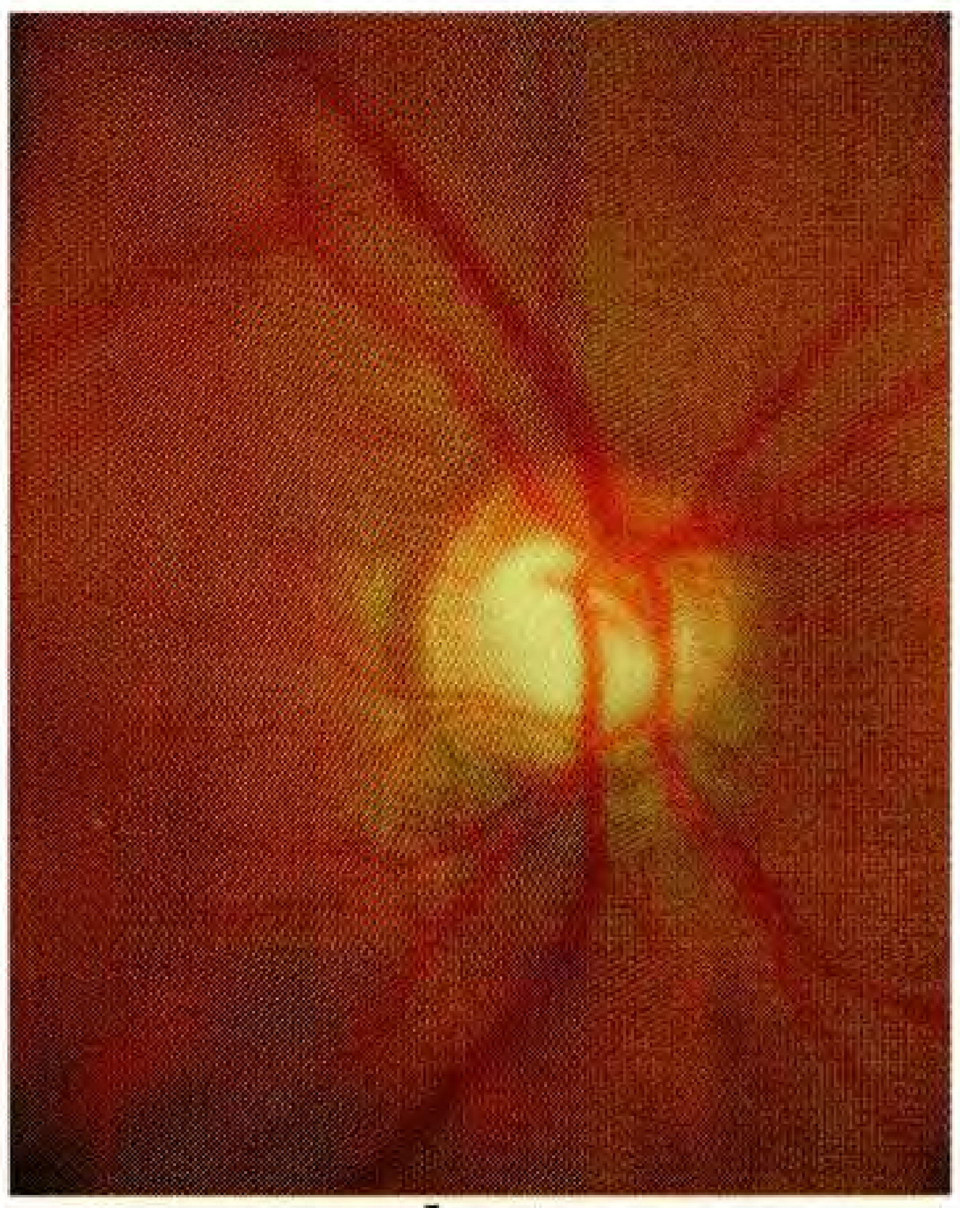

A

B

Case 12-13. Superior Arcuate Scotoma

Clinical Summary

A 65-year-old black woman was taking levobunolol 0.25% in both eyes for primary open-angle glaucoma. On examination of her right eye, the visual acuity was 20/20 with correction and the intraocular pressure was 14 mm Hg. Slit-lamp examination was unremarkable. The angle was open to the ciliary body band on gonioscopy. Dilated fundus examination (A,B) showed moderate to marked cupping and the neuroretinal rim was attenuated from 5:00 to 7:00. A corresponding nerve fiber layer defect was also observed. A Humphrey visual field (D) showed an early superior arcuate scotoma.

Optical Coherence Tomography

A 3.4 mm diameter circular tomogram (E) was acquired around the optic disc. Moderate thinning of the nerve fiber layer was observed diffusely with marked attenuation inferiorly and inferotemporally.

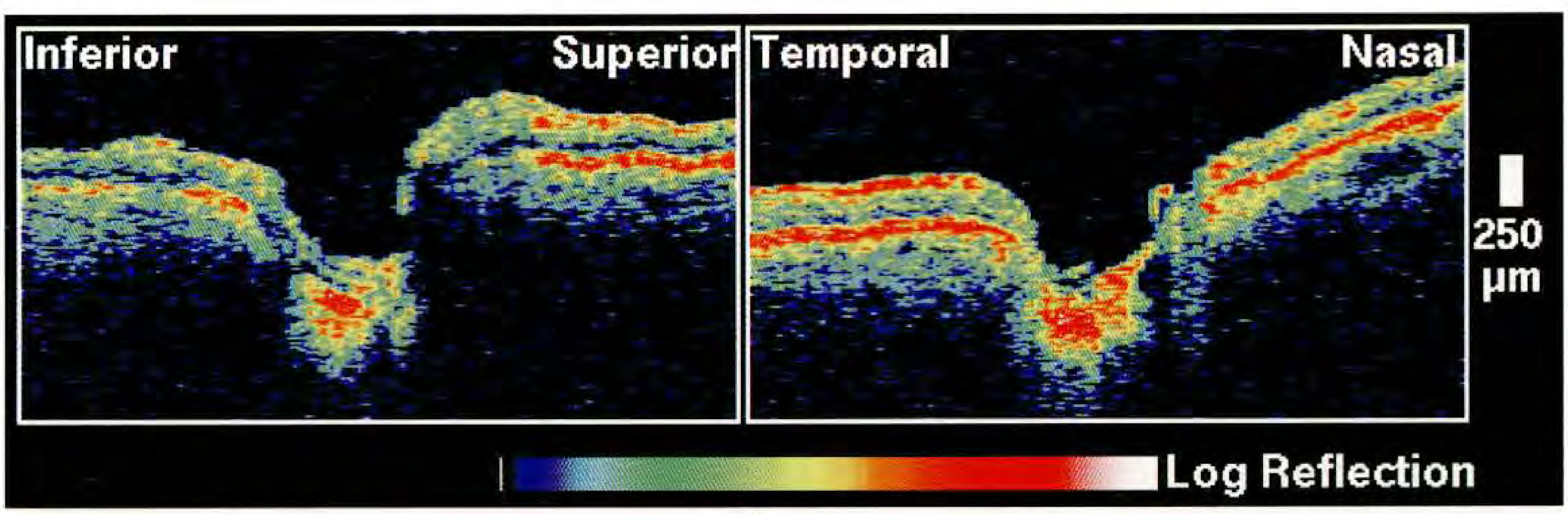

C

VERTICAL		*HORIZONTAL*	
Cup Diameter	**0.97 mm**	**Cup Diameter**	**0.93 mm**
Disc Diameter	**1.44 mm**	**Disc Diameter**	**1.23 mm**
C/D Ratio	**0.67**	**C/D Ratio**	**0.76**
NR Rim Area	**0.89 mm^2**		
Inferior NFL	**100 μm**	**Nasal NFL**	**160 μm**
Superior NFL	**140 μm**	**Temporal NFL**	**160 μm**

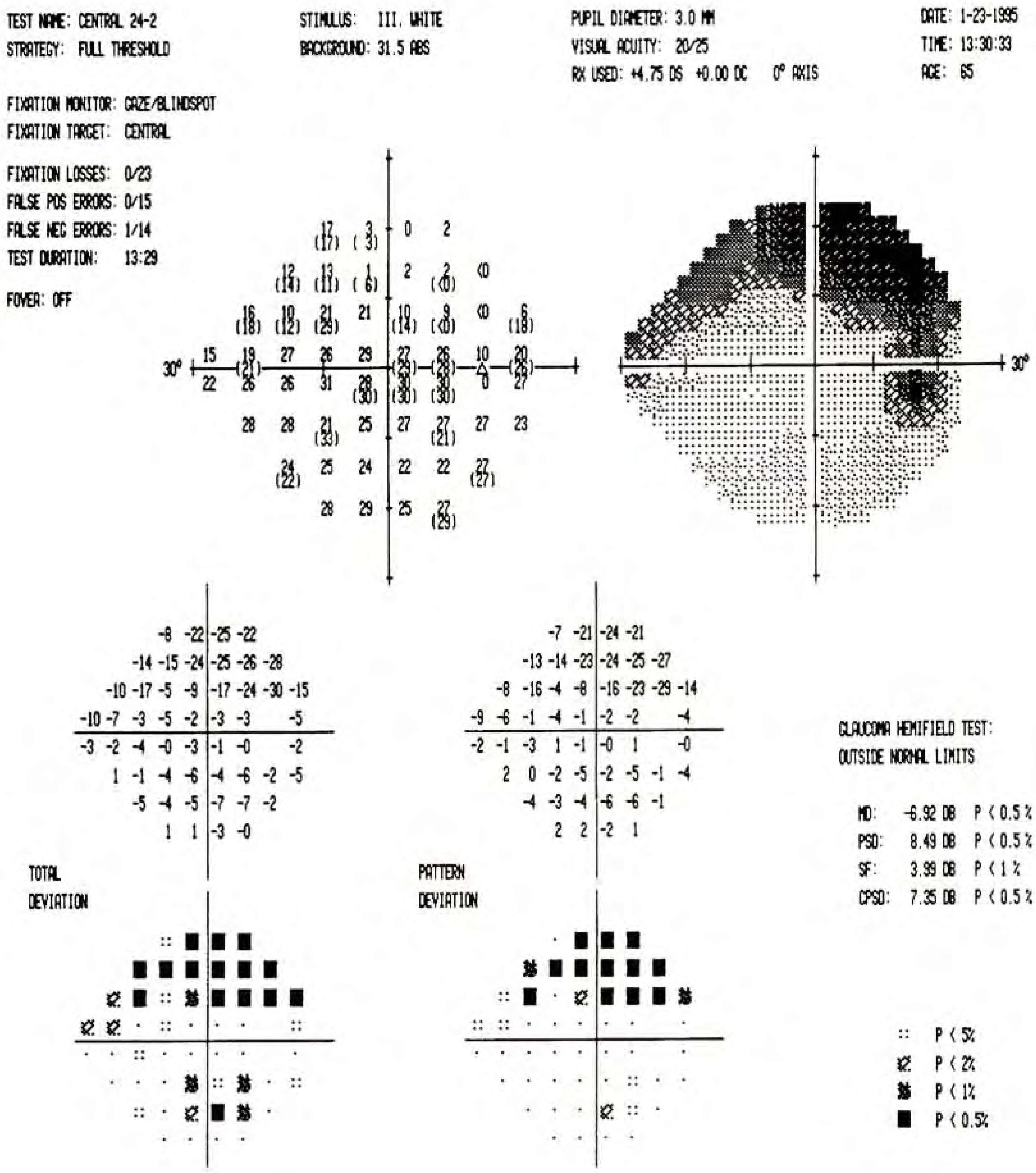
TEST NAME: CENTRAL 24-2
STRATEGY: FULL THRESHOLD
STIMULUS: III, WHITE
BACKGROUND: 31.5 ABS
PUPIL DIAMETER: 3.0 MM
VISUAL ACUITY: 20/25
RX USED: +4.75 DS +0.00 DC 0° AXIS
DATE: 1-23-1995
TIME: 13:30:33
AGE: 65
FIXATION MONITOR: GAZE/BLINDSPOT
FIXATION TARGET: CENTRAL
FIXATION LOSSES: 0/23
FALSE POS ERRORS: 0/15
FALSE NEG ERRORS: 1/14
TEST DURATION: 13:29
FOVEA: OFF
30°
30°
TOTAL
DEVIATION
PATTERN
DEVIATION
GLAUCOMA HEMIFIELD TEST:
OUTSIDE NORMAL LIMITS
MD: -6.92 DB P < 0.5 %
PSD: 8.49 DB P < 0.5 %
SF: 3.99 DB P < 1 %
CPSD: 7.35 DB P < 0.5 %
P < 5%
P < 2%
P < 1%
P < 0.5%

D

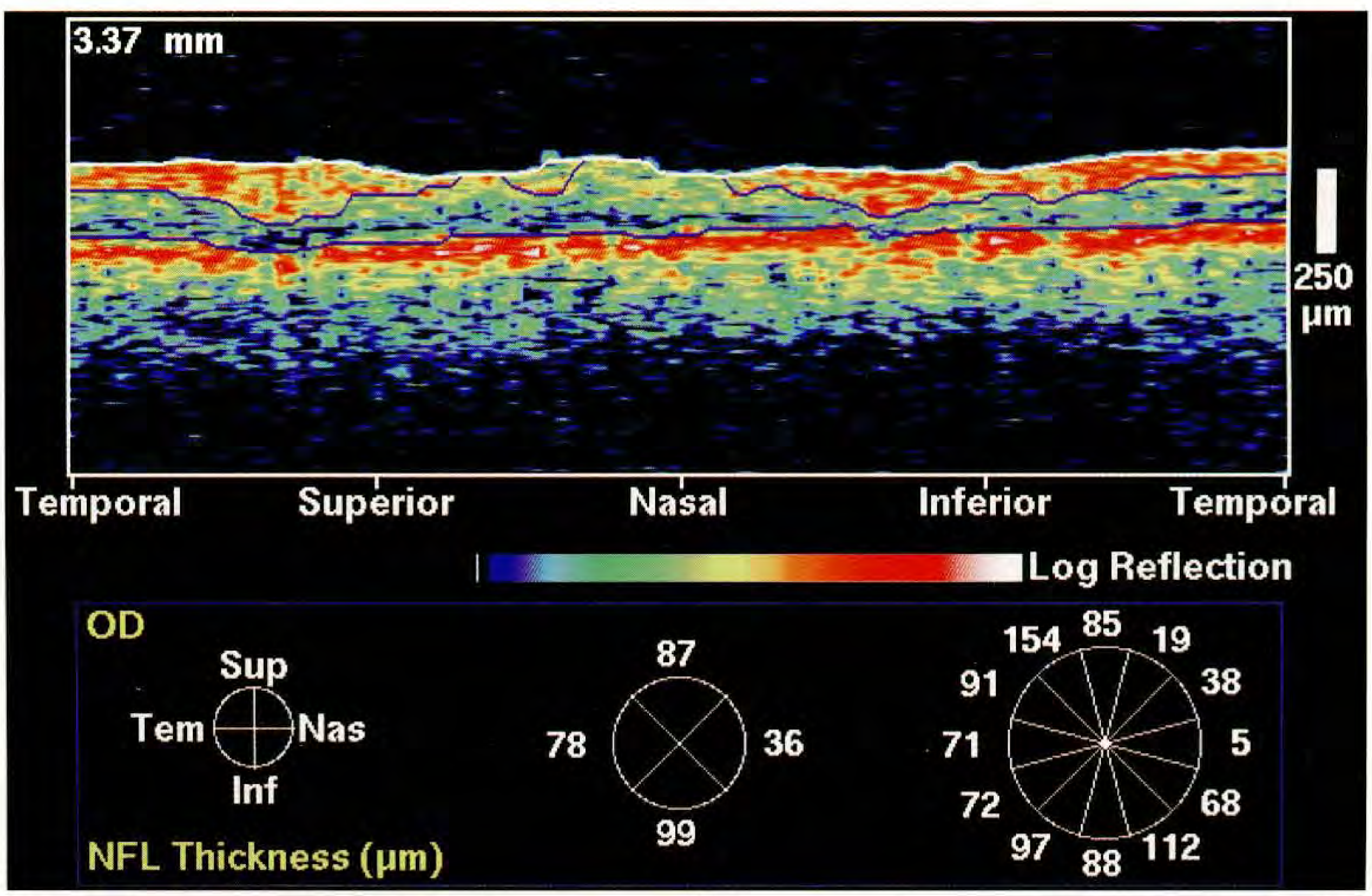
3.37 mm
250 µm
Temporal
Superior
Nasal
Inferior
Temporal
Log Reflection
OD
Sup
Tem
Nas
Inf
NFL Thickness (µm)
87
78
36
99
154
85
19
91
38
71
5
72
68
97
88
112

E

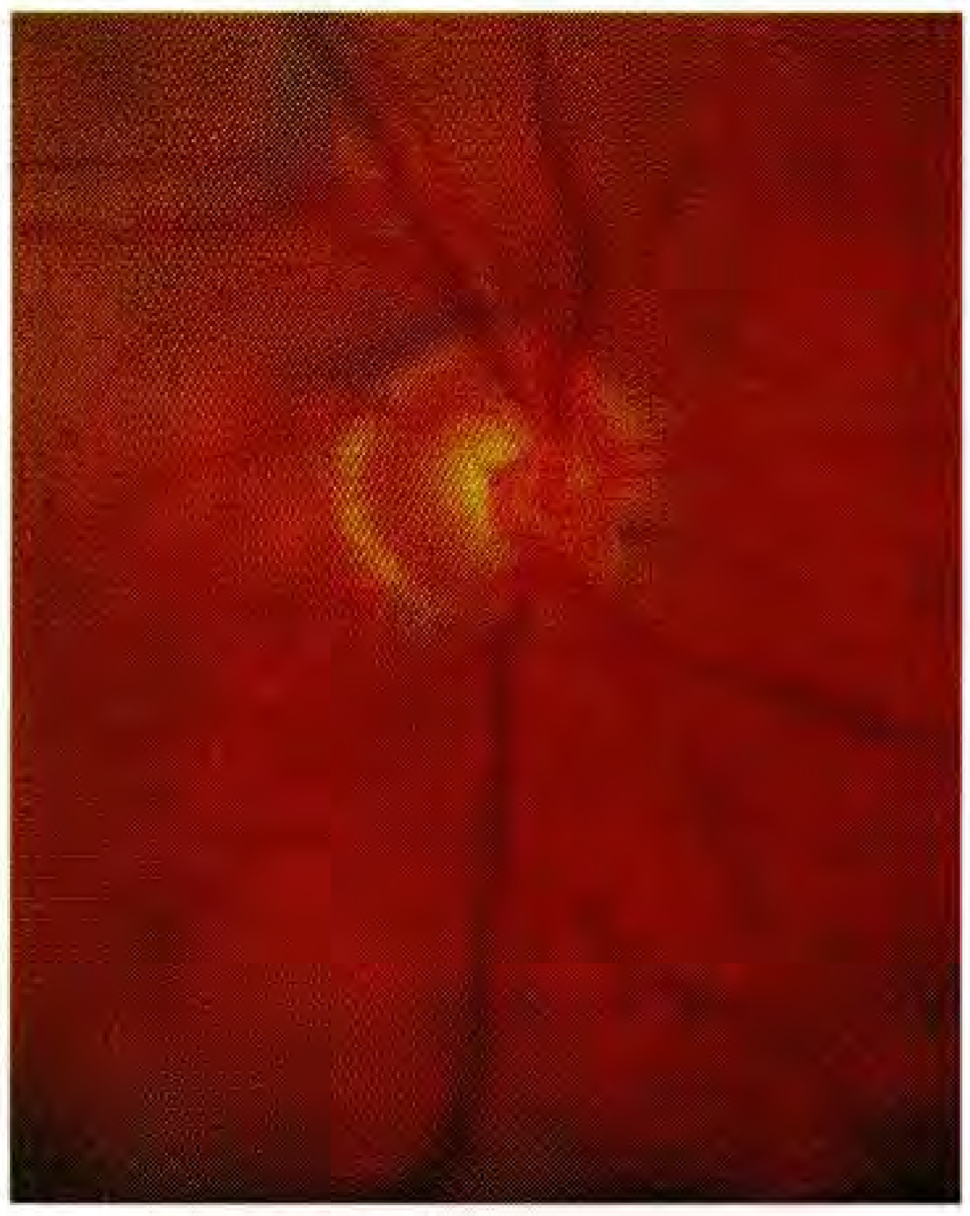

A

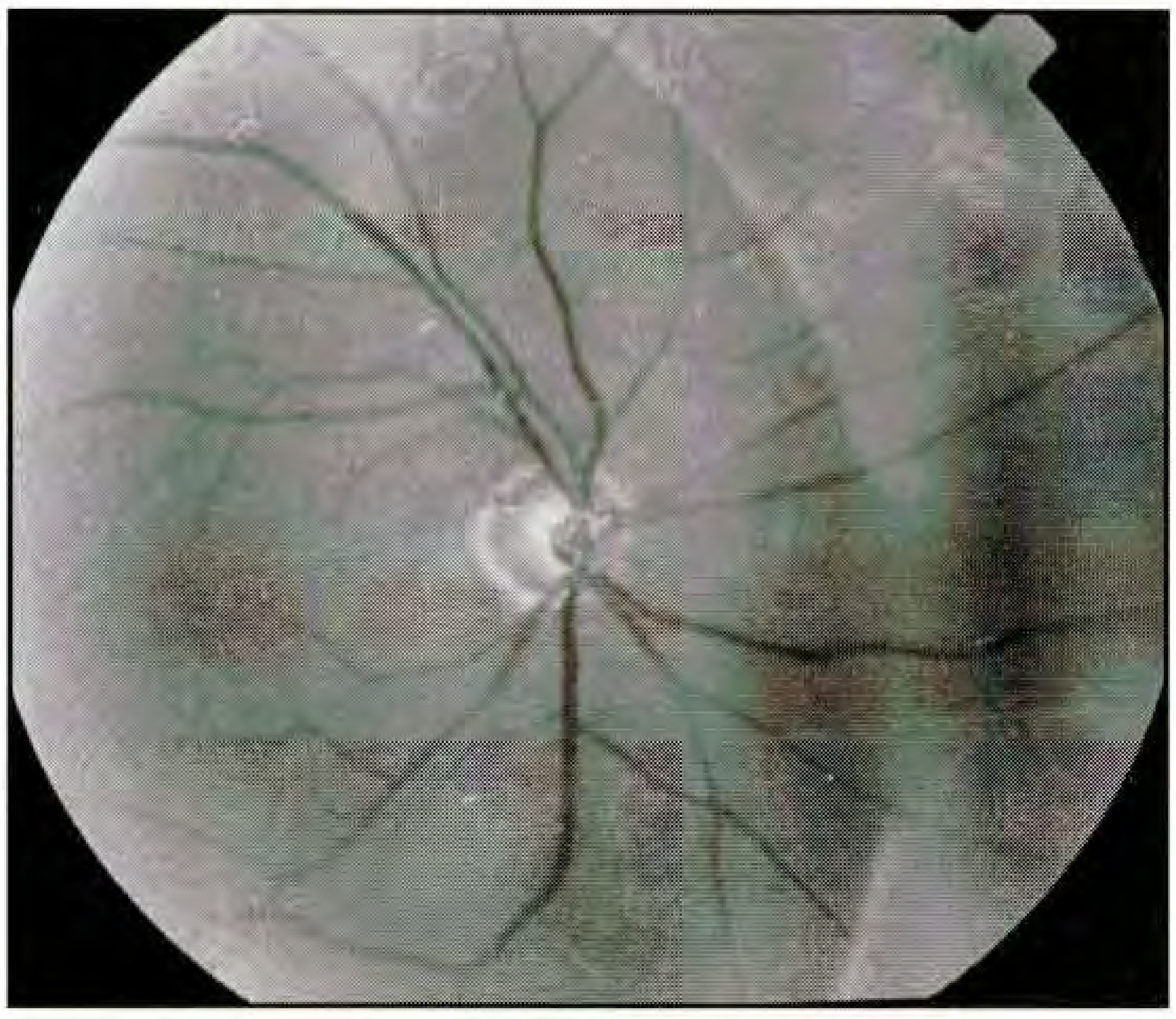

B

Case 12-14. Superior Arcuate Scotomas

Clinical Summary

A 64-year-old white man had primary open-angle glaucoma for the past two and one half years. His current medications included betaxolol 0.5% twice a day in both eyes, pilocarpine 4% four times a day in both eyes, apraclonidine 0.5% three times a day in both eyes, and methazolamide 50 mg orally twice a day. On examination of the right eye, the visual acuity was 20/20 and the intraocular pressure was 30 mm Hg. 1+ nuclear sclerosis of the crystalline lens was noted on slit-lamp exmination, and gonioscopy revealed the angle to be open to the ciliary body band throughout 360°. Marked cupping of the disc was observed (A,B) with loss of the neuroretinal rim from approximately 6:00 to 9:00. A Humphrey visual field (D) showed a dense superior arcuate scotoma splitting fixation.

Optical Coherence Tomography

A 3.4 mm diameter circular tomogram (E) confirmed attenuation of the retinal nerve fiber layer from 6:00 to 9:00, with the most severe thinning occuring at 7:00.

(continued)

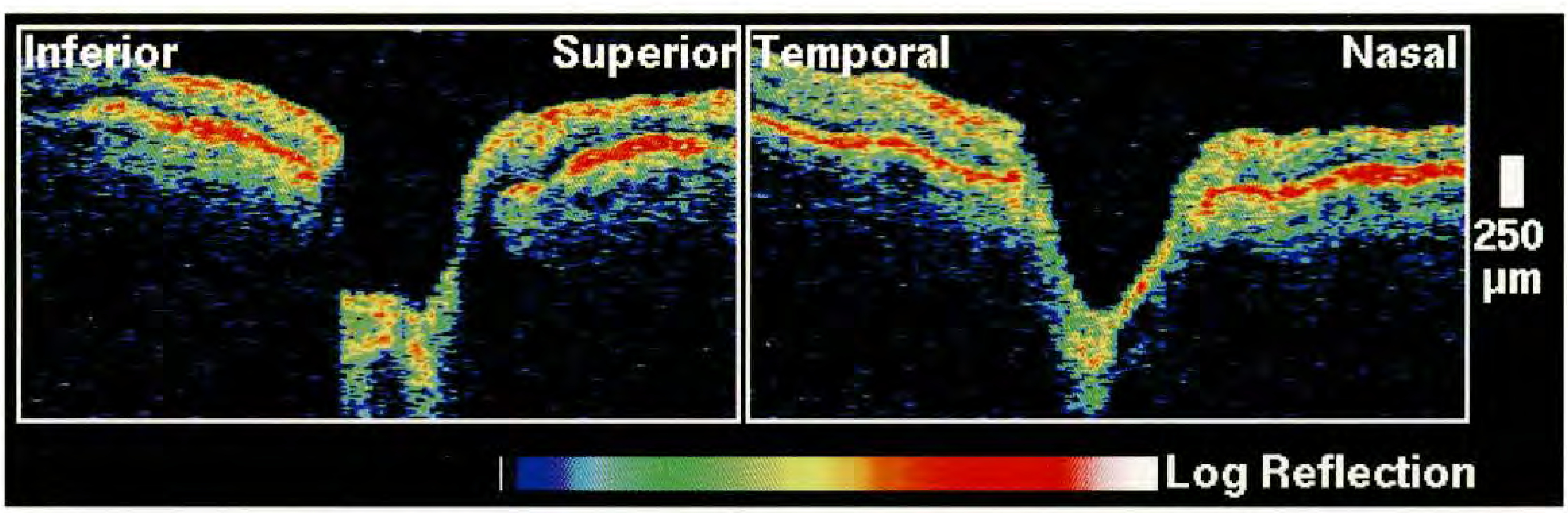

C

VERTICAL		*HORIZONTAL*	
Cup Diameter	1.17 mm	Cup Diameter	1.20 mm
Disc Diameter	1.28 mm	Disc Diameter	1.64 mm
C/D Ratio	0.91	C/D Ratio	0.73
NR Rim Area	0.21 mm^2		
Inferior NFL	130 µm	Temporal NFL	70 µm
Superior NFL	150 µm	Nasal NFL	110 µm

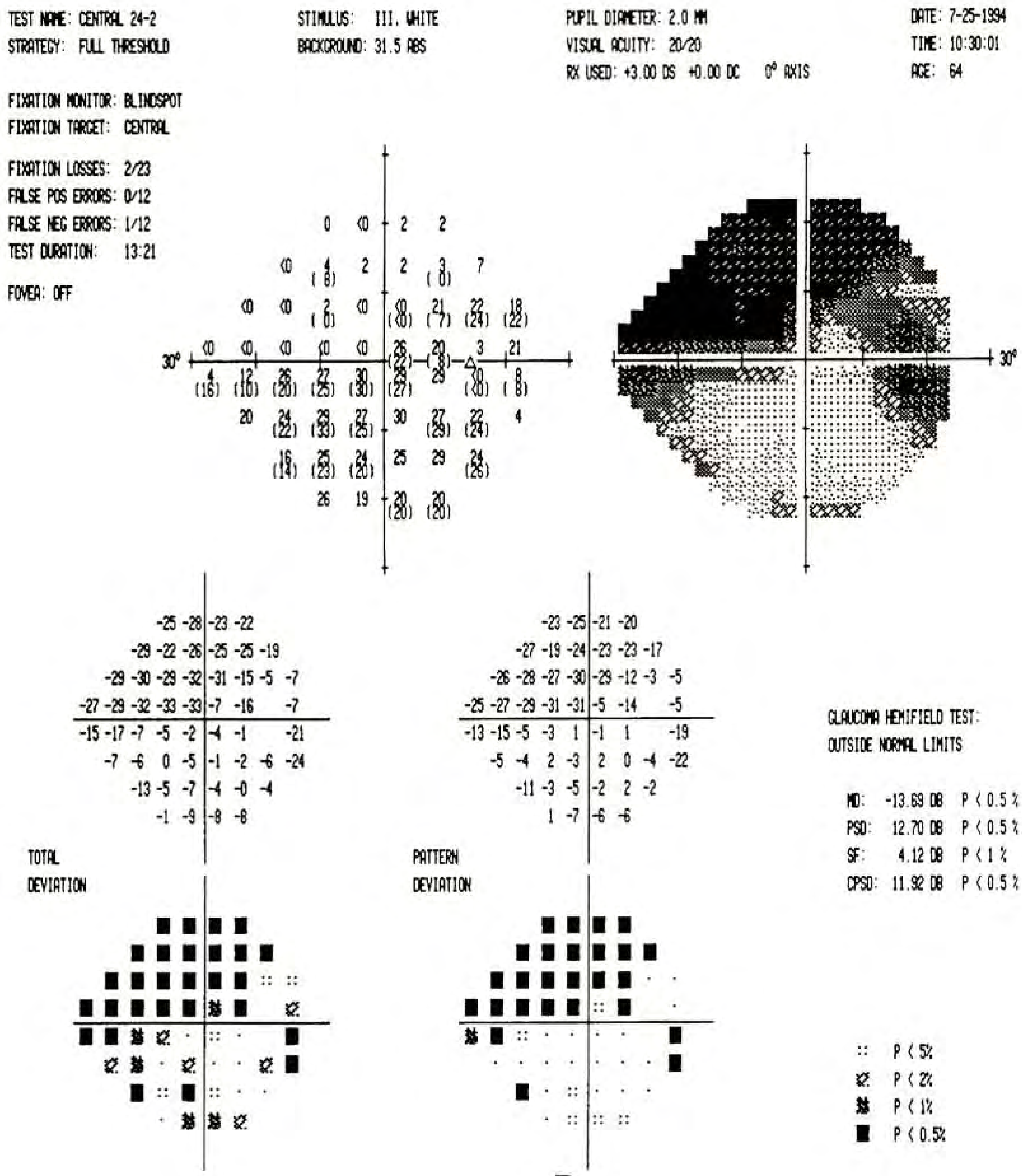
TEST NAME: CENTRAL 24-2
STRATEGY: FULL THRESHOLD
STIMULUS: III, WHITE
BACKGROUND: 31.5 ABS
PUPIL DIAMETER: 2.0 MM
VISUAL ACUITY: 20/20
RX USED: +3.00 DS +0.00 DC 0° AXIS
DATE: 7-25-1994
TIME: 10:30:01
AGE: 64
FIXATION MONITOR: BLINDSPOT
FIXATION TARGET: CENTRAL
FIXATION LOSSES: 2/23
FALSE POS ERRORS: 0/12
FALSE NEG ERRORS: 1/12
TEST DURATION: 13:21
FOVEA: OFF
30°
TOTAL DEVIATION
PATTERN DEVIATION
GLAUCOMA HEMIFIELD TEST: OUTSIDE NORMAL LIMITS
MD: -13.69 DB P < 0.5 %
PSD: 12.70 DB P < 0.5 %
SF: 4.12 DB P < 1 %
CPSD: 11.92 DB P < 0.5 %
P < 5%
P < 2%
P < 1%
P < 0.5%

D

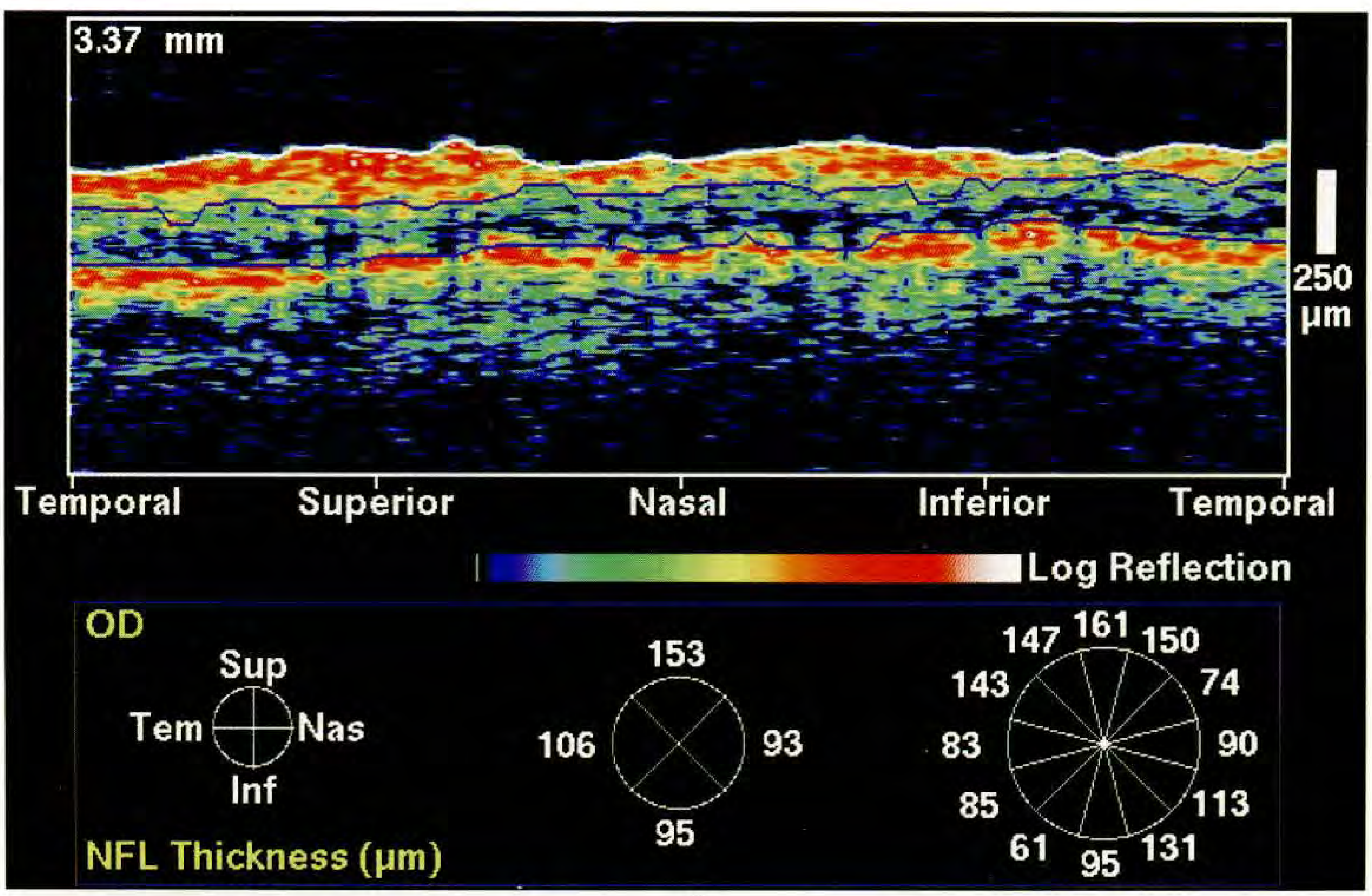
3.37 mm
250 µm
Temporal
Superior
Nasal
Inferior
Temporal
Log Reflection
OD
Sup
Tem
Nas
Inf
NFL Thickness (µm)
153
106
93
95
147
161
150
143
74
83
90
85
113
61
95
131

E

F

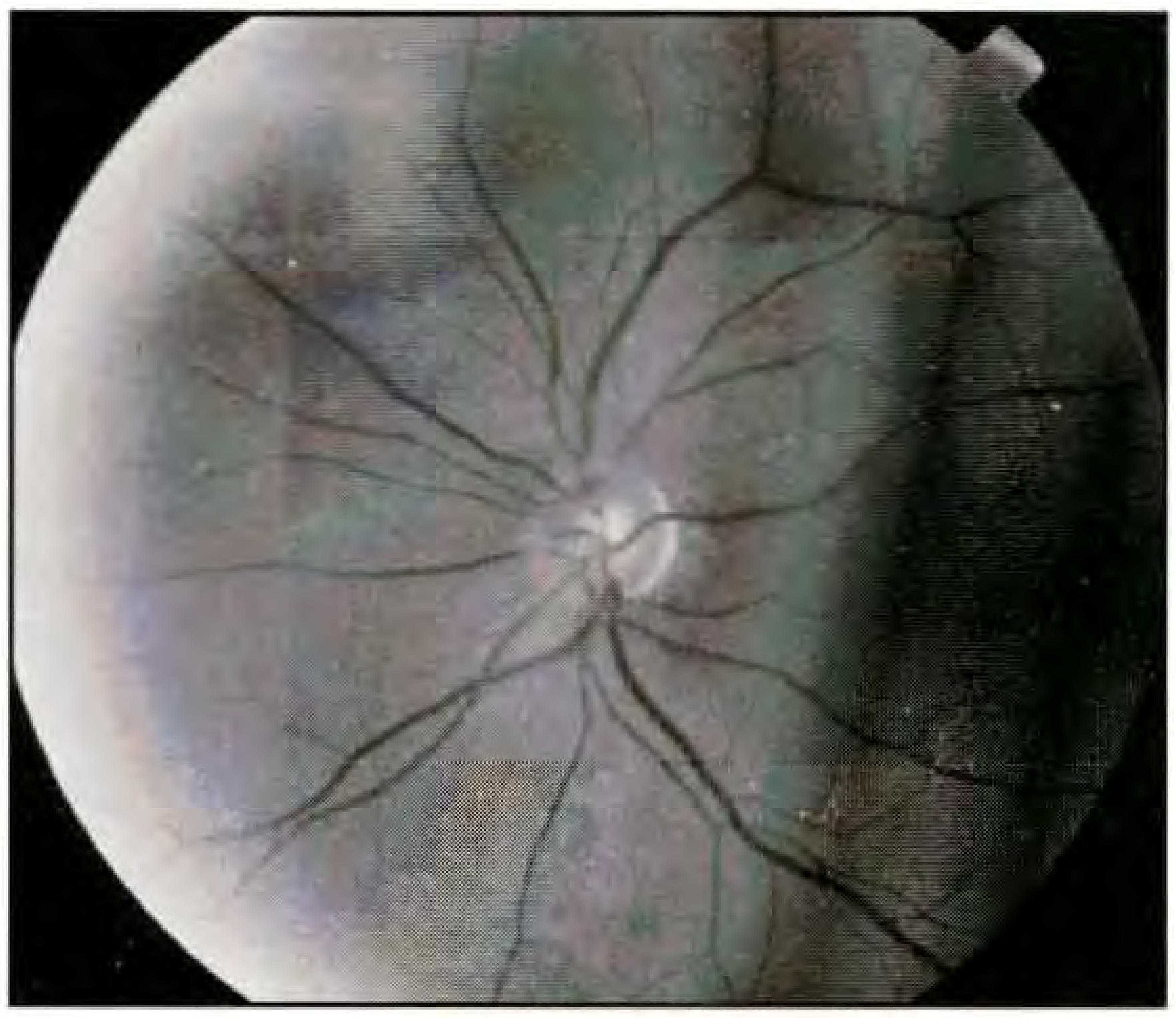

G

Case 12-14 continued

Clinical Summary

The patient's left eye had a visual acuity of 20/20 and an intraocular pressure of 30 mm Hg. Slit-lamp examination again revealed 1+ nuclear sclerosis, and the angles were open to the cililary band body throughout. Dilated fundus examination (F,G) of the left eye showed moderate cupping with an intact neuroretinal rim. Spontaneous venous pulsations were present. The Humphrey visual field (I) showed a suggestion of an early superior arcuate scotoma.

Optical Coherence Tomography

A 3.4 mm diameter circular OCT (J) confirmed slight thinning of the nerve fiber layer between 5:00 and 6:00. Nerve fiber attenuation was also observed inferonasally, which was not detected by the visual field.

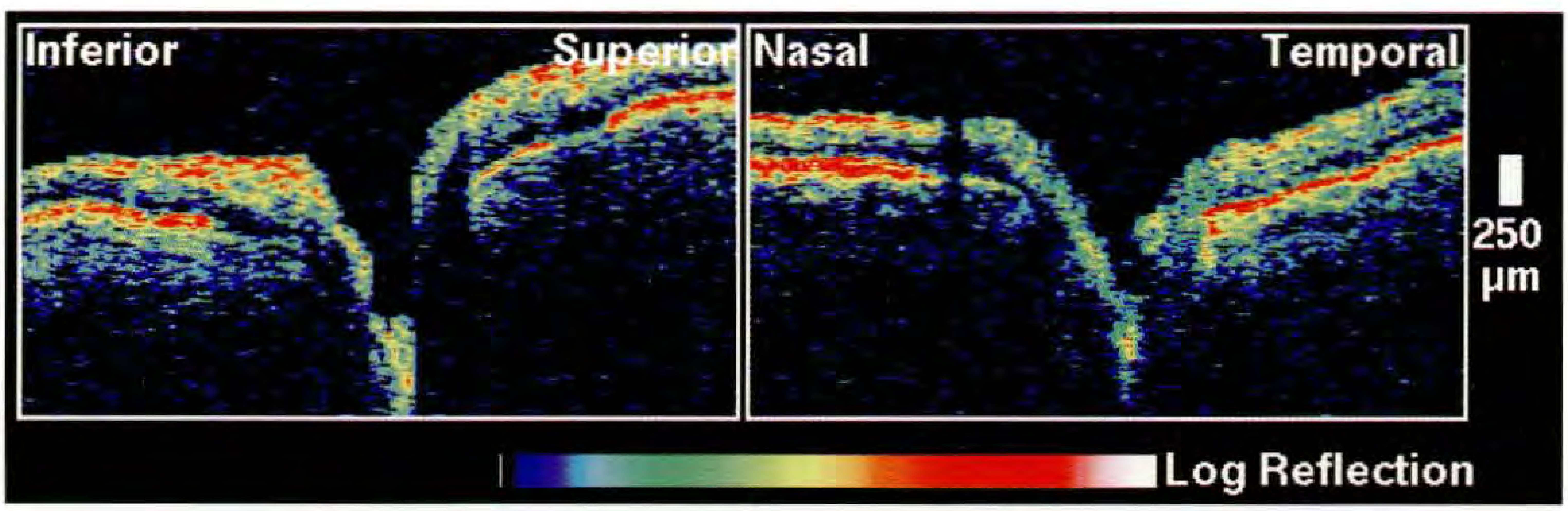

H

VERTICAL		HORIZONTAL	
Cup Diameter	0.89 mm	Cup Diameter	0.83 mm
Disc Diameter	1.16 mm	Disc Diameter	1.23 mm
C/D Ratio	0.77	C/D Ratio	0.67
NR Rim Area	0.43 mm^2		
Inferior NFL	170 µm	Nasal NFL	220 µm
Superior NFL	230 µm	Temporal NFL	150 µm

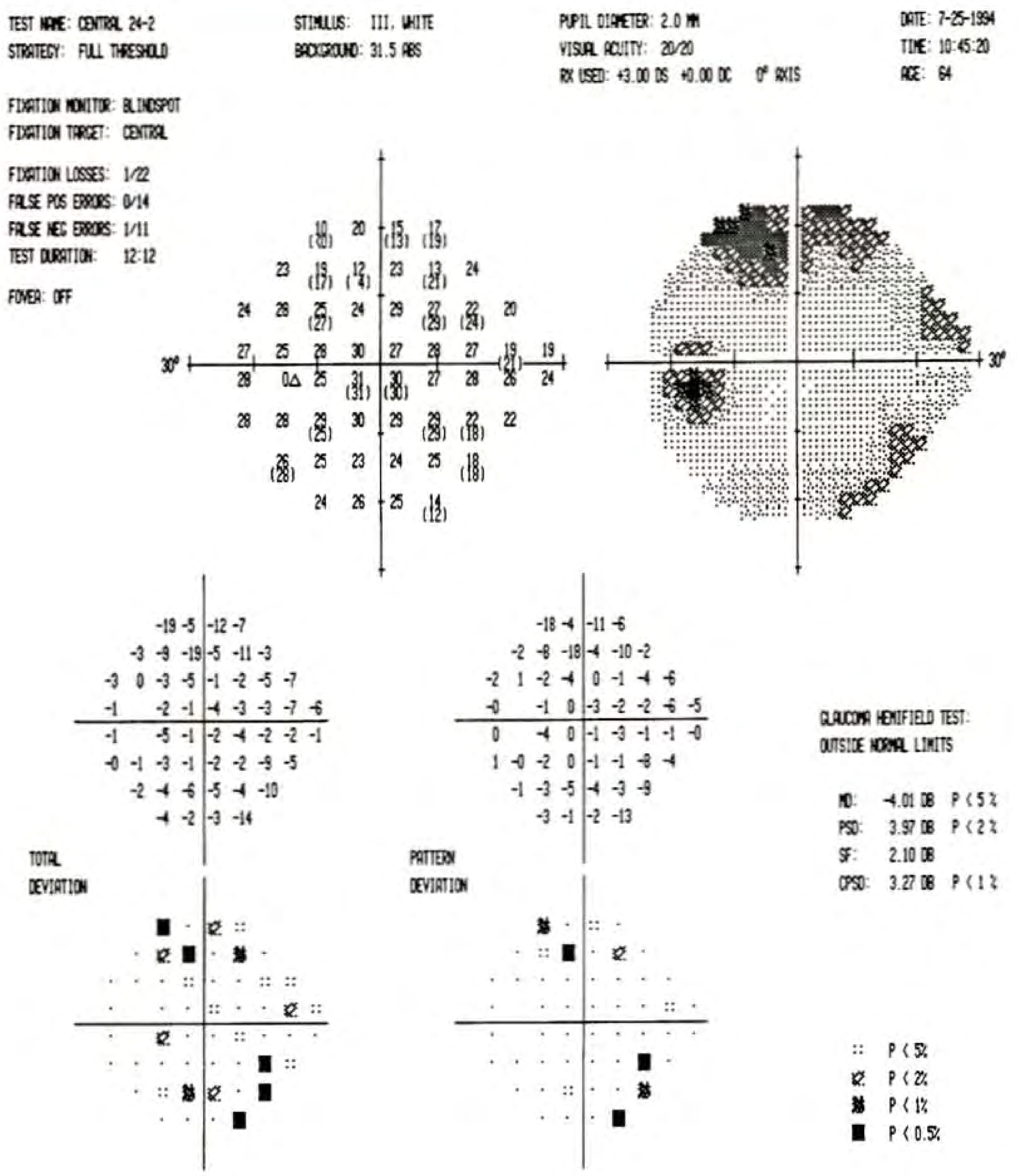
TEST NAME: CENTRAL 24-2
STRATEGY: FULL THRESHOLD
STIMULUS: III, WHITE
BACKGROUND: 31.5 ASB
PUPIL DIAMETER: 2.0 MM
VISUAL ACUITY: 20/20
RX USED: +3.00 DS +0.00 DC 0° AXIS
DATE: 7-25-1994
TIME: 10:45:20
AGE: 64
FIXATION MONITOR: BLINDSPOT
FIXATION TARGET: CENTRAL
FIXATION LOSSES: 1/22
FALSE POS ERRORS: 0/14
FALSE NEG ERRORS: 1/11
TEST DURATION: 12:12
FOVEA: OFF
30°
30°
TOTAL DEVIATION
PATTERN DEVIATION
GLAUCOMA HEMIFIELD TEST:
OUTSIDE NORMAL LIMITS
MD: -4.01 DB P < 5%
PSD: 3.97 DB P < 2%
SF: 2.10 DB
CPSD: 3.27 DB P < 1%
P < 5%
P < 2%
P < 1%
P < 0.5%

I

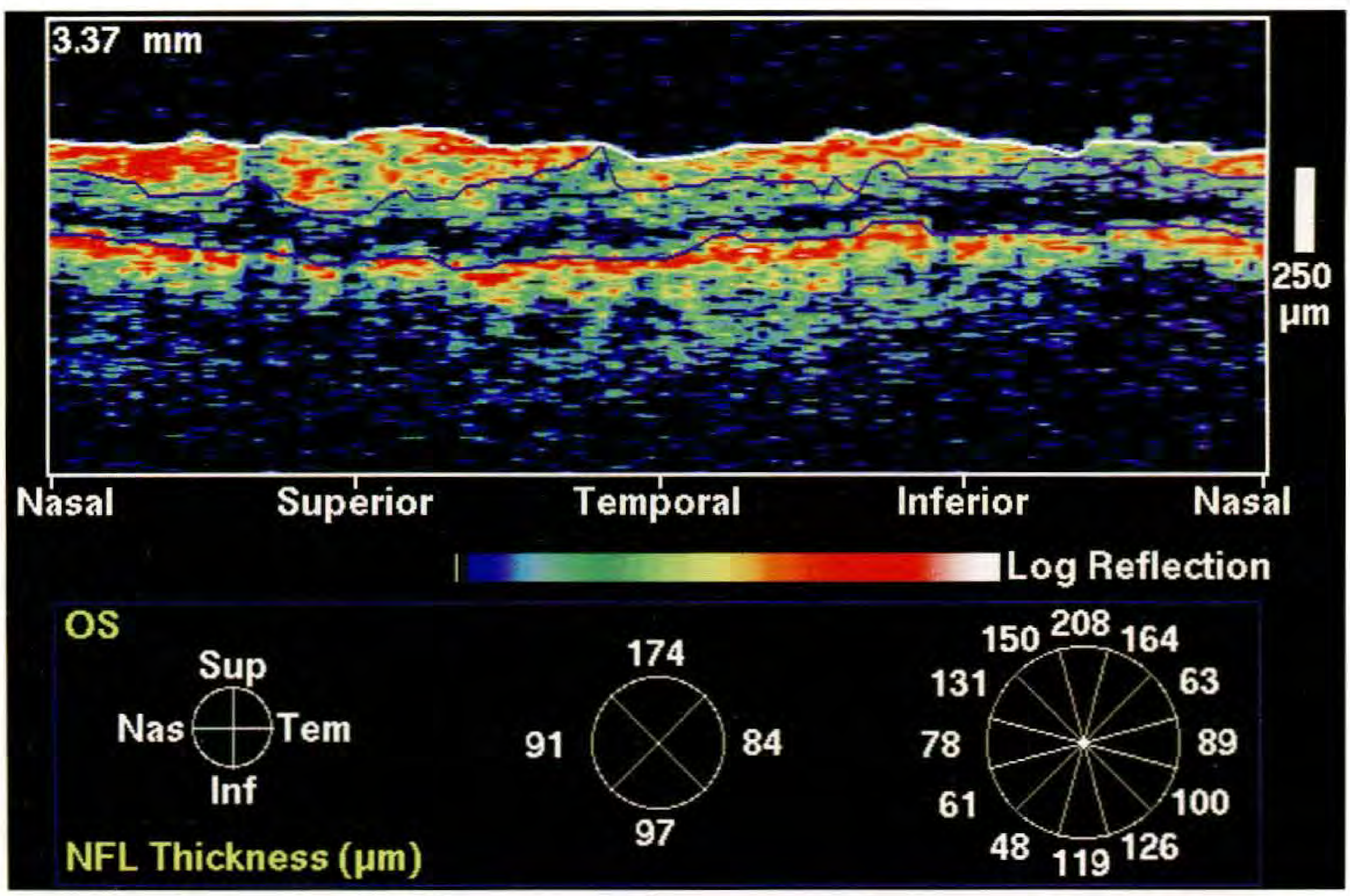
3.37 mm
250 µm
Nasal
Superior
Temporal
Inferior
Nasal
Log Reflection
OS
Sup
Nas
Tem
Inf
NFL Thickness (µm)
174
91
84
97
150
208
164
131
63
78
89
61
100
48
119
126

J

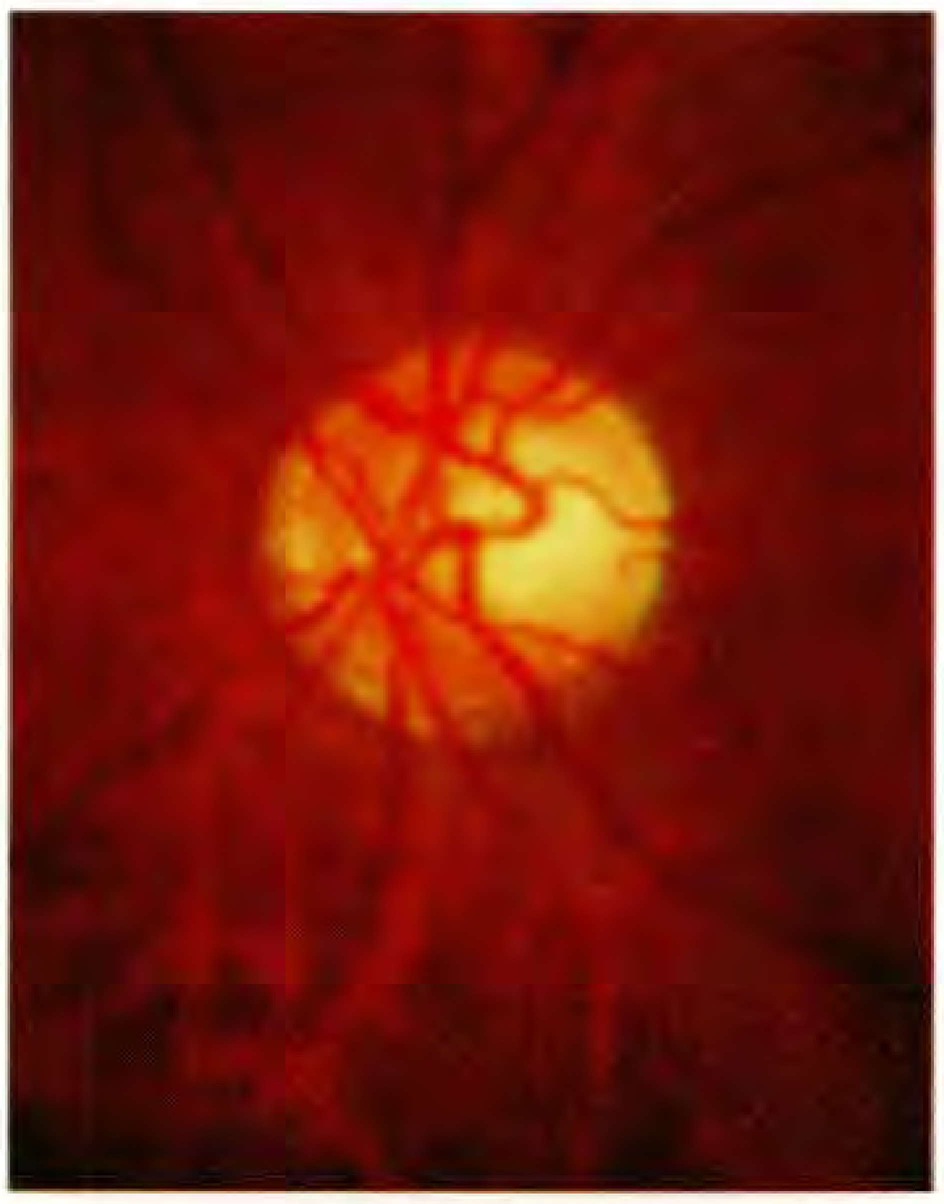

A

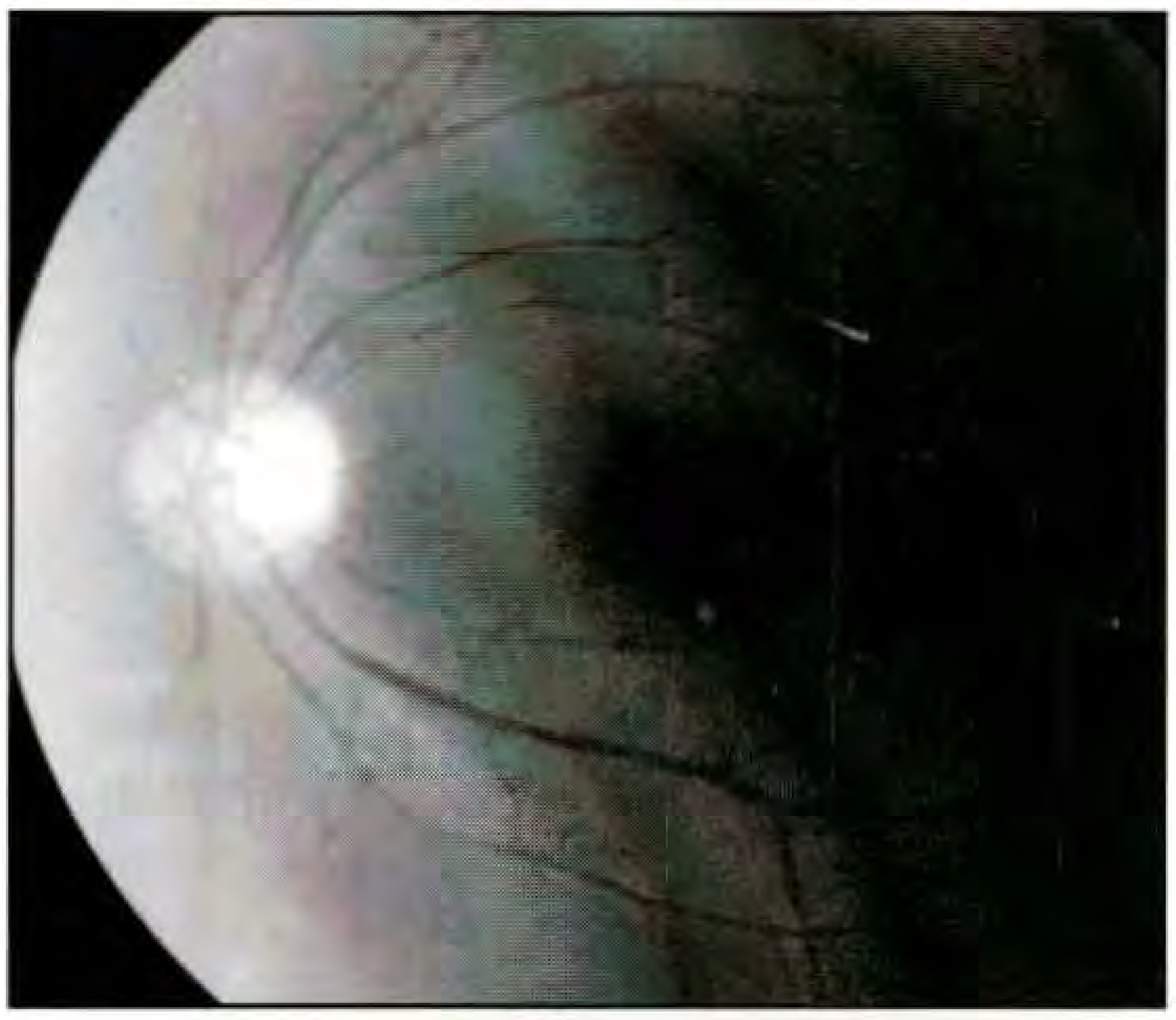

B

Case 12-15. Visual Field Loss Out of Proportion to Nerve Fiber Layer Thickness

Clinical Summary

A 46-year-old asian woman was referred for evaluation of borderline high intraocular pressures. On examination, her left eye had a visual acuity of 20/25 and the intraocular pressure was 19 mm Hg. Slit-lamp observation and gonioscopy were unremarkable with visualization of the ciliary body band through 360°. Indirect biomicroscopy (A,B) revealed moderate disc cupping with mild thinning of the inferotemporal neuroretinal rim. Humphrey visual field testing (D) displayed a dense superior arcuate and an early inferior arcuate scotoma that were out of proportion to the disc findings.

Optical Coherence Tomography

A circular OCT scan (E) centered on the optic disc taken at a diameter of 3.4 mm showed a relatively healthy appearing nerve fiber layer both inferiorly and superiorly. The strong reflection from the nerve fiber layer and the clinically observed disc appearance suggested that the visual field losses were not an accurate measure of nerve fiber layer atrophy, despite the relatively good test parameters.

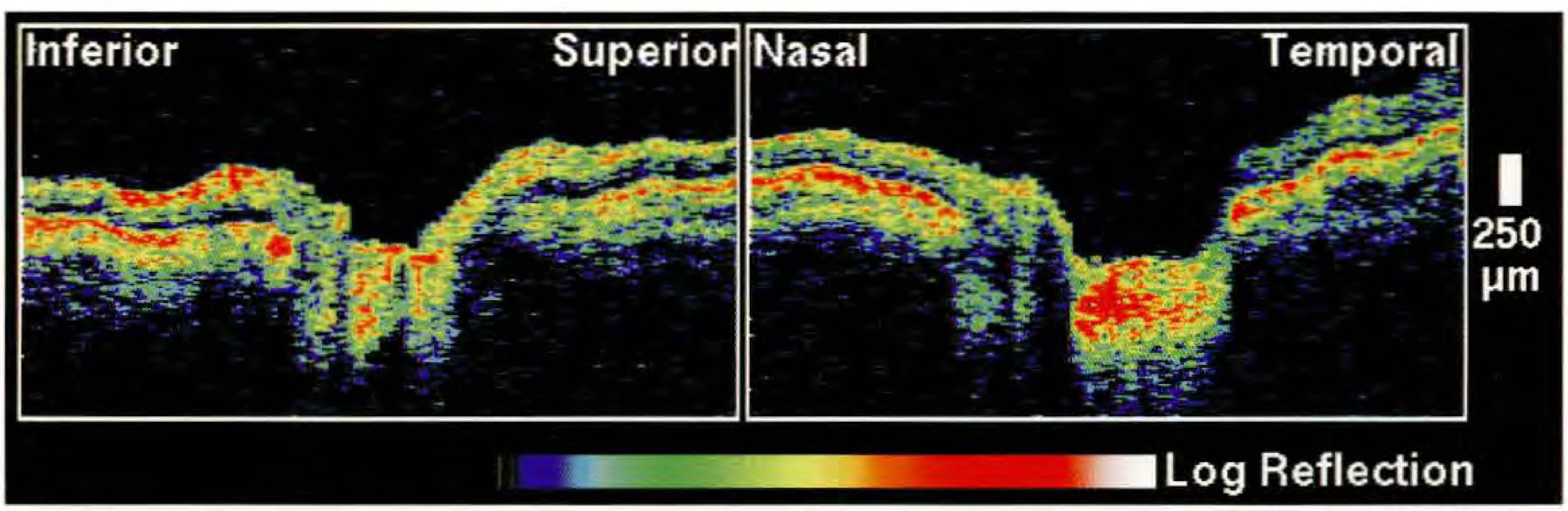

C

VERTICAL		HORIZONTAL	
Cup Diameter	0.87 mm	Cup Diameter	1.36 mm
Disc Diameter	1.65 mm	Disc Diameter	1.59 mm
C/D Ratio	0.53	C/D Ratio	0.86
NR Rim Area	1.54 mm^2		
Inferior NFL	190 µm	Nasal NFL	230 µm
Superior NFL	190 µm	Temporal NFL	110 µm

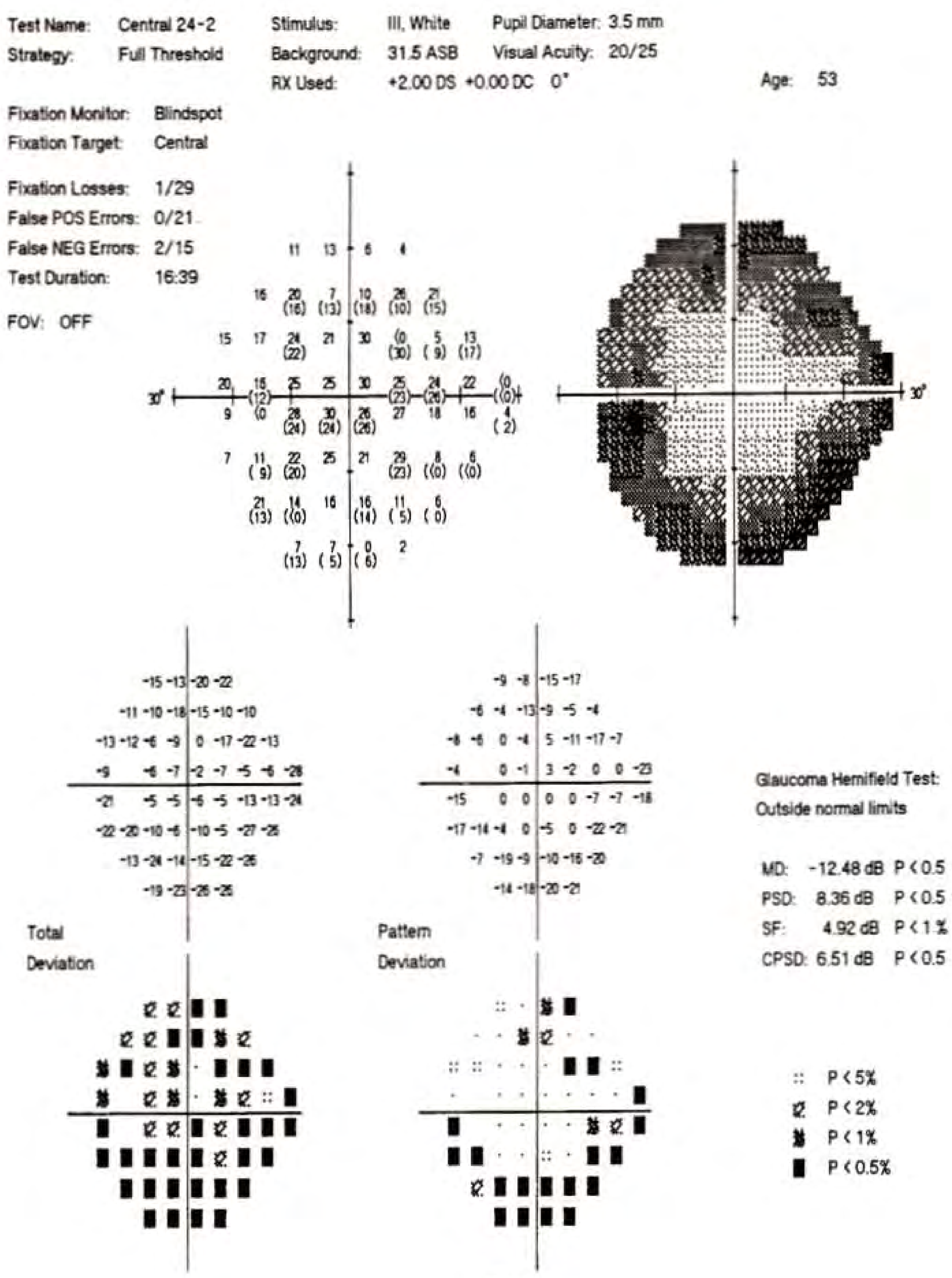

Test Name: Central 24-2
Strategy: Full Threshold
Stimulus: III, White
Background: 31.5 ASB
RX Used: +2.00 DS +0.00 DC 0°
Pupil Diameter: 3.5 mm
Visual Acuity: 20/25
Age: 53
Fixation Monitor: Blindspot
Fixation Target: Central
Fixation Losses: 1/29
False POS Errors: 0/21
False NEG Errors: 2/15
Test Duration: 16:39
FOV: OFF
Total Deviation
Pattern Deviation
Glaucoma Hemifield Test: Outside normal limits
MD: -12.48 dB P < 0.5
PSD: 8.36 dB P < 0.5
SF: 4.92 dB P < 1%
CPSD: 6.51 dB P < 0.5
P < 5%
P < 2%
P < 1%
P < 0.5%

D

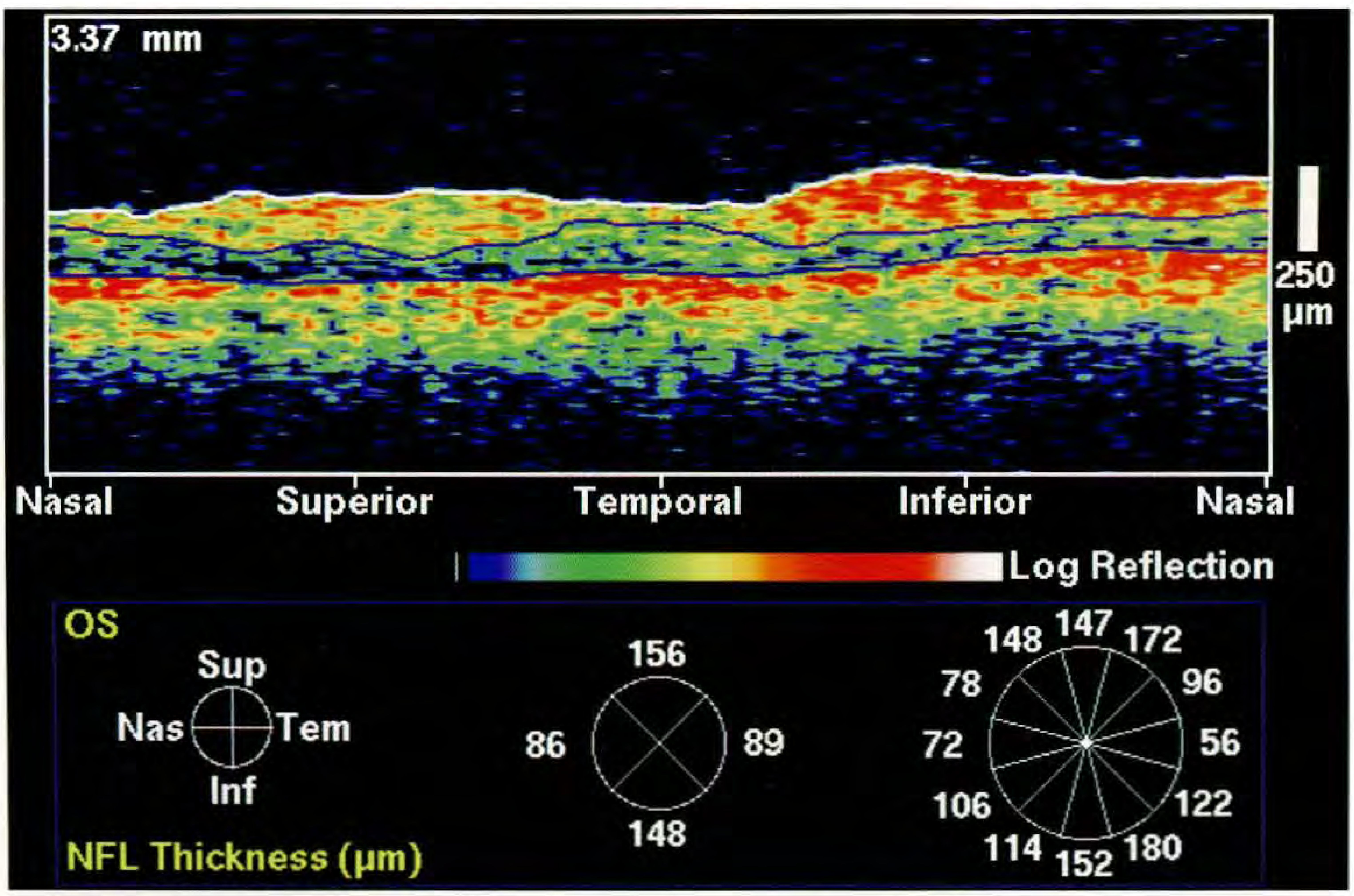

3.37 mm
250 µm
Nasal
Superior
Temporal
Inferior
Nasal
Log Reflection
OS
Sup
Nas
Tem
Inf
NFL Thickness (µm)
156
86
89
148
147
148
172
78
96
72
56
106
122
114
152
180

E

Case 12-16. Inferior Seidel Scotoma due to Chorioretinal Scar

Clinical Summary

A 87-year-old white female glaucoma suspect had age-related macular degeneration associated with a visual acuity of 20/30 in her right eye. She had previously received laser photocoagulation treatment for choroidal neovascularization in this eye. On examination, her intraocular pressure was 21 mm Hg. Slit-lamp observation was remarkable only for an intraocular lens implant. Dilated ophthalmoscopy (A, B) revealed marked cupping of the optic disc with an intact neuroretinal rim, and a chorioretinal scar in the superotemporal arcade. A Goldmann visual field (D) displayed an inferior Seidel scotoma.

Optical Coherence Tomography

A circular OCT image (E) acquired around the optic disc at a diameter of 3.4 mm showed a healthy superior nerve fiber layer and only slight atrophy inferiorly. The lack of nerve fiber layer thinning superiorly suggested that the visual field defect was due to the chorioretinal scar and not to a glaucomatous process.

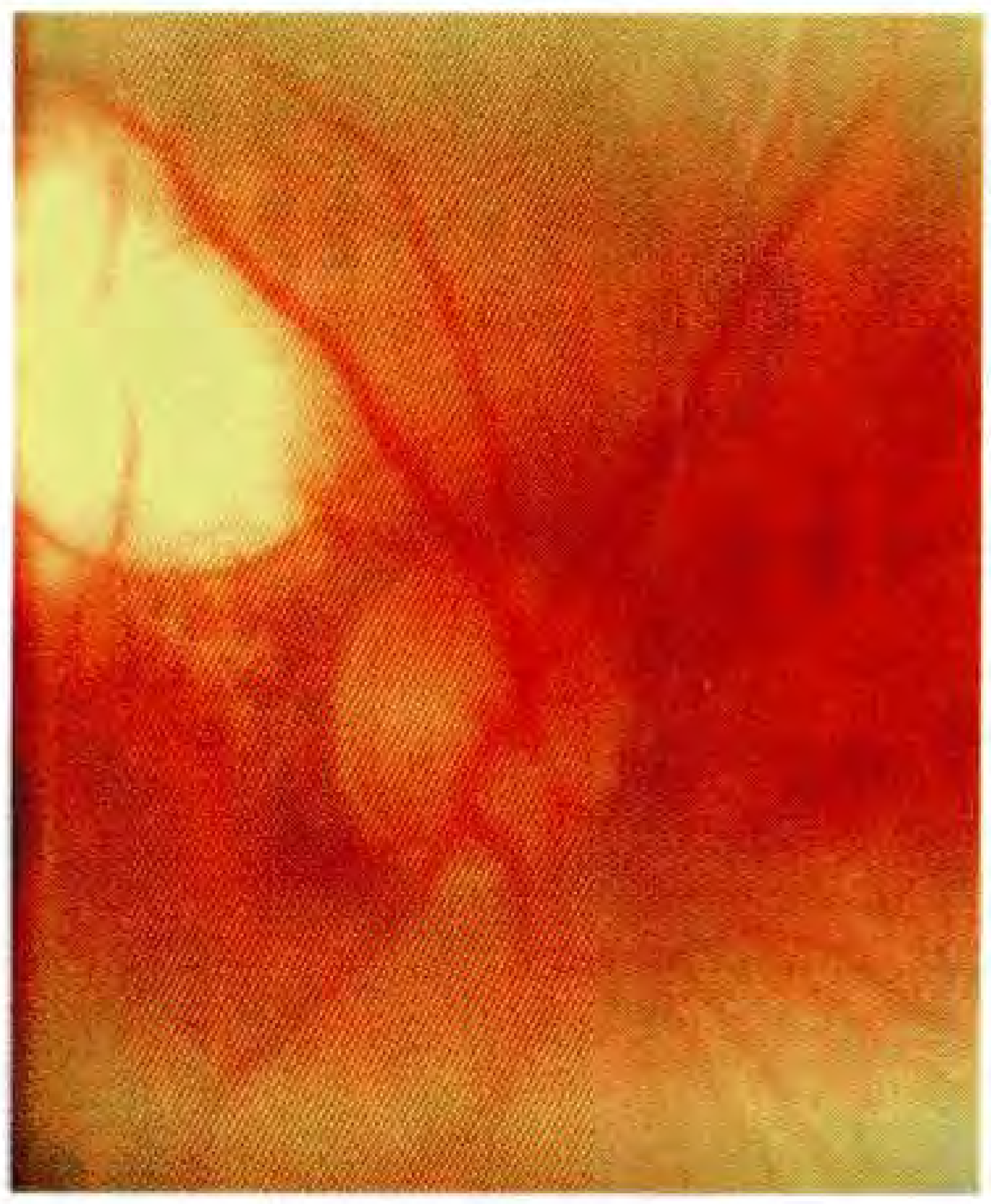

A

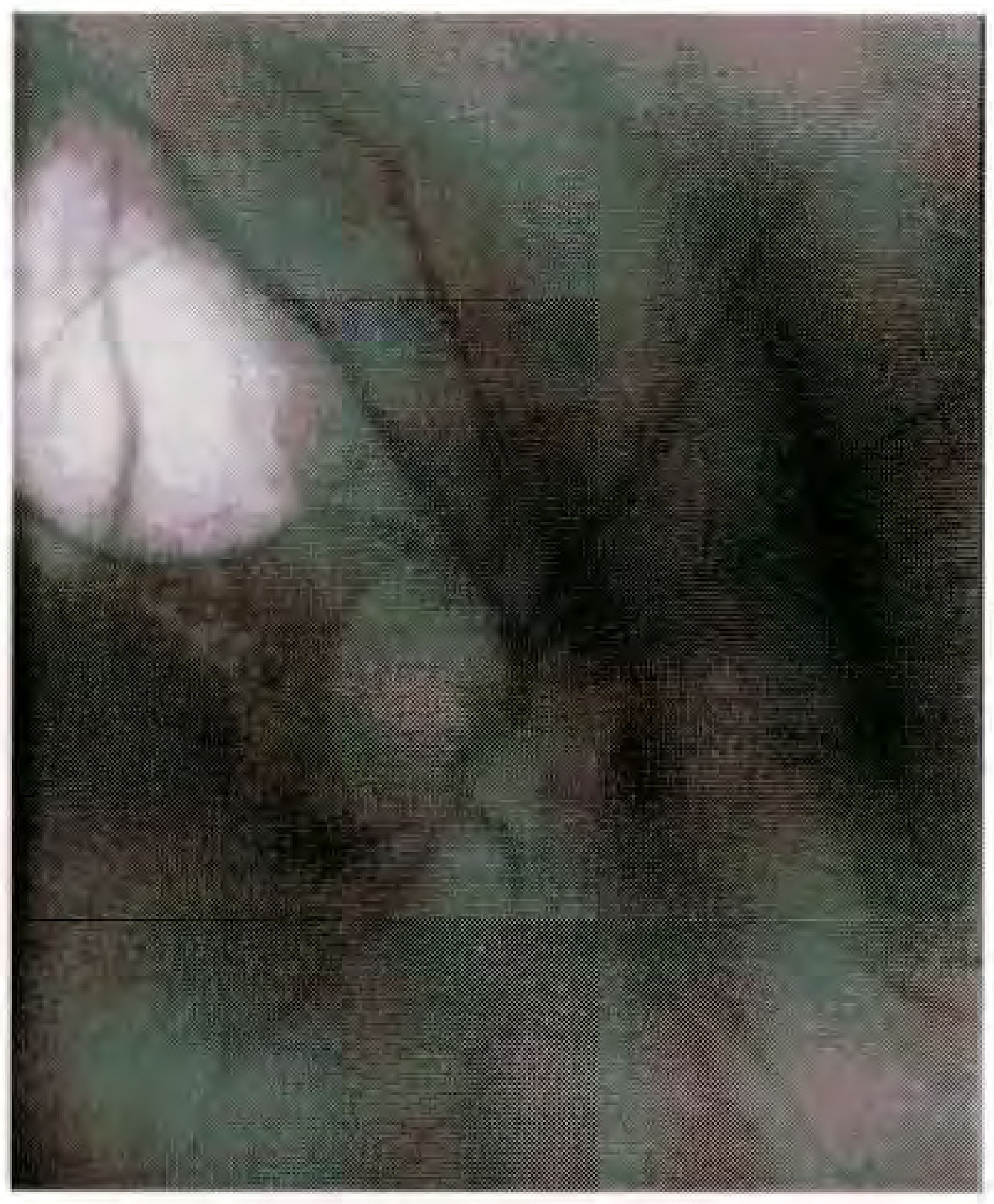

B

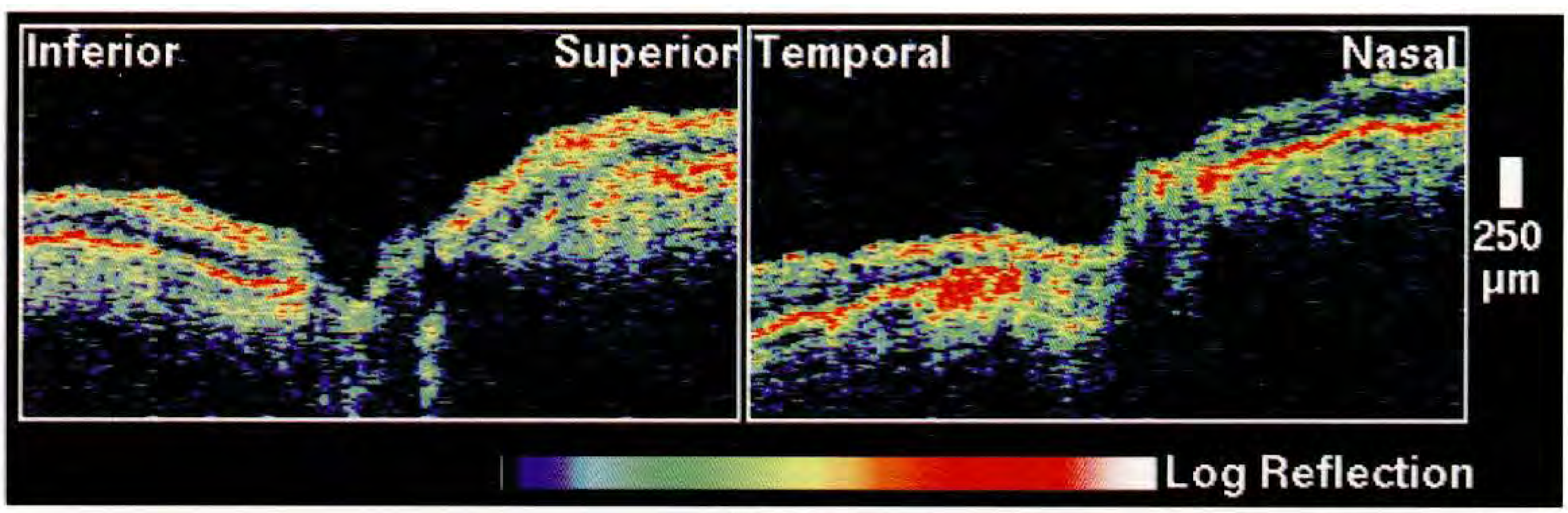

C

VERTICAL		HORIZONTAL	
Cup Diameter	0.59 mm	Cup Diameter	0.74 mm
Disc Diameter	1.46 mm	Disc Diameter	1.26 mm
C/D Ratio	0.40	C/D Ratio	0.59
NR Rim Area	1.40 mm²		
Inferior NFL	170 µm	Temporal NFL	160 µm
Superior NFL	180 µm	Nasal NFL	220 µm

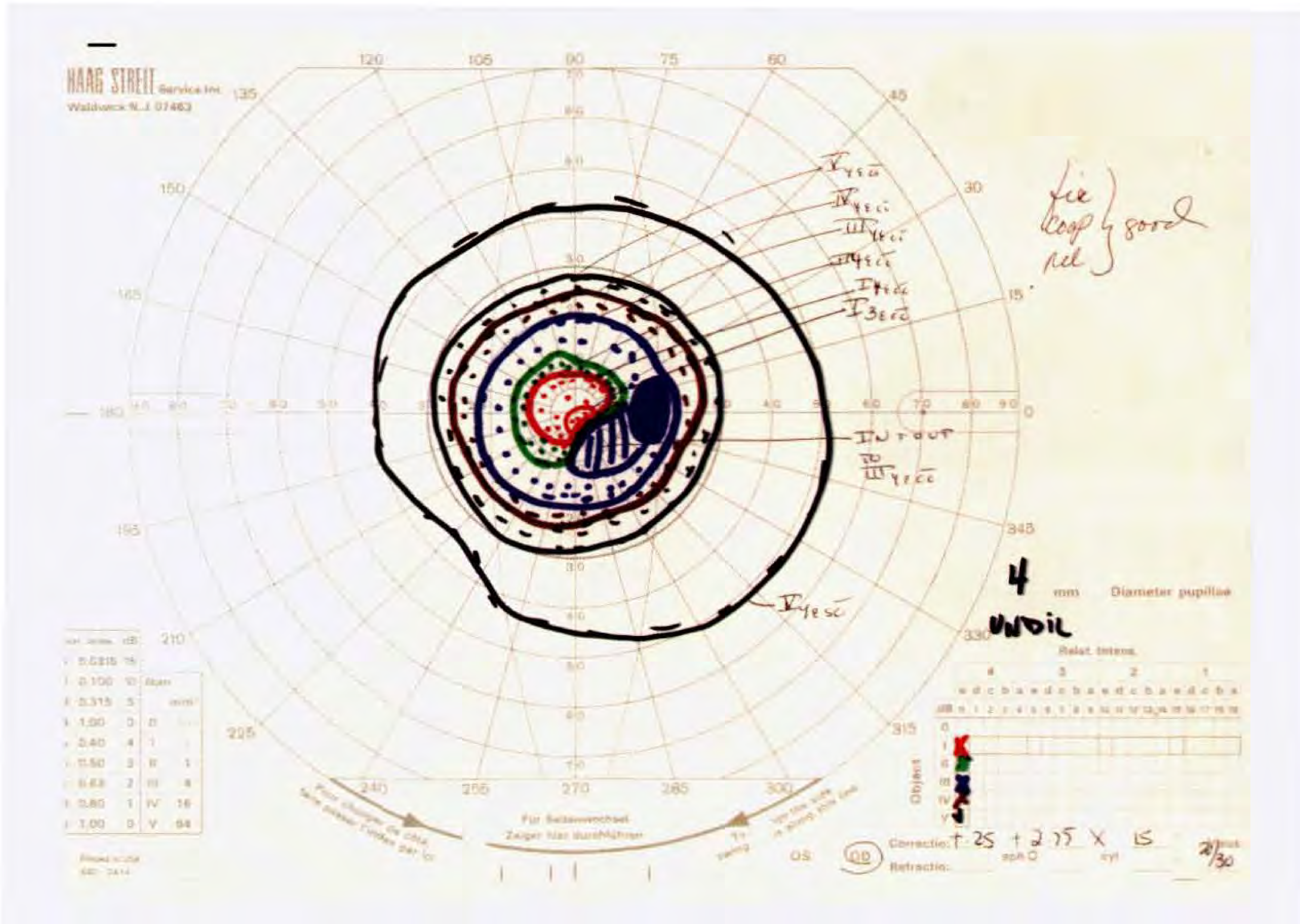
HAAG STREIT Service Inc.
Waldwick N.J. 07463
fix
coop
rel
good
4
mm Diameter pupillae
UNDIL
Relat. Intens.
Object
Correctio
Refractio
OS
OD
Für Seitenwechsel Zeiger hier durchführen

D

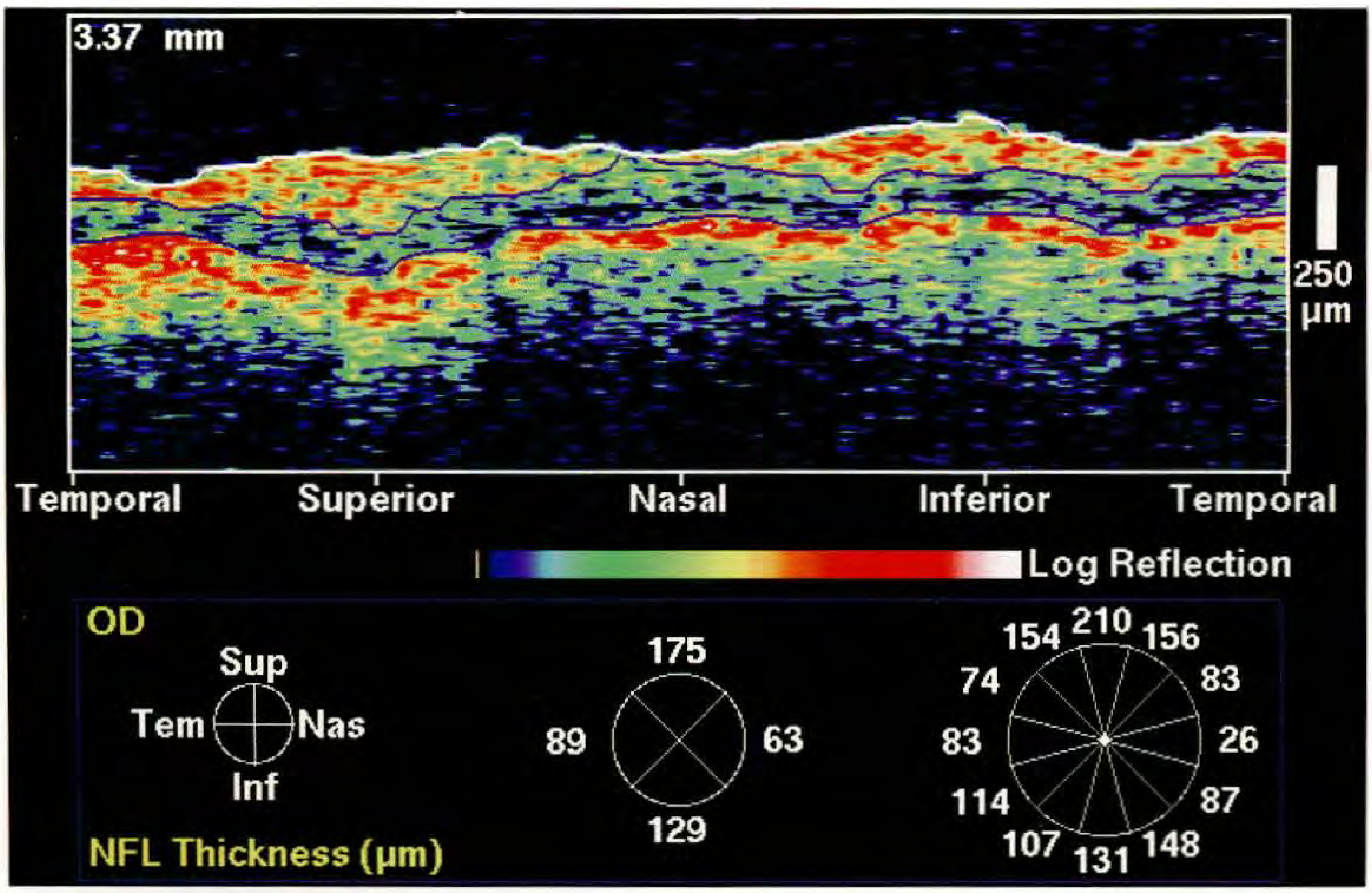
3.37 mm
250
µm
Temporal
Superior
Nasal
Inferior
Temporal
Log Reflection
OD
Sup
Tem
Nas
Inf
NFL Thickness (µm)
175
89
63
129
154
210
156
74
83
83
26
114
87
107
131
148

E

A

B

Case 12-17. Superior Arcuate Scotoma

Clinical Summary

A 70-year-old white woman with primary open-angle glaucoma was taking timolol 0.5% once daily and pilocarpine Ocusert 40s weekly, in both eyes. The right eye had a visual acuity of 20/25 with an intraocular pressure of 12 mm Hg. Slit-lamp examination revealed 2+ nuclear sclerosis of the crystalline lens, but was otherwise normal. The angle was open to the ciliary body band through 360°. Dilated ophthalmoscopy (A,B) showed marked cupping of the optic disc and loss of the neuroretinal rim inferotemporally. A dense superior arcuate defect splitting fixation was noted on the Humphrey visual vield (D).

Optical Coherence Tomography

A 3.4 mm diameter circular tomogram (E) revealed atrophy of the retinal nerve fiber layer inferiorly. The thinning was most significant from 7:00 to 9:00, consistent with the superior visual defect observed clinically.

(continued)

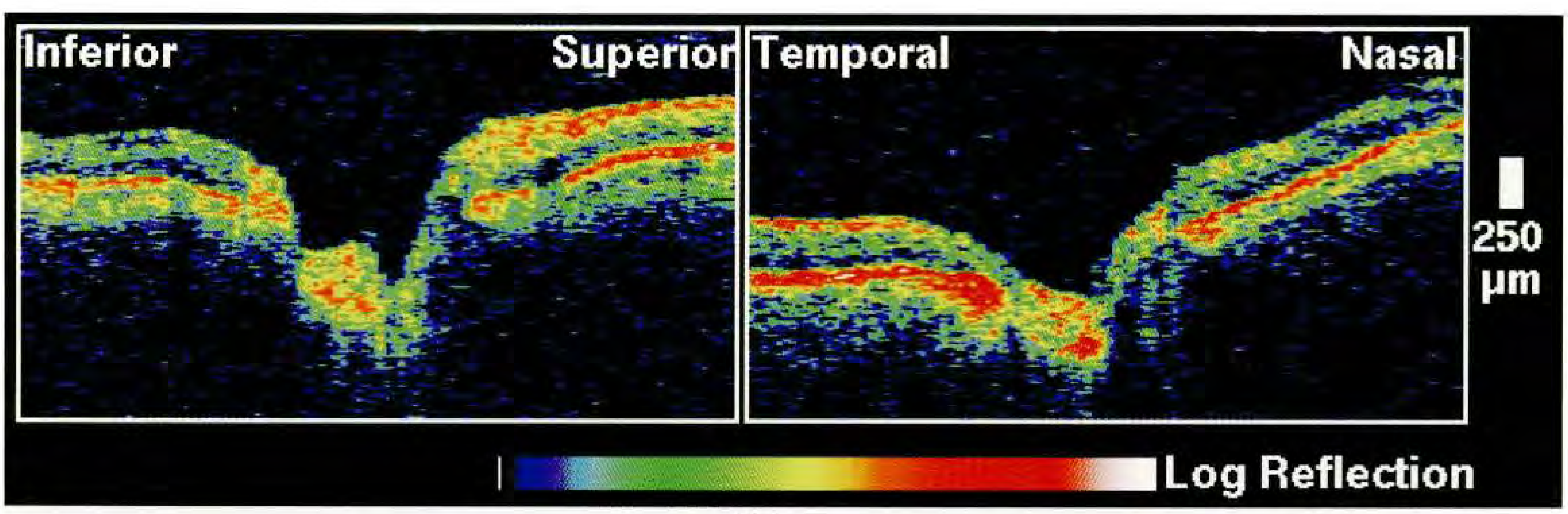

C

VERTICAL		*HORIZONTAL*	
Cup Diameter	**1.40 mm**	**Cup Diameter**	**0.68 mm**
Disc Diameter	**1.70 mm**	**Disc Diameter**	**1.31 mm**
C/D Ratio	**0.82**	**C/D Ratio**	**0.52**
NR Rim Area	**0.73 mm²**		
Inferior NFL	**220 µm**	**Temporal NFL**	**180 µm**
Superior NFL	**250 µm**	**Nasal NFL**	**120 µm**

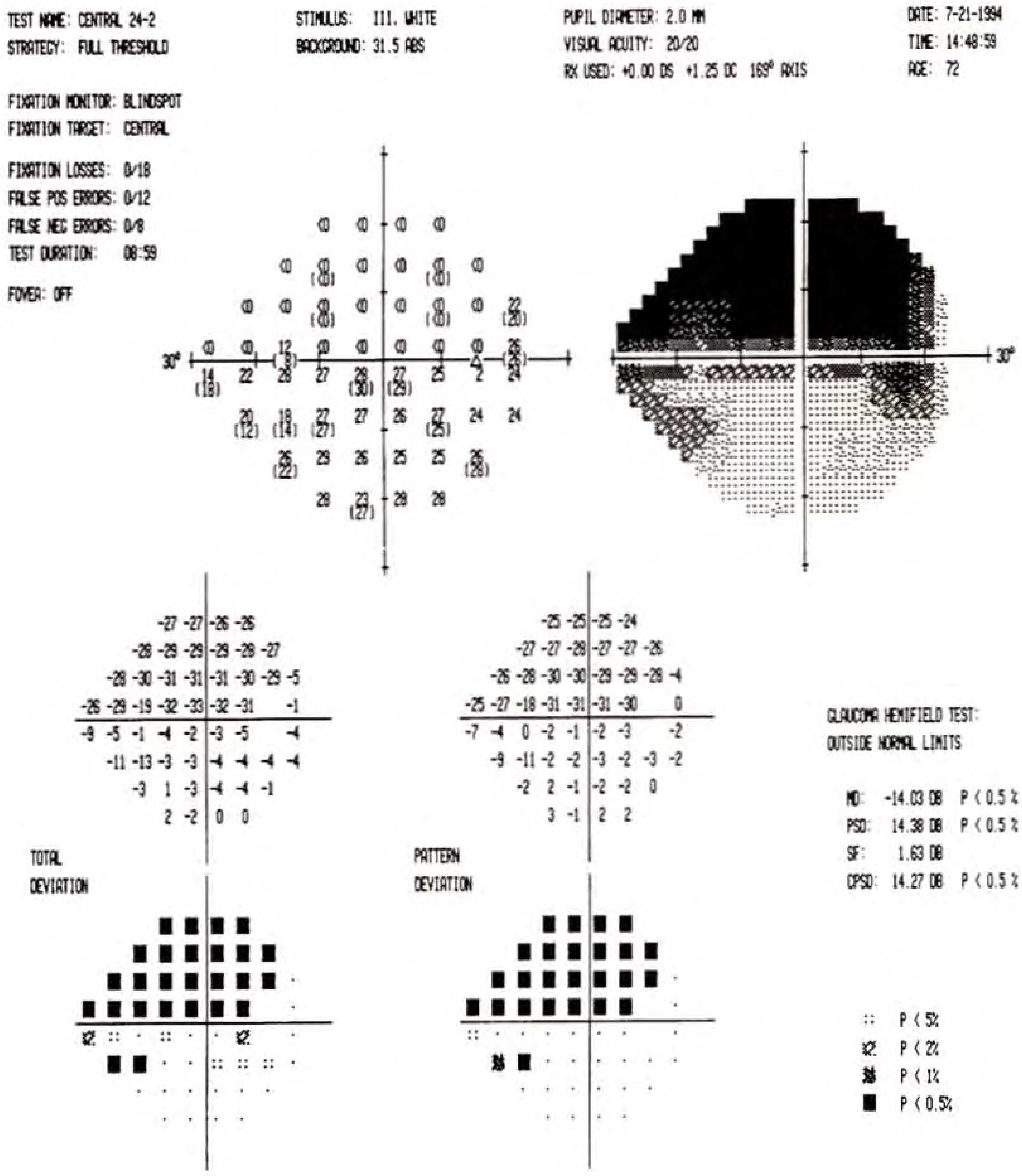
TEST NAME: CENTRAL 24-2
STRATEGY: FULL THRESHOLD
STIMULUS: III, WHITE
BACKGROUND: 31.5 ABS
PUPIL DIAMETER: 2.0 MM
VISUAL ACUITY: 20/20
RX USED: +0.00 DS +1.25 DC 169° AXIS
DATE: 7-21-1994
TIME: 14:48:59
AGE: 72
FIXATION MONITOR: BLINDSPOT
FIXATION TARGET: CENTRAL
FIXATION LOSSES: 0/18
FALSE POS ERRORS: 0/12
FALSE NEG ERRORS: 0/8
TEST DURATION: 08:59
FOVEA: OFF
30°
30°
TOTAL DEVIATION
PATTERN DEVIATION
GLAUCOMA HEMIFIELD TEST: OUTSIDE NORMAL LIMITS
MD: -14.03 DB P < 0.5%
PSD: 14.38 DB P < 0.5%
SF: 1.63 DB
CPSD: 14.27 DB P < 0.5%
P < 5%
P < 2%
P < 1%
P < 0.5%

D

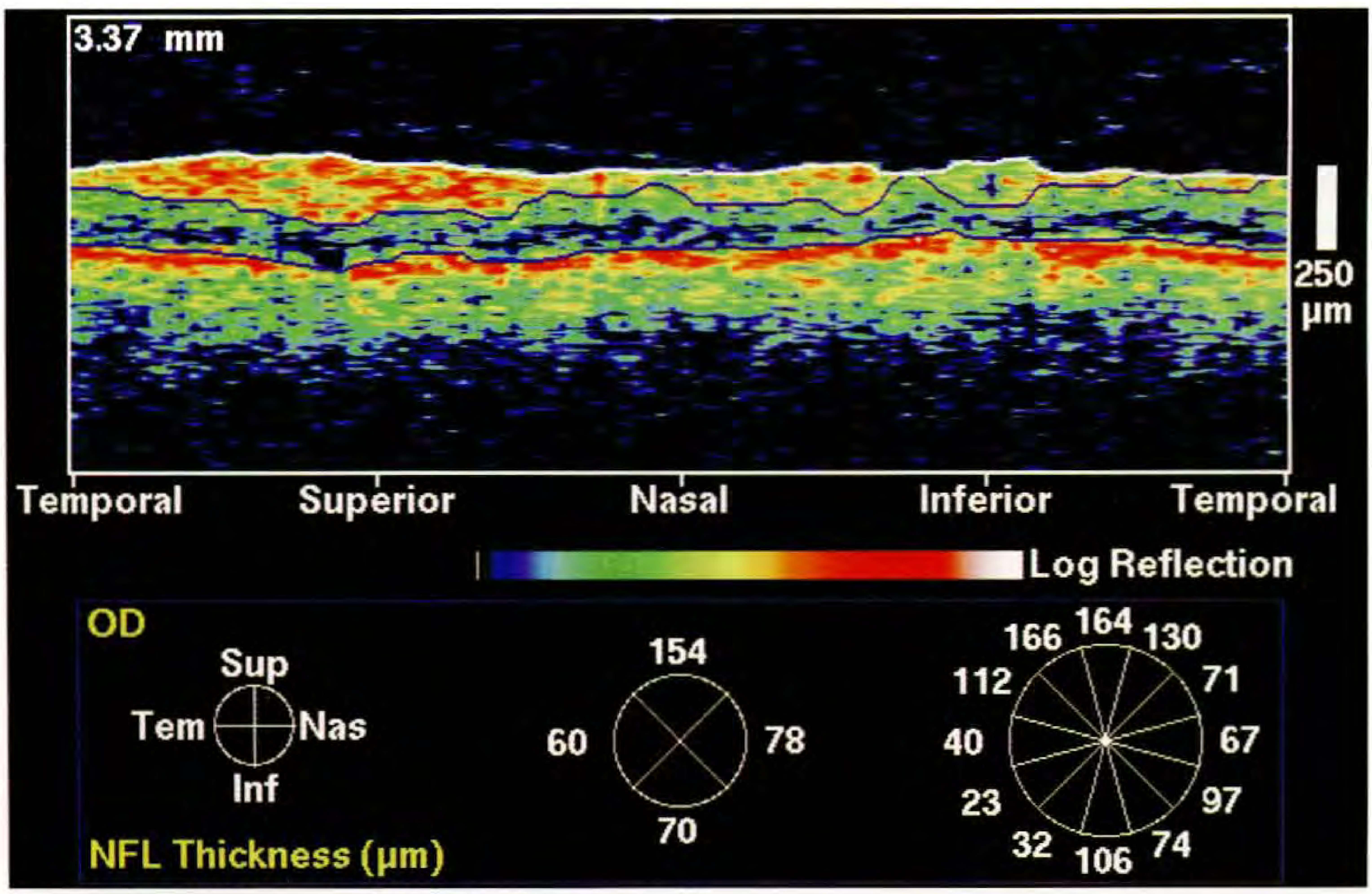
3.37 mm
250 μm
Temporal
Superior
Nasal
Inferior
Temporal
Log Reflection
OD
Sup
Tem
Nas
Inf
NFL Thickness (μm)
154
60
78
70
166
164
130
112
71
40
67
23
97
32
106
74

E

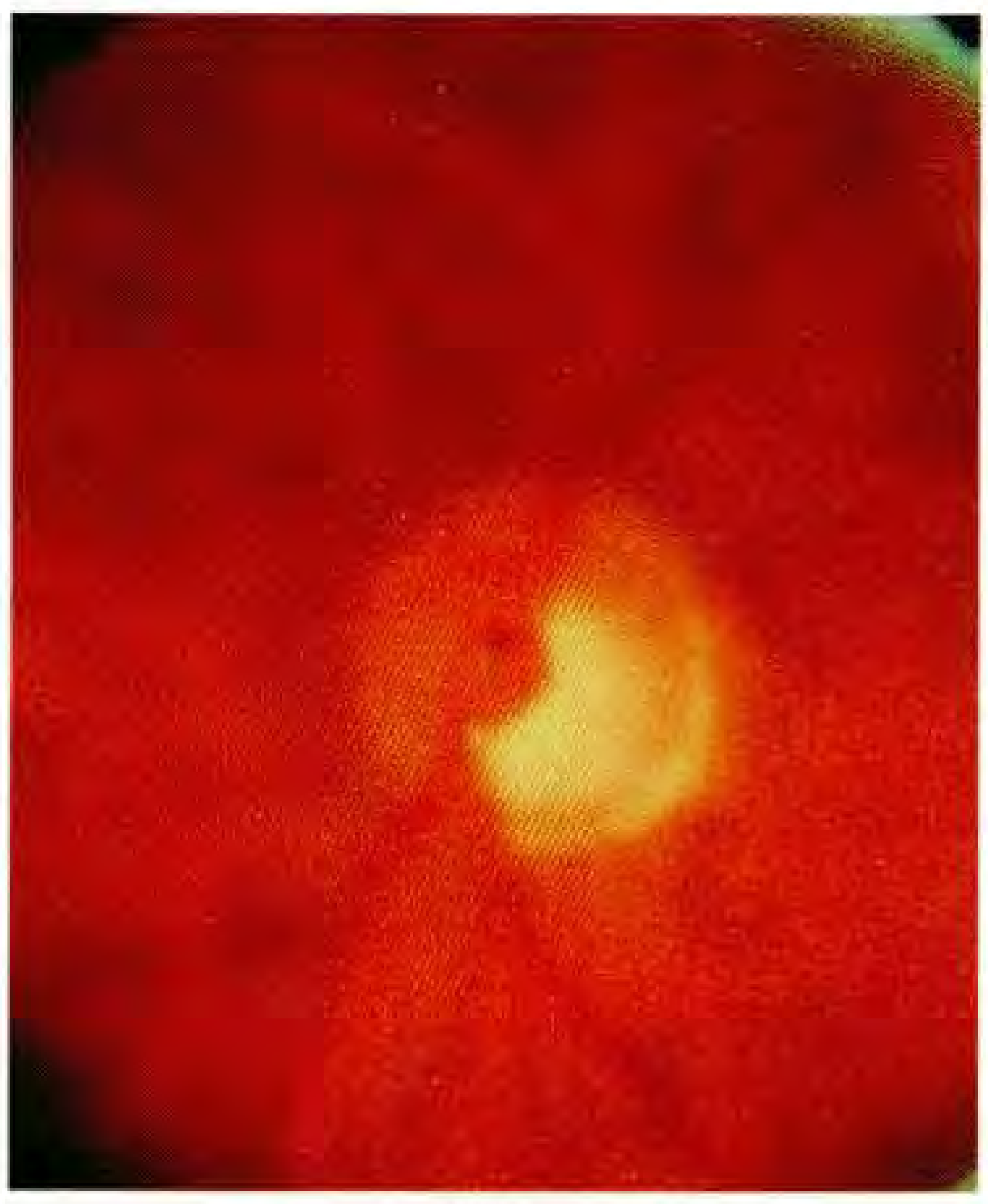

F

G

Case 12-17 continued

Clinical Summary

The patient's left eye had a visual acuity of 20/25 and an intraocular pressure of 11 mm Hg. The anterior segment examination was normal except for 2+ nuclear sclerotic cataracts. The angle was wide open to the ciliary body band through 360°. Marked cupping of the disc was noted on funduscopic examination (F,G), with complete atrophy of the neuroretinal rim inferotemporally. A dense superior arcuate scotoma splitting fixation was also noted in this eye on the Humphrey visual field (I).

Optical Coherence Tomography

A virtual absence of nerve fibers was observed inferotemporally at 5:00 in the circular OCT tomogram (J) corresponding to the area of visual field loss. A narrow, focal notch in the nerve fiber layer was seen superiorly, and did not coincide with a clinically detectable visual field defect.

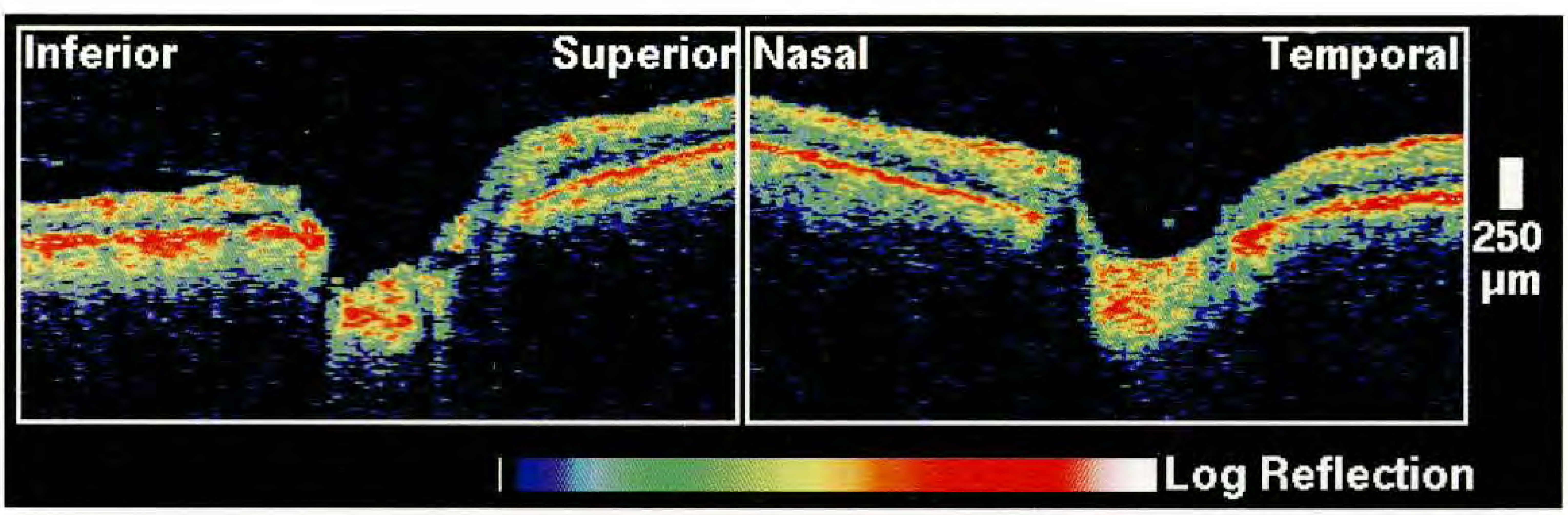

H

VERTICAL		*HORIZONTAL*	
Cup Diameter	**1.38 mm**	**Cup Diameter**	**1.23 mm**
Disc Diameter	**1.70 mm**	**Disc Diameter**	**1.40 mm**
C/D Ratio	**0.81**	**C/D Ratio**	**0.88**
NR Rim Area	**0.77mm²**		
Inferior NFL	**90µm**	**Nasal NFL**	**210 µm**
Superior NFL	**150 µm**	**Temporal NFL**	**150 µm**

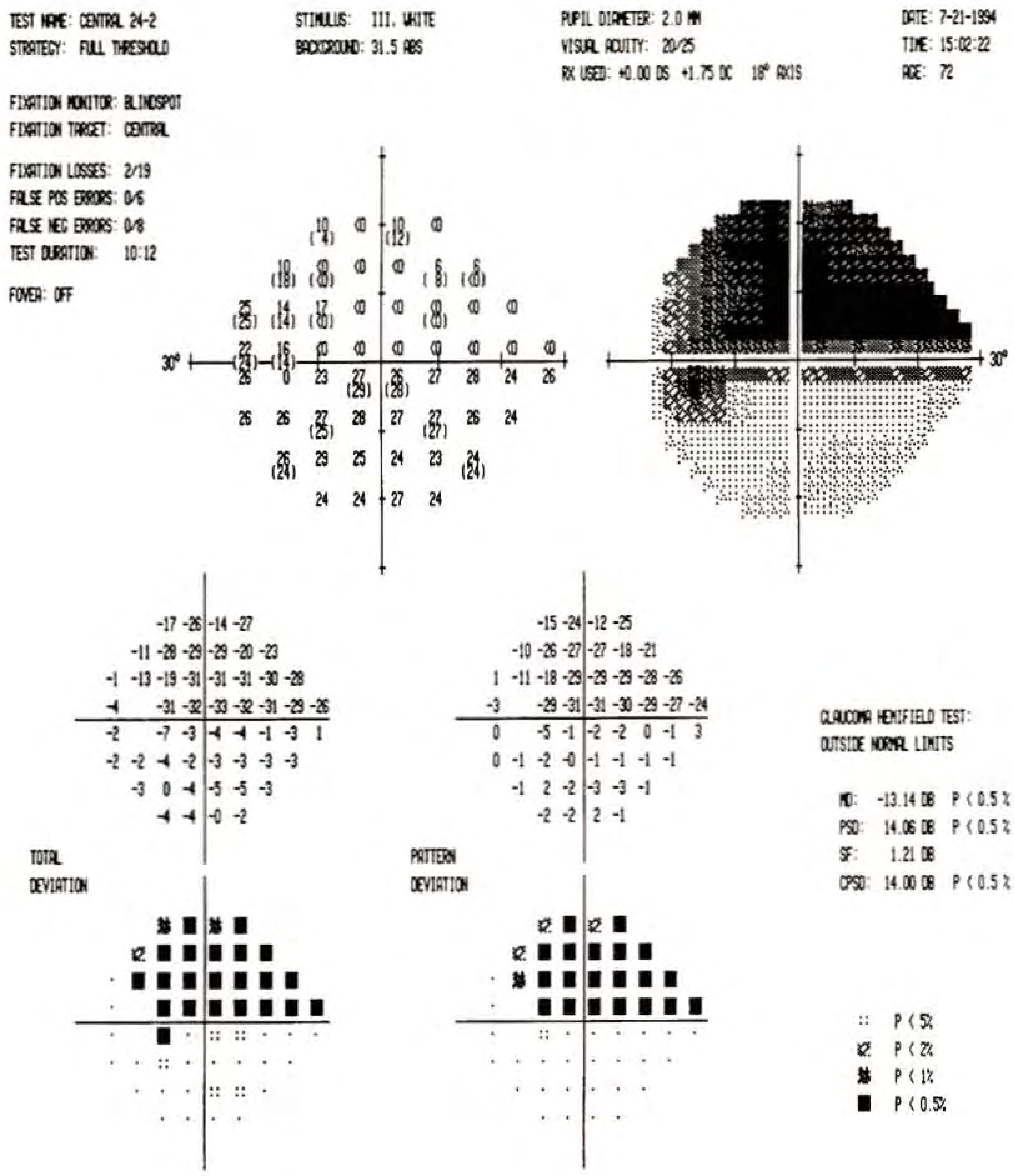
TEST NAME: CENTRAL 24-2
STRATEGY: FULL THRESHOLD
STIMULUS: III, WHITE
BACKGROUND: 31.5 ABS
PUPIL DIAMETER: 2.0 MM
VISUAL ACUITY: 20/25
RX USED: +0.00 DS +1.75 DC 18° AXIS
DATE: 7-21-1994
TIME: 15:02:22
AGE: 72
FIXATION MONITOR: BLINDSPOT
FIXATION TARGET: CENTRAL
FIXATION LOSSES: 2/19
FALSE POS ERRORS: 0/6
FALSE NEG ERRORS: 0/8
TEST DURATION: 10:12
FOVEA: OFF
TOTAL DEVIATION
PATTERN DEVIATION
GLAUCOMA HEMIFIELD TEST: OUTSIDE NORMAL LIMITS
MD: -13.14 DB P < 0.5 %
PSD: 14.06 DB P < 0.5 %
SF: 1.21 DB
CPSD: 14.00 DB P < 0.5 %
P < 5%
P < 2%
P < 1%
P < 0.5%

I

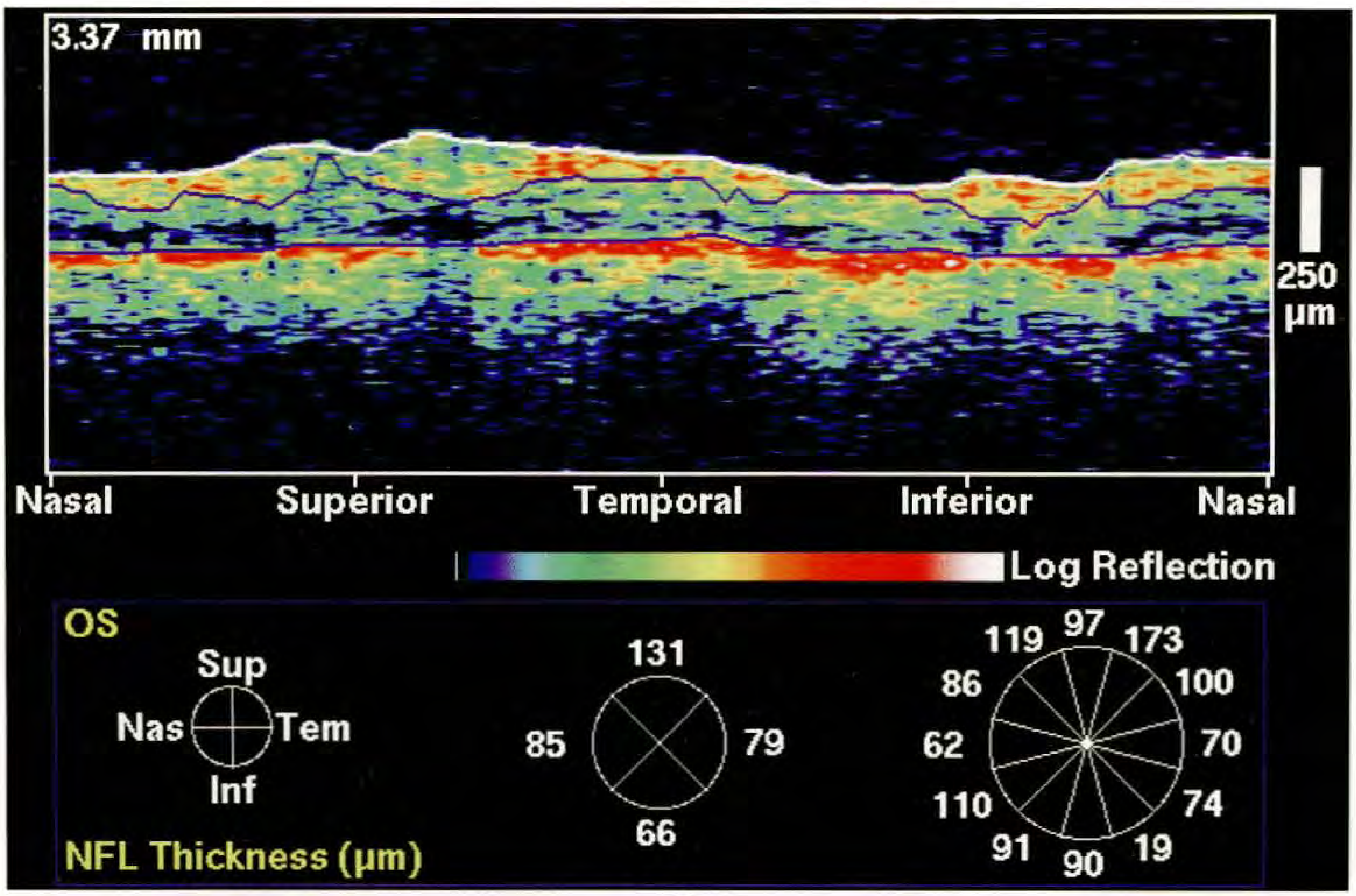
3.37 mm
250 µm
Nasal
Superior
Temporal
Inferior
Nasal
Log Reflection
OS
Sup
Nas
Tem
Inf
NFL Thickness (µm)
131
85
79
66
119
97
173
86
100
62
70
110
74
91
90
19

J

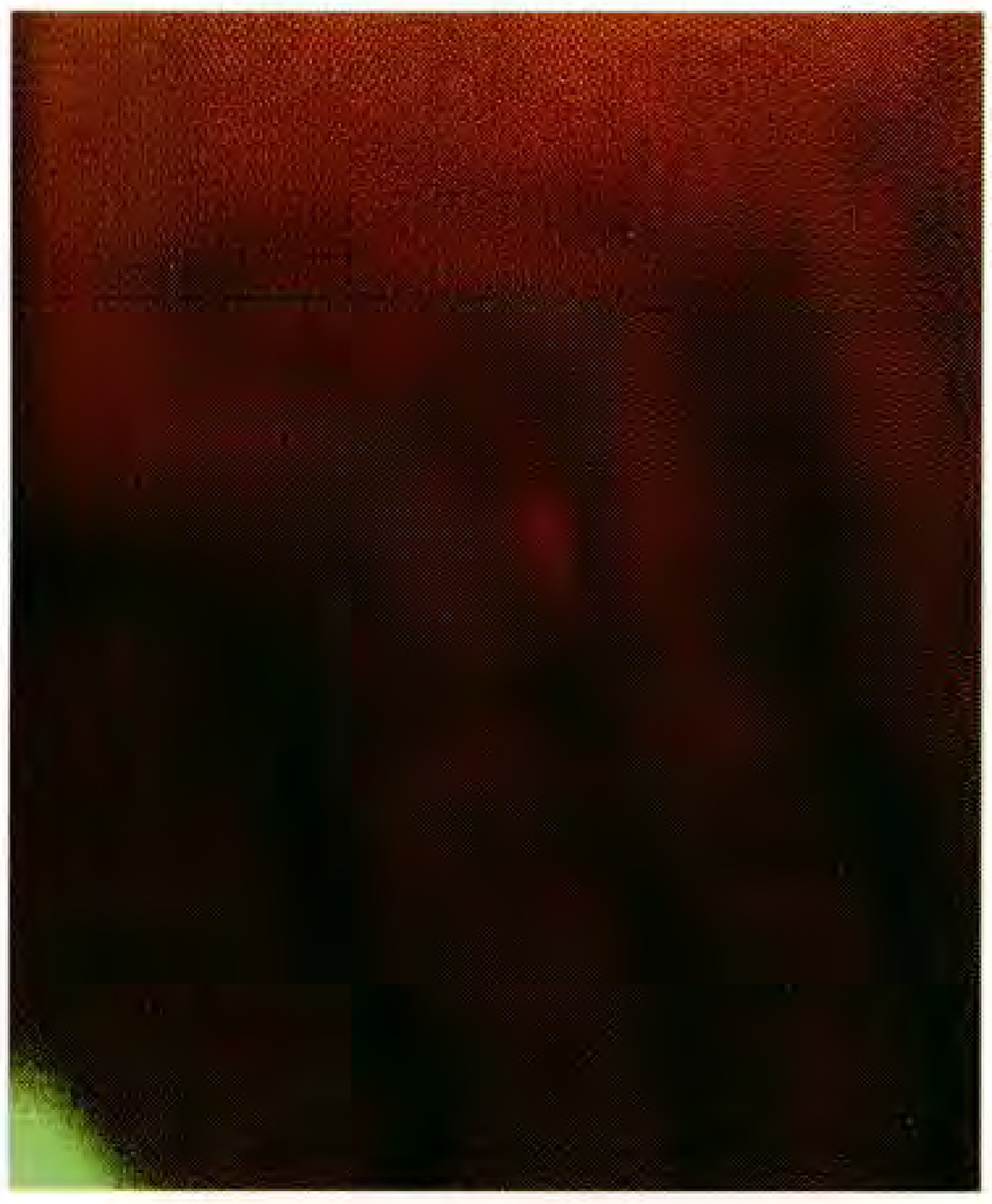

A

Case 12-18. Generalized Depression

Clinical Summary

An 87-year-old white man with pseudoexfoliation glaucoma had an intraocular pressure of 27 mm Hg and a visual acuity of 20/30 in his right eye. He had been taking carteolol 1% twice daily in this eye. Slit-lamp examination revealed pseudoexfoliation and 2-3+ nuclear sclerosis of the crystalline lens. Dilated ophthalmoscopy (A) showed a moderately cupped optic disc and slight superotemporal attenuation of the neuroretinal rim. A Humphrey visual field (C) showed generalized depression with evidence of an inferior nasal step.

Optical Coherence Tomography

The circular OCT image (D) showed a generalized decrease in nerve fiber layer thickness throughout the image, consistent with the depressed field. A focal area of more relative thinning was observed on OCT superotemporally at 11:00, corresponding to the relative inferonasal field defect.

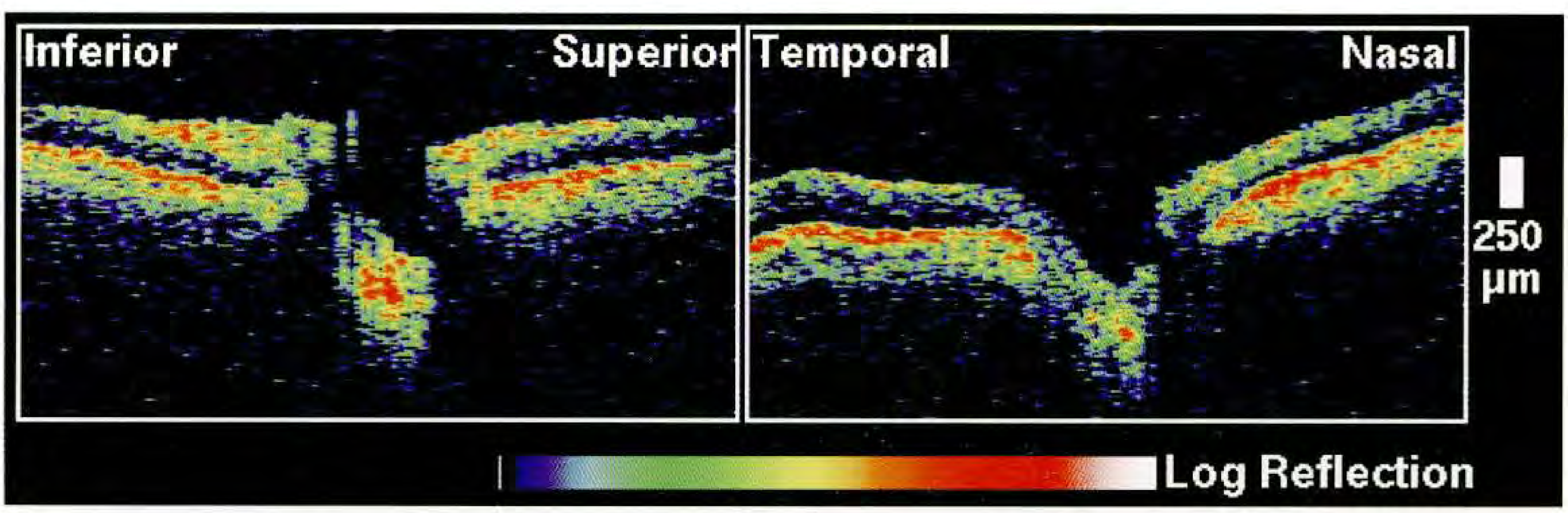

B

VERTICAL		HORIZONTAL	
Cup Diameter	0.85 mm	Cup Diameter	0.76 mm
Disc Diameter	1.11 mm	Disc Diameter	1.19 mm
C/D Ratio	0.77	C/D Ratio	0.64
NR Rim Area	0.40 mm^2		
Inferior NFL	210 µm	Temporal NFL	190 µm
Superior NFL	220 µm	Nasal NFL	230 µm

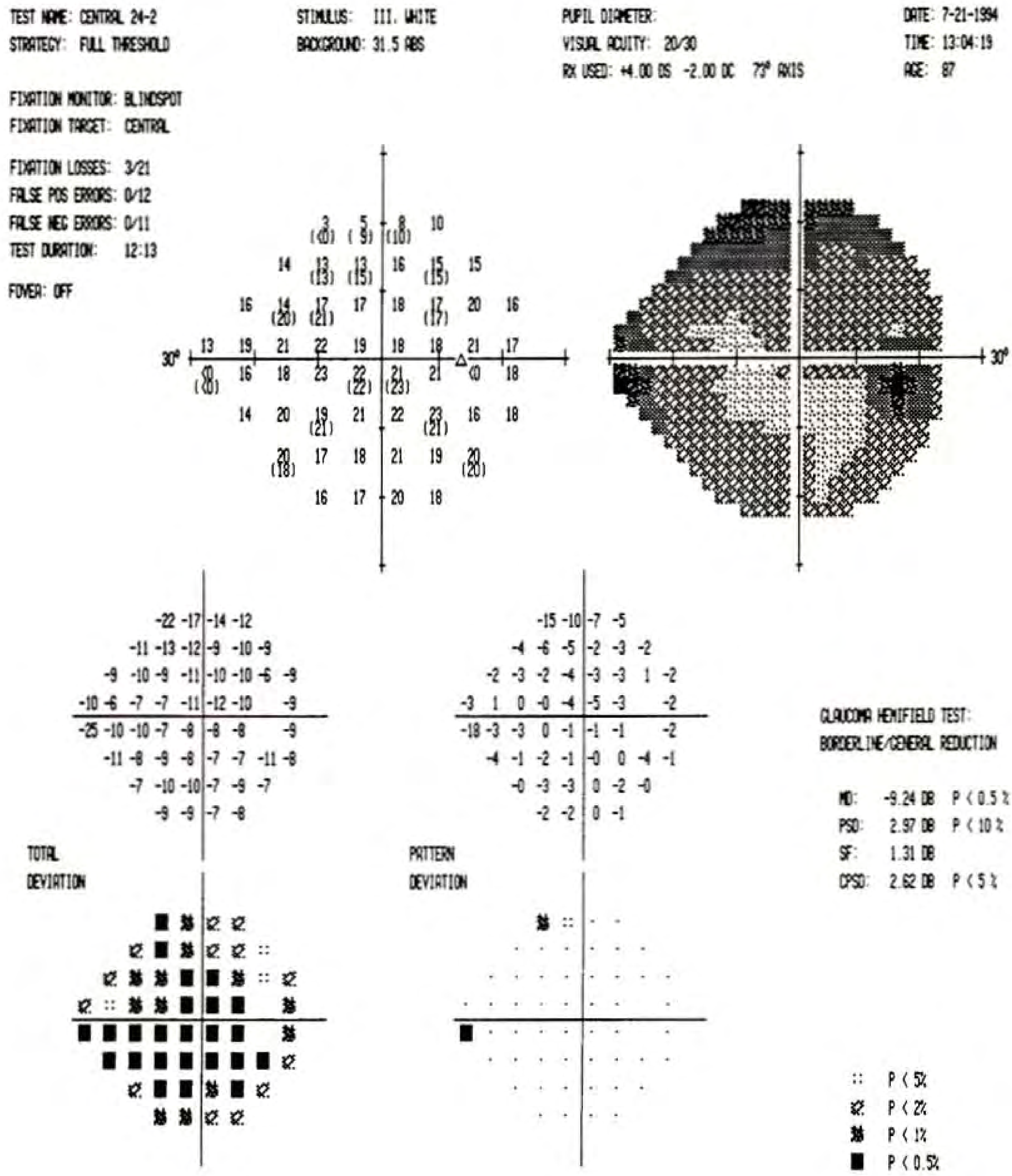
TEST NAME: CENTRAL 24-2
STRATEGY: FULL THRESHOLD
STIMULUS: III, WHITE
BACKGROUND: 31.5 ASB
PUPIL DIAMETER:
VISUAL ACUITY: 20/30
RX USED: +4.00 DS -2.00 DC 73° AXIS
DATE: 7-21-1994
TIME: 13:04:19
AGE: 87
FIXATION MONITOR: BLINDSPOT
FIXATION TARGET: CENTRAL
FIXATION LOSSES: 3/21
FALSE POS ERRORS: 0/12
FALSE NEG ERRORS: 0/11
TEST DURATION: 12:13
FOVEA: OFF
30°
30°
TOTAL DEVIATION
PATTERN DEVIATION
GLAUCOMA HEMIFIELD TEST:
BORDERLINE/GENERAL REDUCTION
MD: -9.24 DB P < 0.5 %
PSD: 2.97 DB P < 10 %
SF: 1.31 DB
CPSD: 2.62 DB P < 5 %
P < 5%
P < 2%
P < 1%
P < 0.5%

C

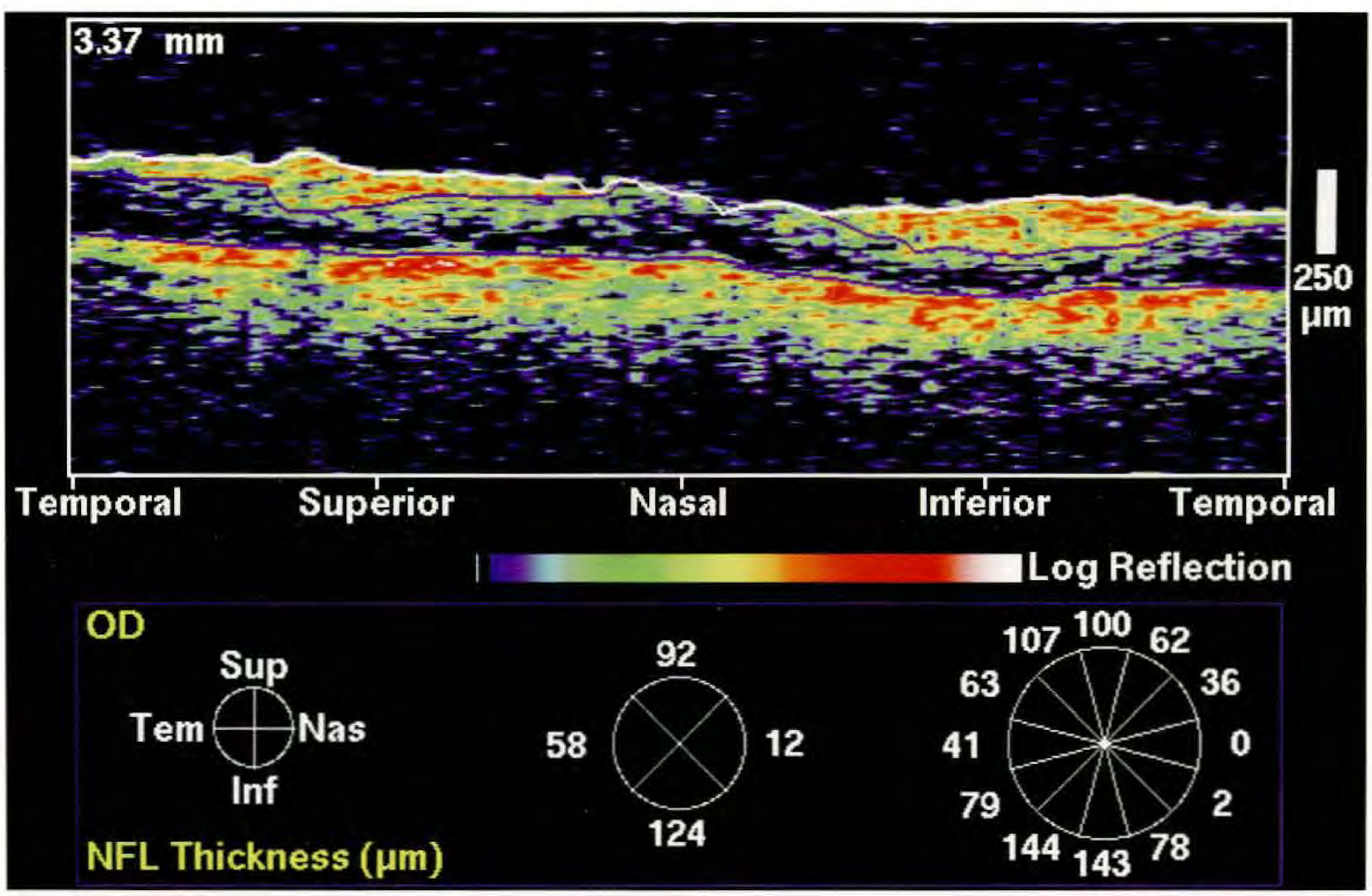
3.37 mm
250 μm
Temporal
Superior
Nasal
Inferior
Temporal
Log Reflection
OD
Sup
Tem
Nas
Inf
NFL Thickness (μm)
92
58
12
124
107
100
62
63
36
41
0
79
2
144
143
78

D

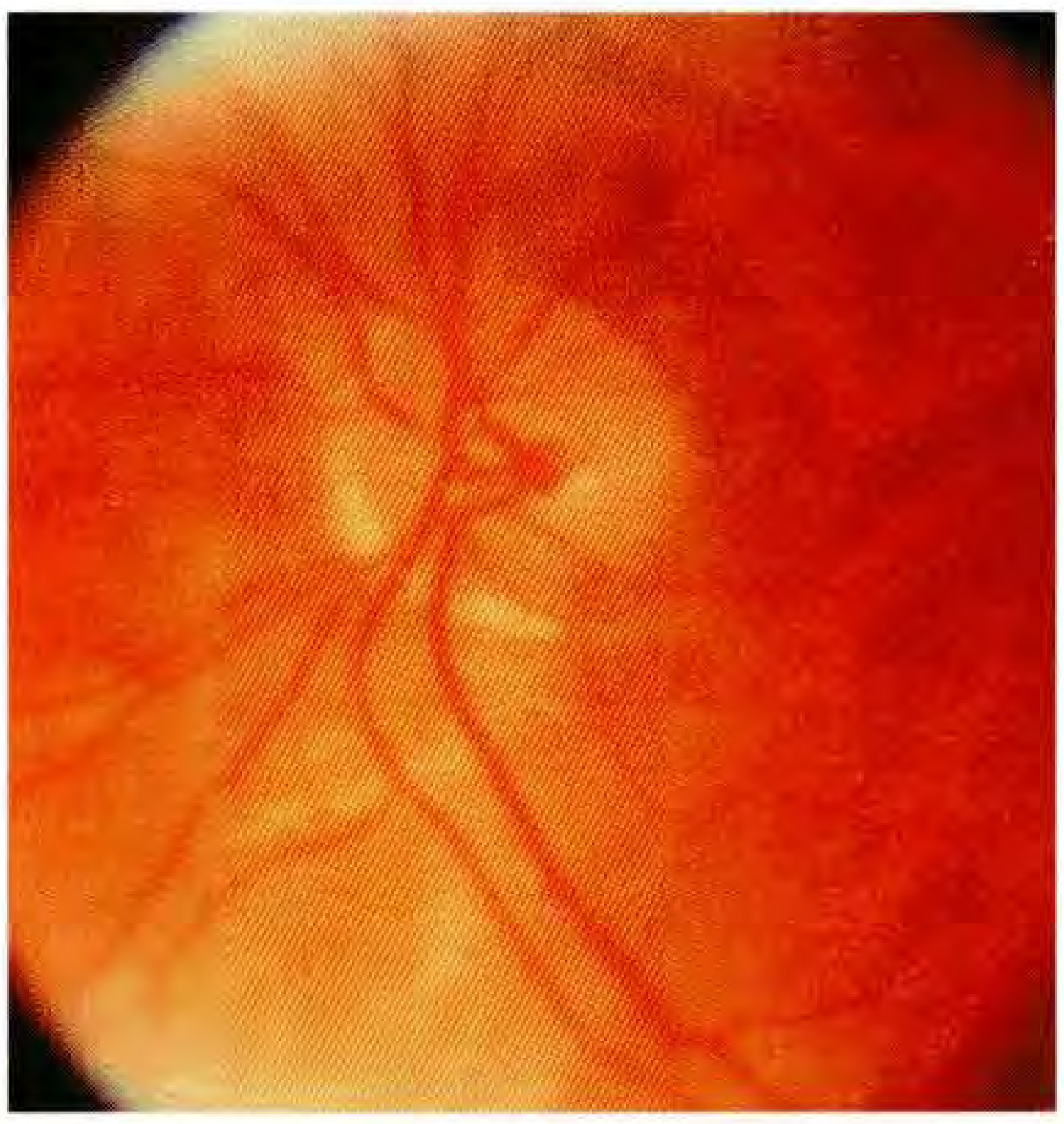

A

Case 12-19. Generalized Depression

Clinical Summary

An 80-year-old white man with primary open-angle glaucoma had borderline control of his intraocular pressure in his left eye. His medications included betaxolol 0.25% twice a day and pilocarpine 4% once daily. On examination, his visual acuity in this eye was 20/20 and the intraocular pressure was 19 mm Hg. Slit-lamp biomicroscopy revealed a normal anterior chamber and 1-2+ nuclear sclerosis of the crystalline lens. Dilated ophthalmoscopy (A) showed moderate to marked cupping of the optic disc and a slightly attenuated neuroretinal rim temporally. Generalized depression was noted on a Humphrey visual field (C).

Optical Coherence Tomography

A 3.4 mm diameter circular OCT tomogram (D) delineated moderate thinning in both the superotemporal (1:00 and 2:00) and inferotemporal (4:00 and 5:00) nerve fiber layer. The nasal nerve fibers, however, appeared to be spared.

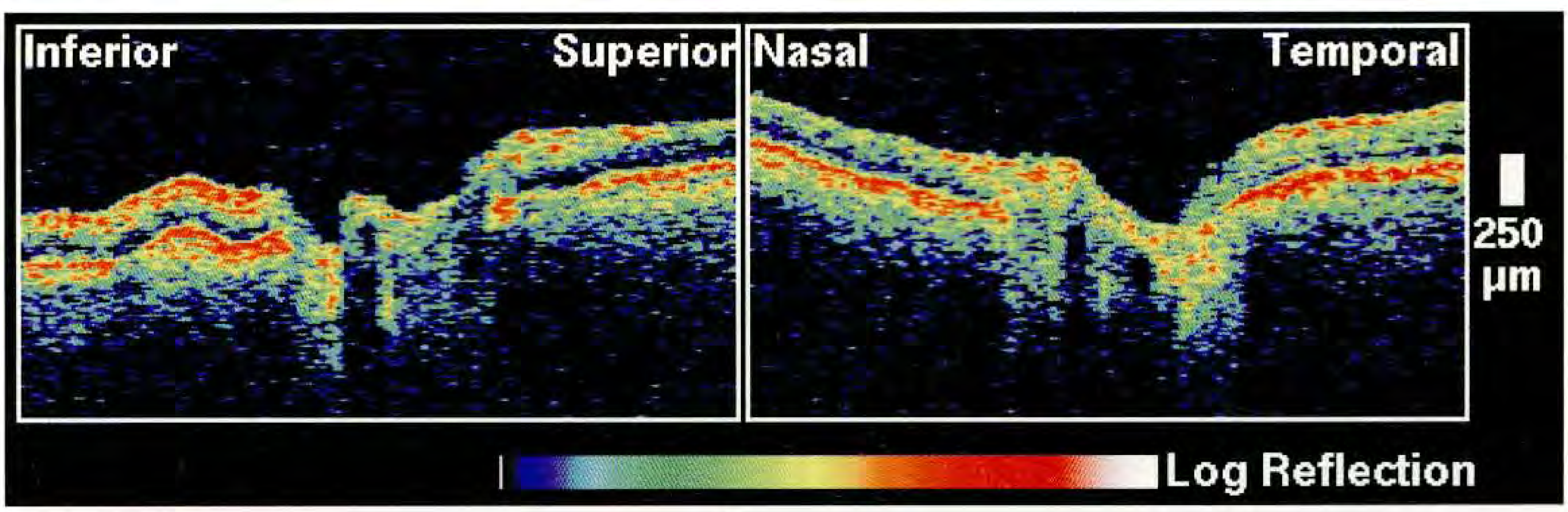

B

VERTICAL		HORIZONTAL	
Cup Diameter	1.59 mm	Cup Diameter	0.79 mm
Disc Diameter	1.86 mm	Disc Diameter	1.20 mm
C/D Ratio	0.85	C/D Ratio	0.66
NR Rim Area	0.73 mm^2		
Inferior NFL	130 μm	Nasal NFL	270 μm
Superior NFL	120 μm	Temporal NFL	120 μm

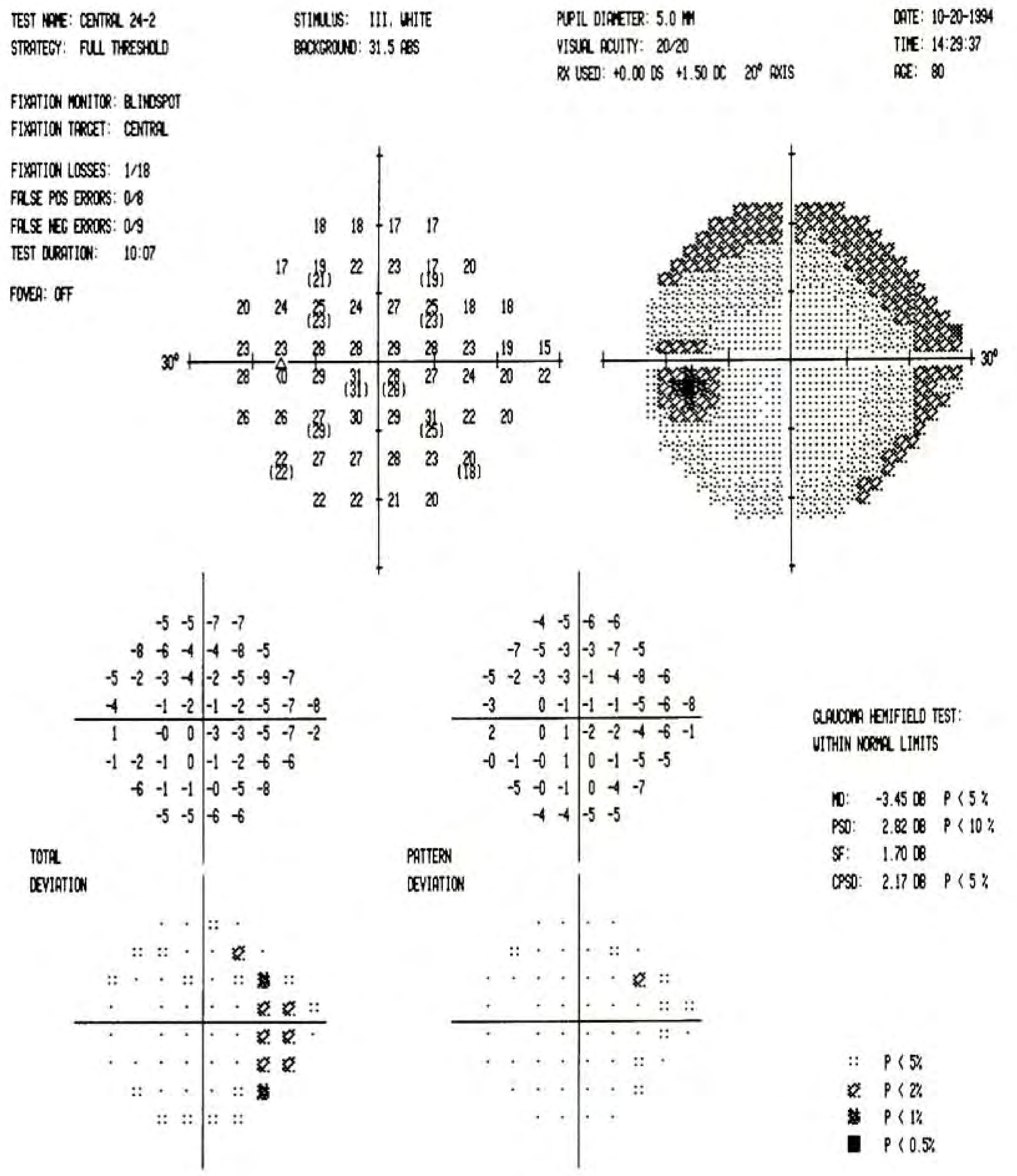
TEST NAME: CENTRAL 24-2
STRATEGY: FULL THRESHOLD
STIMULUS: III, WHITE
BACKGROUND: 31.5 ABS
PUPIL DIAMETER: 5.0 MM
VISUAL ACUITY: 20/20
RX USED: +0.00 DS +1.50 DC 20° AXIS
DATE: 10-20-1994
TIME: 14:29:37
AGE: 80
FIXATION MONITOR: BLINDSPOT
FIXATION TARGET: CENTRAL
FIXATION LOSSES: 1/18
FALSE POS ERRORS: 0/8
FALSE NEG ERRORS: 0/9
TEST DURATION: 10:07
FOVEA: OFF
30°
TOTAL DEVIATION
PATTERN DEVIATION
GLAUCOMA HEMIFIELD TEST:
WITHIN NORMAL LIMITS
MD: -3.45 DB P < 5 %
PSD: 2.82 DB P < 10 %
SF: 1.70 DB
CPSD: 2.17 DB P < 5 %
P < 5%
P < 2%
P < 1%
P < 0.5%

C

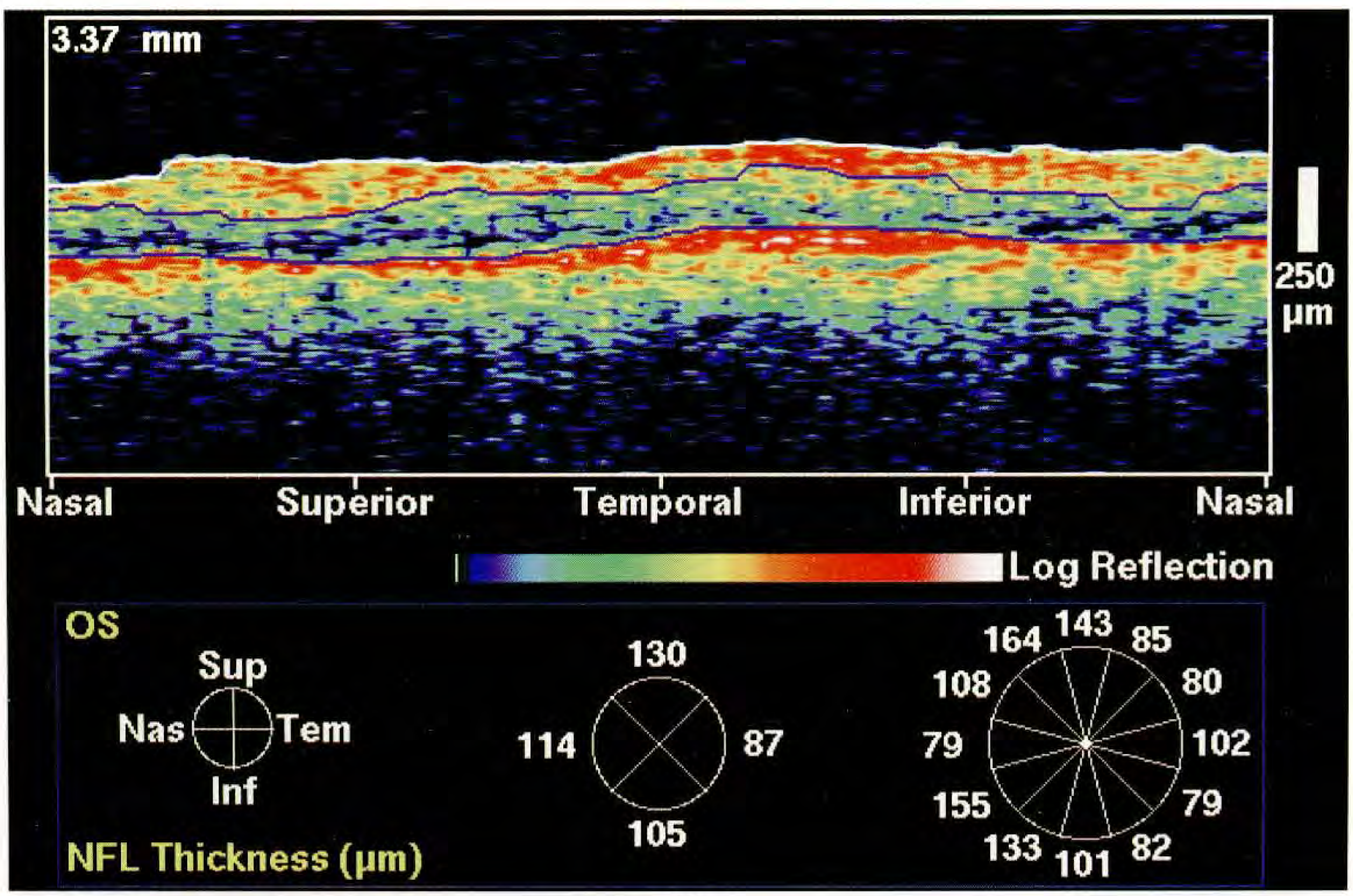
3.37 mm
250 µm
Nasal
Superior
Temporal
Inferior
Nasal
Log Reflection
OS
Sup
Nas
Tem
Inf
NFL Thickness (µm)
130
114
87
105
164
143
85
108
80
79
102
155
79
133
101
82

D

Case 12-20. End-Stage Glaucoma

Clinical Summary

A 77-year-old white woman with advanced glaucoma was taking betaxolol 0.5%, dipivefrin 0.1%, and fluoramethalone, all twice a day in both eyes. Examination of her right eye revealed a visual acuity of 20/30 and an intraocular pressure of 14 mm. Slit-lamp examination showed the angle to be open to the ciliary body band through 360°, 2+ nuclear sclerosis, and 1+ posterior subcapsular cataract. Moderate to marked cupping of the optic disc was observed on fundus examination (A,B), which also showed loss of the neuroretinal rim from approximately 6:00 to 11:00. A Humphrey visual field (D) showed a central island of remaining vision.

Optical Coherence Tomography

Severe thinning of the retinal nerve fiber layer was noted throughout a 3.4 mm diameter OCT image (E) obtained around the optic disc. The attenuation was more marked in the superior compared to the inferior nerve fiber layer.

(continued)

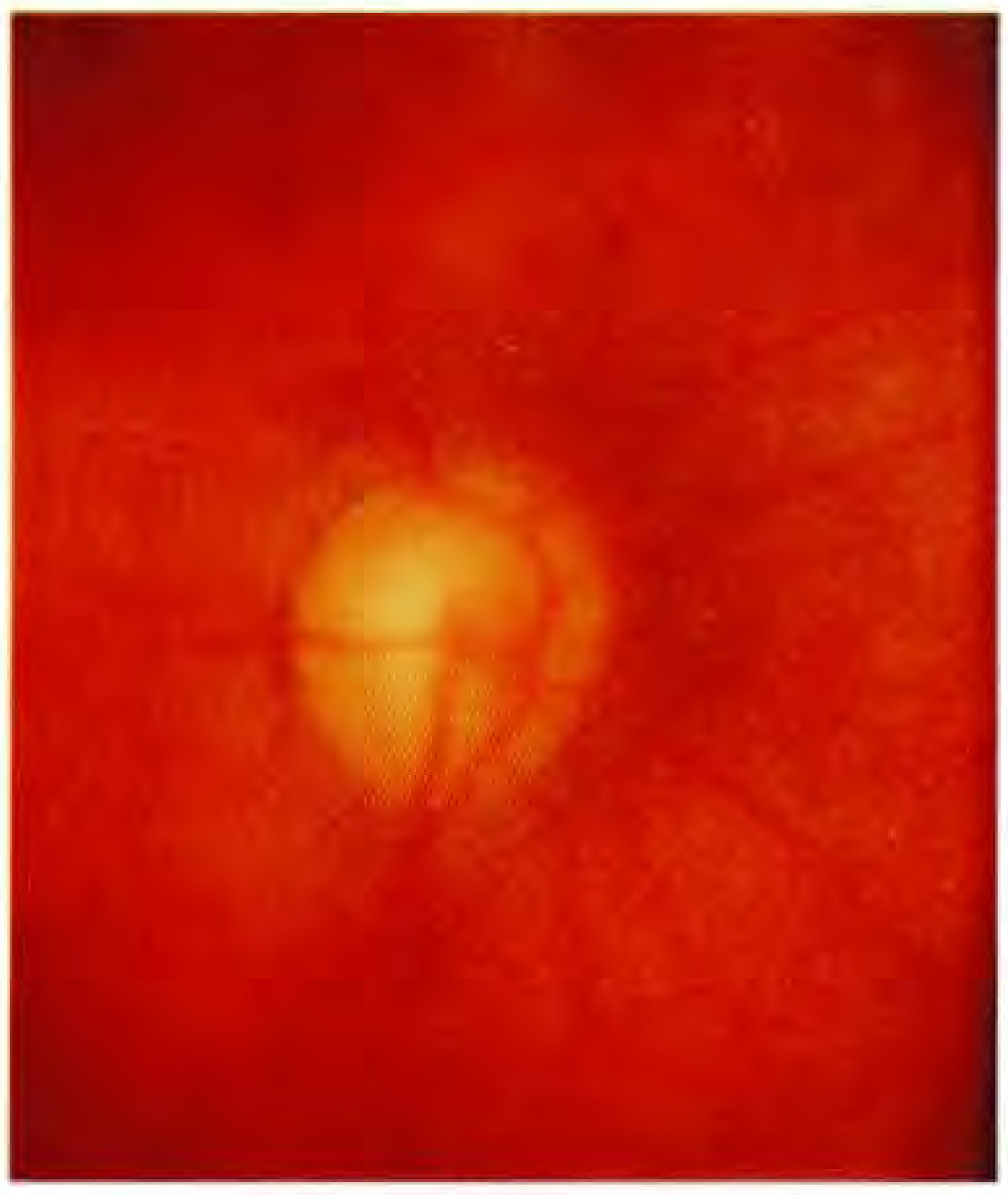

A

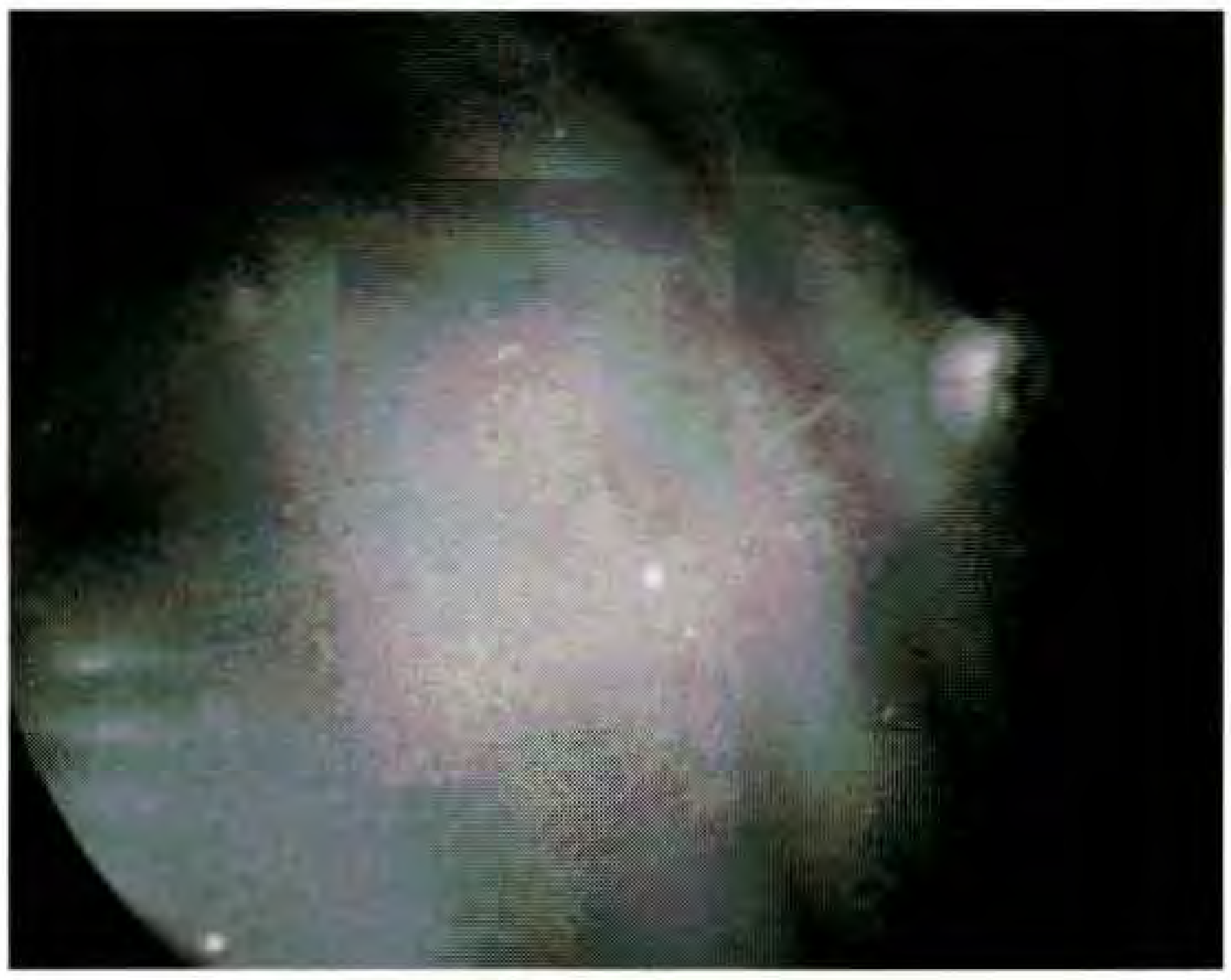

B

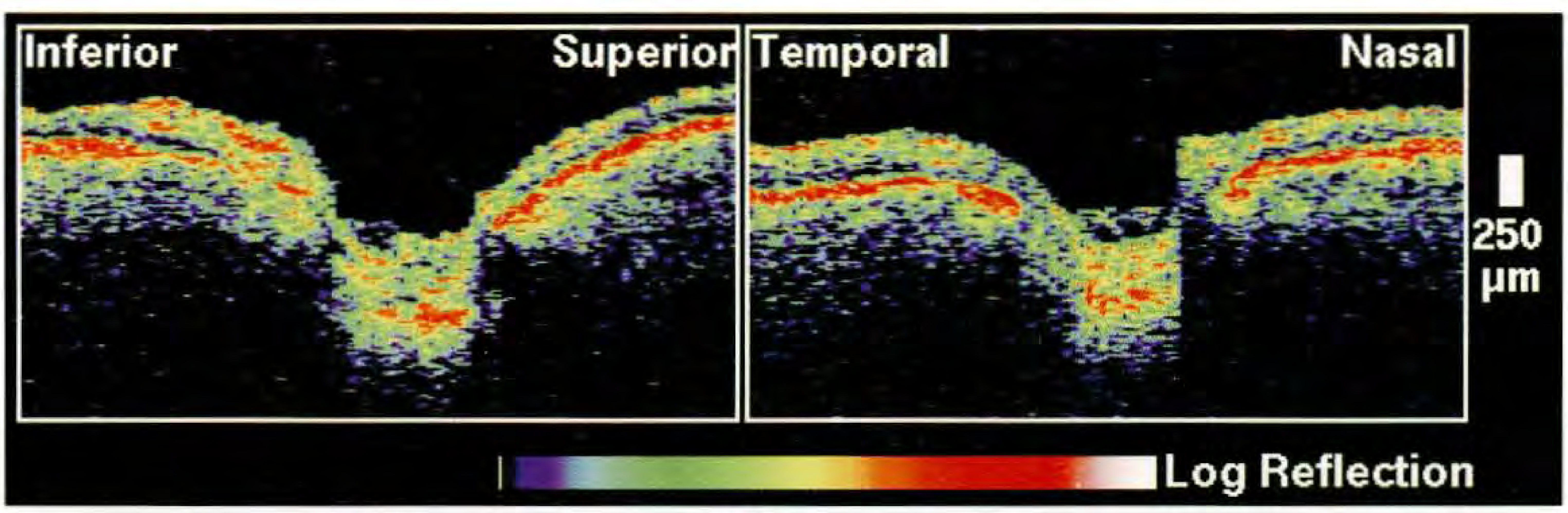

C

VERTICAL		*HORIZONTAL*	
Cup Diameter	**1.26 mm**	**Cup Diameter**	**1.03 mm**
Disc Diameter	**1.38 mm**	**Disc Diameter**	**1.25 mm**
C/D Ratio	**0.91**	**C/D Ratio**	**0.82**
NR Rim Area	**0.25**		
Inferior NFL	**70 µm**	**Temporal NFL**	**60 µm**
Superior NFL	**70 µm**	**Nasal NFL**	**130 µm**

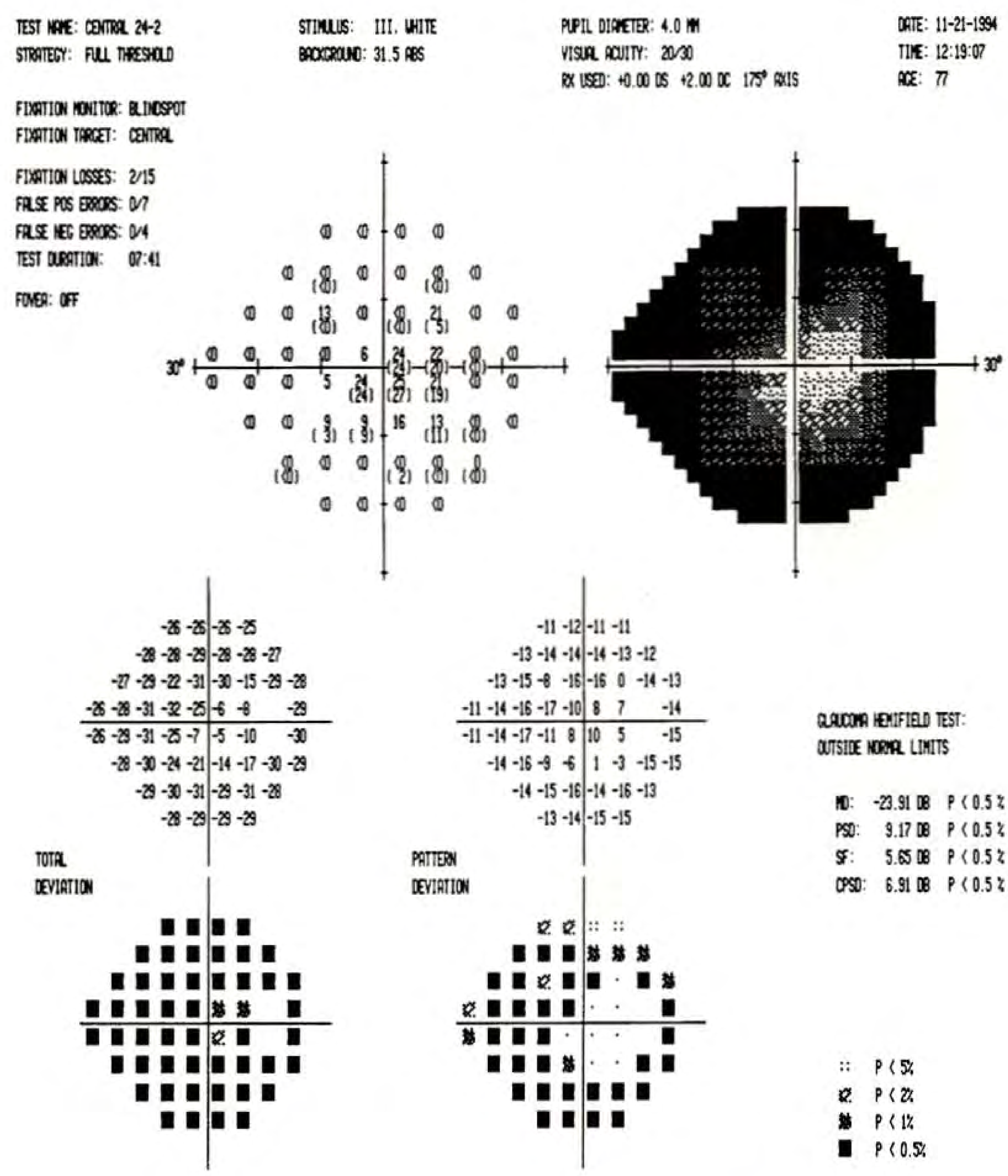
TEST NAME: CENTRAL 24-2
STRATEGY: FULL THRESHOLD
STIMULUS: III, WHITE
BACKGROUND: 31.5 ABS
PUPIL DIAMETER: 4.0 MM
VISUAL ACUITY: 20/30
RX USED: +0.00 DS +2.00 DC 175° AXIS
DATE: 11-21-1994
TIME: 12:19:07
AGE: 77
FIXATION MONITOR: BLINDSPOT
FIXATION TARGET: CENTRAL
FIXATION LOSSES: 2/15
FALSE POS ERRORS: 0/7
FALSE NEG ERRORS: 0/4
TEST DURATION: 07:41
FOVEA: OFF
30°
30°
TOTAL DEVIATION
PATTERN DEVIATION
GLAUCOMA HEMIFIELD TEST: OUTSIDE NORMAL LIMITS
MD: -23.91 DB P < 0.5 %
PSD: 9.17 DB P < 0.5 %
SF: 5.65 DB P < 0.5 %
CPSD: 6.91 DB P < 0.5 %
P < 5%
P < 2%
P < 1%
P < 0.5%

D

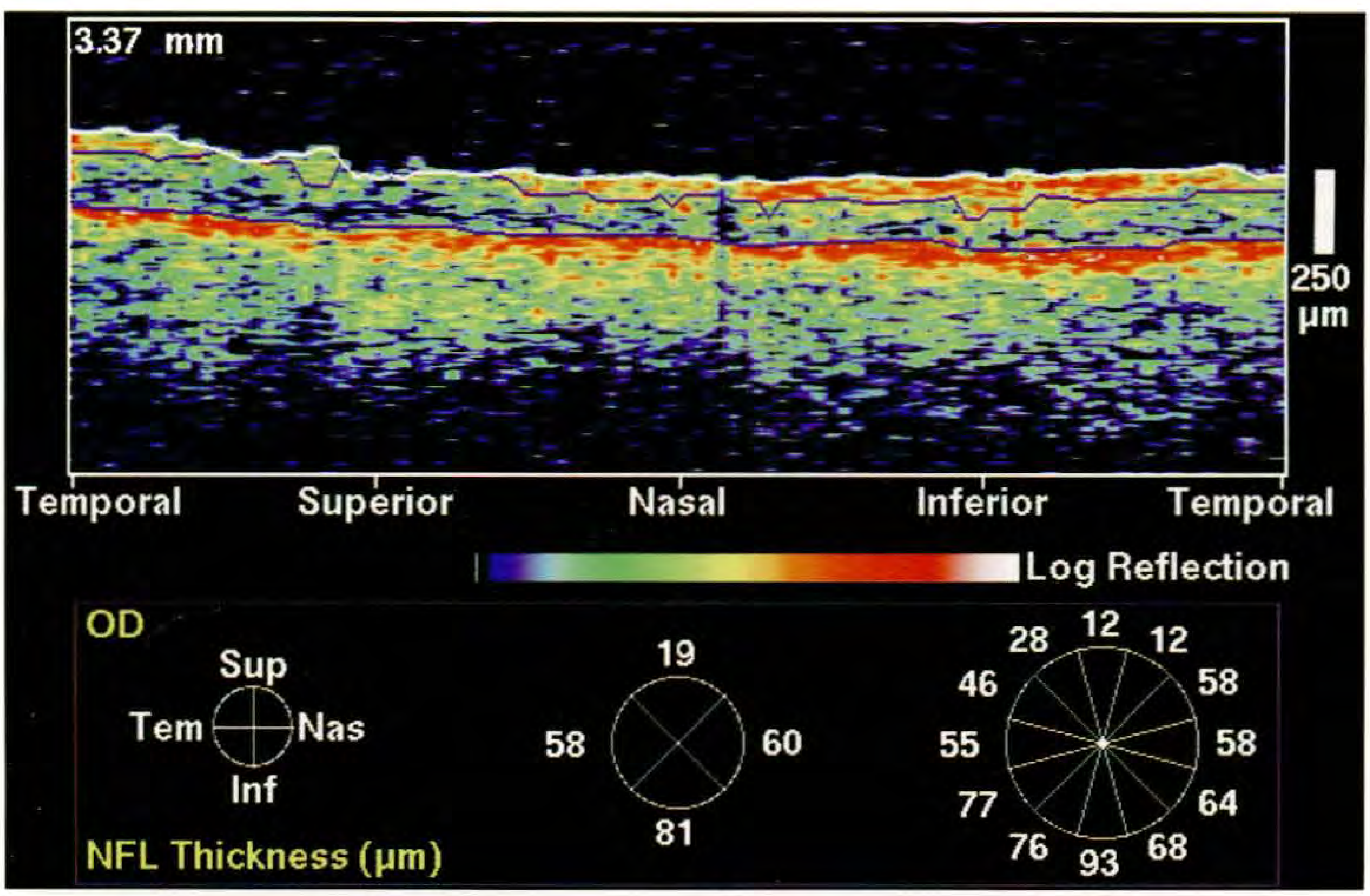
3.37 mm
250 µm
Temporal
Superior
Nasal
Inferior
Temporal
Log Reflection
OD
Sup
Tem
Nas
Inf
NFL Thickness (µm)
19
58
60
81
12
12
28
58
46
58
55
64
77
68
76
93

E

F

G

Case 12-20 continued

Clinical Summary

The patient's left eye had an intraocular pressure of 16 mm Hg and a visual acuity of 20/30. Gonioscopy revealed that the angle was open to the ciliary body band with a narrowed inlet. 2+ nuclear sclerosis of the crystalline lens was also observed. Dilated fundus examination (F,G) showed moderate to marked optic disc cupping and a severely attenuated temporal neuroretinal rim. The Humphrey visual field (I) again displayed loss of peripheral vision with only a central island of vision remaining.

Optical Coherence Tomography

The 3.4 mm diameter OCT image (J) revealed diffuse, severe loss of the nerve fiber layer thickness throughout the image. The thinning was somewhat less marked inferotemporally at 5:00. Note that the thinning was more severe in the right than the left eye, consistent with degree of visual field loss.

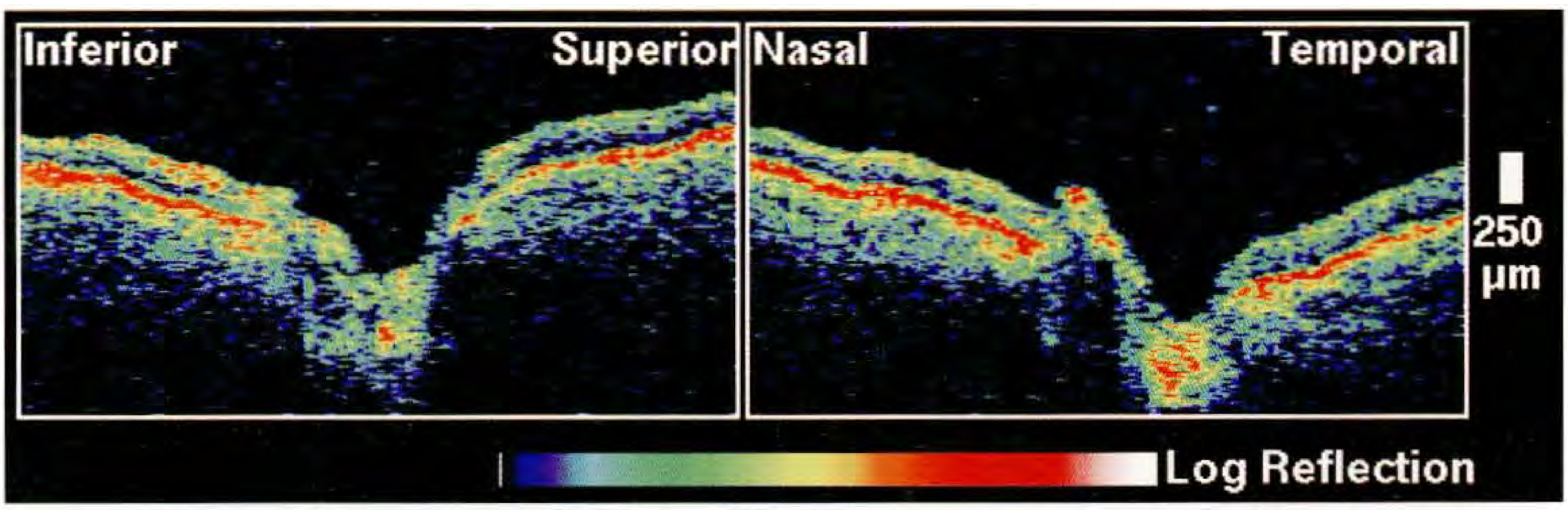

H

VERTICAL		HORIZONTAL	
Cup Diameter	0.74 mm	Cup Diameter	0.63 mm
Disc Diameter	1.14 mm	Disc Diameter	0.96 mm
C/D Ratio	0.65	C/D Ratio	0.66
NR Rim Area	0.59 mm^2		
Inferior NFL	40 µm	Nasal NFL	40 µm
Superior NFL	50 µm	Temporal NFL	20 µm

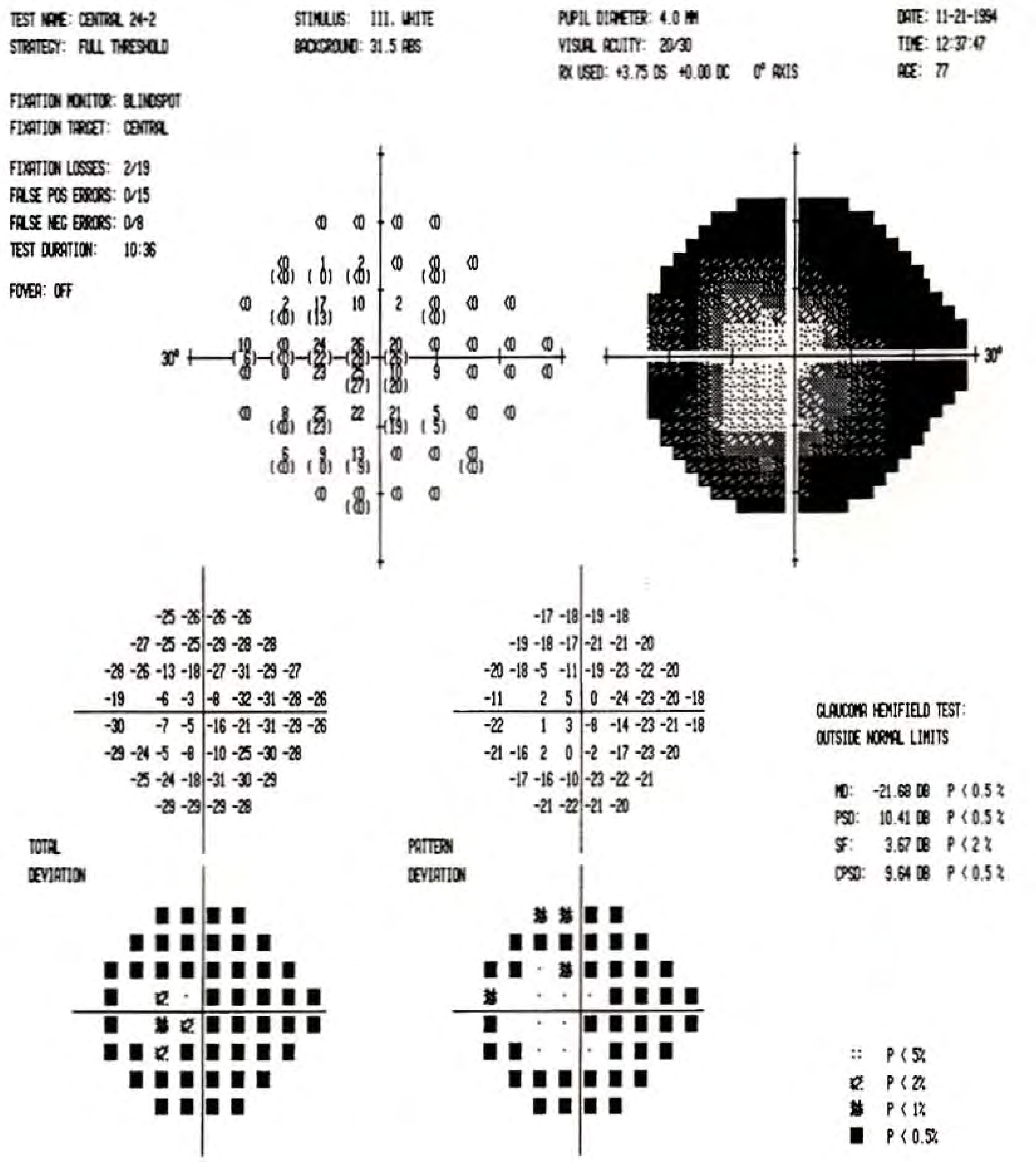

TEST NAME: CENTRAL 24-2
STRATEGY: FULL THRESHOLD
STIMULUS: III, WHITE
BACKGROUND: 31.5 ABS
PUPIL DIAMETER: 4.0 MM
VISUAL ACUITY: 20/30
RX USED: +3.75 DS +0.00 DC 0° AXIS
DATE: 11-21-1994
TIME: 12:37:47
AGE: 77
FIXATION MONITOR: BLINDSPOT
FIXATION TARGET: CENTRAL
FIXATION LOSSES: 2/19
FALSE POS ERRORS: 0/15
FALSE NEG ERRORS: 0/8
TEST DURATION: 10:36
FOVEA: OFF
30°
30°
TOTAL DEVIATION
PATTERN DEVIATION
GLAUCOMA HEMIFIELD TEST: OUTSIDE NORMAL LIMITS
MD: -21.68 DB P < 0.5 %
PSD: 10.41 DB P < 0.5 %
SF: 3.67 DB P < 2 %
CPSD: 9.64 DB P < 0.5 %
P < 5%
P < 2%
P < 1%
P < 0.5%

I

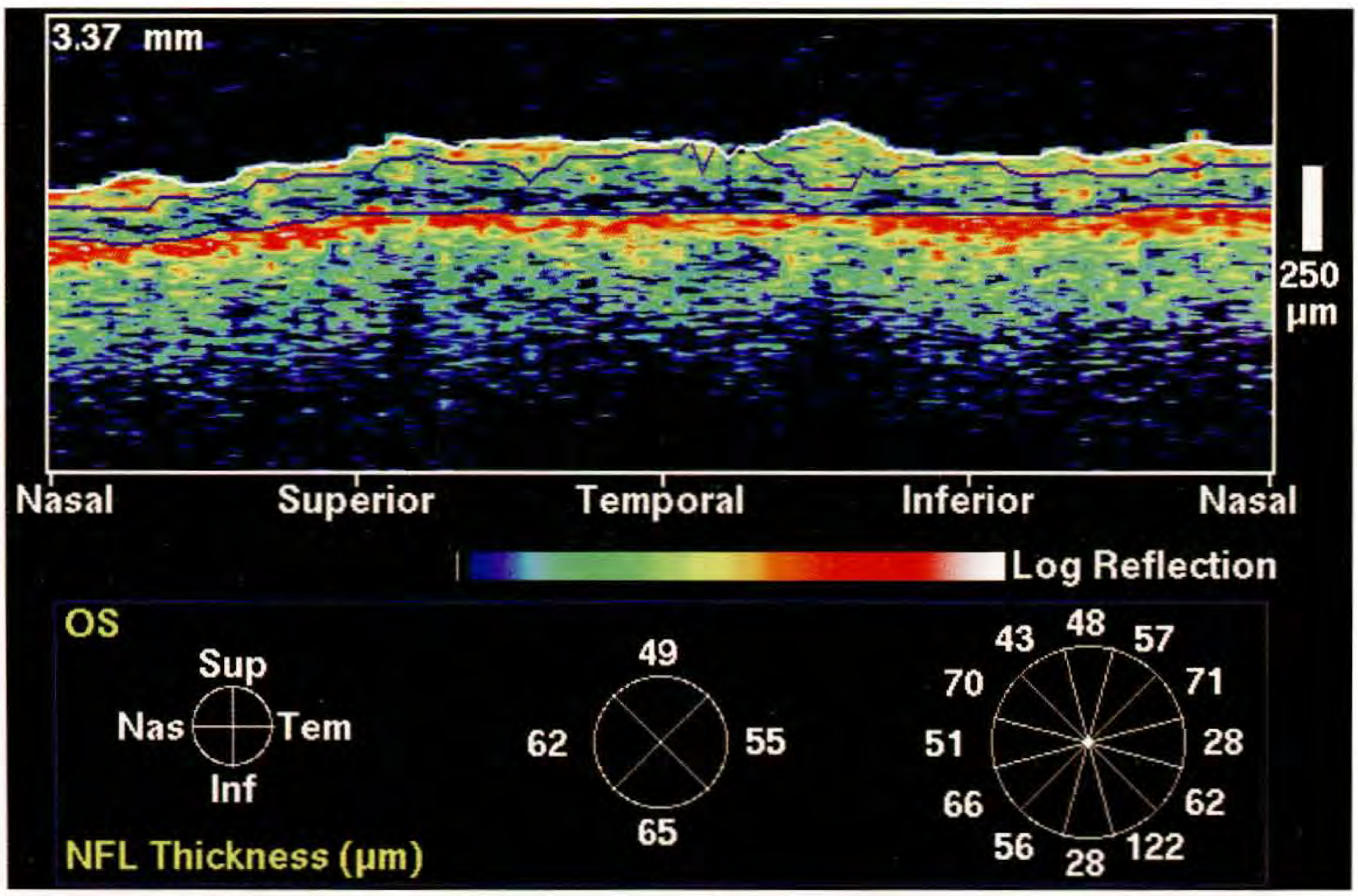

3.37 mm
250 µm
Nasal
Superior
Temporal
Inferior
Nasal
Log Reflection
OS
Sup
Nas
Tem
Inf
NFL Thickness (µm)
49
62
55
65
43
48
57
70
71
51
28
66
62
56
28
122

J

A

Case 12-21. End-Stage Glaucoma

Clinical Summary

A 40-year-old Haitian man was taking pilocarpine 6% four times a day for primary open-angle glaucoma, until four days prior to examination, when he ran out of medication. He had previously undergone laser trabeculoplasty in his right eye. On examination of this eye, the visual acuity was 20/20 and the intraocular pressure was 27 mm Hg. Gonioscopy revealed that the angle was open to the scleral spur, except inferiorly, where it was open to the ciliary body band. Dilated ophthalmoscopy (A) showed a deep, excavated cup with an absence of neuroretinal rim. A Humphrey visual field (C) displayed only a small remaining central island of vision.

Optical Coherence Tomography

Minimal nerve fiber tissue was observed on a 3.4 mm diameter circular OCT tomogram (D) around the optic disc. The dramatic attenuation of the nerve fiber layer was consistent with this patient's degree of cupping and visual field loss.

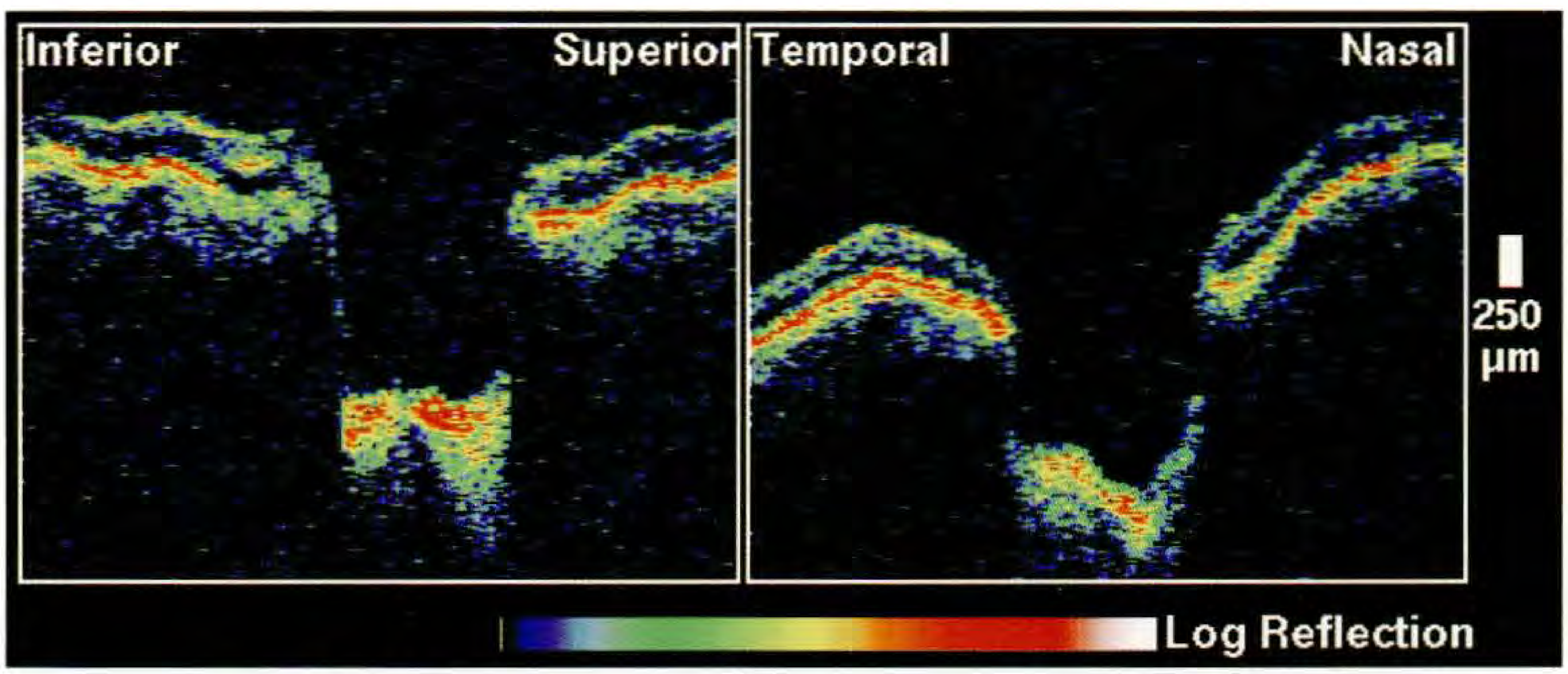

B

VERTICAL		*HORIZONTAL*	
Cup Diameter	**1.64 mm**	**Cup Diameter**	**1.70 mm**
Disc Diameter	**1.74 mm**	**Disc Diameter**	**1.76 mm**
C/D Ratio	**0.94**	**C/D Ratio**	**0.97**
NR Rim Area	**0.27 mm^2**		
Inferior NFL	**30 μm**	**Temporal NFL**	**0 μm**
Superior NFL	**50 μm**	**Nasal NFL**	**20 μm**

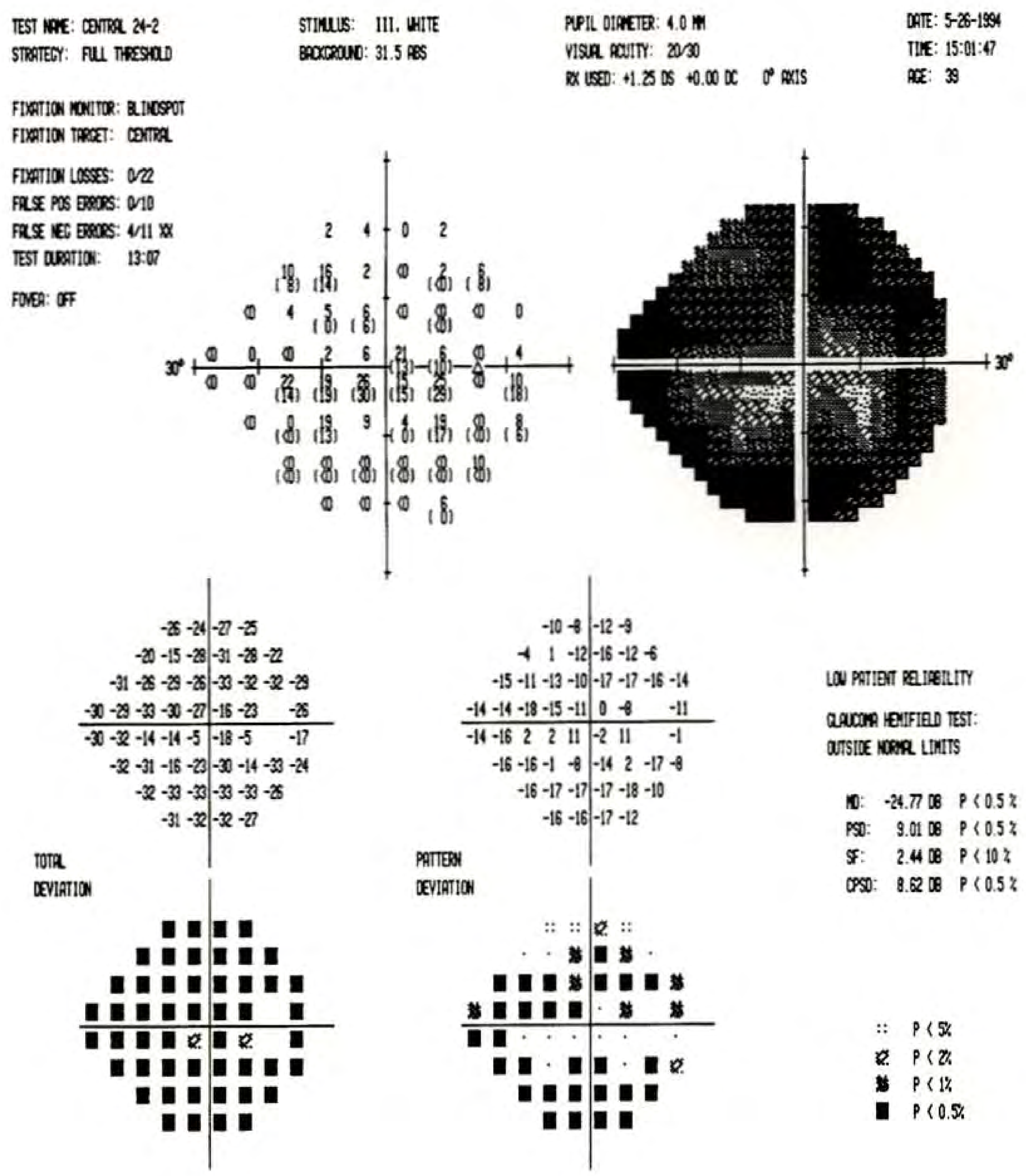
TEST NAME: CENTRAL 24-2
STRATEGY: FULL THRESHOLD
STIMULUS: III, WHITE
BACKGROUND: 31.5 ABS
PUPIL DIAMETER: 4.0 MM
VISUAL ACUITY: 20/30
RX USED: +1.25 DS +0.00 DC 0° AXIS
DATE: 5-26-1994
TIME: 15:01:47
AGE: 39
FIXATION MONITOR: BLINDSPOT
FIXATION TARGET: CENTRAL
FIXATION LOSSES: 0/22
FALSE POS ERRORS: 0/10
FALSE NEG ERRORS: 4/11 XX
TEST DURATION: 13:07
FOVEA: OFF
30°
30°
TOTAL
DEVIATION
PATTERN
DEVIATION
LOW PATIENT RELIABILITY
GLAUCOMA HEMIFIELD TEST:
OUTSIDE NORMAL LIMITS
MD: -24.77 DB P < 0.5 %
PSD: 9.01 DB P < 0.5 %
SF: 2.44 DB P < 10 %
CPSD: 8.62 DB P < 0.5 %
P < 5%
P < 2%
P < 1%
P < 0.5%

C

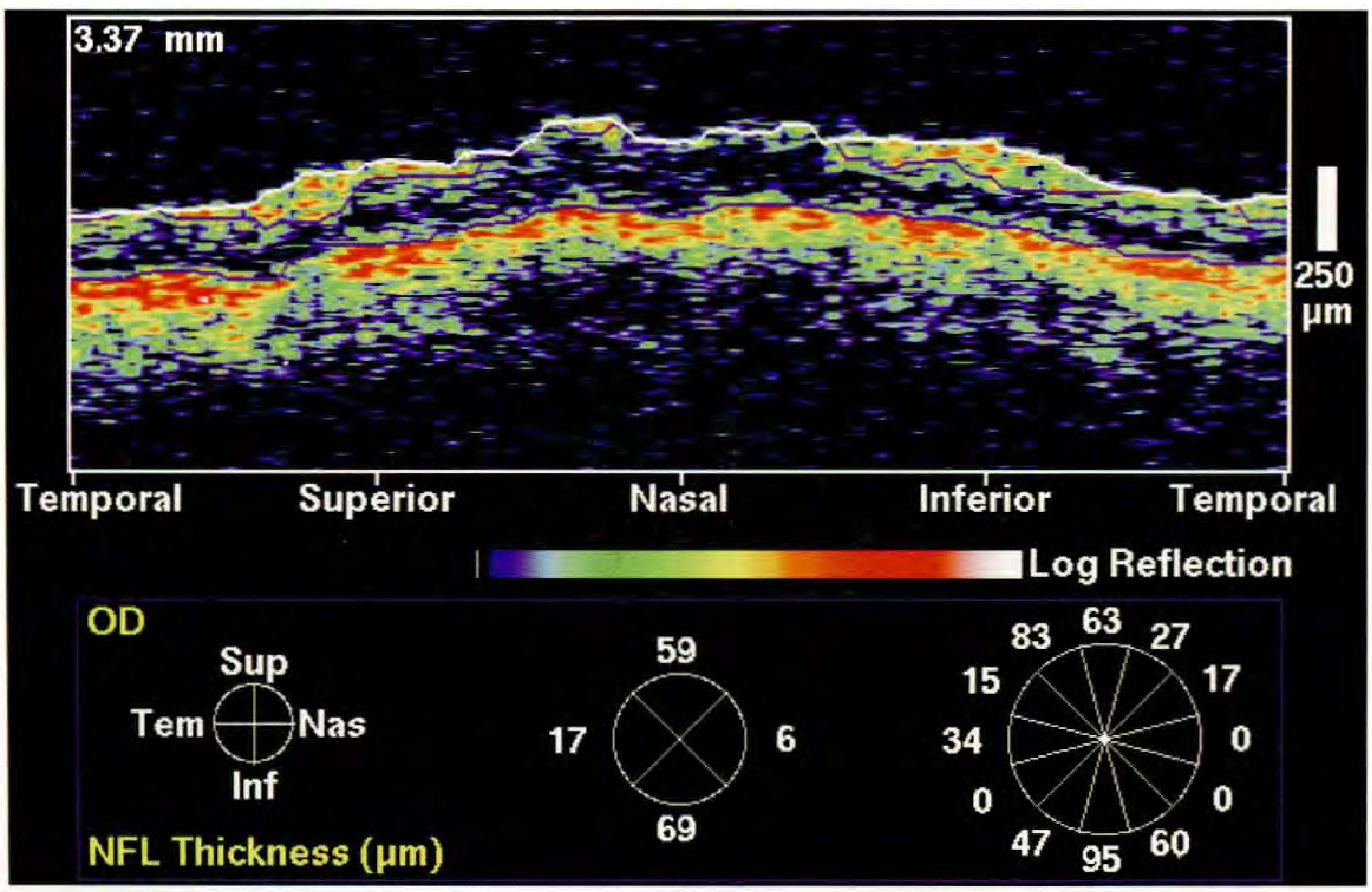
3.37 mm
250 µm
Temporal
Superior
Nasal
Inferior
Temporal
Log Reflection
OD
Sup
Tem
Nas
Inf
NFL Thickness (µm)
59
17
6
69
83
63
27
15
17
34
0
0
0
47
95
60

D

A

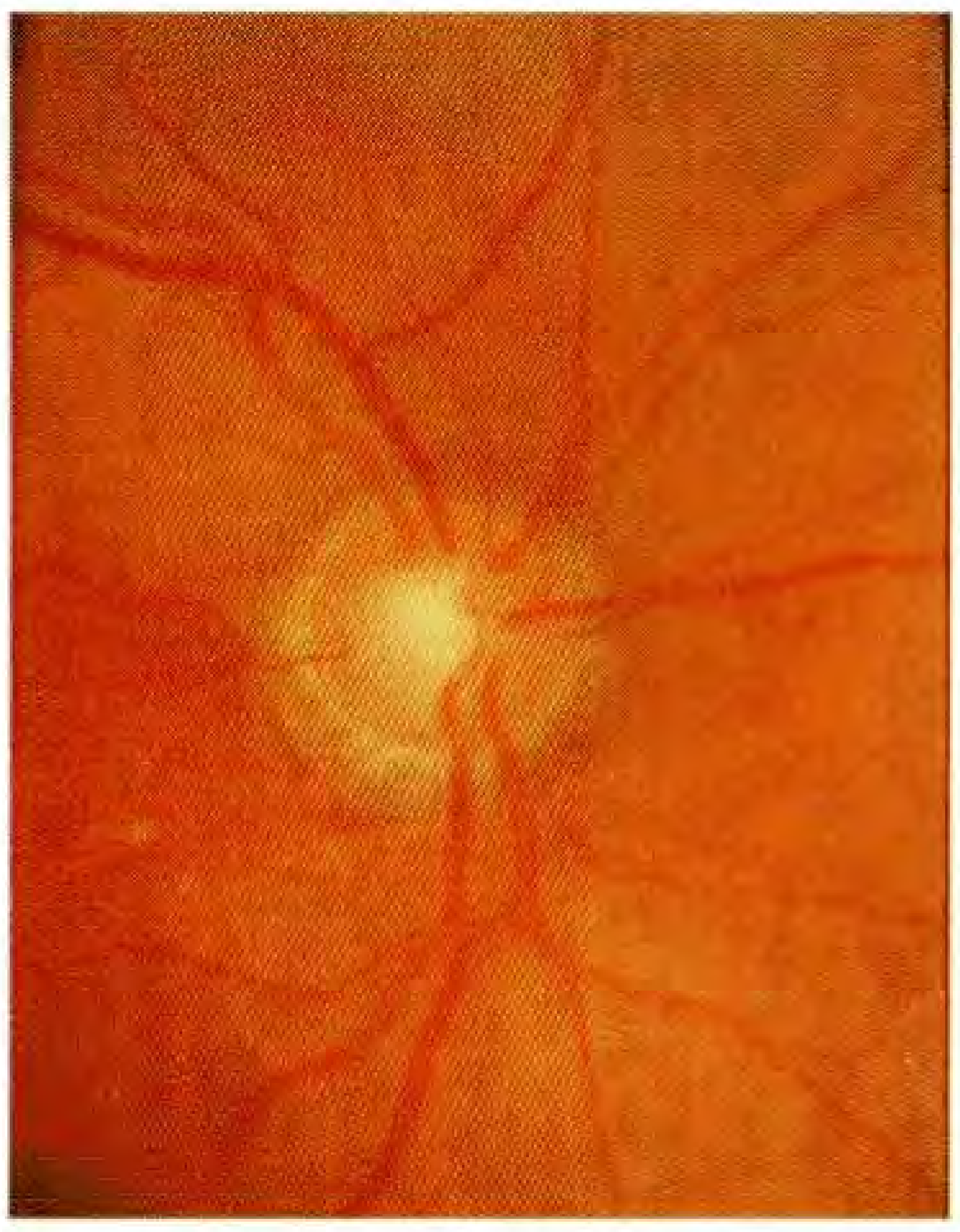

B

Case 12-22. Glaucomatous Progression

Clinical Summary

A 74-year-old man with primary open angle glaucoma was using timolol 0.5% twice daily. Visual acuity was 20/20 bilaterally, and intraocular pressures were 24 mm Hg in each eye. Slit-lamp examination was unremarkable, and both angles were open 360° to the ciliary body band. There was moderate cupping of the optic discs in both eyes with intact neuroretinal rims, both of which were slightly thinned inferotemporally (A,F). Humphrey visual fields showed early superior nasal steps, worse on the left (H) than the right (C).

One year later, there was an increase in the size of the visual field defect bilaterally (H,C), with a minimal increase in cupping (B,G).

(continued)

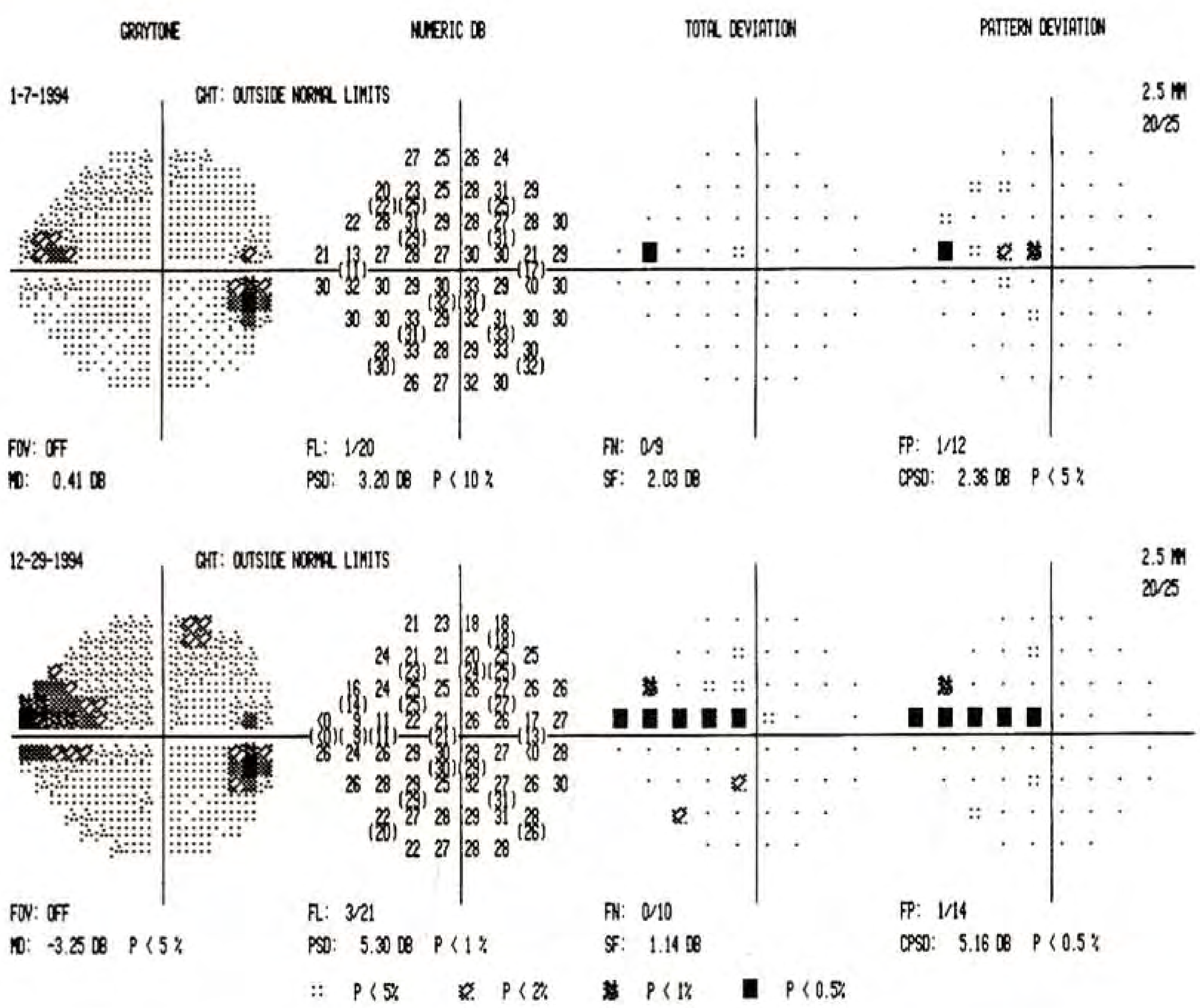

C

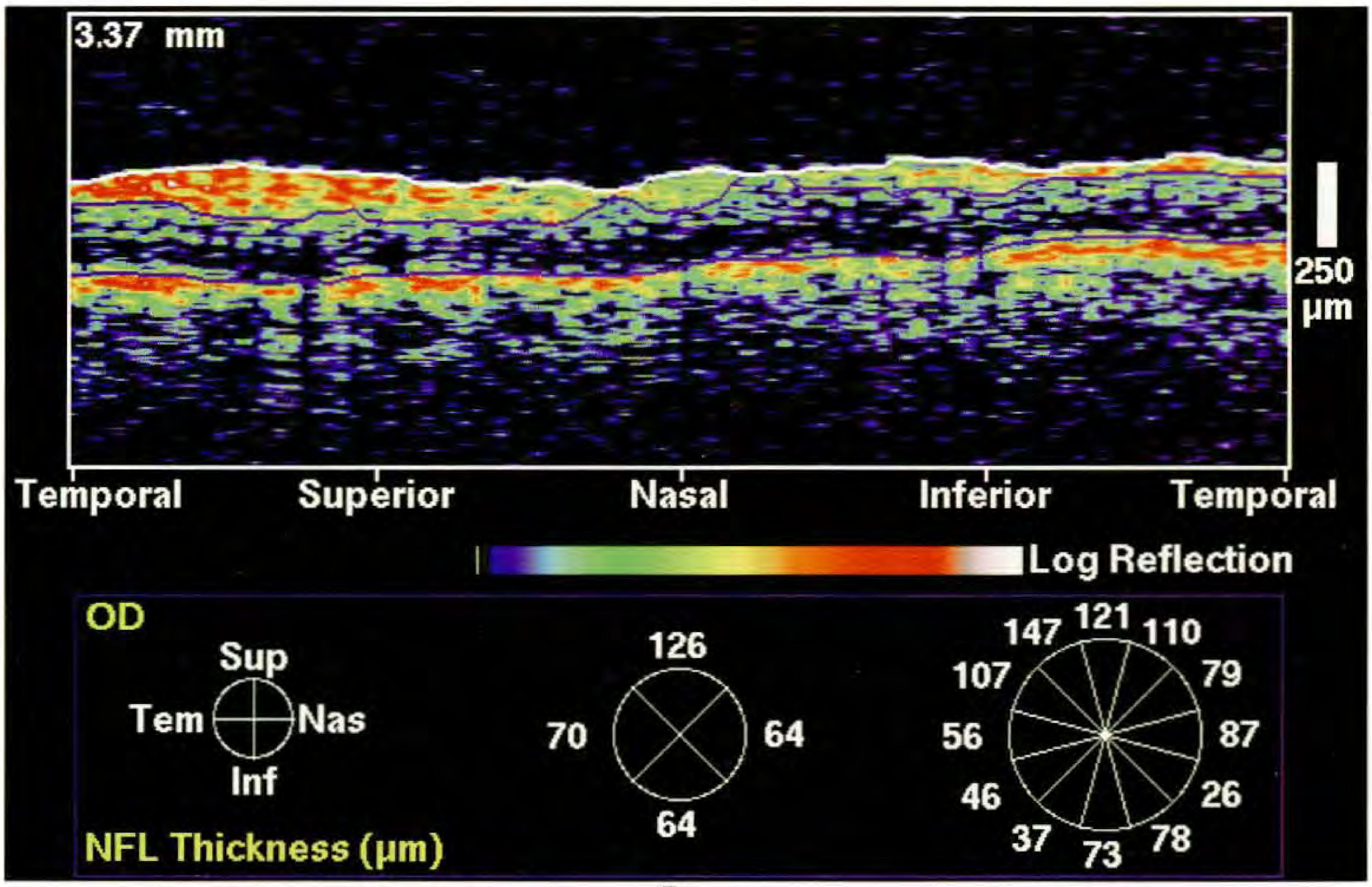
3.37 mm
250 µm
Temporal
Superior
Nasal
Inferior
Temporal
Log Reflection
OD
Sup
Tem
Nas
Inf
NFL Thickness (µm)
126
70
64
64
147
121
110
107
79
56
87
46
26
37
73
78

D

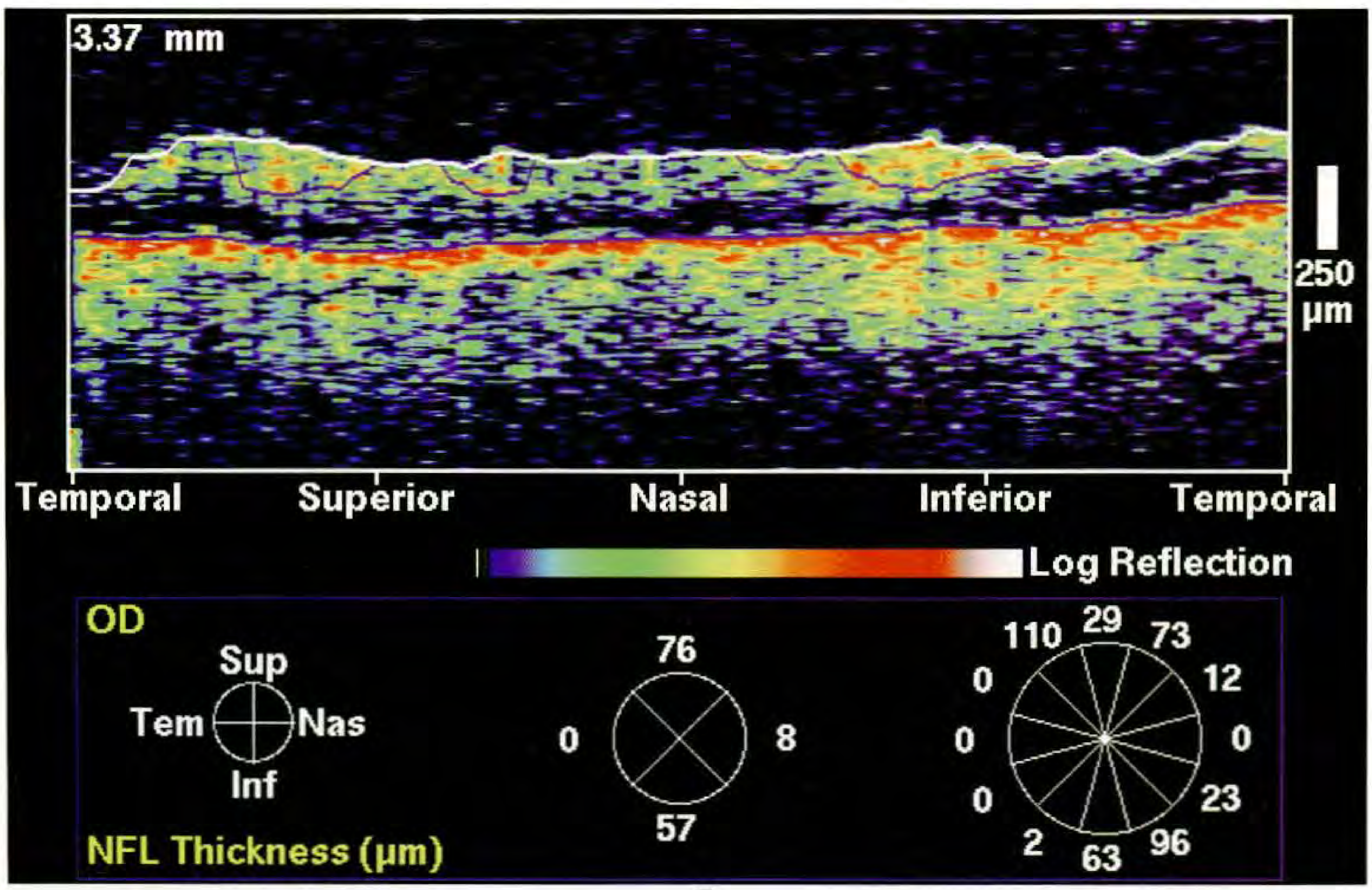
3.37 mm
250 µm
Temporal
Superior
Nasal
Inferior
Temporal
Log Reflection
OD
Sup
Tem
Nas
Inf
NFL Thickness (µm)
76
0
8
57
110
29
73
0
12
0
0
0
23
2
63
96

E

F

G

Case 12-22 continued

Optical Coherence Tomography

Circular OCT images were acquired on the initial visit at a diameter of 3.4 mm around the optic disc of both eyes (D,I). Both tomograms demonstrated thinning of the nerve fiber layer, particularly inferiorly, consistent with the visual field defect.

On follow-up OCT examination one year later, there was evidence of a global decrease in nerve fiber layer thickness in both eyes (E,J). The thinnest region bilaterally was inferotemporally, again corresponding to the visual field change. Of interest was the presence on OCT of nerve fiber layer attenuation, not only in the area of the visual field change, but throughout the tomograms, indicating that the progressive, glaucomatous process affected the entire nerve fiber layer while presenting only as a localized visual field change. These results demonstrate the ability of OCT to document changes in nerve fiber layer thickness associated with glaucomatous progression.

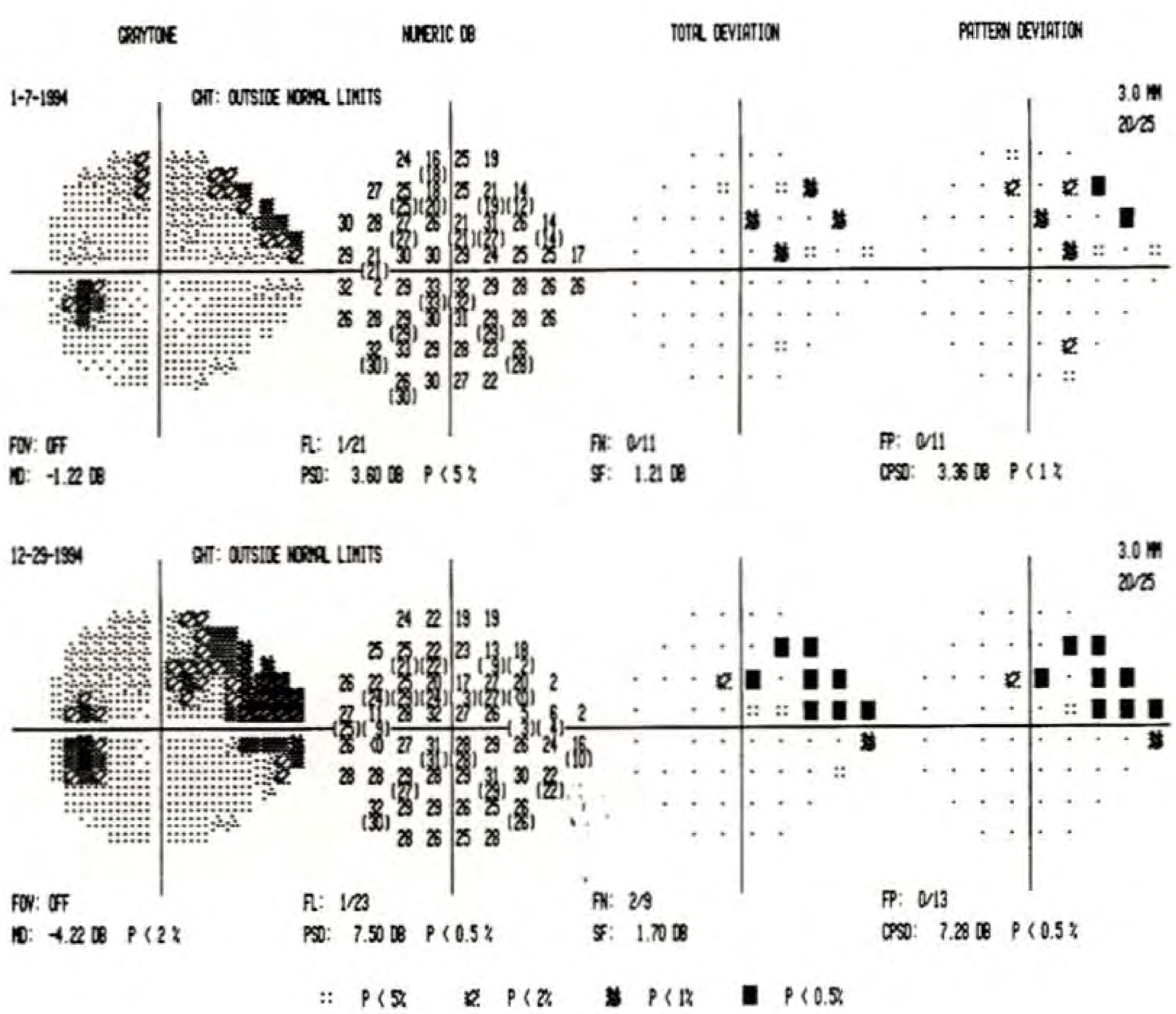

H

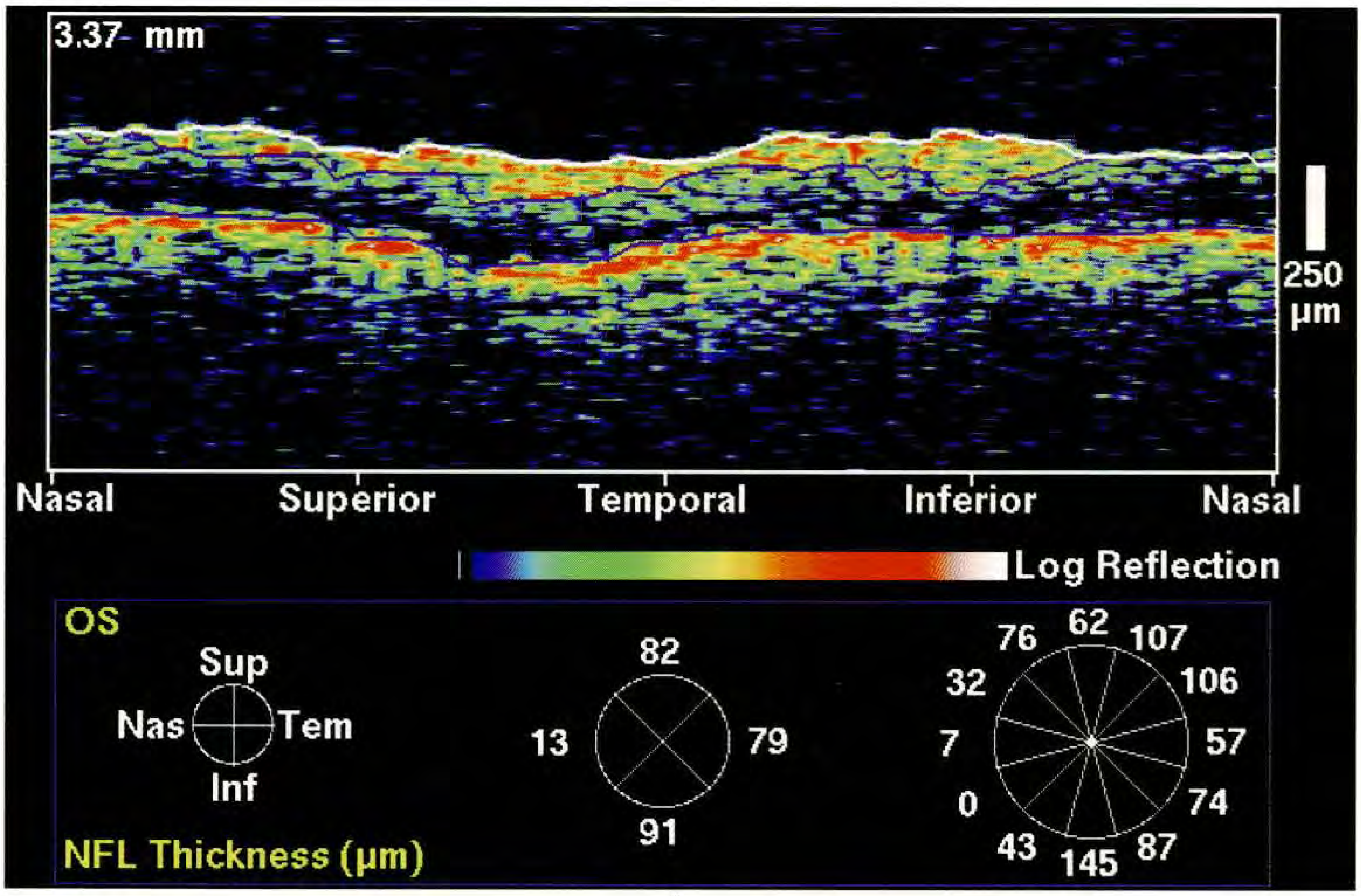

3.37 mm
250 µm
Nasal
Superior
Temporal
Inferior
Nasal
Log Reflection
OS
Sup
Nas
Tem
Inf
NFL Thickness (µm)
82
13
79
91
62
76
107
32
106
7
57
0
74
43
145
87

I

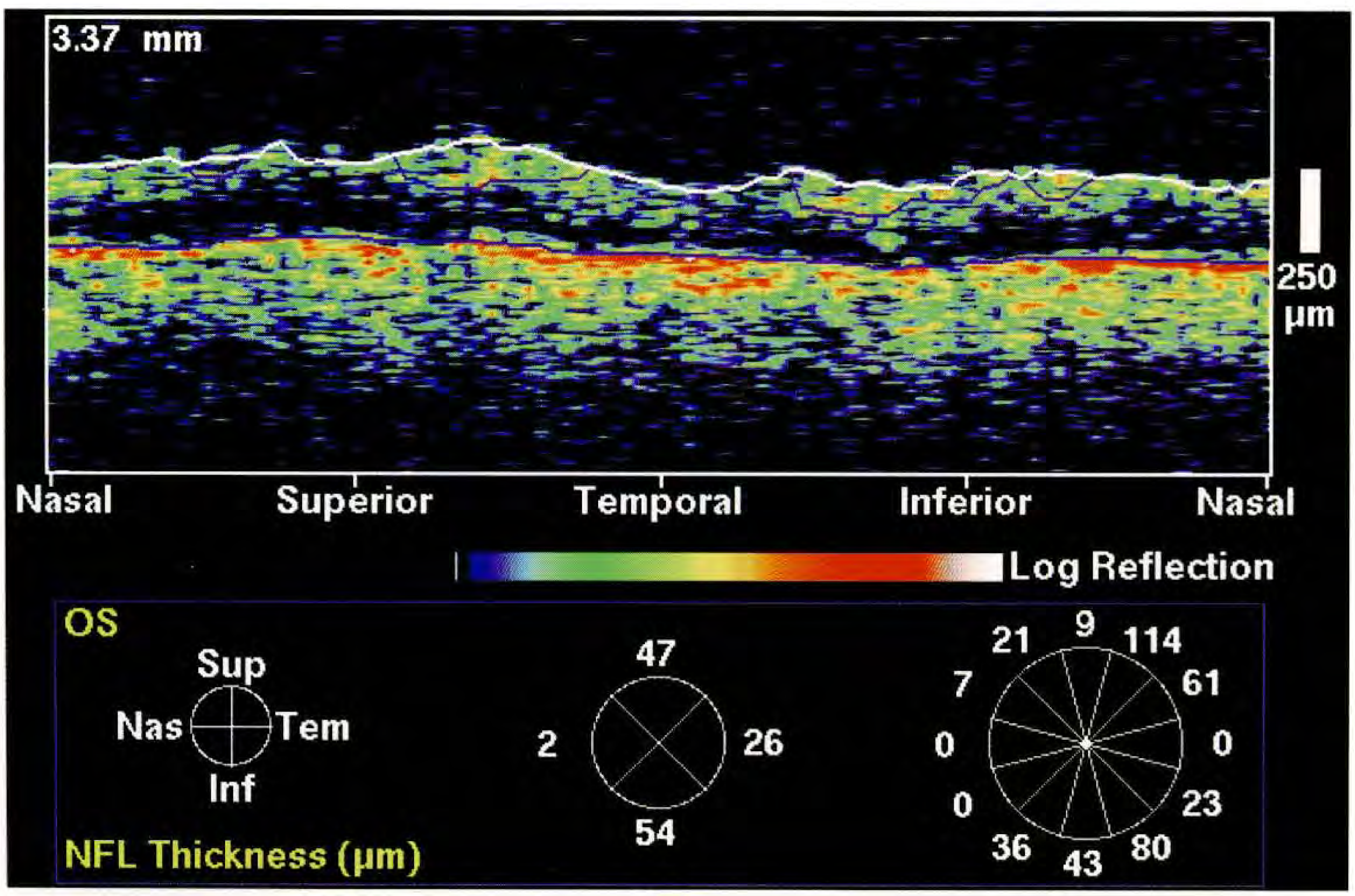

3.37 mm
250 µm
Nasal
Superior
Temporal
Inferior
Nasal
Log Reflection
OS
Sup
Nas
Tem
Inf
NFL Thickness (µm)
47
2
26
54
9
21
114
7
61
0
0
0
23
36
43
80

J

CHAPTER 13

Focal Defects in the Nerve Fiber Layer

Glaucoma may often cause focal regions of retinal nerve fiber layer (NFL) loss [1]. These areas of NFL thinning can be difficult to detect by the traditional methods of ophthalmoscopy, stereoscopic biomicroscopy and optic nerve head photography, or evaluation of the red free NFL reflex [2]. The ability of OCT to profile the NFL in cross-section with high resolution is useful in the identification of focal or diffuse areas of NFL thinning. A circular OCT tomogram acquired around the optic disc provides information on NFL thickness in a cylindrical cross-section surrounding the nerve head. The normal variations in NFL thickness are readily apparent in such a section, and focal or diffuse NFL thinning may be identified by visual inspection. Alternatively, an automated computer image processing algorithm may be used to quantitatively measure the retinal and NFL thickness from the circular tomograms, providing an objective assessment of the size and severity of the NFL loss [3].

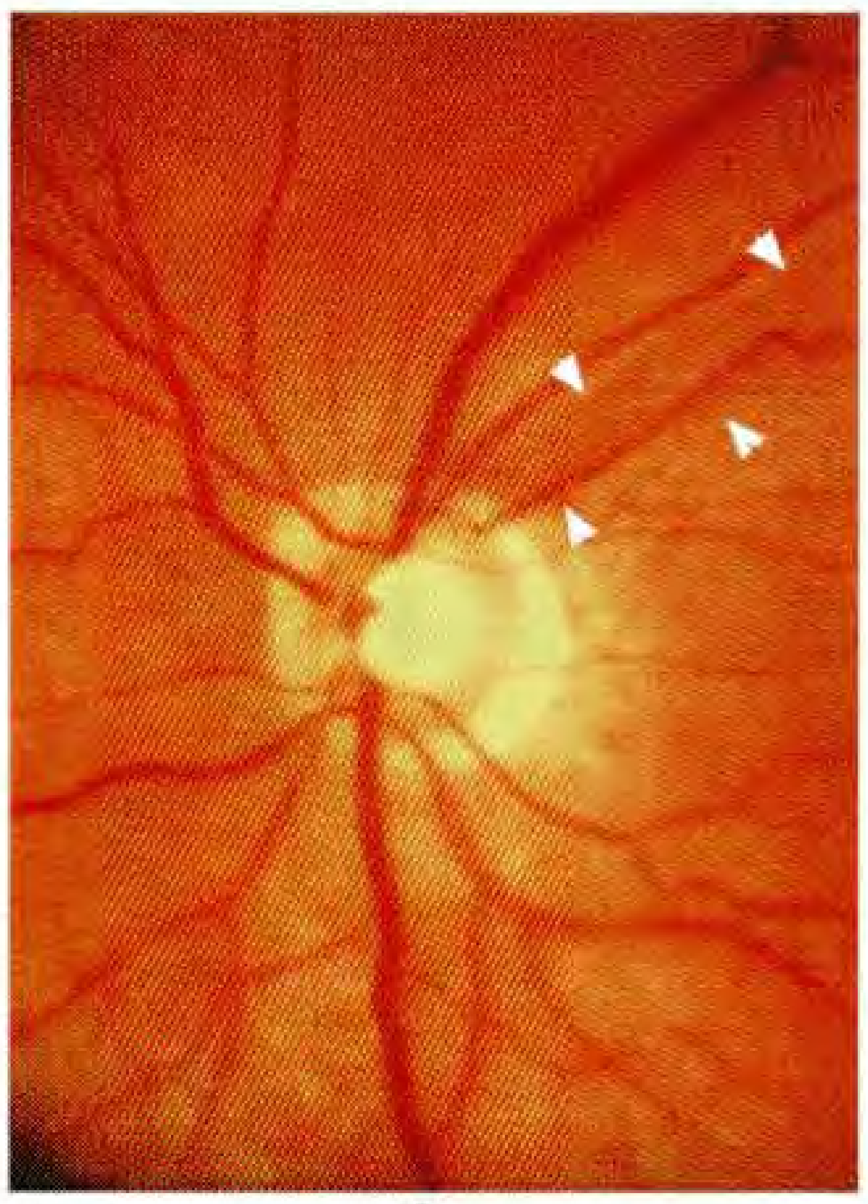

A

B

Case 13-1. Focal Nerve Fiber Layer Defect

Clinical Summary

A 71-year-old white man had primary open angle glaucoma and a focal nerve fiber layer defect in the left eye. Visual acuity in this eye was 20/20 and the intraocular pressure was 14 mm Hg. The pressure had decreased from 19 mm Hg measured one month earlier when the patient began using levobunolol 0.25% twice daily. Slit-lamp examination and gonioscopy revealed a normal anterior chamber and angle. Dilated fundus examination showed a narrow focal defect in the superotemporal nerve fiber layer (A, B; arrows) and a thinning of the neuroretinal rim temporally. A distinct inferonasal step was noted on the Humphrey visual field (D) corresponding to the nerve fiber layer defect observed ophthalmoscopically.

Optical Coherence Tomography

A circular OCT tomogram (E) taken at a diameter of 3.4 mm around the optic disc revealed a generally healthy nerve fiber layer with the exception of a focal area of thinning in the superotemporal nerve fiber layer (arrows), consistent with the defect observed clinically. The thinning was primarily evident at the superficial margin of the nerve fiber layer, and reached a minimum thickness of 90 µm in the image.

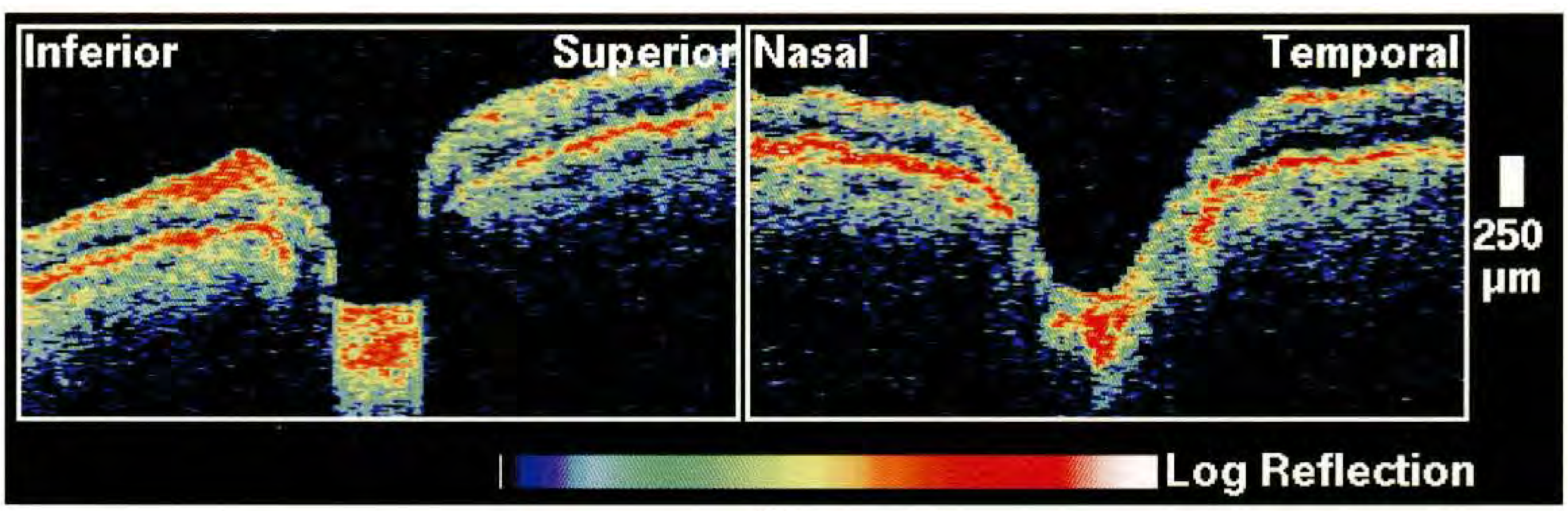

C

VERTICAL		*HORIZONTAL*	
Cup Diameter	1.22 mm	Cup Diameter	1.52 mm
Disc Diameter	1.77 mm	Disc Diameter	1.94 mm
C/D Ratio	0.69	C/D Ratio	0.78
NR Rim Area	1.29 mm^2		
Inferior NFL	210 µm	Nasal NFL	190 µm
Superior NFL	190 µm	Temporal NFL	160 µm

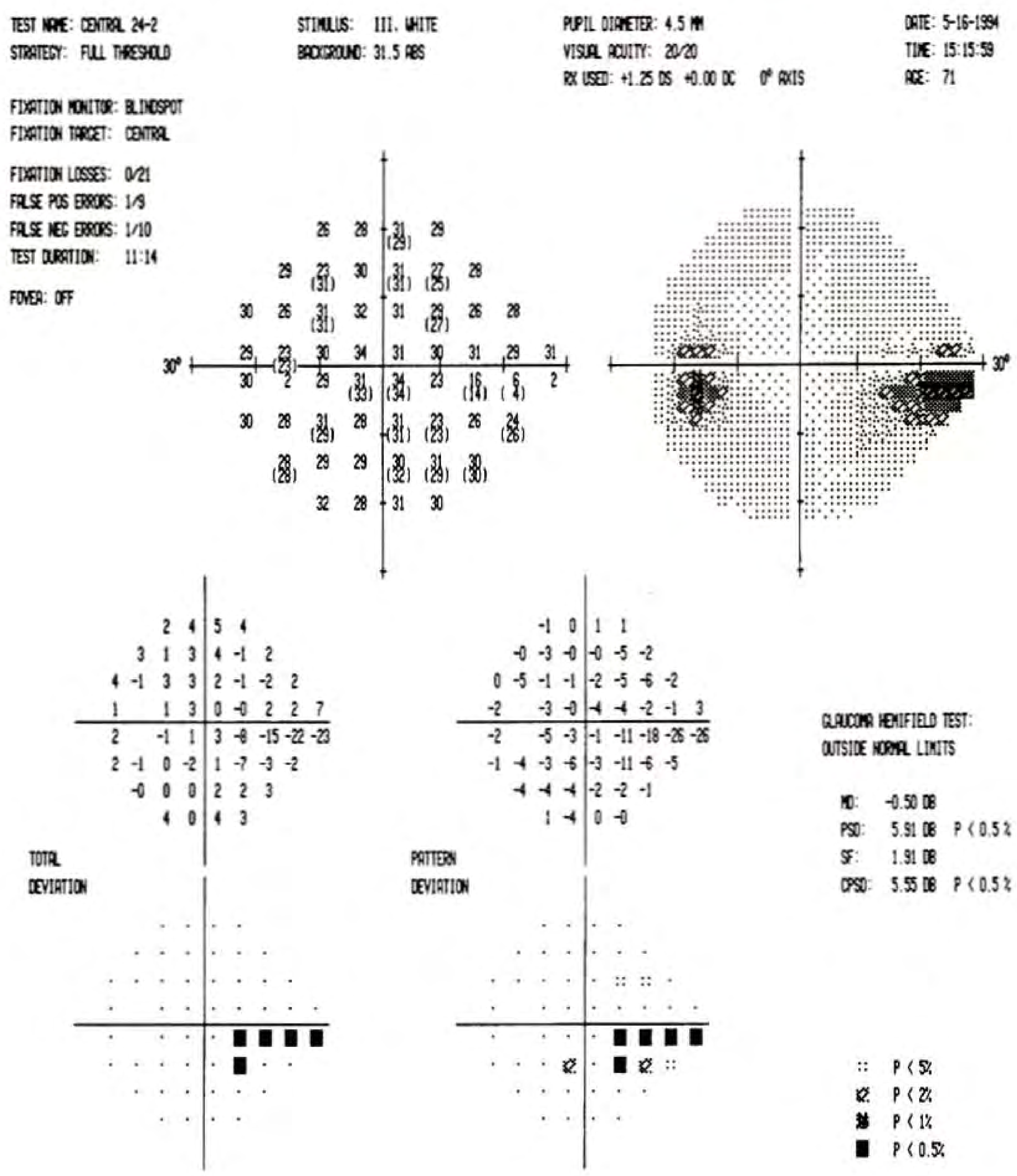
TEST NAME: CENTRAL 24-2
STRATEGY: FULL THRESHOLD
STIMULUS: III, WHITE
BACKGROUND: 31.5 ABS
PUPIL DIAMETER: 4.5 MM
VISUAL ACUITY: 20/20
RX USED: +1.25 DS +0.00 DC 0° AXIS
DATE: 5-16-1994
TIME: 15:15:59
AGE: 71
FIXATION MONITOR: BLINDSPOT
FIXATION TARGET: CENTRAL
FIXATION LOSSES: 0/21
FALSE POS ERRORS: 1/9
FALSE NEG ERRORS: 1/10
TEST DURATION: 11:14
FOVEA: OFF
30°
TOTAL DEVIATION
PATTERN DEVIATION
GLAUCOMA HEMIFIELD TEST:
OUTSIDE NORMAL LIMITS
MD: -0.50 DB
PSD: 5.91 DB P < 0.5%
SF: 1.91 DB
CPSD: 5.55 DB P < 0.5%
P < 5%
P < 2%
P < 1%
P < 0.5%

D

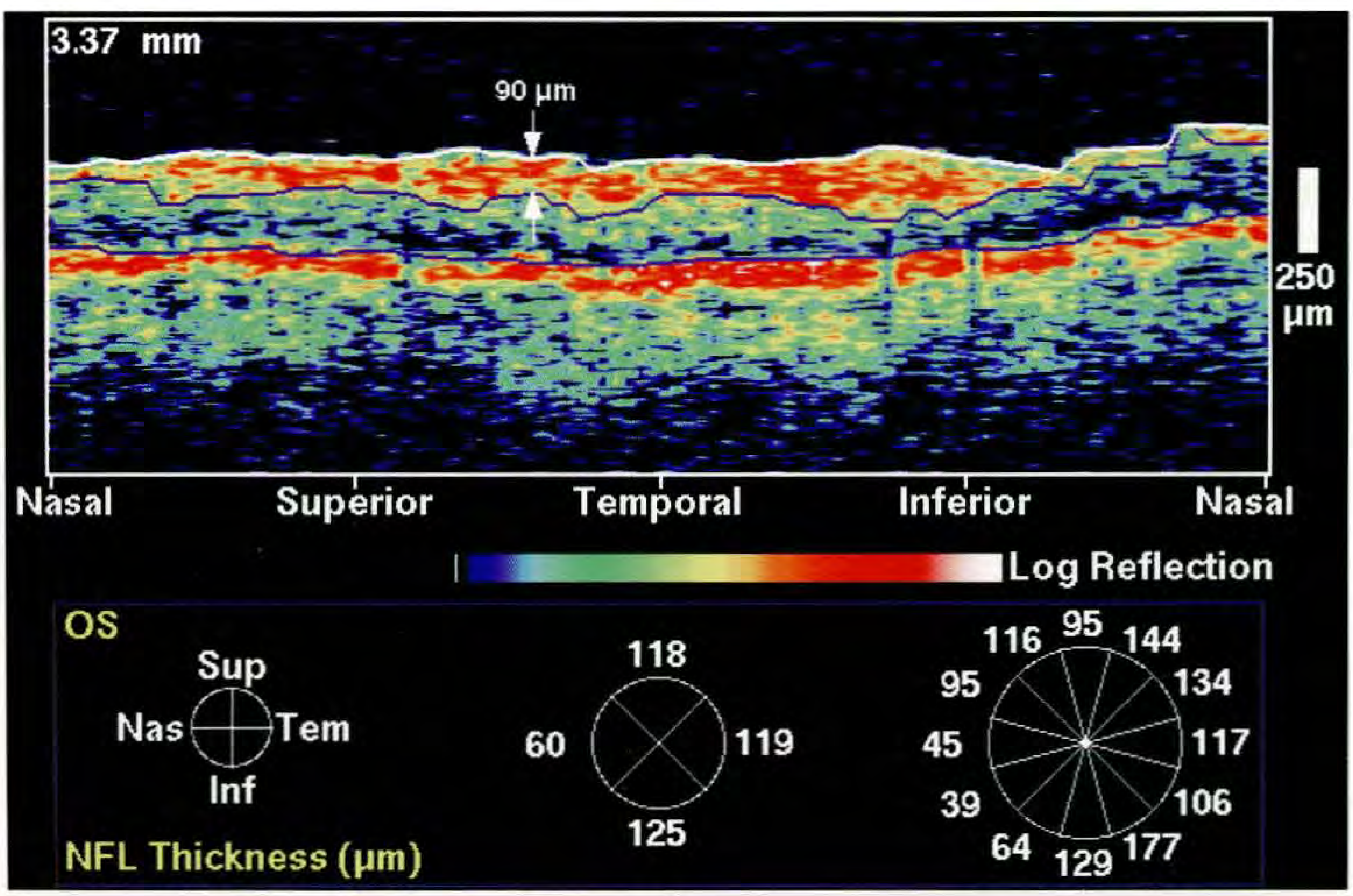
3.37 mm
90 µm
250 µm
Nasal
Superior
Temporal
Inferior
Nasal
Log Reflection
OS
Sup
Nas
Tem
Inf
NFL Thickness (µm)
118
60
119
125
116
95
144
95
134
45
117
39
106
64
129
177

E

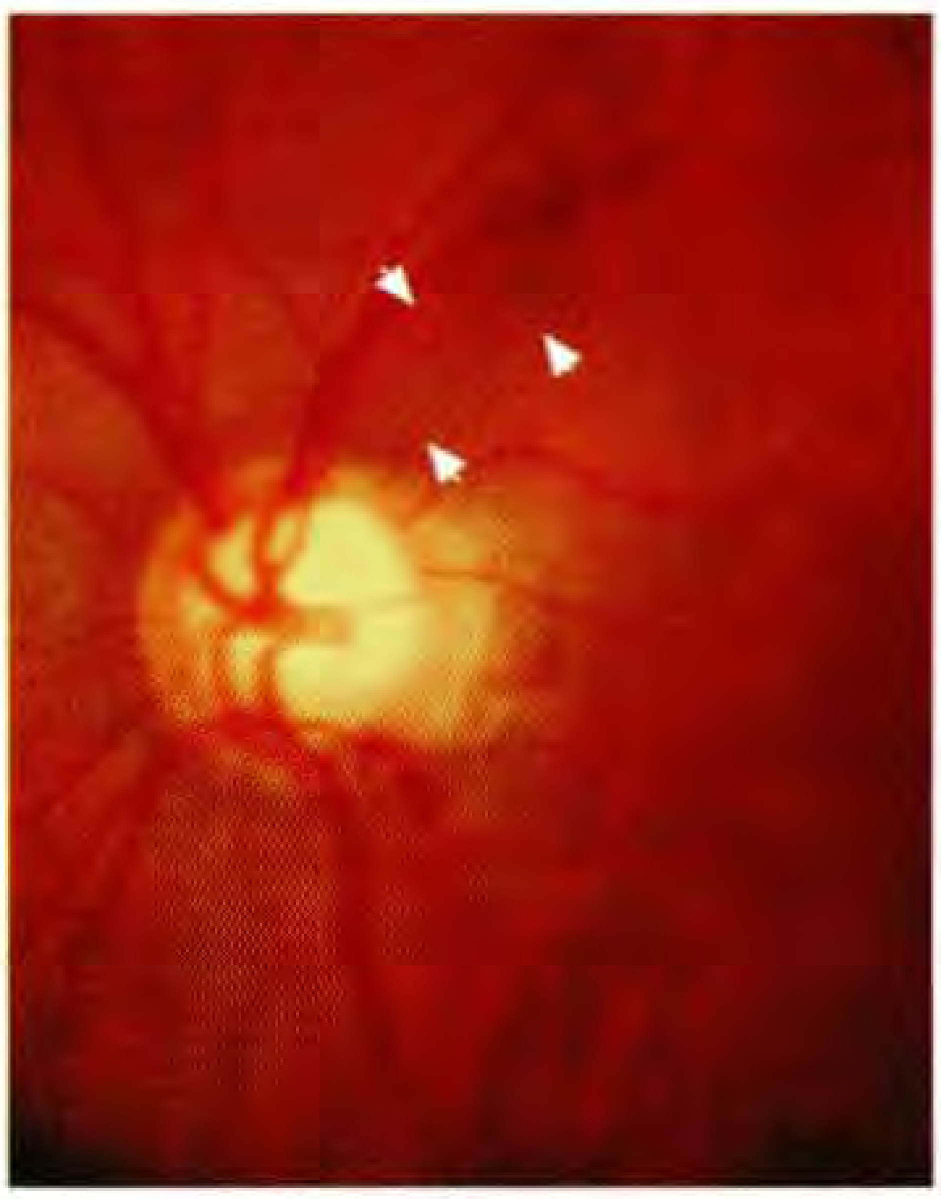

A

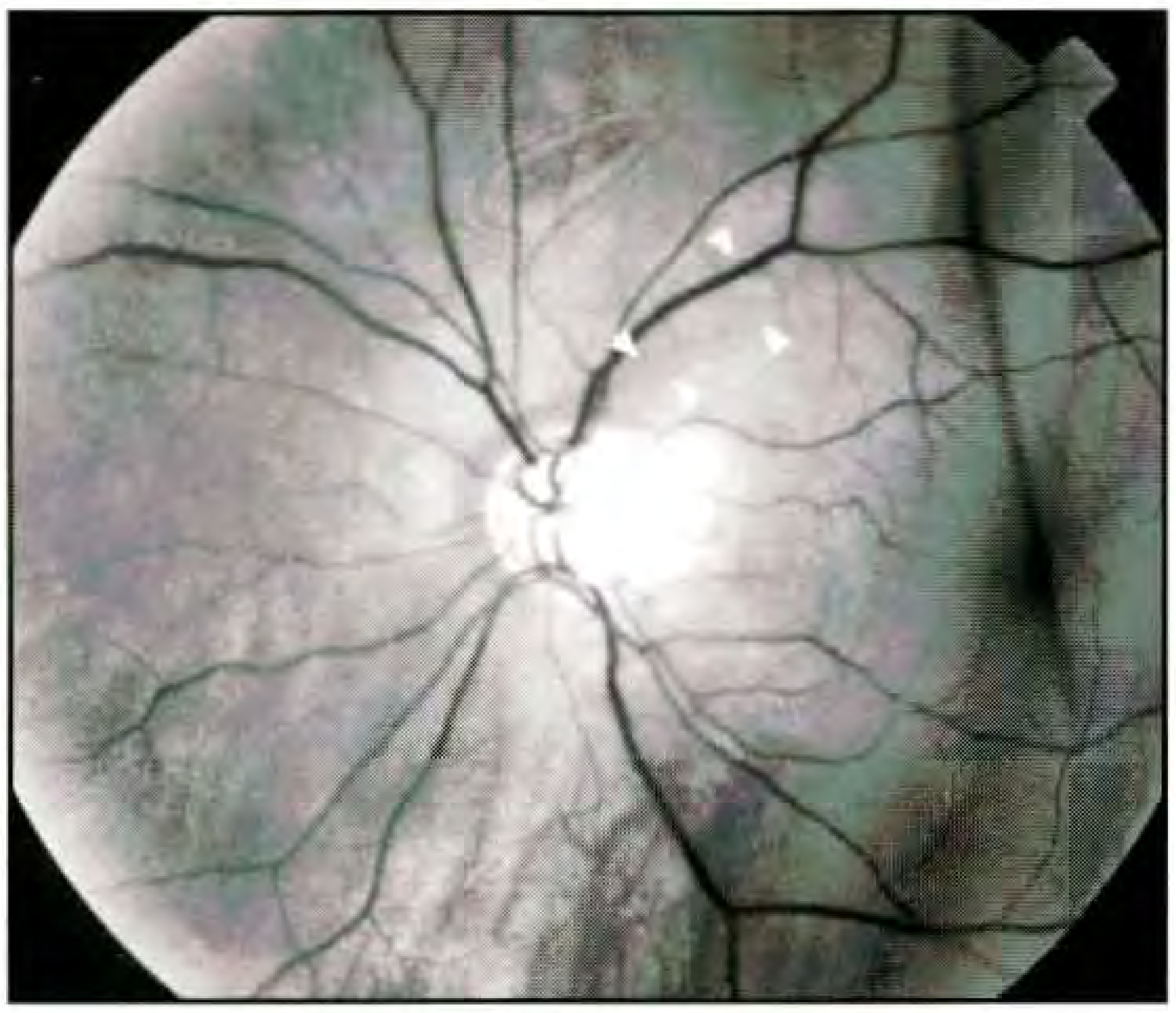

B

Case 13-2. Focal Nerve Fiber Layer Defect

Clinical Summary

A 72-year-old woman with normal tension glaucoma had undergone laser trabeculoplasty four months earlier in her left eye and was taking timolol 0.5% twice daily. The intraocular pressure in this eye was 13 mm Hg and the visual acuity was 20/25. Slit-lamp examination showed an open angle throughout 360°. Ophthalmoscopy (A) revealed a moderately cupped disc with an attenuated neuroretinal rim temporally. The nerve fiber layer reflex (B) displayed a focal reduction in the superotemporal area. A Humphrey visual field (D) revealed an inferior arcuate scotoma consistent with the nerve fiber layer defect and an early superior nasal step as well.

Optical Coherence Tomography

A 3.4 mm diameter circular scan (E) around the optic disc delineated focal thinning of the superotemporal nerve fiber layer consistent with the clinically observed focal nerve fiber layer defect. The depression appeared to arise from both the superficial and deep margins of the nerve fiber layer and reached a minimum thickness of 50 μm in the image. The average nerve fiber layer thickness at 1:00, determined by the computer, was correspondingly reduced to 87 μm.

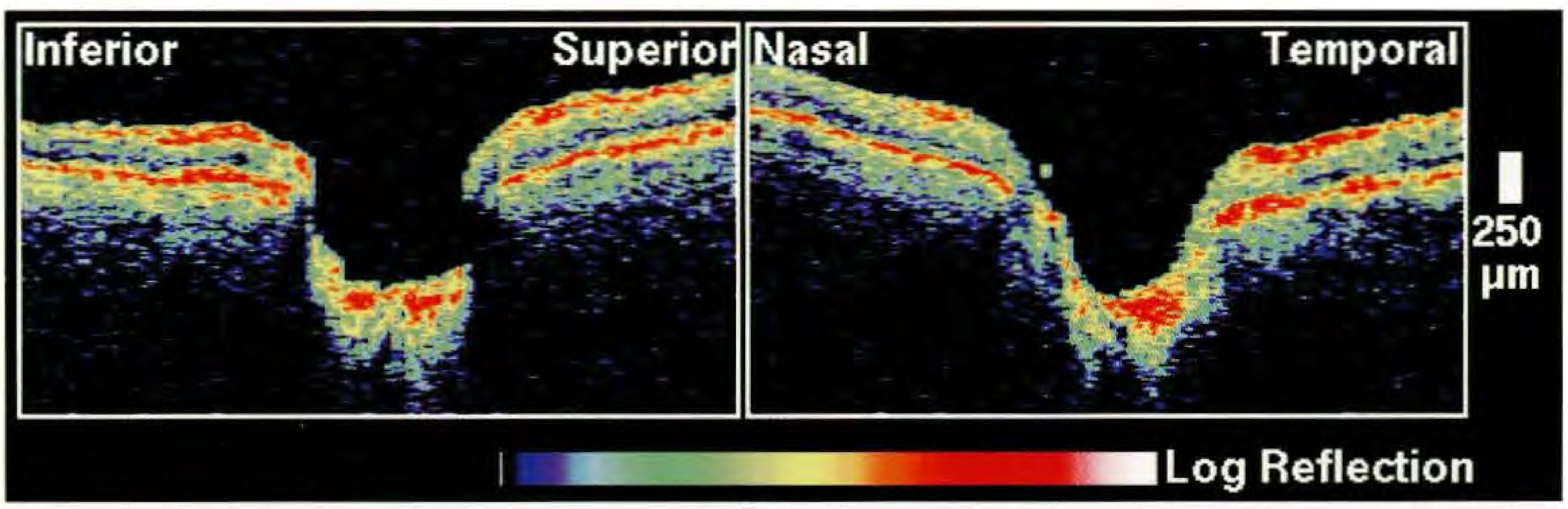

C

VERTICAL		*HORIZONTAL*	
Cup Diameter	**1.44 mm**	**Cup Diameter**	**1.53 mm**
Disc Diameter	**1.82 mm**	**Disc Diameter**	**1.85 mm**
C/D Ratio	**0.79**	**C/D Ratio**	**0.83**
NR Rim Area	**0.97 mm^2**		
Inferior NFL	**120 μm**	**Nasal NFL**	**110 μm**
Superior NFL	**160 μm**	**Temporal NFL**	**100 μm**

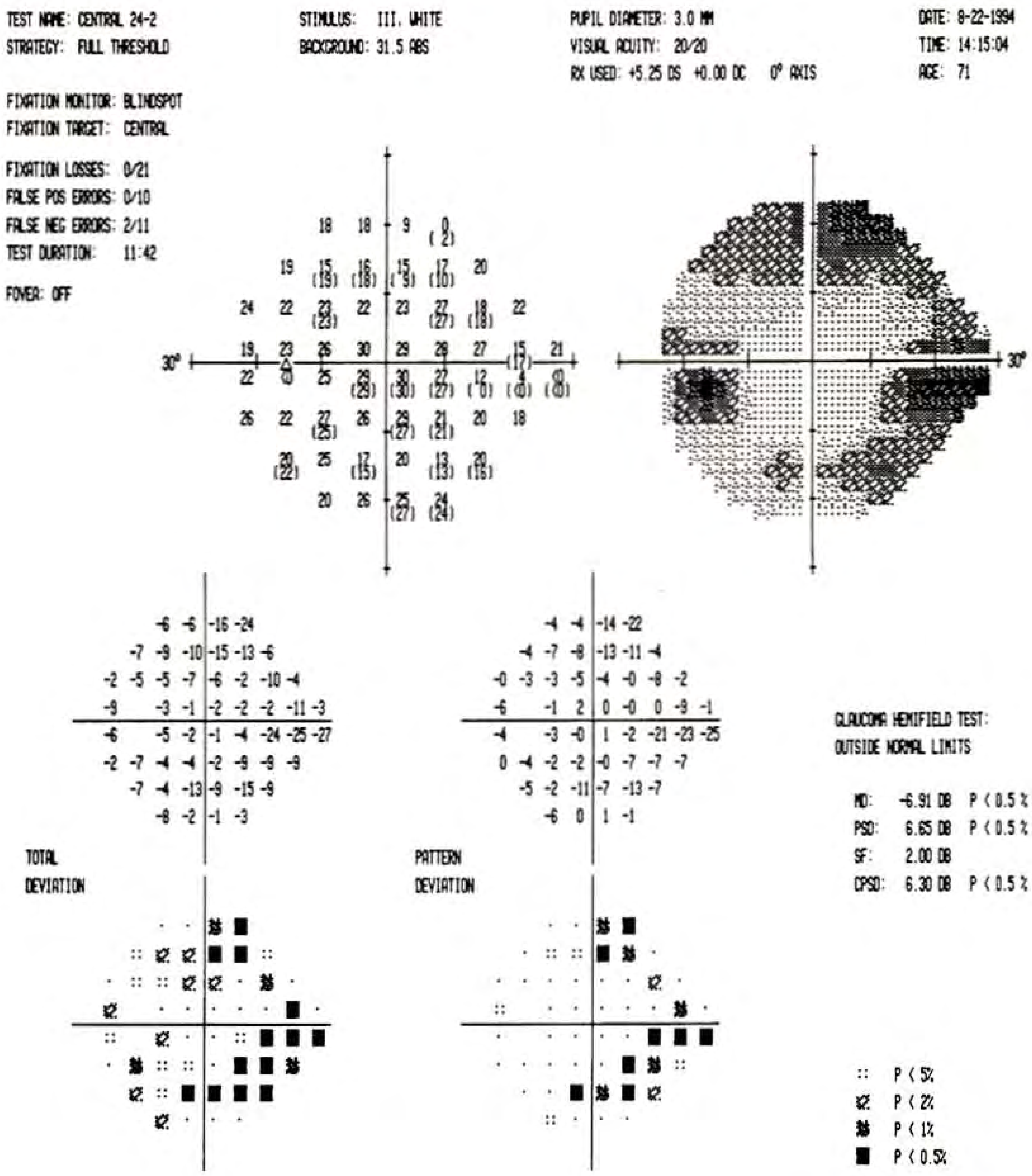
TEST NAME: CENTRAL 24-2
STRATEGY: FULL THRESHOLD
STIMULUS: III, WHITE
BACKGROUND: 31.5 ABS
PUPIL DIAMETER: 3.0 MM
VISUAL ACUITY: 20/20
RX USED: +5.25 DS +0.00 DC 0° AXIS
DATE: 8-22-1994
TIME: 14:15:04
AGE: 71
FIXATION MONITOR: BLINDSPOT
FIXATION TARGET: CENTRAL
FIXATION LOSSES: 0/21
FALSE POS ERRORS: 0/10
FALSE NEG ERRORS: 2/11
TEST DURATION: 11:42
FOVEA: OFF
30°
30°
TOTAL DEVIATION
PATTERN DEVIATION
GLAUCOMA HEMIFIELD TEST: OUTSIDE NORMAL LIMITS
MD: -6.91 DB P < 0.5 %
PSD: 6.65 DB P < 0.5 %
SF: 2.00 DB
CPSD: 6.30 DB P < 0.5 %
P < 5%
P < 2%
P < 1%
P < 0.5%

D

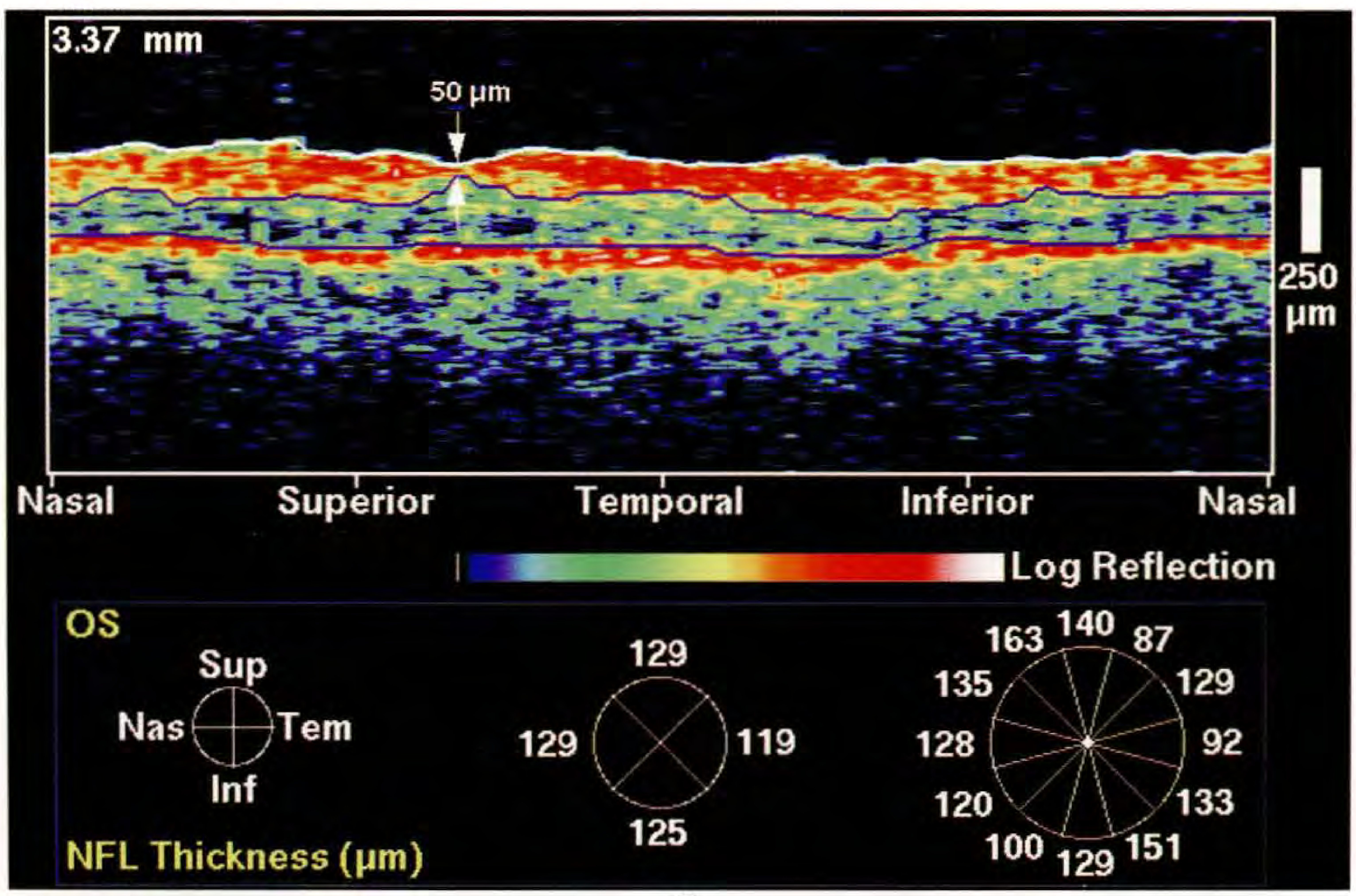
3.37 mm
50 μm
250 μm
Nasal
Superior
Temporal
Inferior
Nasal
Log Reflection
OS
Sup
Nas
Tem
Inf
NFL Thickness (μm)
129
129
119
125
163
140
87
135
129
128
92
120
133
100
129
151

E

A

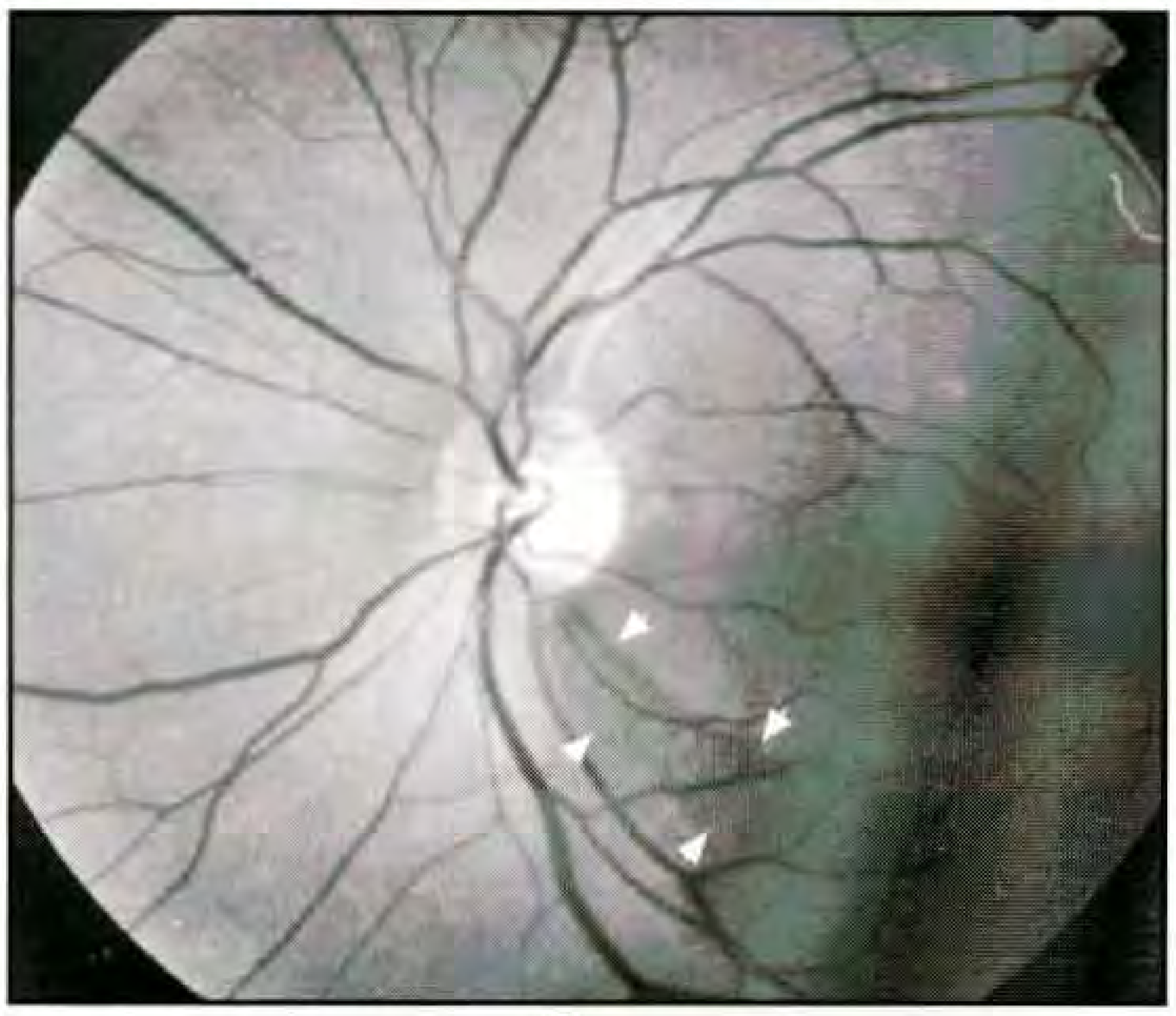

B

Case 13-3. Focal Nerve Fiber Layer Defect

Clinical Summary

A 46-year-old black woman was referred for the evaluation of primary open-angle glaucoma. She had been taking pilocarpine 4% four times daily and timolol 0.5% twice a day in both eyes for the past three weeks. The patient's visual acuity was 20/20 in this eye, with an intraocular pressure of 15 mm Hg. Slit-lamp examination revealed an open angle with a view of the ciliary body band circumferentially. Dilated ophthalmoscopy (A) showed mild cupping of the optic disc with an inferotemporal notch in the neuroretinal rim. A corresponding, focal decrease in the nerve fiber layer (NFL) reflex was also noted inferotemporally (B). A Humphrey visual field (D) showed a superior nasal step and a possible, early inferior nasal step.

Optical Coherence Tomography

The circular OCT tomogram (E) around the optic disc identified a broad, focal thinning of the NFL inferotemporally consistent with the clinical assessment of a focal NFL defect. The minimum NFL thickness in the lesion was 40 µm. The majority of the depression appeared to result from loss of the deeper nerve fibers. Total retinal thickness was not signifcantly affected in this region. The average NFL thickness at 4:00 was reduced to 75 µm. A slight decrease in the superior NFL thickness was also observed at 12:00 in the image consistent with the mild inferonasal depression in the visual field.

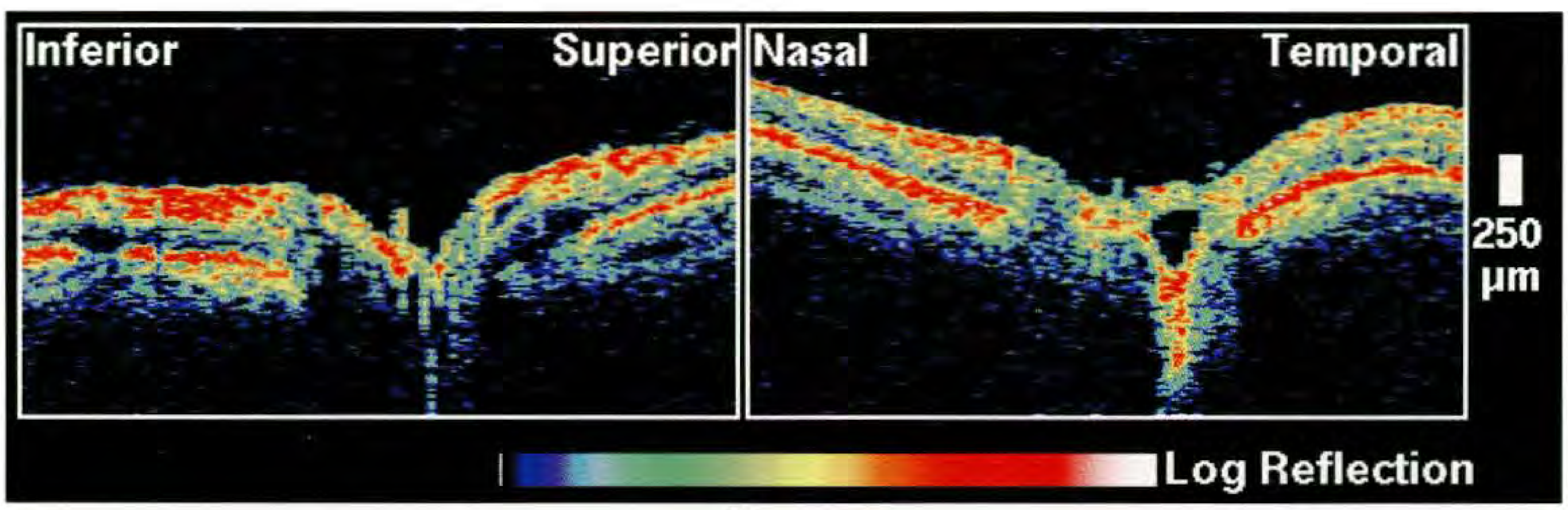

C

VERTICAL		*HORIZONTAL*	
Cup Diameter	**0.80 mm**	**Cup Diameter**	**0.59 mm**
Disc Diameter	**1.59 mm**	**Disc Diameter**	**1.85 mm**
C/D Ratio	**0.50**	**C/D Ratio**	**0.32**
NR Rim Area	**1.48 mm^2**		
Inferior NFL	**210 µm**	**Nasal NFL**	**210 µm**
Superior NFL	**240 µm**	**Temporal NFL**	**180 µm**

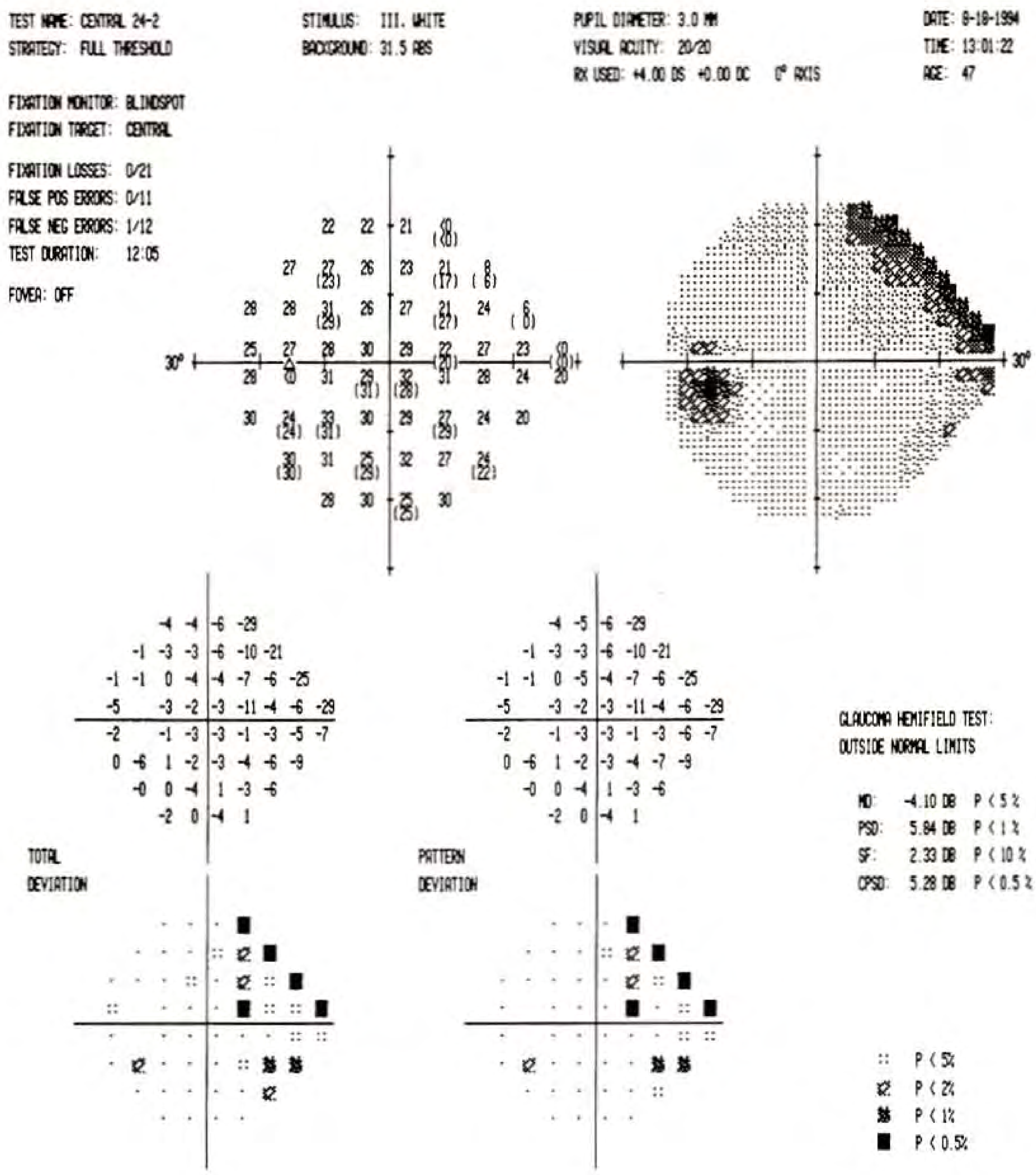
TEST NAME: CENTRAL 24-2
STRATEGY: FULL THRESHOLD
STIMULUS: III, WHITE
BACKGROUND: 31.5 ASB
PUPIL DIAMETER: 3.0 MM
VISUAL ACUITY: 20/20
RX USED: +4.00 DS +0.00 DC 0° AXIS
DATE: 8-18-1994
TIME: 13:01:22
AGE: 47
FIXATION MONITOR: BLINDSPOT
FIXATION TARGET: CENTRAL
FIXATION LOSSES: 0/21
FALSE POS ERRORS: 0/11
FALSE NEG ERRORS: 1/12
TEST DURATION: 12:05
FOVEA: OFF
30°
TOTAL DEVIATION
PATTERN DEVIATION
GLAUCOMA HEMIFIELD TEST: OUTSIDE NORMAL LIMITS
MD: -4.10 DB P < 5 %
PSD: 5.84 DB P < 1 %
SF: 2.33 DB P < 10 %
CPSD: 5.28 DB P < 0.5 %
P < 5%
P < 2%
P < 1%
P < 0.5%

D

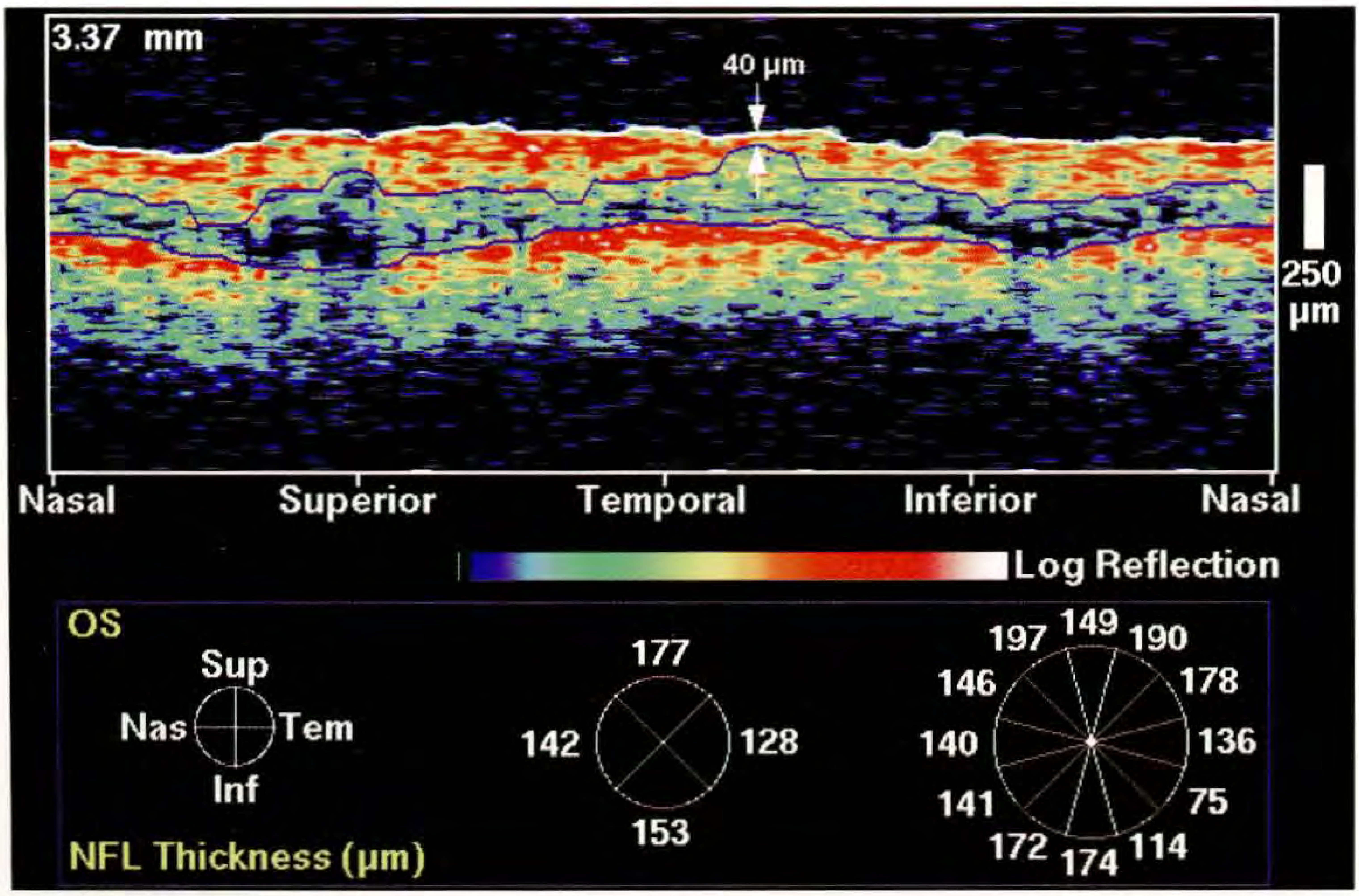
3.37 mm
40 µm
250 µm
Nasal
Superior
Temporal
Inferior
Nasal
Log Reflection
OS
Sup
Nas
Tem
Inf
NFL Thickness (µm)
177
142
128
153
149
197
190
146
178
140
136
141
75
172
174
114

E

CHAPTER 14

Diseases of the Optic Nerve

Optic Disc Pitting
Papilledema

As in glaucoma, OCT is also useful for cross-sectional profiling of the optic nerve head and retinal nerve fiber layer (NFL) in neurological diseases of the optic nerve. Radial tomograms through the optic disc provide information on the disc contour. Optic nerve pits, for example, appear as focal excavations in the nerve head. Quantitative measurements such as cup and disc diameter may be directly extracted from the tomograms, which may be useful in evaluating optic nerve atrophy. The extent of papilledema may be quantified objectively by assessing the protrusion of the nerve head above the surface of the retina in OCT cross-section.

Circular OCT tomograms acquired around the optic nerve head provide information on the cross-sectional structure of the NFL in a cylindrical section surrounding the optic disc. Relative areas of NFL thinning may be quantitatively assessed and correlated with visual field performance, allowing the degeneration of retinal ganglion cell axons to be objectively measured in conditions such as optic atrophy and chronic papilledema. As in the case of glaucoma, an automated computer image processing algorithm may be used to extract measurements of retinal and NFL thickness from the OCT tomograms [1].

Both serous macular detachments and schisis-like macular separations are associated with congenital optic nerve pits [2-4]. The pathogenesis of these lesions, however, has been controversial. The cross-sectional view of OCT is useful in structurally characterizing the development of these lesions. Neurosensory detachments appear as a complete elevation of the sensory retina overlying optically clear serous fluid. In contrast, schisis-like separations are associated with a splitting of the outer retina with vertical, bridging elements between the outer and inner retina. Cystic changes manifest as retinal swelling and reduced intraretinal optical reflectivity associated with weakly backscattering cystic spaces.

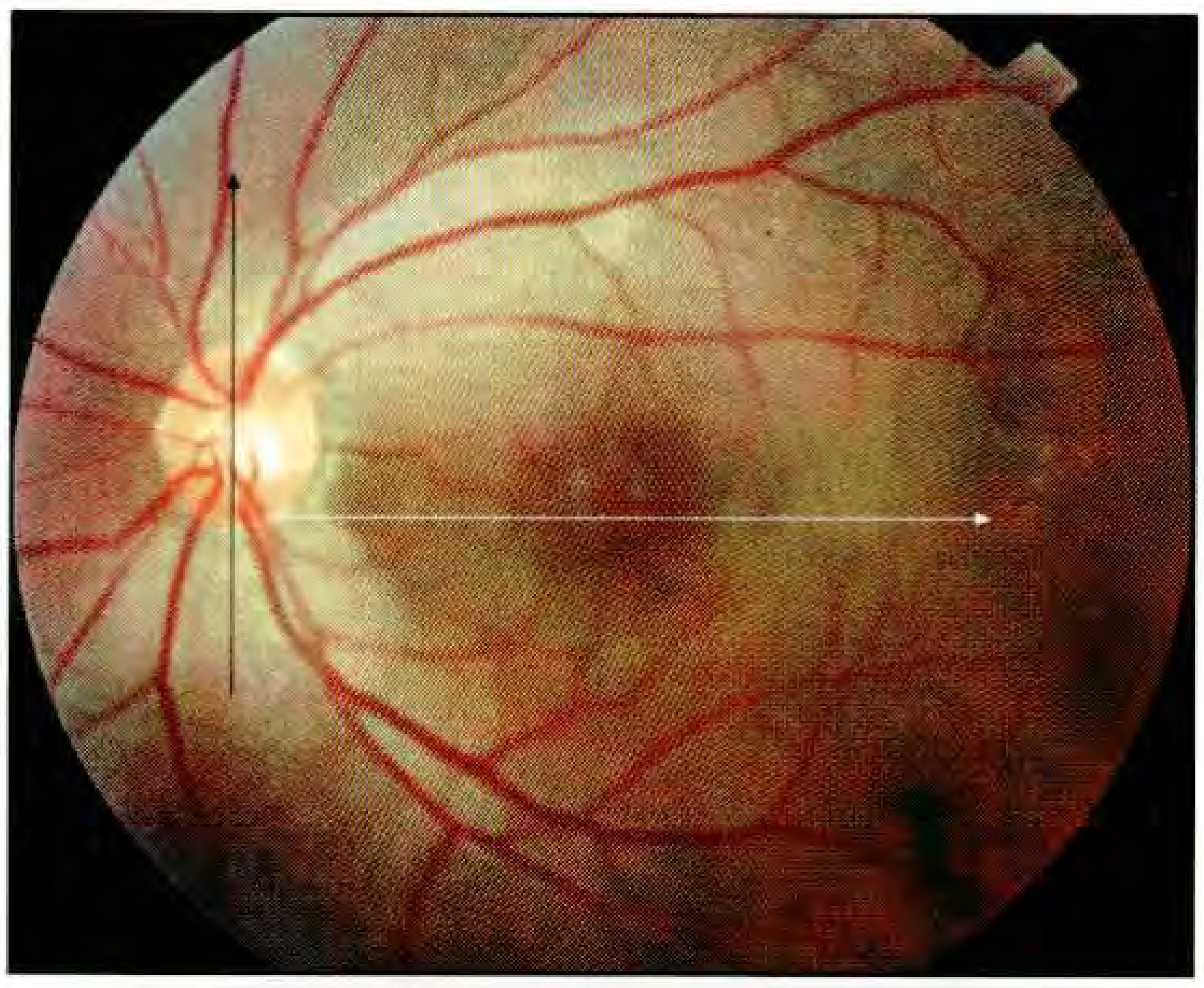

A

Case 14-1. Optic Disc Pitting with Serous Macular Detachment

Clinical Summary

A 63-year-old woman complained of a one day history of blurred vision in her left eye. She reported a prior history of blurring approximately 20 years earlier which took several weeks to resolve. Slit-lamp biomicroscopy (A) showed a large neurosensory detachment in the macula. A deep excavation of the optic nerve head was also observed inferiorly. Visual acuity in this eye was counting fingers.

Optical Coherence Tomography

A vertical scan (B; black line on A) through the optic disc graphically demonstrated pitting of the disc inferiorly. The neurosensory retinal detachment was also visualized in a horizontal scan through fixation (C; white line on A), which showed an elevation of 590 μm above the retinal pigment epithelium. Two weeks later, a repeat image (D) through the fovea demonstrated that the fluid accumulation had decreased to 240 μm beneath the fovea. There was a corresponding improvement in visual acuity to 20/100. Two months later, slit-lamp examination indicated that the detachment had completely resolved. The patient's visual acuity was 20/25. OCT examination (E) demonstrated residual subretinal fluid in the macula, with a height of 80 μm.

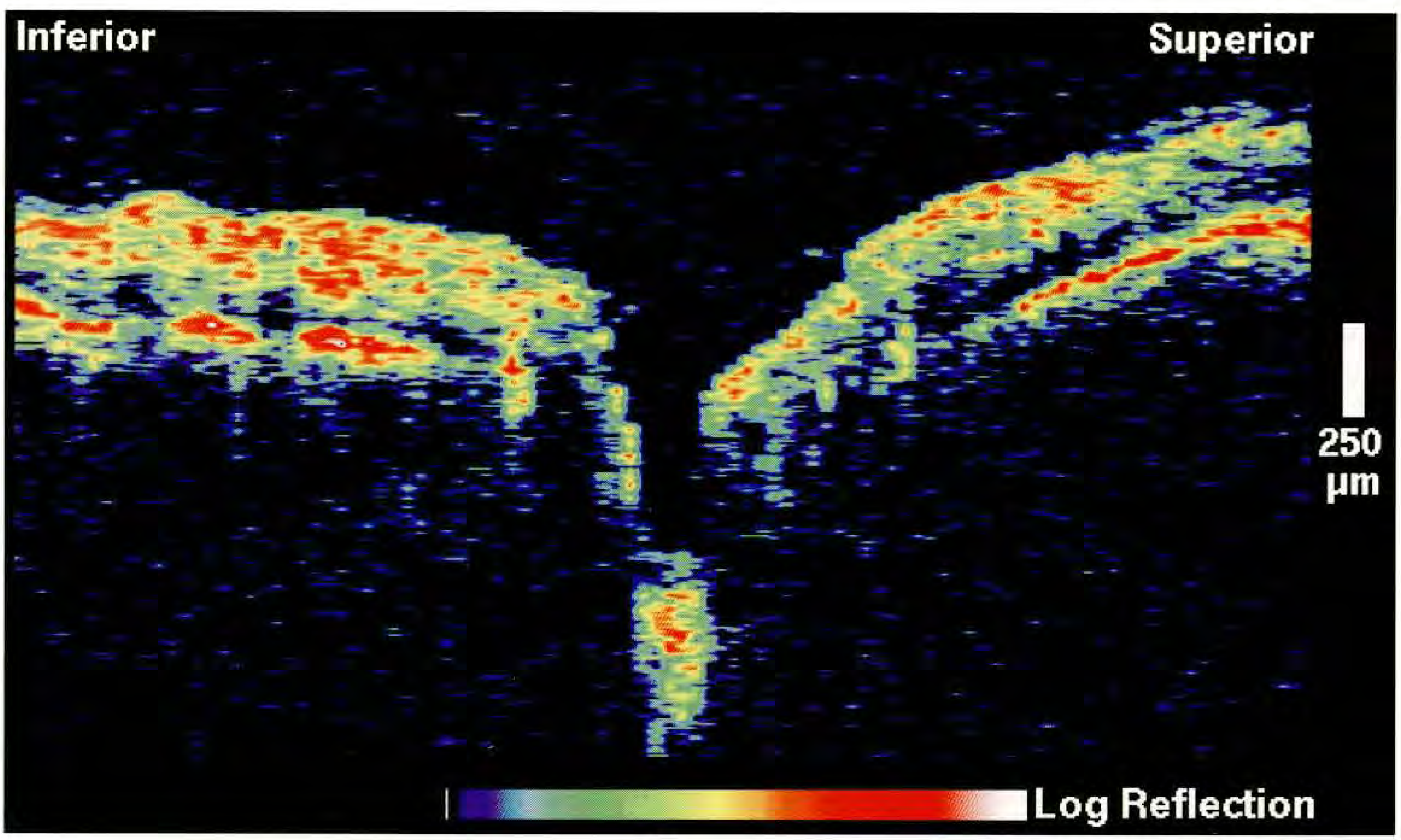

B

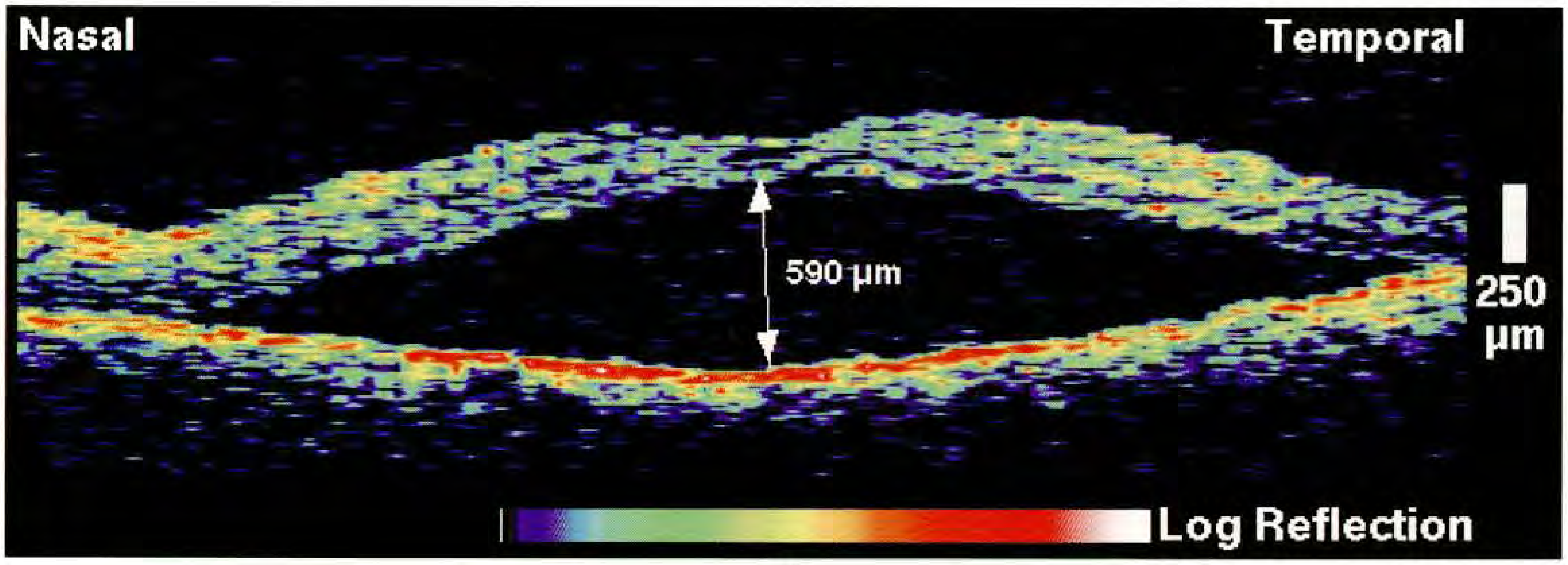
Nasal
Temporal
590 µm
250 µm
Log Reflection

C

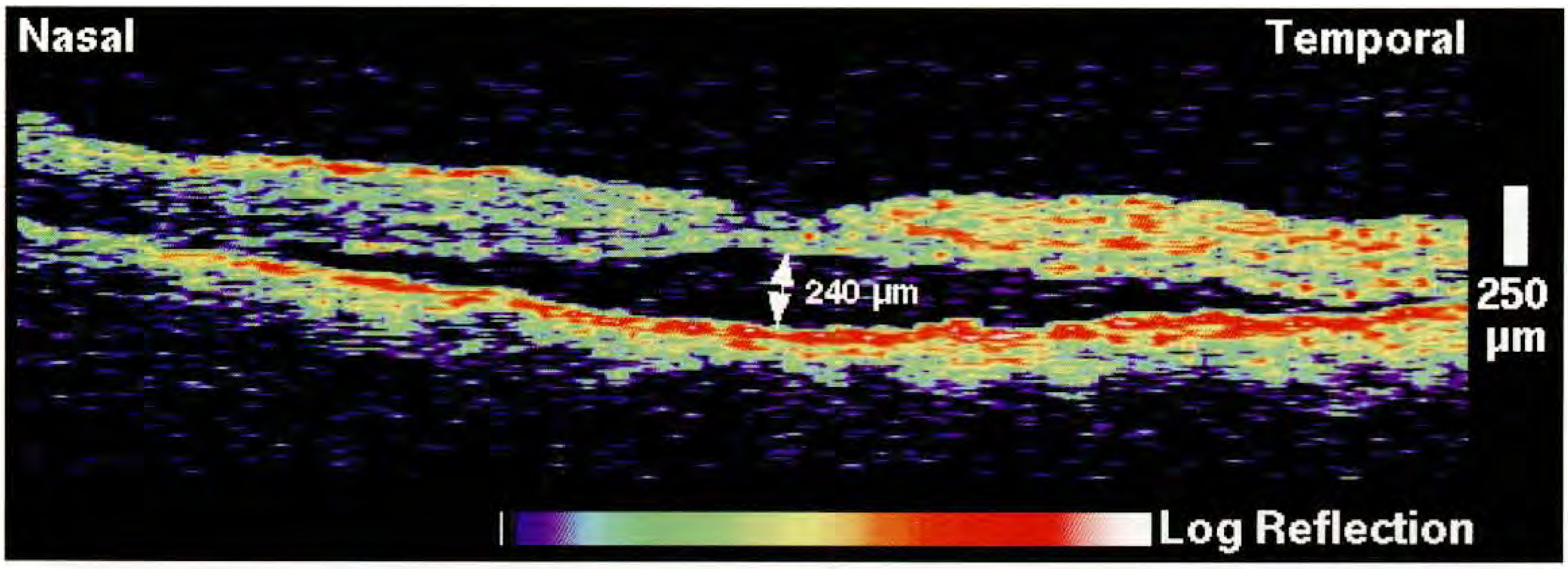
Nasal
Temporal
240 µm
250 µm
Log Reflection

D

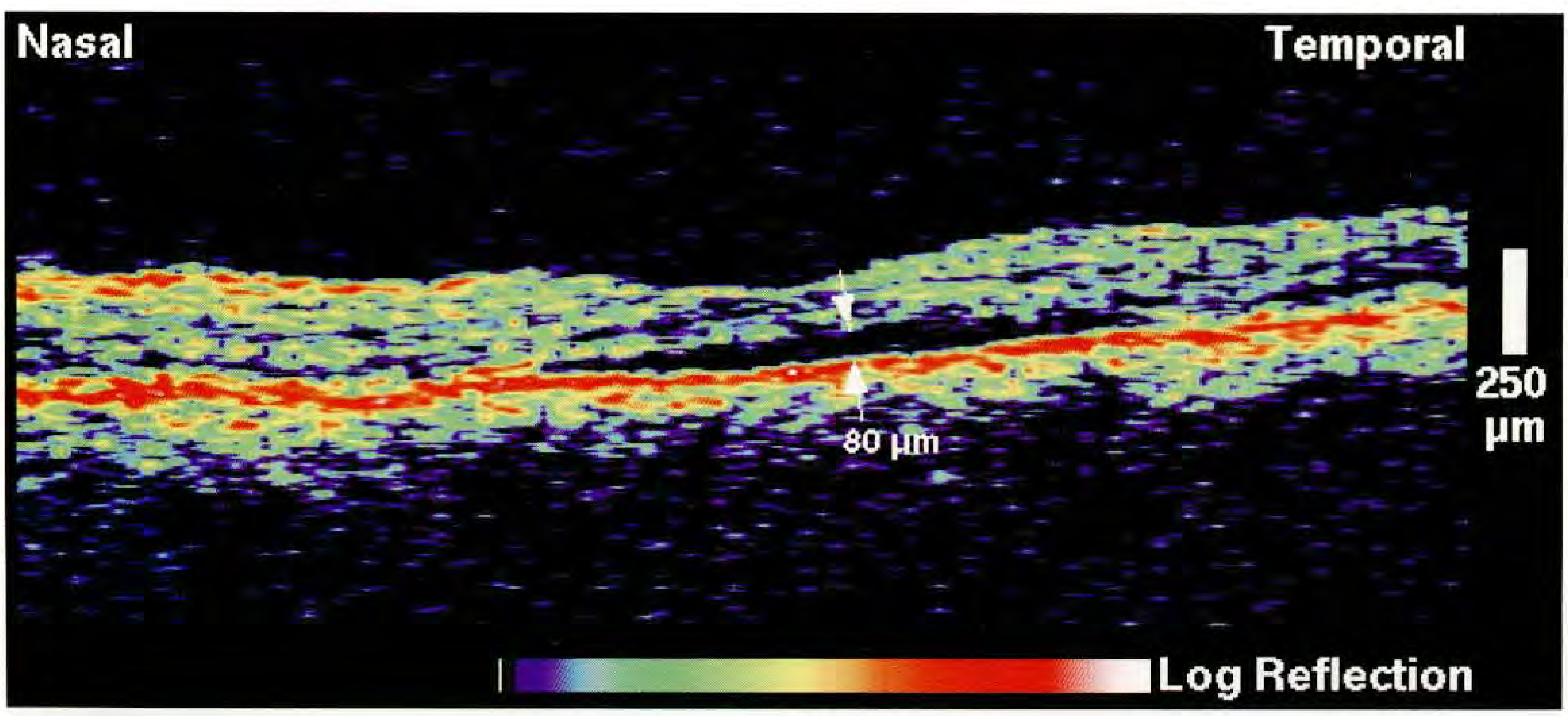
Nasal
Temporal
80 µm
250 µm
Log Reflection

E

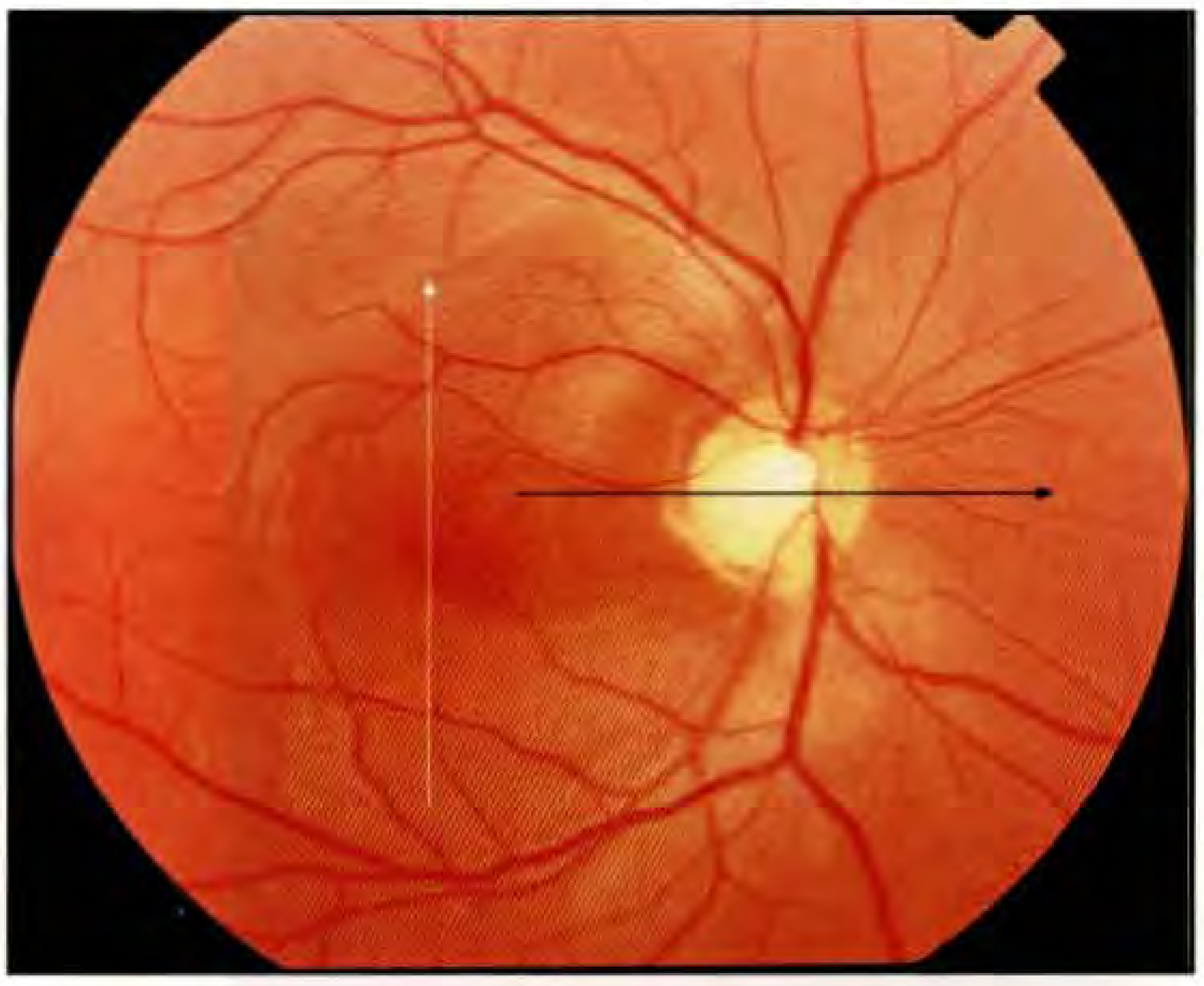

A

Case 14-2. Optic Disc Pitting with Retinal Schisis and Detachment

Clinical Summary

A 21-year-old man was evaluated for a serous macular elevation associated with a pit of the optic nervehead in his right eye. He had received laser treatment four months earlier. On examination, his visual acuity in this eye was 20/50. Slit-lamp biomicroscopy (A) revealed a pit along the inferotemporal rim of the optic disc, a small cyst directly in the fovea, fine superficial retinal striae, and an underlying yellow discoloration of the pigment epithelium.

B

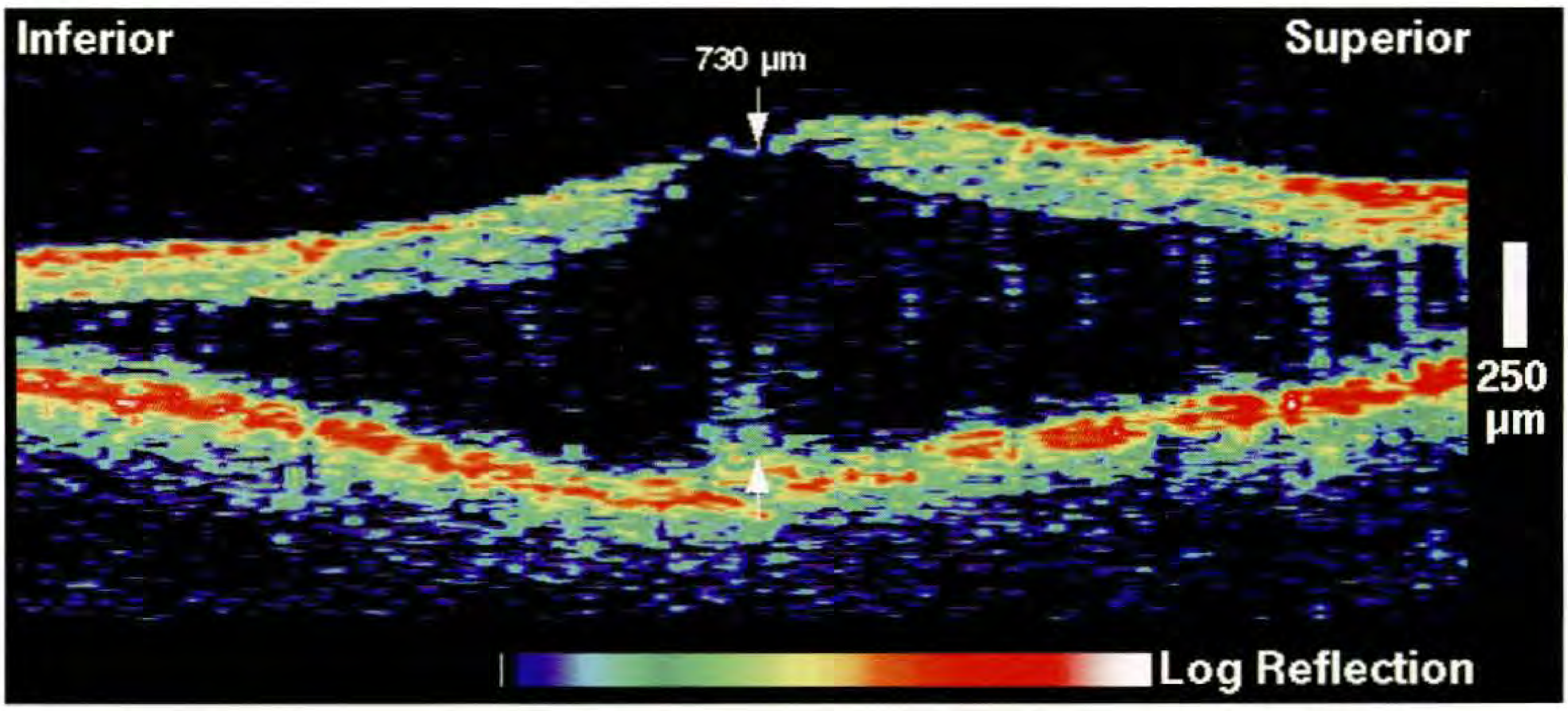

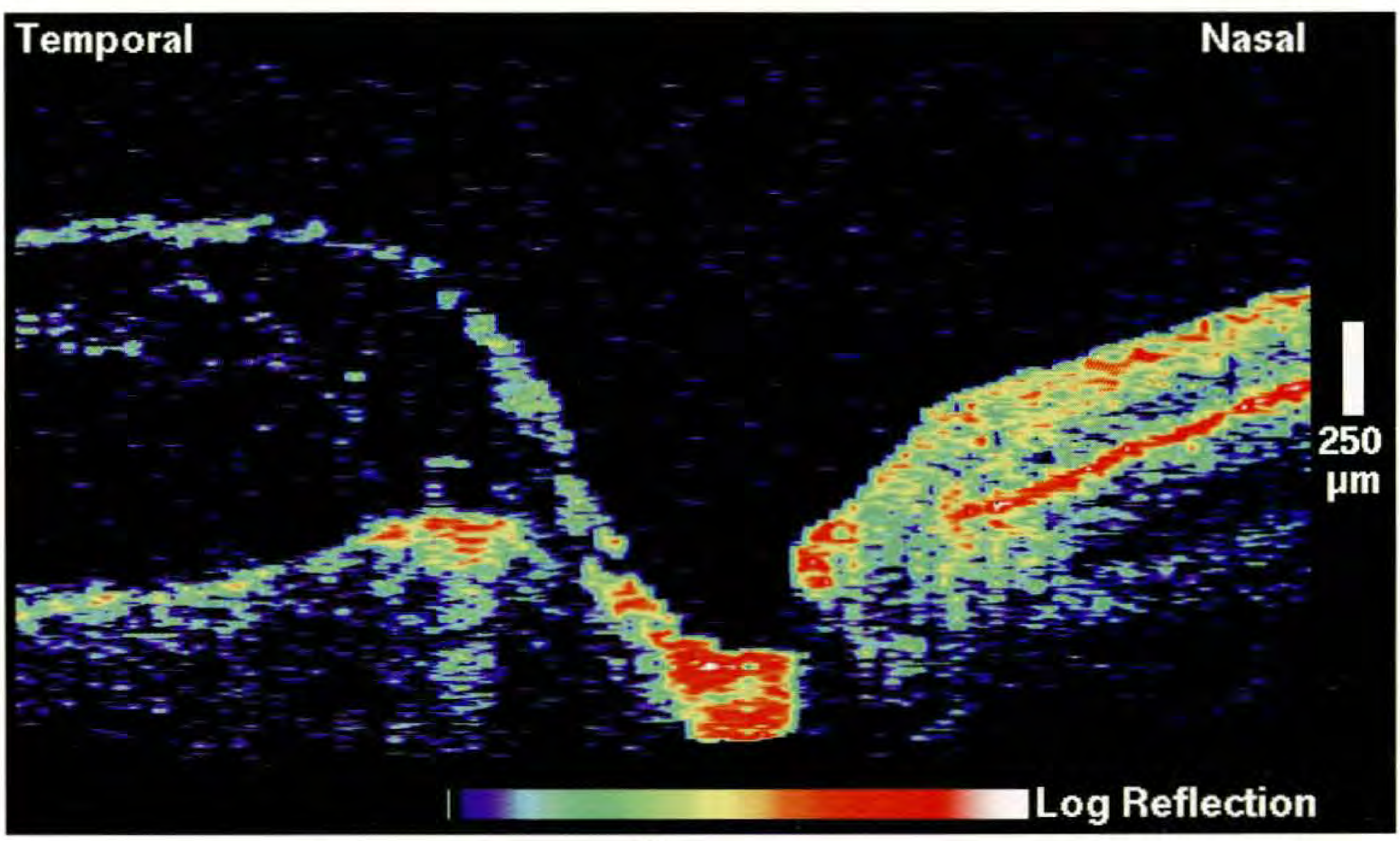

C

Case 14-2 continued

Optical Coherence Tomography

A vertical OCT image through the fovea (B; white line on A) showed thickening of the central macula related to cystic changes or splitting of the outer retina. Vertical structures appeared to bridge the outer and inner retina.

A scan taken through the optic disc (C; black line on A) showed cystic changes in both the inner and outer retina contiguous with the edge of the optic disc.

Follow-up Examination

Two months later, the patient returned with a decline in visual acuity to counting fingers. Dilated fundus examination (D) revealed a new, well-defined serous detachment in the central macula with persistent overlying cystic degeneration.

Follow-up Optical Coherence Tomography

Follow-up OCT examination (E) confirmed the development of a neurosensory detachment centrally beneath intraretinal fluid accumulation in the outer retinal layers. The detachment was well circumscribed and did not communicate with the optic disc.

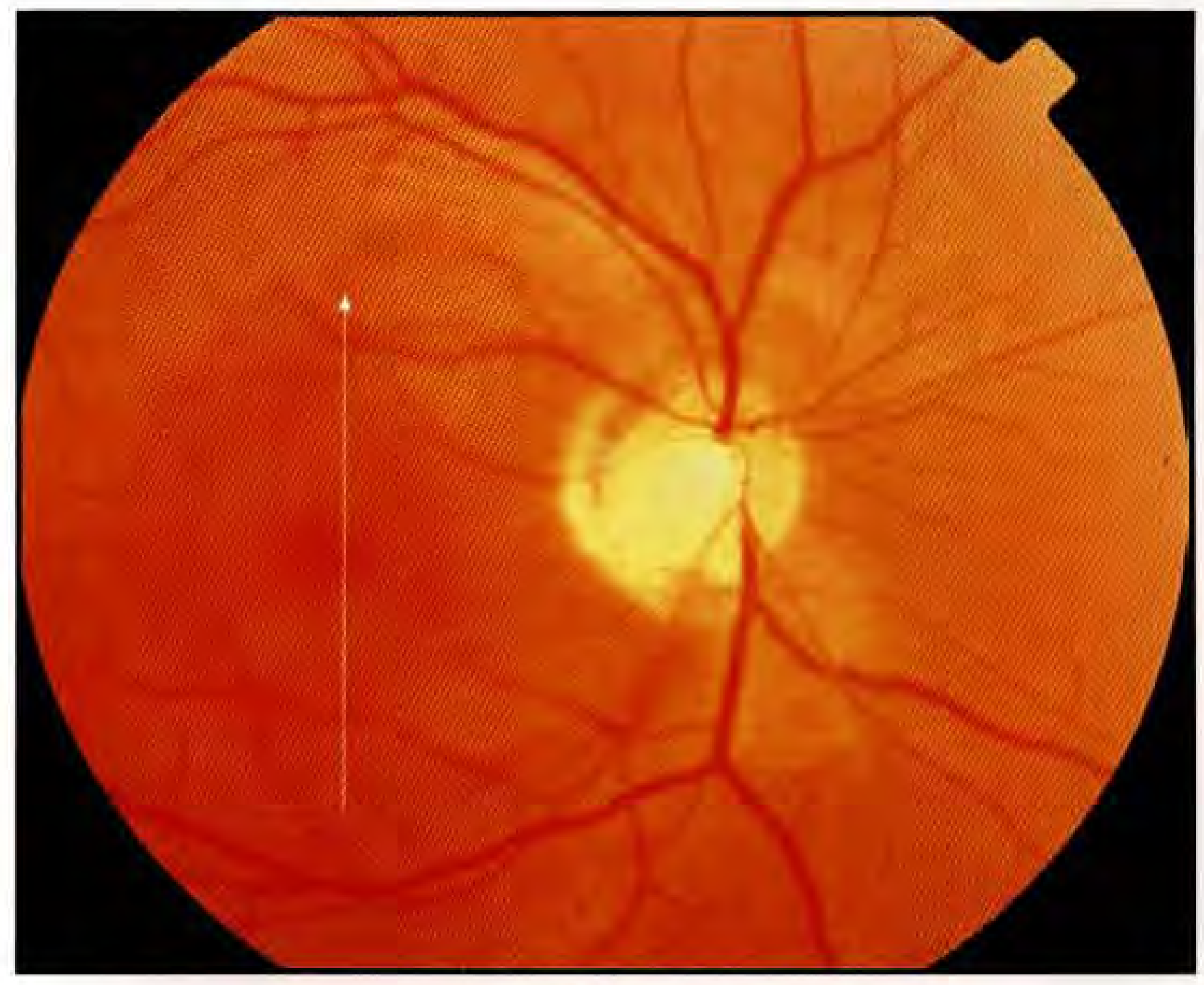

D

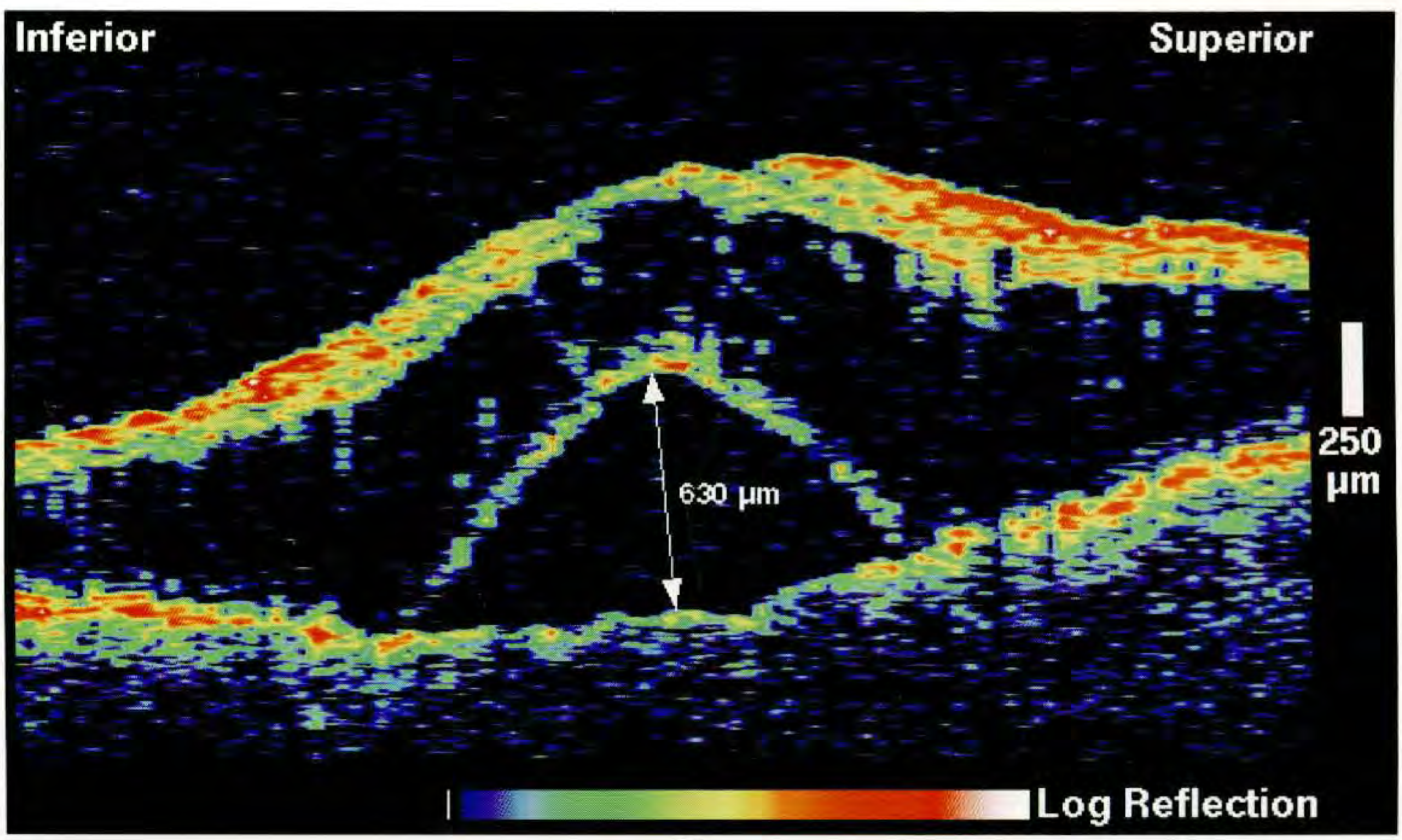

E

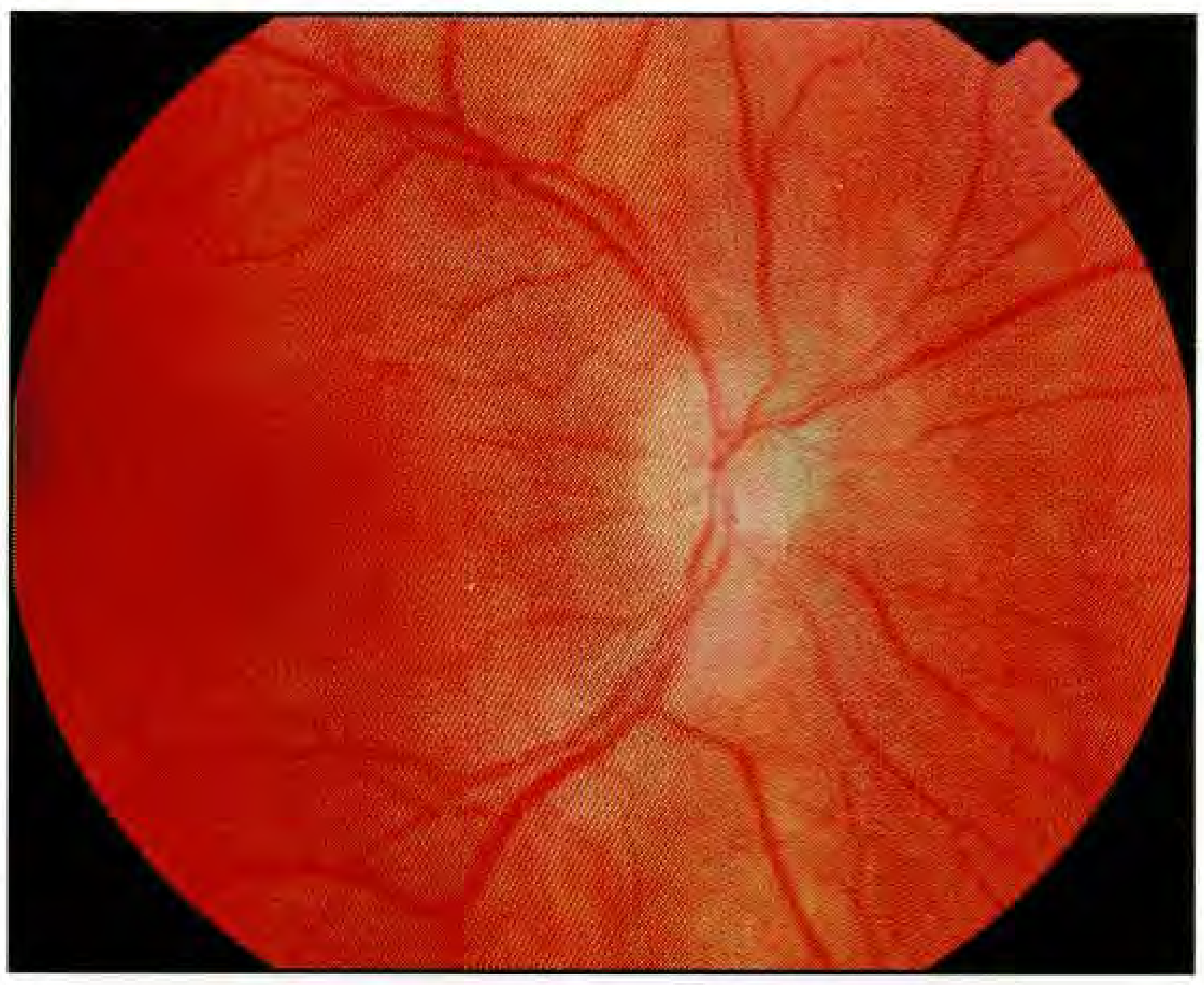

A

Case 14-3. Pseudotumor Cerebri

Clinical Summary

A 16-year-old obese woman reported trouble focusing at near distances and blurred vision in her left eye. Visual acuity in this eye was 20/70 and there was a 3+ relative afferent pupillary defect. Dilated fundus examination revealed papilledema in both eyes with a few peripapillary flame shaped hemorrhages in the left eye inferior to the optic disc. Significant pallor was also noted in the superior portion of the left disc. A clinical diagnosis of pseudotumor cerebri was established after a spinal tap revealed a cerebrospinal fluid pressure of 440 mm Hg. Optic nerve sheath fenestration was performed to relieve the acute optic neuropathy in the left eye, and the patient began taking acetazolamide 500 mg once a day.

Examination of the right eye one month after the procedure showed reduced papilledema with mild blurring of the disc margin (A). No peripapillary hemorrhage was identified. A Humphrey visual field (C) revealed an inferior nasal step. Visual acuity in this eye was 20/20.

Optical Coherence Tomography

A linear OCT tomogram (B) acquired through the center of the right optic disc and peripapillary region following fenestration showed protrusion of the disc contour consistent with papilledema. A circular OCT scan (D) obtained around the disc at a diameter of 3.4 mm revealed that the superotemporal nerve fiber layer (NFL) was thinned compared to the inferotemporal nerve fiber layer, which was relatively preserved. This attenuated NFL thickness superiorly corresponded with the clinical region of visual field loss.

(continued)

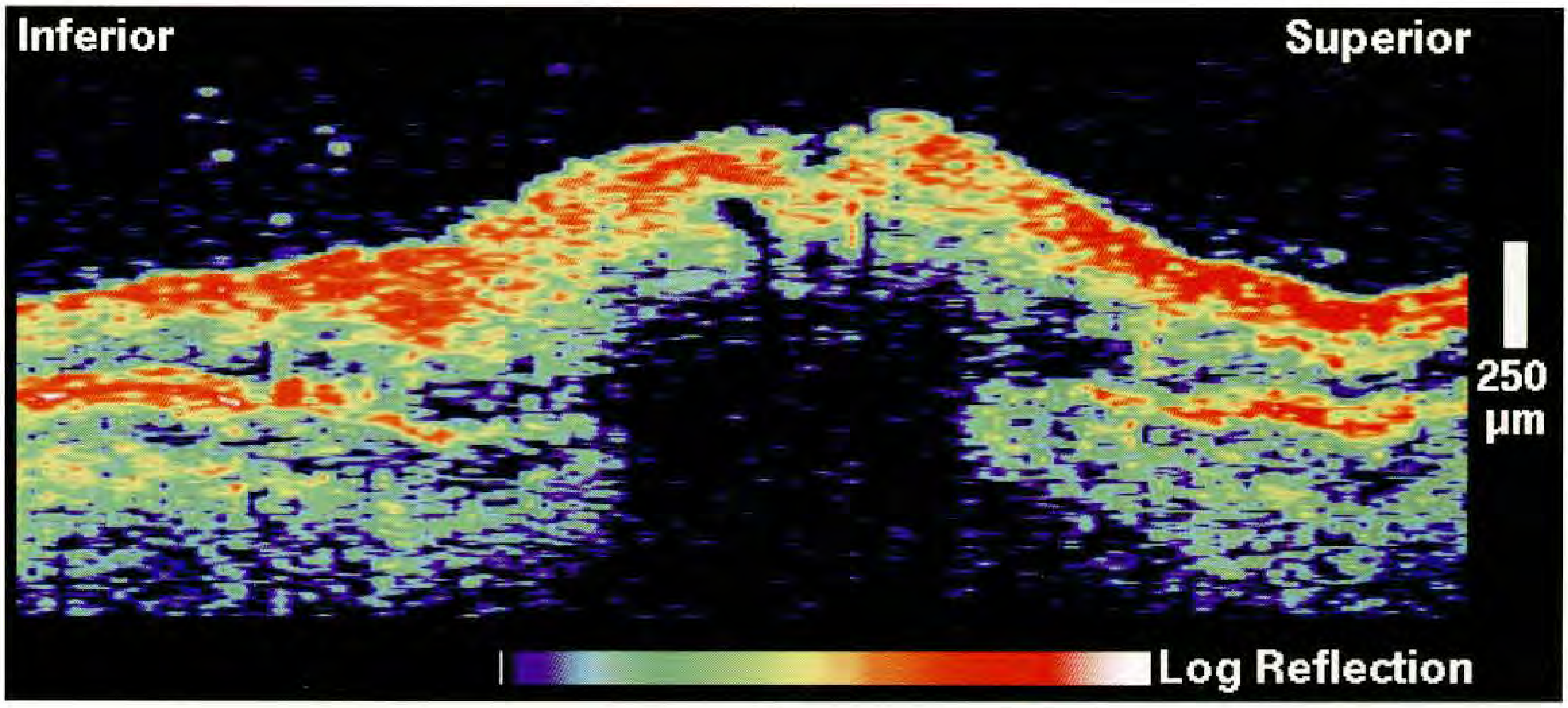

B

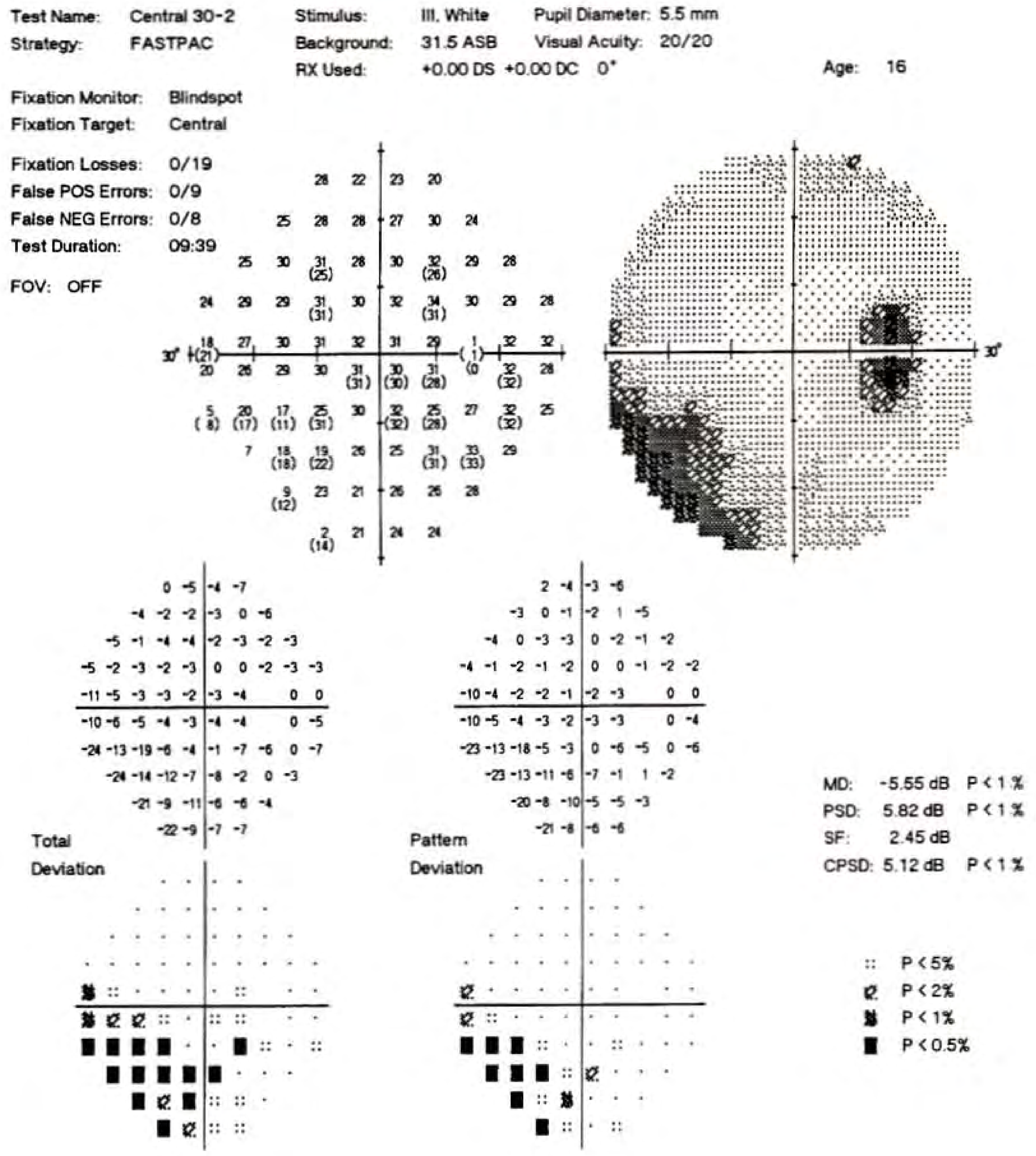

Test Name: Central 30-2
Strategy: FASTPAC
Stimulus: III, White
Background: 31.5 ASB
RX Used: +0.00 DS +0.00 DC 0°
Pupil Diameter: 5.5 mm
Visual Acuity: 20/20
Age: 16
Fixation Monitor: Blindspot
Fixation Target: Central
Fixation Losses: 0/19
False POS Errors: 0/9
False NEG Errors: 0/8
Test Duration: 09:39
FOV: OFF
30°
Total Deviation
Pattern Deviation
MD: -5.55 dB P < 1%
PSD: 5.82 dB P < 1%
SF: 2.45 dB
CPSD: 5.12 dB P < 1%
P < 5%
P < 2%
P < 1%
P < 0.5%

C

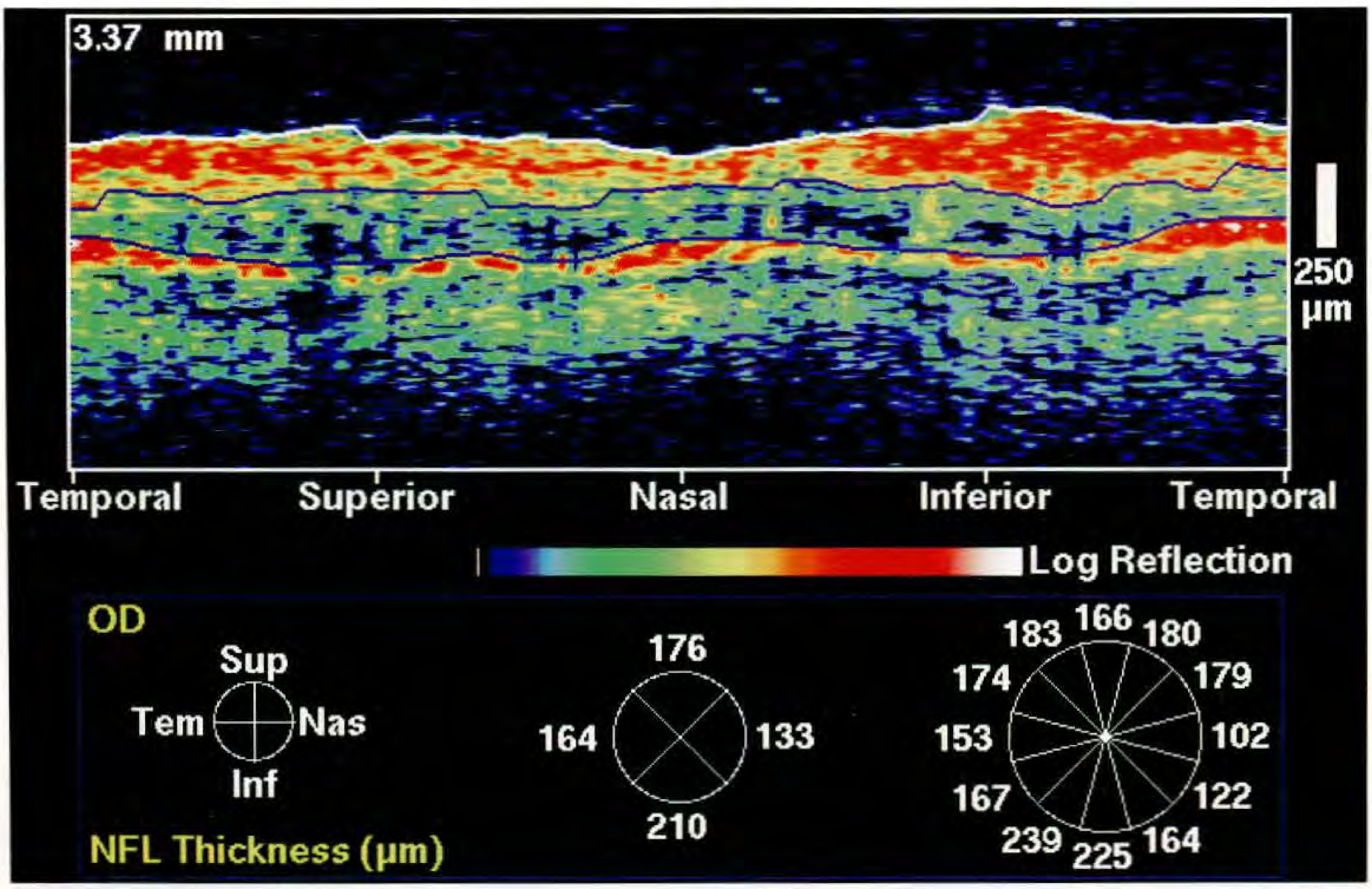

3.37 mm
250 µm
Temporal
Superior
Nasal
Inferior
Temporal
Log Reflection
OD
Sup
Tem
Nas
Inf
NFL Thickness (µm)
176
164
133
210
183
166
180
174
179
153
102
167
122
239
225
164

D

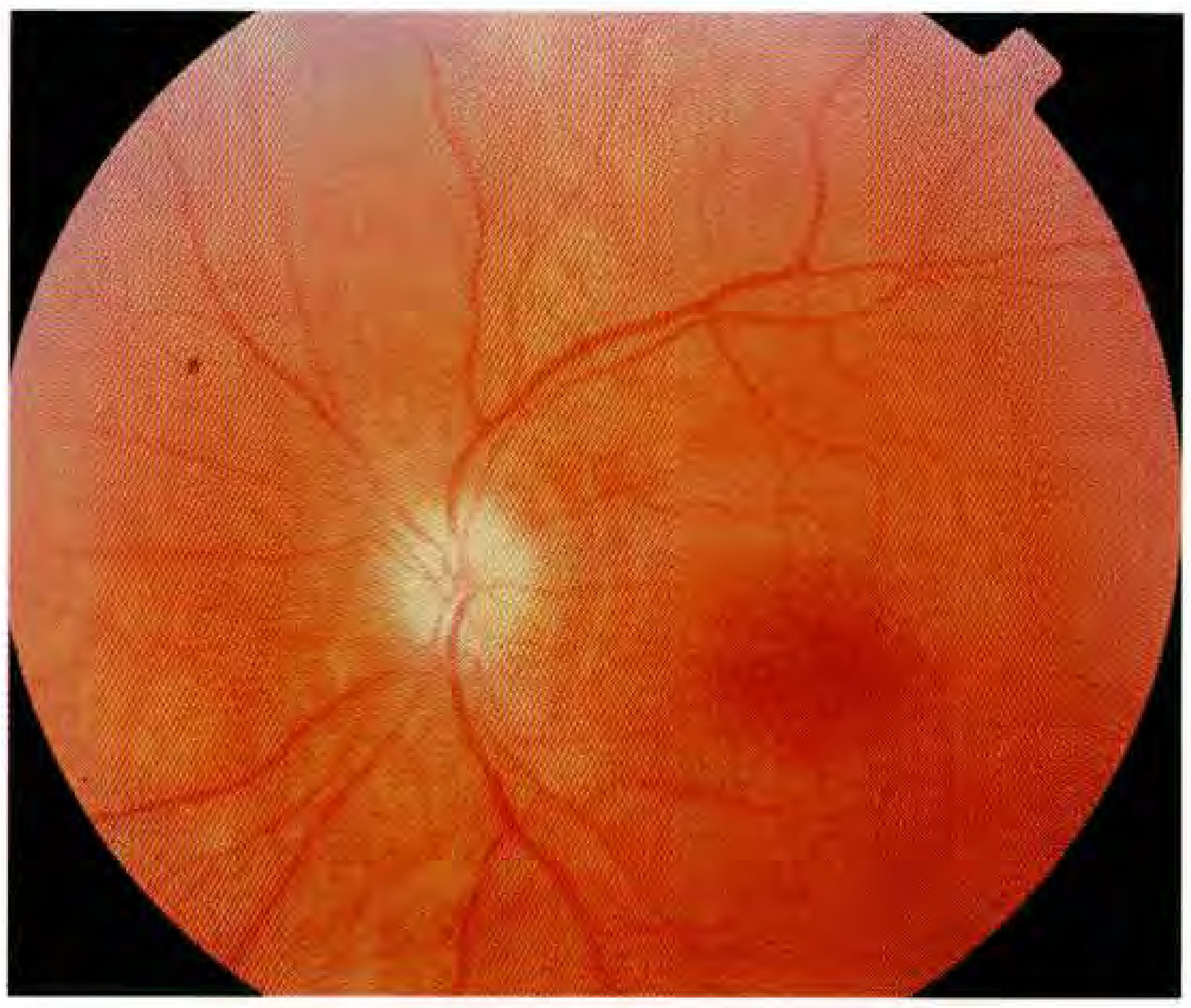

E

Case 14-3 continued

Clinical Summary

Following fenestration, examination of the patient's left eye (E) revealed a 2+afferent pupillary defect and papilledema, which was reduced compared to the preoperative evaluation. Mild blurring of the disc margin was noted; however, no hemorrhage was observed. Visual acuity was 20/30. A Humphrey (G) visual field showed a dense inferior arcuate scotoma and superior quadrant loss.

Optical Coherence Tomography

A linear OCT section (F) taken vertically through the center of the left optic disc again showed significant disc edema. A circular tomogram (H), acquired at a diameter of 3.4 mm surrounding the optic disc, showed generalized thinning of the nerve fiber layer. The thinning was greater superotemporally (2:00 to 3:00), than inferotemporally (4:00 to 5:00) consistent with the relative preservation of the superior compared to the inferior visual field. The overall nerve fiber layer thickness was thinner in the left eye compared to the right throughout all clock hours, corresponding to the clinical observation of asymmetric visual field loss and afferent pupillary defect in the left eye.

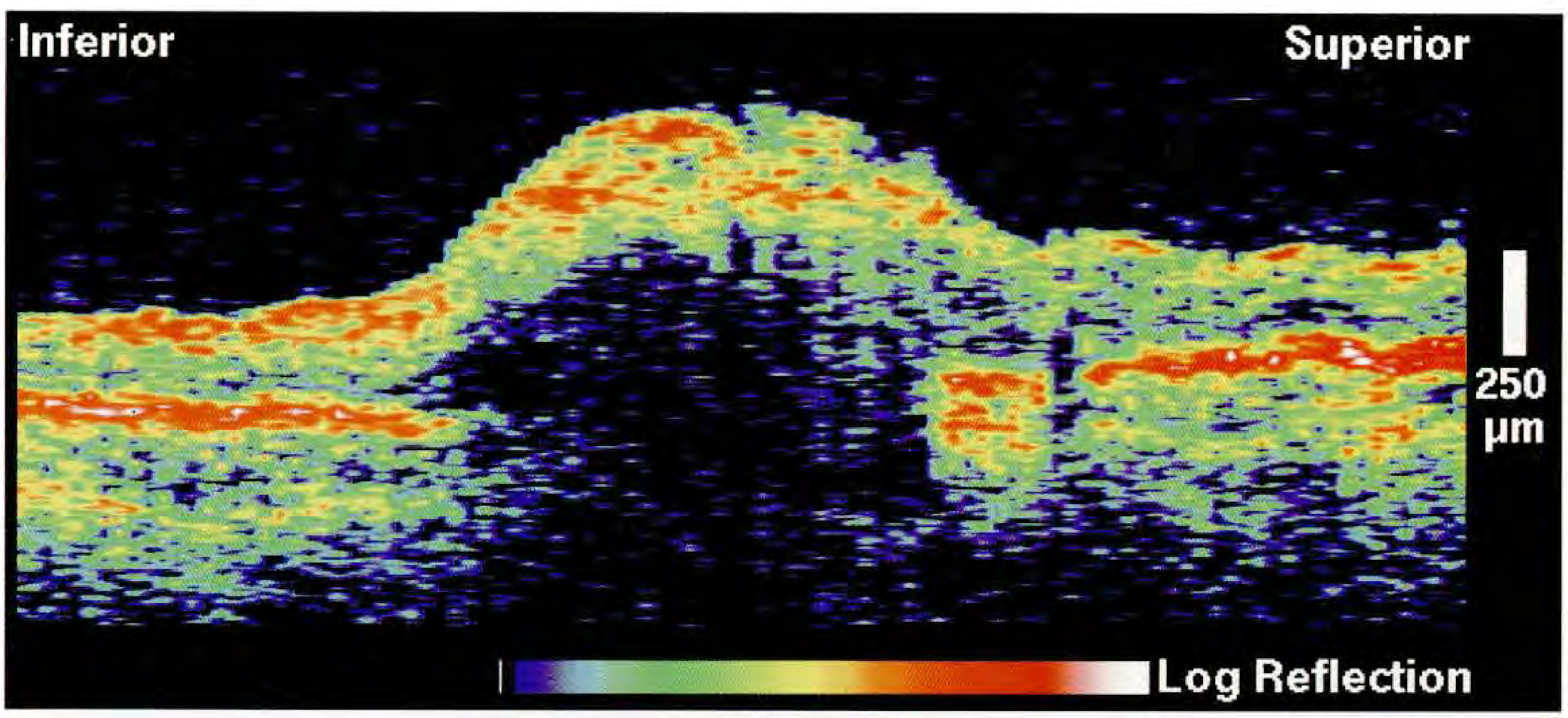

F

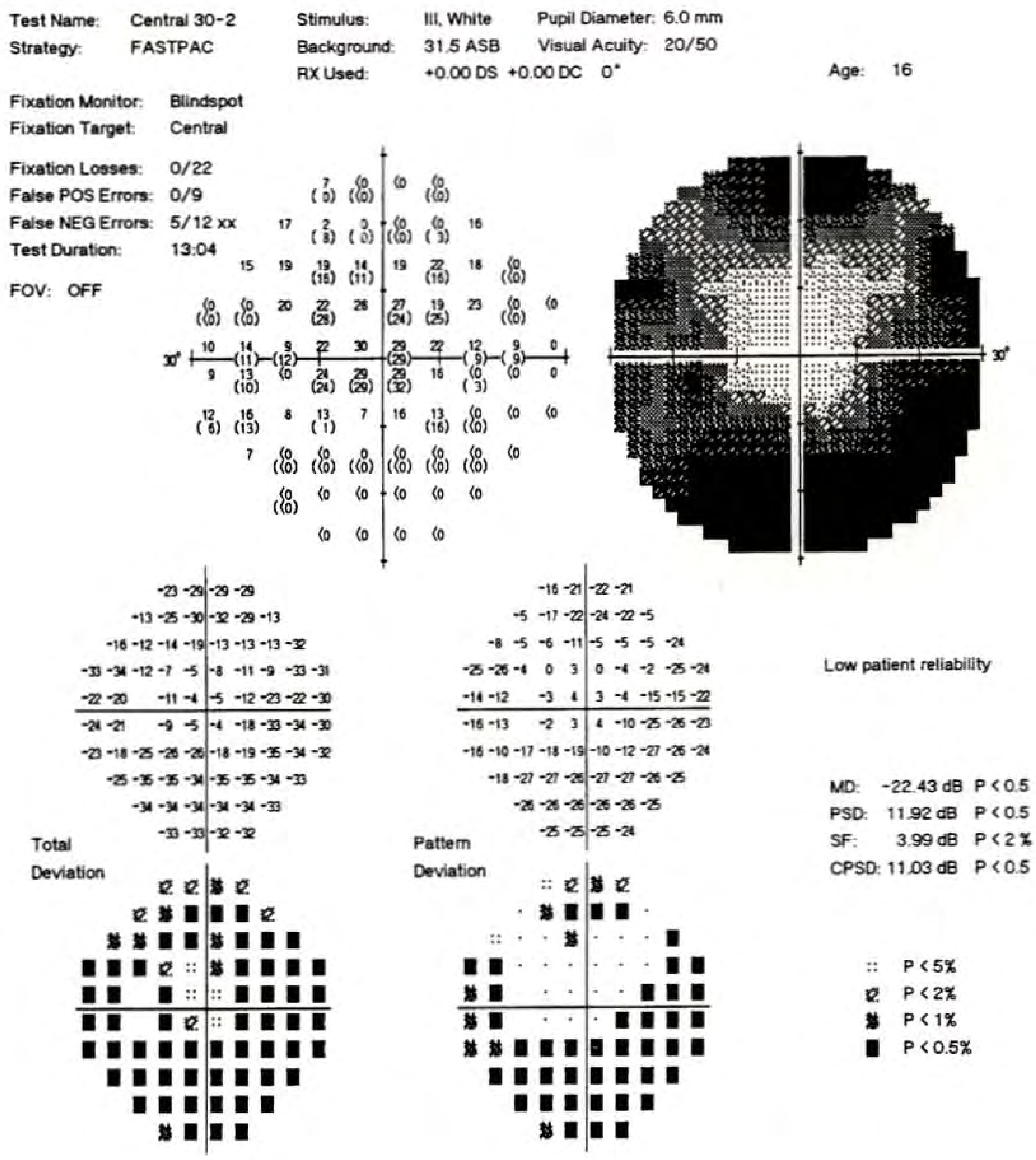
Test Name: Central 30-2
Strategy: FASTPAC
Stimulus: III, White
Background: 31.5 ASB
RX Used: +0.00 DS +0.00 DC 0°
Pupil Diameter: 6.0 mm
Visual Acuity: 20/50
Age: 16
Fixation Monitor: Blindspot
Fixation Target: Central
Fixation Losses: 0/22
False POS Errors: 0/9
False NEG Errors: 5/12 xx
Test Duration: 13:04
FOV: OFF
Low patient reliability
MD: -22.43 dB P < 0.5
PSD: 11.92 dB P < 0.5
SF: 3.99 dB P < 2 %
CPSD: 11.03 dB P < 0.5
Total Deviation
Pattern Deviation
P < 5%
P < 2%
P < 1%
P < 0.5%

G

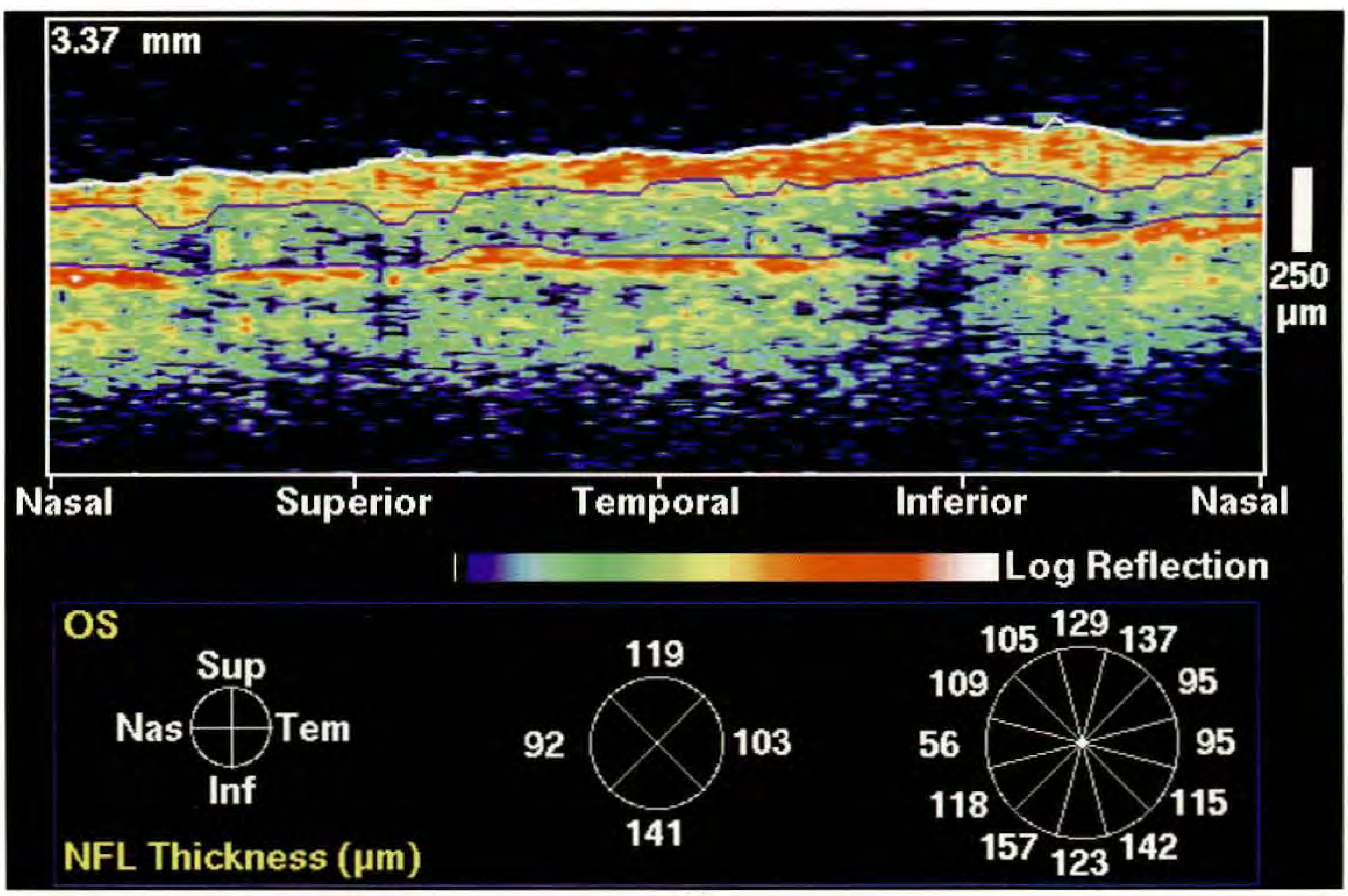
3.37 mm
250 µm
Nasal
Superior
Temporal
Inferior
Nasal
Log Reflection
OS
Sup
Nas
Tem
Inf
NFL Thickness (µm)
119
92
103
141
105 129 137
109
95
56
95
118
115
157 123 142

H

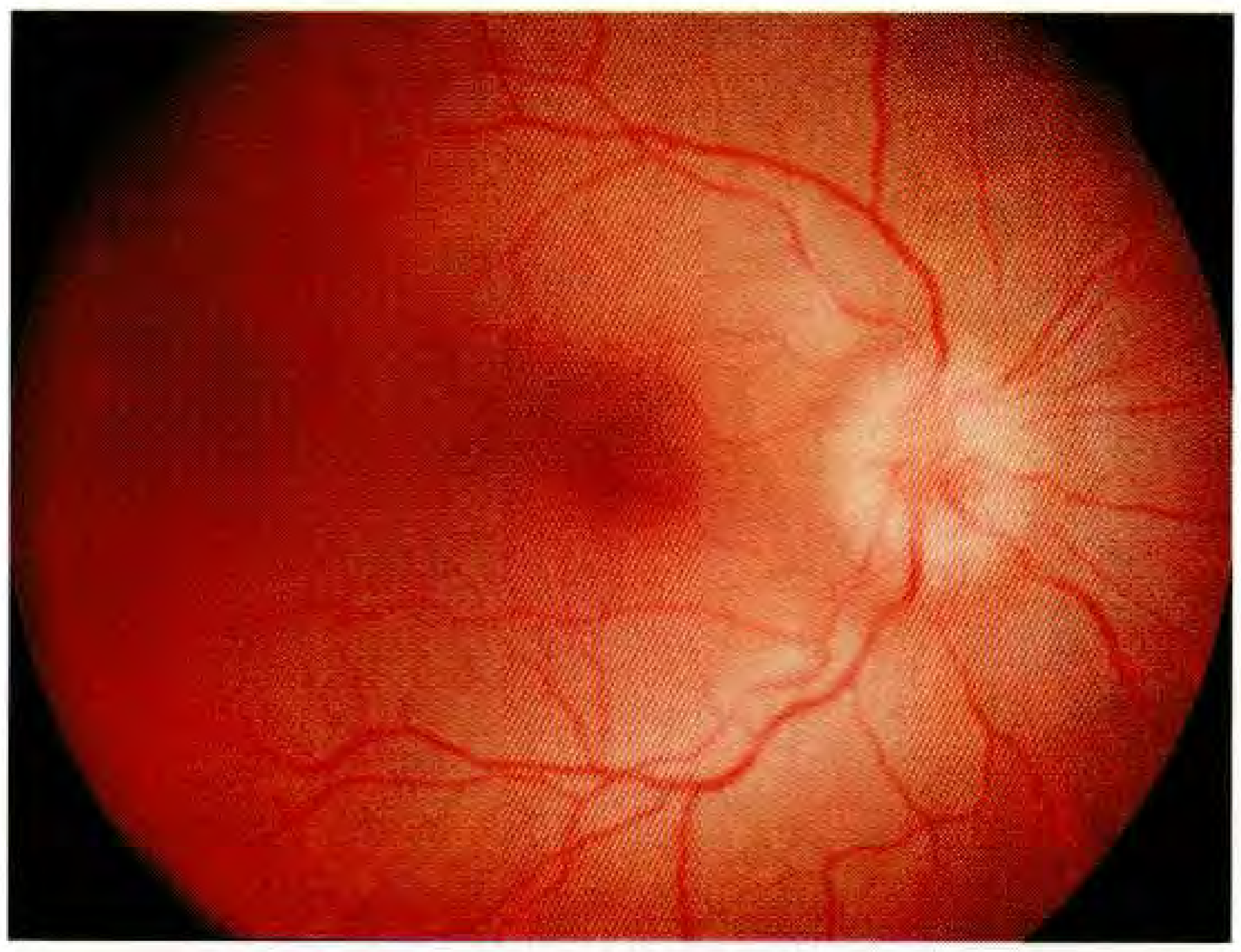

A

B

Case 14-4. Asymmetric Papilledema

Clinical Summary

A 43-year-old obese woman with a history of pseudotumor cerebri was taking acetazolamide 500 mg once daily. On examination, her visual acuity was 20/15 bilaterally. Dilated ophthalmoscopy (A, B) revealed elevation of the optic disc and blurred disc margins, greater in the right eye than the left, and no associated hemorrhage or arteriovenous abnormalities in either eye. There was no relative afferent pupillary defect.

Optical Coherence Tomography

Horizontal and vertical tomograms were acquired through the optic disc in both eyes. In the right eye (C), significant swelling of the disc was noted, with a complete loss of the physiologic cup. In contrast, the left eye (D) exhibited less edema and swelling which primarily affected the disc margins only. There was a relative preservation of the physiologic cup in this eye.

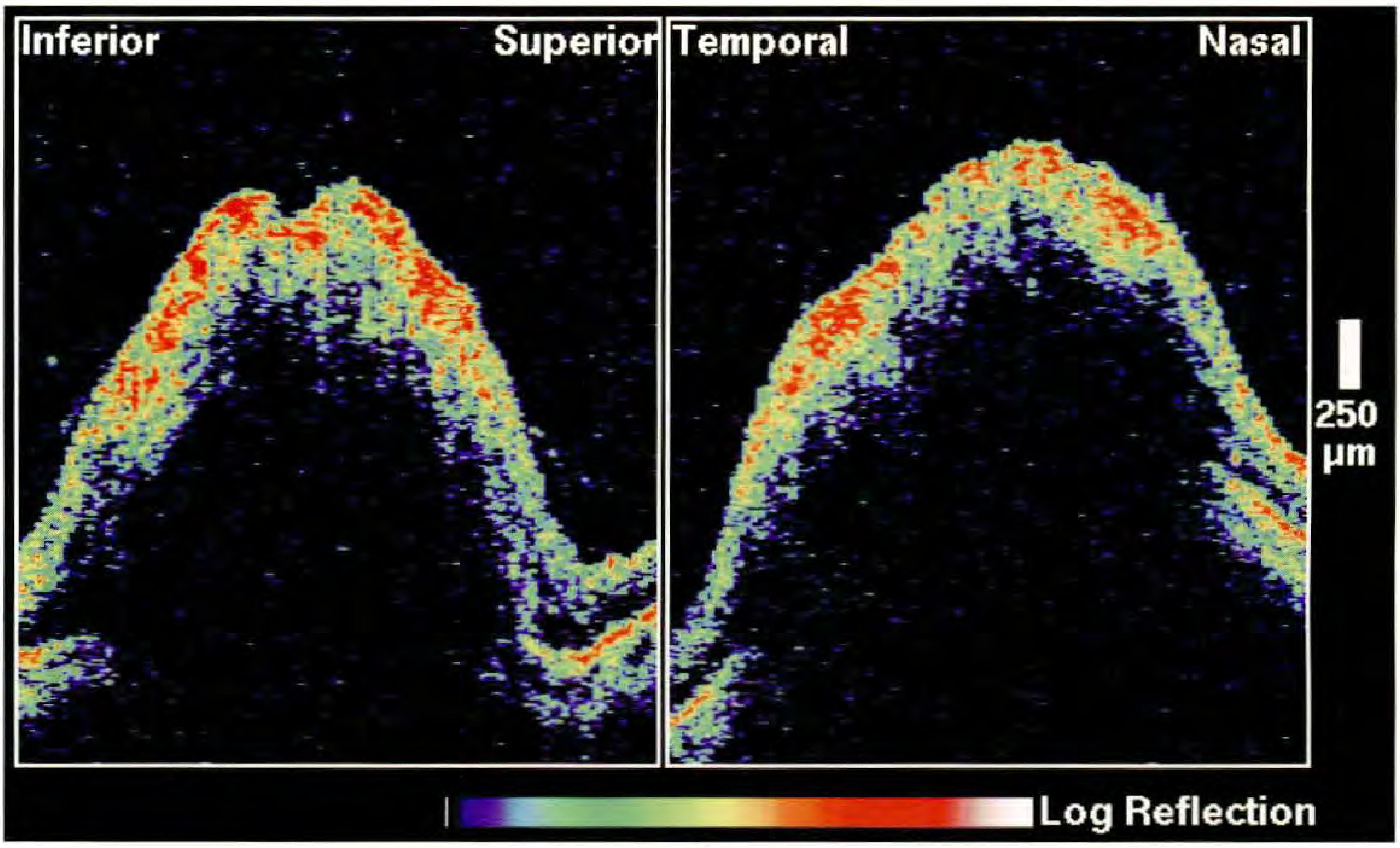
Inferior
Superior
Temporal
Nasal
250 µm
Log Reflection

C

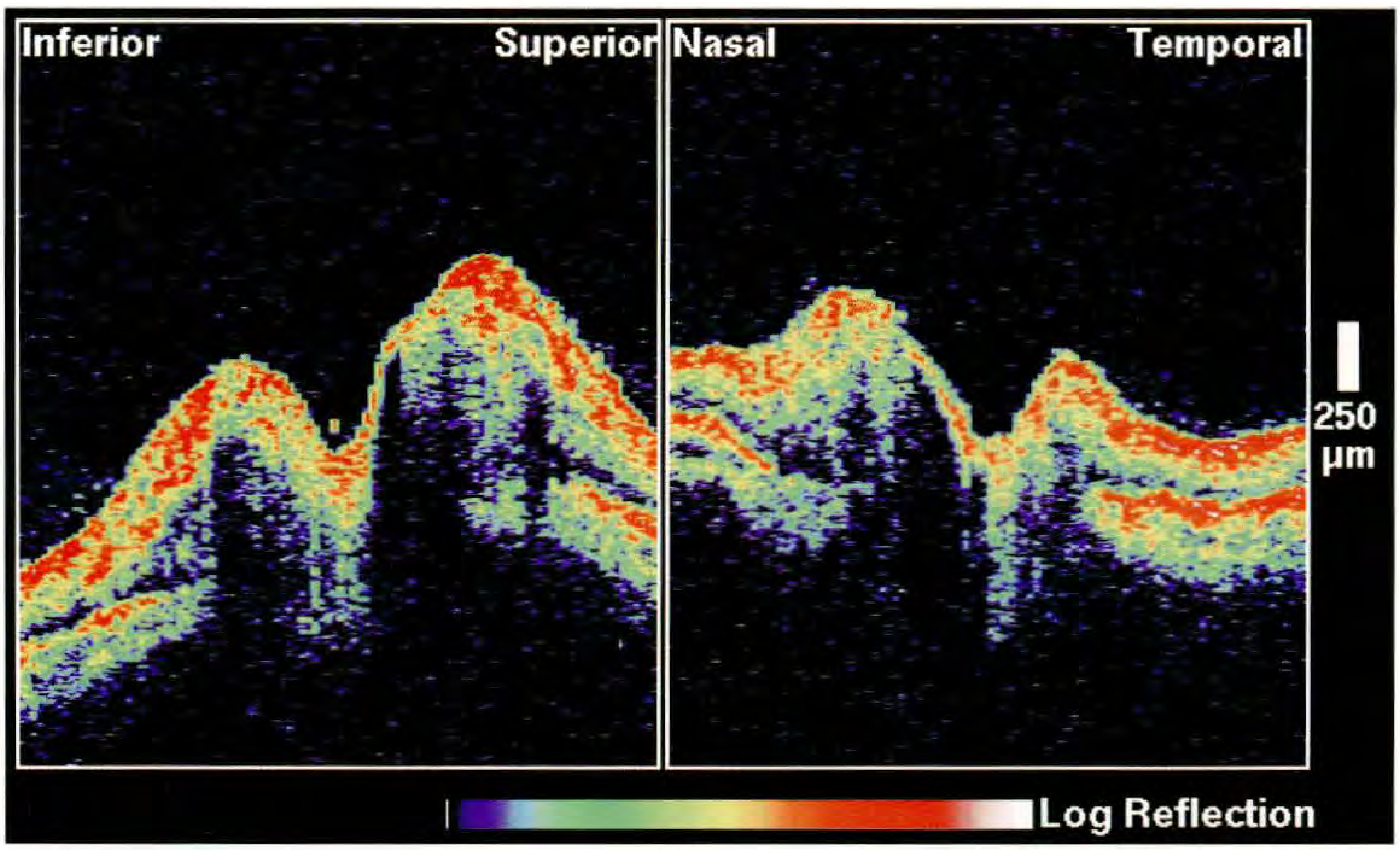
Inferior
Superior
Nasal
Temporal
250 µm
Log Reflection

D

INDEX